Averages of b-hadron, c-hadron, and τ-lepton properties as of summer 2016

Heavy Flavor Averaging Group (HFAG):

Y. Amhis[1], Sw. Banerjee[2], E. Ben-Haim[3], F. Bernlochner[4], A. Bozek[5], C. Bozzi[6], M. Chrząszcz[5,7], J. Dingfelder[4], S. Duell[4], M. Gersabeck[8], T. Gershon[9], P. Goldenzweig[10], R. Harr[11], K. Hayasaka[12], H. Hayashii[13], M. Kenzie[14], T. Kuhr[15], O. Leroy[16], A. Lusiani[17], X.R. Lyu[18], K. Miyabayashi[13], P. Naik[19], T. Nanut[20], A. Oyanguren Campos[21], M. Patel[22], D. Pedrini[23], M. Petrič[24], M. Rama[17], M. Roney[25], M. Rotondo[26], O. Schneider[27], C. Schwanda[28], A. J. Schwartz[29], J. Serrano[16], B. Shwartz[30], R. Tesarek[31], K. Trabelsi[32,33], P. Urquijo[34], R. Van Kooten[35], J. Yelton[36], and A. Zupanc[20,37]

[1] *LAL, Université Paris-Sud, France*
[2] *University of Louisville, USA*
[3] *LPNHE, Université Pierre et Marie Curie-Paris 6, Université Denis Diderot-Paris7, CNRS/IN2P3, France*
[4] *University of Bonn, Germany*
[5] *H. Niewodniczanski Institute of Nuclear Physics, Krakow, Poland*
[6] *INFN Ferrara, Italy*
[7] *Universität Zürich, Switzerland*
[8] *The University of Manchester, UK*
[9] *University of Warwick, UK*
[10] *Karlsruher Institut für Technologie, Germany*
[11] *Wayne State University, Detroit, USA*
[12] *Niigata University, Japan*
[13] *Nara Women's University, Japan*
[14] *University of Cambridge, UK*
[15] *Ludwig-Maximilians-University, Germany*
[16] *CPPM, Aix Marseille Université, CNRS/IN2P3, France*
[17] *Scuola Normale Superiore and INFN Pisa, Italy*
[18] *University of Chinese Academy of Sciences, Beijing, China*
[19] *University of Bristol, UK*
[20] *J. Stefan Institute, Ljubljana, Slovenia*
[21] *IFIC, University of Valencia, Spain*
[22] *Imperial College London, UK*
[23] *INFN Milano-Bicocca, Italy*
[24] *European Organization for Nuclear Research (CERN), Switzerland*
[25] *University of Victoria, Canada*
[26] *INFN Frascati, Italy*
[27] *Ecole Polytechnique Fédérale de Lausanne (EPFL), Switzerland*

Operated by Fermi Research Alliance, LLC under Contract No. DE-AC02-07CH11359 with the United States Department of Energy.

[28] *Institute of High Energy Physics, Vienna, Austria*
[29] *University of Cincinnati, USA*
[30] *Budker Institute of Nuclear Physics, Novosibirsk, Russia*
[31] *Fermilab, Batavia, USA*
[32] *High Energy Accelerator Research Organization (KEK), Tsukuba, Japan*
[33] *SOKENDAI (The Graduate University for Advanced Studies), Hayama, Japan*
[34] *University of Melbourne, Australia*
[35] *Indiana University, USA*
[36] *University of Florida, USA*
[37] *University of Ljubljana, Slovenia*

December 22, 2016

Abstract

This article reports world averages of measurements of b-hadron, c-hadron, and τ-lepton properties obtained by the Heavy Flavor Averaging Group (HFAG) using results available through summer 2016. For the averaging, common input parameters used in the various analyses are adjusted (rescaled) to common values, and known correlations are taken into account. The averages include branching fractions, lifetimes, neutral meson mixing parameters, CP violation parameters, parameters of semileptonic decays and CKM matrix elements.

Contents

1 Introduction

Flavor dynamics is an important element in understanding the nature of particle physics. The accurate knowledge of properties of heavy flavor hadrons, especially b hadrons, plays an essential role for determining the elements of the Cabibbo-Kobayashi-Maskawa (CKM) quark-mixing matrix [1, 2]. The operation of the Belle and *BABAR* e^+e^- B factory experiments led to a large increase in the size of available B-meson, D-hadron and τ-lepton samples, enabling dramatic improvement in the accuracies of related measurements. The CDF and D0 experiments at the Fermilab Tevatron have also provided important results in heavy flavour physics, most notably in the B_s^0 sector. In the D-meson sector, the dedicated e^+e^- charm factory experiments CLEO-c and BESIII have made significant contributions. Run I of the CERN Large Hadron Collider delivered high luminosity, enabling the collection of even larger samples of b and c hadrons, and thus a further leap in precision in many areas, at the ATLAS, CMS, and (especially) LHCb experiments. With the LHC Run II ongoing, further improvements are keenly anticipated.

The Heavy Flavor Averaging Group (HFAG) was formed in 2002 to continue the activities of the LEP Heavy Flavor Steering group [3]. This group was responsible for calculating averages of measurements of b-flavor related quantities. HFAG has evolved since its inception and currently consists of seven subgroups:

- the "B Lifetime and Oscillations" subgroup provides averages for b-hadron lifetimes, b-hadron fractions in $\Upsilon(4S)$ decay and pp or $p\overline{p}$ collisions, and various parameters governing B^0–$\overline{B}^0$ and B_s^0–$\overline{B}_s^0$ mixing;
- the "Unitarity Triangle Parameters" subgroup provides averages for time-dependent CP asymmetry parameters and studies of $B \to DK$ decays, and resulting determinations of the angles of the CKM unitarity triangle;
- the "Semileptonic B Decays" subgroup provides averages for inclusive and exclusive B-decay branching fractions, and subsequent determinations of the CKM matrix elements $|V_{cb}|$ and $|V_{ub}|$;
- the "B to Charm Decays" subgroup provides averages of branching fractions for B decays to final states involving open charm or charmonium mesons;
- the "Rare Decays" subgroup provides averages of branching fractions and CP asymmetries for charmless, radiative, leptonic, and baryonic B-meson and b-baryon decays;
- the "Charm Physics" subgroup provides averages of numerous quantities in the charm sector, including branching fractions, properties of charm baryons and of excited D^{**} and D_{sJ} mesons, averages of D^0–$\overline{D}^0$ mixing and CP and T violation parameters, and an average value for the $\mathcal{D}_s$ decay constant f_{D_s}.
- the "Tau Physics" subgroup provides averages for τ branching fractions using a global fit and elaborates the results to test lepton universality and to determine the CKM matrix element $|V_{us}|$; furthermore, it lists the τ lepton-flavor-violating upper limits and computes the combined upper limits.

The "Lifetime and Oscillations" and "Semileptonic" subgroups were formed from the merger of four LEP working groups. The "Unitary Triangle," "B to Charm Decays," and "Rare Decays" subgroups were formed to provide averages for new results obtained from the B factory

experiments (and now also from the Fermilab Tevatron and CERN LHC experiments). The "Charm" and "Tau" subgroups were formed more recently in response to the wealth of new data concerning D and τ physics. Subgroups typically include representatives from Belle, *BABAR* and LHCb, plus, when relevant, BESIII, CLEO, CDF and D0.

This article is an update of the last HFAG preprint, which used results available by summer 2014 [4]. Here we report world averages using results available by summer 2016. In general, we use all publicly available results that are supported by written documentation, including preliminary results presented at conferences or workshops. However, we do not use preliminary results that remain unpublished for an extended period of time, or for which no publication is planned. Close contacts have been established between representatives from the experiments and members of subgroups that perform averaging to ensure that the data are prepared in a form suitable for combinations.

Chapter 2 describes the methodology used for calculating averages. In the averaging procedure, common input parameters used in the various analyses are adjusted (rescaled) to common values, and, where possible, known correlations are taken into account. Chapters 3–9 present world average values from each of the subgroups listed above. A brief summary of the averages presented is given in Chapter 10. A complete listing of the averages and plots, including updates since this document was prepared, are also available on the HFAG web site:

`http://www.slac.stanford.edu/xorg/hfag`

2 Averaging methodology

The averaging problem that HFAG typically faces is to combine information provided by different measurements of the same parameter to obtain our best estimate of the parameter's value and uncertainty. In this section, the general approach adopted by HFAG is outlined. For some cases, somewhat simplified or more complex algorithms are used; these are noted in the corresponding sections.

The methodology described below in Sec. 2.1 focuses on the problems of combining measurements performed with different systematic assumptions and with potentially correlated systematic uncertainties. Our methodology relies on the close involvement of the people performing the measurements in the averaging process.

This methodology can be trivially extended to the case where multiple parameters are simultaneously averaged, taking account of correlations. Such simultaneous averages are performed for quantities where correlations are known to be important. It is important for any averaging procedure that the quantities determined by experiments are *statistically well-behaved*, which in this context can be interpreted as having a (one- or multi-dimensional) Gaussian likelihood function that is fully described by the central value(s) $\boldsymbol{x}_i$ and covariance matrix $\boldsymbol{V}_i$. If $\boldsymbol{x}$ contains n quantities (*i.e.* n is the number of degrees of freedom, dof), then a χ^2 function of order n is obtained by minimising

$$\chi^2(\boldsymbol{x}) = \sum_i \left(\boldsymbol{x}_i - \boldsymbol{x}\right)^{\mathrm{T}} \boldsymbol{V}_i^{-1} \left(\boldsymbol{x}_i - \boldsymbol{x}\right) \,, \tag{1}$$

where the sum is over the independent determinations of the quantities $\boldsymbol{x}$ (to put it another way, i runs over the different experiments). The results of the average are the central values $\hat{\boldsymbol{x}}$, which are the values of $\boldsymbol{x}$ at the minimum of $\chi^2(\boldsymbol{x})$ and their covariance matrix

$$\hat{\boldsymbol{V}}^{-1} = \sum_i \boldsymbol{V}_i^{-1} \,. \tag{2}$$

We report the covariance matrices, or the correlation matrices derived from them, whereever possible. In some cases where the matrices are large, it is inconvenient to report them in this written document, however, all results can be found on the HFAG web pages. Some discussion of cases where the likelihood function is not statistically well-behaved can be found in Sec. 2.2.

The obtained value of $\chi^2(\hat{\boldsymbol{x}})$ provides a measure of the consistency of the independent determination of $\boldsymbol{x}$. This is typically converted to a confidence level (CL) and reported together with the averages. In cases where the average has a value of $\chi^2/\mathrm{dof} > 1$, we do not usually scale the resulting error, as done by the Particle Data Group [5]. Rather, we examine the systematics of each measurement to better understand them. Unless we find possible systematic discrepancies between the measurements, we do not apply any additional correction to the calculated error. In case some special treatment was necessary to calculate an average, or if an approximation used in an averaging calculation might not be sufficiently accurate (*e.g.*, assuming Gaussian errors when the likelihood function indicates non-Gaussian behavior), we include a warning message. Further modifications to the averaging procedures in the case of non-Gaussian situations are discussed in Sec. 2.2.

For observables such as branching fractions, experiments typically report upper limits when the signal is not significant. Often, there is insufficient information available to combine upper limits for the same quantity obtained by different experiments, which may be obtained using

different statistical approaches. Therefore, we usually follow the convention of reporting the most restrictive upper limit as the average. An exception is made for branching fractions of lepton flavour violating decays of tau leptons, where combined upper limits are obtained as discussed in Sec. 9.6. The reported upper limits are at 90% CL unless stated otherwise.

2.1 Treatment of correlated systematic uncertainties

Consider two hypothetical measurements of a parameter x, which might be summarized as

$$x_1 \pm \delta x_1 \pm \Delta x_{1,1} \pm \Delta x_{2,1} \ldots$$
$$x_2 \pm \delta x_2 \pm \Delta x_{1,2} \pm \Delta x_{2,2} \ldots \, ,$$

where the δx_k are statistical uncertainties, and the $\Delta x_{i,k}$ are contributions to the systematic uncertainty. One popular approach is to combine statistical and systematic uncertainties in quadrature

$$x_1 \pm (\delta x_1 \oplus \Delta x_{1,1} \oplus \Delta x_{2,1} \oplus \ldots)$$
$$x_2 \pm (\delta x_2 \oplus \Delta x_{1,2} \oplus \Delta x_{2,2} \oplus \ldots) \, ,$$

and then perform a weighted average of x_1 and x_2, using their combined uncertainties, as if they were independent. This approach suffers from two potential problems that we attempt to address. First, the values of the x_k may have been obtained using different systematic assumptions. For example, different values of the B^0 lifetime may have been assumed in separate measurements of the oscillation frequency Δm_d. The second potential problem is that some contributions of the systematic uncertainty may be correlated between experiments. For example, separate measurements of Δm_d may both depend on an assumed Monte-Carlo branching fraction used to model a common background.

The problems mentioned above are related since, ideally, any quantity y_i that x_k depends on has a corresponding contribution $\Delta x_{i,k}$ to the systematic error which reflects the uncertainty Δy_i on y_i itself. We assume that this is the case and use the values of y_i and Δy_i assumed by each measurement explicitly in our averaging (we refer to these values as $y_{i,k}$ and $\Delta y_{i,k}$ below). Furthermore, since we do not lump all the systematics together, we require that each measurement used in an average have a consistent definition of the various contributions to the systematic uncertainty. Different analyses often use different decompositions of their systematic uncertainties, so achieving consistent definitions for any potentially correlated contributions requires close coordination between HFAG and the experiments. In some cases, a group of systematic uncertainties must be combined to obtain a coarser description that is consistent between measurements. Systematic uncertainties that are uncorrelated with any other sources of uncertainty appearing in an average are lumped together with the statistical error, so that the only systematic uncertainties treated explicitly are those that are correlated with at least one other measurement via a consistently-defined external parameter y_i. When asymmetric statistical or systematic uncertainties are quoted, we symmetrize them since our combination method implicitly assumes parabolic likelihoods for each measurement.

The fact that a measurement of x is sensitive to the value of y_i indicates that, in principle, the data used to measure x could equally-well be used for a simultaneous measurement of x and y_i, as illustrated by the large contour in Fig. 1(a) for a hypothetical measurement. However, we often have an external constraint Δy_i on the value of y_i (represented by the horizontal band

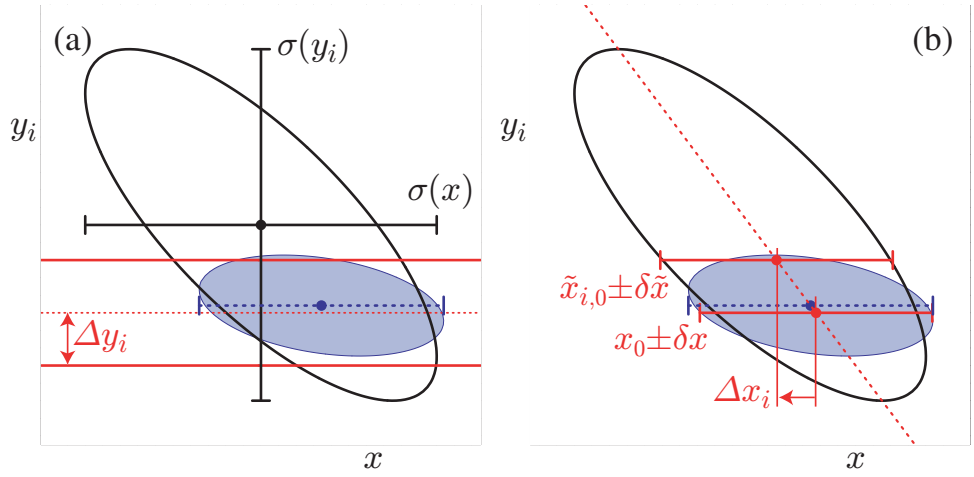

Figure 1: Illustration of the possible dependence of a measured quantity x on a nuisance parameter y_i. The left-hand plot (a) compares the 68% confidence level contours of a hypothetical measurement's unconstrained (large ellipse) and constrained (filled ellipse) likelihoods, using the Gaussian constraint on y_i represented by the horizontal band. The solid error bars represent the statistical uncertainties $\sigma(x)$ and $\sigma(y_i)$ of the unconstrained likelihood. The dashed error bar shows the statistical error on x from a constrained simultaneous fit to x and y_i. The right-hand plot (b) illustrates the method described in the text of performing fits to x with y_i fixed at different values. The dashed diagonal line between these fit results has the slope $\rho(x, y_i)\sigma(y_i)/\sigma(x)$ in the limit of an unconstrained parabolic likelihood. The result of the constrained simultaneous fit from (a) is shown as a dashed error bar on x.

in Fig. 1(a)) that is more precise than the constraint $\sigma(y_i)$ from our data alone. Ideally, in such cases we would perform a simultaneous fit to x and y_i, including the external constraint, obtaining the filled (x, y) contour and corresponding dashed one-dimensional estimate of x shown in Fig. 1(a). Throughout, we assume that the external constraint Δy_i on y_i is Gaussian.

In practice, the added technical complexity of a constrained fit with extra free parameters is not justified by the small increase in sensitivity, as long as the external constraints Δy_i are sufficiently precise when compared with the sensitivities $\sigma(y_i)$ to each y_i of the data alone. Instead, the usual procedure adopted by the experiments is to perform a baseline fit with all y_i fixed to nominal values $y_{i,0}$, obtaining $x = x_0 \pm \delta x$. This baseline fit neglects the uncertainty due to Δy_i, but this error can be mostly recovered by repeating the fit separately for each external parameter y_i with its value fixed at $y_i = y_{i,0} + \Delta y_i$ to obtain $x = \tilde{x}_{i,0} \pm \delta\tilde{x}$, as illustrated in Fig. 1(b). The absolute shift, $|\tilde{x}_{i,0} - x_0|$, in the central value of x is what the experiments usually quote as their systematic uncertainty Δx_i on x due to the unknown value of y_i. Our procedure requires that we know not only the magnitude of this shift but also its sign. In the limit that the unconstrained data is represented by a parabolic likelihood, the signed shift is given by

$$\Delta x_i = \rho(x, y_i)\frac{\sigma(x)}{\sigma(y_i)}\,\Delta y_i\,, \tag{3}$$

where $\sigma(x)$ and $\rho(x, y_i)$ are the statistical uncertainty on x and the correlation between x and y_i in the unconstrained data. While our procedure is not equivalent to the constrained fit with extra parameters, it yields (in the limit of a parabolic unconstrained likelihood) a central value

x_0 that agrees to $\mathcal{O}(\Delta y_i/\sigma(y_i))^2$ and an uncertainty $\delta x \oplus \Delta x_i$ that agrees to $\mathcal{O}(\Delta y_i/\sigma(y_i))^4$.

Another approach, frequently adopted by experiments, is to allow y_i to vary within its uncertainty Δy_i in the fit, by means of a Gaussian constraint added to the likelihood function. In this approach, the resulting uncertainty on the measured parameter Δx_i is absorbed into the statistical uncertainty δx_i. In case this source of systematic uncertainty is shared between experiments, its proper treatment again requires that experiments provide information about the magnitude and sign of Δx_i.

In order to combine two or more measurements that share systematics due to the same external parameters y_i, we would ideally perform a constrained simultaneous fit of all data samples to obtain values of x and each y_i, being careful to only apply the constraint on each y_i once. This is usually not practical since we generally do not have sufficient information to reconstruct the unconstrained likelihoods corresponding to each measurement. Instead, we perform the two-step approximate procedure described below.

Figs. 2(a,b) illustrate two statistically-independent measurements, $x_1 \pm (\delta x_1 \oplus \Delta x_{i,1})$ and $x_2 \pm (\delta x_i \oplus \Delta x_{i,2})$, of the same hypothetical quantity x (for simplicity, we only show the contribution of a single correlated systematic due to an external parameter y_i). As our knowledge of the external parameters y_i evolves, it is natural that the different measurements of x will assume different nominal values and ranges for each y_i. The first step of our procedure is to adjust the values of each measurement to reflect the current best knowledge of the values y'_i and ranges $\Delta y'_i$ of the external parameters y_i, as illustrated in Figs. 2(c,d). We adjust the central values x_k and correlated systematic uncertainties $\Delta x_{i,k}$ linearly for each measurement (indexed by k) and each external parameter (indexed by i):

$$x'_k = x_k + \sum_i \frac{\Delta x_{i,k}}{\Delta y_{i,k}} (y'_i - y_{i,k}) \tag{4}$$

$$\Delta x'_{i,k} = \Delta x_{i,k} \frac{\Delta y'_i}{\Delta y_{i,k}} \,. \tag{5}$$

This procedure is exact in the limit that the unconstrained likelihoods of each measurement is parabolic.

The second step of our procedure is to combine the adjusted measurements, $x'_k \pm (\delta x_k \oplus \Delta x'_{k,1} \oplus \Delta x'_{k,2} \oplus \ldots)$ using

$$\chi^2_{\rm comb}(x, y_1, y_2, \ldots) \equiv \sum_k \frac{1}{\delta x_k^2} \left[x'_k - \left(x + \sum_i (y_i - y'_i) \frac{\Delta x'_{i,k}}{\Delta y'_i} \right) \right]^2 + \sum_i \left(\frac{y_i - y'_i}{\Delta y'_i} \right)^2 \,, \tag{6}$$

and then minimize this χ^2 to obtain the best values of x and y_i and their uncertainties, as illustrated in Fig. 3. Although this method determines new values for the y_i, we do not report them since the $\Delta x_{i,k}$ reported by each experiment are generally not intended for this purpose (for example, they may represent a conservative upper limit rather than a true reflection of a 68% confidence level).

For comparison, the exact method we would perform if we had the unconstrained likelihoods $\mathcal{L}_k(x, y_1, y_2, \ldots)$ available for each measurement is to minimize the simultaneous constrained likelihood

$$\mathcal{L}_{\rm comb}(x, y_1, y_2, \ldots) \equiv \prod_k \mathcal{L}_k(x, y_1, y_2, \ldots) \prod_i \mathcal{L}_i(y_i) \,, \tag{7}$$

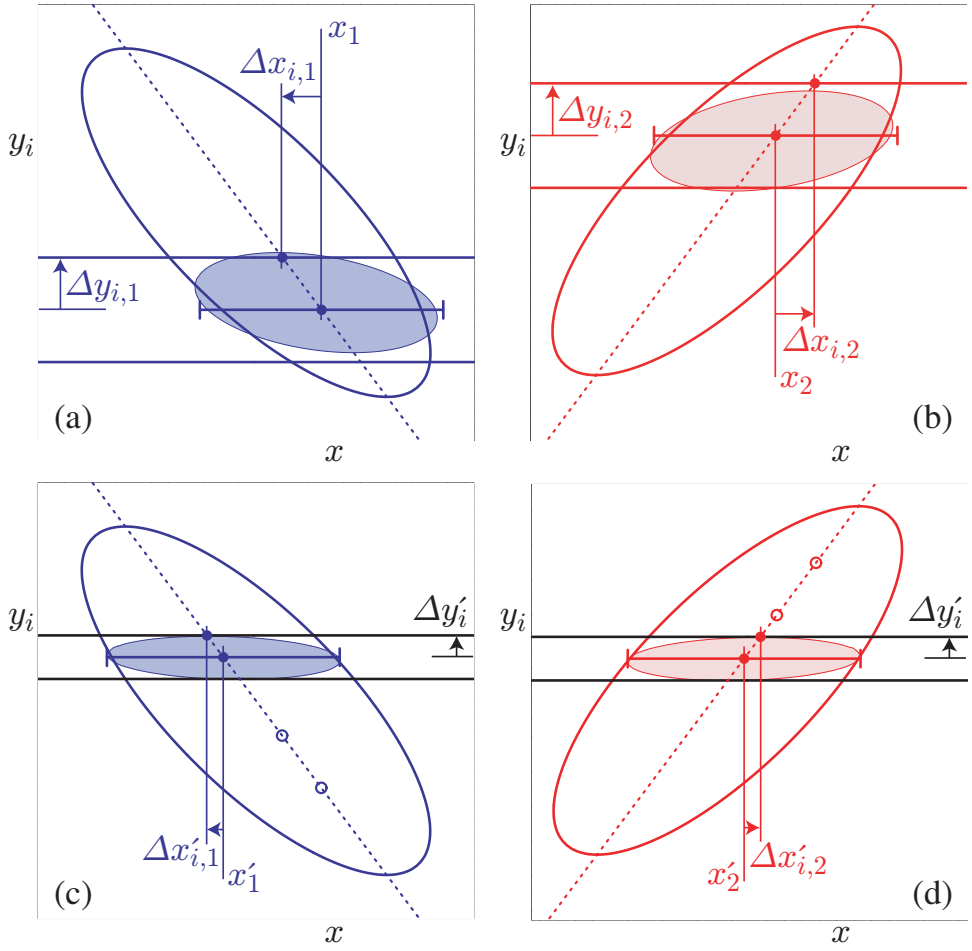

Figure 2: Illustration of the HFAG combination procedure for correlated systematic uncertainties. Upper plots (a) and (b) show examples of two individual measurements to be combined. The large (filled) ellipses represent their unconstrained (constrained) likelihoods, while horizontal bands indicate the different assumptions about the value and uncertainty of y_i used by each measurement. The error bars show the results of the method described in the text for obtaining x by performing fits with y_i fixed to different values. Lower plots (c) and (d) illustrate the adjustments to accommodate updated and consistent knowledge of y_i. Open circles mark the central values of the unadjusted fits to x with y fixed; these determine the dashed line used to obtain the adjusted values.

with an independent Gaussian external constraint on each y_i

$$\mathcal{L}_i(y_i) \equiv \exp\left[-\frac{1}{2}\left(\frac{y_i - y_i'}{\Delta y_i'}\right)^2\right] . \tag{8}$$

The results of this exact method are illustrated by the filled ellipses in Figs. 3(a,b) and agree with our method in the limit that each $\mathcal{L}_k$ is parabolic and that each $\Delta y_i' \ll \sigma(y_i)$. In the case of a non-parabolic unconstrained likelihood, experiments would have to provide a description of $\mathcal{L}_k$ itself to allow an improved combination. In the case of $\sigma(y_i) \simeq \Delta y_i'$, experiments are advised to perform a simultaneous measurement of both x and y so that their data will improve the world knowledge about y.

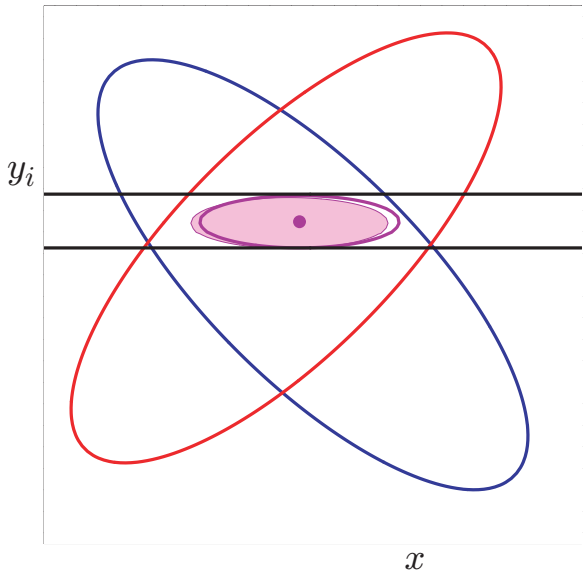

Figure 3: Illustration of the combination of two hypothetical measurements of x using the method described in the text. The ellipses represent the unconstrained likelihoods of each measurement, and the horizontal band represents the latest knowledge about y_i that is used to adjust the individual measurements. The filled small ellipse shows the result of the exact method using $\mathcal{L}_{\rm comb}$, and the hollow small ellipse and dot show the result of the approximate method using $\chi^2_{\rm comb}$.

For averages where common sources of systematic uncertainty are important, central values and uncertainties are rescaled to a common set of input parameters following the prescription described above. We use the most up-to-date values for common inputs, consistently across subgroups, taking values from within HFAG where possible, or from external groups such as the PDG otherwise. The parameters and values used are listed in each subgroup section.

2.2 Treatment of non-Gaussian likelihood functions

For measurements with Gaussian errors, the usual estimator for the average of a set of measurements is obtained by minimizing

$$\chi^2(x) = \sum_i^N \frac{(x_i - x)^2}{\sigma_i^2}\,, \tag{9}$$

where x_i is the $i^{\rm th}$ measured value of x and σ_i^2 is the variance of the distribution from which x_i was drawn. Here, a one-dimensional problem is considered for simplicity. The value $\hat{x}$ of x at minimum χ^2 is the estimator for the average. The true σ_i are unknown but typically the error as assigned by the experiment $\sigma_i^{\rm raw}$ is used as an estimator for it. Caution is advised, however, in the case where $\sigma_i^{\rm raw}$ depends on the value measured for x_i. Examples of this include an uncertainty in any multiplicative factor (like an acceptance) that enters the determination of x_i, *i.e.* the $\sqrt{N}$ dependence of Poisson statistics, where $x_i \propto N$ and $\sigma_i \propto \sqrt{N}$. Failing to account for this type of dependence when averaging leads to a biased average. Biases in the

average can be avoided (or at least reduced) by minimizing

$$\chi^2(x) = \sum_i^N \frac{(x_i - x)^2}{\sigma_i^2(\hat{x})} \,. \tag{10}$$

In the above $\sigma_i(\hat{x})$ is the uncertainty assigned to input i that includes the assumed dependence of the stated error on the value measured. As an example, consider a pure acceptance error, for which $\sigma_i(\hat{x}) = (\hat{x}/x_i) \times \sigma_i^{\rm raw}$. It is easily verified that solving Eq. (10) leads to the correct behavior, namely

$$\hat{x} = \frac{\sum_i^N x_i^3/(\sigma_i^{\rm raw})^2}{\sum_i^N x_i^2/(\sigma_i^{\rm raw})^2} \,,$$

i.e. weighting by the inverse square of the fractional uncertainty, $\sigma_i^{\rm raw}/x_i$. It is sometimes difficult to assess the dependence of $\sigma_i^{\rm raw}$ on $\hat{x}$ from the errors quoted by experiments.

Another issue that needs careful treatment is the question of correlation among different measurements, *e.g.* due to using the same theory for calculating acceptances. A common practice is to set the correlation coefficient to unity to indicate full correlation. However, this is not a "conservative" thing to do, and can in fact lead to a significantly underestimated uncertainty on the average. In the absence of better information, the most conservative choice of correlation coefficient between two measurements i and j is the one that maximizes the uncertainty on $\hat{x}$ due to that pair of measurements:

$$\sigma^2_{\hat{x}(i,j)} = \frac{\sigma_i^2\,\sigma_j^2\,(1-\rho_{ij}^2)}{\sigma_i^2 + \sigma_j^2 - 2\,\rho_{ij}\,\sigma_i\,\sigma_j} \,, \tag{11}$$

namely

$$\rho_{ij} = \min\left(\frac{\sigma_i}{\sigma_j}, \frac{\sigma_j}{\sigma_i}\right) \,, \tag{12}$$

which corresponds to setting $\sigma^2_{\hat{x}(i,j)} = \min(\sigma_i^2, \sigma_j^2)$. Setting $\rho_{ij} = 1$ when $\sigma_i \neq \sigma_j$ can lead to a significant underestimate of the uncertainty on $\hat{x}$, as can be seen from Eq. (11).

Finally, we carefully consider the various sources of error contributing to the overall uncertainty of an average. The overall covariance matrix describing the uncertainties of a number of measurements of the same quantity and their correlations is constructed from a number of individual sources, *e.g.* $\boldsymbol{V} = \boldsymbol{V}_{\rm stat} + \boldsymbol{V}_{\rm sys} + \boldsymbol{V}_{\rm th}$. If the measurements are from independent data samples, then $\boldsymbol{V}_{\rm stat}$ must be diagonal, but $\boldsymbol{V}_{\rm sys}$ and $\boldsymbol{V}_{\rm th}$ may contain non-trivial correlations. The variance on the average $\hat{x}$ can be written

$$\sigma^2_{\hat{x}} \;=\; \frac{\sum_{i,j}\left(\boldsymbol{V}^{-1}\,[\boldsymbol{V}_{\rm stat} + \boldsymbol{V}_{\rm sys} + \boldsymbol{V}_{\rm th}]\,\boldsymbol{V}^{-1}\right)_{ij}}{\left(\sum_{i,j}\boldsymbol{V}^{-1}_{ij}\right)^2} = \sigma^2_{\rm stat} + \sigma^2_{\rm sys} + \sigma^2_{\rm th} \,. \tag{13}$$

Written in this form, one can readily determine the contribution of each source of uncertainty to the overall uncertainty on the average. This breakdown of the uncertainties is used in certain cases in the following sections, but in the majority of cases only a single, combined uncertainty is quoted on the average.

3 b-hadron production fractions, lifetimes and mixing parameters

Quantities such as b-hadron production fractions, b-hadron lifetimes, and neutral B-meson oscillation frequencies have been studied in the nineties at LEP and SLC (e^+e^- colliders at $\sqrt{s} = m_Z$) as well as at the first version of the Tevatron ($p\overline{p}$ collider at $\sqrt{s} = 1.8$ TeV). Since then precise measurements of the B^0 and B^+ mesons have also been performed at the asymmetric B factories, KEKB and PEPII (e^+e^- colliders at $\sqrt{s} = m_{\Upsilon(4S)}$), while measurements related to the other b hadrons, in particular B_s^0, B_c^+ and Λ_b^0, have been performed at the upgraded Tevatron ($\sqrt{s} = 1.96$ TeV). Since a few years, the most precise measurements are coming from the LHC (pp collider at $\sqrt{s} = 7$ and 8 TeV), in particular the LHCb experiment.

In most cases, these basic quantities, although interesting by themselves, became necessary ingredients for the more complicated and refined analyses at both e^+e^- B factories and hadron colliders, in particular the time-dependent CP asymmetry measurements. It is therefore important that the best experimental values of these quantities continue to be kept up-to-date and improved.

In several cases, the averages presented in this chapter are needed and used as input for the results given in the subsequent chapters. Within this chapter, some averages need the knowledge of other averages in a circular way. This coupling, which appears through the b-hadron fractions whenever inclusive or semi-exclusive measurements have to be considered, has been reduced drastically in the past several years with increasingly precise exclusive measurements becoming available and dominating practically all averages.

In addition to b-hadron fractions, lifetimes and mixing parameters, this chapter also deals with the CP-violating phase $\phi_s^{c\bar{c}s} \simeq -2\beta_s$, which is the phase difference between the B_s^0 mixing amplitude and the $b \to c\bar{c}s$ decay amplitude, as well as the parameters of CP violation in the B mixing amplitudes. The angle β, which is the equivalent of β_s for the B^0 system, is discussed in Chapter 4.

3.1 b-hadron production fractions

We consider here the relative fractions of the different b-hadron species found in an unbiased sample of weakly decaying b hadrons produced under some specific conditions. The knowledge of these fractions is useful to characterize the signal composition in inclusive b-hadron analyses, to predict the background composition in exclusive analyses, or to convert (relative) observed rates into (relative) branching fraction measurements. Many B-physics analyses need these fractions as input. We distinguish here the following three conditions: $\Upsilon(4S)$ decays, $\Upsilon(5S)$ decays, and high-energy collisions (including Z^0 decays).

3.1.1 b-hadron production fractions in $\Upsilon(4S)$ decays

Only pairs of the two lightest (charged and neutral) B mesons can be produced in $\Upsilon(4S)$ decays, and it is enough to determine the following branching fractions:

$$f^{+-} = \Gamma(\Upsilon(4S) \to B^+B^-)/\Gamma_{\rm tot}(\Upsilon(4S))\,, \tag{14}$$

$$f^{00} = \Gamma(\Upsilon(4S) \to B^0\overline{B}^0)/\Gamma_{\rm tot}(\Upsilon(4S))\,. \tag{15}$$

Table 1: Published measurements of the B^+/B^0 production ratio in $\Upsilon(4S)$ decays, together with their average (see text). Systematic uncertainties due to the imperfect knowledge of $\tau(B^+)/\tau(B^0)$ are included. The latest *BABAR* result [6] supersedes the earlier *BABAR* measurements [7, 8].

Experiment and year	Ref.	Decay modes or method	Published value of $R^{+-/00} = f^{+-}/f^{00}$	Assumed value of $\tau(B^+)/\tau(B^0)$
CLEO, 2001	[9]	$J/\psi\, K^{(*)}$	$1.04 \pm 0.07 \pm 0.04$	1.066 ± 0.024
BABAR, 2002	[7]	$(c\overline{c})K^{(*)}$	$1.10 \pm 0.06 \pm 0.05$	1.062 ± 0.029
CLEO, 2002	[10]	$D^*\ell\nu$	$1.058 \pm 0.084 \pm 0.136$	1.074 ± 0.028
Belle, 2003	[11]	dilepton events	$1.01 \pm 0.03 \pm 0.09$	1.083 ± 0.017
BABAR, 2004	[8]	$J/\psi\, K$	$1.006 \pm 0.036 \pm 0.031$	1.083 ± 0.017
BABAR, 2005	[6]	$(c\overline{c})K^{(*)}$	$1.06 \pm 0.02 \pm 0.03$	1.086 ± 0.017
Average			1.059 ± 0.027 (tot)	1.076 ± 0.004

In practice, most analyses measure their ratio

$$R^{+-/00} = f^{+-}/f^{00} = \Gamma(\Upsilon(4S) \to B^+B^-)/\Gamma(\Upsilon(4S) \to B^0\overline{B}^0)\,, \tag{16}$$

which is easier to access experimentally. Since an inclusive (but separate) reconstruction of B^+ and B^0 is difficult, exclusive decay modes to specific final states f, $B^+ \to f^+$ and $B^0 \to f^0$, are usually considered to perform a measurement of $R^{+-/00}$, whenever they can be related by isospin symmetry (for example $B^+ \to J/\psi\, K^+$ and $B^0 \to J/\psi\, K^0$). Under the assumption that $\Gamma(B^+ \to f^+) = \Gamma(B^0 \to f^0)$, *i.e.* that isospin invariance holds in these B decays, the ratio of the number of reconstructed $B^+ \to f^+$ and $B^0 \to f^0$ mesons, after correcting for efficiency, is proportional to

$$\frac{f^{+-}\,\mathcal{B}(B^+ \to f^+)}{f^{00}\,\mathcal{B}(B^0 \to f^0)} = \frac{f^{+-}\,\Gamma(B^+ \to f^+)\,\tau(B^+)}{f^{00}\,\Gamma(B^0 \to f^0)\,\tau(B^0)} = \frac{f^{+-}}{f^{00}}\,\frac{\tau(B^+)}{\tau(B^0)}\,, \tag{17}$$

where $\tau(B^+)$ and $\tau(B^0)$ are the B^+ and B^0 lifetimes respectively. Hence the primary quantity measured in these analyses is $R^{+-/00}\,\tau(B^+)/\tau(B^0)$, and the extraction of $R^{+-/00}$ with this method therefore requires the knowledge of the $\tau(B^+)/\tau(B^0)$ lifetime ratio.

The published measurements of $R^{+-/00}$ are listed in Table 1 together with the corresponding assumed values of $\tau(B^+)/\tau(B^0)$. All measurements are based on the above-mentioned method, except the one from Belle, which is a by-product of the B^0 mixing frequency analysis using dilepton events (but note that it also assumes isospin invariance, namely $\Gamma(B^+ \to \ell^+\mathrm{X}) = \Gamma(B^0 \to \ell^+\mathrm{X})$). The latter is therefore treated in a slightly different manner in the following procedure used to combine these measurements:

- each published value of $R^{+-/00}$ from CLEO and *BABAR* is first converted back to the original measurement of $R^{+-/00}\,\tau(B^+)/\tau(B^0)$, using the value of the lifetime ratio assumed in the corresponding analysis;
- a simple weighted average of these original measurements of $R^{+-/00}\,\tau(B^+)/\tau(B^0)$ from CLEO and *BABAR* (which do not depend on the assumed value of the lifetime ratio) is then computed, assuming no statistical or systematic correlations between them;

- the weighted average of $R^{+-/00}\,\tau(B^+)/\tau(B^0)$ is converted into a value of $R^{+-/00}$, using the latest average of the lifetime ratios, $\tau(B^+)/\tau(B^0) = 1.076 \pm 0.004$ (see Sec. 3.2.3);
- the Belle measurement of $R^{+-/00}$ is adjusted to the current values of $\tau(B^0) = 1.520 \pm 0.004$ ps and $\tau(B^+)/\tau(B^0) = 1.076 \pm 0.004$ (see Sec. 3.2.3), using the quoted systematic uncertainties due to these parameters;
- the combined value of $R^{+-/00}$ from CLEO and *BABAR* is averaged with the adjusted value of $R^{+-/00}$ from Belle, assuming a 100% correlation of the systematic uncertainty due to the limited knowledge on $\tau(B^+)/\tau(B^0)$; no other correlation is considered.

The resulting global average,

$$R^{+-/00} = \frac{f^{+-}}{f^{00}} = 1.059 \pm 0.027\,, \tag{18}$$

is consistent with equal production of charged and neutral B mesons, although only at the $2.2\,\sigma$ level.

On the other hand, the *BABAR* collaboration has performed a direct measurement of the f^{00} fraction using an original method, which neither relies on isospin symmetry nor requires the knowledge of $\tau(B^+)/\tau(B^0)$. Its analysis, based on a comparison between the number of events where a single $B^0 \to D^{*-}\ell^+\nu$ decay could be reconstructed and the number of events where two such decays could be reconstructed, yields [12]

$$f^{00} = 0.487 \pm 0.010\,(\text{stat}) \pm 0.008\,(\text{syst})\,. \tag{19}$$

The two results of Eqs. (18) and (19) are of very different natures and completely independent of each other. Their product is equal to $f^{+-} = 0.516 \pm 0.019$, while another combination of them gives $f^{+-} + f^{00} = 1.003 \pm 0.029$, compatible with unity. Assuming[1] $f^{+-} + f^{00} = 1$, also consistent with CLEO's observation that the fraction of $\Upsilon(4S)$ decays to $B\overline{B}$ pairs is larger than 0.96 at 95% CL [14], the results of Eqs. (18) and (19) can be averaged (first converting Eq. (18) into a value of $f^{00} = 1/(R^{+-/00} + 1)$) to yield the following more precise estimates:

$$f^{00} = 0.486 \pm 0.006\,, \quad f^{+-} = 1 - f^{00} = 0.514 \pm 0.006\,, \quad \frac{f^{+-}}{f^{00}} = 1.058 \pm 0.024\,. \tag{20}$$

The latter ratio differs from one by $2.4\,\sigma$.

3.1.2 *b*-hadron production fractions in $\Upsilon(5S)$ decays

Hadronic events produced in e^+e^- collisions at the $\Upsilon(5S)$ (also known as $\Upsilon(10860)$) energy can be classified into three categories: light-quark (u, d, s, c) continuum events, $b\overline{b}$ continuum events, and $\Upsilon(5S)$ events. The latter two cannot be distinguished and will be called $b\overline{b}$ events in the following. These $b\overline{b}$ events, which also include $b\overline{b}\gamma$ events because of possible initial-state radiation, can hadronize in different final states. We define $f_{u,d}^{\Upsilon(5S)}$ as the fraction of $b\overline{b}$

[1] A few non-$B\overline{B}$ decay modes of the $\Upsilon(4S)$ ($\Upsilon(1S)\pi^+\pi^-$, $\Upsilon(2S)\pi^+\pi^-$, $\Upsilon(1S)\eta$) have been observed with branching fractions of the order of 10^{-4} [13], corresponding to a partial width several times larger than that in the e^+e^- channel. However, this can still be neglected and the assumption $f^{+-} + f^{00} = 1$ remains valid in the present context of the determination of f^{+-} and f^{00}.

Table 2: Published measurements of $f_s^{\Upsilon(5S)}$, obtained assuming $f_{\not B}^{\Upsilon(5S)} = 0$ and quoted as in the original publications, except for the 2010 Belle measurement which is quoted as $1 - f_{u,d}^{\Upsilon(5S)}$, with $f_{u,d}^{\Upsilon(5S)}$ from Ref. [15]. Our average of $f_s^{\Upsilon(5S)}$ assuming $f_{\not B}^{\Upsilon(5S)} = 0$, given on the penultimate line, does not include the most recent Belle result quoted on the last line.[2]

Experiment, year, dataset	Decay mode or method	Value of $f_s^{\Upsilon(5S)}$
CLEO, 2006, $0.42\,\text{fb}^{-1}$ [16]	$\Upsilon(5S) \to D_s X$	$0.168 \pm 0.026^{+0.067}_{-0.034}$
	$\Upsilon(5S) \to \phi X$	$0.246 \pm 0.029^{+0.110}_{-0.053}$
	$\Upsilon(5S) \to B\overline{B}X$	$0.411 \pm 0.100 \pm 0.092$
	CLEO average of above 3	$0.21^{+0.06}_{-0.03}$
Belle, 2006, $1.86\,\text{fb}^{-1}$ [17]	$\Upsilon(5S) \to D_s X$	$0.179 \pm 0.014 \pm 0.041$
	$\Upsilon(5S) \to D^0 X$	$0.181 \pm 0.036 \pm 0.075$
	Belle average of above 2	$0.180 \pm 0.013 \pm 0.032$
Belle, 2010, $23.6\,\text{fb}^{-1}$ [15]	$\Upsilon(5S) \to B\overline{B}X$	$0.263 \pm 0.032 \pm 0.051$
Average of all above after adjustments to inputs of Table 3		0.215 ± 0.031
Belle, 2012, $121.4\,\text{fb}^{-1}$ [18]	$\Upsilon(5S) \to D_s X, D^0 X$	0.172 ± 0.030

Table 3: External inputs on which the $f_s^{\Upsilon(5S)}$ averages are based.

Branching fraction	Value	Explanation and reference
$\mathcal{B}(B \to D_s X) \times \mathcal{B}(D_s \to \phi\pi)$	0.00374 ± 0.00014	derived from [5]
$\mathcal{B}(B_s^0 \to D_s X)$	0.92 ± 0.11	model-dependent estimate [19]
$\mathcal{B}(D_s \to \phi\pi)$	0.045 ± 0.004	[5]
$\mathcal{B}(B \to D^0 X) \times \mathcal{B}(D^0 \to K\pi)$	0.0243 ± 0.0011	derived from [5]
$\mathcal{B}(B_s^0 \to D^0 X)$	0.08 ± 0.07	model-dependent estimate [17, 19]
$\mathcal{B}(D^0 \to K\pi)$	0.0393 ± 0.0004	[5]
$\mathcal{B}(B \to \phi X)$	0.0343 ± 0.0012	[5]
$\mathcal{B}(B_s^0 \to \phi X)$	0.161 ± 0.024	model-dependent estimate [16]

events with a pair of non-strange bottom mesons ($B\overline{B}$, $B\overline{B}^*$, $B^*\overline{B}$, $B^*\overline{B}^*$, $B\overline{B}\pi$, $B\overline{B}^*\pi$, $B^*\overline{B}\pi$, $B^*\overline{B}^*\pi$, and $B\overline{B}\pi\pi$ final states, where B denotes a B^0 or B^+ meson and $\overline{B}$ denotes a $\overline{B}^0$ or B^- meson), $f_s^{\Upsilon(5S)}$ as the fraction of $b\bar{b}$ events with a pair of strange bottom mesons ($B_s^0\overline{B}_s^0$, $B_s^0\overline{B}_s^{*0}$, $B_s^{*0}\overline{B}_s^0$, and $B_s^{*0}\overline{B}_s^{*0}$ final states), and $f_{\not B}^{\Upsilon(5S)}$ as the fraction of $b\bar{b}$ events without any bottom meson in the final state. Note that the excited bottom-meson states decay via $B^* \to B\gamma$ and $B_s^{*0} \to B_s^0\gamma$. These fractions satisfy

$$f_{u,d}^{\Upsilon(5S)} + f_s^{\Upsilon(5S)} + f_{\not B}^{\Upsilon(5S)} = 1\,. \tag{21}$$

The CLEO and Belle collaborations have published measurements of several inclusive $\Upsilon(5S)$ branching fractions, $\mathcal{B}(\Upsilon(5S) \to D_s X)$, $\mathcal{B}(\Upsilon(5S) \to \phi X)$ and $\mathcal{B}(\Upsilon(5S) \to D^0 X)$, from which they extracted the model-dependent estimates of $f_s^{\Upsilon(5S)}$ reported in Table 2. This extraction

was performed under the implicit assumption $f_{\not B}^{\Upsilon(5S)} = 0$, using the relation

$$\frac{1}{2}\mathcal{B}(\Upsilon(5S) \to D_s X) = f_s^{\Upsilon(5S)} \times \mathcal{B}(B_s^0 \to D_s X) + \left(1 - f_s^{\Upsilon(5S)} - f_{\not B}^{\Upsilon(5S)}\right) \times \mathcal{B}(B \to D_s X)\,, \quad (22)$$

and similar relations for $\mathcal{B}(\Upsilon(5S) \to D^0 X)$ and $\mathcal{B}(\Upsilon(5S) \to \phi X)$. In Table 2 we list also the values of $f_s^{\Upsilon(5S)}$ derived from measurements of $f_{u,d}^{\Upsilon(5S)} = \mathcal{B}(\Upsilon(5S) \to B\overline{B}X)$ [15, 16], as well as our average value of $f_s^{\Upsilon(5S)}$, all obtained under the assumption $f_{\not B}^{\Upsilon(5S)} = 0$.

However, the assumption $f_{\not B}^{\Upsilon(5S)} = 0$ is known to be invalid since the observation of the following final states in e^+e^- collisions at the $\Upsilon(5S)$ energy: $\Upsilon(1S)\pi^+\pi^-$, $\Upsilon(2S)\pi^+\pi^-$, $\Upsilon(3S)\pi^+\pi^-$ and $\Upsilon(1S)K^+K^-$ [20, 21], $h_b(1P)\pi^+\pi^-$ and $h_b(2P)\pi^+\pi^-$ [22], and more recently $\Upsilon(1S)\pi^0\pi^0$, $\Upsilon(2S)\pi^0\pi^0$ and $\Upsilon(3S)\pi^0\pi^0$ [23]. The sum of the measurements of the corresponding visible cross-sections, adding also the contributions of the unmeasured $\Upsilon(1S)K^0\overline{K}^0$, $h_b(1P)\pi^0\pi^0$ and $h_b(2P)\pi^0\pi^0$ final states assuming isospin conservation, amounts to

$$\sigma^{\rm vis}(e^+e^- \to (b\bar{b})hh) = 13.2 \pm 1.4 \text{ pb}\,, \quad \text{for } (b\bar{b}) = \Upsilon(1S, 2S, 3S), h_b(1P, 2P) \text{ and } hh = \pi\pi, KK\,.$$

We divide this by the $b\bar{b}$ production cross section, $\sigma(e^+e^- \to b\bar{b}X) = 337 \pm 15$ pb, obtained as the average of the CLEO [19] and Belle [18][2]measurements, to obtain

$$\mathcal{B}(\Upsilon(5S) \to (b\bar{b})hh) = 0.039 \pm 0.004\,, \quad \text{for } (b\bar{b}) = \Upsilon(1S, 2S, 3S), h_b(1P, 2P) \text{ and } hh = \pi\pi, KK\,,$$

which is to be considered as a lower bound for $f_{\not B}^{\Upsilon(5S)}$.

Following the method described in Ref. [24], we perform a χ^2 fit of the original measurements of the $\Upsilon(5S)$ branching fractions of Refs. [15–17],[2] using the inputs of Table 3, the relations of Eqs. (21) and (22) and the one-sided Gaussian constraint $f_{\not B}^{\Upsilon(5S)} \geq \mathcal{B}(\Upsilon(5S) \to (b\bar{b})hh)$, to simultaneously extract $f_{u,d}^{\Upsilon(5S)}$, $f_s^{\Upsilon(5S)}$ and $f_{\not B}^{\Upsilon(5S)}$. Taking all known correlations into account, the best fit values are

$$f_{u,d}^{\Upsilon(5S)} = 0.761^{+0.027}_{-0.042}\,, \quad (23)$$

$$f_s^{\Upsilon(5S)} = 0.200^{+0.030}_{-0.031}\,, \quad (24)$$

$$f_{\not B}^{\Upsilon(5S)} = 0.039^{+0.050}_{-0.004}\,, \quad (25)$$

where the strongly asymmetric uncertainty on $f_{\not B}^{\Upsilon(5S)}$ is due to the one-sided constraint from the observed $(b\bar{b})hh$ decays. These results, together with their correlation, imply

$$f_s^{\Upsilon(5S)}/f_{u,d}^{\Upsilon(5S)} = 0.263^{+0.052}_{-0.044}\,, \quad (26)$$

in fair agreement with the results of a *BABAR* analysis [25], performed as a function of centre-of-mass energy.[3]

The production of B_s^0 mesons at the $\Upsilon(5S)$ is observed to be dominated by the $B_s^{*0}\overline{B}_s^{*0}$ channel, with $\sigma(e^+e^- \to B_s^{*0}\overline{B}_s^{*0})/\sigma(e^+e^- \to B_s^{(*)0}\overline{B}_s^{(*)0}) = (87.0 \pm 1.7)\%$ [26, 27]. The proportions of the various production channels for non-strange B mesons have also been measured [15].

[2] Belle updated the analysis of Ref. [17] with the full $\Upsilon(5S)$ dataset. The resulting measurements of $\sigma(e^+e^- \to b\bar{b}X)$ and $f_s^{\Upsilon(5S)}$, which supersede those of Ref. [17], are quoted and used in Ref. [18]. However, no details are given. Because of the lack of relevant information, this measurement of $f_s^{\Upsilon(5S)}$ cannot be included in the averages presented here.

[3] The results of Ref. [25] are not included in the average since no numerical value is given for $f_s^{\Upsilon(5S)}/f_{u,d}^{\Upsilon(5S)}$.

3.1.3 *b*-hadron production fractions at high energy

At high energy, all species of weakly decaying b hadrons may be produced, either directly or in strong and electromagnetic decays of excited b hadrons. It is often assumed that the fractions of these different species are the same in unbiased samples of high-$p_{\rm T}$ b jets originating from Z^0 decays, from $p\overline{p}$ collisions at the Tevatron, or from pp collisions at the LHC. This hypothesis is plausible under the condition that the square of the momentum transfer to the produced b quarks, Q^2, is large compared with the square of the hadronization energy scale, $Q^2 \gg \Lambda^2_{\rm QCD}$. On the other hand, there is no strong argument that the fractions at different machines should be strictly equal, so this assumption should be checked experimentally. The available data show that the fractions depend on the kinematics of the produced b hadron. A simple phenomenological model appears to agree with all data and indicates that the fractions are constant if the b hadron is produced with sufficiently high transverse momentum from any collider. Unless otherwise indicated, these fractions are assumed to be equal at all high-energy colliders until demonstrated otherwise by experiment. Both CDF and LHCb report a $p_{\rm T}$ dependence for Λ_b^0 production relative to B^+ and B^0; the number of Λ_b^0 baryons observed at low $p_{\rm T}$ is enhanced with respect to that seen at LEP's higher $p_{\rm T}$. Therefore we present three sets of complete averages: one set including only measurements performed at LEP, a second set including only measurements performed at the Tevatron, a third set including measurements performed at LEP, Tevatron and LHC. The LHCb production fractions results by themselves are still incomplete, lacking measurements of the production of weakly-decaying baryons heavier than Λ_b^0.

Contrary to what happens in the charm sector where the fractions of D^+ and D^0 are different, the relative amount of B^+ and B^0 is not affected by the electromagnetic decays of excited B^{*+} and B^{*0} states and strong decays of excited B^{**+} and B^{**0} states. Decays of the type $B_s^{**0} \to B^{(*)}K$ also contribute to the B^+ and B^0 rates, but with the same magnitude if mass effects can be neglected. We therefore assume equal production of B^+ and B^0 mesons. We also neglect the production of weakly decaying states made of several heavy quarks (like B_c^+ and doubly heavy baryons) which is known to be very small. Hence, for the purpose of determining the b-hadron fractions, we use the constraints

$$f_u = f_d \quad \text{and} \quad f_u + f_d + f_s + f_{\rm baryon} = 1\,, \tag{27}$$

where f_u, f_d, f_s and $f_{\rm baryon}$ are the unbiased fractions of B^+, B^0, B_s^0 and b baryons, respectively.

We note that there are many measurements of the production cross-sections of different species of b hadrons. In principle these could be included in a global fit to determine the production fractions. We do not perform such a fit at the current time, and instead average only the explicit measurements of the production fractions.

The LEP experiments have measured $f_s \times \mathcal{B}(B_s^0 \to D_s^- \ell^+ \nu_\ell X)$ [28], $\mathcal{B}(b \to \Lambda_b^0) \times \mathcal{B}(\Lambda_b^0 \to \Lambda_c^+ \ell^- \overline{\nu}_\ell X)$ [29,30] and $\mathcal{B}(b \to \Xi_b^-) \times \mathcal{B}(\Xi_b^- \to \Xi^- \ell^- \overline{\nu}_\ell X)$ [31,32][4] from partially reconstructed final states including a lepton, $f_{\rm baryon}$ from protons identified in b events [34], and the production rate of charged b hadrons [35]. Ratios of b-hadron fractions have been measured at CDF using lepton+charm final states [36–38][5], double semileptonic decays with $K^*\mu\mu$ and $\phi\mu\mu$ final states [39], and fully reconstructed $B_s^0 \to J/\psi\,\phi$ decays [40]. Measurements of the production of

[4] The DELPHI result of Ref. [32] is considered to supersede an older one [33].

[5] CDF updated their measurement of $f_{\Lambda_b^0}/f_d$ [36] to account for a measured $p_{\rm T}$ dependence between exclusively reconstructed Λ_b^0 and B^0 [38].

other heavy flavour baryons at the Tevatron are included in the determination of $f_{\rm baryon}$ [41–43][6] using the constraint

$$\begin{aligned} f_{\rm baryon} &= f_{\Lambda_b^0} + f_{\Xi_b^0} + f_{\Xi_b^-} + f_{\Omega_b^-} \\ &= f_{\Lambda_b^0}\left(1 + 2\frac{f_{\Xi_b^-}}{f_{\Lambda_b^0}} + \frac{f_{\Omega_b^-}}{f_{\Lambda_b^0}}\right), \end{aligned} \tag{28}$$

where isospin invariance is assumed in the production of Ξ_b^0 and Ξ_b^-. Other b baryons are expected to decay strongly or electromagnetically to those baryons listed. For the production measurements, both CDF and D0 reconstruct their b baryons exclusively to final states which include a J/ψ and a hyperon ($\Lambda_b^0 \to J/\psi\,\Lambda$, $\Xi_b^- \to J/\psi\,\Xi^-$ and $\Omega_b^- \to J/\psi\,\Omega^-$). We assume that the partial decay width of a b baryon to a J/ψ and the corresponding hyperon is equal to the partial width of any other b baryon to a J/ψ and the corresponding hyperon. LHCb has also measured ratios of b-hadron fractions in charm+lepton final states [44] and in fully reconstructed hadronic two-body decays $B^0 \to D^-\pi^+$, $B_s^0 \to D_s^-\pi^+$ and $\Lambda_b^0 \to \Lambda_c^+\pi^-$ [45, 46].

Both CDF and LHCb observe that the ratio $f_{\Lambda_b^0}/f_d$ depends on the $p_{\rm T}$ of the charm+lepton system [38, 44].[7] CDF chose to correct an older result to account for the $p_{\rm T}$ dependence. In a second result, CDF binned their data in $p_{\rm T}$ of the charm+electron system [37]. The more recent LHCb measurement using hadronic decays [46] obtains the scale for $R_{\Lambda_b^0} = f_{\Lambda_b^0}/f_d$ from their previous charm + lepton data [44]. The LHCb measurement using hadronic data also bins the same data in pseudorapidity (η) and sees a linear dependence of $R_{\Lambda_b^0}$. Since η is not entirely independent of $p_{\rm T}$ it is impossible to tell at this time whether this dependence is just an artifact of the $p_{\rm T}$ dependence. Figure 4 shows the ratio $R_{\Lambda_b^0}$ as a function of $p_{\rm T}$ for the b hadron, as measured by LHCb. LHCb fits their scaled hadronic data to obtain

$$R_{\Lambda_b^0} = (0.151 \pm 0.030) + \exp\left\{-(0.57 \pm 0.11) - (0.095 \pm 0.016)[\mathrm{GeV}/c]^{-1} \times p_{\rm T}\right\}. \tag{29}$$

A value of $R_{\Lambda_b^0}$ is also calculated for LEP and placed at the approximate $p_{\rm T}$ for the charm+lepton system, but this value does not participate in any fit.[8] Because the two LHCb results for $R_{\Lambda_b^0}$ are not independent, we use only their semileptonic data for the averages. Note that the $p_{\rm T}$ dependence of $R_{\Lambda_b^0}$ combined with the constraint from Eq. (27) implies a compensating $p_{\rm T}$ dependence in one or more of the production fractions, f_u, f_d, or f_s.

CDF[9], LHCb and ATLAS have investigated the $p_{\rm T}$ dependence of f_s/f_d using fully reconstructed B_s^0 and B^0 decays. LHCb reported 3σ evidence that the ratio $R_s = f_s/f_d$ decreases with $p_{\rm T}$ using fully reconstructed B_s^0 and B^0 decays and theoretical predictions for branching ratios [45]. Data from the ATLAS experiment [47] using decays of B_s^0 and B^0 to J/ψ final states and using theoretical predictions for branching ratios [48] indicates that R_s is consistent with no p_T dependence. Figure 5 shows the ratio R_s as a function of $p_{\rm T}$ measured by LHCb

[6] D0 reports $f_{\Omega_b^-}/f_{\Xi_b^-}$. We use the CDF+D0 average of $f_{\Xi_b^-}/f_{\Lambda_b^0}$ to obtain $f_{\Omega_b^-}/f_{\Lambda_b^0}$ and then combine it with the CDF result.

[7] CDF compares the $p_{\rm T}$ distribution of fully reconstructed $\Lambda_b^0 \to \Lambda_c^+\pi^-$ with $\overline{B}^0 \to D^+\pi^-$, which gives $f_{\Lambda_b^0}/f_d$ up to a scale factor. LHCb compares the $p_{\rm T}$ in the charm+lepton system between Λ_b^0 and B^0 and B^+, giving $R_{\Lambda_b^0}/2 = f_{\Lambda_b^0}/(f_u + f_d) = f_{\Lambda_b^0}/2f_d$.

[8] The CDF semileptonic data would require significant corrections to obtain the $p_{\rm T}$ of the b hadron and be included on the same plot with the LHCb data. We do not have these corrections at this time.

[9] The analysis of Ref. [40] is unpublished, therefore not further discussed here nor included in the averages.

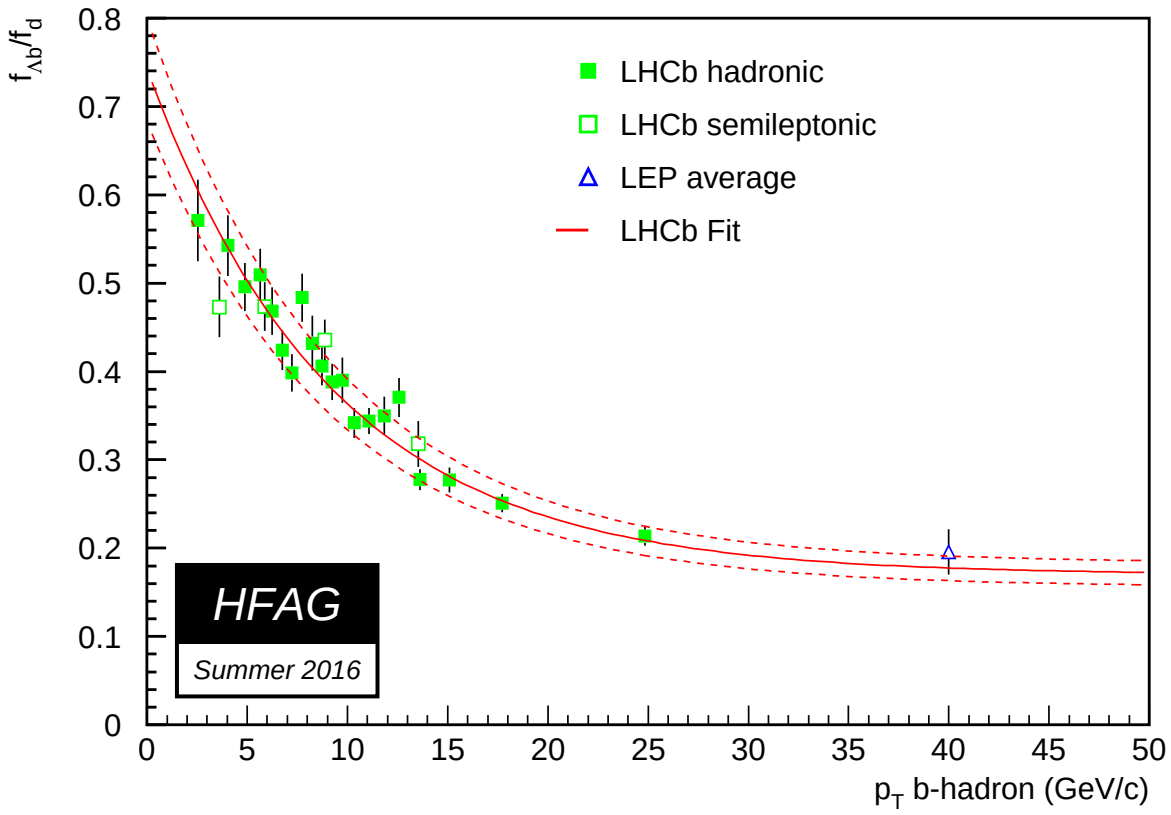

Figure 4: Ratio of production fractions $f_{\Lambda_b^0}/f_d$ as a function of $p_{\rm T}$ of the b hadron from LHCb data for b hadrons decaying semileptonically [44] and fully reconstructed in hadronic decays [46]. The curve represents a fit to the LHCb hadronic data [46]. The computed LEP ratio is included at an approximate $p_{\rm T}$ in Z decays, but does not participate in any fit.

and ATLAS. Two fits are performed. The first fit, using a linear parameterization, yields $R_s = (0.2701 \pm 0.0058) - (0.00139 \pm 0.00044)[\text{GeV}/c]^{-1} \times p_{\rm T}$. A second fit, using a simple exponential, yields $R_s = \exp\{(-1.304 \pm 0.024) - (0.0058 \pm 0.0019)[\text{GeV}/c]^{-1} \times p_{\rm T}\}$. The two fits are nearly indistinguishable over the $p_{\rm T}$ range of the results, but the second gives a physical value for all $p_{\rm T}$. R_s is also calculated for LEP and placed at the approximate $p_{\rm T}$ for the b hadron, though the LEP result doesn't participate in the fit. Our world average for R_s is also included in the figure for reference.

In order to combine or compare LHCb results with other experiments, the $p_{\rm T}$-dependent $f_{\Lambda_b^0}/(f_u + f_d)$ is weighted by the $p_{\rm T}$ spectrum.[10] Table 4 compares the $p_{\rm T}$-weighted LHCb data with comparable averages from CDF. The average CDF and LHCb data are in agreement despite the b hadrons being produced in different kinematic regimes.

[10] In practice the LHCb data are given in 14 bins in $p_{\rm T}$ and η with a full covariance matrix [44]. The weighted average is calculated as $D^T C^{-1} M/\sigma$, where $\sigma = D^T C^{-1} D$, M is a vector of measurements, C^{-1} is the inverse covariance matrix and D^T is the transpose of the design matrix (vector of 1's).

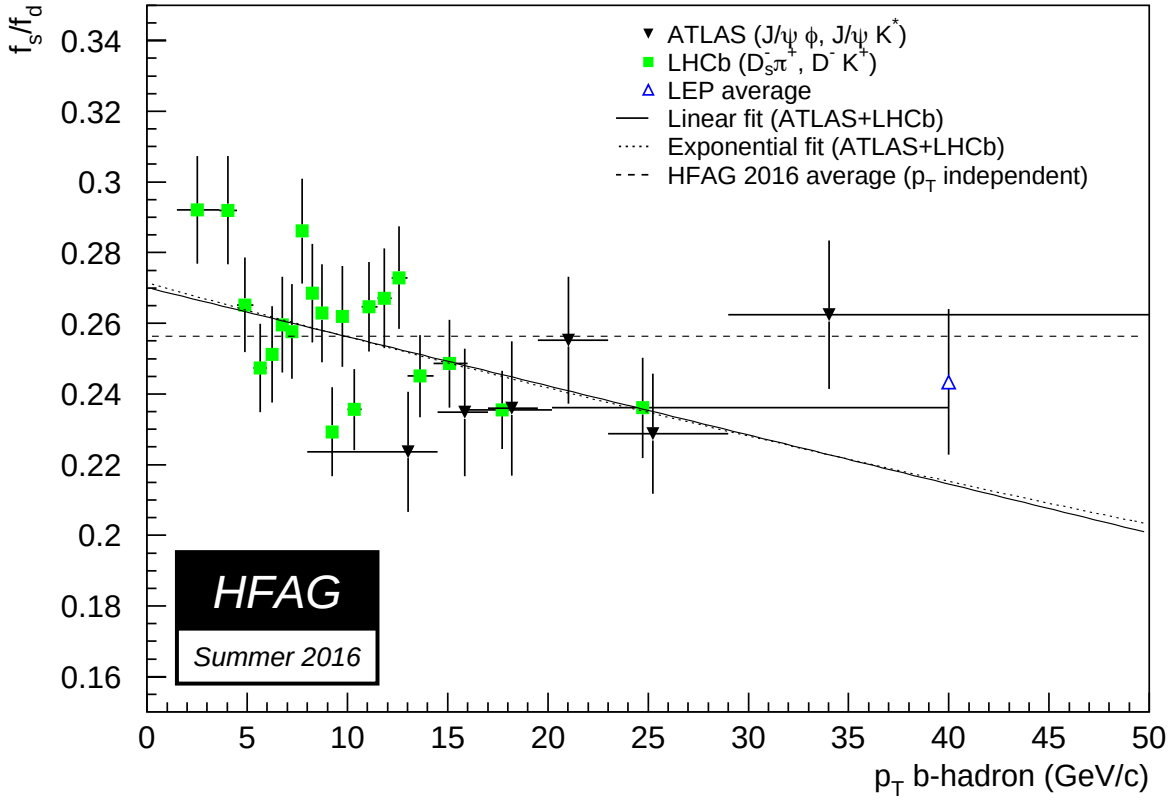

Figure 5: Ratio of production fractions f_s/f_d as a function of p_{T} of the reconstructed b hadrons for the LHCb [45] and ATLAS [47] data. Note the suppressed zero for the vertical axis. The curves represent fits to the data: a linear fit (solid), and an exponential fit described in the text (dotted). The p_{T} independent value average of R_s (dashed) is shown for comparison. The computed LEP ratio is included at an approximate p_{T} in Z decays, but does not participate in any fit.

Table 4: Comparison of average production fraction ratios from CDF [37, 38] and LHCb [44]. The kinematic regime of the charm+lepton system reconstructed in each experiment is also shown.

Quantity	CDF	LHCb
$f_s/(f_u + f_d)$	0.224 ± 0.057	0.134 ± 0.009
$f_{\Lambda_b^0}/(f_u + f_d)$	0.229 ± 0.062	0.240 ± 0.022
Average charm+lepton p_{T}	~ 13 GeV/c	~ 7 GeV/c
Pseudorapidity range	$-1 < \eta < 1$	$2 < \eta < 5$

Ignoring $p_{\rm T}$ dependence, all these published results have been adjusted to the latest branching fraction averages [5] and combined following the procedure and assumptions described in Ref. [3], to yield $f_u = f_d = 0.404 \pm 0.006$, $f_s = 0.102 \pm 0.005$ and $f_{\rm baryon} = 0.090 \pm 0.012$ under the constraints of Eq. (27). Repeating the combinations for LEP and the Tevatron, we obtain $f_u = f_d = 0.412 \pm 0.008$, $f_s = 0.088 \pm 0.013$ and $f_{\rm baryon} = 0.089 \pm 0.012$ when using the LEP data only, and $f_u = f_d = 0.340 \pm 0.021$, $f_s = 0.101 \pm 0.015$ and $f_{\rm baryon} = 0.218 \pm 0.047$ when using the Tevatron data only. As noted previously, the LHCb data are insufficient to determine a complete set of b-hadron production fractions. The world averages (LEP, Tevatron and LHC) for the various fractions are presented here for comparison with previous averages. Significant differences exist between the LEP and Tevatron fractions, therefore use of the world averages should be taken with some care. For these combinations other external inputs are used, *e.g.* the branching ratios of B mesons to final states with a D or D^* in semileptonic decays, which are needed to evaluate the fraction of semileptonic B^0_s decays with a D^-_s in the final state.

Time-integrated mixing analyses performed with lepton pairs from $b\overline{b}$ events produced at high-energy colliders measure the quantity

$$\overline{\chi} = f'_d\,\chi_d + f'_s\,\chi_s\,, \tag{30}$$

where f'_d and f'_s are the fractions of B^0 and B^0_s hadrons in a sample of semileptonic b-hadron decays, and where χ_d and χ_s are the B^0 and B^0_s time-integrated mixing probabilities. Assuming that all b hadrons have the same semileptonic decay width implies $f'_i = f_i R_i$, where $R_i = \tau_i/\tau_b$ is the ratio of the lifetime τ_i of species i to the average b-hadron lifetime $\tau_b = \sum_i f_i \tau_i$. Hence measurements of the mixing probabilities $\overline{\chi}$, χ_d and χ_s can be used to improve our knowledge of f_u, f_d, f_s and $f_{\rm baryon}$. In practice, the above relations yield another determination of f_s obtained from $f_{\rm baryon}$ and mixing information,

$$f_s = \frac{1}{R_s}\frac{(1+r)\overline{\chi} - (1 - f_{\rm baryon}R_{\rm baryon})\chi_d}{(1+r)\chi_s - \chi_d}\,, \tag{31}$$

where $r = R_u/R_d = \tau(B^+)/\tau(B^0)$.

The published measurements of $\overline{\chi}$ performed by the LEP experiments have been combined by the LEP Electroweak Working Group to yield $\overline{\chi} = 0.1259 \pm 0.0042$ [49]. This can be compared with the Tevatron average, $\overline{\chi} = 0.147 \pm 0.011$, obtained from D0 [50] and CDF [51].[11] The two averages deviate from each other by $1.8\,\sigma$; this could be an indication that the production fractions of b hadrons at the Z peak or at the Tevatron are not the same. We choose to combine these two results in a simple weighted average, assuming no correlations, and, following the PDG prescription, we multiply the combined uncertainty by 1.8 to account for the discrepancy. Our world average is then $\overline{\chi} = 0.1284 \pm 0.0069$.

Introducing the $\overline{\chi}$ average in Eq. (31), together with our world average $\chi_d = 0.1860 \pm 0.0011$ (see Eq. (60) of Sec. 3.3.1), the assumption $\chi_s = 1/2$ (justified by Eq. (69) in Sec. 3.3.2), the best knowledge of the lifetimes (see Sec. 3.2) and the estimate of $f_{\rm baryon}$ given above, yields $f_s = 0.118 \pm 0.018$ (or $f_s = 0.111 \pm 0.011$ using only LEP data, or $f_s = 0.166 \pm 0.029$ using only Tevatron data), an estimate dominated by the mixing information. Taking into account all known correlations (including that introduced by $f_{\rm baryon}$), this result is then combined with the set of fractions obtained from direct measurements (given above), to yield the improved

[11] The CDF result of Ref. [51] is from Run I data. A preliminary CDF measurement based on Run II data [52] is still unpublished and therefore no longer included in our averages.

Table 5: Time-integrated mixing probability $\overline{\chi}$ (defined in Eq. (30)), and fractions of the different b-hadron species in an unbiased sample of weakly decaying b hadrons, obtained from both direct and mixing measurements. The correlation coefficients between the fractions are also given. The last column includes measurements performed at LEP, Tevatron and LHC.

Quantity		Z decays	Tevatron	LHCb [45]	all
Mixing probability $\overline{\chi}$		0.1259 ± 0.0042	0.147 ± 0.011		0.1284 ± 0.0069
B^+ or B^0 fraction	$f_u = f_d$	0.407 ± 0.007	0.344 ± 0.021		0.404 ± 0.006
B_s^0 fraction	f_s	0.101 ± 0.008	0.115 ± 0.013		0.103 ± 0.005
b-baryon fraction	$f_{\rm baryon}$	0.084 ± 0.011	0.196 ± 0.046		0.088 ± 0.012
B_s^0/B^0 ratio	f_s/f_d	0.249 ± 0.023	0.333 ± 0.041	0.256 ± 0.020^u	0.256 ± 0.013
$\rho(f_s, f_u) = \rho(f_s, f_d)$		-0.629	$+0.153$		-0.143
$\rho(f_{\rm baryon}, f_u) = \rho(f_{\rm baryon}, f_d)$		-0.822	-0.959		-0.921
$\rho(f_{\rm baryon}, f_s)$		$+0.075$	-0.426		-0.254

^{u} This value has been updated with new inputs by LHCb to yield 0.259 ± 0.015 [53].

estimates of Table 5, still under the constraints of Eq. (27). As can be seen, our knowledge on the mixing parameters reduces the uncertainty on f_s, quite substantially in the case of LEP data. It should be noted that the results are correlated, as indicated in Table 5.

3.2 *b*-hadron lifetimes

In the spectator model the decay of b-flavoured hadrons H_b is governed entirely by the flavour changing $b \to Wq$ transition ($q = c, u$). For this very reason, lifetimes of all b-flavoured hadrons are the same in the spectator approximation regardless of the (spectator) quark content of the H_b. In the early 1990's experiments became sophisticated enough to start seeing the differences of the lifetimes among various H_b species. The first theoretical calculations of the spectator quark effects on H_b lifetime emerged only few years earlier.

Currently, most such calculations are performed in the framework of the Heavy Quark Expansion, HQE. In the HQE, under certain assumptions (the most important of which is that of quark-hadron duality [54]), the decay rate of an H_b to an inclusive final state f is expressed as the sum of a series of expectation values of operators of increasing dimension, multiplied by the correspondingly higher powers of $\Lambda_{\rm QCD}/m_b$:

$$\Gamma_{H_b \to f} = |{\rm CKM}|^2 \sum_n c_n^{(f)} \Big(\frac{\Lambda_{\rm QCD}}{m_b} \Big)^n \langle H_b | O_n | H_b \rangle, \tag{32}$$

where $|{\rm CKM}|^2$ is the relevant combination of the CKM matrix elements. The coefficients $c_n^{(f)}$ of this expansion, known as the Operator Product Expansion [55], can be calculated perturbatively. Hence, the HQE predicts $\Gamma_{H_b \to f}$ in the form of an expansion in both $\Lambda_{\rm QCD}/m_b$ and $\alpha_s(m_b)$. The precision of current experiments makes it mandatory to go to the next-to-leading order in QCD, *i.e.* to include corrections of the order of $\alpha_s(m_b)$ to the $c_n^{(f)}$ terms. All non-perturbative physics is shifted into the expectation values $\langle H_b | O_n | H_b \rangle$ of operators O_n. These can be calculated using lattice QCD or QCD sum rules, or can be related to other observables via the HQE [56]. One may reasonably expect that powers of $\Lambda_{\rm QCD}/m_b$ provide enough suppression that only the first few terms of the sum in Eq. (32) matter.

Theoretical predictions are usually made for the ratios of the lifetimes (with $\tau(B^0)$ often chosen as the common denominator) rather than for the individual lifetimes, for this allows several uncertainties to cancel. The precision of the HQE calculations (see Refs. [57–59], and Ref. [60] for the latest updates) is in some instances already surpassed by the measurements, *e.g.* in the case of $\tau(B^+)/\tau(B^0)$. Also, HQE calculations are not assumption-free. More accurate predictions are a matter of progress in the evaluation of the non-perturbative hadronic matrix elements and verifying the assumptions that the calculations are based upon. However, the HQE, even in its present shape, draws a number of important conclusions, which are in agreement with experimental observations:

- The heavier the mass of the heavy quark, the smaller is the variation in the lifetimes among different hadrons containing this quark, which is to say that as $m_b \to \infty$ we retrieve the spectator picture in which the lifetimes of all H_b states are the same. This is well illustrated by the fact that lifetimes are rather similar in the b sector, while they differ by large factors in the charm sector ($m_c < m_b$).

- The non-perturbative corrections arise only at the order of $\Lambda^2_{\rm QCD}/m_b^2$, which translates into differences among H_b lifetimes of only a few percent.

- It is only the difference between meson and baryon lifetimes that appears at the $\Lambda^2_{\rm QCD}/m_b^2$ level. The splitting of the meson lifetimes occurs at the $\Lambda^3_{\rm QCD}/m_b^3$ level, yet it is enhanced by a phase space factor $16\pi^2$ with respect to the leading free b decay.

To ensure that certain sources of systematic uncertainty cancel, lifetime analyses are sometimes designed to measure ratios of lifetimes. However, because of the differences in decay topologies, abundance (or lack thereof) of decays of a certain kind, *etc.*, measurements of the individual lifetimes are also common. In the following section we review the most common types of lifetime measurements. This discussion is followed by the presentation of the averaging of the various lifetime measurements, each with a brief description of its particularities.

3.2.1 Lifetime measurements, uncertainties and correlations

In most cases, the lifetime of an H_b state is estimated from a flight distance measurement and a $\beta\gamma$ factor which is used to convert the geometrical distance into the proper decay time. Methods of accessing lifetime information can roughly be divided in the following five categories:

1. ***Inclusive (flavour-blind) measurements***. These early measurements were aimed at extracting the lifetime from a mixture of b-hadron decays, without distinguishing the decaying species. Often the knowledge of the mixture composition was limited, which made these measurements experiment-specific. Also, these measurements had to rely on Monte Carlo simulation for estimating the $\beta\gamma$ factor, because the decaying hadrons are not fully reconstructed. These were usually the largest statistics b-hadron lifetime measurements accessible to a given experiment, and could therefore serve as an important performance benchmark.

2. ***Measurements in semileptonic decays of a specific H_b***. The W boson from $b \to Wc$ produces a $\ell\nu_l$ pair ($\ell = e, \mu$) in about 21% of the cases. The electron or muon from such decays provides a clean and efficient trigger signature. The c quark from the $b \to Wc$

transition and the other quark(s) making up the decaying H_b combine into a charm hadron, which is reconstructed in one or more exclusive decay channels. Knowing what this charmed hadron is allows one to separate, at least statistically, different H_b species. The advantage of these measurements is in statistics, which is usually superior to the case of exclusively reconstructed H_b decays. Some of the main disadvantages are related to the difficulty of estimating the lepton+charm sample composition and to the Monte Carlo reliance for the momentum (and hence $\beta\gamma$ factor) estimate.

3. ***Measurements in exclusively reconstructed hadronic decays***. These have the advantage of complete reconstruction of the decaying H_b state, which allows one to infer the decaying species as well as to perform precise measurement of the $\beta\gamma$ factor. Both lead to generally smaller systematic uncertainties than in the above two categories. The downsides are smaller branching ratios and larger combinatorial backgrounds, especially in $H_b \to H_c\pi(\pi\pi)$ and multi-body H_c decays, or in a hadron collider environment with non-trivial underlying event. Decays of the type $H_b \to J/\psi\, H_s$ are relatively clean and easy to trigger, due to the $J/\psi \to \ell^+\ell^-$ signature, but their branching fraction is only about 1%.

4. ***Measurements at asymmetric B factories***. In the $\Upsilon(4S) \to B\overline{B}$ decay, the B mesons (B^+ or B^0) are essentially at rest in the $\Upsilon(4S)$ frame. This makes direct lifetime measurements impossible in experiments at symmetric colliders producing $\Upsilon(4S)$ at rest. At asymmetric B factories the $\Upsilon(4S)$ meson is boosted resulting in B and $\overline{B}$ moving nearly parallel to each other with the same boost. The lifetime is inferred from the distance Δz separating the B and $\overline{B}$ decay vertices along the beam axis and from the $\Upsilon(4S)$ boost known from the beam energies. This boost is equal to $\beta\gamma \approx 0.55$ (0.43) in the *BABAR* (Belle) experiment, resulting in an average B decay length of approximately 250 (190) μm.

   In order to determine the charge of the B mesons in each event, one of them is fully reconstructed in a semileptonic or hadronic decay mode. The other B is typically not fully reconstructed, only the position of its decay vertex is determined from the remaining tracks in the event. These measurements benefit from large statistics, but suffer from poor proper time resolution, comparable to the B lifetime itself. This resolution is dominated by the uncertainty on the decay vertices, which is typically 50 (100) μm for a fully (partially) reconstructed B meson. With very large future statistics, the resolution and purity could be improved (and hence the systematics reduced) by fully reconstructing both B mesons in the event.

5. ***Direct measurement of lifetime ratios***. This method, initially applied in the measurement of $\tau(B^+)/\tau(B^0)$, is now also used for other b-hadron species at the LHC. The ratio of the lifetimes is extracted from the proper time dependence of the ratio of the observed yields of of two different b-hadron species, both reconstructed in decay modes with similar topologies. The advantage of this method is that subtle efficiency effects (partially) cancel in the ratio.

In some of the latest analyses, measurements of two (*e.g.* $\tau(B^+)$ and $\tau(B^+)/\tau(B^0)$) or three (*e.g.* $\tau(B^+)$, $\tau(B^+)/\tau(B^0)$, and Δm_d) quantities are combined. This introduces correlations

among measurements. Another source of correlations among the measurements are the systematic effects, which could be common to an experiment or to an analysis technique across the experiments. When calculating the averages, such correlations are taken into account following the general procedure described in Ref. [61].

3.2.2 Inclusive *b*-hadron lifetimes

The inclusive b hadron lifetime is defined as $\tau_b = \sum_i f_i \tau_i$ where τ_i are the individual species lifetimes and f_i are the fractions of the various species present in an unbiased sample of weakly decaying b hadrons produced at a high-energy collider.[12] This quantity is certainly less fundamental than the lifetimes of the individual species, the latter being much more useful in comparisons of the measurements with the theoretical predictions. Nonetheless, we perform the averaging of the inclusive lifetime measurements for completeness as well as for the reason that they might be of interest as "technical numbers."

In practice, an unbiased measurement of the inclusive lifetime is difficult to achieve, because it would imply an efficiency which is guaranteed to be the same across species. So most of the measurements are biased. In an attempt to group analyses which are expected to select the same mixture of b hadrons, the available results (given in Table 6) are divided into the following three sets:

1. measurements at LEP and SLD that accept any b-hadron decay, based on topological reconstruction (secondary vertex or track impact parameters);

2. measurements at LEP based on the identification of a lepton from a b decay; and

3. measurements at hadron colliders based on inclusive $H_b \to J/\psi X$ reconstruction, where the J/ψ is fully reconstructed.

The measurements of the first set are generally considered as estimates of τ_b, although the efficiency to reconstruct a secondary vertex most probably depends, in an analysis-specific way, on the number of tracks coming from the vertex, thereby depending on the type of the H_b. Even though these efficiency variations can in principle be accounted for using Monte Carlo simulations (which inevitably contain assumptions on branching fractions), the H_b mixture in that case can remain somewhat ill-defined and could be slightly different among analyses in this set.

On the contrary, the mixtures corresponding to the other two sets of measurements are better defined in the limit where the reconstruction and selection efficiency of a lepton or a J/ψ from an H_b does not depend on the decaying hadron type. These mixtures are given by the production fractions and the inclusive branching fractions for each H_b species to give a lepton or a J/ψ. In particular, under the assumption that all b hadrons have the same semileptonic decay width, the analyses of the second set should measure $\tau(b \to \ell) = (\sum_i f_i \tau_i^3)/(\sum_i f_i \tau_i^2)$ which is necessarily larger than τ_b if lifetime differences exist. Given the present knowledge on τ_i and f_i, $\tau(b \to \ell) - \tau_b$ is expected to be of the order of 0.003 ps. On the other hand, the third set measuring $\tau(b \to J/\psi)$ is expected to give an average smaller than τ_b because of the B_c^+ meson which has a significantly larger probability to decay to a J/ψ than other b-hadron species.

[12] In principle such a quantity could be slightly different in Z decays, at the Tevatron or at the LHC, in case the fractions of b-hadron species are not exactly the same; see the discussion in Sec. 3.1.3.

Table 6: Measurements of average b-hadron lifetimes.

Experiment	Method	Data set	τ_b (ps)	Ref.
ALEPH	Dipole	91	$1.511 \pm 0.022 \pm 0.078$	[62]
DELPHI	All track i.p. (2D)	91–92	$1.542 \pm 0.021 \pm 0.045$	[63][a]
DELPHI	Sec. vtx	91–93	$1.582 \pm 0.011 \pm 0.027$	[64][a]
DELPHI	Sec. vtx	94–95	$1.570 \pm 0.005 \pm 0.008$	[65]
L3	Sec. vtx + i.p.	91–94	$1.556 \pm 0.010 \pm 0.017$	[66][b]
OPAL	Sec. vtx	91–94	$1.611 \pm 0.010 \pm 0.027$	[67]
SLD	Sec. vtx	93	$1.564 \pm 0.030 \pm 0.036$	[68]
Average set 1 (b vertex)			1.572 ± 0.009	
ALEPH	Lepton i.p. (3D)	91–93	$1.533 \pm 0.013 \pm 0.022$	[69]
L3	Lepton i.p. (2D)	91–94	$1.544 \pm 0.016 \pm 0.021$	[66][b]
OPAL	Lepton i.p. (2D)	90–91	$1.523 \pm 0.034 \pm 0.038$	[70]
Average set 2 ($b \to \ell$)			1.537 ± 0.020	
CDF1	J/ψ vtx	92–95	$1.533 \pm 0.015^{+0.035}_{-0.031}$	[71]
Average set 3 ($b \to J/\psi$)			1.533 ± 0.036	

[a] The combined DELPHI result quoted in [64] is $1.575 \pm 0.010 \pm 0.026$ ps.
[b] The combined L3 result quoted in [66] is $1.549 \pm 0.009 \pm 0.015$ ps.

Measurements by SLC and LEP experiments are subject to a number of common systematic uncertainties, such as those due to (lack of knowledge of) b and c fragmentation, b and c decay models, $\mathcal{B}(B \to \ell)$, $\mathcal{B}(B \to c \to \ell)$, $\mathcal{B}(c \to \ell)$, τ_c, and H_b decay multiplicity. In the averaging, these systematic uncertainties are assumed to be 100% correlated. The averages for the sets defined above (also given in Table 6)[13] are

$$\tau(b \text{ vertex}) = 1.572 \pm 0.009 \text{ ps}, \quad (33)$$

$$\tau(b \to \ell) = 1.537 \pm 0.020 \text{ ps}, \quad (34)$$

$$\tau(b \to J/\psi) = 1.533 \pm 0.036 \text{ ps}. \quad (35)$$

The differences between these averages are consistent both with zero and with expectations within less than $2\,\sigma$.

3.2.3 B^0 and B^+ lifetimes and their ratio

After a number of years of dominating these averages the LEP experiments yielded the scene to the asymmetric B factories and the Tevatron experiments. The B factories have been very successful in utilizing their potential – in only a few years of running, *BABAR* and, to a greater extent, Belle, have struck a balance between the statistical and the systematic uncertainties, with both being close to (or even better than) an impressive 1% level. In the meanwhile, CDF and D0 have emerged as significant contributors to the field as the Tevatron Run II data flowed in. Recently, the LHCb experiment reached a further step in precision, improving by a factor ~ 2 over the previous best measurements.

[13] We do not include here an unpublished measurement from ATLAS [72].

Table 7: Measurements of the B^0 lifetime.

Experiment	Method	Data set	$\tau(B^0)$ (ps)	Ref.
ALEPH	$D^{(*)}\ell$	91–95	$1.518 \pm 0.053 \pm 0.034$	[73]
ALEPH	Exclusive	91–94	$1.25^{+0.15}_{-0.13} \pm 0.05$	[74]
ALEPH	Partial rec. $\pi^+\pi^-$	91–94	$1.49^{+0.17+0.08}_{-0.15-0.06}$	[74]
DELPHI	$D^{(*)}\ell$	91–93	$1.61^{+0.14}_{-0.13} \pm 0.08$	[75]
DELPHI	Charge sec. vtx	91–93	$1.63 \pm 0.14 \pm 0.13$	[76]
DELPHI	Inclusive $D^*\ell$	91–93	$1.532 \pm 0.041 \pm 0.040$	[77]
DELPHI	Charge sec. vtx	94–95	$1.531 \pm 0.021 \pm 0.031$	[65]
L3	Charge sec. vtx	94–95	$1.52 \pm 0.06 \pm 0.04$	[78]
OPAL	$D^{(*)}\ell$	91–93	$1.53 \pm 0.12 \pm 0.08$	[79]
OPAL	Charge sec. vtx	93–95	$1.523 \pm 0.057 \pm 0.053$	[80]
OPAL	Inclusive $D^*\ell$	91–00	$1.541 \pm 0.028 \pm 0.023$	[81]
SLD	Charge sec. vtx ℓ	93–95	$1.56^{+0.14}_{-0.13} \pm 0.10$	[82][a]
SLD	Charge sec. vtx	93–95	$1.66 \pm 0.08 \pm 0.08$	[82][a]
CDF1	$D^{(*)}\ell$	92–95	$1.474 \pm 0.039^{+0.052}_{-0.051}$	[83]
CDF1	Excl. $J/\psi K^{*0}$	92–95	$1.497 \pm 0.073 \pm 0.032$	[84]
CDF2	Excl. $J/\psi K^0_S$, $J/\psi K^{*0}$	02–09	$1.507 \pm 0.010 \pm 0.008$	[85]
D0	Excl. $J/\psi K^{*0}$	03–07	$1.414 \pm 0.018 \pm 0.034$	[86]
D0	Excl. $J/\psi K^0_S$	02–11	$1.508 \pm 0.025 \pm 0.043$	[87]
D0	Inclusive $D^-\mu^+$	02–11	$1.534 \pm 0.019 \pm 0.021$	[88]
BABAR	Exclusive	99–00	$1.546 \pm 0.032 \pm 0.022$	[89]
BABAR	Inclusive $D^*\ell$	99–01	$1.529 \pm 0.012 \pm 0.029$	[90]
BABAR	Exclusive $D^*\ell$	99–02	$1.523^{+0.024}_{-0.023} \pm 0.022$	[91]
BABAR	Incl. $D^*\pi$, $D^*\rho$	99–01	$1.533 \pm 0.034 \pm 0.038$	[92]
BABAR	Inclusive $D^*\ell$	99–04	$1.504 \pm 0.013^{+0.018}_{-0.013}$	[93]
Belle	Exclusive	00–03	$1.534 \pm 0.008 \pm 0.010$	[94]
ATLAS	Excl. $J/\psi K^0_S$	2011	$1.509 \pm 0.012 \pm 0.018$	[95]
LHCb	Excl. $J/\psi K^{*0}$	2011	$1.524 \pm 0.006 \pm 0.004$	[96]
LHCb	Excl. $J/\psi K^0_S$	2011	$1.499 \pm 0.013 \pm 0.005$	[96]
LHCb	$K^+\pi^-$	2011	$1.524 \pm 0.011 \pm 0.004$	[97]
Average			1.520 ± 0.004	

[a] The combined SLD result quoted in [82] is $1.64 \pm 0.08 \pm 0.08$ ps.

At present time we are in an interesting position of having three sets of measurements (from LEP/SLC, B factories and Tevatron/LHC) that originate from different environments, obtained using substantially different techniques and are precise enough for incisive comparison.

The averaging of $\tau(B^+)$, $\tau(B^0)$ and $\tau(B^+)/\tau(B^0)$ measurements is summarized[14] in Tables 7, 8, and 9. For $\tau(B^+)/\tau(B^0)$ we average only the measurements of this quantity provided by experiments rather than using all available knowledge, which would have included, for example, $\tau(B^+)$ and $\tau(B^0)$ measurements which did not contribute to any of the ratio measurements.

[14]We do not include the old unpublished measurements of Refs. [100–102].

The following sources of correlated (within experiment/machine) systematic uncertainties have been considered:

- for SLC/LEP measurements – D^{**} branching ratio uncertainties [3], momentum estimation of b mesons from Z^0 decays (b-quark fragmentation parameter $\langle X_E \rangle = 0.702 \pm 0.008$ [3]), B_s^0 and b-baryon lifetimes (see Secs. 3.2.4 and 3.2.6), and b-hadron fractions at high energy (see Table 5);
- for B-factory measurements – alignment, z scale, machine boost, sample composition (where applicable);
- for Tevatron/LHC measurements – alignment (separately within each experiment).

The resultant averages are:

$$\tau(B^0) = 1.520 \pm 0.004 \text{ ps}, \quad (36)$$

$$\tau(B^+) = 1.638 \pm 0.004 \text{ ps}, \quad (37)$$

$$\tau(B^+)/\tau(B^0) = 1.076 \pm 0.004. \quad (38)$$

3.2.4 B_s^0 lifetimes

Like neutral kaons, neutral B mesons contain short- and long-lived components, since the light (L) and heavy (H) eigenstates, $B_{\rm L}$ and $B_{\rm H}$, differ not only in their masses, but also in their total decay widths, with a decay width difference defined as $\Delta\Gamma = \Gamma_{\rm L} - \Gamma_{\rm H}$. Neglecting *CP* violation in $B - \overline{B}$ mixing, which is expected to be very small [103–105] (see also Sec. 3.3.3), the mass eigenstates are also *CP* eigenstates, with the light $B_{\rm L}$ state being *CP*-even and the heavy $B_{\rm H}$ state being *CP*-odd. While the decay width difference $\Delta\Gamma_d$ can be neglected in the B^0 system, the B_s^0 system exhibits a significant value of $\Delta\Gamma_s$: the sign of $\Delta\Gamma_s$ is known to be positive [106], *i.e.* the heavy eigenstate lives longer than the light eigenstate. Specific measurements of $\Delta\Gamma_s$ and $\Gamma_s = (\Gamma_{\rm L} + \Gamma_{\rm H})/2$ are explained and averaged in Sec. 3.3.2, but the results for $1/\Gamma_{\rm L}$, $1/\Gamma_{\rm H}$ and the mean B_s^0 lifetime, defined as $\tau(B_s^0) = 1/\Gamma_s$, are also quoted at the end of this section.

Many B_s^0 lifetime analyses, in particular the early ones performed before the non-zero value of $\Delta\Gamma_s$ was firmly established, ignore $\Delta\Gamma_s$ and fit the proper time distribution of a sample of B_s^0 candidates reconstructed in a certain final state f with a model assuming a single exponential function for the signal. We denote such effective lifetime measurements [107] as $\tau_{\rm single}(B_s^0 \to f)$; their true values may lie *a priori* anywhere between $1/\Gamma_{\rm L} = 1/(\Gamma_s + \Delta\Gamma_s/2)$ and $1/\Gamma_{\rm H} = 1/(\Gamma_s - \Delta\Gamma_s/2)$, depending on the proportion of $B_{\rm L}$ and $B_{\rm H}$ in the final state f. More recent determinations of effective lifetimes may be interpreted as measurements of the relative composition of $B_{\rm L}$ and $B_{\rm H}$ decaying to the final state f. Table 10 summarizes the effective lifetime measurements.

Averaging measurements of $\tau_{\rm single}(B_s^0 \to f)$ over several final states f will yield a result corresponding to an ill-defined observable when the proportions of $B_{\rm L}$ and $B_{\rm H}$ differ. Therefore, the effective B_s^0 lifetime measurements are broken down into several categories and averaged separately.

- ***$B_s^0 \to D_s^\mp X$ decays*** include mostly flavour-specific decays but also decays with an unknown mixture of light and heavy components. Measurements performed with such inclusive states are no longer used in averages.

Table 8: Measurements of the B^+ lifetime.

Experiment	Method	Data set	$\tau(B^+)$ (ps)	Ref.
ALEPH	$D^{(*)}\ell$	91–95	$1.648 \pm 0.049 \pm 0.035$	[73]
ALEPH	Exclusive	91–94	$1.58^{+0.21+0.04}_{-0.18-0.03}$	[74]
DELPHI	$D^{(*)}\ell$	91–93	$1.61 \pm 0.16 \pm 0.12$	[75][a]
DELPHI	Charge sec. vtx	91–93	$1.72 \pm 0.08 \pm 0.06$	[76][a]
DELPHI	Charge sec. vtx	94–95	$1.624 \pm 0.014 \pm 0.018$	[65]
L3	Charge sec. vtx	94–95	$1.66 \pm 0.06 \pm 0.03$	[78]
OPAL	$D^{(*)}\ell$	91–93	$1.52 \pm 0.14 \pm 0.09$	[79]
OPAL	Charge sec. vtx	93–95	$1.643 \pm 0.037 \pm 0.025$	[80]
SLD	Charge sec. vtx ℓ	93–95	$1.61^{+0.13}_{-0.12} \pm 0.07$	[82][b]
SLD	Charge sec. vtx	93–95	$1.67 \pm 0.07 \pm 0.06$	[82][b]
CDF1	$D^{(*)}\ell$	92–95	$1.637 \pm 0.058^{+0.045}_{-0.043}$	[83]
CDF1	Excl. $J/\psi K$	92–95	$1.636 \pm 0.058 \pm 0.025$	[84]
CDF2	Excl. $J/\psi K$	02–09	$1.639 \pm 0.009 \pm 0.009$	[85]
CDF2	Excl. $D^0\pi$	02–06	$1.663 \pm 0.023 \pm 0.015$	[98]
BABAR	Exclusive	99–00	$1.673 \pm 0.032 \pm 0.023$	[89]
Belle	Exclusive	00–03	$1.635 \pm 0.011 \pm 0.011$	[94]
LHCb	Excl. $J/\psi K$	2011	$1.637 \pm 0.004 \pm 0.003$	[96]
Average			1.638 ± 0.004	

[a] The combined DELPHI result quoted in [76] is 1.70 ± 0.09 ps.
[b] The combined SLD result quoted in [82] is $1.66 \pm 0.06 \pm 0.05$ ps.

Table 9: Measurements of the ratio $\tau(B^+)/\tau(B^0)$.

Experiment	Method	Data set	Ratio $\tau(B^+)/\tau(B^0)$	Ref.
ALEPH	$D^{(*)}\ell$	91–95	$1.085 \pm 0.059 \pm 0.018$	[73]
ALEPH	Exclusive	91–94	$1.27^{+0.23+0.03}_{-0.19-0.02}$	[74]
DELPHI	$D^{(*)}\ell$	91–93	$1.00^{+0.17}_{-0.15} \pm 0.10$	[75]
DELPHI	Charge sec. vtx	91–93	$1.06^{+0.13}_{-0.11} \pm 0.10$	[76]
DELPHI	Charge sec. vtx	94–95	$1.060 \pm 0.021 \pm 0.024$	[65]
L3	Charge sec. vtx	94–95	$1.09 \pm 0.07 \pm 0.03$	[78]
OPAL	$D^{(*)}\ell$	91–93	$0.99 \pm 0.14^{+0.05}_{-0.04}$	[79]
OPAL	Charge sec. vtx	93–95	$1.079 \pm 0.064 \pm 0.041$	[80]
SLD	Charge sec. vtx ℓ	93–95	$1.03^{+0.16}_{-0.14} \pm 0.09$	[82][a]
SLD	Charge sec. vtx	93–95	$1.01^{+0.09}_{-0.08} \pm 0.05$	[82][a]
CDF1	$D^{(*)}\ell$	92–95	$1.110 \pm 0.056^{+0.033}_{-0.030}$	[83]
CDF1	Excl. $J/\psi K$	92–95	$1.093 \pm 0.066 \pm 0.028$	[84]
CDF2	Excl. $J/\psi K^{(*)}$	02–09	$1.088 \pm 0.009 \pm 0.004$	[85]
D0	$D^{*+}\mu$ $D^0\mu$ ratio	02–04	$1.080 \pm 0.016 \pm 0.014$	[99]
BABAR	Exclusive	99–00	$1.082 \pm 0.026 \pm 0.012$	[89]
Belle	Exclusive	00–03	$1.066 \pm 0.008 \pm 0.008$	[94]
LHCb	Excl. $J/\psi K^{(*)}$	2011	$1.074 \pm 0.005 \pm 0.003$	[96]
Average			1.076 ± 0.004	

[a] The combined SLD result quoted in [82] is $1.01 \pm 0.07 \pm 0.06$.

Table 10: Measurements of the effective B_s^0 lifetimes obtained from single exponential fits.

Experiment	Final state f		Data set		$\tau_{\rm single}(B_s^0 \to f)$ (ps)	Ref.
ALEPH	$D_s h$	ill-defined	91–95		$1.47 \pm 0.14 \pm 0.08$	[108]
DELPHI	$D_s h$	ill-defined	91–95		$1.53^{+0.16}_{-0.15} \pm 0.07$	[109]
OPAL	D_s incl.	ill-defined	90–95		$1.72^{+0.20+0.18}_{-0.19-0.17}$	[110]
ALEPH	$D_s^- \ell^+$	flavour-specific	91–95		$1.54^{+0.14}_{-0.13} \pm 0.04$	[111]
CDF1	$D_s^- \ell^+$	flavour-specific	92–96		$1.36 \pm 0.09^{+0.06}_{-0.05}$	[112]
DELPHI	$D_s^- \ell^+$	flavour-specific	91–95		$1.42^{+0.14}_{-0.13} \pm 0.03$	[113]
OPAL	$D_s^- \ell^+$	flavour-specific	90–95		$1.50^{+0.16}_{-0.15} \pm 0.04$	[114]
D0	$D_s^- \mu^+ X$	flavour-specific	Run II	10.4 fb^{-1}	$1.479 \pm 0.010 \pm 0.021$	[88]
CDF2	$D_s^- \pi^+(X)$	flavour-specific	02–06	1.3 fb^{-1}	$1.518 \pm 0.041 \pm 0.027$	[115]
LHCb	$D_s^- D^+$	flavour-specific	11–12	3 fb^{-1}	$1.52 \pm 0.15 \pm 0.01$	[116]
LHCb	$D_s^- \pi^+$	flavour-specific	11	1 fb^{-1}	$1.535 \pm 0.015 \pm 0.014$	[117]
LHCb	$\pi^+ K^-$	flavour-specific	11	1.0 fb^{-1}	$1.60 \pm 0.06 \pm 0.01$	[97]
Average of above 9 flavour-specific lifetime measurements					1.516 ± 0.014	
CDF1	$J/\psi\,\phi$	CP even+odd	92–95		$1.34^{+0.23}_{-0.19} \pm 0.05$	[71]
D0	$J/\psi\,\phi$	CP even+odd	02–04		$1.444^{+0.098}_{-0.090} \pm 0.02$	[118]
LHCb	$J/\psi\,\phi$	CP even+odd	11	1 fb^{-1}	$1.480 \pm 0.011 \pm 0.005$	[96]
Average of above 3 $J/\psi\,\phi$ lifetime measurements					1.479 ± 0.012	
ALEPH	$D_s^{(*)+} D_s^{(*)-}$	mostly CP even	91–95		$1.27 \pm 0.33 \pm 0.08$	[119]
LHCb	$K^+ K^-$	CP-even	10	0.037 fb^{-1}	$1.440 \pm 0.096 \pm 0.009$	[120]
LHCb	$K^+ K^-$	CP-even	11	1.0 fb^{-1}	$1.407 \pm 0.016 \pm 0.007$	[97]
Average of above 2 K^+K^- lifetime measurements					1.408 ± 0.017	
LHCb	$D_s^+ D_s^-$	CP-even	11–12	3 fb^{-1}	$1.379 \pm 0.026 \pm 0.017$	[116]
LHCb	$J/\psi\,\eta$	CP-even	11–12	3 fb^{-1}	$1.479 \pm 0.034 \pm 0.011$	[121]
Average of above 2 measurements of $1/\Gamma_{\rm L}$					1.422 ± 0.023	
LHCb	$J/\psi\,K_{\rm S}^0$	CP-odd	11	1.0 fb^{-1}	$1.75 \pm 0.12 \pm 0.07$	[122]
CDF2	$J/\psi\,f_0(980)$	CP-odd	02–08	3.8 fb^{-1}	$1.70^{+0.12}_{-0.11} \pm 0.03$	[123]
D0	$J/\psi\,f_0(980)$	CP-odd	Run II	10.4 fb^{-1}	$1.70 \pm 0.14 \pm 0.05$	[124]
LHCb	$J/\psi\,\pi^+\pi^-$	CP-odd	11	1.0 fb^{-1}	$1.652 \pm 0.024 \pm 0.024$	[125]
Average of above 3 measurements of $1/\Gamma_{\rm H}$					1.658 ± 0.032	

- ***Decays to flavour-specific final states***, *i.e.* decays to final states f with instantaneous decay amplitudes satisfying $A(B_s^0 \to f) \neq 0$, $A(\overline{B}_s^0 \to \overline{f}) \neq 0$, $A(B_s^0 \to \overline{f}) = 0$ and $A(\overline{B}_s^0 \to f) = 0$, have equal fractions of $B_{\rm L}$ and $B_{\rm H}$ at time zero. Their total untagged time-dependent decay rates $\Gamma(t)$ have a mean value $\int_0^\infty t\Gamma(t)dt / \int_0^\infty \Gamma(t)dt$, called the *flavour-specific lifetime*, equal to [126]

$$\tau_{\rm single}(B_s^0 \to \text{flavour specific}) = \frac{1/\Gamma_{\rm L}^2 + 1/\Gamma_{\rm H}^2}{1/\Gamma_{\rm L} + 1/\Gamma_{\rm H}} = \frac{1}{\Gamma_s} \frac{1 + \left(\frac{\Delta\Gamma_s}{2\Gamma_s}\right)^2}{1 - \left(\frac{\Delta\Gamma_s}{2\Gamma_s}\right)^2} \,. \tag{39}$$

  Because of the fast $B_s^0 - \overline{B}_s^0$ oscillations, possible biases of the flavour-specific lifetime due to a combination of $B_s^0/\overline{B}_s^0$ production asymmetry, *CP* violation in the decay amplitudes ($|A(B_s^0 \to f)| \neq |A(\overline{B}_s^0 \to \overline{f})|$), and *CP* violation in $B_s^0 - \overline{B}_s^0$ mixing ($|q/p|_s \neq 1$) are strongly suppressed, by a factor $\sim x_s^2$ (given in Eq. (68)). The $B_s^0/\overline{B}_s^0$ production asymmetry at LHCb and the *CP* asymmetry due to mixing have been measured to be compatible with zero with a precision below 3% [127] and 0.3% (see Eq. (76)), respectively. The corresponding effects on the flavour-specific lifetime, which therefore have a relative size of the order of 10^{-5} or smaller, can be neglected at the current level of experimental precision. Under the assumption of no production asymmetry and no *CP* violation in mixing, Eq. (39) is exact even for a flavour-specific decay with *CP* violation in the decay amplitudes. Hence any flavour-specific decay mode can be used to measure the flavour-specific lifetime.

  The average of all flavour-specific B_s^0 lifetime measurements [88, 97, 111–117][15] is

$$\tau_{\rm single}(B_s^0 \to \text{flavour specific}) = 1.516 \pm 0.014 \text{ ps} \,. \tag{40}$$

- ***$B_s^0 \to J/\psi\,\phi$ decays*** contain a well-measured mixture of *CP*-even and *CP*-odd states. There are no known correlations between the existing $B_s^0 \to J/\psi\,\phi$ effective lifetime measurements; these are combined into the average[16] $\tau_{\rm single}(B_s^0 \to J/\psi\,\phi) = 1.479 \pm 0.012$ ps. A caveat is that different experimental acceptances may lead to different admixtures of the *CP*-even and *CP*-odd states, and simple fits to a single exponential may result in inherently different values of $\tau_{\rm single}(B_s^0 \to J/\psi\,\phi)$. Analyses that separate the *CP*-even and *CP*-odd components in this decay through a full angular study, outlined in Sec. 3.3.2, provide directly precise measurements of $1/\Gamma_s$ and $\Delta\Gamma_s$ (see Table 21).

- ***Decays to CP eigenstates*** have also been measured, in the *CP*-even modes $B_s^0 \to D_s^{(*)+} D_s^{(*)-}$ by ALEPH [119], $B_s^0 \to K^+K^-$ by LHCb [97, 120][17], $B_s^0 \to D_s^+ D_s^-$ by LHCb [116] and $B_s^0 \to J/\psi\eta$ by LHCb [121], as well as in the *CP*-odd modes $B_s^0 \to J/\psi\, f_0(980)$ by CDF [123] and D0 [124], $B_s^0 \to J/\psi\,\pi^+\pi^-$ by LHCb [125] and $B_s^0 \to J/\psi\, K_{\rm S}^0$ by LHCb [122]. If these decays are dominated by a single weak phase and if *CP* violation can be neglected, then $\tau_{\rm single}(B_s^0 \to CP\text{-even}) = 1/\Gamma_{\rm L}$ and $\tau_{\rm single}(B_s^0 \to CP\text{-odd}) = 1/\Gamma_{\rm H}$

[15] An old unpublished measurement [128] is not included.

[16] The old unpublished measurements of Refs. [102, 129] are not included.

[17] An old unpublished measurement of the $B_s^0 \to K^+K^-$ effective lifetime by CDF [130] is no longer considered.

(see Eqs. (63) and (64) for approximate relations in presence of mixing-induced *CP* violation). However, not all these modes can be considered as pure *CP* eigenstates: a small *CP*-odd component is most probably present in $B_s^0 \to D_s^{(*)+} D_s^{(*)-}$ decays. Furthermore the decays $B_s^0 \to K^+K^-$ and $B_s^0 \to J/\psi\, K_{\rm S}^0$ may suffer from direct *CP* violation due to interfering tree and loop amplitudes. The averages for the effective lifetimes obtained for decays to pure *CP*-even ($D_s^+ D_s^-$, $J/\psi\,\eta$) and *CP*-odd ($J/\psi\, f_0(980)$, $J/\psi\,\pi^+\pi^-$) final states, where *CP* conservation can be assumed, are

$$\tau_{\rm single}(B_s^0 \to CP\text{-even}) = 1.422 \pm 0.023 \text{ ps}\,, \quad (41)$$

$$\tau_{\rm single}(B_s^0 \to CP\text{-odd}) = 1.658 \pm 0.032 \text{ ps}\,. \quad (42)$$

As described in Sec. 3.3.2, the effective lifetime averages of Eqs. (40), (41), and (42) are used as ingredients to improve the determination of $1/\Gamma_s$ and $\Delta\Gamma_s$ obtained from the full angular analyses of $B_s^0 \to J/\psi\,\phi$ and $B_s^0 \to J/\psi\, K^+K^-$ decays. The resulting world averages for the B_s^0 lifetimes are

$$\tau(B_{s\rm L}) = \frac{1}{\Gamma_{\rm L}} = \frac{1}{\Gamma_s + \Delta\Gamma_s/2} = 1.414 \pm 0.006 \text{ ps}\,, \quad (43)$$

$$\tau(B_{s\rm H}) = \frac{1}{\Gamma_{\rm H}} = \frac{1}{\Gamma_s - \Delta\Gamma_s/2} = 1.609 \pm 0.010 \text{ ps}\,, \quad (44)$$

$$\tau(B_s^0) = \frac{1}{\Gamma_s} = \frac{2}{\Gamma_{\rm L} + \Gamma_{\rm H}} = 1.505 \pm 0.005 \text{ ps}\,. \quad (45)$$

3.2.5 B_c^+ lifetime

Early measurements of the B_c^+ meson lifetime, from CDF [131–133] and D0 [134], use the semileptonic decay mode $B_c^+ \to J/\psi\,\ell^+\nu$ and are based on a simultaneous fit to the mass and lifetime using the vertex formed with the leptons from the decay of the J/ψ and the third lepton. Correction factors to estimate the boost due to the missing neutrino are used. Correlated systematic errors include the impact of the uncertainty of the B_c^+ p_T spectrum on the correction factors, the level of feed-down from $\psi(2S)$ decays, Monte Carlo modeling of the decay model varying from phase space to the ISGW model, and mass variations. With more statistics, CDF2 was able to perform the first B_c^+ lifetime based on fully reconstructed $B_c^+ \to J/\psi\pi^+$ decays [135], which does not suffer from a missing neutrino. Recent measurements from LHCb, both with $B_c^+ \to J/\psi\,\mu^+\nu$ [136] and $B_c^+ \to J/\psi\,\pi^+$ [137] decays, achieve the highest level of precision.

All the measurements[18] are summarized in Table 11 and the world average, dominated by the LHCb measurements, is determined to be

$$\tau(B_c^+) = 0.507 \pm 0.009 \text{ ps}\,. \quad (46)$$

3.2.6 Λ_b^0 and b-baryon lifetimes

The first measurements of b-baryon lifetimes, performed at LEP, originate from two classes of partially reconstructed decays. In the first class, decays with an exclusively reconstructed Λ_c^+

[18] We do not list (nor include in the average) an unpublished result from CDF2 [132].

Table 11: Measurements of the B_c^+ lifetime.

Experiment	Method	Data set		$\tau(B_c^+)$ (ps)	Ref.
CDF1	$J/\psi\,\ell$	92–95	0.11 fb^{-1}	$0.46^{+0.18}_{-0.16} \pm 0.03$	[131]
CDF2	$J/\psi\,e$	02–04	0.36 fb^{-1}	$0.463^{+0.073}_{-0.065} \pm 0.036$	[133]
D0	$J/\psi\,\mu$	02–06	1.3 fb^{-1}	$0.448^{+0.038}_{-0.036} \pm 0.032$	[134]
CDF2	$J/\psi\,\pi$		6.7 fb^{-1}	$0.452 \pm 0.048 \pm 0.027$	[135]
LHCb	$J/\psi\,\mu$	12	2 fb^{-1}	$0.509 \pm 0.008 \pm 0.012$	[136]
LHCb	$J/\psi\,\pi$	11–12	3 fb^{-1}	$0.5134 \pm 0.0110 \pm 0.0057$	[137]
Average				0.507 ± 0.009	

baryon and a lepton of opposite charge are used. These products are more likely to occur in the decay of Λ_b^0 baryons. In the second class, more inclusive final states with a baryon (p, $\overline{p}$, Λ, or $\overline{\Lambda}$) and a lepton have been used, and these final states can generally arise from any b baryon. With the large b-hadron samples available at the Tevatron and the LHC, the most precise measurements of b baryons now come from fully reconstructed exclusive decays.

The following sources of correlated systematic uncertainties have been considered: experimental time resolution within a given experiment, b-quark fragmentation distribution into weakly decaying b baryons, Λ_b^0 polarization, decay model, and evaluation of the b-baryon purity in the selected event samples. In computing the averages the central values of the masses are scaled to $M(\Lambda_b^0) = 5619.51 \pm 0.23$ MeV/c^2 [5].

For measurements with partially reconstructed decays, the meaning of the decay model systematic uncertainties and the correlation of these uncertainties between measurements are not always clear. Uncertainties related to the decay model are dominated by assumptions on the fraction of n-body semileptonic decays. To be conservative, it is assumed that these are 100% correlated whenever given as an error. DELPHI varies the fraction of 4-body decays from 0.0 to 0.3. In computing the average, the DELPHI result is corrected to a value of 0.2 ± 0.2 for this fraction. Furthermore the semileptonic decay results from LEP are corrected for a Λ_b^0 polarization of $-0.45^{+0.19}_{-0.17}$ [3] and a b fragmentation parameter $\langle x_E \rangle_b = 0.702 \pm 0.008$ [49].

The list of all measurements are given in Table 12. We do not attempt to average measurements performed with $p\ell$ or $\Lambda\ell$ correlations, which select unknown mixtures of b baryons. Measurements performed with $\Lambda_c\ell$ or $\Lambda\ell^+\ell^-$ correlations can be assumed to correspond to semileptonic Λ_b^0 decays. Their average ($1.247^{+0.071}_{-0.069}$ ps) is significantly different from the average using only measurements performed with exclusively reconstructed hadronic Λ_b^0 decays (1.470 ± 0.010 ps). The latter is much more precise and less prone to potential biases than the former. The discrepancy between the two averages is at the level of $3.1\,\sigma$ and assumed to be due to an experimental systematic effect in the semileptonic measurements or to a rare statistical fluctuation. The best estimate of the Λ_b^0 lifetime is therefore taken as the average of the exclusive measurements only. The CDF $\Lambda_b^0 \to J/\psi\,\Lambda$ lifetime result [144] is larger than the average of all other exclusive measurements by $2.4\,\sigma$. It is nonetheless kept in the average without adjustment of input errors. The world average Λ_b^0 lifetime is then

$$\tau(\Lambda_b^0) = 1.470 \pm 0.010 \text{ ps}\,. \tag{47}$$

For the strange b baryons, we do not include the LEP measurements based on inclusive $\Xi^\mp\ell^\mp$ [31–33] final states, which consist of a mixture of Ξ_b^- and Ξ_b^0 baryons. Instead we only

Table 12: Measurements of the b-baryon lifetimes.

Experiment	Method	Data set	Lifetime (ps)	Ref.
ALEPH	$\Lambda\ell$	91–95	$1.20 \pm 0.08 \pm 0.06$	[30]
DELPHI	$\Lambda\ell\pi$ vtx	91–94	$1.16 \pm 0.20 \pm 0.08$	[138][b]
DELPHI	$\Lambda\mu$ i.p.	91–94	$1.10^{+0.19}_{-0.17} \pm 0.09$	[139][b]
DELPHI	$p\ell$	91–94	$1.19 \pm 0.14 \pm 0.07$	[138][b]
OPAL	$\Lambda\ell$ i.p.	90–94	$1.21^{+0.15}_{-0.13} \pm 0.10$	[140][c]
OPAL	$\Lambda\ell$ vtx	90–94	$1.15 \pm 0.12 \pm 0.06$	[140][c]
ALEPH	$\Lambda_c^+\ell$	91–95	$1.18^{+0.13}_{-0.12} \pm 0.03$	[30][a]
ALEPH	$\Lambda\ell^-\ell^+$	91–95	$1.30^{+0.26}_{-0.21} \pm 0.04$	[30][a]
DELPHI	$\Lambda_c^+\ell$	91–94	$1.11^{+0.19}_{-0.18} \pm 0.05$	[138][b]
OPAL	$\Lambda_c^+\ell$, $\Lambda\ell^-\ell^+$	90–95	$1.29^{+0.24}_{-0.22} \pm 0.06$	[114]
CDF1	$\Lambda_c^+\ell$	91–95	$1.32 \pm 0.15 \pm 0.07$	[141]
D0	$\Lambda_c^+\mu$	02–06	$1.290^{+0.119+0.087}_{-0.110-0.091}$	[142]
Average of above 6			$1.247^{+0.071}_{-0.069}$	
CDF2	$\Lambda_c^+\pi$	02–06	$1.401 \pm 0.046 \pm 0.035$	[143]
CDF2	$J/\psi\,\Lambda$	02–11	$1.565 \pm 0.035 \pm 0.020$	[144]
D0	$J/\psi\,\Lambda$	02–11	$1.303 \pm 0.075 \pm 0.035$	[87]
ATLAS	$J/\psi\,\Lambda$	2011	$1.449 \pm 0.036 \pm 0.017$	[95]
CMS	$J/\psi\,\Lambda$	2011	$1.503 \pm 0.052 \pm 0.031$	[145]
LHCb	$J/\psi\,\Lambda$	2011	$1.415 \pm 0.027 \pm 0.006$	[96]
LHCb	$J/\psi\,pK$ (w.r.t. B^0)	11–12	$1.479 \pm 0.009 \pm 0.010$	[146]
Average of above 7:	Λ_b^0 lifetime =		1.470 ± 0.010	
ALEPH	$\Xi^-\ell^-X$	90–95	$1.35^{+0.37+0.15}_{-0.28-0.17}$	[31]
DELPHI	$\Xi^-\ell^-X$	91–93	$1.5^{+0.7}_{-0.4} \pm 0.3$	[33][d]
DELPHI	$\Xi^-\ell^-X$	92–95	$1.45^{+0.55}_{-0.43} \pm 0.13$	[32][d]
CDF2	$J/\psi\,\Xi^-$	02–11	$1.32 \pm 0.14 \pm 0.02$	[144]
LHCb	$J/\psi\,\Xi^-$	11–12	$1.55^{+0.10}_{-0.09} \pm 0.03$	[147]
LHCb	$\Xi_c^0\pi^-$ (w.r.t. Λ_b^0)	11–12	$1.599 \pm 0.041 \pm 0.022$	[148]
Average of above 3:	Ξ_b^- lifetime =		1.571 ± 0.040	
LHCb	$\Xi_c^+\pi^-$ (w.r.t. Λ_b^0)	11–12	$1.477 \pm 0.026 \pm 0.019$	[149]
Average of above 1:	Ξ_b^0 lifetime =		1.479 ± 0.031	
CDF2	$J/\psi\,\Omega^-$	02–11	$1.66^{+0.53}_{-0.40} \pm 0.02$	[144]
LHCb	$J/\psi\,\Omega^-$	11–12	$1.54^{+0.26}_{-0.21} \pm 0.05$	[147]
LHCb	$\Omega_c^0\pi^-$ (w.r.t. Ξ_b^-)	11–12	$1.78 \pm 0.26 \pm 0.05 \pm 0.06$	[150]
Average of above 3:	Ω_b^- lifetime =		$1.64^{+0.18}_{-0.17}$	

[a] The combined ALEPH result quoted in [30] is 1.21 ± 0.11 ps.
[b] The combined DELPHI result quoted in [138] is $1.14 \pm 0.08 \pm 0.04$ ps.
[c] The combined OPAL result quoted in [140] is $1.16 \pm 0.11 \pm 0.06$ ps.
[d] The combined DELPHI result quoted in [32] is $1.48^{+0.40}_{-0.31} \pm 0.12$ ps.

Table 13: Summary of the lifetime averages for the different b-hadron species.

b-hadron species		Measured lifetime
B^+		1.638 ± 0.004 ps
B^0		1.520 ± 0.004 ps
B_s^0	$1/\Gamma_s =$	1.505 ± 0.005 ps
$B_{s\mathrm{L}}$	$1/\Gamma_{\mathrm{L}} =$	1.414 ± 0.006 ps
$B_{s\mathrm{H}}$	$1/\Gamma_{\mathrm{H}} =$	1.609 ± 0.010 ps
B_c^+		0.507 ± 0.009 ps
Λ_b^0		1.470 ± 0.010 ps
Ξ_b^-		1.571 ± 0.040 ps
Ξ_b^0		1.479 ± 0.031 ps
Ω_b^-		$1.64^{+0.18}_{-0.17}$ ps

Table 14: Experimental averages of b-hadron lifetime ratios and Heavy-Quark Expansion (HQE) predictions [60].

Lifetime ratio	Experimental average	HQE prediction
$\tau(B^+)/\tau(B^0)$	1.076 ± 0.004	$1.04^{+0.05}_{-0.01} \pm 0.02 \pm 0.01$
$\tau(B_s^0)/\tau(B^0)$	0.990 ± 0.004	1.001 ± 0.002
$\tau(\Lambda_b^0)/\tau(B^0)$	0.967 ± 0.007	0.935 ± 0.054
$\tau(\Xi_b^0)/\tau(\Xi_b^-)$	0.929 ± 0.028	0.95 ± 0.06

average results obtained with fully reconstructed Ξ_b^-, Ξ_b^0 and Ω_b^- baryons, and obtain

$$\tau(\Xi_b^-) = 1.571 \pm 0.040 \text{ ps}, \quad (48)$$

$$\tau(\Xi_b^0) = 1.479 \pm 0.031 \text{ ps}, \quad (49)$$

$$\tau(\Omega_b^-) = 1.64^{+0.18}_{-0.17} \text{ ps}. \quad (50)$$

It should be noted that several b-baryon lifetime measurements from LHCb [146, 148–150] were made with respect to the lifetime of another b hadron (*i.e.* the original measurement is that of a decay width difference). Before these measurements are included in the averages quoted above, we rescale them according to our latest lifetime average of that reference b hadron. This introduces correlations between our averages, in particular between the Ξ_b^- and Ξ_b^0 lifetimes. Taking this correlation into account leads to

$$\tau(\Xi_b^0)/\tau(\Xi_b^-) = 0.929 \pm 0.028. \quad (51)$$

3.2.7 Summary and comparison with theoretical predictions

Averages of lifetimes of specific b-hadron species are collected in Table 13. As described in the introduction to Sec. 3.2, the HQE can be employed to explain the hierarchy of $\tau(B_c^+) \ll \tau(\Lambda_b^0) < \tau(B_s^0) \approx \tau(B^0) < \tau(B^+)$, and used to predict the ratios between lifetimes. Recent predictions are compared to the measured lifetime ratios in Table 14.

The predictions of the ratio between the B^+ and B^0 lifetimes, 1.06 ± 0.02 [58] or $1.04^{+0.05}_{-0.01} \pm 0.02 \pm 0.01$ [60], are in good agreement with experiment.

The total widths of the B_s^0 and B^0 mesons are expected to be very close and differ by at most 1% [59,60,151]. This prediction is consistent with the experimental ratio $\tau(B_s^0)/\tau(B^0) = \Gamma_d/\Gamma_s$,

which is smaller than 1 by $(1.0 \pm 0.4)\%$. The authors of Ref. [103] predict $\tau(B_s^0)/\tau(B^0) = 1.00050 \pm 0.00108 \pm 0.0225 \times \delta$, where δ quantifies a possible breaking of the quark-hadron duality. In this context, they interpret the 2.5σ difference between theory and experiment as being due to either new physics or a sizable duality violation. The key message is that improved experimental precision on this ratio is very welcome.

The ratio $\tau(\Lambda_b^0)/\tau(B^0)$ has particularly been the source of theoretical scrutiny since earlier calculations using the HQE [55, 152] predicted a value larger than 0.90, almost $2\,\sigma$ above the world average at the time. Many predictions cluster around a most likely central value of 0.94 [153]. Calculations of this ratio that include higher-order effects predict a lower ratio between the Λ_b^0 and B^0 lifetimes [58,59] and reduce this difference. Since then the experimental average is now definitely settling at a value significantly larger than initially, in agreement with the latest theoretical predictions. A recent review [60] concludes that the long-standing Λ_b lifetime puzzle is resolved, with a nice agreement between the precise experimental determination of $\tau(\Lambda_b^0)/\tau(B^0)$ and the less precise HQE prediction which needs new lattice calculations. There is also good agreement for the $\tau(\Xi_b^0)/\tau(\Xi_b^-)$ ratio.

As already mentioned, the CDF measurement of the Λ_b^0 lifetime in the exclusive decay mode $J/\psi\,\Lambda$ [144] is significantly higher than the world average before inclusion, with a ratio to the $\tau(B^0)$ world average of $\tau(\Lambda_b^0)/\tau(B^0) = 1.030 \pm 0.027$, resulting in continued interest in lifetimes of b baryons.

The lifetimes of the most abundant b-hadron species are now all known to sub-percent precision. Neglecting the contributions of the rarer species (B_c^+ meson and b baryons other than the Λ_b^0), one can compute the average b-hadron lifetime from the individual lifetimes and production fractions as

$$\tau_b = \frac{f_d\tau(B^0)^2 + f_u\tau(B^+)^2 + 0.5 f_s\tau(B_{s\mathrm{H}})^2 + 0.5 f_s\tau(B_{s\mathrm{L}})^2 + f_{\mathrm{baryon}}\tau(\Lambda_b^0)^2}{f_d\tau(B^0) + f_u\tau(B^+) + 0.5 f_s\tau(B_{s\mathrm{H}}) + 0.5 f_s\tau(B_{s\mathrm{L}}) + f_{\mathrm{baryon}}\tau(\Lambda_b^0)}\,. \tag{52}$$

Using the lifetimes of Table 13 and the fractions in Z decays of Table 5, taking into account the correlations between the fractions (Table 5) as well as the correlation between $\tau(B_{s\mathrm{H}})$ and $\tau(B_{s\mathrm{L}})$ (-0.389), one obtains

$$\tau_b(Z) = 1.566 \pm 0.003 \text{ ps}\,. \tag{53}$$

This is in very good agreement with (and three times more precise than) the average of Eq. (33) for the inclusive measurements performed at LEP.

3.3 Neutral B-meson mixing

The $B^0 - \overline{B}^0$ and $B_s^0 - \overline{B}_s^0$ systems both exhibit the phenomenon of particle-antiparticle mixing. For each of them, there are two mass eigenstates which are linear combinations of the two flavour states, B and $\overline{B}$. The heaviest (lightest) of these mass states is denoted B_{H} (B_{L}), with mass m_{H} (m_{L}) and total decay width Γ_{H} (Γ_{L}). We define

$$\Delta m = m_{\mathrm{H}} - m_{\mathrm{L}}\,, \qquad x = \Delta m/\Gamma\,, \tag{54}$$

$$\Delta\Gamma = \Gamma_{\mathrm{L}} - \Gamma_{\mathrm{H}}\,, \qquad y = \Delta\Gamma/(2\Gamma)\,, \tag{55}$$

where $\Gamma = (\Gamma_{\rm H}+\Gamma_{\rm L})/2 = 1/\overline{\tau}(B)$ is the average decay width. Δm is positive by definition, and $\Delta\Gamma$ is expected to be positive within the Standard Model.[19]

There are four different time-dependent probabilities describing the case of a neutral B meson produced as a flavour state and decaying without *CP* violation to a flavour-specific final state. If *CPT* is conserved (which will be assumed throughout), they can be written as

$$\left\{\begin{array}{lcl} \mathcal{P}(B \to B) & = & \frac{e^{-\Gamma t}}{2}\left[\cosh\left(\frac{\Delta\Gamma}{2}t\right) + \cos(\Delta m t)\right] \\ \mathcal{P}(B \to \overline{B}) & = & \frac{e^{-\Gamma t}}{2}\left[\cosh\left(\frac{\Delta\Gamma}{2}t\right) - \cos(\Delta m t)\right] \left|\frac{q}{p}\right|^2 \\ \mathcal{P}(\overline{B} \to B) & = & \frac{e^{-\Gamma t}}{2}\left[\cosh\left(\frac{\Delta\Gamma}{2}t\right) - \cos(\Delta m t)\right] \left|\frac{p}{q}\right|^2 \\ \mathcal{P}(\overline{B} \to \overline{B}) & = & \frac{e^{-\Gamma t}}{2}\left[\cosh\left(\frac{\Delta\Gamma}{2}t\right) + \cos(\Delta m t)\right] \end{array}\right. , \tag{56}$$

where t is the proper time of the system (*i.e.* the time interval between the production and the decay in the rest frame of the B meson). At the B factories, only the proper-time difference Δt between the decays of the two neutral B mesons from the $\Upsilon(4S)$ can be determined, but, because the two B mesons evolve coherently (keeping opposite flavours as long as neither of them has decayed), the above formulae remain valid if t is replaced with Δt and the production flavour is replaced by the flavour at the time of the decay of the accompanying B meson in a flavour-specific state. As can be seen in the above expressions, the mixing probabilities depend on three mixing observables: Δm, $\Delta\Gamma$, and $|q/p|^2$, which signals *CP* violation in the mixing if $|q/p|^2 \neq 1$.

In the next sections we review in turn the experimental knowledge on the B^0 decay-width and mass differences, the B^0_s decay-width and mass differences, *CP* violation in B^0 and B^0_s mixing, and mixing-induced *CP* violation in B^0_s decays.

3.3.1 B^0 mixing parameters $\Delta\Gamma_d$ and Δm_d

A large number of time-dependent B^0–$\overline{B}^0$ oscillation analyses have been performed since almost 20 years by the ALEPH, DELPHI, L3, OPAL, CDF, D0, *BABAR*, Belle and LHCb collaborations. The corresponding measurements of Δm_d are summarized in Table 15, where only the most recent results are listed (*i.e.* measurements superseded by more recent ones are omitted[20]). Although a variety of different techniques have been used, the individual Δm_d results obtained at different colliders have remarkably similar precision. The systematic uncertainties are comparable to the statistical uncertainties; they are often dominated by sample composition, mistag probability, or b-hadron lifetime contributions. Before being combined, the measurements are adjusted on the basis of a common set of input values, including the averages of the b-hadron fractions and lifetimes given in this report (see Secs. 3.1 and 3.2). Some measurements are statistically correlated. Systematic correlations arise both from common physics sources (fractions, lifetimes, branching ratios of b hadrons), and from purely experimental or algorithmic effects (efficiency, resolution, flavour tagging, background description). Combining all published measurements listed in Table 15 and accounting for all identified correlations as described in Ref. [3] yields $\Delta m_d = 0.5065 \pm 0.0016 \pm 0.0011$ ps^{-1}.

[19] For reasons of symmetry in Eqs. (54) and (55), $\Delta\Gamma$ is sometimes defined with the opposite sign. The definition adopted here, *i.e.* Eq. (55), is the one used by most experimentalists and many phenomenologists in B physics.

[20] Two old unpublished CDF2 measurements [173, 174] are also omitted from our averages, Table 15 and Fig. 6.

Table 15: Time-dependent measurements included in the Δm_d average. The results obtained from multi-dimensional fits involving also the B^0 (and B^+) lifetimes as free parameter(s) [91, 93, 94] have been converted into one-dimensional measurements of Δm_d. All the measurements have then been adjusted to a common set of physics parameters before being combined.

Experiment	Method		Δm_d in ps^{-1}	Δm_d in ps^{-1}
and Ref.	rec.	tag	before adjustment	after adjustment
ALEPH [154]	ℓ	$Q_{\rm jet}$	$0.404 \pm 0.045 \pm 0.027$	
ALEPH [154]	ℓ	ℓ	$0.452 \pm 0.039 \pm 0.044$	
ALEPH [154]	above two combined		$0.422 \pm 0.032 \pm 0.026$	$0.440 \pm 0.032 ^{+0.020}_{-0.019}$
ALEPH [154]	D^*	$\ell, Q_{\rm jet}$	$0.482 \pm 0.044 \pm 0.024$	$0.482 \pm 0.044 \pm 0.024$
DELPHI [155]	ℓ	$Q_{\rm jet}$	$0.493 \pm 0.042 \pm 0.027$	$0.499 \pm 0.042 \pm 0.024$
DELPHI [155]	$\pi^*\ell$	$Q_{\rm jet}$	$0.499 \pm 0.053 \pm 0.015$	$0.500 \pm 0.053 \pm 0.015$
DELPHI [155]	ℓ	ℓ	$0.480 \pm 0.040 \pm 0.051$	$0.494 \pm 0.040 ^{+0.042}_{-0.040}$
DELPHI [155]	D^*	$Q_{\rm jet}$	$0.523 \pm 0.072 \pm 0.043$	$0.518 \pm 0.072 \pm 0.043$
DELPHI [156]	vtx	comb	$0.531 \pm 0.025 \pm 0.007$	$0.525 \pm 0.025 \pm 0.006$
L3 [157]	ℓ	ℓ	$0.458 \pm 0.046 \pm 0.032$	$0.467 \pm 0.046 \pm 0.028$
L3 [157]	ℓ	$Q_{\rm jet}$	$0.427 \pm 0.044 \pm 0.044$	$0.439 \pm 0.044 \pm 0.042$
L3 [157]	ℓ	ℓ(IP)	$0.462 \pm 0.063 \pm 0.053$	$0.470 \pm 0.063 \pm 0.044$
OPAL [158]	ℓ	ℓ	$0.430 \pm 0.043 ^{+0.028}_{-0.030}$	$0.466 \pm 0.043 ^{+0.017}_{-0.016}$
OPAL [159]	ℓ	$Q_{\rm jet}$	$0.444 \pm 0.029 ^{+0.020}_{-0.017}$	$0.481 \pm 0.029 \pm 0.013$
OPAL [160]	$D^*\ell$	$Q_{\rm jet}$	$0.539 \pm 0.060 \pm 0.024$	$0.544 \pm 0.060 \pm 0.023$
OPAL [160]	D^*	ℓ	$0.567 \pm 0.089 ^{+0.029}_{-0.023}$	$0.572 \pm 0.089 ^{+0.028}_{-0.022}$
OPAL [81]	$\pi^*\ell$	$Q_{\rm jet}$	$0.497 \pm 0.024 \pm 0.025$	$0.496 \pm 0.024 \pm 0.025$
CDF1 [161]	$D\ell$	SST	$0.471 ^{+0.078}_{-0.068} ^{+0.033}_{-0.034}$	$0.470 ^{+0.078}_{-0.068} ^{+0.033}_{-0.034}$
CDF1 [162]	μ	μ	$0.503 \pm 0.064 \pm 0.071$	$0.514 \pm 0.064 ^{+0.070}_{-0.069}$
CDF1 [163]	ℓ	$\ell, Q_{\rm jet}$	$0.500 \pm 0.052 \pm 0.043$	$0.546 \pm 0.052 \pm 0.036$
CDF1 [164]	$D^*\ell$	ℓ	$0.516 \pm 0.099 ^{+0.029}_{-0.035}$	$0.523 \pm 0.099 ^{+0.028}_{-0.035}$
D0 [165]	$D^{(*)}\mu$	OST	$0.506 \pm 0.020 \pm 0.016$	$0.506 \pm 0.020 \pm 0.016$
BABAR [166]	B^0	$\ell, K, {\rm NN}$	$0.516 \pm 0.016 \pm 0.010$	$0.521 \pm 0.016 \pm 0.008$
BABAR [167]	ℓ	ℓ	$0.493 \pm 0.012 \pm 0.009$	$0.487 \pm 0.012 \pm 0.006$
BABAR [91]	$D^*\ell\nu$	$\ell, K, {\rm NN}$	$0.492 \pm 0.018 \pm 0.014$	$0.493 \pm 0.018 \pm 0.013$
BABAR [93]	$D^*\ell\nu$(part)	ℓ	$0.511 \pm 0.007 \pm 0.007$	$0.513 \pm 0.007 \pm 0.007$
Belle [94]	$B^0, D^*\ell\nu$	comb	$0.511 \pm 0.005 \pm 0.006$	$0.513 \pm 0.005 \pm 0.006$
Belle [168]	$D^*\pi$(part)	ℓ	$0.509 \pm 0.017 \pm 0.020$	$0.513 \pm 0.017 \pm 0.019$
Belle [11]	ℓ	ℓ	$0.503 \pm 0.008 \pm 0.010$	$0.506 \pm 0.008 \pm 0.008$
LHCb [169]	B^0	OST	$0.499 \pm 0.032 \pm 0.003$	$0.499 \pm 0.032 \pm 0.003$
LHCb [170]	B^0	OST,SST	$0.5156 \pm 0.0051 \pm 0.0033$	$0.5156 \pm 0.0051 \pm 0.0033$
LHCb [171]	$D\mu$	OST,SST	$0.503 \pm 0.011 \pm 0.013$	$0.503 \pm 0.011 \pm 0.013$
LHCb [172]	$D^{(*)}\mu$	OST	$0.5050 \pm 0.0021 \pm 0.0010$	$0.5050 \pm 0.0021 \pm 0.0010$
World average (all above measurements included):				$0.5065 \pm 0.0016 \pm 0.0011$
– ALEPH, DELPHI, L3, OPAL and CDF1 only:				$0.496 \pm 0.010 \pm 0.009$
– *BABAR* and Belle only:				$0.509 \pm 0.003 \pm 0.003$
– LHCb only:				$0.5063 \pm 0.0019 \pm 0.0010$

On the other hand, ARGUS and CLEO have published measurements of the time-integrated mixing probability χ_d [175–177], which average to $\chi_d = 0.182 \pm 0.015$. Following Ref. [177], the decay width difference $\Delta\Gamma_d$ could in principle be extracted from the measured value of $\Gamma_d = 1/\tau(B^0)$ and the above averages for Δm_d and χ_d (provided that $\Delta\Gamma_d$ has a negligible impact on the Δm_d and $\tau(B^0)$ analyses that have assumed $\Delta\Gamma_d = 0$), using the relation

$$\chi_d = \frac{x_d^2 + y_d^2}{2(x_d^2+1)} \quad \text{with} \quad x_d = \frac{\Delta m_d}{\Gamma_d} \quad \text{and} \quad y_d = \frac{\Delta\Gamma_d}{2\Gamma_d}\,. \tag{57}$$

However, direct time-dependent studies provide much stronger constraints: $|\Delta\Gamma_d|/\Gamma_d < 18\%$ at 95% CL from DELPHI [156], $-6.8\% < \mathrm{sign}(\mathrm{Re}\lambda_{CP})\Delta\Gamma_d/\Gamma_d < 8.4\%$ at 90% CL from *BABAR* [178], and $\mathrm{sign}(\mathrm{Re}\lambda_{CP})\Delta\Gamma_d/\Gamma_d = (1.7 \pm 1.8 \pm 1.1)\%$ [179] from Belle, where $\lambda_{CP} = (q/p)_d(\overline{A}_{CP}/A_{CP})$ is defined for a *CP*-even final state (the sensitivity to the overall sign of $\mathrm{sign}(\mathrm{Re}\lambda_{CP})\Delta\Gamma_d/\Gamma_d$ comes from the use of B^0 decays to *CP* final states). In addition LHCb has obtained $\Delta\Gamma_d/\Gamma_d = (-4.4 \pm 2.5 \pm 1.1)\%$ [96] by comparing measurements of the $B^0 \to J/\psi\, K^{*0}$ and $B^0 \to J/\psi\, K^0_S$ decays, following the method of Ref. [180]. More recently ATLAS has measured $\Delta\Gamma_d/\Gamma_d = (-0.1 \pm 1.1 \pm 0.9)\%$ [181] using a similar method. Assuming $\mathrm{Re}\lambda_{CP} > 0$, as expected from the global fits of the Unitarity Triangle within the Standard Model [182], a combination of these five results (after adjusting the DELPHI and *BABAR* results to $1/\Gamma_d = \tau(B^0) = 1.520 \pm 0.004$ ps) yields

$$\Delta\Gamma_d/\Gamma_d = -0.002 \pm 0.010\,, \tag{58}$$

an average consistent with zero. An independent result, $\Delta\Gamma_d/\Gamma_d = (0.50 \pm 1.38)\%$ [183], was obtained by the D0 collaboration from their measurements of the single muon and same-sign dimuon charge asymmetries, under the interpretation that the observed asymmetries are due to *CP* violation in neutral B-meson mixing and interference. This indirect determination was called into question [184] and is therefore not included in the above average.

Assuming $\Delta\Gamma_d = 0$ and using $1/\Gamma_d = \tau(B^0) = 1.520 \pm 0.004$ ps, the Δm_d and χ_d results are combined through Eq. (57) to yield the world average

$$\Delta m_d = 0.5064 \pm 0.0019 \text{ ps}^{-1}\,, \tag{59}$$

or, equivalently,

$$x_d = 0.770 \pm 0.004 \quad \text{and} \quad \chi_d = 0.1860 \pm 0.0011\,. \tag{60}$$

Figure 6 compares the Δm_d values obtained by the different experiments.

The B^0 mixing averages given in Eqs. (59) and (60) and the b-hadron fractions of Table 5 have been obtained in a fully consistent way, taking into account the fact that the fractions are computed using the χ_d value of Eq. (60) and that many individual measurements of Δm_d at high energy depend on the assumed values for the b-hadron fractions. Furthermore, this set of averages is consistent with the lifetime averages of Sec. 3.2.

3.3.2 B^0_s mixing parameters $\Delta\Gamma_s$ and Δm_s

Definitions and an introduction to $\Delta\Gamma_s$ have been given in Sec. 3.2.4. Neglecting *CP* violation, the mass eigenstates are also *CP* eigenstates, with the short-lived state being *CP*-even and the long-lived state being *CP*-odd.

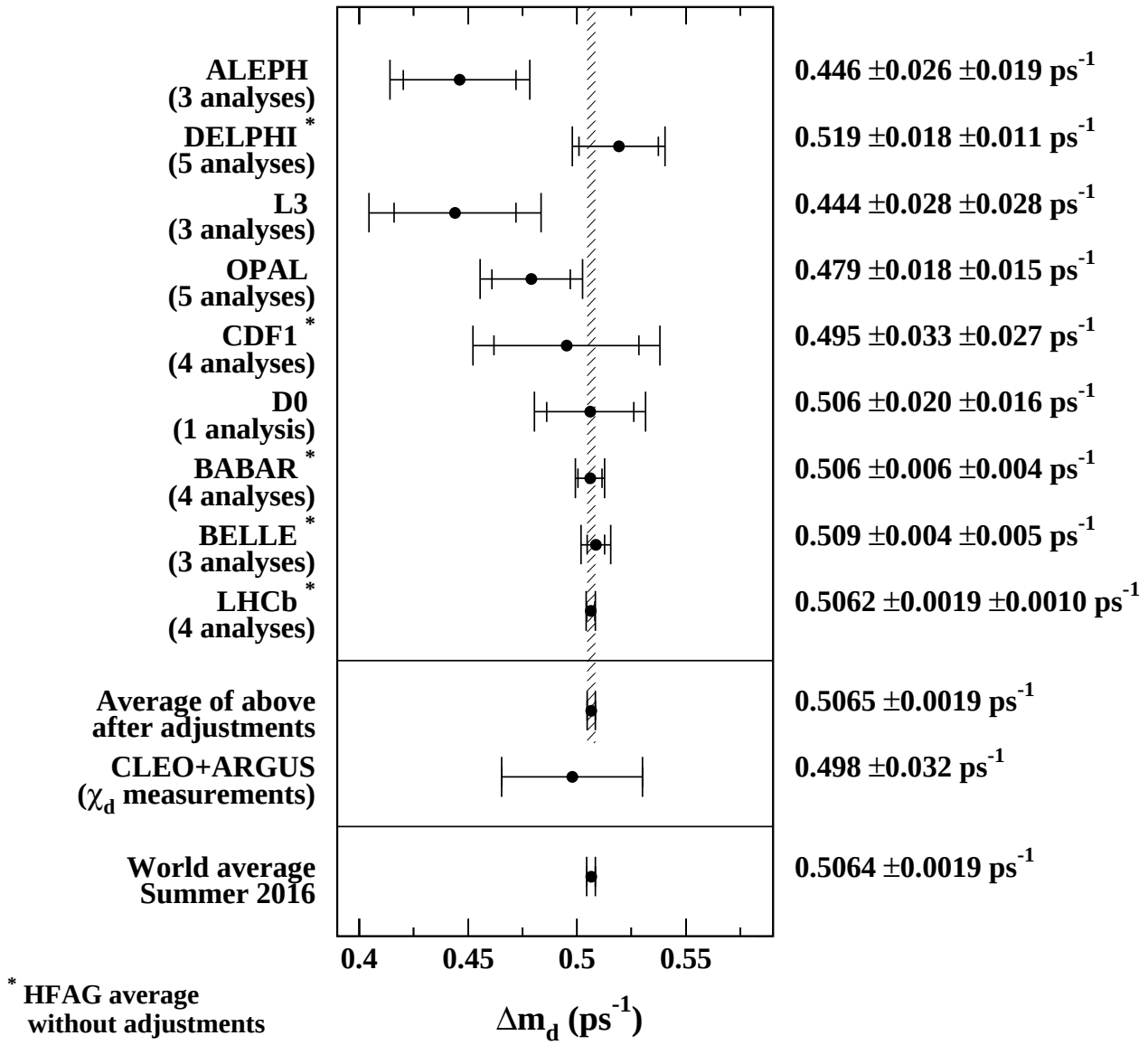

Figure 6: The B^0–$\overline{B}^0$ oscillation frequency Δm_d as measured by the different experiments. The averages quoted for ALEPH, L3 and OPAL are taken from the original publications, while the ones for DELPHI, CDF, *BABAR*, Belle and LHCb have been computed from the individual results listed in Table 15 without performing any adjustments. The time-integrated measurements of χ_d from the symmetric B factory experiments ARGUS and CLEO have been converted to a Δm_d value using $\tau(B^0) = 1.520 \pm 0.004$ ps. The two global averages have been obtained after adjustments of all the individual Δm_d results of Table 15 (see text).

Table 16: Measurements of $\Delta\Gamma_s$ and Γ_s using $B_s^0 \to J/\psi\,\phi$, $B_s^0 \to J/\psi\,K^+K^-$ and $B_s^0 \to \psi(2S)\phi$ decays. Only the solution with $\Delta\Gamma_s > 0$ is shown, since the two-fold ambiguity has been resolved in Ref. [106]. The first error is due to statistics, the second one to systematics. The last line gives our average.

Exp.	Mode	Dataset	$\Delta\Gamma_s$ (ps^{-1})	Γ_s (ps^{-1})	Ref.
CDF	$J/\psi\,\phi$	$9.6\,\mathrm{fb}^{-1}$	$+0.068 \pm 0.026 \pm 0.009$	$0.654 \pm 0.008 \pm 0.004$	[185]
D0	$J/\psi\,\phi$	$8.0\,\mathrm{fb}^{-1}$	$+0.163^{+0.065}_{-0.064}$	$0.693^{+0.018}_{-0.017}$	[186]
ATLAS	$J/\psi\,\phi$	$4.9\,\mathrm{fb}^{-1}$	$+0.053 \pm 0.021 \pm 0.010$	$0.677 \pm 0.007 \pm 0.004$	[187]
ATLAS	$J/\psi\,\phi$	$14.3\,\mathrm{fb}^{-1}$	$+0.101 \pm 0.013 \pm 0.007$	$0.676 \pm 0.004 \pm 0.004$	[188]
ATLAS	above 2 combined		$+0.085 \pm 0.011 \pm 0.007$	$0.675 \pm 0.003 \pm 0.003$	[188]
CMS	$J/\psi\,\phi$	$19.7\,\mathrm{fb}^{-1}$	$+0.095 \pm 0.013 \pm 0.007$	$0.6704 \pm 0.0043 \pm 0.0055$	[190]
LHCb	$J/\psi\,K^+K^-$	$3.0\,\mathrm{fb}^{-1}$	$+0.0805 \pm 0.0091 \pm 0.0033$	$0.6603 \pm 0.0027 \pm 0.0015$	[191]
LHCb	$\psi(2S)\phi$	$3.0\,\mathrm{fb}^{-1}$	$+0.066^{+0.041}_{-0.044} \pm 0.007$	$0.668 \pm 0.011 \pm 0.006$	[192]
All combined			$+0.083 \pm 0.007$	0.6654 ± 0.0022	

The best sensitivity to $\Delta\Gamma_s$ is currently achieved by the recent time-dependent measurements of the $B_s^0 \to J/\psi\,\phi$ (or more generally $B_s^0 \to (c\bar{c})K^+K^-$) decay rates performed at CDF [185], D0 [186], ATLAS [187, 188], CMS [189, 190] and LHCb [191, 192], where the *CP*-even and *CP*-odd amplitudes are statistically separated through a full angular analysis. With the exception of the first CMS analysis [189][21], these studies use both untagged and tagged B_s^0 candidates and are optimized for the measurement of the *CP*-violating phase $\phi_s^{c\bar{c}s}$, defined later in Sec. 3.3.4. The LHCb collaboration analyzed the $B_s^0 \to J/\psi\,K^+K^-$ decay, considering that the K^+K^- system can be in a P-wave or S-wave state, and measured the dependence of the strong phase difference between the P-wave and S-wave amplitudes as a function of the K^+K^- invariant mass [106]. This allowed, for the first time, the unambiguous determination of the sign of $\Delta\Gamma_s$, which was found to be positive at the $4.7\,\sigma$ level. The following averages present only the $\Delta\Gamma_s > 0$ solutions.

The published results [185–188, 190–192] are shown in Table 16. They are combined, taking into account, in each analysis, the correlation between $\Delta\Gamma_s$ and Γ_s. The results, displayed as the red contours labelled "$B_s^0 \to (c\bar{c})KK$ measurements" in the plots of Fig. 7, are given in the first column of numbers of Table 17.

An alternative approach, which is directly sensitive to first order in $\Delta\Gamma_s/\Gamma_s$, is to determine the effective lifetime of untagged B_s^0 candidates decaying to pure *CP* eigenstates; we use here measurements with $B_s^0 \to D_s^+D_s^-$ [116], $B_s^0 \to J/\psi\eta$ [121], $B_s^0 \to J/\psi\,f_0(980)$ [123, 124] and $B_s^0 \to J/\psi\,\pi^+\pi^-$ [125] decays. The precise extraction of $1/\Gamma_s$ and $\Delta\Gamma_s$ from such measurements, discussed in detail in Ref. [107], requires additional information in the form of theoretical assumptions or external inputs on weak phases and hadronic parameters. If f designates a final state in which both B_s^0 and $\overline{B}_s^0$ can decay, the ratio of the effective B_s^0 lifetime decaying

[21] The CMS result of Ref. [189] is statistically independent of that of Ref. [190] but, since it has not been published, it is not included in Table 16 nor in our averages.

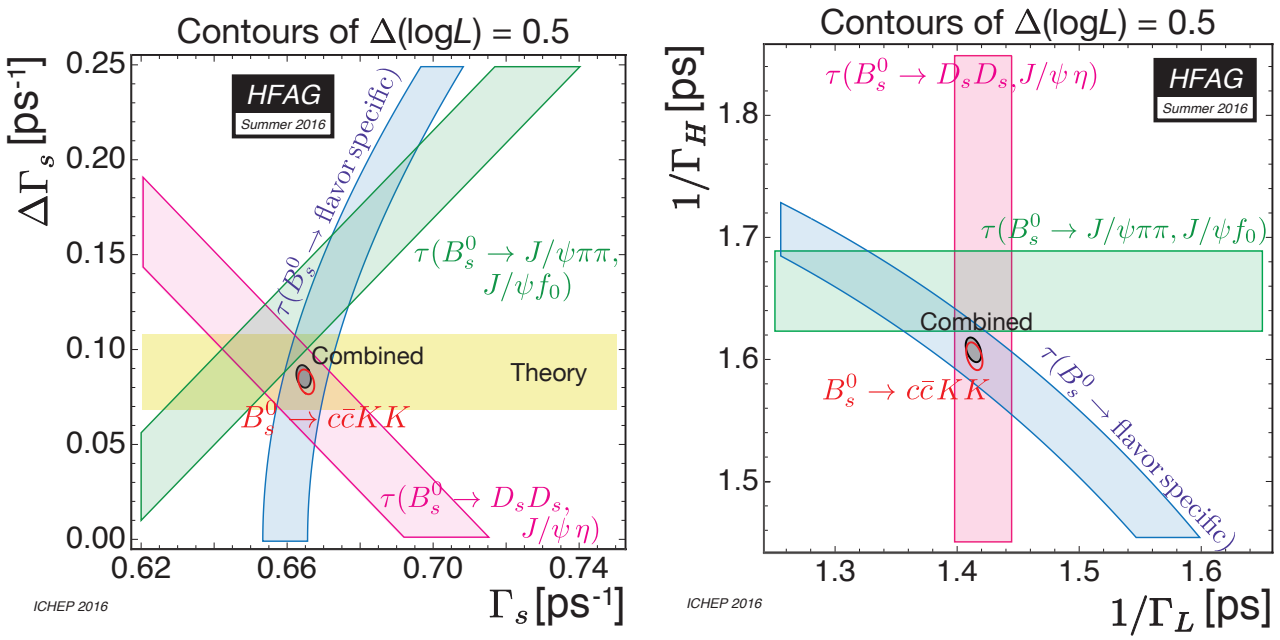

Figure 7: Contours of $\Delta \ln L = 0.5$ (39% CL for the enclosed 2D regions, 68% CL for the bands) shown in the (Γ_s, $\Delta\Gamma_s$) plane on the left and in the ($1/\Gamma_{\rm L}$, $1/\Gamma_{\rm H}$) plane on the right. The average of all the $B_s^0 \to J/\psi\phi$, $B_s^0 \to J/\psi K^+K^-$ and $B_s^0 \to \psi(2S)\phi$ results is shown as the red contour, and the constraints given by the effective lifetime measurements of B_s^0 to flavour-specific, pure *CP*-odd and pure *CP*-even final states are shown as the blue, green and purple bands, respectively. The average taking all constraints into account is shown as the grey-filled contour. The yellow band is a theory prediction $\Delta\Gamma_s = 0.088 \pm 0.020$ ps^{-1} [103] that assumes no new physics in B_s^0 mixing.

Table 17: Averages of $\Delta\Gamma_s$, Γ_s and related quantities, obtained from $B_s^0 \to J/\psi\phi$, $B_s^0 \to J/\psi K^+K^-$ and $B_s^0 \to \psi(2S)\phi$ alone (first column), adding the constraints from the effective lifetimes measured in pure *CP* modes $B_s^0 \to D_s^+D_s^-, J/\psi\eta$ and $B_s^0 \to J/\psi\, f_0(980), J/\psi\pi^+\pi^-$ (second column), and adding the constraint from the effective lifetime measured in flavour-specific modes $B_s^0 \to D_s^-\ell^+\nu X$, $D_s^-\pi^+$, $D_s^-D^+$ (third column, recommended world averages).

	$B_s^0 \to (c\bar{c})K^+K^-$ modes only (see Table 16)	$B_s^0 \to (c\bar{c})K^+K^-$ modes + pure *CP* modes	$B_s^0 \to (c\bar{c})K^+K^-$ modes + pure *CP* modes + flavour-specific modes
Γ_s	0.6654 ± 0.0022 ps^{-1}	0.6644 ± 0.0021 ps^{-1}	0.6645 ± 0.0020 ps^{-1}
$1/\Gamma_s$	1.503 ± 0.005 ps	1.505 ± 0.005 ps	1.505 ± 0.005 ps
$1/\Gamma_{\rm L}$	1.414 ± 0.007 ps	1.414 ± 0.006 ps	1.414 ± 0.006 ps
$1/\Gamma_{\rm H}$	1.603 ± 0.011 ps	1.609 ± 0.011 ps	1.609 ± 0.010 ps
$\Delta\Gamma_s$	$+0.083 \pm 0.007$ ps^{-1}	$+0.086 \pm 0.006$ ps^{-1}	$+0.086 \pm 0.006$ ps^{-1}
$\Delta\Gamma_s/\Gamma_s$	$+0.125 \pm 0.010$	$+0.129 \pm 0.009$	$+0.129 \pm 0.009$
$\rho(\Gamma_s, \Delta\Gamma_s)$	-0.292	-0.273	-0.217

to f relative to the mean B_s^0 lifetime is [107][22]

$$\frac{\tau_{\rm single}(B_s^0 \to f)}{\tau(B_s^0)} = \frac{1}{1-y_s^2}\left[\frac{1-2A_f^{\Delta\Gamma}y_s+y_s^2}{1-A_f^{\Delta\Gamma}y_s}\right], \tag{61}$$

where

$$A_f^{\Delta\Gamma} = -\frac{2{\rm Re}(\lambda_f)}{1+|\lambda_f|^2}\,. \tag{62}$$

To include the measurements of the effective $B_s^0 \to D_s^+D_s^-$ (CP-even), $B_s^0 \to J/\psi\, f_0(980)$ (CP-odd) and $B_s^0 \to J/\psi\,\pi^+\pi^-$ (CP-odd) lifetimes as constraints in the $\Delta\Gamma_s$ fit,[23] we neglect sub-leading penguin contributions and possible direct CP violation. Explicitly, in Eq. (62), we set $A_{CP\text{-even}}^{\Delta\Gamma} = \cos\phi_s^{c\bar{c}s}$ and $A_{CP\text{-odd}}^{\Delta\Gamma} = -\cos\phi_s^{c\bar{c}s}$. Given the small value of $\phi_s^{c\bar{c}s}$, we have, to first order in y_s:

$$\tau_{\rm single}(B_s^0 \to CP\text{-even}) \;\approx\; \frac{1}{\Gamma_{\rm L}}\left(1+\frac{(\phi_s^{c\bar{c}s})^2 y_s}{2}\right), \tag{63}$$

$$\tau_{\rm single}(B_s^0 \to CP\text{-odd}) \;\approx\; \frac{1}{\Gamma_{\rm H}}\left(1-\frac{(\phi_s^{c\bar{c}s})^2 y_s}{2}\right). \tag{64}$$

The numerical inputs are taken from Eqs. (41) and (42) and the resulting averages, combined with the $B_s^0 \to J/\psi\, K^+K^-$ information, are indicated in the second column of numbers of Table 17. These averages assume $\phi_s^{c\bar{c}s} = 0$, which is compatible with the $\phi_s^{c\bar{c}s}$ average presented in Sec. 3.3.4.

Information on $\Delta\Gamma_s$ can also be obtained from the study of the proper time distribution of untagged samples of flavour-specific B_s^0 decays [126], where the flavour (*i.e.* B_s^0 or $\overline{B}{}_s^0$) at the time of decay can be determined by the decay products. In such decays, *e.g.* semileptonic B_s^0 decays, there is an equal mix of the heavy and light mass eigenstates at time zero. The proper time distribution is then a superposition of two exponential functions with decay constants $\Gamma_{\rm L,H} = \Gamma_s \pm \Delta\Gamma_s/2$. This provides sensitivity to both $1/\Gamma_s$ and $(\Delta\Gamma_s/\Gamma_s)^2$. Ignoring $\Delta\Gamma_s$ and fitting for a single exponential leads to an estimate of Γ_s with a relative bias proportional to $(\Delta\Gamma_s/\Gamma_s)^2$, as shown in Eq. (39). Including the constraint from the world-average flavour-specific B_s^0 lifetime, given in Eq. (40), leads to the results shown in the last column of Table 17. These world averages are displayed as the grey contours labelled "Combined" in the plots of Fig. 7. They correspond to the lifetime averages $1/\Gamma_s = 1.505 \pm 0.005$ ps, $1/\Gamma_{\rm L} = 1.414 \pm 0.006$ ps, $1/\Gamma_{\rm H} = 1.609 \pm 0.010$ ps, and to the decay-width difference

$$\Delta\Gamma_s = +0.086 \pm 0.006 \text{ ps}^{-1} \quad \text{and} \quad \Delta\Gamma_{\rm s}/\Gamma_{\rm s} = +0.129 \pm 0.009\,, \tag{65}$$

which is in good agreement with the Standard Model prediction $\Delta\Gamma_s = 0.088 \pm 0.020$ ps^{-1} [103].

Estimates of $\Delta\Gamma_s/\Gamma_s$ obtained from measurements of the $B_s^0 \to D_s^{(*)+}D_s^{(*)-}$ branching fraction [119, 193–195][24] have not been used, since they are based on the questionable [104] assumption that these decays account for all CP-even final states. The results of early lifetime analyses attempting to measure $\Delta\Gamma_s/\Gamma_s$ [71, 78, 109, 113] have not been used either.

[22] The definition of $A_f^{\Delta\Gamma}$ given in Eq. (62) has the sign opposite to that given in Ref. [107].

[23] The effective lifetimes measured in $B_s^0 \to K^+K^-$ (mostly CP-even) and $B_s^0 \to J/\psi K_{\rm S}^0$ (mostly CP-odd) are not used because we can not quantify the penguin contributions in those modes.

[24] The result of Ref. [194] supersedes that of Ref. [196].

Table 18: Measurements of Δm_s.

Experiment	Method	Data set		Δm_s (ps^{-1})	Ref.
CDF2	$D_s^{(*)-}\ell^+\nu$, $D_s^{(*)-}\pi^+$, $D_s^-\rho^+$		1 fb^{-1}	$17.77 \pm 0.10 \pm 0.07$	[205]
D0	$D_s^-\ell^+X$, $D_s^-\pi^+X$		2.4 fb^{-1}	$18.53 \pm 0.93 \pm 0.30$	[206][u]
LHCb	$D_s^-\pi^+$, $D_s^-\pi^+\pi^-\pi^+$	2010	0.034 fb^{-1}	$17.63 \pm 0.11 \pm 0.02$	[207]
LHCb	$D_s^-\mu^+X$	2011	1.0 fb^{-1}	$17.93 \pm 0.22 \pm 0.15$	[171]
LHCb	$D_s^-\pi^+$	2011	1.0 fb^{-1}	$17.768 \pm 0.023 \pm 0.006$	[208]
LHCb	$J/\psi K^+K^-$	2011–2012	3.0 fb^{-1}	$17.711\,^{+0.055}_{-0.057} \pm 0.011$	[191]
Average of CDF and LHCb measurements				$17.757 \pm 0.020 \pm 0.007$	

[u] Unpublished.

The strength of B_s^0 mixing is known to be large since more than 20 years. Indeed the time-integrated measurements of $\overline{\chi}$ (see Sec. 3.1.3), when compared to our knowledge of χ_d and the b-hadron fractions, indicated that χ_s should be close to its maximal possible value of 1/2. Many searches of the time dependence of this mixing were performed by ALEPH [197], CDF (Run I) [198], DELPHI [109, 113, 156, 199], OPAL [200, 201] and SLD [202–204], but did not have enough statistical power and proper time resolution to resolve the small period of the B_s^0 oscillations.

B_s^0 oscillations have been observed for the first time in 2006 by the CDF collaboration [205], based on samples of flavour-tagged hadronic and semileptonic B_s^0 decays (in flavour-specific final states), partially or fully reconstructed in 1 fb^{-1} of data collected during Tevatron's Run II. This was shortly followed by independent evidence obtained by the D0 collaboration with 2.4 fb^{-1} of data [206]. More recently the LHCb collaboration obtained the most precise results using fully reconstructed $B_s^0 \to D_s^-\pi^+$ and $B_s^0 \to D_s^-\pi^+\pi^-\pi^+$ decays at the LHC [207, 208]. LHCb has also observed B_s^0 oscillations with $B_s^0 \to J/\psi K^+K^-$ decays [191] and with semileptonic $B_s^0 \to D_s^-\mu^+X$ decays [171]. The measurements of Δm_s are summarized in Table 18.

A simple average of the CDF and LHCb results[25], taking into account the correlated systematic uncertainties between the three LHCb measurements, yields

$$\Delta m_s = 17.757 \pm 0.020 \pm 0.007 \text{ ps}^{-1} = 17.757 \pm 0.021 \text{ ps}^{-1} \tag{66}$$

and is illustrated in Figure 8. The Standard Model prediction $\Delta m_s = 18.3 \pm 2.7$ ps^{-1} [103] is consistent with the experimental value, but has a much larger error. The ratio $\Delta\Gamma_s/\Delta m_s$ can be predicted more accurately, 0.0048 ± 0.0008 [103], and is in good agreement with the experimental determination of

$$\Delta\Gamma_s/\Delta m_s = 0.00483 \pm 0.00034\,. \tag{67}$$

Multiplying the Δm_s result of Eq. (66) with the mean B_s^0 lifetime of Eq. (45), $1/\Gamma_s = 1.505 \pm 0.005$ ps, yields

$$x_s = \frac{\Delta m_s}{\Gamma_s} = 26.72 \pm 0.09\,. \tag{68}$$

[25] We do not include the old unpublished D0 [206] result in the average.

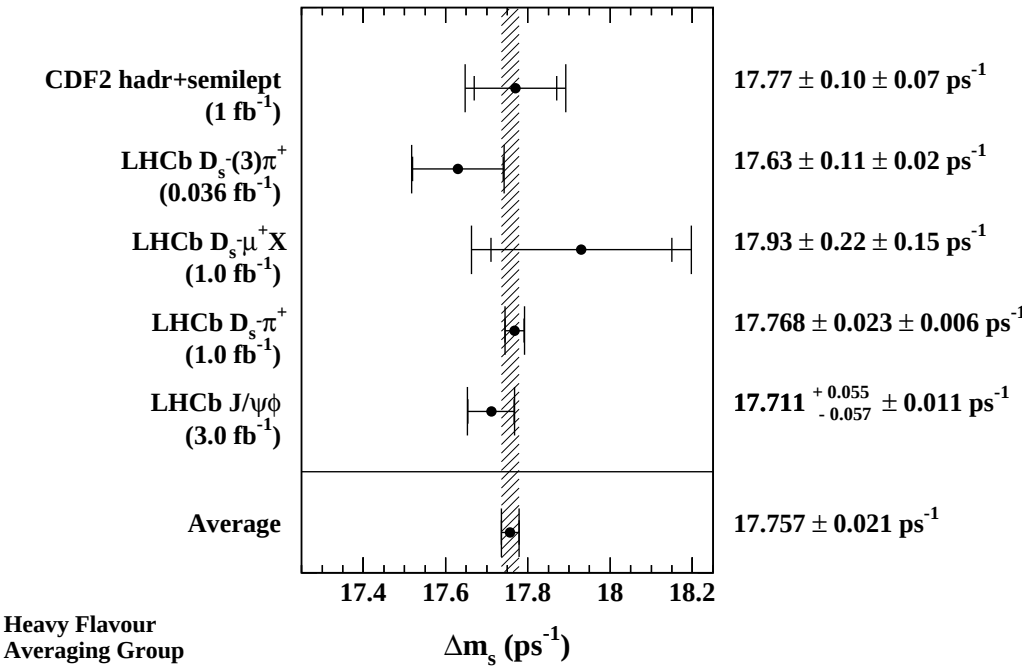

Figure 8: Published measurements of Δm_s, together with their average.

With $2y_s = \Delta\Gamma_s/\Gamma_s = +0.129 \pm 0.009$ (see Eq. (65)) and under the assumption of no *CP* violation in B_s^0 mixing, this corresponds to

$$\chi_s = \frac{x_s^2 + y_s^2}{2(x_s^2+1)} = 0.499304 \pm 0.000005\,. \tag{69}$$

The ratio of the B^0 and B_s^0 oscillation frequencies, obtained from Eqs. (59) and (66),

$$\frac{\Delta m_d}{\Delta m_s} = 0.02852 \pm 0.00011\,, \tag{70}$$

can be used to extract the following ratio of CKM matrix elements,

$$\left|\frac{V_{td}}{V_{ts}}\right| = \xi \sqrt{\frac{\Delta m_d}{\Delta m_s}\frac{m(B_s^0)}{m(B^0)}} = 0.2053 \pm 0.0004 \pm 0.0032\,, \tag{71}$$

where the first quoted error is from experimental uncertainties (with the masses $m(B_s^0)$ and $m(B^0)$ taken from Ref. [5]), and where the second quoted error is from theoretical uncertainties in the estimation of the SU(3) flavour-symmetry breaking factor $\xi = 1.206 \pm 0.018 \pm 0.006$, obtained from recent three-flavour lattice QCD calculations [209,210]. Note that Eq. (71) assumes that Δm_s and Δm_d only receive Standard Model contributions. An alternative approach would be to take V_{td}/V_{ts} from global fits to predict $\Delta m_d/\Delta m_s$, and then compare the prediction with the measurement of Eq. (70) to set limits on new physics effects.

3.3.3 *CP* violation in B^0 and B^0_s mixing

Evidence for *CP* violation in B^0 mixing has been searched for, both with flavour-specific and inclusive B^0 decays, in samples where the initial flavour state is tagged. In the case of semileptonic (or other flavour-specific) decays, where the final state tag is also available, the asymmetry

$$\mathcal{A}^d_{\rm SL} = \frac{N(\overline{B}^0(t) \to \ell^+\nu_\ell X) - N(B^0(t) \to \ell^-\overline{\nu}_\ell X)}{N(\overline{B}^0(t) \to \ell^+\nu_\ell X) + N(B^0(t) \to \ell^-\overline{\nu}_\ell X)} = \frac{|p/q|^2_d - |q/p|^2_d}{|p/q|^2_d + |q/p|^2_d} \tag{72}$$

has been measured, either in decay-time-integrated analyses at CLEO [177, 211], *BABAR* [212], CDF [213,214] and D0 [183], or in decay-time-dependent analyses at OPAL [159], ALEPH [215], *BABAR* [178, 216, 217] and Belle [218]. Note that the asymmetry of time-dependent decay rates in Eq. (72) is time-independent. In the inclusive case, also investigated and published at ALEPH [215] and OPAL [80], no final state tag is used, and the asymmetry [219]

$$\frac{N(B^0(t) \to \text{all}) - N(\overline{B}^0(t) \to \text{all})}{N(B^0(t) \to \text{all}) + N(\overline{B}^0(t) \to \text{all})} \simeq \mathcal{A}^d_{\rm SL}\left[\frac{\Delta m_d}{2\Gamma_d}\sin(\Delta m_d\, t) - \sin^2\left(\frac{\Delta m_d\, t}{2}\right)\right] \tag{73}$$

must be measured as a function of the proper time to extract information on *CP* violation.

On the other hand, D0 [220] and LHCb [221] have studied the time-dependence of the charge asymmetry of $B^0 \to D^{(*)-}\mu^+\nu_\mu X$ decays without tagging the initial state, which would be equal to

$$\frac{N(D^{(*)-}\mu^+\nu_\mu X) - N(D^{(*)+}\mu^-\overline{\nu}_\mu X)}{N(D^{(*)-}\mu^+\nu_\mu X) + N(D^{(*)+}\mu^-\overline{\nu}_\mu X)} = \mathcal{A}^d_{\rm SL}\frac{1-\cos(\Delta m_d\, t)}{2} \tag{74}$$

in absence of detection and production asymmetries.

Table 19 summarizes the different measurements[26] of $\mathcal{A}^d_{\rm SL}$ and $|q/p|_d$: in all cases asymmetries compatible with zero have been found, with a precision limited by the available statistics. A simple average of all measurements performed at the B factories [177, 178, 211, 212, 216, 218] yields $\mathcal{A}^d_{\rm SL} = -0.0019 \pm 0.0027$. Adding also the D0 [220] and LHCb [221] measurements obtained with reconstructed semileptonic B^0 decays yields $\mathcal{A}^d_{\rm SL} = +0.0001 \pm 0.0020$. As discussed in more detail later in this section, the D0 analysis with single muons and like-sign dimuons [183] separates the B^0 and B^0_s contributions by exploiting the dependence on the muon impact parameter cut; including the $\mathcal{A}^d_{\rm SL}$ result quoted by D0 in the average yields $\mathcal{A}^d_{\rm SL} = -0.0010 \pm 0.0018$. All the other B^0 analyses performed at high energy, either at LEP or at the Tevatron, did not separate the contributions from the B^0 and B^0_s mesons. Under the assumption of no *CP* violation in B^0_s mixing ($\mathcal{A}^s_{\rm SL} = 0$), a number of these early analyses [50, 80, 159, 215] quote a measurement of $\mathcal{A}^d_{\rm SL}$ or $|q/p|_d$ for the B^0 meson. However, these imprecise determinations no longer improve the world average of $\mathcal{A}^d_{\rm SL}$. The latter assumption makes sense within the Standard Model, since $\mathcal{A}^s_{\rm SL}$ is predicted to be much smaller than $\mathcal{A}^d_{\rm SL}$ [103], but may not be suitable in the presence of new physics.

The Tevatron experiments have measured linear combinations of $\mathcal{A}^d_{\rm SL}$ and $\mathcal{A}^s_{\rm SL}$ using inclusive semileptonic decays of b hadrons, $\mathcal{A}^b_{\rm SL} = +0.0015 \pm 0.0038(\text{stat}) \pm 0.0020(\text{syst})$ [213] and $\mathcal{A}^b_{\rm SL} = -0.00496 \pm 0.00153(\text{stat}) \pm 0.00072(\text{syst})$ [183], at CDF1 and D0 respectively. While

[26] A low-statistics result published by CDF using the Run I data [213] and an unpublished result by CDF using Run II data [214] are not included in our averages, nor in Table 19.

Table 19: Measurements[26] of *CP* violation in B^0 mixing and their average in terms of both $\mathcal{A}^d_{\rm SL}$ and $|q/p|_d$. The individual results are listed as quoted in the original publications, or converted[29] to an $\mathcal{A}^d_{\rm SL}$ value. When two errors are quoted, the first one is statistical and the second one systematic. The ALEPH and OPAL results assume no *CP* violation in B^0_s mixing.

Exp. & Ref.	Method	Measured $\mathcal{A}^d_{\rm SL}$	Measured $\lvert q/p\rvert_d$
CLEO [177]	partial hadronic rec.	$+0.017 \pm 0.070 \pm 0.014$	
CLEO [211]	dileptons	$+0.013 \pm 0.050 \pm 0.005$	
CLEO [211]	average of above two	$+0.014 \pm 0.041 \pm 0.006$	
BABAR [178]	full hadronic rec.		$1.029 \pm 0.013 \pm 0.011$
BABAR [216]	part. rec. $D^*X\ell\nu$	$+0.0006 \pm 0.0017^{+0.0038}_{-0.0032}$	$0.99971 \pm 0.00084 \pm 0.00175$
BABAR [212]	dileptons	$-0.0039 \pm 0.0035 \pm 0.0019$	
Belle [218]	dileptons	$-0.0011 \pm 0.0079 \pm 0.0085$	$1.0005 \pm 0.0040 \pm 0.0043$
Average of above 6 B-factory results		-0.0019 ± 0.0027 (tot)	1.0009 ± 0.0013 (tot)
D0 [220]	$B^0 \to D^{(*)-}\mu^+\nu X$	$+0.0068 \pm 0.0045 \pm 0.0014$	
LHCb [221]	$B^0 \to D^{(*)-}\mu^+\nu X$	$-0.0002 \pm 0.0019 \pm 0.0030$	
Average of above 8 pure B^0 results		$+0.0001 \pm 0.0020$ (tot)	1.0000 ± 0.0010 (tot)
D0 [183]	muons & dimuons	-0.0062 ± 0.0043 (tot)	
Average of above 9 direct measurements		-0.0010 ± 0.0018 (tot)	1.0005 ± 0.0009 (tot)
OPAL [159]	leptons	$+0.008 \pm 0.028 \pm 0.012$	
OPAL [80]	inclusive (Eq. (73))	$+0.005 \pm 0.055 \pm 0.013$	
ALEPH [215]	leptons	$-0.037 \pm 0.032 \pm 0.007$	
ALEPH [215]	inclusive (Eq. (73))	$+0.016 \pm 0.034 \pm 0.009$	
ALEPH [215]	average of above two	-0.013 ± 0.026 (tot)	
Average of above 13 results		-0.0010 ± 0.0018 (tot)	1.0005 ± 0.0009 (tot)
Best fit value from 2D combination of $\mathcal{A}^d_{\rm SL}$ and $\mathcal{A}^s_{\rm SL}$ results (see Eq. (75))		-0.0021 ± 0.0017 (tot)	1.0010 ± 0.0008 (tot)

the imprecise CDF1 result is compatible with no *CP* violation[27], the D0 result, obtained by measuring the single muon and like-sign dimuon charge asymmetries, differs by 2.8 standard deviations from the Standard Model expectation of $\mathcal{A}^b_{\rm SL}({\rm SM}) = (-2.3 \pm 0.4) \times 10^{-4}$ [104, 183]. With a more sophisticated analysis in bins of the muon impact parameters, D0 conclude that the overall deviation of their measurements from the SM is at the level of $3.6\,\sigma$. Interpreting the observed asymmetries in bins of the muon impact parameters in terms of *CP* violation in B-meson mixing and interference, and using the mixing parameters and the world b-hadron fractions of Ref. [222], the D0 collaboration extracts [183] values for $\mathcal{A}^d_{\rm SL}$ and $\mathcal{A}^s_{\rm SL}$ and their correlation coefficient[28], as shown in Table 20. However, the various contributions to the total quoted errors from this analysis and from the external inputs are not given, so the adjustment of these results to different or more recent values of the external inputs cannot (easily) be done.

Finally, direct determinations of $\mathcal{A}^s_{\rm SL}$, also shown in Table 20, are obtained by D0 [223] and LHCb [224] from the time-integrated charge asymmetry of untagged $B^0_s \to D^-_s\mu^+\nu X$ decays.

Using a two-dimensional fit, all measurements of $\mathcal{A}^s_{\rm SL}$ and $\mathcal{A}^d_{\rm SL}$ obtained by D0 and LHCb

[27] An unpublished measurement from CDF2, $\mathcal{A}^b_{\rm SL} = +0.0080 \pm 0.0090({\rm stat}) \pm 0.0068({\rm syst})$ [214], more precise than the D0 measurement, is also compatible with no *CP* violation.

[28] They also extract at the same time a value for $\Delta\Gamma_d/\Gamma_d$ (see Sec. 3.3.1).

Table 20: Measurements of CP violation in B^0_s and B^0 mixing, together with their correlations $\rho(\mathcal{A}^s_{\rm SL}, \mathcal{A}^d_{\rm SL})$ and their two-dimensional average. Only total errors are quoted.

Exp. & Ref.	Method	Measured $\mathcal{A}^s_{\rm SL}$	Measured $\mathcal{A}^d_{\rm SL}$	$\rho(\mathcal{A}^s_{\rm SL}, \mathcal{A}^d_{\rm SL})$
B-factory average of Table 19			-0.0019 ± 0.0027	
D0 [220, 223]	$B^0_{(s)} \to D^{(*)-}_{(s)} \mu^+ \nu X$	-0.0112 ± 0.0076	$+0.0068 \pm 0.0047$	$+0.$
LHCb [221, 224]	$B^0_{(s)} \to D^{(*)-}_{(s)} \mu^+ \nu X$	$+0.0039 \pm 0.0033$	-0.0002 ± 0.0036	$+0.13$
Average of above		$+0.0016 \pm 0.0030$	$+0.0000 \pm 0.0019$	$+0.066$
D0 [183]	muons & dimuons	-0.0082 ± 0.0099	-0.0062 ± 0.0043	-0.61
Average of all above		-0.0006 ± 0.0028	-0.0021 ± 0.0017	-0.054

are combined with the B-factory average of Table 19. Correlations are taken into account as shown in Table 20. The results, displayed graphically in Fig. 9, are

$$\mathcal{A}^d_{\rm SL} = -0.0021 \pm 0.0017 \iff |q/p|_d = 1.0010 \pm 0.0008\,, \quad (75)$$

$$\mathcal{A}^s_{\rm SL} = -0.0006 \pm 0.0028 \iff |q/p|_s = 1.0003 \pm 0.0014\,, \quad (76)$$

$$\rho(\mathcal{A}^d_{\rm SL}, \mathcal{A}^s_{\rm SL}) = -0.054\,, \quad (77)$$

where the relation between $\mathcal{A}^d_{\rm SL}$ and $|q/p|_d$ is given in Eq. (72), and similarly for $\mathcal{A}^s_{\rm SL}$ and $|q/p|_s$.[29] However, the confidence level of the fit is only 4.5%. This is mostly due to an overall discrepancy between the D0 and LHCb averages at the level of $2.2\,\sigma$.

The above averages show no evidence of CP violation in B^0 or B^0_s mixing. They deviate by $0.5\,\sigma$ from the very small predictions of the Standard Model (SM), ${\mathcal{A}^d_{\rm SL}}^{\rm SM} = -(4.7 \pm 0.6) \times 10^{-4}$ and ${\mathcal{A}^s_{\rm SL}}^{\rm SM} = +(2.22 \pm 0.27) \times 10^{-5}$ [103]. Given the current size of the experimental uncertainties, there is still significant room for a possible new physics contribution, in particular in the B^0_s system. In this respect, the deviation of the D0 dimuon asymmetry [183] from expectation has generated a lot of excitement. However, the recent $\mathcal{A}^s_{\rm SL}$ and $\mathcal{A}^d_{\rm SL}$ results from LHCb are not precise enough yet to settle the issue. It was pointed out [225] that the D0 dimuon result can be reconciled with the SM expectations of $\mathcal{A}^s_{\rm SL}$ and $\mathcal{A}^d_{\rm SL}$ if there were non-SM sources of CP violation in the semileptonic decays of the b and c quarks. A recent Run 1 ATLAS study [226] of charge asymmetries in muon+jets $t\bar{t}$ events, in which a b-hadron decays semileptonically to a soft muon, yields results with limited statistical precision, compatible both with the D0 dimuon asymmetry and with the SM predictions. More experimental data, especially from Run 2 of LHC, is awaited eagerly.

At the more fundamental level, CP violation in B^0_s mixing[30] is caused by the weak phase difference

$$\phi_{12} = \arg\left[-M_{12}/\Gamma_{12}\right], \quad (78)$$

where M_{12} and Γ_{12} are the off-diagonal elements of the mass and decay matrices of the $B^0_s - \overline{B}^0_s$

[29] Early analyses and the PDG use the complex parameter $\epsilon_B = (p-q)/(p+q)$; if CP violation in the mixing is small, $\mathcal{A}^d_{\rm SL} \cong 4{\rm Re}(\epsilon_B)/(1+|\epsilon_B|^2)$ and the average of Eq. (75) corresponds to ${\rm Re}(\epsilon_B)/(1+|\epsilon_B|^2) = -0.0005 \pm 0.0004$.

[30] Of course, a similar formalism exists for the B^0 system; for simplicity we omit here the subscript s for ϕ_{12}, M_{12} and Γ_{12}.

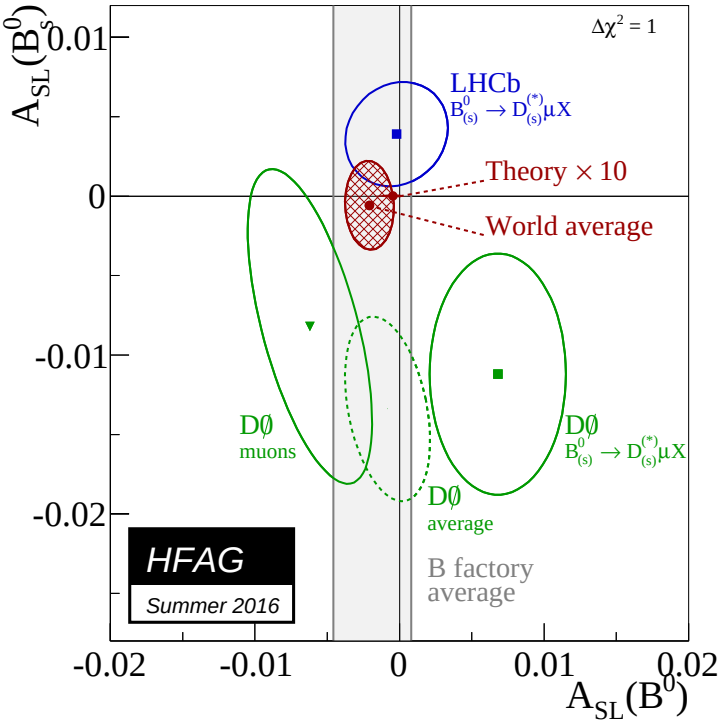

Figure 9: Measurements of $\mathcal{A}^s_{\rm SL}$ and $\mathcal{A}^d_{\rm SL}$ listed in Table 20 (B-factory average as the grey band, D0 measurements as the green ellipses, LHCb measurements as the blue ellipse) together with their two-dimensional average (red hatched ellipse). The red point close to $(0,0)$ is the Standard Model prediction of Ref. [103] with error bars multiplied by 10. The prediction and the experimental world average deviate from each other by $0.5\,\sigma$.

system. This is related to the observed decay-width difference through the relation

$$\Delta\Gamma_s = 2|\Gamma_{12}|\cos\phi_{12} + \mathcal{O}\left(\left|\frac{\Gamma_{12}}{M_{12}}\right|^2\right), \tag{79}$$

where quadratic (or higher-order) terms in the small quantity $|\Gamma_{12}/M_{12}| \sim \mathcal{O}(m_b^2/m_t^2)$ can be neglected. The SM prediction for this phase is tiny [103],

$$\phi_{12}^{\rm SM} = 0.0046 \pm 0.0012\,; \tag{80}$$

however, new physics in B^0_s mixing could change this observed phase to

$$\phi_{12} = \phi_{12}^{\rm SM} + \phi_{12}^{\rm NP}\,. \tag{81}$$

The B^0_s semileptonic asymmetry can be expressed as [227]

$$\mathcal{A}^s_{\rm SL} = {\rm Im}\left(\frac{\Gamma_{12}}{M_{12}}\right) + \mathcal{O}\left(\left|\frac{\Gamma_{12}}{M_{12}}\right|^2\right) = \frac{\Delta\Gamma_s}{\Delta m_s}\tan\phi_{12} + \mathcal{O}\left(\left|\frac{\Gamma_{12}}{M_{12}}\right|^2\right). \tag{82}$$

Using this relation, the current knowledge of $\mathcal{A}_{\rm SL}^s$, $\Delta\Gamma_s$ and Δm_s, given in Eqs. (76), (65), and (66) respectively, yield an experimental determination of ϕ_{12},

$$\tan\phi_{12} = \mathcal{A}_{\rm SL}^s \frac{\Delta m_s}{\Delta\Gamma_s} = -0.1 \pm 0.6\,, \tag{83}$$

which represents only a very weak constraint at present.

3.3.4 Mixing-induced *CP* violation in B_s^0 decays

CP violation induced by $B_s^0 - \overline{B}_s^0$ mixing has been a field of very active study and fast experimental progress in the past few years. The main observable is the *CP*-violating phase $\phi_s^{c\bar{c}s}$, defined as the weak phase difference between the $B_s^0 - \overline{B}_s^0$ mixing amplitude and the $b \to c\bar{c}s$ decay amplitude.

The golden mode for such studies is $B_s^0 \to J/\psi\,\phi$, followed by $J/\psi \to \mu^+\mu^-$ and $\phi \to K^+K^-$, for which a full angular analysis of the decay products is performed to separate statistically the *CP*-even and *CP*-odd contributions in the final state. As already mentioned in Sec. 3.3.2, CDF [185], D0 [186], ATLAS [187,188], CMS [190] and LHCb [191,192] have used both untagged and tagged $B_s^0 \to J/\psi\,\phi$ (and more generally $B_s^0 \to (c\bar{c})K^+K^-$) events for the measurement of $\phi_s^{c\bar{c}s}$. LHCb [228] has used $B_s^0 \to J/\psi\,\pi^+\pi^-$ events, analyzed with a full amplitude model including several $\pi^+\pi^-$ resonances (*e.g.* $f_0(980)$), although the $J/\psi\,\pi^+\pi^-$ final state had already been shown to be almost *CP* pure with a *CP*-odd fraction larger than 0.977 at 95% CL [229]. In addition, LHCb has used the $B_s^0 \to D_s^+D_s^-$ channel [230] to measure $\phi_s^{c\bar{c}s}$.

All CDF, D0, ATLAS and CMS analyses provide two mirror solutions related by the transformation $(\Delta\Gamma_s, \phi_s^{c\bar{c}s}) \to (-\Delta\Gamma_s, \pi - \phi_s^{c\bar{c}s})$. However, the LHCb analysis of $B_s^0 \to J/\psi\,K^+K^-$ resolves this ambiguity and rules out the solution with negative $\Delta\Gamma_s$ [106], a result in agreement with the Standard Model expectation. Therefore, in what follows, we only consider the solution with $\Delta\Gamma_s > 0$.

We perform a combination of the CDF [185], D0 [186], ATLAS [187, 188], CMS [190] and LHCb [191,192,228] results summarized in Table 21. This is done by adding the two-dimensional log profile-likelihood scans of $\Delta\Gamma_s$ and $\phi_s^{c\bar{c}s}$ from all $B_s^0 \to (c\bar{c})K^+K^-$ analyses and a one-dimensional log profile-likelihood of $\phi_s^{c\bar{c}s}$ from the $B_s^0 \to J/\psi\,\pi^+\pi^-$ and $B_s^0 \to D_s^+D_s^-$ analyses; the combined likelihood is then maximized with respect to $\Delta\Gamma_s$ and $\phi_s^{c\bar{c}s}$.

In the $B_s^0 \to J/\psi\,\phi$ and $B_s^0 \to J/\psi\,K^+K^-$ analyses, $\phi_s^{c\bar{c}s}$ and $\Delta\Gamma_s$ come from a simultaneous fit that determines also the B_s^0 lifetime, the polarisation amplitudes and strong phases. While the correlation between $\phi_s^{c\bar{c}s}$ and all other parameters is small, the correlations between $\Delta\Gamma_s$ and the polarisation amplitudes are sizeable. However, since the various experiments use different conventions for the amplitudes and phases, a full combination including all correlations is not performed. Instead, our average only takes into account the correlation between $\phi_s^{c\bar{c}s}$ and $\Delta\Gamma_s$.

In the recent LHCb $B_s^0 \to J/\psi\,K^+K^-$ analysis [191], the $\phi_s^{c\bar{c}s}$ values are measured for the first time for each polarization of the final state. Since those values are compatible within each other, we still use the unique value of $\phi_s^{c\bar{c}s}$ for our world average, corresponding to the one measured by the other-than-LHCb analyses. In the same analysis, the statistical correlation coefficient between $\phi_s^{c\bar{c}s}$ and $|\lambda|$ (which signals *CP* violation in the decay if different from unity) is measured to be very small (-0.02). We neglect this correlation in our average. Furthermore, the statistical correlation coefficient between $\phi_s^{c\bar{c}s}$ and $\Delta\Gamma_s$ is measured to be small (-0.08). When averaging LHCb results of $B_s^0 \to J/\psi\,K^+K^-$, $B_s^0 \to J/\psi\,\pi^+\pi^-$ and $B_s^0 \to D_s^+D_s^-$, we neglect

Table 21: Direct experimental measurements of $\phi_s^{c\bar{c}s}$, $\Delta\Gamma_s$ and Γ_s using $B_s^0 \to J/\psi\phi$, $J/\psi K^+K^-$, $\psi(2S)\phi$, $J/\psi\pi^+\pi^-$ and $D_s^+D_s^-$ decays. Only the solution with $\Delta\Gamma_s > 0$ is shown, since the two-fold ambiguity has been resolved in Ref. [106]. The first error is due to statistics, the second one to systematics. The last line gives our average.

Exp.	Mode	Dataset	$\phi_s^{c\bar{c}s}$	$\Delta\Gamma_s$ (ps^{-1})	Ref.
CDF	$J/\psi\phi$	9.6 fb^{-1}	$[-0.60, +0.12]$, 68% CL	$+0.068 \pm 0.026 \pm 0.009$	[185]
D0	$J/\psi\phi$	8.0 fb^{-1}	$-0.55^{+0.38}_{-0.36}$	$+0.163^{+0.065}_{-0.064}$	[186]
ATLAS	$J/\psi\phi$	4.9 fb^{-1}	$+0.12 \pm 0.25 \pm 0.05$	$+0.053 \pm 0.021 \pm 0.010$	[187]
ATLAS	$J/\psi\phi$	14.3 fb^{-1}	$-0.110 \pm 0.082 \pm 0.042$	$+0.101 \pm 0.013 \pm 0.007$	[188]
ATLAS	above 2 combined		$-0.090 \pm 0.078 \pm 0.041$	$+0.085 \pm 0.011 \pm 0.007$	[188]
CMS	$J/\psi\phi$	19.7 fb^{-1}	$-0.075 \pm 0.097 \pm 0.031$	$+0.095 \pm 0.013 \pm 0.007$	[190]
LHCb	$J/\psi K^+K^-$	3.0 fb^{-1}	$-0.058 \pm 0.049 \pm 0.006$	$+0.0805 \pm 0.0091 \pm 0.0033$	[191]
LHCb	$J/\psi\pi^+\pi^-$	3.0 fb^{-1}	$+0.070 \pm 0.068 \pm 0.008$	—	[228]
LHCb	above 2 combined		-0.010 ± 0.039(tot)	—	[191]
LHCb	$\psi(2S)\phi$	3.0 fb^{-1}	$+0.23^{+0.29}_{-0.28} \pm 0.02$	$+0.066^{+0.41}_{-0.44} \pm 0.007$	[192]
LHCb	$D_s^+D_s^-$	3.0 fb^{-1}	$+0.02 \pm 0.17 \pm 0.02$	—	[230]
All combined			-0.030 ± 0.033	$+0.084 \pm 0.007$	

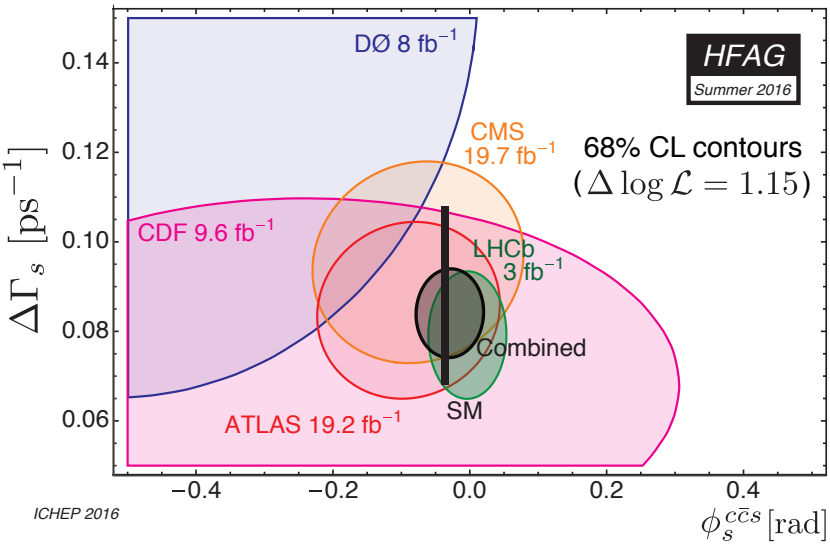

Figure 10: 68% CL regions in B_s^0 width difference $\Delta\Gamma_s$ and weak phase $\phi_s^{c\bar{c}s}$ obtained from individual and combined CDF [185], D0 [186], ATLAS [187, 188], CMS [190] and LHCb [191, 192, 228, 230] likelihoods of $B_s^0 \to J/\psi\phi$, $B_s^0 \to J/\psi K^+K^-$, $B_s^0 \to \psi(2S)\phi$, $B_s^0 \to J/\psi\pi^+\pi^-$ and $B_s^0 \to D_s^+D_s^-$ samples. The expectation within the Standard Model [103, 182] is shown as the black rectangle.

this correlation coefficient (putting it to zero). Given the increasing experimental precision, we have also stopped using the two-dimensional $\Delta\Gamma_s - \phi_s^{c\bar{c}s}$ histograms provided by the CDF and D0 collaborations: we are now approximating those with two-dimensional Gaussian likelihoods.

We obtain the individual and combined contours shown in Fig. 10. Maximizing the likelihood, we find, as summarized in Table 21:

$$\Delta\Gamma_s = +0.084 \pm 0.007 \text{ ps}^{-1}\,, \tag{84}$$

$$\phi_s^{c\bar{c}s} = -0.030 \pm 0.033\,. \tag{85}$$

The above $\Delta\Gamma_s$ average is consistent, but highly correlated with the average of Eq. (65). Our final recommended average for $\Delta\Gamma_s$ is the one of Eq. (65), which includes all available information on $\Delta\Gamma_s$.

In the Standard Model and ignoring sub-leading penguin contributions, $\phi_s^{c\bar{c}s}$ is expected to be equal to $-2\beta_s$, where $\beta_s = \arg\left[-\left(V_{ts}V_{tb}^*\right)/\left(V_{cs}V_{cb}^*\right)\right]$ is a phase analogous to the angle β of the usual CKM unitarity triangle (aside from a sign change). An indirect determination via global fits to experimental data gives [182]

$$(\phi_s^{c\bar{c}s})^{\rm SM} = -2\beta_s = -0.0376^{+0.0008}_{-0.0007}\,. \tag{86}$$

The average value of $\phi_s^{c\bar{c}s}$ from Eq. (85) is consistent with this Standard Model expectation.

New physics could contribute to $\phi_s^{c\bar{c}s}$. Assuming that new physics only enters in M_{12} (rather than in Γ_{12}), one can write [104]

$$\phi_s^{c\bar{c}s} = -2\beta_s + \phi_{12}^{\rm NP}\,, \tag{87}$$

where the new physics phase $\phi_{12}^{\rm NP}$ is the same as that appearing in Eq. (81). In this case

$$\phi_{12} = \phi_{12}^{\rm SM} + 2\beta_s + \phi_s^{c\bar{c}s} = 0.013 \pm 0.033\,, \tag{88}$$

where the numerical estimation was performed with the values of Eqs. (80), (86), and (85). This can serve as a reference value to which the measurement of Eq. (83) can be compared.

4 Measurements related to Unitarity Triangle angles

The charge of the "$CP(t)$ and Unitarity Triangle angles" group is to provide averages of measurements from time-dependent asymmetry analyses, and other quantities that are related to the angles of the Unitarity Triangle (UT). In cases where considerable theoretical input is required to extract the fundamental quantities, no attempt to do so is made. However, straightforward interpretations of the averages are given, where possible.

In Sec. 4.1 a brief introduction to the relevant phenomenology is given. In Sec. 4.2 an attempt is made to clarify the various different notations in use. In Sec. 4.3 the common inputs to which experimental results are rescaled in the averaging procedure are listed. We also briefly introduce the treatment of experimental errors. In the remainder of this section, the experimental results and their averages are given, divided into subsections based on the underlying quark-level decays. All the measurements reported are quantities determined from decay-time-dependent analyses, with the exception of several in Sec. 4.14, which are related to the UT angle γ and are obtained from decay-time-integrated analyses. In the compilations of measurements, indications of the sizes of the data samples used by each experiment are given. For the e^+e^- B factory experiments, this is quoted in terms of the number of $B\overline{B}$ pairs in the data sample, while for hadron colliders the quantity given is the integrated luminosity.

4.1 Introduction

The Standard Model Cabibbo-Kobayashi-Maskawa (CKM) quark mixing matrix V must be unitary. The CKM matrix has four free parameters and these are conventionally written by the product of three (complex) rotation matrices [231], where the rotations are characterised by the Euler mixing angles between the generations, θ_{12}, θ_{13} and θ_{23}, and one overall phase δ,

$$V = \begin{pmatrix} V_{ud} & V_{us} & V_{ub} \\ V_{cd} & V_{cs} & V_{cb} \\ V_{td} & V_{ts} & V_{tb} \end{pmatrix} = \begin{pmatrix} c_{12}c_{13} & s_{12}c_{13} & s_{13}e^{-i\delta} \\ -s_{12}c_{23} - c_{12}s_{23}s_{13}e^{i\delta} & c_{12}c_{23} - s_{12}s_{23}s_{13}e^{i\delta} & s_{23}c_{13} \\ s_{12}s_{23} - c_{12}c_{23}s_{13}e^{i\delta} & -c_{12}s_{23} - s_{12}c_{23}s_{13}e^{i\delta} & c_{23}c_{13} \end{pmatrix} \quad (89)$$

where $c_{ij} = \cos\theta_{ij}$, $s_{ij} = \sin\theta_{ij}$ for $i < j = 1, 2, 3$.

Following the observation of a hierarchy between the different matrix elements, the Wolfenstein parametrisation [232] is an expansion of V in terms of the four real parameters λ (the expansion parameter), A, ρ and η. Defining to all orders in λ [233]

$$\begin{aligned} s_{12} &\equiv \lambda\,, \\ s_{23} &\equiv A\lambda^2\,, \\ s_{13}e^{-i\delta} &\equiv A\lambda^3(\rho - i\eta)\,, \end{aligned} \quad (90)$$

and inserting these into the representation of Eq. (89), unitarity of the CKM matrix is achieved to all orders. A Taylor expansion of V leads to the familiar approximation

$$V = \begin{pmatrix} 1 - \lambda^2/2 & \lambda & A\lambda^3(\rho - i\eta) \\ -\lambda & 1 - \lambda^2/2 & A\lambda^2 \\ A\lambda^3(1 - \rho - i\eta) & -A\lambda^2 & 1 \end{pmatrix} + \mathcal{O}\left(\lambda^4\right)\,. \quad (91)$$

At order λ^5, the obtained CKM matrix in this extended Wolfenstein parametrisation is:

$$V = \begin{pmatrix} 1 - \frac{1}{2}\lambda^2 - \frac{1}{8}\lambda^4 & \lambda & A\lambda^3(\rho - i\eta) \\ -\lambda + \frac{1}{2}A^2\lambda^5\left[1 - 2(\rho + i\eta)\right] & 1 - \frac{1}{2}\lambda^2 - \frac{1}{8}\lambda^4(1 + 4A^2) & A\lambda^2 \\ A\lambda^3\left[1 - (1 - \frac{1}{2}\lambda^2)(\rho + i\eta)\right] & -A\lambda^2 + \frac{1}{2}A\lambda^4\left[1 - 2(\rho + i\eta)\right] & 1 - \frac{1}{2}A^2\lambda^4 \end{pmatrix} + \mathcal{O}\left(\lambda^6\right)\,. \quad (92)$$

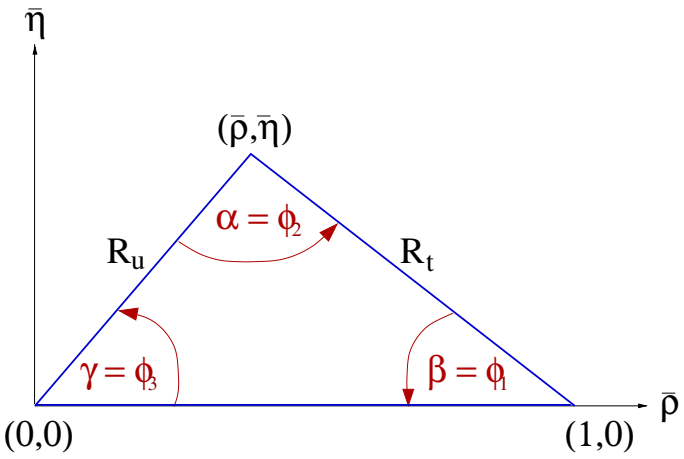

Figure 11: The Unitarity Triangle.

The non-zero imaginary part of the CKM matrix, which is the origin of *CP* violation in the Standard Model, is encapsulated in a non-zero value of η.

The unitarity relation $V^\dagger V = 1$ results in a total of nine expressions, that can be written as $\sum_{i=u,c,t} V_{ij}^* V_{ik} = \delta_{jk}$, where δ_{jk} is the Kronecker symbol. Of the off-diagonal expressions ($j \neq k$), three can be transformed into the other three leaving six relations, in which three complex numbers sum to zero, which therefore can be expressed as triangles in the complex plane. More details about unitarity triangles can be found in Refs. [234–239].

One of these relations,

$$V_{ud}V_{ub}^* + V_{cd}V_{cb}^* + V_{td}V_{tb}^* = 0\,, \tag{93}$$

is of particular importance to the B system, being specifically related to flavour changing neutral current $b \to d$ transitions. The three terms in Eq. (93) are of the same order, $\mathcal{O}(\lambda^3)$, and this relation is commonly known as the Unitarity Triangle. For presentational purposes, it is convenient to rescale the triangle by $(V_{cd}V_{cb}^*)^{-1}$, as shown in Fig. 11.

Two popular naming conventions for the UT angles exist in the literature:

$$\alpha \equiv \phi_2 = \arg\left[-\frac{V_{td}V_{tb}^*}{V_{ud}V_{ub}^*}\right], \quad \beta \equiv \phi_1 = \arg\left[-\frac{V_{cd}V_{cb}^*}{V_{td}V_{tb}^*}\right], \quad \gamma \equiv \phi_3 = \arg\left[-\frac{V_{ud}V_{ub}^*}{V_{cd}V_{cb}^*}\right]. \tag{94}$$

In this document the (α, β, γ) set is used. The sides R_u and R_t of the Unitarity Triangle (the third side being normalised to unity) are given by

$$R_u = \left|\frac{V_{ud}V_{ub}^*}{V_{cd}V_{cb}^*}\right| = \sqrt{\overline{\rho}^2 + \overline{\eta}^2}\,, \quad R_t = \left|\frac{V_{td}V_{tb}^*}{V_{cd}V_{cb}^*}\right| = \sqrt{(1-\overline{\rho})^2 + \overline{\eta}^2}\,. \tag{95}$$

where $\overline{\rho}$ and $\overline{\eta}$ define the apex of the Unitarity Triangle [233]

$$\overline{\rho} + i\overline{\eta} \equiv -\frac{V_{ud}V_{ub}^*}{V_{cd}V_{cb}^*} \equiv 1 + \frac{V_{td}V_{tb}^*}{V_{cd}V_{cb}^*} = \frac{\sqrt{1-\lambda^2}\,(\rho + i\eta)}{\sqrt{1 - A^2\lambda^4} + \sqrt{1-\lambda^2}A^2\lambda^4(\rho + i\eta)}\,. \tag{96}$$

The exact relation between (ρ, η) and $(\overline{\rho}, \overline{\eta})$ is

$$\rho + i\eta \;=\; \frac{\sqrt{1 - A^2\lambda^4}(\overline{\rho} + i\overline{\eta})}{\sqrt{1-\lambda^2}\,[1 - A^2\lambda^4(\overline{\rho} + i\overline{\eta})]}\,. \tag{97}$$

By expanding in powers of λ, several useful approximate expressions can be obtained, including

$$\overline{\rho} = \rho(1 - \frac{1}{2}\lambda^2) + \mathcal{O}(\lambda^4)\,, \quad \overline{\eta} = \eta(1 - \frac{1}{2}\lambda^2) + \mathcal{O}(\lambda^4)\,, \quad V_{td} = A\lambda^3(1 - \overline{\rho} - i\overline{\eta}) + \mathcal{O}(\lambda^6)\,. \tag{98}$$

Recent world average values for the Wolfenstein parameters, evaluated using many of the measurements reported in this document, are [240]

$$A = 0.8227\,^{+0.0066}_{-0.0136}\,, \quad \lambda = 0.22543\,^{+0.00042}_{-0.00031}\,, \quad \overline{\rho} = 0.1504\,^{+0.0121}_{-0.0062}\,, \quad \overline{\eta} = 0.3540\,^{+0.0069}_{-0.0076}\,. \tag{99}$$

The relevant unitarity triangle for the $b \to s$ transition is obtained by replacing $d \leftrightarrow s$ in Eq. (93). Definitions of the set of angles $(\alpha_s, \beta_s, \gamma_s)$ can be obtained using equivalent relations to those of Eq. (94). However, this gives a value of β_s that is negative in the Standard Model, so that the sign is usually flipped in the literature; this convention, *i.e.* $\beta_s = \arg\left[-(V_{ts}V_{tb}^*)/(V_{cs}V_{cb}^*)\right]$, is also followed here and in Sec. 3. Since the sides of the $b \to s$ Unitarity Triangle are not all of the same order of λ, the triangle is squashed and $\beta_s \sim \lambda^2\eta$.

4.2 Notations

Several different notations for *CP* violation parameters are commonly used. This section reviews those found in the experimental literature, in the hope of reducing the potential for confusion, and to define the frame that is used for the averages.

In some cases, when B mesons decay into multibody final states via broad resonances (ρ, K^*, *etc.*), the experimental analyses ignore the effects of interference between the overlapping structures. This is referred to as the quasi-two-body (Q2B) approximation in the following.

4.2.1 *CP* asymmetries

The *CP* asymmetry is defined as the difference between the rate involving a b quark and that involving a $\overline{b}$ quark, divided by the sum. For example, the partial rate (or charge) asymmetry for a charged B decay would be given as

$$\mathcal{A}_f \;\equiv\; \frac{\Gamma(B^- \to f) - \Gamma(B^+ \to \overline{f})}{\Gamma(B^- \to f) + \Gamma(B^+ \to \overline{f})}. \tag{100}$$

4.2.2 Time-dependent *CP* asymmetries in decays to *CP* eigenstates

If the amplitudes for B^0 and $\overline{B}^0$ to decay to a final state f, which is a *CP* eigenstate with eigenvalue η_f, are given by A_f and $\overline{A}_f$, respectively, then the decay distributions for neutral B mesons, with known flavour at time $\Delta t = 0$, are given by

$$\Gamma_{\overline{B}^0 \to f}(\Delta t) \;=\; \frac{e^{-|\Delta t|/\tau(B^0)}}{4\tau(B^0)}\left[1 + \frac{2\,\mathrm{Im}(\lambda_f)}{1+|\lambda_f|^2}\sin(\Delta m \Delta t) - \frac{1-|\lambda_f|^2}{1+|\lambda_f|^2}\cos(\Delta m \Delta t)\right], \tag{101}$$

$$\Gamma_{B^0 \to f}(\Delta t) \;=\; \frac{e^{-|\Delta t|/\tau(B^0)}}{4\tau(B^0)}\left[1 - \frac{2\,\mathrm{Im}(\lambda_f)}{1+|\lambda_f|^2}\sin(\Delta m \Delta t) + \frac{1-|\lambda_f|^2}{1+|\lambda_f|^2}\cos(\Delta m \Delta t)\right]. \tag{102}$$

Here $\lambda_f = \frac{q}{p}\frac{\bar{A}_f}{A_f}$ contains terms related to B^0–$\overline{B}^0$ mixing and to the decay amplitude (the eigenstates of the effective Hamiltonian in the $B^0\overline{B}^0$ system are $|B_\pm\rangle = p\,|B^0\rangle \pm q\,|\overline{B}^0\rangle$). This

formulation assumes *CPT* invariance, and neglects possible lifetime differences (between the eigenstates of the effective Hamiltonian; see Sec. 3.3 where the mass difference Δm is also defined) in the neutral B meson system. The case where non-zero lifetime differences are taken into account is discussed in Sec. 4.2.3. Note that the notation and normalisation used here is that which is relevant for the e^+e^- B factory experiments. At hadron collider experiments, the flavour tagging is done at production ($\Delta t = t = 0$), and therefore t is usually used in place of Δt. Moreover, since negative values of t are not possible, the normalisation is such that $\int_0^{+\infty} \left(\Gamma_{\overline{B}^0\to f}(t) + \Gamma_{B^0\to f}(t)\right) dt = 1$, rather than $\int_{-\infty}^{+\infty} \left(\Gamma_{\overline{B}^0\to f}(\Delta t) + \Gamma_{B^0\to f}(\Delta t)\right) d(\Delta t) = 1$, as in Eqs. (101) and (102).

The time-dependent *CP* asymmetry, again defined as the difference between the rate involving a b quark and that involving a $\overline{b}$ quark, is then given by

$$\mathcal{A}_f\,(\Delta t) \;\equiv\; \frac{\Gamma_{\overline{B}^0\to f}(\Delta t) - \Gamma_{B^0\to f}(\Delta t)}{\Gamma_{\overline{B}^0\to f}(\Delta t) + \Gamma_{B^0\to f}(\Delta t)} \;=\; \frac{2\,\mathrm{Im}(\lambda_f)}{1+|\lambda_f|^2}\sin(\Delta m\Delta t) - \frac{1-|\lambda_f|^2}{1+|\lambda_f|^2}\cos(\Delta m\Delta t). \quad (103)$$

While the coefficient of the $\sin(\Delta m\Delta t)$ term in Eq. (103) is everywhere[31] denoted S_f:

$$S_f \;\equiv\; \frac{2\,\mathrm{Im}(\lambda_f)}{1+|\lambda_f|^2}, \quad (104)$$

different notations are in use for the coefficient of the $\cos(\Delta m\Delta t)$ term:

$$C_f \;\equiv\; -A_f \;\equiv\; \frac{1-|\lambda_f|^2}{1+|\lambda_f|^2}. \quad (105)$$

The C notation has been used by the *BABAR* collaboration (see *e.g.* Ref. [241]), and is also adopted in this document. The A notation has been used by the Belle collaboration (see *e.g.* Ref. [242]). When the final state is a *CP* eigenstate, the notation S_{CP} and C_{CP} is widely used.

Neglecting effects due to *CP* violation in mixing (by taking $|q/p| = 1$), if the decay amplitude contains terms with a single weak (*i.e. CP* violating) phase then $|\lambda_f| = 1$ and one finds $S_f = -\eta_f \sin(\phi_{\rm mix} + \phi_{\rm dec})$, $C_f = 0$, where $\phi_{\rm mix} = \arg(q/p)$ and $\phi_{\rm dec} = \arg(\overline{A}_f/A_f)$. Note that the B^0–$\overline{B}^0$ mixing phase $\phi_{\rm mix} \approx 2\beta$ in the Standard Model (in the usual phase convention) [243,244].

If amplitudes with different weak phases contribute to the decay, no clean interpretation of S_f is possible without further input. If the decay amplitudes have in addition different *CP* conserving strong phases, then $|\lambda_f| \neq 1$ and additional input is required for interpretation. The coefficient of the cosine term becomes non-zero, indicating *CP* violation in decay.

Due to the fact that $\sin(\Delta m\Delta t)$ and $\cos(\Delta m\Delta t)$ are respectively odd and even functions of Δt, only small correlations (that can be induced by backgrounds, for example) between S_f and C_f are expected at an e^+e^- B factory experiment, where the range of Δt is $-\infty < \Delta t < +\infty$. The situation is different for measurements at hadron collider experiments, where the range of the time variable is $0 < t < +\infty$, so that more sizable correlations can be expected. We include the correlations in the averages where available.

Frequently, we are interested in combining measurements governed by similar or identical short-distance physics, but with different final states (*e.g.*, $B^0 \to J/\psi\, K^0_S$ and $B^0 \to J/\psi\, K^0_L$). In this case, we remove the dependence on the *CP* eigenvalue of the final state by quoting $-\eta S_f$. In cases where the final state is not a *CP* eigenstate but has an effective *CP* content (see below), the reported $-\eta S$ is corrected by the effective *CP*.

[31] Occasionally one also finds Eq. (103) written as $\mathcal{A}_f\,(\Delta t) = \mathcal{A}_f^{\rm mix}\sin(\Delta m\Delta t) + \mathcal{A}_f^{\rm dir}\cos(\Delta m\Delta t)$, or similar.

4.2.3 Time-dependent distributions with non-zero decay width difference

A complete analysis of the time-dependent decay rates of neutral B mesons must also take into account the lifetime difference between the eigenstates of the effective Hamiltonian, denoted by $\Delta\Gamma$. This is particularly important in the B_s^0 system, since a non-negligible value of $\Delta\Gamma_s$ has been established (see Sec. 3.3 for the latest experimental constraints). Neglecting *CP* violation in mixing, the relevant replacements for Eqs. (101) and (102) are [245]

$$\begin{aligned}\Gamma_{\overline{B}{}_s^0\to f}(\Delta t) = \mathcal{N}\frac{e^{-|\Delta t|/\tau(B_s^0)}}{4\tau(B_s^0)}\Big[\cosh(\tfrac{\Delta\Gamma\Delta t}{2})+ \\ \tfrac{2\,\mathrm{Im}(\lambda_f)}{1+|\lambda_f|^2}\sin(\Delta m\Delta t) - \tfrac{1-|\lambda_f|^2}{1+|\lambda_f|^2}\cos(\Delta m\Delta t) - \tfrac{2\,\mathrm{Re}(\lambda_f)}{1+|\lambda_f|^2}\sinh(\tfrac{\Delta\Gamma\Delta t}{2})\Big],\end{aligned} \tag{106}$$

and

$$\begin{aligned}\Gamma_{B_s^0\to f}(\Delta t) = \mathcal{N}\frac{e^{-|\Delta t|/\tau(B_s^0)}}{4\tau(B_s^0)}\Big[\cosh(\tfrac{\Delta\Gamma\Delta t}{2})- \\ \tfrac{2\,\mathrm{Im}(\lambda_f)}{1+|\lambda_f|^2}\sin(\Delta m\Delta t) + \tfrac{1-|\lambda_f|^2}{1+|\lambda_f|^2}\cos(\Delta m\Delta t) - \tfrac{2\,\mathrm{Re}(\lambda_f)}{1+|\lambda_f|^2}\sinh(\tfrac{\Delta\Gamma\Delta t}{2})\Big].\end{aligned} \tag{107}$$

To be consistent with our earlier notation,[32] we write here the coefficient of the sinh term as

$$A_f^{\Delta\Gamma} = -\frac{2\,\mathrm{Re}(\lambda_f)}{1+|\lambda_f|^2}\,. \tag{108}$$

A time-dependent analysis of *CP* asymmetries in flavour-tagged B_s^0 decays to a *CP* eigenstate f can thus obtain the parameters S_f, C_f and $A_f^{\Delta\Gamma}$. Note that, by definition,

$$(S_f)^2 + (C_f)^2 + \left(A_f^{\Delta\Gamma}\right)^2 = 1\,, \tag{109}$$

and this constraint can be imposed or not in the fits. Since these parameters have sensitivity to both $\mathrm{Im}(\lambda_f)$ and $\mathrm{Re}(\lambda_f)$, alternative choices of parametrisation, including those directly involving *CP* violating phases (such as β_s), are possible. These can also be adopted for vector-vector final states.

The *untagged* time-dependent decay rate is given by

$$\Gamma_{\overline{B}{}_s^0\to f}(\Delta t) + \Gamma_{B_s^0\to f}(\Delta t) = \mathcal{N}\frac{e^{-|\Delta t|/\tau(B_s^0)}}{2\tau(B_s^0)}\Big[\cosh\left(\frac{\Delta\Gamma\Delta t}{2}\right) + A_f^{\Delta\Gamma}\sinh\left(\frac{\Delta\Gamma\Delta t}{2}\right)\Big]\,. \tag{110}$$

With the requirement $\int_{-\infty}^{+\infty}\left\{\Gamma_{\overline{B}{}_s^0\to f}(\Delta t) + \Gamma_{B_s^0\to f}(\Delta t)\right\}d(\Delta t) = 1$, the normalisation factor $\mathcal{N}$ is fixed to $1-(\frac{\Delta\Gamma}{2\Gamma})^2$. Note that an untagged time-dependent analysis can probe λ_f, through the dependence of $A_f^{\Delta\Gamma}$ on $\mathrm{Re}(\lambda_f)$, when $\Delta\Gamma \neq 0$. This is equivalent to determining the "*effective lifetime*" [107], as discussed in Sec. 3.2.4. The tagged analysis is, of course, more sensitive. Other expressions can be similarly modified to take into account non-zero lifetime differences.

4.2.4 Time-dependent *CP* asymmetries in decays to vector-vector final states

Consider B decays to states consisting of two spin-1 particles, such as $J/\psi K^{*0}(\to K_S^0\pi^0)$, $J/\psi\,\phi$, $D^{*+}D^{*-}$ and $\rho^+\rho^-$, which are eigenstates of charge conjugation but not of parity.[33] In

[32] As ever, alternative and conflicting notations appear in the literature. One popular alternative notation for this parameter is $\mathcal{A}_{\Delta\Gamma}$. Particular care must be taken over the signs.

[33] This is not true of all vector-vector final states, *e.g.*, $D^{*\pm}\rho^{\mp}$ is clearly not an eigenstate of charge conjugation.

fact, for such a system, there are three possible final states; in the helicity basis these can be written h_{-1}, h_0, h_{+1}. The h_0 state is an eigenstate of parity, and hence of *CP*; however, *CP* transforms $h_{+1} \leftrightarrow h_{-1}$ (up to an unobservable phase). In the transversity basis, these states are transformed into $h_\parallel = (h_{+1} + h_{-1})/2$ and $h_\perp = (h_{+1} - h_{-1})/2$. In this basis all three states are *CP* eigenstates, and $h_\perp$ has the opposite *CP* to the others.

The amplitudes to these states are usually given by $A_{0,\perp,\parallel}$, with normalisation such that $|A_0|^2 + |A_\perp|^2 + |A_\parallel|^2 = 1$. Then the effective *CP* of the vector-vector state is known if $|A_\perp|^2$ is measured. An alternative strategy is to measure just the longitudinally polarised component, $|A_0|^2$ (sometimes denoted by $f_{\rm long}$), which allows a limit to be set on the effective *CP* since $|A_\perp|^2 \leq |A_\perp|^2 + |A_\parallel|^2 = 1 - |A_0|^2$. The most complete treatment for neutral B decays to vector-vector final states is time-dependent angular analysis (also known as time-dependent transversity analysis). In such an analysis, interference between *CP*-even and *CP*-odd states provides additional sensitivity to the weak and strong phases involved. When non-negligible, the finite widths of the decaying vector particles should also be taken into account.

In most analyses of time-dependent *CP* asymmetries in decays to vector-vector final states carried out to date, an assumption has been made that each helicity (or transversity) amplitude has the same weak phase. This is a good approximation for decays that are dominated by amplitudes with a single weak phase, such $B^0 \to J/\psi K^{*0}$, and is a reasonable approximation in any mode for which only very limited statistics are available. However, for modes that have contributions from amplitudes with different weak phases, the relative size of these contributions can be different for each helicity (or transversity) amplitude, and therefore the time-dependent *CP* asymmetry parameters can also differ. The most generic analysis, suitable for modes with sufficient statistics, allows for this effect; such an analysis has been carried out by LHCb for the $B^0 \to J/\psi \rho^0$ decay [246]. An intermediate analysis can allow different parameters for the *CP*-even and *CP*-odd components; such an analysis has been carried out by *BABAR* for the decay $B^0 \to D^{*+}D^{*-}$ [247]. The independent treatment of each helicity (or transversity) amplitude, as in the latest result on $B_s^0 \to J/\psi \phi$ [191] (discussed in Sec. 3), becomes increasingly important for high precision measurements.

4.2.5 Time-dependent asymmetries: self-conjugate multiparticle final states

Amplitudes for neutral B decays into self-conjugate multiparticle final states such as $\pi^+\pi^-\pi^0$, $K^+K^-K_S^0$, $\pi^+\pi^-K_S^0$, $J/\psi\,\pi^+\pi^-$ or $D\pi^0$ with $D \to K_S^0\pi^+\pi^-$ may be written in terms of *CP*-even and *CP*-odd amplitudes. As above, the interference between these terms provides additional sensitivity to the weak and strong phases involved in the decay, and the time-dependence depends on both the sine and cosine of the weak phase difference. In order to perform unbinned maximum likelihood fits, and thereby extract as much information as possible from the distributions, it is necessary to select a model for the multiparticle decay, and therefore the results acquire some model dependence. In certain cases, model-independent methods are also possible, but the binning of the Dalitz plot that is required leads to some loss of statistical precision. The number of observables depends on the final state (and on the model used); the key feature is that as long as there are regions where both *CP*-even and *CP*-odd amplitudes contribute, the interference terms will be sensitive to the cosine of the weak phase difference. Therefore, these measurements allow distinction between multiple solutions for, *e.g.*, the two values of 2β from the measurement of $\sin(2\beta)$.

We now consider the various notations which have been used in experimental studies of

time-dependent asymmetries in decays to self-conjugate multiparticle final states.

$B^0 \to D^{(*)}h^0$ with $D \to K^0_S\pi^+\pi^-$

The states $D\pi^0$, $D^*\pi^0$, $D\eta$, $D^*\eta$, $D\omega$ are collectively denoted $D^{(*)}h^0$. When the D decay model is fixed, fits to the time-dependent decay distributions can be performed to extract the weak phase difference. However, it is experimentally advantageous to use the sine and cosine of this phase as fit parameters, since these behave as essentially independent parameters, with low correlations and (potentially) rather different uncertainties. A parameter representing *CP* violation in the B decay can also be floated. For consistency with other analyses, this could be chosen to be C_f, but could equally well be $|\lambda_f|$, or other possibilities.

Belle performed an analysis of these channels with $\sin(2\phi_1)$ and $\cos(2\phi_1)$ as free parameters [248]. *BABAR* has performed an analysis floating also $|\lambda_f|$ [249] (and, of course, replacing ϕ_1 with β).

Belle have in addition performed a model-independent analysis [250], using as input information about the average strong phase difference between symmetric bins of the Dalitz plot determined by CLEO-c [251].[34] The results of this analysis are measurements of $\sin(2\phi_1)$ and $\cos(2\phi_1)$.

$B^0 \to D^{*+}D^{*-}K^0_S$

The hadronic structure of the $B^0 \to D^{*+}D^{*-}K^0_S$ decay is not sufficiently well understood to perform a full time-dependent Dalitz plot analysis. Instead, following Ref. [252], *BABAR* [253] and Belle [254] divide the Dalitz plane in two: $m(D^{*+}K^0_S)^2 > m(D^{*-}K^0_S)^2$ ($\eta_y = +1$) and $m(D^{*+}K^0_S)^2 < m(D^{*-}K^0_S)^2$ ($\eta_y = -1$); and then fit to a decay time distribution with asymmetry given by

$$\mathcal{A}_f\,(\Delta t) = \eta_y \frac{J_c}{J_0}\cos(\Delta m \Delta t) - \left[\frac{2J_{s1}}{J_0}\sin(2\beta) + \eta_y \frac{2J_{s2}}{J_0}\cos(2\beta)\right]\sin(\Delta m \Delta t)\,. \tag{111}$$

The measured values are $\frac{J_c}{J_0}$, $\frac{2J_{s1}}{J_0}\sin(2\beta)$ and $\frac{2J_{s2}}{J_0}\cos(2\beta)$, where the parameters J_0, J_c, J_{s1} and J_{s2} are the integrals over the half Dalitz plane $m(D^{*+}K^0_S)^2 < m(D^{*-}K^0_S)^2$ of the functions $|a|^2+|\overline{a}|^2$, $|a|^2-|\overline{a}|^2$, $\mathrm{Re}(\overline{a}a^*)$ and $\mathrm{Im}(\overline{a}a^*)$ respectively, where a and $\overline{a}$ are the decay amplitudes of $B^0 \to D^{*+}D^{*-}K^0_S$ and $\overline{B}^0 \to D^{*+}D^{*-}K^0_S$ respectively. The parameter J_{s2} (and hence J_{s2}/J_0) is predicted to be positive; assuming this prediction to be correct, it is possible to determine the sign of $\cos(2\beta)$.

$B^0 \to J/\psi\,\pi^+\pi^-$

Amplitude analyses of $B^0 \to J/\psi\,\pi^+\pi^-$ decays [246, 255] show large contributions from the $\rho(770)^0$ and $f_0(500)$ states, together with smaller contributions from higher resonances. Since modelling the $f_0(500)$ structure is challenging [256], it is difficult to determine reliably its associated *CP* violation parameters. Corresponding parameters for the $J/\psi\,\rho^0$ decay can, however, be determined. In the LHCb analysis [246], $2\beta^{\rm eff}$ is determined from the fit; results are then converted into values for S_{CP} and C_{CP} to allow comparison with other modes. Here, the notation S_{CP} and C_{CP} denotes parameters obtained for the $J/\psi\,\rho^0$ final state accounting

[34] The external input needed for this analysis is the same as in the model-independent analysis of $B^+ \to DK^+$ with $D \to K^0_S\pi^+\pi^-$, discussed in Sec. 4.14.5.

for the composition of *CP*-even and *CP*-odd amplitudes (while assuming that all amplitudes involve the same phases), so that no dilution occurs. Possible *CP* violation effects in the other amplitudes contributing to the Dalitz plot are treated as a source of systematic uncertainty.

Amplitude analyses have also been done for the $B^0_s \to J/\psi\pi^+\pi^-$ decay, where the final state is dominated by scalar resonances including the $f_0(980)$ [228,229]. Time-dependent analyses of this B^0_s decay allow a determination of $2\beta_s$, as discussed in Sec. 3.

$B^0 \to K^+K^-K^0$

Studies of $B^0 \to K^+K^-K^0$ [257–259] and of the related decay $B^+ \to K^+K^-K^+$ [259–261], show that the decay is dominated by a large nonresonant contribution with significant components from the intermediate K^+K^- resonances $\phi(1020)$, $f_0(980)$, and other higher resonances, as well a contribution from χ_{c0}.

The full time-dependent Dalitz plot analysis allows the complex amplitudes of each contributing term to be determined from data, including *CP* violation effects (*i.e.* allowing the complex amplitude for the B^0 decay to be independent from that for $\overline{B}^0$ decay), although one amplitude must be fixed to give a reference point. There are several choices for parametrisation of the complex amplitudes (*e.g.* real and imaginary part, or magnitude and phase). Similarly, there are various approaches to include *CP* violation effects. Note that positive definite parameters such as magnitudes are disfavoured in certain circumstances (they inevitably lead to biases for small values). In order to compare results between analyses, it is useful for each experiment to present results in terms of the parameters that can be measured in a Q2B analysis (such as $\mathcal{A}_f$, S_f, C_f, $\sin(2\beta^{\rm eff})$, $\cos(2\beta^{\rm eff})$, *etc.*)

In the *BABAR* analysis of $B^0 \to K^+K^-K^0$ [259], the complex amplitude for each resonant contribution is written as

$$A_f = c_f(1+b_f)e^{i(\phi_f+\delta_f)}\,, \qquad \overline{A}_f = c_f(1-b_f)e^{i(\phi_f-\delta_f)}\,, \tag{112}$$

where b_f and δ_f introduce *CP* violation in the magnitude and phase respectively. Belle [258] use the same parametrisation but with a different notation for the parameters.[35] [The weak phase in B^0–$\overline{B}^0$ mixing (2β) also appears in the full formula for the time-dependent decay distribution.] The Q2B parameter of *CP* violation in decay is directly related to b_f

$$\mathcal{A}_f = \frac{-2b_f}{1+b_f^2} \approx C_f\,, \tag{113}$$

and the mixing-induced *CP* violation parameter can be used to obtain $\sin(2\beta^{\rm eff})$

$$-\eta_f S_f \approx \frac{1-b_f^2}{1+b_f^2}\sin(2\beta_f^{\rm eff})\,, \tag{114}$$

where the approximations are exact in the case that $|q/p| = 1$.

Both *BABAR* [259] and Belle [258] present results for c_f and ϕ_f, for each resonant contribution, and in addition present results for $\mathcal{A}_f$ and $\beta_f^{\rm eff}$ for $\phi(1020)K^0$, $f_0(980)K^0$ and for the remainder of the contributions to the $K^+K^-K^0$ Dalitz plot combined. *BABAR* also present results for the Q2B parameter S_f for these channels. The models used to describe the resonant

[35] $(c, b, \phi, \delta) \leftrightarrow (a, c, b, d)$. See Eq. (116).

structure of the Dalitz plot differ, however. Both analyses suffer from multiple solutions, from which we select only one for averaging.

$B^0 \to \pi^+\pi^- K^0_S$

Studies of $B^0 \to \pi^+\pi^- K^0_S$ [262, 263] and of the related decay $B^+ \to \pi^+\pi^- K^+$ [260, 264–266] show that the decay is dominated by components from intermediate resonances in the $K\pi$ ($K^*(892)$, $K^*_0(1430)$) and $\pi\pi$ ($\rho(770)$, $f_0(980)$, $f_2(1270)$) spectra, together with a poorly understood scalar structure that peaks near $m(\pi\pi) \sim 1300$ MeV/c^2 and is denoted $f_X(1300)$ (that could be identified as either the $f_0(1370)$ or $f_0(1500)$), and a large nonresonant component. There is also a contribution from the χ_{c0} state.

The full time-dependent Dalitz plot analysis allows the complex amplitudes of each contributing term to be determined from data, including *CP* violation effects. In the *BABAR* analysis [262], the magnitude and phase of each component (for both B^0 and $\overline{B}^0$ decays) are measured relative to $B^0 \to f_0(980)K^0_S$, using the following parametrisation

$$A_f = |A_f|\, e^{i\arg(A_f)} \ , \quad \overline{A}_f = \left|\overline{A}_f\right| e^{i\arg(\overline{A}_f)} \, . \tag{115}$$

In the Belle analysis [263], the $B^0 \to K^{*+}\pi^-$ amplitude is chosen as the reference, and the amplitudes are parametrised as

$$A_f = a_f(1+c_f)e^{i(b_f+d_f)} \ , \quad \overline{A}_f = a_f(1-c_f)e^{i(b_f-d_f)} \, . \tag{116}$$

In both cases, the results are translated into Q2B parameters such as $2\beta^{\rm eff}_f$, S_f, C_f for each *CP* eigenstate f, and parameters of *CP* violation in decay for each flavour-specific state. Relative phase differences between resonant terms are also extracted.

$B^0 \to \pi^+\pi^-\pi^0$

The $B^0 \to \pi^+\pi^-\pi^0$ decay is dominated by intermediate ρ resonances. Though it is possible, as above, to determine directly the complex amplitudes for each component, an alternative approach [267,268] has been used by both *BABAR* [269,270] and Belle [271,272]. The amplitudes for B^0 and $\overline{B}^0$ decays to $\pi^+\pi^-\pi^0$ are written

$$A_{3\pi} = f_+A_+ + f_-A_- + f_0A_0 \ , \quad \overline{A}_{3\pi} = f_+\overline{A}_+ + f_-\overline{A}_- + f_0\overline{A}_0 \tag{117}$$

respectively. The symbols A_+, A_- and A_0 represent the complex decay amplitudes for $B^0 \to \rho^+\pi^-$, $B^0 \to \rho^-\pi^+$ and $B^0 \to \rho^0\pi^0$ while $\overline{A}_+$, $\overline{A}_-$ and $\overline{A}_0$ represent those for $\overline{B}^0 \to \rho^+\pi^-$, $\overline{B}^0 \to \rho^-\pi^+$ and $\overline{B}^0 \to \rho^0\pi^0$ respectively. The terms f_+, f_- and f_0 incorporate kinematic and dynamical factors and depend on the Dalitz plot coordinates. The full time-dependent decay distribution can then be written in terms of 27 free parameters, one for each coefficient of the form factor bilinears, as listed in Table 22. These parameters are sometimes referred to as "the Us and Is", and can be expressed in terms of A_+, A_-, A_0, $\overline{A}_+$, $\overline{A}_-$ and $\overline{A}_0$. If the full set of parameters is determined, together with their correlations, other parameters, such as weak and strong phases, parameters of *CP* violation in decay, *etc.*, can be subsequently extracted. Note that one of the parameters (typically U^+_+) is often fixed to unity to provide a reference point; this does not affect the analysis.

Table 22: Definitions of the U and I coefficients. Modified from Ref. [269].

Parameter	Description
U_+^+	Coefficient of $\lvert f_+\rvert^2$
U_0^+	Coefficient of $\lvert f_0\rvert^2$
U_-^+	Coefficient of $\lvert f_-\rvert^2$
U_0^-	Coefficient of $\lvert f_0\rvert^2 \cos(\Delta m \Delta t)$
U_-^-	Coefficient of $\lvert f_-\rvert^2 \cos(\Delta m \Delta t)$
U_+^-	Coefficient of $\lvert f_+\rvert^2 \cos(\Delta m \Delta t)$
I_0	Coefficient of $\lvert f_0\rvert^2 \sin(\Delta m \Delta t)$
I_-	Coefficient of $\lvert f_-\rvert^2 \sin(\Delta m \Delta t)$
I_+	Coefficient of $\lvert f_+\rvert^2 \sin(\Delta m \Delta t)$
$U_{+-}^{+,\mathrm{Im}}$	Coefficient of $\mathrm{Im}[f_+ f_-^*]$
$U_{+-}^{+,\mathrm{Re}}$	Coefficient of $\mathrm{Re}[f_+ f_-^*]$
$U_{+-}^{-,\mathrm{Im}}$	Coefficient of $\mathrm{Im}[f_+ f_-^*] \cos(\Delta m \Delta t)$
$U_{+-}^{-,\mathrm{Re}}$	Coefficient of $\mathrm{Re}[f_+ f_-^*] \cos(\Delta m \Delta t)$
I_{+-}^{Im}	Coefficient of $\mathrm{Im}[f_+ f_-^*] \sin(\Delta m \Delta t)$
I_{+-}^{Re}	Coefficient of $\mathrm{Re}[f_+ f_-^*] \sin(\Delta m \Delta t)$
$U_{+0}^{+,\mathrm{Im}}$	Coefficient of $\mathrm{Im}[f_+ f_0^*]$
$U_{+0}^{+,\mathrm{Re}}$	Coefficient of $\mathrm{Re}[f_+ f_0^*]$
$U_{+0}^{-,\mathrm{Im}}$	Coefficient of $\mathrm{Im}[f_+ f_0^*] \cos(\Delta m \Delta t)$
$U_{+0}^{-,\mathrm{Re}}$	Coefficient of $\mathrm{Re}[f_+ f_0^*] \cos(\Delta m \Delta t)$
I_{+0}^{Im}	Coefficient of $\mathrm{Im}[f_+ f_0^*] \sin(\Delta m \Delta t)$
I_{+0}^{Re}	Coefficient of $\mathrm{Re}[f_+ f_0^*] \sin(\Delta m \Delta t)$
$U_{-0}^{+,\mathrm{Im}}$	Coefficient of $\mathrm{Im}[f_- f_0^*]$
$U_{-0}^{+,\mathrm{Re}}$	Coefficient of $\mathrm{Re}[f_- f_0^*]$
$U_{-0}^{-,\mathrm{Im}}$	Coefficient of $\mathrm{Im}[f_- f_0^*] \cos(\Delta m \Delta t)$
$U_{-0}^{-,\mathrm{Re}}$	Coefficient of $\mathrm{Re}[f_- f_0^*] \cos(\Delta m \Delta t)$
I_{-0}^{Im}	Coefficient of $\mathrm{Im}[f_- f_0^*] \sin(\Delta m \Delta t)$
I_{-0}^{Re}	Coefficient of $\mathrm{Re}[f_- f_0^*] \sin(\Delta m \Delta t)$

4.2.6 Time-dependent *CP* asymmetries in decays to non-*CP* eigenstates

Consider a non-*CP* eigenstate f, and its conjugate $\overline{f}$. For neutral B decays to these final states, there are four amplitudes to consider: those for B^0 to decay to f and $\overline{f}$ (A_f and $A_{\overline{f}}$, respectively), and the equivalents for $\overline{B}^0$ ($\overline{A}_f$ and $\overline{A}_{\overline{f}}$). If *CP* is conserved in the decay, then $A_f = \overline{A}_{\overline{f}}$ and $A_{\overline{f}} = \overline{A}_f$.

The time-dependent decay distributions can be written in many different ways. Here, we follow Sec. 4.2.2 and define $\lambda_f = \frac{q}{p}\frac{\overline{A}_f}{A_f}$ and $\lambda_{\overline{f}} = \frac{q}{p}\frac{\overline{A}_{\overline{f}}}{A_{\overline{f}}}$. The time-dependent *CP* asymmetries

that are sensitive to mixing-induced *CP* violation effects then follow Eq. (103):

$$\mathcal{A}_f(\Delta t) \equiv \frac{\Gamma_{\overline{B}^0\to f}(\Delta t) - \Gamma_{B^0\to f}(\Delta t)}{\Gamma_{\overline{B}^0\to f}(\Delta t) + \Gamma_{B^0\to f}(\Delta t)} = S_f \sin(\Delta m \Delta t) - C_f \cos(\Delta m \Delta t), \tag{118}$$

$$\mathcal{A}_{\overline{f}}(\Delta t) \equiv \frac{\Gamma_{\overline{B}^0\to \overline{f}}(\Delta t) - \Gamma_{B^0\to \overline{f}}(\Delta t)}{\Gamma_{\overline{B}^0\to \overline{f}}(\Delta t) + \Gamma_{B^0\to \overline{f}}(\Delta t)} = S_{\overline{f}} \sin(\Delta m \Delta t) - C_{\overline{f}} \cos(\Delta m \Delta t), \tag{119}$$

with the definitions of the parameters C_f, S_f, $C_{\overline{f}}$ and $S_{\overline{f}}$, following Eqs. (104) and (105).

The time-dependent decay rates are given by

$$\Gamma_{\overline{B}^0\to f}(\Delta t) = \frac{e^{-|\Delta t|/\tau(B^0)}}{8\tau(B^0)}(1 + \langle \mathcal{A}_{f\overline{f}} \rangle) \left\{1 + S_f \sin(\Delta m \Delta t) - C_f \cos(\Delta m \Delta t)\right\}, \tag{120}$$

$$\Gamma_{B^0\to f}(\Delta t) = \frac{e^{-|\Delta t|/\tau(B^0)}}{8\tau(B^0)}(1 + \langle \mathcal{A}_{f\overline{f}} \rangle) \left\{1 - S_f \sin(\Delta m \Delta t) + C_f \cos(\Delta m \Delta t)\right\}, \tag{121}$$

$$\Gamma_{\overline{B}^0\to \overline{f}}(\Delta t) = \frac{e^{-|\Delta t|/\tau(B^0)}}{8\tau(B^0)}(1 - \langle \mathcal{A}_{f\overline{f}} \rangle) \left\{1 + S_{\overline{f}} \sin(\Delta m \Delta t) - C_{\overline{f}} \cos(\Delta m \Delta t)\right\}, \tag{122}$$

$$\Gamma_{B^0\to \overline{f}}(\Delta t) = \frac{e^{-|\Delta t|/\tau(B^0)}}{8\tau(B^0)}(1 - \langle \mathcal{A}_{f\overline{f}} \rangle) \left\{1 - S_{\overline{f}} \sin(\Delta m \Delta t) + C_{\overline{f}} \cos(\Delta m \Delta t)\right\}, \tag{123}$$

where the time-independent parameter $\langle \mathcal{A}_{f\overline{f}} \rangle$ represents an overall asymmetry in the production of the f and $\overline{f}$ final states,[36]

$$\langle \mathcal{A}_{f\overline{f}} \rangle = \frac{\left(|A_f|^2 + \left|\overline{A}_f\right|^2\right) - \left(\left|A_{\overline{f}}\right|^2 + \left|\overline{A}_{\overline{f}}\right|^2\right)}{\left(|A_f|^2 + \left|\overline{A}_f\right|^2\right) + \left(\left|A_{\overline{f}}\right|^2 + \left|\overline{A}_{\overline{f}}\right|^2\right)}. \tag{124}$$

Assuming $|q/p| = 1$, *i.e.* absence of *CP* violation in mixing, the parameters C_f and $C_{\overline{f}}$ can also be written in terms of the decay amplitudes as follows:

$$C_f = \frac{|A_f|^2 - \left|\overline{A}_f\right|^2}{|A_f|^2 + \left|\overline{A}_f\right|^2} \quad \text{and} \quad C_{\overline{f}} = \frac{\left|A_{\overline{f}}\right|^2 - \left|\overline{A}_{\overline{f}}\right|^2}{\left|A_{\overline{f}}\right|^2 + \left|\overline{A}_{\overline{f}}\right|^2}, \tag{125}$$

giving asymmetries in the decay amplitudes of B^0 and $\overline{B}^0$ to the final states f and $\overline{f}$ respectively. In this notation, the conditions for absence of *CP* violation in decay are $\langle \mathcal{A}_{f\overline{f}} \rangle = 0$ and $C_f = -C_{\overline{f}}$. Note that C_f and $C_{\overline{f}}$ are typically non-zero; *e.g.*, for a flavour-specific final state, $\overline{A}_f = A_{\overline{f}} = 0$ ($A_f = \overline{A}_{\overline{f}} = 0$), they take the values $C_f = -C_{\overline{f}} = 1$ ($C_f = -C_{\overline{f}} = -1$).

The coefficients of the sine terms contain information about the weak phase. In the case that each decay amplitude contains only a single weak phase (*i.e.*, no *CP* violation in decay as well as none in mixing), these terms can be written

$$S_f = \frac{-2\,|A_f|\,\left|\overline{A}_f\right| \sin(\phi_{\rm mix} + \phi_{\rm dec} - \delta_f)}{|A_f|^2 + \left|\overline{A}_f\right|^2} \quad \text{and} \quad S_{\overline{f}} = \frac{-2\,\left|A_{\overline{f}}\right|\,\left|\overline{A}_{\overline{f}}\right| \sin(\phi_{\rm mix} + \phi_{\rm dec} + \delta_f)}{\left|A_{\overline{f}}\right|^2 + \left|\overline{A}_{\overline{f}}\right|^2}, \tag{126}$$

[36] This parameter is often denoted $\mathcal{A}_f$ (or $\mathcal{A}_{CP}$), but here we avoid this notation to prevent confusion with the time-dependent *CP* asymmetry.

where δ_f is the strong phase difference between the decay amplitudes. If there is no *CP* violation, the condition $S_f = -S_{\overline{f}}$ holds. If decay amplitudes with different weak and strong phases contribute, no clean interpretation of S_f and $S_{\overline{f}}$ is possible.

Since two of the *CP* invariance conditions are $C_f = -C_{\overline{f}}$ and $S_f = -S_{\overline{f}}$, there is motivation for a rotation of the parameters:

$$S_{f\overline{f}} = \frac{S_f + S_{\overline{f}}}{2}, \quad \Delta S_{f\overline{f}} = \frac{S_f - S_{\overline{f}}}{2}, \quad C_{f\overline{f}} = \frac{C_f + C_{\overline{f}}}{2}, \quad \Delta C_{f\overline{f}} = \frac{C_f - C_{\overline{f}}}{2}. \tag{127}$$

With these parameters, the *CP* invariance conditions become $S_{f\overline{f}} = 0$ and $C_{f\overline{f}} = 0$. The parameter $\Delta C_{f\overline{f}}$ gives a measure of the "flavour-specificity" of the decay: $\Delta C_{f\overline{f}} = \pm 1$ corresponds to a completely flavour-specific decay, in which no interference between decays with and without mixing can occur, while $\Delta C_{f\overline{f}} = 0$ results in maximum sensitivity to mixing-induced *CP* violation. The parameter $\Delta S_{f\overline{f}}$ is related to the strong phase difference between the decay amplitudes of B^0 to f and to $\overline{f}$. We note that the observables of Eq. (127) exhibit experimental correlations (typically of $\sim 20\%$, depending on the tagging purity, and other effects) between $S_{f\overline{f}}$ and $\Delta S_{f\overline{f}}$, and between $C_{f\overline{f}}$ and $\Delta C_{f\overline{f}}$. On the other hand, the final state specific observables of Eqs. (120)–(123) tend to have low correlations.

Alternatively, if we recall that the *CP* invariance conditions at the decay amplitude level are $A_f = \overline{A}_{\overline{f}}$ and $A_{\overline{f}} = \overline{A}_f$, we are led to consider the parameters [240]

$$\mathcal{A}_{f\overline{f}} = \frac{\left|\overline{A}_{\overline{f}}\right|^2 - |A_f|^2}{\left|\overline{A}_{\overline{f}}\right|^2 + |A_f|^2} \quad \text{and} \quad \mathcal{A}_{\overline{f}f} = \frac{\left|\overline{A}_f\right|^2 - \left|A_{\overline{f}}\right|^2}{\left|\overline{A}_f\right|^2 + \left|A_{\overline{f}}\right|^2}. \tag{128}$$

These are sometimes considered more physically intuitive parameters since they characterise *CP* violation in decay in decays with particular topologies. For example, in the case of $B^0 \to \rho^\pm\pi^\mp$ (choosing $f = \rho^+\pi^-$ and $\overline{f} = \rho^-\pi^+$), $\mathcal{A}_{f\overline{f}}$ (also denoted $\mathcal{A}_{\rho\pi}^{+-}$) parametrises *CP* violation in decays in which the produced ρ meson does not contain the spectator quark, while $\mathcal{A}_{\overline{f}f}$ (also denoted $\mathcal{A}_{\rho\pi}^{-+}$) parametrises *CP* violation in decays in which it does. Note that we have again followed the sign convention that the asymmetry is the difference between the rate involving a b quark and that involving a $\overline{b}$ quark, *cf.* Eq. (100). Of course, these parameters are not independent of the other sets of parameters given above, and can be written

$$\mathcal{A}_{f\overline{f}} = -\frac{\langle\mathcal{A}_{f\overline{f}}\rangle + C_{f\overline{f}} + \langle\mathcal{A}_{f\overline{f}}\rangle\Delta C_{f\overline{f}}}{1 + \Delta C_{f\overline{f}} + \langle\mathcal{A}_{f\overline{f}}\rangle C_{f\overline{f}}} \quad \text{and} \quad \mathcal{A}_{\overline{f}f} = \frac{-\langle\mathcal{A}_{f\overline{f}}\rangle + C_{f\overline{f}} + \langle\mathcal{A}_{f\overline{f}}\rangle\Delta C_{f\overline{f}}}{-1 + \Delta C_{f\overline{f}} + \langle\mathcal{A}_{f\overline{f}}\rangle C_{f\overline{f}}}. \tag{129}$$

They usually exhibit strong correlations.

We now consider the various notations which have been used in experimental studies of time-dependent *CP* asymmetries in decays to non-*CP* eigenstates.

$B^0 \to D^{*\pm}D^\mp$

The ($\langle\mathcal{A}_{f\overline{f}}\rangle$, C_f, S_f, $C_{\overline{f}}$, $S_{\overline{f}}$) set of parameters was used in early publications by both *BABAR* [273] and Belle [274] (albeit with slightly different notations) in the $D^{*\pm}D^\mp$ system ($f = D^{*+}D^-$, $\overline{f} = D^{*-}D^+$). In their most recent paper on this topic Belle [275] instead used the parametrisation (A_{D^*D}, S_{D^*D}, ΔS_{D^*D}, C_{D^*D}, ΔC_{D^*D}), while *BABAR* [247] give results in both sets of parameters. We therefore use the (A_{D^*D}, S_{D^*D}, ΔS_{D^*D}, C_{D^*D}, ΔC_{D^*D}) set.

$B^0 \to \rho^\pm\pi^\mp$

In the $\rho^\pm\pi^\mp$ system, the ($\langle\mathcal{A}_{f\overline{f}}\rangle$, $C_{f\overline{f}}$, $S_{f\overline{f}}$, $\Delta C_{f\overline{f}}$, $\Delta S_{f\overline{f}}$) set of parameters has been used originally by *BABAR* [276] and Belle [277], in the Q2B approximation; the exact names[37] used in this case are ($\mathcal{A}_{CP}^{\rho\pi}, C_{\rho\pi}, S_{\rho\pi}, \Delta C_{\rho\pi}, \Delta S_{\rho\pi}$), and these names are also used in this document.

Since $\rho^\pm\pi^\mp$ is reconstructed in the final state $\pi^+\pi^-\pi^0$, the interference between the ρ resonances can provide additional information about the phases (see Sec. 4.2.5). Both *BABAR* [269] and Belle [271, 272] have performed time-dependent Dalitz plot analyses, from which the weak phase α is directly extracted. In such an analysis, the measured Q2B parameters are also naturally corrected for interference effects.

$B^0 \to D^\mp\pi^\pm, D^{*\mp}\pi^\pm, D^\mp\rho^\pm$

Time-dependent *CP* analyses have also been performed for the final states $D^\mp\pi^\pm$, $D^{*\mp}\pi^\pm$ and $D^\mp\rho^\pm$. In these theoretically clean cases, no penguin contributions are possible, so there is no *CP* violation in decay. Furthermore, due to the smallness of the ratio of the magnitudes of the suppressed ($b \to u$) and favoured ($b \to c$) amplitudes (denoted R_f), to a very good approximation, $C_f = -C_{\overline{f}} = 1$ (using $f = D^{(*)-}h^+$, $\overline{f} = D^{(*)+}h^-$ $h = \pi, \rho$), and the coefficients of the sine terms are given by

$$S_f = -2R_f \sin(\phi_{\rm mix} + \phi_{\rm dec} - \delta_f) \quad \text{and} \quad S_{\overline{f}} = -2R_f \sin(\phi_{\rm mix} + \phi_{\rm dec} + \delta_f). \tag{130}$$

Thus weak phase information can be cleanly obtained from measurements of S_f and $S_{\overline{f}}$, although external information on at least one of R_f or δ_f is necessary. (Note that $\phi_{\rm mix} + \phi_{\rm dec} = 2\beta + \gamma \equiv 2\phi_1 + \phi_3$ for all the decay modes in question, while R_f and δ_f depend on the decay mode.)

Again, different notations have been used in the literature. *BABAR* [278, 279] defines the time-dependent probability function by

$$f^\pm(\eta, \Delta t) = \frac{e^{-|\Delta t|/\tau}}{4\tau}\left[1 \mp S_\zeta \sin(\Delta m \Delta t) \mp \eta C_\zeta \cos(\Delta m \Delta t)\right], \tag{131}$$

where the upper (lower) sign corresponds to the tagging meson being a B^0 ($\overline{B}^0$). Note here that a tagging B^0 ($\overline{B}^0$) corresponds to $-S_\zeta$ ($+S_\zeta$). The parameters η and ζ take the values $+1$ and $+$ (-1 and $-$) when the final state is, *e.g.*, $D^-\pi^+$ ($D^+\pi^-$). However, in the fit, the substitutions $C_\zeta = 1$ and $S_\zeta = a \mp \eta b_i - \eta c_i$ are made, where the subscript i denotes tagging category. Neglecting b terms,

$$S_+ = a - c \quad \text{and} \quad S_- = a + c \;\Leftrightarrow\; a = (S_+ + S_-)/2 \quad \text{and} \quad c = (S_- - S_+)/2\,, \tag{132}$$

in analogy to the parameters of Eq. (127). These are motivated by the possibility of *CP* violation on the tag side [280], which is absent for semileptonic B decays (mostly lepton tags). The parameter a is not affected by tag side *CP* violation. The parameter b only depends on tag side *CP* violation parameters and is not directly useful for determining UT angles. A clean interpretation of the c parameter is only possible for lepton-tagged events, so the *BABAR* measurements report c measured with those events only.

[37] *BABAR* has used the notations $A_{CP}^{\rho\pi}$ [276] and $\mathcal{A}_{\rho\pi}$ [269] in place of $\mathcal{A}_{CP}^{\rho\pi}$.

Table 23: Conversion between the various notations used for *CP* violation parameters in the $D^{\pm}\pi^{\mp}$, $D^{*\pm}\pi^{\mp}$ and $D^{\pm}\rho^{\mp}$ systems. The b_i terms used by *BABAR* have been neglected. Recall that $(\alpha, \beta, \gamma) \equiv (\phi_2, \phi_1, \phi_3)$.

	BABAR	Belle partial rec.	Belle full rec.
$S_{D^+\pi^-}$	$-S_- = -(a + c_i)$	N/A	$2R_{D\pi}\sin(2\phi_1 + \phi_3 + \delta_{D\pi})$
$S_{D^-\pi^+}$	$-S_+ = -(a - c_i)$	N/A	$2R_{D\pi}\sin(2\phi_1 + \phi_3 - \delta_{D\pi})$
$S_{D^{*+}\pi^-}$	$-S_- = -(a + c_i)$	S^+	$-2R_{D^*\pi}\sin(2\phi_1 + \phi_3 + \delta_{D^*\pi})$
$S_{D^{*-}\pi^+}$	$-S_+ = -(a - c_i)$	S^-	$-2R_{D^*\pi}\sin(2\phi_1 + \phi_3 - \delta_{D^*\pi})$
$S_{D^+\rho^-}$	$-S_- = -(a + c_i)$	N/A	N/A
$S_{D^-\rho^+}$	$-S_+ = -(a - c_i)$	N/A	N/A

Table 24: Translations used to convert the parameters measured by Belle to the parameters used for averaging in this document. The angular momentum factor L is -1 for $D^*\pi$ and $+1$ for $D\pi$. Recall that $(\alpha, \beta, \gamma) \equiv (\phi_2, \phi_1, \phi_3)$.

	$D^*\pi$ partial rec.	$D^{(*)}\pi$ full rec.
a	$-(S^+ + S^-)$	$\frac{1}{2}(-1)^{L+1}\left(2R_{D^{(*)}\pi}\sin(2\phi_1 + \phi_3 + \delta_{D^{(*)}\pi}) + 2R_{D^{(*)}\pi}\sin(2\phi_1 + \phi_3 - \delta_{D^{(*)}\pi})\right)$
c	$-(S^+ - S^-)$	$\frac{1}{2}(-1)^{L+1}\left(2R_{D^{(*)}\pi}\sin(2\phi_1 + \phi_3 + \delta_{D^{(*)}\pi}) - 2R_{D^{(*)}\pi}\sin(2\phi_1 + \phi_3 - \delta_{D^{(*)}\pi})\right)$

The parameters used by Belle in the analysis using partially reconstructed B decays [281], are similar to the S_ζ parameters defined above. However, in the Belle convention, a tagging B^0 corresponds to a + sign in front of the sine coefficient; furthermore the correspondence between the super/subscript and the final state is opposite, so that $S_\pm$ (*BABAR*) $= -S^\mp$ (Belle). In this analysis, only lepton tags are used, so there is no effect from tag side *CP* violation. In the Belle analysis using fully reconstructed B decays [282], this effect is measured and taken into account using $D^*\ell\nu$ decays; in neither Belle analysis are the a, b and c parameters used. In the latter case, the measured parameters are $2R_{D^{(*)}\pi}\sin(2\phi_1 + \phi_3 \pm \delta_{D^{(*)}\pi})$; the definition is such that $S^\pm$ (Belle) $= -2R_{D^*\pi}\sin(2\phi_1 + \phi_3 \pm \delta_{D^*\pi})$. However, the definition includes an angular momentum factor $(-1)^L$ [283], and so for the results in the $D\pi$ system, there is an additional factor of -1 in the conversion.

Explicitly, the conversion then reads as given in Table 23, where we have neglected the b_i terms used by *BABAR* (which are zero in the absence of tag side *CP* violation). For the averages in this document, we use the a and c parameters, and give the explicit translations used in Table 24. It is to be fervently hoped that the experiments will converge on a common notation in future.

$B_s^0 \to D_s^\mp K^\pm$

The phenomenology of $B_s^0 \to D_s^\mp K^\pm$ decays is similar to that for $B^0 \to D^\mp\pi^\pm$, with some important caveats. The larger size of the ratio R of the magnitudes of the suppressed and favoured amplitudes allows it to be determined from the data, as the deviation of C_f and $C_{\overline{f}}$ from unity (in magnitude) can be observed. Moreover, the non-zero value of $\Delta\Gamma_s$ allows the determination of additional terms, $A_f^{\Delta\Gamma}$ and $A_{\overline{f}}^{\Delta\Gamma}$ (see Sec. 4.2.3), that break ambiguities in the

solutions for $\phi_{\rm mix} + \phi_{\rm dec}$, which for $B^0_s \to D^\mp_s K^\pm$ decays is equal to $\gamma - 2\beta_s$.

LHCb [284] have performed such an analysis with $B^0_s \to D^\mp_s K^\pm$ decays. The absence of *CP* violation in decay is assumed, and the parameters that are determined from the fit are labelled C, $A^{\Delta\Gamma}$, $\overline{A}^{\Delta\Gamma}$, S, $\overline{S}$. These are trivially related to the definitions used in this Section.

Time-dependent asymmetries in radiative B decays

As a special case of decays to non-*CP* eigenstates, let us consider radiative B decays. Here, the emitted photon has a distinct helicity, which is in principle observable, but in practise is not usually measured. Thus the measured time-dependent decay rates for B^0 decays are given by [285, 286]

$$\begin{aligned}
\Gamma_{\overline{B}^0 \to X\gamma}(\Delta t) &= \Gamma_{\overline{B}^0 \to X\gamma_L}(\Delta t) + \Gamma_{\overline{B}^0 \to X\gamma_R}(\Delta t) \qquad (133)\\
&= \frac{e^{-|\Delta t|/\tau(B^0)}}{4\tau(B^0)} \left\{1 + (S_L + S_R)\sin(\Delta m \Delta t) - (C_L + C_R)\cos(\Delta m \Delta t)\right\},\\
\Gamma_{B^0 \to X\gamma}(\Delta t) &= \Gamma_{B^0 \to X\gamma_L}(\Delta t) + \Gamma_{B^0 \to X\gamma_R}(\Delta t) \qquad (134)\\
&= \frac{e^{-|\Delta t|/\tau(B^0)}}{4\tau(B^0)} \left\{1 - (S_L + S_R)\sin(\Delta m \Delta t) + (C_L + C_R)\cos(\Delta m \Delta t)\right\},
\end{aligned}$$

where in place of the subscripts f and $\overline{f}$ we have used L and R to indicate the photon helicity. In order for interference between decays with and without B^0-$\overline{B}^0$ mixing to occur, the X system must not be flavour-specific, *e.g.*, in case of $B^0 \to K^{*0}\gamma$, the final state must be $K^0_S\pi^0\gamma$. The sign of the sine term depends on the C eigenvalue of the X system. At leading order, the photons from $b \to q\gamma$ ($\overline{b} \to \overline{q}\gamma$) are predominantly left (right) polarised, with corrections of order of m_q/m_b, thus interference effects are suppressed. Higher order effects can lead to corrections of order $\Lambda_{\rm QCD}/m_b$ [287, 288], though explicit calculations indicate such corrections are small for exclusive final states [289, 290]. The predicted smallness of the S terms in the Standard Model results in sensitivity to new physics contributions.

The formalism discussed above is valid from any radiative decay to a final state where the hadronic system is an eigenstate of C. In addition to $K^0_S\pi^0\gamma$, experiments have presented results using B^0 decays to $K^0_S\eta\gamma$, $K^0_S\rho\gamma$ and $K^0_S\phi\gamma$. For the case of the $K^0_S\rho\gamma$ final state, particular care is needed, as due to the non-negligible width of the ρ^0 meson, decays selected as $B^0 \to K^0_S\rho^0\gamma$ can include a significant contribution from $K^{*\pm}\pi^\mp\gamma$ decays, which are flavour-specific and do not have the same oscillation phenomenology. It is therefore necessary to correct the fitted asymmetry parameter for a "dilution factor".

In the case of radiative B^0_s decays, the time-dependent decay rates of Eqs. (133) and (134) must be modified, in a similar way as discussed in Sec. 4.2.3, to account for the non-zero value of $\Delta\Gamma_s$. Thus, for decays such as $B^0_s \to \phi\gamma$, there is an additional observable, $A^{\Delta\Gamma}_{\phi\gamma}$, which can be determined from an untagged effective lifetime measurement [291].

4.2.7 Asymmetries in $B \to D^{(*)}K^{(*)}$ decays

CP asymmetries in $B \to D^{(*)}K^{(*)}$ decays are sensitive to γ. The neutral $D^{(*)}$ meson produced is an admixture of $D^{(*)0}$ (produced by a $b \to c$ transition) and $\overline{D}^{(*)0}$ (produced by a colour-suppressed $b \to u$ transition) states. If the final state is chosen so that both $D^{(*)0}$ and $\overline{D}^{(*)0}$ can contribute, the two amplitudes interfere, and the resulting observables are sensitive to γ,

the relative weak phase between the two B decay amplitudes [292]. Various methods have been proposed to exploit this interference, including those where the neutral D meson is reconstructed as a *CP* eigenstate (GLW) [293, 294], in a suppressed final state (ADS) [295, 296], or in a self-conjugate three-body final state, such as $K^0_S\pi^+\pi^-$ (GGSZ or Dalitz) [297, 298]. It should be emphasised that while each method differs in the choice of D decay, they are all sensitive to the same parameters of the B decay, and can be considered as variations of the same technique.

Consider the case of $B^\mp \to DK^\mp$, with D decaying to a final state f, which is accessible to both D^0 and $\overline{D}^0$. We can write the decay rates for B^- and B^+ ($\Gamma_\mp$), the charge averaged rate ($\Gamma = (\Gamma_- + \Gamma_+)/2$) and the charge asymmetry ($\mathcal{A} = (\Gamma_- - \Gamma_+)/(\Gamma_- + \Gamma_+)$, see Eq. (100)) as

$$\Gamma_\mp \propto r_B^2 + r_D^2 + 2r_B r_D \cos(\delta_B + \delta_D \mp \gamma), \tag{135}$$

$$\Gamma \propto r_B^2 + r_D^2 + 2r_B r_D \cos(\delta_B + \delta_D)\cos(\gamma), \tag{136}$$

$$\mathcal{A} = \frac{2r_B r_D \sin(\delta_B + \delta_D)\sin(\gamma)}{r_B^2 + r_D^2 + 2r_B r_D \cos(\delta_B + \delta_D)\cos(\gamma)}, \tag{137}$$

where the ratio of B decay amplitudes[38] is usually defined to be less than one,

$$r_B = \frac{\left|A\left(B^- \to \overline{D}^0 K^-\right)\right|}{\left|A\left(B^- \to D^0 K^-\right)\right|}, \tag{138}$$

and the ratio of D decay amplitudes is correspondingly defined by

$$r_D = \frac{\left|A\left(D^0 \to f\right)\right|}{\left|A\left(\overline{D}^0 \to f\right)\right|}. \tag{139}$$

The strong phase differences between the B and D decay amplitudes are given by δ_B and δ_D, respectively. The values of r_D and δ_D depend on the final state f: for the GLW analysis, $r_D = 1$ and δ_D is trivial (either zero or π); for other modes, values of r_D and δ_D are not trivial and for multibody final states they vary across the phase-space. This can be quantified either by an explicit D decay amplitude model or by model-independent information. In the case that the multibody final state is treated inclusively, the formalism is modified by the inclusion of a coherence factor, usually denoted κ, while r_D and δ_D become effectively parameters corresponding to amplitude-weighted averages across the phase-space.

Note that, for given values of r_B and r_D, the maximum size of $\mathcal{A}$ (at $\sin(\delta_B + \delta_D) = 1$) is $2r_B r_D \sin(\gamma) / (r_B^2 + r_D^2)$. Thus even for D decay modes with small r_D, large asymmetries, and hence sensitivity to γ, may occur for B decay modes with similar values of r_B. For this reason, the ADS analysis of the decay $B^\mp \to D\pi^\mp$ is also of interest.

In the GLW analysis, the measured quantities are the partial rate asymmetry and the charge averaged rate, which are measured both for *CP*-even and *CP*-odd D decays. The latter is defined as

$$R_{CP} = \frac{2\,\Gamma\left(B^- \to D_{CP} K^-\right)}{\Gamma\left(B^- \to D^0 K^-\right)}. \tag{140}$$

[38] Note that here we use the notation r_B to denote the ratio of B decay amplitudes, whereas in Sec. 4.2.6 we used, *e.g.*, $R_{D\pi}$, for a rather similar quantity. The reason is that here we need to be concerned also with D decay amplitudes, and so it is convenient to use the subscript to denote the decaying particle. Hopefully, using r in place of R will reduce the potential for confusion.

It is experimentally convenient to measure R_{CP} using a double ratio,

$$R_{CP} = \frac{\Gamma\left(B^- \to D_{CP}K^-\right) / \Gamma\left(B^- \to D^0K^-\right)}{\Gamma\left(B^- \to D_{CP}\pi^-\right) / \Gamma\left(B^- \to D^0\pi^-\right)} \tag{141}$$

that is normalised both to the rate for the favoured $D^0 \to K^-\pi^+$ decay, and to the equivalent quantities for $B^- \to D\pi^-$ decays (charge conjugate processes are implicitly included in Eqs. (140) and (141)). In this way the constant of proportionality drops out of Eq. (136). Eq. (141) is exact in the limit that the contribution of the $b \to u$ decay amplitude to $B^- \to D\pi^-$ vanishes and when the flavour-specific rates $\Gamma\left(B^- \to D^0h^-\right)$ $(h = \pi, K)$ are determined using appropriately flavour-specific D decays. In reality, the decay $D \to K\pi$ is used, leading to a small source of systematic uncertainty. The CP asymmetry is defined as

$$A_{CP} = \frac{\Gamma\left(B^- \to D_{CP}K^-\right) - \Gamma\left(B^+ \to D_{CP}K^+\right)}{\Gamma\left(B^- \to D_{CP}K^-\right) + \Gamma\left(B^+ \to D_{CP}K^+\right)}\,. \tag{142}$$

For the ADS analysis, using a suppressed $D \to f$ decay, the measured quantities are again the partial rate asymmetry, and the charge averaged rate. In this case it is sufficient to measure the rate in a single ratio (normalised to the favoured $D \to \overline{f}$ decay) since detection systematics cancel naturally; the observed quantity is then

$$R_{\rm ADS} = \frac{\Gamma\left(B^- \to [f]_D\,K^-\right) + \Gamma\left(B^+ \to \left[\overline{f}\right]_D\,K^+\right)}{\Gamma\left(B^- \to \left[\overline{f}\right]_D\,K^-\right) + \Gamma\left(B^+ \to [f]_D\,K^+\right)}\,, \tag{143}$$

where the inclusion of charge conjugate modes has been made explicit. The CP asymmetry is defined as

$$A_{\rm ADS} = \frac{\Gamma\left(B^- \to [f]_D\,K^-\right) - \Gamma\left(B^+ \to [f]_D\,K^+\right)}{\Gamma\left(B^- \to [f]_D\,K^-\right) + \Gamma\left(B^+ \to [f]_D\,K^+\right)}\,. \tag{144}$$

Since the uncertainty of $A_{\rm ADS}$ depends on the central value of $R_{\rm ADS}$, for some statistical treatments it is preferable to use an alternative pair of parameters [299])

$$R_- = \frac{\Gamma\left(B^- \to [f]_D\,K^-\right)}{\Gamma\left(B^- \to \left[\overline{f}\right]_D\,K^-\right)} \qquad R_+ = \frac{\Gamma\left(B^+ \to \left[\overline{f}\right]_D\,K^+\right)}{\Gamma\left(B^+ \to [f]_D\,K^+\right)}\,, \tag{145}$$

where there is no inclusion of charge conjugated processes. These parameters are statistically uncorrelated but may be effected by common sources of systematic uncertainty. We use the $(R_{\rm ADS}, A_{\rm ADS})$ set in our compilation where available.

In the ADS analysis, there are an additional two unknowns (r_D and δ_D) compared to the GLW case. However, the value of r_D can be measured using decays of D mesons of known flavour, and δ_D can be measured from interference effects in decays of quantum-correlated $D\overline{D}$ pairs produced at the $\psi(3770)$ resonance. More generally, one needs access to two different linear admixtures of D^0 and $\overline{D}^0$ states in order to determine the relative phase: one such sample can be flavour tagged D mesons which are available in abundant quantities in many experiments; the other can be CP-tagged D mesons from $\psi(3770)$ decays or could be mixed D mesons, or could for that matter be the combination of D^0 and $\overline{D}^0$ that is found in $B \to DK$ decays. In fact, the most precise information on both r_D and δ_D currently comes from global fits on charm mixing parameters, as discussed in Sec. 8.1.

The relation of $\mathcal{A}_{\rm ADS}$ to the underlying parameters given in Eq. (137) and Table 25 is exact for a two-body D decay. For multibody decays, a similar formalism can be used with the introduction of a coherence factor [300]. This is most appropriate for doubly-Cabibbo-suppressed decays to non-self-conjugate final states, but can also be modified for use with singly-Cabibbo-suppressed decays [301]. For multibody self-conjugate final states, such as $K^0_S\pi^+\pi^-$, a Dalitz plot analysis (discussed below) is often more appropriate. However, in certain cases where the final state has a high net *CP* content, a modified version of the GLW formalism can be used [302]. In such cases the observables are denoted $A_{\rm qGLW}$ and $R_{\rm qGLW}$ to indicate that the final state is not a pure *CP* eigenstate.

Additional coherence factors enter the expressions when the B decay is to a multibody final state. In particular, experiments have studied $B^+ \to DK^*(892)^+$, $B^0 \to DK^*(892)^0$ and $B^+ \to DK^+\pi^+\pi^-$ decays. Considering, for concreteness, the $B \to DK^*(892)$ case, the non-negligible width of the $K^*(892)$ resonance implies that contributions from other $B \to DK\pi$ decays can pass the selection requirements. Their effect on the Q2B analysis can be accounted for with a coherence factor [303], usually denoted κ, which tends to unity in the limit that the $K^*(892)$ resonance is the only signal amplitude contributing in the selected region of phase space. In this case, the hadronic parameters r_B and δ_B become effectively weighted averages across the selected phase space of the magnitude ratio and relative strong phase between the CKM-suppressed and -favoured amplitudes; these effective parameters are denoted $\overline{r}_B$ and $\overline{\delta}_B$ (the notations r_s, δ_s and r_S, δ_S are also found in the literature). An alternative, and in certain cases more advantageous, approach is Dalitz plot analysis of the full $B \to DK\pi$ phase space [304, 305].

In the Dalitz plot (or GGSZ) analysis of D decays to multibody self-conjugate final states, once a model is assumed for the D decay, which gives the values of r_D and δ_D across the Dalitz plot, it is possible to perform a simultaneous fit to the B^+ and B^- samples and directly extract γ, r_B and δ_B. However, the uncertainties on the phases depend approximately inversely on r_B. Furthermore, r_B is positive definite and therefore tends to be overestimated (unless $\sigma(r_B) \ll r_B$), which leads to an underestimation of the uncertainty on γ that must be corrected statistically. An alternative approach is to extract from the data the "Cartesian" variables

$$(x_\pm, y_\pm) = \left({\rm Re}(r_B e^{i(\delta_B \pm \gamma)}), {\rm Im}(r_B e^{i(\delta_B \pm \gamma)})\right) = (r_B \cos(\delta_B \pm \gamma), r_B \sin(\delta_B \pm \gamma)) \,. \qquad (146)$$

These variables are tend to be statistically well-behaved, and are therefore appropriate for combination of results. The pairs of variables $(x_\pm, y_\pm)$ can be extracted from independent fits of the $B^\pm$ data samples.

The assumption of a model for the D decay however leads to a non-negligible, and hard to quantify, source of uncertainty. To obviate this, it is possible to use instead a model-independent approach, in which the Dalitz plot (or, more generally, the phase-space) is binned [297,306,307]. In this case, hadronic parameters describing the average strong phase difference in each bin between the suppressed and favoured decay amplitudes enter the equations. These parameters can be determined from interference effects in decays of quantum-correlated $D\overline{D}$ pairs produced at the $\psi(3770)$ resonance. Measurements of such parameters have been made for various different hadronic D decays by CLEO-c and BESIII.

If a multibody decay is dominated by one *CP* state there will be additional sensitivity to γ in the numbers of events in the $B^\pm$ data samples. This can be taken into account in various ways. One possibility is to perform a GLW-like analysis, as mentioned above. An alternative approach proceeds by defining $z_\pm = x_\pm + iy_\pm$ and $x_0 = -\int {\rm Re}\left[f(s_1,s_2)f^*(s_2,s_1)\right] ds_1 ds_2$, where s_1, s_2 are

the coordinates of invariant mass squared that define the Dalitz plot and f is the complex amplitude for D decay as a function of the Dalitz plot coordinates.[39] The fitted parameters $(\rho^{\pm}, \theta^{\pm})$ are then defined by

$$\rho^{\pm} e^{i\theta^{\pm}} = z_{\pm} - x_0 \,. \tag{147}$$

Note that the yields of $B^{\pm}$ decays are proportional to $1 + (\rho^{\pm})^2 - (x_0)^2$. This choice of variables has been used by *BABAR* in the analysis of $B^{\mp} \to DK^{\mp}$ with $D \to \pi^+\pi^-\pi^0$ [309]; for this D decay, and with the assumed amplitude model, a value of $x_0 = 0.850$ is obtained.

The relations between the measured quantities and the underlying parameters are summarised in Table 25. It must be emphasised that the hadronic factors r_B and δ_B are different, in general, for each B decay mode.

Table 25: Summary of relations between measured and physical parameters in GLW, ADS and Dalitz analyses of $B \to D^{(*)}K^{(*)}$.

GLW analysis	
$R_{CP\pm}$	$1 + r_B^2 \pm 2r_B \cos(\delta_B)\cos(\gamma)$
$A_{CP\pm}$	$\pm 2r_B \sin(\delta_B)\sin(\gamma)\,/R_{CP\pm}$
ADS analysis	
$R_{\rm ADS}$	$r_B^2 + r_D^2 + 2r_B r_D \cos(\delta_B + \delta_D)\cos(\gamma)$
$A_{\rm ADS}$	$2r_B r_D \sin(\delta_B + \delta_D)\sin(\gamma)\,/R_{\rm ADS}$
GGSZ Dalitz analysis ($D \to K^0_S\pi^+\pi^-$)	
$x_{\pm}$	$r_B \cos(\delta_B \pm \gamma)$
$y_{\pm}$	$r_B \sin(\delta_B \pm \gamma)$
Dalitz analysis ($D \to \pi^+\pi^-\pi^0$)	
$\rho^{\pm}$	$\lvert z_{\pm} - x_0\rvert$
$\theta^{\pm}$	$\tan^{-1}(\mathrm{Im}(z_{\pm})/(\mathrm{Re}(z_{\pm}) - x_0))$

4.3 Common inputs and error treatment

The common inputs used for rescaling are listed in Table 26. The B^0 lifetime ($\tau(B^0)$), mixing parameter (Δm_d) and relative width difference ($\Delta\Gamma_d/\Gamma_d$) averages are provided by the HFAG Lifetimes and Oscillations subgroup (Sec. 3). The fraction of the perpendicularly polarised component ($|A_\perp|^2$) in $B \to J/\psi K^*(892)$ decays, which determines the *CP* composition in these decays, is averaged from results by *BABAR* [310], Belle [311], CDF [312], D0 [86] and LHCb [313]. See also the HFAG B to Charm Decay Parameters subgroup (Sec. 6).

At present, we only rescale to a common set of input parameters for modes with reasonably small statistical errors ($b \to c\bar{c}s$ transitions). Correlated systematic errors are taken into account in these modes as well. For all other modes, the effect of such a procedure is currently negligible.

As explained in Sec. 1, we do not apply a rescaling factor on the error of an average that has $\chi^2/\mathrm{dof} > 1$ (unlike the procedure currently used by the PDG [314]). We provide a confidence

[39] The x_0 parameter gives a model-dependent measure of the net *CP* content of the final state [302, 308]. It is closely related to the c_i parameters of the model dependent Dalitz plot analysis [297, 306, 307], and the coherence factor of inclusive ADS-type analyses [300], integrated over the entire Dalitz plot.

Table 26: Common inputs used in calculating the averages.

$\tau(B^0)$ (ps)	1.520 ± 0.004
Δm_d (ps^{-1})	0.5064 ± 0.0019
$\Delta\Gamma_d/\Gamma_d$	-0.002 ± 0.010
$\lvert A_\perp \rvert^2 (J/\psi K^*)$	0.209 ± 0.006

level of the fit so that one can know the consistency of the measurements included in the average, and attach comments in case some care needs to be taken in the interpretation. Note that, in general, results obtained from data samples with low statistics will exhibit some non-Gaussian behaviour. We average measurements with asymmetric errors using the PDG [314] prescription. In cases where several measurements are correlated (*e.g.* S_f and C_f in measurements of time-dependent *CP* violation in B decays to a particular *CP* eigenstate) we take these into account in the averaging procedure if the uncertainties are sufficiently Gaussian. For measurements where one error is given, it represents the total error, where statistical and systematic uncertainties have been added in quadrature. If two errors are given, the first is statistical and the second systematic. If more than two errors are given, the origin of the additional uncertainty will be explained in the text.

4.4 Time-dependent asymmetries in $b \to c\bar{c}s$ transitions

4.4.1 Time-dependent *CP* asymmetries in $b \to c\bar{c}s$ decays to *CP* eigenstates

In the Standard Model, the time-dependent parameters for B^0 decays governed by $b \to c\bar{c}s$ transitions are predicted to be: $S_{b\to c\bar{c}s} = -\eta \sin(2\beta)$, $C_{b\to c\bar{c}s} = 0$ to very good accuracy. Deviations from this relation are currently limited to the level of $\lesssim 1^\circ$ on 2β [315–317]. The averages for $-\eta S_{b\to c\bar{c}s}$ and $C_{b\to c\bar{c}s}$ are provided in Table 27. The averages for $-\eta S_{b\to c\bar{c}s}$ are shown in Fig. 12.

Both *BABAR* and Belle have used the $\eta = -1$ modes $J/\psi K^0_S$, $\psi(2S)K^0_S$, $\chi_{c1}K^0_S$ and $\eta_c K^0_S$, as well as $J/\psi K^0_L$, which has $\eta = +1$ and $J/\psi K^{*0}(892)$, which is found to have η close to $+1$ based on the measurement of $|A_\perp|$ (see Sec. 4.3). The most recent Belle result does not use $\eta_c K^0_S$ or $J/\psi K^{*0}(892)$ decays.[40] ALEPH, OPAL, CDF and LHCb have used only the $J/\psi K^0_S$ final state. *BABAR* has also determined the *CP* violation parameters of the $B^0 \to \chi_{c0}K^0_S$ decay from the time-dependent Dalitz plot analysis of $B^0 \to \pi^+\pi^- K^0_S$ (see Sec. 4.7.2). In addition, Belle has performed a measurement with data accumulated at the $\Upsilon(5S)$ resonance, using the $J/\psi K^0_S$ final state – this involves a different flavour tagging method compared to the measurements performed with data accumulated at the $\Upsilon(4S)$ resonance. A breakdown of results in each charmonium-kaon final state is given in Table 28.

It should be noted that, while the uncertainty in the average for $-\eta S_{b\to c\bar{c}s}$ is still limited by statistics, the uncertainty for $C_{b\to c\bar{c}s}$ is close to being dominated by systematics particularly for measurements from the e^+e^- B factory experiments. This occurs due to the possible effect of tag side interference [280] on the $C_{b\to c\bar{c}s}$ measurement, an effect which is correlated between

[40] Previous analyses from Belle did include these channels [94], but it is not possible to obtain separate results for those modes from the published information.

Table 27: $S_{b\to c\bar{c}s}$ and $C_{b\to c\bar{c}s}$.

Experiment		Sample size	$-\eta S_{b\to c\bar{c}s}$	$C_{b\to c\bar{c}s}$
BABAR	[318]	$N(B\overline{B}) = 465$M	$0.687 \pm 0.028 \pm 0.012$	$0.024 \pm 0.020 \pm 0.016$
BABAR $\chi_{c0}K^0_S$	[262]	$N(B\overline{B}) = 383$M	$0.69 \pm 0.52 \pm 0.04 \pm 0.07$	$-0.29\,^{+0.53}_{-0.44} \pm 0.03 \pm 0.05$
BABAR $J/\psi K^0_S$ (*)	[319]	$N(B\overline{B}) = 88$M	$1.56 \pm 0.42 \pm 0.21$	–
Belle	[320]	$N(B\overline{B}) = 772$M	$0.667 \pm 0.023 \pm 0.012$	$-0.006 \pm 0.016 \pm 0.012$
***B* factory average**			0.679 ± 0.020	0.005 ± 0.017
Confidence level			0.28 (1.2σ)	0.47 (0.5σ)
ALEPH	[321]	$N(Z \to \text{hadrons}) = 4$M	$0.84\,^{+0.82}_{-1.04} \pm 0.16$	–
OPAL	[322]	$N(Z \to \text{hadrons}) = 4.4$M	$3.2\,^{+1.8}_{-2.0} \pm 0.5$	–
CDF	[323]	$\int \mathcal{L}\,dt = 110$ pb^{-1}	$0.79\,^{+0.41}_{-0.44}$	–
LHCb	[324]	$\int \mathcal{L}\,dt = 3$ fb^{-1}	$0.731 \pm 0.035 \pm 0.020$	$-0.038 \pm 0.032 \pm 0.005$
Belle $\Upsilon(5S)$	[325]	$\int \mathcal{L}\,dt = 121$ fb^{-1}	$0.57 \pm 0.58 \pm 0.06$	–
Average			0.691 ± 0.017	-0.004 ± 0.015

* This result uses "*hadronic and previously unused muonic decays of the* J/ψ". We neglect a small possible correlation of this result with the main *BABAR* result [318] that could be caused by reprocessing of the data.

different $e^+e^- \to \Upsilon(4S) \to B\overline{B}$ experiments. Understanding of this effect may continue to improve in future, allowing the uncertainty to reduce.

From the average for $-\eta S_{b\to c\bar{c}s}$ above, we obtain the following solutions for β (in $[0, \pi]$):

$$\beta = (21.9 \pm 0.7)^\circ \quad \text{or} \quad \beta = (68.1 \pm 0.7)^\circ \tag{148}$$

In radians, these values are $\beta = (0.382 \pm 0.012)$, $\beta = (1.189 \pm 0.012)$.

This result gives a precise constraint on the $(\overline{\rho}, \overline{\eta})$ plane, as shown in Fig. 12. The measurement is in remarkable agreement with other constraints from *CP* conserving quantities, and with *CP* violation in the kaon system, in the form of the parameter ϵ_K. Such comparisons have been performed by various phenomenological groups, such as CKMfitter [240] and UTFit [326] (see also Refs. [327, 328]).

4.4.2 Time-dependent transversity analysis of $B^0 \to J/\psi K^{*0}$

B meson decays to the vector-vector final state $J/\psi K^{*0}$ are also mediated by the $b \to c\bar{c}s$ transition. When a final state that is not flavour-specific ($K^{*0} \to K^0_S\pi^0$) is used, a time-dependent transversity analysis can be performed allowing sensitivity to both $\sin(2\beta)$ and $\cos(2\beta)$ [329]. Such analyses have been performed by both B factory experiments. In principle, the strong phases between the transversity amplitudes are not uniquely determined by such an analysis, leading to a discrete ambiguity in the sign of $\cos(2\beta)$. The *BABAR* collaboration resolves this ambiguity using the known variation [330] of the P-wave phase (fast) relative to the S-wave phase (slow) with the invariant mass of the $K\pi$ system in the vicinity of the $K^*(892)$ resonance. The result is in agreement with the prediction from s quark helicity conservation, and corresponds to Solution II defined by Suzuki [331]. We use this phase convention for the averages given in Table 29 and Fig. 13.

Table 28: Breakdown of B factory results on $S_{b\to c\bar{c}s}$ and $C_{b\to c\bar{c}s}$.

Mode		$N(B\overline{B})$	$-\eta S_{b\to c\bar{c}s}$	$C_{b\to c\bar{c}s}$
			BABAR	
$J/\psi K^0_S$	[318]	465M	$0.657 \pm 0.036 \pm 0.012$	$0.026 \pm 0.025 \pm 0.016$
$J/\psi K^0_L$	[318]	465M	$0.694 \pm 0.061 \pm 0.031$	$-0.033 \pm 0.050 \pm 0.027$
$\boldsymbol{J/\psi K^0}$	[318]	465M	$0.666 \pm 0.031 \pm 0.013$	$0.016 \pm 0.023 \pm 0.018$
$\psi(2S)K^0_S$	[318]	465M	$0.897 \pm 0.100 \pm 0.036$	$0.089 \pm 0.076 \pm 0.020$
$\chi_{c1}K^0_S$	[318]	465M	$0.614 \pm 0.160 \pm 0.040$	$0.129 \pm 0.109 \pm 0.025$
$\eta_c K^0_S$	[318]	465M	$0.925 \pm 0.160 \pm 0.057$	$0.080 \pm 0.124 \pm 0.029$
$J/\psi\, K^{*0}(892)$	[318]	465M	$0.601 \pm 0.239 \pm 0.087$	$0.025 \pm 0.083 \pm 0.054$
All	[318]	465M	$0.687 \pm 0.028 \pm 0.012$	$0.024 \pm 0.020 \pm 0.016$
			Belle	
$J/\psi K^0_S$	[320]	772M	$0.670 \pm 0.029 \pm 0.013$	$0.015 \pm 0.021\,^{+0.023}_{-0.045}$
$J/\psi K^0_L$	[320]	772M	$0.642 \pm 0.047 \pm 0.021$	$-0.019 \pm 0.026\,^{+0.041}_{-0.017}$
$\psi(2S)K^0_S$	[320]	772M	$0.738 \pm 0.079 \pm 0.036$	$-0.104 \pm 0.055\,^{+0.027}_{-0.047}$
$\chi_{c1}K^0_S$	[320]	772M	$0.640 \pm 0.117 \pm 0.040$	$0.017 \pm 0.083\,^{+0.026}_{-0.046}$
All	[320]	772M	$0.667 \pm 0.023 \pm 0.012$	$-0.006 \pm 0.016 \pm 0.012$
			Averages	
$J/\psi K^0_S$			0.665 ± 0.024	0.024 ± 0.026
$J/\psi K^0_L$			0.663 ± 0.041	-0.023 ± 0.030
$\psi(2S)K^0_S$			0.807 ± 0.067	-0.009 ± 0.055
$\chi_{c1}K^0_S$			0.632 ± 0.099	0.066 ± 0.074

At present the results are dominated by large and non-Gaussian statistical errors, and exhibit significant correlations. We perform uncorrelated averages, the interpretation of which has to be done with the greatest care. Nonetheless, it is clear that $\cos(2\beta) > 0$ is preferred by the experimental data in $J/\psi K^{*0}$ (for example, *BABAR* [332] find a confidence level for $\cos(2\beta) > 0$ of 89%).

4.4.3 Time-dependent *CP* asymmetries in $B^0 \to D^{*+}D^{*-}K^0_S$ decays

Both *BABAR* [253] and Belle [254] have performed time-dependent analyses of the $B^0 \to D^{*+}D^{*-}K^0_S$ decay, to obtain information on the sign of $\cos(2\beta)$. More information can be found in Sec. 4.2.5. The results are given in Table 30, and shown in Fig. 14.

From the above result and the assumption that $J_{s2} > 0$, *BABAR* infer that $\cos(2\beta) > 0$ at the 94% confidence level [253].

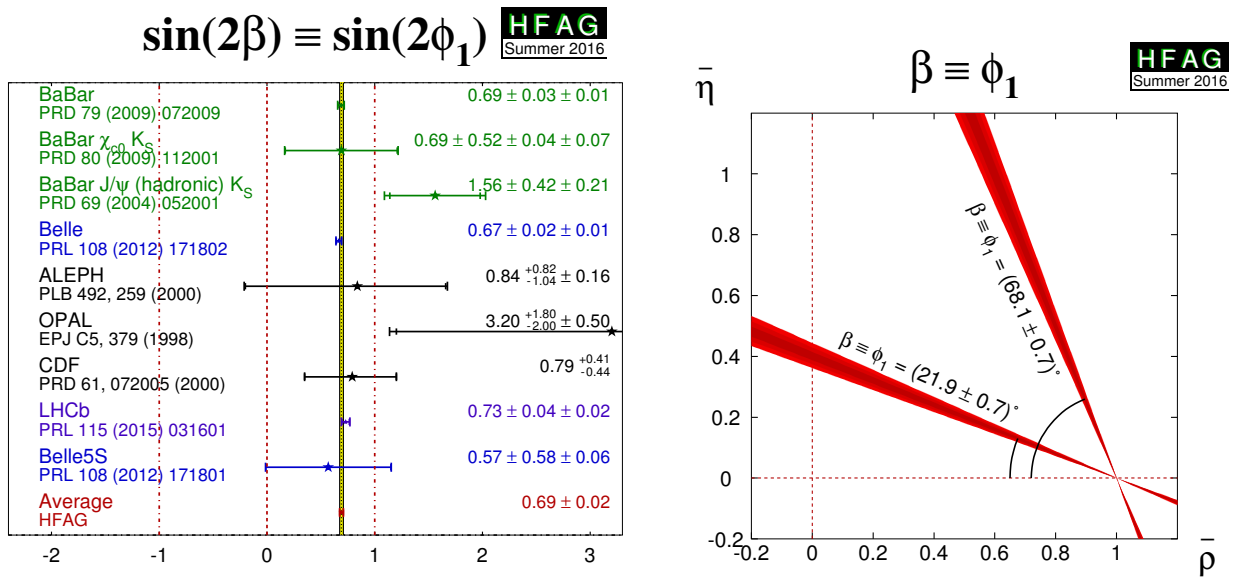

Figure 12: (Left) Average of measurements of $S_{b\to c\bar{c}s}$. (Right) Constraints on the $(\overline{\rho},\overline{\eta})$ plane, obtained from the average of $-\eta S_{b\to c\bar{c}s}$ and Eq. (148). Note that the solution with the smaller (larger) value of β has $\cos(2\beta) > 0$ (< 0).

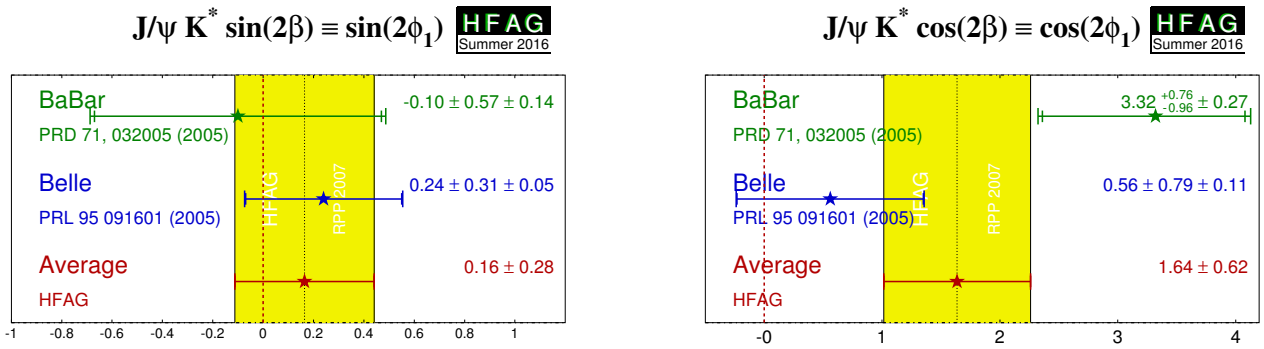

Figure 13: Averages of (left) $\sin(2\beta) \equiv \sin(2\phi_1)$ and (right) $\cos(2\beta) \equiv \cos(2\phi_1)$ from time-dependent analyses of $B^0 \to J/\psi\, K^{*0}$ decays.

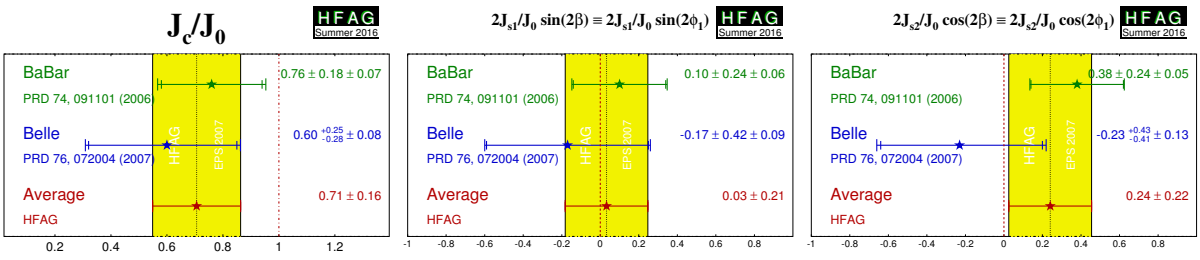

Figure 14: Averages of (left) (J_c/J_0), (middle) $(2J_{s1}/J_0)\sin(2\beta)$ and (right) $(2J_{s2}/J_0)\cos(2\beta)$ from time-dependent analyses of $B^0 \to D^{*+}D^{*-}K^0_S$ decays.

Table 29: Averages from $B^0 \to J/\psi K^{*0}$ transversity analyses.

Experiment		$N(B\overline{B})$	$\sin 2\beta$	$\cos 2\beta$	Correlation
BABAR	[332]	88M	$-0.10 \pm 0.57 \pm 0.14$	$3.32^{+0.76}_{-0.96} \pm 0.27$	-0.37
Belle	[311]	275M	$0.24 \pm 0.31 \pm 0.05$	$0.56 \pm 0.79 \pm 0.11$	0.22
Average			0.16 ± 0.28	1.64 ± 0.62	uncorrelated averages
Confidence level			0.61 (0.5σ)	0.03 (2.2σ)	

Table 30: Results from time-dependent analysis of $B^0 \to D^{*+}D^{*-}K^0_S$.

Experiment		$N(B\overline{B})$	$\frac{J_c}{J_0}$	$\frac{2J_{s1}}{J_0}\sin(2\beta)$	$\frac{2J_{s2}}{J_0}\cos(2\beta)$
BABAR	[253]	230M	$0.76 \pm 0.18 \pm 0.07$	$0.10 \pm 0.24 \pm 0.06$	$0.38 \pm 0.24 \pm 0.05$
Belle	[254]	449M	$0.60\,^{+0.25}_{-0.28} \pm 0.08$	$-0.17 \pm 0.42 \pm 0.09$	$-0.23\,^{+0.43}_{-0.41} \pm 0.13$
Average			0.71 ± 0.16	0.03 ± 0.21	0.24 ± 0.22
Confidence level			0.63 (0.5σ)	0.59 (0.5σ)	0.23 (1.2σ)

4.4.4 Time-dependent analysis of B^0_s decays through the $b \to c\bar{c}s$ transition

As described in Sec. 4.2.3, time-dependent analysis of decays such as $B^0_s \to J/\psi\phi$ probes the *CP* violating phase of B^0_s–$\overline{B}^0_s$ oscillations, ϕ_s.[41] Within the Standard Model, this parameter is predicted to be small. The combination of results on $B^0_s \to J/\psi\,\phi$ decays, including also results from $B^0_s \to J/\psi\,\pi^+\pi^-$ and $B^0_s \to D^+_s D^-_s$ decays, is performed by the HFAG Lifetimes and Oscillations subgroup, see Sec. 3.

4.5 Time-dependent *CP* asymmetries in colour-suppressed $b \to c\bar{u}d$ transitions

4.5.1 Time-dependent *CP* asymmetries: $b \to c\bar{u}d$ decays to *CP* eigenstates

Decays of B mesons to final states such as $D\pi^0$ are governed by $b \to c\bar{u}d$ transitions. If the final state is a *CP* eigenstate, *e.g.* $D_{CP}\pi^0$, the usual time-dependence formulae are recovered, with the sine coefficient sensitive to $\sin(2\beta)$. Since there is no penguin contribution to these decays, there is even less associated theoretical uncertainty than for $b \to c\bar{c}s$ decays such as $B \to J/\psi\,K^0_S$. Such measurements therefore allow to test the Standard Model prediction that the *CP* violation parameters in $b \to c\bar{u}d$ transitions are the same as those in $b \to c\bar{c}s$ [333].

Note that there is an additional contribution from CKM suppressed $b \to u\bar{c}d$ decays. The effect of this contribution is small, and can be taken into account in the analysis [334, 335].

Results are available from a joint analysis of *BABAR* and Belle data [336]. The following *CP*-even final states are included: $D\pi^0$ and $D\eta$ with $D \to K^0_S\pi^0$ and $D \to K^0_S\omega$; $D\omega$ with $D \to K^0_S\pi^0$; $D^*\pi^0$ and $D^*\eta$ with $D^* \to D\pi^0$ and $D \to K^+K^-$. The following *CP*-odd final

[41] We use ϕ_s here to denote the same quantity labelled $\phi_s^{c\bar{c}s}$ in Sec. 3. It should not be confused with the parameter $\phi_{12} \equiv \arg\left[-M_{12}/\Gamma_{12}\right]$, which historically was also often referred to as ϕ_s.

states are included: $D\pi^0$, $D\eta$ and $D\omega$ with $D \to K^+K^-$, $D^*\pi^0$ and $D^*\eta$ with $D^* \to D\pi^0$ and $D \to K^0_S\pi^0$. All $B^0 \to D^{(*)}h^0$ decays are analysed together, taking into account the different CP factors (denoted $D^{(*)}_{CP}h^0$). The results are summarised in Table 31.

Table 31: Results from analyses of $B^0 \to D^{(*)}h^0$, $D \to CP$ eigenstates decays.

Experiment		$N(B\overline{B})$	S_{CP}	C_{CP}	Correlation
			$D^{(*)}_{CP}h^0$		
BABAR & Belle	[336]	1243M	$0.66 \pm 0.10 \pm 0.06$	$-0.02 \pm 0.07 \pm 0.03$	-0.05

4.5.2 Time-dependent Dalitz plot analyses of $b \to c\bar{u}d$ decays

When multibody D decays, such as $D \to K^0_S\pi^+\pi^-$ are used, a time-dependent analysis of the Dalitz plot of the neutral D decay allows for a direct determination of the weak phase: 2β. (Equivalently, both $\sin(2\beta)$ and $\cos(2\beta)$ can be measured.) This information can be used to resolve the ambiguity in the measurement of 2β from $\sin(2\beta)$ [337].

Results of such analyses are available from both Belle [248] and *BABAR* [249]. The decays $B \to D\pi^0$, $B \to D\eta$, $B \to D\omega$, $B \to D^*\pi^0$ and $B \to D^*\eta$ are used. (This collection of states is denoted by $D^{(*)}h^0$.) The daughter decays are $D^* \to D\pi^0$ and $D \to K^0_S\pi^+\pi^-$. The results are given in Table 32, and shown in Fig. 15. Note that *BABAR* quote uncertainties due to the D decay model separately from other systematic errors as a third source of uncertainty, while Belle do not.

Table 32: Averages from $B^0 \to D^{(*)}h^0$, $D \to K^0_S\pi^+\pi^-$ analyses.

Experiment		$N(B\overline{B})$	$\sin 2\beta$	$\cos 2\beta$	$\lvert\lambda\rvert$
				Model dependent	
BABAR	[249]	383M	$0.29 \pm 0.34 \pm 0.03 \pm 0.05$	$0.42 \pm 0.49 \pm 0.09 \pm 0.13$	$1.01 \pm 0.08 \pm 0.02$
Belle	[248]	386M	$0.78 \pm 0.44 \pm 0.22$	$1.87\,^{+0.40\ +0.22}_{-0.53\ -0.32}$	–
Average			0.45 ± 0.28	1.01 ± 0.40	1.01 ± 0.08
Confidence level			0.59 (0.5σ)	0.12 (1.6σ)	–
				Model independent	
Belle	[250]	772M	$0.43 \pm 0.27 \pm 0.08$	$1.06 \pm 0.33\,^{+0.21}_{-0.15}$	–

Again, it is clear that the data prefer $\cos(2\beta) > 0$. Indeed, Belle [248] determine the sign of $\cos(2\phi_1)$ to be positive at 98.3% confidence level, while *BABAR* [249] favour the solution of β with $\cos(2\beta) > 0$ at 87% confidence level. Note, however, that the Belle measurement has strongly non-Gaussian behaviour. Therefore, we perform uncorrelated averages, from which any interpretation has to be done with the greatest care.

A model-independent time-dependent analysis of $B^0 \to D^{(*)}h^0$ decays, with $D \to K^0_S\pi^+\pi^-$, has been performed by Belle [250]. The decays $B^0 \to D\pi^0$, $B^0 \to D\eta$, $B^0 \to D\eta'$, $B^0 \to D\omega$, $B^0 \to D^*\pi^0$ and $B^0 \to D^*\eta$ are used. The results are also included in Table 32. From

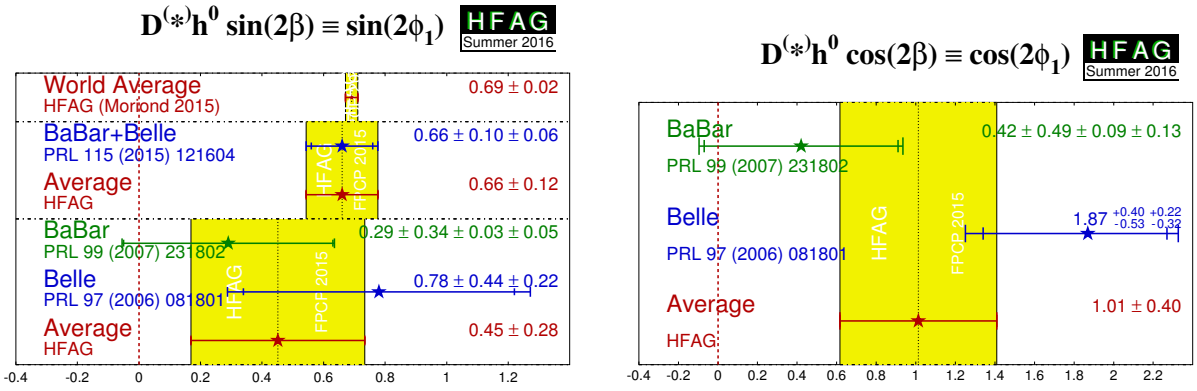

Figure 15: Averages of (left) $\sin(2\beta)$ and (right) $\cos(2\beta)$ measured in colour-suppressed $b \to c\bar{u}d$ transitions.

these results, Belle disfavour the solution with the charmonium-kaon value of $\sin(2\phi_1)$ and a negative value for $\cos(2\phi_1)$, at $5.1\,\sigma$ significance. The solution with the charmonium-kaon value of $\sin(2\phi_1)$ and positive $\cos(2\phi_1)$ is consistent with the data at the level of $1.3\,\sigma$. Note that due to the strong statistical and systematic correlations, model-dependent results and model-independent results from the same experiment cannot be combined.

4.6 Time-dependent *CP* asymmetries in $b \to c\bar{c}d$ transitions

The transition $b \to c\bar{c}d$ can occur via either a $b \to c$ tree or a $b \to d$ penguin amplitude. Similarly to Eq. (151), the amplitude for the $b \to d$ penguin can be written

$$\begin{aligned} A_{b\to d} &= F_u V_{ub}V_{ud}^* + F_c V_{cb}V_{cd}^* + F_t V_{tb}V_{td}^*\,, \\ &= (F_u - F_c)V_{ub}V_{ud}^* \;+\; (F_t - F_c)V_{tb}V_{td}^*\,, \\ &= \quad \mathcal{O}(\lambda^3) \quad\;\; + \quad\;\; \mathcal{O}(\lambda^3)\,. \end{aligned} \tag{149}$$

From this it can be seen that the $b \to d$ penguin amplitude contains terms with different weak phases at the same order of CKM suppression.

In the above, we have chosen to eliminate the F_c term using unitarity. However, we could equally well write

$$\begin{aligned} A_{b\to d} &= (F_u - F_t)V_{ub}V_{ud}^* \;+\; (F_c - F_t)V_{cb}V_{cd}^*\,, \\ &= (F_c - F_u)V_{cb}V_{cd}^* \;+\; (F_t - F_u)V_{tb}V_{td}^*\,. \end{aligned} \tag{150}$$

Since the $b \to c\bar{c}d$ tree amplitude has the weak phase of $V_{cb}V_{cd}^*$, either of the above expressions allow the penguin to be decomposed into parts with weak phases the same and different to the tree amplitude (the relative weak phase can be chosen to be either β or γ). The choice of parametrisation cannot, of course, affect the physics [338]. In any case, if the tree amplitude dominates, there is little sensitivity to any phase other than that from B^0–$\overline{B}^0$ mixing.

The $b \to c\bar{c}d$ transitions can be investigated with studies of various different final states. Results are available from both *BABAR* and Belle using the final states $J/\psi\pi^0$, D^+D^-, $D^{*+}D^{*-}$ and $D^{*\pm}D^{\mp}$, and from LHCb using the final states $J/\psi\rho^0$ and D^+D^-; the averages of these results are given in Tables 33 and 34. The results using the *CP* eigenstate ($\eta = +1$) modes $J/\psi\pi^0$

and D^+D^- are shown in Fig. 16 and Fig. 17 respectively, with two-dimensional constraints shown in Fig. 18.

Results for the vector-vector mode $J/\psi\,\rho^0$ are obtained from a full time-dependent amplitude analysis of $B^0 \to J/\psi\,\pi^+\pi^-$ decays. LHCb [246] find a $J/\psi\,\rho^0$ fit fraction of $65.6 \pm 1.9\%$ and a longitudinal polarisation fraction of $56.7 \pm 1.8\%$ (uncertainties are statistical only; both results are consistent with those from a time-integrated amplitude analysis [255] where systematic uncertainties were also evaluated). Fits are performed to obtain $2\beta^{\rm eff}$ in the cases that all transversity amplitudes are assumed to have the same *CP* violation parameter. A separate fit is performed allowing different parameters. The results in the former case are presented in terms of S_{CP} and C_{CP} in Table 34.

The vector-vector mode $D^{*+}D^{*-}$ is found to be dominated by the *CP*-even longitudinally polarised component; *BABAR* measures a *CP*-odd fraction of $0.158 \pm 0.028 \pm 0.006$ [247] while Belle measures a *CP*-odd fraction of $0.125 \pm 0.043 \pm 0.023$ [339]. These values, listed as $R_\perp$, are included in the averages which ensures that the correlations are taken into account.[42] *BABAR* has also performed an additional fit in which the *CP*-even and *CP*-odd components are allowed to have different *CP* violation parameters S and C. These results are included in Table 34. Results using $D^{*+}D^{*-}$ are shown in Fig. 19.

As discussed in Sec. 4.2.6, the most recent papers on the non-*CP* eigenstate mode $D^{*\pm}D^{\mp}$ use the (A, S, ΔS, C, ΔC) set of parameters, and we therefore perform the averages with this choice.

Table 33: Averages for the $b \to c\bar{c}d$ modes, $B^0 \to J/\psi\pi^0$ and D^+D^-.

Experiment		Sample size	S_{CP}	C_{CP}	Correlation
			$J/\psi\pi^0$		
BABAR	[340]	$N(B\overline{B}) = 466$M	$-1.23 \pm 0.21 \pm 0.04$	$-0.20 \pm 0.19 \pm 0.03$	0.20
Belle	[341]	$N(B\overline{B}) = 535$M	$-0.65 \pm 0.21 \pm 0.05$	$-0.08 \pm 0.16 \pm 0.05$	-0.10
Average			-0.93 ± 0.15	-0.10 ± 0.13	0.04
Confidence level			0.15 (1.4σ)		
			D^+D^-		
BABAR	[247]	$N(B\overline{B}) = 467$M	$-0.65 \pm 0.36 \pm 0.05$	$-0.07 \pm 0.23 \pm 0.03$	-0.01
Belle	[275]	$N(B\overline{B}) = 772$M	$-1.06\,^{+0.21}_{-0.14} \pm 0.08$	$-0.43 \pm 0.16 \pm 0.05$	-0.12
LHCb	[342]	$\int \mathcal{L}\,dt = 3\,\text{fb}^{-1}$	$-0.54\,^{+0.17}_{-0.16} \pm 0.05$	$0.26\,^{+0.18}_{-0.17} \pm 0.02$	0.48
Average			-0.84 ± 0.12	-0.13 ± 0.10	0.18
Confidence level			0.027 (2.2σ)		

In the absence of the penguin contribution (tree dominance), the time-dependent parameters would be given by $S_{b\to c\bar{c}d} = -\eta \sin(2\beta)$, $C_{b\to c\bar{c}d} = 0$, $S_{+-} = \sin(2\beta + \delta)$, $S_{-+} = \sin(2\beta - \delta)$, $C_{+-} = -C_{-+}$ and $\mathcal{A} = 0$, where δ is the strong phase difference between the $D^{*+}D^-$ and $D^{*-}D^+$ decay amplitudes. In the presence of the penguin contribution, there is no clean interpretation in terms of CKM parameters, however direct *CP* violation may be observed as any of $C_{b\to c\bar{c}d} \neq 0$, $C_{+-} \neq -C_{-+}$ or $A_{+-} \neq 0$.

[42] Note that the *BABAR* value given in Table 34 differs from the value quoted here, since that in the table is not corrected for efficiency.

Table 34: Averages for the $b \to c\bar{c}d$ modes, $J/\psi\,\rho^0$, $D^{*+}D^{*-}$ and $D^{*\pm}D^{\mp}$.

Experiment		$N(B\overline{B})$	S_{CP}	C_{CP}	$R_\perp$
			$J/\psi\,\rho^0$		
LHCb	[246]	3 fb^{-1}	$-0.66\,^{+0.13\ +0.09}_{-0.12\ -0.03}$	$-0.06 \pm 0.06\,^{+0.02}_{-0.01}$	0.198 ± 0.017
			$D^{*+}D^{*-}$		
BABAR	[247]	467M	$-0.70 \pm 0.16 \pm 0.03$	$0.05 \pm 0.09 \pm 0.02$	0.17 ± 0.03
BABAR part. rec.	[343]	471M	$-0.49 \pm 0.18 \pm 0.07 \pm 0.04$	$0.15 \pm 0.09 \pm 0.04$	—
Belle	[344]	772M	$-0.79 \pm 0.13 \pm 0.03$	$-0.15 \pm 0.08 \pm 0.02$	$0.14 \pm 0.02 \pm 0.01$
Average			-0.71 ± 0.09	-0.01 ± 0.05	0.15 ± 0.02
Confidence level				0.72 (0.4σ)	

Experiment		$N(B\overline{B})$	S_{CP+}	C_{CP+}	S_{CP-}	C_{CP-}	$R_\perp$
				$D^{*+}D^{*-}$			
BABAR	[247]	467M	$-0.76 \pm 0.16 \pm 0.04$	$0.02 \pm 0.12 \pm 0.02$	$-1.81 \pm 0.71 \pm 0.16$	$0.41 \pm 0.50 \pm 0.08$	0.15 ± 0.03

Experiment		$N(B\overline{B})$	S	C	ΔS	ΔC	$\mathcal{A}$
				$D^{*\pm}D^{\mp}$			
BABAR	[247]	467M	$-0.68 \pm 0.15 \pm 0.04$	$0.04 \pm 0.12 \pm 0.03$	$0.05 \pm 0.15 \pm 0.02$	$0.04 \pm 0.12 \pm 0.03$	$0.01 \pm 0.05 \pm 0.01$
Belle	[275]	772M	$-0.78 \pm 0.15 \pm 0.05$	$-0.01 \pm 0.11 \pm 0.04$	$-0.13 \pm 0.15 \pm 0.04$	$0.12 \pm 0.11 \pm 0.03$	$0.06 \pm 0.05 \pm 0.02$
Average			-0.73 ± 0.11	0.01 ± 0.09	-0.04 ± 0.11	0.08 ± 0.08	0.03 ± 0.04
Confidence level			0.65 (0.5σ)	0.77 (0.3σ)	0.41 (0.8σ)	0.63 (0.5σ)	0.48 (0.7σ)

The averages for the $b \to c\bar{c}d$ modes are shown in Figs. 20 and 21. Results are consistent with tree dominance, and with the Standard Model, though the Belle results in $B^0 \to D^+D^-$ [345] show an indication of CP violation in decay, and hence a non-zero penguin contribution. The average of $S_{b\to c\bar{c}d}$ in each of the $J/\psi\pi^0$, D^+D^- and $D^{*+}D^{*-}$ final states is more than 5σ from zero, corresponding to observations of CP violation in these decay channels. Possible non-Gaussian effects due to some of the inputs measurements being outside the physical region ($S_{CP}^2 + C_{CP}^2 \leq 1$) should, however, be borne in mind.

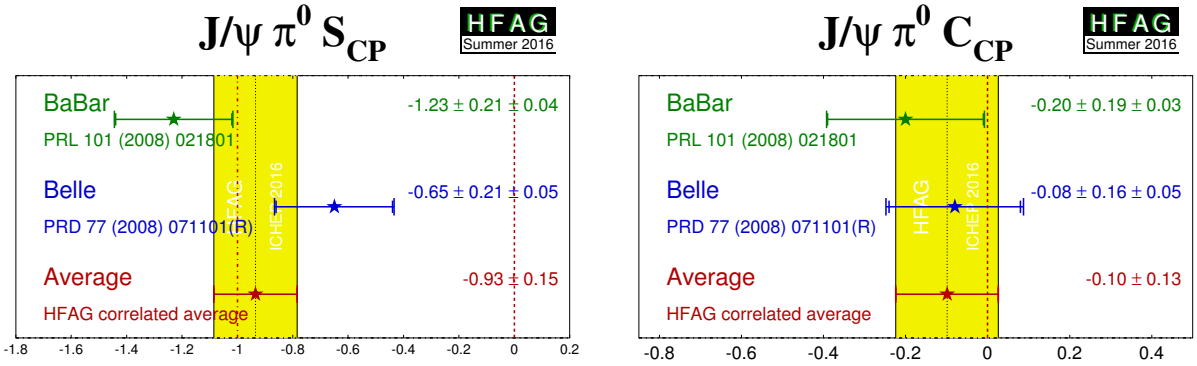

Figure 16: Averages of (left) $S_{b\to c\bar{c}d}$ and (right) $C_{b\to c\bar{c}d}$ for the mode $B^0 \to J/\psi\pi^0$.

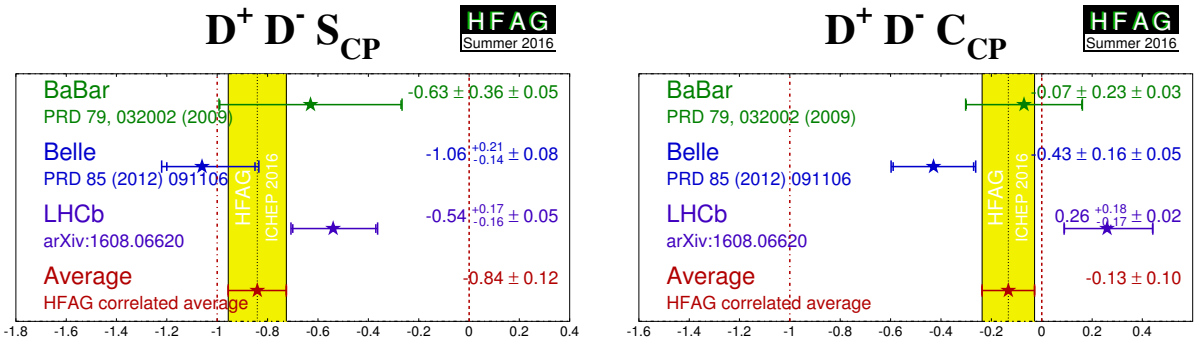

Figure 17: Averages of (left) $S_{b\to c\bar{c}d}$ and (right) $C_{b\to c\bar{c}d}$ for the mode $B^0 \to D^+D^-$.

4.6.1 Time-dependent CP asymmetries in B_s^0 decays mediated by $b \to c\bar{c}d$ transitions

Time-dependent CP asymmetries in B_s^0 decays mediated by $b \to c\bar{c}d$ transitions provide a determination of $2\beta_s^{\rm eff}$ where possible effects from penguin amplitudes may cause a shift from the value of $2\beta_s$ seen in $b \to c\bar{c}s$ transitions. Results in the $b \to c\bar{c}d$ case, with larger penguin effects, can be used together with flavour symmetries to derive limits on the possible size of penguin effects in the $b \to c\bar{c}s$ transitions [346, 347]. If the penguin effect is large, it may also be possible to determine $\gamma \equiv \phi_3$.

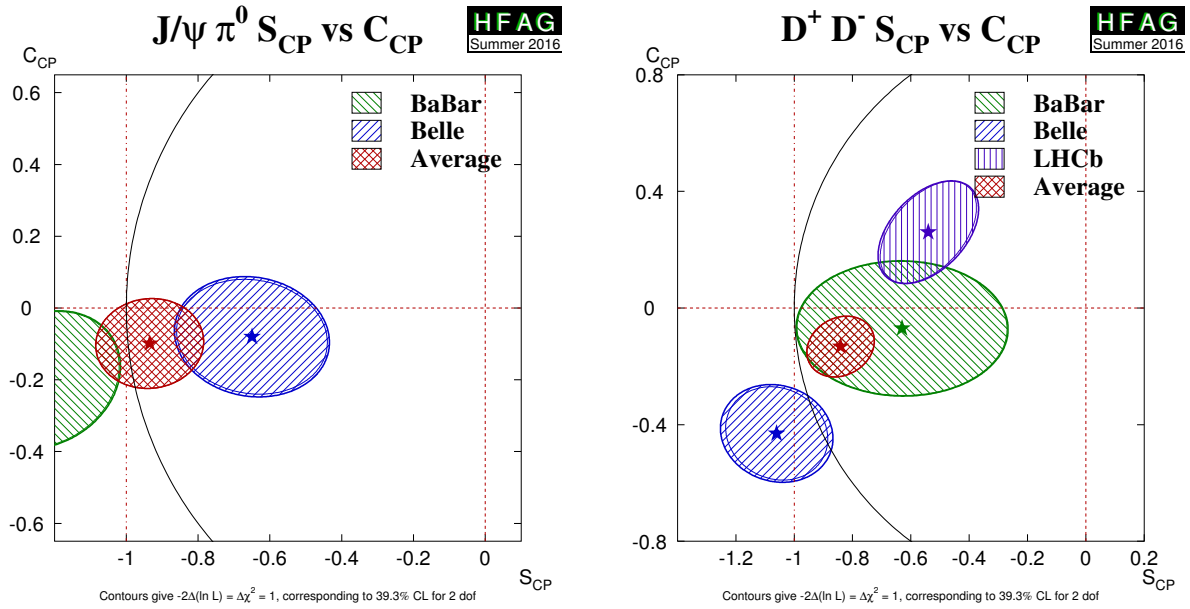

Figure 18: Averages of two $b \to c\bar{c}d$ dominated channels, for which correlated averages are performed, in the S_{CP} *vs.* C_{CP} plane. (Left) $B^0 \to J/\psi\pi^0$ and (right) $B^0 \to D^+D^-$.

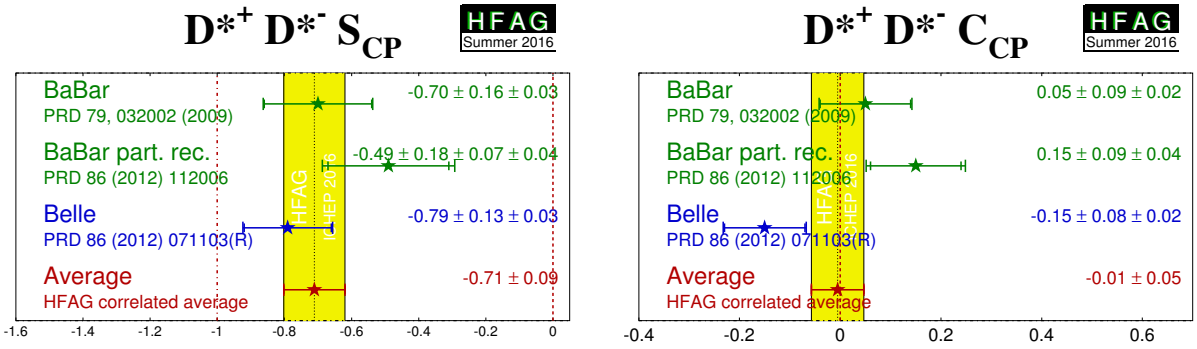

Figure 19: Averages of (left) $S_{b\to c\bar{c}d}$ and (right) $C_{b\to c\bar{c}d}$ for the mode $B^0 \to D^{*+}D^{*-}$.

The parameters have been measured in $B_s^0 \to J/\psi K_S^0$ decays by LHCb, as summarised in Table 35. The results supersede an earlier measurement of the effective lifetime, which is directly related to $A^{\Delta\Gamma}$, in the same mode [122], which is discussed in Sec. 3.

Table 35: Averages for measurements of *CP* violation paramters from $B_s^0 \to J/\psi K_S^0$.

Experiment		$\int \mathcal{L}\, dt$	S_{CP}	C_{CP}	$A^{\Delta\Gamma}$
LHCb	[348]	3fb^{-1}	$0.49\,^{+0.77}_{-0.65} \pm 0.06$	$-0.28 \pm 0.41 \pm 0.08$	$-0.08 \pm 0.40 \pm 0.08$

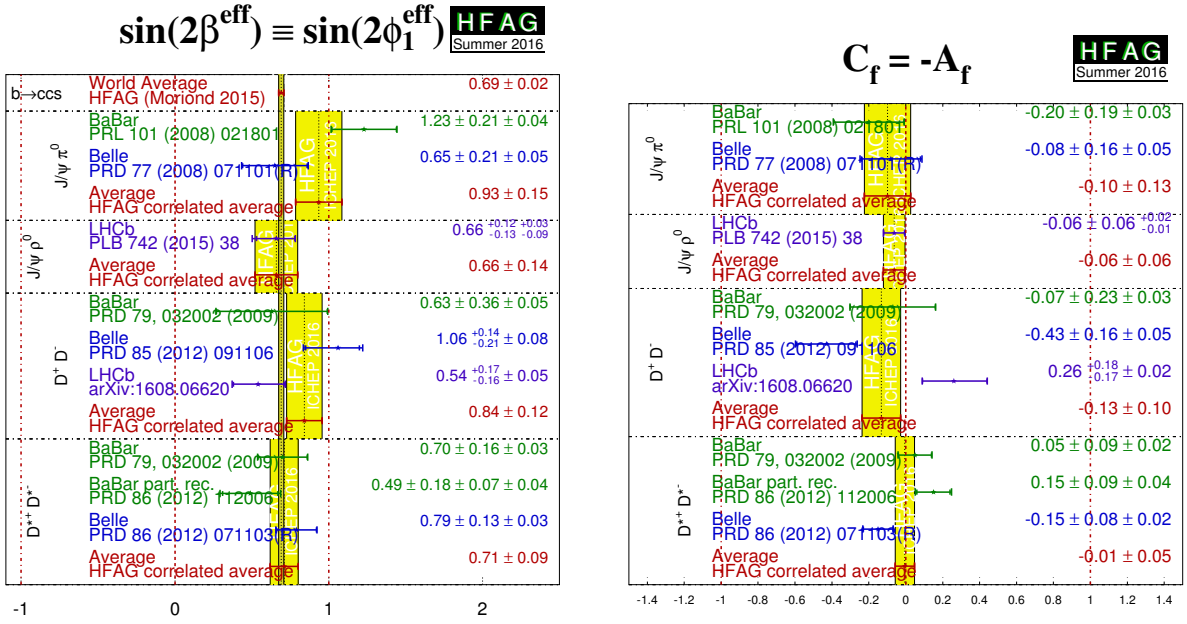

Figure 20: Averages of (left) $-\eta S_{b\to c\bar{c}d}$ and (right) $C_{b\to c\bar{c}d}$. The $-\eta S_{b\to q\bar{q}s}$ figure compares the results to the world average for $-\eta S_{b\to c\bar{c}s}$ (see Sec. 4.4.1).

4.7 Time-dependent *CP* asymmetries in charmless $b \to q\bar{q}s$ transitions

The flavour changing neutral current $b \to s$ penguin can be mediated by any up-type quark in the loop, and hence the amplitude can be written as

$$\begin{aligned} A_{b\to s} &= F_u V_{ub} V_{us}^* + F_c V_{cb} V_{cs}^* + F_t V_{tb} V_{ts}^* \,, \\ &= (F_u - F_c) V_{ub} V_{us}^* \;+\; (F_t - F_c) V_{tb} V_{ts}^* \,, \\ &= \quad \mathcal{O}(\lambda^4) \quad + \quad \mathcal{O}(\lambda^2) \,, \end{aligned} \tag{151}$$

using the unitarity of the CKM matrix to eliminate the F_c term. Therefore, in the Standard Model, this amplitude is dominated by $V_{tb}V_{ts}^*$, and to within a few degrees ($\delta\beta \lesssim 2^\circ$ for $\beta \approx 20^\circ$) the time-dependent parameters can be written[43] $S_{b\to q\bar{q}s} \approx -\eta \sin(2\beta)$, $C_{b\to q\bar{q}s} \approx 0$, assuming $b \to s$ penguin contributions only ($q = u, d, s$).

Due to the suppression of the Standard Model amplitude, contributions of additional diagrams from physics beyond the Standard Model, with heavy virtual particles in the penguin loops, may have observable effects. In general, these contributions will affect the values of $S_{b\to q\bar{q}s}$ and $C_{b\to q\bar{q}s}$. A discrepancy between the values of $S_{b\to c\bar{c}s}$ and $S_{b\to q\bar{q}s}$ can therefore provide a clean indication of new physics [333, 349–351].

However, there is an additional consideration to take into account. The above argument assumes that only the $b \to s$ penguin contributes to the $b \to q\bar{q}s$ transition. For $q = s$ this

[43] The presence of a small ($\mathcal{O}(\lambda^2)$) weak phase in the dominant amplitude of the s penguin decays introduces a phase shift given by $S_{b\to q\bar{q}s} = -\eta \sin(2\beta) \cdot (1 + \Delta)$. Using the CKMfitter results for the Wolfenstein parameters [240], one finds: $\Delta \simeq 0.033$, which corresponds to a shift of 2β of $+2.1$ degrees. Nonperturbative contributions can alter this result.

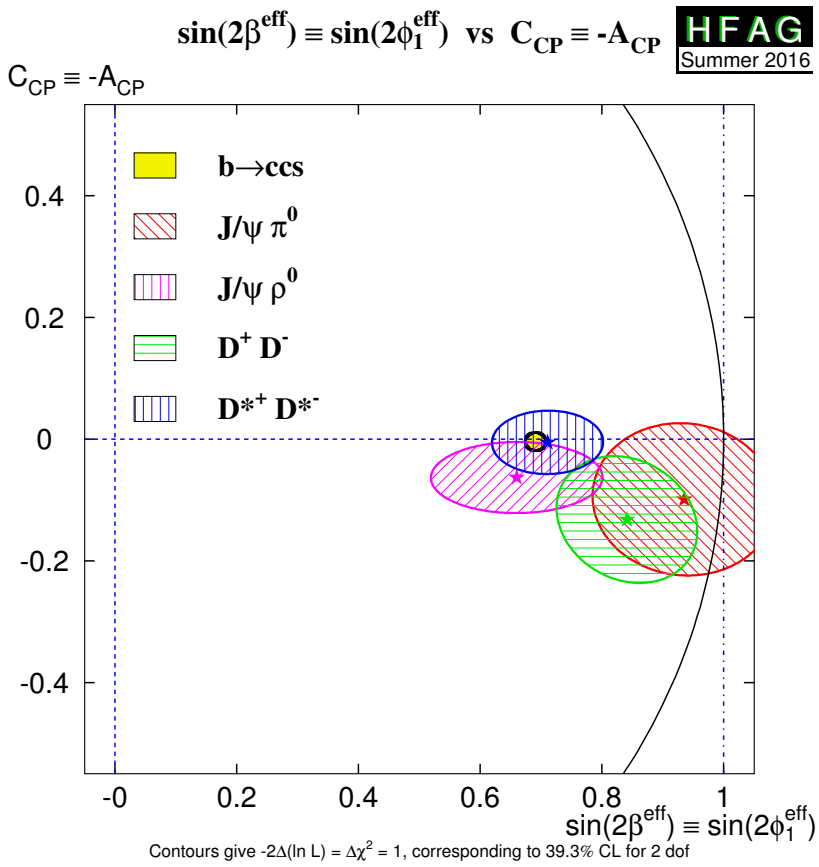

Figure 21: Compilation of constraints in the $-\eta S_{b\to c\bar{c}d}$ *vs.* $C_{b\to c\bar{c}d}$ plane.

is a good assumption, which neglects only rescattering effects. However, for $q = u$ there is a colour-suppressed $b \to u$ tree diagram (of order $\mathcal{O}(\lambda^4)$), which has a different weak (and possibly strong) phase. In the case $q = d$, any light neutral meson that is formed from $d\overline{d}$ also has a $u\overline{u}$ component, and so again there is "tree pollution". The B^0 decays to $\pi^0 K^0_S$, $\rho^0 K^0_S$ and ωK^0_S belong to this category. The mesons ϕ, f_0 and η' are expected to have predominant $s\overline{s}$ parts, which reduces the relative size of the possible tree pollution. If the inclusive decay $B^0 \to K^+K^-K^0$ (excluding ϕK^0) is dominated by a nonresonant three-body transition, an OZI-rule suppressed tree-level diagram can occur through insertion of an $s\overline{s}$ pair. The corresponding penguin-type transition proceeds via insertion of a $u\overline{u}$ pair, which is expected to be favoured over the $s\overline{s}$ insertion by fragmentation models. Neglecting rescattering, the final state $K^0\overline{K}^0K^0$ (reconstructed as $K^0_SK^0_SK^0_S$) has no tree pollution [352]. Various estimates, using different theoretical approaches, of the values of $\Delta S = S_{b\to q\bar{q}s} - S_{b\to c\bar{c}s}$ exist in the literature [353–366]. In general, there is agreement that the modes ϕK^0, $\eta' K^0$ and $K^0\overline{K}^0K^0$ are the cleanest, with values of $|\Delta S|$ at or below the few percent level (ΔS is usually predicted to be positive).

4.7.1 Time-dependent *CP* asymmetries: $b \to q\bar{q}s$ decays to *CP* eigenstates

The averages for $-\eta S_{b\to q\bar{q}s}$ and $C_{b\to q\bar{q}s}$ can be found in Table 36, and are shown in Figs. 22, 23 and 24. Results from both *BABAR* and Belle are averaged for the modes $\eta' K^0$ (K^0 indicates that

both K^0_S and K^0_L are used) $K^0_S K^0_S K^0_S$, $\pi^0 K^0_S$ and ωK^0_S.[44] Results on ϕK^0_S and $K^+K^-K^0_S$ (implicitly excluding ϕK^0_S and $f_0 K^0_S$) are taken from time-dependent Dalitz plot analyses of $K^+K^-K^0_S$; results on $\rho^0 K^0_S$, $f_2 K^0_S$, $f_X K^0_S$ and $\pi^+\pi^- K^0_S$ nonresonant are taken from time-dependent Dalitz plot analyses of $\pi^+\pi^- K^0_S$ (see Sec. 4.7.2). The results on $f_0 K^0_S$ are from combinations of both Dalitz plot analyses. *BABAR* has also presented results with the final states $\pi^0\pi^0 K^0_S$ and $\phi K^0_S \pi^0$.

Of these final states, ϕK^0_S, $\eta' K^0_S$, $\pi^0 K^0_S$, $\rho^0 K^0_S$, ωK^0_S and $f_0 K^0_L$ have *CP* eigenvalue $\eta = -1$, while ϕK^0_L, $\eta' K^0_L$, $K^0_S K^0_S K^0_S$, $f_0 K^0_S$, $f_2 K^0_S$, $f_X K^0_S$, $\pi^0\pi^0 K^0_S$ and $\pi^+\pi^- K^0_S$ nonresonant have $\eta = +1$. The final state $K^+K^-K^0_S$ (with ϕK^0_S and $f_0 K^0_S$ implicitly excluded) is not a *CP* eigenstate, but the *CP*-content can be absorbed in the amplitude analysis to allow the determination of a single effective S parameter. (In earlier analyses of the $K^+K^-K^0$ final state, its *CP* composition was determined using an isospin argument [368] and a moments analysis [369].) Throughout this section, $f_0 \equiv f_0(980)$ and $f_2 \equiv f_2(1270)$. Details of the assumed lineshapes of these states, and of the f_X (which is taken to have even spin), can be found in the relevant experimental papers [258, 259, 262, 263].

The final state $\phi K^0_S \pi^0$ is also not a *CP* eigenstate but its *CP*-composition can be determined from an angular analysis. Since the parameters are common to the $B^0 \to \phi K^0_S \pi^0$ and $B^0 \to \phi K^+\pi^-$ decays (because only $K\pi$ resonances contribute), *BABAR* perform a simultaneous analysis of the two final states [376] (see Sec. 4.7.3).

It must be noted that Q2B parameters extracted from Dalitz plot analyses are constrained to lie within the physical boundary ($S^2_{CP} + C^2_{CP} < 1$) and consequently the obtained errors are highly non-Gaussian when the central value is close to the boundary. This is particularly evident in the *BABAR* results for $B^0 \to f_0 K^0$ with $f_0 \to \pi^+\pi^-$ [262]. These results must be treated with extreme caution.

As explained above, each of the modes listed in Table 36 has potentially different subleading contributions within the Standard Model, and thus each may have a different value of $-\eta S_{b\to q\bar{q}s}$. Therefore, there is no strong motivation to make a combined average over the different modes. We refer to such an average as a "naïve s-penguin average." It is naïve not only because of the theoretical uncertainties are neglected, but also since possible correlations of systematic effects between different modes are not included. In spite of these caveats there remains interest in the value of this quantity and therefore it is given here: $\langle -\eta S_{b\to q\bar{q}s} \rangle = 0.655 \pm 0.032$, with confidence level 0.77 (0.3σ). This value is in agreement with the average $-\eta S_{b\to c\bar{c}s}$ given in Sec. 4.4.1. (The average for $C_{b\to q\bar{q}s}$ is $\langle C_{b\to q\bar{q}s} \rangle = -0.006 \pm 0.026$ with confidence level 0.53 (0.6σ).) We emphasise again that we do not advocate the use of these averages.

From Table 36 it may be noted that the averages for $-\eta S_{b\to q\bar{q}s}$ in ϕK^0_S, $\eta' K^0$, $f_0 K^0_S$ and $K^+K^-K^0_S$ are all now more than 5σ away from zero, so that *CP* violation in these modes can be considered well established. There is no evidence (above 2σ) for *CP* violation in any $b \to q\bar{q}s$ decay.

4.7.2 Time-dependent Dalitz plot analyses: $B^0 \to K^+K^-K^0$ and $B^0 \to \pi^+\pi^- K^0_S$

As mentioned in Sec. 4.2.5 and above, both *BABAR* and Belle have performed time-dependent Dalitz plot analysis of $B^0 \to K^+K^-K^0$ and $B^0 \to \pi^+\pi^- K^0_S$ decays. The results are summarised in Tables 38 and 39. Averages for the $B^0 \to f_0 K^0_S$ decay, which contributes to both Dalitz plots, are shown in Fig. 25. Results are presented in terms of the effective weak phase (from mixing

[44] Belle [367] include the $\pi^0 K^0_L$ final state together with $\pi^0 K^0_S$ in order to improve the constraint on the parameter of *CP* violation in decay; these events cannot be used for time-dependent analysis.

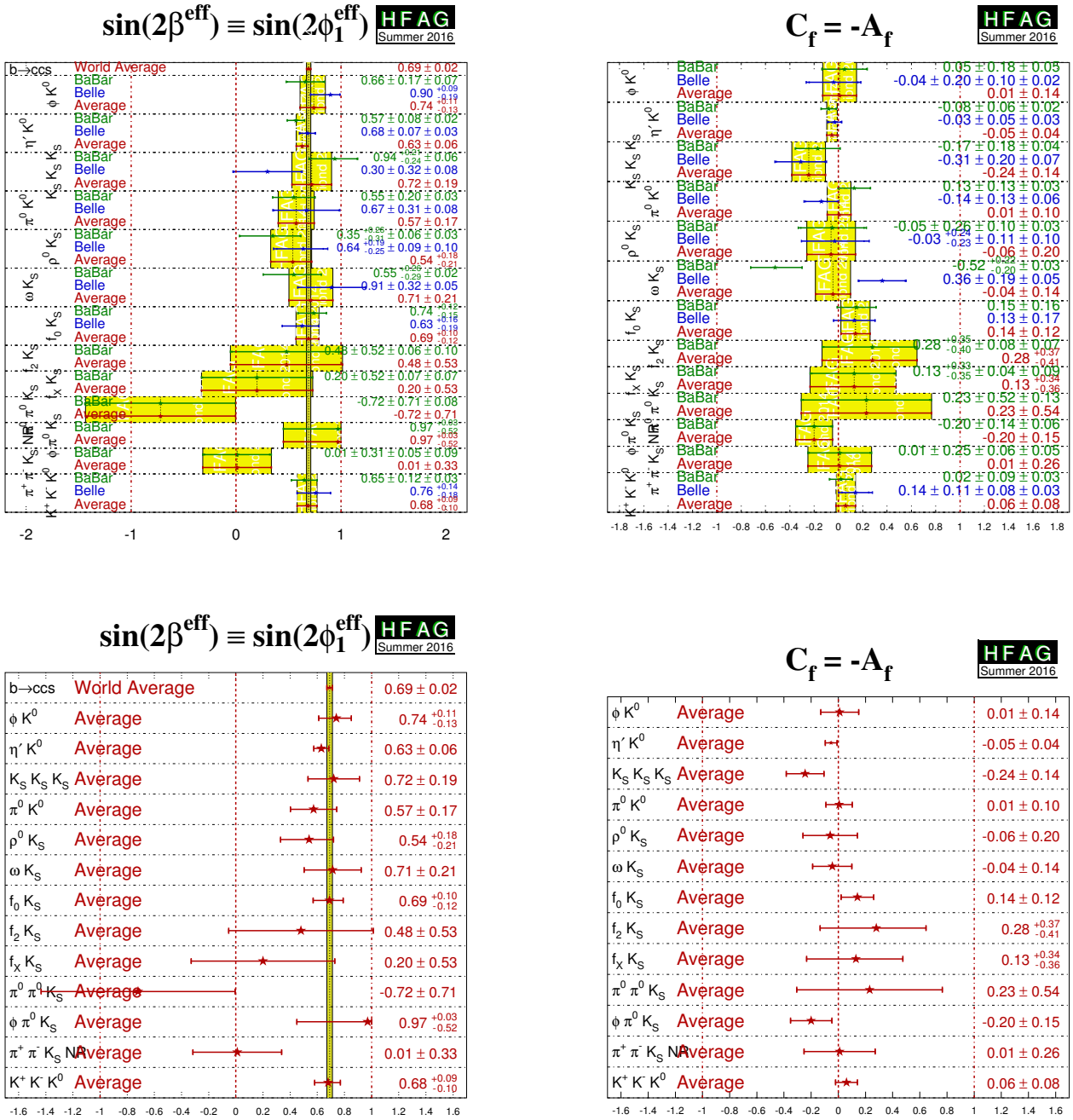

Figure 22: (Top) Averages of (left) $-\eta S_{b\to q\bar{q}s}$ and (right) $C_{b\to q\bar{q}s}$. The $-\eta S_{b\to q\bar{q}s}$ figure compares the results to the world average for $-\eta S_{b\to c\bar{c}s}$ (see Sec. 4.4.1). (Bottom) Same, but only averages for each mode are shown. More figures are available from the HFAG web pages.

Table 36: Averages of $-\eta S_{b\to q\bar{q}s}$ and $C_{b\to q\bar{q}s}$. Where a third source of uncertainty is given, it is due to model uncertainties arising in Dalitz plot analyses.

Experiment		$N(B\overline{B})$	$-\eta S_{b\to q\bar{q}s}$	$C_{b\to q\bar{q}s}$	Correlation
			ϕK^0		
BABAR	[259]	470M	$0.66 \pm 0.17 \pm 0.07$	$0.05 \pm 0.18 \pm 0.05$	–
Belle	[258]	657M	$0.90\,^{+0.09}_{-0.19}$	$-0.04 \pm 0.20 \pm 0.10 \pm 0.02$	–
Average			$0.74\,^{+0.11}_{-0.13}$	0.01 ± 0.14	uncorrelated averages
			$\eta' K^0$		
BABAR	[370]	467M	$0.57 \pm 0.08 \pm 0.02$	$-0.08 \pm 0.06 \pm 0.02$	0.03
Belle	[371]	772M	$0.68 \pm 0.07 \pm 0.03$	$-0.03 \pm 0.05 \pm 0.03$	0.03
Average			0.63 ± 0.06	-0.05 ± 0.04	0.02
Confidence level			0.53 (0.6σ)		
			$K^0_S K^0_S K^0_S$		
BABAR	[372]	468M	$0.94\,^{+0.21}_{-0.24} \pm 0.06$	$-0.17 \pm 0.18 \pm 0.04$	0.16
Belle	[373]	535M	$0.30 \pm 0.32 \pm 0.08$	$-0.31 \pm 0.20 \pm 0.07$	–
Average			0.72 ± 0.19	-0.24 ± 0.14	0.09
Confidence level			0.26 (1.1σ)		
			$\pi^0 K^0$		
BABAR	[370]	467M	$0.55 \pm 0.20 \pm 0.03$	$0.13 \pm 0.13 \pm 0.03$	0.06
Belle	[367]	657M	$0.67 \pm 0.31 \pm 0.08$	$-0.14 \pm 0.13 \pm 0.06$	-0.04
Average			0.57 ± 0.17	0.01 ± 0.10	0.02
Confidence level			0.37 (0.9σ)		
			$\rho^0 K^0_S$		
BABAR	[262]	383M	$0.35\,^{+0.26}_{-0.31} \pm 0.06 \pm 0.03$	$-0.05 \pm 0.26 \pm 0.10 \pm 0.03$	–
Belle	[263]	657M	$0.64\,^{+0.19}_{-0.25} \pm 0.09 \pm 0.10$	$-0.03\,^{+0.24}_{-0.23} \pm 0.11 \pm 0.10$	–
Average			$0.54\,^{+0.18}_{-0.21}$	-0.06 ± 0.20	uncorrelated averages
			ωK^0_S		
BABAR	[370]	467M	$0.55\,^{+0.26}_{-0.29} \pm 0.02$	$-0.52\,^{+0.22}_{-0.20} \pm 0.03$	0.03
Belle	[374]	772M	$0.91 \pm 0.32 \pm 0.05$	$0.36 \pm 0.19 \pm 0.05$	-0.00
Average			0.71 ± 0.21	-0.04 ± 0.14	0.01
Confidence level			0.007 (2.7σ)		
			$f_0 K^0$		
BABAR	[259, 262]	–	$0.74\,^{+0.12}_{-0.15}$	0.15 ± 0.16	–
Belle	[258, 263]	–	$0.63\,^{+0.16}_{-0.19}$	0.13 ± 0.17	–
Average			$0.69\,^{+0.10}_{-0.12}$	0.14 ± 0.12	uncorrelated averages
			$f_2 K^0_S$		
BABAR	[262]	383M	$0.48 \pm 0.52 \pm 0.06 \pm 0.10$	$0.28\,^{+0.35}_{-0.40} \pm 0.08 \pm 0.07$	–
			$f_X K^0_S$		
BABAR	[262]	383M	$0.20 \pm 0.52 \pm 0.07 \pm 0.07$	$0.13\,^{+0.33}_{-0.35} \pm 0.04 \pm 0.09$	–

and decay) difference $\beta^{\rm eff}$ and the parameter of *CP* violation in decay $\mathcal{A}$ ($\mathcal{A} = -C$) for each of the resonant contributions. Note that Dalitz plot analyses, including all those included in these averages, often suffer from ambiguous solutions – we quote the results corresponding to those presented as solution 1 in all cases. Results on flavour specific amplitudes that may contribute to these Dalitz plots (such as $K^{*+}\pi^-$) are averaged by the HFAG Rare Decays subgroup (Sec. 7).

For the $B^0 \to K^+K^-K^0$ decay, both *BABAR* and Belle measure the *CP* violation parameters

Table 37: Averages of $-\eta S_{b\to q\bar{q}s}$ and $C_{b\to q\bar{q}s}$ (continued). Where a third source of uncertainty is given, it is due to model uncertainties arising in Dalitz plot analyses.

Experiment	$N(B\overline{B})$	$-\eta S_{b\to q\bar{q}s}$	$C_{b\to q\bar{q}s}$	Correlation
		$\pi^0\pi^0 K^0_S$		
BABAR [375]	227M	$-0.72 \pm 0.71 \pm 0.08$	$0.23 \pm 0.52 \pm 0.13$	-0.02
		$\phi K^0_S \pi^0$		
BABAR [376]	465M	$0.97\,^{+0.03}_{-0.52}$	$-0.20 \pm 0.14 \pm 0.06$	–
		$\pi^+\pi^- K^0_S$ nonresonant		
BABAR [262]	383M	$0.01 \pm 0.31 \pm 0.05 \pm 0.09$	$0.01 \pm 0.25 \pm 0.06 \pm 0.05$	–
		$K^+K^-K^0$		
BABAR [259]	470M	$0.65 \pm 0.12 \pm 0.03$	$0.02 \pm 0.09 \pm 0.03$	–
Belle [258]	657M	$0.76\,^{+0.14}_{-0.18}$	$0.14 \pm 0.11 \pm 0.08 \pm 0.03$	–
Average		$0.68\,^{+0.09}_{-0.10}$	0.06 ± 0.08	uncorrelated averages

for the ϕK^0, $f_0 K^0$ and "other $K^+K^-K^0$" amplitudes, where the latter includes all remaining resonant and nonresonant contributions to the charmless three-body decay. For the $B^0 \to \pi^+\pi^- K^0_S$ decay, *BABAR* report *CP* violation parameters for all of the *CP* eigenstate components in the Dalitz plot model ($\rho^0\ K^0_S$, $f_0 K^0_S$, $f_2 K^0_S$, $f_X K^0_S$ and nonresonant decays[45]), while Belle report the *CP* violation parameters for only the $\rho^0\ K^0_S$ and $f_0 K^0_S$ amplitudes, although the used Dalitz plot model is rather similar.

4.7.3 Time-dependent analyses of $B^0 \to \phi K^0_S \pi^0$

The final state in the decay $B^0 \to \phi K^0_S \pi^0$ is a mixture of *CP*-even and *CP*-odd amplitudes. However, since only ϕK^{*0} resonant states contribute (in particular, $\phi K^{*0}(892)$, $\phi K^{*0}_0(1430)$ and $\phi K^{*0}_2(1430)$ are seen), the composition can be determined from the analysis of $B \to \phi K^+\pi^-$, assuming only that the ratio of branching fractions $\mathcal{B}(K^{*0} \to K^0_S\pi^0)/\mathcal{B}(K^{*0} \to K^+\pi^-)$ is the same for each exited kaon state.

BABAR [376] have performed a simultaneous analysis of $B^0 \to \phi K^0_S \pi^0$ and $B^0 \to \phi K^+\pi^-$ that is time-dependent for the former mode and time-integrated for the latter. Such an analysis allows, in principle, all parameters of the $B^0 \to \phi K^{*0}$ system to be determined, including mixing-induced *CP* violation effects. The latter is determined to be $\Delta\phi_{00} = 0.28 \pm 0.42 \pm 0.04$, where $\Delta\phi_{00}$ is half the weak phase difference between B^0 and $\overline{B}^0$ decays to $\phi K^{*0}_0(1430)$. As discussed above, this can also be presented in terms of the Q2B parameter $\sin(2\beta^{\rm eff}_{00}) = \sin(2\beta + 2\Delta\phi_{00}) = 0.97\,^{+0.03}_{-0.52}$. The highly asymmetric uncertainty arises due to the conversion from the phase to the sine of the phase, and the proximity of the physical boundary.

Similar $\sin(2\beta^{\rm eff})$ parameters can be defined for each of the helicity amplitudes for both $\phi K^{*0}(892)$ and $\phi K^{*0}_2(1430)$. However, the relative phases between these decays are constrained due to the nature of the simultaneous analysis of $B^0 \to \phi K^0_S\pi^0$ and $B^0 \to \phi K^+\pi^-$, and therefore these measurements are highly correlated. Instead of quoting all these results, *BABAR* provide

[45] The f_X resonance included in the model is a poorly understood excess in the $m(\pi^+\pi^-)$ distribution, that may originate from interference between other states in this region and nonresonant amplitudes.

Table 38: Results from time-dependent Dalitz plot analyses of the $B^0 \to K^+K^-K^0$ decay. Correlations (not shown) are taken into account in the average.

Experiment	$N(B\overline{B})$	ϕK^0_S		$f_0 K^0_S$		$K^+K^-K^0_S$	
		$\beta^{\rm eff}$ (°)	$\mathcal{A}$	$\beta^{\rm eff}$ (°)	$\mathcal{A}$	$\beta^{\rm eff}$ (°)	$\mathcal{A}$
BABAR [259]	470M	$21 \pm 6 \pm 2$	$-0.05 \pm 0.18 \pm 0.05$	$18 \pm 6 \pm 4$	$-0.28 \pm 0.24 \pm 0.09$	$20.3 \pm 4.3 \pm 1.2$	$-0.02 \pm 0.09 \pm 0.03$
Belle [258]	657M	$32.2 \pm 9.0 \pm 2.6 \pm 1.4$	$0.04 \pm 0.20 \pm 0.10 \pm 0.02$	$31.3 \pm 9.0 \pm 3.4 \pm 4.0$	$-0.30 \pm 0.29 \pm 0.11 \pm 0.09$	$24.9 \pm 6.4 \pm 2.1 \pm 2.5$	$-0.14 \pm 0.11 \pm 0.08 \pm 0.03$
Average		24 ± 5	-0.01 ± 0.14	22 ± 6	-0.29 ± 0.20	21.6 ± 3.7	-0.06 ± 0.08
Confidence level				0.93 (0.1σ)			

Table 39: Results from time-dependent Dalitz plot analysis of the $B^0 \to \pi^+\pi^- K^0_S$ decay. Correlations (not shown) are taken into account in the average.

Experiment	$N(B\overline{B})$	$\rho^0 K^0_S$		$f_0 K^0_S$	
		$\beta^{\rm eff}$	$\mathcal{A}$	$\beta^{\rm eff}$	$\mathcal{A}$
BABAR [262]	383M	$(10.2 \pm 8.9 \pm 3.0 \pm 1.9)^\circ$	$0.05 \pm 0.26 \pm 0.10 \pm 0.03$	$(36.0 \pm 9.8 \pm 2.1 \pm 2.1)^\circ$	$-0.08 \pm 0.19 \pm 0.03 \pm 0.04$
Belle [263]	657M	$(20.0\,^{+8.6}_{-8.5} \pm 3.2 \pm 3.5)^\circ$	$0.03\,^{+0.23}_{-0.24} \pm 0.11 \pm 0.10$	$(12.7\,^{+6.9}_{-6.5} \pm 2.8 \pm 3.3)^\circ$	$-0.06 \pm 0.17 \pm 0.07 \pm 0.09$
Average		16.4 ± 6.8	0.06 ± 0.20	20.6 ± 6.2	-0.07 ± 0.14
Confidence level			0.39 (0.9σ)		

Experiment	$N(B\overline{B})$	$f_2 K^0_S$		$f_{\rm X} K^0_S$	
		$\beta^{\rm eff}$	$\mathcal{A}$	$\beta^{\rm eff}$	$\mathcal{A}$
BABAR [262]	383M	$(14.9 \pm 17.9 \pm 3.1 \pm 5.2)^\circ$	$-0.28\,^{+0.40}_{-0.35} \pm 0.08 \pm 0.07$	$(5.8 \pm 15.2 \pm 2.2 \pm 2.3)^\circ$	$-0.13\,^{+0.35}_{-0.33} \pm 0.04 \pm 0.09$

Experiment	$N(B\overline{B})$	$B^0 \to \pi^+\pi^- K^0_S$ nonresonant		$\chi_{c0} K^0_S$	
		$\beta^{\rm eff}$	$\mathcal{A}$	$\beta^{\rm eff}$	$\mathcal{A}$
BABAR [262]	383M	$(0.4 \pm 8.8 \pm 1.9 \pm 3.8)^\circ$	$-0.01 \pm 0.25 \pm 0.06 \pm 0.05$	$(23.2 \pm 22.4 \pm 2.3 \pm 4.2)^\circ$	$0.29\,^{+0.44}_{-0.53} \pm 0.03 \pm 0.05$

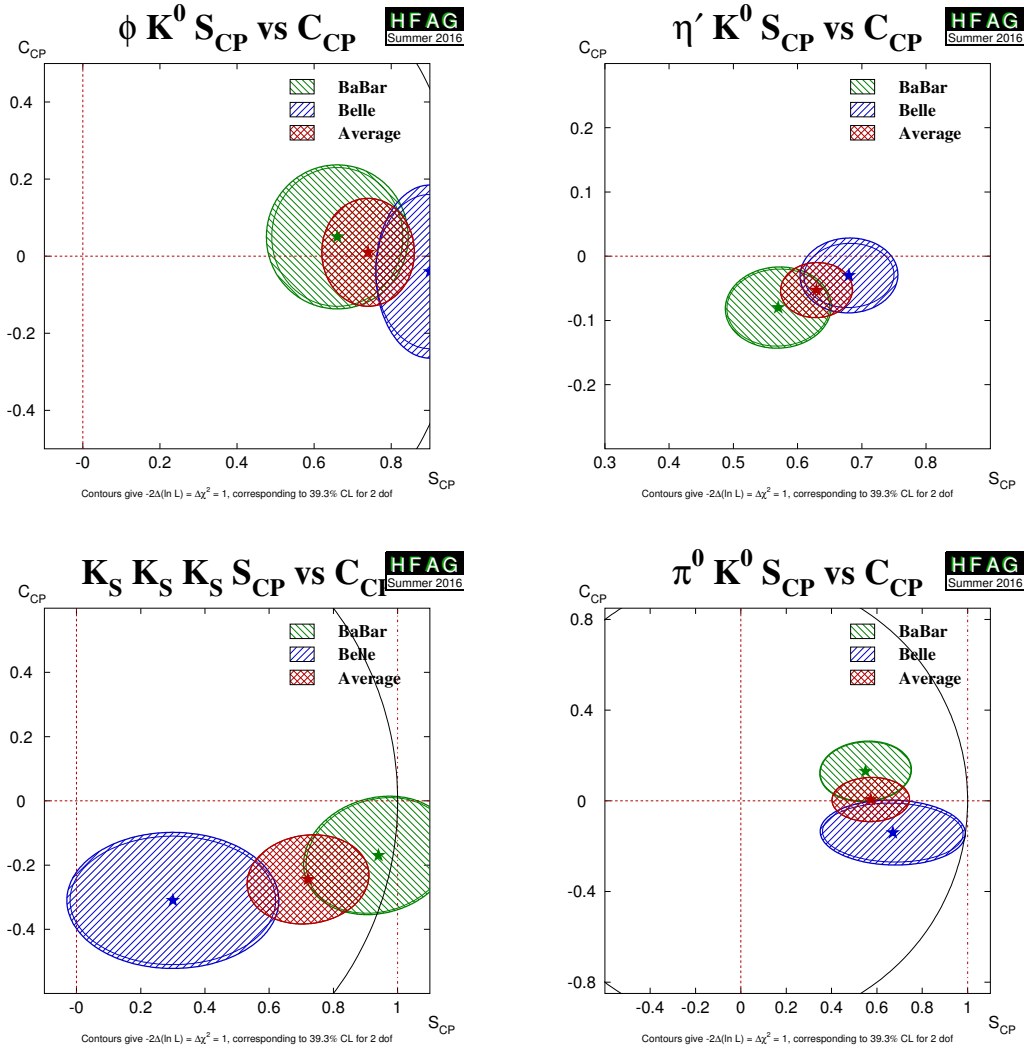

Figure 23: Averages of four $b \to q\bar{q}s$ dominated channels, for which correlated averages are performed, in the S_{CP} *vs.* C_{CP} plane, where S_{CP} has been corrected by the *CP* eigenvalue to give $\sin(2\beta^{\rm eff})$. (Top left) $B^0 \to \phi K^0$, (top right) $B^0 \to \eta' K^0$, (bottom left) $B^0 \to K^0_S K^0_S K^0_S$, (bottom right) $B^0 \to \pi^0 K^0_S$. More figures are available from the HFAG web pages.

an illustration of their measurements with the following differences:

$$\sin(2\beta - 2\Delta\delta_{01}) - \sin(2\beta) = -0.42\,^{+0.26}_{-0.34}\,, \quad (152)$$

$$\sin(2\beta - 2\Delta\phi_{\|1}) - \sin(2\beta) = -0.32\,^{+0.22}_{-0.30}\,, \quad (153)$$

$$\sin(2\beta - 2\Delta\phi_{\perp 1}) - \sin(2\beta) = -0.30\,^{+0.23}_{-0.32}\,, \quad (154)$$

$$\sin(2\beta - 2\Delta\phi_{\perp 1}) - \sin(2\beta - 2\Delta\phi_{\|1}) = 0.02 \pm 0.23\,, \quad (155)$$

$$\sin(2\beta - 2\Delta\delta_{02}) - \sin(2\beta) = -0.10\,^{+0.18}_{-0.29}\,, \quad (156)$$

where the first subscript indicates the helicity amplitude and the second indicates the spin of the kaon resonance. For the complete definitions of the $\Delta\delta$ and $\Delta\phi$ parameters, please refer to the *BABAR* paper [376].

Parameters of *CP* violation in decay for each of the contributing helicity amplitudes can also

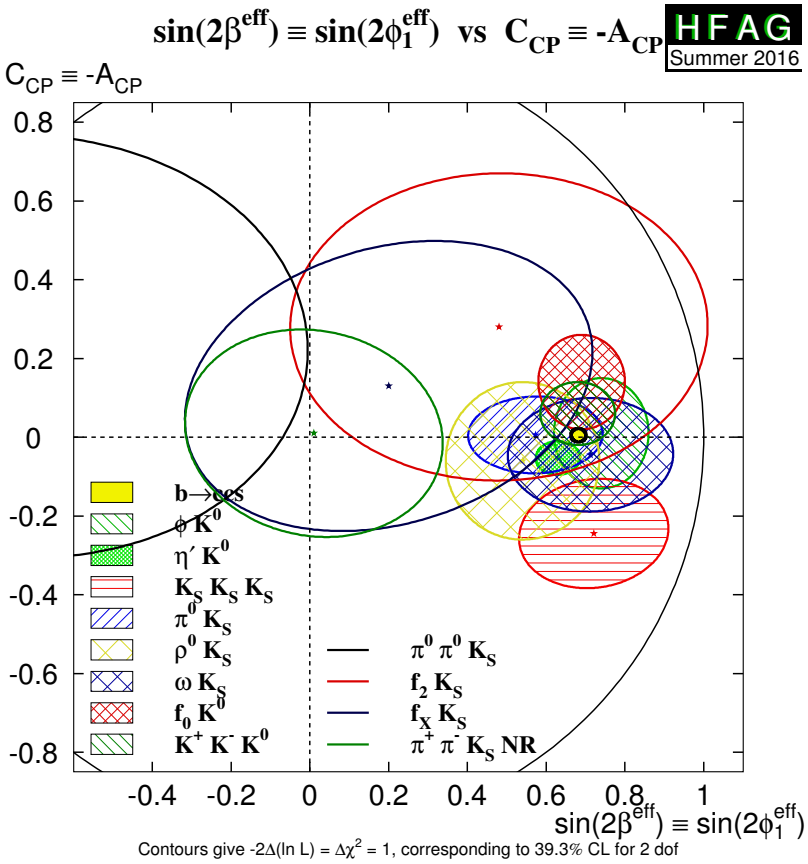

Figure 24: Compilation of constraints in the $-\eta S_{b\to q\bar{q}s}$ *vs.* $C_{b\to q\bar{q}s}$ plane.

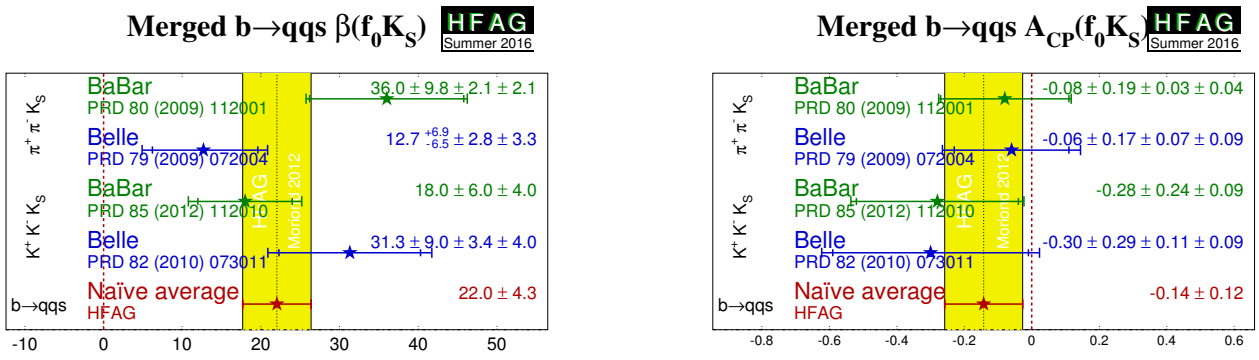

Figure 25: Averages of (left) $\beta^{\rm eff} \equiv \phi_1^{\rm eff}$ and (right) A_{CP} for the $B^0 \to f_0 K_S^0$ decay including measurements from Dalitz plot analyses of both $B^0 \to K^+K^-K_S^0$ and $B^0 \to \pi^+\pi^-K_S^0$.

be measured. Again, these are determined from a simultaneous fit of $B^0 \to \phi K^0_S \pi^0$ and $B^0 \to \phi K^+\pi^-$, with the precision being dominated by the statistics of the latter mode. Measurements of *CP* violation in decay, obtained from decay-time-integrated analyses, are tabulated by the HFAG Rare Decays subgroup (Sec. 7).

4.7.4 Time-dependent *CP* asymmetries in $B^0_s \to K^+K^-$

The decay $B^0_s \to K^+K^-$ involves a $b \to u\overline{u}s$ transition, and hence has both penguin and tree contributions. Both mixing-induced and *CP* violation in decay effects may arise, and additional input is needed to disentangle the contributions and determine γ and $\beta_s^{\rm eff}$. For example, the observables in $B^0 \to \pi^+\pi^-$ can be related using U-spin, as proposed by Fleischer [377].

The observables are $A_{\rm mix} = S_{CP}$, $A_{\rm dir} = -C_{CP}$, and $A_{\Delta\Gamma}$. They can all be treated as free parameters, but are physically constrained to satisfy $A^2_{\rm mix} + A^2_{\rm dir} + A^2_{\Delta\Gamma} = 1$. Note that the untagged decay distribution, from which an "effective lifetime" can be measured, retains sensitivity to $A_{\Delta\Gamma}$; measurements of the $B^0_s \to K^+K^-$ effective lifetime have been made by LHCb [97, 120]. Compilations and averages of effective lifetimes are performed by the HFAG Lifetimes and Oscillations subgroup, see Sec. 3.

The observables in $B^0_s \to K^+K^-$ have been measured by LHCb [378], who do not impose the constraint mentioned above to eliminate $A_{\Delta\Gamma}$. The results are shown in Table 40, and correspond to evidence for *CP* violation both in the interference between mixing and decay, and in the $B^0_s \to K^+K^-$ decay.

Table 40: Results from time-dependent analysis of the $B^0_s \to K^+K^-$ decay.

Experiment		Sample size	S_{CP}	C_{CP}	$A^{\Delta\Gamma}$
LHCb	[378]	$\int \mathcal{L}\,dt = 3.0$ fb^{-1}	$0.22 \pm 0.06 \pm 0.02$	$0.24 \pm 0.06 \pm 0.02$	$-0.75 \pm 0.07 \pm 0.11$

Interpretations of an earlier set of results [379], in terms of constraints on γ and $2\beta_s$, have been separately published by LHCb [380].

4.7.5 Time-dependent *CP* asymmetries in $B^0_s \to \phi\phi$

The decay $B^0_s \to \phi\phi$ involves a $b \to s\overline{s}s$ transition, and hence is a "pure penguin" mode (in the limit that the ϕ meson is considered a pure $s\overline{s}$ state). Since the mixing phase and the decay phase are expected to cancel in the Standard Model, the prediction for the phase from the interference of mixing and decay is predicted to be $\phi_s(\phi\phi) = 0$ with low uncertainty [381]. Due to the vector-vector nature of the final state, angular analysis is needed to separate the *CP*-even and *CP*-odd contributions. Such an analysis also makes it possible to fit directly for $\phi_s(\phi\phi)$.

A constraint on $\phi_s(\phi\phi)$ has been obtained by LHCb using $3.0\,\text{fb}^{-1}$ of data [382]. The result is $\phi_s(\phi\phi) = -0.17 \pm 0.15 \pm 0.03\,\text{rad}$ where the first uncertainty is statistical and the second is systematic.

4.8 Time-dependent *CP* asymmetries in $b \to q\bar{q}d$ transitions

Decays such as $B^0 \to K^0_S K^0_S$ are pure $b \to q\bar{q}d$ penguin transitions. As shown in Eq. (149), this diagram has different contributing weak phases, and therefore the observables are sensitive to the difference (which can be chosen to be either β or γ). Note that if the contribution with the top quark in the loop dominates, the weak phase from the decay amplitudes should cancel that from mixing, so that no *CP* violation (neither mixing-induced nor in decay) occurs. Non-zero contributions from loops with intermediate up and charm quarks can result in both types of effect (as usual, a strong phase difference is required for *CP* violation in decay to occur).

Both *BABAR* [383] and Belle [384] have performed time-dependent analyses of $B^0 \to K^0_S K^0_S$. The results are given in Table 41 and shown in Fig. 26.

Table 41: Results for $B^0 \to K^0_S K^0_S$.

Experiment		$N(B\overline{B})$	S_{CP}	C_{CP}	Correlation
BABAR	[383]	350M	$-1.28\,^{+0.80}_{-0.73}\,^{+0.11}_{-0.16}$	$-0.40 \pm 0.41 \pm 0.06$	-0.32
Belle	[384]	657M	$-0.38\,^{+0.69}_{-0.77} \pm 0.09$	$0.38 \pm 0.38 \pm 0.05$	0.48
Average			-1.08 ± 0.49	-0.06 ± 0.26	0.14
Confidence level			0.29 (1.1σ)		

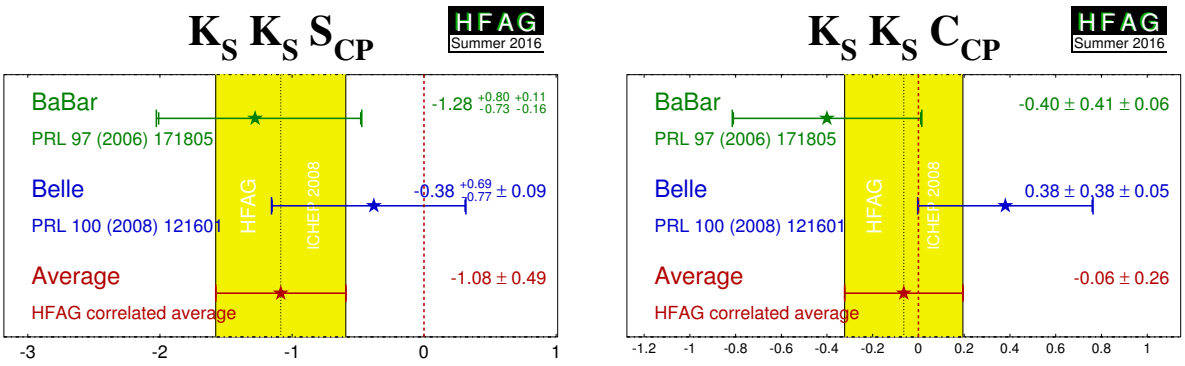

Figure 26: Averages of (left) $S_{b\to q\bar{q}d}$ and (right) $C_{b\to q\bar{q}d}$ for the mode $B^0 \to K^0_S K^0_S$.

4.9 Time-dependent asymmetries in $b \to s\gamma$ transitions

The radiative decays $b \to s\gamma$ produce photons which are highly polarised in the Standard Model. The decays $B^0 \to F\gamma$ and $\overline{B}^0 \to F\gamma$ produce photons with opposite helicities, and since the polarisation is, in principle, observable, these final states cannot interfere. The finite mass of the s quark introduces small corrections to the limit of maximum polarisation, but any large mixing-induced *CP* violation would be a signal for new physics. Since a single weak phase dominates the $b \to s\gamma$ transition in the Standard Model, the cosine term is also expected to be small.

Atwood *et al.* [286] have shown that an inclusive analysis with respect to $K^0_S\pi^0\gamma$ can be performed, since the properties of the decay amplitudes are independent of the angular momentum of the $K^0_S\pi^0$ system. However, if non-dipole operators contribute significantly to the amplitudes, then the Standard Model mixing-induced *CP* violation could be larger than the naïve expectation $S \simeq -2(m_s/m_b)\sin(2\beta)$ [287,288]. In this case, the *CP* parameters may vary over the $K^0_S\pi^0\gamma$ Dalitz plot, for example as a function of the $K^0_S\pi^0$ invariant mass. Explicit calculations indicate such corrections are small for exclusive final states [289, 290].

With the above in mind, we quote two averages: one for $K^*(892)$ candidates only, and the other one for the inclusive $K^0_S\pi^0\gamma$ decay (including the $K^*(892)$). If the Standard Model dipole operator is dominant, both should give the same quantities (the latter naturally with smaller statistical error). If not, care needs to be taken in interpretation of the inclusive parameters, while the results on the $K^*(892)$ resonance remain relatively clean. Results from *BABAR* and Belle are used for both averages; both experiments use the invariant mass range $0.60\ \mathrm{GeV}/c^2 < M_{K^0_S\pi^0} < 1.80\ \mathrm{GeV}/c^2$ in the inclusive analysis.

In addition to the $K^0_S\pi^0\gamma$ decay, both *BABAR* and Belle have presented results using $K^0_S\rho\gamma$, while *BABAR* (Belle) has in addition presented results using $K^0_S\eta\gamma$ ($K^0_S\phi\gamma$). For the $K^0_S\rho\gamma$ case, due to the non-negligible width of the ρ^0 meson, decays selected as $B^0 \to K^0_S\rho^0\gamma$ can include a significant contribution from $K^{*\pm}\pi^\mp\gamma$ decays, which are flavour-specific and do not have the same oscillation phenomenology. Both *BABAR* and Belle measure $S_{\rm eff}$ for all B decay candidates with the ρ^0 selection being $0.6 < m(\pi^+\pi^-) < 0.9\ \mathrm{GeV}/c^2$, obtaining $0.14 \pm 0.25\,^{+0.04}_{-0.03}$ (*BABAR*) and $0.09 \pm 0.27\,^{+0.04}_{-0.07}$ (Belle). These values are then corrected for a "dilution factor", that is evaluated with different methods in the two experiments: *BABAR* [385, 386] obtain a dilution factor of $-0.78\,^{+0.19}_{-0.17}$ while Belle [387] obtain $+0.83\,^{+0.19}_{-0.03}$. Until the discrepancy between these values is understood, the average of the results should be treated with caution.

The results are given in Table 42, and shown in Figs. 27 and 28. No significant *CP* violation results are seen; the results are consistent with the Standard Model and with other measurements in the $b \to s\gamma$ system (see Sec. 7).

A similar analysis can be performed for radiative B^0_s decays to, for example, the $\phi\gamma$ final state. As for other observables determined with self-conjugate final states produced in B^0_s decays, the effective lifetime also provides sensitivity, and can be determined without tagging the initial flavour of the decaying meson. The LHCb collaboration have determined the associated parameter $A_{\Delta\Gamma}(\phi\gamma) = -0.98\,^{+0.46}_{-0.52}\,^{+0.23}_{-0.20}$ [392].

4.10 Time-dependent asymmetries in $b \to d\gamma$ transitions

The formalism for the radiative decays $b \to d\gamma$ is much the same as that for $b \to s\gamma$ discussed above. Assuming dominance of the top quark in the loop, the weak phase in decay should cancel with that from mixing, so that the mixing-induced *CP* violation parameter S_{CP} should be very small. Corrections due to the finite light quark mass are smaller compared to $b \to s\gamma$, since $m_d < m_s$, and although QCD corrections may still play a role, they cannot significantly affect the prediction $S_{b\to d\gamma} \simeq 0$. Large *CP* violation effects could, however, be seen through a non-zero value of $C_{b\to d\gamma}$, since the top loop is not the only contribution.

Results using the mode $B^0 \to \rho^0\gamma$ are available from Belle and are given in Table 43.

Table 42: Averages for $b \to s\gamma$ modes.

Experiment		$N(B\overline{B})$	$S_{CP}(b \to s\gamma)$	$C_{CP}(b \to s\gamma)$	Correlation
			$K^*(892)\gamma$		
BABAR	[388]	467M	$-0.03 \pm 0.29 \pm 0.03$	$-0.14 \pm 0.16 \pm 0.03$	0.05
Belle	[389]	535M	$-0.32\,^{+0.36}_{-0.33} \pm 0.05$	$0.20 \pm 0.24 \pm 0.05$	0.08
Average			-0.16 ± 0.22	-0.04 ± 0.14	0.06
Confidence level			0.40 (0.9σ)		
			$K^0_S\pi^0\gamma$ (including $K^*(892)\gamma$)		
BABAR	[388]	467M	$-0.17 \pm 0.26 \pm 0.03$	$-0.19 \pm 0.14 \pm 0.03$	0.04
Belle	[389]	535M	$-0.10 \pm 0.31 \pm 0.07$	$0.20 \pm 0.20 \pm 0.06$	0.08
Average			-0.15 ± 0.20	-0.07 ± 0.12	0.05
Confidence level			0.30 (1.0σ)		
			$K^0_S\eta\gamma$		
BABAR	[390]	465M	$-0.18\,^{+0.49}_{-0.46} \pm 0.12$	$-0.32\,^{+0.40}_{-0.39} \pm 0.07$	-0.17
			$K^0_S\rho^0\gamma$		
BABAR	[386]	471M	$-0.18 \pm 0.32\,^{+0.06}_{-0.05}$	$-0.39 \pm 0.20\,^{+0.03}_{-0.02}$	-0.09
Belle	[387]	657M	$0.11 \pm 0.33\,^{+0.05}_{-0.09}$	$-0.05 \pm 0.18 \pm 0.06$	0.04
Average			-0.06 ± 0.23	-0.22 ± 0.14	-0.02
Confidence level			0.38 (0.9σ)		
			$K^0_S\phi\gamma$		
Belle	[391]	772M	$0.74\,^{+0.72\,+0.10}_{-1.05\,-0.24}$	$-0.35 \pm 0.58\,^{+0.10}_{-0.23}$	–

Table 43: Averages for $B^0 \to \rho^0\gamma$.

Experiment		$N(B\overline{B})$	S_{CP}	C_{CP}	Correlation
Belle	[393]	657M	$-0.83 \pm 0.65 \pm 0.18$	$0.44 \pm 0.49 \pm 0.14$	-0.08

4.11 Time-dependent *CP* asymmetries in $b \to u\overline{u}d$ transitions

The $b \to u\overline{u}d$ transition can be mediated by either a $b \to u$ tree amplitude or a $b \to d$ penguin amplitude. These transitions can be investigated using the time dependence of B^0 decays to final states containing light mesons. Results are available from both *BABAR* and Belle for the *CP* eigenstate ($\eta = +1$) $\pi^+\pi^-$ final state and for the vector-vector final state $\rho^+\rho^-$, which is found to be dominated by the *CP*-even longitudinally polarised component (*BABAR* measure $f_{\rm long} = 0.992 \pm 0.024\,^{+0.026}_{-0.013}$ [394] while Belle measure $f_{\rm long} = 0.988 \pm 0.012 \pm 0.023$ [395]). *BABAR* has also performed a time-dependent analysis of the vector-vector final state $\rho^0\rho^0$ [396], in which they measure $f_{\rm long} = 0.70 \pm 0.14 \pm 0.05$; Belle measure a smaller branching fraction than *BABAR* for $B^0 \to \rho^0\rho^0$ [397] with corresponding signal yields too small to perform a time-dependent analysis; for the longitudinal polarisation they measure $f_{\rm long} = 0.21\,^{+0.18}_{-0.22} \pm 0.13$. LHCb has measured the branching fraction and longitudinal polarisation for $B^0 \to \rho^0\rho^0$, and for the latter

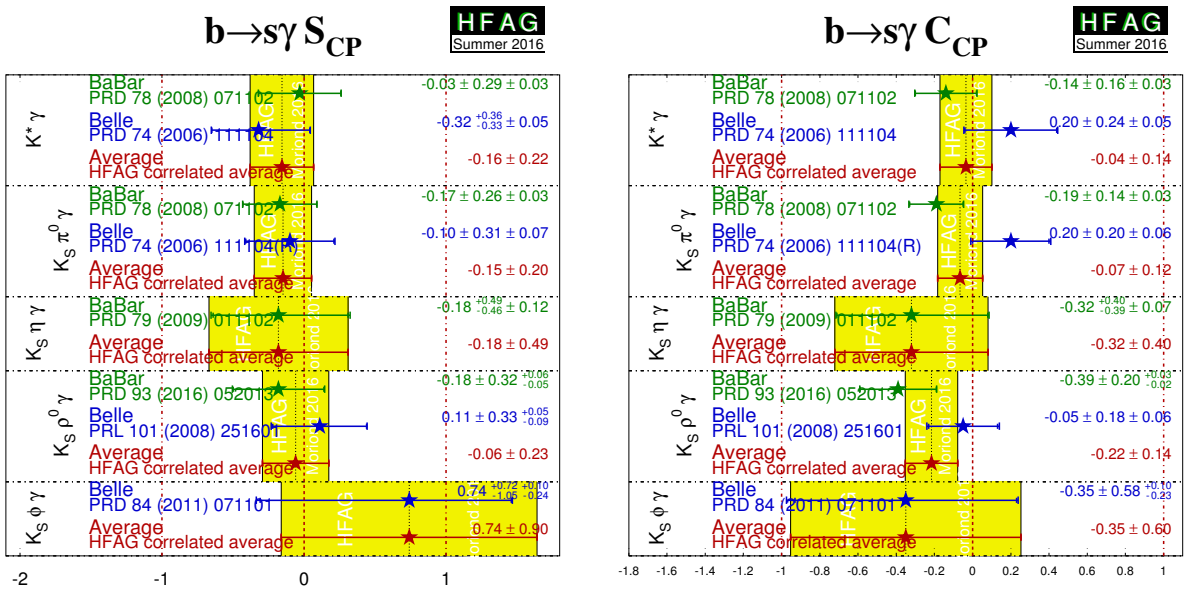

Figure 27: Averages of (left) $S_{b\to s\gamma}$ and (right) $C_{b\to s\gamma}$. Recall that the data for $K^*\gamma$ is a subset of that for $K^0_S\pi^0\gamma$.

finds $f_{\rm long} = 0.745\,^{+0.048}_{-0.058} \pm 0.034$ [398], but has not yet performed a time-dependent analysis of this decay. The Belle measurement for $f_{\rm long}$ is thus in some tension with the other results. *BABAR* has furthermore performed a time-dependent analysis of the $B^0 \to a_1^\pm\pi^\mp$ decay [399]; further experimental input for the extraction of α from this channel is reported in a later publication [400].

Results, and averages, of time-dependent *CP* violation parameters in $b \to u\bar{u}d$ transitions are listed in Table 44. The averages for $\pi^+\pi^-$ are shown in Fig. 29, and those for $\rho^+\rho^-$ are shown in Fig. 30, with the averages in the S_{CP} *vs.* C_{CP} plane shown in Fig. 31 and averages of *CP* violation parameters in $B^0 \to a_1^\pm\pi^\mp$ decay shown in Fig. 32.

If the penguin contribution is negligible, the time-dependent parameters for $B^0 \to \pi^+\pi^-$ and $B^0 \to \rho^+\rho^-$ are given by $S_{b\to u\bar{u}d} = \eta\sin(2\alpha)$ and $C_{b\to u\bar{u}d} = 0$. In the presence of the penguin contribution, *CP* violation in decay may arise, and there is no straightforward interpretation of $S_{b\to u\bar{u}d}$ and $C_{b\to u\bar{u}d}$. An isospin analysis [404] can be used to disentangle the contributions and extract α.

For the non-*CP* eigenstate $\rho^\pm\pi^\mp$, both *BABAR* [269] and Belle [271, 272] have performed time-dependent Dalitz plot analyses of the $\pi^+\pi^-\pi^0$ final state [267]; such analyses allow direct measurements of the phases. Both experiments have measured the U and I parameters discussed in Sec. 4.2.5 and defined in Table 22. We have performed a full correlated average of these parameters, the results of which are summarised in Fig. 33.

Both experiments have also extracted the Q2B parameters. We have performed a full correlated average of these parameters, which is equivalent to determining the values from the averaged U and I parameters. The results are given in Table 45.[46] Averages of the $B^0 \to \rho^0\pi^0$

[46] The $B^0 \to \rho^\pm\pi^\mp$ Q2B parameters are comparable to the parameters used for $B^0 \to a_1^\pm\pi^\mp$ decays, reported in Table 44. For the $B^0 \to a_1^\pm\pi^\mp$ case there has not yet been a full amplitude analysis of $B^0 \to \pi^+\pi^-\pi^+\pi^-$ and therefore only the Q2B parameters are available.

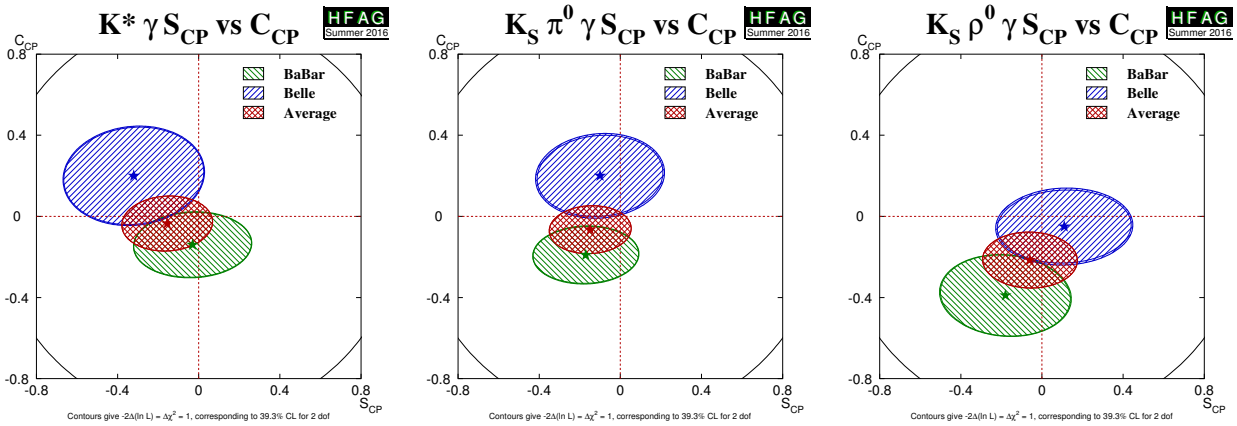

Figure 28: Averages of three $b \to s\gamma$ dominated channels, for which correlated averages are performed, in the S_{CP} *vs.* C_{CP} plane. (Left) $B^0 \to K^*\gamma$, (middle) $B^0 \to K^0_S\pi^0\gamma$ (including $K^*\gamma$), (right) $B^0 \to K^0_S\rho\gamma$.

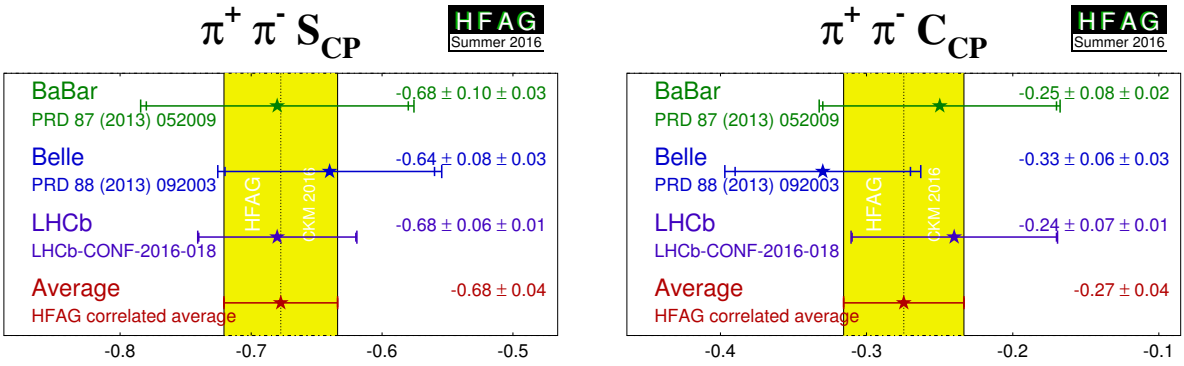

Figure 29: Averages of (left) $S_{b\to u\bar{u}d}$ and (right) $C_{b\to u\bar{u}d}$ for the mode $B^0 \to \pi^+\pi^-$.

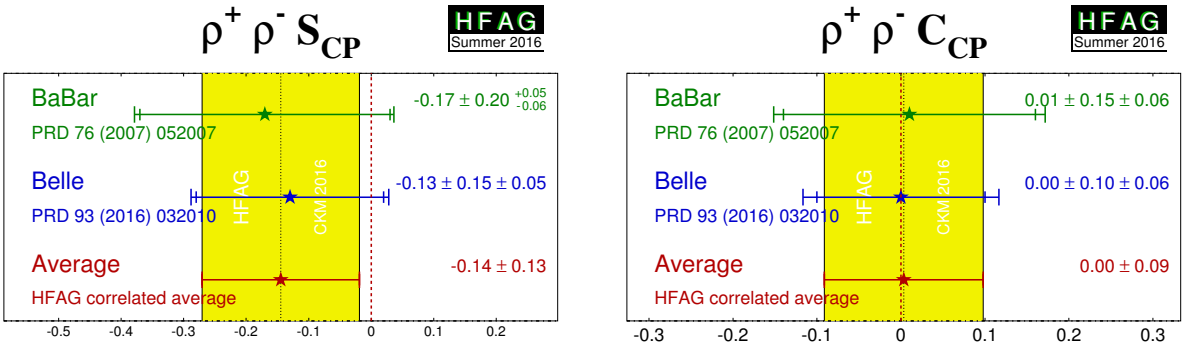

Figure 30: Averages of (left) $S_{b\to u\bar{u}d}$ and (right) $C_{b\to u\bar{u}d}$ for the mode $B^0 \to \rho^+\rho^-$.

Table 44: Averages for $b \to u\overline{u}d$ modes.

Experiment		Sample size	S_{CP}	C_{CP}	Correlation
			$\pi^+\pi^-$		
BABAR	[401]	$N(B\overline{B}) = 467$M	$-0.68 \pm 0.10 \pm 0.03$	$-0.25 \pm 0.08 \pm 0.02$	-0.06
Belle	[402]	$N(B\overline{B}) = 772$M	$-0.64 \pm 0.08 \pm 0.03$	$-0.33 \pm 0.06 \pm 0.03$	-0.10
LHCb	[378]	$\int \mathcal{L}\, dt = 3.0\,\text{fb}^{-1}$	$-0.68 \pm 0.06 \pm 0.01$	$-0.24 \pm 0.07 \pm 0.01$	0.38
Average			-0.68 ± 0.04	-0.27 ± 0.04	0.14
Confidence level			0.88 (0.2σ)		
			$\rho^+\rho^-$		
BABAR	[394]	$N(B\overline{B}) = 387$M	$-0.17 \pm 0.20\,^{+0.05}_{-0.06}$	$0.01 \pm 0.15 \pm 0.06$	-0.04
Belle	[395]	$N(B\overline{B}) = 772$M	$-0.13 \pm 0.15 \pm 0.05$	$0.00 \pm 0.10 \pm 0.06$	-0.02
Average			-0.14 ± 0.13	0.00 ± 0.09	-0.02
Confidence level			0.99 (0.02σ)		
			$\rho^0\rho^0$		
BABAR	[396]	$N(B\overline{B}) = 465$M	$0.3 \pm 0.7 \pm 0.2$	$0.2 \pm 0.8 \pm 0.3$	-0.04

Experiment		$N(B\overline{B})$	$A_{CP}^{a_1\pi}$	$C_{a_1\pi}$	$S_{a_1\pi}$	$\Delta C_{a_1\pi}$	$\Delta S_{a_1\pi}$
				$a_1^\pm\pi^\mp$			
BABAR	[399]	384M	$-0.07 \pm 0.07 \pm 0.02$	$-0.10 \pm 0.15 \pm 0.09$	$0.37 \pm 0.21 \pm 0.07$	$0.26 \pm 0.15 \pm 0.07$	$-0.14 \pm 0.21 \pm 0.06$
Belle	[403]	772M	$-0.06 \pm 0.05 \pm 0.07$	$-0.01 \pm 0.11 \pm 0.09$	$-0.51 \pm 0.14 \pm 0.08$	$0.54 \pm 0.11 \pm 0.07$	$-0.09 \pm 0.14 \pm 0.06$
Average			-0.06 ± 0.06	-0.05 ± 0.11	-0.20 ± 0.13	0.43 ± 0.10	-0.10 ± 0.12
Confidence level					0.03 (2.1σ)		

Experiment		$N(B\overline{B})$	$\mathcal{A}_{a_1\pi}^{-+}$	$\mathcal{A}_{a_1\pi}^{+-}$	Correlation
BABAR	[399]	384M	$0.07 \pm 0.21 \pm 0.15$	$0.15 \pm 0.15 \pm 0.07$	0.63
Belle	[403]	772M	$-0.04 \pm 0.26 \pm 0.19$	$0.07 \pm 0.08 \pm 0.10$	0.61
Average			0.02 ± 0.20	0.10 ± 0.10	0.38
Confidence level			0.92 (0.1σ)		

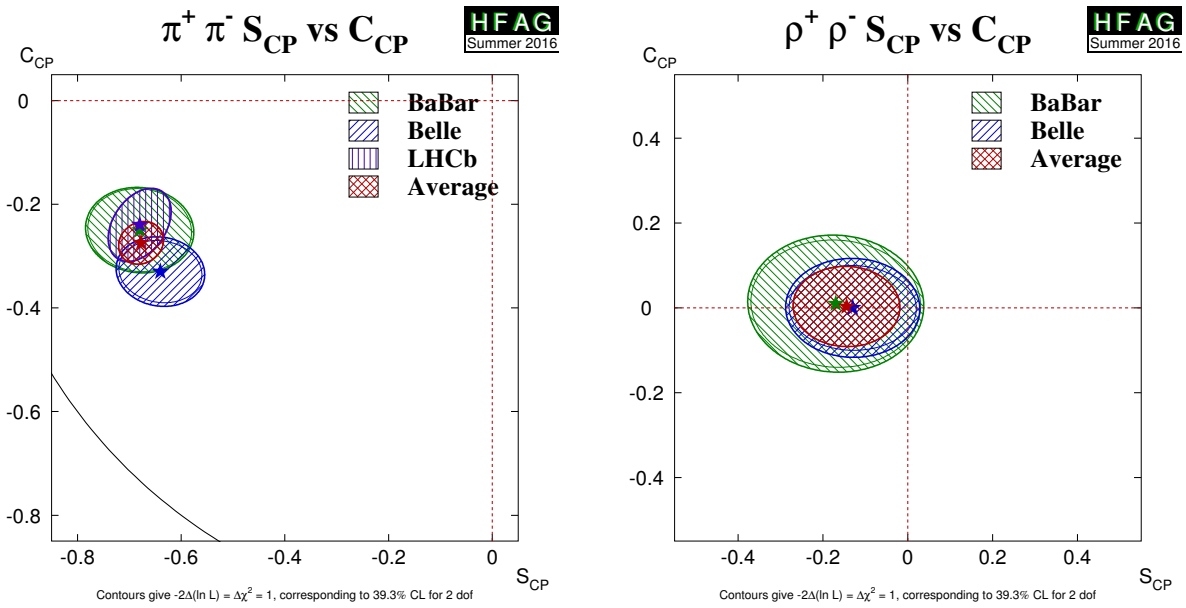

Figure 31: Averages of $b \to u\overline{u}d$ dominated channels, for which correlated averages are performed, in the S_{CP} *vs.* C_{CP} plane. (Left) $B^0 \to \pi^+\pi^-$ and (right) $B^0 \to \rho^+\rho^-$.

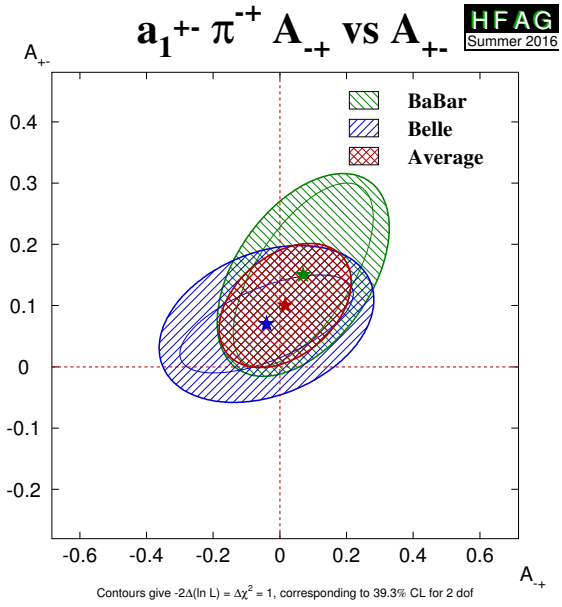

Figure 32: Averages of CP violation parameters in $B^0 \to a_1^{\pm}\pi^{\mp}$ in $\mathcal{A}_{a_1\pi}^{-+}$ *vs.* $\mathcal{A}_{a_1\pi}^{+-}$ space.

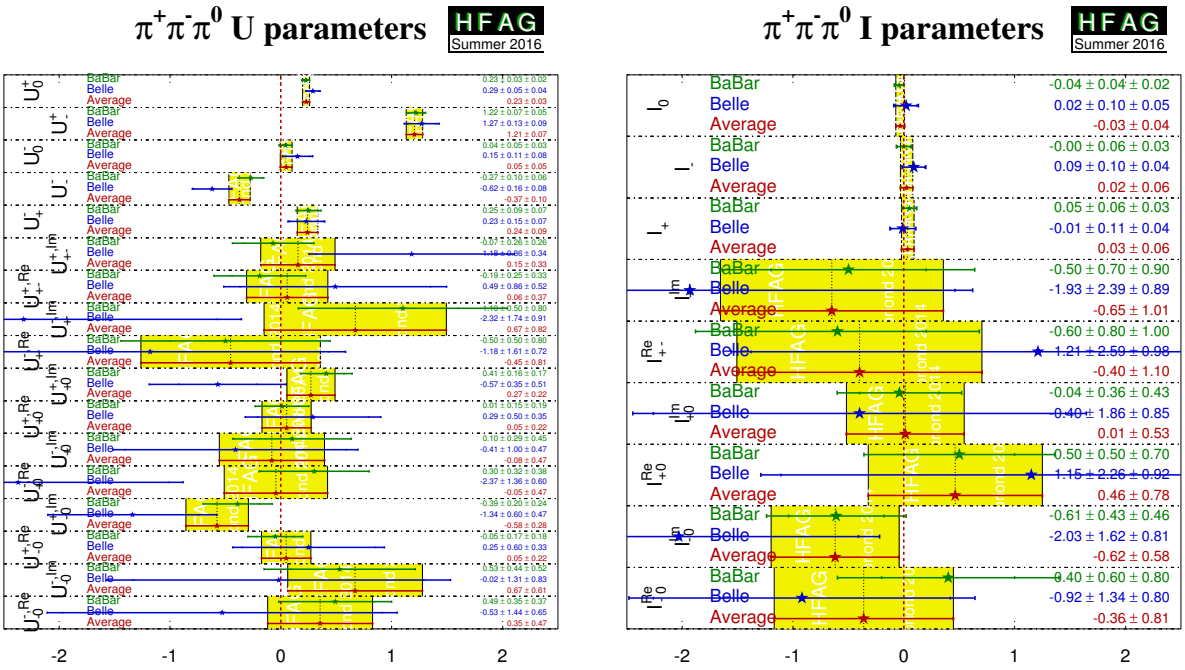

Figure 33: Summary of the U and I parameters measured in the time-dependent $B^0 \to \pi^+\pi^-\pi^0$ Dalitz plot analysis.

Q2B parameters are shown in Figs. 34 and 35.

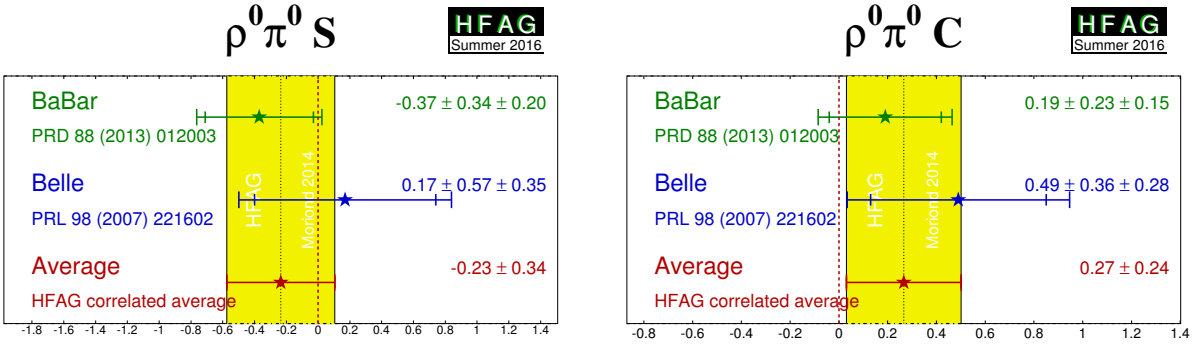

Figure 34: Averages of (left) $S_{b\to u\bar{u}d}$ and (right) $C_{b\to u\bar{u}d}$ for the mode $B^0 \to \rho^0\pi^0$.

With the notation described in Sec. 4.2 (Eq. (127)), the time-dependent parameters for the Q2B $B^0 \to \rho^\pm\pi^\mp$ analysis are, neglecting penguin contributions, given by

$$S_{\rho\pi} = \sqrt{1-\left(\frac{\Delta C}{2}\right)^2}\sin(2\alpha)\cos(\delta)\ , \quad \Delta S_{\rho\pi} = \sqrt{1-\left(\frac{\Delta C}{2}\right)^2}\cos(2\alpha)\sin(\delta) \tag{157}$$

and $C_{\rho\pi} = \mathcal{A}_{CP}^{\rho\pi} = 0$, where $\delta = \arg(A_{-+}A_{+-}^*)$ is the strong phase difference between the $\rho^-\pi^+$ and $\rho^+\pi^-$ decay amplitudes. In the presence of the penguin contribution, there is no

Table 45: Averages of quasi-two-body parameters extracted from time-dependent Dalitz plot analysis of $B^0 \to \pi^+\pi^-\pi^0$.

Experiment		$N(B\overline{B})$	$\mathcal{A}_{CP}^{\rho\pi}$	$C_{\rho\pi}$	$S_{\rho\pi}$	$\Delta C_{\rho\pi}$	$\Delta S_{\rho\pi}$
BABAR	[270]	471M	$-0.10 \pm 0.03 \pm 0.02$	$0.02 \pm 0.06 \pm 0.04$	$0.05 \pm 0.08 \pm 0.03$	$0.23 \pm 0.06 \pm 0.05$	$0.05 \pm 0.08 \pm 0.04$
Belle	[271, 272]	449M	$-0.12 \pm 0.05 \pm 0.04$	$-0.13 \pm 0.09 \pm 0.05$	$0.06 \pm 0.13 \pm 0.05$	$0.36 \pm 0.10 \pm 0.05$	$-0.08 \pm 0.13 \pm 0.05$
Average			-0.11 ± 0.03	-0.03 ± 0.06	0.06 ± 0.07	0.27 ± 0.06	0.01 ± 0.08
Confidence level					0.63 (0.5σ)		

Experiment		$N(B\overline{B})$	$\mathcal{A}_{\rho\pi}^{-+}$	$\mathcal{A}_{\rho\pi}^{+-}$	Correlation
BABAR	[270]	471M	$-0.12 \pm 0.08\,^{+0.04}_{-0.05}$	$0.09\,^{+0.05}_{-0.06} \pm 0.04$	0.55
Belle	[271, 272]	449M	$0.08 \pm 0.16 \pm 0.11$	$0.21 \pm 0.08 \pm 0.04$	0.47
Average			-0.08 ± 0.08	0.13 ± 0.05	0.37
Confidence level				0.47 (0.7σ)	

Experiment		$N(B\overline{B})$	$C_{\rho^0\pi^0}$	$S_{\rho^0\pi^0}$	Correlation
BABAR	[270]	471M	$0.19 \pm 0.23 \pm 0.15$	$-0.37 \pm 0.34 \pm 0.20$	0.00
Belle	[271, 272]	449M	$0.49 \pm 0.36 \pm 0.28$	$0.17 \pm 0.57 \pm 0.35$	0.08
Average			0.27 ± 0.24	-0.23 ± 0.34	0.02
Confidence level				0.68 (0.4σ)	

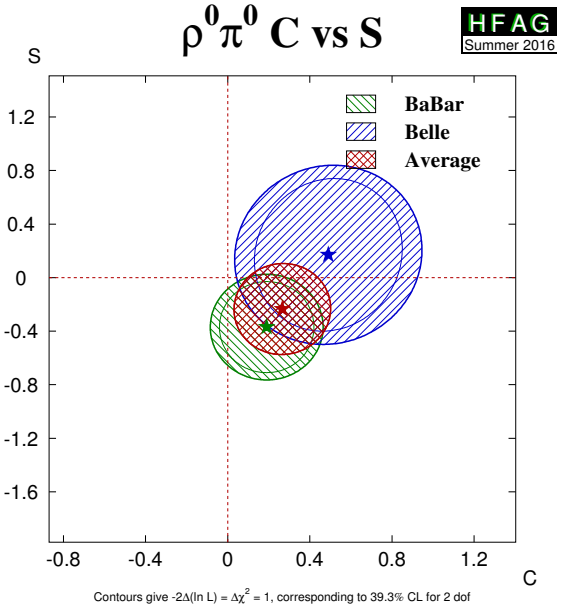

Figure 35: Averages of $b \to u\bar{u}d$ dominated channels, for the mode $B^0 \to \rho^0\pi^0$ in the S_{CP} *vs.* C_{CP} plane.

straightforward interpretation of the Q2B observables in the $B^0 \to \rho^\pm\pi^\mp$ system in terms of CKM parameters. However, *CP* violation in decay may arise, resulting in either or both of $C_{\rho\pi} \neq 0$ and $\mathcal{A}_{CP}^{\rho\pi} \neq 0$. Equivalently, *CP* violation in decay may be seen by either of the decay-type-specific observables $\mathcal{A}_{\rho\pi}^{+-}$ and $\mathcal{A}_{\rho\pi}^{-+}$, defined in Eq. (128), deviating from zero. Results and averages for these parameters are also given in Table 45. Averages of *CP* violation parameters in $B^0 \to \rho^\pm\pi^\mp$ decays are shown in Fig. 36, both in $\mathcal{A}_{CP}^{\rho\pi}$ *vs.* $C_{\rho\pi}$ space and in $\mathcal{A}_{\rho\pi}^{-+}$ *vs.* $\mathcal{A}_{\rho\pi}^{+-}$ space.

The averages for $S_{b\to u\bar{u}d}$ and $C_{b\to u\bar{u}d}$ in $B^0 \to \pi^+\pi^-$ are both more than 5σ away from zero, suggesting that both mixing-induced and *CP* violation in decay are well-established in this channel. The discrepancy between results from *BABAR* and Belle that used to exist in this channel (see, for example, Ref. [405]) is no longer apparent, and the results from LHCb are also fully consistent with other measurements. Some difference is, however, seen between the *BABAR* and Belle measurements in the $a_1^\pm\pi^\mp$ system. The confidence level of the five-dimensional average is 0.03, which corresponds to a 2.1σ discrepancy. As seen in Table 44, this discrepancy is primarily in the values of $S_{a_1\pi}$, and is not evident in the $\mathcal{A}_{a_1\pi}^{-+}$ *vs.* $\mathcal{A}_{a_1\pi}^{+-}$ projection shown in Fig. 32. Since there is no evidence of systematic problems in either analysis, we do not rescale the errors of the averages.

In $B^0 \to \rho^\pm\pi^\mp$ decays, both experiments see an indication of *CP* violation in the $\mathcal{A}_{CP}^{\rho\pi}$ parameter (as seen in Fig. 36). The average is more than 3σ from zero, providing evidence of direct *CP* violation in this channel. In $B^0 \to \rho^+\rho^-$ decays there is no evidence for *CP* violation, either mixing-induced or in decay. The absence of evidence of penguin contributions in this mode leads to strong constraints on $\alpha \equiv \phi_2$.

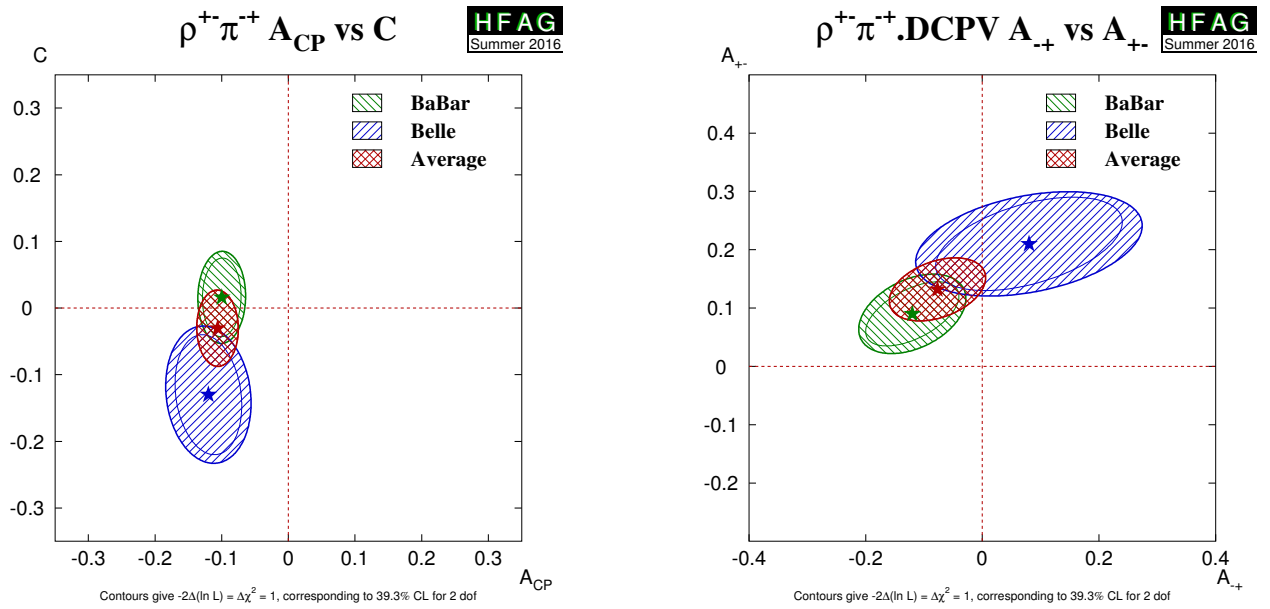

Figure 36: *CP* violation in $B^0 \to \rho^{\pm}\pi^{\mp}$ decays. (Left) $\mathcal{A}_{CP}^{\rho\pi}$ *vs.* $C_{\rho\pi}$ space, (right) $\mathcal{A}_{\rho\pi}^{-+}$ *vs.* $\mathcal{A}_{\rho\pi}^{+-}$ space.

4.11.1 Constraints on $\alpha \equiv \phi_2$

The precision of the measured *CP* violation parameters in $b \to u\overline{u}d$ transitions allows constraints to be set on the UT angle $\alpha \equiv \phi_2$. Constraints have been obtained with various methods:

- Both *BABAR* [401] and Belle [402] have performed isospin analyses in the $\pi\pi$ system. Belle exclude $23.8^\circ < \phi_2 < 66.8^\circ$ at the 68% CL while *BABAR* give a confidence level interpretation for α, and constrain $\alpha \in [71^\circ, 109^\circ]$ at the 68% CL considering only the solution consistent with the Standard Model. Values in the range $[23^\circ, 67^\circ]$ at the 90% CL are excluded. In both cases, only solutions in 0°–180° are considered.

- Both experiments have also performed isospin analyses in the $\rho\rho$ system. The most recent result from *BABAR* is given in an update of the measurements of the $B^+ \to \rho^+\rho^0$ decay [406], and sets the constraint $\alpha = \left(92.4\,^{+6.0}_{-6.5}\right)^\circ$. The most recent result from Belle is given in their paper on time-dependent *CP* violation parameters in $B^0 \to \rho^+\rho^-$ decays, and sets the constraint $\phi_2 = (93.7 \pm 10.6)^\circ$ [395].

- The time-dependent Dalitz plot analysis of the $B^0 \to \pi^+\pi^-\pi^0$ decay allows a determination of α without input from any other channels. *BABAR* [270] present a scan, but not an interval, for α, since their studies indicate that the scan is not statistically robust and cannot be interpreted as $1-$CL. Belle [271,272] have obtained a constraint on α using additional information from the SU(2) partners of $B \to \rho\pi$, which can be used to constrain α via an isospin pentagon relation [407]. With this analysis, Belle obtain the constraint $\phi_2 = (83\,^{+12}_{-23})^\circ$ (where the errors correspond to 1σ, *i.e.* 68.3% confidence level).

- The results from *BABAR* on $B^0 \to a_1^{\pm}\pi^{\mp}$ [399] can be combined with results from modes related by flavour symmetries ($a_1 K$ and $K_1\pi$) [408]. This has been done by *BABAR* [400], resulting in the constraint $\alpha = (79 \pm 7 \pm 11)^\circ$, where the first uncertainty is from the

analysis of $B^0 \to a_1^\pm \pi^\mp$ that obtains $\alpha^{\rm eff}$, and the second is due to the constraint on $\left|\alpha^{\rm eff} - \alpha\right|$. This approach gives a result with several ambiguous solutions; that consistent with the global fit is quoted here.

- The CKMfitter [240] and UTFit [326] groups use the measurements from Belle and *BABAR* given above with other branching fractions and *CP* asymmetries in $B \to \pi\pi$, $\rho\pi$ and $\rho\rho$ modes, to perform isospin analyses for each system, and to make combined constraints on α.

- The *BABAR* and Belle collaborations have combined their results on $B \to \pi\pi$, $\pi\pi\pi^0$ and $\rho\rho$ to obtain [409]

$$\alpha \equiv \phi_2 = (88 \pm 5)^\circ \,. \tag{158}$$

  The above solution is that consistent with the Standard Model (an ambiguous solution shifted by 180° exists). The strongest constraint currently comes from the $B \to \rho\rho$ system. The inclusion of results from $B^0 \to a_1^\pm \pi^\mp$ does not significantly affect the average.

Note that methods based on isospin symmetry make extensive use of measurements of branching fractions and *CP* asymmetries, as averaged by the HFAG Rare Decays subgroup (Sec. 7). Note also that each method suffers from discrete ambiguities in the solutions. The model assumption in the $B^0 \to \pi^+\pi^-\pi^0$ analysis helps resolve some of the multiple solutions, and results in a single preferred value for α in $[0, \pi]$. All the above measurements correspond to the choice that is in agreement with the global CKM fit.

At present we make no attempt to provide an HFAG average for $\alpha \equiv \phi_2$. More details on procedures to calculate a best fit value for α can be found in Refs. [240, 326].

4.12 Time-dependent *CP* asymmetries in $b \to c\bar{u}d/u\bar{c}d$ transitions

Non-*CP* eigenstates such as $D^\mp\pi^\pm$, $D^{*\mp}\pi^\pm$ and $D^\mp\rho^\pm$ can be produced in decays of B^0 mesons either via Cabibbo favoured ($b \to c$) or doubly Cabibbo suppressed ($b \to u$) tree amplitudes. Since no penguin contribution is possible, these modes are theoretically clean. The ratio of the magnitudes of the suppressed and favoured amplitudes, R, is sufficiently small (predicted to be about 0.02), that terms of $\mathcal{O}(R^2)$ can be neglected, and the sine terms give sensitivity to the combination of UT angles $2\beta + \gamma$.

As described in Sec. 4.2.6, the averages are given in terms of the parameters a and c of Eq. (132). *CP* violation would appear as $a \neq 0$. Results are available from both *BABAR* and Belle in the modes $D^\mp\pi^\pm$ and $D^{*\mp}\pi^\pm$; for the latter mode both experiments have used both full and partial reconstruction techniques. Results are also available from *BABAR* using $D^\mp\rho^\pm$. These results, and their averages, are listed in Table 46, and are shown in Fig. 37. The constraints in c *vs.* a space for the $D\pi$ and $D^*\pi$ modes are shown in Fig. 38. It is notable that the average value of a from $D^*\pi$ is more than 3σ from zero, providing evidence of *CP* violation in this channel.

For each mode, $D\pi$, $D^*\pi$ and $D\rho$, there are two measurements (a and c, or S^+ and S^-) which depend on three unknowns (R, δ and $2\beta + \gamma$), of which two are different for each decay mode. Therefore, there is not enough information to solve directly for $2\beta + \gamma$. However, for each choice of R and $2\beta + \gamma$, one can find the value of δ that allows a and c to be closest to their measured values, and calculate the distance in terms of numbers of standard deviations. (We currently neglect experimental correlations in this analysis.) These values of $N(\sigma)_{\rm min}$ can

Table 46: Averages for $b \to c\bar{u}d/u\bar{c}d$ modes.

Experiment		$N(B\overline{B})$	a	c
			$D^{\mp}\pi^{\pm}$	
BABAR (full rec.)	[278]	232M	$-0.010 \pm 0.023 \pm 0.007$	$-0.033 \pm 0.042 \pm 0.012$
Belle (full rec.)	[282]	386M	$-0.050 \pm 0.021 \pm 0.012$	$-0.019 \pm 0.021 \pm 0.012$
Average			-0.030 ± 0.017	-0.022 ± 0.021
Confidence level			0.24 (1.2σ)	0.78 (0.3σ)
			$D^{*\mp}\pi^{\pm}$	
BABAR (full rec.)	[278]	232M	$-0.040 \pm 0.023 \pm 0.010$	$0.049 \pm 0.042 \pm 0.015$
BABAR (partial rec.)	[279]	232M	$-0.034 \pm 0.014 \pm 0.009$	$-0.019 \pm 0.022 \pm 0.013$
Belle (full rec.)	[282]	386M	$-0.039 \pm 0.020 \pm 0.013$	$-0.011 \pm 0.020 \pm 0.013$
Belle (partial rec.)	[281]	657M	$-0.046 \pm 0.013 \pm 0.015$	$-0.015 \pm 0.013 \pm 0.015$
Average			-0.039 ± 0.010	-0.010 ± 0.013
Confidence level			0.97 (0.03σ)	0.59 (0.6σ)
			$D^{\mp}\rho^{\pm}$	
BABAR (full rec.)	[278]	232M	$-0.024 \pm 0.031 \pm 0.009$	$-0.098 \pm 0.055 \pm 0.018$

then be plotted as a function of R and $2\beta + \gamma$ (and can trivially be converted to confidence levels). These plots are given for the $D\pi$ and $D^*\pi$ modes in Fig. 38; the uncertainties in the $D\rho$ mode are currently too large to give any meaningful constraint.

The constraints can be tightened if one is willing to use theoretical input on the values of R and/or δ. One popular choice is the use of SU(3) symmetry to obtain R by relating the suppressed decay mode to B decays involving D_s mesons. More details can be found in Refs. [283, 410–413].

4.13 Time-dependent *CP* asymmetries in $b \to c\bar{u}s/u\bar{c}s$ transitions

4.13.1 Time-dependent *CP* asymmetries in $B^0 \to D^{\mp}K^0_S\pi^{\pm}$

Time-dependent analyses of transitions such as $B^0 \to D^{\mp}K^0_S\pi^{\pm}$ can be used to probe $\sin(2\beta+\gamma)$ in a similar way to that discussed above (Sec. 4.12). Since the final state contains three particles, a Dalitz plot analysis is necessary to maximise the sensitivity. *BABAR* [414] have carried out such an analysis. They obtain $2\beta+\gamma = (83 \pm 53 \pm 20)^\circ$ (with an ambiguity $2\beta+\gamma \leftrightarrow 2\beta+\gamma+\pi$) assuming the ratio of the $b \to u$ and $b \to c$ amplitude to be constant across the Dalitz plot at 0.3.

4.13.2 Time-dependent *CP* asymmetries in $B^0_s \to D^{\mp}_s K^{\pm}$

Time-dependent analysis of $B^0_s \to D^{\mp}_s K^{\pm}$ decays can be used to determine $\gamma - 2\beta_s$ [283,415,416]. Compared to the situation for $B^0 \to D^{(*)\mp}\pi^{\pm}$ discussed in Sec. 4.12, the larger value of the ratio R of the magnitudes of the suppressed and favoured amplitudes allows it to be determined from the data. Moreover, the non-zero value of $\Delta\Gamma_s$ allows the determination of additional terms, labelled $A^{\Delta\Gamma}$ and $\overline{A}^{\Delta\Gamma}$, that break ambiguities in the solutions for $\gamma - 2\beta_s$.

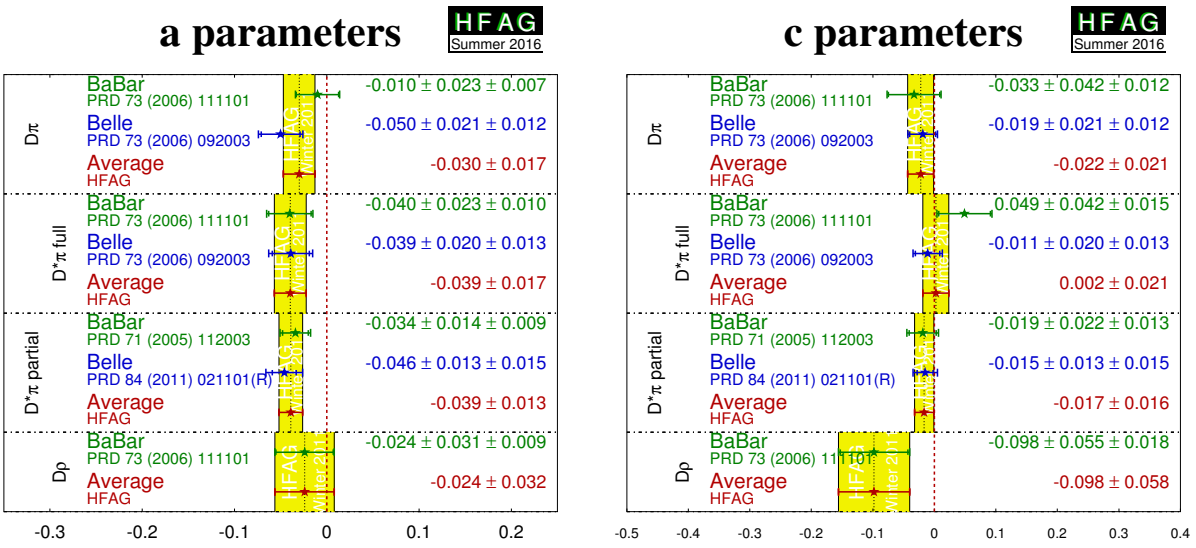

Figure 37: Averages for $b \to c\bar{u}d/u\bar{c}d$ modes.

LHCb [284,417] have measured the time-dependent *CP* violation parameters in $B_s^0 \to D_s^{\mp} K^{\pm}$ decays, using 3.0 fb^{-1} of data. The results are given in Table 47, and correspond to $3.6\,\sigma$ evidence for *CP* violation in the interference between mixing and $B_s^0 \to D_s^{\mp} K^{\pm}$ decays. From these results, and a constraint on $2\beta_s$ from independent LHCb measurements [191], LHCb determine $\gamma = (127\,^{+17}_{-22})^\circ$, $\delta_{D_s K} = (358\,^{+15}_{-16})^\circ$ and $R_{D_s K} = 0.37\,^{+0.10}_{-0.09}$.

Table 47: Results for $B_s^0 \to D_s^{\mp} K^{\pm}$.

Experiment		$\int \mathcal{L}\,dt$	C	$A^{\Delta\Gamma}$	$\overline{A}^{\Delta\Gamma}$	S	$\overline{S}$
LHCb	[417]	3 fb^{-1}	$0.74 \pm 0.14 \pm 0.05$	$0.40 \pm 0.28 \pm 0.12$	$0.31 \pm 0.27 \pm 0.11$	$-0.52 \pm 0.20 \pm 0.07$	$-0.50 \pm 0.20 \pm 0.07$

4.14 Rates and asymmetries in $B \to D^{(*)} K^{(*)}$ decays

As explained in Sec. 4.2.7, rates and asymmetries in $B^{\mp} \to D^{(*)} K^{(*)\mp}$ decays are sensitive to γ, and have negligible theoretical uncertainty [418]. Various methods using different $D^{(*)}$ final states have been used.

4.14.1 *D* decays to *CP* eigenstates

Results are available from *BABAR*, Belle, CDF and LHCb on GLW analyses in the decay mode $B^{\mp} \to DK^{\mp}$. All experiments use the *CP*-even D decay final states K^+K^- and $\pi^+\pi^-$; *BABAR* and Belle in addition use the *CP*-odd decay modes $K^0_S\pi^0$, $K^0_S\omega$ and $K^0_S\phi$, though care is taken to avoid statistical overlap with the $K^0_S K^+ K^-$ sample used for Dalitz plot analyses (see Sec. 4.14.4). *BABAR* and Belle also have results in the decay mode $B^{\mp} \to D^* K^{\mp}$, using both the $D^* \to D\pi^0$ decay, which gives $CP(D^*) = CP(D)$, and the $D^* \to D\gamma$ decays, which gives $CP(D^*) = -CP(D)$. In addition, *BABAR* and LHCb have results in the decay mode

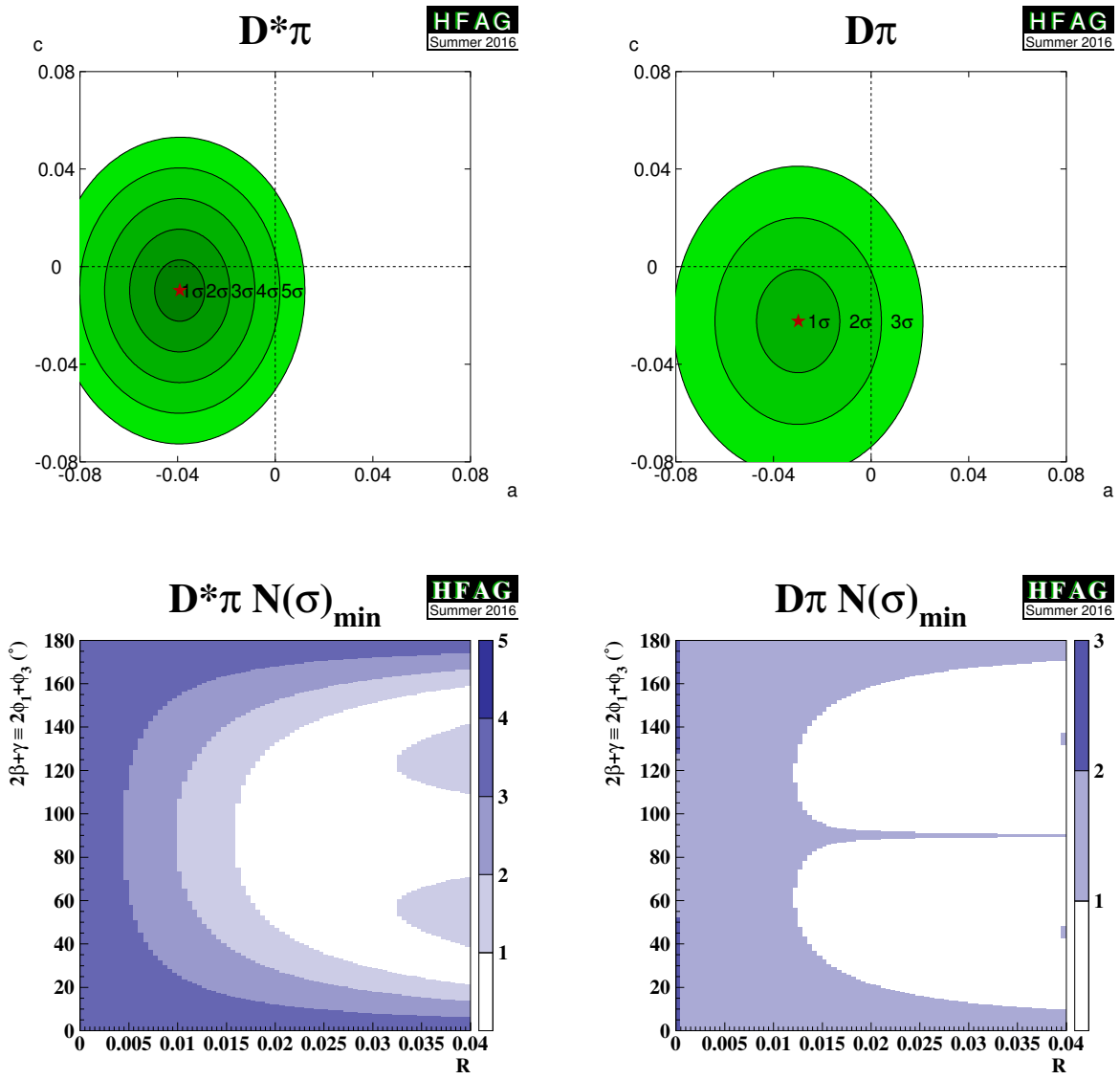

Figure 38: Results from $b \to c\bar{u}d/u\bar{c}d$ modes. (Top) Constraints in c *vs.* a space. (Bottom) Constraints in $2\beta+\gamma$ *vs.* R space. (Left) $D^*\pi$ and (right) $D\pi$ modes.

$B^\mp \to DK^{*\mp}$, and LHCb have results in the decay mode $B^\mp \to DK^\mp\pi^+\pi^-$. The results and averages are given in Table 48 and shown in Fig. 39.

LHCb have performed a GLW analysis using the $B^0 \to DK^{*0}$ decay with the *CP*-even $D \to K^+K^-$ and $D \to \pi^+\pi^-$ channels [427]. The results are presented separately to allow for possible *CP* violation effects in the charm decays, which are, however, known to be small. The results are given in Table 49 where an average is also reported.

As pointed out in Refs. [304, 305], a Dalitz plot analysis of $B^0 \to DK^+\pi^-$ decays provides more sensitivity to $\gamma \equiv \phi_3$ than the quasi-two-body DK^{*0} approach. The analysis provides direct sensitivity to the hadronic parameters r_B and δ_B associated with the $B^0 \to DK^{*0}$ decay amplitudes, rather than effective hadronic parameters averaged over the K^{*0} selection window as in the quasi-two-body case.

Such an analysis has been performed by LHCb. A simultaneous fit is performed to the

Table 48: Averages from GLW analyses of $b \to c\bar{u}s/u\bar{c}s$ modes. The sample size is given in terms of number of $B\overline{B}$ pairs, $N(B\overline{B})$, for the e^+e^- B factory experiments *BABAR* and Belle, and in terms of integrated luminosity, $\int \mathcal{L}\,dt$, for the hadron collider experiments CDF and LHCb.

Experiment		Sample size	A_{CP+}	A_{CP-}	R_{CP+}	R_{CP-}
			$D_{CP}K^-$			
BABAR	[419]	467M	$0.25 \pm 0.06 \pm 0.02$	$-0.09 \pm 0.07 \pm 0.02$	$1.18 \pm 0.09 \pm 0.05$	$1.07 \pm 0.08 \pm 0.04$
Belle	[420]	275M	$0.06 \pm 0.14 \pm 0.05$	$-0.12 \pm 0.14 \pm 0.05$	$1.13 \pm 0.16 \pm 0.08$	$1.17 \pm 0.14 \pm 0.14$
CDF	[421]	$1\,\text{fb}^{-1}$	$0.39 \pm 0.17 \pm 0.04$	–	$1.30 \pm 0.24 \pm 0.12$	–
LHCb KK	[422]	$3\,\text{fb}^{-1}$	$0.087 \pm 0.020 \pm 0.008$	–	$0.968 \pm 0.022 \pm 0.021$	–
LHCb $\pi\pi$	[422]	$3\,\text{fb}^{-1}$	$0.128 \pm 0.037 \pm 0.012$	–	$1.002 \pm 0.040 \pm 0.026$	–
LHCb average	[422]	$3\,\text{fb}^{-1}$	$0.097 \pm 0.018 \pm 0.009$	–	$0.978 \pm 0.019 \pm 0.018$	–
Average			0.111 ± 0.018	-0.10 ± 0.07	0.995 ± 0.025	1.09 ± 0.08
Confidence level			0.063 (1.9σ)	0.86 (0.2σ)	0.21 (1.3σ)	0.65 (0.5σ)
			$D^*_{CP}K^-$			
BABAR	[423]	383M	$-0.11 \pm 0.09 \pm 0.01$	$0.06 \pm 0.10 \pm 0.02$	$1.31 \pm 0.13 \pm 0.03$	$1.09 \pm 0.12 \pm 0.04$
Belle	[420]	275M	$-0.20 \pm 0.22 \pm 0.04$	$0.13 \pm 0.30 \pm 0.08$	$1.41 \pm 0.25 \pm 0.06$	$1.15 \pm 0.31 \pm 0.12$
Average			-0.12 ± 0.07	0.13 ± 0.07	1.25 ± 0.09	1.06 ± 0.09
Confidence level			0.82 (0.2σ)	0.29 (1.1σ)	0.52 (0.6σ)	0.74 (0.3σ)
			$D_{CP}K^{*-}$			
BABAR	[424]	379M	$0.09 \pm 0.13 \pm 0.06$	$-0.23 \pm 0.21 \pm 0.07$	$2.17 \pm 0.35 \pm 0.09$	$1.03 \pm 0.27 \pm 0.13$
LHCb KK	[425]	$4\,\text{fb}^{-1}$	$0.12 \pm 0.08 \pm 0.01$	–	$1.31 \pm 0.11 \pm 0.05$	–
LHCb $\pi\pi$	[425]	$4\,\text{fb}^{-1}$	$0.08 \pm 0.16 \pm 0.02$	–	$0.98 \pm 0.17 \pm 0.04$	–
LHCb average	[425]	$4\,\text{fb}^{-1}$	0.11 ± 0.07	–	1.21 ± 0.10	–
Average			0.11 ± 0.06	-0.23 ± 0.22	1.27 ± 0.10	1.03 ± 0.30
Confidence level			0.97 (0.04σ)		0.01 (2.6σ)	
			$D_{CP}K^-\pi^+\pi^-$			
LHCb KK	[426]	$3\,\text{fb}^{-1}$	$-0.045 \pm 0.064 \pm 0.011$	–	$1.043 \pm 0.069 \pm 0.034$	–
LHCb $\pi\pi$	[426]	$3\,\text{fb}^{-1}$	$-0.054 \pm 0.101 \pm 0.011$	–	$1.035 \pm 0.108 \pm 0.038$	–
LHCb average	[426]	$3\,\text{fb}^{-1}$	-0.048 ± 0.055	–	1.040 ± 0.064	–

Table 49: Results from GLW analysis of $B^0 \to DK^{*0}$.

Experiment		Sample size	A_{CP+}	R_{CP+}
LHCb KK	[427]	$\int \mathcal{L}\,dt = 3\,\text{fb}^{-1}$	$-0.20 \pm 0.15 \pm 0.02$	$1.05\,^{+0.17}_{-0.15} \pm 0.04$
LHCb $\pi\pi$	[427]	$\int \mathcal{L}\,dt = 3\,\text{fb}^{-1}$	$-0.09 \pm 0.22 \pm 0.02$	$1.21\,^{+0.28}_{-0.25} \pm 0.05$
Average			-0.16 ± 0.12	1.10 ± 0.14

$B^0 \to DK^+\pi^-$ Dalitz plots with the neutral D meson reconstructed in the $K^+\pi^-$, K^+K^- and $\pi^+\pi^-$ final states. The reported results in Table 50 are for the Cartesian parameters, defined in Eq. (146) associated with the $B^0 \to DK^*(892)^0$ decay. Note that, since the measurements use overlapping data samples, these results cannot be combined with the LHCb results for GLW observables in $B^0 \to DK^*(892)^0$ decays reported in Table 49.

LHCb use these results to obtain confidence levels for γ, $r_B(DK^{*0})$ and $\delta_B(DK^{*0})$. In

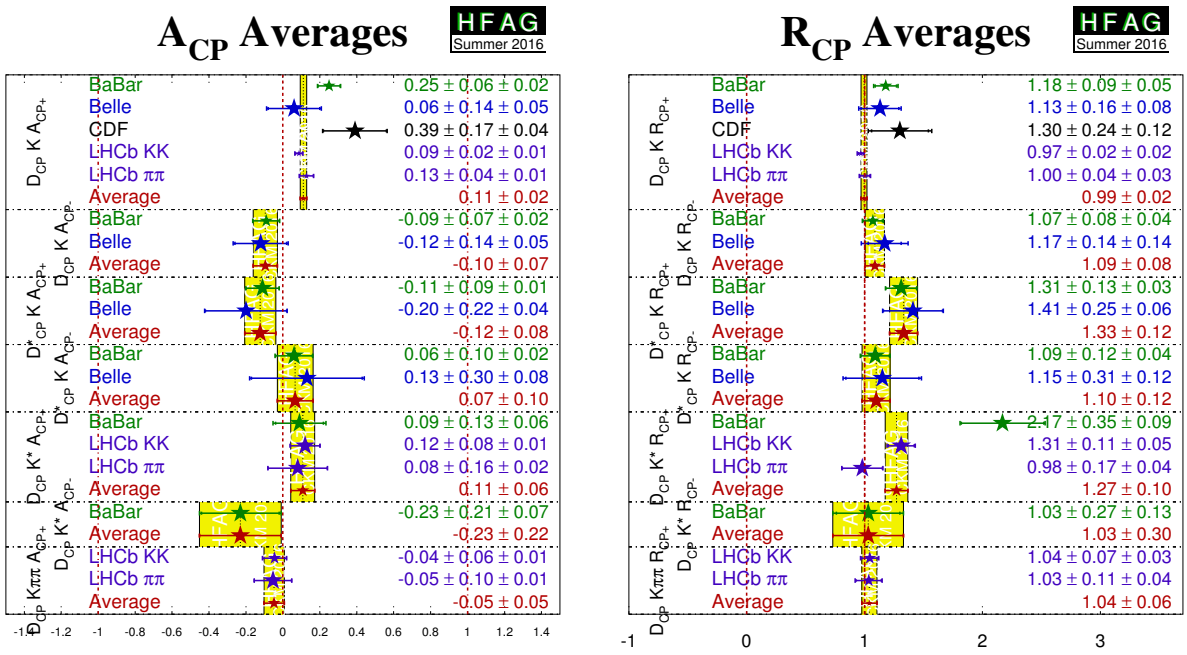

Figure 39: Averages of A_{CP} and R_{CP} from GLW analyses.

Table 50: Averages from Dalitz plot analysis of $B^0 \to D_{CP}K^+\pi^-$ decays.

Experiment	$\int \mathcal{L}\,dt$	x_+	y_+	x_-	y_-
LHCb [428]	$3\,\text{fb}^{-1}$	$0.04 \pm 0.16 \pm 0.11$	$-0.47 \pm 0.28 \pm 0.22$	$-0.02 \pm 0.13 \pm 0.14$	$-0.35 \pm 0.26 \pm 0.41$

addition, results are reported for the hadronic parameters needed to relate these results to quasi-two-body measurements of $B^0 \to DK^*(892)^0$ decays, where a selection window of $m(K^+\pi^-)$ within $50\text{MeV}/c^2$ of the pole mass and helicity angle satisfying $|\cos(\theta_{K^{*0}})| > 0.4$ is assumed. These parameters are the coherence factor κ, the ratio of quasi-two-body and amplitude level r_B values, $\overline{R}_B = \overline{r}_B/r_B$, and the difference between quasi-two-body and amplitude level δ_B values, $\Delta\overline{\delta}_B = \overline{\delta}_B - \delta_B$. LHCb [428] obtain

$$\gamma = 0.958\,^{+0.005\ +0.002}_{-0.010\ -0.045}\,, \quad \overline{R}_B = 1.02\,^{+0.03}_{-0.01} \pm 0.06\,, \quad \Delta\overline{\delta}_B = 0.02\,^{+0.03}_{-0.02} \pm 0.11\,. \tag{159}$$

4.14.2 *D* decays to quasi-*CP* eigenstates

As discussed in Sec. 4.2.7, if a multibody neutral D meson decay can be shown to be dominated by one CP eigenstate, it can be used in a "GLW-like" (sometimes called "quasi-GLW") analysis [302]. The same observables R_{CP}, A_{CP} as for the GLW case are measured, but an additional factor of $(2F_+ - 1)$, where F_+ is the fractional CP-even content, enters the expressions relating these observables to $\gamma \equiv \phi_3$. The F_+ factors have been measured using CLEO-c data to be $F_+(\pi^+\pi^-\pi^0) = 0.973 \pm 0.017$, $F_+(K^+K^-\pi^0) = 0.732 \pm 0.055$, $F_+(\pi^+\pi^-\pi^+\pi^-) = 0.737 \pm 0.028$ [429].

The GLW-like observables for $D \to \pi^+\pi^-\pi^0$, $K^+K^-\pi^0$ and $D \to \pi^+\pi^-\pi^+\pi^-$ have been

measured by LHCb. The $A_{\rm qGLW}$ observable for $D \to \pi^+\pi^-\pi^0$ was measured in an earlier analysis by *BABAR*, from which additional observables, discussed in Sec. 4.2.7 and reported in Table 55 below, were reported. The results are given in Table 51.

Table 51: Averages from GLW-like analyses of $b \to c\bar{u}s/u\bar{c}s$ modes.

Experiment		Sample size	$A_{\rm qGLW}$	$R_{\rm qGLW}$
		$D_{\pi^+\pi^-\pi^0}K^-$		
LHCb	[430]	$\int \mathcal{L}\,dt = 3\,\text{fb}^{-1}$	$0.05 \pm 0.09 \pm 0.01$	$0.98 \pm 0.11 \pm 0.05$
BABAR	[309]	$N(B\overline{B}) = 324\text{M}$	$-0.02 \pm 0.15 \pm 0.03$	–
Average			0.03 ± 0.08	0.98 ± 0.12
Confidence level			0.68 (0.4σ)	–
		$D_{K^+K^-\pi^0}K^-$		
LHCb	[430]	$\int \mathcal{L}\,dt = 3\,\text{fb}^{-1}$	$0.30 \pm 0.20 \pm 0.02$	$0.95 \pm 0.22 \pm 0.04$
		$D_{\pi^+\pi^-\pi^+\pi^-}K^-$		
LHCb	[422]	$\int \mathcal{L}\,dt = 3\,\text{fb}^{-1}$	$0.10 \pm 0.03 \pm 0.02$	$0.97 \pm 0.04 \pm 0.02$

4.14.3 *D* decays to suppressed final states

For ADS analyses, all of *BABAR*, Belle, CDF and LHCb have studied the modes $B^\mp \to DK^\mp$ and $B^\mp \to D\pi^\mp$. *BABAR* have also analysed the $B^\mp \to D^*K^\mp$ mode. There is an effective shift of π in the strong phase difference between the cases that the D^* is reconstructed as $D\pi^0$ and $D\gamma$ [299], therefore these modes are studied separately. *BABAR* has also studied the $B^\mp \to DK^{*\mp}$ mode, where $K^{*\mp}$ is reconstructed as $K^0_S\pi^\mp$, and LHCb have studied the $B^\mp \to DK^\mp\pi^+\pi^-$ mode. In all the above cases the suppressed decay $D \to K^+\pi^-$ has been used. *BABAR*, Belle and LHCb also have results using $B^\mp \to DK^\mp$ with $D \to K^+\pi^-\pi^0$, while LHCb have results using $B^\mp \to DK^\mp$ with $D \to K^+\pi^-\pi^+\pi^-$. The results and averages are given in Table 52 and shown in Fig. 40.

Similar phenomenology as for $B \to DK$ decays holds for $B \to D\pi$ decays, though in this case the interference is between $b \to c\bar{u}d$ and $b \to u\bar{c}d$ transitions, and the ratio of suppressed to favoured amplitudes is expected to be much smaller, $\mathcal{O}(1\%)$. For most D meson final states this implies that the interference effect is too small to be of interest, but in the case of ADS analysis it is possible that effects due to γ may be observable. Accordingly, the experiments now measure the corresponding observables in the $D\pi$ final states. The results and averages are given in Table 53 and shown in Fig. 41.

BABAR, Belle and LHCb have also presented results from a similar analysis method with self-tagging neutral B decays: $B^0 \to DK^{*0}$ with $D \to K^-\pi^+$ (all), $D \to K^-\pi^+\pi^0$ and $D \to K^-\pi^+\pi^+\pi^-$ (*BABAR* only). All these results are obtained with the $K^{*0} \to K^+\pi^-$ decay. Effects due to the natural width of the K^{*0} are handled using the parametrisation suggested by Gronau [303].

The following 95% CL limits are set by *BABAR* [436]:

$$R_{\rm ADS}(K\pi) < 0.244 \quad R_{\rm ADS}(K\pi\pi^0) < 0.181 \quad R_{\rm ADS}(K\pi\pi\pi) < 0.391\,, \tag{160}$$

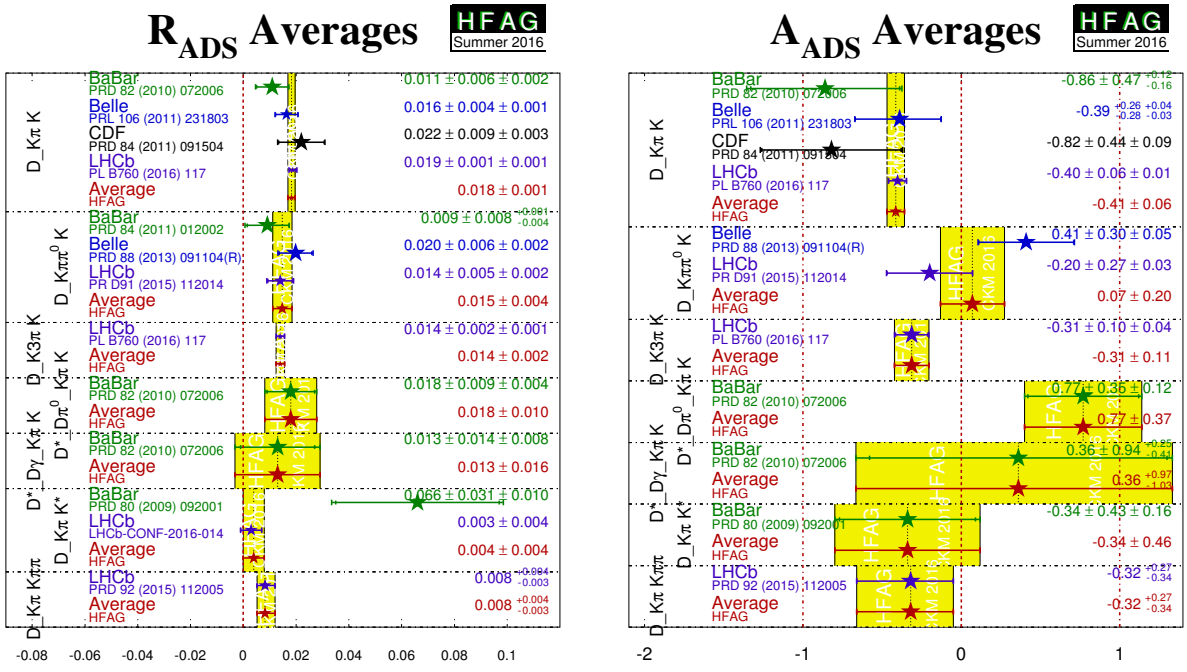

Figure 40: Averages of $R_{\rm ADS}$ and $A_{\rm ADS}$ for $B \to D^{(*)}K^{(*)}$ decays.

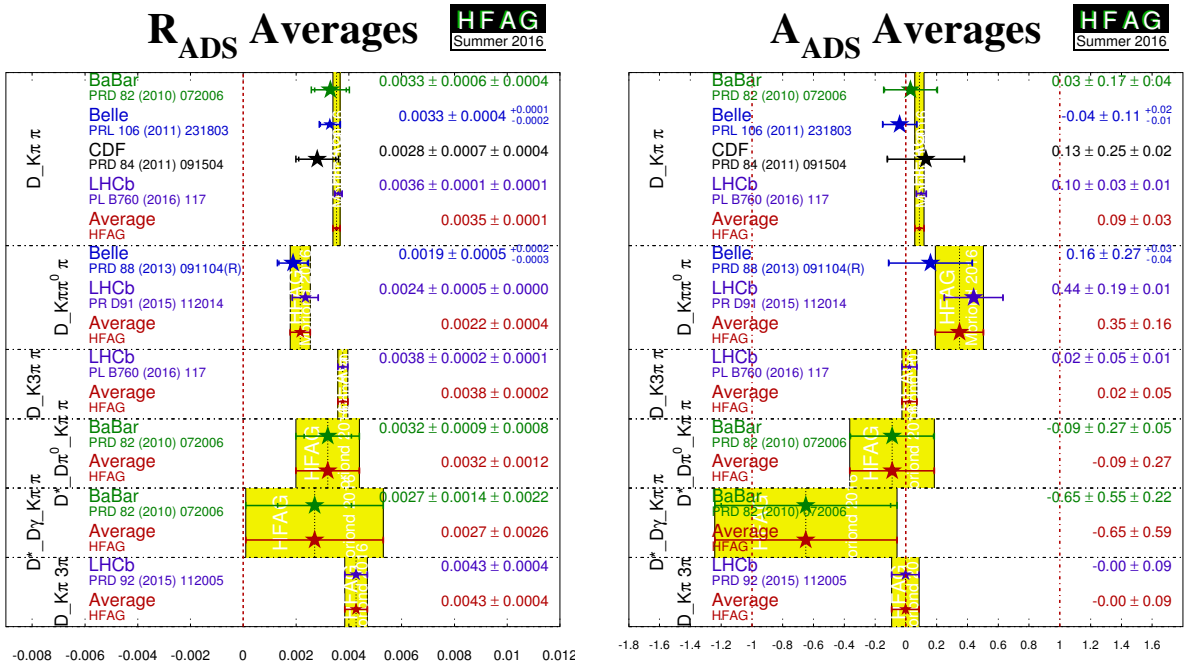

Figure 41: Averages of $R_{\rm ADS}$ and $A_{\rm ADS}$ for $B \to D^{(*)}\pi$ decays.

Table 52: Averages from ADS analyses of $b \to c\overline{u}s/u\overline{c}s$ modes.

Experiment		Sample size	$A_{\rm ADS}$	$R_{\rm ADS}$
		DK^-, $D \to K^+\pi^-$		
BABAR	[431]	$N(B\overline{B}) = 467$M	$-0.86 \pm 0.47\,^{+0.12}_{-0.16}$	$0.011 \pm 0.006 \pm 0.002$
Belle	[432]	$N(B\overline{B}) = 772$M	$-0.39\,^{+0.26\,+0.04}_{-0.28\,-0.03}$	$0.0163\,^{+0.0044\,+0.0007}_{-0.0041\,-0.0013}$
CDF	[433]	$\int \mathcal{L}\,dt = 7\,\text{fb}^{-1}$	$-0.82 \pm 0.44 \pm 0.09$	$0.0220 \pm 0.0086 \pm 0.0026$
LHCb	[422]	$\int \mathcal{L}\,dt = 3\,\text{fb}^{-1}$	$-0.403 \pm 0.056 \pm 0.011$	$0.0188 \pm 0.0011 \pm 0.0010$
Average			-0.415 ± 0.055	0.0183 ± 0.0014
Confidence level			0.64 (0.5σ)	0.61 (0.5σ)
		DK^-, $D \to K^+\pi^-\pi^0$		
BABAR	[434]	474M	–	$0.0091\,^{+0.0082\,+0.0014}_{-0.0076\,-0.0037}$
Belle	[435]	772M	$0.41 \pm 0.30 \pm 0.05$	$0.0198 \pm 0.0062 \pm 0.0024$
LHCb	[430]	$\int \mathcal{L}\,dt = 3\,\text{fb}^{-1}$	$-0.20 \pm 0.27 \pm 0.03$	$0.0140 \pm 0.0047 \pm 0.0019$
Average			0.07 ± 0.20	0.0148 ± 0.0036
Confidence level			0.13 (1.5σ)	0.59 (0.5σ)
		DK^-, $D \to K^+\pi^-\pi^+\pi^-$		
LHCb	[422]	$\int \mathcal{L}\,dt = 3\,\text{fb}^{-1}$	$-0.313 \pm 0.102 \pm 0.038$	$0.0140 \pm 0.0015 \pm 0.0006$
		D^*K^-, $D^* \to D\pi^0$, $D \to K^+\pi^-$		
BABAR	[431]	$N(B\overline{B}) = 467$M	$0.77 \pm 0.35 \pm 0.12$	$0.018 \pm 0.009 \pm 0.004$
		D^*K^-, $D^* \to D\gamma$, $D \to K^+\pi^-$		
BABAR	[431]	$N(B\overline{B}) = 467$M	$0.36 \pm 0.94\,^{+0.25}_{-0.41}$	$0.013 \pm 0.014 \pm 0.008$
		DK^{*-}, $D \to K^+\pi^-$, $K^{*-} \to K^0_S\pi^-$		
BABAR	[424]	$N(B\overline{B}) = 379$M	$-0.34 \pm 0.43 \pm 0.16$	$0.066 \pm 0.031 \pm 0.010$
LHCb	[425]	$\int \mathcal{L}\,dt = 4\,\text{fb}^{-1}$	–	0.003 ± 0.004
Average			-0.34 ± 0.46	0.004 ± 0.004
Confidence level			–	0.06 (1.9σ)
		$DK^-\pi^+\pi^-$, $D \to K^+\pi^-$		
LHCb	[426]	$\int \mathcal{L}\,dt = 3\,\text{fb}^{-1}$	$-0.32\,^{+0.27}_{-0.34}$	$0.0082\,^{+0.0038}_{-0.0030}$

while Belle [437] obtain

$$R_{\rm ADS}(K\pi) < 0.16\,. \tag{161}$$

The results from LHCb, which are presented in terms of the parameters R_+ and R_- instead of $R_{\rm ADS}$ and $A_{\rm ADS}$, are given in Table 54.

Combining the results and using additional input from CLEO-c [438, 439] a limit on the ratio between the $b \to u$ and $b \to c$ amplitudes of $\overline{r}_B(DK^{*0}) \in [0.07, 0.41]$ at 95% CL limit is set by *BABAR*. Belle set a limit of $\overline{r}_B < 0.4$ at 95% CL. LHCb take input from Sec. 8 and obtain $\overline{r}_B = 0.240\,^{+0.055}_{-0.048}$ (different from zero with 2.7σ significance).

Table 53: Averages from ADS analyses of $b \to c\overline{u}d/u\overline{c}d$ modes.

Experiment		Sample size	$A_{\rm ADS}$	$R_{\rm ADS}$
			$D\pi^-$, $D \to K^+\pi^-$	
BABAR	[431]	$N(B\overline{B}) = 467$M	$0.03 \pm 0.17 \pm 0.04$	$0.0033 \pm 0.0006 \pm 0.0004$
Belle	[432]	$N(B\overline{B}) = 772$M	$-0.04 \pm 0.11\,^{+0.02}_{-0.01}$	$0.00328\,^{+0.00038\ +0.00012}_{-0.00036\ -0.00018}$
CDF	[433]	$\int \mathcal{L}\,dt = 7\,\text{fb}^{-1}$	$0.13 \pm 0.25 \pm 0.02$	$0.0028 \pm 0.0007 \pm 0.0004$
LHCb	[422]	$\int \mathcal{L}\,dt = 3\,\text{fb}^{-1}$	$0.100 \pm 0.031 \pm 0.009$	$0.00360 \pm 0.00012 \pm 0.00009$
Average			0.088 ± 0.030	0.00353 ± 0.00014
Confidence level			0.66 (0.4σ)	0.68 (0.4σ)
			$D\pi^-$, $D \to K^+\pi^-\pi^0$	
Belle	[435]	772M	$0.16 \pm 0.27\,^{+0.03}_{-0.04}$	$0.00189 \pm 0.00054\,^{+0.00022}_{-0.00025}$
LHCb	[430]	$\int \mathcal{L}\,dt = 3\,\text{fb}^{-1}$	$0.44 \pm 0.19 \pm 0.01$	$0.00235 \pm 0.00049 \pm 0.00004$
Average			0.35 ± 0.16	0.00216 ± 0.00038
Confidence level			0.40 (0.8σ)	0.55 (0.6σ)
			$D\pi^-$, $D \to K^+\pi^-\pi^+\pi^-$	
LHCb	[422]	$\int \mathcal{L}\,dt = 3\,\text{fb}^{-1}$	$0.023 \pm 0.048 \pm 0.005$	$0.00377 \pm 0.00018 \pm 0.00006$
			$D^*\pi^-$, $D^* \to D\pi^0$, $D \to K^+\pi^-$	
BABAR	[431]	467M	$-0.09 \pm 0.27 \pm 0.05$	$0.0032 \pm 0.0009 \pm 0.0008$
			$D^*\pi^-$, $D^* \to D\gamma$, $D \to K^+\pi^-$	
BABAR	[431]	467M	$-0.65 \pm 0.55 \pm 0.22$	$0.0027 \pm 0.0014 \pm 0.0022$
			$D\pi^-\pi^+\pi^-$, $D \to K^+\pi^-$	
LHCb	[426]	$\int \mathcal{L}\,dt = 3\,\text{fb}^{-1}$	-0.003 ± 0.090	0.00427 ± 0.00043

Table 54: Results from ADS analysis of $B^0 \to DK^{*0}$, $D \to K^+\pi^-$.

Experiment		Sample size	R_+	R_-
LHCb	[427]	$\int \mathcal{L}\,dt = 3\text{fb}^{-1}$	$0.06 \pm 0.03 \pm 0.01$	$0.06 \pm 0.03 \pm 0.01$

4.14.4 *D* decays to multiparticle self-conjugate final states (model-dependent analysis)

For the model-dependent Dalitz plot analysis, both *BABAR* and Belle have studied the modes $B^\mp \to DK^\mp$, $B^\mp \to D^*K^\mp$ and $B^\mp \to DK^{*\mp}$. For $B^\mp \to D^*K^\mp$, both experiments have used both D^* decay modes, $D^* \to D\pi^0$ and $D^* \to D\gamma$, taking the effective shift in the strong phase difference into account.[47] In all cases the decay $D \to K^0_S\pi^+\pi^-$ has been used. *BABAR* also used the decay $D \to K^0_S K^+K^-$. LHCb has also studied $B^\mp \to DK^\mp$ decays with $D \to K^0_S\pi^+\pi^-$.

[47] Belle [440] quote separate results for $B^\mp \to D^*K^\mp$ with $D^* \to D\pi^0$ and $D^* \to D\gamma$. The results quoted in Table 55 are from our average, performed using the statistical correlations provided, and neglecting all systematic correlations; model uncertainties are not included. The first uncertainty on the quoted results is combined statistical and systematic, the second is the model error (taken from the Belle results on $B^\mp \to D^*K^\mp$ with $D^* \to D\pi^0$).

BABAR has also performed an analysis of $B^\mp \to DK^\mp$ with $D \to \pi^+\pi^-\pi^0$. Results and averages are given in Table 55, and shown in Figs. 42 and 43. The third error on each measurement is due to D decay model uncertainty.

The parameters measured in the analyses are explained in Sec. 4.2.7. All experiments measure the Cartesian variables, defined in Eq. (146), and perform frequentist statistical procedures, to convert these into measurements of γ, r_B and δ_B. In the $B^\mp \to DK^\mp$ with $D \to \pi^+\pi^-\pi^0$ analysis, the parameters $(\rho^\pm, \theta^\pm)$ are used instead.

Both experiments reconstruct $K^{*\mp}$ as $K^0_S\pi^\mp$, but the treatment of possible nonresonant $K^0_S\pi^\mp$ differs: Belle assign an additional model uncertainty, while *BABAR* use a parametrisation suggested by Gronau [303]. The parameters r_B and δ_B are replaced with effective parameters $\kappa\overline{r}_B$ and $\overline{\delta}_B$; no attempt is made to extract the true hadronic parameters of the $B^\mp \to DK^{*\mp}$ decay.

We perform averages using the following procedure, which is based on a set of reasonable, though imperfect, assumptions.

- It is assumed that effects due to the different D decay models used by the two experiments are negligible. Therefore, we do not rescale the results to a common model.
- It is further assumed that the model uncertainty is 100% correlated between experiments, and therefore this source of error is not used in the averaging procedure. (This approximation is comprimised by the fact that the *BABAR* results include $D \to K^0_S K^+K^-$ decays in addition to $D \to K^0_S\pi^+\pi^-$.)
- We include in the average the effect of correlations within each experiment's set of measurements.
- At present it is unclear how to assign an average model uncertainty. We have not attempted to do so. Our average includes only statistical and systematic errors. An unknown amount of model uncertainty should be added to the final error.
- We follow the suggestion of Gronau [303] in making the DK^* averages. Explicitly, we assume that the selection of $K^{*\mp} \to K^0_S\pi^\mp$ is the same in both experiments (so that κ, $\overline{r}_B$ and $\overline{\delta}_B$ are the same), and drop the additional source of model uncertainty assigned by Belle due to possible nonresonant decays.
- We do not consider common systematic errors, other than the D decay model.

Constraints on $\gamma \equiv \phi_3$

The measurements of $(x_\pm, y_\pm)$ can be used to obtain constraints on γ, as well as the hadronic parameters r_B and δ_B. *BABAR* [441], Belle [440, 443] and LHCb [442] have all done so using a frequentist procedure (there are some differences in the details of the techniques used).

- *BABAR* obtain $\gamma = (68\,^{+15}_{-14} \pm 4 \pm 3)^\circ$ from $DK^\pm$, $D^*K^\pm$ and $DK^{*\pm}$.
- Belle obtain $\phi_3 = (78\,^{+11}_{-12} \pm 4 \pm 9)^\circ$ from $DK^\pm$ and $D^*K^\pm$.
- LHCb obtain $\gamma = (84\,^{+49}_{-42})^\circ$ from $DK^\pm$ using 1 fb^{-1} of data (a more precise result using 3 fb^{-1} and the model-independent method is reported below).
- The experiments also obtain values for the hadronic parameters as detailed in Table 56.

Table 55: Averages from model-dependent Dalitz plot analyses of $b \to c\bar{u}s/u\bar{c}s$ modes. Note that the uncertainities assigned to the averages do not include model errors.

Experiment		Sample size	x_+	y_+	x_-	y_-
			DK^-, $D \to K^0_S\pi^+\pi^-$			
BABAR	[441]	$N(B\overline{B}) = 468$M	$-0.103 \pm 0.037 \pm 0.006 \pm 0.007$	$-0.021 \pm 0.048 \pm 0.004 \pm 0.009$	$0.060 \pm 0.039 \pm 0.007 \pm 0.006$	$0.062 \pm 0.045 \pm 0.004 \pm 0.006$
Belle	[440]	$N(B\overline{B}) = 657$M	$-0.107 \pm 0.043 \pm 0.011 \pm 0.055$	$-0.067 \pm 0.059 \pm 0.018 \pm 0.063$	$0.105 \pm 0.047 \pm 0.011 \pm 0.064$	$0.177 \pm 0.060 \pm 0.018 \pm 0.054$
LHCb	[442]	$\int \mathcal{L}\,dt = 1\text{fb}^{-1}$	$-0.084 \pm 0.045 \pm 0.009 \pm 0.005$	$-0.032 \pm 0.048\,^{+0.010}_{-0.009} \pm 0.008$	$0.027 \pm 0.044\,^{+0.010}_{-0.008} \pm 0.001$	$0.013 \pm 0.048\,^{+0.009}_{-0.007} \pm 0.003$
Average			-0.098 ± 0.024	-0.036 ± 0.030	0.070 ± 0.025	0.075 ± 0.029
Confidence level				0.52 (0.7σ)		
			D^*K^-, $D^* \to D\pi^0$ or $D\gamma$, $D \to K^0_S\pi^+\pi^-$			
BABAR	[441]	$N(B\overline{B}) = 468$M	$0.147 \pm 0.053 \pm 0.017 \pm 0.003$	$-0.032 \pm 0.077 \pm 0.008 \pm 0.006$	$-0.104 \pm 0.051 \pm 0.019 \pm 0.002$	$-0.052 \pm 0.063 \pm 0.009 \pm 0.007$
Belle	[440]	$N(B\overline{B}) = 657$M	$0.100 \pm 0.074 \pm 0.081$	$0.155 \pm 0.101 \pm 0.063$	$-0.023 \pm 0.112 \pm 0.090$	$-0.252 \pm 0.112 \pm 0.049$
Average			0.132 ± 0.044	0.037 ± 0.061	-0.081 ± 0.049	-0.107 ± 0.055
Confidence level				0.22 (1.2σ)		
			DK^{*-}, $D \to K^0_S\pi^+\pi^-$			
BABAR	[441]	$N(B\overline{B}) = 468$M	$-0.151 \pm 0.083 \pm 0.029 \pm 0.006$	$0.045 \pm 0.106 \pm 0.036 \pm 0.008$	$0.075 \pm 0.096 \pm 0.029 \pm 0.007$	$0.127 \pm 0.095 \pm 0.027 \pm 0.006$
Belle	[443]	$N(B\overline{B}) = 386$M	$-0.105\,^{+0.177}_{-0.167} \pm 0.006 \pm 0.088$	$-0.004\,^{+0.164}_{-0.156} \pm 0.013 \pm 0.095$	$-0.784\,^{+0.249}_{-0.295} \pm 0.029 \pm 0.097$	$-0.281\,^{+0.440}_{-0.335} \pm 0.046 \pm 0.086$
Average			-0.152 ± 0.077	0.024 ± 0.091	-0.043 ± 0.094	0.091 ± 0.096
Confidence level				0.011 (2.5σ)		
			DK^{*0}, $D \to K^0_S\pi^+\pi^-$, $K^{*0} \to K^+\pi^-$			
LHCb	[444]	$\int \mathcal{L}\,dt = 3\,\text{fb}^{-1}$	$0.05 \pm 0.24 \pm 0.04 \pm 0.01$	$-0.65\,^{+0.24}_{-0.23} \pm 0.08 \pm 0.01$	$-0.15 \pm 0.14 \pm 0.03 \pm 0.01$	$0.25 \pm 0.15 \pm 0.06 \pm 0.01$

Experiment		$N(B\overline{B})$	ρ^+	θ^+	ρ^-	θ^-
			DK^-, $D \to \pi^+\pi^-\pi^0$			
BABAR	[309]	324M	$0.75 \pm 0.11 \pm 0.04$	$147 \pm 23 \pm 1$	$0.72 \pm 0.11 \pm 0.04$	$173 \pm 42 \pm 2$

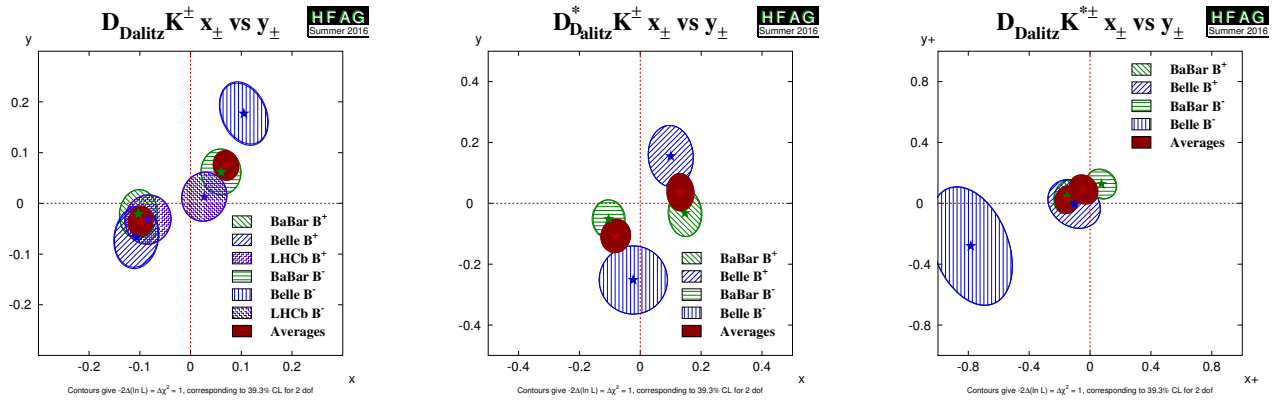

Figure 42: Contours in the $(x_\pm, y_\pm)$ from model-dependent analysis of $B^\mp \to D^{(*)}K^{(*)\pm}$, $D \to K^0_S h^+h^-$ $(h = \pi, K)$. (Left) $B^\mp \to DK^\mp$, (middle) $B^\mp \to D^*K^\mp$, (right) $B^\mp \to DK^{*\mp}$. Note that the uncertainties assigned to the averages given in these plots do not include model errors.

- In the *BABAR* analysis of $B^\mp \to DK^\mp$ with $D \to \pi^+\pi^-\pi^0$ [309], a constraint of $-30° < \gamma < 76°$ is obtained at the 68% confidence level.
- The results discussed here are included in the HFAG combination to obtain a world average value for $\gamma \equiv \phi_3$, as discussed in Sec. 4.14.7.

BABAR and LHCb have performed a similar analysis using the self-tagging neutral B decay $B^0 \to DK^{*0}$ (with $K^{*0} \to K^+\pi^-$). Effects due to the natural width of the K^{*0} are handled using the parametrisation suggested by Gronau [303]. LHCb give results in terms of the Cartesian parameters, as shown in Table 55. *BABAR* [445] present results only in terms of γ and the hadronic parameters. The obtained constraints on $\gamma \equiv \phi_3$ are

- *BABAR* obtain $\gamma = (162 \pm 56)°$
- LHCb obtain $\gamma = (80\,^{+21}_{-22})°$
- Values for the hadronic parameters are given in Table 56.

4.14.5 *D* decays to multiparticle self-conjugate final states (model-independent analysis)

A model-independent approach to the analysis of $B^- \to D^{(*)}K^-$ with multibody D decays was proposed by Giri, Grossman, Soffer and Zupan [297], and further developed by Bondar and Poluektov [306, 307]. The method relies on information on the average strong phase difference between D^0 and $\overline{D}^0$ decays in bins of Dalitz plot position that can be obtained from quantum-correlated $\psi(3770) \to D^0\overline{D}^0$ events. This information is measured in the form of parameters c_i and s_i that are the amplitude weighted averages of the cosine and sine of the strong phase difference in a Dalitz plot bin labelled by i, respectively. These quantities have been obtained for $D \to K^0_S\pi^+\pi^-$ (and $D \to K^0_S K^+K^-$) by CLEO-c [251, 446].

Belle [447] and LHCb [448] have used the model-independent Dalitz plot analysis approach to study the mode $B^\mp \to DK^\mp$. Both Belle [449] and LHCb [450] have also used this approach to study $B^0 \to DK^*(892)^0$ decays. In both cases, both experiments use $D \to K^0_S\pi^+\pi^-$ decays

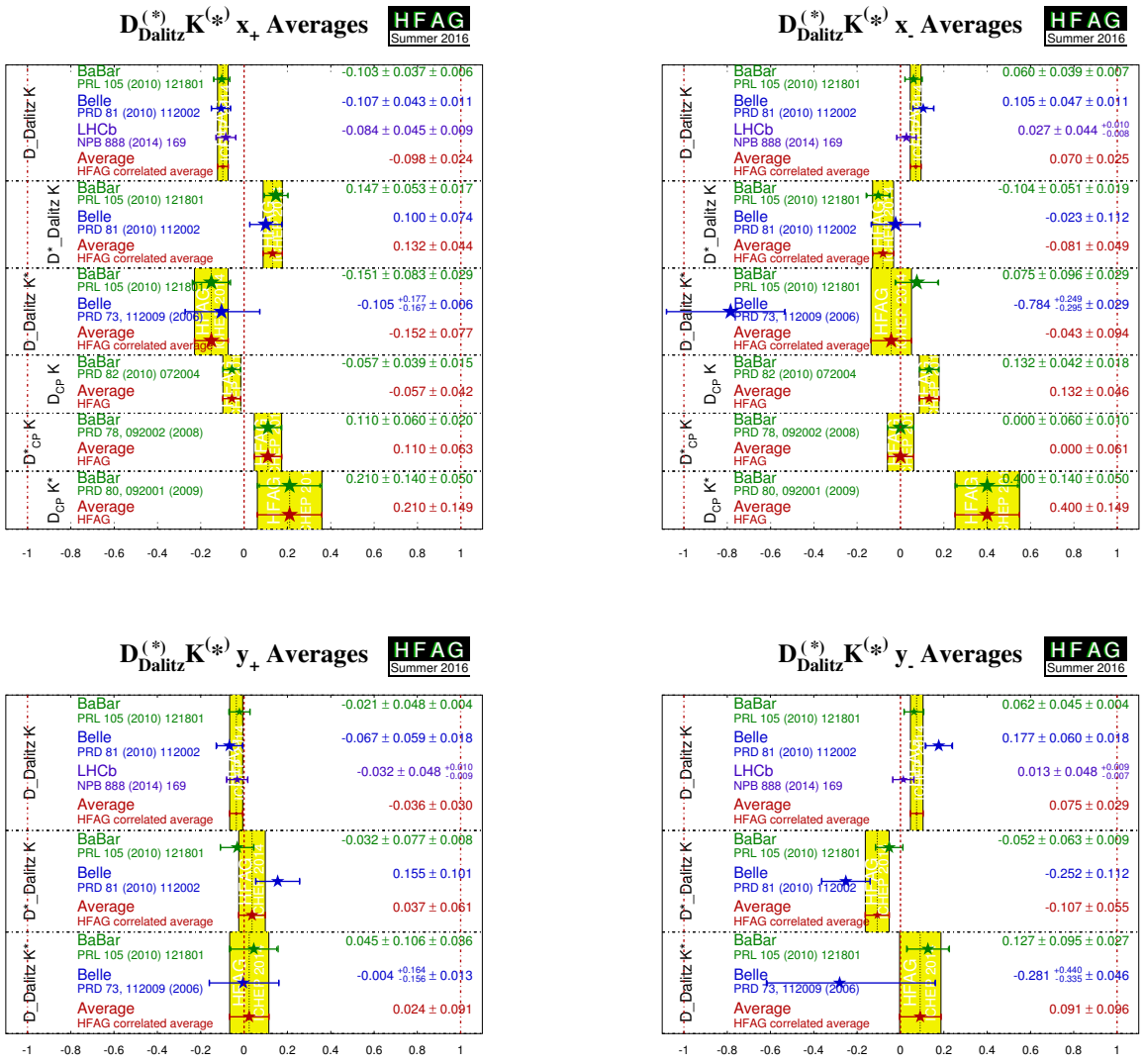

Figure 43: Averages of $(x_\pm, y_\pm)$ from model-dependent analyses of $B^\pm \to D^{(*)}K^{(*)\pm}$ with $D \to K^0_S h^+ h^-$ $(h = \pi, K)$. (Top left) x_+, (top right) x_-, (bottom left) y_+, (bottom right) y_-. The top plots include constraints on $x_\pm$ obtained from GLW analyses (see Sec. 4.14.1). Note that the uncertainties assigned to the averages given in these plots do not include model errors.

while LHCb have also included the $D \to K^0_S K^+ K^-$ decay. The Cartesian variables $(x_\pm, y_\pm)$, defined in Eq. (146), are determined from the data. Note that due to the strong statistical and systematic correlations with the model-dependent results given in Sec. 4.14.4, these results cannot be combined.

The results and averages are given in Table 57, and shown in Figs. 44. Most results have three sets of errors, which are statistical, systematic, and uncertainty coming from the knowledge of c_i and s_i respectively. To perform the average, we remove the last uncertainty, which should be 100% correlated between the measurements. Since the size of the uncertainty from c_i and s_i is found to depend on the size of the $B \to DK$ data sample, we assign the LHCb uncertainties (which are mostly the smaller of the Belle and LHCb values) to the averaged result. This procedure should be conservative. In the LHCb $B^0 \to DK^*(892)^0$ results [450],

Table 56: Summary of constraints on hadronic parameters in $B^\pm \to D^{(*)}K^{(*)\pm}$ decays. Note the alternative parametrisation of the hadronic parameters used by *BABAR* in the $DK^{*\pm}$ mode.

	r_B	δ_B
	In $DK^\pm$	
BABAR	$0.096 \pm 0.029 \pm 0.005 \pm 0.004$	$(119\,^{+19}_{-20} \pm 3 \pm 3)^\circ$
Belle	$0.160\,^{+0.040}_{-0.038} \pm 0.011\,^{+0.05}_{-0.010}$	$(138\,^{+13}_{-16} \pm 4 \pm 23)^\circ$
LHCb	0.06 ± 0.04	$(115\,^{+41}_{-51})^\circ$
	In $D^*K^\pm$	
BABAR	$0.133\,^{+0.042}_{-0.039} \pm 0.014 \pm 0.003$	$(-82 \pm 21 \pm 5 \pm 3)^\circ$
Belle	$0.196\,^{+0.072}_{-0.069} \pm 0.012\,^{+0.062}_{-0.012}$	$(342\,^{+19}_{-21} \pm 3 \pm 23)^\circ$
	$\overline{r}_B$	$\overline{\delta}_B$
	In $DK^{*\pm}$	
BABAR	$\kappa\overline{r}_B = 0.149\,^{+0.066}_{-0.062} \pm 0.026 \pm 0.006$	$(111 \pm 32 \pm 11 \pm 3)^\circ$
Belle	$0.56\,^{+0.22}_{-0.16} \pm 0.04 \pm 0.08$	$(243\,^{+20}_{-23} \pm 3 \pm 50)^\circ$
	In DK^{*0}	
BABAR	< 0.55 at 95% probability	$(62 \pm 57)^\circ$
LHCb	0.39 ± 0.13	$(197\,^{+24}_{-20})^\circ$

the values of c_i and s_i are constrained to their measured values within uncertainties in the fit to data, and hence the effect is absorbed in their statistical uncertainties. The $B^0 \to DK^*(892)^0$ average is performed neglecting the model uncertainties on the Belle results.

Constraints on $\gamma \equiv \phi_3$

The measurements of $(x_\pm, y_\pm)$ can be used to obtain constraints on γ, as well as the hadronic parameters r_B and δ_B. The experiments have done so using frequentist procedures (there are some differences in the details of the techniques used).

- From $B^\mp \to DK^\mp$, Belle [447] obtain $\phi_3 = (77.3\,^{+15.1}_{-14.9} \pm 4.1 \pm 4.3)^\circ$.
- From $B^\mp \to DK^\mp$, LHCb [448] obtain $\gamma = (62\,^{+15}_{-14})^\circ$.
- From $B^0 \to DK^*(892)^0$, LHCb [450] obtain $\gamma = (71 \pm 20)^\circ$.
- The experiments also obtain values for the hadronic parameters as detailed in Table 59.
- The results discussed here are included in the HFAG combination to obtain a world average value for $\gamma \equiv \phi_3$, as discussed in Sec. 4.14.7.

4.14.6 *D* decays to multiparticle non-self-conjugate final states (model-independent analysis)

Following the original suggestion of Grossman, Ligeti and Soffer [301], decays of D mesons to $K^0_S K^\pm \pi^\mp$ can be used in a similar approach to that discussed above to determine $\gamma \equiv \phi_3$. Since these decays are less abundant, the event samples available to date have not been

Table 57: Averages from model-independent Dalitz plot analyses of $b \to c\overline{u}s/u\overline{c}s$ modes.

Experiment	Sample size	x_+	y_+	x_-	y_-
		DK^-, $D \to K^0_S\pi^+\pi^-$			
Belle [447]	$N(B\overline{B}) = 772$M	$-0.110 \pm 0.043 \pm 0.014 \pm 0.007$	$-0.050\,^{+0.052}_{-0.055} \pm 0.011 \pm 0.007$	$0.095 \pm 0.045 \pm 0.014 \pm 0.010$	$0.137\,^{+0.053}_{-0.057} \pm 0.015 \pm 0.023$
LHCb [448]	$\int \mathcal{L}\,dt = 3\text{fb}^{-1}$	$-0.077 \pm 0.024 \pm 0.010 \pm 0.004$	$-0.022 \pm 0.025 \pm 0.004 \pm 0.010$	$0.025 \pm 0.025 \pm 0.010 \pm 0.005$	$0.075 \pm 0.029 \pm 0.005 \pm 0.014$
Average		$-0.085 \pm 0.023 \pm 0.04$	$-0.027 \pm 0.023 \pm 0.010$	$0.044 \pm 0.023 \pm 0.005$	$0.090 \pm 0.026 \pm 0.014$
Confidence level			0.39 (0.9σ)		
		DK^{*0}, $D \to K^0_S\pi^+\pi^-$			
Belle [449]	$N(B\overline{B}) = 772$M	$0.1\,^{+0.7\,+0.0}_{-0.4\,-0.1} \pm 0.1$	$0.3\,^{+0.5\,+0.0}_{-0.8\,-0.1} \pm 0.1$	$0.4\,^{+1.0\,+0.0}_{-0.6\,-0.1} \pm 0.0$	$-0.6\,^{+0.8\,+0.1}_{-1.0\,-0.0} \pm 0.1$
LHCb [450]	$\int \mathcal{L}\,dt = 3\text{fb}^{-1}$	$0.05 \pm 0.35 \pm 0.02$	$-0.81 \pm 0.28 \pm 0.06$	$-0.31 \pm 0.20 \pm 0.04$	$0.31 \pm 0.21 \pm 0.05$
Average		0.10 ± 0.30	-0.63 ± 0.26	-0.27 ± 0.20	0.27 ± 0.21
Confidence level			0.38 (0.9σ)		

Table 58: Results from model-independent Dalitz plot analysis of $B^- \to DK^-$, $D \to K^0_S K^\pm \pi^\mp$.

Experiment		$\int \mathcal{L}\, dt$	$R_{\rm SS}$	$R_{\rm OS}$	$A_{{\rm SS},DK}$	$A_{{\rm OS},DK}$	$A_{{\rm SS},D\pi}$	$A_{{\rm OS},D\pi}$
				$D \to K^0_S K^\pm \pi^\mp$ (whole Dalitz plot)				
LHCb	[451]	3 fb^{-1}	$0.092 \pm 0.009 \pm 0.004$	$0.066 \pm 0.009 \pm 0.002$	$0.040 \pm 0.091 \pm 0.018$	$0.233 \pm 0.129 \pm 0.024$	$-0.025 \pm 0.024 \pm 0.010$	$-0.052 \pm 0.029 \pm 0.017$
				$D \to K^*(892)^\pm \pi^\mp$				
LHCb	[451]	3 fb^{-1}	$0.084 \pm 0.011 \pm 0.003$	$0.056 \pm 0.013 \pm 0.002$	$0.026 \pm 0.109 \pm 0.029$	$0.336 \pm 0.208 \pm 0.026$	$-0.012 \pm 0.028 \pm 0.010$	$-0.054 \pm 0.043 \pm 0.017$

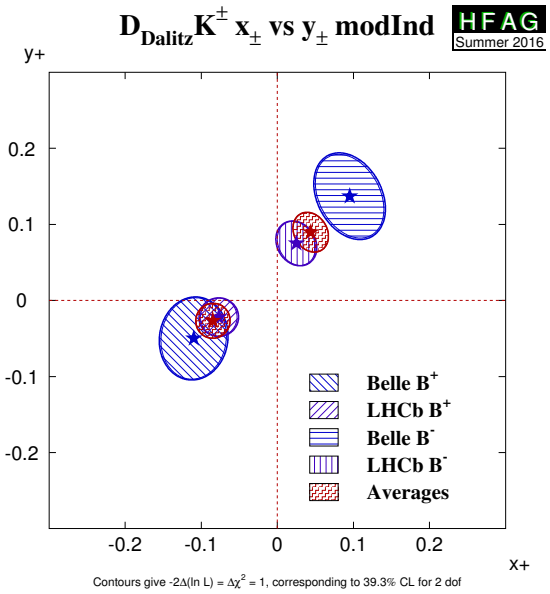

Figure 44: Contours in the $(x_\pm, y_\pm)$ plane from model-independent analysis of $B^\mp \to DK^\mp$ with $D \to K^0_S h^+ h^-$,$(h = \pi, K)$.

Table 59: Summary of constraints on hadronic parameters from model-independent analyses of $B^\pm \to DK^\pm$, $D \to K^0_S h^+ h^-$ $(h = \pi, K)$ decays.

	$r_B(DK^\pm)$	$\delta_B(DK^\pm)$
Belle	$0.145 \pm 0.030 \pm 0.010 \pm 0.011$	$(129.9 \pm 15.0 \pm 3.8 \pm 4.7)^\circ$
LHCb	$0.080\,^{+0.019}_{-0.021}$	$(134\,^{+14}_{-15})^\circ$
	$\overline{r}_B(DK^{*0})$	$\overline{\delta}_B(DK^{*0})$
Belle	< 0.87 at 68% confidence level	
LHCb	0.56 ± 0.17	$(204\,^{+21}_{-20})^\circ$

sufficient for a fine binning of the Dalitz plots, but the analysis can be performed using only an overall coherence factor and related strong phase difference for the decay. These quantities have been determined by CLEO-c [452] both for the full Dalitz plots and in a restricted region ± 100 MeV/c^2 around the peak of the $K^*(892)^\pm$ resonance.

LHCb [451] have reported results of an analysis of $B^- \to DK^-$ and $B^- \to D\pi^-$ decays with $D \to K^0_S K^\pm \pi^\mp$. The decays with different final states of the D meson are distinguished by the charge of the kaon from the decay of the D meson relative to the charge of the B meson, and are labelled "same sign" (SS) and "opposite sign" (OS). Six observables potentially sensitive to $\gamma \equiv \phi_3$ are measured: two ratios of rates for DK and $D\pi$ decays (one each for SS and OS) and four asymmetries (for DK & $D\pi$, SS & OS). This is done both for the full Dalitz plot and for the $K^*(892)^\pm$-dominated region (with the same boundaries as used by CLEO-c). Note that there is a significant overlap of events between the two samples. The results, shown in Table 58 do not yet have sufficient precision to set significant constraints on $\gamma \equiv \phi_3$.

Table 60: Summary of constraints on hadronic parameters obtained from global combinations of results in $B^\pm \to D^{(*)}K^{(*)\pm}$ and $B^0 \to DK^{*0}$ decays.

	$r_B(DK^\pm)$	$\delta_B(DK^\pm)$
BABAR	$0.092\,^{+0.013}_{-0.012}$	$(105\,^{+16}_{-17})^\circ$
LHCb	0.1019 ± 0.0056	$(142.6\,^{+5.7}_{-6.6})^\circ$
	$r_B(DK^{*0})$	$\delta_B(DK^{*0})$
LHCb	$0.218\,^{+0.045}_{-0.047}$	$(189\,^{+23}_{-20})^\circ$

4.14.7 Combinations of results on rates and asymmetries in $B \to D^{(*)}K^{(*)}$ decays to obtain constraints on $\gamma \equiv \phi_3$

BABAR and LHCb have both produced constraints on $\gamma \equiv \phi_3$ from combinations of their results on $B^- \to DK^-$ and related processes. The experiments use a frequentist procedure (there are some differences in the details of the techniques used).

- *BABAR* [453] use results from DK, D^*K and DK^* modes with GLW, ADS and GGSZ analyses, to obtain $\gamma = (69\,^{+17}_{-16})^\circ$.
- LHCb [454] use results from the DK^+ mode with GLW, GLW-like, ADS, GGSZ ($K^0_S h^+h^-$) and GLS ($K^0_S K^\pm\pi^\mp$) analyses, as well as DK^{*0} with GLW, ADS and GGSZ analyses, $DK^+\pi^-$ GLW Dalitz plot analysis, $DK^+\pi^-\pi^+$ with GLW and ADS analyses and $B^0_s \to D^\mp_s K^\pm$ decays. The LHCb combination takes into account subleading effects due to charm mixing and *CP* violation [455]. The result is $\gamma = (72.2\,^{+6.8}_{-7.3})^\circ$.
- All the combinations use inputs determined from $\psi(3770) \to D^0\overline{D}^0$ data samples (and/or from the HFAG Charm Physics subgroup global fits on charm mixing parameters, see Sec. 8.1) to constrain the hadronic parameters in the charm system.
- Constraints are also obtained on the hadronic parameters involved in the decays. A summary of these is given in Table 60.
- The CKMfitter [240] and UTFit [326] groups perform similar combinations of all available results to make combined constraints on $\gamma \equiv \phi_3$.

Independently from the constraints on $\gamma \equiv \phi_3$ obtained by the experiments, the results summarised in Sec. 4.14 are statistically combined to produce world average constraints on $\gamma \equiv \phi_3$ and the hadronic parameters involved. The combination is performed with the GAMMACOMBO framework [456] and follows a frequentist procedure, similar to those used by the experiments [453, 454, 457].

The input measurements used in the combination are listed in Table 61. Individual measurements are used as inputs, rather than the HFAG averages presented in Sec. 4.14, in order to facilitate cross-checks and to ensure the most appropriate treatment of correlations. A combination based on the HFAG averages for each of the quantities measured by experiments gives consistent results. All results from GLW and GLW-like analyses of $B^- \to D^{(\star)}K^{(\star)-}$ modes, as listed in Tables 48 and 51, are used. All results from ADS analyses of $B^- \to D^{(\star)}K^{(\star)-}$ as listed in Table 52 are also used. Concerning results of GGSZ analyses of $B^- \to D^{(\star)}K^{(\star)-}$

with $D \to K^0_S h^+ h^-$ the model-dependent results, as listed in Table 55, are used for the *BABAR* and Belle experiments, whilst the model-independent results, as listed in Table 57 are used for LHCb. This choice is made in order to maintain consistency of the approach across experiments whilst maximising the size of the samples used to obtain inputs for the combination. The result of the GLS analysis of $B^- \to DK^-$ with $D \to K^{*\pm}K^\mp$ from LHCb (Table 58) are used. The results of the LHCb ADS analysis of $B^0 \to DK^{*0}$ (Table 54) are included. The GLW equivalent is not used because of the overlap with the GLW-Dalitz analysis (Table 50) which is used instead. For GGSZ analyses of $B^0 \to DK^{*0}$ with $D \to K^0_S h^+ h^-$ the model-independent result from LHCb (Table 57) is used for consistency with the treatment of the LHCb $B^- \to DK^-$ GGSZ result. Finally, results from the time-dependent analysis of $B^0_s \to D^\mp_s K^\pm$ from LHCb (Table 47) are used. Results from time-dependent analyses of $B^0 \to D^{(*)\mp}\pi^\pm$ and $D^\mp\rho^\pm$ (Table 46) are not used as there are insufficient constraints on the associated hadronic parameters. Similarly, results from $B^0 \to D^\mp K^0_S \pi^\pm$ (Sec. 4.13) are not used.

Table 61: List of measurements used in the combination.

B decay	D decay	Method	Experiment	Ref.
$B^- \to DK^-$	$D \to K^+K^-$, $D \to \pi^+\pi^-$, $D \to K^0_S\pi^0$, $D \to K^0_S\omega$, $D \to K^0_S\phi$	GLW	*BABAR*	[419]
$B^- \to DK^-$	$D \to K^+K^-$, $D \to \pi^+\pi^-$, $D \to K^0_S\pi^0$, $D \to K^0_S\omega$, $D \to K^0_S\phi$	GLW	Belle	[420]
$B^- \to DK^-$	$D \to K^+K^-$, $D \to \pi^+\pi^-$	GLW	CDF	[421]
$B^- \to DK^-$	$D \to K^+K^-$, $D \to \pi^+\pi^-$	GLW	LHCb	[422]
$B^- \to D^*K^-$, $D^* \to D\gamma$ (π^0)	$D \to K^+K^-$, $D \to \pi^+\pi^-$, $D \to K^0_S\pi^0$, $D \to K^0_S\omega$, $D \to K^0_S\phi$	GLW	*BABAR*	[423]
$B^- \to D^*K^-$, $D^* \to D\gamma$ (π^0)	$D \to K^+K^-$, $D \to \pi^+\pi^-$, $D \to K^0_S\pi^0$, $D \to K^0_S\omega$, $D \to K^0_S\phi$	GLW	Belle	[420]
$B^- \to DK^{*-}$	$D \to K^+K^-$, $D \to \pi^+\pi^-$, $D \to K^0_S\pi^0$, $D \to K^0_S\omega$, $D \to K^0_S\phi$	GLW	*BABAR*	[424]
$B^- \to DK^{*-}$	$D \to K^+K^-$, $D \to \pi^+\pi^-$,	GLW	LHCb	[425]
$B^- \to DK^-\pi^+\pi^-$	$D \to K^+K^-$, $D \to \pi^+\pi^-$	GLW	LHCb	[426]
$B^- \to DK^-$	$D \to \pi^+\pi^-\pi^0$	GLW-like	*BABAR*	[309]
$B^- \to DK^-$	$D \to h^+h^-\pi^0$	GLW-like	LHCb	[430]
$B^- \to DK^-$	$D \to \pi^+\pi^-\pi^+\pi^-$	GLW-like	LHCb	[422]
$B^- \to DK^-$	$D \to K^\pm\pi^\mp$	ADS	*BABAR*	[431]
$B^- \to DK^-$	$D \to K^\pm\pi^\mp$	ADS	Belle	[432]
$B^- \to DK^-$	$D \to K^\pm\pi^\mp$	ADS	CDF	[433]
$B^- \to DK^-$	$D \to K^\pm\pi^\mp$	ADS	LHCb	[422]
$B^- \to DK^-$	$D \to K^\pm\pi^\mp\pi^0$	ADS	*BABAR*	[434]
$B^- \to DK^-$	$D \to K^\pm\pi^\mp\pi^0$	ADS	Belle	[435]
$B^- \to DK^-$	$D \to K^\pm\pi^\mp\pi^0$	ADS	LHCb	[430]
$B^- \to DK^-$	$D \to K^\pm\pi^\mp\pi^+\pi^-$	ADS	LHCb	[422]
$B^- \to D^*K^-$, $D^* \to D\gamma$	$D \to K^\pm\pi^\mp$	ADS	*BABAR*	[431]
$B^- \to D^*K^-$, $D^* \to D\pi^0$	$D \to K^\pm\pi^\mp$	ADS	*BABAR*	[431]

List of measurements used in the combination – continued from previous page.

$B^- \to DK^{*-}$	$D \to K^\pm\pi^\mp$	ADS	*BABAR*	[424]
$B^- \to DK^{*-}$	$D \to K^\pm\pi^\mp$	ADS	LHCb	[425]
$B^- \to DK^-\pi^+\pi^-$	$D \to K^\pm\pi^\mp$	ADS	LHCb	[426]
$B^- \to DK^-$	$D \to K^0_S\pi^+\pi^-$	GGSZ MD	*BABAR*	[441]
$B^- \to DK^-$	$D \to K^0_S\pi^+\pi^-$	GGSZ MD	Belle	[440]
$B^- \to D^*K^-$ $D^* \to D\gamma$ (π^0)	$D \to K^0_S\pi^+\pi^-$	GGSZ MD	*BABAR*	[441]
$B^- \to D^*K^-$ $D^* \to D\gamma$ (π^0)	$D \to K^0_S\pi^+\pi^-$	GGSZ MD	Belle	[440]
$B^- \to DK^{*-}$	$D \to K^0_S\pi^+\pi^-$	GGSZ MD	*BABAR*	[441]
$B^- \to DK^{*-}$	$D \to K^0_S\pi^+\pi^-$	GGSZ MD	Belle	[443]
$B^- \to DK^-$	$D \to K^0_S\pi^+\pi^-$	GGSZ MI	LHCb	[448]
$B^- \to DK^-$	$D \to K^0_SK^+\pi^-$	GLS	LHCb	[451]
$B^0 \to DK^{*0}$	$D \to K^\pm\pi^\mp$	ADS	LHCb	[427]
$B^0 \to DK^+\pi^-$	$D \to h^+h^-$	GLW-Dalitz	LHCb	[428]
$B^0 \to DK^+\pi^-$	$D \to K^0_Sh^+h^-$	GGSZ MI	LHCb	[450]
$B^0_s \to D^\mp_sK^\pm$	$D^+_s \to h^+h^-\pi^+$	TD	LHCb	[417]

Auxiliary inputs are used in the combination in order to constrain the D system parameters and subsequently improve the determination of $\gamma \equiv \phi_3$. These include the ratio of suppressed to favoured decay amplitudes and the strong phase difference for $D \to K^\pm\pi^\mp$ decays, taken from the HFAG Charm Physics subgroup global fits (see Sec. 8). The amplitude ratios, strong phase differences and coherence factors of $D \to K^\pm\pi^\mp\pi^0$, $D \to K^\pm\pi^\mp\pi^+\pi^-$ and $D \to K^0_SK^\pm\pi^\pm$ decays are taken from CLEO-c and LHCb measurements [452,458,459]. The fraction of *CP*-even content for quasi-GLW $D \to \pi^+\pi^-\pi^+\pi^-$, $D \to K^+K^-\pi^0$ and $D \to \pi^+\pi^-\pi^0$ decays are taken from CLEO-c measurements [429]. Constraints required to relate the hadronic parameters of the $B^0 \to DK^{*0}$ GLW-Dalitz analysis to the effective hadronic parameters of the quasi-two-body approaches are taken from LHCb measurements [428]. Finally, the value of $-2\beta_s$ is taken from the HFAG Lifetimes and Oscillations subgroup (see Sec. 3); this is required to obtain sensitivity to $\gamma \equiv \phi_3$ from the time-dependent analysis of $B^0_s \to D^\mp_sK^\pm$ decays. A summary of

Table 62: List of the auxiliary inputs used in the combinations.

Decay	Parameters	Source	Ref.
$D \to K^\pm\pi^\mp$	$r_D^{K\pi}$, $\delta_D^{K\pi}$	HFAG	Sec. 8
$D \to K^\pm\pi^\mp\pi^+\pi^-$	$\delta_D^{K3\pi}$, $\kappa_D^{K3\pi}$, $r_D^{K3\pi}$	CLEO+LHCb	[458]
$D \to \pi^+\pi^-\pi^+\pi^-$	$F_{\pi\pi\pi\pi}$	CLEO	[429]
$D \to K^\pm\pi^\mp\pi^0$	$\delta_D^{K2\pi}$, $\kappa_D^{K2\pi}$, $r_D^{K2\pi}$	CLEO+LHCb	[458]
$D \to h^+h^-\pi^0$	$F_{\pi\pi\pi^0}$, $F_{KK\pi^0}$	CLEO	[429]
$D \to K^0_SK^+\pi^-$	$\delta_D^{K_SK\pi}$, $\kappa_D^{K_SK\pi}$, $r_D^{K_SK\pi}$	CLEO	[452]
	$r_D^{K_SK\pi}$	LHCb	[459]
$B^0 \to DK^{*0}$	$\kappa_B(DK^{*0})$, $\overline{R}_B^{DK^{*0}}$, $\overline{\Delta}_B^{DK^{*0}}$	LHCb	[428]
$B^0_s \to D^\mp_sK^\pm$	ϕ_s	HFAG	Sec. 3

Table 63: Averages values obtained for the hadronic parameters in $B \to D^{(*)}K^{(*)}$ decays.

Parameter	Value
$r_B(DK^-)$	0.104 ± 0.005
$r_B(D^*K^-)$	0.12 ± 0.02
$r_B(DK^{*-})$	0.05 ± 0.03
$r_B(DK^{*0})$	0.55 ± 0.16
$\delta_B(DK^-)$	$(137.7\,^{+5.1}_{-6.0})^\circ$
$\delta_B(D^*K^-)$	$(311\,^{+13}_{-17})^\circ$
$\delta_B(DK^{*-})$	$(108\,^{+33}_{-74})^\circ$
$\delta_B(DK^{*0})$	$(203\,^{+22}_{-20})^\circ$

the auxiliary constraints is given in Table 62.

The following reasonable, although imperfect, assumptions are made when performing the averages.

- *CP* violation in $D \to K^+K^-$ and $D \to \pi^+\pi^-$ decays is assumed to be zero. The results of Sec. 8 anyhow suggest such effects to be negligible.

- The combination is potentially sensitive to subleading effects from D^0–$\overline{D}^0$ mixing which is not accounted for [455, 460, 461]. The effect is expected to be small given that $r_B \gtrsim 0.1$ (for all B modes) whilst $r_D \approx 0.05$.

- All $B^- \to DK^{*-}$ modes are treated as two-body decays. In other words any dilution caused by non-K^{*-} contributions in the selected regions of the $DK^0_S\pi^-$ or $DK^-\pi^0$ Dalitz plots is assumed to be negligible. As a check of this assumption, it was found that including a coherence factor for $B^- \to DK^{*-}$ modes, $\kappa_B(DK^{*-}) = 0.9$, had negligible impact on the results.

- All of the inputs are assumed to be completely uncorrelated. Whilst this is true of the statistical uncertainties, it is not necessarily the case for systematic uncertainties. In particular, the model uncertainties for different model-dependent GGSZ analyses are fully correlated (when the same model is used) and similarly the model-independent GGSZ analyses have correlated systematic uncertainties originating from the knowledge of the strong phase variation across the Dalitz plot. The effect of including these correlations is estimated to be $< 1^\circ$.

The obtained world average for the Unitarity Triangle angle $\gamma \equiv \phi_3$ is

$$\gamma \equiv \phi_3 = (74.0\,^{+5.8}_{-6.4})^\circ\,. \tag{162}$$

An ambiguous solution at $\gamma \equiv \phi_3 \longrightarrow \gamma \equiv \phi_3 + \pi$ also exists. The results for the hadronic parameters are listed in Table 63. Results for input analyses as split by B meson decay mode are shown in Table 64 and Fig. 45. Results for input analyses as split by the method are shown in Table 65 and Fig. 46. Results for the hadronic ratios, r_B, are shown in Fig. 47. A demonstration of how the various analyses contribute to the combination is shown in Fig. 48.

Table 64: Averages of $\gamma \equiv \phi_3$ split by B meson decay mode.

Decay Mode	Value
$B_s^0 \to D_s^{\mp} K^{\pm}$	$(128\,^{+18}_{-22})^\circ$
$B^- \to DK^{*-}$	$(33\,^{+30}_{-20})^\circ$
$B^- \to D^* K^-$	$(64\,^{+18}_{-19})^\circ$
$B^0 \to DK^{*0}$	$(92\,^{+23}_{-21})^\circ$
$B^- \to DK^-$	$(72.2\,^{+5.9}_{-7.0})^\circ$

Table 65: Averages of $\gamma \equiv \phi_3$ split by method. For GLW method only the solution nearest the combined average is shown.

Method	Value
GLW	$(82.7\,^{+5.5}_{-6.9})^\circ$
ADS	$(72\,^{+12}_{-18})^\circ$
GGSZ	$(67.3\,^{+8.1}_{-7.8})^\circ$

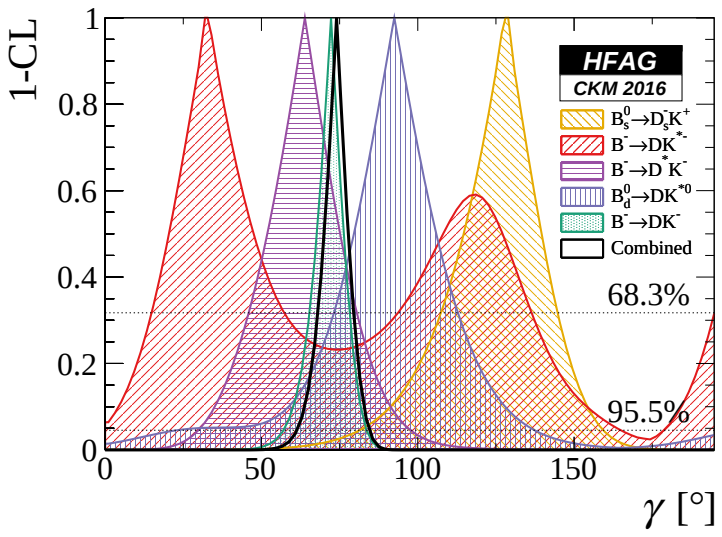

Figure 45: World average of $\gamma \equiv \phi_3$, in terms of $1-\mathrm{CL}$, split by decay mode.

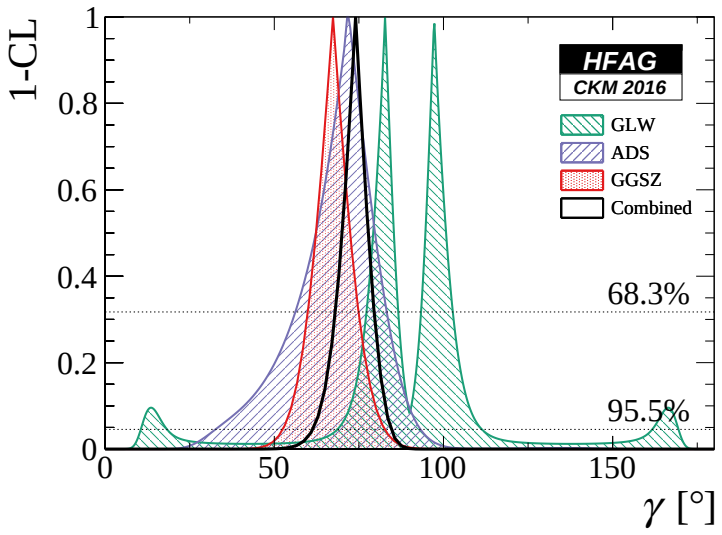

Figure 46: World average of $\gamma \equiv \phi_3$, in terms of 1−CL, split by analysis method.

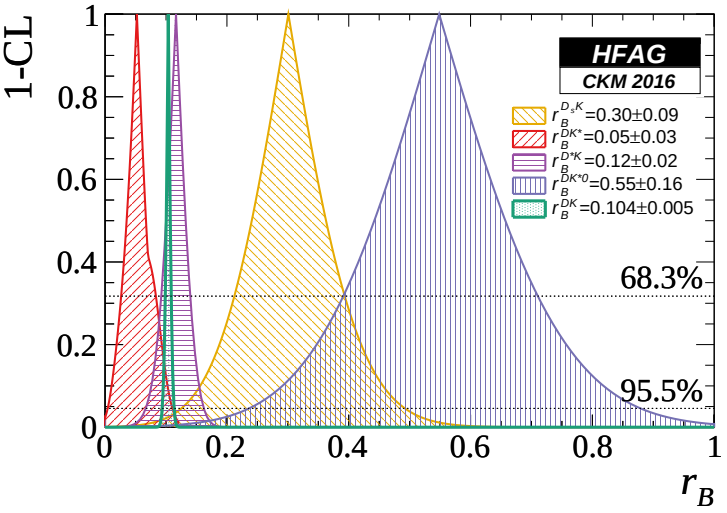

Figure 47: World average for the hadronic parameters r_B in the different decay modes, in terms of 1−CL.

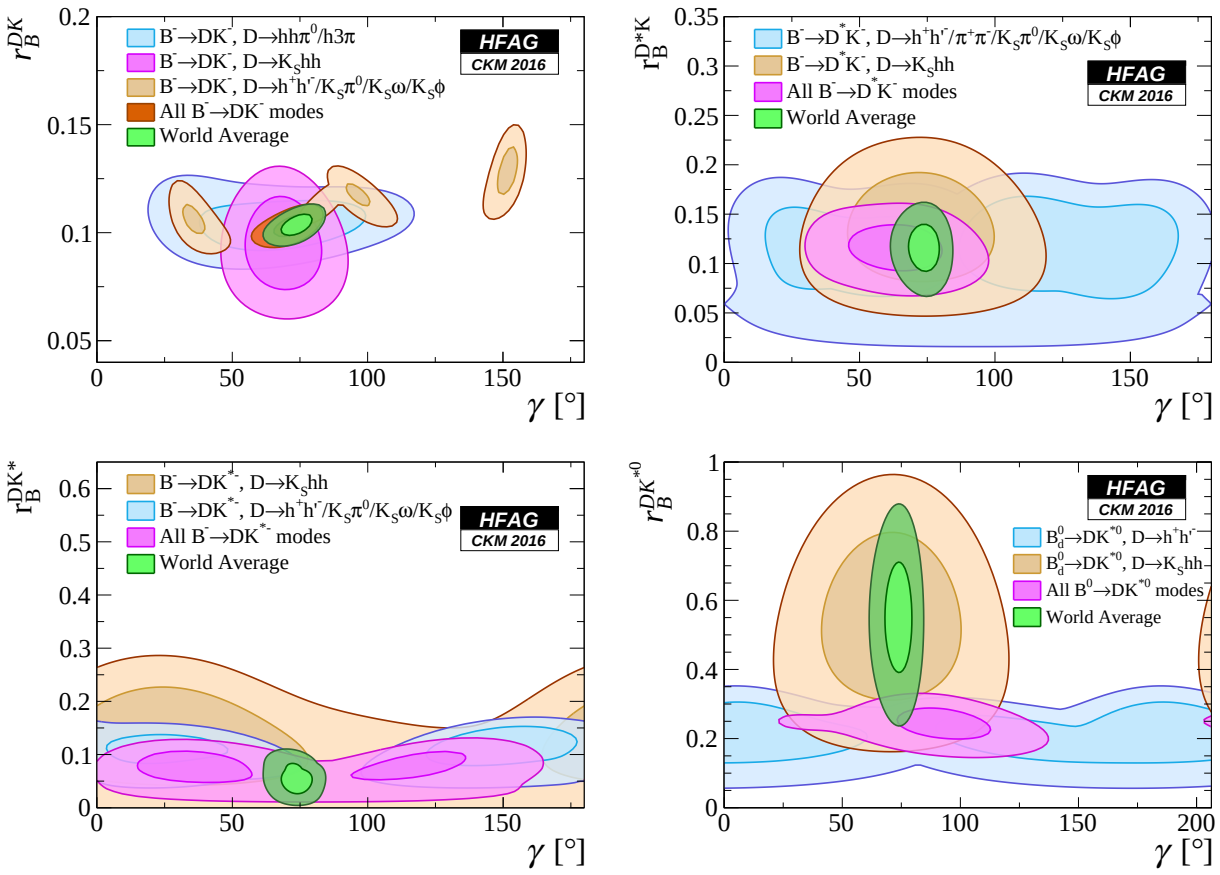

Figure 48: Contributions to the combination from different input measurements, shown in the plane of the relevant r_B parameter *vs.* $\gamma \equiv \phi_3$. From left to right, top to bottom: $B^- \to DK^-$, $B^- \to D^*K^-$, $B^- \to DK^{*-}$ and $B^0 \to DK^{*0}$. Contours show the two-dimensional 68 % and 95 % CL regions.

5 Semileptonic B decays

This section contains our averages for semileptonic B meson decays, *i.e.* decays of the type $B \to X\ell\nu_\ell$, where X is a hadronic system, ℓ a charged lepton and ν_ℓ its corresponding neutrino. Unless otherwise stated, ℓ stands for an electron *or* a muon, lepton universality is assumed, and both charge conjugate states are included. Some averages assume isospin symmetry and this will be explicitly mentioned at every instance.

The averages are organized by the flavour changing transition (the CKM-favoured $b \to c$ transition and the CKM-suppressed $b \to u$ transition) and by the experimental definition of the hadronic X system. Measurements which are sensitive to only a specific hadronic state ($X = D, D^*, \pi, \dots$) are called *exclusive* while analyses that measure all hadronic states within a given region of phase space are *inclusive*. The principal reason why semileptonic B decays are studied in experiments is the determination of the CKM matrix element magnitudes $|V_{cb}|$ and $|V_{ub}|$. The averages in the different subsections thus focus very much on these two fundamental parameters of the Standard Model. In the last subsection, we discuss semileptonic B decays with a τ-lepton. These decays are relevant to the search for physics beyond the Standard Model, *e.g.* in the context of the type II Two-Higgs-Doublet-Model (2HDM).

The technique for obtaining the averages follows the general HFAG procedure (Sec. 2) unless otherwise stated. More information on the averages, in particular the common input parameters is available on the HFAG semileptonic webpage:

`http://www.slac.stanford.edu/xorg/hfag/semi/summer16/main.shtml`

5.1 Exclusive CKM-favoured decays

This section is organized as follows: First, we present averages for the decays $\overline{B} \to D^*\ell^-\overline{\nu}_\ell$ and $\overline{B} \to D\ell^-\overline{\nu}_\ell$. In addition to the branching fractions, the CKM element $|V_{cb}|$ is extracted. We then provide averages for the inclusive branching fractions $\mathcal{B}(\overline{B} \to D^{(*)}\pi\ell^-\overline{\nu}_\ell)$ and for B semileptonic decays into orbitally-excited P-wave charm mesons (D^{**}). As the D^{**} branching fraction is poorly known, we report the averages for the products $\mathcal{B}(B^- \to D^{**}(D^{(*)}\pi)\ell^-\overline{\nu}_\ell) \times \mathcal{B}(D^{**} \to D^{(*)}\pi)$.

5.1.1 $\overline{B} \to D^*\ell^-\overline{\nu}_\ell$

The kinematic of the decay $\overline{B} \to D^*\ell^-\overline{\nu}_\ell$ is described by the form factor $\eta_{\rm EW}\mathcal{F}(w)$, where η_{EW} is a known electro-weak correction factor and w is the product of the B and D^* meson 4-velocities, $w = v_B \cdot v_{D^*}$. Experiments measure the differential decay width as a function of w and determine the product of the form factor $\eta_{\rm EW}\mathcal{F}(w)$ times $|V_{cb}|$. The form factor is parametrized according to the model by from Caprini, Lelouch and Neubert (CLN), which describes the shape and normalization in terms of four quantities: the normalization $\eta_{\rm EW}\mathcal{F}(1)$, the slope ρ^2, and the amplitude ratios $R_1(1)$ and $R_2(1)$ [462]. Our main average and the determination of $|V_{cb}|$ are based on this parameterization.

We use the measurements of these form factor parameters shown in Table 66 and rescale them to the latest values of the input parameters (mainly branching fractions of charmed mesons) [463]. Most of the measurements in Table 66 are based exclusively on the decay $\overline{B}^0 \to D^{*+}\ell^-\overline{\nu}_\ell$. Some measurements [464, 465] are sensitive also to $B^- \to D^{*0}\ell^-\overline{\nu}_\ell$ and one

measurement [466] is based exclusively on the decay $B^- \to D^{*0}\ell^-\overline{\nu}_\ell$. Our analysis thus assumes isospin symmetry.

Table 66: Measurements of the Caprini, Lellouch and Neubert (CLN) [462] form factor parameters in $\overline{B} \to D^*\ell^-\overline{\nu}_\ell$ before and after rescaling. Most analyses (except [467,468]) measure only $\eta_{\rm EW}\mathcal{F}(1)|V_{cb}|$, and ρ^2, so only these two parameters are shown here. The average is the result of a 4-dimensional fit to the rescaled measurements of $\eta_{\rm EW}\mathcal{F}(1)|V_{cb}|$, ρ^2, $R_1(1)$ and $R_2(1)$ – see the text for more details. The χ^2 value of the combination is 30.2 for 23 degrees of freedom (CL=14.4%).

Experiment	$\eta_{\rm EW}\mathcal{F}(1)\lvert V_{cb}\rvert[10^{-3}]$ (rescaled) $\eta_{\rm EW}\mathcal{F}(1)\lvert V_{cb}\rvert[10^{-3}]$ (published)	ρ^2 (rescaled) ρ^2 (published)
ALEPH [469]	$30.97 \pm 1.78_{\rm stat} \pm 1.29_{\rm syst}$ $31.9 \pm 1.8_{\rm stat} \pm 1.9_{\rm syst}$	$0.491 \pm 0.227_{\rm stat} \pm 0.146_{\rm syst}$ $0.37 \pm 0.26_{\rm stat} \pm 0.14_{\rm syst}$
CLEO [464]	$39.67 \pm 1.22_{\rm stat} \pm 1.62_{\rm syst}$ $43.1 \pm 1.3_{\rm stat} \pm 1.8_{\rm syst}$	$1.366 \pm 0.085_{\rm stat} \pm 0.087_{\rm syst}$ $1.61 \pm 0.09_{\rm stat} \pm 0.21_{\rm syst}$
OPAL excl [470]	$35.81 \pm 1.57_{\rm stat} \pm 1.62_{\rm syst}$ $36.8 \pm 1.6_{\rm stat} \pm 2.0_{\rm syst}$	$1.205 \pm 0.207_{\rm stat} \pm 0.153_{\rm syst}$ $1.31 \pm 0.21_{\rm stat} \pm 0.16_{\rm syst}$
OPAL partial reco [470]	$36.98 \pm 1.19_{\rm stat} \pm 2.32_{\rm syst}$ $37.5 \pm 1.2_{\rm stat} \pm 2.5_{\rm syst}$	$1.149 \pm 0.145_{\rm stat} \pm 0.296_{\rm syst}$ $1.12 \pm 0.14_{\rm stat} \pm 0.29_{\rm syst}$
DELPHI partial reco [471]	$35.15 \pm 1.39_{\rm stat} \pm 2.30_{\rm syst}$ $35.5 \pm 1.4_{\rm stat}\ ^{+2.3}_{-2.4{\rm syst}}$	$1.168 \pm 0.126_{\rm stat} \pm 0.381_{\rm syst}$ $1.34 \pm 0.14_{\rm stat}\ ^{+0.24}_{-0.22{\rm syst}}$
DELPHI excl [472]	$35.85 \pm 1.68_{\rm stat} \pm 1.98_{\rm syst}$ $39.2 \pm 1.8_{\rm stat} \pm 2.3_{\rm syst}$	$1.084 \pm 0.143_{\rm stat} \pm 0.151_{\rm syst}$ $1.32 \pm 0.15_{\rm stat} \pm 0.33_{\rm syst}$
Belle [467]	$34.39 \pm 0.17_{\rm stat} \pm 1.01_{\rm syst}$ $34.6 \pm 0.2_{\rm stat} \pm 1.0_{\rm syst}$	$1.213 \pm 0.034_{\rm stat} \pm 0.008_{\rm syst}$ $1.214 \pm 0.034_{\rm stat} \pm 0.009_{\rm syst}$
BABAR excl [468]	$33.59 \pm 0.29_{\rm stat} \pm 1.03_{\rm syst}$ $34.7 \pm 0.3_{\rm stat} \pm 1.1_{\rm syst}$	$1.184 \pm 0.048_{\rm stat} \pm 0.029_{\rm syst}$ $1.18 \pm 0.05_{\rm stat} \pm 0.03_{\rm syst}$
BABAR D^{*0} [466]	$34.96 \pm 0.58_{\rm stat} \pm 1.32_{\rm syst}$ $35.9 \pm 0.6_{\rm stat} \pm 1.4_{\rm syst}$	$1.126 \pm 0.058_{\rm stat} \pm 0.055_{\rm syst}$ $1.16 \pm 0.06_{\rm stat} \pm 0.08_{\rm syst}$
BABAR global fit [465]	$35.49 \pm 0.20_{\rm stat} \pm 1.09_{\rm syst}$ $35.7 \pm 0.2_{\rm stat} \pm 1.2_{\rm syst}$	$1.185 \pm 0.020_{\rm stat} \pm 0.061_{\rm syst}$ $1.21 \pm 0.02_{\rm stat} \pm 0.07_{\rm syst}$
Average	$\mathbf{35.61 \pm 0.11_{stat} \pm 0.41_{syst}}$	$\mathbf{1.205 \pm 0.015_{stat} \pm 0.021_{syst}}$

In the next step, we perform a four-dimensional fit of the parameters $\eta_{\rm EW}\mathcal{F}(1)|V_{cb}|$, ρ^2, $R_1(1)$ and $R_2(1)$ using the rescaled measurements and taking into account correlated statistical and systematic uncertainties. Only two measurements constrain all four parameters [467,468], the remaining measurements determine only the normalization $\eta_{\rm EW}\mathcal{F}(1)|V_{cb}|$ and the slope ρ^2. The result of the fit is

$$\eta_{\rm EW}\mathcal{F}(1)|V_{cb}| = (35.61 \pm 0.43) \times 10^{-3} , \quad (163)$$
$$\rho^2 = 1.205 \pm 0.026 , \quad (164)$$
$$R_1(1) = 1.404 \pm 0.032 , \quad (165)$$
$$R_2(1) = 0.854 \pm 0.020 , \quad (166)$$

and the correlation coefficients are

$$\rho_{\eta_{\rm EW}\mathcal{F}(1)|V_{cb}|,\rho^2} = 0.338 \ , \tag{167}$$
$$\rho_{\eta_{\rm EW}\mathcal{F}(1)|V_{cb}|,R_1(1)} = -0.104 \ , \tag{168}$$
$$\rho_{\eta_{\rm EW}\mathcal{F}(1)|V_{cb}|,R_2(1)} = -0.071 \ , \tag{169}$$
$$\rho_{\rho^2,R_1(1)} = 0.570 \ , \tag{170}$$
$$\rho_{\rho^2,R_2(1)} = -0.810 \ , \tag{171}$$
$$\rho_{R_1(1),R_2(1)} = -0.758 \ . \tag{172}$$

The uncertainties and correlations quoted here include both statistical and systematic contributions. The χ^2 of the fit is 30.2 for 23 degrees of freedom, which corresponds to a confidence level of 14.4%. An illustration of this fit result is given in Fig. 49.

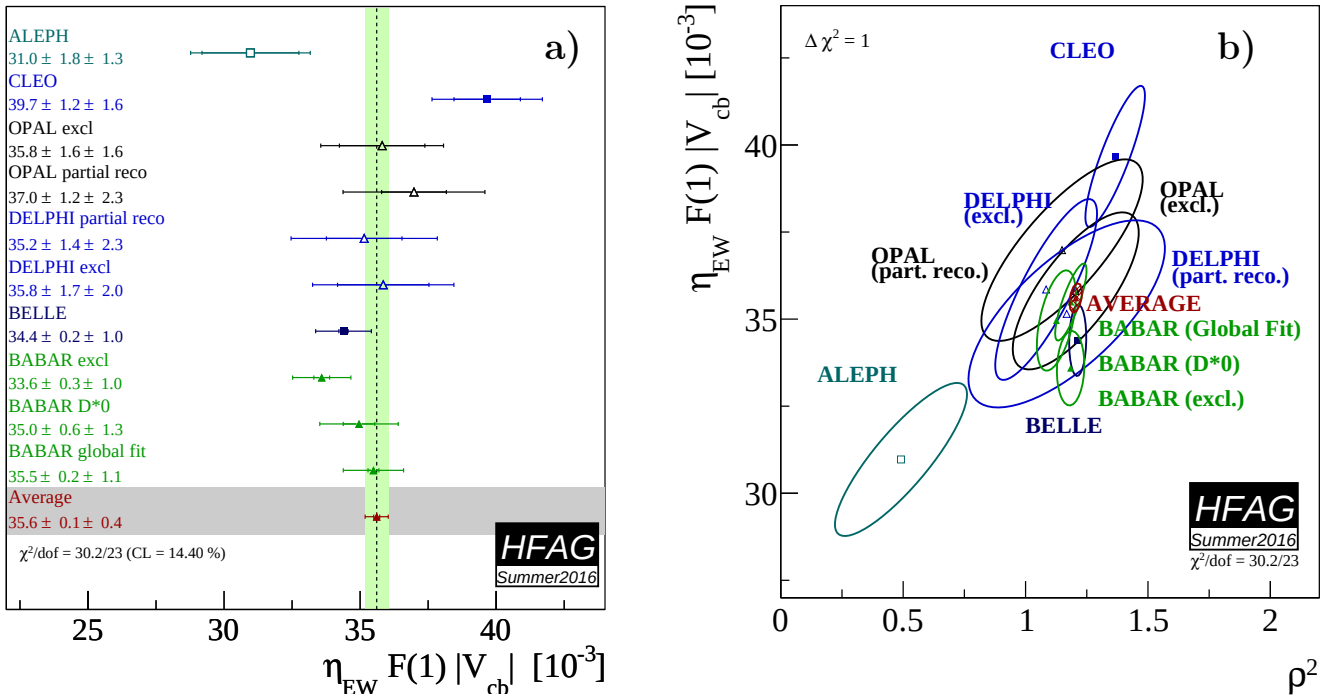

Figure 49: (a) Illustration of the $\eta_{\rm EW}\mathcal{F}(1)|V_{cb}|$ average. (b) Illustration of the $\eta_{\rm EW}\mathcal{F}(1)|V_{cb}|$ vs. ρ^2 average. The error ellipses correspond to $\Delta\chi^2 = 1$ (CL=39%).

Using the lastest update from the FNAL/MILC group [473], the form factor normalization $\eta_{\rm EW}\mathcal{F}(1)$ is

$$\eta_{\rm EW}\mathcal{F}(1) = 0.920 \pm 0.014 \ , \tag{173}$$

which results in the following determination of $|V_{cb}|$ from Eq. 163,

$$|V_{cb}| = (38.71 \pm 0.47_{\rm exp} \pm 0.59_{\rm th}) \times 10^{-3} \ , \tag{174}$$

where the first uncertainty is experimental and the second error is theoretical (lattice QCD calculation and electro-weak correction).

From each rescaled measurement in Table 66, we calculate the $\overline{B} \to D^* \ell^- \overline{\nu}_\ell$ form factor $\eta_{\rm EW}\mathcal{F}(w)$ and, by numerical integration, the branching ratio of the decay $\overline{B}^0 \to D^{*+}\ell^-\overline{\nu}_\ell$. For measurements which do not determine the parameters $R_1(1)$ and $R_2(1)$ we assume the average values Eqs. 165 and 166. The results are quoted in Table 67. The branching ratio found for the average values of $\eta_{\rm EW}\mathcal{F}(1)|V_{cb}|$, ρ^2, $R_1(1)$ and $R_2(1)$ is

$$\mathcal{B}(\overline{B}^0 \to D^{*+}\ell^-\overline{\nu}_\ell) = (4.88 \pm 0.10)\% \ . \tag{175}$$

To test isospin symmetry, we have performed a simple 1-dimensional average of measurements sensitive to the decay $B^- \to D^{*0}\ell^-\overline{\nu}_\ell$ only, which is shown in Table 68. Figure 50 illustrates our two averages of $\overline{B} \to D^*\ell^-\overline{\nu}_\ell$.

Table 67: $\overline{B}^0 \to D^{*+}\ell^-\overline{\nu}_\ell$ branching fractions calculated from the rescaled CLN pameters in Table 66. For Ref. [466] the published value of $\mathcal{B}(B^- \to D^{*0}\ell^-\overline{\nu}_\ell)$ has been rescaled by the factor $\tau(B^0)/\tau(B^+)$ for comparison to the other measurements.

Experiment	$\mathcal{B}(\overline{B}^0 \to D^{*+}\ell^-\overline{\nu}_\ell)$ [%] (calculated)	$\mathcal{B}(\overline{B}^0 \to D^{*+}\ell^-\overline{\nu}_\ell)$ [%] (published)
ALEPH [469]	$5.26 \pm 0.25_{\rm stat} \pm 0.30_{\rm syst}$	$5.53 \pm 0.26_{\rm stat} \pm 0.52_{\rm syst}$
CLEO [464]	$5.55 \pm 0.17_{\rm stat} \pm 0.24_{\rm syst}$	$6.09 \pm 0.19_{\rm stat} \pm 0.40_{\rm syst}$
OPAL excl [470]	$4.93 \pm 0.18_{\rm stat} \pm 0.43_{\rm syst}$	$5.11 \pm 0.19_{\rm stat} \pm 0.49_{\rm syst}$
OPAL partial reco [470]	$5.42 \pm 0.25_{\rm stat} \pm 0.52_{\rm syst}$	$5.92 \pm 0.27_{\rm stat} \pm 0.68_{\rm syst}$
DELPHI partial reco [471]	$4.85 \pm 0.13_{\rm stat} \pm 0.72_{\rm syst}$	$4.70 \pm 0.13_{\rm stat}\ ^{+0.36}_{-0.31}\ _{\rm syst}$
DELPHI excl [472]	$5.27 \pm 0.20_{\rm stat} \pm 0.37_{\rm syst}$	$5.90 \pm 0.22_{\rm stat} \pm 0.50_{\rm syst}$
Belle [467]	$4.51 \pm 0.03_{\rm stat} \pm 0.26_{\rm syst}$	$4.58 \pm 0.03_{\rm stat} \pm 0.26_{\rm syst}$
BABAR excl [468]	$4.45 \pm 0.04_{\rm stat} \pm 0.26_{\rm syst}$	$4.69 \pm 0.04_{\rm stat} \pm 0.34_{\rm syst}$
BABAR D^{*0} [466]	$4.90 \pm 0.07_{\rm stat} \pm 0.34_{\rm syst}$	$5.15 \pm 0.07_{\rm stat} \pm 0.38_{\rm syst}$
BABAR global fit [465]	$4.90 \pm 0.02_{\rm stat} \pm 0.19_{\rm syst}$	$5.00 \pm 0.02_{\rm stat} \pm 0.19_{\rm syst}$
Average	$\mathbf{4.88 \pm 0.01_{stat} \pm 0.10_{syst}}$	$\boldsymbol{\chi^2/\mathrm{dof} = 30.2/23}$ (CL=**14.4%**)

Table 68: Average of the $B^- \to D^{*0}\ell^-\overline{\nu}_\ell$ branching fraction measurements. This fit uses only measurements of $B^- \to D^{*0}\ell^-\overline{\nu}_\ell$.

Experiment	$\mathcal{B}(B^- \to D^{*0}\ell^-\overline{\nu}_\ell)$ [%] (rescaled)	$\mathcal{B}(B^- \to D^{*0}\ell^-\overline{\nu}_\ell)$ [%] (published)
CLEO [464]	$6.52 \pm 0.20_{\rm stat} \pm 0.39_{\rm syst}$	$6.50 \pm 0.20_{\rm stat} \pm 0.43_{\rm syst}$
BABAR tagged [474]	$5.48 \pm 0.15_{\rm stat} \pm 0.35_{\rm syst}$	$5.83 \pm 0.15_{\rm stat} \pm 0.30_{\rm syst}$
BABAR [466]	$5.28 \pm 0.08_{\rm stat} \pm 0.40_{\rm syst}$	$5.56 \pm 0.08_{\rm stat} \pm 0.41_{\rm syst}$
BABAR [465]	$5.36 \pm 0.02_{\rm stat} \pm 0.21_{\rm syst}$	$5.40 \pm 0.02_{\rm stat} \pm 0.21_{\rm syst}$
Average	$\mathbf{5.59 \pm 0.02_{stat} \pm 0.19_{syst}}$	$\boldsymbol{\chi^2/\mathrm{dof} = 8.3/3}$ (CL=**3.94%**)

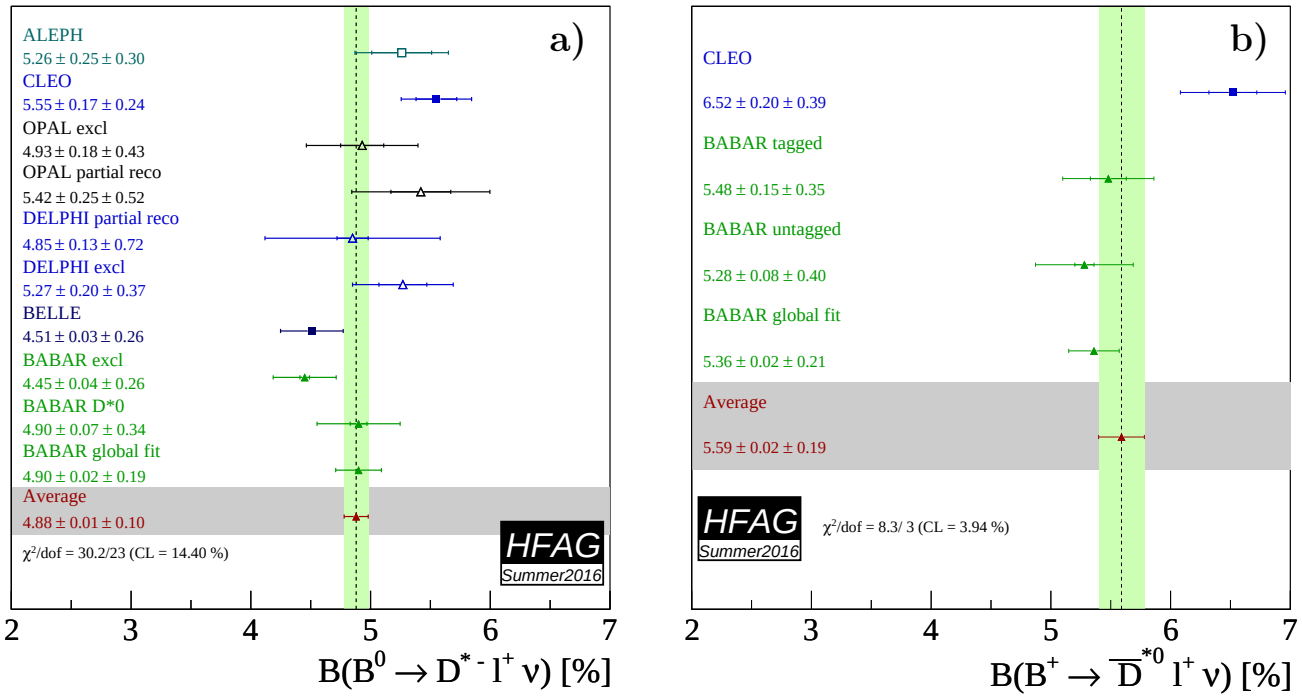

Figure 50: (a) Average branching fractions of exclusive semileptonic B decays $\overline{B} \to D^* \ell^- \overline{\nu}_\ell$: (a) $\overline{B}^0 \to D^{*+} \ell^- \overline{\nu}_\ell$ (Table 67) and (b) $B^- \to D^{*0} \ell^- \overline{\nu}_\ell$ (Table 68).

5.1.2 $\overline{B} \to D \ell^- \overline{\nu}_\ell$

The relevant form factor for the decay $\overline{B} \to D \ell^- \overline{\nu}_\ell$ is $\eta_{\rm EW} \mathcal{G}(w)$, which in CLN [462] is described by only two parameters: the normalization $\eta_{\rm EW} \mathcal{G}(1)|V_{cb}|$ and the slope ρ^2.

Experiments measure the differential decay width as a function of w and determine these two form factor parameters. We use the analyses shown in Table 69 and correct them to match the latest values of the input parameters [463]. These measurements are sensitive to both isospin states ($\overline{B}^0 \to D^+ \ell^- \overline{\nu}_\ell$ and $B^- \to D^0 \ell^- \overline{\nu}_\ell$), so isospin symmetry is assumed in the analysis.

The form factor parameters are extracted by a two-dimensional fit to the rescaled measurements of $\eta_{\rm EW} \mathcal{G}(1)|V_{cb}|$ and ρ^2 taking into account correlated statistical and systematic uncertainties. The result of the fit reads

$$\eta_{\rm EW} \mathcal{G}(1)|V_{cb}| = (41.57 \pm 1.00) \times 10^{-3} \,, \tag{176}$$

$$\rho^2 = 1.128 \pm 0.033 \,, \tag{177}$$

with a correlation of

$$\rho_{\eta_{\rm EW} \mathcal{G}(1)|V_{cb}|, \rho^2} = 0.751 \,. \tag{178}$$

The uncertainties and the correlation coefficient include both statistical and systematic contributions. The χ^2 of the fit is 4.7 for 8 degrees of freedom, which corresponds to a confidence level of 79.3%. An illustration of this fit result is given in Fig. 51.

The most recent lattice QCD result obtained for the form factor normalization is [478]

$$\mathcal{G}(1) = 1.0541 \pm 0.0083 \,. \tag{179}$$

Table 69: Measurements of the Caprini, Lellouch and Neubert (CLN) [462] form factor parameters in $\overline{B} \to D\ell^-\overline{\nu}_\ell$ before and after rescaling. The average is the result of a 2-dimensional fit to the rescaled measurements of $\eta_{\rm EW}\mathcal{G}(1)|V_{cb}|$ and ρ^2 – see the text for more details. The χ^2 value of the combination is 4.7 for 8 degrees of freedom (CL=79.3%).

Experiment	$\mathcal{G}(1)\|V_{cb}\|$ $[10^{-3}]$ (rescaled) $\mathcal{G}(1)\|V_{cb}\|$ $[10^{-3}]$ (published)	ρ^2 (rescaled) ρ^2 (published)
ALEPH [469]	$36.67 \pm 10.05_{\rm stat} \pm 7.33_{\rm syst}$ $31.1 \pm 9.9_{\rm stat} \pm 8.6_{\rm syst}$	$0.845 \pm 0.879_{\rm stat} \pm 0.448_{\rm syst}$ $0.70 \pm 0.98_{\rm stat} \pm 0.50_{\rm syst}$
CLEO [475]	$44.18 \pm 5.70_{\rm stat} \pm 3.47_{\rm syst}$ $44.8 \pm 6.1_{\rm stat} \pm 3.7_{\rm syst}$	$1.270 \pm 0.215_{\rm stat} \pm 0.121_{\rm syst}$ $1.30 \pm 0.27_{\rm stat} \pm 0.14_{\rm syst}$
Belle [476]	$41.94 \pm 0.60_{\rm stat} \pm 1.21_{\rm syst}$ 42.29 ± 1.37	$1.090 \pm 0.036_{\rm stat} \pm 0.019_{\rm syst}$ 1.09 ± 0.05
BABAR global fit [465]	$42.23 \pm 0.74_{\rm stat} \pm 2.14_{\rm syst}$ $43.1 \pm 0.8_{\rm stat} \pm 2.3_{\rm syst}$	$1.186 \pm 0.035_{\rm stat} \pm 0.062_{\rm syst}$ $1.20 \pm 0.04_{\rm stat} \pm 0.07_{\rm syst}$
BABAR tagged [477]	$42.60 \pm 1.71_{\rm stat} \pm 1.26_{\rm syst}$ $42.3 \pm 1.9_{\rm stat} \pm 1.0_{\rm syst}$	$1.200 \pm 0.088_{\rm stat} \pm 0.043_{\rm syst}$ $1.20 \pm 0.09_{\rm stat} \pm 0.04_{\rm syst}$
Average	$\mathbf{41.57 \pm 0.45_{stat} \pm 0.89_{syst}}$	$\mathbf{1.128 \pm 0.024_{stat} \pm 0.023_{syst}}$

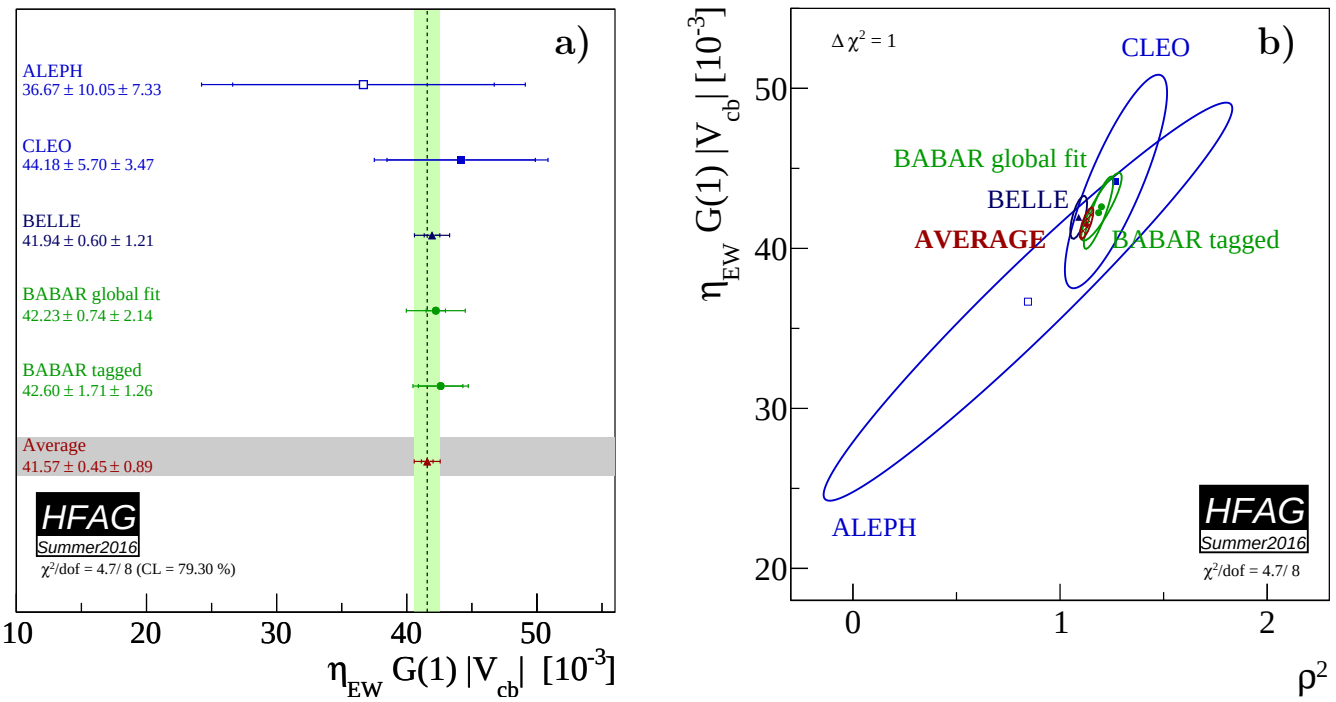

Figure 51: (a) Illustration of the $\eta_{\rm EW}\mathcal{G}(1)|V_{cb}|$ average. (b) Illustration of the $\eta_{\rm EW}\mathcal{G}(1)|V_{cb}|$ vs. ρ^2 average. The error ellipses correspond to $\Delta\chi^2 = 1$ (CL=39%).

Assuming $\eta_{\rm EW} = 1.0066 \pm 0.0016$ [479], we determine $|V_{cb}|$ from Eq. 176,

$$|V_{cb}| = (39.18 \pm 0.94_{\rm exp} \pm 0.31_{\rm th}) \times 10^{-3} \ , \tag{180}$$

where the first error is experimental and the second theoretical. This number is in excellent agreement with $|V_{cb}|$ obtained from decays $\overline{B} \to D^* \ell^- \overline{\nu}_\ell$ (Eq. 174).

From each rescaled measurement in Table 69, we have calculated the $\overline{B} \to D \ell^- \overline{\nu}_\ell$ form factor $\mathcal{G}(w)$ and, by numerical integration, the branching ratio of the decay $\overline{B}^0 \to D^+ \ell^- \overline{\nu}_\ell$. The results are quoted in Table 70 and illustrated in Fig. 52. The branching ratio found for the average values of $\eta_{\rm EW}\mathcal{G}(1)|V_{cb}|$ and ρ^2 is

$$\mathcal{B}(\overline{B}^0 \to D^+ \ell^- \overline{\nu}_\ell) = (2.13 \pm 0.07)\% \ . \tag{181}$$

Table 70: $\overline{B}^0 \to D^+ \ell^- \overline{\nu}_\ell$ branching fractions calculated from the rescaled CLN pameters in Table 69.

Experiment	$\mathcal{B}(\overline{B}^0 \to D^+ \ell^- \overline{\nu}_\ell)$ [%] (calculated)	$\mathcal{B}(\overline{B}^0 \to D^+ \ell^- \overline{\nu}_\ell)$ [%] (published)
ALEPH [469]	$2.09 \pm 0.15_{\rm stat} \pm 0.37_{\rm syst}$	$2.35 \pm 0.20_{\rm stat} \pm 0.44_{\rm syst}$
CLEO [475]	$2.12 \pm 0.23_{\rm stat} \pm 0.29_{\rm syst}$	$2.20 \pm 0.16_{\rm stat} \pm 0.19_{\rm syst}$
Belle [476]	$2.24 \pm 0.03_{\rm stat} \pm 0.11_{\rm syst}$	$2.31 \pm 0.03_{\rm stat} \pm 0.11_{\rm syst}$
BABAR global fit [465]	$2.09 \pm 0.03_{\rm stat} \pm 0.13_{\rm syst}$	$2.34 \pm 0.03_{\rm stat} \pm 0.13_{\rm syst}$
BABAR tagged [477]	$2.10 \pm 0.07_{\rm stat} \pm 0.08_{\rm syst}$	$2.23 \pm 0.11_{\rm stat} \pm 0.11_{\rm syst}$
Average	$\mathbf{2.13 \pm 0.02_{stat} \pm 0.07_{syst}}$	$\boldsymbol{\chi^2/\mathrm{dof} = 4.7/8}$ (CL=**79.3%**)

We have also performed simple 1-dimensional averages of measurements of $\overline{B}^0 \to D^+ \ell^- \overline{\nu}_\ell$ and $B^- \to D^0 \ell^- \overline{\nu}_\ell$ decays. The results are shown in Tables 71 and 72.

Table 71: Average of $\overline{B}^0 \to D^+ \ell^- \overline{\nu}_\ell$ branching fraction measurements. This fit uses only measurements of the neutral mode.

Experiment	$\mathcal{B}(\overline{B}^0 \to D^+ \ell^- \overline{\nu}_\ell)$ [%] (rescaled)	$\mathcal{B}(\overline{B}^0 \to D^+ \ell^- \overline{\nu}_\ell)$ [%] (published)
ALEPH [469]	$2.14 \pm 0.18_{\rm stat} \pm 0.36_{\rm syst}$	$2.35 \pm 0.20_{\rm stat} \pm 0.44_{\rm syst}$
CLEO [475]	$2.09 \pm 0.13_{\rm stat} \pm 0.16_{\rm syst}$	$2.20 \pm 0.16_{\rm stat} \pm 0.19_{\rm syst}$
Belle [476]	$2.30 \pm 0.04_{\rm stat} \pm 0.12_{\rm syst}$	$2.39 \pm 0.04_{\rm stat} \pm 0.11_{\rm syst}$
BABAR [474]	$2.08 \pm 0.11_{\rm stat} \pm 0.14_{\rm syst}$	$2.21 \pm 0.11_{\rm stat} \pm 0.12_{\rm syst}$
Average	$\mathbf{2.20 \pm 0.04_{stat} \pm 0.09_{syst}}$	$\boldsymbol{\chi^2/\mathrm{dof} = 1.7/3}$ (CL=**63.9%**)

5.1.3 $\overline{B} \to D^{(*)} \pi \ell^- \overline{\nu}_\ell$

The average inclusive branching fractions for $\overline{B} \to D^* \pi \ell^- \overline{\nu}_\ell$ decays, where no constraint is applied to the hadronic $D^{(*)}\pi$ system, are determined by the combination of the results provided

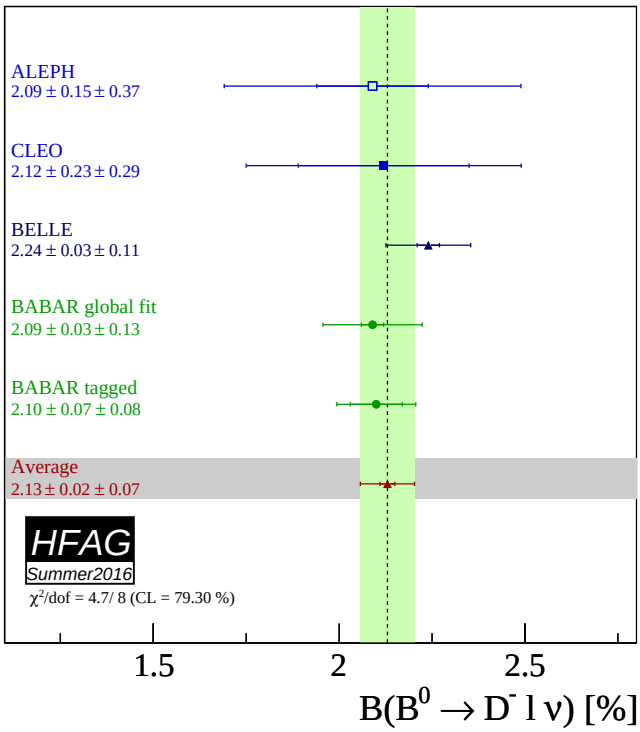

Figure 52: Illustration of Table 70.

Table 72: Average of $B^- \to D^0\ell^-\overline{\nu}_\ell$ branching fraction measurements. This fit uses only measurements of the charged mode.

Experiment	$\mathcal{B}(B^- \to D^0\ell^-\overline{\nu}_\ell)$ [%] (rescaled)	$\mathcal{B}(B^- \to D^0\ell^-\overline{\nu}_\ell)$ [%] (published)
CLEO [475]	$2.16 \pm 0.13_{\rm stat} \pm 0.17_{\rm syst}$	$2.32 \pm 0.17_{\rm stat} \pm 0.20_{\rm syst}$
BABAR [474]	$2.21 \pm 0.09_{\rm stat} \pm 0.12_{\rm syst}$	$2.33 \pm 0.09_{\rm stat} \pm 0.09_{\rm syst}$
Belle [476]	$2.48 \pm 0.04_{\rm stat} \pm 0.12_{\rm syst}$	$2.54 \pm 0.04_{\rm stat} \pm 0.13_{\rm syst}$
Average	$\mathbf{2.33 \pm 0.04_{stat} \pm 0.09_{syst}}$	$\boldsymbol{\chi^2/\mathrm{dof} = 2.8/2}$ (CL=**25.2%**)

in Table 73 for $\overline{B}^0 \to D^0\pi^+\ell^-\overline{\nu}_\ell$, $\overline{B}^0 \to D^{*0}\pi^+\ell^-\overline{\nu}_\ell$, $B^- \to D^+\pi^-\ell^-\overline{\nu}_\ell$, and $B^- \to D^{*+}\pi^-\ell^-\overline{\nu}_\ell$ decays. The measurements included in the average are scaled to a consistent set of input parameters and their errors [463]. For both the *BABAR* and Belle results, the B semileptonic signal yields are extracted from a fit to the missing mass squared in a sample of fully reconstructed $B\overline{B}$ events. Figure 53 illustrates the measurements and the resulting average.

5.1.4 $\overline{B} \to D^{**}\ell^-\overline{\nu}_\ell$

The D^{**} mesons contain one charm quark and one light quark with relative angular momentum $L = 1$. According to Heavy Quark Symmetry (HQS) [481], they form one doublet of states with angular momentum $j \equiv s_q + L = 3/2$ $[D_1(2420), D_2^*(2460)]$ and another doublet with $j = 1/2$ $[D_0^*(2400), D_1'(2430)]$, where s_q is the light quark spin. Parity and angular momentum

Table 73: Averages of the $B \to D^{(*)}\pi^-\ell^-\overline{\nu}_\ell$ branching fractions and individual results.

Experiment	$\mathcal{B}(B^- \to D^+\pi^-\ell^-\overline{\nu}_\ell)[\%]$ (rescaled)	$\mathcal{B}(B^- \to D^+\pi^-\ell^-\overline{\nu}_\ell)[\%]$ (published)
Belle [480]	$0.42 \pm 0.04_{\rm stat} \pm 0.05_{\rm syst}$	$0.40 \pm 0.04_{\rm stat} \pm 0.06_{\rm syst}$
BABAR [474]	$0.40 \pm 0.06_{\rm stat} \pm 0.03_{\rm syst}$	$0.42 \pm 0.06_{\rm stat} \pm 0.03_{\rm syst}$
Average	$\mathbf{0.41 \pm 0.04}$	$\boldsymbol{\chi^2/\rm dof = 0.073}$ (CL=**78.9%**)
Experiment	$\mathcal{B}(B^- \to D^{*+}\pi^-\ell^-\overline{\nu}_\ell)[\%]$ (rescaled)	$\mathcal{B}(B^- \to D^{*+}\pi^-\ell^-\overline{\nu}_\ell)[\%]$ (published)
Belle [480]	$0.68 \pm 0.08_{\rm stat} \pm 0.07_{\rm syst}$	$0.64 \pm 0.08_{\rm stat} \pm 0.09_{\rm syst}$
BABAR [474]	$0.57 \pm 0.05_{\rm stat} \pm 0.04_{\rm syst}$	$0.59 \pm 0.05_{\rm stat} \pm 0.04_{\rm syst}$
Average	$\mathbf{0.60 \pm 0.06}$	$\boldsymbol{\chi^2/\rm dof = 0.778}$ (CL=**37.9%**)
Experiment	$\mathcal{B}(\overline{B}^0 \to D^0\pi^+\ell^-\overline{\nu}_\ell)[\%]$ (rescaled)	$\mathcal{B}(\overline{B}^0 \to D^0\pi^+\ell^-\overline{\nu}_\ell)[\%]$ (published)
Belle [480]	$0.43 \pm 0.07_{\rm stat} \pm 0.05_{\rm syst}$	$0.42 \pm 0.07_{\rm stat} \pm 0.06_{\rm syst}$
BABAR [474]	$0.40 \pm 0.08_{\rm stat} \pm 0.03_{\rm syst}$	$0.43 \pm 0.08_{\rm stat} \pm 0.03_{\rm syst}$
Average	$\mathbf{0.42 \pm 0.06}$	$\boldsymbol{\chi^2/\rm dof = 0.061}$ (CL=**80.5%**)
Experiment	$\mathcal{B}(\overline{B}^0 \to D^{*0}\pi^+\ell^-\overline{\nu}_\ell)[\%]$ (rescaled)	$\mathcal{B}(\overline{B}^0 \to D^{*0}\pi^+\ell^-\overline{\nu}_\ell)[\%]$ (published)
Belle [480]	$0.58 \pm 0.21_{\rm stat} \pm 0.07_{\rm syst}$	$0.56 \pm 0.21_{\rm stat} \pm 0.08_{\rm syst}$
BABAR [474]	$0.46 \pm 0.08_{\rm stat} \pm 0.04_{\rm syst}$	$0.48 \pm 0.08_{\rm stat} \pm 0.04_{\rm syst}$
Average	$\mathbf{0.47 \pm 0.08}$	$\boldsymbol{\chi^2/\rm dof = 0.262}$ (CL=**60.9%**)

conservation constrain the decays allowed for each state. The D_1 and D_2^* states decay through a D-wave to $D^*\pi$ and $D^{(*)}\pi$, respectively, and have small decay widths, while the D_0^* and D_1' states decay through an S-wave to $D\pi$ and $D^*\pi$ and are very broad. For the narrow states, the averages are determined by the combination of the results provided in Table 74 and 75 for $\mathcal{B}(B^- \to D_1^0\ell^-\overline{\nu}_\ell) \times \mathcal{B}(D_1^0 \to D^{*+}\pi^-)$ and $\mathcal{B}(B^- \to D_2^0\ell^-\overline{\nu}_\ell) \times \mathcal{B}(D_2^0 \to D^{*+}\pi^-)$. For the broad states, the averages are determined by the combination of the results provided in Table 76 and 77 for $\mathcal{B}(B^- \to D_1'^0\ell^-\overline{\nu}_\ell) \times \mathcal{B}(D_1'^0 \to D^{*+}\pi^-)$ and $\mathcal{B}(B^- \to D_0^{*0}\ell^-\overline{\nu}_\ell) \times \mathcal{B}(D_0^{*0} \to D^+\pi^-)$. The measurements included in the average are scaled to a consistent set of input parameters and their errors [463].

For both the B-factory and the LEP and Tevatron results, the B semileptonic signal yields are extracted from a fit to the invariant mass distribution of the $D^{(*)+}\pi^-$ system. Apart for the CLEO, Belle and *BABAR* results, the other measurements are for the $\overline{B} \to D^{**}(D^*\pi^-)X\ell^-\overline{\nu}_\ell$ final state and we assume that no particles are left in the X system. The *BABAR* tagged measurement [482] measures $\overline{B} \to D_2^*(D\pi)X\ell^-\overline{\nu}_\ell$ and it has been translated in a result on $D_2^* \to D^*\pi$ decay mode, assuming $\mathcal{B}(D_2^* \to D\pi)/\mathcal{B}(D_2^* \to D^*\pi) = 1.54 \pm 0.15$ [314]. Figure 54 and 55 illustrate the measurements and the resulting averages.

5.2 Inclusive CKM-favored decays

5.2.1 Global analysis of $\overline{B} \to X_c\ell^-\overline{\nu}_\ell$

The semileptonic width $\Gamma(\overline{B} \to X_c\ell^-\overline{\nu}_\ell)$ has been calculated in the framework of the Operator Product Expansion [55]. The result is a double-expansion in $\Lambda_{\rm QCD}/m_b$ and α_s, which depends on a number of non-perturbative parameters. These parameters give information on the dynamics

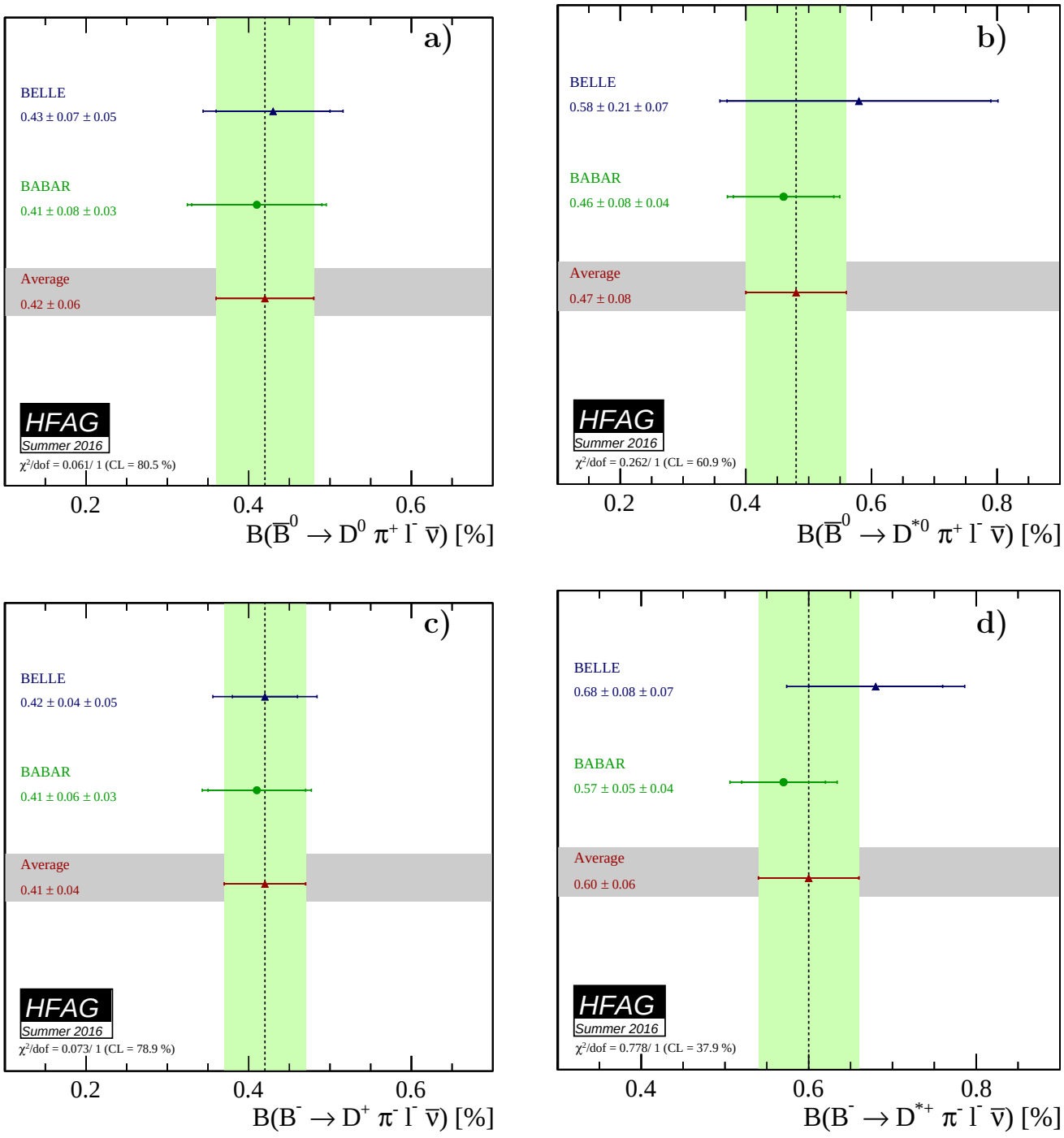

Figure 53: Average branching fraction of exclusive semileptonic B decays (a) $\overline{B}^0 \to D^0\pi^+\ell^-\overline{\nu}_\ell$, (b) $\overline{B}^0 \to D^{*0}\pi^+\ell^-\overline{\nu}_\ell$, (c) $B^- \to D^+\pi^-\ell^-\overline{\nu}_\ell$, and (d) $B^- \to D^{*+}\pi^-\ell^-\overline{\nu}_\ell$. The corresponding individual results are also shown.

of the b-quark inside the B hadron and can be measured using other observables in $\overline{B} \to X_c\ell^-\overline{\nu}_\ell$ decays, such as the moments of the lepton energy and the hadronic mass spectrum.

Table 74: Average of the branching fraction $\mathcal{B}(B^- \to D_1^0 \ell^- \overline{\nu}_\ell) \times \mathcal{B}(D_1^0 \to D^{*+}\pi^-)$ and individual results. The ALEPH, OPAL and D0 measurements are for the $D_1(D^*\pi)X$ final state and we assume that no particles are left in the X system.

Experiment	$\mathcal{B}(B^- \to D_1^0(D^{*+}\pi^-)\ell^-\overline{\nu}_\ell)[\%]$ (rescaled)	$\mathcal{B}(B^- \to D_1^0(D^{*+}\pi^-)\ell^-\overline{\nu}_\ell)[\%]$ (published)
ALEPH [483]	$0.437 \pm 0.085_{\rm stat} \pm 0.056_{\rm syst}$	$0.47 \pm 0.10_{\rm stat} \pm 0.07_{\rm syst}$
OPAL [484]	$0.570 \pm 0.210_{\rm stat} \pm 0.101_{\rm syst}$	$0.70 \pm 0.21_{\rm stat} \pm 0.10_{\rm syst}$
CLEO [485]	$0.347 \pm 0.085_{\rm stat} \pm 0.056_{\rm syst}$	$0.373 \pm 0.085_{\rm stat} \pm 0.057_{\rm syst}$
D0 [486]	$0.214 \pm 0.018_{\rm stat} \pm 0.035_{\rm syst}$	$0.219 \pm 0.018_{\rm stat} \pm 0.035_{\rm syst}$
Belle Tagged B^- [480]	$0.443 \pm 0.070_{\rm stat} \pm 0.059_{\rm syst}$	$0.42 \pm 0.07_{\rm stat} \pm 0.07_{\rm syst}$
Belle Tagged B^0 [480]	$0.612 \pm 0.200_{\rm stat} \pm 0.077_{\rm syst}$	$0.42 \pm 0.07_{\rm stat} \pm 0.07_{\rm syst}$
BABAR Tagged [482]	$0.274 \pm 0.030_{\rm stat} \pm 0.029_{\rm syst}$	$0.29 \pm 0.03_{\rm stat} \pm 0.03_{\rm syst}$
BABAR Untagged B^- [487]	$0.290 \pm 0.017_{\rm stat} \pm 0.016_{\rm syst}$	$0.30 \pm 0.02_{\rm stat} \pm 0.02_{\rm syst}$
BABAR Untagged B^0 [487]	$0.294 \pm 0.026_{\rm stat} \pm 0.027_{\rm syst}$	$0.30 \pm 0.02_{\rm stat} \pm 0.02_{\rm syst}$
Average	$\mathbf{0.281 \pm 0.010 \pm 0.015}$	$\boldsymbol{\chi^2}$**/dof = 12.7/8** (CL=**11.7%**)

Table 75: Average of the branching fraction $\mathcal{B}(B^- \to D_2^0 \ell^- \overline{\nu}_\ell) \times \mathcal{B}(D_2^0 \to D^{*+}\pi^-)$ and individual results. The D0 measurement is for the $D_2^*(D^*\pi)X$ final state and we assume that no particles are left in the X system. The *BABAR* tagged measurement has been translated in a result on $D_2^* \to D^*\pi$ decay mode, assuming $\mathcal{B}(D_2^* \to D\pi)/\mathcal{B}(D_2^* \to D^*\pi) = 1.54 \pm 0.15$ [314].

Experiment	$\mathcal{B}(B^- \to D_2^0(D^{*+}\pi^-)\ell^-\overline{\nu}_\ell)[\%]$ (rescaled)	$\mathcal{B}(B^- \to D_2^0(D^{*+}\pi^-)\ell^-\overline{\nu}_\ell)[\%]$ (published)
CLEO [485]	$0.055 \pm 0.066_{\rm stat} \pm 0.011_{\rm syst}$	$0.059 \pm 0.066_{\rm stat} \pm 0.011_{\rm syst}$
D0 [486]	$0.086 \pm 0.018_{\rm stat} \pm 0.020_{\rm syst}$	$0.088 \pm 0.018_{\rm stat} \pm 0.020_{\rm syst}$
Belle [480]	$0.190 \pm 0.060_{\rm stat} \pm 0.025_{\rm syst}$	$0.18 \pm 0.06_{\rm stat} \pm 0.03_{\rm syst}$
BABAR tagged [482]	$0.075 \pm 0.013_{\rm stat} \pm 0.009_{\rm syst}$	$0.078 \pm 0.013_{\rm stat} \pm 0.010_{\rm syst}$
BABAR untagged B^- [487]	$0.087 \pm 0.009_{\rm stat} \pm 0.007_{\rm syst}$	$0.087 \pm 0.013_{\rm stat} \pm 0.007_{\rm syst}$
BABAR untagged B^0 [487]	$0.065 \pm 0.010_{\rm stat} \pm 0.004_{\rm syst}$	$0.087 \pm 0.013_{\rm stat} \pm 0.007_{\rm syst}$
Average	$\mathbf{0.077 \pm 0.006 \pm 0.004}$	$\boldsymbol{\chi^2}$**/dof = 5.3/5** (CL=**37.7%**)

Two independent sets of theoretical expressions, named after the definition of the b-quark mass used, are available for this kind of analysis: the kinetic [489–492] and 1S scheme expressions [493]. The non-perturbative parameters in the kinetic scheme are: the quark masses m_b and m_c, μ_π^2 and μ_G^2 at $O(1/m_b^2)$, and ρ_D^3 and ρ_{LS}^3 at $O(1/m_b^3)$. In the 1S scheme, the parameters are: m_b, λ_1 at $O(1/m_b^2)$, and ρ_1, τ_1, τ_2 and τ_3 at $O(1/m_b^3)$. Note that due to the different definitions, the results for the quark masses cannot be compared directly between the two schemes.

Our analysis uses all available measurements of moments in $\overline{B} \to X_c \ell^- \overline{\nu}_\ell$, excluding only points with too high correlation to avoid numerical issues. The list of included measurements is given in Table 78. The only external input is the average lifetime τ_B of neutral and charged B mesons, taken to be (1.579 ± 0.004) ps (Sec. 3).

Table 76: Average of the branching fraction $\mathcal{B}(B^- \to D_1^{\prime 0}\ell^-\overline{\nu}_\ell) \times \mathcal{B}(D_1^{\prime 0} \to D^{*+}\pi^-)$ and individual results. The DELPHI measurement is for the final state $D_1'(D^*\pi)X$ and we assume that no particles are left in the X system.

Experiment	$\mathcal{B}(B^- \to D_1^{\prime 0}(D^{*+}\pi^-)\ell^-\overline{\nu}_\ell)[\%]$ (rescaled)	$\mathcal{B}(B^- \to D_1^{\prime 0}(D^{*+}\pi^-)\ell^-\overline{\nu}_\ell)[\%]$ (published)
DELPHI [488]	$0.71 \pm 0.17_{\rm stat} \pm 0.18_{\rm syst}$	$0.83 \pm 0.17_{\rm stat} \pm 0.18_{\rm syst}$
Belle [480]	$-0.03 \pm 0.06_{\rm stat} \pm 0.07_{\rm syst}$	$-0.03 \pm 0.06_{\rm stat} \pm 0.07_{\rm syst}$
BABAR [482]	$0.26 \pm 0.04_{\rm stat} \pm 0.04_{\rm syst}$	$0.27 \pm 0.04_{\rm stat} \pm 0.05_{\rm syst}$
Average	$\mathbf{0.13 \pm 0.03 \pm 0.02}$	$\boldsymbol{\chi^2/\mathrm{dof} = 18./2}$ (CL=**0.0001%**)

Table 77: Average of the branching fraction $\mathcal{B}(B^- \to D_0^{*0}\ell^-\overline{\nu}_\ell) \times \mathcal{B}(D_0^{*0} \to D^+\pi^-)$ and individual results.

Experiment	$\mathcal{B}(B^- \to D_0^{*0}(D^+\pi^-)\ell^-\overline{\nu}_\ell)[\%]$ (rescaled)	$\mathcal{B}(B^- \to D_0^{*0}(D^+\pi^-)\ell^-\overline{\nu}_\ell)[\%]$ (published)
Belle Tagged B^- [480]	$0.25 \pm 0.04_{\rm stat} \pm 0.06_{\rm syst}$	$0.24 \pm 0.04_{\rm stat} \pm 0.06_{\rm syst}$
Belle Tagged B^0 [480]	$0.23 \pm 0.08_{\rm stat} \pm 0.06_{\rm syst}$	$0.24 \pm 0.04_{\rm stat} \pm 0.06_{\rm syst}$
BABAR Tagged [482]	$0.31 \pm 0.04_{\rm stat} \pm 0.05_{\rm syst}$	$0.26 \pm 0.05_{\rm stat} \pm 0.04_{\rm syst}$
Average	$\mathbf{0.28 \pm 0.03 \pm 0.04}$	$\boldsymbol{\chi^2/\mathrm{dof} = 0.49/2}$ (CL=**78.0%**)

Both in the kinetic and 1S schemes, the moments in $\overline{B} \to X_c\ell^-\overline{\nu}_\ell$ are not sufficient to determine the b-quark mass precisely. In the kinetic scheme analysis we constrain the c-quark mass (defined in the $\overline{\rm MS}$ scheme) to the value of Ref. [500],

$$m_c^{\overline{\rm MS}}(3\ {\rm GeV}) = 0.986 \pm 0.013\ {\rm GeV}\ . \tag{182}$$

In the 1S scheme analysis, the b-quark mass is constrained with measurements of the photon energy moments in $B \to X_s\gamma$ [501–504].

5.2.2 Analysis in the kinetic scheme

The fit relies on the calculations of the spectral moments in $\overline{B} \to X_c\ell^-\overline{\nu}_\ell$ decays described in Ref. [491,492] and closely follows the procedure of Ref. [505]. The analysis determines $|V_{cb}|$ and the 6 non-perturbative parameters mentioned above.

The result in terms of the main parameters is

$$|V_{cb}| = (42.19 \pm 0.78) \times 10^{-3}\ , \tag{183}$$
$$m_b^{\rm kin} = 4.554 \pm 0.018\ {\rm GeV}\ , \tag{184}$$
$$\mu_\pi^2 = 0.464 \pm 0.076\ {\rm GeV}^2\ , \tag{185}$$

with a χ^2 of 15.6 for $50 - 7$ degrees of freedom. The detailed result and the matrix of the correlation coefficients is given in Table 79. The fit to the lepton energy and hadronic mass moments is shown in Figs. 56 and 57, respectively.

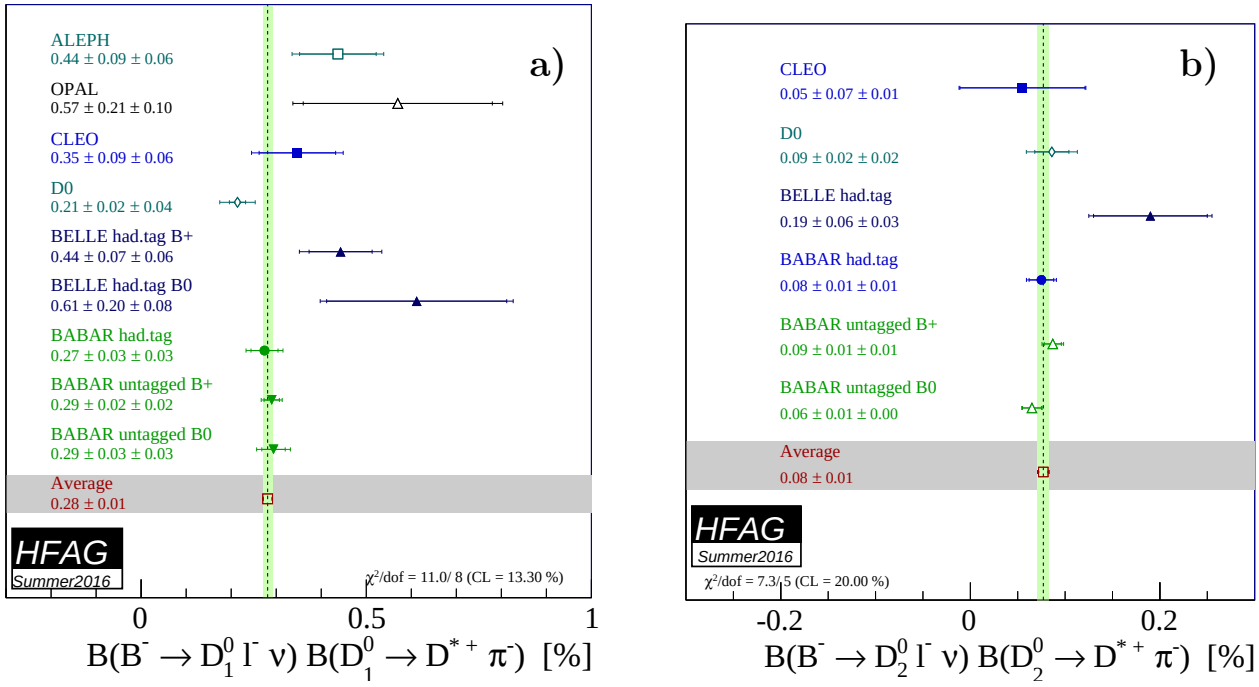

Figure 54: Average of the product of branching fraction (a) $\mathcal{B}(B^- \to D_1^0 \ell^- \overline{\nu}_\ell) \times \mathcal{B}(D_1^0 \to D^{*+}\pi^-)$ and (b) $\mathcal{B}(B^- \to D_2^0 \ell^- \overline{\nu}_\ell) \times \mathcal{B}(D_2^0 \to D^{*+}\pi^-)$. The corresponding individual results are also shown.

The inclusive $\overline{B} \to X_c \ell^- \overline{\nu}_\ell$ branching fraction determined by this analysis is

$$\mathcal{B}(\overline{B} \to X_c \ell^- \overline{\nu}_\ell) = (10.65 \pm 0.16)\% \ . \tag{186}$$

Correcting for charmless semileptonic decays (Sec. 5.4), $\mathcal{B}(\overline{B} \to X_u \ell^- \overline{\nu}_\ell) = (2.13 \pm 0.31) \times 10^{-3}$, we obtain the semileptonic branching fraction,

$$\mathcal{B}(\overline{B} \to X \ell^- \overline{\nu}_\ell) = (10.86 \pm 0.16)\% \ . \tag{187}$$

5.2.3 Analysis in the 1S scheme

The fit relies on the calculations of the spectral moments described in Ref. [493]. The theoretical uncertainties are estimated as explained in Ref. [506]. Only trivial theory correlations, *i.e.* between the same moment at the same threshold are included in the analysis. The fit determines $|V_{cb}|$ and the 6 non-perturbative parameters mentioned above.

The result of the fit using the $B \to X_s\gamma$ constraint is

$$|V_{cb}| = (41.98 \pm 0.45) \times 10^{-3} \ , \tag{188}$$
$$m_b^{1S} = 4.691 \pm 0.037 \text{ GeV} \ , \tag{189}$$
$$\lambda_1 = -0.362 \pm 0.067 \text{ GeV}^2 \ , \tag{190}$$

with a χ^2 of 23.0 for $66-7$ degrees of freedom. The detailed result of the fit is given in Table 80.

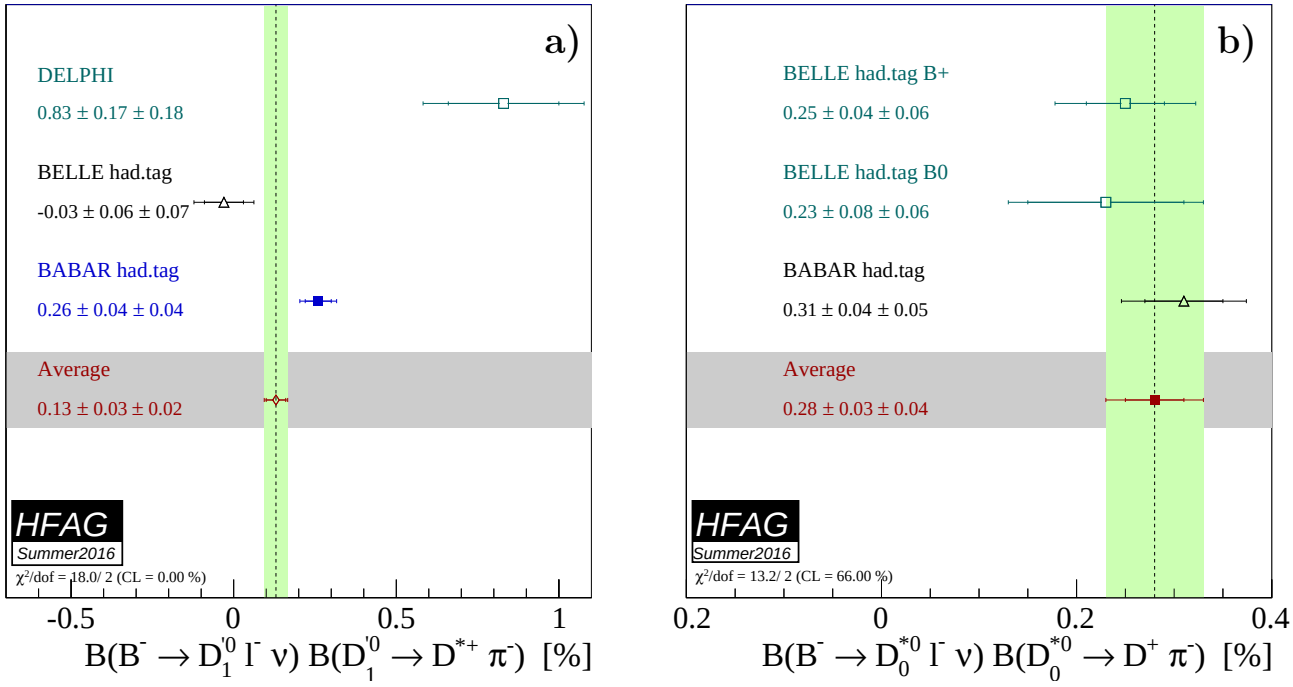

Figure 55: Average of the product of branching fraction (a) $\mathcal{B}(B^- \to D_1'^0 \ell^- \overline{\nu}_\ell) \times \mathcal{B}(D_1'^0 \to D^{*+}\pi^-)$ and (b) $\mathcal{B}(B^- \to D_0^{*0} \ell^- \overline{\nu}_\ell) \times \mathcal{B}(D_0^{*0} \to D^+\pi^-)$. The corresponding individual results are also shown.

5.3 Exclusive CKM-suppressed decays

In this section, we give results on exclusive charmless semileptonic branching fractions and the determination of $|V_{ub}|$ based on $B \to \pi l \nu$ decays. The measurements are based on two different event selections: tagged events, in which the second B meson in the event is fully (or partially) reconstructed, and untagged events, for which the momentum of the undetected neutrino is inferred from measurements of the total momentum sum of the detected particles and the knowledge of the initial state. The LHCb experiment recently reported a direct measurement of $|V_{ub}|/|V_{cb}|$ [507] reconstructing the $\Lambda_b \to p\mu\nu$ decays and normalizing the branching fraction to the $\Lambda_b \to \Lambda_c(\to pK\pi)\mu\nu$ decays. We show a combination of $|V_{ub}|$-$|V_{cb}|$ using the LHCb constraint on $|V_{ub}|/|V_{cb}|$, the exclusive determination of $|V_{ub}|$ from $B \to \pi l \nu$ and $|V_{cb}|$ from both $B \to D^* \ell \nu$ and $B \to D \ell \nu$. We also present branching fraction averages for $B^0 \to \rho \ell^+ \nu$, $B^+ \to \omega \ell^+ \nu$, $B^+ \to \eta \ell^+ \nu$ and $B^+ \to \eta' \ell^+ \nu$.

The experimental average of $|V_{ub}|$ from $B \to \pi l \nu$ decays is performed in a two-step procedure. First the experimental information from the four most precise $B \to \pi l \nu$ measurements from *BABAR* and Belle [508–511] is averaged to produce an average q^2 spectrum. From the two untagged *BABAR* analyses [510, 511], the combined results for $B^0 \to \pi^- \ell^+ \nu$ and $B^+ \to \pi^0 \ell^+ \nu$ decays based on isospin symmetry are used. The hadronic-tag analysis by Belle [509] provides results for $B^0 \to \pi^- \ell^+ \nu$ and $B^+ \to \pi^0 \ell^+ \nu$ separately, but not for the combination of both channels. In the untagged analysis by Belle [508], only $B^0 \to \pi^- \ell^+ \nu$ decays were measured. The average is determined by constructing a likelihood that combines the information from the various measurements. The experimental measurements use different binnings in q^2, but have matching bin edges, which allows them to be easily combined. In the second step, a χ^2 fit of

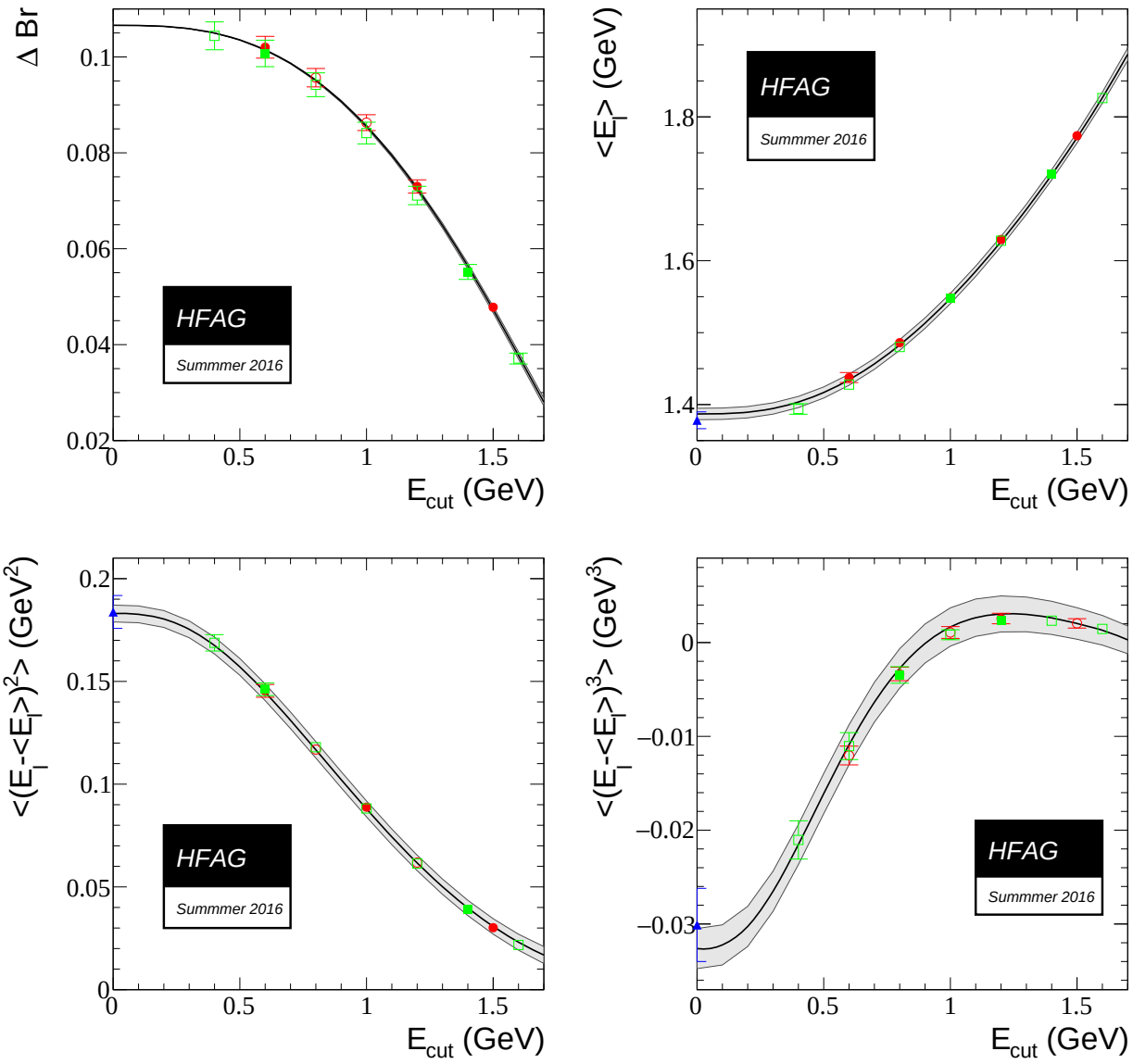

Figure 56: Fit to the partial semileptonic branching ratios and to the lepton energy moments in the kinetic mass scheme. In all plots, the grey band is the theory prediction with total theory error. *BABAR* data are shown by circles, Belle by squares and other experiments (DELPHI, CDF, CLEO) by triangles. Filled symbols mean that the point was used in the fit. Open symbols are measurements that were not used in the fit.

Table 78: Experimental inputs used in the global analysis of $\overline{B} \to X_c \ell^- \overline{\nu}_\ell$. n is the order of the moment, c is the threshold value of the lepton momentum in GeV. In total, there are 23 measurements from *BABAR*, 15 measurements from Belle and 12 from other experiments.

Experiment	Hadron moments $\langle M_X^n \rangle$	Lepton moments $\langle E_\ell^n \rangle$
BABAR	$n = 2$, $c = 0.9, 1.1, 1.3, 1.5$ $n = 4$, $c = 0.8, 1.0, 1.2, 1.4$ $n = 6$, $c = 0.9, 1.3$ [494]	$n = 0$, $c = 0.6, 1.2, 1.5$ $n = 1$, $c = 0.6, 0.8, 1.0, 1.2, 1.5$ $n = 2$, $c = 0.6, 1.0, 1.5$ $n = 3$, $c = 0.8, 1.2$ [494, 495]
Belle	$n = 2$, $c = 0.7, 1.1, 1.3, 1.5$ $n = 4$, $c = 0.7, 0.9, 1.3$ [496]	$n = 0$, $c = 0.6, 1.4$ $n = 1$, $c = 1.0, 1.4$ $n = 2$, $c = 0.6, 1.4$ $n = 3$, $c = 0.8, 1.2$ [497]
CDF	$n = 2$, $c = 0.7$ $n = 4$, $c = 0.7$ [498]	
CLEO	$n = 2$, $c = 1.0, 1.5$ $n = 4$, $c = 1.0, 1.5$ [499]	
DELPHI	$n = 2$, $c = 0.0$ $n = 4$, $c = 0.0$ $n = 6$, $c = 0.0$ [488]	$n = 1$, $c = 0.0$ $n = 2$, $c = 0.0$ $n = 3$, $c = 0.0$ [488]

Table 79: Fit result in the kinetic scheme, using a precise c-quark mass constraint. The error matrix of the fit contains experimental and theoretical contributions. In the lower part of the table, the correlation matrix of the parameters is given.

	$\lvert V_{cb}\rvert$ [10^{-3}]	$m_b^{\rm kin}$ [GeV]	$m_c^{\overline{\rm MS}}$ [GeV]	μ_π^2 [GeV^2]	ρ_D^3 [GeV^3]	μ_G^2 [GeV^2]	ρ_{LS}^3 [GeV^3]
value	42.19	4.554	0.987	0.464	0.169	0.333	−0.153
error	0.78	0.018	0.015	0.076	0.043	0.053	0.096
$\lvert V_{cb}\rvert$	1.000	−0.257	−0.078	0.354	0.289	−0.080	−0.051
$m_b^{\rm kin}$		1.000	0.769	−0.054	0.097	0.360	−0.087
$m_c^{\overline{\rm MS}}$			1.000	−0.021	0.027	0.059	−0.013
μ_π^2				1.000	0.732	0.012	0.020
ρ_D^3					1.000	−0.173	−0.123
μ_G^2						1.000	0.066
ρ_{LS}^3							1.000

the BCL form-factor parametrization [512] to the averaged q^2 spectrum is performed, taking into account the full experimental covariance matrix obtained from the averaging. Constraints on the form factors from lattice QCD (LQCD) or light-cone sum rule (LCSR) calculations are included by adding constraint terms to the fit.

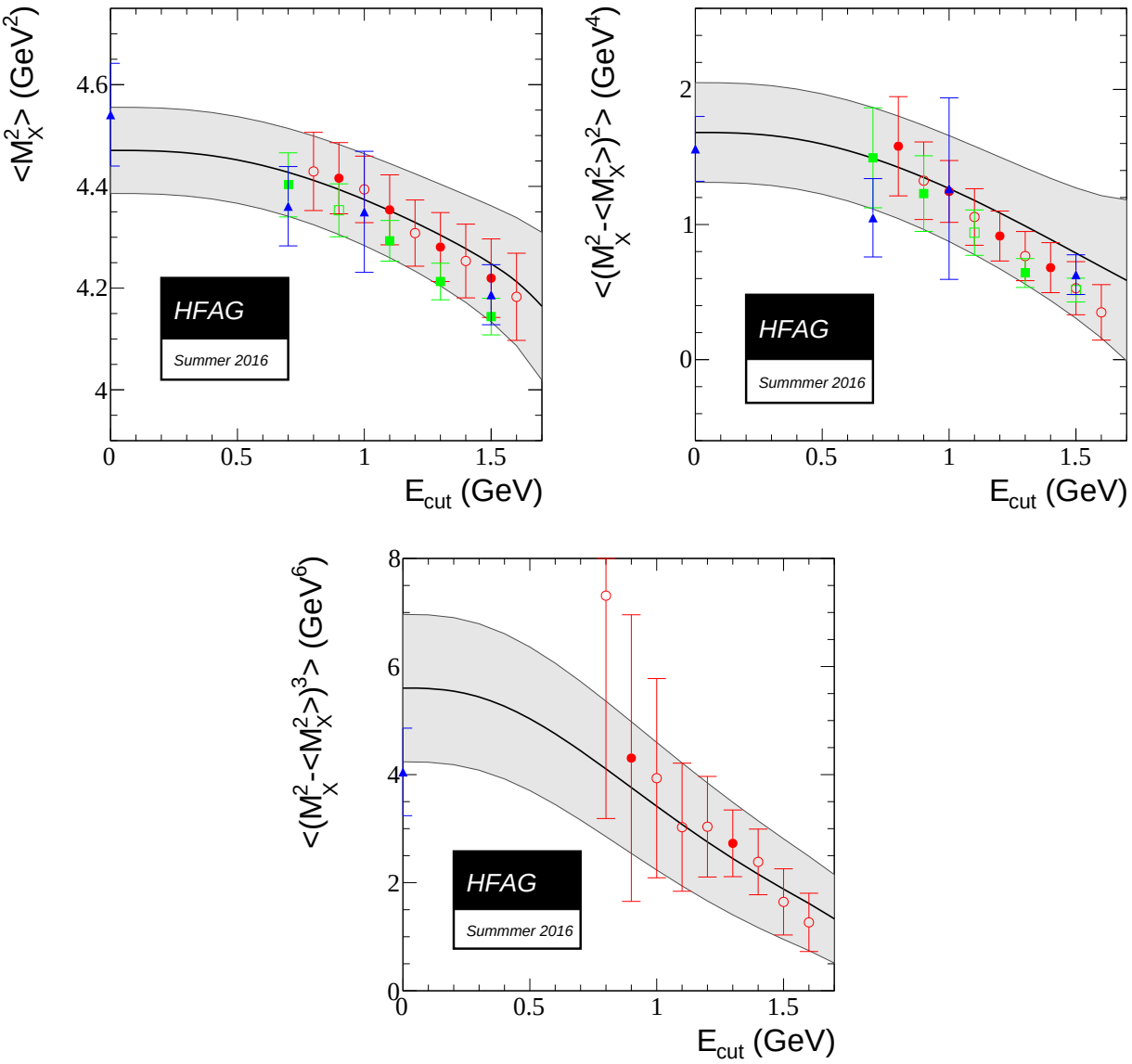

Figure 57: Same as Fig. 56 for the fit to the hadronic mass moments in the kinetic mass scheme.

5.3.1 $B \to \pi l \nu$ branching fraction and q^2 spectrum

A global likelihood is constructed using the experimental measurements of the differential branching fractions of $B \to \pi l \nu$ decays of Refs. [508–511]. Its general form is given by:

$$\mathcal{L} = \prod_{\mathrm{m}} \mathcal{L}_m \prod_n \mathcal{G}_n \tag{191}$$

with $\mathcal{L}_m$ denoting the likelihood of a single measurement m, and $\mathcal{G}_n$ denoting a range of shared nuisance parameters between the measurements. The free parameters of the likelihood are the differential partial branching fractions $\mathcal{B}_i$ for a q^2 bin size corresponding to the one used in the measurement with the finest binning in q^2. A single experimental measurement is modelled

Table 80: Fit result in the 1S scheme, using $B \to X_s\gamma$ moments as a constraint. In the lower part of the table, the correlation matrix of the parameters is given.

	m_b^{1S} [GeV]	λ_1 [GeV^2]	ρ_1 [GeV^3]	τ_1 [GeV^3]	τ_2 [GeV^3]	τ_3 [GeV^3]	$\lvert V_{cb}\rvert$ [10^{-3}]
value	4.691	−0.362	0.043	0.161	−0.017	0.213	41.98
error	0.037	0.067	0.048	0.122	0.062	0.102	0.45
m_b^{1S}	1.000	0.434	0.213	−0.058	−0.629	−0.019	−0.215
λ_1		1.000	−0.467	−0.602	−0.239	−0.547	−0.403
ρ_1			1.000	0.129	−0.624	0.494	0.286
τ_1				1.000	0.062	−0.148	0.194
τ_2					1.000	−0.009	−0.145
τ_3						1.000	0.376
$\lvert V_{cb}\rvert$							1.000

using a multivariate normal distribution,

$$\mathcal{L}_m = \frac{1}{\sqrt{|2\pi\, C_m|}} \exp\left(-\frac{1}{2}\,(\vec{x}-\vec{\mu})^T\, C_m^{-1}\,(\vec{x}-\vec{\mu})\right) \tag{192}$$

with C_m denoting the experimental covariance, $\vec{x}$ the measurement vector of partial branching fractions as a function of q^2, and $\vec{\mu}$ the vector of the desired averaged branching fractions. If measurement m has a larger bin size than the measurement with the smallest bin size for q^2 bin i, the element i of the vector $\vec{\mu}$ for measurement m is expressed as the sum of the branching fractions in the finer binning,

$$\mu_i = \sum_j b_j\,, \tag{193}$$

i.e. larger bins constrain the sum of smaller bins. Shared sources of systematic uncertainty of all measurements are not included in the individual covariances C_m, but are modelled using nuisance parameters. These enter Eq. 192 via a replacement

$$\vec{\mu} \to \prod_n \vec{\mu}(1+\epsilon_n\theta_n), \tag{194}$$

where n is a given source of uncertainty with amplitude ϵ_n and θ_n the corresponding nuisance parameter. The nuisance parameters are constrained in the likelihood in Eq. 191 using standard normal distributions,

$$\mathcal{G}_n = \mathcal{G}_n(\theta_n; \mu=0, \nu=1)\,. \tag{195}$$

The benefit of the replacement according to Eq. 194 over including systematic variations in a large covariance matrix between all measurements is that uncertainty sources can be constrained by the sum of all measurements. The most important shared sources of uncertainty are due to continuum subtraction, branching fractions, the number of B-meson pairs (only correlated among measurement by the same experiment), tracking efficiency (only correlated

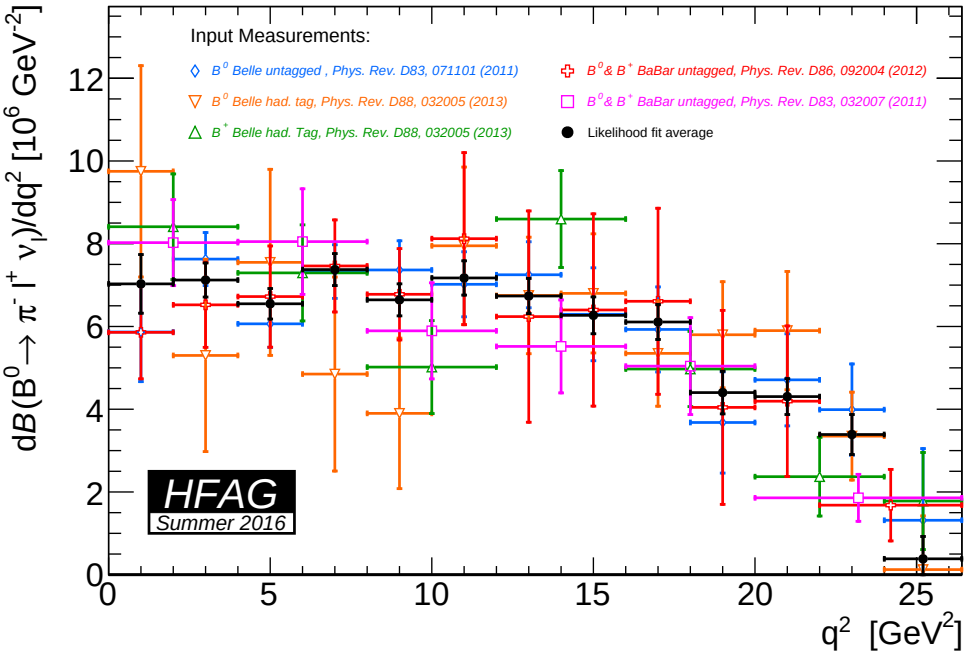

Figure 58: The $B \to \pi l \nu$ q^2 spectrum measurements and the average spectrum obtained from the likelihood combination (shown in black).

among measurements by the same experiment), uncertainties from modelling the $b \to u\,\ell\,\overline{\nu}_\ell$ contamination, modelling of final state radiation, and contamination from $b \to c\,\ell\overline{\nu}_\ell$ decays. The averaged spectrum together with the input spectra are shown in Figure 58. The probability for the average is 4%. The numerical values and the full covariance matrix are given in Tables 81 and 82. The average for the total $B^0 \to \pi^-\ell^+\nu_\ell$ branching fraction is obtained by summing up the partial branching fractions:

$$\mathcal{B}(B^0 \to \pi^-\ell^+\nu_\ell) = (1.47 \pm 0.02_{\rm stat} \pm 0.06_{\rm syst}) \times 10^{-4}. \tag{196}$$

5.3.2 $|V_{ub}|$ from $B \to \pi l \nu$

The value of $|V_{ub}|$ is extracted by constructing a χ^2 function of the form

$$\chi^2 = \left(\vec{\mathcal{B}} - \Delta\vec{\Gamma}\,\tau\right)^2 C^{-1} \left(\vec{\mathcal{B}} - \Delta\vec{\Gamma}\,\tau\right) + \chi^2_{\rm LQCD} + \chi^2_{\rm LCSR} \tag{197}$$

with C denoting the covariance matrix given in Table 82, $\vec{\mathcal{B}}$ the vector of averaged branching fractions and $\Delta\vec{\Gamma}\,\tau$ the product of the vector of theoretical predictions of the partial decay rates and the B^0-meson lifetime. The expression of the theoretical decay rate for light leptons (e, μ) is given by

$$\Delta\Gamma = \Delta\Gamma(q^2_{\rm low}, q^2_{\rm high}) = \int_{q^2_{\rm low}}^{q^2_{\rm high}} {\rm d}q^2 \left[\frac{8\,|\vec{p}_\pi|}{3} \frac{G_F^2\,|V_{ub}|^2\,q^2}{256\,\pi^3\,m_B^2} H_0^2(q^2)\right], \tag{198}$$

Table 81: Averaged partial branching fractions per GeV^2 obtained from the likelihood fit. The uncertainties are the combined statistical and systematic uncertainties.

Δq^2 [GeV^2]	$\Delta\mathcal{B}(B^0 \to \pi^-\ell^+\nu_\ell)/\Delta q^2 \quad [10^{-7}]$
0-2	70.3 ± 7.1
2-4	71.2 ± 4.1
4-6	65.5 ± 3.7
6-8	73.8 ± 3.9
8-10	66.4 ± 3.9
10-12	71.7 ± 4.2
12-14	67.3 ± 4.3
14-16	62.7 ± 4.5
16-18	61.1 ± 4.2
18-20	44.0 ± 5.2
20-22	43.1 ± 4.3
22-24	33.9 ± 4.8
24-26.4	3.8 ± 5.3

where G_F is Fermi's constant, $|\vec{p}_\pi|$ is the absolute four-momentum of the final state π (a function of q^2), m_B the B^0-meson mass, and $H_0(q^2)$ the only non-zero helicity amplitude. The helicity amplitude is a function of the form factor f_+,

$$H_0 = \frac{2m_B\ |\vec{p}_\pi|}{\sqrt{q^2}}\, f_+(q^2). \tag{199}$$

The form factor f_+ can only be calculated with non-perturbative methods, but its general form can be constrained by the differential $B \to \pi l\nu$ spectrum. It is parametrized using the BCL parametrization [512].

The minimal information needed to determine $|V_{ub}|$ is the normalization of the form factor at a single point in q^2, as $|V_{ub}|$ is degenerate with the overall normalization of f_+. This information is added in the fit by the two extra terms in Eq. 197: χ_{LQCD} uses the latest FLAG lattice average [210] from two state-of-the-art unquenched lattice QCD calculations. The resulting constraints are quoted directly in terms of the expansion parameters b_j^+ and enter Eq. 197 as

$$\chi^2_{\mathrm{LQCD}} = \left(\vec{b}^+ - \vec{b}^+_{\mathrm{LQCD}}\right)^T\, C^{-1}_{\mathrm{LQCD}}\, \left(\vec{b}^+ - \vec{b}^+_{\mathrm{LQCD}}\right)\,, \tag{200}$$

with $\vec{b}^+$ the vector containing the free parameters of the χ^2 fit constraining the form factor, $\vec{b}^+_{\mathrm{LQCD}}$ the averaged values from Ref. [210], and C_{LQCD} their covariance matrix. Additional information about the form factor can be obtained from light-cone sum rule calculations. The state-of-the-art calculation includes up to two-loops contributions [513]. It is included in Eq. 197 via

$$\chi^2_{\mathrm{LQCR}} = \left(f_+^{\mathrm{LCSR}} - f_+(q^2 = 0; \vec{b}^+)\right)^2 / \sigma^2_{f_+^{\mathrm{LCSR}}}\,. \tag{201}$$

The $|V_{ub}|$ average is obtained for two scenarios: the first combines the data with the lattice QCD constraints and the second additionally includes the information from the LCSR calculation.

Table 82: Covariance matrix of the averaged partial branching fractions per GeV^2 in units of 10^{-14}.

Δq^2 [GeV^2]	0-2	2-4	4-6	6-8	8-10	10-12	12-14	14-16	16-18	18-20	20-22	22-24	24-26.4
0-2	50.463	5.709	9.719	10.581	10.812	12.437	10.844	12.400	11.184	10.150	9.179	7.501	4.722
2-4	5.709	17.018	3.001	8.447	6.621	7.354	6.656	6.308	5.991	4.508	4.696	3.625	1.304
4-6	9.719	3.001	13.704	3.430	6.990	6.310	6.053	5.294	5.222	4.039	4.193	3.179	1.249
6-8	10.581	8.447	3.430	15.032	6.024	9.392	8.147	7.391	6.945	5.211	5.120	4.177	1.117
8-10	10.812	6.621	6.990	6.024	15.058	6.619	9.180	7.282	7.279	5.702	5.474	4.555	1.872
10-12	12.437	7.354	6.310	9.392	6.619	17.276	7.756	9.194	8.354	6.588	6.127	5.065	1.942
12-14	10.844	6.656	6.053	8.147	9.180	7.756	18.157	4.677	7.771	5.389	5.528	4.430	1.787
14-16	12.400	6.308	5.294	7.391	7.282	9.194	4.677	19.881	6.940	7.281	5.332	4.699	1.899
16-18	11.184	5.991	5.222	6.945	7.279	8.354	7.771	6.940	17.977	2.485	5.545	4.328	1.755
18-20	10.150	4.508	4.039	5.211	5.702	6.588	5.389	7.281	2.485	26.614	3.452	3.780	2.423
20-22	9.179	4.696	4.193	5.120	5.474	6.127	5.528	5.332	5.545	3.452	18.920	1.296	−1.490
22-24	7.501	3.625	3.179	4.177	4.555	5.065	4.430	4.699	4.328	3.780	1.296	23.504	−6.517
24-26.4	4.722	1.304	1.249	1.117	1.872	1.942	1.787	1.899	1.755	2.423	−1.490	−6.517	29.270

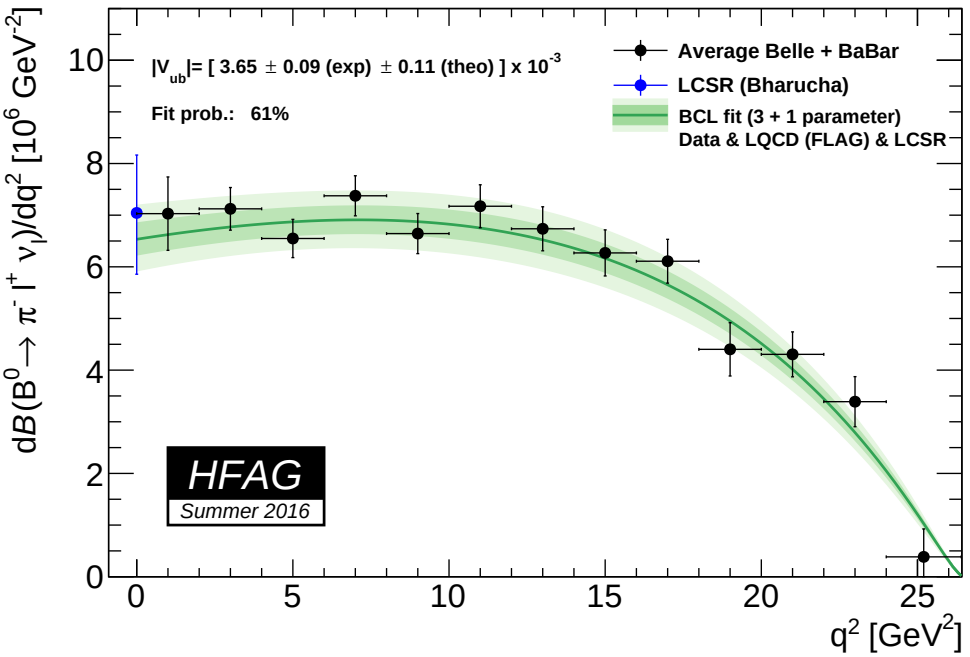

Figure 59: Fit of the BCL parametrization to the averaged q^2 spectrum from *BABAR* and Belle and the LQCD and LCSR calculations. The error band shows the 1 σ (dark green) and 2 σ (light green) uncertainties on the fitted parametrization.

Table 83: Best fit values and uncertainties for the combined fit to data, LQCD and LCSR results.

Parameter	Value
$\lvert V_{ub}\rvert$	$(3.65 \pm 0.14) \times 10^{-3}$
b_1^+	0.421 ± 0.017
b_2^+	-0.390 ± 0.033
b_3^+	-0.650 ± 0.126

The resulting values for $|V_{ub}|$ are

$$|V_{ub}| = (3.68 \pm 0.10\,(\text{exp}) \pm 0.12\,(\text{theo})) \times 10^{-3} \quad (\text{data} + \text{LQCD}), \tag{202}$$
$$|V_{ub}| = (3.65 \pm 0.09\,(\text{exp}) \pm 0.11\,(\text{theo})) \times 10^{-3} \quad (\text{data} + \text{LQCD} + \text{LCSR}), \tag{203}$$

for the first and second fit scenario, respectively. The result of the fit in the second scenario is shown in Figure 59. The χ^2 probability of the fit is 61%. We quote the result of the fit including both LQCD and LCSR calculations as our average for $|V_{ub}|$. The best fit values for $|V_{ub}|$ and the BCL parameters and their covariance matrix are given in Tables 83 and 84.

5.3.3 Combined extraction of $|V_{ub}|$ and $|V_{cb}|$

The LHCb experiment reported the first observation of $\Lambda_b \to p\mu\nu$ decays [507] and the measurement of the ratio of partial branching fractions at high q^2 for $\Lambda_b \to p\mu\nu$ and $\Lambda_b \to \Lambda_c(\to pK\pi)\mu\nu$ decays

Table 84: Covariance matrix for the combined fit to data, LQCD and LCSR results.

Parameter	$\lvert V_{ub}\rvert$	b_1^+	b_2^+	b_3^+
$\lvert V_{ub}\rvert$	2.088×10^{-8}	-1.291×10^{-6}	-1.808×10^{-6}	7.274×10^{-6}
b_1^+	-1.291×10^{-6}	1.377×10^{-4}	7.922×10^{-5}	-8.681×10^{-4}
b_2^+	-1.808×10^{-6}	7.922×10^{-5}	1.068×10^{-3}	-2.873×10^{-3}
b_3^+	7.274×10^{-6}	-8.681×10^{-4}	-2.873×10^{-3}	1.588×10^{-2}

$$R = \frac{\mathcal{B}(\Lambda_b \to p\mu\nu)_{q^2>15\ GeV^2}}{\mathcal{B}(\Lambda_b \to \Lambda_c\mu\nu)_{q^2>7\ GeV^2}} = (1.00 \pm 0.04 \pm 0.08) \times 10^{-2}. \tag{204}$$

The ratio R is proportional to $(|V_{ub}|/|V_{cb}|)^2$ through a factor that depends on the form factors of $\Lambda_b \to p$ and $\Lambda_b \to \Lambda_c$ transitions that have to be computed with non perturbative methods, like lattice QCD. The measured ratio R depends on the branching fraction of the Λ_c in the $pK\pi$ decay mode used to reconstruct the normalization decay. The uncertainty on $\mathcal{B}(\Lambda_c \to pK\pi)$ is the largest source of systematics on R. Using the recent HFAG average $\mathcal{B}(\Lambda_c \to pK\pi) = (6.46 \pm 0.24)\%$, that includes the recent BESIII measurements, the rescaled value for R is

$$R = (0.95 \pm 0.04 \pm 0.07) \times 10^{-2} \tag{205}$$

The lattice QCD prediction [514] of the form factors in the restricted q^2 region considered, allows to extract $|V_{ub}|/|V_{cb}|$,

$$\frac{|V_{ub}|}{|V_{cb}|} = 0.080 \pm 0.004_{Exp.} \pm 0.004_{F.F.} \tag{206}$$

where the first uncertainty is the total experimental error and the second one is due to the knowledge of the form factors. A combined fit for $|V_{ub}|$ and $|V_{cb}|$ that includes the constraint from LHCb, and the exclusive determination of $|V_{ub}|$ and $|V_{cb}|$ only, gives the following results

$$|V_{ub}| = (3.55 \pm 0.12) \times 10^{-3} \tag{207}$$
$$|V_{cb}| = (39.16 \pm 0.58) \times 10^{-3} \tag{208}$$
$$\rho(|V_{ub}||, |V_{cb}|) = 0.14 \tag{209}$$

where the uncertainties are considered uncorrelated. The χ^2 of the fit is 5.2 for 2 d.o.f corresponding to a $P(\chi^2)$ of 7.4%. The fit result is shown in Fig. 60, where both the 1-σ and the 68% C.L. contours are reported. The $|V_{ub}|/|V_{cb}|$ value extracted from R is more compatible with the exclusive determinations of $|V_{ub}|$. Another recent calculation, by Faustov and Galkin [515], based on a relativistic quark model, gives a value of $|V_{ub}|/|V_{cb}|$ closer to the inclusive determinations. More calculations of the relevant form factors for $\Lambda_b \to p\ell\nu$ and $\Lambda_b \to \Lambda_c\ell\nu$ are highly desirable.

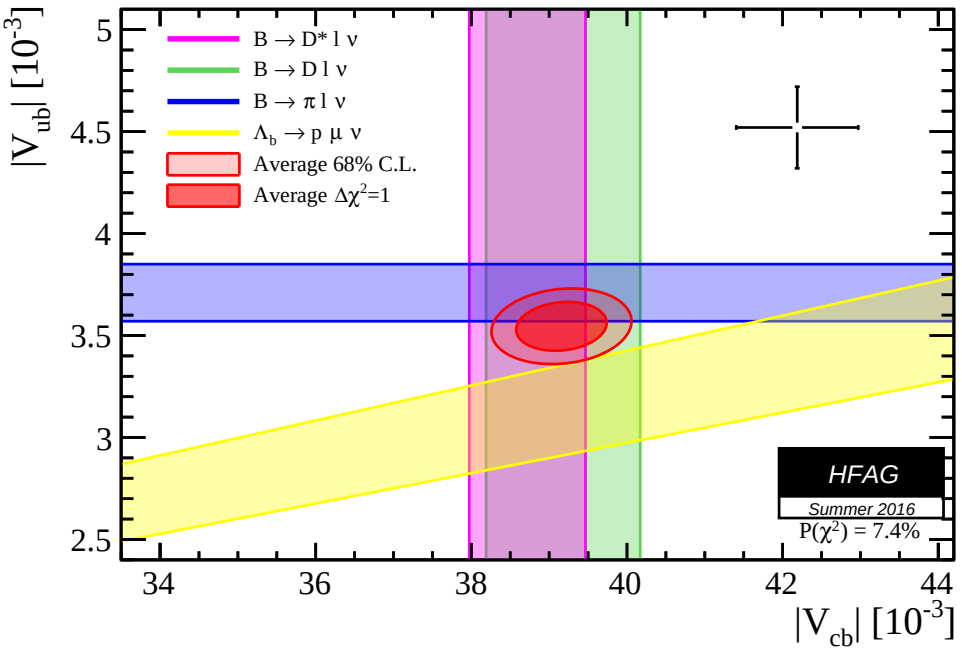

Figure 60: $|V_{ub}|$-$|V_{cb}|$ combined average including the LHCb measurement of $|V_{ub}|/|V_{cb}|$, the exclusive $|V_{ub}|$ measurement from $B \to \pi l \nu$, and $|V_{cb}|$ measurements from both $B \to D^* \ell \nu$ and $B \to D \ell \nu$. The point with the error bars corresponds to the inclusive $|V_{cb}|$ from the kinetic scheme, and the inclusive $|V_{ub}|$ from GGOU calculation which are reported for comparisons.

5.3.4 Other exclusive charmless semileptonic B decays

We report the branching fraction average for $B^0 \to \rho \ell^+ \nu$, $B^+ \to \omega \ell^+ \nu$, $B^+ \to \eta \ell^+ \nu$ and $B^+ \to \eta' \ell^+ \nu$. The measurements for $B^0 \to \rho \ell^+ \nu$ are reported in Table 85 and shown in Fig. 61 (a). In the average both the $B^0 \to \rho^- \ell^+ \nu$ and $B^+ \to \rho^0 \ell^+ \nu$ are used, where the $B^+ \to \rho^0 \ell^+ \nu$ are rescaled by $2\tau_{B^0}/\tau_{B^+}$ to account for the isospin symmetry. The measurement for $B^+ \to \omega \ell^+ \nu$ and their average, are reported in Table 86 and shown in Fig. 61 (b), while the ones for $B^+ \to \eta \ell^+ \nu$ and $B^+ \to \eta' \ell^+ \nu$ are reported in Table 87 and 88, and are shown in Fig. 62.

Table 85: Summary of exclusive determinations of $B^0 \to \rho\ell^+\nu$. The errors quoted correspond to statistical and systematic uncertainties, respectively.

	$\mathcal{B}[10^{-4}]$
CLEO (Untagged) ρ^+ [516]	$2.77 \pm 0.41 \pm 0.52$
CLEO (Untagged) ρ^+ [517]	$2.93 \pm 0.37 \pm 0.37$
Belle (Hadronic Tag) ρ^+ [509]	$3.22 \pm 0.27 \pm 0.24$
Belle (Hadronic Tag) ρ^0 [509]	$3.39 \pm 0.18 \pm 0.18$
Belle (Semileptonic Tag) ρ^+ [518]	$2.24 \pm 0.54 \pm 0.31$
Belle (Semileptonic Tag) ρ^0 [518]	$2.50 \pm 0.43 \pm 0.33$
BABAR (Untagged) ρ^+ [510]	$1.96 \pm 0.21 \pm 0.38$
BABAR (Untagged) ρ^0 [510]	$1.86 \pm 0.19 \pm 0.32$
Average	$\mathbf{2.94 \pm 0.09 \pm 0.17}$

Table 86: Summary of exclusive determinations of $B^+ \to \omega\ell^+\nu$. The errors quoted correspond to statistical and systematic uncertainties, respectively.

	$\mathcal{B}[10^{-4}]$
Belle (Untagged) [519]	$1.30 \pm 0.40 \pm 0.36$
BABAR (Loose ν reco.) [511]	$1.19 \pm 0.16 \pm 0.09$
BABAR (Untagged) [520]	$1.21 \pm 0.14 \pm 0.08$
Belle (Hadronic Tag) [509]	$1.07 \pm 0.16 \pm 0.07$
BABAR (Semileptonic Tag) [521]	$1.35 \pm 0.21 \pm 0.11$
Average	$\mathbf{1.19 \pm 0.08 \pm 0.06}$

Table 87: Summary of exclusive determinations of $B^+ \to \eta\ell^+\nu$. The errors quoted correspond to statistical and systematic uncertainties, respectively.

	$\mathcal{B}[10^{-4}]$
CLEO [522]	$0.45 \pm 0.23 \pm 0.11$
BABAR (Untagged) [523]	$0.31 \pm 0.06 \pm 0.08$
BABAR (Semileptonic Tag) [524]	$0.64 \pm 0.20 \pm 0.04$
BABAR (Loose ν-reco.) [511]	$0.38 \pm 0.05 \pm 0.05$
Average	$\mathbf{0.38 \pm 0.04 \pm 0.04}$

Table 88: Summary of exclusive determinations of $B^+ \to \eta'\ell^+\nu$. The errors quoted correspond to statistical and systematic uncertainties, respectively.

	$\mathcal{B}[10^{-4}]$
CLEO [522]	$2.71 \pm 0.80 \pm 0.56$
BABAR (Semileptonic Tag) [524]	$0.04 \pm 0.22 \pm 0.04$, (< 0.47 @ 90%$C.L.$)
BABAR (Untagged) [511]	$0.24 \pm 0.08 \pm 0.03$
Average	$\mathbf{0.23 \pm 0.08 \pm 0.03}$

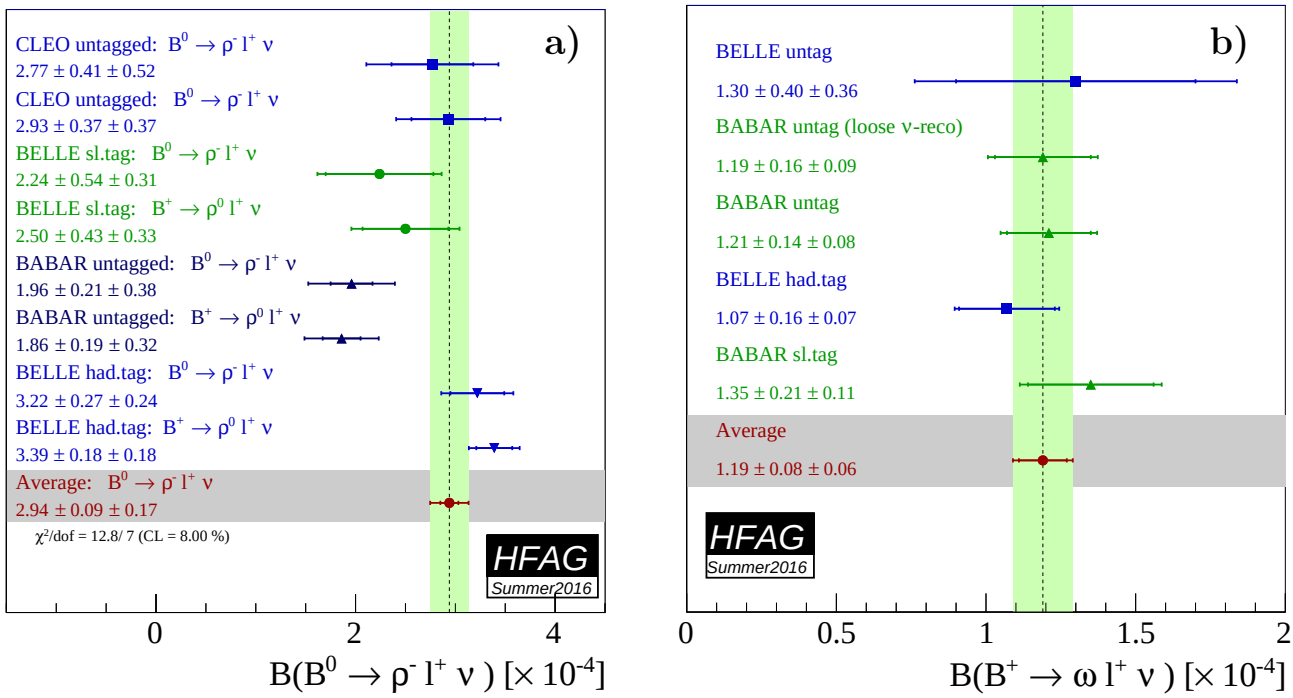

Figure 61: (a) Summary of exclusive determinations of $\mathcal{B}(B^0 \to \rho\ell^+\nu)$ and their average. Measurements of $B^+ \to \rho^0\ell^+\nu$ branching fractions have been multiplied by $2\tau_{B^0}/\tau_{B^+}$ in accordance with isospin symmetry. (b) Summary of exclusive determinations of $B^+ \to \omega\ell^+\nu$ and their average.

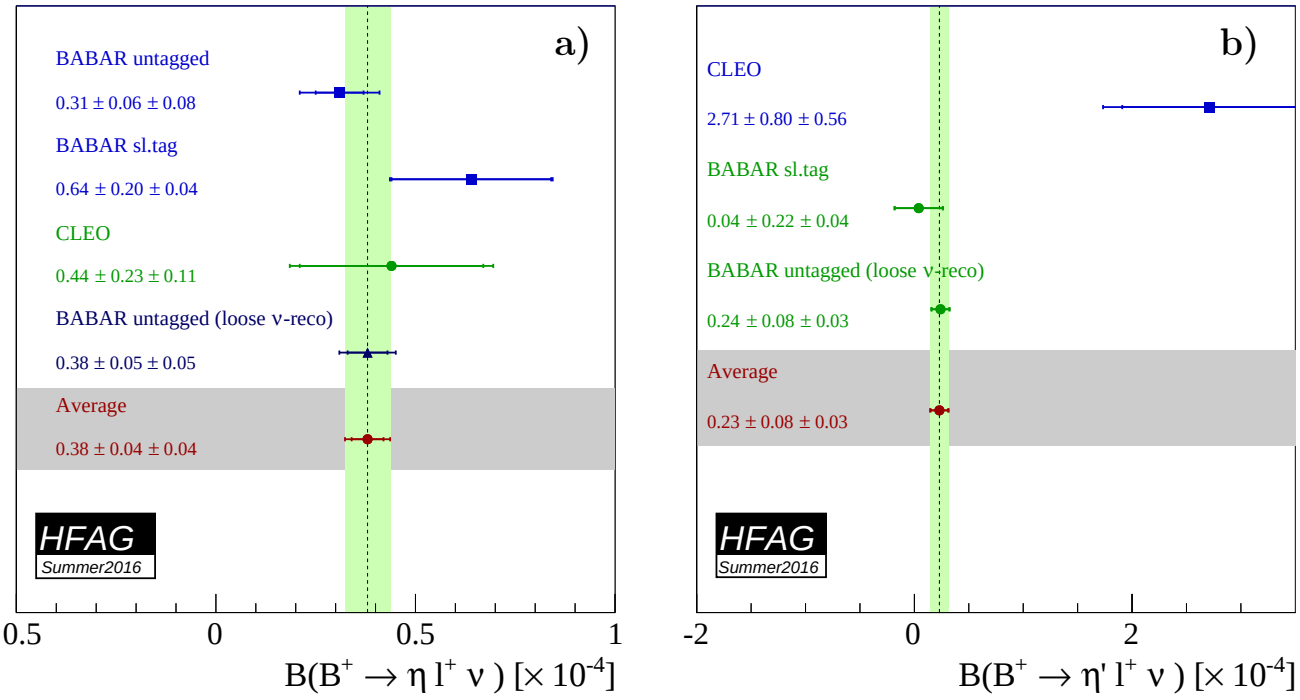

Figure 62: (a) Summary of exclusive determinations of $\mathcal{B}(B^+ \to \eta \ell^+ \nu)$ and their average. (b) Summary of exclusive determinations of $\mathcal{B}(B^+ \to \eta' \ell^+ \nu)$ and their average.

5.4 Inclusive CKM-suppressed decays

The large background from $B \to X_c \ell^+ \nu_\ell$ decays is the chief experimental limitation in determinations of $|V_{ub}|$. Cuts designed to reject this background limit the acceptance for $B \to X_u \ell^+ \nu_\ell$ decays. The calculation of partial rates for these restricted acceptances is more complicated and requires substantial theoretical machinery. In this update, we use several theoretical calculations to extract $|V_{ub}|$. We do not advocate the use of one method over another. The authors of the different calculations have provided codes to compute the partial rates in limited regions of phase space covered by the measurements. Latest results by Belle [525] and *BABAR* [526] explore bigger and bigger portions of phase space, with a consequent reduction of the theoretical uncertainties.

When computing the averages, the systematic errors associated with the modeling of $B \to X_c \ell^+ \nu_\ell$ and $B \to X_u \ell^+ \nu_\ell$ decays and the theoretical uncertainties are taken as fully correlated among all measurements. Reconstruction-related uncertainties are taken as fully correlated within a given experiment. We use all results published by *BABAR* in Ref. [526], since the statistical correlations are given. To make use of the theoretical calculations of Ref. [527], we restrict the kinematic range of the invariant mass of the hadronic system, M_X, and the square of the invariant mass of the lepton pair, q^2. This reduces the size of the data sample significantly, but also the theoretical uncertainty, as stated by the authors [527]. The dependence of the quoted error on the measured value for each source of uncertainty is taken into account in the calculation of the averages. Measurements of partial branching fractions for $B \to X_u \ell^+ \nu_\ell$ transitions from $\Upsilon(4S)$ decays, together with the corresponding selected region, are given in Table 89. The signal yields for all the measurements shown in Table 89 are not rescaled to common input values of the B meson lifetime (see Sec. 3) and the semileptonic width [314].

It has been first suggested by Neubert [528] and later detailed by Leibovich, Low, and Rothstein (LLR) [529] and Lange, Neubert and Paz (LNP) [530], that the uncertainty of the leading shape functions can be eliminated by comparing inclusive rates for $B \to X_u \ell^+ \nu_\ell$ decays with the inclusive photon spectrum in $B \to X_s \gamma$, based on the assumption that the shape functions for transitions to light quarks, u or s, are the same at first order. However, shape function uncertainties are only eliminated at the leading order and they still enter via the signal models used for the determination of efficiency. For completeness, we provide at the end of this section a comparison of the results using calculations with reduced dependence on the shape function, as just introduced, with our averages based on different theoretical approaches. Results are presented by *BABAR* in Ref. [531] using the LLR prescription. In another work (Ref. [532]), $|V_{ub}|$ was extracted from the endpoint spectrum of $B \to X_u \ell^+ \nu_\ell$ from *BABAR* [533], using several theoretical approaches with reduced dependence on the shape function. In both cases, the photon energy spectrum in the rest frame of the B-meson by *BABAR* [501] has been used.

In the following, the different theoretical methods and the resulting averages are described.

5.4.1 BLNP

Bosch, Lange, Neubert and Paz (BLNP) [540–543] provide theoretical expressions for the triple differential decay rate for $B \to X_u \ell^+ \nu_\ell$ events, incorporating all known contributions, whilst smoothly interpolating between the "shape-function region" of large hadronic energy and small invariant mass, and the "OPE region" in which all hadronic kinematical variables scale with the b-quark mass. BLNP assign uncertainties to the b-quark mass which enters through the leading

Table 89: Summary of inclusive determinations of partial branching fractions for $B \to X_u \ell^+ \nu_\ell$ decays. The errors quoted on $\Delta\mathcal{B}$ correspond to statistical and systematic uncertainties. E_e is the electron energy in the B rest frame, p^* the lepton momentum in the B frame and m_X is the invariant mass of the hadronic system. The light-cone momentum P_+ is defined in the B rest frame as $P_+ = E_X - |\vec{p}_X|$. The $s_{\rm h}^{\rm max}$ variable is described in Refs. [534, 535].

Measurement	Accepted region	$\Delta\mathcal{B}[10^{-4}]$	Notes
CLEO [536]	$E_e > 2.1\,\text{GeV}$	$3.3 \pm 0.2 \pm 0.7$	
BABAR [535]	$E_e > 2.0\,\text{GeV}$, $s_{\rm h}^{\rm max} < 3.5\,\text{GeV}^2$	$4.4 \pm 0.4 \pm 0.4$	
BABAR [533]	$E_e > 2.0\,\text{GeV}$	$5.7 \pm 0.4 \pm 0.5$	
Belle [537]	$E_e > 1.9\,\text{GeV}$	$8.5 \pm 0.4 \pm 1.5$	
BABAR [526]	$M_X < 1.7\,\text{GeV}/c^2, q^2 > 8\,\text{GeV}^2/c^2$	$6.9 \pm 0.6 \pm 0.4$	
Belle [538]	$M_X < 1.7\,\text{GeV}/c^2, q^2 > 8\,\text{GeV}^2/c^2$	$7.4 \pm 0.9 \pm 1.3$	
Belle [539]	$M_X < 1.7\,\text{GeV}/c^2, q^2 > 8\,\text{GeV}^2/c^2$	$8.5 \pm 0.9 \pm 1.0$	used only in BLL average
BABAR [526]	$P_+ < 0.66\,\text{GeV}$	$9.9 \pm 0.9 \pm 0.8$	
BABAR [526]	$M_X < 1.7\,\text{GeV}/c^2$	$11.6 \pm 1.0 \pm 0.8$	
BABAR [526]	$M_X < 1.55\,\text{GeV}/c^2$	$10.9 \pm 0.8 \pm 0.6$	
Belle [525]	$p_\ell^* > 1\text{GeV}/c$	$19.6 \pm 1.7 \pm 1.6$	
BABAR [526]	(M_X, q^2) fit, $p_\ell^* > 1\text{GeV}/c$	$18.2 \pm 1.3 \pm 1.5$	
BABAR [526]	$p_\ell^* > 1.3\text{GeV}/c$	$15.5 \pm 1.3 \pm 1.4$	

shape function, to sub-leading shape function forms, to possible weak annihilation contribution, and to matching scales. The BLNP calculation uses the shape function renormalization scheme; the heavy quark parameters determined from the global fit in the kinetic scheme, described in 5.2.2, were therefore translated into the shape function scheme by using a prescription by Neubert [544,545]. The resulting parameters are $m_b(SF) = (4.582 \pm 0.023 \pm 0.018)$ GeV, $\mu_\pi^2(SF) = (0.202 \pm 0.089^{+0.020}_{-0.040})$ GeV^2, where the second uncertainty is due to the scheme translation. The extracted values of $|V_{ub}|$ for each measurement along with their average are given in Table 90 and illustrated in Fig. 63(a). The total uncertainty is $^{+5.8}_{-6.0}\%$ and is due to: statistics ($^{+2.1}_{-2.1}\%$), detector effects ($^{+1.7}_{-1.8}\%$), $B \to X_c \ell^+ \nu_\ell$ model ($^{+1.2}_{-1.2}\%$), $B \to X_u \ell^+ \nu_\ell$ model ($^{+1.8}_{-1.7}\%$), heavy quark parameters ($^{+2.6}_{-2.6}\%$), SF functional form ($^{+0.2}_{-0.3}\%$), sub-leading shape functions ($^{+0.6}_{-0.7}\%$), BLNP theory: matching scales μ, μ_i, μ_h ($^{+3.8}_{-3.7}\%$), and weak annihilation ($^{+0.0}_{-1.4}\%$). The error assigned to the matching scales is the source of the largest uncertainty, while the uncertainty due to HQE parameters (b-quark mass and μ_π^2) is second. The uncertainty due to weak annihilation has been assumed to be asymmetric, *i.e.* it only tends to decrease $|V_{ub}|$.

5.4.2 DGE

Andersen and Gardi (Dressed Gluon Exponentiation, DGE) [546] provide a framework where the on-shell b-quark calculation, converted into hadronic variables, is directly used as an approximation to the meson decay spectrum without the use of a leading-power non-perturbative function (or, in other words, a shape function). The on-shell mass of the b-quark within the B-meson (m_b) is required as input. The DGE calculation uses the $\overline{MS}$ renormalization scheme; the heavy quark parameters determined from the global fit in the kinetic scheme, described in 5.2.2, were therefore translated into the $\overline{MS}$ scheme by using a calculation by Gardi, giving

Table 90: Summary of input parameters used by the different theory calculations, corresponding inclusive determinations of $|V_{ub}|$ and their average. The errors quoted on $|V_{ub}|$ correspond to experimental and theoretical uncertainties, respectively.

	BLNP	DGE	GGOU	ADFR	BLL
Input parameters					
scheme	SF	$\overline{MS}$	kinetic	$\overline{MS}$	$1S$
Ref.	[544, 545]	Ref. [546]	see Sec. 5.2.2	Ref. [547]	Ref. [527]
m_b (GeV)	4.582 ± 0.026	4.188 ± 0.043	4.554 ± 0.018	4.188 ± 0.043	4.704 ± 0.029
μ_π^2 (GeV^2)	$0.145\ ^{+0.091}_{-0.097}$	-	0.414 ± 0.078	-	-
Ref.	$\|V_{ub}\|$ values $[10^{-3}]$				
CLEO E_e [536]	$4.22 \pm 0.49^{+0.29}_{-0.34}$	$3.86 \pm 0.45^{+0.25}_{-0.27}$	$4.23 \pm 0.49^{+0.22}_{-0.31}$	$3.42 \pm 0.40^{+0.17}_{-0.17}$	-
Belle M_X, q^2 [538]	$4.51 \pm 0.47^{+0.27}_{-0.29}$	$4.43 \pm 0.47^{+0.19}_{-0.21}$	$4.52 \pm 0.48^{+0.25}_{-0.28}$	$3.93 \pm 0.41^{+0.18}_{-0.17}$	$4.68 \pm 0.49^{+0.30}_{-0.30}$
Belle E_e [537]	$4.93 \pm 0.46^{+0.26}_{-0.29}$	$4.82 \pm 0.45^{+0.23}_{-0.23}$	$4.95 \pm 0.46^{+0.16}_{-0.21}$	$4.48 \pm 0.42^{+0.20}_{-0.20}$	-
BABAR E_e [533]	$4.52 \pm 0.26^{+0.26}_{-0.30}$	$4.30 \pm 0.24^{+0.23}_{-0.25}$	$4.52 \pm 0.26^{+0.17}_{-0.24}$	$3.93 \pm 0.22^{+0.20}_{-0.20}$	-
BABAR $E_e, s_{\rm h}^{\rm max}$ [535]	$4.71 \pm 0.32^{+0.33}_{-0.38}$	$4.35 \pm 0.29^{+0.28}_{-0.30}$	-	$3.81 \pm 0.19^{+0.19}_{-0.18}$	
Belle p_ℓ^* [525]	$4.50 \pm 0.27^{+0.20}_{-0.22}$	$4.62 \pm 0.28^{+0.13}_{-0.13}$	$4.62 \pm 0.28^{+0.09}_{-0.10}$	$4.50 \pm 0.30^{+0.20}_{-0.20}$	-
BABAR M_X [526]	$4.24 \pm 0.19^{+0.25}_{-0.25}$	$4.47 \pm 0.20^{+0.19}_{-0.24}$	$4.30 \pm 0.20^{+0.20}_{-0.21}$	$3.83 \pm 0.18^{+0.20}_{-0.19}$	-
BABAR M_X [526]	$4.03 \pm 0.22^{+0.22}_{-0.22}$	$4.22 \pm 0.23^{+0.21}_{-0.27}$	$4.10 \pm 0.23^{+0.16}_{-0.17}$	$3.75 \pm 0.21^{+0.18}_{-0.18}$	-
BABAR M_X, q^2 [526]	$4.32 \pm 0.23^{+0.26}_{-0.28}$	$4.24 \pm 0.22^{+0.18}_{-0.21}$	$4.33 \pm 0.23^{+0.24}_{-0.27}$	$3.75 \pm 0.20^{+0.17}_{-0.17}$	$4.50 \pm 0.24^{+0.29}_{-0.29}$
BABAR P_+ [526]	$4.09 \pm 0.25^{+0.25}_{-0.25}$	$4.17 \pm 0.25^{+0.28}_{-0.37}$	$4.25 \pm 0.26^{+0.26}_{-0.27}$	$3.57 \pm 0.22^{+0.19}_{-0.18}$	-
BABAR p_ℓ^*, (M_X, q^2) fit [526]	$4.33 \pm 0.24^{+0.19}_{-0.21}$	$4.45 \pm 0.24^{+0.12}_{-0.13}$	$4.44 \pm 0.24^{+0.09}_{-0.10}$	$4.33 \pm 0.24^{+0.19}_{-0.19}$	-
BABAR p_ℓ^* [526]	$4.34 \pm 0.27^{+0.20}_{-0.21}$	$4.43 \pm 0.27^{+0.13}_{-0.13}$	$4.43 \pm 0.27^{+0.09}_{-0.11}$	$4.28 \pm 0.27^{+0.19}_{-0.19}$	-
Belle M_X, q^2 [539]	-	-	-	-	$5.01 \pm 0.39^{+0.32}_{-0.32}$
Average	$4.44 \pm 0.15^{+0.21}_{-0.22}$	$4.52 \pm 0.16^{+0.15}_{-0.16}$	$4.52 \pm 0.15^{+0.11}_{-0.14}$	$4.08 \pm 0.13^{+0.18}_{-0.12}$	$4.62 \pm 0.20^{+0.29}_{-0.29}$

$m_b(\overline{MS}) = (4.188 \pm 0.043)$ GeV. The extracted values of $|V_{ub}|$ for each measurement along with their average are given in Table 90 and illustrated in Fig. 63(b). The total error is $^{+4.8}_{-4.8}\%$, whose breakdown is: statistics ($^{+1.9}_{-1.9}\%$), detector effects ($^{+1.7}_{-1.7}\%$), $B \to X_c\ell^+\nu_\ell$ model ($^{+1.3}_{-1.3}\%$), $B \to X_u\ell^+\nu_\ell$ model ($^{+2.1}_{-1.7}\%$), strong coupling α_s ($^{+0.5}_{-0.5}\%$), m_b ($^{+3.2}_{-2.9}\%$), weak annihilation ($^{+0.0}_{-1.8}\%$), DGE theory: matching scales ($^{+0.5}_{-0.4}\%$). The largest contribution to the total error is due to the effect of the uncertainty on m_b. The uncertainty due to weak annihilation has been assumed to be asymmetric, *i.e.* it only tends to decrease $|V_{ub}|$.

5.4.3 GGOU

Gambino, Giordano, Ossola and Uraltsev (GGOU) [548] compute the triple differential decay rates of $B \to X_u\ell^+\nu_\ell$, including all perturbative and non–perturbative effects through $O(\alpha_s^2\beta_0)$ and $O(1/m_b^3)$. The Fermi motion is parameterized in terms of a single light–cone function for each structure function and for any value of q^2, accounting for all subleading effects. The calculations are performed in the kinetic scheme, a framework characterized by a Wilsonian treatment with a hard cutoff $\mu \sim 1$ GeV. GGOU have not included calculations for the "(E_e, s_h^{max})" analysis. The heavy quark parameters determined from the global fit in the kinetic scheme, described in 5.2.2, are used as inputs: $m_b(kin) = (4.554 \pm 0.018)$ GeV, $\mu_\pi^2(kin) = (0.464 \pm 0.076)$ GeV^2. The extracted values of $|V_{ub}|$ for each measurement along with their average are given in Table 90 and illustrated in Fig. 64(a). The total error is $^{+4.2}_{-4.6}\%$ whose breakdown is: statistics ($^{+2.0}_{-2.0}\%$), detector effects ($^{+1.7}_{-1.7}\%$), $B \to X_c\ell^+\nu_\ell$ model ($^{+1.3}_{-1.3}\%$), $B \to X_u\ell^+\nu_\ell$ model ($^{+1.8}_{-1.8}\%$), α_s, m_b and other non–perturbative parameters ($^{+1.4}_{-1.4}\%$), higher order perturbative and non–perturbative corrections ($^{+1.5}_{-1.5}\%$), modelling of the q^2 tail ($^{+1.2}_{-1.2}\%$), weak annihilations matrix

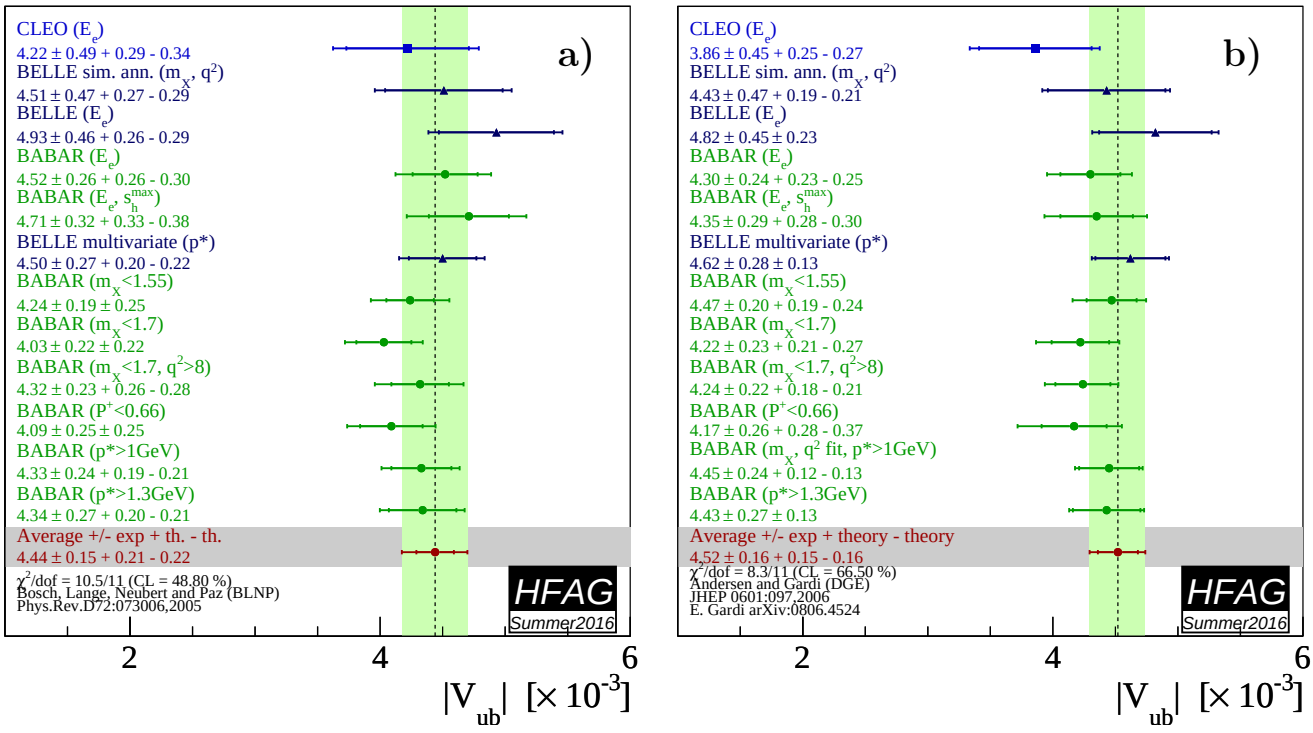

Figure 63: Measurements of $|V_{ub}|$ from inclusive semileptonic decays and their average based on the BLNP (a) and DGE (b) prescription. The labels indicate the variabless and selections used to define the signal regions in the different analyses.

element $(^{+0.0}_{-1.9}\%)$, functional form of the distribution functions $(^{+0.2}_{-0.2}\%)$. The leading uncertainties on $|V_{ub}|$ are both from theory, and are due to perturbative and non–perturbative parameters and the modelling of the q^2 tail. The uncertainty due to weak annihilation has been assumed to be asymmetric, *i.e.* it only tends to decrease $|V_{ub}|$.

5.4.4 ADFR

Aglietti, Di Lodovico, Ferrera and Ricciardi (ADFR) [549] use an approach to extract $|V_{ub}|$, that makes use of the ratio of the $B \to X_c \ell^+ \nu_\ell$ and $B \to X_u \ell^+ \nu_\ell$ widths. The normalized triple differential decay rate for $B \to X_u \ell^+ \nu_\ell$ [547,550–552] is calculated with a model based on (i) soft–gluon resummation to next–to–next–leading order and (ii) an effective QCD coupling without Landau pole. This coupling is constructed by means of an extrapolation to low energy of the high–energy behaviour of the standard coupling. More technically, an analyticity principle is used. The lower cut on the electron energy for the endpoint analyses is 2.3 GeV [547]. The ADFR calculation uses the $\overline{MS}$ renormalization scheme; the heavy quark parameters determined from the global fit in the kinetic scheme, described in 5.2.2, were therefore translated into the $\overline{MS}$ scheme by using a calculation by Gardi, giving $m_b(\overline{MS}) = (4.188 \pm 0.043)$ GeV. The extracted values of $|V_{ub}|$ for each measurement along with their average are given in Table 90 and illustrated in Fig. 64(b). The total error is $^{+5.5}_{-5.5}\%$ whose breakdown is: statistics $(^{+1.9}_{-1.9}\%)$, detector effects $(^{+1.7}_{-1.7}\%)$, $B \to X_c \ell^+ \nu_\ell$ model $(^{+1.3}_{-1.3}\%)$, $B \to X_u \ell^+ \nu_\ell$ model $(^{+1.3}_{-1.3}\%)$, α_s $(^{+1.1}_{-1.0}\%)$, $|V_{cb}|$ $(^{+1.9}_{-1.9}\%)$, m_b $(^{+0.7}_{-0.7}\%)$, m_c $(^{+1.3}_{-1.3}\%)$, semileptonic branching fraction $(^{+0.8}_{-0.7}\%)$, theory model

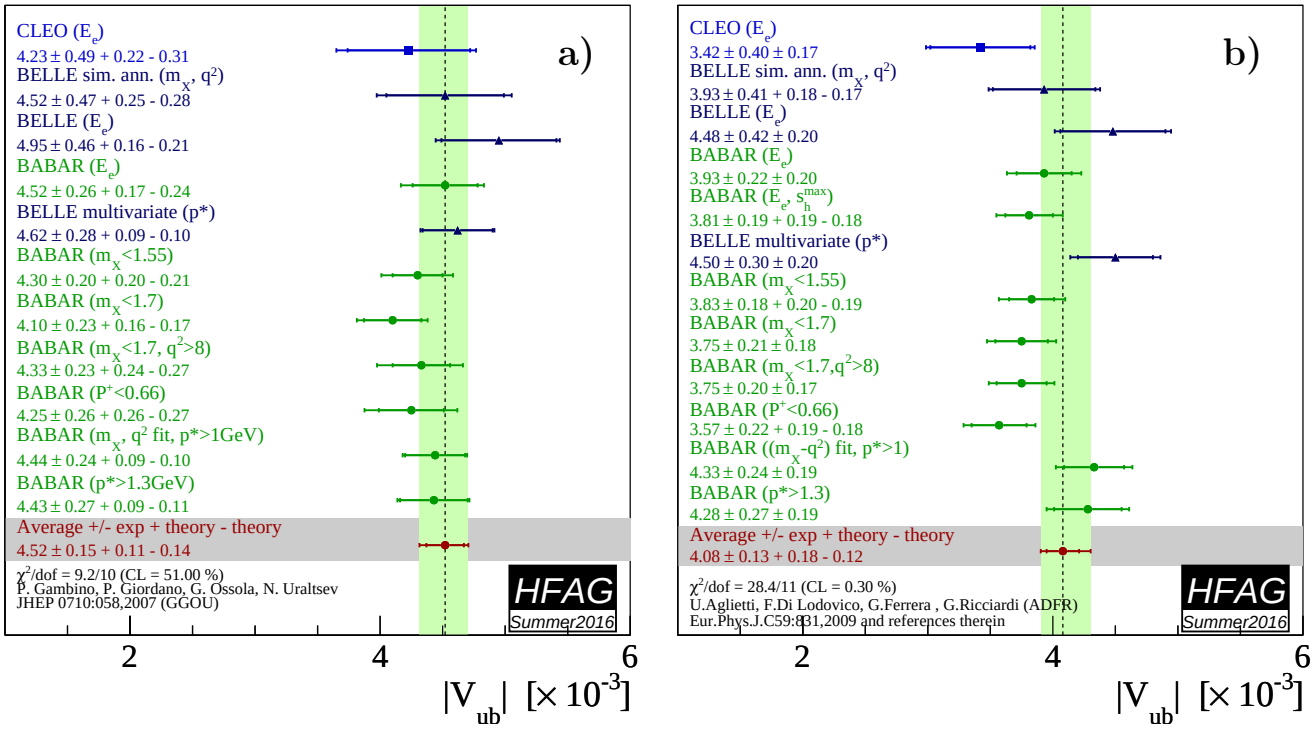

Figure 64: Measurements of $|V_{ub}|$ from inclusive semileptonic decays and their average based on the GGOU (a) and ADFR (b) prescription. The labels indicate the variables and selections used to define the signal regions in the different analyses .

$(^{+3.6}_{-3.6}\%)$. The leading uncertainty is due to the theory model.

5.4.5 BLL

Bauer, Ligeti, and Luke (BLL) [527] give a HQET-based prescription that advocates combined cuts on the dilepton invariant mass, q^2, and hadronic mass, m_X, to minimise the overall uncertainty on $|V_{ub}|$. In their reckoning a cut on m_X only, although most efficient at preserving phase space ($\sim$80%), makes the calculation of the partial rate untenable due to uncalculable corrections to the b-quark distribution function or shape function. These corrections are suppressed if events in the low q^2 region are removed. The cut combination used in measurements is $M_x < 1.7$ GeV/c^2 and $q^2 > 8$ GeV$^2/c^2$. The extracted values of $|V_{ub}|$ for each measurement along with their average are given in Table 90 and illustrated in Fig. 65. The total error is $^{+7.7}_{-7.7}\%$ whose breakdown is: statistics $(^{+3.3}_{-3.3}\%)$, detector effects $(^{+3.0}_{-3.0}\%)$, $B \to X_c\ell^+\nu_\ell$ model $(^{+1.6}_{-1.6}\%)$, $B \to X_u\ell^+\nu_\ell$ model $(^{+1.1}_{-1.1}\%)$, spectral fraction (m_b) $(^{+3.0}_{-3.0}\%)$, perturbative approach: strong coupling α_s $(^{+3.0}_{-3.0}\%)$, residual shape function $(^{+2.5}_{-2.5}\%)$, third order terms in the OPE $(^{+4.0}_{-4.0}\%)$. The leading uncertainties, both from theory, are due to residual shape function effects and third order terms in the OPE expansion. The leading experimental uncertainty is due to statistics.

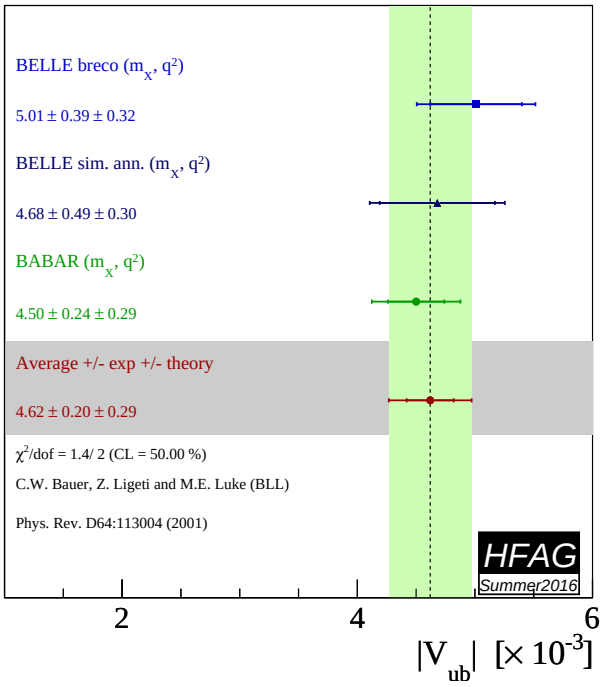

Figure 65: Measurements of $|V_{ub}|$ from inclusive semileptonic decays and their average in the BLL prescription.

5.4.6 Summary

A summary of the averages presented in several different frameworks and results by Golubev, Luth and Skovpen [532], based on prescriptions by LLR [529] and LNP [530] to reduce the leading shape function uncertainties are presented in Table 91. Experimental and theoretical uncertainties play out differently between the schemes and the theoretical assumptions for the theory calculations are different. Therefore, it is difficult to perform an average between the various determinations of $|V_{ub}|$. Since the methodology is similar to that used to determine the inclusive $|V_{cb}|$ average, we choose to quote as reference value the average determined by the GGOU calculation, which gives $|V_{ub}| = (4.52 \pm 0.15^{+0.11}_{-0.14}) \times 10^{-3}$.

5.5 $B \to D^{(*)}\tau\nu_\tau$ decays

The leptonic and semileptonic decays with τ in the final state are probes of physics beyond the SM. In the SM these decays proceed via the W emission diagrams. In models with extended Higgs sectors, such as the Two Higgs Doublet Models (2HDM) or the MSSM, charged Higgs can contribute to the decay amplitude at the tree level. Compared to $B^+ \to \tau\nu_\tau$, the $B \to D^{(*)}\tau\nu_\tau$ decay has advantages: the branching fraction is relatively high, because it is not Cabibbo-suppressed, and it is a three-body decay allowing access to many observables beside the branching fraction, such as the D^* and the τ polarisation, or the q^2 distribution (see Ref. [553] and reference therein for recent calculations).

Table 91: Summary of inclusive determinations of $|V_{ub}|$. The errors quoted on $|V_{ub}|$ correspond to experimental and theoretical uncertainties, except for the last two measurements where the errors are due to the *BABAR* endpoint analysis, the *BABAR* $b \to s\gamma$ analysis [531], the theoretical errors. For the next-to-last measurement, the fourth error is due to the uncertainty on V_{ts}.

Framework	$\lvert V_{ub}\rvert[10^{-3}]$
BLNP	$4.44 \pm 0.15^{+0.21}_{-0.22}$
DGE	$4.52 \pm 0.16^{+0.15}_{-0.16}$
GGOU	$4.52 \pm 0.15^{+0.11}_{-0.14}$
ADFR	$4.08 \pm 0.13^{+0.18}_{-0.12}$
BLL (m_X/q^2 only)	$4.62 \pm 0.20 \pm 0.29$
LLR (*BABAR*) [531]	$4.43 \pm 0.45 \pm 0.29$
LLR (*BABAR*) [532]	$4.28 \pm 0.29 \pm 0.29 \pm 0.26 \pm 0.28$
LNP (*BABAR*) [532]	$4.40 \pm 0.30 \pm 0.41 \pm 0.23$

The ratio of branching fractions defined as

$$\mathcal{R}(D) = \frac{\mathcal{B}(B \to D\tau\nu_\tau)}{\mathcal{B}(B \to D\ell\nu_\ell)}, \tag{210}$$

$$\mathcal{R}(D^*) = \frac{\mathcal{B}(B \to D^*\tau\nu_\tau)}{\mathcal{B}(B \to D^*\ell\nu_\ell)} \tag{211}$$

where ℓ is an electron or a μ, are independent of $|V_{cb}|$ and to a large extent, from the $B \to D^{(*)}$ form factors. As consequences the SM predictions for these ratios are quite precise:

- $\mathcal{R}(D) = 0.300 \pm 0.008$: average obtained by FLAG [210] combining the most recent lattice calculations of the $B \to D\ell\nu$ form factors [478, 554];
- $\mathcal{R}(D^*) = 0.252 \pm 0.003$: prediction obtained in Ref. [555, 556] updating the calculations in Ref. [557, 558] with the recent $B \to D^*$ measurements from the B-Factories.

From the experimental side, in the case of the leptonic τ decay, the ratios $\mathcal{R}(D^{(*)})$ can be directly measured, and many systematic uncertainties cancel in the measurement.

The $B^0 \to D^{*+}\tau\nu_\tau$ decay was first observed by Belle [559] performing an inclusive reconstruction of the B_{tag} candidates using all the particles remaining after the selection of the B_{sig} decay products. Since then, both *BABAR* and Belle have published improved measurements and have found evidence for the $B \to D\tau\nu_\tau$ decays [560–562]. The most powerful way to study these decays at the B-Factories is the full hadronic B_{tag}. Using the full dataset and an improved B_{tag} selection, *BABAR* measured [555]:

$$\mathcal{R}(D) = 0.440 \pm 0.058 \pm 0.042, \ \mathcal{R}(D^*) = 0.332 \pm 0.024 \pm 0.018 \tag{212}$$

where $\ell = e, \mu$ and the B^0 and B^+ are combined in a isospin-constrained fit. The fact that the *BABAR* result exceeded SM predictions by 3.4σ, raised huge interest for these channels.

Belle published various measurements using different techniques, and LHCb also joined the effort with a measurement of $R(D^*)$. The results obtained by *BABAR*, Belle and LHCb on $\mathcal{R}(D)$

and $\mathcal{R}(D^*)$ are reported in Table 92 together with their average. In Fig.66 all the measurements and the result of the combined average in the $\mathcal{R}(D)$ and $\mathcal{R}(D^*)$ plane are reported. The average results, projected separately on $\mathcal{R}(D)$ and $\mathcal{R}(D^*)$, are reported in Figs.67(a) and Figs.67(b) respectively. The most important sources of systematics correlated between the various measurement is due to the $B \to D^{**}$ background components that are difficult to disentangle from the signal. In the average the systematics due to the $B \to D^{**}$ composition and model, are considered fully correlated between the various measurements.

The averaged $\mathcal{R}(D)$ and $\mathcal{R}(D^*)$ exceed the SM predictions by 2.2σ and 3.4σ respectively. Considering the $\mathcal{R}(D)$ and $\mathcal{R}(D^*)$ total correlation of -0.23, the resulting combined χ^2 is 18.83 for 2 degree of freedom, corresponding to a p-value of 8.3×10^{-5}. The difference with the SM predictions is at about 3.9σ.

Table 92: Input measurements and combined average of $\mathcal{R}(D^*)$ and $\mathcal{R}(D)$. The experimental correlation between $\mathcal{R}(D)$ and $\mathcal{R}(D^*)$ is also reported.

Experiment	$\mathcal{R}(D^*)$	$\mathcal{R}(D)$	ρ
BaBar [555, 556]	$0.332 \pm 0.024_{\text{stat}} \pm 0.018_{\text{syst}}$	$0.440 \pm 0.058_{\text{stat}} \pm 0.042_{\text{syst}}$	-0.27
Belle [563]	$0.293 \pm 0.038_{\text{stat}} \pm 0.015_{\text{syst}}$	$0.375 \pm 0.064_{\text{stat}} \pm 0.026_{\text{syst}}$	-0.49
LHCb [564]	$0.336 \pm 0.027_{\text{stat}} \pm 0.030_{\text{syst}}$		
Belle [565]	$0.302 \pm 0.030_{\text{stat}} \pm 0.011_{\text{syst}}$		
Belle [566]	$0.276 \pm 0.034_{\text{stat}}{}^{+0.034}_{-0.026_{\text{syst}}}$		
Average	$\mathbf{0.310 \pm 0.015 \pm 0.008}$	$\mathbf{0.403 \pm 0.040 \pm 0.024}$	-0.23

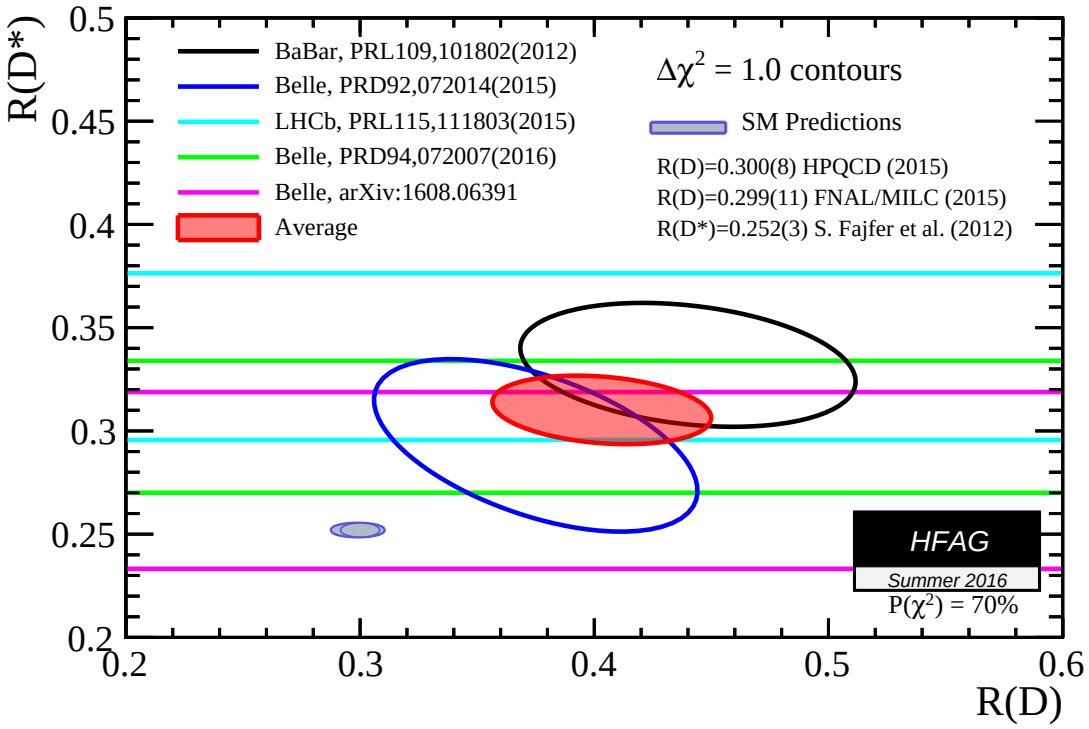

Figure 66: Measurement of $\mathcal{R}(D)$ and $\mathcal{R}(D^*)$ and their average. For $\mathcal{R}(D^*)$ we report the prediction from Ref. [558], and for $\mathcal{R}(D)$ the predictions from both MILC/FNAL and HPQCD collaborations.

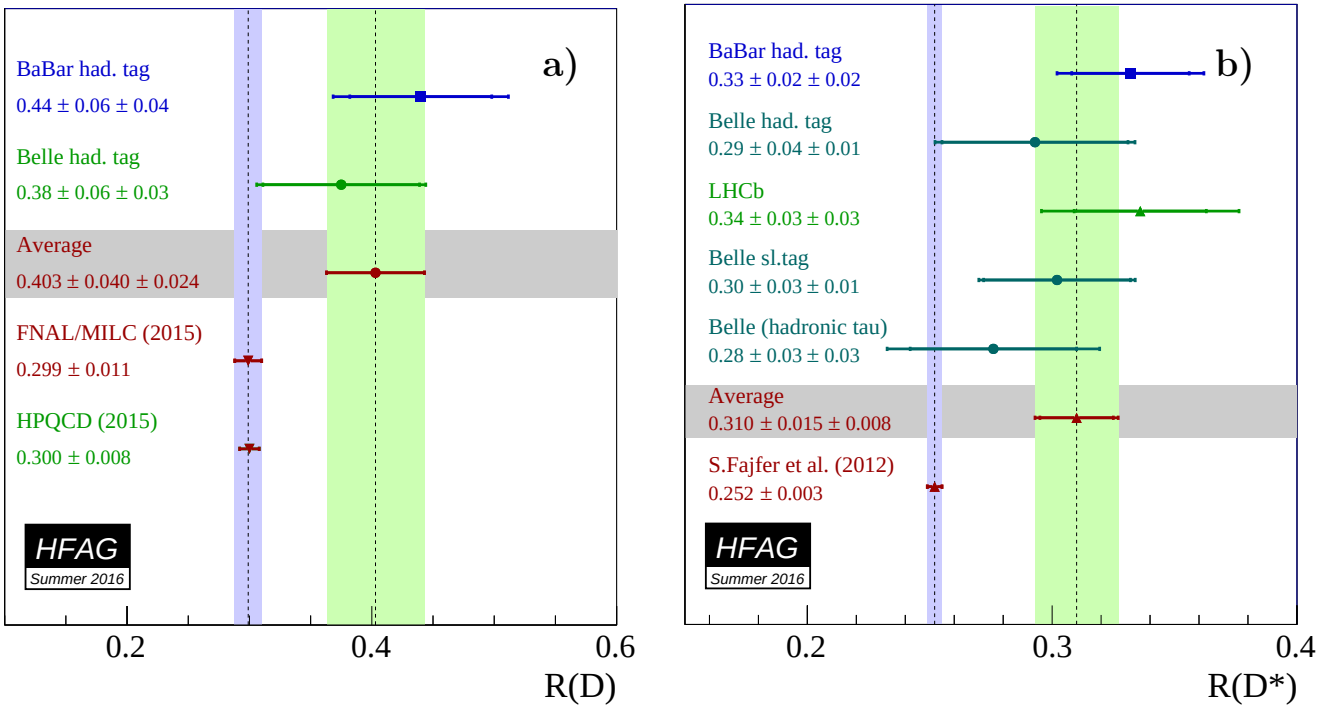

Figure 67: (a) Measurement of $\mathcal{R}(D)$ and (b) $\mathcal{R}(D^*)$. The average is the projection of the average obtained from the combined fit.

6 b-hadron decays to charmed hadrons

Ground state B mesons and b baryons dominantly decay to particles containing a charm quark via the $b \to c$ quark transition. Therefore these decays are sensitive to the CKM matrix element $|V_{cb}|$. Usually semileptonic modes are used for $|V_{cb}|$ measurements, as discussed in Section 5. Some B meson decays to open charmed hadrons are fundamental decays for the measurements of CP-violation phases like $\phi_s^{c\bar{c}s}$ (Section 3), $\beta \equiv \phi_1$ and $\gamma \equiv \phi_3$ (Section 4).

The fact that decays to charmed hadrons are the dominant b-hadron decays makes them a very important part of the experimental programme. Understanding the rate of charm production in b-hadron decays is crucial to validate the HQE that underpins much of the theoretical framework for b physics (see, for example, Ref. [567] for a review). Moreover, such decays are often used as the normalization mode for measurements of rarer decays. In addition, they are the dominant background in many analyses. To accurately model the background with simulated data it is essential to have a precise knowledge of the contributing decay modes. In particular, with the expected increase in the data samples at LHCb and Belle II, the enhanced statistical sensitivity has to be matched by low systematic uncertainties due to knowledge of the dominant b-hadron decay modes. For multibody decays, knowledge of the distribution of decays across the phase-space (*e.g.* the Dalitz plot density for three-body decays or the polarization amplitudes for vector-vector final states) is required in addition to the total branching fraction.

The large yields of b-hadron decays to multibody final states containing charm makes them ideal to study the spectroscopy of both open charm and charmonia (or charmonia-like) mesons. In particular, they have been used to both discover and measure the properties of exotic particles such as the $X(3872)$ [568,569] and $Z(4430)$ [570,571] states. The large yields available similarly make decays involving $b \to c$ transitions very useful to study baryon-antibaryon pair production.

In addition to the dominant b-hadron decays to final states containing charmed hadrons, there are several decays in this category that are expected to be highly suppressed in the Standard Model. These are of interest to probe particular decay topologies (*e.g.* the $B^- \to D_s^- \phi$ decay, which is dominated by the annihilation diagram) and thereby constrain effects in other hadronic decays or to search for new physics. There are also other decays involving $b \to c$ transitions, such as $\overline{B}^0 \to D_s^- \pi^+$, that are mediated by the W emission involving the $|V_{ub}|$ CKM matrix element. Finally, some $b \to c$ decays involving lepton flavour or number violation are completely forbidden in the Standard Model, and therefore provide highly sensitive null tests.

In this section, we give an exhaustive list of measured branching ratios of decay modes to charmed hadrons. The averaging procedure follows the methodology described in Section 2. Where available, correlations between measurements are taken into account. We provide averages of the polarization amplitudes of B meson decays to vector-vector states, but we do not currently provide detailed averages of quantities obtained from Dalitz plot analyses, due to the complications arising from the dependence on the model used.

The results are presented in subsections organized according to the type of decaying bottom hadron: $\overline{B}^0$ (Sec. 6.1), B^- (Sec. 6.2), $\overline{B}^0/B^-$ admixture (Sec. 6.3), $\overline{B}_s^0$ (Sec. 6.4), B_c^- (Sec. 6.5), b baryons (Sec. 6.6). For each subsection the measurements are arranged according to the final state into the following groups: a single charmed meson, two charmed mesons, a charmonium state, a charm baryon, or other states, like for example the $X(3872)$ meson. The individual measurements and averages are shown as numerical values in tables followed by a

graphical representation of the averages. The symbol $\mathcal{B}$ is used for branching ratios, f for production fractions (see Section 3), and σ for cross sections. The decay amplitudes for longitudinal, parallel, and perpendicular transverse polarization in pseudoscalar to vector-vector decays are denoted $\mathcal{A}_0$, $\mathcal{A}_\parallel$, and $\mathcal{A}_\perp$, respectively, and the definitions $\delta_\parallel = \arg(\mathcal{A}_\parallel/\mathcal{A}_0)$ and $\delta_\perp = \arg(\mathcal{A}_\perp/\mathcal{A}_0)$ are used for their relative phases. The inclusion of charge conjugate modes is always implied.

Following the approach used by the PDG [314], for decays that involve neutral kaons we mainly quote results in terms of final states including either a K^0 or $\overline{K}^0$ meson (instead of a K^0_S or K^0_L). In some cases where the decay is not flavour-specific and the final state is not self-conjugate, the inclusion of the conjugate final state is implied – in fact, the flavour of the neutral kaon is never determined experimentally, and so the specification as K^0 or $\overline{K}^0$ simply follows the quark model expectation for the dominant decay. An exception occurs for some B^0_s decays, specifically those to CP eigenstates, where the width difference between the mass eigenstates (see Sec. 3) means that the measured branching fraction, integrated over decay time, is specific to the studied final state [572]. Therefore it is appropriate to quote the branching fraction for, *e.g.*, $\overline{B}^0_s \to J/\psi\, K^0_S$ instead of $\overline{B}^0_s \to J/\psi\, \overline{K}^0$.

6.1 Decays of $\overline{B}^0$ mesons

Measurements of $\overline{B}^0$ decays to charmed hadrons are summarized in Sections 6.1.1 to 6.1.5.

6.1.1 Decays to a single open charm meson

Averages of $\overline{B}^0$ decays to a single open charm meson are shown in Tables 93–101 and Figs. 68–76. In this section D^{**} refers to the sum of all the non-strange charm meson states with masses in the range $2.2 - 2.8$ GeV/c^2.

Table 93: Decays to a $D^{(*)}$ meson and one or more pions [10^{-3}].

Parameter	**Measurements**	**Average**
$\mathcal{B}(\overline{B}^0 \to D^0\pi^0)$	Belle [573]: $0.225 \pm 0.014 \pm 0.035$ *BABAR* [574]: $0.269 \pm 0.009 \pm 0.013$	0.262 ± 0.015
$\mathcal{B}(\overline{B}^0 \to D^*(2007)^0\pi^0)$	Belle [573]: $0.139 \pm 0.018 \pm 0.026$ *BABAR* [574]: $0.305 \pm 0.014 \pm 0.028$	0.223 ± 0.022
$\mathcal{B}(\overline{B}^0 \to D^+\pi^-)$	*BABAR* [575]: $2.55 \pm 0.05 \pm 0.16$ *BABAR* [576]: $3.03 \pm 0.23 \pm 0.23$	2.65 ± 0.15
$\mathcal{B}(\overline{B}^0 \to D^*(2010)^+\pi^-)$	*BABAR* [575]: $2.79 \pm 0.08 \pm 0.17$ *BABAR* [576]: $2.99 \pm 0.23 \pm 0.24$	2.84 ± 0.16
$\mathcal{B}(\overline{B}^0 \to D^0\pi^+\pi^-)$	LHCb [577]: $0.846 \pm 0.014 \pm 0.049$ Belle [578]: $0.80 \pm 0.06 \pm 0.15$	0.842 ± 0.049
$\mathcal{B}(\overline{B}^0 \to D^*(2007)^0\pi^+\pi^-)$	Belle [578]: $0.62 \pm 0.12 \pm 0.18$	0.62 ± 0.22
$\mathcal{B}(\overline{B}^0 \to D^*(2010)^+\pi^-\pi^+\pi^-)$	Belle [579]: $6.81 \pm 0.23 \pm 0.72$ *BABAR* [580]: $7.26 \pm 0.11 \pm 0.31$	7.19 ± 0.30
$\mathcal{B}(\overline{B}^0 \to D^*(2007)^0\pi^-\pi^+\pi^-\pi^+)$	Belle [579]: $2.60 \pm 0.47 \pm 0.37$	2.60 ± 0.60
$\mathcal{B}(\overline{B}^0 \to D^*(2010)^+\pi^-\pi^+\pi^-\pi^+\pi^-)$	Belle [579]: $4.72 \pm 0.59 \pm 0.71$	4.72 ± 0.92
$\mathcal{B}(\overline{B}^0 \to D^*(2010)^+\omega(782)\pi^-)$	Belle [581]: $2.31 \pm 0.11 \pm 0.14$ *BABAR* [582]: $2.88 \pm 0.21 \pm 0.31$	2.41 ± 0.16

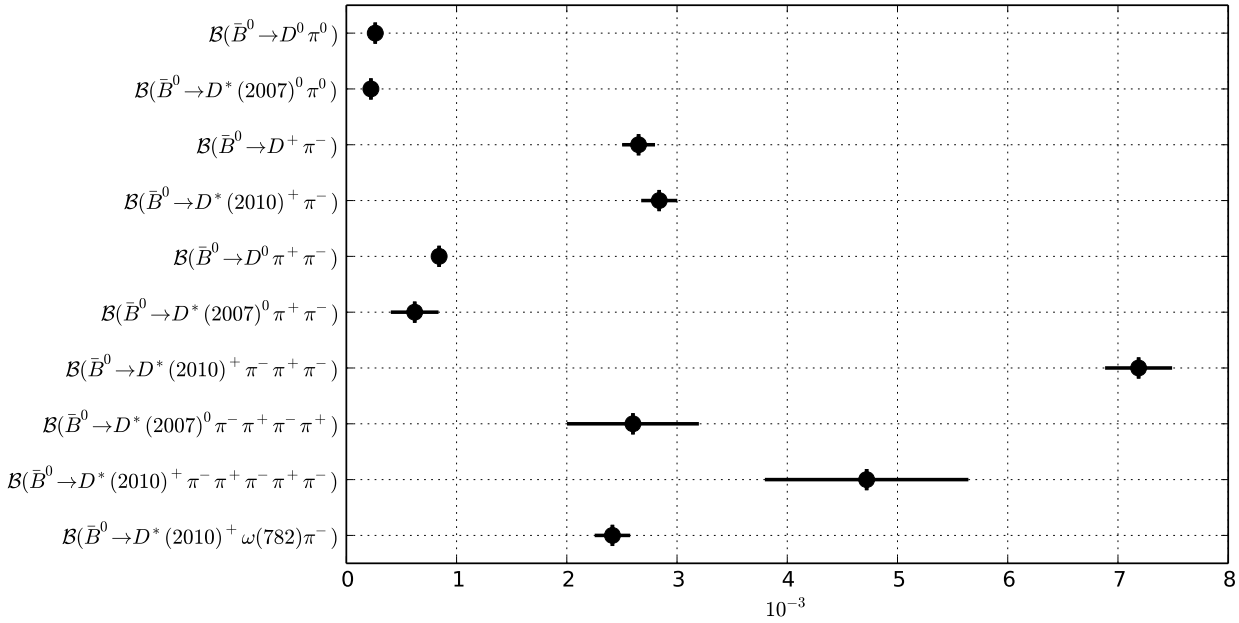

Figure 68: Summary of the averages from Table 93.

Table 94: Decays to a $D^{(*)0}$ meson and a light meson [10^{-4}].

Parameter	**Measurements**	**Average**
$\mathcal{B}(\overline{B}^0 \to D^0\rho(770)^0)$	Belle [578]: $2.9 \pm 1.0 \pm 0.4$	2.9 ± 1.1
$\mathcal{B}(\overline{B}^0 \to D^*(2007)^0\rho(770)^0)$	Belle [578]: < 5.1	< 5.1
$\mathcal{B}(\overline{B}^0 \to D^0\eta)$	Belle [573]: $1.77 \pm 0.16 \pm 0.21$ *BABAR* [574]: $2.53 \pm 0.09 \pm 0.11$	2.36 ± 0.13
$\mathcal{B}(\overline{B}^0 \to D^*(2007)^0\eta)$	Belle [573]: $1.40 \pm 0.28 \pm 0.26$ *BABAR* [574]: $2.69 \pm 0.14 \pm 0.23$	2.26 ± 0.22
$\mathcal{B}(\overline{B}^0 \to D^0\eta'(958))$	Belle [583]: $1.14 \pm 0.20\,^{+0.10}_{-0.13}$ *BABAR* [574]: $1.48 \pm 0.13 \pm 0.07$	1.38 ± 0.12
$\mathcal{B}(\overline{B}^0 \to D^*(2007)^0\eta'(958))$	Belle [583]: $1.21 \pm 0.34 \pm 0.22$ *BABAR* [574]: $1.48 \pm 0.22 \pm 0.13$	1.40 ± 0.22
$\mathcal{B}(\overline{B}^0 \to D^0\omega(782))$	LHCb [577]: $2.81 \pm 0.72\,^{+0.30}_{-0.33}$ Belle [573]: $2.37 \pm 0.23 \pm 0.28$ *BABAR* [574]: $2.57 \pm 0.11 \pm 0.14$	2.54 ± 0.16
$\mathcal{B}(\overline{B}^0 \to D^*(2007)^0\omega(782))$	Belle [573]: $2.29 \pm 0.39 \pm 0.40$ *BABAR* [574]: $4.55 \pm 0.24 \pm 0.39$	3.64 ± 0.35
$\mathcal{B}(\overline{B}^0 \to D^0 f_2(1270))$	LHCb [577]: $1.61 \pm 0.11\,^{+0.19}_{-0.18}$	$1.61\,^{+0.22}_{-0.21}$

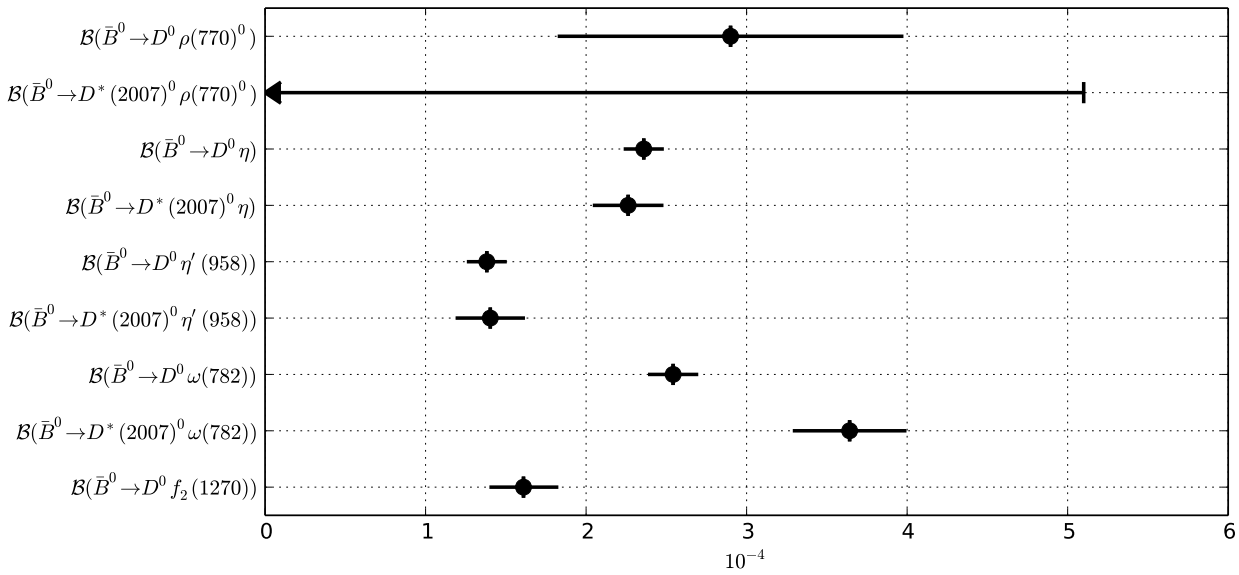

Figure 69: Summary of the averages from Table 94.

Table 95: Decays to a $D^{(*)+}$ meson and one or more kaons [10^{-3}].

Parameter	**Measurements**	**Average**
$\mathcal{B}(\overline{B}^0 \to D^+ K^-)$	LHCb [45]: $0.220 \pm 0.003 \pm 0.013$ Belle [584]: $0.204 \pm 0.045 \pm 0.034$	0.219 ± 0.013
$\mathcal{B}(\overline{B}^0 \to D^*(2010)^+ K^-)$	Belle [584]: $0.204 \pm 0.041 \pm 0.023$	0.204 ± 0.047
$\mathcal{B}(\overline{B}^0 \to D^+ K^*(892)^-)$	*BABAR* [585]: $0.46 \pm 0.06 \pm 0.05$	0.46 ± 0.08
$\mathcal{B}(\overline{B}^0 \to D^*(2010)^+ K^*(892)^-)$	*BABAR* [585]: $0.32 \pm 0.06 \pm 0.03$	0.32 ± 0.07
$\mathcal{B}(\overline{B}^0 \to D^+ K^0 \pi^-)$	*BABAR* [585]: $0.49 \pm 0.07 \pm 0.05$	0.49 ± 0.09
$\mathcal{B}(\overline{B}^0 \to D^*(2010)^+ K^0 \pi^-)$	*BABAR* [585]: $0.30 \pm 0.07 \pm 0.03$	0.30 ± 0.08
$\mathcal{B}(\overline{B}^0 \to D^+ K^- K^0)$	Belle [586]: < 0.31	< 0.31
$\mathcal{B}(\overline{B}^0 \to D^*(2010)^+ K^- K^0)$	Belle [586]: < 0.47	< 0.47
$\mathcal{B}(\overline{B}^0 \to D^+ K^- K^*(892)^0)$	Belle [586]: $0.88 \pm 0.11 \pm 0.15$	0.88 ± 0.19
$\mathcal{B}(\overline{B}^0 \to D^*(2010)^+ K^- K^*(892)^0)$	Belle [586]: $1.29 \pm 0.22 \pm 0.25$	1.29 ± 0.33

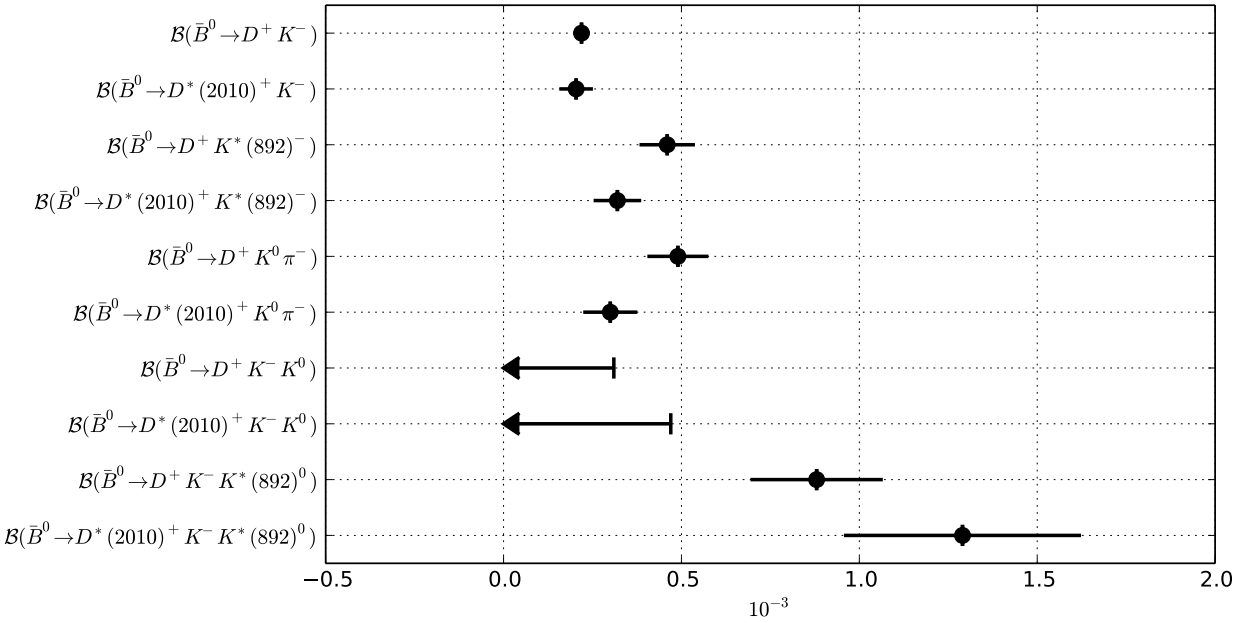

Figure 70: Summary of the averages from Table 95.

Table 96: Decays to a $D^{(*)0}$ meson and a kaon [10^{-4}].

Parameter	**Measurements**	**Average**
$\mathcal{B}(\overline{B}^0 \to D^0\overline{K}^0)$	Belle [587]: $0.50\,^{+0.13}_{-0.12} \pm 0.06$ *BABAR* [588]: $0.53 \pm 0.07 \pm 0.03$	0.52 ± 0.07
$\mathcal{B}(\overline{B}^0 \to D^*(2007)^0\overline{K}^0)$	Belle [587]: < 0.66 *BABAR* [588]: $0.36 \pm 0.12 \pm 0.03$	0.36 ± 0.12
$\mathcal{B}(\overline{B}^0 \to D^0 K^-\pi^+)$	*BABAR* [589]: $0.88 \pm 0.15 \pm 0.09$	0.88 ± 0.17
$\mathcal{B}(\overline{B}^0 \to D^0\overline{K}^*(892)^0)$	Belle [587]: $0.48\,^{+0.11}_{-0.10} \pm 0.05$ *BABAR* [588]: $0.40 \pm 0.07 \pm 0.03$	0.42 ± 0.06
$\mathcal{B}(\overline{B}^0 \to D^0\overline{K}^*(892)^0) \times \mathcal{B}(\overline{K}^*(892)^0 \to K^-\pi^+)$		
	BABAR [589]: $0.38 \pm 0.06 \pm 0.04$	0.38 ± 0.07
$\mathcal{B}(\overline{B}^0 \to D^*(2007)^0\overline{K}^*(892)^0)$	Belle [587]: < 0.69	< 0.69
$\mathcal{B}(\overline{B}^0 \to \overline{D}^*(2007)^0\overline{K}^*(892)^0)$	Belle [587]: < 0.40	< 0.40
$\mathcal{B}(\overline{B}^0 \to \overline{D}^0 K^-\pi^+)$	*BABAR* [589]: < 0.19	< 0.19
$\mathcal{B}(\overline{B}^0 \to \overline{D}^0\overline{K}^*(892)^0)$	Belle [587]: < 0.18 *BABAR* [588]: $0.00 \pm 0.05 \pm 0.03$	0.00 ± 0.06

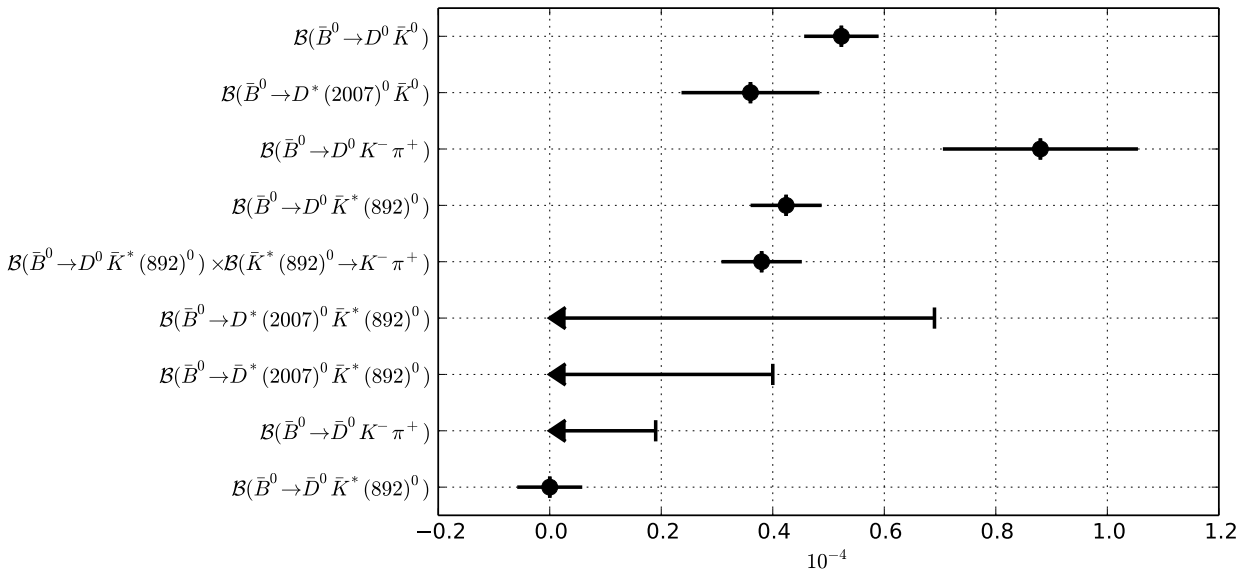

Figure 71: Summary of the averages from Table 96.

Table 97: Decays to a $D_s^{(*)}$ meson [10^{-4}].

Parameter	**Measurements**	**Average**
$\mathcal{B}(\overline{B}^0 \to D_s^- \pi^+)$	Belle [590]: $0.199 \pm 0.026 \pm 0.018$ *BABAR* [591]: $0.25 \pm 0.04 \pm 0.02$	0.216 ± 0.026
$\mathcal{B}(\overline{B}^0 \to D_s^{*-} \pi^+)$	Belle [592]: $0.175 \pm 0.034 \pm 0.020$ *BABAR* [591]: $0.26 \,^{+0.05}_{-0.04} \pm 0.02$	0.207 ± 0.032
$\mathcal{B}(\overline{B}^0 \to D_s^- \rho(770)^+)$	*BABAR* [591]: $0.11 \,^{+0.09}_{-0.08} \pm 0.03$	$0.11 \,^{+0.09}_{-0.09}$
$\mathcal{B}(\overline{B}^0 \to D_s^{*-} \rho(770)^+)$	*BABAR* [591]: $0.41 \,^{+0.13}_{-0.12} \pm 0.04$	$0.41 \,^{+0.14}_{-0.13}$
$\mathcal{B}(\overline{B}^0 \to D_s^- a_0(980)^+)$	*BABAR* [593]: $0.06 \,^{+0.14}_{-0.11} \pm 0.01$	$0.06 \,^{+0.14}_{-0.11}$
$\mathcal{B}(\overline{B}^0 \to D_s^{*-} a_0(980)^+)$	*BABAR* [593]: $0.14 \,^{+0.21}_{-0.16} \pm 0.03$	$0.14 \,^{+0.21}_{-0.16}$
$\mathcal{B}(\overline{B}^0 \to D_s^- a_2(1320)^+)$	*BABAR* [593]: $0.64 \,^{+1.04}_{-0.57} \pm 0.15$	$0.64 \,^{+1.05}_{-0.59}$
$\mathcal{B}(\overline{B}^0 \to D_s^{*-} a_2(1320)^+)$	*BABAR* [593]: < 2.0	< 2.0
$\mathcal{B}(\overline{B}^0 \to D_s^+ K^-)$	Belle [590]: $0.191 \pm 0.024 \pm 0.017$ *BABAR* [591]: $0.29 \pm 0.04 \pm 0.02$	0.221 ± 0.025
$\mathcal{B}(\overline{B}^0 \to D_s^{*+} K^-)$	Belle [592]: $0.202 \pm 0.033 \pm 0.022$ *BABAR* [591]: $0.24 \pm 0.04 \pm 0.02$	0.219 ± 0.031
$\mathcal{B}(\overline{B}^0 \to D_s^+ K^*(892)^-)$	*BABAR* [591]: $0.35 \,^{+0.10}_{-0.09} \pm 0.04$	$0.35 \,^{+0.11}_{-0.10}$
$\mathcal{B}(\overline{B}^0 \to D_s^{*+} K^*(892)^-)$	*BABAR* [591]: $0.32 \,^{+0.14}_{-0.12} \pm 0.04$	$0.32 \,^{+0.15}_{-0.13}$
$\mathcal{B}(\overline{B}^0 \to D_s^+ K_S^0 \pi^-)$	*BABAR* [594]: $0.55 \pm 0.13 \pm 0.10$	0.55 ± 0.17
$\mathcal{B}(\overline{B}^0 \to D_s^{*+} K^0 \pi^-)$	*BABAR* [594]: < 0.55	< 0.55

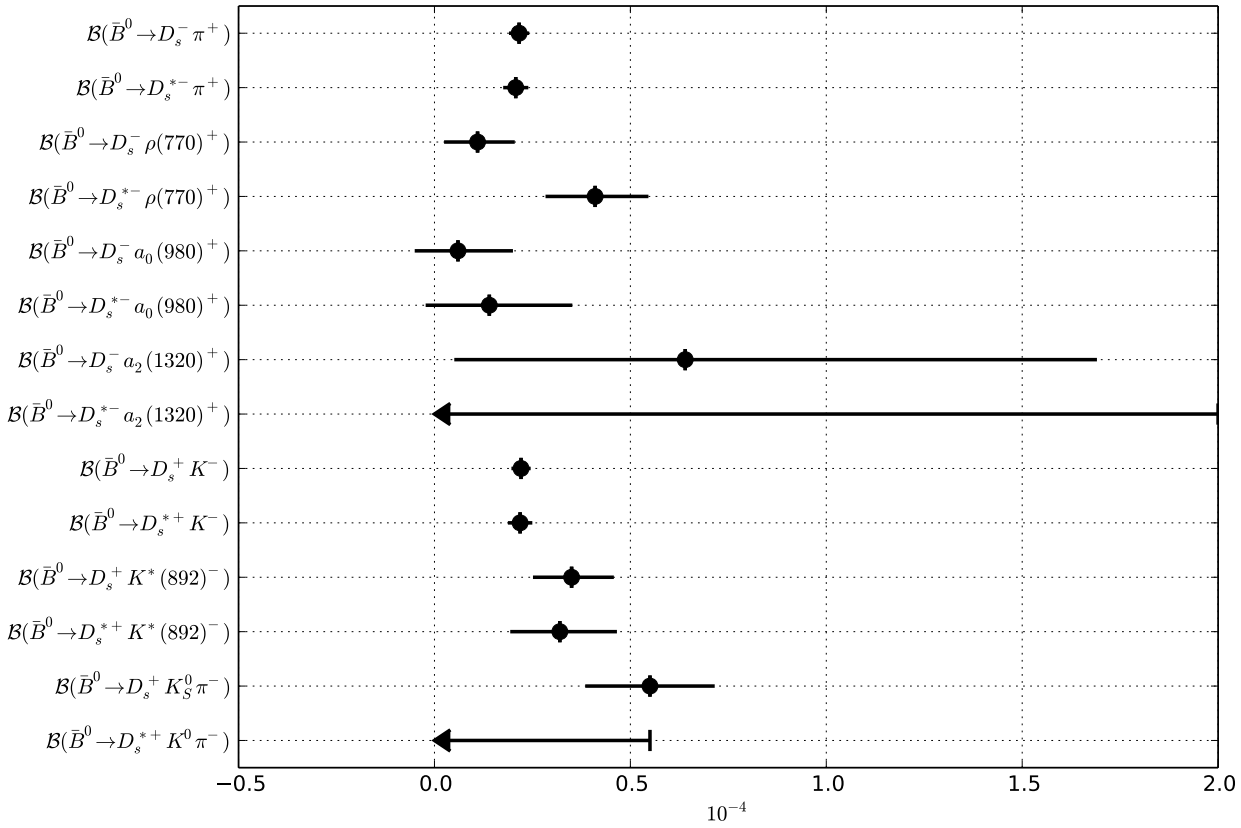

Figure 72: Summary of the averages from Table 97.

Table 98: Relative decay rates.

Parameter	Measurements	Average
$\mathcal{B}(\overline{B}^0 \to D^0\rho(770)^0)/\mathcal{B}(\overline{B}^0 \to D^0\omega(782))$		
	Belle [578]: 1.6 ± 0.8	1.6 ± 0.8
$\mathcal{B}(\overline{B}^0 \to \overline{D}^0 K^-\pi^+)/\mathcal{B}(\overline{B}^0 \to \overline{D}^0\pi^-\pi^+)$		
	LHCb [595]: $0.106 \pm 0.007 \pm 0.008$	0.106 ± 0.011
$\mathcal{B}(\overline{B}^0 \to \overline{D}^0 K^- K^+)/\mathcal{B}(\overline{B}^0 \to \overline{D}^0\pi^-\pi^+)$		
	LHCb [596]: $0.056 \pm 0.110 \pm 0.007$	0.056 ± 0.110
$\mathcal{B}(\overline{B}^0 \to D^+\pi^+\pi^-\pi^-)/\mathcal{B}(\overline{B}^0 \to D^+\pi^-)$		
	LHCb [597]: $2.38 \pm 0.11 \pm 0.21$	2.38 ± 0.24
$\mathcal{B}(\overline{B}^0 \to D^+K^-)/\mathcal{B}(\overline{B}^0 \to D^+\pi^-)$		
	LHCb [45]: $0.0822 \pm 0.0011 \pm 0.0025$	0.0818 ± 0.0027
	Belle [584]: $0.068 \pm 0.015 \pm 0.007$	
$\mathcal{B}(\overline{B}^0 \to D^+K^-\pi^+\pi^-)/\mathcal{B}(\overline{B}^0 \to D^+\pi^+\pi^-\pi^-)$		
	LHCb [598]: $0.059 \pm 0.011 \pm 0.005$	0.059 ± 0.012
$\mathcal{B}(\overline{B}^0 \to D^*(2010)^+\pi^-)/\mathcal{B}(\overline{B}^0 \to D^+\pi^-)$		
	BABAR [576]: $0.99 \pm 0.11 \pm 0.08$	0.99 ± 0.14
$\mathcal{B}(\overline{B}^0 \to D^*(2010)^+K^-)/\mathcal{B}(\overline{B}^0 \to D^*(2010)^+\pi^-)$		
	Belle [584]: $0.074 \pm 0.015 \pm 0.006$	0.0773 ± 0.0043
	BABAR [589]: $0.0776 \pm 0.0034 \pm 0.0029$	
$\mathcal{B}(\overline{B}^0 \to D^{**+}\pi^-)/\mathcal{B}(\overline{B}^0 \to D^+\pi^-)$		
	BABAR [576]: $0.77 \pm 0.22 \pm 0.29$	0.77 ± 0.36
$\mathcal{B}(\overline{B}^0 \to D_s^+K^-\pi^+\pi^-)/\mathcal{B}(\overline{B}_s^0 \to D_s^+K^-\pi^+\pi^-)$		
	LHCb [599]: $0.54 \pm 0.07 \pm 0.07$	0.54 ± 0.10
$\mathcal{B}(\overline{B}^0 \to D_s^+K^-)/\mathcal{B}(\overline{B}^0 \to D_s^+\pi^-)$		
	LHCb [600]: $0.0129 \pm 0.0005 \pm 0.0008$	0.0129 ± 0.0009

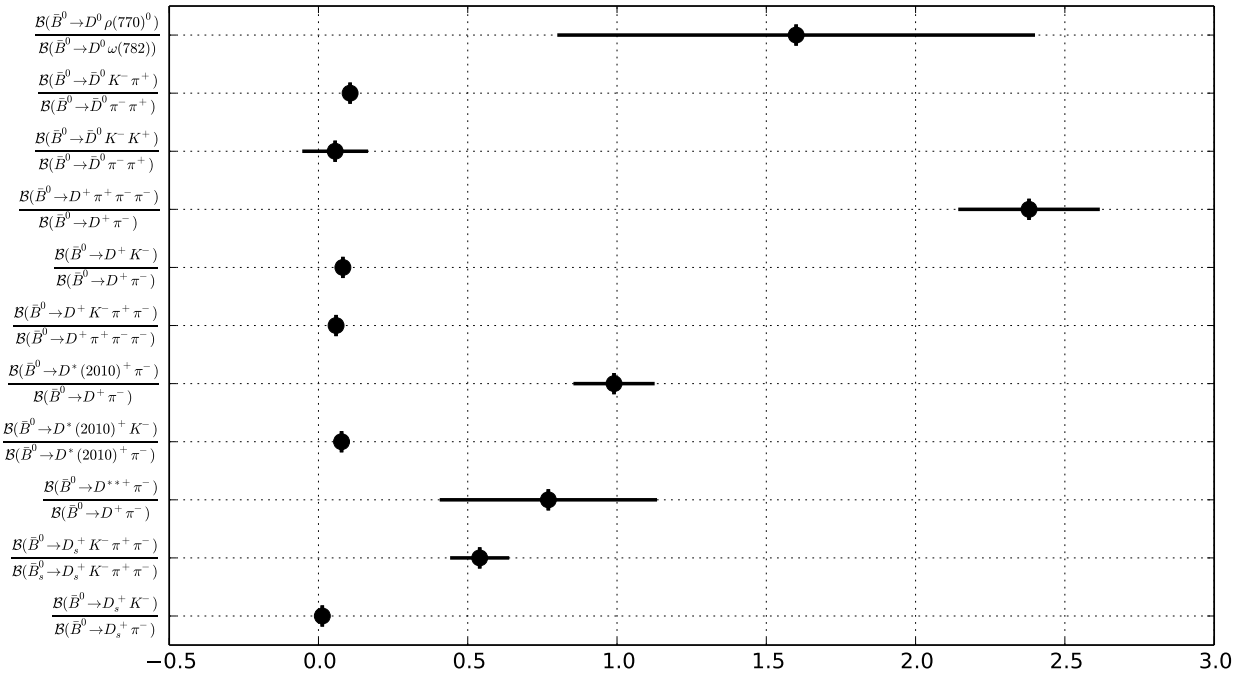

Figure 73: Summary of the averages from Table 98.

Table 99: Absolute product decay rates to excited D mesons [10^{-3}].

Parameter	**Measurements**	**Average**
$\mathcal{B}(\overline{B}^0 \to D_1(2420)^+\pi^-) \times \mathcal{B}(D_1(2420)^+ \to D^+\pi^-\pi^+)$		
	Belle [601]: $0.089 \pm 0.015\,^{+0.017}_{-0.031}$	$0.089\,^{+0.023}_{-0.034}$
$\mathcal{B}(\overline{B}^0 \to D_1(2420)^+\pi^-) \times \mathcal{B}(D_1(2420)^+ \to D^*(2010)^+\pi^-\pi^+)$		
	Belle [601]: < 0.033	< 0.033
$\mathcal{B}(\overline{B}^0 \to D_2^*(2460)^+\pi^-) \times \mathcal{B}(D_2^*(2460)^+ \to D^*(2010)^+\pi^-\pi^+)$		
	Belle [601]: < 0.024	< 0.024
$\mathcal{B}(\overline{B}^0 \to D_2^*(2460)^+K^-) \times \mathcal{B}(D_2^*(2460)^+ \to D^0\pi^+)$		
	BABAR [589]: $0.0183 \pm 0.0040 \pm 0.0031$	0.0183 ± 0.0051
$\mathcal{B}(\overline{B}^0 \to D_1^0(H)\omega(782)) \times \mathcal{B}(D_1^0(H) \to D^*(2010)^+\pi^-)$		
	BABAR [582]: $0.41 \pm 0.12 \pm 0.11$	0.41 ± 0.16
$\mathcal{B}(\overline{B}^0 \to D_{sJ}(2460)^-\pi^+) \times \mathcal{B}(D_{sJ}(2460)^- \to D_s^-\gamma)$		
	Belle [602]: < 0.0040	< 0.0040
$\mathcal{B}(\overline{B}^0 \to D_{sJ}^+(2460)K^-) \times \mathcal{B}(D_{sJ}^+(2460) \to D_s^+\gamma)$		
	Belle [603]: $0.0053 \pm 0.0020\,^{+0.0016}_{-0.0015}$	$0.0053\,^{+0.0026}_{-0.0025}$
$\mathcal{B}(\overline{B}^0 \to D_{sJ}^*(2317)^-\pi^+) \times \mathcal{B}(D_{sJ}^*(2317)^- \to D_s^-\pi^0)$		
	Belle [602]: < 0.025	< 0.025
$\mathcal{B}(\overline{B}^0 \to D_{sJ}^*(2317)^+K^-) \times \mathcal{B}(D_{sJ}^*(2317)^+ \to D_s^+\pi^0)$		
	Belle [603]: $0.044 \pm 0.008 \pm 0.013$	0.044 ± 0.015

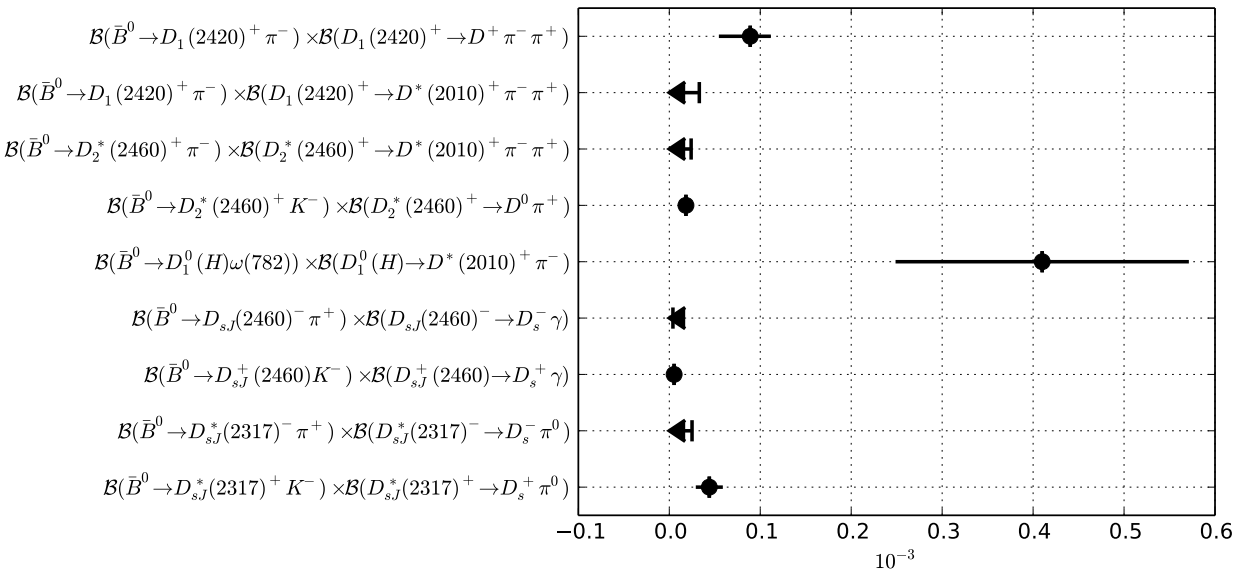

Figure 74: Summary of the averages from Table 99.

Table 100: Absolute and relative decay rates to excited D mesons [10^{-2}].

Parameter	Measurements	Average
$\mathcal{B}(\overline{B}^0 \to D^{**+}\pi^-)$	*BABAR* [576]: $0.234 \pm 0.065 \pm 0.088$	0.234 ± 0.109
$\mathcal{B}(\overline{B}^0 \to D_1^+\pi^-) \times \mathcal{B}(D_1^+ \to D^+\pi^+\pi^-)/\mathcal{B}(\overline{B}^0 \to D^+\pi^+\pi^-\pi^-)$		
	LHCb [597]: $2.1 \pm 0.5\,^{+0.3}_{-0.5}$	$2.1\,^{+0.6}_{-0.7}$

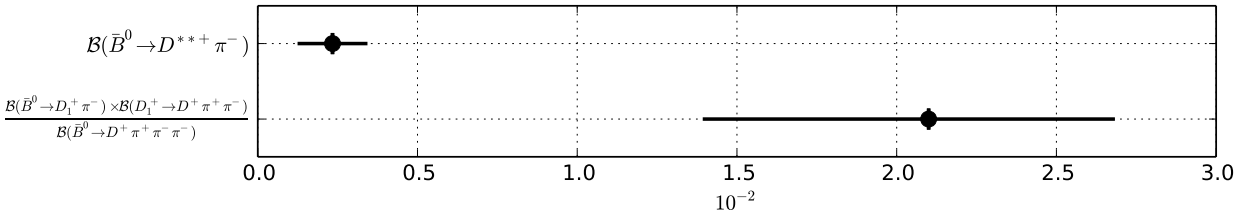

Figure 75: Summary of the averages from Table 100.

Table 101: Baryonic decays [10^{-4}].

Parameter	Measurements	Average
$\mathcal{B}(\overline{B}^0 \to D^0 p\overline{p})$	Belle [604]: $1.18 \pm 0.15 \pm 0.16$ *BABAR* [605]: $1.02 \pm 0.04 \pm 0.06$	1.04 ± 0.07
$\mathcal{B}(\overline{B}^0 \to D^*(2007)^0 p\overline{p})$	Belle [604]: $1.20\,^{+0.33}_{-0.29} \pm 0.21$ *BABAR* [605]: $0.97 \pm 0.07 \pm 0.09$	0.99 ± 0.11
$\mathcal{B}(\overline{B}^0 \to D^+ p\overline{p}\pi^-)$	*BABAR* [605]: $3.32 \pm 0.10 \pm 0.29$	3.32 ± 0.31
$\mathcal{B}(\overline{B}^0 \to D^*(2010)^+ p\overline{p}\pi^-)$	*BABAR* [605]: $4.55 \pm 0.16 \pm 0.39$	4.55 ± 0.42
$\mathcal{B}(\overline{B}^0 \to D^0 p\overline{p}\pi^-\pi^+)$	*BABAR* [605]: $2.99 \pm 0.21 \pm 0.45$	2.99 ± 0.50
$\mathcal{B}(\overline{B}^0 \to D^*(2007)^0 p\overline{p}\pi^-\pi^+)$	*BABAR* [605]: $1.91 \pm 0.36 \pm 0.29$	1.91 ± 0.46
$\mathcal{B}(\overline{B}^0 \to D_s^+ \Lambda\overline{p})$	Belle [606]: $0.29 \pm 0.07 \pm 0.06$	0.29 ± 0.09
$\mathcal{B}(\overline{B}^0 \to D^0 \Lambda^0 \overline{\Lambda}^0)$	Belle [607]: $0.105\,^{+0.057}_{-0.044} \pm 0.014$ *BABAR* [608]: $0.098\,^{+0.029}_{-0.026} \pm 0.019$	0.100 ± 0.028
$\mathcal{B}(\overline{B}^0 \to D^0 \Sigma^0 \overline{\Lambda} + \overline{B}^0 \to D^0 \Lambda \overline{\Sigma}^0)$		
	BABAR [608]: $0.15\,^{+0.09}_{-0.08} \pm 0.03$	$0.15\,^{+0.09}_{-0.09}$
$\mathcal{B}(\overline{B}^0 \to D^+ \Lambda\overline{p})$	Belle [609]: $0.336 \pm 0.063 \pm 0.044$	0.336 ± 0.077
$\mathcal{B}(\overline{B}^0 \to D^{*+} \Lambda\overline{p})$	Belle [609]: $0.251 \pm 0.026 \pm 0.035$	0.251 ± 0.044

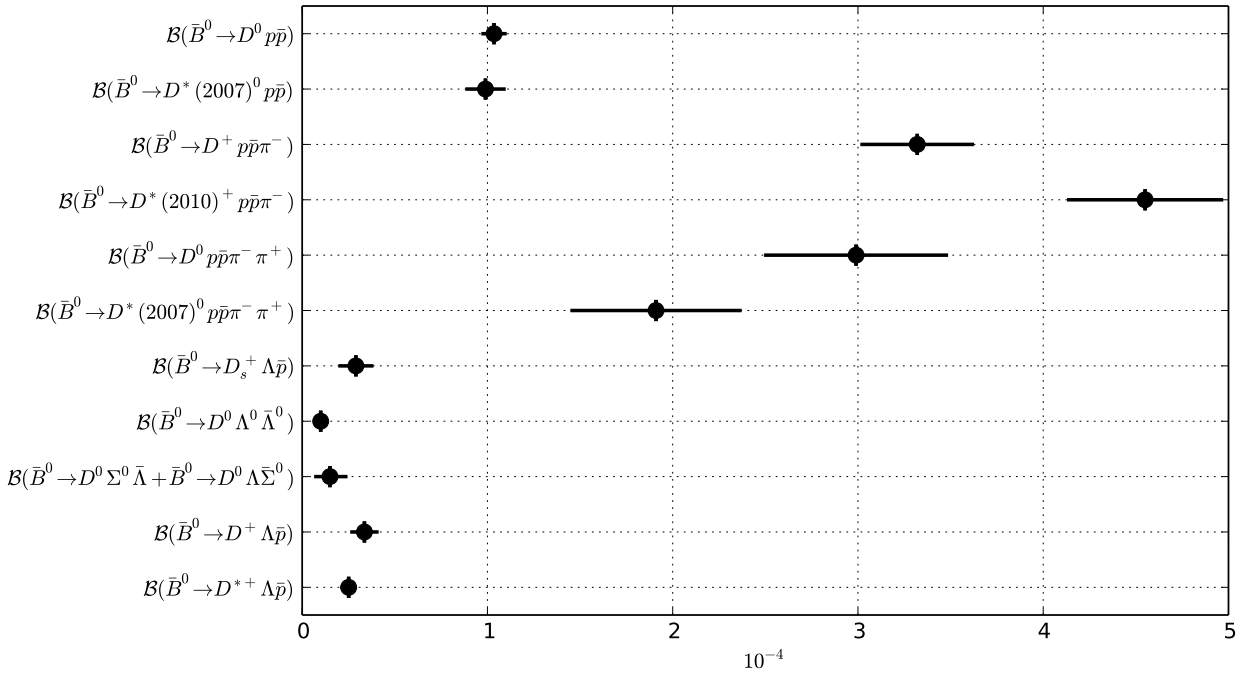

Figure 76: Summary of the averages from Table 101.

6.1.2 Decays to two open charm mesons

Averages of $\overline{B}^0$ decays to two open charm mesons are shown in Tables 102–108 and Figs. 77–83.

Table 102: Decays to $D^{(*)+}D^{(*)-}$ $[10^{-3}]$.

Parameter	**Measurements**	**Average**
$\mathcal{B}(\overline{B}^0 \to D^+D^-)$	Belle [275]: $0.212 \pm 0.016 \pm 0.018$ *BABAR* [610]: $0.28 \pm 0.04 \pm 0.05$	0.220 ± 0.023
$\mathcal{B}(\overline{B}^0 \to D_s^-D^+)$	Belle [275]: $0.614 \pm 0.029 \pm 0.050$ *BABAR* [610]: $0.57 \pm 0.07 \pm 0.07$	0.603 ± 0.050
$\mathcal{B}(\overline{B}^0 \to D^{*-}D^*(2010)^+)$	Belle [344]: $0.782 \pm 0.038 \pm 0.060$ *BABAR* [610]: $0.81 \pm 0.06 \pm 0.10$	0.790 ± 0.061
$\mathcal{B}(\overline{B}^0 \to D^0\overline{D}^0)$	Belle [611]: < 0.043 *BABAR* [610]: < 0.06	< 0.043
$\mathcal{B}(\overline{B}^0 \to D^0\overline{D}^*(2007)^0)$	*BABAR* [610]: < 0.29	< 0.29
$\mathcal{B}(\overline{B}^0 \to D^*(2007)^0\overline{D}^*(2007)^0)$	*BABAR* [610]: < 0.09	< 0.09

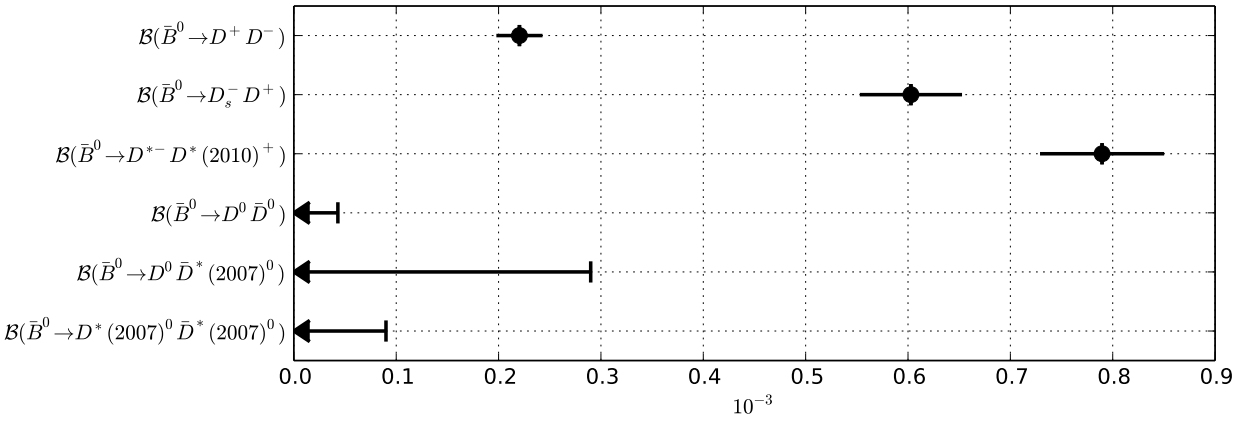

Figure 77: Summary of the averages from Table 102.

Table 103: Decays to two D mesons and a kaon [10^{-3}].

Parameter	**Measurements**	**Average**
$\mathcal{B}(\overline{B}^0 \to D^+ D^- \overline{K}^0)$	*BABAR* [612]: $0.75 \pm 0.12 \pm 0.12$	0.75 ± 0.17
$\mathcal{B}(\overline{B}^0 \to D^*(2010)^+ D^- \overline{K}^0)$	*BABAR* [612]: $6.41 \pm 0.36 \pm 0.39$	6.41 ± 0.53
$\mathcal{B}(\overline{B}^0 \to D^*(2010)^- D^*(2010)^+ \overline{K}^0)$	*BABAR* [612]: $8.26 \pm 0.43 \pm 0.67$	8.26 ± 0.80
$\mathcal{B}(\overline{B}^0 \to D^*(2010)^+ D^*(2010)^- K_S^0)$	Belle [254]: $3.4 \pm 0.4 \pm 0.7$ *BABAR* [253]: $4.4 \pm 0.4 \pm 0.7$	3.9 ± 0.6
$\mathcal{B}(\overline{B}^0 \to D^+ \overline{D}^0 K^-)$	*BABAR* [612]: $1.07 \pm 0.07 \pm 0.09$	1.07 ± 0.11
$\mathcal{B}(\overline{B}^0 \to D^*(2010)^+ \overline{D}^0 K^-)$	*BABAR* [612]: $2.47 \pm 0.10 \pm 0.18$	2.47 ± 0.21
$\mathcal{B}(\overline{B}^0 \to D^+ \overline{D}^*(2007)^0 K^-)$	*BABAR* [612]: $3.46 \pm 0.18 \pm 0.37$	3.46 ± 0.41
$\mathcal{B}(\overline{B}^0 \to D^*(2010)^+ \overline{D}^*(2007)^0 K^-)$	*BABAR* [612]: $10.6 \pm 0.3 \pm 0.9$	10.6 ± 0.9
$\mathcal{B}(\overline{B}^0 \to D^0 \overline{D}^0 \overline{K}^0)$	*BABAR* [612]: $0.27 \pm 0.10 \pm 0.05$	0.27 ± 0.11
$\mathcal{B}(\overline{B}^0 \to D^0 \overline{D}^*(2007)^0 \overline{K}^0)$	*BABAR* [612]: $1.08 \pm 0.32 \pm 0.36$	1.08 ± 0.48
$\mathcal{B}(\overline{B}^0 \to D^*(2007)^0 \overline{D}^*(2007)^0 \overline{K}^0)$	*BABAR* [612]: $2.40 \pm 0.55 \pm 0.67$	2.40 ± 0.87
$\mathcal{B}(\overline{B}^0 \to D^0 \overline{D}^0 \pi^0 \overline{K}^0)$	Belle [613]: $0.173 \pm 0.070\,^{+0.031}_{-0.053}$	$0.173\,^{+0.077}_{-0.088}$

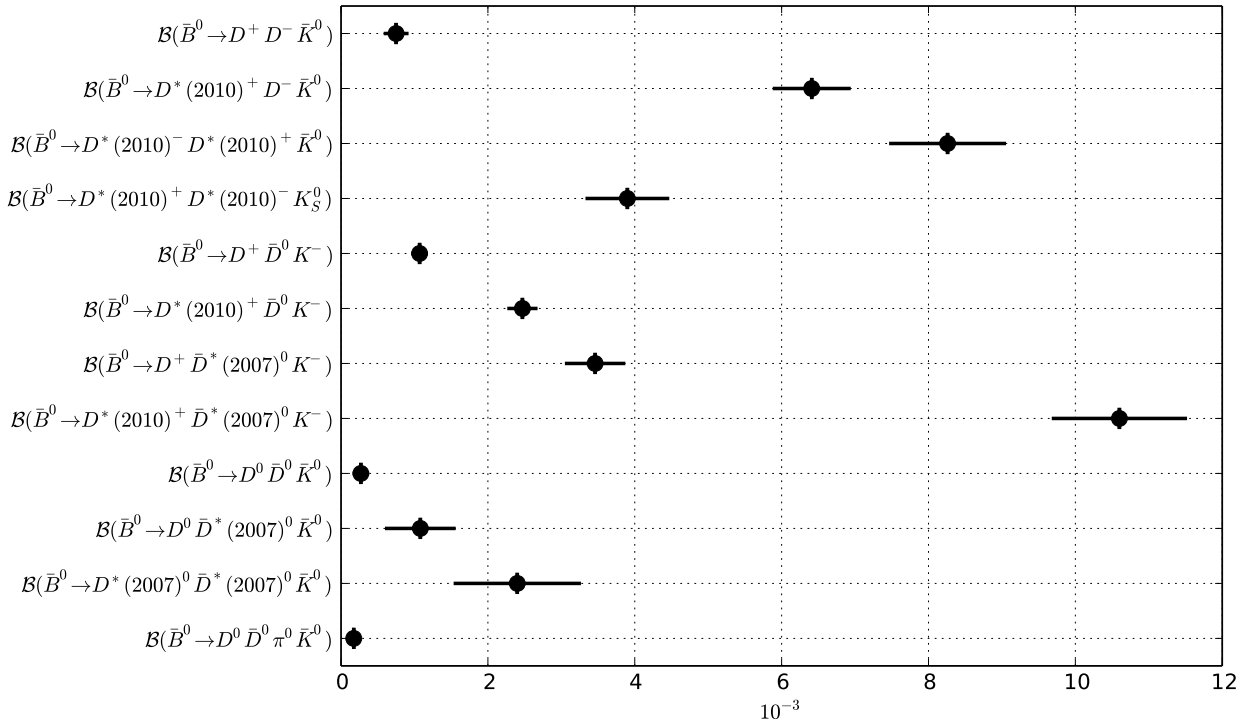

Figure 78: Summary of the averages from Table 103.

Table 104: Decays to $D_s^{(*)-}D^{(*)+}$ [10^{-3}].

Parameter	Measurements	Average
$\mathcal{B}(\overline{B}^0 \to D_s^- D^+)$	Belle [614]: $7.5 \pm 0.2 \pm 1.1$ *BABAR* [615]: $9.0 \pm 1.8 \pm 1.4$	7.8 ± 1.0
$\mathcal{B}(\overline{B}^0 \to D_s^- D^*(2010)^+)$	*BABAR* [615]: $5.7 \pm 1.6 \pm 0.9$ *BABAR* [616]: $10.3 \pm 1.4 \pm 2.9$	6.8 ± 1.6
$\mathcal{B}(\overline{B}^0 \to D_s^{*-} D^*(2010)^+)$	*BABAR* [615]: $16.5 \pm 2.3 \pm 1.9$ *BABAR* [617]: $18.8 \pm 0.9 \pm 1.7$ *BABAR* [616]: $19.7 \pm 1.5 \pm 5.7$	18.1 ± 1.6
$\mathcal{B}(\overline{B}^0 \to D_s^{*-} D^+)$	*BABAR* [615]: $6.7 \pm 2.0 \pm 1.1$	6.7 ± 2.3
$\mathcal{B}(\overline{B}^0 \to D_s^- D^+) \times \mathcal{B}(D_s^- \to \phi(1020)\pi^-) \times \mathcal{B}(\phi(1020) \to K^+K^-)$ Belle [618]: $0.147 \pm 0.005 \pm 0.021$		0.147 ± 0.022
$\mathcal{B}(\overline{B}^0 \to D_s^- D^+) \times \mathcal{B}(D_s^- \to \phi(1020)\pi^-)$ *BABAR* [615]: $0.267 \pm 0.061 \pm 0.047$		0.267 ± 0.077
$\mathcal{B}(\overline{B}^0 \to D_s^- D^*(2010)^+) \times \mathcal{B}(D_s^- \to \phi(1020)\pi^-)$ *BABAR* [615]: $0.511 \pm 0.094 \pm 0.072$		0.511 ± 0.118
$\mathcal{B}(\overline{B}^0 \to D_s^{*-} D^+) \times \mathcal{B}(D_s^- \to \phi(1020)\pi^-)$ *BABAR* [615]: $0.414 \pm 0.119 \pm 0.094$		0.414 ± 0.152
$\mathcal{B}(\overline{B}^0 \to D_s^{*-} D^*(2010)^+) \times \mathcal{B}(D_s^- \to \phi(1020)\pi^-)$ *BABAR* [615]: $1.22 \pm 0.22 \pm 0.22$		1.22 ± 0.31

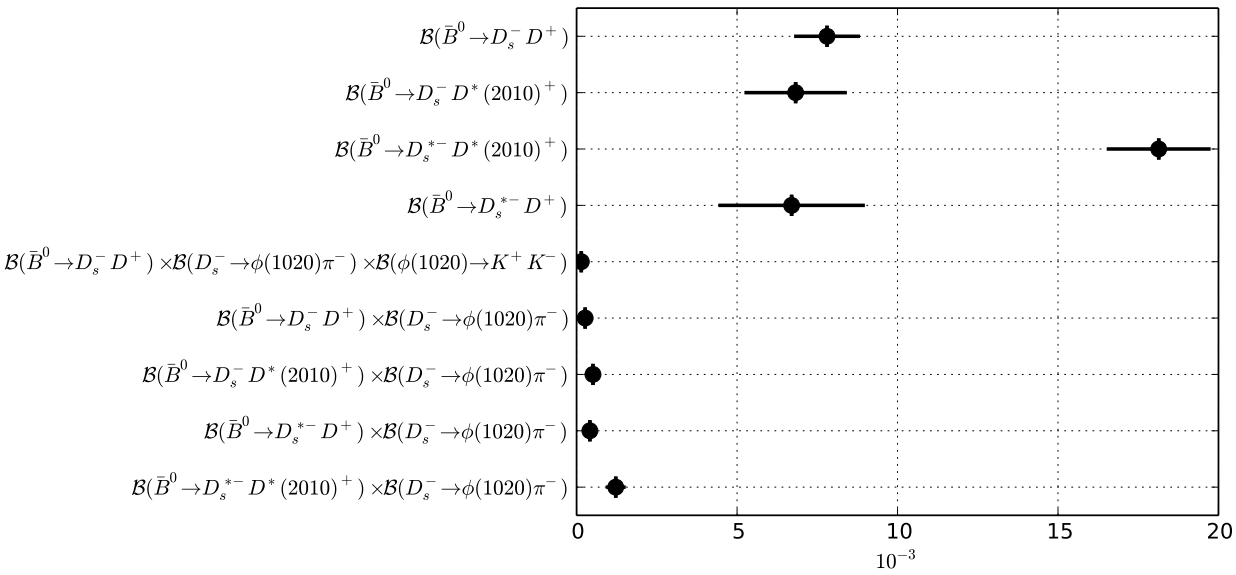

Figure 79: Summary of the averages from Table 104.

Table 105: Decays to $D_s^{(*)+} D_s^{(*)-}$ [10^{-3}].

Parameter	Measurements	Average
$\mathcal{B}(\overline{B}^0 \to D_s^- D_s^+)$	Belle [614]: < 0.036 *BABAR* [619]: < 0.10	< 0.036
$\mathcal{B}(\overline{B}^0 \to D_s^- D_s^{*+})$	*BABAR* [619]: < 0.13	< 0.13
$\mathcal{B}(\overline{B}^0 \to D_s^{*+} D_s^{*-})$	*BABAR* [619]: < 0.24	< 0.24

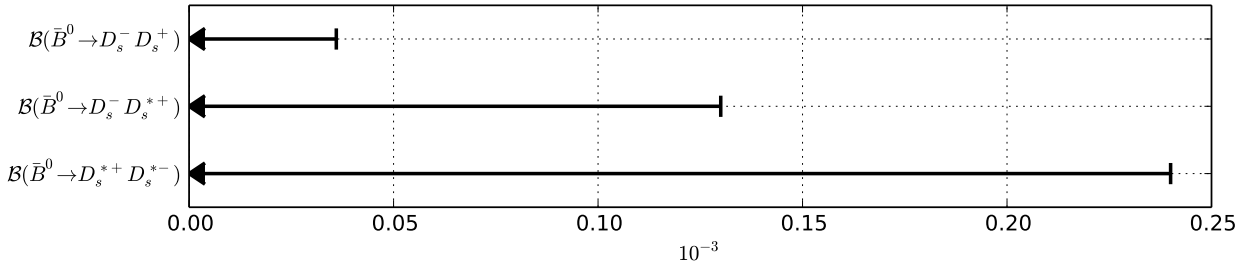

Figure 80: Summary of the averages from Table 105.

Table 106: Relative decay rates.

Parameter	Measurements	Average
$\mathcal{B}(\overline{B}^0 \to D^0 \overline{D}^0)/\mathcal{B}(\overline{B}^- \to D^0 \overline{D}_s^-)$		
	LHCb [620]: $0.0014 \pm 0.0006 \pm 0.0002$	0.0014 ± 0.0006
$\mathcal{B}(\overline{B}^0 \to D_s^- D^+)/\mathcal{B}(\overline{B}^0 \to D^+ \pi^+ \pi^- \pi^-)$		
	CDF [621]: $1.99 \pm 0.13 \pm 0.46$	1.99 ± 0.48
$\mathcal{B}(\overline{B}^0 \to D_s^- D^*(2010)^+)/\mathcal{B}(\overline{B}^0 \to D_s^- D^+)$		
	CDF [621]: $1.5 \pm 0.4 \pm 0.1$	1.5 ± 0.4
$\mathcal{B}(\overline{B}^0 \to D_s^{*-} D^+)/\mathcal{B}(\overline{B}^0 \to D_s^- D^+)$		
	CDF [621]: $0.9 \pm 0.2 \pm 0.1$	0.9 ± 0.2
$\mathcal{B}(\overline{B}^0 \to D_s^{*-} D^*(2010)^+)/\mathcal{B}(\overline{B}^0 \to D_s^- D^+)$		
	CDF [621]: $2.6 \pm 0.5 \pm 0.2$	2.6 ± 0.5

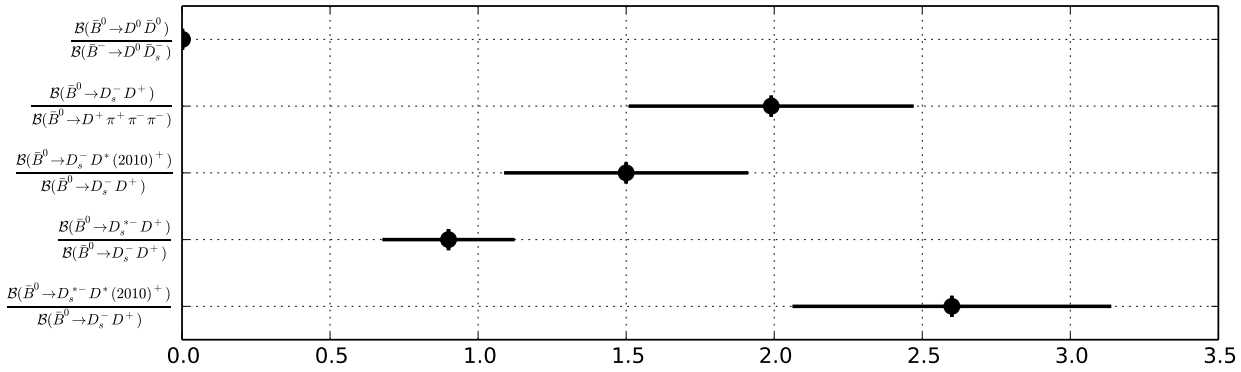

Figure 81: Summary of the averages from Table 106.

Table 107: Absolute decays rates to excited D_s mesons $[10^{-3}]$.

Parameter	**Measurements**	**Average**
$\mathcal{B}(\overline{B}^0 \to D_{sJ}(2460)^- D^+)$	*BABAR* [615]: $2.6 \pm 1.5 \pm 0.7$	2.6 ± 1.7
$\mathcal{B}(\overline{B}^0 \to D_{sJ}(2460)^- D^*(2010)^+)$	*BABAR* [615]: $8.8 \pm 2.0 \pm 1.4$	8.8 ± 2.4
$\mathcal{B}(\overline{B}^0 \to D_{s1}(2536)^- D^*(2010)^+)$	*BABAR* [253]: $92 \pm 24 \pm 1$	92 ± 24

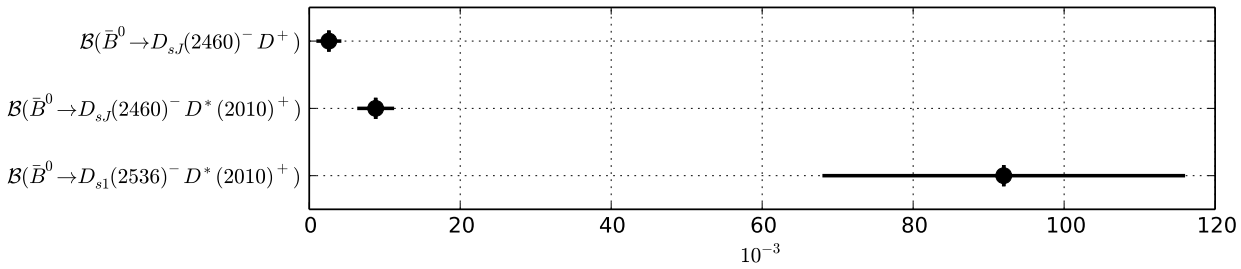

Figure 82: Summary of the averages from Table 107.

Table 108: Product decays rates to excited D_s mesons [10^{-3}].

Parameter	Measurements	Average
$\mathcal{B}(\overline{B}^0 \to D_{s1}(2536)^- D^+) \times \mathcal{B}(D_{s1}(2536)^- \to D^*(2010)^- \overline{K}^0)$		
	BABAR [622]: $0.261 \pm 0.103 \pm 0.031$	0.261 ± 0.108
$\mathcal{B}(\overline{B}^0 \to D_{s1}(2536)^- D^+) \times \mathcal{B}(D_{s1}(2536)^- \to K^- \overline{D}^*(2007)^0)$		
	BABAR [622]: $0.171 \pm 0.048 \pm 0.032$	0.171 ± 0.058
$\mathcal{B}(\overline{B}^0 \to D_{s1}(2536)^- D^*(2010)^+) \times \mathcal{B}(D_{s1}(2536)^- \to D^*(2010)^- \overline{K}^0)$		
	BABAR [622]: $0.500 \pm 0.151 \pm 0.067$	0.500 ± 0.165
$\mathcal{B}(\overline{B}^0 \to D_{s1}(2536)^- D^*(2010)^+) \times \mathcal{B}(D_{s1}(2536)^- \to \overline{D}^*(2007)^0 K^+)$		
	BABAR [622]: $0.332 \pm 0.088 \pm 0.066$	0.332 ± 0.110
$\mathcal{B}(\overline{B}^0 \to D_{s1}(2536)^+ D^-) \times \mathcal{B}(D_{s1}(2536)^+ \to D^*(2007)^0 K^+ + D^*(2010)^+ K^0)$		
	Belle [623]: $0.275 \pm 0.062 \pm 0.036$	0.275 ± 0.072
$\mathcal{B}(\overline{B}^0 \to D_{s1}(2536)^+ D^*(2010)^-) \times \mathcal{B}(D_{s1}(2536)^+ \to D^*(2007)^0 K^+ + D^*(2010)^+ K^0)$		
	Belle [623]: $0.501 \pm 0.121 \pm 0.070$	0.501 ± 0.140
$\mathcal{B}(\overline{B}^0 \to D_{s1}(2536)^+ D^*(2010)^-) \times \mathcal{B}(D_{s1}(2536)^+ \to D^*(2010)^+ K^0_S)$		
	Belle [254]: < 0.60	< 0.60
$\mathcal{B}(\overline{B}^0 \to D^+ D_{sJ}(2460)^-) \times \mathcal{B}(D_{sJ}(2460)^- \to D_s^- \pi^+ \pi^-)$		
	Belle [624]: < 0.20	< 0.20
$\mathcal{B}(\overline{B}^0 \to D^+ D_{sJ}(2460)^-) \times \mathcal{B}(D_{sJ}(2460)^- \to D_s^- \pi^0)$		
	Belle [624]: < 0.36	< 0.36
$\mathcal{B}(\overline{B}^0 \to D^+ D_{sJ}(2460)^-) \times \mathcal{B}(D_{sJ}(2460)^- \to D_s^- \gamma)$		
	Belle [624]: $0.82 \,^{+0.22}_{-0.19} \pm 0.25$	0.81 ± 0.23
	BABAR [625]: $0.8 \pm 0.2 \,^{+0.3}_{-0.2}$	
$\mathcal{B}(\overline{B}^0 \to D^+ D_{sJ}(2460)^-) \times \mathcal{B}(D_{sJ}(2460)^- \to D_s^{*-} \pi^0)$		
	Belle [624]: $2.27 \,^{+0.73}_{-0.62} \pm 0.68$	2.47 ± 0.76
	BABAR [625]: $2.8 \pm 0.8 \,^{+1.1}_{-0.8}$	
$\mathcal{B}(\overline{B}^0 \to D^+ D_{sJ}(2460)^-) \times \mathcal{B}(D_{sJ}(2460)^- \to D_s^{*-} \gamma)$		
	Belle [624]: < 0.60	< 0.60
$\mathcal{B}(\overline{B}^0 \to D_{sJ}(2460)^- D^*(2010)^+) \times \mathcal{B}(D_{sJ}(2460)^- \to D_s^{*-} \pi^0)$		
	BABAR [625]: $5.5 \pm 1.2 \,^{+2.1}_{-1.6}$	$5.5 \,^{+2.5}_{-2.0}$
$\mathcal{B}(\overline{B}^0 \to D_{sJ}(2460)^- D^*(2010)^+) \times \mathcal{B}(D_{sJ}(2460)^- \to D_s^- \gamma)$		
	BABAR [625]: $2.3 \pm 0.3 \,^{+0.9}_{-0.6}$	$2.3 \,^{+0.9}_{-0.7}$
$\mathcal{B}(\overline{B}^0 \to D^+ D^*_{sJ}(2317)^-) \times \mathcal{B}(D^*_{sJ}(2317)^- \to D_s^- \pi^0)$		
	Belle [626]: $1.02 \,^{+0.13}_{-0.12} \pm 0.11$	1.03 ± 0.16
	BABAR [625]: $1.8 \pm 0.4 \,^{+0.7}_{-0.5}$	
$\mathcal{B}(\overline{B}^0 \to D^+ D^*_{sJ}(2317)^-) \times \mathcal{B}(D^*_{sJ}(2317)^- \to D_s^{*-} \gamma)$		
	Belle [624]: < 0.95	< 0.95
$\mathcal{B}(\overline{B}^0 \to D^*_{sJ}(2317)^- D^*(2010)^+) \times \mathcal{B}(D^*_{sJ}(2317)^- \to D_s^- \pi^0)$		
	BABAR [625]: $1.5 \pm 0.4 \,^{+0.5}_{-0.4}$	$1.5 \,^{+0.7}_{-0.5}$

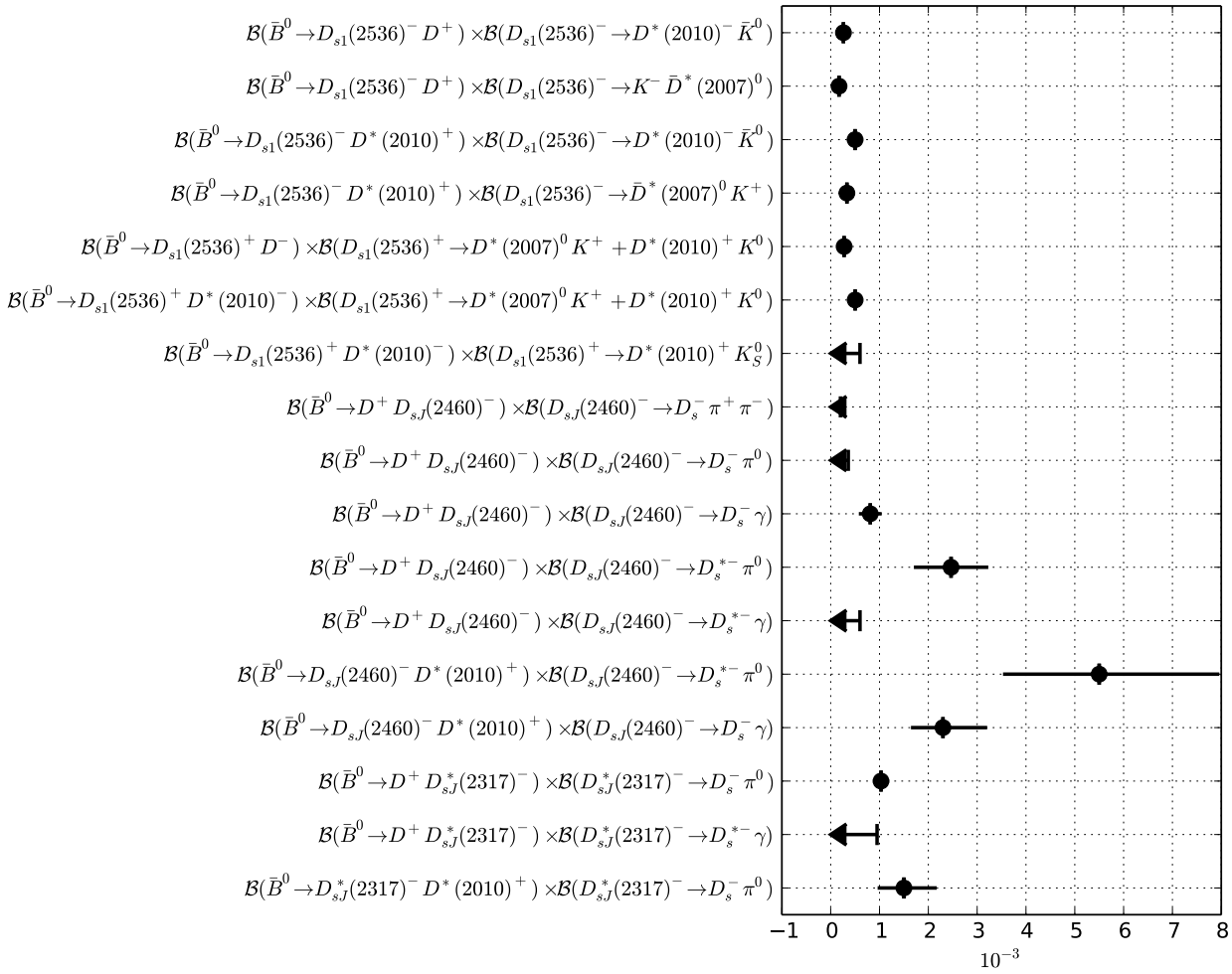

Figure 83: Summary of the averages from Table 108.

6.1.3 Decays to charmonium states

Averages of $\overline{B}^0$ decays to charmonium states are shown in Tables 109–114 and Figs. 84–89.

Table 109: Decays to J/ψ and one kaon [10^{-3}].

Parameter	**Measurements**	**Average**
$\mathcal{B}(\overline{B}^0 \to J/\psi \overline{K}^0)$	CDF [627]: $1.15 \pm 0.23 \pm 0.17$ Belle [628]: $0.79 \pm 0.04 \pm 0.09$ *BABAR* [6]: $0.869 \pm 0.022 \pm 0.030$	0.863 ± 0.035
$\mathcal{B}(\overline{B}^0 \to J/\psi K^- \pi^+)$	Belle [629]: $1.15 \pm 0.01 \pm 0.05$	1.15 ± 0.05
$\mathcal{B}(\overline{B}^0 \to J/\psi \overline{K}^*(892)^0)$	CDF [630]: $1.74 \pm 0.20 \pm 0.18$ Belle [629]: $1.19 \pm 0.01 \pm 0.08$ *BABAR* [6]: $1.309 \pm 0.026 \pm 0.077$	1.270 ± 0.056
$\mathcal{B}(\overline{B}^0 \to J/\psi \overline{K}^0 \pi^+ \pi^-)$	LHCb [631]: $0.430 \pm 0.030 \pm 0.037$ CDF [632]: $1.03 \pm 0.33 \pm 0.15$	0.440 ± 0.047
$\mathcal{B}(\overline{B}^0 \to J/\psi \overline{K}^0 \rho(770)^0)$	CDF [632]: $0.54 \pm 0.29 \pm 0.09$	0.54 ± 0.30
$\mathcal{B}(\overline{B}^0 \to J/\psi K^*(892)^- \pi^+)$	CDF [632]: $0.77 \pm 0.41 \pm 0.13$	0.77 ± 0.43
$\mathcal{B}(\overline{B}^0 \to J/\psi \omega(782) \overline{K}^0)$	*BABAR* [633]: $0.23 \pm 0.03 \pm 0.03$	0.23 ± 0.04
$\mathcal{B}(\overline{B}^0 \to J/\psi \phi(1020) \overline{K}^0)$	*BABAR* [634]: $0.102 \pm 0.038 \pm 0.010$	0.102 ± 0.039
$\mathcal{B}(\overline{B}^0 \to J/\psi \overline{K}^0_1(1270))$	Belle [635]: $1.30 \pm 0.34 \pm 0.31$	1.30 ± 0.46
$\mathcal{B}(\overline{B}^0 \to J/\psi \eta K^0_S)$	Belle [636]: $0.0522 \pm 0.0078 \pm 0.0049$ *BABAR* [637]: $0.084 \pm 0.026 \pm 0.027$	0.0540 ± 0.0089
$\mathcal{B}(\overline{B}^0 \to J/\psi \overline{K}^*(892)^0 \pi^+ \pi^-)$	CDF [632]: $0.66 \pm 0.19 \pm 0.11$	0.66 ± 0.22

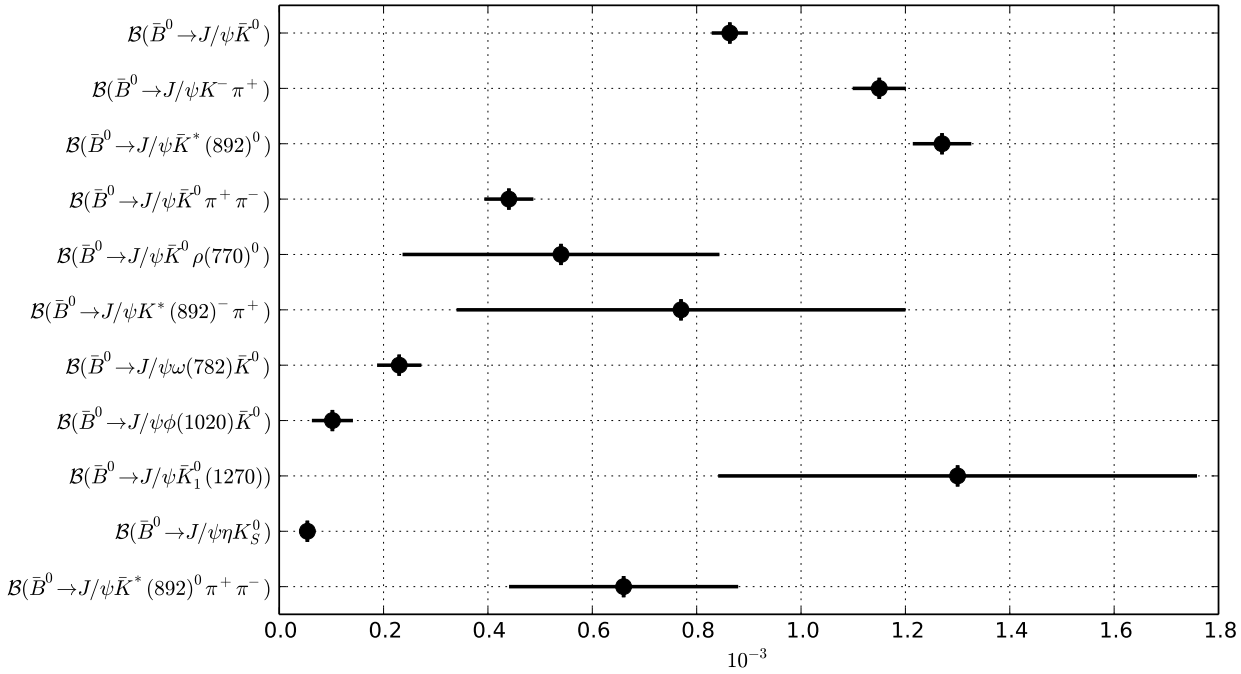

Figure 84: Summary of the averages from Table 109.

Table 110: Decays to charmonium other than J/ψ and one kaon [10^{-3}].

Parameter	**Measurements**	**Average**
$\mathcal{B}(\overline{B}^0 \to \psi(2S)\overline{K}^0)$	Belle [628]: 0.67 ± 0.11 *BABAR* [6]: $0.646 \pm 0.065 \pm 0.051$	0.655 ± 0.066
$\mathcal{B}(\overline{B}^0 \to \psi(2S)\overline{K}^*(892)^0)$	CDF [630]: $0.90 \pm 0.22 \pm 0.09$ Belle [638]: $0.720 \pm 0.043 \pm 0.065$ *BABAR* [6]: $0.649 \pm 0.059 \pm 0.097$	0.711 ± 0.062
$\mathcal{B}(\overline{B}^0 \to \psi(2S)K^0)$	LHCb [631]: $0.47 \pm 0.07 \pm 0.07$	0.47 ± 0.10
$\mathcal{B}(\overline{B}^0 \to K^*(892)^0\psi(2S))$	Belle [639]: $0.552\,^{+0.035\ +0.053}_{-0.032\ -0.058}$	$0.552\,^{+0.064}_{-0.066}$
$\mathcal{B}(\overline{B}^0 \to \psi(2S)K^0) \times \mathcal{B}(\psi(2S) \to \chi_{c1}\gamma)$	Belle [640]: $0.68 \pm 0.10 \pm 0.07$	0.68 ± 0.12
$\mathcal{B}(\overline{B}^0 \to \psi(2S)K^0) \times \mathcal{B}(\psi(2S) \to \chi_{c2}\gamma)$	Belle [640]: $0.47 \pm 0.16 \pm 0.08$	0.47 ± 0.18
$\mathcal{B}(\overline{B}^0 \to \psi(3770)\overline{K}^0) \times \mathcal{B}(\psi(3770) \to D^0\overline{D}^0)$	*BABAR* [622]: < 0.123	< 0.123
$\mathcal{B}(\overline{B}^0 \to \psi(3770)\overline{K}^0) \times \mathcal{B}(\psi(3770) \to D^+D^-)$	*BABAR* [622]: < 0.188	< 0.188
$\mathcal{B}(\overline{B}^0 \to \chi_{c0}\overline{K}^0)$	*BABAR* [641]: < 1.24	< 1.24
$\mathcal{B}(\overline{B}^0 \to \chi_{c0}\overline{K}^*(892)^0)$	*BABAR* [641]: < 0.77 *BABAR* [642]: $0.17 \pm 0.03 \pm 0.02$	0.17 ± 0.04
$\mathcal{B}(\overline{B}^0 \to \chi_{c1}\overline{K}^0)$	Belle [643]: $0.378\,^{+0.017}_{-0.016} \pm 0.033$ *BABAR* [644]: $0.42 \pm 0.03 \pm 0.03$	0.396 ± 0.028
$\mathcal{B}(\overline{B}^0 \to \chi_{c1}K^-\pi^+)$	Belle [645]: $0.497 \pm 0.012 \pm 0.028$ *BABAR* [646]: $0.511 \pm 0.014 \pm 0.058$	0.500 ± 0.027
$\mathcal{B}(\overline{B}^0 \to \chi_{c1}\overline{K}^*(892)^0)$	Belle [647]: $0.31 \pm 0.03 \pm 0.07$ *BABAR* [644]: $0.25 \pm 0.02 \pm 0.02$	0.26 ± 0.03
$\mathcal{B}(\overline{B}^0 \to \chi_{c1}K^-\pi^+\pi^0)$	Belle [645]: $0.352 \pm 0.052 \pm 0.024$	0.352 ± 0.057
$\mathcal{B}(\overline{B}^0 \to \chi_{c1}\overline{K}^0\pi^+\pi^-)$	Belle [645]: $0.316 \pm 0.035 \pm 0.032$	0.316 ± 0.047
$\mathcal{B}(\overline{B}^0 \to \chi_{c2}\overline{K}^0)$	Belle [643]: < 0.015 *BABAR* [644]: $0.015 \pm 0.009 \pm 0.003$	0.015 ± 0.009
$\mathcal{B}(\overline{B}^0 \to \chi_{c2}\overline{K}^*(892)^0)$	*BABAR* [644]: $0.066 \pm 0.018 \pm 0.005$	0.066 ± 0.019
$\mathcal{B}(\overline{B}^0 \to \chi_{c2}K^-\pi^+)$	Belle [645]: $0.072 \pm 0.009 \pm 0.005$	0.072 ± 0.010
$\mathcal{B}(\overline{B}^0 \to \eta_c\overline{K}^0)$	Belle [648]: $1.23 \pm 0.23\,^{+0.40}_{-0.41}$ *BABAR* [649]: $0.64\,^{+0.22\ +0.28}_{-0.20\ -0.16}$ *BABAR* [650]: $1.14 \pm 0.15 \pm 0.34$	0.85 ± 0.24
$\mathcal{B}(\overline{B}^0 \to \eta_c\overline{K}^*(892)^0)$	Belle [648]: $1.62 \pm 0.32\,^{+0.55}_{-0.60}$ *BABAR* [651]: $0.57 \pm 0.06 \pm 0.09$ *BABAR* [649]: $0.80\,^{+0.21\ +0.37}_{-0.19\ -0.23}$	0.61 ± 0.10
$\mathcal{B}(\overline{B}^0 \to \eta_c(2S)\overline{K}^*(892)^0)$	*BABAR* [651]: < 0.39	< 0.39
$\mathcal{B}(\overline{B}^0 \to h_c(1P)\overline{K}^*(892)^0) \times \mathcal{B}(h_c(1P) \to \eta_c\gamma)$	*BABAR* [651]: < 0.22	< 0.22

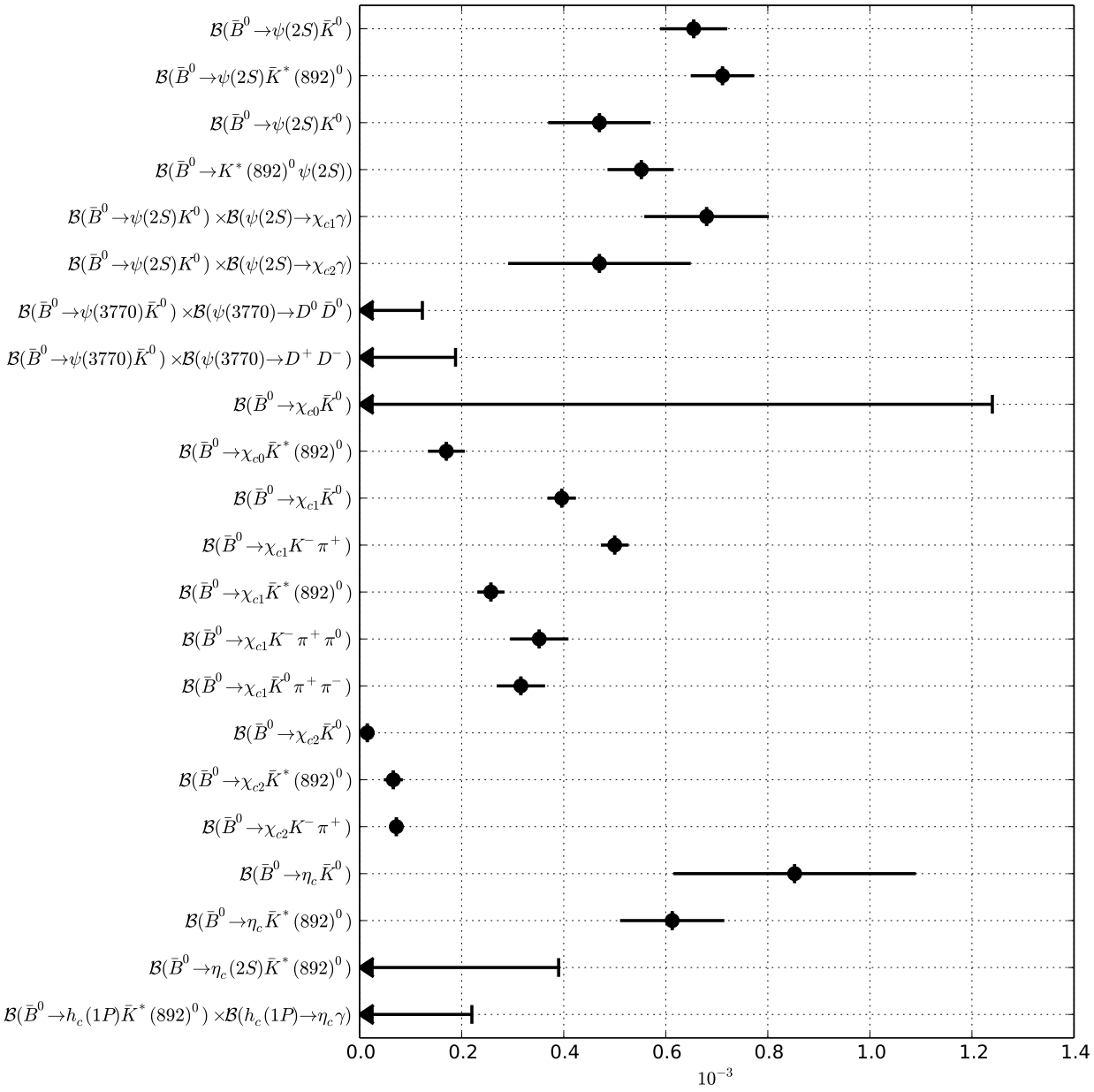

Figure 85: Summary of the averages from Table 110.

Table 111: Decays to charmonium and light mesons [10^{-5}].

Parameter	**Measurements**	**Average**
$\mathcal{B}(\overline{B}^0 \to J/\psi\pi^0)$	Belle [628]: $2.3 \pm 0.5 \pm 0.2$ *BABAR* [340]: $1.69 \pm 0.14 \pm 0.07$	1.74 ± 0.15
$\mathcal{B}(\overline{B}^0 \to J/\psi\pi^+\pi^-)$	Belle [652]: < 1 *BABAR* [653]: < 1.2	< 1
$\mathcal{B}(\overline{B}^0 \to J/\psi\rho(770)^0)$	Belle [652]: $2.8 \pm 0.3 \pm 0.3$ *BABAR* [653]: $2.7 \pm 0.3 \pm 0.2$	2.7 ± 0.3
$\mathcal{B}(\overline{B}^0 \to J/\psi\eta)$	Belle [654]: $1.23\,^{+0.18}_{-0.17} \pm 0.07$ *BABAR* [634]: < 2.7	$1.23\,^{+0.19}_{-0.18}$
$\mathcal{B}(\overline{B}^0 \to J/\psi\eta'(958))$	Belle [654]: < 0.74 *BABAR* [634]: < 6.3	< 0.74
$\mathcal{B}(\overline{B}^0 \to J/\psi f_2(1270))$	Belle [652]: $0.98 \pm 0.39 \pm 0.20$ *BABAR* [653]: < 0.46	0.98 ± 0.44
$\mathcal{B}(\overline{B}^0 \to J/\psi a_0(980)) \times \mathcal{B}(a_0(980) \to K^+K^-)$		
	LHCb [655]: < 0.090	< 0.090
$\mathcal{B}(\overline{B}^0 \to J/\psi f_0(980)) \times \mathcal{B}(f_0(980) \to \pi^+\pi^-)$		
	LHCb [656]: < 0.11	< 0.11
$\mathcal{B}(\overline{B}^0 \to J/\psi f_1(1285))$	LHCb [657]: $0.837 \pm 0.195\,^{+0.079}_{-0.075}$	$0.837\,^{+0.210}_{-0.209}$
$\mathcal{B}(\overline{B}^0 \to J/\psi f_1(1285)) \times \mathcal{B}(f_1(1285) \to \pi^+\pi^-\pi^+\pi^-)$		
	LHCb [657]: $0.0921 \pm 0.0214 \pm 0.0064$	0.0921 ± 0.0223
$\mathcal{B}(\overline{B}^0 \to J/\psi K^+K^-)$	LHCb [655]: $0.253 \pm 0.031 \pm 0.019$	0.253 ± 0.036
$\mathcal{B}(\overline{B}^0 \to J/\psi\phi(1020))$	LHCb [655]: < 0.019 Belle [658]: < 0.094 *BABAR* [634]: < 0.9	< 0.019
$\mathcal{B}(\overline{B}^0 \to J/\psi K^0 K^\pm\pi^\mp)$	LHCb [631]: < 2.1	< 2.1
$\mathcal{B}(\overline{B}^0 \to J/\psi K^0 K^+K^-)$	LHCb [631]: $2.02 \pm 0.43 \pm 0.19$	2.02 ± 0.47
$\mathcal{B}(\overline{B}^0 \to \chi_{c1}\pi^0)$	Belle [659]: $1.12 \pm 0.25 \pm 0.12$	1.12 ± 0.28

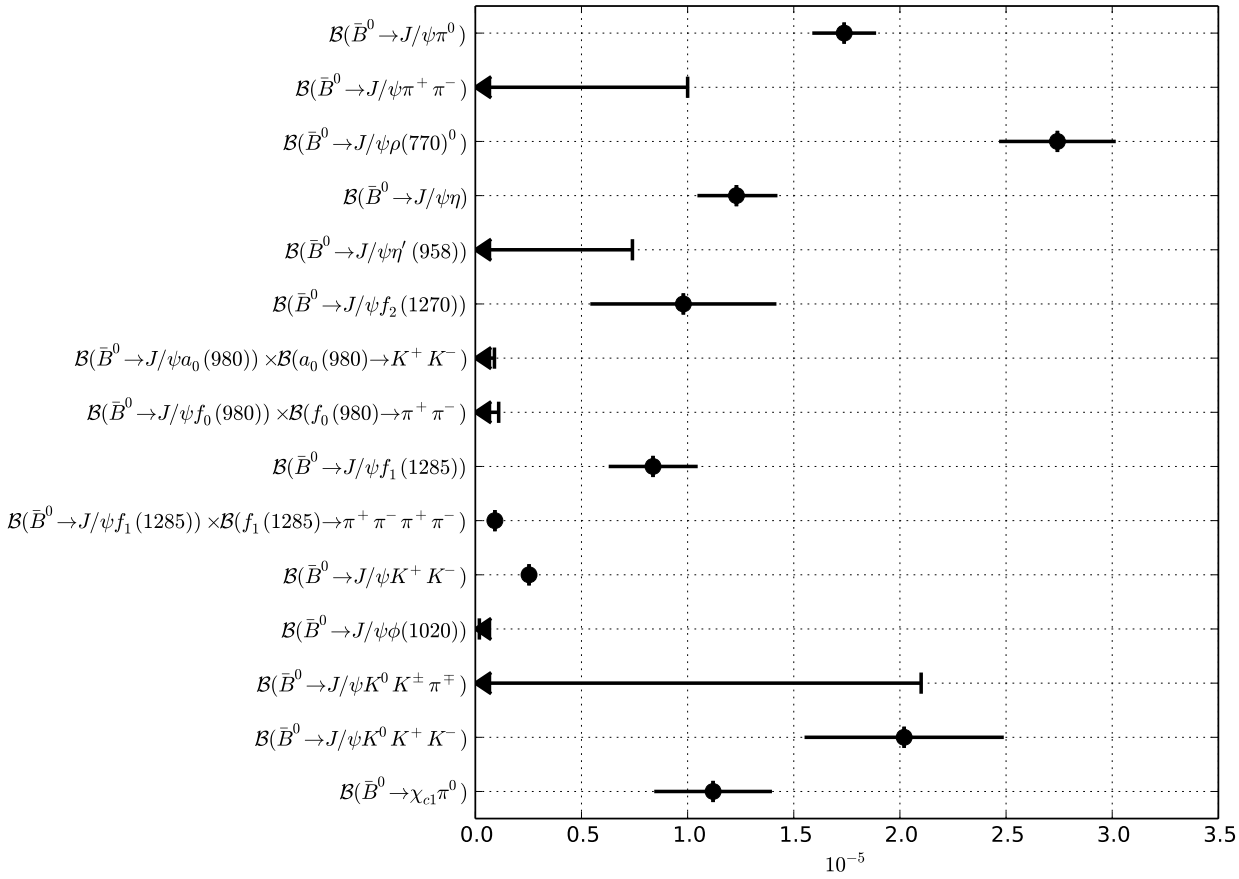

Figure 86: Summary of the averages from Table 111.

Table 112: Decays to J/ψ and photons, baryons, or heavy mesons [10^{-5}].

Parameter	**Measurements**	**Average**
$\mathcal{B}(\overline{B}^0 \to J/\psi\gamma)$	LHCb [660]: < 0.15 *BABAR* [661]: < 0.16	< 0.15
$\mathcal{B}(\overline{B}^0 \to J/\psi\overline{p}p)$	LHCb [662]: < 0.052 Belle [663]: < 0.083 *BABAR* [664]: < 0.19	< 0.052
$\mathcal{B}(\overline{B}^0 \to J/\psi D^0)$	Belle [665]: < 2.0 *BABAR* [666]: < 1.3	< 1.3

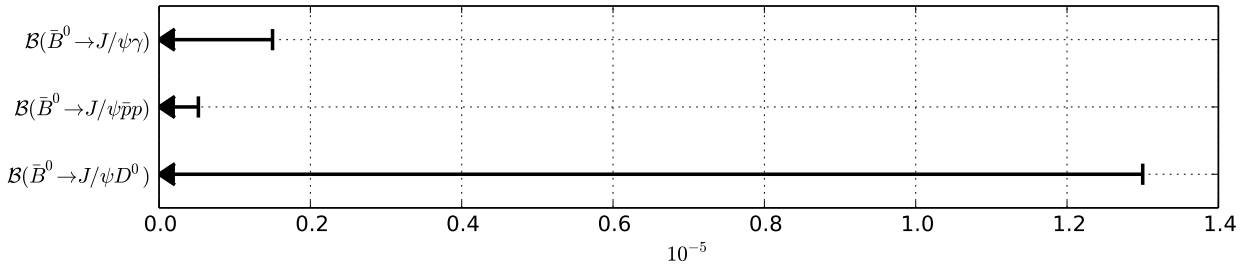

Figure 87: Summary of the averages from Table 112.

Table 113: Relative decay rates

Parameter	**Measurements**	**Average**
$\mathcal{B}(\overline{B}^0 \to J/\psi \overline{K}_1^0(1270))/\mathcal{B}(B^- \to J/\psi K^-)$		
	Belle [635]: $1.30 \pm 0.34 \pm 0.28$	1.30 ± 0.44
$\mathcal{B}(\overline{B}^0 \to J/\psi \overline{K}^*(892)^0)/\mathcal{B}(\overline{B}^0 \to J/\psi \overline{K}^0)$		
	CDF [667]: $1.39 \pm 0.36 \pm 0.10$	
	BABAR [6]: $1.51 \pm 0.05 \pm 0.08$	1.50 ± 0.09
$\mathcal{B}(\overline{B}^0 \to J/\psi\omega(782))/\mathcal{B}(\overline{B}^0 \to J/\psi\rho)$		
	LHCb [668]: $0.89 \pm 0.19\,^{+0.07}_{-0.13}$	$0.89\,^{+0.20}_{-0.23}$
$\mathcal{B}(\overline{B}^0 \to J/\psi\omega(782)\overline{K}^0)/\mathcal{B}(B^- \to J/\psi\omega(782)K^-)$		
	BABAR [633]: $0.7 \pm 0.1 \pm 0.1$	0.7 ± 0.1
$\mathcal{B}(\overline{B}^0 \to J/\psi\eta)/\mathcal{B}(\overline{B}_s^0 \to J/\psi\eta)$		
	LHCb [669]: $0.0185 \pm 0.0061 \pm 0.0014$	0.0185 ± 0.0063
$\mathcal{B}(\overline{B}^0 \to J/\psi\eta')/\mathcal{B}(\overline{B}_s^0 \to J/\psi\eta')$		
	LHCb [669]: $0.0228 \pm 0.0065 \pm 0.0016$	0.0228 ± 0.0067
$\mathcal{B}(\overline{B}^0 \to J/\psi K_S^0\pi^-\pi^+)/\mathcal{B}(\overline{B}^0 \to J/\psi K_S^0)$		
	LHCb [631]: $0.493 \pm 0.034 \pm 0.027$	0.493 ± 0.043
$\mathcal{B}(\overline{B}^0 \to J/\psi K_S^0 K^\pm\pi^\mp)/\mathcal{B}(\overline{B}^0 \to J/\psi K_S^0\pi^+\pi^-)$		
	LHCb [631]: < 0.048	< 0.048
$\mathcal{B}(\overline{B}^0 \to J/\psi K_S^0 K^+K^-)/\mathcal{B}(\overline{B}^0 \to J/\psi K_S^0\pi^+\pi^-)$		
	LHCb [631]: $0.047 \pm 0.010 \pm 0.004$	0.047 ± 0.011
$\mathcal{B}(\overline{B}^0 \to \psi(2S)K_S^0) \times \mathcal{B}(\psi(2S) \to J/\psi\pi^-\pi^+)/\mathcal{B}(\overline{B}^0 \to J/\psi K_S^0)$		
	LHCb [631]: $0.183 \pm 0.027 \pm 0.015$	0.183 ± 0.031
$\mathcal{B}(\overline{B}^0 \to \psi(2S)\overline{K}^*(892)^0)/\mathcal{B}(\overline{B}^0 \to \psi(2S)\overline{K}^0)$		
	BABAR [6]: $1.00 \pm 0.14 \pm 0.09$	1.00 ± 0.17
$\mathcal{B}(\overline{B}^0 \to \psi(2S)K(892)^{*0})/\mathcal{B}(\overline{B}^0 \to J/\psi K(892)^{*0})$		
	LHCb [670]: $0.476 \pm 0.014 \pm 0.016$	0.476 ± 0.021
$\mathcal{B}\overline{B}^0 \to \psi(2S)\pi^+\pi^-/\mathcal{B}\overline{B}^0 \to J/\psi\pi^+\pi^-$		
	LHCb [671]: $0.56 \pm 0.07 \pm 0.05$	0.56 ± 0.09
$\mathcal{B}(\overline{B}^0 \to \eta_c\overline{K}^0)/\mathcal{B}(B^- \to \eta_c K^-)$		

continued from previous page

	BABAR [650]: $0.87 \pm 0.13 \pm 0.07$	0.87 ± 0.15
$\mathcal{B}(\overline{B}^0 \to \eta_c \overline{K}^0)/\mathcal{B}(\overline{B}^0 \to J/\psi \overline{K}^0)$		
	BABAR [650]: $1.34 \pm 0.19 \pm 0.40$	1.34 ± 0.44
$\mathcal{B}(\overline{B}^0 \to \eta_c \overline{K}^*(892)^0)/\mathcal{B}(B^- \to \eta_c K^-)$		
	BABAR [672]: $0.67 \pm 0.09 \pm 0.07$	0.67 ± 0.11
$\mathcal{B}(\overline{B}^0 \to \eta_c \overline{K}^*(892)^0)/\mathcal{B}(\overline{B}^0 \to \eta_c \overline{K}^0)$		
	Belle [648]: $1.33 \pm 0.36\,^{+0.24}_{-0.33}$	$1.33\,^{+0.43}_{-0.49}$
$\mathcal{B}(\overline{B}^0 \to \chi_{c1} K^- \pi^+)/\mathcal{B}(\overline{B}^0 \to J/\psi K^- \pi^+)$		
	BABAR [646]: $0.474 \pm 0.013 \pm 0.054$	0.474 ± 0.056
$\mathcal{B}(\overline{B}^0 \to \chi_{c1} \overline{K}^*(892)^0)/\mathcal{B}(\overline{B}^0 \to \chi_{c1} \overline{K}^0)$		
	BABAR [6]: $0.72 \pm 0.11 \pm 0.12$	0.72 ± 0.16
$\mathcal{B}(\overline{B}^0 \to h_c(1P) \overline{K}^*(892)^0) \times \mathcal{B}(h_c(1P) \to \eta_c \gamma)/\mathcal{B}(B^- \to \eta_c K^-)$		
	BABAR [672]: < 0.26	< 0.26
$\mathcal{B}(\overline{B}^0 \to h_c(1P) \overline{K}^*(892)^0) \times \mathcal{B}(h_c(1P) \to \eta_c \gamma)/\mathcal{B}(\overline{B}^0 \to \eta_c \overline{K}^*(892)^0)$		
	BABAR [672]: < 0.39	< 0.39

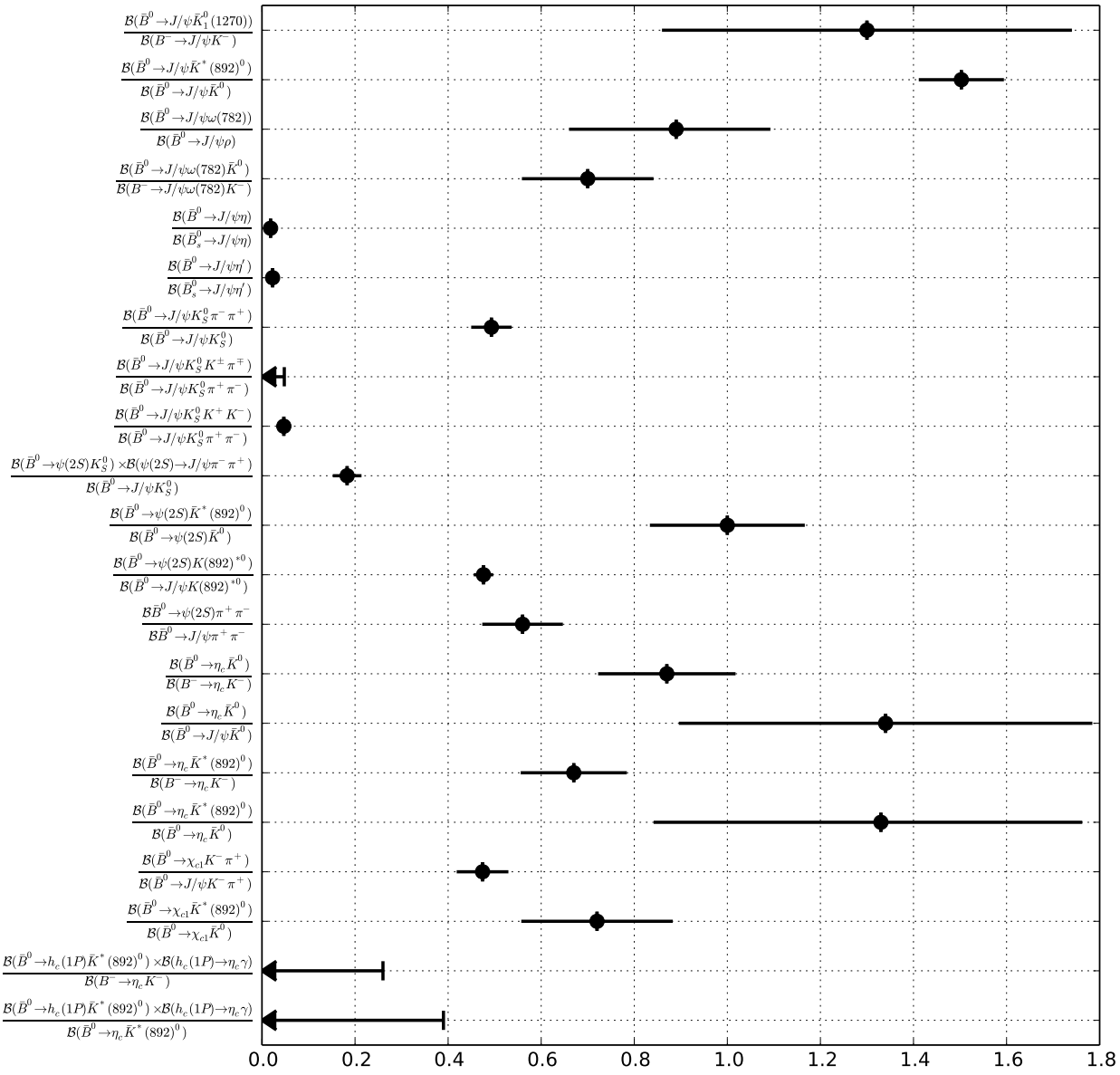

Figure 88: Summary of the averages from Table 113.

Table 114: Polarization fractions.

Parameter	**Measurements**	**Average**
$\lvert\mathcal{A}_0\rvert^2(B^0\to J/\psi\overline{K}^*(892)^0)/\lvert\mathcal{A}_0\rvert^2(\overline{B}^0\to J/\psi\overline{K}^*(892)^0)$		
	BABAR [673]: < 0.32	< 0.32
$\lvert\mathcal{A}_0\rvert^2(\overline{B}^0\to J/\psi K^*(892)^0)/\lvert\mathcal{A}_0\rvert^2(B^0\to J/\psi K^*(892)^0)$		
	BABAR [673]: < 0.26	< 0.26

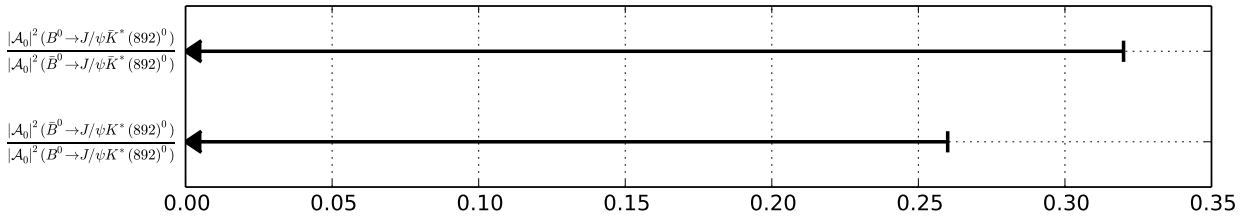

Figure 89: Summary of the averages from Table 114.

6.1.4 Decays to charm baryons

Averages of $\overline{B}^0$ decays to charm baryons are shown in Tables 115–116 and Fig. 90.

Table 115: Absolute decay rates to charm baryons [10^{-4}].

Parameter	**Measurements**	**Average**
$\mathcal{B}(\overline{B}^0 \to \Lambda_c^+ \overline{p}\pi^0)$	*BABAR* [674]: $1.94 \pm 0.17 \pm 0.52$	1.94 ± 0.55
$\mathcal{B}(\overline{B}^0 \to \Lambda_c^+ \overline{p}\pi^+\pi^-)$	Belle [675]: $11.0\,^{+1.2}_{-1.2} \pm 3.5$ *BABAR* [676]: $12.3 \pm 0.5 \pm 3.3$	11.9 ± 3.2
$\mathcal{B}(\overline{B}^0 \to \Lambda_c^+ \overline{p}K^+K^-)$	*BABAR* [677]: $0.25 \pm 0.04 \pm 0.06$	0.25 ± 0.07
$\mathcal{B}(\overline{B}^0 \to \Lambda_c^+ \overline{p}\phi(1020))$	*BABAR* [677]: < 0.12	< 0.12
$\mathcal{B}(\overline{B}^0 \to \Sigma_c^{++} \overline{p}\pi^-)$	Belle [678]: $2.1 \pm 0.2 \pm 0.6$ *BABAR* [676]: $2.13 \pm 0.10 \pm 0.56$	2.12 ± 0.55
$\mathcal{B}(\overline{B}^0 \to \Sigma_c^{*++} \overline{p}\pi^-)$	Belle [678]: $1.2 \pm 0.1 \pm 0.4$ *BABAR* [676]: $1.15 \pm 0.10 \pm 0.30$	1.16 ± 0.32
$\mathcal{B}(\overline{B}^0 \to \Sigma_c^{0} \overline{p}\pi^+)$	Belle [678]: $1.4 \pm 0.2 \pm 0.4$ *BABAR* [676]: $0.91 \pm 0.07 \pm 0.24$	0.77 ± 0.23
$\mathcal{B}(\overline{B}^0 \to \Sigma_c^{*0} \overline{p}\pi^+)$	Belle [678]: < 0.33 *BABAR* [676]: $0.22 \pm 0.07 \pm 0.06$	0.22 ± 0.09
$\mathcal{B}(\overline{B}^0 \to \Sigma_c^{+} \overline{p}) \times \mathcal{B}(\Lambda_c^+ \to pK^-\pi^+)$	*BABAR* [674]: < 0.015	< 0.015
$\mathcal{B}(\overline{B}^0 \to \Lambda_c^+ \overline{p})$	Belle [679]: $0.219\,^{+0.056}_{-0.049} \pm 0.065$ *BABAR* [680]: $0.189 \pm 0.021 \pm 0.049$	0.190 ± 0.054
$\mathcal{B}(\overline{B}^0 \to \Lambda_c^+ \overline{p}\overline{K}^*(892)^0)$	*BABAR* [681]: $0.160 \pm 0.061 \pm 0.044$	0.160 ± 0.075
$\mathcal{B}(\overline{B}^0 \to \Sigma_c^{++} \overline{p}K^-)$	*BABAR* [681]: $0.111 \pm 0.030 \pm 0.030$	0.111 ± 0.043
$\mathcal{B}(\overline{B}^0 \to \Xi_c^+ \Lambda_c^-) \times \mathcal{B}(\Xi_c^+ \to \Xi^-\pi^+\pi^+)$	Belle [682]: $0.93\,^{+0.37}_{-0.28} \pm 0.31$ *BABAR* [683]: $0.15 \pm 0.11 \pm 0.04$	0.17 ± 0.12
$\mathcal{B}(\overline{B}^0 \to \Lambda_c^+ \Lambda_c^-)$	Belle [684]: < 0.57	< 0.57
$\mathcal{B}(\overline{B}^0 \to \Lambda_c^+ \overline{\Lambda}K^-)$	*BABAR* [685]: $0.38 \pm 0.08 \pm 0.10$	0.38 ± 0.13
$\mathcal{B}(\overline{B}^0 \to \Lambda_c^+ \overline{p}K^-\pi^+)$	*BABAR* [681]: $0.433 \pm 0.082 \pm 0.118$	0.433 ± 0.143
$\mathcal{B}(\overline{B}^0 \to \Lambda_c^+ \Lambda_c^- \overline{K}^0)$	Belle [686]: $7.9\,^{+2.9}_{-2.3} \pm 4.3$ *BABAR* [683]: $3.8 \pm 3.1 \pm 2.1$	4.8 ± 3.5
$\mathcal{B}(\overline{B}^0 \to \Lambda_c^+ \overline{p}\pi^+\pi^-_{\mathrm{non-\Sigma_c}})$	*BABAR* [676]: $7.9 \pm 0.4 \pm 2.0$	7.9 ± 2.1
$\mathcal{B}(\overline{B}^0 \to \Lambda_c^+ \overline{p}p\overline{p}) \times \mathcal{B}(\Lambda_c^+ \to pK^-\pi^+)$	*BABAR* [687]: < 0.0014	< 0.0014

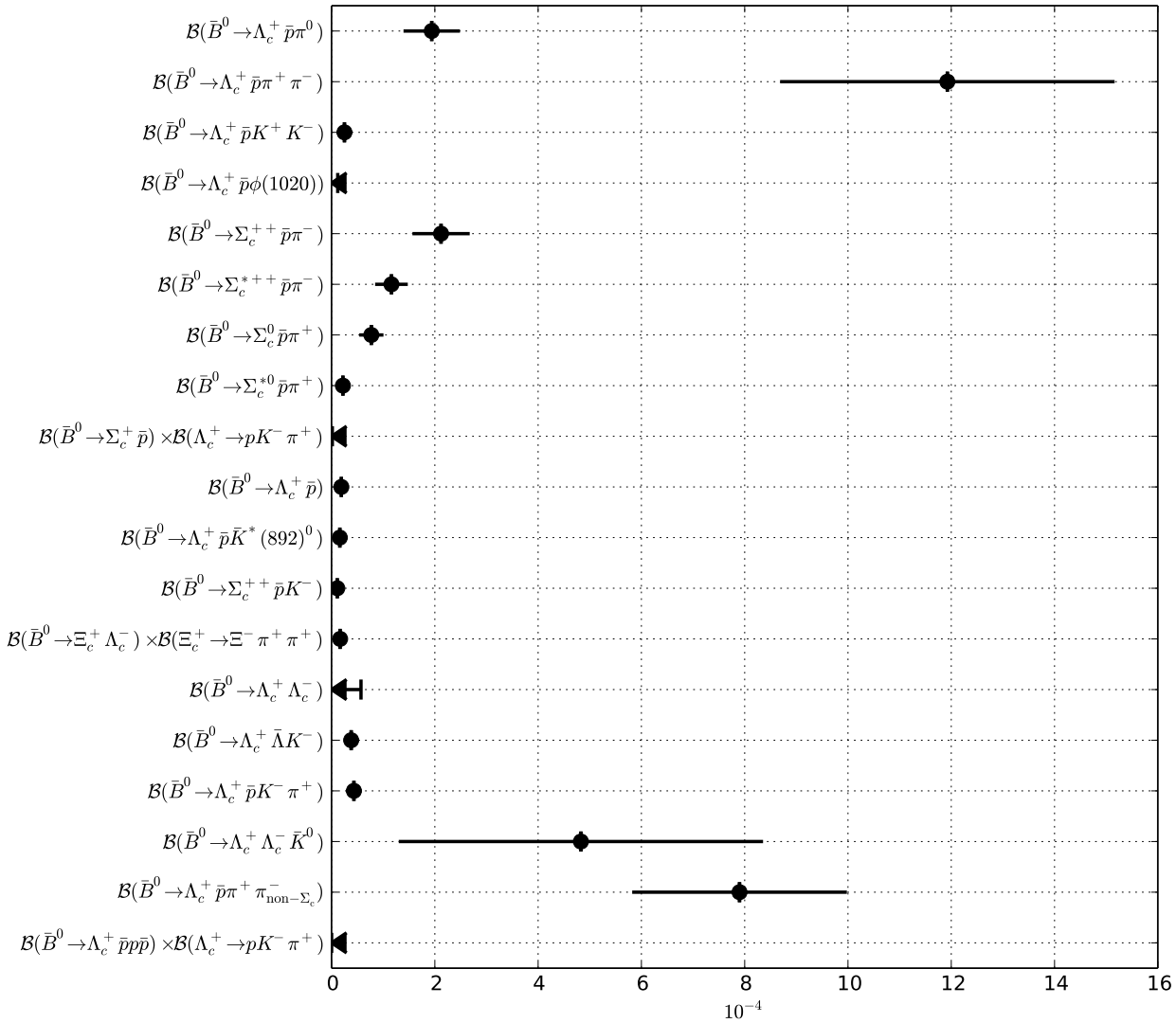

Figure 90: Summary of the averages from Table 115.

Table 116: Relative decay rates to charm baryons [10^{-3}].

Parameter	Measurements	Average
$\mathcal{B}(\overline{B}^0 \to \Lambda_c^- \Lambda_c^+)/\mathcal{B}(\overline{B}^0 \to D^+ D_s^-)$		
	LHCb [688]: < 2	< 2

6.1.5 Decays to other (XYZ) states

Averages of $\overline{B}^0$ decays to other (XYZ) states are shown in Tables 117–121 and Figs. 92–94.

Table 117: Decays to $X(3872)$ [10^{-5}].

Parameter	Measurements	Average
$\mathcal{B}(\overline{B}^0 \to X(3872)\overline{K}^0) \times \mathcal{B}(X(3872) \to J/\psi\pi^+\pi^-)$		
	BABAR [689]: $0.35 \pm 0.19 \pm 0.04$	0.35 ± 0.19
$\mathcal{B}(\overline{B}^0 \to X(3872)\overline{K}^0) \times \mathcal{B}(X(3872) \to J/\psi\omega(782))$		
	BABAR [633]: $0.6 \pm 0.3 \pm 0.1$	0.6 ± 0.3
$\mathcal{B}(\overline{B}^0 \to X(3872)\overline{K}^0) \times \mathcal{B}(X(3872) \to J/\psi\gamma)$		
	Belle [643]: $0.24\,^{+0.13}_{-0.14} \pm 0.07$	
	BABAR [644]: $0.26 \pm 0.18 \pm 0.02$	0.25 ± 0.12
$\mathcal{B}(\overline{B}^0 \to X(3872)\overline{K}^*(892)^0) \times \mathcal{B}(X(3872) \to J/\psi\gamma)$		
	BABAR [644]: $0.07 \pm 0.14 \pm 0.01$	0.07 ± 0.14
$\mathcal{B}(\overline{B}^0 \to X(3872)\overline{K}^0) \times \mathcal{B}(X(3872) \to \psi(2S)\gamma)$		
	Belle [643]: $0.662\,^{+0.130}_{-0.140} \pm 0.070$	
	BABAR [644]: $1.14 \pm 0.55 \pm 0.10$	0.695 ± 0.147
$\mathcal{B}(\overline{B}^0 \to X(3872)\overline{K}^*(892)^0) \times \mathcal{B}(X(3872) \to \psi(2S)\gamma)$		
	BABAR [644]: $-0.13 \pm 0.31 \pm 0.03$	-0.13 ± 0.31
$\mathcal{B}(\overline{B}^0 \to X(3872)K^0) \times \mathcal{B}(X(3872) \to \chi_{c1}\gamma)$		
	Belle [640]: < 0.96	< 0.96
$\mathcal{B}(\overline{B}^0 \to X(3872)K^0) \times \mathcal{B}(X(3872) \to \chi_{c2}\gamma)$		
	Belle [640]: < 1.22	< 1.22

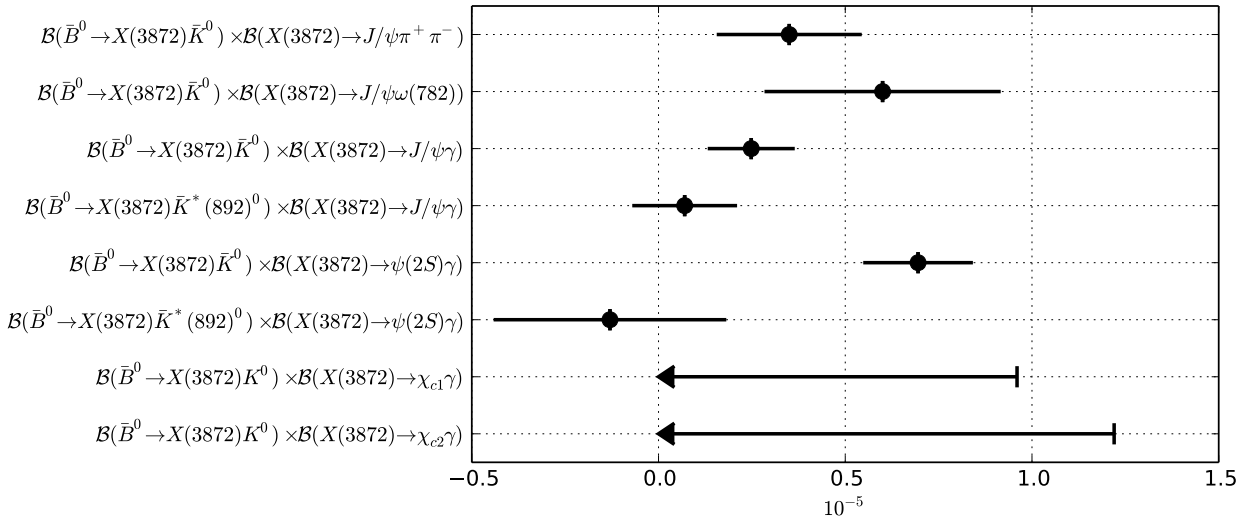

Figure 91: Summary of the averages from Table 117.

Table 118: Decays to $X(3872)$ with $X(3872) \to D\overline{D}$ [10^{-4}].

Parameter	Measurements	Average
$\mathcal{B}(\overline{B}^0 \to X(3872)\overline{K}^0) \times \mathcal{B}(X(3872) \to \overline{D}^*(2007)^0 D^0)$		
	BABAR [622]: < 4.37	< 4.37

Table 119: Decays to neutral states other than $X(3872)$ [10^{-4}].

Parameter	Measurements	Average
$\mathcal{B}(\overline{B}^0 \to X(3823)K^0) \times \mathcal{B}(X(3823) \to \chi_{c1}\gamma)$		
	Belle [640]: < 0.099	< 0.099
$\mathcal{B}(\overline{B}^0 \to X(3823)K^0) \times \mathcal{B}(X(3823) \to \chi_{c2}\gamma)$		
	Belle [640]: < 0.228	< 0.228
$\mathcal{B}(\overline{B}^0 \to Y(3940)\overline{K}^0) \times \mathcal{B}(Y(3940) \to J/\psi\omega(782))$		
	BABAR [633]: $0.21 \pm 0.09 \pm 0.03$	0.21 ± 0.09
$\mathcal{B}(\overline{B}^0 \to Z_1(4050)K^-) \times \mathcal{B}(Z_1(4050) \to \chi_{c1}\pi^+)$		
	Belle [690]: $0.30\,^{+0.15\ +0.37}_{-0.08\ -0.16}$	$0.30\,^{+0.40}_{-0.18}$
	BABAR [646]: < 0.18	
$\mathcal{B}(\overline{B}^0 \to Z_2(4250)K^-) \times \mathcal{B}(Z_2(4250) \to \chi_{c1}\pi^+)$		
	Belle [690]: $0.40\,^{+0.23\ +1.97}_{-0.09\ -0.05}$	$0.40\,^{+1.98}_{-0.10}$
	BABAR [646]: < 0.47	

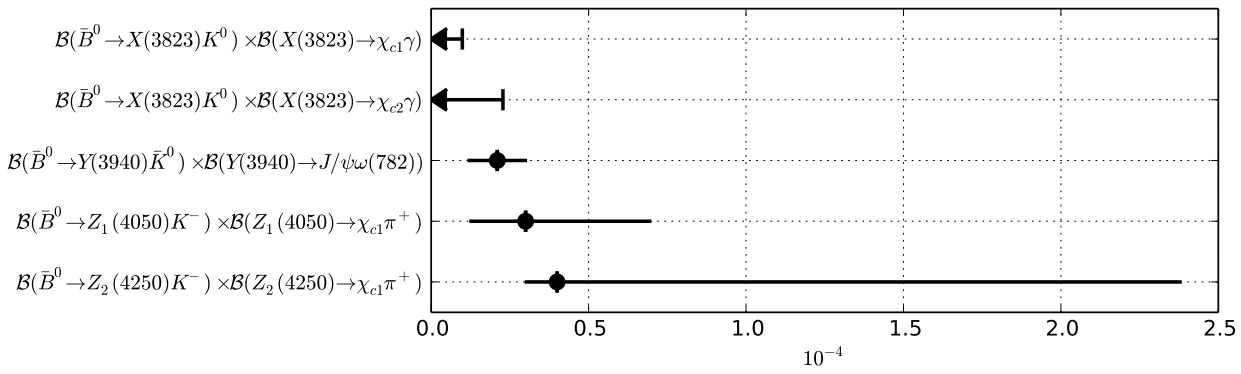

Figure 92: Summary of the averages from Table 119.

Table 120: Decays to charged states [10^{-4}].

Parameter	Measurements	Average
$\mathcal{B}(\overline{B}^0 \to X(3872)^+ K^-)$	*BABAR* [691]: < 5.0	< 5.0
$\mathcal{B}(\overline{B}^0 \to X(3872)^+ K^-) \times \mathcal{B}(X(3872)^+ \to J/\psi\pi^+\pi^0)$	*BABAR* [692]: < 0.054	< 0.054
$\mathcal{B}(\overline{B}^0 \to Z(4430)^+ K^-) \times \mathcal{B}(Z(4430)^+ \to J/\psi\pi^+)$	Belle [629]: $0.054\,^{+0.040\ +0.011}_{-0.010\ -0.009}$ *BABAR* [693]: $-0.12 \pm 0.04 \pm 0.00$	-0.011 ± 0.024
$\mathcal{B}(\overline{B}^0 \to Z(4430)^+ K^-) \times \mathcal{B}(Z(4430)^+ \to \psi(2S)\pi^+)$	Belle [639]: $0.32\,^{+0.18\ +0.53}_{-0.09\ -0.16}$ *BABAR* [693]: $0.19 \pm 0.08 \pm 0.00$	0.19 ± 0.08
$\mathcal{B}(\overline{B}^0 \to Z_c(3900)^+ K^-) \times \mathcal{B}(Z_c(3900)^+ \to J/\psi\pi^+)$	Belle [629]: < 0.009	< 0.009
$\mathcal{B}(\overline{B}^0 \to Z_c(4200)^+ K^-) \times \mathcal{B}(Z_c(4200)^+ \to J/\psi\pi^+)$	Belle [629]: $0.22\,^{+0.07\ +0.11}_{-0.05\ -0.06}$	$0.22\,^{+0.13}_{-0.08}$

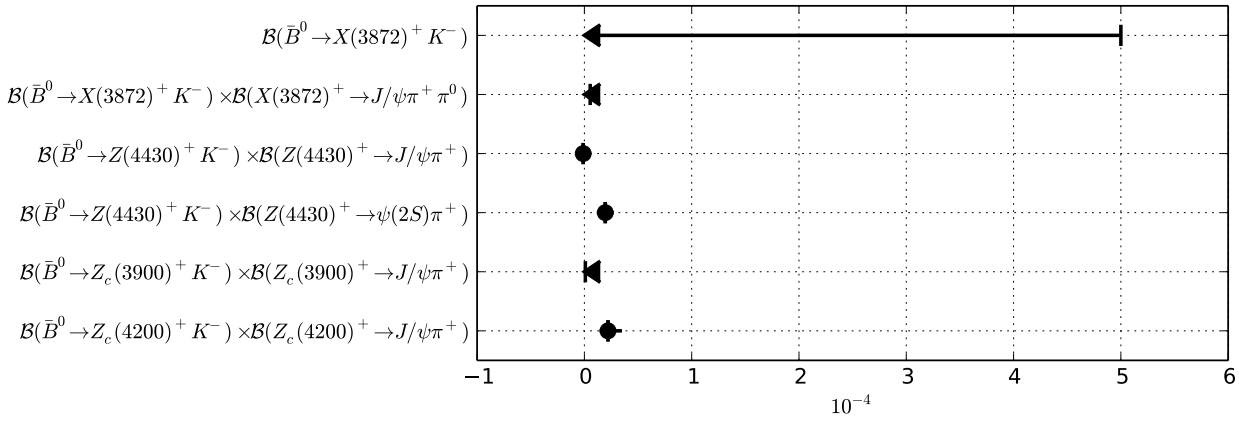

Figure 93: Summary of the averages from Table 120.

Table 121: Relative decay rates.

Parameter	Measurements	Average
$\mathcal{B}(\overline{B}^0 \to X(3872)\overline{K}^0)/\mathcal{B}(B^- \to X(3872)K^-)$	*BABAR* [633]: $1.0\,^{+0.8\ +0.1}_{-0.6\ -0.2}$ *BABAR* [689]: $0.41 \pm 0.24 \pm 0.05$	0.47 ± 0.23
$\mathcal{B}(\overline{B}^0 \to Y(3940)\overline{K}^0)/\mathcal{B}(B^- \to Y(3940)K^-)$	*BABAR* [633]: $0.7\,^{+0.4}_{-0.3} \pm 0.1$	$0.7\,^{+0.4}_{-0.3}$

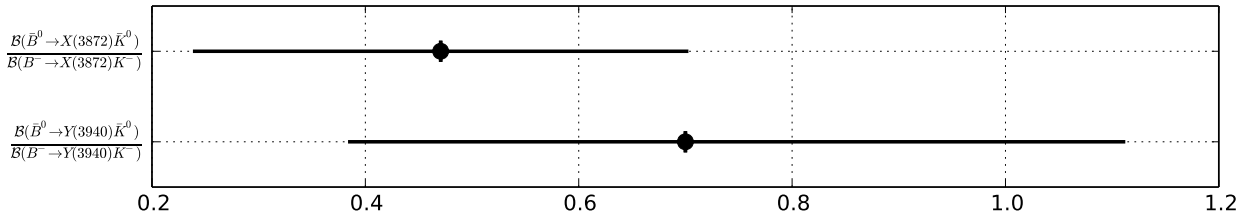

Figure 94: Summary of the averages from Table 121.

6.2 Decays of B^- mesons

Measurements of B^- decays to charmed hadrons are summarized in Sections 6.2.1 to 6.2.5.

6.2.1 Decays to a single open charm meson

Averages of B^- decays to a single open charm meson are shown in Tables 122–132 and Figs. 95–104. In this ection D^{**} refers to the sum of all the non-strange charm meson states with masses in the range $2.2 - 2.8$ GeV/c^2.

Table 122: Decays to a $D^{(*)}$ meson and one or more pions [10^{-2}].

Parameter	**Measurements**	**Average**
$\mathcal{B}(B^- \to D_s^- \pi^0)$	Belle [694]: < 0.00036	< 0.00036
$\mathcal{B}(B^- \to D^0 \pi^-)$	*BABAR* [575]: $0.490 \pm 0.007 \pm 0.022$ *BABAR* [576]: $0.449 \pm 0.021 \pm 0.023$	0.475 ± 0.019
$\mathcal{B}(B^- \to D^*(2007)^0 \pi^-)$	*BABAR* [575]: $0.552 \pm 0.017 \pm 0.042$ *BABAR* [576]: $0.513 \pm 0.022 \pm 0.028$	0.528 ± 0.028
$\mathcal{B}(B^- \to D^+ \pi^- \pi^-)$	Belle [695]: $0.102 \pm 0.004 \pm 0.015$ *BABAR* [696]: $0.108 \pm 0.003 \pm 0.005$	0.107 ± 0.005
$\mathcal{B}(B^- \to D^*(2010)^+ \pi^- \pi^-)$	Belle [695]: $0.125 \pm 0.008 \pm 0.022$ *BABAR* [697]: $0.122 \pm 0.005 \pm 0.018$	0.123 ± 0.015
$\mathcal{B}(B^- \to D^*(2007)^0 \pi^- \pi^+ \pi^-)$	Belle [579]: $1.055 \pm 0.047 \pm 0.129$	1.055 ± 0.137
$\mathcal{B}(B^- \to D^*(2010)^+ \pi^- \pi^+ \pi^- \pi^-)$	Belle [579]: $0.256 \pm 0.026 \pm 0.033$	0.256 ± 0.042
$\mathcal{B}(B^- \to D^*(2007)^0 \pi^- \pi^+ \pi^- \pi^+ \pi^-)$	Belle [579]: $0.567 \pm 0.091 \pm 0.085$	0.567 ± 0.125

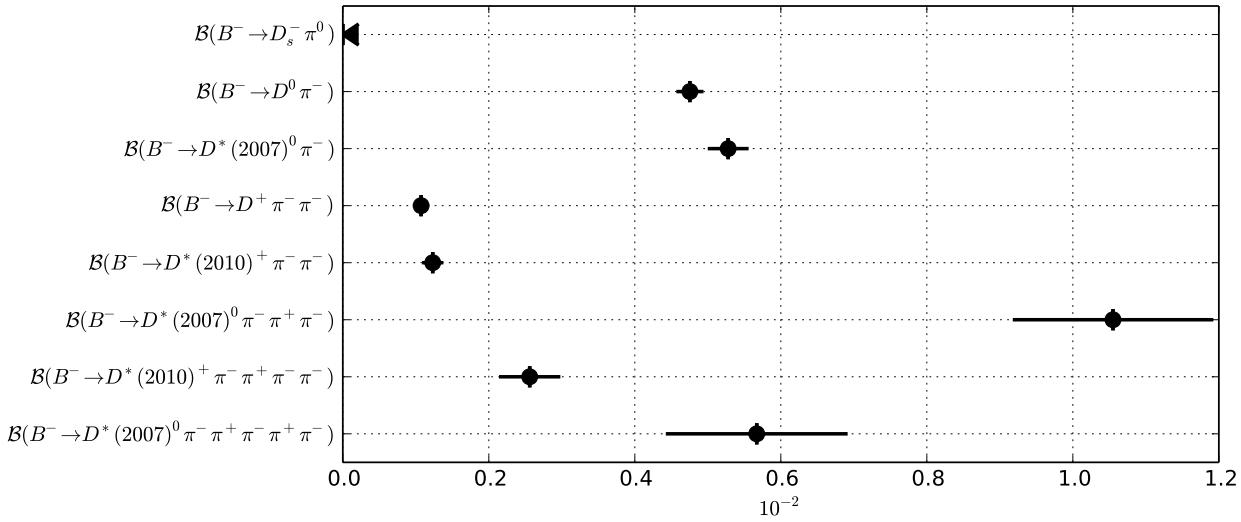

Figure 95: Summary of the averages from Table 122.

Table 123: Decays to a $D^{(*)0}$ meson and one or more kaons [10^{-3}].

Parameter	**Measurements**	**Average**
$\mathcal{B}(B^- \to D^0 K^-)$	Belle [698]: $0.383 \pm 0.025 \pm 0.037$	0.383 ± 0.045
$\mathcal{B}(B^- \to D^*(2007)^0 K^-)$	Belle [584]: $0.359 \pm 0.087 \pm 0.051$	0.359 ± 0.101
$\mathcal{B}(B^- \to D^0 K^- K^0)$	Belle [586]: $0.55 \pm 0.14 \pm 0.08$	0.55 ± 0.16
$\mathcal{B}(B^- \to D^*(2007)^0 K^- K^0)$	Belle [586]: < 1.06	< 1.06
$\mathcal{B}(B^- \to D^0 K^- K^*(892)^0)$	Belle [586]: $0.75 \pm 0.13 \pm 0.11$	0.75 ± 0.17
$\mathcal{B}(B^- \to D^*(2007)^0 K^- K^*(892)^0)$	Belle [586]: $1.53 \pm 0.31 \pm 0.29$	1.53 ± 0.42
$\mathcal{B}(B^- \to D^0 K^*(892)^-)$	*BABAR* [699]: $0.529 \pm 0.030 \pm 0.034$	0.529 ± 0.045
$\mathcal{B}(B^- \to D^*(2007)^0 K^*(892)^-)$	*BABAR* [700]: $0.83 \pm 0.11 \pm 0.10$	0.83 ± 0.15
$\mathcal{B}(B^- \to D^+ K^- \pi^-)$	LHCb [701]: $0.0731 \pm 0.0019 \pm 0.0045$	0.0731 ± 0.0049

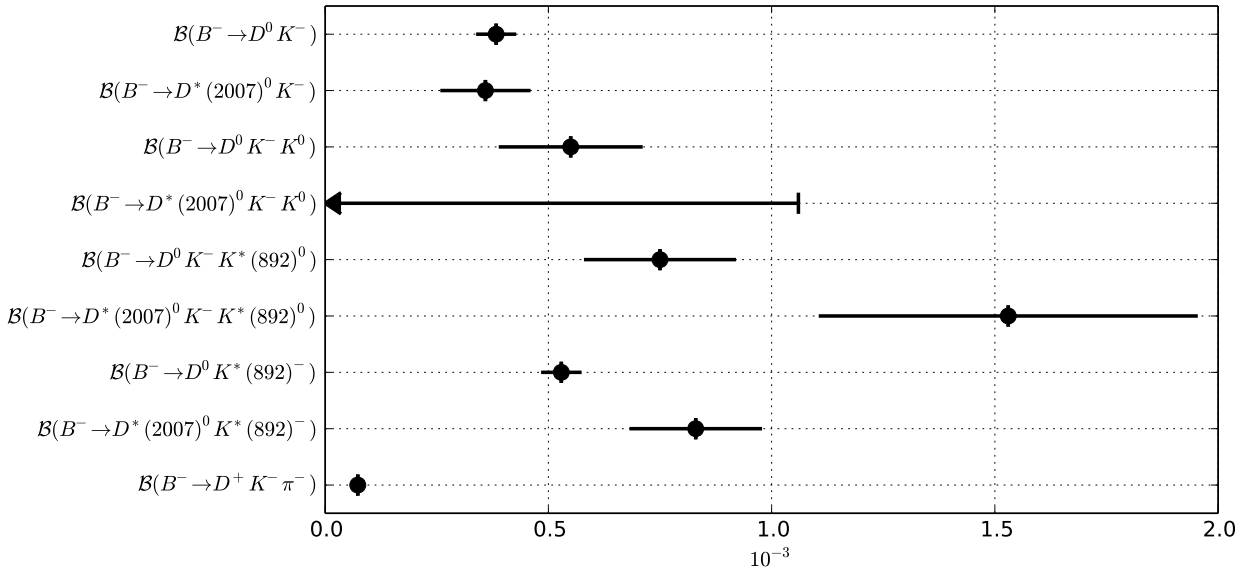

Figure 96: Summary of the averages from Table 123.

Table 124: Decays to a $D^{(*)-}$ meson and a neutral kaon or a kaon and a pion $[10^{-4}]$.

Parameter	**Measurements**	**Average**
$\mathcal{B}(B^- \to D^- \overline{K}^0)$	*BABAR* [702]: $-0.038\,^{+0.022\,+0.012}_{-0.018\,-0.016}$	$-0.038\,^{+0.025}_{-0.024}$
$\mathcal{B}(B^- \to D^- \overline{K}^*(892)^0)$	*BABAR* [702]: $-0.053\,^{+0.023\,+0.014}_{-0.020\,-0.018}$	$-0.053\,^{+0.027}_{-0.027}$
$\mathcal{B}(B^- \to D^- K^- \pi^+)$	LHCb [703]: $0.0531 \pm 0.0090 \pm 0.0059$	0.0531 ± 0.0108
$\mathcal{B}(B^- \to D^*(2010)^- \overline{K}^0)$	*BABAR* [704]: < 0.09	< 0.09

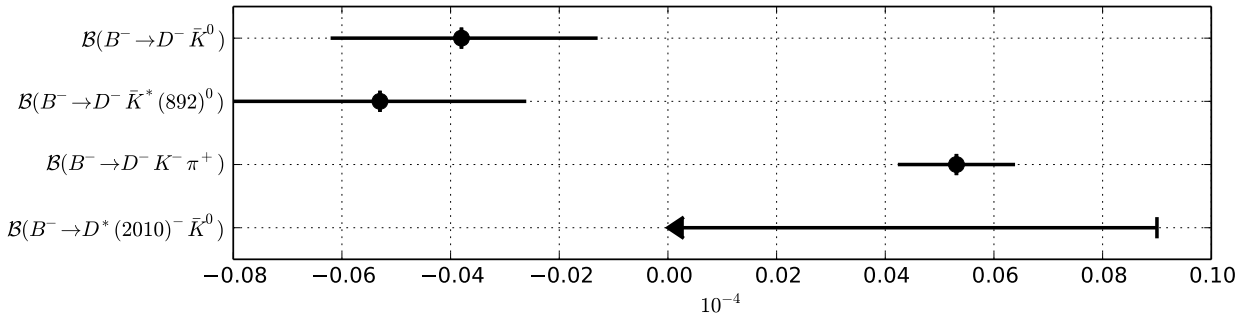

Figure 97: Summary of the averages from Table 124.

Table 125: Relative decay rates to D^0 mesons.

Parameter	Measurements	Average
$\mathcal{B}(B^- \to D^0\pi^-)/\mathcal{B}(\overline{B}^0 \to D^+\pi^-)$		
	CDF [705]: $1.97 \pm 0.10 \pm 0.21$	1.97 ± 0.23
$\mathcal{B}(B^- \to D^0\pi^+\pi^-\pi^-)/\mathcal{B}(B^- \to D^0\pi^-)$		
	LHCb [597]: $1.27 \pm 0.06 \pm 0.11$	1.27 ± 0.13
$\mathcal{B}(B^- \to \overline{D}^0 K^-)/\mathcal{B}(B^- \to D^0 K^-)$		
	Belle [706]: < 0.19	< 0.19
$\mathcal{B}(B^- \to D^0 K^-)/\mathcal{B}(B^- \to D^0\pi^-)$		
	LHCb [707]: $0.063 \pm 0.004 \pm 0.004$	
	CDF [708]: $0.065 \pm 0.007 \pm 0.004$	
	Belle [706]: $0.0677 \pm 0.0023 \pm 0.0030$	0.0723 ± 0.0023
	Belle [698]: $0.077 \pm 0.005 \pm 0.006$	
	BABAR [709]: $0.0831 \pm 0.0035 \pm 0.0020$	
$\mathcal{B}(B^- \to D^0 K^-\pi^+\pi^-)/\mathcal{B}(B^- \to D^0\pi^+\pi^-\pi^-)$		
	LHCb [598]: $0.094 \pm 0.013 \pm 0.009$	0.094 ± 0.016

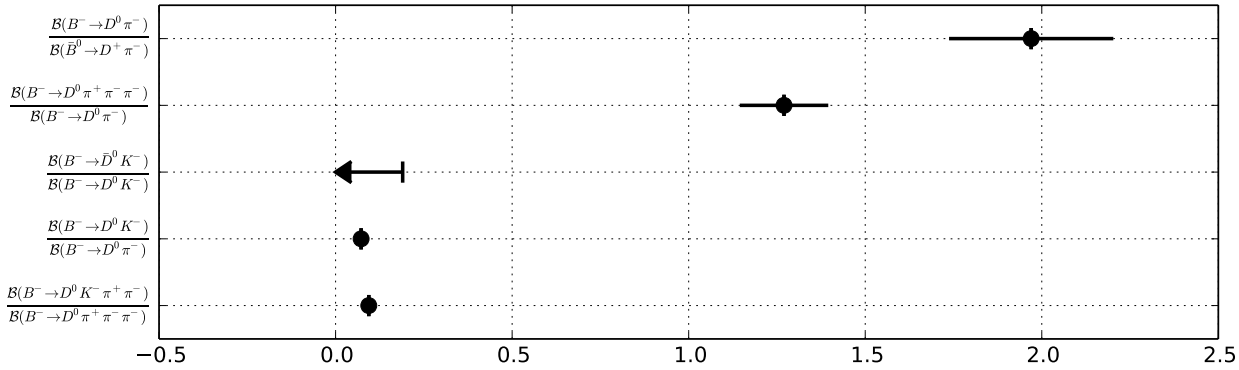

Figure 98: Summary of the averages from Table 125.

Table 126: Absolute decay rates to excited D mesons $[10^{-2}]$.

Parameter	Measurements	Average
$\mathcal{B}(B^- \to D^{**0}\pi^-)$	*BABAR* [576]: $0.550 \pm 0.052 \pm 0.104$	0.550 ± 0.116

Table 127: Absolute product decay rates to excited D mesons [10^{-3}].

Parameter	Measurements	Average
$\mathcal{B}(B^- \to D_1^0(2420)\pi^-) \times \mathcal{B}(D_1^0(2420) \to D^*(2010)^+\pi^-)$		
	Belle [695]: $0.68 \pm 0.07 \pm 0.13$	0.62 ± 0.09
	BABAR [697]: $0.59 \pm 0.03 \pm 0.11$	
$\mathcal{B}(B^- \to D_1^0(2420)\pi^-) \times \mathcal{B}(D_1^0(2420) \to D^0\pi^-\pi^+)$		
	Belle [601]: $0.185 \pm 0.029\,^{+0.035}_{-0.058}$	$0.185\,^{+0.045}_{-0.065}$
$\mathcal{B}(B^- \to D_1^0(2420)\pi^-) \times \mathcal{B}(D_1^0(2420) \to D^*(2007)^0\pi^-\pi^+)$		
	Belle [601]: < 0.006	< 0.006
$\mathcal{B}(B^- \to D_0^{*0}\pi^-) \times \mathcal{B}(D_0^{*0} \to D^+\pi^-)$		
	Belle [695]: $0.61 \pm 0.06 \pm 0.18$	0.63 ± 0.19
	BABAR [696]: $0.68 \pm 0.03 \pm 0.20$	
$\mathcal{B}(B^- \to D_1^0(H)\pi^-) \times \mathcal{B}(D_1^0(H) \to D^*(2010)^+\pi^-)$		
	Belle [695]: $0.50 \pm 0.04 \pm 0.11$	0.50 ± 0.11
$\mathcal{B}(B^- \to D_2^{*0}(2460)\pi^-) \times \mathcal{B}(D_2^{*0}(2460) \to D^*(2010)^+\pi^-)$		
	Belle [695]: $0.18 \pm 0.03 \pm 0.04$	0.18 ± 0.04
	BABAR [697]: $0.18 \pm 0.03 \pm 0.05$	
$\mathcal{B}(B^- \to D_2^{*0}(2460)\pi^-) \times \mathcal{B}(D_2^{*0}(2460) \to D^+\pi^-)$		
	Belle [695]: $0.34 \pm 0.03 \pm 0.07$	0.35 ± 0.05
	BABAR [696]: $0.35 \pm 0.02 \pm 0.04$	
$\mathcal{B}(B^- \to D_2^{*0}(2460)\pi^-) \times \mathcal{B}(D_2^{*0}(2460) \to D^*(2007)^0\pi^-\pi^+)$		
	Belle [601]: < 0.022	< 0.022

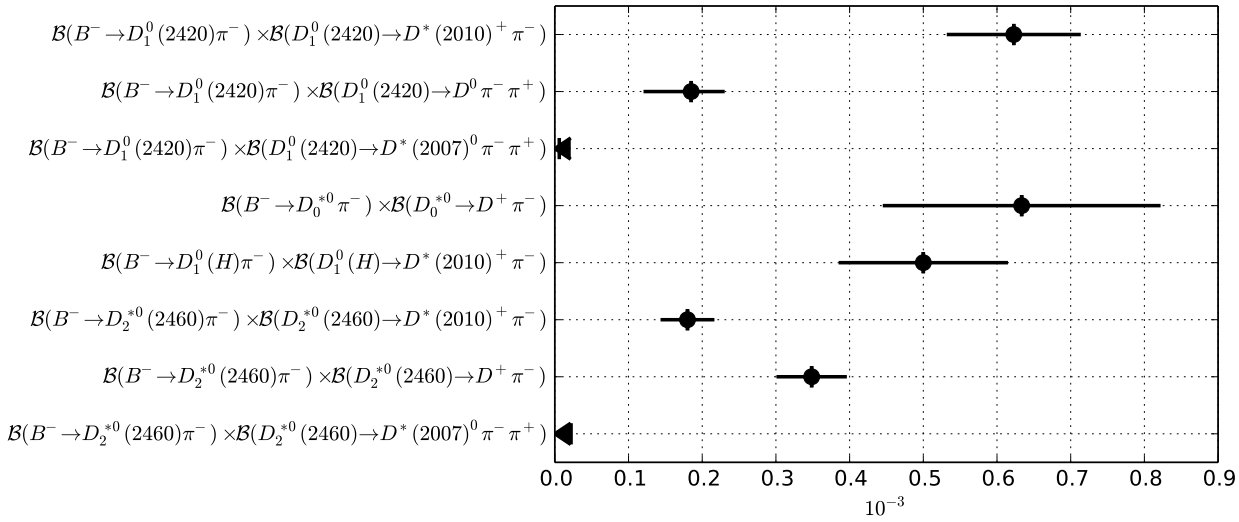

Figure 99: Summary of the averages from Table 127.

Table 128: Relative decay rates to excited D mesons.

Parameter	Measurements	Average
$\mathcal{B}(B^- \to D^*(2007)^0\pi^-)/\mathcal{B}(B^- \to D^0\pi^-)$		
	BABAR [576]: $1.14 \pm 0.07 \pm 0.04$	1.14 ± 0.08
$\mathcal{B}(B^- \to D^{**0}\pi^-)/\mathcal{B}(B^- \to D^0\pi^-)$		
	BABAR [576]: $1.22 \pm 0.13 \pm 0.23$	1.22 ± 0.26
$\mathcal{B}(B^- \to D_2^{*0}(2460)\pi^-)/\mathcal{B}(B^- \to D_1^0(2420)\pi^-)$		
	BABAR [697]: $0.80 \pm 0.07 \pm 0.16$	0.80 ± 0.17
$\mathcal{B}(B^- \to D^*(2007)^0K^-)/\mathcal{B}(B^- \to D^*(2007)^0\pi^-)$		
	Belle [584]: $0.078 \pm 0.019 \pm 0.009$	0.0811 ± 0.0053
	BABAR [710]: $0.0813 \pm 0.0040\,^{+0.0042}_{-0.0031}$	

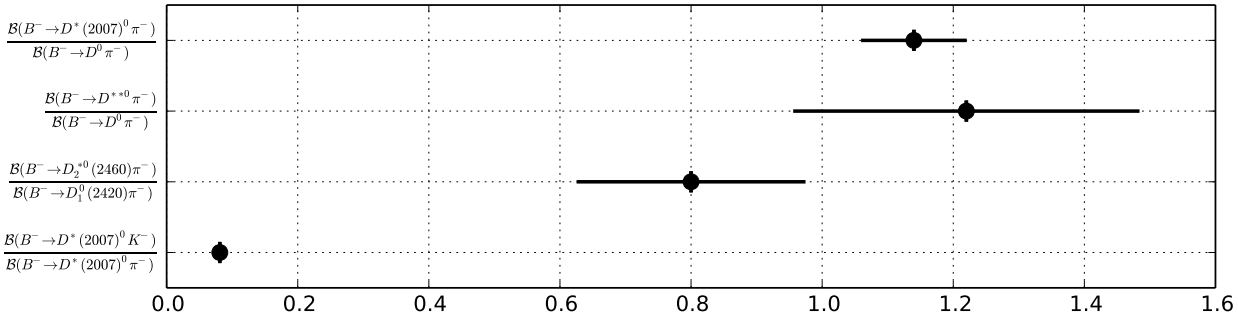

Figure 100: Summary of the averages from Table 128.

Table 129: Relative product decay rates to excited D mesons.

Parameter	Measurements	Average
$\mathcal{B}(B^- \to D_1^0\pi^-) \times \mathcal{B}(D_1^0 \to D^0\pi^+\pi^-)/\mathcal{B}(B^- \to D^0\pi^+\pi^-\pi^-)$		
	LHCb [597]: $0.040 \pm 0.007 \pm 0.005$	0.040 ± 0.009
$\mathcal{B}(B^- \to D_1^{*0}\pi^-) \times \mathcal{B}(D_1^{*0} \to D^{*+}\pi^-)/\mathcal{B}(B^- \to D^0\pi^+\pi^-\pi^-)$		
	LHCb [597]: $0.093 \pm 0.016 \pm 0.009$	0.093 ± 0.018
$\mathcal{B}(B^- \to D_1^{*0}\pi^-) \times \mathcal{B}(D_1^{*0} \to D^0\pi^+\pi^-)/\mathcal{B}(B^- \to D^0\pi^+\pi^-\pi^-)$		
	LHCb [597]: $0.103 \pm 0.015 \pm 0.009$	0.103 ± 0.017
$\mathcal{B}(B^- \to D_2^{*0}\pi^-) \times \mathcal{B}(D_2^{*0} \to D^{*+}\pi^-)/\mathcal{B}(B^- \to D^0\pi^+\pi^-\pi^-)$		
	LHCb [597]: $0.039 \pm 0.012 \pm 0.004$	0.039 ± 0.013
$\mathcal{B}(B^- \to D_2^{*0}\pi^-) \times \mathcal{B}(D_2^{*0} \to D^0\pi^+\pi^-)/\mathcal{B}(B^- \to D^0\pi^+\pi^-\pi^-)$		
	LHCb [597]: $0.040 \pm 0.010 \pm 0.004$	0.040 ± 0.011
$\mathcal{B}(B^- \to D_2^{*+}\pi^-) \times \mathcal{B}(D_2^{*+} \to D^0\pi^-\pi^+)/\mathcal{B}(B^- \to D^0\pi^+\pi^-\pi^-)$		
	LHCb [597]: $0.014 \pm 0.006 \pm 0.002$	0.014 ± 0.006

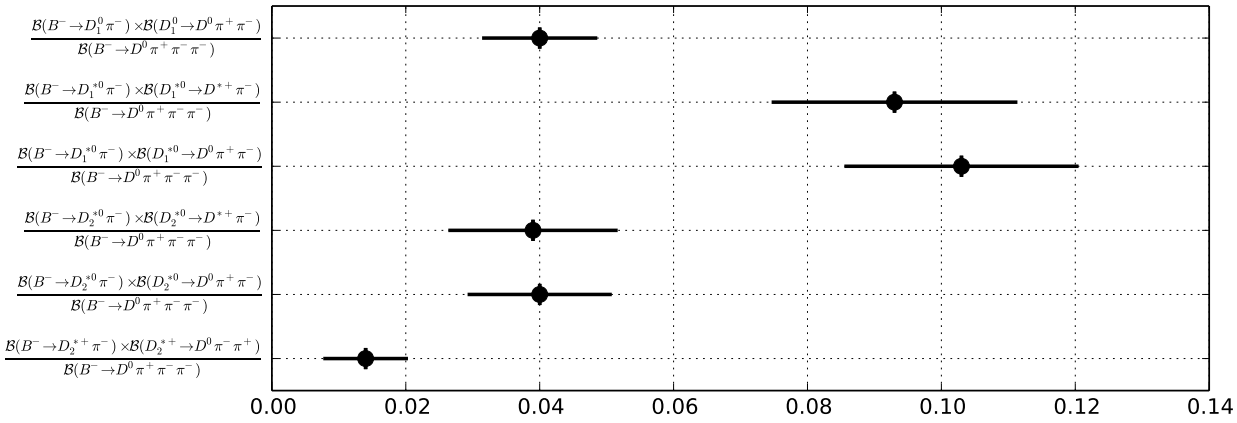

Figure 101: Summary of the averages from Table 129.

Table 130: Decays to $D_s^{(*)}$ mesons $[10^{-4}]$.

Parameter	**Measurements**	**Average**
$\mathcal{B}(B^- \to D_s^+ K^-\pi^-)$	Belle [711]: $1.94\,^{+0.09\,+0.26}_{-0.08\,-0.26}$ *BABAR* [594]: $2.02 \pm 0.13 \pm 0.38$	1.97 ± 0.23
$\mathcal{B}(B^- \to D_s^{*+} K^-\pi^-)$	Belle [711]: $1.47\,^{+0.15\,+0.23}_{-0.14\,-0.23}$ *BABAR* [594]: $1.67 \pm 0.16 \pm 0.35$	1.54 ± 0.22
$\mathcal{B}(B^- \to D_s^+ K^- K^-)$	*BABAR* [594]: $0.11 \pm 0.04 \pm 0.02$	0.11 ± 0.04
$\mathcal{B}(B^- \to D_s^{*+} K^- K^-)$	*BABAR* [594]: < 0.15	< 0.15
$\mathcal{B}(B^- \to D_s^- \pi^0)$	*BABAR* [712]: $0.15\,^{+0.05}_{-0.04} \pm 0.02$	$0.15\,^{+0.05}_{-0.05}$
$\mathcal{B}(B^- \to D_s^- \phi(1020))$	LHCb [713]: $0.0187\,^{+0.0125}_{-0.0073} \pm 0.0037$ *BABAR* [714]: < 0.019	$0.0187\,^{+0.0130}_{-0.0082}$
$\mathcal{B}(B^- \to D_s^{*-} \phi(1020))$	*BABAR* [714]: < 0.12	< 0.12

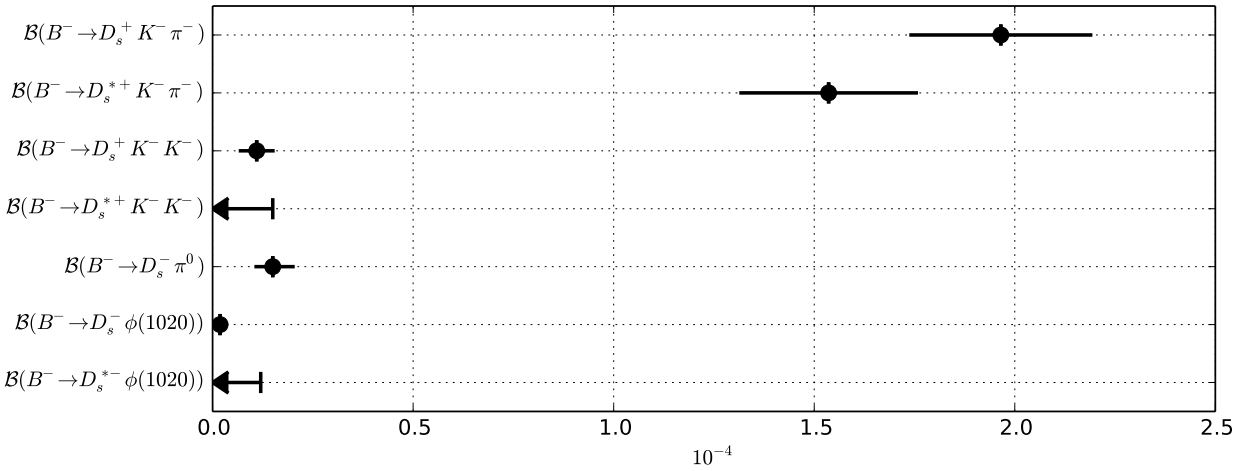

Figure 102: Summary of the averages from Table 130.

Table 131: Baryonic decays [10^{-4}].

Parameter	**Measurements**	**Average**
$\mathcal{B}(B^- \to D^0 p\overline{p}\pi^-)$	*BABAR* [605]: $3.72 \pm 0.11 \pm 0.25$	3.72 ± 0.27
$\mathcal{B}(B^- \to D^*(2007)^0 p\overline{p}\pi^-)$	*BABAR* [605]: $3.73 \pm 0.17 \pm 0.27$	3.73 ± 0.32
$\mathcal{B}(B^- \to D^+ p\overline{p}\pi^-\pi^-)$	*BABAR* [605]: $1.66 \pm 0.13 \pm 0.27$	1.66 ± 0.30
$\mathcal{B}(B^- \to D^*(2010)^+ p\overline{p}\pi^-\pi^-)$	*BABAR* [605]: $1.86 \pm 0.16 \pm 0.19$	1.86 ± 0.25
$\mathcal{B}(B^- \to D^0 \Lambda\overline{p})$	Belle [715]: $0.143\,^{+0.028}_{-0.025} \pm 0.018$	$0.143\,^{+0.033}_{-0.031}$
$\mathcal{B}(B^- \to D^*(2007)^0 \Lambda\overline{p})$	Belle [715]: < 0.48	< 0.48
$\mathcal{B}(B^- \to D^- p\overline{p})$	Belle [604]: < 0.15	< 0.15
$\mathcal{B}(B^- \to D^*(2010)^- p\overline{p})$	Belle [604]: < 0.15	< 0.15

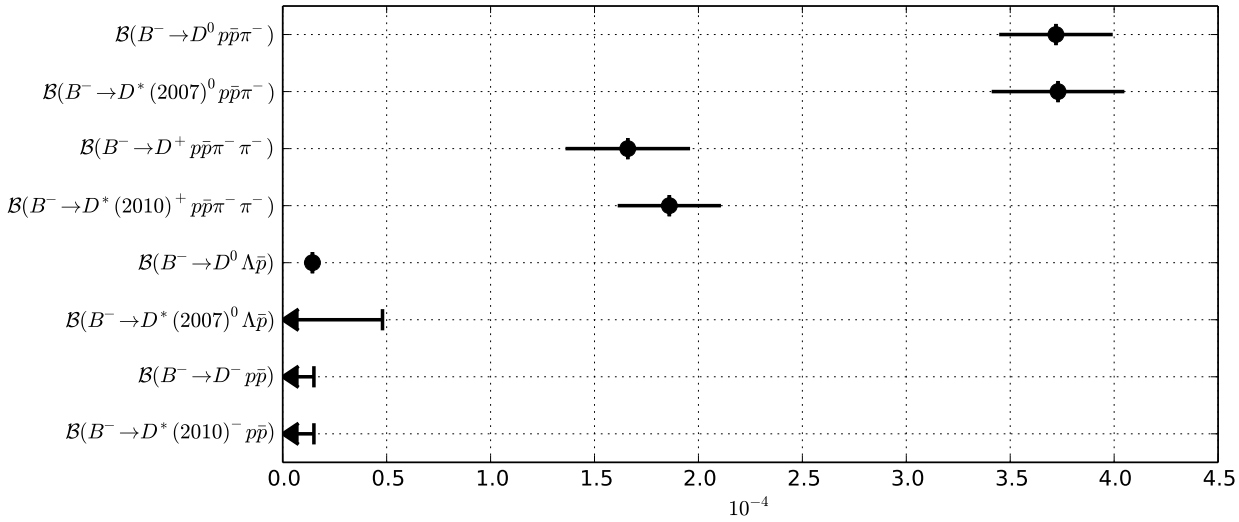

Figure 103: Summary of the averages from Table 131.

Table 132: Lepton number violating decays [10^{-6}].

Parameter	**Measurements**	**Average**
$\mathcal{B}(B^- \to D^- e^+ e^+)$	Belle [716]: < 2.6	< 2.6
$\mathcal{B}(B^- \to D^- e^+ \mu^+)$	Belle [716]: < 1.8	< 1.8
$\mathcal{B}(B^- \to D^- \mu^+ \mu^+)$	Belle [716]: < 1.0	< 1.0

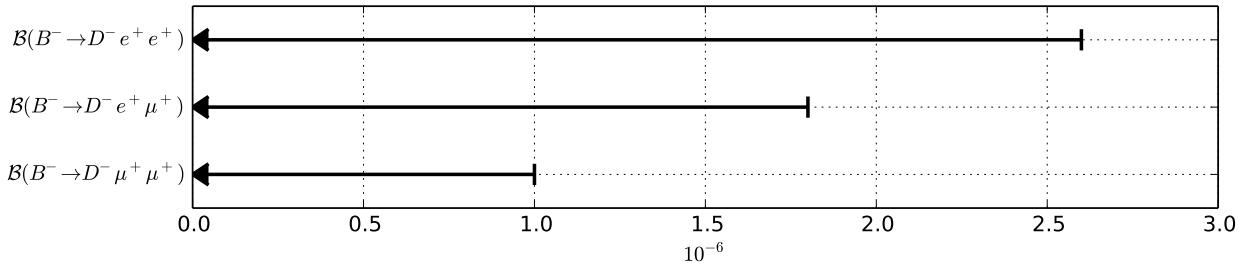

Figure 104: Summary of the averages from Table 132.

6.2.2 Decays to two open charm mesons

Averages of B^- decays to two open charm mesons are shown in Tables 133–138 and Figs. 105–109.

Table 133: Decays to $D^{(*)-}D^{(*)0}$ [10^{-3}].

Parameter	Measurements	Average
$\mathcal{B}(B^- \to D^- D^0)$	Belle [611]: $0.385 \pm 0.031 \pm 0.038$ *BABAR* [610]: $0.38 \pm 0.06 \pm 0.05$	0.384 ± 0.042
$\mathcal{B}(B^- \to D^{*0} D^-)$	*BABAR* [610]: $0.63 \pm 0.14 \pm 0.10$	0.63 ± 0.17
$\mathcal{B}(B^- \to D_s^- D^0)$	Belle [717]: $0.459 \pm 0.072 \pm 0.056$ *BABAR* [610]: $0.36 \pm 0.05 \pm 0.04$	0.385 ± 0.046
$\mathcal{B}(B^- \to D^*(2007)^0 D^*(2010)^-)$	*BABAR* [610]: $0.81 \pm 0.12 \pm 0.12$	0.81 ± 0.17

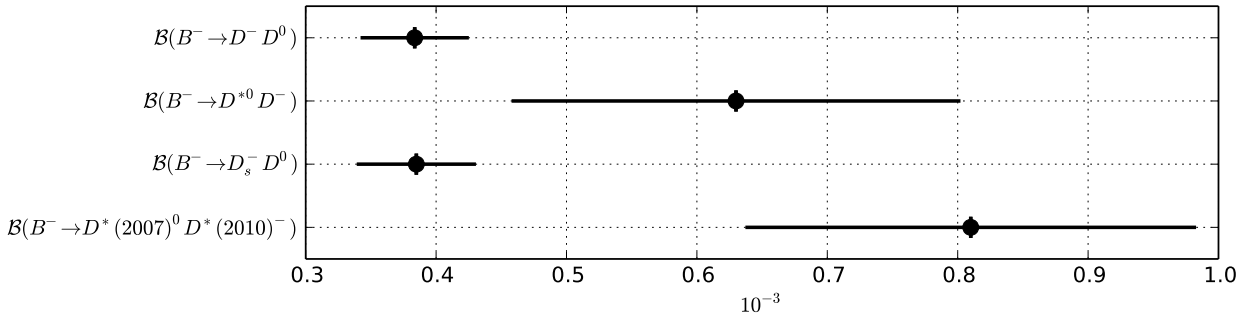

Figure 105: Summary of the averages from Table 133.

Table 134: Decays to two D mesons and a kaon [10^{-3}].

Parameter	Measurements	Average
$\mathcal{B}(B^- \to D^0 \overline{D}^0 K^-)$	Belle [718]: $2.22 \pm 0.22\,^{+0.26}_{-0.24}$ *BABAR* [612]: $1.31 \pm 0.07 \pm 0.12$	1.44 ± 0.13
$\mathcal{B}(B^- \to D^*(2007)^0 \overline{D}^0 K^-)$	*BABAR* [612]: $2.26 \pm 0.16 \pm 0.17$	2.26 ± 0.23
$\mathcal{B}(B^- \to D^0 \overline{D}^*(2007)^0 K^-)$	*BABAR* [612]: $6.32 \pm 0.19 \pm 0.45$	6.32 ± 0.49
$\mathcal{B}(B^- \to \overline{D}^*(2007)^0 D^*(2007)^0 K^-)$	*BABAR* [612]: $11.23 \pm 0.36 \pm 1.26$	11.23 ± 1.31
$\mathcal{B}(B^- \to D^0 \overline{D}^0 \pi^0 K^-)$	Belle [613]: $0.107 \pm 0.031\,^{+0.019}_{-0.033}$	$0.107\,^{+0.036}_{-0.045}$
$\mathcal{B}(B^- \to D^+ D^- K^-)$	Belle [719]: < 0.90 *BABAR* [612]: $0.22 \pm 0.05 \pm 0.05$	0.22 ± 0.07
$\mathcal{B}(B^- \to D^*(2010)^+ D^- K^-)$	*BABAR* [612]: $0.60 \pm 0.10 \pm 0.08$	0.60 ± 0.13
$\mathcal{B}(B^- \to D^+ D^*(2010)^- K^-)$	*BABAR* [612]: $0.63 \pm 0.09 \pm 0.06$	0.63 ± 0.11
$\mathcal{B}(B^- \to D^*(2010)^- D^*(2010)^+ K^-)$	*BABAR* [612]: $1.32 \pm 0.13 \pm 0.12$	1.32 ± 0.18
$\mathcal{B}(B^- \to D^0 D^- \overline{K}^0)$	*BABAR* [612]: $1.55 \pm 0.17 \pm 0.13$	1.55 ± 0.21
$\mathcal{B}(B^- \to D^*(2007)^0 D^- \overline{K}^0)$	*BABAR* [612]: $2.06 \pm 0.38 \pm 0.30$	2.06 ± 0.48
$\mathcal{B}(B^- \to D^0 D^*(2010)^- \overline{K}^0)$	*BABAR* [612]: $3.81 \pm 0.31 \pm 0.23$	3.81 ± 0.39
$\mathcal{B}(B^- \to D^*(2007)^0 D^*(2010)^- \overline{K}^0)$	*BABAR* [612]: $9.17 \pm 0.83 \pm 0.90$	9.17 ± 1.22

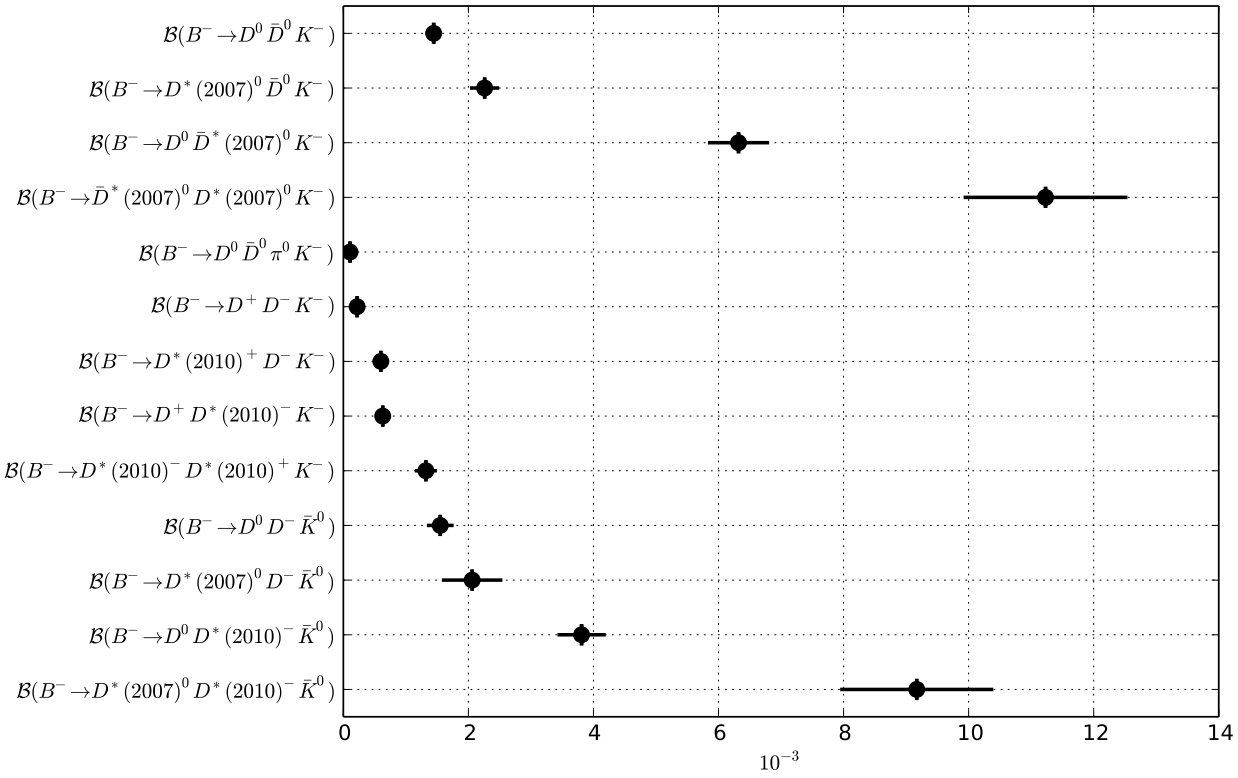

Figure 106: Summary of the averages from Table 134.

Table 135: Decays to $D_s^{(*)-} D^{(*)+}$ $[10^{-2}]$.

Parameter	**Measurements**	**Average**
$\mathcal{B}(B^- \to D_s^- D^0)$	Belle [720]: $0.852^{+0.039}_{-0.038} \pm 0.000$ *BABAR* [615]: $1.33 \pm 0.18 \pm 0.32$	0.857 ± 0.038
$\mathcal{B}(B^- \to D_s^- D^0) \times \mathcal{B}(D_s^- \to \phi(1020)\pi^-)$		
	BABAR [615]: $0.0400 \pm 0.0061 \pm 0.0061$	0.0400 ± 0.0086
$\mathcal{B}(B^- \to D_s^- D^*(2007)^0)$	*BABAR* [615]: $1.21 \pm 0.23 \pm 0.20$	1.21 ± 0.30
$\mathcal{B}(B^- \to D_s^- D^*(2007)^0) \times \mathcal{B}(D_s^- \to \phi(1020)\pi^-)$		
	BABAR [615]: $0.0295 \pm 0.0065 \pm 0.0036$	0.0295 ± 0.0074
$\mathcal{B}(B^- \to D_s^{*-} D^0)$	*BABAR* [615]: $0.93 \pm 0.18 \pm 0.19$	0.93 ± 0.26
$\mathcal{B}(B^- \to D_s^{*-} D^0) \times \mathcal{B}(D_s^- \to \phi(1020)\pi^-)$		
	BABAR [615]: $0.0313 \pm 0.0119 \pm 0.0058$	0.0313 ± 0.0132
$\mathcal{B}(B^- \to D_s^{*-} D^*(2007)^0)$	*BABAR* [615]: $1.70 \pm 0.26 \pm 0.24$	1.70 ± 0.35
$\mathcal{B}(B^- \to D_s^{*-} D^*(2007)^0) \times \mathcal{B}(D_s^- \to \phi(1020)\pi^-)$		
	BABAR [615]: $0.0857 \pm 0.0148 \pm 0.0112$	0.0857 ± 0.0186

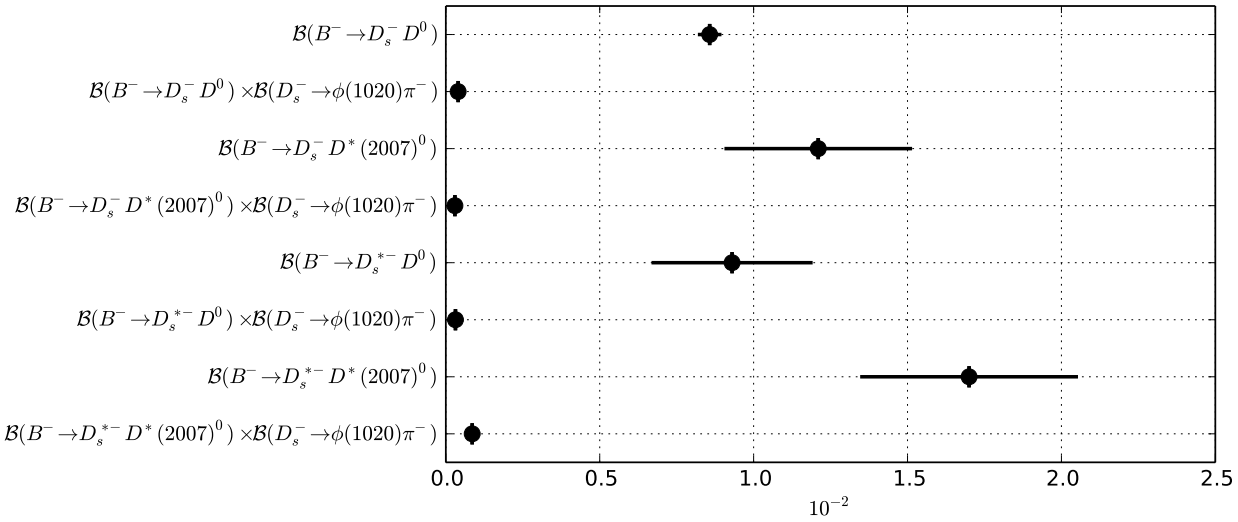

Figure 107: Summary of the averages from Table 135.

Table 136: Relative decay rates.

Parameter	**Measurements**	**Average**
$\mathcal{B}(B^- \to D_s^- D^0)/\mathcal{B}(\overline{B}^0 \to D_s^+ D^-)$		
	LHCb [620]: $1.22 \pm 0.02 \pm 0.07$	1.22 ± 0.07

Table 137: Absolute decays rates to excited D_s mesons $[10^{-3}]$.

Parameter	**Measurements**	**Average**
$\mathcal{B}(B^- \to D_{sJ}(2460)^- D^0)$	*BABAR* [615]: $4.3 \pm 1.6 \pm 1.3$	4.3 ± 2.1
$\mathcal{B}(B^- \to D_{sJ}(2460)^- D^*(2007)^0)$	*BABAR* [615]: $11.2 \pm 2.6 \pm 2.0$	11.2 ± 3.3

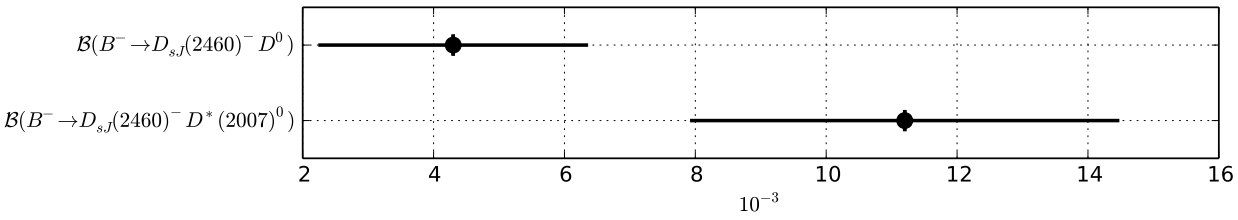

Figure 108: Summary of the averages from Table 137.

Table 138: Product decays rates to excited D_s mesons [10^{-3}].

Parameter	Measurements	Average
$\mathcal{B}(B^- \to D^0 D^*_{sJ}(2317)^-) \times \mathcal{B}(D^*_{sJ}(2317)^- \to D^-_s \pi^0)$		
	Belle [626]: $0.80^{+0.13}_{-0.12} \pm 0.12$	0.82 ± 0.17
	BABAR [625]: $1.0 \pm 0.3^{+0.4}_{-0.2}$	
$\mathcal{B}(B^- \to D^0 D^*_{sJ}(2317)^-) \times \mathcal{B}(D^*_{sJ}(2317)^- \to D^{*-}_s \gamma)$		
	Belle [624]: < 0.76	< 0.76
$\mathcal{B}(B^- \to D^*_{sJ}(2317)^- D^*(2007)^0) \times \mathcal{B}(D^*_{sJ}(2317)^- \to D^-_s \pi^0)$		
	BABAR [625]: $0.9 \pm 0.6^{+0.4}_{-0.3}$	$0.9^{+0.7}_{-0.7}$
$\mathcal{B}(B^- \to D^0 D_{sJ}(2460)^-) \times \mathcal{B}(D_{sJ}(2460)^- \to D^-_s \gamma)$		
	Belle [624]: $0.56^{+0.16}_{-0.15} \pm 0.17$	0.58 ± 0.18
	BABAR [625]: $0.6 \pm 0.2^{+0.2}_{-0.1}$	
$\mathcal{B}(B^- \to D^0 D_{sJ}(2460)^-) \times \mathcal{B}(D_{sJ}(2460)^- \to D^{*-}_s \gamma)$		
	Belle [624]: < 0.98	< 0.98
$\mathcal{B}(B^- \to D^0 D_{sJ}(2460)^-) \times \mathcal{B}(D_{sJ}(2460)^- \to D^-_s \pi^0)$		
	Belle [624]: < 0.27	< 0.27
$\mathcal{B}(B^- \to D^0 D_{sJ}(2460)^-) \times \mathcal{B}(D_{sJ}(2460)^- \to D^{*-}_s \pi^0)$		
	Belle [624]: $1.19^{+0.61}_{-0.49} \pm 0.36$	1.56 ± 0.57
	BABAR [625]: $2.7 \pm 0.7^{+1.0}_{-0.8}$	
$\mathcal{B}(B^- \to D^0 D_{sJ}(2460)^-) \times \mathcal{B}(D_{sJ}(2460)^- \to D^-_s \pi^+ \pi^-)$		
	Belle [624]: < 0.22	< 0.22
$\mathcal{B}(B^- \to D_{sJ}(2460)^- D^*(2007)^0) \times \mathcal{B}(D_{sJ}(2460)^- \to D^-_s \gamma)$		
	BABAR [625]: $1.4 \pm 0.4^{+0.6}_{-0.4}$	$1.4^{+0.7}_{-0.6}$
$\mathcal{B}(B^- \to D_{sJ}(2460)^- D^*(2007)^0) \times \mathcal{B}(D_{sJ}(2460)^- \to D^{*-}_s \pi^0)$		
	BABAR [625]: $7.6 \pm 1.7^{+3.2}_{-2.4}$	$7.6^{+3.6}_{-2.9}$
$\mathcal{B}(B^+ \to D_{s1}(2536)^+ \overline{D}^0) \times \mathcal{B}(D_{s1}(2536)^+ \to D^*(2007)^0 K^+ + D^*(2010)^+ K^0)$		
	Belle [623]: $0.397 \pm 0.085 \pm 0.056$	0.397 ± 0.102
$\mathcal{B}(B^- \to D_{s1}(2536)^- D^0) \times \mathcal{B}(D_{s1}(2536)^- \to \overline{D}^*(2007)^0 K^-)$		
	BABAR [622]: $0.216 \pm 0.052 \pm 0.045$	0.216 ± 0.069
$\mathcal{B}(B^- \to D_{s1}(2536)^- D^0) \times \mathcal{B}(D_{s1}(2536)^- \to D^*(2010)^- \overline{K}^0)$		
	BABAR [622]: $0.230 \pm 0.098 \pm 0.043$	0.230 ± 0.107
$\mathcal{B}(B^- \to D_{s1}(2536)^- \overline{D}^*(2007)^0) \times \mathcal{B}(D_{s1}(2536)^- \to \overline{D}^*(2007)^0 K^-)$		
	BABAR [622]: $0.546 \pm 0.117 \pm 0.104$	0.546 ± 0.157
$\mathcal{B}(B^- \to D_{s1}(2536)^- D^*(2007)^0) \times \mathcal{B}(D_{s1}(2536)^- \to D^*(2010)^- \overline{K}^0)$		
	BABAR [622]: < 1.069	< 1.069

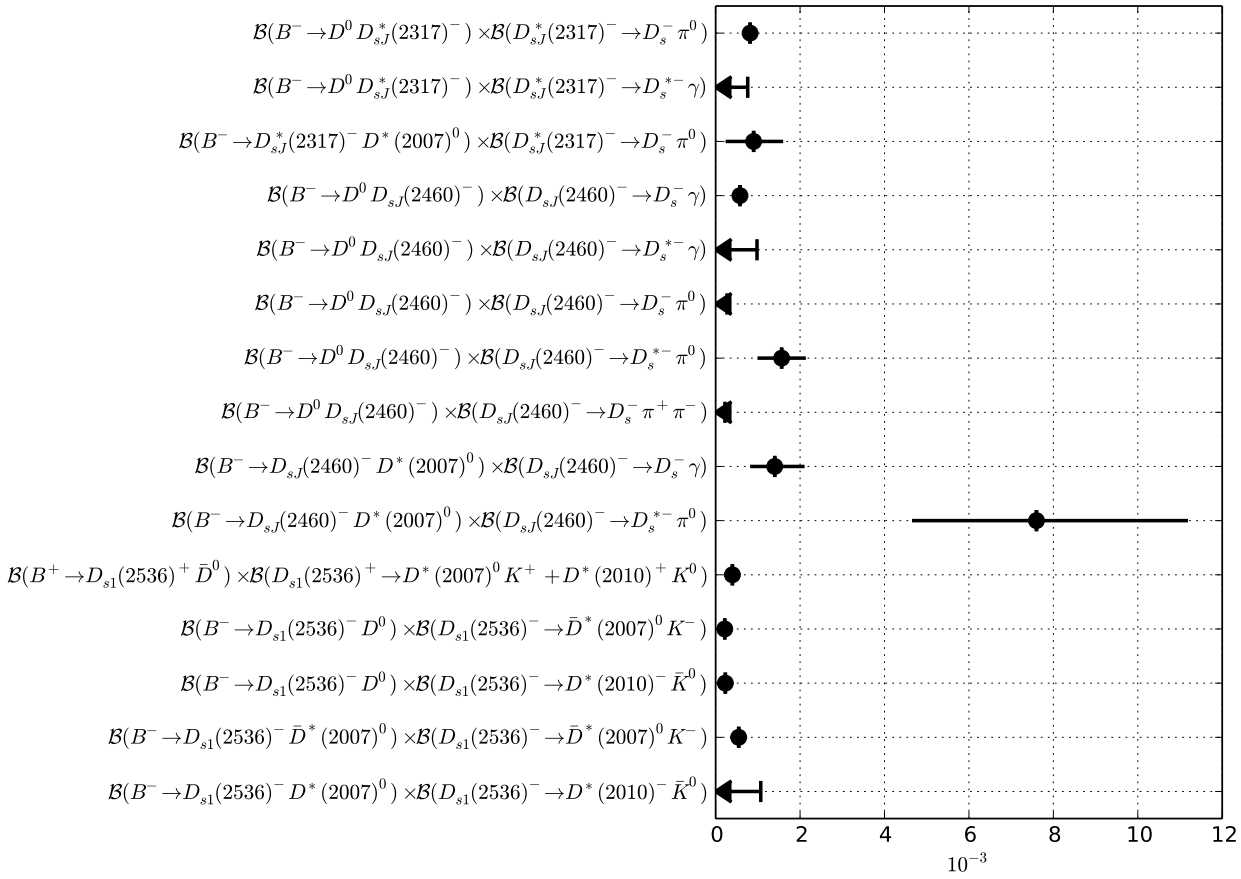

Figure 109: Summary of the averages from Table 138.

6.2.3 Decays to charmonium states

Averages of B^- decays to charmonium states are shown in Tables 139–144 and Figs. 110–115.

Table 139: Decays to J/ψ and one kaon [10^{-3}].

Parameter	Measurements	Average
$\mathcal{B}(B^- \to J/\psi K^-)$	Belle [628]: $1.01 \pm 0.02 \pm 0.07$ *BABAR* [691]: $0.81 \pm 0.13 \pm 0.07$ *BABAR* [6]: $1.061 \pm 0.015 \pm 0.048$	1.028 ± 0.040
$\mathcal{B}(B^- \to J/\psi K^*(892)^-)$	CDF [627]: $1.58 \pm 0.47 \pm 0.27$ Belle [721]: $1.28 \pm 0.07 \pm 0.14$ *BABAR* [6]: $1.454 \pm 0.047 \pm 0.097$	1.404 ± 0.089
$\mathcal{B}(B^- \to J/\psi K_1(1270)^-)$	Belle [635]: $1.80 \pm 0.34 \pm 0.39$	1.80 ± 0.52
$\mathcal{B}(B^- \to J/\psi K^-\pi^+\pi^-)$	CDF [722]: $0.69 \pm 0.18 \pm 0.12$ Belle [723]: $0.716 \pm 0.010 \pm 0.060$ *BABAR* [724]: $1.16 \pm 0.07 \pm 0.09$	0.807 ± 0.052
$\mathcal{B}(B^- \to J/\psi \eta K^-)$	Belle [636]: $0.127 \pm 0.011 \pm 0.011$ *BABAR* [637]: $0.108 \pm 0.023 \pm 0.024$	0.124 ± 0.014
$\mathcal{B}(B^- \to J/\psi \omega(782) K^-)$	*BABAR* [633]: $0.32 \pm 0.01\,^{+0.06}_{-0.03}$	$0.32\,^{+0.06}_{-0.03}$
$\mathcal{B}(B^- \to J/\psi \phi(1020) K^-)$	*BABAR* [634]: $0.044 \pm 0.014 \pm 0.005$	0.044 ± 0.015

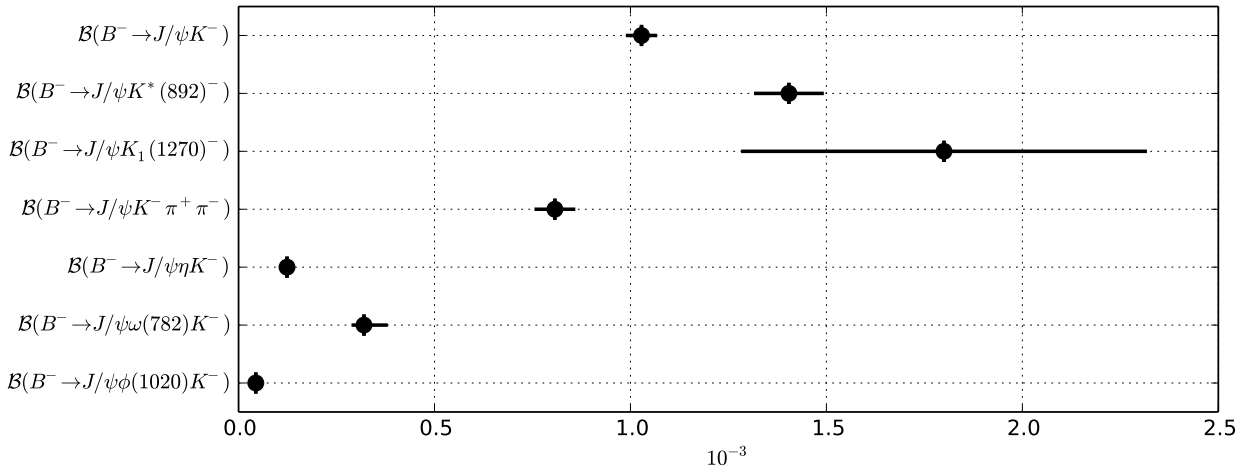

Figure 110: Summary of the averages from Table 139.

Table 140: Decays to charmonium other than J/ψ and one kaon [10^{-3}]

Parameter	Measurements	Average
$\mathcal{B}(B^- \to \psi(2S) K^-)$	CDF [630]: $0.55 \pm 0.10 \pm 0.06$ Belle [628]: 0.69 ± 0.06 *BABAR* [691]: $0.49 \pm 0.16 \pm 0.04$ *BABAR* [6]: $0.617 \pm 0.032 \pm 0.044$	0.632 ± 0.037
$\mathcal{B}(B^- \to \psi(2S) K^-) \times \mathcal{B}(\psi(2S) \to \chi_{c1}\gamma)$		
	Belle [640]: $0.77 \pm 0.08 \pm 0.09$	0.77 ± 0.12

continued from previous page

$\mathcal{B}(B^- \to \psi(2S)K^-) \times \mathcal{B}(\psi(2S) \to \chi_{c2}\gamma)$		
	Belle [640]: $0.63 \pm 0.09 \pm 0.06$	0.63 ± 0.11
$\mathcal{B}(B^- \to \psi(2S)K^*(892)^-)$	Belle [638]: $0.813 \pm 0.077 \pm 0.089$ *BABAR* [6]: $0.592 \pm 0.085 \pm 0.089$	0.707 ± 0.085
$\mathcal{B}(B^- \to \psi(2S)K^-\pi^+\pi^-)$	Belle [723]: $0.431 \pm 0.020 \pm 0.050$	0.431 ± 0.054
$\mathcal{B}(B^- \to \psi(3770)K^-)$	Belle [719]: $0.48 \pm 0.11 \pm 0.07$ *BABAR* [691]: $0.35 \pm 0.25 \pm 0.03$	0.45 ± 0.12
$\mathcal{B}(B^- \to \psi(3770)K^-) \times \mathcal{B}(\psi(3770) \to D^+D^-)$		
	BABAR [622]: $0.084 \pm 0.032 \pm 0.021$	0.084 ± 0.038
$\mathcal{B}(B^- \to \psi(3770)K^-) \times \mathcal{B}(\psi(3770) \to D^0\overline{D}^0)$		
	BABAR [622]: $0.141 \pm 0.030 \pm 0.022$	0.141 ± 0.037
$\mathcal{B}(B^- \to \chi_{c0}K^-)$	Belle [725]: $0.60\,^{+0.21}_{-0.18} \pm 0.11$ *BABAR* [691]: < 0.18 *BABAR* [261]: $0.184 \pm 0.032 \pm 0.031$	0.200 ± 0.044
$\mathcal{B}(B^- \to \chi_{c0}K^*(892)^-)$	*BABAR* [641]: < 2.86 *BABAR* [642]: $0.14 \pm 0.05 \pm 0.02$	0.14 ± 0.05
$\mathcal{B}(B^- \to \chi_{c1}K^-)$	CDF [722]: $1.55 \pm 0.54 \pm 0.20$ Belle [643]: $0.494 \pm 0.011 \pm 0.033$ *BABAR* [691]: $0.80 \pm 0.14 \pm 0.07$ *BABAR* [644]: $0.45 \pm 0.01 \pm 0.03$	0.479 ± 0.023
$\mathcal{B}(B^- \to \chi_{c1}K^*(892)^-)$	Belle [647]: $0.41 \pm 0.06 \pm 0.09$ *BABAR* [644]: $0.26 \pm 0.05 \pm 0.04$	0.30 ± 0.06
$\mathcal{B}(B^- \to \chi_{c1}K^-\pi^0)$	Belle [645]: $0.329 \pm 0.029 \pm 0.019$	0.329 ± 0.035
$\mathcal{B}(B^- \to \chi_{c1}\overline{K}^0\pi^-)$	Belle [645]: $0.575 \pm 0.026 \pm 0.032$ *BABAR* [646]: $0.552 \pm 0.026 \pm 0.061$	0.569 ± 0.035
$\mathcal{B}(B^- \to \chi_{c1}K^-\pi^+\pi^-)$	Belle [645]: $0.374 \pm 0.018 \pm 0.024$	0.374 ± 0.030
$\mathcal{B}(B^- \to \chi_{c2}K^-)$	Belle [643]: $0.0111\,^{+0.0036}_{-0.0034} \pm 0.0009$ *BABAR* [644]: $0.01 \pm 0.01 \pm 0.00$	0.0108 ± 0.0031
$\mathcal{B}(B^- \to \chi_{c2}K^*(892)^-)$	*BABAR* [644]: $0.011 \pm 0.043 \pm 0.055$	0.011 ± 0.070
$\mathcal{B}(B^- \to \chi_{c2}\overline{K}^0\pi^-)$	Belle [645]: $0.116 \pm 0.022 \pm 0.012$	0.116 ± 0.025
$\mathcal{B}(B^- \to \chi_{c2}K^-\pi^+\pi^-)$	Belle [645]: $0.134 \pm 0.017 \pm 0.009$	0.134 ± 0.019
$\mathcal{B}(B^- \to \eta_c K^-)$	Belle [648]: $1.25 \pm 0.14\,^{+0.39}_{-0.40}$ *BABAR* [691]: 0.87 ± 0.15 *BABAR* [650]: $1.29 \pm 0.09 \pm 0.38$	0.92 ± 0.14
$\mathcal{B}(B^- \to \eta_c K^-) \times \mathcal{B}(\eta_c \to K^0K^+\pi^+)$		
	Belle [726]: $0.000267 \pm 0.000014\,^{+0.000057}_{-0.000055}$	$0.000267\,^{+0.000059}_{-0.000057}$
$\mathcal{B}(B^- \to \eta_c K^-) \times \mathcal{B}(\eta_c \to p\overline{p})$		
	Belle [727]: $0.00142 \pm 0.00011\,^{+0.00016}_{-0.00020}$ *BABAR* [728]: $0.0018\,^{+0.0003}_{-0.0002} \pm 0.0002$	0.00153 ± 0.00018
$\mathcal{B}(B^- \to \eta_c K^-) \times \mathcal{B}(\eta_c \to \Lambda\overline{\Lambda})$		
	Belle [727]: $0.00095\,^{+0.00025\,+0.00008}_{-0.00022\,-0.00011}$	$0.00095\,^{+0.00026}_{-0.00025}$
$\mathcal{B}(B^- \to \eta_c K^*(892)^-)$	*BABAR* [649]: $1.21\,^{+0.43\,+0.64}_{-0.35\,-0.40}$	$1.21\,^{+0.77}_{-0.53}$
$\mathcal{B}(B^- \to \eta_c(2S)K^-)$	*BABAR* [691]: $0.34 \pm 0.18 \pm 0.03$	0.34 ± 0.18
$\mathcal{B}(B^- \to \eta_c(2S)K^-) \times \mathcal{B}(\eta_c(2S) \to K^0K^-\pi^+)$		

continued from previous page

	Belle [726]: $0.000034\,^{+0.000022\ +0.000005}_{-0.000015\ -0.000004}$	$0.000034\,^{+0.000023}_{-0.000016}$
$\mathcal{B}(B^- \to h_c(1P)K^-)$	Belle [729]: < 0.0038	< 0.0038
$\mathcal{B}(B^- \to h_c(1P)K^-) \times \mathcal{B}(h_c(1P) \to \eta_c\gamma)$		
	BABAR [651]: < 0.048	< 0.048
$\mathcal{B}(B^- \to h_c(1P)K^-) \times \mathcal{B}(h_c(1P) \to J/\psi\pi^+\pi^-)$		
	BABAR [724]: < 0.0034	< 0.0034

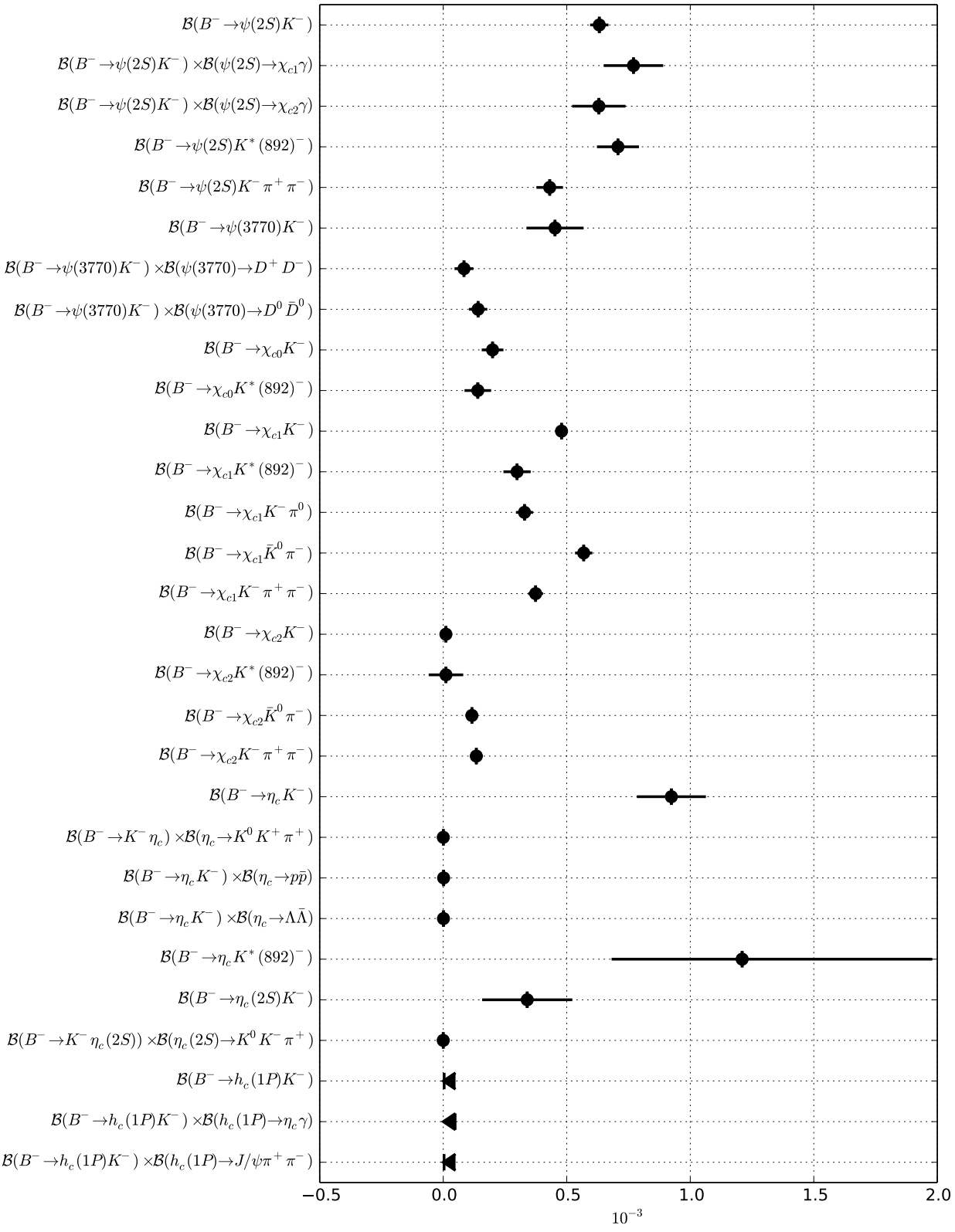

Figure 111: Summary of the averages from Table 140.

Table 141: Decays to charmonium and light mesons [10^{-5}].

Parameter	Measurements	Average
$\mathcal{B}(B^- \to J/\psi\pi^-)$	LHCb [730]: $3.88 \pm 0.11 \pm 0.15$ Belle [628]: $3.8 \pm 0.6 \pm 0.3$ *BABAR* [731]: $5.37 \pm 0.45 \pm 0.24$	4.04 ± 0.17
$\mathcal{B}(B^- \to J/\psi\pi^-\pi^0)$	*BABAR* [653]: < 0.73	< 0.73
$\mathcal{B}(B^- \to J/\psi\rho^-(770))$	*BABAR* [653]: $5 \pm 1 \pm 0$	5 ± 1
$\mathcal{B}(B^- \to \psi(2S)\pi^-)$	LHCb [730]: $2.52 \pm 0.26 \pm 0.15$	2.52 ± 0.30
$\mathcal{B}(B^- \to \chi_{c0}\pi^-)$	*BABAR* [732]: < 6.1	< 6.1
$\mathcal{B}(B^- \to \chi_{c1}\pi^-)$	Belle [733]: $2.2 \pm 0.4 \pm 0.3$	2.2 ± 0.5

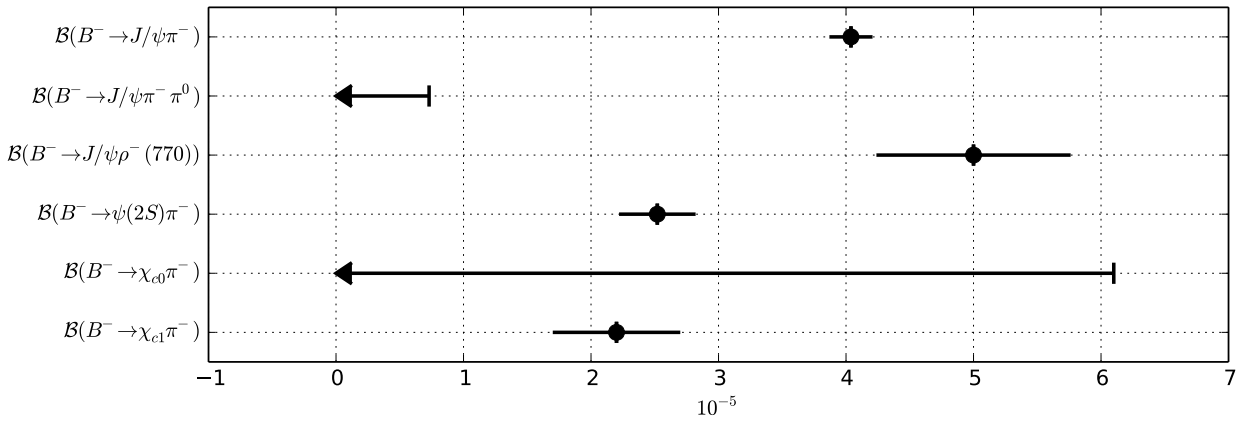

Figure 112: Summary of the averages from Table 141.

Table 142: Decays to J/ψ and a heavy mesons [10^{-4}].

Parameter	Measurements	Average
$\mathcal{B}(B^- \to J/\psi D^-)$	*BABAR* [666]: < 1.2	< 1.2
$\mathcal{B}(B^- \to J/\psi D^0\pi^-)$	Belle [665]: < 0.25 *BABAR* [724]: < 0.52	< 0.25

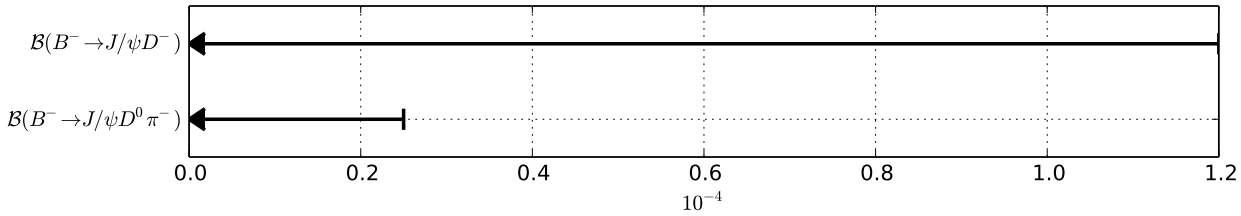

Figure 113: Summary of the averages from Table 142.

Table 143: Decays with baryons $[10^{-5}]$.

Parameter	**Measurements**	**Average**
$\mathcal{B}(B^- \to J/\psi p\overline{p}\pi^-)$	LHCb [662]: < 0.050	< 0.050
$\mathcal{B}(B^- \to J/\psi \Lambda\overline{p})$	Belle [663]: $1.16 \pm 0.28\,^{+0.18}_{-0.23}$ *BABAR* [664]: $1.16\,^{+0.74\ +0.42}_{-0.53\ -0.18}$	1.16 ± 0.31
$\mathcal{B}(B^- \to J/\psi \Sigma^0\overline{p})$	Belle [663]: < 1.1	< 1.1
$\mathcal{B}(B^- \to J/\psi K^-) \times \mathcal{B}(J/\psi \to \Lambda\overline{\Lambda})$	Belle [727]: $0.20\,^{+0.03}_{-0.03} \pm 0.03$	$0.20\,^{+0.05}_{-0.04}$
$\mathcal{B}(B^- \to J/\psi K^-) \times \mathcal{B}(J/\psi \to p\overline{p})$	Belle [727]: $0.221 \pm 0.013 \pm 0.010$ *BABAR* [728]: $0.22 \pm 0.02 \pm 0.01$	0.221 ± 0.013

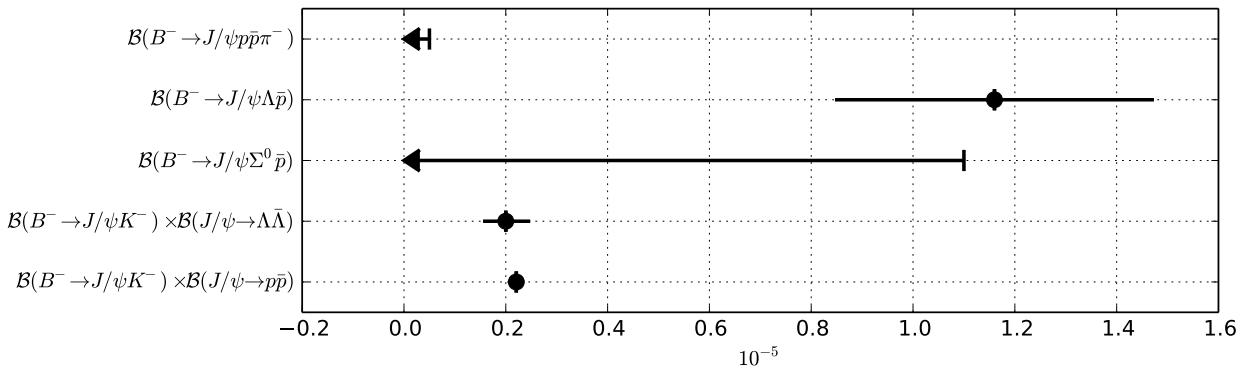

Figure 114: Summary of the averages from Table 143.

Table 144: Relative decay rates.

Parameter	Measurements	Average
$\mathcal{B}(B^- \to J/\psi K^*(892)^-)/\mathcal{B}(B^- \to J/\psi K^-)$		
	CDF [667]: $1.92 \pm 0.60 \pm 0.17$	1.38 ± 0.09
	BABAR [6]: $1.37 \pm 0.05 \pm 0.08$	
$\mathcal{B}(B^- \to J/\psi K_1(1270)^-)/\mathcal{B}(B^- \to J/\psi K^-)$		
	Belle [635]: $1.80 \pm 0.34 \pm 0.34$	1.80 ± 0.48
$\mathcal{B}(B^- \to J/\psi K_1^-(1400))/\mathcal{B}(B^- \to J/\psi K_1(1270)^-)$		
	Belle [635]: < 0.30	< 0.30
$\frac{\mathcal{B}(B^- \to J/\psi \pi^-)}{\mathcal{B}(B^- \to J/\psi K^-)}$	LHCb [734]: $0.0394 \pm 0.0039 \pm 0.0017$	
	CDF [735]: $0.050\,^{+0.019}_{-0.017} \pm 0.001$	0.0464 ± 0.0029
	CDF [736]: $0.0486 \pm 0.0082 \pm 0.0015$	
	BABAR [731]: $0.0537 \pm 0.0045 \pm 0.0011$	
$\mathcal{B}(B^- \to \psi(2S)K^-)/\mathcal{B}(B^- \to J/\psi K^-)$		
	LHCb [670]: $0.594 \pm 0.006 \pm 0.022$	0.598 ± 0.022
	D0 [737]: $0.65 \pm 0.04 \pm 0.08$	
$\mathcal{B}(B^- \to \psi(2S)K^-) \times \mathcal{B}(\psi(2S) \to p\overline{p})/\mathcal{B}(B^- \to J/\psi K^-) \times \mathcal{B}(J/\psi \to p\overline{p})$		
	LHCb [738]: $0.080 \pm 0.012 \pm 0.009$	0.080 ± 0.015
$\mathcal{B}(B^- \to \psi(2S)K^*(892)^-)/\mathcal{B}(B^- \to \psi(2S)K^-)$		
	BABAR [6]: $0.96 \pm 0.15 \pm 0.09$	0.96 ± 0.17
$\mathcal{B}(B^- \to \chi_{c0}K^-)/\mathcal{B}(B^- \to J/\psi K^-)$		
	Belle [725]: $0.60\,^{+0.21}_{-0.18} \pm 0.09$	$0.60\,^{+0.23}_{-0.20}$
$\mathcal{B}(B^- \to \chi_{c1}K^*(892)^-)/\mathcal{B}(B^- \to \chi_{c1}K^-)$		
	BABAR [6]: $0.51 \pm 0.17 \pm 0.16$	0.51 ± 0.23
$\mathcal{B}(B^- \to \chi_{c1}\pi^-)/\mathcal{B}(B^- \to \chi_{c1}K^-)$		
	Belle [733]: $0.043 \pm 0.008 \pm 0.003$	0.043 ± 0.009
$\mathcal{B}(B^- \to \chi_{c1}\overline{K}^0\pi^-)/\mathcal{B}(B^- \to J/\psi\overline{K}^0\pi^-)$		
	BABAR [646]: $0.501 \pm 0.024 \pm 0.055$	0.501 ± 0.060
$\frac{\mathcal{B}(B^- \to \eta_c K^-)}{\mathcal{B}(B^- \to J/\psi K^-)}$	*BABAR* [691]: $1.06 \pm 0.23 \pm 0.04$	1.12 ± 0.20
	BABAR [650]: $1.28 \pm 0.10 \pm 0.38$	
$\mathcal{B}(B^- \to \eta_c K^-) \times \mathcal{B}(\eta_c \to p\overline{p})/\mathcal{B}(B^- \to J/\psi K^-) \times \mathcal{B}(J/\psi \to p\overline{p})$		
	LHCb [738]: $0.578 \pm 0.035 \pm 0.027$	0.578 ± 0.044
$\mathcal{B}(B^- \to h_c(1P)K^-) \times \mathcal{B}(h_c(1P) \to \eta_c\gamma)/\mathcal{B}(B^- \to \eta_c K^-)$		
	BABAR [672]: < 0.058	< 0.058

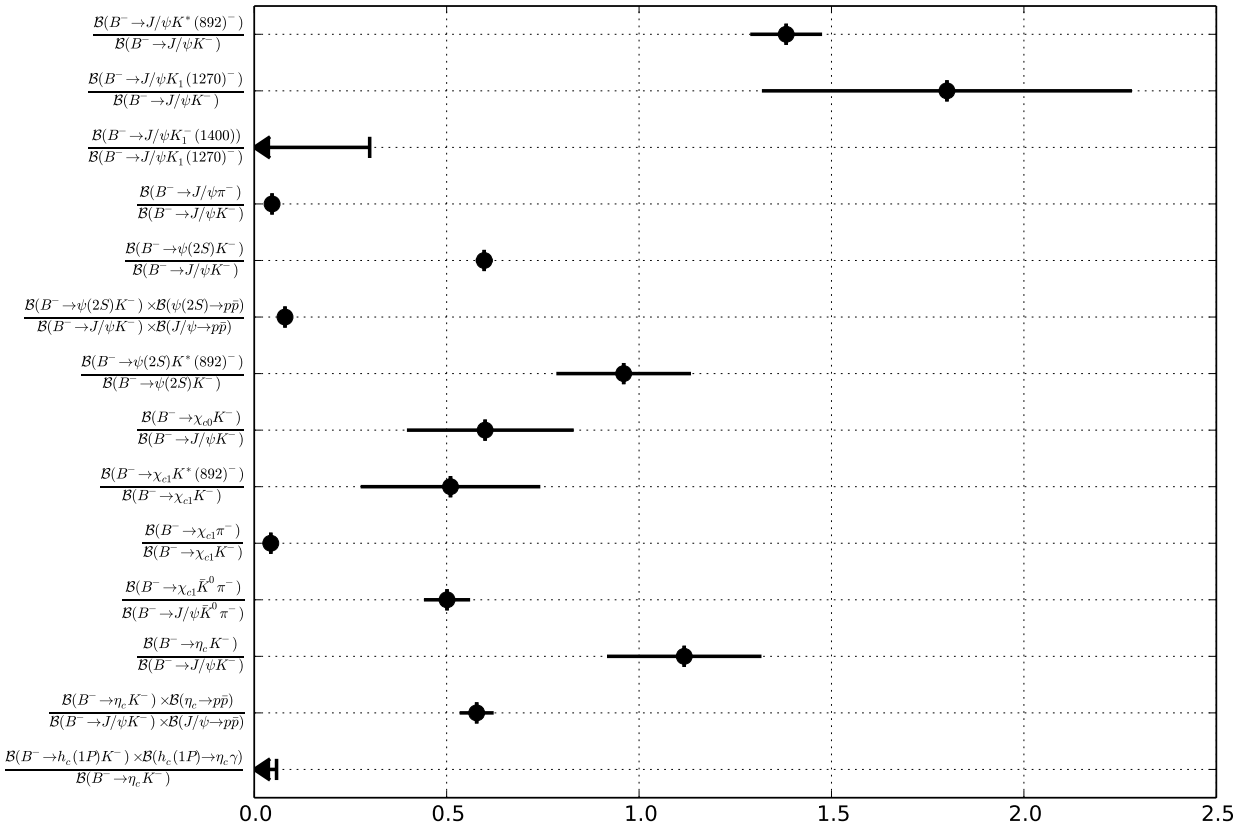

Figure 115: Summary of the averages from Table 144.

6.2.4 Decays to charm baryons

Averages of B^- decays to charm baryons are shown in Tables 145–146 and Figs. 116–117.

Table 145: Absolute (product) decay rates [10^{-3}].

Parameter	Measurements	Average
$\mathcal{B}(B^-\to\Lambda_c^+\Lambda_c^-K^-)$	Belle [686]: $0.65\,^{+0.10}_{-0.09}\pm0.36$ *BABAR* [683]: $1.14\pm0.15\pm0.62$	0.41 ± 0.32
$\mathcal{B}(B^-\to\Xi_c^0\Lambda_c^-)\times\mathcal{B}(\Xi_c^0\to\Xi^-\pi^+)$	Belle [682]: $0.048\,^{+0.010}_{-0.009}\pm0.016$ *BABAR* [683]: $0.0208\pm0.0065\pm0.0061$	0.0221 ± 0.0089
$\mathcal{B}(B^-\to\Lambda_c^+\overline{p}\pi^-)$	Belle [675]: $0.187\,^{+0.043}_{-0.040}\pm0.056$ *BABAR* [680]: $0.338\pm0.012\pm0.089$	0.208 ± 0.069
$\mathcal{B}(B^-\to\Sigma_c^0\overline{p})$	Belle [675]: $0.045\,^{+0.026}_{-0.019}\pm0.014$	$0.045\,^{+0.029}_{-0.024}$
$\mathcal{B}(B^-\to\Sigma_c^{*0}\overline{p})$	Belle [675]: <0.046	<0.046
$\mathcal{B}(B^-\to\Sigma_c^{++}\overline{p}\pi^-\pi^-)$	*BABAR* [739]: $0.298\pm0.016\pm0.078$	0.298 ± 0.080

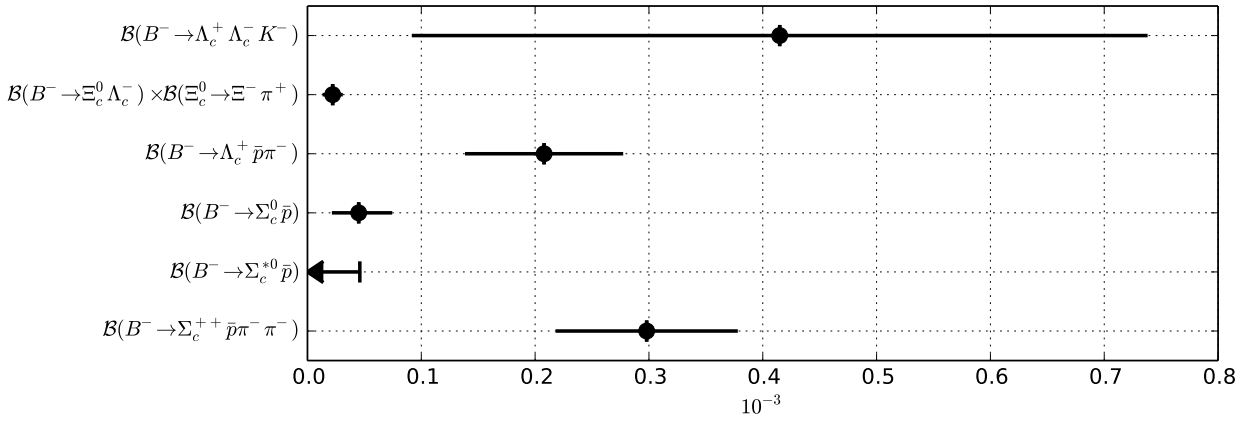

Figure 116: Summary of the averages from Table 145.

Table 146: Relative decay rates.

Parameter	**Measurements**	**Average**
$\mathcal{B}(B^- \to \Lambda_c^+ \overline{p}\pi^-)/\mathcal{B}(\overline{B}^0 \to \Lambda_c^+ \overline{p})$		
	BABAR [680]: $15.4 \pm 1.8 \pm 0.3$	15.4 ± 1.8
$\mathcal{B}(B^- \to \Sigma_c(2455)^0 \overline{p})/\mathcal{B}(B^- \to \Lambda_c^+ \overline{p}\pi^-)$		
	BABAR [680]: $0.123 \pm 0.012 \pm 0.008$	0.123 ± 0.014
$\mathcal{B}(B^- \to \Sigma_c(2800)^0 \overline{p})/\mathcal{B}(B^- \to \Lambda_c^+ \overline{p}\pi^-)$		
	BABAR [680]: $0.117 \pm 0.023 \pm 0.024$	0.117 ± 0.033

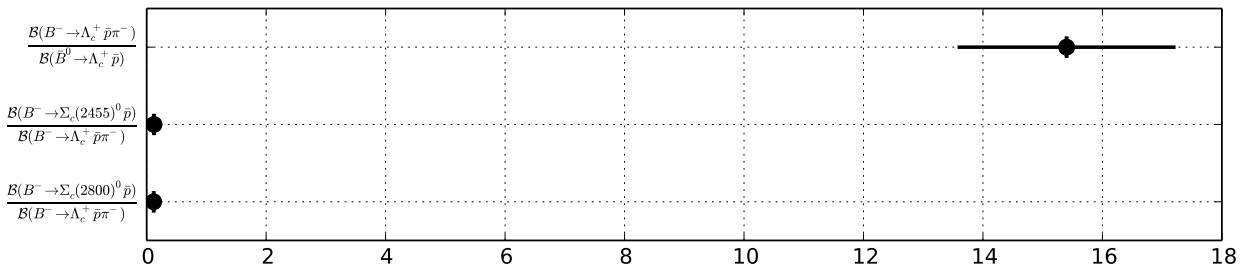

Figure 117: Summary of the averages from Table 146.

6.2.5 Decays to other (XYZ) states

Averages of B^- decays to other (XYZ) states are shown in Tables 147–151 and Figs. 118–121.

Table 147: Absolute decay rates [10^{-4}].

Parameter	Measurements	Average
$\mathcal{B}(B^- \to X(3872)K^-)$	*BABAR* [691]: < 3.2	< 3.2

Table 148: Product decay rates to $X(3872)$ [10^{-4}].

Parameter	Measurements	Average
$\mathcal{B}(B^- \to X(3872)K^-) \times \mathcal{B}(X(3872) \to \overline{D}^*(2007)^0 D^0)$		
	BABAR [622]: $1.67 \pm 0.36 \pm 0.47$	1.67 ± 0.59
$\mathcal{B}(B^- \to X(3872)K^-) \times \mathcal{B}(X(3872) \to D^0 \overline{D}^0 \pi^0)$		
	Belle [719]: < 0.6	< 0.6
$\mathcal{B}(B^- \to X(3872)K^-) \times \mathcal{B}(X(3872) \to D^0 \overline{D}^0)$		
	Belle [719]: < 0.6	< 0.6
$\mathcal{B}(B^- \to X(3872)K^-) \times \mathcal{B}(X(3872) \to D^+ D^-)$		
	Belle [719]: < 0.4	< 0.4
$\mathcal{B}(B^- \to K^- X(3872)) \times \mathcal{B}(X(3872) \to J/\psi \pi^+ \pi^-)$		
	Belle [740]: $0.131 \pm 0.024 \pm 0.013$ *BABAR* [689]: $0.084 \pm 0.015 \pm 0.007$	0.097 ± 0.014
$\mathcal{B}(B^- \to X(3872)K^-) \times \mathcal{B}(X(3872) \to J/\psi \omega(782))$		
	BABAR [633]: $0.06 \pm 0.02 \pm 0.01$	0.06 ± 0.02
$\mathcal{B}(B^- \to X(3872)K^-) \times \mathcal{B}(X(3872) \to J/\psi \eta)$	*BABAR* [637]: < 0.077	< 0.077
$\mathcal{B}(B^- \to X(3872)K^-) \times \mathcal{B}(X(3872) \to J/\psi \gamma)$		
	Belle [643]: $0.0178\,^{+0.0048}_{-0.0044} \pm 0.0012$ *BABAR* [644]: $0.028 \pm 0.008 \pm 0.001$	0.0204 ± 0.0041
$\mathcal{B}(B^- \to X(3872)K^*(892)^-) \times \mathcal{B}(X(3872) \to J/\psi \gamma)$		
	BABAR [644]: $0.007 \pm 0.026 \pm 0.001$	0.007 ± 0.026
$\mathcal{B}(B^- \to X(3872)K^-) \times \mathcal{B}(X(3872) \to \psi(2S) \gamma)$		
	Belle [643]: < 0.0345 *BABAR* [644]: $0.095 \pm 0.027 \pm 0.006$	0.095 ± 0.028
$\mathcal{B}(B^- \to X(3872)K^*(892)^-) \times \mathcal{B}(X(3872) \to \psi(2S) \gamma)$		
	BABAR [644]: $0.064 \pm 0.098 \pm 0.096$	0.064 ± 0.137
$\mathcal{B}(B^- \to X(3872)K^-) \times \mathcal{B}(X(3872) \to \chi_{c1} \gamma)$		
	Belle [640]: < 0.019	< 0.019
$\mathcal{B}(B^- \to X(3872)K^-) \times \mathcal{B}(X(3872) \to \chi_{c2} \gamma)$		
	Belle [640]: < 0.067	< 0.067

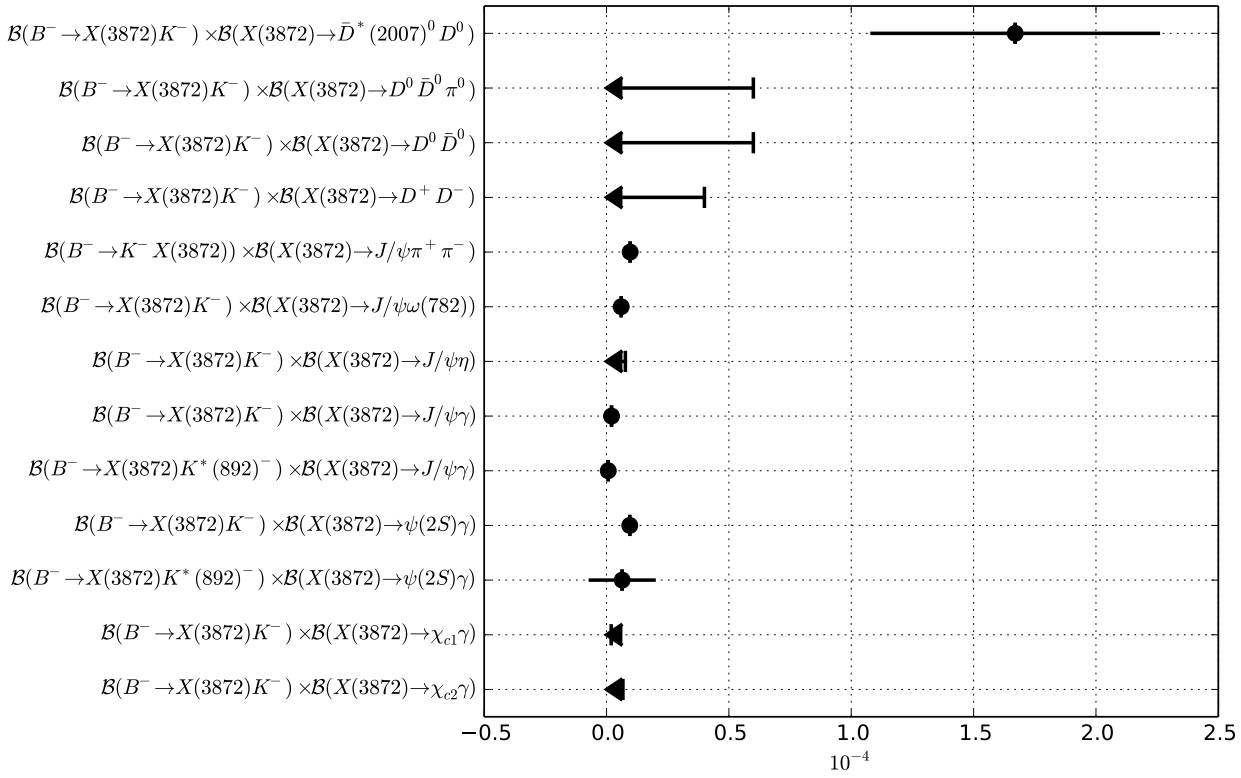

Figure 118: Summary of the averages from Table 148.

Table 149: Product decay rates to neutral states other than $X(3872)$ [10^{-5}].

Parameter	**Measurements**	**Average**
$\mathcal{B}(B^- \to X(3823)K^-) \times \mathcal{B}(X(3823) \to \chi_{c1}\gamma)$		
	Belle [640]: $0.97 \pm 0.28 \pm 0.11$	0.97 ± 0.30
$\mathcal{B}(B^- \to X(3823)K^-) \times \mathcal{B}(X(3823) \to \chi_{c2}\gamma)$		
	Belle [640]: < 0.36	< 0.36
$\mathcal{B}(B^- \to Y(3940)K^-) \times \mathcal{B}(Y(3940) \to J/\psi\gamma)$		
	BABAR [741]: < 1.4	< 1.4
$\mathcal{B}(B^- \to Y(3940)K^-) \times \mathcal{B}(Y(3940) \to J/\psi\omega(782))$		
	BABAR [633]: $3.0\,^{+0.7\ +0.5}_{-0.6\ -0.3}$	$3.0\,^{+0.9}_{-0.7}$
$\mathcal{B}(B^- \to Y(4260)K^-) \times \mathcal{B}(Y(4260) \to J/\psi\pi^+\pi^-)$		
	BABAR [742]: $2.0 \pm 0.7 \pm 0.2$	2.0 ± 0.7

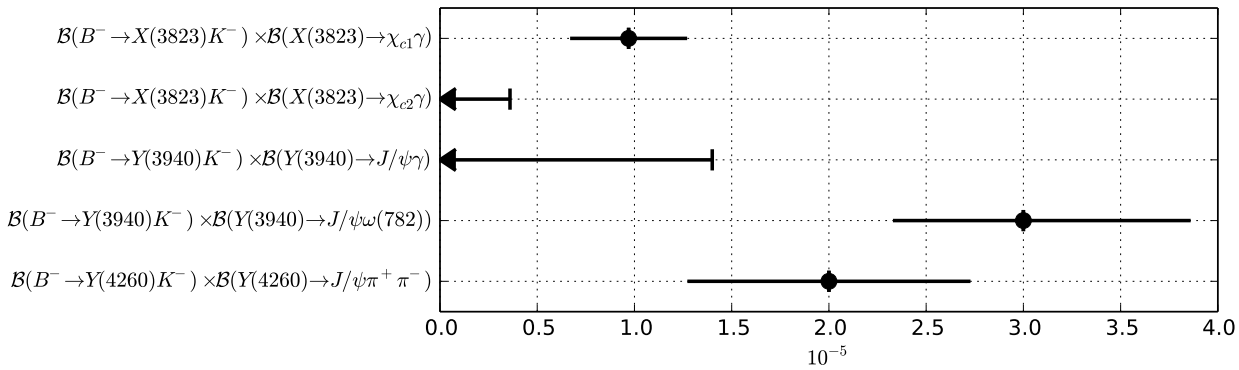

Figure 119: Summary of the averages from Table 149.

Table 150: Relative product decay rates to states with $s\overline{s}$ component.

Parameter	**Measurements**	**Average**
$\mathcal{B}(B^- \to X(4140)K^-) \times \mathcal{B}(X(4140) \to J/\psi\phi(1020))/\mathcal{B}(B^- \to J/\psi\phi(1020)K^-)$		
	LHCb [743]: $0.130 \pm 0.032\,^{+0.047}_{-0.020}$	
	D0 [744]: $0.21 \pm 0.08 \pm 0.04$	0.149 ± 0.031
	CDF [745]: $0.149 \pm 0.039 \pm 0.024$	
$\mathcal{B}(B^- \to X(4274)K^-) \times \mathcal{B}(X(4274) \to J/\psi\phi(1020))/\mathcal{B}(B^- \to J/\psi\phi(1020)K^-)$		
	LHCb [743]: $0.071 \pm 0.025\,^{+0.035}_{-0.024}$	$0.071\,^{+0.043}_{-0.035}$

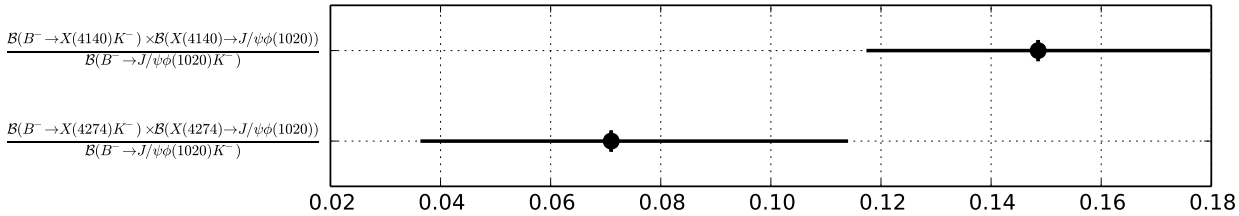

Figure 120: Summary of the averages from Table 150.

Table 151: Product decay rates to charged states [10^{-5}].

Parameter	Measurements	Average
$\mathcal{B}(B^- \to X(3872)^- \overline{K}^0) \times \mathcal{B}(X(3872)^- \to J/\psi\pi^-\pi^0)$		
	BABAR [692]: < 2.2	< 2.2
$\mathcal{B}(B^- \to Z(4430)^- \overline{K}^0) \times \mathcal{B}(Z(4430)^- \to J/\psi\pi^-)$		
	BABAR [693]: $-0.1 \pm 0.8 \pm 0.0$	-0.1 ± 0.8
$\mathcal{B}(B^- \to Z(4430)^- \overline{K}^0) \times \mathcal{B}(Z(4430)^- \to \psi(2S)\pi^-)$		
	BABAR [693]: $2.0 \pm 1.7 \pm 0.0$	2.0 ± 1.7

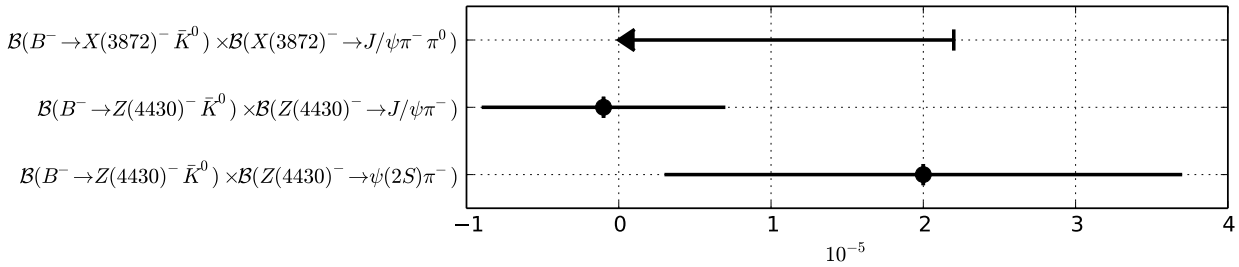

Figure 121: Summary of the averages from Table 151.

6.3 Decays of admixtures of $\overline{B}^0$ / B^- mesons

Measurements of $\overline{B}^0$ / B^- decays to charmed hadrons are summarized in Sections 6.3.1 to 6.3.3.

6.3.1 Decays to two open charm mesons

Averages of $\overline{B}^0$ / B^- decays to two open charm mesons are shown in Table 152.

Table 152: B decays to double charm [10^{-4}].

Parameter	Measurements	Average
$\mathcal{B}(B \to D^0\overline{D}^0\pi^0 K)$	Belle [613]: $1.27 \pm 0.31\,^{+0.22}_{-0.39}$	$1.27\,^{+0.38}_{-0.50}$

6.3.2 Decays to charmonium states

Averages of $\overline{B}^0$ / B^- decays to charmonium states are shown in Tables 153–157 and Figs. 122–126.

Table 153: Decay amplitudes for parallel transverse polarization.

Parameter	Measurements	Average
$\|\mathcal{A}_\parallel\|^2(B \to J/\psi K^*)$	Belle [311]: $0.231 \pm 0.012 \pm 0.008$ *BABAR* [310]: $0.211 \pm 0.010 \pm 0.006$	0.219 ± 0.009
$\|\mathcal{A}_\parallel\|^2(B \to \chi_{c1} K^*)$	*BABAR* [310]: $0.20 \pm 0.07 \pm 0.04$	0.20 ± 0.08
$\|\mathcal{A}_\parallel\|^2(B \to \psi(2S) K^*)$	*BABAR* [310]: $0.22 \pm 0.06 \pm 0.02$	0.22 ± 0.06

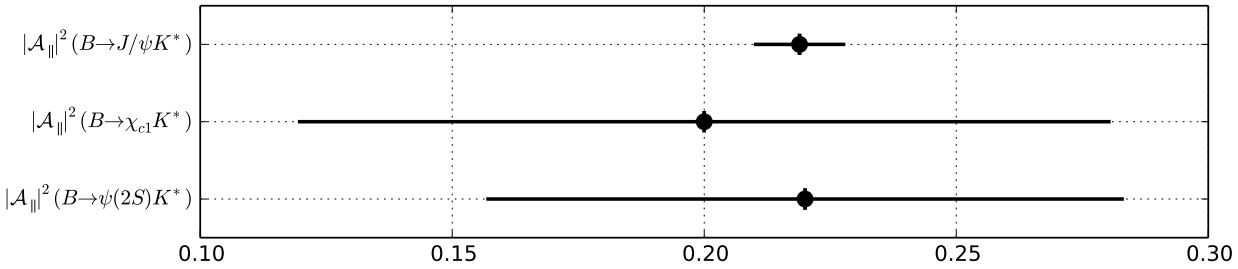

Figure 122: Summary of the averages from Table 153.

Table 154: Decay amplitudes for perpendicular transverse polarization.

Parameter	Measurements	Average
$\|\mathcal{A}_\perp\|^2(B \to J/\psi K^*)$	Belle [311]: $0.195 \pm 0.012 \pm 0.008$ *BABAR* [310]: $0.233 \pm 0.010 \pm 0.005$	0.219 ± 0.009
$\|\mathcal{A}_\perp\|^2(B \to \chi_{c1} K^*)$	*BABAR* [310]: $0.03 \pm 0.04 \pm 0.02$	0.03 ± 0.04
$\|\mathcal{A}_\perp\|^2(B \to \psi(2S) K^*)$	*BABAR* [310]: $0.30 \pm 0.06 \pm 0.02$	0.30 ± 0.06

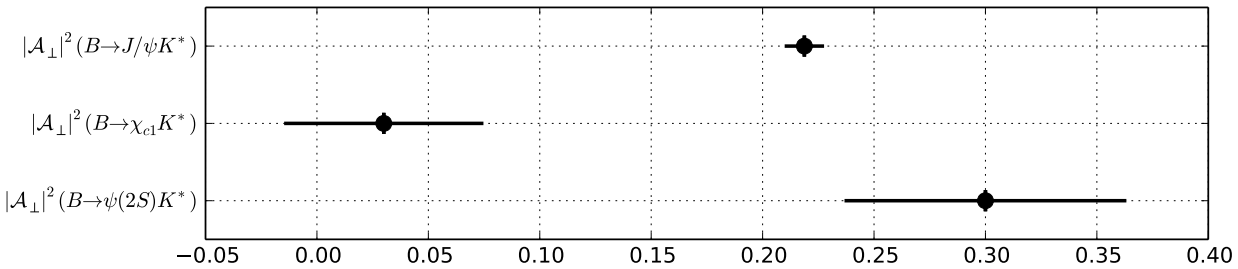

Figure 123: Summary of the averages from Table 154.

Table 155: Decay amplitudes for longitudinal polarization.

Parameter	Measurements	Average
$\|\mathcal{A}_0\|^2(B \to J/\psi K^*)$	Belle [311]: $0.574 \pm 0.012 \pm 0.009$ *BABAR* [310]: $0.556 \pm 0.009 \pm 0.010$	0.564 ± 0.010
$\|\mathcal{A}_0\|^2(B \to \chi_{c1} K^*)$	*BABAR* [310]: $0.77 \pm 0.07 \pm 0.04$	0.77 ± 0.08
$\|\mathcal{A}_0\|^2(B \to \psi(2S) K^*)$	*BABAR* [310]: $0.48 \pm 0.05 \pm 0.02$	0.48 ± 0.05

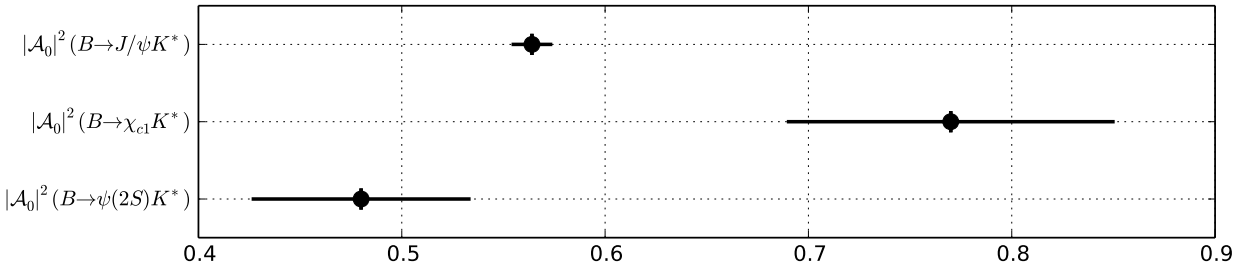

Figure 124: Summary of the averages from Table 155.

Table 156: Relative phases of parallel transverse polarization decay amplitudes.

Parameter	Measurements	Average
$\delta_\parallel(B \to J/\psi K^*)$	Belle [311]: $-2.887 \pm 0.090 \pm 0.008$ *BABAR* [310]: $-2.93 \pm 0.08 \pm 0.04$	-2.909 ± 0.064
$\delta_\parallel(B \to \chi_{c1} K^*)$	*BABAR* [310]: $0.0 \pm 0.3 \pm 0.1$	0.0 ± 0.3
$\delta_\parallel(B \to \psi(2S) K^*)$	*BABAR* [310]: $-2.8 \pm 0.4 \pm 0.1$	-2.8 ± 0.4

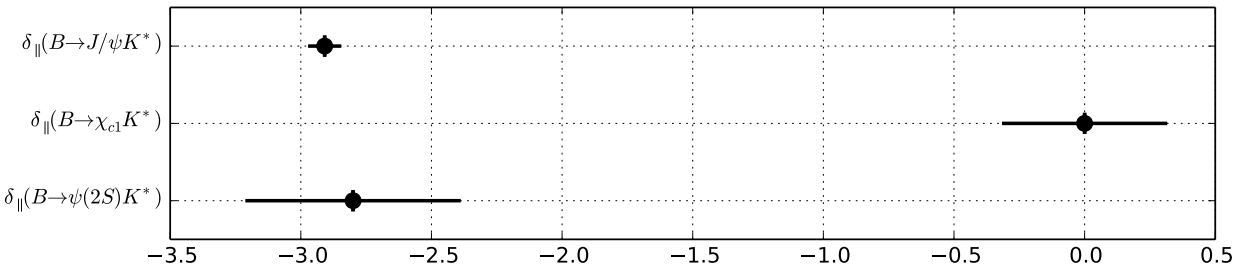

Figure 125: Summary of the averages from Table 156.

Table 157: Relative phases of perpendicular transverse polarization decay amplitudes.

Parameter	Measurements	Average
$\delta_\perp(B \to J/\psi K^*)$	Belle [311]: $2.938 \pm 0.064 \pm 0.010$ *BABAR* [310]: $2.91 \pm 0.05 \pm 0.03$	2.923 ± 0.043
$\delta_\perp(B \to \psi(2S) K^*)$	*BABAR* [310]: $2.8 \pm 0.3 \pm 0.1$	2.8 ± 0.3

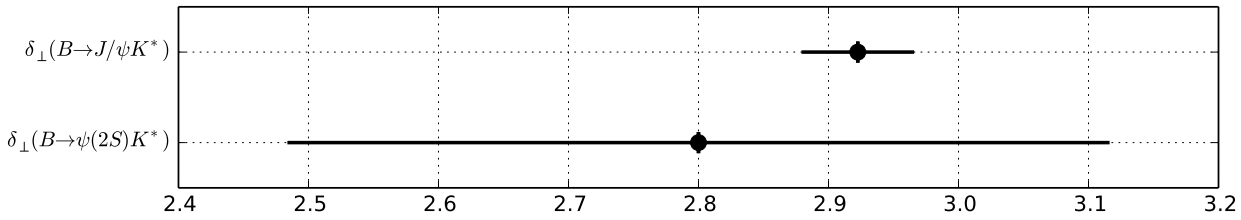

Figure 126: Summary of the averages from Table 157.

6.3.3 Decays to other (XYZ) states

Averages of $\overline{B}^0$ / B^- decays to other (XYZ) states are shown in Table 158 and Fig. 127.

Table 158: Absolute decay rates to X/Y states [10^{-4}].

Parameter	Measurements	Average
$\mathcal{B}(B \to X(3872)K) \times \mathcal{B}(X(3872) \to D^*(2007)^0 \overline{D}^0)$		
	Belle [746]: $0.80 \pm 0.20 \pm 0.10$	0.80 ± 0.22
$\mathcal{B}(B \to Y(3940)K) \times \mathcal{B}(Y(3940) \to D^*(2007)^0 \overline{D}^0)$		
	Belle [746]: < 0.67	< 0.67
$\mathcal{B}(B \to KY(3940)) \times \mathcal{B}(Y(3940) \to J/\psi\omega(782))$	Belle [747]: $0.71 \pm 0.13 \pm 0.31$	0.71 ± 0.34

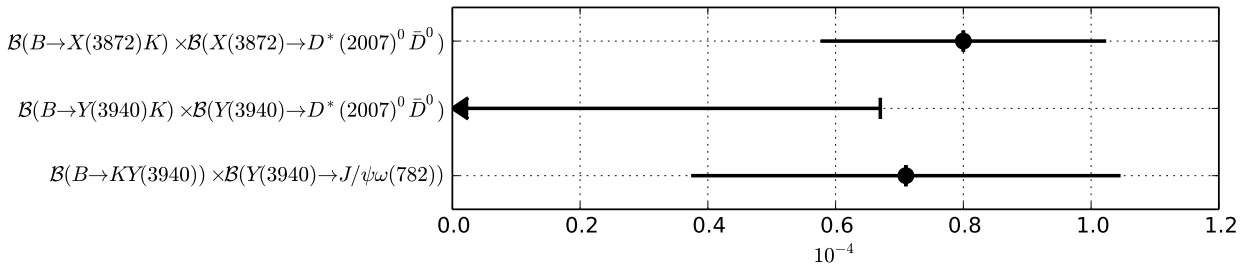

Figure 127: Summary of the averages from Table 158.

6.4 Decays of $\overline{B}{}^0_s$ mesons

Measurements of $\overline{B}{}^0_s$ decays to charmed hadrons are summarized in Sections 6.4.1 to 6.4.4.

6.4.1 Decays to a single open charm meson

Averages of $\overline{B}{}^0_s$ decays to a single open charm meson are shown in Tables 159–161 and Figs. 128–130.

Table 159: Decays to a $D_s^{(*)}$ and a light meson [10^{-3}].

Parameter	Measurements	Average
$\mathcal{B}(\overline{B}{}^0_s \to D_s^+\pi^-)$	LHCb [748]: $2.95 \pm 0.05\,^{+0.25}_{-0.28}$ Belle [27]: $3.67\,^{+0.35\,+0.65}_{-0.33\,-0.65}$	3.03 ± 0.25
$\mathcal{B}(\overline{B}{}^0_s \to D_s^{*+}\pi^-)$	Belle [749]: $2.4\,^{+0.5}_{-0.4} \pm 0.4$	$2.4\,^{+0.7}_{-0.6}$
$\mathcal{B}(\overline{B}{}^0_s \to D_s^+\rho^-(770))$	Belle [749]: $8.5\,^{+1.3}_{-1.2} \pm 1.7$	$8.5\,^{+2.1}_{-2.1}$
$\mathcal{B}(\overline{B}{}^0_s \to D_s^{*+}\rho^-(770))$	Belle [749]: $11.8\,^{+2.2}_{-2.0} \pm 2.5$	$11.8\,^{+3.3}_{-3.2}$
$\mathcal{B}(\overline{B}{}^0_s \to D_s^+K^-)$	LHCb [748]: $0.190 \pm 0.012\,^{+0.018}_{-0.019}$ Belle [27]: $0.24\,^{+0.12}_{-0.10} \pm 0.04$	0.192 ± 0.022
$\mathcal{B}(\overline{B}{}^0_s \to D_s^{*+}K^-)$	LHCb [750]: $0.163 \pm 0.012\,^{+0.049}_{-0.048}$	$0.163\,^{+0.050}_{-0.050}$

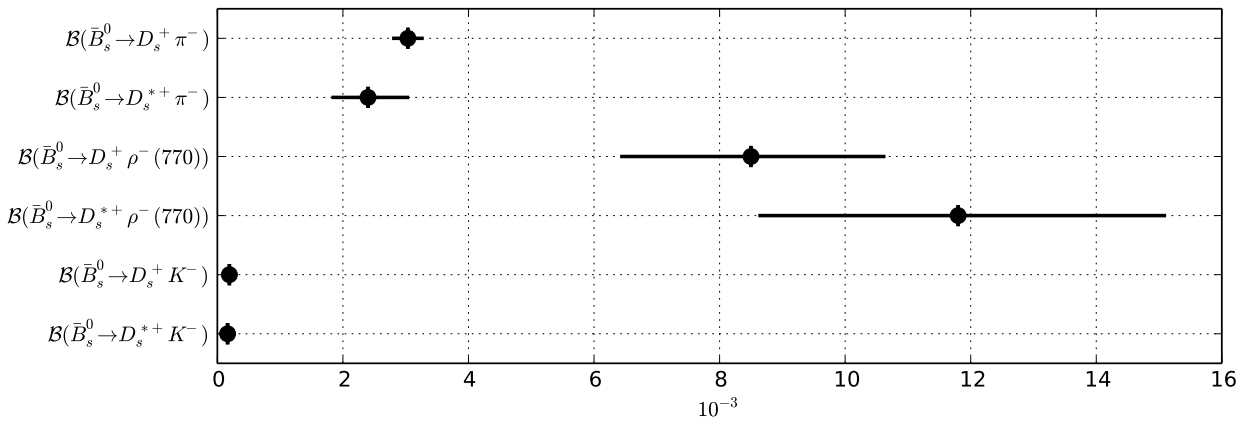

Figure 128: Summary of the averages from Table 159.

Table 160: Decays to a $D^{(*)}$ and a light meson $[10^{-4}]$.

Parameter	**Measurements**	**Average**
$\mathcal{B}(\overline{B}_s^0 \to D^*(2010)^{\pm}\pi^{\mp})$	LHCb [751]: < 0.061	< 0.061
$\mathcal{B}(\overline{B}_s^0 \to D^0 K^0)$	LHCb [752]: $4.3 \pm 0.5 \pm 0.8$	4.3 ± 0.9
$\mathcal{B}(\overline{B}_s^0 \to D^{*0} K^0)$	LHCb [752]: $2.8 \pm 1.0 \pm 0.5$	2.8 ± 1.1
$\mathcal{B}(\overline{B}_s^0 \to D^0 \overline{K}^{*0})$	LHCb [753]: $4.72 \pm 1.07 \pm 0.96$	4.72 ± 1.44
$\mathcal{B}(\overline{B}_s^0 \to D^0 f_0(980))$	LHCb [754]: < 0.031	< 0.031

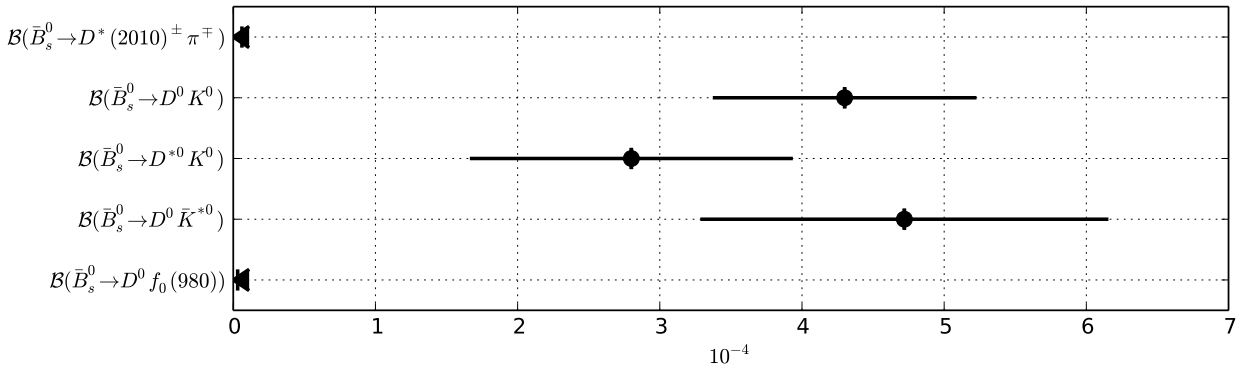

Figure 129: Summary of the averages from Table 160.

Table 161: Relative decay rates.

Parameter	Measurements	Average
$\mathcal{B}(\overline{B}_s^0 \to D_s^+\pi^-)/\mathcal{B}(\overline{B}^0 \to D^+\pi^-)$		
	CDF [755]: $1.13 \pm 0.08 \pm 0.23$	1.13 ± 0.25
$\mathcal{B}(\overline{B}_s^0 \to D_s^+\pi^+\pi^-\pi^-)/\mathcal{B}(\overline{B}_s^0 \to D_s^+\pi^-)$		
	LHCb [597]: $2.01 \pm 0.37 \pm 0.20$	2.01 ± 0.42
$\mathcal{B}(\overline{B}_s^0 \to D_s^+\pi^+\pi^-\pi^-)/\mathcal{B}(\overline{B}^0 \to D^+\pi^+\pi^-\pi^-)$		
	CDF [755]: $1.05 \pm 0.10 \pm 0.22$	1.05 ± 0.24
$\mathcal{B}(\overline{B}_s^0 \to D_s^+K^-)/\mathcal{B}(\overline{B}_s^0 \to D_s^+\pi^-)$		
	LHCb [600]: $0.0752 \pm 0.0015 \pm 0.0019$ CDF [756]: $0.097 \pm 0.018 \pm 0.009$	0.0755 ± 0.0024
$\mathcal{B}(\overline{B}_s^0 \to D_s^{*+}K^-)/\mathcal{B}(\overline{B}_s^0 \to D_s^{*+}\pi^-)$		
	LHCb [750]: $0.068 \pm 0.005\,^{+0.003}_{-0.002}$	$0.068\,^{+0.006}_{-0.005}$
$\mathcal{B}(\overline{B}_s^0 \to D_s^+K^-\pi^+\pi^-)/\mathcal{B}(\overline{B}^0 \to D_s^+\pi^-\pi^+\pi^-)$		
	LHCb [599]: $0.052 \pm 0.005 \pm 0.003$	0.052 ± 0.006
$\mathcal{B}(\overline{B}_s^0 \to D^0K^{*0})/\mathcal{B}(B^- \to D^0\rho^0)$		
	LHCb [753]: $1.48 \pm 0.34 \pm 0.19$	1.48 ± 0.39
$\mathcal{B}(\overline{B}_s^0 \to D^0K^{*0})/\mathcal{B}(\overline{B}^0 \to D^0K^{*0})$		
	LHCb [757]: $7.8 \pm 0.7 \pm 0.7$	7.8 ± 1.0
$\mathcal{B}(\overline{B}_s^0 \to D^0\phi(1020))/\mathcal{B}(\overline{B}_s^0 \to D^0K^{*0})$		
	LHCb [757]: $0.069 \pm 0.013 \pm 0.007$	0.069 ± 0.015
$\mathcal{B}(\overline{B}_s^0 \to \overline{D}^0K^-\pi^+)/\mathcal{B}(\overline{B}^0 \to \overline{D}^0\pi^-\pi^+)$		
	LHCb [595]: $1.18 \pm 0.05 \pm 0.12$	1.18 ± 0.13
$\mathcal{B}(\overline{B}_s^0 \to D_{s1}^+\pi^-) \times (D_{s1}^+ \to D_s^+\pi^-\pi^+)/\mathcal{B}(\overline{B}^0 \to D_s^+\pi^-\pi^+\pi^-)$		
	LHCb [599]: $0.0040 \pm 0.0010 \pm 0.0004$	0.0040 ± 0.0011

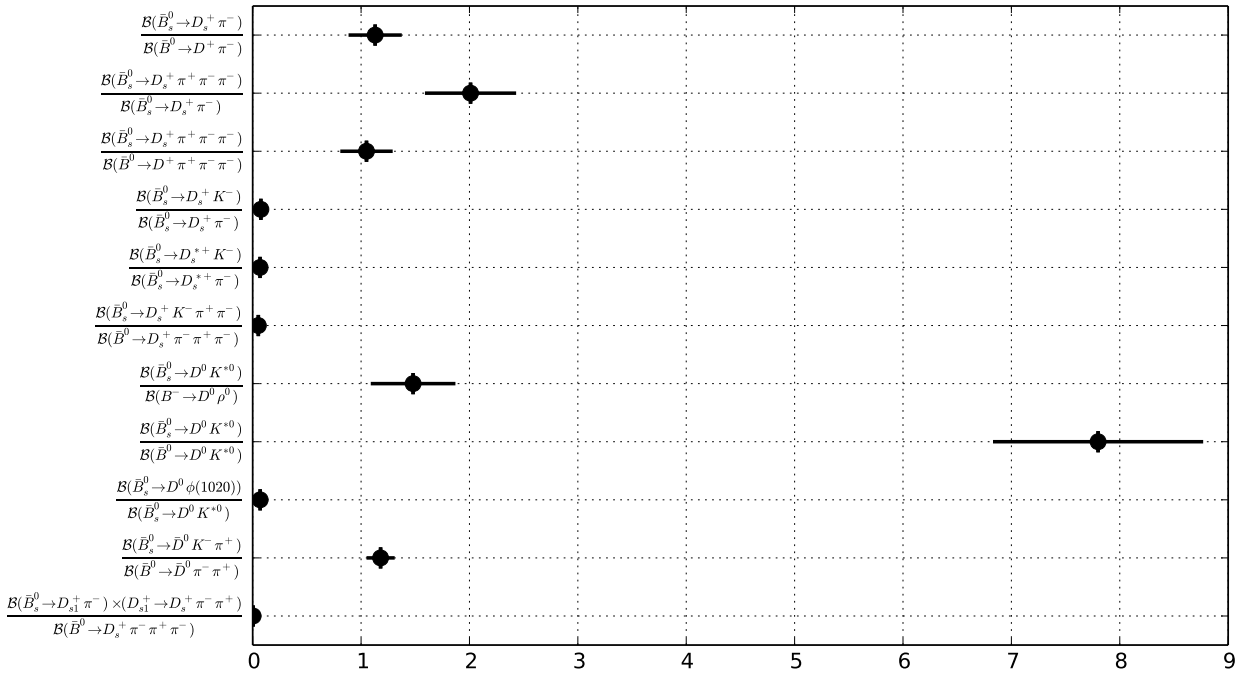

Figure 130: Summary of the averages from Table 161.

6.4.2 Decays to two open charm mesons

Averages of $\overline{B}_s^0$ decays to two open charm mesons are shown in Tables 162–163 and Figs. 131–132.

Table 162: Absolute branching fractions $[10^{-2}]$.

Parameter	**Measurements**	**Average**
$\mathcal{B}(\overline{B}_s^0 \to D_s^+ D_s^-)$	CDF [758]: $0.49 \pm 0.06 \pm 0.09$ Belle [18]: $0.58\,^{+0.11}_{-0.09} \pm 0.13$	0.52 ± 0.09
$\mathcal{B}(\overline{B}_s^0 \to D_s^+ D_s^{*-})$	LHCb [759]: $1.35 \pm 0.06 \pm 0.17$ CDF [758]: $1.13 \pm 0.12 \pm 0.21$ Belle [18]: $1.76\,^{+0.23}_{-0.22} \pm 0.40$	1.38 ± 0.17
$\mathcal{B}(\overline{B}_s^0 \to D_s^{*+} D_s^{*-})$	LHCb [759]: $1.27 \pm 0.08 \pm 0.17$ CDF [758]: $1.75 \pm 0.19 \pm 0.34$ Belle [18]: $1.98\,^{+0.33\ +0.51}_{-0.31\ -0.50}$	1.32 ± 0.18
$\mathcal{B}(\overline{B}_s^0 \to D_s^{(*)+} D_s^{(*)-})$	LHCb [759]: $3.05 \pm 0.10 \pm 0.39$ D0 [194]: $3.5 \pm 1.0 \pm 1.1$ CDF [758]: $3.38 \pm 0.25 \pm 0.64$ Belle [18]: $4.32\,^{+0.42\ +1.04}_{-0.39\ -1.03}$	3.19 ± 0.37

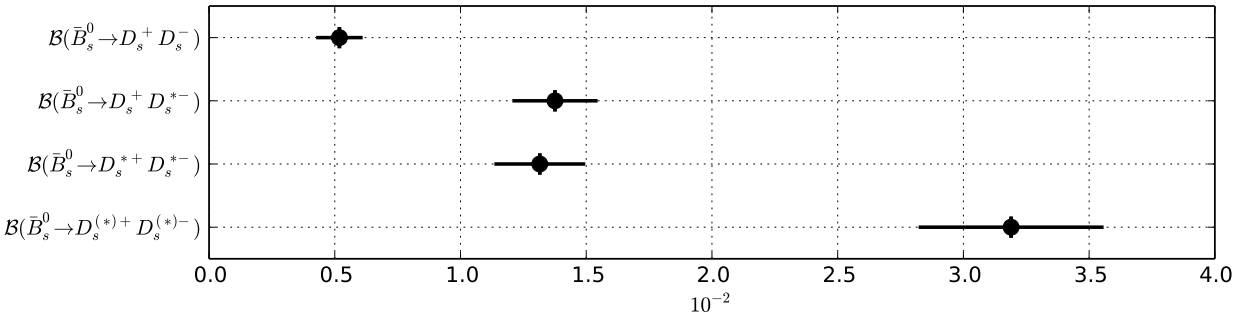

Figure 131: Summary of the averages from Table 162.

Table 163: Relative branching fractions.

Parameter	Measurements	Average
$\mathcal{B}(\overline{B}_s^0 \to D^- D^+)/\mathcal{B}(\overline{B}^0 \to D^- D^+)$		
	LHCb [620]: $1.08 \pm 0.20 \pm 0.10$	1.08 ± 0.22
$\mathcal{B}(\overline{B}_s^0 \to D_s^- D_s^+)/\mathcal{B}(\overline{B}^0 \to D_s^- D^+)$		
	LHCb [620]: $0.56 \pm 0.03 \pm 0.04$	0.56 ± 0.05
$\mathcal{B}(\overline{B}_s^0 \to D_s^+ D^-)/\mathcal{B}(B^0 \to D_s^+ D^-)$		
	LHCb [620]: $0.050 \pm 0.008 \pm 0.004$	0.050 ± 0.009
$\mathcal{B}(\overline{B}_s^0 \to \overline{D}^0 D^0)/\mathcal{B}(B^- \to D^0 D_s^-)$		
	LHCb [620]: $0.019 \pm 0.003 \pm 0.003$	0.019 ± 0.004

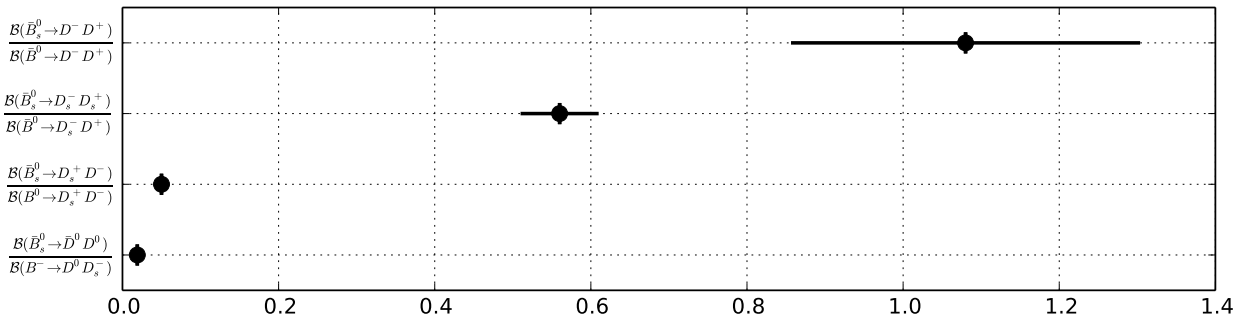

Figure 132: Summary of the averages from Table 163.

6.4.3 Decays to charmonium states

Averages of $\overline{B}_s^0$ decays to charmonium states are shown in Tables 164–167 and Figs. 133–136.

Table 164: Absolute decay rates I [10^{-4}].

Parameter	**Measurements**	**Average**
$\mathcal{B}(\overline{B}_s^0 \to J/\psi\eta)$	Belle [760]: $5.10 \pm 0.50\,^{+1.17}_{-0.83}$	$5.10\,^{+1.27}_{-0.97}$
$\mathcal{B}(\overline{B}_s^0 \to J/\psi\eta')$	Belle [760]: $3.71 \pm 0.61\,^{+0.85}_{-0.60}$	$3.71\,^{+1.05}_{-0.85}$
$\mathcal{B}(\overline{B}_s^0 \to J/\psi\phi(1020))$	LHCb [761]: $10.5 \pm 0.1 \pm 1.0$ CDF [667]: $9.3 \pm 2.8 \pm 1.7$ Belle [762]: $12.5 \pm 0.7 \pm 2.3$	10.0 ± 0.9
$\mathcal{B}(\overline{B}_s^0 \to J/\psi K^0 K^\pm \pi^\mp)$	LHCb [631]: $9.1 \pm 0.6 \pm 0.7$	9.1 ± 0.9
$\mathcal{B}(\overline{B}_s^0 \to J/\psi f_0(980)) \times \mathcal{B}(f_0(980) \to \pi^+\pi^-)$	Belle [26]: $1.16\,^{+0.31\,+0.30}_{-0.19\,-0.25}$	$1.16\,^{+0.43}_{-0.32}$

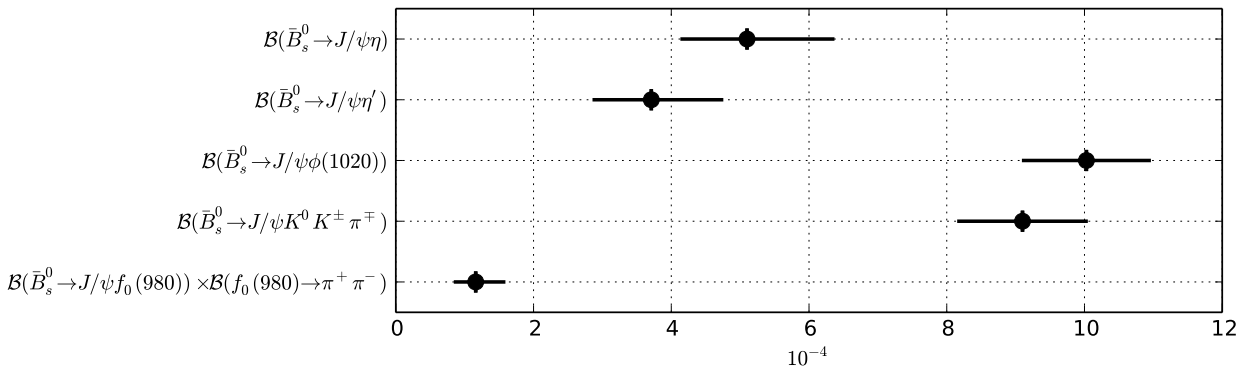

Figure 133: Summary of the averages from Table 164.

Table 165: Absolute decay rates II [10^{-5}].

Parameter	**Measurements**	**Average**
$\mathcal{B}(\overline{B}_s^0 \to J/\psi \overline{K}^0)$	LHCb [763]: $3.66 \pm 0.42 \pm 0.37$ CDF [764]: $3.5 \pm 0.6 \pm 0.6$	3.61 ± 0.46
$\mathcal{B}(\overline{B}_s^0 \to J/\psi K^{*0})$	LHCb [765]: $4.17 \pm 0.18 \pm 0.35$ CDF [764]: $8.3 \pm 1.2 \pm 3.6$	4.15 ± 0.40
$\mathcal{B}(\overline{B}_s^0 \to J/\psi p\bar{p})$	LHCb [662]: < 0.48	< 0.48
$\mathcal{B}(\overline{B}_s^0 \to J/\psi K^+\pi^-)$	LHCb [766]: $3.94\,^{+0.71}_{-0.62} \pm 0.66$	$3.94\,^{+0.97}_{-0.91}$
$\mathcal{B}(\overline{B}_s^0 \to J/\psi f_1(1285))$	LHCb [657]: $7.14 \pm 0.99\,^{+0.93}_{-1.00}$	$7.14\,^{+1.36}_{-1.41}$
$\mathcal{B}(\overline{B}_s^0 \to J/\psi K^0\pi^+\pi^-)$	LHCb [631]: < 4.4	< 4.4
$\mathcal{B}(\overline{B}_s^0 \to J/\psi K^0 K^+ K^-)$	LHCb [631]: < 1.2	< 1.2
$\mathcal{B}(\overline{B}_s^0 \to J/\psi f_0(1370)) \times \mathcal{B}(f_0(1370) \to \pi^+\pi^-)$	Belle [26]: $3.4\,^{+1.1\,+0.9}_{-1.4\,-0.5}$	$3.4\,^{+1.4}_{-1.5}$
$\mathcal{B}(\overline{B}_s^0 \to J/\psi f_1(1285)) \times \mathcal{B}(f_1(1285) \to \pi^+\pi^-\pi^+\pi^-)$	LHCb [657]: $0.785 \pm 0.109\,^{+0.089}_{-0.101}$	$0.785\,^{+0.141}_{-0.149}$
$\mathcal{B}(\overline{B}_s^0 \to J/\psi\gamma)$	LHCb [660]: < 0.73	< 0.73

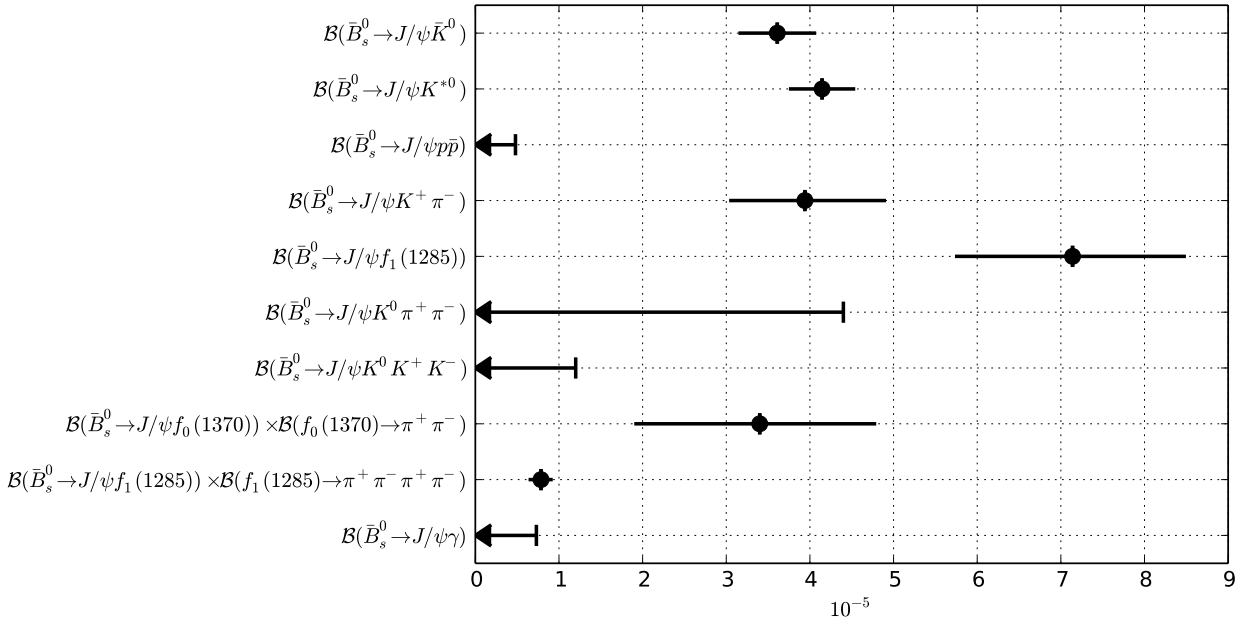

Figure 134: Summary of the averages from Table 165.

Table 166: Relative decay rates I.

Parameter	Measurements	Average
$\mathcal{B}(\overline{B}_s^0 \to J/\psi\eta)/\mathcal{B}(\overline{B}^0 \to J/\psi\rho)$		
	LHCb [668]: $14.0 \pm 1.2\,^{+1.6}_{-1.8}$	$14.0\,^{+2.0}_{-2.2}$
$\mathcal{B}(\overline{B}_s^0 \to J/\psi\eta')/\mathcal{B}(\overline{B}^0 \to J/\psi\rho)$		
	LHCb [668]: $12.7 \pm 1.1\,^{+1.1}_{-0.9}$	$12.7\,^{+1.6}_{-1.4}$
$\mathcal{B}(\overline{B}_s^0 \to J/\psi K_S^0 K^\pm\pi^\mp)/\mathcal{B}(\overline{B}^0 \to J/\psi\pi^+\pi^-)$		
	LHCb [631]: $2.12 \pm 0.15 \pm 0.18$	2.12 ± 0.23

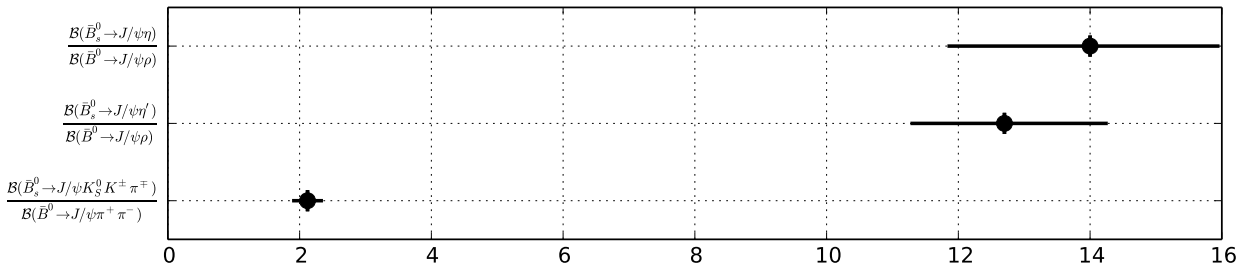

Figure 135: Summary of the averages from Table 166.

Table 167: Relative decay rates II.

Parameter	Measurements	Average
$\mathcal{B}(\overline{B}_s^0 \to J/\psi K_S^0)/\mathcal{B}(\overline{B}^0 \to J/\psi K_S^0)$		
	LHCb [763]: $0.0420 \pm 0.0049 \pm 0.0040$	0.0420 ± 0.0063
$\mathcal{B}(\overline{B}_s^0 \to J/\psi\eta)/\mathcal{B}(\overline{B}^0 \to J/\psi\eta')$		
	Belle [760]: $0.73 \pm 0.14 \pm 0.02$	0.73 ± 0.14
$\mathcal{B}(\overline{B}_s^0 \to J/\psi\eta')/\mathcal{B}(\overline{B}_s^0 \to J/\psi\eta)$		
	LHCb [668]: $0.90 \pm 0.09\,^{+0.06}_{-0.02}$	$0.90\,^{+0.11}_{-0.09}$
$\mathcal{B}(\overline{B}_s^0 \to J/\psi f_2')/\mathcal{B}(\overline{B}_s^0 \to J/\psi\phi(1020))$		
	LHCb [767]: $0.264 \pm 0.027 \pm 0.024$	0.246 ± 0.031
	D0 [768]: $0.19 \pm 0.05 \pm 0.04$	
$\mathcal{B}(\overline{B}_s^0 \to J/\psi\phi(1020))/\mathcal{B}(\overline{B}^0 \to J/\psi\overline{K}^{*0})$		
	CDF [769]: $0.89 \pm 0.01 \pm 0.13$	0.89 ± 0.13
$\mathcal{B}(\overline{B}_s^0 \to J/\psi\pi^+\pi^-)/\mathcal{B}(\overline{B}_s^0 \to J/\psi\phi(1020))$		
	LHCb [770]: $0.162 \pm 0.022 \pm 0.016$	0.162 ± 0.027
$\mathcal{B}\overline{B}_s^0 \to \psi(2S)\pi^+\pi^-/\mathcal{B}\overline{B}_s^0 \to J/\psi\pi^+\pi^-$		
	LHCb [671]: $0.34 \pm 0.04 \pm 0.03$	0.34 ± 0.05
$\mathcal{B}(\overline{B}_s^0 \to \psi(2S)\phi(1020))/\mathcal{B}(\overline{B}_s^0 \to J/\psi\phi(1020))$		
	LHCb [670]: $0.489 \pm 0.026 \pm 0.024$	
	D0 [737]: $0.55 \pm 0.11 \pm 0.09$	0.494 ± 0.034
	CDF [771]: $0.52 \pm 0.13 \pm 0.07$	
$\mathcal{B}(\overline{B}_s^0 \to J/\psi\phi(1020)\phi(1020))/\mathcal{B}(\overline{B}_s^0 \to J/\psi\phi(1020))$		
	LHCb [772]: $0.0115 \pm 0.0012\,^{+0.0005}_{-0.0009}$	$0.0115\,^{+0.0013}_{-0.0015}$
$\mathcal{B}(\overline{B}_s^0 \to \psi(2S)K^+\pi^-)/\mathcal{B}(\overline{B}^0 \to \psi(2S)K^+\pi^-)$		
	LHCb [773]: $0.0538 \pm 0.0036 \pm 0.0038$	0.0538 ± 0.0052
$\mathcal{B}(\overline{B}_s^0 \to \psi(2S)K^{*0})/\mathcal{B}(\overline{B}^0 \to \psi(2S)K^{*0})$		
	LHCb [773]: $0.0538 \pm 0.0057 \pm 0.0051$	0.0538 ± 0.0077
$\mathcal{B}(\overline{B}_s^0 \to J/\psi K_S^0\pi^+\pi^-)/\mathcal{B}(\overline{B}^0 \to J/\psi\pi^+\pi^-)$		
	LHCb [631]: < 0.10	< 0.10
$\mathcal{B}(\overline{B}_s^0 \to J/\psi K_S^0 K^+K^-)/\mathcal{B}(\overline{B}^0 \to J/\psi\pi^+\pi^-)$		
	LHCb [631]: < 0.027	< 0.027
$\mathcal{B}(\overline{B}_s^0 \to J/\psi f_0(980)) \times \mathcal{B}(f_0(980) \to \pi^+\pi^-)/\mathcal{B}(\overline{B}_s^0 \to J/\psi\phi(1020))) \times \mathcal{B}(\phi \to K^+K^-)$		
	LHCb [770]: $0.252\,^{+0.046\,+0.027}_{-0.032\,-0.033}$	
	D0 [774]: $0.275 \pm 0.041 \pm 0.061$	0.207 ± 0.016
	CMS [775]: $0.140 \pm 0.008 \pm 0.023$	
	CDF [123]: $0.257 \pm 0.020 \pm 0.014$	
$\mathcal{B}(\overline{B}_s^0 \to J/\psi f_0(500)) \times \mathcal{B}(f_0(500) \to \pi^+\pi^-)/\mathcal{B}(\overline{B}_s^0 \to J/\psi f_0(980))) \times \mathcal{B}(f_0(500) \to \pi^+\pi^-)$		
	LHCb [776]: < 0.034	< 0.034

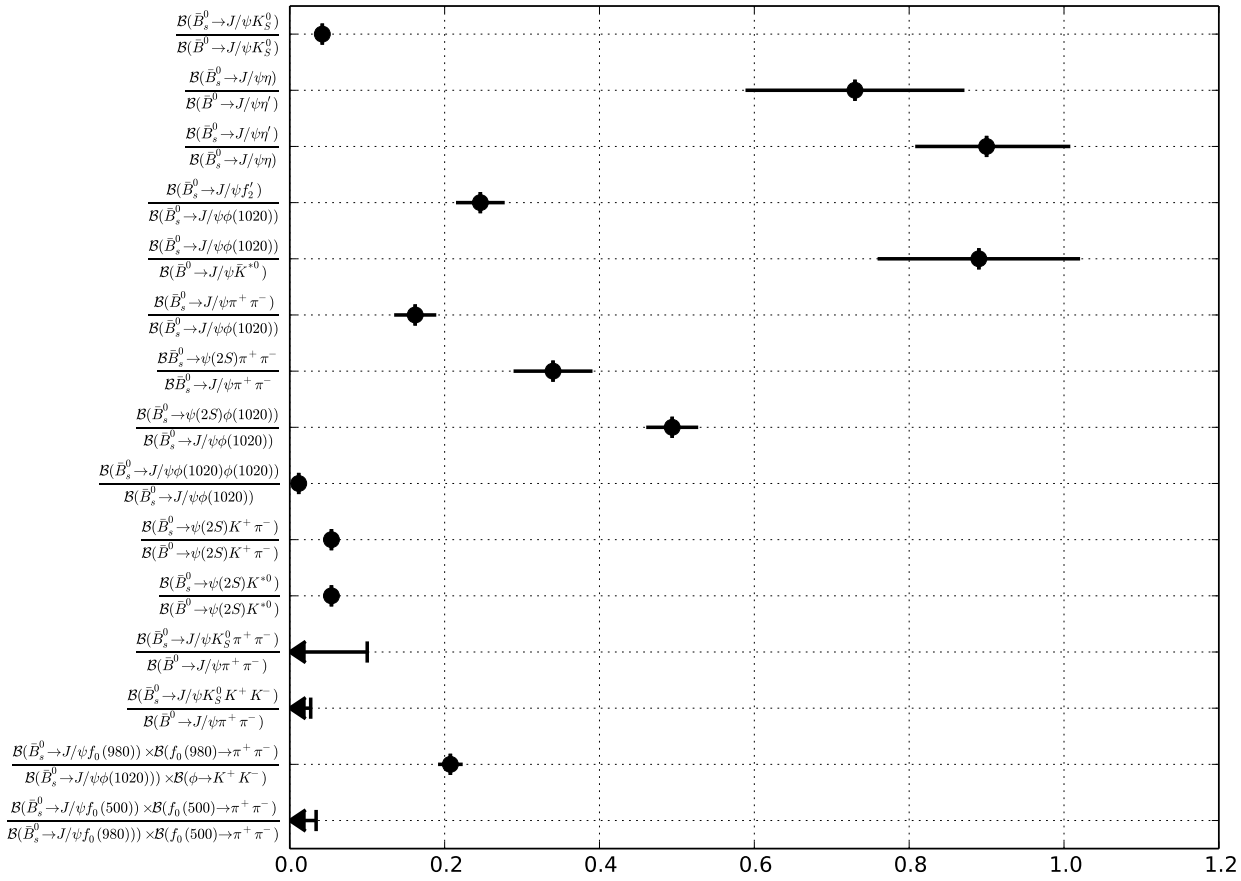

Figure 136: Summary of the averages from Table 167.

6.4.4 Decays to charm baryons

Averages of $\overline{B}_s^0$ decays to charm baryons are shown in Tables 168–169.

Table 168: Decays to one charm baryon $[10^{-4}]$.

Parameter	Measurements	Average
$\mathcal{B}(\overline{B}_s^0 \to \Lambda_c^+\overline{\Lambda}\pi^-)$	Belle [777]: $3.6 \pm 1.1\,^{+1.2}_{-1.2}$	$3.6\,^{+1.6}_{-1.7}$

Table 169: Decays to two charm baryons.

Parameter	Measurements	Average
$\mathcal{B}(\overline{B}_s^0 \to \Lambda_c^-\Lambda_c^+)/\mathcal{B}(\overline{B}_s^0 \to D^-D_s^+)$		
	LHCb [688]: < 0.30	< 0.30

6.5 Decays of B_c^- mesons

Measurements of B_c^- decays to charmed hadrons are summarized in Sections 6.5.1 to 6.5.2.

6.5.1 Decays to charmonium states

Averages of B_c^- decays to charmonium states are shown in Tables 170–171 and Fig. 137.

Table 170: Relative decay rates.

Parameter	Measurements	Average
$\mathcal{B}(B_c^- \to J/\psi D_s^-)/\mathcal{B}(B_c^- \to J/\psi\pi^-)$		
	LHCb [778]: $2.90 \pm 0.57 \pm 0.24$	3.09 ± 0.55
	ATLAS [779]: $3.8 \pm 1.1 \pm 0.4$	
$\mathcal{B}(B_c^- \to J/\psi D_s^{*-})/\mathcal{B}(B_c^- \to J/\psi D_s^-)$		
	ATLAS [779]: $2.8\,^{+1.2}_{-0.8} \pm 0.3$	$2.8\,^{+1.2}_{-0.9}$
$\mathcal{B}(B_c^- \to J/\psi D_s^{*-})/\mathcal{B}(B_c^- \to J/\psi\pi^-)$		
	ATLAS [779]: $10.4 \pm 3.1 \pm 1.6$	10.4 ± 3.5
$\mathcal{B}(B_c^- \to J/\psi K^-)/\mathcal{B}(B_c^- \to J/\psi\pi^-)$		
	LHCb [780]: $0.069 \pm 0.019 \pm 0.005$	0.069 ± 0.020
$\mathcal{B}(B_c^- \to J/\psi K^- K^+\pi^-)/\mathcal{B}(B_c^- \to J/\psi\pi^-)$		
	LHCb [781]: $0.53 \pm 0.10 \pm 0.05$	0.53 ± 0.11
$\mathcal{B}(B_c^- \to J/\psi\pi^+\pi^-\pi^-)/\mathcal{B}(B_c^- \to J/\psi\pi^-)$		
	LHCb [782]: $3.0 \pm 0.6 \pm 0.4$	
	LHCb [783]: $2.41 \pm 0.30 \pm 0.33$	2.57 ± 0.35
	CMS [784]: $2.55 \pm 0.80\,^{+0.33}_{-0.33}$	
$\mathcal{B}(B_c^- \to \psi(2S)\pi^-)/\mathcal{B}(B_c^- \to J/\psi\pi^-)$		
	LHCb [785]: $0.268 \pm 0.032 \pm 0.009$	0.268 ± 0.033

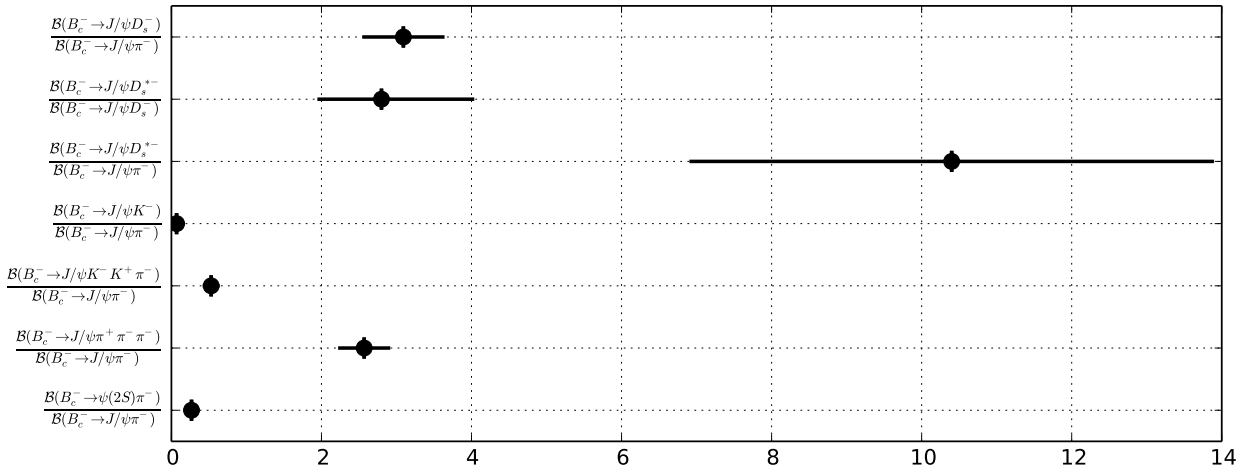

Figure 137: Summary of the averages from Table 170.

Table 171: Relative production times decay rates [10^{-3}].

Parameter	Measurements	Average
$\sigma(B_c^-) \times \mathcal{B}(B_c^- \to J/\psi\pi^-)/\sigma(B^-) \times \mathcal{B}(B^- \to J/\psi K^-)$		
	LHCb [786]: $22 \pm 8 \pm 2$	5.0 ± 0.8
	CMS [784]: $4.8 \pm 0.5 \pm 0.6$	

6.5.2 Decays to a B meson

Averages of B_c^- decays to a B meson are shown in Table 172.

Table 172: Decays to B_s^0 meson [10^{-3}].

Parameter	Measurements	Average
$\sigma(B_c^+)/\sigma(B_s^0) \times \mathcal{B}(B_c^+ \to B_s^0\pi^+)$		
	LHCb [787]: $2.37 \pm 0.31\,^{+0.20}_{-0.17}$	$2.37\,^{+0.37}_{-0.35}$

6.6 Decays of b baryons

Measurements of b baryons decays to charmed hadrons are summarized in Sections 6.6.1 to 6.6.3.

6.6.1 Decays to a single open charm meson

Averages of b baryons decays to a single open charm meson are shown in Table 173 and Fig. 138.

Table 173: Relative decay rates to D^0 mesons.

Parameter	Measurements	Average
$\mathcal{B}(\Lambda_b^0 \to D^0 pK^-)/\mathcal{B}(\Lambda_b^0 \to D^0 p\pi^-)$		
	LHCb [788]: $0.073 \pm 0.008\,^{+0.005}_{-0.006}$	$0.073\,^{+0.009}_{-0.010}$
$\mathcal{B}(\Lambda_b^0 \to D^0 p\pi^-) \times \mathcal{B}(D^0 \to K^+\pi^-)/\mathcal{B}(\Lambda_b^0 \to \Lambda_c^+\pi^-) \times \mathcal{B}(\Lambda_c^+ \to pK^-\pi^+)$		
	LHCb [788]: $0.0806 \pm 0.0023 \pm 0.0035$	0.0806 ± 0.0042
$f_{\Xi_b^0} \times \mathcal{B}(\Xi_b^0 \to D^0 pK^-)/f_{\Lambda_b^0} \times \mathcal{B}(\Lambda_b^0 \to D^0 pK^-)$		
	LHCb [788]: $0.44 \pm 0.09 \pm 0.06$	0.44 ± 0.11

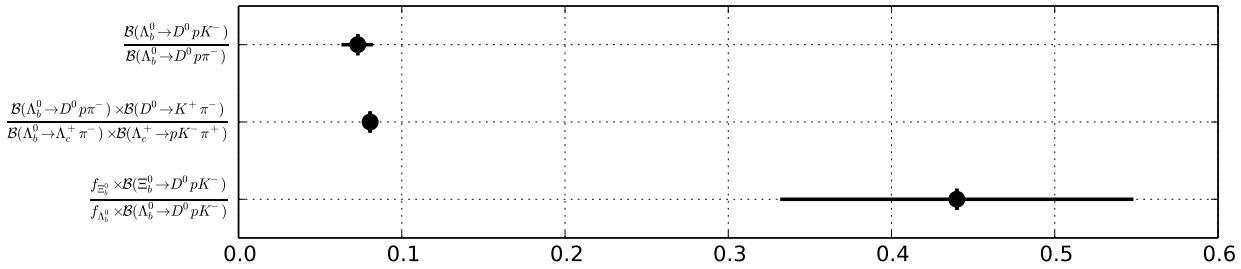

Figure 138: Summary of the averages from Table 173.

6.6.2 Decays to charmonium states

Averages of b baryons decays to charmonium states are shown in Tables 174–178 and Figs. 139–141.

Table 174: Λ_b^0 decays to charmonium $[10^{-4}]$.

Parameter	**Measurements**	**Average**
$\mathcal{B}(\Lambda_b^0 \to J/\psi p K^-)$	LHCb [789]: $3.17 \pm 0.04\,^{+0.46}_{-0.29}$	$3.17\,^{+0.46}_{-0.29}$
$\mathcal{B}(\Lambda_b^0 \to J/\psi \Lambda)$	CDF [790]: $4.7 \pm 2.1 \pm 1.9$	4.7 ± 2.8

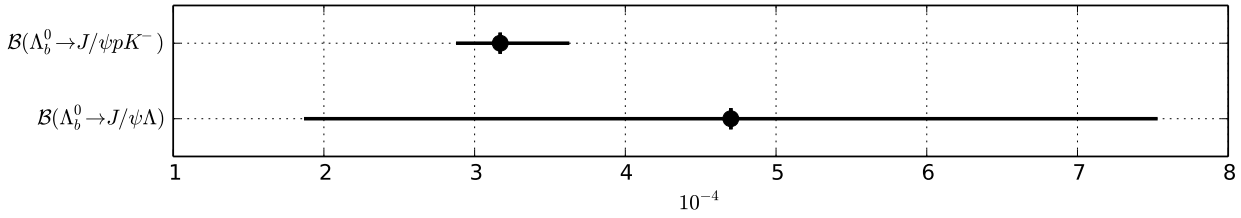

Figure 139: Summary of the averages from Table 174.

Table 175: f_b times Λ_b^0 decay to charmonium $[10^{-5}]$.

Parameter	**Measurements**	**Average**
$f_b \times \mathcal{B}(\Lambda_b^0 \to J/\psi \Lambda)$	D0 [791]: $6.01 \pm 0.60 \pm 0.64$	6.01 ± 0.88

Table 176: Relative Λ_b^0 decay rates.

Parameter	Measurements	Average
$\mathcal{B}(\Lambda_b^0 \to \psi(2S)\Lambda)/\mathcal{B}(\Lambda_b^0 \to J/\psi\Lambda)$		
	ATLAS [792]: $0.501 \pm 0.033 \pm 0.019$	0.501 ± 0.038
$\mathcal{B}(\Lambda_b^0 \to J/\psi p\pi^-)/\mathcal{B}(\Lambda_b^0 \to J/\psi pK^-)$		
	LHCb [793]: $0.0824 \pm 0.0025 \pm 0.0042$	0.0824 ± 0.0049
$\mathcal{B}(\Lambda_b^0 \to J/\psi\pi^+\pi^- pK^-)/\mathcal{B}(\Lambda_b^0 \to J/\psi pK^-)$		
	LHCb [794]: $0.2086 \pm 0.0096 \pm 0.0134$	0.2086 ± 0.0165
$\mathcal{B}(\Lambda_b^0 \to \psi(2s)pK^-)/\mathcal{B}(\Lambda_b^0 \to J/\psi pK^-)$		
	LHCb [794]: $0.2070 \pm 0.0076 \pm 0.0059$	0.2070 ± 0.0096

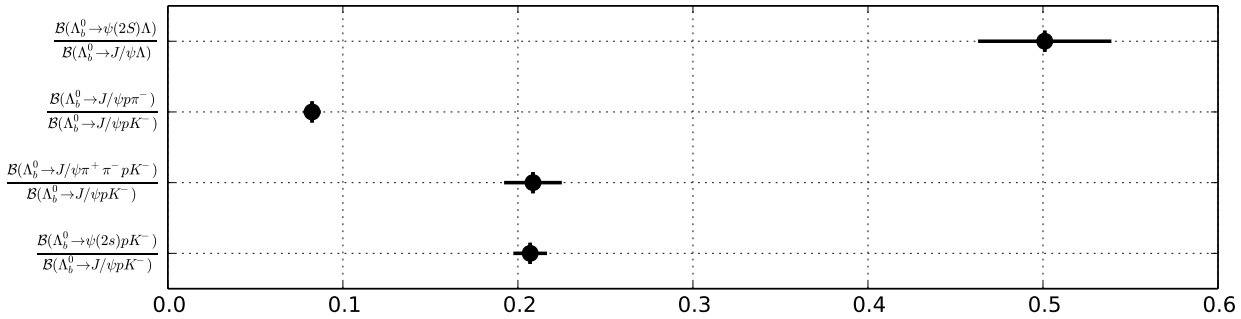

Figure 140: Summary of the averages from Table 176.

Table 177: Ξ_b^- and Ω_b^- decays to charmonium.

Parameter	Measurements	Average
$\sigma(\Xi_b^-) \times \mathcal{B}(\Xi_b^- \to J/\psi\Xi^-)/\sigma(\Lambda_b^0) \times \mathcal{B}(\Lambda_b^0 \to J/\psi\Lambda)$		
	CDF [43]: $0.167\,^{+0.037}_{-0.025} \pm 0.012$	$0.167\,^{+0.039}_{-0.028}$
$\sigma(\Omega_b^-) \times \mathcal{B}(\Omega_b^- \to J/\psi\Omega^-)/\sigma(\Lambda_b^0) \times \mathcal{B}(\Lambda_b^0 \to J/\psi\Lambda)$		
	CDF [43]: $0.045\,^{+0.017}_{-0.012} \pm 0.004$	$0.045\,^{+0.017}_{-0.013}$

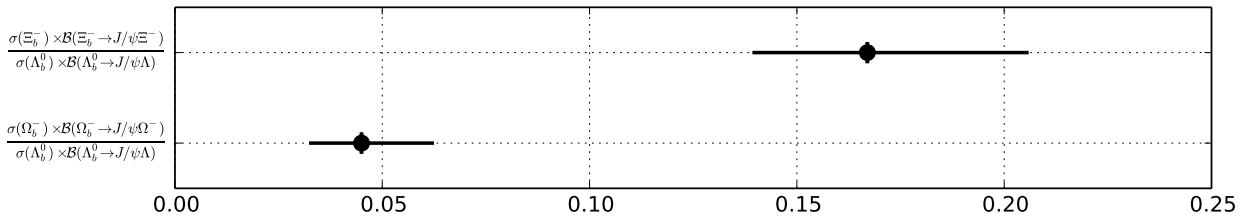

Figure 141: Summary of the averages from Table 177.

Table 178: Parity violation in Λ_b^0 decays to charmonium.

Parameter	Measurements	Average
$\alpha_b(\Lambda_b^0 \to J/\psi\Lambda)$	ATLAS [795]: $0.30 \pm 0.16 \pm 0.06$	0.30 ± 0.17

6.6.3 Decays to charm baryons

Averages of b baryons decays to charm baryons are shown in Tables 179–182 and Figs. 142–144.

Table 179: Absolute decay rates [10^{-2}].

Parameter	Measurements	Average
$\mathcal{B}(\Lambda_b^0 \to \Lambda_c^+\pi^-)$	LHCb [46]: $0.430 \pm 0.003\,^{+0.036}_{-0.035}$	$0.430\,^{+0.036}_{-0.035}$
$\mathcal{B}(\Lambda_b^0 \to \Lambda_c^+\pi^+\pi^-\pi^-)$	CDF [796]: $2.68 \pm 0.29\,^{+1.15}_{-1.09}$	$2.68\,^{+1.19}_{-1.12}$

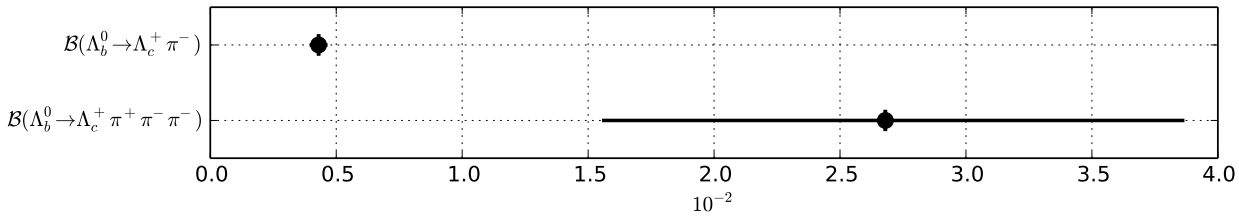

Figure 142: Summary of the averages from Table 179.

Table 180: Relative decay rates to Λ_c.

Parameter	Measurements	Average
$\mathcal{B}(\Lambda_b^0 \to \Lambda_c^+\pi^-)/\mathcal{B}(\overline{B}^0 \to D^+\pi^-)$		
	CDF [797]: $3.3 \pm 0.3 \pm 1.2$	3.3 ± 1.2
$\mathcal{B}(\Lambda_b^0 \to \Lambda_c^+\pi^+\pi^-\pi^-)/\mathcal{B}(\Lambda_b^0 \to \Lambda_c^+\pi^-)$		
	LHCb [597]: $1.43 \pm 0.16 \pm 0.13$	
	CDF [796]: $3.04 \pm 0.33\,^{+0.70}_{-0.55}$	1.55 ± 0.20
$\mathcal{B}(\Lambda_b^0 \to \Lambda_c^+K^-)/\mathcal{B}(\Lambda_b^0 \to \Lambda_c^+\pi^-)$		
	LHCb [788]: $0.0731 \pm 0.0016 \pm 0.0016$	0.0731 ± 0.0023
$\mathcal{B}(\Lambda_b^0 \to \Lambda_c^+D^-)/\mathcal{B}(\Lambda_b^0 \to \Lambda_c^+D_s^-)$		
	LHCb [688]: $0.042 \pm 0.003 \pm 0.003$	0.042 ± 0.004
$\mathcal{B}(\Xi_b^0 \to \Lambda_c^+K^-) \times \mathcal{B}(\Lambda_c^+ \to pK^-\pi^+)/\mathcal{B}(\Xi_b^0 \to D^0pK^-) \times \mathcal{B}(D^0 \to K^+\pi^-)$		
	LHCb [788]: $0.57 \pm 0.22 \pm 0.21$	0.57 ± 0.30

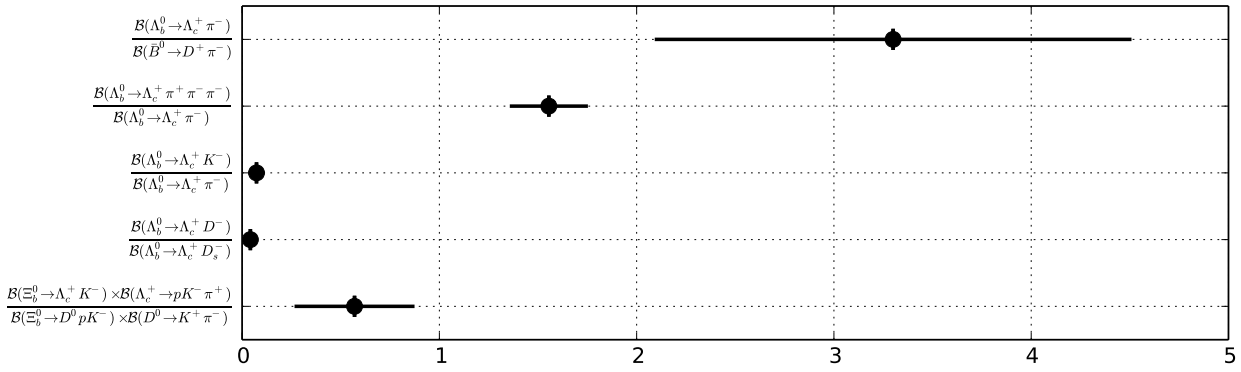

Figure 143: Summary of the averages from Table 180.

Table 181: Relative decay rates to excited or Σ_c states.

Parameter	**Measurements**	**Average**
$\mathcal{B}(\Lambda_b^0 \to \Lambda_c(2595)^+\pi^-) \times \mathcal{B}(\Lambda_c(2595)^+ \to \Lambda_c^+\pi^+\pi^-)/\mathcal{B}(\Lambda_b^0 \to \Lambda_c^+\pi^+\pi^-\pi^-)$		
	LHCb [597]: $0.044 \pm 0.017\,^{+0.006}_{-0.004}$	$0.044\,^{+0.018}_{-0.017}$
$\mathcal{B}(\Lambda_b^0 \to \Lambda_c(2625)^+\pi^-) \times \mathcal{B}(\Lambda_c(2625)^+ \to \Lambda_c^+\pi^+\pi^-)/\mathcal{B}(\Lambda_b^0 \to \Lambda_c^+\pi^+\pi^-\pi^-)$		
	LHCb [597]: $0.043 \pm 0.015 \pm 0.004$	0.043 ± 0.016
$\mathcal{B}(\Lambda_b^0 \to \Sigma_c^0\pi^+\pi^-) \times \mathcal{B}(\Sigma_c^0 \to \Lambda_c^+\pi^-)/\mathcal{B}(\Lambda_b^0 \to \Lambda_c^+\pi^+\pi^-\pi^-)$		
	LHCb [597]: $0.074 \pm 0.024 \pm 0.012$	0.074 ± 0.027
$\mathcal{B}(\Lambda_b^0 \to \Sigma_c^{++}\pi^-\pi^-) \times \mathcal{B}(\Sigma_c^{++} \to \Lambda_c^+\pi^+)/\mathcal{B}(\Lambda_b^0 \to \Lambda_c^+\pi^+\pi^-\pi^-)$		
	LHCb [597]: $0.042 \pm 0.018 \pm 0.007$	0.042 ± 0.019

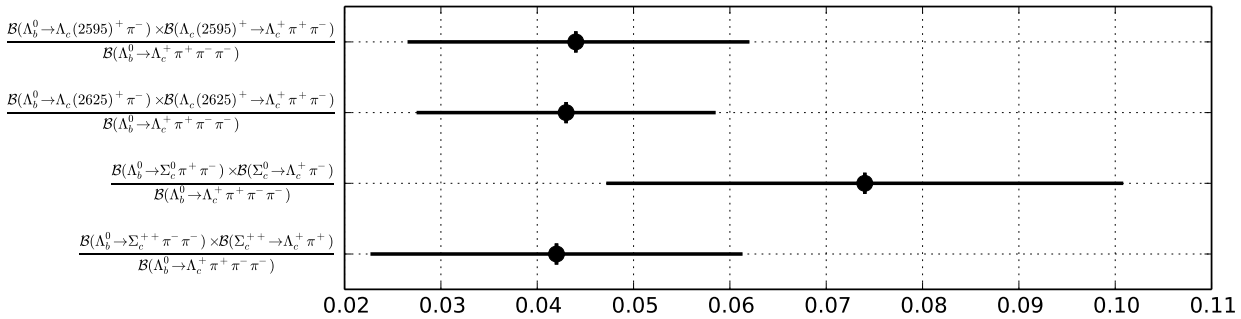

Figure 144: Summary of the averages from Table 181.

Table 182: Ξ_b decay rates [10^{-4}].

Parameter	Measurements	Average
$f_{\Xi_b^-}/f_{\Lambda_b^0}\mathcal{B}(\Xi_b^- \to \Lambda_b^0\pi^-)$		
	LHCb [798]: $5.7 \pm 1.8\,^{+0.8}_{-0.9}$	$5.7\,^{+2.0}_{-2.0}$

7 B decays to charmless final states

This section provides the branching fractions, polarization fractions, the partial rate asymmetries (A_{CP}) and other observables of B decays to final states that do not contain charm hadrons or charmonia mesons. The order of entries in the tables corresponds to that in the PDG [5], and the quoted RPP numbers are the PDG numbers of the corresponding branching fractions. The asymmetry is defined as

$$A_{CP} = \frac{N_{\overline{B}} - N_B}{N_{\overline{B}} + N_B}, \tag{213}$$

where $N_{\overline{B}}$ and N_B are, respectively, the number of $\overline{B}^0/B^-$ mesons (or of heavier mesons containing a b quark) and B^0/B^+ mesons (containing a $\bar{b}$ quark) decaying into a specific final state. This definition is consistent with that of Eq. (100) in Sec. 4.2.1. Four different B^0 and B^+ decay categories are considered: charmless mesonic (*i.e.* final states containing only mesons), baryonic (only hadrons, but including a baryon-antibaryon pair), radiative (including a photon or a lepton anti-lepton pair) and semileptonic/leptonic (including/only leptons). We also include measurements of B_s^0, B_c^+ and b-baryon decays. Measurements supported with written documents are accepted in the averages; written documents include journal papers, conference contributed papers, preprints or conference proceedings. Results from A_{CP} measurements obtained from time-dependent analyses are listed and described in Sec. 4.

Most of the branching fractions from *BABAR* and Belle assume equal production of charged and neutral B pairs. The best measurements to date show that this is still a reasonable approximation (see Sec. 3). For branching fractions, we provide either averages or the most stringent upper limits. If one or more experiments have measurements with $> 4\sigma$ for a decay channel, all available central values for that channel are used in the averaging. We also give central values and errors for cases where the significance of the average value is at least 3σ, even if no single measurement is above 4σ. For A_{CP} we provide averages in all cases. At the end of some of the tables we include a list of results that were not included. Typical cases are the measurements of distributions, such as differential branching fractions or longitudinal polarizations, which are measured in different binning schemes by the different collaborations, and thus cannot be directly used to obtain averages.

Our averaging is performed by maximizing the likelihood, $\mathcal{L} = \prod_i \mathcal{P}_i(x)$, where $\mathcal{P}_i$ is the probability density function (PDF) of the i^{th} measurement, and x is the branching fraction or A_{CP}. The PDF is modelled by an asymmetric Gaussian function with the measured central value as its mean and the quadratic sum of the statistical and systematic errors as the standard deviations. The experimental uncertainties are considered to be uncorrelated with each other when the averaging is performed. As mentioned in Sec. 2, no error scaling is applied when the fit χ^2 is greater than 1, except for cases of extreme disagreement (at present we have no such cases).

At present, this section contains measurements of more than 500 decay modes, reported in hundreds of papers. Because the number of references is so large, we do not include them with the tables shown here but the full set of references is available from active GIF files at the rare decays HFAG web page: `http://www.slac.stanford.edu/xorg/hfag/rare/index.html`. The largest improvement since the last report has come from the inclusion of a variety of new measurements from the LHC, especially LHCb. The measurements of B_s^0 decays are particularly noteworthy.

Sections 7.1 and 7.2 provide compilations of branching fractions of B^0 and B^+ to mesonic and baryonic charmless final states, respectively, while Sec. 7.3 gives branching fractions of b-baryons decays. In Sec. 7.4 and 7.5 different observables of interest are detailed in addition to branching fractions: in the former for B_s^0-meson charmless decays, and in the latter for leptonic and radiative B^0 and B^+ meson decays, including processes in which the photon yields a pair of charged of neutral leptons. This section also contains limits from searches for lepton-number-violating decays. Sections 7.6 and 7.7 give CP asymmetries and results of polarization measurements, respectively, in different b-hadron charmless decays. Finally, Sec. 7.8 gives branching fractions of B_c^+ meson decays to charmless final states.

7.1 Mesonic decays of B^0 and B^+ mesons

This section provides branching fractions of charmless mesonic decays: Tables 183 to 185 for B^+ and Tables 186 to 188 for B^0 mesons. The tables are separated according to the presence or absence of kaons in the final state. Finally, Table 189 details several relative branching fractions of B^0 decays.

Figure 145 gives a graphic representation of a selection of high precision branching fractions given in this section. For comments in the plot, marked with a symbol or a number, refer to the corresponding table.

Table 183: Branching fractions (BF) of charmless mesonic B^+ decays with kaons (part 1) in units of $\times 10^{-6}$. Upper limits are at 90% CL. Values in red (blue) are new published (preliminary) results since PDG2014.

RPP#	Mode	PDG2014 Avg.	*BABAR*	Belle	CLEO	CDF	LHCb	Our Avg.
262	$K^0\pi^+$	23.7 ± 0.8	$23.9 \pm 1.1 \pm 1.0$	$23.97 \pm 0.53 \pm 0.71$	$18.8^{+3.7+2.1}_{-3.3-1.8}$			23.79 ± 0.75
263	$K^+\pi^0$	12.9 ± 0.5	$13.6 \pm 0.6 \pm 0.7$	$12.62 \pm 0.31 \pm 0.56$	$12.9^{+2.4+1.2}_{-2.2-1.1}$			$12.94^{+0.52}_{-0.51}$
264	$\eta' K^+$	70.6 ± 2.5	$71.5 \pm 1.3 \pm 3.2$	$69.2 \pm 2.2 \pm 3.7$	$80^{+10}_{-9} \pm 7$			71.1 ± 2.6
265	$\eta' K^{*+}$	$4.8^{+1.8}_{-1.6}$	$4.8^{+1.6}_{-1.4} \pm 0.8$	< 2.9	< 35			$4.8^{+1.8}_{-1.6}$
266	$\eta' K_0^*(1430)^+$	5.2 ± 2.1	$5.2 \pm 1.9 \pm 1.0$					5.2 ± 2.1
267	$\eta' K_2^*(1430)^+$	28 ± 5	$28.0^{+4.6}_{-4.3} \pm 2.6$					$28.0^{+5.3}_{-5.0}$
268	ηK^+	2.4 ± 0.4	$2.94^{+0.39}_{-0.34} \pm 0.21$	$2.12 \pm 0.23 \pm 0.11$	$2.2^{+2.8}_{-2.2}$			$2.36^{+0.22}_{-0.21}$
269	ηK^{*+}	19.3 ± 1.6	$18.9 \pm 1.8 \pm 1.3$	$19.3^{+2.0}_{-1.9} \pm 1.5$	$26.4^{+9.6}_{-8.2} \pm 3.3$			19.3 ± 1.6
270	$\eta K_0^*(1430)^+$	18 ± 4	$18.2 \pm 2.6 \pm 2.6$					18.2 ± 3.7
271	$\eta K_2^*(1430)^+$	9.1 ± 3.0	$9.1 \pm 2.7 \pm 1.4$					9.1 ± 3.0
272	$\eta(1295) K^+$ †	$2.9^{+0.8}_{-0.7}$	$2.9^{+0.8}_{-0.7} \pm 0.2$ §					$2.9^{+0.8}_{-0.7}$
274	$\eta(1405) K^+$ †	< 1.2	< 1.2					< 1.2
275	$\eta(1475) K^+$ †	$13.8^{+2.1}_{-1.8}$	$13.8^{+1.8+1.0}_{-1.7-0.6}$					$13.8^{+2.1}_{-1.8}$
276	$f_1(1285) K^+$	< 2.0	< 2.0					< 2.0
277	$f_1(1420) K^+$ †	< 2.9	< 2.9					< 2.9
279	$\phi(1680) K^+$ †	< 3.4	< 3.4					< 3.4
280	$f_0(1500) K^+$	3.7 ± 2.2	3.7 ± 2.2 ‡					3.7 ± 2.2
281	ωK^+	6.7 ± 0.8	$6.3 \pm 0.5 \pm 0.3$	$6.8 \pm 0.4 \pm 0.4$	$3.2^{+2.4}_{-1.9} \pm 0.8$			6.5 ± 0.4
282	ωK^{*+}	< 7.4	< 7.4		< 87			< 7.4
283	$\omega (K\pi)_0^{*+}$	28 ± 4	$27.5^{+3.0}_{-2.6}$					$27.5^{+3.0}_{-2.6}$
284	$\omega K_0^*(1430)^+$	24 ± 5	$24.0 \pm 2.6 \pm 4.4$					24.0 ± 5.1
285	$\omega K_2^*(1430)^+$	21 ± 4	$21.5 \pm 3.6 \pm 2.4$					21.5 ± 4.3
286	$a_0(980)^+ K^0$ †	< 3.9	< 3.9					< 3.9
287	$a_0(980)^0 K^+$ †	< 2.5	< 2.5					< 2.5
288	$K^{*0}\pi^+$	10.1 ± 0.9	$10.8 \pm 0.6^{+1.2}_{-1.4}$	$9.7 \pm 0.6^{+0.8}_{-0.9}$	< 16			$10.1^{+0.8}_{-0.9}$
289	$K^{*+}\pi^0$	8.2 ± 1.9	$8.2 \pm 1.5 \pm 1.1$		$7.1^{+11.4}_{-7.1} \pm 1.0$			8.2 ± 1.8
290	$K^+\pi^+\pi^-$	51 ± 2.9	$54.4 \pm 1.1 \pm 4.6$	$48.8 \pm 1.1 \pm 3.6$				51.0 ± 3.0
291	$K^+\pi^+\pi^-$ (NR)	$16.3^{+2.1}_{-1.5}$	$9.3 \pm 1.0^{+6.9}_{-1.7}$	$16.9 \pm 1.3^{+1.7}_{-1.6}$	< 28			16.3 ± 2.0
292	$\omega(782) K^+$ $(K^+\pi^+\pi^-)$	6 ± 9	$5.9^{+8.8+0.5}_{-9.0-0.4}$					$5.9^{+8.8}_{-9.0}$
293	$f_0(980) K^+$ $(K^+\pi^+\pi^-)$ †	$9.4^{+1.0}_{-1.2}$	$10.3 \pm 0.5^{+2.0}_{-1.4}$	$8.8 \pm 0.8^{+0.9}_{-1.8}$				$9.4^{+0.9}_{-1.0}$
294	$f_2(1270)^0 K^+$ $(K^+\pi^+\pi^-)$	1.07 ± 0.27	$0.88^{+0.38+0.01}_{-0.33-0.03}$	$1.33 \pm 0.30^{+0.23}_{-0.34}$				1.07 ± 0.29
295	$f_0(1370)^0 K^+$ $(K^+\pi^+\pi^-)$ †	< 10.7	< 10.7					< 10.7
296	$\rho(1450)^0 K^+$ $(K^+\pi^+\pi^-)$	< 11.7	< 11.7					< 11.7
297	$f_2'(1525) K^+$ $(K^+\pi^+\pi^-)$	< 3.4	< 3.4					< 3.4
298	$\rho^0 K^+$ $(K^+\pi^+\pi^-)$	3.7 ± 0.5	$3.56 \pm 0.45^{+0.57}_{-0.46}$	$3.89 \pm 0.47^{+0.43}_{-0.41}$	< 17			$3.74^{+0.49}_{-0.45}$
299	$K_0^*(1430)^0\pi^+$ $(K^+\pi^+\pi^-)$	45^{+9}_{-7}	$32.0 \pm 1.2^{+10.8}_{-6.0}$	$51.6 \pm 1.7^{+7.0}_{-7.5}$				45.1 ± 6.3
300	$K_2^*(1430)^0\pi^+$ $(K^+\pi^+\pi^-)$	$5.6^{+2.2}_{-1.5}$	$5.6 \pm 1.2^{+1.8}_{-0.8}$	< 6.9				$5.6^{+2.2}_{-1.4}$
301	$K^*(1410)^0\pi^+$ $(K^+\pi^+\pi^-)$	< 45		< 45				< 45
302	$K^*(1680)^0\pi^+$ $(K^+\pi^+\pi^-)$	< 12	< 15	< 12				< 12
303	$K^+\pi^0\pi^0$	16.2 ± 1.9	$16.2 \pm 1.2 \pm 1.5$					16.2 ± 1.9
304	$f_0(980) K^+$ $(K^+\pi^0\pi^0)$	2.8 ± 0.8	$2.8 \pm 0.6 \pm 0.5$					2.8 ± 0.8
305	$K^-\pi^+\pi^+$	< 0.95	< 0.95	< 4.5			< 0.046	< 0.046
306	$K^-\pi^+\pi^+$ (NR)	< 56			< 56			< 56
307	$K_1(1270)^0\pi^+$	< 40	< 40					< 40
308	$K_1(1400)^0\pi^+$	< 39	< 39					< 39
309	$K^0\pi^+\pi^0$	< 66			< 66			< 66
310	$\rho^+ K^0 (K^0\pi^+\pi^0)$	8.0 ± 1.5	$8.0^{+1.4}_{-1.3} \pm 0.6$		< 48			$8.0^{+1.5}_{-1.4}$
311	$K^{*+}\pi^+\pi^-$	75 ± 10	$75.3 \pm 6.0 \pm 8.1$					75.3 ± 10.1
312	$K^{*+}\rho^0$	4.6 ± 1.1	$4.6 \pm 1.0 \pm 0.4$		< 74			4.6 ± 1.1
313	$f_0(980) K^{*+}$ †	4.2 ± 0.7	$4.2 \pm 0.6 \pm 0.3$					4.2 ± 0.7

† Product BF - daughter BF taken to be 100%
§ Product BF $\times \mathcal{B}(\eta(1295) \to \eta\pi\pi)$
‡ Average of results in $K_S^0 K^+ K^-$, $K_S^0 K_S^0 K^+$ [259] and $K^+\pi^+\pi^-$ [266]. Reference [266] includes an f_X resonance with parameters that are compatible with $f_0(1500)$.

Table 184: Branching fractions (BF) of charmless mesonic B^+ decays with kaons (part 2) in units of $\times 10^{-6}$. Upper limits are at 90% CL. Values in red (blue) are new published (preliminary) results since PDG2014.

RPP#	Mode	PDG2014 Avg.	*BABAR*	Belle	CLEO	CDF	LHCb	Our Avg.
314	$a_1^+ K^0$	35 ± 7	$34.9 \pm 5.0 \pm 4.4$					34.9 ± 6.7
315	$b_1^+ K^0$ †	9.6 ± 1.9	$9.6 \pm 1.7 \pm 0.9$					9.6 ± 1.9
317	$K_1(1400)^+ \rho^0$	< 780	< 780 ◦					< 780 ◦
318	$K_2(1430)^+ \rho^0$	< 1500	< 1500 ◦					< 1500 ◦
319	$b_1^0 K^+$ †	9.1 ± 2.0	$9.1 \pm 1.7 \pm 1.0$					9.1 ± 2.0
320	$b_1^+ K^{*0}$ †	< 5.9	< 5.9					< 5.9
321	$b_1^0 K^{*+}$ †	< 6.7	< 6.7					< 6.7
322	$K^+ \overline{K}^0$	1.31 ± 0.17	$1.61 \pm 0.44 \pm 0.09$	$1.11 \pm 0.19 \pm 0.05$	< 3.3		$1.52 \pm 0.21 \pm 0.05$	1.32 ± 0.14
323	$\overline{K}^0 K^+ \pi^0$	< 24			< 24			< 24
324	$K^+ K_S K_S$	10.8 ± 0.6	$10.6 \pm 0.5 \pm 0.3$	$13.4 \pm 1.9 \pm 1.5$				10.8 ± 0.6
325	$f_0(980) K^+$ $(K^+ K_S K_S)$	14.7 ± 3.3	$14.7 \pm 2.8 \pm 1.8$					14.7 ± 3.3
326	$f_0(1710) K^+$ $(K^+ K_S K_S)$	$0.48^{+0.40}_{-0.26}$	$0.48^{+0.40}_{-0.24} \pm 0.11$					$0.48^{+0.41}_{-0.26}$
327	$K^+ K_S K_S$ (NR)	20 ± 4	$19.8 \pm 3.7 \pm 2.5$					19.8 ± 4.5
328	$K_S K_S \pi^+$	< 0.51	< 0.51	< 3.2				< 0.51
329	$K^+ K^- \pi^+$	5.0 ± 0.7	$5.0 \pm 0.5 \pm 0.5$	< 13				5.0 ± 0.7
330	$K^+ K^- \pi^+$ (NR)	< 75			< 75			< 75
331	$\overline{K}^{*0} K^+$ $(K^+ K^- \pi^+)$	< 1.1	< 1.1		< 5.3			< 1.1
332	$\overline{K}_0^*(1430)^0 K^+$ $(K^+ K^- \pi^+)$	< 2.2	< 2.2					< 2.2
333	$K^+ K^+ \pi^-$	< 0.16	< 0.16	< 2.4			< 0.011	< 0.011
334	$K^+ K^+ \pi^-$ (NR)	< 87.9						< 87.9
335	$f_2'(1525) K^+$	1.8 ± 0.5	1.8 ± 0.5 ‡	< 8				1.8 ± 0.5
336	$f_J(2220) K^+$	< 1.2		< 1.2				< 1.2
337	$K^{*+} \pi^+ K^-$	< 11.8	< 11.8					< 11.8
338	$K^{*+} \overline{K}^{*0}$	1.2 ± 0.5	$1.2 \pm 0.5 \pm 0.1$	< 1.31	< 71			1.2 ± 0.5
339	$K^{*+} K^+ \pi^-$	< 6.1	< 6.1					< 6.1
340	$K^+ K^- K^+$	34.0 ± 1.4	$34.6 \pm 0.6 \pm 0.9$	$30.6 \pm 1.2 \pm 2.3$				34.0 ± 1.0
341	ϕK^+ $(K^+ K^- K^+)$	$8.8^{+0.7}_{-0.6}$	$9.2 \pm 0.4^{+0.7}_{-0.5}$	$9.6 \pm 0.9^{+1.1}_{-0.8}$	$5.5^{+2.1}_{-1.8} \pm 0.6$	$7.6 \pm 1.3 \pm 0.6$		8.8 ± 0.5
342	$f_0(980) K^+$ $(K^+ K^- K^+)$	9.4 ± 3.2	$9.4^{+1.6}_{-2.8}$					$9.4^{+1.6}_{-2.8}$
343	$a_2(1320) K^+$ $(K^+ K^- K^+)$ †	< 1.1		< 1.1				< 1.1
344	$X_0(1550) K^+$ $(K^+ K^- K^+)$	4.3 ± 0.7	$4.3 \pm 0.60 \pm 0.30$					4.30 ± 0.67
345	$\phi(1680) K^+$ $(K^+ K^- K^+)$ †	< 0.8		< 0.8				< 0.8
346	$f_0(1710) K^+$ $(K^+ K^- K^+)$ †	1.1 ± 0.6	$1.12 \pm 0.25 \pm 0.50$					1.12 ± 0.56
347	$K^+ K^- K^+$ (NR)	$23.8^{+2.8}_{-5.0}$	$22.8 \pm 2.7 \pm 7.6$	$24.0 \pm 1.5^{+2.6}_{-6.0}$				$23.8^{+2.9}_{-5.1}$
348	$K^{*+} K^+ K^-$	36 ± 5	$36.2 \pm 3.3 \pm 3.6$					36.2 ± 4.9
349	ϕK^{*+}	10.0 ± 2.0	$11.2 \pm 1.0 \pm 0.9$	$6.7^{+2.1+0.7}_{-1.9-1.0}$	$10.6^{+6.4+1.8}_{-4.9-1.6}$			10.0 ± 1.1
350	$\phi(K\pi)_0^{*+}$	8.3 ± 1.6	$8.3^{+1.4}_{-0.8}$					$8.3^{+1.4}_{-0.8}$
351	$\phi K_1(1270)^+$	6.1 ± 1.9	$6.1 \pm 1.6 \pm 1.1$					6.1 ± 1.9
352	$\phi K_1(1400)^+$	< 3.2	< 3.2					< 3.2
353	$\phi K^*(1410)^+$	< 4.3	< 4.3					< 4.3
354	$\phi K_0^*(1430)^+$	7.0 ± 1.6	$7.0 \pm 1.3 \pm 0.9$					7.0 ± 1.6
355	$\phi K_2^*(1430)^+$	8.4 ± 2.1	$8.4 \pm 1.8 \pm 1.0$					8.4 ± 2.1
356	$\phi K_2(1770)^+$	< 15	< 15					< 15
357	$\phi K_2(1820)^+$	< 16.3	< 16.3					< 16.3
358	$a_1^+ K^{*0}$	< 3.6	< 3.6					< 3.6
359	$\phi\phi K^+$ §	5.0 ± 1.2	$5.6 \pm 0.5 \pm 0.3$	$2.6^{+1.1}_{-0.9} \pm 0.3$				5.0 ± 0.5
360	$\eta'\eta' K^+$	< 25	< 25					< 25
361	$K^+ \omega\phi$	< 1.9		< 1.9				< 1.9
362	$K^+ X(1812)$ †	< 0.32		< 0.32				< 0.32

† Product BF - daughter BF taken to be 100%; § $M_{\phi\phi} < 2.85$ GeV/c^2
‡ Average of results in $K_S^0 K^+ K^-$, $K_S^0 K_S^0 K^+$ [259].
◦ Result from ARGUS. Cited in the *BABAR* column to avoid adding a column to the table.

Table 185: Branching fractions (BF) of charmless mesonic B^+ decays without kaons in units of $\times 10^{-6}$. Upper limits are at 90% CL. Values in red (blue) are new published (preliminary) results since PDG2014.

RPP#	Mode	PDG2014 Avg.	*BABAR*	Belle	CLEO	CDF	LHCb	Our Avg.
379	$\pi^+\pi^0$	5.5 ± 0.4	$5.02 \pm 0.46 \pm 0.29$	$5.86 \pm 0.26 \pm 0.38$	$4.6^{+1.8+0.6}_{-1.6-0.7}$			$5.48^{+0.35}_{-0.34}$
380	$\pi^+\pi^+\pi^-$	15.2 ± 1.4	$15.2 \pm 0.6 \pm 1.3$					15.2 ± 1.4
381	$\rho^0\pi^+$	8.3 ± 1.2	$8.1 \pm 0.7^{+1.3}_{-1.6}$	$8.0^{+2.3}_{-2.0} \pm 0.7$	$10.4^{+3.3}_{-3.4} \pm 2.1$			$8.3^{+1.2}_{-1.3}$
382	$f_0(980)\pi^+$ †	< 1.5	< 1.5					< 1.5
383	$f_2(1270)\pi^+$	$1.6^{+0.7}_{-0.4}$	$1.57 \pm 0.42^{+0.55}_{-0.25}$					$1.57^{+0.69}_{-0.49}$
384	$\rho(1450)^0\pi^+$ †	$1.4^{+0.6}_{-0.9}$	$1.4 \pm 0.4^{+0.5}_{-0.8}$					$1.4^{+0.6}_{-0.9}$
385	$f_0(1370)\pi^+$ †	< 4.0	< 4.0					< 4.0
386	$f_0(500)\pi^+$ †	< 4.1	< 4.1					< 4.1
387	$\pi^+\pi^-\pi^+(NR)$	$5.3^{+1.5}_{-1.1}$	$5.3 \pm 0.7^{+1.3}_{-0.8}$					$5.3^{+1.5}_{-1.1}$
388	$\pi^+\pi^0\pi^0$	< 890	< 890 ◇					< 890 ◇
389	$\rho^+\pi^0$	10.9 ± 1.4	$10.2 \pm 1.4 \pm 0.9$	$13.2 \pm 2.3^{+1.4}_{-1.9}$	< 43			$10.9^{+1.4}_{-1.5}$
391	$\rho^+\rho^0$	24.0 ± 1.9	$23.7 \pm 1.4 \pm 1.4$	$31.7 \pm 7.1^{+3.8}_{-6.7}$				$24.0^{+1.9}_{-2.0}$
392	$f_0(980)\rho^+$ †	< 2.0	< 2.0					< 2.0
393	$a_1^+\pi^0$	26 ± 7	$26.4 \pm 5.4 \pm 4.1$					26.4 ± 6.8
394	$a_1^0\pi^+$	20 ± 6	$20.4 \pm 4.7 \pm 3.4$					20.4 ± 5.8
395	$\omega\pi^+$	6.9 ± 0.5	$6.7 \pm 0.5 \pm 0.4$	$6.9 \pm 0.6 \pm 0.5$	$11.3^{+3.3}_{-2.9} \pm 1.4$			6.9 ± 0.5
396	$\omega\rho^+$	15.9 ± 2.1	$15.9 \pm 1.6 \pm 1.4$		< 61			15.9 ± 2.1
397	$\eta\pi^+$	4.02 ± 0.27	$4.00 \pm 0.40 \pm 0.24$	$4.07 \pm 0.26 \pm 0.21$	$1.2^{+2.8}_{-1.2}$			4.02 ± 0.27
398	$\eta\rho^+$	7.0 ± 2.9	$9.9 \pm 1.2 \pm 0.8$	$4.1^{+1.4}_{-1.3} \pm 0.4$	$4.8^{+5.2}_{-3.8}$			6.9 ± 1.0
399	$\eta'\pi^+$	2.7 ± 0.9	$3.5 \pm 0.6 \pm 0.2$	$1.8^{+0.7}_{-0.6} \pm 0.1$	$1.0^{+5.8}_{-1.0}$			$2.7^{+0.5}_{-0.4}$
400	$\eta'\rho^+$	9.7 ± 2.2	$9.7^{+1.9}_{-1.8} \pm 1.1$	< 5.8	< 33			$9.7^{+2.2}_{-2.1}$
401	$\phi\pi^+$	< 0.15	< 0.24	< 0.33	< 5		< 0.15	< 0.15
402	$\phi\rho^+$	< 3.0	< 3.0		< 16			< 3.0
403	$a_0(980)^0\pi^+$ †	< 5.8	< 5.8					< 5.8
404	$a_0(980)^+\pi^0$ †	< 1.4	< 1.4					< 1.4
405	$\pi^+\pi^+\pi^+\pi^-\pi^-$	< 860	< 860 ◇					< 860 ◇
406	$\rho^0 a_1(1260)^+$	< 620			< 620			< 620
407	$\rho^0 a_2(1320)^+$	< 720			< 720			< 720
408	$b_1^0\pi^+$ †	6.7 ± 2.0	$6.7 \pm 1.7 \pm 1.0$					6.7 ± 2.0
409	$b_1^+\pi^0$ †	< 3.3	< 3.3					< 3.3
410	$\pi^+\pi^+\pi^+\pi^-\pi^-\pi^0$	< 6300	< 6300 ◇					< 6300 ◇
411	$b_1^+\rho^0$ †	< 5.2	< 5.2					< 5.2
413	$b_1^0\rho^+$ †	< 3.3	< 3.3					< 3.3

† Product BF - daughter BF taken to be 100%;

Table 186: Branching fractions (BF) of charmless mesonic B^0 decays with kaons (part 1) in units of $\times 10^{-6}$. Upper limits are at 90% CL. Values in red (blue) are new published (preliminary) results since PDG2014.

RPP#	Mode	PDG2014 Avg.	*BABAR*	Belle	CLEO	CDF	LHCb	Our Avg.
227	$K^+\pi^-$	19.6 ± 0.5	$19.1 \pm 0.6 \pm 0.6$	$20.0 \pm 0.34 \pm 0.60$	$18.0^{+2.3+1.2}_{-2.1-0.9}$			$19.57^{+0.53}_{-0.52}$
228	$K^0\pi^0$	9.9 ± 0.5	$10.1 \pm 0.6 \pm 0.4$	$9.68 \pm 0.46 \pm 0.50$	$12.8^{+4.0+1.7}_{-3.3-1.4}$			9.93 ± 0.49
229	$\eta' K^0$	66 ± 4	$68.5 \pm 2.2 \pm 3.1$	$58.9^{+3.6}_{-3.5} \pm 4.3$	$89^{+18}_{-16} \pm 9$			66.1 ± 3.1
230	$\eta' K^{*0}$	3.1 ± 0.9	$3.1^{+0.9}_{-0.8} \pm 0.3$	$2.6 \pm 0.7 \pm 0.2$	$7.8^{+7.7}_{-5.7}$			$2.8^{+0.6}_{-0.5}$
231	$\eta' K_0^*(1430)^0$	6.3 ± 1.6	$6.3 \pm 1.3 \pm 0.9$					6.3 ± 1.6
232	$\eta' K_2^*(1430)^0$	13.7 ± 3.2	$13.7^{+3.0}_{-1.9} \pm 1.2$					$13.7^{+3.2}_{-2.2}$
233	ηK^0	$1.23^{+0.27}_{-0.24}$	$1.15^{+0.43}_{-0.38} \pm 0.09$	$1.27^{+0.33}_{-0.29} \pm 0.08$	$0.0^{+3.0}_{-0.0}$			$1.23^{+0.27}_{-0.24}$
234	ηK^{*0}	15.9 ± 1.0	$16.5 \pm 1.1 \pm 0.8$	$15.2 \pm 1.2 \pm 1.0$	$13.8^{+5.5}_{-4.6} \pm 1.6$			15.9 ± 1.0
235	$\eta K_0^*(1430)^0$	11.0 ± 2.2	$11.0 \pm 1.6 \pm 1.5$					11.0 ± 2.2
236	$\eta K_2^*(1430)^0$	9.6 ± 2.1	$9.6 \pm 1.8 \pm 1.1$					9.6 ± 2.1
237	ωK^0	5.0 ± 0.6	$5.4 \pm 0.8 \pm 0.3$	$4.5 \pm 0.4 \pm 0.3$	$10.0^{+5.4}_{-4.2} \pm 1.4$			4.8 ± 0.4
238	$a_0(980)^0 K^0$ †	< 7.8	< 7.8					< 7.8
239	$b_1^0 K^0$ †	< 7.8	< 7.8					< 7.8
240	$a_0(980)^- K^+$ †	< 1.9	< 1.9					< 1.9
241	$b_1^- K^+$ †	7.4 ± 1.4	$7.4 \pm 1.0 \pm 1.0$					7.4 ± 1.4
242	$b_1^0 K^{*0}$ †	< 8.0	< 8.0					< 8.0
243	$b_1^- K^{*+}$ †	< 5.0	< 5.0					< 5.0
244	$a_0(1450)^- K^+$ †	< 3.1	< 3.1					< 3.1
245	$K_S X^0(\text{Familon})$ †	< 53			< 53			< 53
246	ωK^{*0}	2.0 ± 0.5	$2.2 \pm 0.6 \pm 0.2$	$1.8 \pm 0.7^{+0.3}_{-0.2}$	< 23			2.0 ± 0.5
247	ωK^{*0}	18.4 ± 2.5	$18.4^{+1.8}_{-1.7}$					$18.4^{+1.8}_{-1.7}$
248	$\omega K_0^*(1430)^0$	16.0 ± 3.4	$16.0 \pm 1.6 \pm 3.0$					16.0 ± 3.4
249	$\omega K_2^*(1430)^0$	10.1 ± 2.3	$10.1 \pm 2.0 \pm 1.1$					10.1 ± 2.3
250	$\omega K^+\pi^-$ (NR)[1]	5.1 ± 1.0		$5.1 \pm 0.7 \pm 0.7$				5.1 ± 1.0
251	$K^+\pi^-\pi^0$	37.8 ± 3.2	$38.5 \pm 1.0 \pm 3.9$	$36.6^{+4.2}_{-4.3} \pm 3.0$	< 40			37.8 ± 3.2
252	$\rho^- K^+$	7.0 ± 0.9	$6.6 \pm 0.5 \pm 0.8$	$15.1^{+3.4+2.4}_{-3.3-2.6}$	< 32			7.0 ± 0.9
253	$\rho(1450)^- K^+$	2.4 ± 1.2	$2.4 \pm 1.0 \pm 0.6$					2.4 ± 1.2
254	$\rho(1700)^- K^+$	0.6 ± 0.7	$0.6 \pm 0.6 \pm 0.4$					0.6 ± 0.7
255	$K^+\pi^-\pi^0$ (NR)	2.8 ± 0.6	$2.8 \pm 0.5 \pm 0.4$	< 9.4				2.8 ± 0.6
256	$(K\pi)_0^{*+}\pi^-$	34 ± 5	$34.2 \pm 2.4 \pm 4.1$					34.2 ± 4.8
257	$(K\pi)_0^{*+}\pi^0$	8.5 ± 1.7	$8.6^{+1.1}_{-1.3}$					$8.6^{+1.1}_{-1.3}$
258	$K_2^*(1430)^0\pi^0$	< 4.0	< 4.0					< 4.0
259	$K^*(1680)^0\pi^0$	< 7.5	< 7.5					< 7.5
260	$K_x^{*0}\pi^0$ [2]	6.1 ± 1.6		$6.1^{+1.6+0.5}_{-1.5-0.6}$				$6.1^{+1.7}_{-1.6}$
261	$K^0\pi^+\pi^-$	65 ± 8	$50.2 \pm 1.5 \pm 1.8$	$47.5 \pm 2.4 \pm 3.7$	$50^{+10}_{-9} \pm 7$		$65.2^{+6.0}_{-5.1}$ ◇	51.8 ± 1.9
262	$K^0\pi^+\pi^-$ (NR)	$14.7^{+4.0}_{-2.6}$	$11.1^{+2.5}_{-1.0} \pm 0.9$	$19.9 \pm 2.5^{+1.7}_{-2.0}$				14.7 ± 2.0
263	$\rho^0 K^0$	4.7 ± 0.6	$4.4 \pm 0.7 \pm 0.3$	$6.1 \pm 1.0^{+1.1}_{-1.2}$	< 39			4.7 ± 0.7
264	$K^{*+}\pi^-$	8.4 ± 0.8	8.2 ± 0.9 [3]	$8.4 \pm 1.1^{+1.0}_{-0.9}$	$16^{+6}_{-5} \pm 2$			8.4 ± 0.8
265	$K_0^*(1430)^+\pi^-$	33 ± 7	$29.9^{+2.3}_{-1.7} \pm 3.6$	$49.7 \pm 3.8^{+6.8}_{-8.2}$				$33.5^{+3.9}_{-3.8}$
266	$K_x^{*+}\pi^-$ [2]	5.1 ± 1.6		$5.1^{+1.5+0.6}_{-1.5-0.7}$				$5.1^{+1.6}_{-1.7}$
267	$K^*(1410)^+\pi^-$ †	< 3.8		< 3.8				< 3.8
268	$f_0(980) K^0$ †	7.0 ± 0.9	$6.9 \pm 0.8 \pm 0.6$	$7.6 \pm 1.7^{+0.9}_{-1.3}$				7.0 ± 0.9
269	$f_2(1270)^0 K^0$	$2.7^{+1.3}_{-1.2}$	$2.7^{+1.0}_{-0.8} \pm 0.9$	< 2.5†				$2.7^{+1.3}_{-1.2}$
270	$f_x(1300)^0 K^0$	1.8 ± 0.7	$1.81^{+0.55}_{-0.45} \pm 0.48$					$1.81^{+0.73}_{-0.66}$

† Product BF - daughter BF taken to be 100%; ‡ Relative BF converted to absolute BF; [1] $0.755 < M(K\pi) < 1.250$ GeV/c^2; [2] K_x^{*0} stands for the possible candidates for $K^*(1410), K_0^*(1430), K_2^*(1430)$;
[3] Average of *BABAR* results from $B^0 \to K^+\pi^-\pi^0$ and $B^0 \to K^0\pi^+\pi^-$.
◇ Obtained from a fit to the ratios of BFs measured by LHCb (Ref. [799]) and to the averages of the BFs in their numerators, as measured by other experiments (RPP 292 and 298).

Table 187: Branching fractions (BF) of charmless mesonic B^0 decays with kaons (part 2) in units of $\times 10^{-6}$. Upper limits are at 90% CL. Values in red (blue) are new published (preliminary) results since PDG2014.

RPP#	Mode	PDG2014 Avg.	*BABAR*	Belle	CLEO	CDF	LHCb	Our Avg.
271	$K^{*0}\pi^0$	3.3 ± 0.6	$3.3 \pm 0.5 \pm 0.4$	< 3.5	< 3.6			3.3 ± 0.6
272	$K_2^*(1430)^+\pi^-$	< 6	< 16.2	< 6.3				< 6.3
273	$K^*(1680)^+\pi^-$	< 10	< 25	< 10.1				< 10.1
275	$\rho^0 K^+\pi^-$	2.8 ± 0.7		$2.8 \pm 0.5 \pm 0.5$ [2]				2.8 ± 0.7
276	$f_0(980)K^+\pi^-$	$1.4^{+0.5}_{-0.6}$		$1.4 \pm 0.4^{+0.3}_{-0.4}$ [2]				$1.4^{+0.5}_{-0.6}$
277	$K^+\pi^-\pi^+\pi^-$	< 2.1		< 2.1				< 2.1
278	$K^{*0}\pi^+\pi^-$	55 ± 5	$54.5 \pm 2.9 \pm 4.3$					54.5 ± 5.2
279	$K^{*0}\rho^0$	3.9 ± 1.3	$5.1 \pm 0.6^{+0.6}_{-0.8}$	$2.1^{+0.8+0.9}_{-0.7-0.5}$	< 34			3.9 ± 0.8
280	$f_0(980)K^{*0}$ †	$3.9^{+2.1}_{-1.8}$	$5.7 \pm 0.6 \pm 0.4$	$1.4^{+0.6+0.6}_{-0.5-0.4}$				3.9 ± 0.5
281	$K_1(1270)^+\pi^-$	< 30	17^{+6}_{-25}					17^{+6}_{-25}
282	$K_1(1400)^+\pi^-$	< 27	16^{+8}_{-24}					16^{+8}_{-24}
283	$a_1^- K^+$	16 ± 4	$16.3 \pm 2.9 \pm 2.3$					16.3 ± 3.7
284	$K^{*+}\rho^-$	10.3 ± 0.26	$10.3 \pm 2.3 \pm 1.3$					10.3 ± 2.6
285	$K_0(1430)^+\rho^-$	28 ± 12	$28 \pm 10 \pm 6$					28 ± 11
287	$K_0^*(1430)^0\rho^0$	27 ± 6	$27 \pm 4 \pm 4$					27 ± 5
288	$K_0^*(1430)^0 f_0(980)$	2.7 ± 0.9	$2.7 \pm 0.7 \pm 0.6$					2.7 ± 0.9
289	$K_2^*(1430)^0 f_0(980)$	8.6 ± 2.0	$8.6 \pm 1.7 \pm 1.0$					8.6 ± 2.0
290	K^+K^-	0.13 ± 0.05	< 0.5	$0.10 \pm 0.08 \pm 0.04$	< 0.8	$0.23 \pm 0.10 \pm 0.10$‡	$0.0780 \pm 0.0127 \pm 0.084$‡	0.1111 ± 0.0565
291	$K^0\overline{K}^0$	1.21 ± 0.16	$1.08 \pm 0.28 \pm 0.11$	$1.26 \pm 0.19 \pm 0.05$	< 3.3			1.21 ± 0.16
292	$K^0K^-\pi^+$	7.3 ± 1.1	$6.4 \pm 1.0 \pm 0.6$	< 18	< 21		6.64 ± 0.99 ◇	6.54 ± 0.75
293	$K^{*0}\overline{K}^0$ ¶	< 1.9	< 1.9				< 0.96 ‡	< 0.96 ‡
–	$K^{*\mp}K^{\pm}$	New					< 0.4 ‡	< 0.4 ‡
294	$K^+K^-\pi^0$	2.2 ± 0.6		$2.17 \pm 0.60 \pm 0.24$	< 19			2.17 ± 0.65
295	$K_SK_S\pi^0$	< 0.9	< 0.9					< 0.9
296	$K_SK_S\eta$	< 1.0	< 1.0					< 1.0
297	$K_SK_S\eta'$	< 2.0	< 2.0					< 2.0
298	$K^+K^-K^0$	26.3 ± 1.5	$26.5 \pm 0.9 \pm 0.8$	$28.3 \pm 3.3 \pm 4.0$			19.1 ± 1.9 ◇	24.5 ± 1.0
299	ϕK^0	7.3 ± 0.7	$7.1 \pm 0.6^{+0.4}_{-0.3}$	$9.0^{+2.2}_{-1.8} \pm 0.7$	$5.4^{+3.7}_{-2.7} \pm 0.7$			$7.3^{+0.7}_{-0.6}$
300	$f_0(980)K^0$ †	$7.0^{+3.5}_{-3.0}$	$7.0^{+2.6}_{-1.8} \pm 2.4$					$7.0^{+3.5}_{-3.0}$
301	$f_0(1500)K^0$ †	13^{+7}_{-5}	$13.3^{+5.8}_{-4.4} \pm 3.2$					$13.3^{+6.6}_{-5.4}$
302	$f_2'(1525)K^0$	$0.3^{+0.5}_{-0.4}$	$0.29^{+0.27}_{-0.18} \pm 0.36$					$0.29^{+0.45}_{-0.40}$
303	$f_0(1710)K^0$†	4.4 ± 0.9	$4.4 \pm 0.7 \pm 0.5$					4.4 ± 0.9
304	$K^0K^+K^-$ (NR)	33 ± 10	$33 \pm 5 \pm 9$					33 ± 10
305	$K_SK_SK_S$	$6.2^{+1.2}_{-1.1}$	$6.19 \pm 0.48 \pm 0.19$	$4.2^{+1.6}_{-1.3} \pm 0.8$				6.04 ± 0.50
306	$f_0(980)K_S$ †	2.7 ± 1.8	$2.7^{+1.3}_{-1.2} \pm 1.3$ †					2.7 ± 1.8
307	$f_0(1710)K_S$ †	$0.50^{+0.050}_{-0.026}$	$0.50^{+0.46}_{-0.24} \pm 0.11$ †					$0.50^{+0.47}_{-0.26}$
308	$f_0(2010)K_S$ †	0.5 ± 0.6	$0.54^{+0.21}_{-0.20} \pm 0.52$ †					0.54 ± 0.56
309	$K_SK_SK_S(NR)$	13.3 ± 3.1	$13.3^{+2.2}_{-2.3} \pm 2.2$					$13.3^{+3.1}_{-3.2}$
310	$K_SK_SK_L$	< 16	< 16 [2]					< 16 [2]
311	$K^{*0}K^+K^-$	27.5 ± 2.6	$27.5 \pm 1.3 \pm 2.2$					27.5 ± 2.6
312	ϕK^{*0}	10.0 ± 0.5	$9.7 \pm 0.5 \pm 0.6$	$10.4 \pm 0.5 \pm 0.6$	$11.5^{+4.5+1.8}_{-3.7-1.7}$			$10.1^{+0.6}_{-0.5}$
313	$K^+\pi^-\pi^+K^-$	< 72		< 72 [3]				< 72 [3]
314	$K^{*0}\pi^+K^-$	4.5 ± 1.3	$4.6 \pm 1.1 \pm 0.8$	< 13.9 [3]				4.6 ± 1.4
315	$K^{*0}\overline{K}^{*0}$	0.8 ± 0.5	$1.28^{+0.35}_{-0.30} \pm 0.11$	$0.26^{+0.33+0.10}_{-0.29-0.08}$	< 22			0.81 ± 0.23
316	$K^+\pi^-K^+\pi^-(NR)$	< 6.0		< 6.0 [3]				< 6.0 [3]
317	$K^{*0}K^+\pi^-$	< 2.2	< 2.2	< 7.6 [3]				< 2.2
318	$K^{*0}K^{*0}$	< 0.2	< 0.41	< 0.2	< 37			< 0.2
319	$K^{*+}K^{*-}$	< 2.0	< 2.0		< 141			< 2.0
320	$K_1^*(1400)^0\phi$	< 5000	< 5000 [5]					< 5000 [5]
321	$(K\pi)_0^{*0}\phi$	4.3 ± 0.4	$4.3 \pm 0.4 \pm 0.4$	$4.3 \pm 0.4 \pm 0.4$				4.3 ± 0.4
322	$(K\pi)_0^{*0}\phi$ [4]	< 1.7	< 1.7					< 1.7
323	$K_0^*(1430)^0\pi^+K^-$	< 31.8		< 31.8 [3]				< 31.8 [3]
324	$K_0^*(1430)^0\overline{K}^{*0}$	< 3.3		< 3.3				< 3.3
325	$K_0^*(1430)^0\overline{K}_0^*(1430)^0$	< 8.4		< 8.4				< 8.4
326	$\phi K_0^*(1430)^0$	3.9 ± 0.8	$3.9 \pm 0.5 \pm 0.6$	$4.3 \pm 0.4 \pm 0.4$				4.2 ± 0.5
327	$K_0^*(1430)^0K^{*0}$	< 1.7		< 1.7				< 1.7
328	$K_0^*(1430)^0K_0^*(1430)^0$	< 4.7		< 4.7				< 4.7
329	$\phi K^*(1680)^0$	< 3.5	< 3.5					< 3.5
330	$\phi K_3^*(1780)^0$	< 2.7	< 2.7					< 2.7
331	$\phi K_4^*(2045)^0$	< 15.3	< 15.3					< 15.3
332	$\rho^0 K_2^*(1430)^0$	< 1100	< 1100 [5]					< 1100 [5]
333	$\phi K_2^*(1430)^0$	6.8 ± 0.9	$7.5 \pm 0.9 \pm 0.5$	$5.5^{+0.9}_{-0.7} \pm 1.0$				6.8 ± 0.8
334	$\phi\phi K^0$ §	4.5 ± 0.9	$4.5 \pm 0.8 \pm 0.3$					4.5 ± 0.9
335	$\eta'\eta' K^0$	< 31	< 31					< 31

† Product BF - daughter BF taken to be 100%; § $M_{\phi\phi} < 2.85$ GeV/c^2; ‡ Relative BF converted to absolute BF; ◇ Obtained from a fit to the ratios of BFs measured by LHCb (Ref. [799]) and to the averages of the BFs therein, as measured by other experiments (excluding the present line);
¶ Sum of charge conjugate states; [1] $0.55 < M(\pi\pi) < 1.42$ GeV/c^2; [2] $0.75 < M(K\pi) < 1.20$ GeV/c^2; [3] $0.70 < M(K\pi) < 1.70$ GeV/c^2; [4] $1.60 < M(K\pi) < 2.15$ GeV/c^2; [5] Result from ARGUS.

Table 188: Branching fractions (BF) of charmless mesonic B^0 decays without kaons in units of $\times 10^{-6}$. Upper limits are at 90% CL. Values in red (blue) are new published (preliminary) results since PDG2014.

RPP#	Mode	PDG2014 Avg.	*BABAR*	Belle	CLEO	CDF	LHCb	Our Avg.
356	$\pi^+\pi^-$	5.15 ± 0.19	$5.5 \pm 0.4 \pm 0.3$	$5.04 \pm 0.21 \pm 0.18$	$4.5^{+1.4+0.5}_{-1.2-0.4}$	$5.02 \pm 0.33 \pm 0.35^{\ddagger}$	$5.08 \pm 0.17 \pm 0.37^{\ddagger}$	5.10 ± 0.19
357	$\pi^0\pi^0$	1.91 ± 0.22	$1.83 \pm 0.21 \pm 0.13$	$0.90 \pm 0.12 \pm 0.10$	< 4.4			1.17 ± 0.13
358	$\eta\pi^0$	< 1.5	< 1.5	$4.1^{+1.7+0.5}_{-1.5-0.7}$	< 2.9			$4.1^{+1.8}_{-1.7}$
359	$\eta\eta$	< 1.0	< 1.0	$0.76^{+0.27+0.14}_{-0.23-0.16}$	< 18			$0.76^{+0.30}_{-0.28}$
360	$\eta'\pi^0$	1.2 ± 0.6	$0.9 \pm 0.4 \pm 0.1$	$2.8 \pm 1.0 \pm 0.3$	$0.0^{+1.8}_{-0.0}$			1.2 ± 0.4
361	$\eta'\eta'$	< 1.7	< 1.7	< 6.5	< 47			< 1.7
362	$\eta'\eta$	< 1.2	< 1.2	< 4.5	< 27			< 1.2
363	$\eta'\rho^0$	< 1.3	< 2.8	< 1.3	< 12			< 1.3
364	$f_0(980)\eta'$ †	< 0.9	< 0.9					< 0.9
365	$\eta\rho^0$	< 1.5	< 1.5	< 1.9	< 10			< 1.5
366	$f_0(980)\eta$ †	< 0.4	< 0.4					< 0.4
367	$\omega\eta$	$0.94^{+0.40}_{-0.31}$	$0.94^{+0.35}_{-0.30} \pm 0.09$		< 12			$0.94^{+0.36}_{-0.31}$
368	$\omega\eta'$	$1.0^{+0.5}_{-0.4}$	$1.01^{+0.46}_{-0.38} \pm 0.09$	< 2.2	< 60			$1.01^{+0.47}_{-0.39}$
369	$\omega\rho^0$	< 1.6	< 1.6		< 11			< 1.6
370	$f_0(980)\omega$ †	< 1.5	< 1.5					< 1.5
371	$\omega\omega$	1.2 ± 0.4	$1.2 \pm 0.3^{+0.3}_{-0.2}$		< 19			1.2 ± 0.4
372	$\phi\pi^0$	< 0.15	< 0.28	< 0.15	< 5			< 0.15
373	$\phi\eta$	< 0.5	< 0.5		< 9			< 0.5
374	$\phi\eta'$	< 0.5	< 1.1	< 0.5	< 31			< 0.5
375	$\phi\rho^0$	< 0.33	< 0.33		< 13			< 0.33
376	$f_0(980)\phi$ †	< 0.38	< 0.38					< 0.38
377	$\omega\phi$	< 0.7	< 0.7		< 21			< 0.7
378	$\phi\phi$	< 0.2	< 0.2		< 12		< 0.028	< 0.028
379	$a_0^{\mp}(980)\pi^{\pm}$ †	< 3.1	< 3.1					< 3.1
379	$a_0^{\mp}(1450)\pi^{\pm}$	< 2.3	< 2.3					< 2.3
380	$a_0^{\mp}(1450)\pi^{\pm}$ †	< 2.3	< 2.3					< 2.3
382	$\rho^0\pi^0$	2.0 ± 0.5	$1.4 \pm 0.6 \pm 0.3$	$3.0 \pm 0.5 \pm 0.7$	$1.6^{+2.0}_{-1.4} \pm 0.8$			2.0 ± 0.5
383	$\rho^{\mp}\pi^{\pm}$	23.0 ± 2.3	$22.6 \pm 1.8 \pm 2.2$	$22.6 \pm 1.1 \pm 4.4$	$27.6^{+8.4}_{-7.4} \pm 4.2$			23.0 ± 2.3
384	$\pi^+\pi^-\pi^+\pi^-$	< 19.3	< 23.1	< 11.2				< 11.2
385	$\rho^0\pi^+\pi^-(NR)$	< 8.8	< 8.8	< 12				< 8.8
386	$\rho^0\rho^0$	0.73 ± 0.28	$0.92 \pm 0.32 \pm 0.14$	$1.02 \pm 0.30 \pm 0.15$	< 18		$0.94 \pm 0.17 \pm 0.11$ *	0.95 ± 0.16
387	$f_0(980)\pi^+\pi^-(NR)$ †	< 3.8		< 3.0				< 3.0
388	$f_0(980)\rho^0$ †	< 0.3	< 0.40	$0.78 \pm 0.22 \pm 0.11$				0.78 ± 0.25
389	$f_0(980)f_0(980)$ †	< 0.1	< 0.19	< 0.2				< 0.19
391	$a_1^{\mp}\pi^{\pm}$	26 ± 5	$33.2 \pm 3.8 \pm 3.0$	$22.2 \pm 2.0 \pm 2.8$				25.9 ± 2.8
392	$a_2^{\mp}\pi^{\pm}$	< 6.3		< 6.3				< 6.3
393	$\pi^+\pi^-\pi^0\pi^0$	< 3100	< 3100 °					< 3100 °
394	$\rho^+\rho^-$	24.2 ± 3.1	$25.5 \pm 2.1^{+3.6}_{-3.9}$	$22.8 \pm 3.8^{+2.3}_{-2.6}$				$24.2^{+3.1}_{-3.2}$
395	$a_1(1260)^0\pi^0$	< 1100	< 1100 °					< 1100 °
396	$\omega\pi^0$	< 0.5	< 0.5	< 2.0	< 5.5			< 0.5
397	$\pi + \pi^+\pi^-\pi^-\pi^0$	< 9000	< 9000 °					< 9000 °
398	$a_1^{\pm}\rho^{\mp}$	< 61	< 61					< 61
399	$a_1^{\pm}\rho^0$	< 600	< 6000 °					< 6000 °
400	$b_1^{\mp}\pi^{\pm}$ †	10.9 ± 1.5	$10.9 \pm 1.2 \pm 0.9$					10.9 ± 1.5
401	$b_1^0\pi^0$ †	< 1.9	< 1.9					< 1.9
402	$b_1^{\pm}\rho^{\mp}$ †	< 1.4	< 1.4					< 1.4
403	$b_1^0\rho^0$ †	< 3.4	< 3.4					< 3.4
404	$\pi^+\pi^+\pi^+\pi^-\pi^-\pi^-$	< 3000	< 3000 °					< 3000 °
405	$a_1^{\pm}a_1^{\mp}$	11.8 ± 2.6	11.8 ± 2.6					11.8 ± 2.6
406	$\pi + \pi^+\pi^+\pi^-\pi^-\pi^-\pi^0$	< 11000	< 11000 °					< 11000 °
	$\phi\pi^+\pi^-$						$0.182 \pm 0.048 \pm 0.014^{\ddagger\P}$	0.182 ± 0.050

† Product BF - daughter BF taken to be 100%;
‡ Relative BF converted to absolute BF;
* Result given as $0.94 \pm 0.17 \pm 0.09 \pm 0.06$ where last error is from $\mathcal{B}(B^0 \to \phi K^{*0})$;
¶ In the mass range $400 < m(\pi^+\pi^-) < 1600$ GeV/c^2.

Table 189: Relative branching fractions (BF) of charmless mesonic B^0 decays. Upper limits are at 90% CL. Values in red (blue) are new published (preliminary) results since PDG2014.

RPP#	Mode	PDG2014 Avg.	CDF	LHCb	Our Avg.
273	$\mathcal{B}(B^0 \to K^+K^-)/\mathcal{B}(B^0 \to K^+\pi^-)$		$0.012 \pm 0.005 \pm 0.005$	$(3.98 \pm 0.65 \pm 0.42) \times 10^{-3}$	0.012 ± 0.007
356	$\mathcal{B}(B^0 \to \pi^+\pi^-)/\mathcal{B}(B^0 \to K^+\pi^-)$	0.261 ± 0.010	$0.259 \pm 0.017 \pm 0.016$	$0.262 \pm 0.009 \pm 0.017$	0.261 ± 0.015
–	$\mathcal{B}(B^0 \to K^{*\mp}K^{\pm})/\mathcal{B}(B^0 \to K^{*+}\pi^-)$	New		< 0.05	< 0.05
–	$\mathcal{B}(B^0 \to K_S^0K^{*0})/\mathcal{B}(B^0 \to K_S^0\pi^+\pi^-)$ †			< 0.020	< 0.020

† Sum of charge conjugate states in the numerator and denominator.

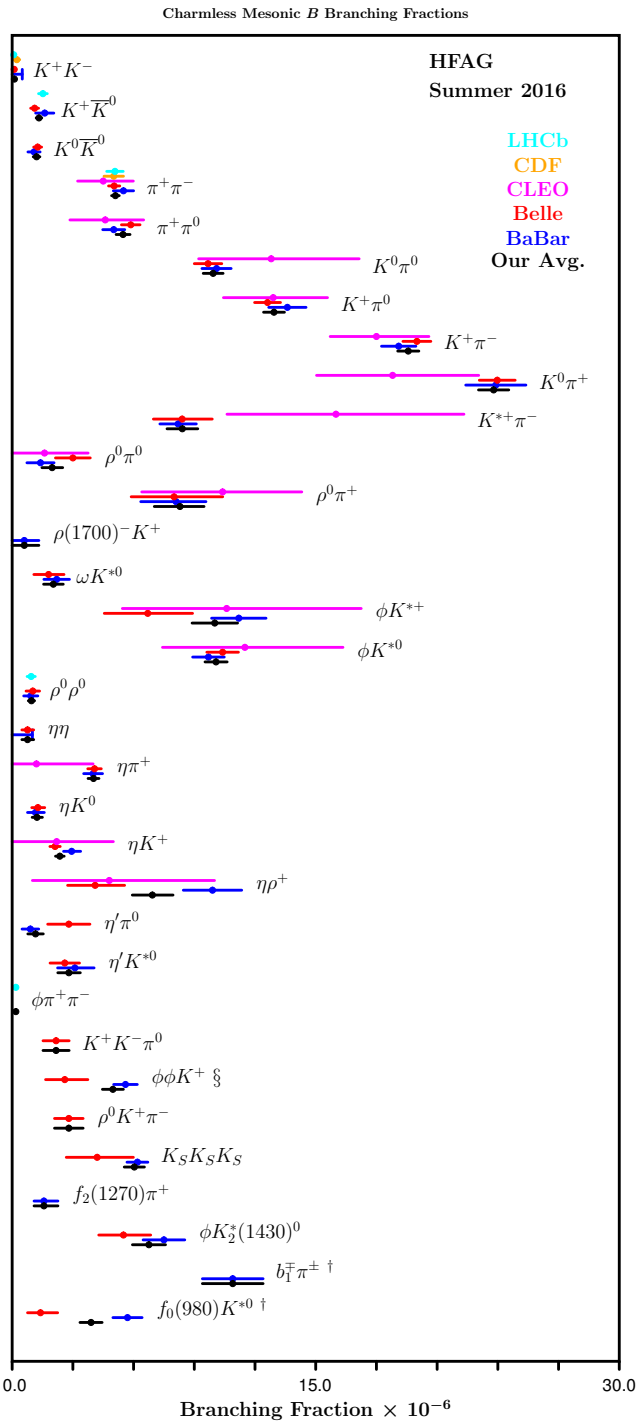

Figure 145: Selection of high precision charmless mesonic B meson branching fraction measurements.

7.2 Baryonic decays of B^0 and B^+ mesons

This section provides branching fractions of charmless baryonic decays of B^0 and B^+ mesons in Tables 190 and 191, respectively. Relative branching fractions are given in Table 192.

Figures 146 and 147 show a graphic representation of a selection of results given in this section. For comments in the plots, marked with a symbol or a number, refer to the corresponding table.

Table 190: Branching fractions (BF) of charmless baryonic B^+ decays in units of $\times 10^{-6}$. Upper limits are at 90% CL. Values in red (blue) are new published (preliminary) results since PDG2014.

RPP#	Mode	PDG2014 Avg.	*BABAR*	Belle	LHCb	Our Avg.
417	$p\bar{p}\pi^+$	1.62 ± 0.20	$1.69 \pm 0.29 \pm 0.26$ †	$1.60^{+0.22}_{-0.19} \pm 0.12$		$1.62^{+0.21}_{-0.20}$
417	$p\bar{p}\pi^+$ §				$1.07 \pm 0.11 \pm 0.11$ ¶	1.07 ± 0.16
420	$p\bar{p}K^+$	5.9 ± 0.5	$6.7 \pm 0.5 \pm 0.4$ †	$5.54^{+0.27}_{-0.25} \pm 0.36$	$4.46 \pm 0.21 \pm 0.27$ ¶ ◇	5.14 ± 0.25
421	$\Theta^{++}\bar{p}$ [1]	< 0.091	< 0.09	< 0.091		< 0.09
422	$f_J(2221)K^+$ [2]	< 0.41		< 0.41		< 0.41
423	$p\overline{\Lambda}(1520)$	< 1.5	< 1.5		$0.315 \pm 0.048 \pm 0.027$ ¶	0.315 ± 0.055
425	$p\bar{p}K^{*+}$	$3.6^{+0.8}_{-0.7}$	$5.3 \pm 1.5 \pm 1.3$ †	$3.38^{+0.73}_{-0.60} \pm 0.39$ ‡		$3.64^{+0.79}_{-0.70}$
426	$f_J(2221)K^{*+}$ [2]	< 0.77	< 0.77			< 0.77
427	$p\overline{\Lambda}$	< 0.32		< 0.32		< 0.32
429	$p\overline{\Lambda}\pi^0$	$3.00^{+0.7}_{-0.6}$		$3.00^{+0.61}_{-0.53} \pm 0.33$		$3.00^{+0.69}_{-0.62}$
430	$p\overline{\Sigma}(1385)^0$	< 0.47		< 0.47		< 0.47
431	$\Delta^+\overline{\Lambda}$	< 0.82		< 0.82		< 0.82
433	$p\overline{\Lambda}\pi^+\pi^-$ (NR)	5.9 ± 1.1		$5.92^{+0.88}_{-0.84} \pm 0.69$		$5.92^{+1.12}_{-1.09}$
434	$p\overline{\Lambda}\rho^0$	4.8 ± 0.9		$4.78^{+0.67}_{-0.64} \pm 0.60$		$4.78^{+0.90}_{-0.88}$
435	$p\overline{\Lambda}f_2(1270)$	2.0 ± 0.8		$2.03^{+0.77}_{-0.72} \pm 0.27$		$2.03^{+0.82}_{-0.77}$
436	$\Lambda\overline{\Lambda}\pi^+$	< 0.94		< 0.94 §		< 0.94 §
437	$\Lambda\overline{\Lambda}K^+$	3.4 ± 0.6		$3.38^{+0.41}_{-0.36} \pm 0.41$ ‡		$3.38^{+0.58}_{-0.55}$
438	$\Lambda\overline{\Lambda}K^{*+}$	$2.2^{+1.2}_{-0.9}$		$2.19^{+1.13}_{-0.88} \pm 0.33$ §		$2.19^{+1.18}_{-0.94}$
439	$\overline{\Delta}^0 p$	< 1.38		< 1.38 §		< 1.38 §
440	$\Delta^{++}\bar{p}$	< 0.14		< 0.14 §		< 0.14 §

§ Di-baryon mass is less than 2.85GeV/c^2.
† Charmonium decays to $p\bar{p}$ have been statistically subtracted;
¶ Relative BF converted to absolute BF.
◇ Includes contribution where $p\bar{p}$ is produced in charmonia decays.
[1] $\Theta(1540)^{++} \to K^+p$ (pentaquark candidate);
[2] Product BF — daughter BF taken to be 100%;
‡ The charmonium mass region has been vetoed;

Table 191: Branching fractions (BF) of charmless baryonic B^0 decays in units of $\times 10^{-6}$. Upper limits are at 90% CL. Values in red (blue) are new published (preliminary) results since PDG2014.

RPP#	Mode	PDG2014 Avg.	*BABAR*	Belle	LHCb	Our Avg.
407	$p\overline{p}$	$0.015^{+0.007}_{-0.005}$	< 0.27	< 0.11	$0.0147^{+0.0062+0.0035}_{-0.0051-0.0014}$	$0.0150^{+0.0070}_{-0.0050}$
409	$p\overline{p}K^0$	2.66 ± 0.32	$3.0 \pm 0.5 \pm 0.3$ †	$2.51^{+0.35}_{-0.29} \pm 0.21$ ‡		$2.66^{+0.34}_{-0.32}$
410	$\Theta^+\overline{p}$ [1]	< 0.05	< 0.05	< 0.23		< 0.05
411	$f_J(2221)K^0$ [2]	< 0.45	< 0.45			< 0.45
412	$p\overline{p}K^{*0}$	$1.24^{+0.28}_{-0.25}$	$1.47 \pm 0.45 \pm 0.40$ †	$1.18^{+0.29}_{-0.25} \pm 0.11$ ‡		$1.24^{+0.28}_{-0.25}$
413	$f_J(2221)K^{*0}$ [2]	< 0.15	< 0.15			< 0.15
414	$p\overline{\Lambda}\pi^-$	3.14 ± 0.29	$3.07 \pm 0.31 \pm 0.23$	$3.23^{+0.33}_{-0.29} \pm 0.29$		$3.14^{+0.29}_{-0.28}$
415	$p\overline{\Sigma}(1385)^-$	< 0.26		< 0.26		< 0.26
416	$\Delta^0\overline{\Lambda}$	< 0.93		< 0.93		< 0.93
417	$p\overline{\Lambda}K^-$	< 0.82		< 0.82		< 0.82
418	$p\overline{\Sigma}^0\pi^-$	< 3.8		< 3.8		< 3.8
419	$\overline{\Lambda}\Lambda$	< 0.32		< 0.32		< 0.32
420	$\overline{\Lambda}\Lambda K^0$	$4.8^{+1.0}_{-0.9}$		$4.76^{+0.84}_{-0.68} \pm 0.61$ ‡		$4.76^{+1.04}_{-0.91}$
421	$\Lambda\overline{\Lambda}K^{*0}$	$2.5^{+0.9}_{-0.8}$		$2.46^{+0.87}_{-0.72} \pm 0.34$ ‡		$2.46^{+0.93}_{-0.80}$

† Charmonium decays to $p\overline{p}$ have been statistically subtracted.
‡ The charmonium mass region has been vetoed.
[1] $\Theta(1540)^+ \to pK^0$ (pentaquark candidate).
[2] Product BF — daughter BF taken to be 100%.

Table 192: Relative branching fractions (BF) of charmless baryonic B decays. Values in red (blue) are new published (preliminary) results since PDG2014.

RPP#	Mode	PDG2014 Avg.	LHCb	Our Avg.
417	$\mathcal{B}(B^+ \to p\overline{p}\pi^+, m_{p\overline{p}} < 2.85\text{GeV}/c^2)/\mathcal{B}(B^+ \to J/\psi(\to p\overline{p})\pi^+)$		$12.0 \pm 1.2 \pm 0.3$	12.0 ± 1.2
420	$\mathcal{B}(B^+ \to p\overline{p}K^+)/\mathcal{B}(B^+ \to J/\psi(\to p\overline{p})K^+)$		$4.91 \pm 0.19 \pm 0.14$ †	4.91 ± 0.24
420	$\mathcal{B}(B^+ \to p\overline{p}K^+)/\mathcal{B}(B^+ \to J/\psi K^+)$	$0.0104 \pm 0.0005 \pm 0.0001$	$0.0104 \pm 0.0005 \pm 0.0001$ † §	0.0100 ± 0.0010
423	$\mathcal{B}(B^+ \to \overline{\Lambda}(1520)(\to K^+\overline{p})p)/\mathcal{B}(B^+ \to J/\psi(\to p\overline{p})\pi^+)$		$0.033 \pm 0.005 \pm 0.007$	0.033 ± 0.009

† Includes contribution where $p\overline{p}$ is produced in charmonia decays.
§ Original experimental relative BF multiplied by the best values (PDG2014) of certain reference BFs. The first error is experimental, the second is from reference BF.

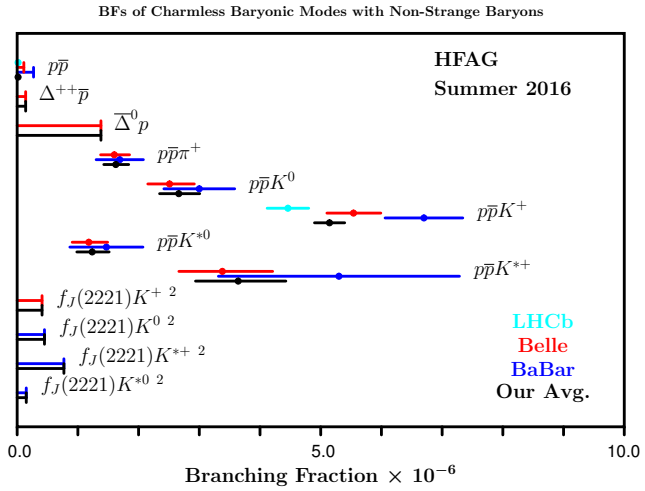

Figure 146: Branching fractions of charmless baryonic modes with non-strange baryons.

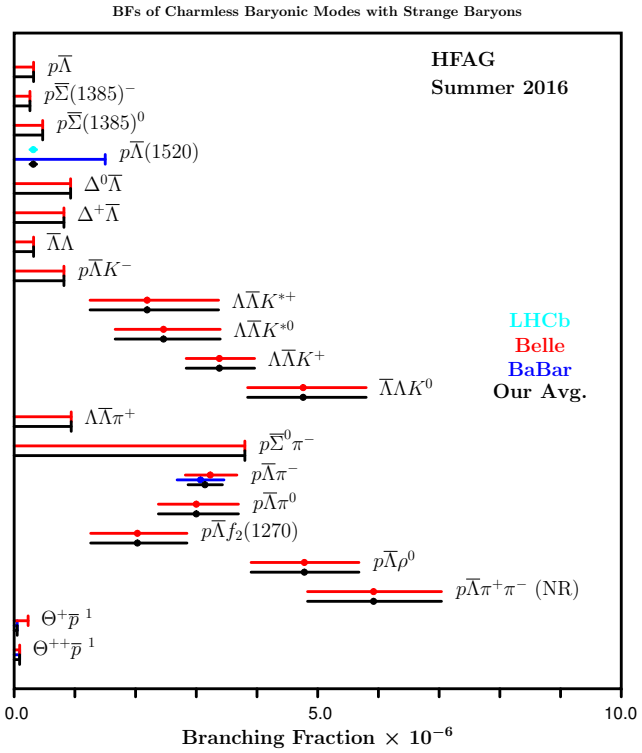

Figure 147: Branching fractions of charmless baryonic modes with strange baryons.

7.3 Decays of b baryons

A compilation of branching fractions of Λ_b^0 baryon decays is given in Table 193. Table 194 provides the partial branching fractions of $\Lambda_b^0 \to \Lambda\mu^+\mu^-$ decays. A compilation of branching fractions of Ξ_b^0 baryon decays is given in Table 195.

Figure 148 shows a graphic representation of branching fractions of Λ_b^0 decays. For comments in the plot, marked with a symbol or a number, refer to the corresponding table.

Table 193: Branching fractions (BF) of charmless Λ_b^0 decays in units of $\times 10^{-6}$. Values in red (blue) are new published (preliminary) results since PDG2014.

RPP#	Mode	PDG2014 Avg.	CDF	LHCb	Our Avg.
19	$p\pi^-$	$3.5 \pm 0.8 \pm 0.6$	$3.5 \pm 0.8 \pm 0.6$		3.5 ± 1.0
20	pK^-	$5.5 \pm 1.0 \pm 1.0$	$5.5 \pm 1.0 \pm 1.0$		5.5 ± 1.4
21	$\Lambda\mu^+\mu^-$	$1.73 \pm 0.42 \pm 0.55$	$1.73 \pm 0.42 \pm 0.55$	$0.96 \pm 0.16 \pm 0.25$	1.08 ± 0.27
–	$\Lambda\eta$	New		$9.3^{+7.3}_{-5.3}$ $^\diamond$	$9.3^{+7.3}_{-5.3}$
–	$\Lambda\eta'$	New		< 3.1	< 3.1
–	$\Lambda\phi$	New		$5.18 \pm 1.04 \pm 0.35^{+0.67}_{-0.62}$ ‡	$5.18^{+1.29}_{-1.26}$
–	$\overline{K}^0 p\pi^-$	New		$1.26 \pm 0.19 \pm 0.09 \pm 0.34 \pm 0.05$ §	1.26 ± 0.21
–	$K^0 pK^-$	New		$< 3.5(4.0)$ *	$< 3.5(4.0)$ *
–	$\Lambda\pi^+\pi^-$	New		$4.6 \pm 1.2 \pm 1.4 \pm 0.6$ †	4.6 ± 1.8
–	$\Lambda K^+\pi^-$	New		$5.6 \pm 0.8 \pm 0.8 \pm 0.7$ †	5.6 ± 1.1
–	ΛK^+K^-	New		$15.9 \pm 1.2 \pm 1.2 \pm 2.0$ †	15.9 ± 1.7

$^\diamond$ Result at 68% CL interval.
* Limits quoted at 90 (95%) confidence level.
‡ Third uncertainty is related to external inputs.
§ Third uncertainty is from the ratio of fragmentation fractions $f_{\Lambda_b^0}/f_d$, and the fourth is due to the uncertainty on $\mathcal{B}(B^0 \to K^0\pi^+\pi^-)$.
† Last quoted uncertainty is due to the precision with which the normalisation channel branching fraction is known.

Table 194: Partial branching fractions (BF) of $\Lambda_b^0 \to \mu^+\mu^-$ decays in intervals of $q^2 = m^2_{\mu\mu}$ in units of $\times 10^{-6}$. Values in red (blue) are new published (preliminary) results since PDG2014.

RPP#	Mode	q^2 $[(\mathrm{GeV}/c^2)^2]$ †	PDG2014 Avg.	CDF	LHCb	Our Avg.
21	$\Lambda\mu^+\mu^-$ ‡	< 2.0	$0.15 \pm 2.01 \pm 0.05$	$0.15 \pm 2.01 \pm 0.05$	$0.56 \pm 0.76 \pm 0.80$	0.41 ± 0.87
	$\Lambda\mu^+\mu^-$	$[2.0, 4.3]$	$1.8 \pm 1.7 \pm 0.6$	$1.8 \pm 1.7 \pm 0.6$	$0.71 \pm 0.60 \pm 0.10$	0.91 ± 0.55
	$\Lambda\mu^+\mu^-$	$[4.3, 8.68]$	$-0.2 \pm 1.6 \pm 0.1$	$-0.2 \pm 1.6 \pm 0.1$	$0.66 \pm 0.72 \pm 0.16$	0.40 ± 0.62
	$\Lambda\mu^+\mu^-$	$[10.09, 12.86]$	$3.0 \pm 1.5 \pm 1.0$	$3.0 \pm 1.5 \pm 1.0$	$1.55 \pm 0.58 \pm 0.55$	1.96 ± 0.68
	$\Lambda\mu^+\mu^-$	$[14.18, 16.00]$	$1.0 \pm 0.7 \pm 0.3$	$1.0 \pm 0.7 \pm 0.3$	$1.44 \pm 0.44 \pm 0.42$	1.19 ± 0.40
	$\Lambda\mu^+\mu^-$	> 16.00	$7.0 \pm 1.9 \pm 2.2$	$7.0 \pm 1.9 \pm 2.2$	$4.7 \pm 0.8 \pm 1.2$	5.5 ± 1.2

† See the original paper for the exact q^2 selection.
‡ The LHCb measurement was superseded with a more accurate result in different q^2 bins (see list of not-included results).

Table 195: Branching fractions (BF) of charmless Ξ_b^0 decays in units of $\times 10^{-6}$. Values in red (blue) are new published (preliminary) results since PDG2014.

RPP#	Mode	PDG2014 Avg.	CDF	LHCb	Our Avg.
–	$\Lambda\pi^+\pi^-$	New		$< 1.7(2.1)$ †	$< 1.7(2.1)$ †
–	$\Lambda K^+\pi^-$	New		$< 0.8(1.0)$ †	$< 0.8(1.0)$ †
–	ΛK^+K^-	New		$< 0.3(0.4)$ †	$< 0.3(0.4)$ †
–	$\overline{K}^0 p\pi^-$	New		$< 1.6(1.8)$ †	$< 1.6(1.8)$ †
–	$\overline{K}^0 pK^-$	New		$< 1.1(1.2)$ †	$< 1.1(1.2)$ †

† Limits quoted at 90 (95%) confidence level.

List of other measurements that are not included in the tables:

- In Ref. [800], LHCb provides a measurement of the differential $\Lambda_b^0 \to \Lambda\mu^+\mu^-$ branching fraction. It is given in bins of q^2 that are different from those used in the past by LHCb and CDF collaboration (see table of differential branching fractions).
- In the paper [801], LHCb measures the ratios

$$\frac{\sigma(pp \to \Xi_b'^- X)\mathcal{B}(\Xi_b'^- \to \Xi_b^0\pi^-)}{\sigma(pp \to \Xi_b^0 X)}, \frac{\sigma(pp \to \Xi_b'^- X)\mathcal{B}(\Xi_b^{*-} \to \Xi_b^0\pi^-)}{\sigma(pp \to \Xi_b'^- X)\mathcal{B}(\Xi_b'^- \to \Xi_b^0\pi^-)}.$$

- In the paper [802], LHCb measures the ratio

$$\frac{\sigma(pp \to \Xi_b^{*-} X)\mathcal{B}(\Xi_b^{*-} \to \Xi_b^0\pi^-)}{\sigma(pp \to \Xi_b^0 X)}.$$

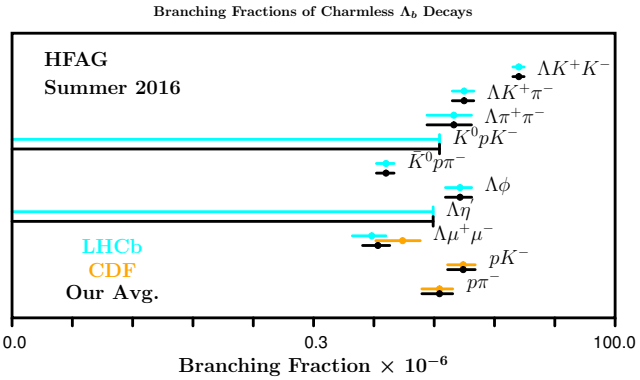

Figure 148: Branching fractions of charmless Λ_b decays

7.4 Decays of B_s^0 mesons

Tables 196 and 197 detail branching fractions and relative branching fractions of B_s^0 meson decays, respectively.

Figures 149 and 150 show a graphic representation of a selection of results given in this section. For comments in the plots, marked with a symbol or a number, refer to the corresponding table.

Table 196: Branching fractions (BF) of charmless B_s^0 decays in units of $\times 10^{-6}$. Upper limits are at 90% CL. Values in red (blue) are new published (preliminary) results since PDG2014.

RPP#	Mode	PDG2014 Avg.	Belle	CDF	D0	LHCb	CMS	ATLAS	Our Avg.
45	$\pi^+\pi^-$	0.76 ± 0.19	< 12	$0.60 \pm 0.17 \pm 0.04$ ‡		$0.691 \pm 0.083 \pm 0.044$ ‡			0.671 ± 0.083
51	$\phi\phi$	19.1 ± 3.1		$19.1 \pm 2.6 \pm 1.6$ ‡		$18.4 \pm 0.5 \pm 1.8$*			18.6 ± 1.6
52	π^+K^-	5.5 ± 0.6	< 26	$5.3 \pm 0.9 \pm 0.3$ ‡		$5.6 \pm 0.6 \pm 0.3$ ‡			5.5 ± 0.5
53	K^+K^-	24.9 ± 1.7	$38^{+10}_{-9} \pm 7$	$25.9 \pm 2.2 \pm 1.7$ ‡		$23.7 \pm 1.6 \pm 1.5$ ‡			24.8 ± 1.7
54	$K^0\overline{K}^0$	< 66	$19.6^{+5.8}_{-5.1} \pm 1.0 \pm 2.0$ ◇						$19.6^{+9.7}_{-9.3}$
55	$K^0\pi^+\pi^-$	19 ± 5				$19 \pm 5 \pm 2$ ‡			19 ± 5
56	$K^0K^-\pi^+$ ¶	97 ± 17				$97 \pm 12 \pm 12$ ‡			97 ± 16
57	$K^0K^+K^-$	< 4				< 4 ‡			< 4 ‡
–	$K^{*\pm}K^{\mp}$	New				$12.7 \pm 1.9 \pm 1.9$ †			12.7 ± 2.7
–	$K^{*-}\pi^+$	New				$3.3 \pm 1.1 \pm 0.5$ †			3.3 ± 1.2
59	$K^{*0}\overline{K}^{*0}$	$28.1 \pm 4.6 \pm 5.6$				$10.8 \pm 1.4 \pm 1.5$ *†			10.8 ± 2.1
60	$\phi\overline{K}^{*0}$	1.13 ± 0.3				$1.13 \pm 0.29 \pm 0.06$ ‡			1.13 ± 0.30
61	$p\overline{p}$	$0.028^{+0.022}_{-0.017}$				$0.0284^{+0.0203+0.0085}_{-0.0168-0.0018}$ †			$0.0280^{+0.0220}_{-0.0170}$
63	$\gamma\gamma$	< 8.7	< 3.1						< 3.1
64	$\phi\gamma$	36 ± 4	$36 \pm 5 \pm 7$			$35.1 \pm 3.5 \pm 1.2$ ‡			35.2 ± 3.4
65	$\mu^+\mu^-$	0.0031 ± 0.0007		$0.013^{+0.009}_{-0.007}$ †	< 0.012 †	$0.0029^{+0.0011+0.0003}_{-0.0010-0.0001}$	$0.0030^{+0.0010}_{-0.0009}$	< 0.003 †1	$0.0029^{+0.0007}_{-0.0006}$ 3
66	e^+e^-	< 0.28		< 0.28					< 0.28
67	$e^{\pm}\mu^{\mp}$	< 0.011		< 0.20		< 0.011 †			< 0.011 †
68	$\mu^+\mu^-\mu^+\mu^-$	< 0.012				< 0.012			< 0.012
70	$\phi\mu^+\mu^-$	0.76 ± 0.15			< 3.2 †	$0.797^{+0.045}_{-0.043} \pm 0.068$ †			$0.797^{+0.082}_{-0.080}$
	$\eta'\eta'$					$33.1 \pm 7.0 \pm 1.2$ ‡			33.1 ± 7.1
	$\pi^+\pi^-\mu^+\mu^-$					$0.086 \pm 0.015 \pm 0.010$ 2			0.086 ± 0.018
	$K^0\overline{K}^{*0}$ ¶					$16.4 \pm 3.4 \pm 2.3$ †			16.4 ± 4.1
	$\phi\pi^+\pi^-$					$3.48 \pm 0.29 \pm 0.35$ 4†			3.48 ± 0.46
	$\phi f_0(980), f_0(980) \to \pi^+\pi^-$					$1.12 \pm 0.18 \pm 0.11$†			1.12 ± 0.21
	$\phi f_2(1270), f_2(1270) \to \pi^+\pi^-$					$0.61^{+0.18}_{-0.14} \pm 0.06$†			$0.61^{+0.19}_{-0.15}$
	$\phi\rho^0(770)$					$0.27 \pm 0.07 \pm 0.02$†			0.27 ± 0.07

‡ The first error is experimental, the second is from reference BF.

† Relative BF converted to absolute BF.

¶ Sum of charge conjugate states.

* Last error takes into account $BF(B^0 \to \phi K^{*0})$ and f_d/f_s

◇ Last error represents the uncertainty due to the total number of $B_s^0\overline{B}_s^0$ pairs.

1 Limit at 95% C.L

2 Muon pairs do not originate from resonances and $0.5 < m(\pi^+\pi-) < 1.3$ GeV/c^2.

3 The average is done between the combined LHCb and CMS result, $0.0028^{+0.0007}_{-0.0006}$ (Ref. [803]) and CDF.

4 In the mass range $400 < m(\pi^+\pi^-) < 1600$ GeV/c^2.

Table 197: Relative branching fractions (BF) of charmless B_s^0 decays. Upper limits are at 90% CL. Values in red (blue) are new published (preliminary) results since PDG2014.

RPP#	Mode	PDG2014 Avg.	CDF	LHCb	Our Avg.
45	$f_s\mathcal{B}(B_s^0 \to \pi^+\pi^-)/f_d\mathcal{B}(B^0 \to K^+\pi^-)$		$0.008 \pm 0.002 \pm 0.001$	$(9.15 \pm 0.71 \pm 0.83) \times 10^{-3}$	0.008 ± 0.002
45	$f_s\mathcal{B}(B_s^0 \to \pi^+\pi^-)/f_d\mathcal{B}(B^0 \to \pi^+\pi^-)$			$0.050^{+0.011}_{-0.009} \pm 0.004$	$0.050^{+0.012}_{-0.010}$
51	$\mathcal{B}(B_s^0 \to \phi\phi)/\mathcal{B}(B_s^0 \to J/\psi\phi)$		$0.0178 \pm 0.0014 \pm 0.0020$		0.0180 ± 0.0020
	$\mathcal{B}(B_s^0 \to \phi\phi)/\mathcal{B}(B^0 \to \phi K^*)$			$1.84 \pm 0.05 \pm 0.13$	1.84 ± 0.14
52	$f_s\mathcal{B}(B_s^0 \to K^+\pi^-)/f_d\mathcal{B}(B_d^0 \to K^+\pi^-)$		$0.071 \pm 0.010 \pm 0.007$	$0.074 \pm 0.006 \pm 0.006$	0.073 ± 0.007
53	$f_s\mathcal{B}(B_s^0 \to K^+K^-)/f_d\mathcal{B}(B_d^0 \to K^+\pi^-)$		$0.347 \pm 0.020 \pm 0.021$	$0.316 \pm 0.009 \pm 0.019$	0.327 ± 0.017
55	$f_s\mathcal{B}(B_s^0 \to K^0\pi^+\pi^-)/f_d\mathcal{B}(B^0 \to K^0\pi^+\pi^-)$			$0.29 \pm 0.06 \pm 0.04$	0.29 ± 0.07
56	$f_s\mathcal{B}(B_s^0 \to K^0K^-\pi^+)/f_d\mathcal{B}(B^0 \to K^0K^-\pi^+)$ ¶			$1.48 \pm 0.12 \pm 0.14$	1.48 ± 0.18
57	$f_s\mathcal{B}(B_s^0 \to K^0K^+K^-)/f_d\mathcal{B}(B^0 \to K^0K^+K^-)$			< 0.068	< 0.068
–	$\mathcal{B}(B_s^0 \to K^{*-}K^+)/\mathcal{B}(B^0 \to K^{*+}\pi^-)$	New		$1.49 \pm 0.22 \pm 0.18$	1.49 ± 0.28
–	$\mathcal{B}(B_s^0 \to K^{*-}\pi^+)/\mathcal{B}(B^0 \to K^{*+}\pi^-)$	New		$0.39 \pm 0.13 \pm 0.05$	0.39 ± 0.14
59	$\mathcal{B}(B_s^0 \to K^{*0}\overline{K}^{*0})/\mathcal{B}(B^0 \to K^{*+}\pi^-)$	New		$1.11 \pm 0.22 \pm 0.13$	1.11 ± 0.26
60	$\mathcal{B}(B_s^0 \to \phi\overline{K}^{*0})/\mathcal{B}(B^0 \to \phi K^{*0})$			$0.113 \pm 0.024 \pm 0.016$	0.113 ± 0.029
64	$\mathcal{B}(B_s^0 \to \phi\gamma)/\mathcal{B}(B^0 \to K^{*0}\gamma)$			$0.81 \pm 0.04 \pm 0.07$	0.81 ± 0.08
70	$\mathcal{B}(B_s^0 \to \phi\mu^+\mu^-)/\mathcal{B}(B_s^0 \to J/\psi\phi) \times 10^4$	7.1 ± 1.3		$7.41^{+0.42}_{-0.40} \pm 0.29$	$7.41^{+0.51}_{-0.49}$
–	$\mathcal{B}(B_s^0 \to K_S^0K^{*0})/\mathcal{B}(B^0 \to K_S^0\pi^+\pi^-)$			$0.33 \pm 0.07 \pm 0.04$†	0.33 ± 0.08

¶ Sum of charge conjugate states in the numerator.

† Sum of charge conjugate states in the numerator and denominator.

List of other measurements that are not included in the tables:

- $B_s^0 \to \phi\mu^+\mu^-$: LHCb measures the differential BF in bins of q^2. It also performs an angular analysis and measures F_L, S_3, S_4, S_7, A_5, A_6, A_8 and A_9 in bins of q^2 [804].
- $B_s^0 \to \phi\gamma$: LHCb has measured the photon polarization [392].

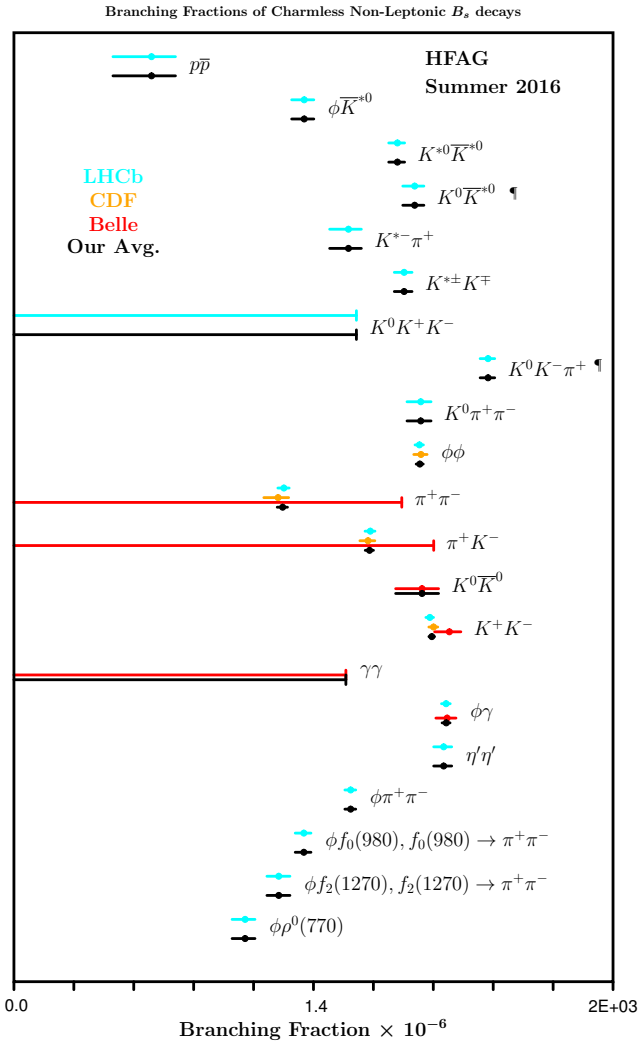

Figure 149: Branching fractions of charmless non-leptonic B_s decays

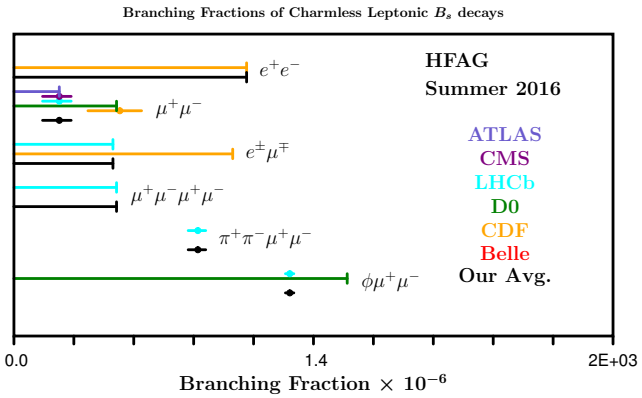

Figure 150: Branching fractions of charmless leptonic B_s decays

7.5 Radiative and leptonic decays of B^0 and B^+ mesons

This section gives different observables for leptonic and radiative B^0 and B^+ meson decays, including processes in which the photon yields a pair of charged of neutral leptons. Tables 198, 199, 200 and 201 provide compilations of branching fractions of B^+, B^0, and $B^\pm/B^0$ admixture, respectively. Table 202 contains branching fractions of leptonic and radiative-leptonic B^+ and B^0 decays. It is followed by Tables 203 and 204, which give relative branching fractions of B^+ decays and a compilations of inclusive decays, respectively. Table 205 contains isospin asymmetry measurements.

Figures 151 to 156 show a graphic representation of a selection of results given in this section. For comments in the plots, marked with a symbol or a number, refer to the corresponding table.

Table 198: Branching fractions (BF) of charmless semileptonic and radiative B^+ decays (part 1) in units of $\times 10^{-6}$. Upper limits are at 90% CL. Values in red (blue) are new published (preliminary) results since PDG2014.

RPP#	Mode	PDG2014 Avg.	*BABAR*	Belle	CLEO	LHCb	Our Avg.
363	$K^{*+}\gamma$	42.1 ± 1.8	$42.2 \pm 1.4 \pm 1.6$	$42.5 \pm 3.1 \pm 2.4$	$37.6^{+8.9}_{-8.3} \pm 2.8$		42.1 ± 1.8
364	$K_1^+(1270)\gamma$	43 ± 13	$44.1^{+6.3}_{-4.4} \pm 5.8$ †	$43 \pm 9 \pm 9$			$43.8^{+7.1}_{-6.3}$
365	$K^+\eta\gamma$	7.9 ± 0.9	$7.7 \pm 1.0 \pm 0.4$	$8.4^{+1.5}_{-1.2} \pm 0.9$			7.9 ± 0.9
366	$K^+\eta'\gamma$	$2.9^{+1.0}_{-0.9}$	$1.9^{+1.5}_{-1.2} \pm 0.1$	$3.6 \pm 1.2 \pm 0.4$			$2.9^{+1.0}_{-0.9}$
367	$K^+\phi\gamma$	2.7 ± 0.4	$3.5 \pm 0.6 \pm 0.4$	$2.48 \pm 0.30 \pm 0.24$			2.71 ± 0.34
368	$K^+\pi^-\pi^+\gamma$	27.6 ± 2.2	$24.5 \pm 0.9 \pm 1.2$ †	$25.0 \pm 1.8 \pm 2.2$ ‡			24.6 ± 1.3
369	$K^{*0}\pi^+\gamma$ §	20^{+7}_{-6}	$23.4 \pm 0.9^{+0.8}_{-0.7}$ †	$20^{+7}_{-6} \pm 2$			$23.3^{+1.2}_{-1.1}$
370	$K^+\rho^0\gamma$ §	< 20	$8.2 \pm 0.4 \pm 0.8$ †	< 20			8.2 ± 0.9
–	$(K\pi)_0^{*0}\pi^+\gamma$	New	$10.3^{+0.7+1.5}_{-0.8-2.0}$ †				$10.3^{+1.7}_{-2.2}$
371	$K^+\pi^-\pi^+\gamma$(N.R.)§	< 9.2	$9.9 \pm 0.7^{+1.5}_{-1.9}$ †	< 9.2			$9.9^{+1.7}_{-2.0}$
–	$K_0^*(1430)\pi^+\gamma$	New	$1.32^{+0.09+0.24}_{-0.10-0.30}$ †				$1.32^{+0.26}_{-0.32}$
372	$K^0\pi^+\pi^0\gamma$	46 ± 5	$45.6 \pm 4.2 \pm 3.1$ †				45.6 ± 5.2
373	$K_1^+(1400)\gamma$	< 15	$9.7^{+4.6+2.9}_{-2.9-2.4}$ †	< 15			$9.7^{+5.4}_{-3.8}$
–	$K^{*+}(1410)\gamma$	New	$27.1^{+5.4+5.9}_{-4.8-3.7}$ †				$27.1^{+8.0}_{-6.1}$
374	$K_2^*(1430)^+\gamma$	14 ± 4	$8.7^{+7.0+8.7}_{-5.3-10.4}$ †				$8.7^{+11.2}_{-11.7}$
375	$K^{*+}(1680)\gamma$	< 1900	$66.7^{+9.3+14.4}_{-7.8-11.4}$ †				$66.7^{+17.1}_{-13.8}$
376	$K_3^*(1780)^+\gamma$	< 39		< 39			< 39
378	$\rho^+\gamma$	0.98 ± 0.25	$1.20^{+0.42}_{-0.37} \pm 0.20$	$0.87^{+0.29+0.09}_{-0.27-0.11}$	< 13		$0.98^{+0.25}_{-0.24}$
428	$p\overline{\Lambda}\gamma$	$2.4^{+0.5}_{-0.4}$		$2.45^{+0.44}_{-0.38} \pm 0.22$			$2.45^{+0.49}_{-0.44}$
432	$p\overline{\Sigma^0}\gamma$	< 4.6		< 4.6			< 4.6
467	$\pi^+\ell^+\ell^-$	< 0.049	< 0.066	< 0.049			< 0.049
468	$\pi^+e^+e^-$	< 0.080	< 0.125	< 0.080			< 0.080
469	$\pi^+\mu^+\mu^-$	< 0.055	< 0.055	< 0.069		$0.0183 \pm 0.0024 \pm 0.0005$ ¶1	0.0180 ± 0.0020
470	$\pi^+\nu\overline{\nu}$	< 98	< 100	< 98			< 98
471	$K^+\ell^+\ell^-$	0.451 ± 0.023	$0.48 \pm 0.09 \pm 0.02$	$0.53^{+0.06}_{-0.05} \pm 0.03$		[4]	0.51 ± 0.05
472	$K^+e^+e^-$	0.55 ± 0.07	$0.51^{+0.12}_{-0.11} \pm 0.02$	$0.57^{+0.09}_{-0.08} \pm 0.03$	< 2.4		0.55 ± 0.07
473	$K^+\mu^+\mu^-$	0.449 ± 0.023	$0.41^{+0.16}_{-0.15} \pm 0.02$	$0.53 \pm 0.08^{+0.07}_{-0.03}$	< 3.68	$0.429 \pm 0.007 \pm 0.021$	0.435 ± 0.021
–	$K^+\tau^+\tau^-$		< 2250				< 2250
476	$K^+\nu\overline{\nu}$	< 16	< 16	< 55	< 240		< 16
477	$\rho^+\nu\overline{\nu}$	< 213		< 213			< 213
478	$K^{*+}\ell^+\ell^-$	1.29 ± 0.21	$1.40^{+0.40}_{-0.37} \pm 0.09$	$1.24^{+0.23}_{-0.21} \pm 0.13$			$1.29^{+0.22}_{-0.21}$
479	$K^{*+}e^+e^-$	$1.55^{+0.40}_{-0.31}$	$1.38^{+0.47}_{-0.42} \pm 0.08$	$1.73^{+0.50}_{-0.42} \pm 0.20$			$1.55^{+0.35}_{-0.32}$
480	$K^{*+}\mu^+\mu^-$	1.12 ± 0.15	$1.46^{+0.79}_{-0.75} \pm 0.12$	$1.11^{+0.32}_{-0.27} \pm 0.10$		$0.924 \pm 0.093 \pm 0.067$	$0.958^{+0.107}_{-0.104}$
481	$K^{*+}\nu\overline{\nu}$	< 40	< 64	< 40			< 40
–	$K^+\pi^+\pi^-\mu^+\mu^-$	New				$0.436^{+0.029}_{-0.027} \pm 0.028$ ¶2	$0.436^{+0.040}_{-0.039}$
–	$K^+\phi\mu^+\mu^-$	New				$0.082^{+0.019+0.029}_{-0.017-0.027}$ ¶	$0.082^{+0.035}_{-0.032}$

See next table (part 2) for footnotes.

Table 199: Branching fractions (BF) of charmless semileptonic and radiative B^+ decays (part 2) in units of $\times 10^{-6}$. Upper limits are at 90% CL. Values in red (blue) are new published (preliminary) results since PDG2014.

RPP#	Mode	PDG2014 Avg.	*BABAR*	Belle	CLEO	LHCb	Our Avg.
484	$\pi^+ e^\pm \mu^\mp$	< 0.17	< 0.17				< 0.17
485	$\pi^+ e^+ \tau^-$	< 74	< 74				< 74
486	$\pi^+ e^- \tau^+$	< 20	< 20				< 20
487	$\pi^+ e^\pm \tau^\mp$	< 75	< 75				< 75
488	$\pi^+ \mu^+ \tau^-$	< 62	< 62				< 62
489	$\pi^+ \mu^- \tau^+$	< 45	< 45				< 45
490	$\pi^+ \mu^\pm \tau^\mp$	< 72	< 72				< 72
491	$K^+ e^+ \mu^-$	< 0.091	< 0.091				< 0.091
492	$K^+ e^- \mu^+$	< 0.13	< 0.13				< 0.13
493	$K^+ e^\pm \mu^\mp$	< 0.091	< 0.091				< 0.091
494	$K^+ e^+ \tau^-$	< 43	< 43				< 43
495	$K^+ e^- \tau^+$	< 15	< 15				< 15
496	$K^+ e^\pm \tau^\mp$	< 30	< 30				< 30
497	$K^+ \mu^+ \tau^-$	< 45	< 45				< 45
498	$K^+ \mu^- \tau^+$	< 28	< 28				< 28
499	$K^+ \mu^\pm \tau^\mp$	< 48	< 48				< 48
500	$K^{*+} e^+ \mu^-$	< 1.3	< 1.3				< 1.3
501	$K^{*+} e^- \mu^+$	< 0.99	< 0.99				< 0.99
502	$K^{*+} e^\pm \mu^\mp$	< 1.4	< 1.4				< 1.4
503	$\pi^- e^+ e^+$	< 0.023	< 0.023		< 1.6		< 0.023
504	$\pi^- \mu^+ \mu^+$	< 0.013	< 0.107		< 1.4	< 0.004 [3]	< 0.004 [3]
505	$\pi^- e^+ \mu^+$	< 0.15	< 0.15		< 1.3		< 0.15
506	$\rho^- e^+ e^+$	< 0.17	< 0.17		< 2.6		< 0.17
507	$\rho^- \mu^+ \mu^+$	< 0.42	< 0.42		< 5.0		< 0.42
508	$\rho^- e^+ \mu^+$	< 0.47	< 0.47		< 3.3		< 0.47
509	$K^- e^+ e^+$	< 0.03	< 0.03		< 1.0		< 0.03
510	$K^- \mu^+ \mu^+$	< 0.041	< 0.067		< 1.8	< 0.041	< 0.041
511	$K^- e^+ \mu^+$	< 0.16	< 0.16		< 2.0		< 0.16
512	$K^{*-} e^+ e^+$	< 0.40	< 0.40		< 2.8		< 0.40
513	$K^{*-} \mu^+ \mu^+$	< 0.59	< 0.59		< 8.3		< 0.59
514	$K^{*-} e^+ \mu^+$	< 0.30	< 0.30		< 4.4		< 0.30

† $M_{K\pi\pi} < 1.8$ GeV/c^2; ‡ $1.0 < M_{K\pi\pi} < 2.0$ GeV/c^2; § $M_{K\pi\pi} < 2.4$ GeV/c^2.
¶ Relative BF converted to absolute BF.
[1] PDG2014 cites only the measurement: $\mathcal{B}(\pi^+\mu^+\mu^-)/\mathcal{B}(K^+\mu^+\mu^-) = 0.053 \pm 0.014 \pm 0.01$.
[2] Differential BF in bins of $m(\mu\mu)$ is also available.
[3] At 95% C.L.
[4] PDG considers here the BF measured in $B^+ \to K^+\mu^+\mu^-$.

Table 200: Branching fractions (BF) of charmless semileptonic and radiative B^0 decays in units of $\times 10^{-6}$. Upper limits are at 90% CL. Values in red (blue) are new published (preliminary) results since PDG2014.

RPP#	Mode	PDG2014 Avg.	*BABAR*	Belle	CLEO	LHCb	Our Avg.
336	$K^0\eta\gamma$	7.6 ± 1.8	$7.1^{+2.1}_{-2.0} \pm 0.4$	$8.7^{+3.1+1.9}_{-2.7-1.6}$			$7.6^{+1.8}_{-1.7}$
337	$K^0\eta'\gamma$	< 6.4	< 6.6	< 6.4			< 6.4
338	$K^0\phi\gamma$	2.7 ± 0.7	< 2.7	$2.74 \pm 0.60 \pm 0.32$			2.74 ± 0.68
339	$K^+\pi^-\gamma$ §	4.6 ± 1.4		$4.6^{+1.3+0.5}_{-1.2-0.7}$			4.6 ± 1.4
340	$K^{*0}\gamma$	43.3 ± 1.5	$44.7 \pm 1.0 \pm 1.6$	$40.1 \pm 2.1 \pm 1.7$	$45.5^{+7.2}_{-6.8} \pm 3.4$		43.3 ± 1.5
341	$K^*(1410)^0\gamma$	< 130		< 130			< 130
342	$K^+\pi^-\gamma$ (N.R.) §	< 2.6		< 2.6			< 2.6
344	$K^0\pi^+\pi^-\gamma$	19.5 ± 2.2	$18.5 \pm 2.1 \pm 1.2$ †	$24 \pm 4 \pm 3$ ‡			19.5 ± 2.2
345	$K^+\pi^-\pi^0\gamma$	41 ± 4	$40.7 \pm 2.2 \pm 3.1$ †				40.7 ± 3.8
346	$K_1^0(1270)\gamma$	< 58		< 58			< 58
347	$K_1^0(1400)\gamma$	< 12		< 12			< 12
348	$K_2^*(1430)^0\gamma$	12.4 ± 2.4	$12.2 \pm 2.5 \pm 1.0$	$13 \pm 5 \pm 1$			12.4 ± 2.4
350	$K_3^*(1780)^0\gamma$	< 83		< 83			< 83
352	$\rho^0\gamma$	0.86 ± 0.15	$0.97^{+0.24}_{-0.22} \pm 0.06$	$0.78^{+0.17+0.09}_{-0.16-0.10}$	< 17		$0.86^{+0.15}_{-0.14}$
354	$\omega\gamma$	$0.44^{+0.18}_{-0.16}$	$0.50^{+0.27}_{-0.23} \pm 0.09$	$0.40^{+0.19}_{-0.17} \pm 0.13$	< 9.2		$0.44^{+0.18}_{-0.16}$
355	$\phi\gamma$	< 0.85	< 0.85	< 0.1	< 3.3		< 0.1
–	$p\overline{\Lambda}\pi^-\gamma$	New		< 0.65			< 0.65
465	$\pi^0\ell^+\ell^-$	< 0.053	< 0.053	< 0.154			< 0.053
466	$\pi^0e^+e^-$	< 0.084	< 0.084	< 0.227			< 0.084
467	$\pi^0\mu^+\mu^-$	< 0.069	< 0.069	< 0.184			< 0.069
468	$\eta\ell^+\ell^-$	< 0.064	< 0.064				< 0.064
469	ηe^+e^-	< 0.108	< 0.108				< 0.108
470	$\eta\mu^+\mu^-$	< 0.112	< 0.112				< 0.112
471	$\pi^0\nu\overline{\nu}$	< 69		< 69			< 69
472	$K^0\ell^+\ell^-$	$0.31^{+0.08}_{-0.07}$	$0.21^{+0.15}_{-0.13} \pm 0.02$	$0.34^{+0.09}_{-0.08} \pm 0.02$			$0.31^{+0.08}_{-0.07}$
473	$K^0e^+e^-$	$0.16^{+0.10}_{-0.08}$	$0.08^{+0.15}_{-0.12} \pm 0.01$	$0.20^{+0.14}_{-0.10} \pm 0.01$	< 8.45		$0.16^{+0.10}_{-0.08}$
474	$K^0\mu^+\mu^-$	0.34 ± 0.05	$0.49^{+0.29}_{-0.25} \pm 0.03$	$0.44^{+0.13}_{-0.10} \pm 0.03$	< 6.64	$0.327 \pm 0.034 \pm 0.017$	$0.343^{+0.036}_{-0.035}$
475	$K^0\nu\overline{\nu}$	< 49	< 49	< 194			< 49
476	$\rho^0\nu\overline{\nu}$	< 208		< 208			< 208
477	$K^{*0}\ell^+\ell^-$	$0.99^{+0.12}_{-0.11}$	$1.03^{+0.22}_{-0.21} \pm 0.07$	$0.97^{+0.13}_{-0.11} \pm 0.07$			$0.99^{+0.13}_{-0.11}$
478	$K^{*0}e^+e^-$	$1.03^{+0.19}_{-0.17}$	$0.86^{+0.26}_{-0.24} \pm 0.05$	$1.18^{+0.27}_{-0.22} \pm 0.09$			$1.03^{+0.19}_{-0.17}$
479	$K^{*0}\mu^+\mu^-$	1.05 ± 0.10	$1.35^{+0.40}_{-0.37} \pm 0.10$	$1.06^{+0.19}_{-0.14} \pm 0.07$		$1.036^{+0.018}_{-0.017} \pm 0.071$*	$1.049^{+0.067}_{-0.065}$
480	$K^{*0}\nu\overline{\nu}$	< 55	< 120	< 55			< 55
481	$\phi\nu\overline{\nu}$	< 127		< 127			< 127
	$\pi^+\pi^-\mu^+\mu^-$					$0.0211 \pm 0.0051 \pm 0.0022$ [1]	0.0210 ± 0.0060
483	$\pi^0e^\pm\mu^\mp$	< 0.14	< 0.14				< 0.14
484	$K^0e^\pm\mu^\mp$	< 0.27	< 0.27				< 0.27
485	$K^{*0}e^\pm\mu^\mp$	< 0.53	< 0.53				< 0.53

† $M_{K\pi\pi} < 1.8$ GeV/c^2; ‡ $1.0 < M_{K\pi\pi} < 2.0$ GeV/c^2.
§ 1.25 GeV/$c^2 < M_{K\pi} < 1.6$ GeV/c^2.
* This result takes into account the Swave fraction in the $K\pi$ system.
[1] Muon pairs do not originate from resonances and $0.5 < m(\pi^+\pi^-) < 1.3$ GeV/c^2.

Table 201: Branching fractions (BF) of charmless semileptonic and radiative decays of $B^{\pm}/B^0$ admixture in units of $\times 10^{-6}$. Upper limits are at 90% CL. Values in red (blue) are new published (preliminary) results since PDG2014.

RPP#	Mode	PDG2014 Avg.	*BABAR*	Belle	CLEO	CDF	Our Avg.
66	$K\eta\gamma$	$8.5^{+1.8}_{-1.6}$		$8.5^{+1.3}_{-1.2} \pm 0.9$			$8.5^{+1.6}_{-1.5}$
68	$K_2^*(1430)\gamma$	17^{+6}_{-5}			$17 \pm 6 \pm 1$		17 ± 6
70	$K_3^*(1780)\gamma$	< 37		< 2.8 §			< 2.8 §
77	$s\gamma$ †	349 ± 19	341 ± 28 [1]	328 ± 20 [1]	$329 \pm 44 \pm 29$		332 ± 15
77	$s\gamma$ [2]		336 ± 46 [1]	305 ± 16 [1]			308 ± 15
78	$d\gamma$	9.2 ± 3.0	$9.2 \pm 2.0 \pm 2.3$				9.2 ± 3.0
84	$\rho\gamma$	1.39 ± 0.25	$1.73^{+0.34}_{-0.32} \pm 0.17$	$1.21^{+0.24}_{-0.22} \pm 0.12$	< 14		$1.39^{+0.22}_{-0.21}$
85	$\rho/\omega\gamma$	1.30 ± 0.23	$1.63^{+0.30}_{-0.28} \pm 0.16$	$1.14 \pm 0.20^{+0.10}_{-0.12}$	< 14		$1.30^{+0.18}_{-0.19}$
119	se^+e^- ‡	4.7 ± 1.3	$7.69^{+0.82+0.71}_{-0.77-0.60}$		< 57		$7.69^{+1.08}_{-0.98}$
120	$s\mu^+\mu^-$ ‡	4.3 ± 1.2	$4.41^{+1.31+0.63}_{-1.17-0.50}$		< 58		$4.41^{+1.45}_{-1.27}$
121	$s\ell^+\ell^-$ ‡	4.5 ± 1.0	$6.73^{+0.70+0.60}_{-0.64-0.56}$		< 42		$6.73^{+0.92}_{-0.85}$
122	$\pi\ell^+\ell^-$	< 0.059	< 0.059	< 0.062			< 0.059
123	πe^+e^-	< 0.110	< 0.110				< 0.110
124	$\pi\mu^+\mu^-$	< 0.050	< 0.050				< 0.050
125	Ke^+e^-	0.44 ± 0.06	$0.39^{+0.09}_{-0.08} \pm 0.02$	$0.48^{+0.08}_{-0.07} \pm 0.03$			0.44 ± 0.06
126	$K^*e^+e^-$	1.19 ± 0.20	$0.99^{+0.23}_{-0.21} \pm 0.06$	$1.39^{+0.23}_{-0.20} \pm 0.12$			$1.19^{+0.17}_{-0.16}$
127	$K\mu^+\mu^-$	0.44 ± 0.04	$0.41^{+0.13}_{-0.12} \pm 0.02$	$0.50 \pm 0.06 \pm 0.03$		$0.42 \pm 0.04 \pm 0.02$	0.44 ± 0.04
128	$K^*\mu^+\mu^-$	1.06 ± 0.09	$1.35^{+0.35}_{-0.33} \pm 0.10$	$1.10^{+0.16}_{-0.14} \pm 0.08$		$1.01 \pm 0.10 \pm 0.05$	1.06 ± 0.09
129	$K\ell^+\ell^-$	0.48 ± 0.04	$0.47 \pm 0.06 \pm 0.02$	$0.48^{+0.05}_{-0.04} \pm 0.03$	< 1.7		0.48 ± 0.04
130	$K^*\ell^+\ell^-$	1.05 ± 0.10	$1.02^{+0.14}_{-0.13} \pm 0.05$	$1.07^{+0.11}_{-0.10} \pm 0.09$	< 3.3		1.05 ± 0.10
131	$K\nu\bar{\nu}$	< 17	< 17				< 17
132	$K^*\nu\bar{\nu}$	< 76	< 76				< 76
134	$\pi e^{\pm}\mu^{\mp}$	< 0.092	< 0.092		< 1.6		< 0.092
135	$\rho e^{\pm}\mu^{\mp}$	< 3.2			< 3.2		< 3.2
136	$Ke^{\pm}\mu^{\mp}$	< 0.038	< 0.038		< 1.6		< 0.038
137	$K^*e^{\pm}\mu^{\mp}$	< 0.51	< 0.51		< 6.2		< 0.51

† Results extrapolated to $E_\gamma > 1.6$ GeV, using the method of Ref. [805].
[1] Average of several results, obtained with different methods.
[2] Only results originally measured in the interval $E_\gamma > 1.9$ GeV (also taken into account in the previous line).
‡ Belle: $m(\ell^+\ell^-) > 0.2$ GeV/c^2, *BABAR*: $m^2(\ell^+\ell^-) > 0.1$ GeV$^2/c^4$.
§ Product BF ($\times\mathcal{B}(K_3^* \to K\eta)$). PDG gives the BF assuming $\mathcal{B}(K_3^* \to K\eta) = 11^{+5}_{-4}\%$.
¶ $E_\gamma > 2.0$ GeV.

List of other measurements that are not included in the tables:

- $B^+ \to K^+\pi^-\pi^+\gamma$: LHCb has measured the up-down asymmetries in bins of the $K\pi\pi\gamma$ mass [808].
- In [809], LHCb has also measured the BR of $B^+ \to K^+e^-e^+$ in the $m^2(\ell\ell)$ bin [1, 6] $(\text{GeV}/c^2)^2$.
- In the $B^+ \to \pi^+\mu^+\mu^-$ paper [810], LHCb has also measured the differential BR in bins of $m^2(\ell\ell)$.
- For $B \to K\ell^-\ell^+$, LHCb has measured F_H and A_{FB} in 17 (5) bins of $m^2(\ell\ell)$ for the K^+ (K_S^0) final state [811]. Belle has measured F_L and A_{FB} in 6 $m^2(\ell\ell)$ bins [812].
- For the $B \to K^*\ell^-\ell^+$ analyses, partial branching fractions and angular observables in bins of $m^2(\ell\ell)$ are also available:
  - $B^0 \to K^{*0}e^-e^+$: LHCb has measured F_L, $A_T^{(2)}$, A_T^{Im}, A_T^{Re} in the $m^2(\ell\ell)$ bin [0.002, 1.120] $(\text{GeV}/c^2)^2$ [813], and the BR in the dilepton mass region [10,1000]

Table 202: Branching fractions (BF) of leptonic and radiative-leptonic B^+ and B^0 decays in units of $\times 10^{-6}$. Upper limits are at 90% CL. Values in red (blue) are new published (preliminary) results since PDG2014.

RPP#	Mode	PDG2014 Avg.	*BABAR*	Belle	CDF	LHCb	CMS	ATLAS	Our Avg.
29	$e^+\nu$	< 0.98	< 1.9	< 0.98 †					< 0.98 †
30	$\mu^+\nu$	< 1.0	< 1.0	< 1.7 †					< 1.0
31	$\tau^+\nu$	114 ± 27	179 ± 48 ‡	$91 \pm 19 \pm 11$ ‡					106 ± 19
32	$\ell^+\nu_\ell\gamma$	< 15.6	< 15.6	< 3.5					< 3.5
33	$e^+\nu_e\gamma$	< 17	< 17	< 6.1					< 6.1
34	$\mu^+\nu_\mu\gamma$	< 24	< 24	< 3.4					< 3.4
457	$\gamma\gamma$	< 0.32	< 0.32	< 0.62					< 0.32
458	e^+e^-	< 0.083	< 0.113	< 0.19	< 0.083				< 0.083
459	$e^+e^-\gamma$	< 0.12	< 0.12						< 0.12
460	$\mu^+\mu^-$	< 0.00063	< 0.052	< 0.16	< 0.0038	< 00074 *	< 00110 *	< 0.00042 *	$0.00039^{+0.00016}_{-0.00014}$ §
461	$\mu^+\mu^-\gamma$	< 0.16	< 0.16						< 0.16
462	$\mu^+\mu^-\mu^+\mu^-$	< 0.0053				< 0.0053			< 0.0053
464	$\tau^+\tau^-$	< 4100	< 4100						< 4100
482	$e^\pm\mu^\mp$	< 0.0028	< 0.092	< 0.17	< 0.064	< 0.0028			< 0.0028
488	$e^\pm\tau^\mp$	< 28	< 28						< 28
489	$\mu^\pm\tau^\mp$	< 22	< 22						< 22
490	$\nu\overline{\nu}$	< 24	< 24	< 130					< 24
491	$\nu\overline{\nu}\gamma$	< 17	< 17						< 17

† More recent results exist, with hadronic tagging (PRD 91, 052016 (Belle)). It does not improve the limits (< 3.5 and < 2.7 for $e^+\nu$ and $\mu^+\nu$, respectively).
‡ The authors make the average with their previous results, derived from statistically independent samples. *BABAR*: [806], Belle: [807].
* Limit at 95% C.L.
§ This is the combined result obtained by the LHCb and CMS collaborations (Ref. [803]).

Table 203: Relative branching fractions (BF) of semileptonic and radiative B^+ decays. Values in red (blue) are new published (preliminary) results since PDG2014.

RPP#	Mode	PDG2014 AVG.	Belle	*BABAR*	LHCb	Our Avg.
–	$10^4 \times \mathcal{B}(K^+\pi^+\pi^-\mu^+\mu^-)/\mathcal{B}(\psi(2S)K^+)$	New			$6.95^{+0.46}_{-0.43} \pm 0.34$	$6.95^{+0.57}_{-0.55}$
–	$10^4 \times \mathcal{B}(K^+\phi\mu^+\mu^-)/\mathcal{B}(\psi(2S)K^+)$	New			$1.58^{+0.36+0.19}_{-0.32-0.07}$	$1.58^{+0.41}_{-0.33}$
469	$\mathcal{B}(\pi^+\mu^+\mu^-)/\mathcal{B}(K^+\mu^+\mu^-)$[1]	$0.053 \pm 0.014 \pm 0.01$			$0.038 \pm 0.009 \pm 0.001$	0.038 ± 0.009
473	$\mathcal{B}(K^+\mu^+\mu^-)/\mathcal{B}(K^+e^+e^-)$[2]	New			$0.745^{+0.090}_{-0.074} \pm 0.036$	$0.745^{+0.097}_{-0.082}$
473	$\mathcal{B}(K^+\mu^+\mu^-)/\mathcal{B}(K^+e^+e^-)$[3]	New	$1.03 \pm 0.19 \pm 0.06$			1.03 ± 0.20
473	$\mathcal{B}(K^+\mu^+\mu^-)/\mathcal{B}(K^+e^+e^-)$[4]	New		$1.00^{+0.31}_{-0.25} \pm 0.07$		$1.00^{+0.32}_{-0.26}$
–	$\mathcal{B}(K^*\mu^+\mu^-)/\mathcal{B}(K^*e^+e^-)$[3]	New	$0.83 \pm 0.17 \pm 0.08$			0.83 ± 0.19
–	$\mathcal{B}(K^*\mu^+\mu^-)/\mathcal{B}(K^*e^+e^-)$[4]	New		$1.013^{+0.34}_{-0.26} \pm 0.010$		$1.013^{+0.340}_{-0.260}$

[1] For $0.1 < m^2(\ell^+\ell^-) < 6.0\,\mathrm{GeV}^2/c^4$
[2] For $1.0 < m^2(\ell^+\ell^-) < 6.0\,\mathrm{GeV}^2/c^4$
[3] For the full $m^2(\ell^+\ell^-)$ range
[4] For $0.10 < m^2(\ell^+\ell^-) < 8.12\,\mathrm{GeV}^2/c^4$ and $m^2(\ell^+\ell^-) > 10.11\,\mathrm{GeV}^2/c^4$

(MeV/c^2) [809].

- $B \to K^*\ell^-\ell^+$: Belle has measured F_L, A_{FB}, isospin asymmetry in 6 $m^2(\ell\ell)$ bins [814] and P_4', P_5', P_6', P_8' in 4 $m^2(\ell\ell)$ bins [812]. *BABAR* has measured F_L, A_{FB}, P_2 in 5 $m^2(\ell\ell)$ bins [815].
- $B^0 \to K^{*0}\mu^-\mu^+$: LHCb has measured F_L, A_{FB}, $S_3 - S_9$, $A_3 - A_9$, $P_1 - P_3$, $P_4' - P_8'$ in 8 $m^2(\ell\ell)$ bins [816]. CMS has measured F_L and A_{FB} in 7 $m^2(\ell\ell)$ bins [817].

- For $B \to X_s\ell^-\ell^+$ (X_s is a hadronic system with an s quark), Belle has measured A_{FB} in bins of $m^2(\ell\ell)$ with a sum of 10 exclusive final states [818].

Table 204: Branching fractions (BF) of $B \to \bar{b} \to \bar{q}$ gluon decays in units of $\times 10^{-6}$. Upper limits are at 90% CL. Values in red (blue) are new published (preliminary) results since PDG2014.

RPP#	Mode	PDG2014 Avg.	*BABAR*	Belle	CLEO	Our Avg.
80	ηX	260^{+50}_{-80}		$261 \pm 30^{+44}_{-74}$ §	< 440	261^{+53}_{-79}
81	$\eta' X$	420 ± 90	$390 \pm 80 \pm 90$ †		$460 \pm 110 \pm 60$ †	423 ± 86
82	$K^+ X$	< 187	< 187 ‡			< 187 ‡
83	$K^0 X$	195^{+71}_{-67}	$195^{+51}_{-45} \pm 50$ ‡			195^{+71}_{-67}
94	$\pi^+ X$	370 ± 80	$372^{+50}_{-47} \pm 59$ ¶			372^{+77}_{-75}

§ $0.4 < m_X < 2.6$ GeV/c^2.
† $2.0 < p^*(\eta') < 2.7$ GeV/c.
‡ $m_X < 1.69$ GeV/c^2.
¶ $m_X < 1.71$ GeV/c^2.

Table 205: Isospin asymmetry in radiative and semileptonic B meson decays. The notations are those adopted by the PDG. Values in red (blue) are new published (preliminary) results since PDG2014.

Parameter	PDG2014 Avg.	*BABAR*	Belle	LHCb	Our Avg.
$\Delta_{0^-}(X_s\gamma)$	-0.01 ± 0.06	-0.01 ± 0.06 §			-0.01 ± 0.06
$\Delta_{0^+}(K^*\gamma)$	0.052 ± 0.026	$0.066 \pm 0.021 \pm 0.022$	$0.012 \pm 0.044 \pm 0.026$		0.012 ± 0.051
$\Delta_{\rho\gamma}$	-0.46 ± 0.17	$-0.43^{+0.25}_{-0.22} \pm 0.10$	$-0.48^{+0.21+0.08}_{-0.19-0.09}$		$-0.48^{+0.23}_{-0.21}$
$\Delta_{0-}(K\ell\ell)$ †	-0.37 ± 0.13	$-0.41 \pm 0.25 \pm 0.01$	$-0.41^{+0.25}_{-0.20} \pm 0.07$	$-0.10^{+0.08}_{-0.09} \pm 0.02^*$	$-0.13^{+0.08}_{-0.09}$
$\Delta_{0-}(K^*\ell\ell)$ †	-0.22 ± 0.10	$-0.20^{+0.30}_{-0.23} \pm 0.03$	$0.33^{+0.37}_{-0.43} \pm 0.08$	$0.00^{+0.12}_{-0.10} \pm 0.02^*$	$0.02^{+0.12}_{-0.10}$

§ Average of two independent measurements from *BABAR*.
† Results given for the bin $1 < m^2(\ell^+\ell^-) < 6\,\text{GeV}^2/c^2$, see references for the other bins.
*Only muons are used.

- $B^0 \to K^+\pi^-\mu^+\mu^-$, with 1330< $m(K^+\pi^-)$ <1530 GeV/c^2 : LHCb has measured the partial BR in bins of $m^2(\mu^-\mu^+)$ in the range [0.1,8.0] (GeV/c^2)^2, as well as angular moments [819].

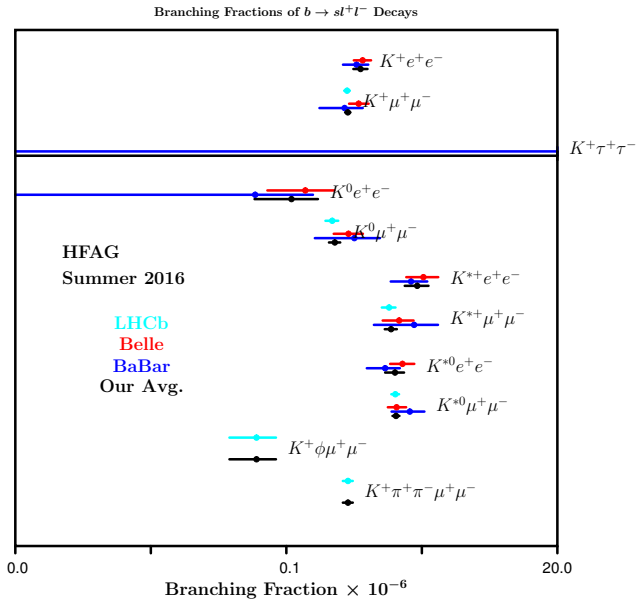

Figure 151: Branching fractions of $b \to sl^+l^-$ decays.

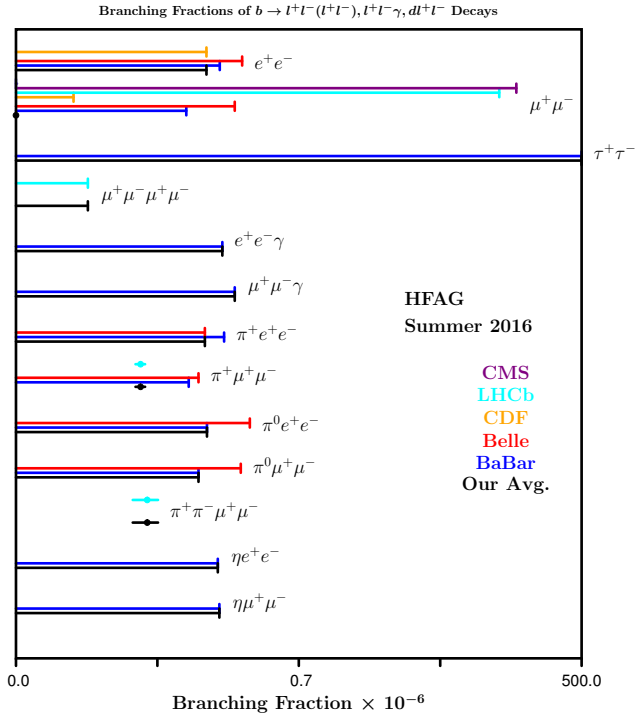

Figure 152: Branching fractions of $b \to l^+l^-(l^+l^-), l^+l^-\gamma and dl^+l^-$ decays.

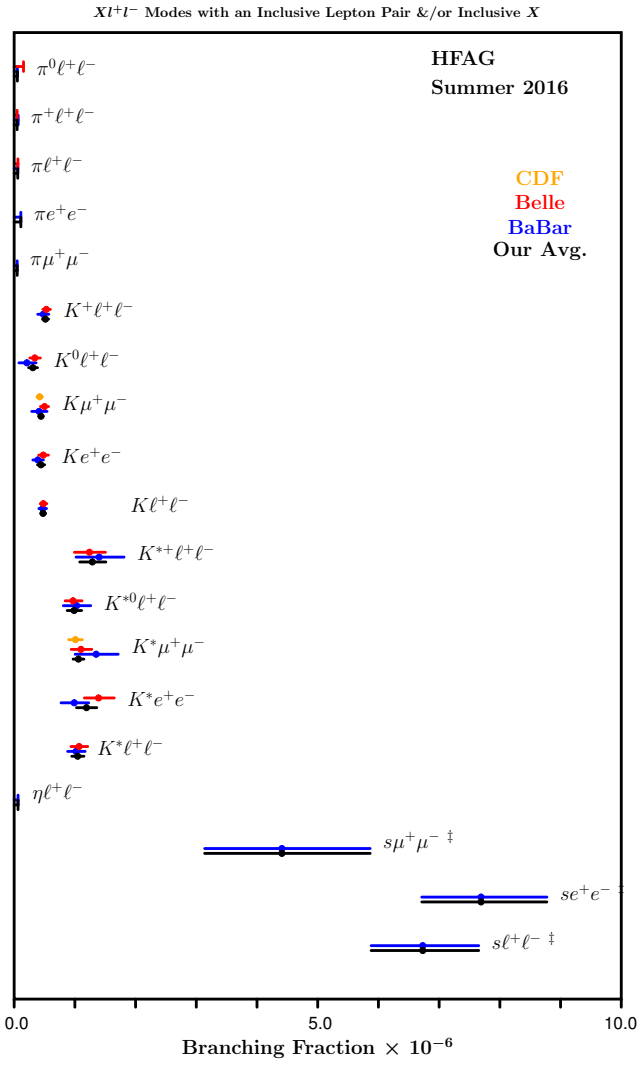

Figure 153: Xl^+l^- modes with an inclusive lepton pair and/or inclusive X.

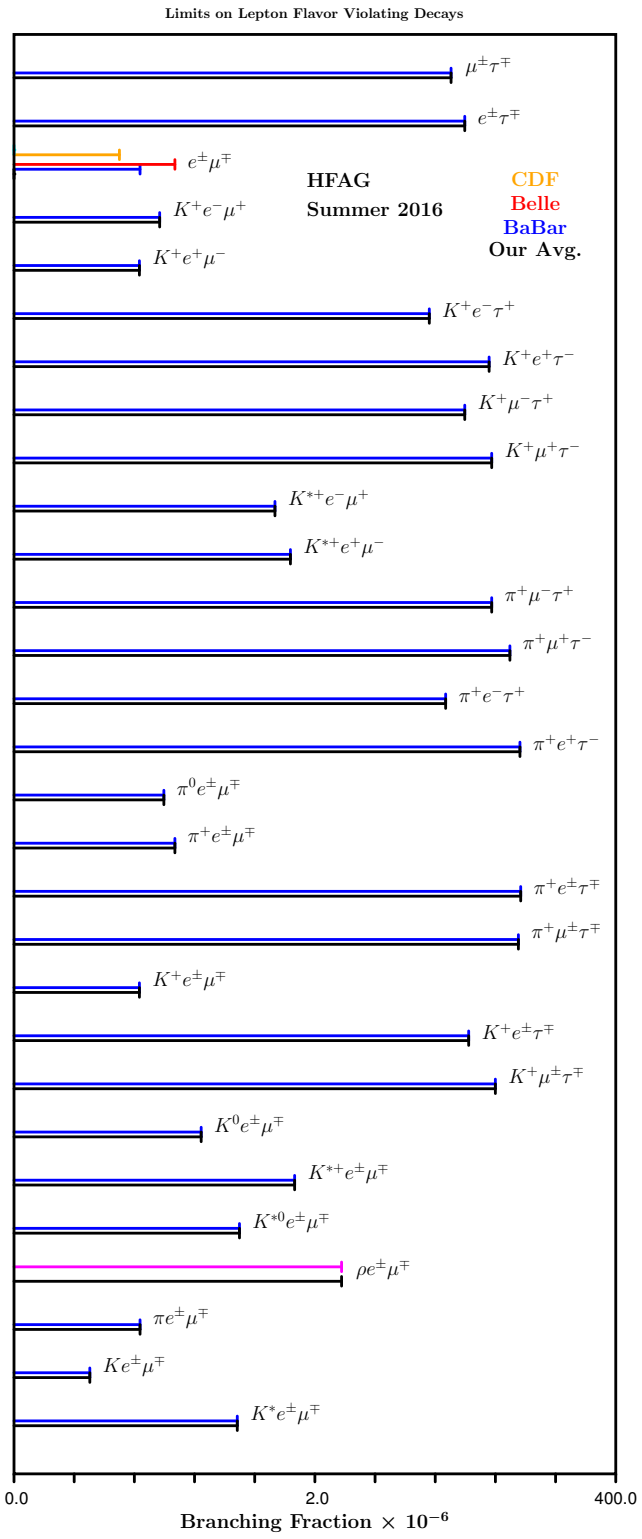

Figure 154: Limits on lepton flavor violating decays.

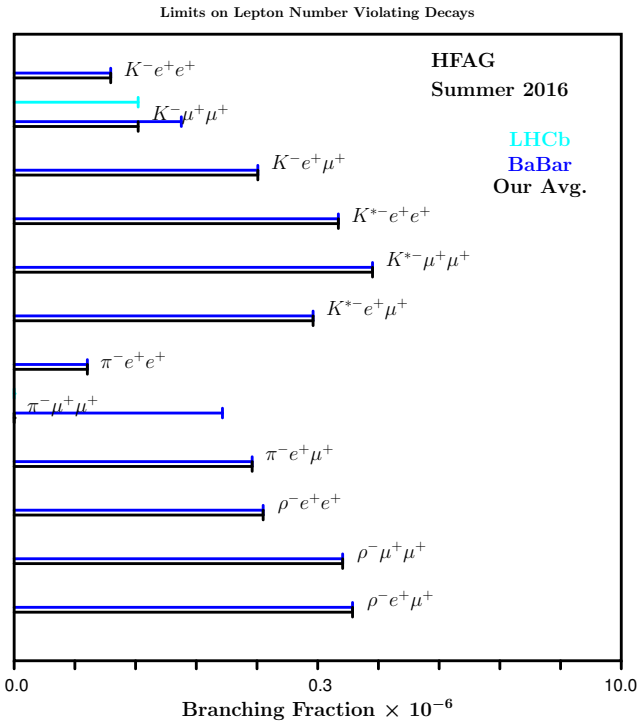

Figure 155: Limits on lepton number violating decays.

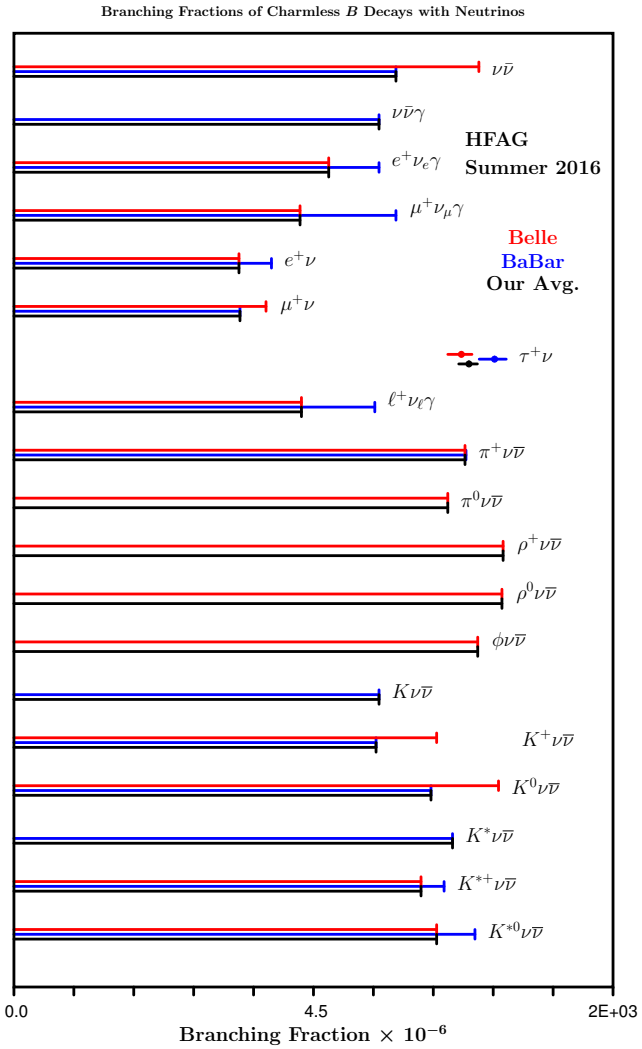

Figure 156: Branching fractions of charmless B decays with neutrinos.

7.6 Charge asymmetries in *b*-hadron decays

This section contains, in Tables 206 to 210 compilations of *CP* asymmetries in decays of different b-hadrons: B^+, B^0 mesons, $B^\pm/B^0$ admixtures, B_s^0 mesons and finally Λ_b^0 baryons. Measurements of time-dependent *CP* asymmetries are not listed here but are discussed in Sec. 4.

Figure 157 shows a graphic representation of a selection of results given in this section. For comments in the plot, marked with a symbol or a number, refer to the corresponding table.

Table 206: *CP* asymmetries of charmless hadronic B^+ decays. Values in red (blue) are new published (preliminary) results since PDG2014.

RPP#	Mode	PDG2014 Avg.	*BABAR*	Belle	CDF	LHCb	Our Avg.
262	$K^0\pi^+$	-0.017 ± 0.016	$-0.029 \pm 0.039 \pm 0.010$	$-0.011 \pm 0.021 \pm 0.006$		$-0.022 \pm 0.025 \pm 0.010$	-0.017 ± 0.016
263	$K^+\pi^0$	0.037 ± 0.021 1	$0.030 \pm 0.039 \pm 0.010$	$0.043 \pm 0.024 \pm 0.002$			0.040 ± 0.021
264	$\eta' K^+$	0.013 ± 0.017	$0.008^{+0.017}_{-0.018} \pm 0.009$	$0.028 \pm 0.028 \pm 0.021$			0.013 ± 0.017
265	$\eta' K^{*+}$	-0.26 ± 0.27	$-0.26 \pm 0.27 \pm 0.02$				-0.26 ± 0.27
266	$\eta' K_0^*(1430)^+$	0.06 ± 0.20	$0.06 \pm 0.20 \pm 0.02$				0.06 ± 0.20
267	$\eta' K_2^*(1430)^+$	0.15 ± 0.13	$0.15 \pm 0.13 \pm 0.02$				0.15 ± 0.13
268	ηK^+	-0.37 ± 0.08	$-0.36 \pm 0.11 \pm 0.03$	$-0.38 \pm 0.11 \pm 0.01$			-0.37 ± 0.08
269	ηK^{*+}	0.02 ± 0.06	$0.01 \pm 0.08 \pm 0.02$	$0.03 \pm 0.10 \pm 0.01$			0.02 ± 0.06
270	$\eta K_0^*(1430)^+$	$0.05 \pm 0.13 \pm 0.02$	$0.05 \pm 0.13 \pm 0.02$				0.05 ± 0.13
271	$\eta K_2^*(1430)^+$	$-0.45 \pm 0.30 \pm 0.02$	$-0.45 \pm 0.30 \pm 0.02$				-0.45 ± 0.30
281	ωK^+	0.02 ± 0.05	$-0.01 \pm 0.07 \pm 0.01$	$-0.03 \pm 0.04 \pm 0.01$			-0.02 ± 0.04
282	ωK^{*+}	0.29 ± 0.35	$0.29 \pm 0.35 \pm 0.02$				0.29 ± 0.35
284	$\omega K_0^*(1430)^+$	-0.10 ± 0.09	$-0.10 \pm 0.09 \pm 0.02$				-0.10 ± 0.09
285	$\omega K_2^*(1430)^+$	0.14 ± 0.15	$0.14 \pm 0.15 \pm 0.02$				0.14 ± 0.15
288	$K^{*0}\pi^+$	-0.04 ± 0.09	$0.032 \pm 0.052^{+0.016}_{-0.013}$	$-0.149 \pm 0.064 \pm 0.022$			-0.038 ± 0.042
289	$K^{*+}\pi^0$	-0.06 ± 0.24	$-0.06 \pm 0.24 \pm 0.04$				-0.06 ± 0.24
290	$K^+\pi^+\pi^-$	0.033 ± 0.010	$0.028 \pm 0.020 \pm 0.023$	$0.049 \pm 0.026 \pm 0.020$		$0.025 \pm 0.004 \pm 0.008$	0.027 ± 0.008
293	$f_0(980)K^+$	$-0.08 \pm 0.09^{\dagger}$	$-0.106 \pm 0.050^{+0.036}_{-0.015}$	$-0.077 \pm 0.065^{+0.046}_{-0.026}$			$-0.095^{+0.049}_{-0.042}$
294	$f_2(1270)K^+$	$-0.68^{+0.19}_{-0.017}$	$-0.85 \pm 0.22^{+0.26}_{-0.13}$	$-0.59 \pm 0.22 \pm 0.04$			$-0.68^{+0.20}_{-0.18}$
295	$f_0(1370)K^+$	$0.28^{+0.30}_{-0.29}$	$0.28 \pm 0.26^{+0.15}_{-0.14}$				$0.28^{+0.30}_{-0.29}$
298	$\rho^0 K^+$	0.37 ± 0.10	$0.44 \pm 0.10^{+0.06}_{-0.14}$	$0.30 \pm 0.11^{+0.11}_{-0.05}$			0.37 ± 0.11
299	$K_0^*(1430)^0\pi^+$	0.055 ± 0.033	$0.032 \pm 0.035^{+0.034}_{-0.028}$	$0.076 \pm 0.038^{+0.028}_{-0.022}$			$0.055^{+0.034}_{-0.032}$
300	$K_2^*(1430)^0\pi^+$	$0.05^{+0.29}_{-0.24}$	$0.05 \pm 0.23^{+0.18}_{-0.08}$				$0.05^{+0.29}_{-0.24}$
303	$K^+\pi^0\pi^0$	-0.06 ± 0.07	$-0.06 \pm 0.06 \pm 0.04$				-0.06 ± 0.07
310	$\rho^+ K^0$	-0.12 ± 0.17	$-0.12 \pm 0.17 \pm 0.02$				-0.12 ± 0.17
311	$K^{*+}\pi^+\pi^-$	0.07 ± 0.08	$0.07 \pm 0.07 \pm 0.04$				0.07 ± 0.08
312	$K^{*+}\rho^0$	0.31 ± 0.13	$0.31 \pm 0.13 \pm 0.03$				0.31 ± 0.13
313	$f_0(980)K^{*+}$	-0.15 ± 0.12	$-0.15 \pm 0.12 \pm 0.03$				-0.15 ± 0.12
314	$a_1^+ K^0$	0.12 ± 0.11	$0.12 \pm 0.11 \pm 0.02$				0.12 ± 0.11
315	$b_1^+ K^0$	-0.03 ± 0.15	$-0.03 \pm 0.15 \pm 0.02$				-0.03 ± 0.15
312	$K^{*0}\rho^+$	-0.01 ± 0.16	$-0.01 \pm 0.16 \pm 0.02$				-0.01 ± 0.16
319	$b_1^0 K^+$	-0.46 ± 0.20	$-0.46 \pm 0.20 \pm 0.02$				-0.46 ± 0.20
322	$K^+\overline{K}^0$	0.04 ± 0.14	$0.10 \pm 0.26 \pm 0.03$	$0.014 \pm 0.168 \pm 0.002$		$-0.21 \pm 0.14 \pm 0.01$	-0.087 ± 0.100
324	$K^+K_SK_S$	$0.04^{+0.04}_{-0.05}$	$0.04^{+0.04}_{-0.05} \pm 0.02$				$0.04^{+0.04}_{-0.05}$
329	$K^+K^-\pi^+$	-0.12 ± 0.05	$0.00 \pm 0.10 \pm 0.03$			$-0.123 \pm 0.017 \pm 0.014$	-0.118 ± 0.022
340	$K^+K^-K^+$	-0.036 ± 0.012	$-0.017^{+0.019}_{-0.014} \pm 0.014$			$-0.036 \pm 0.004 \pm 0.007$	-0.033 ± 0.007
341	ϕK^+	0.04 ± 0.04	$0.128 \pm 0.044 \pm 0.013$	$0.01 \pm 0.12 \pm 0.05$	$-0.07 \pm 0.17^{+0.03}_{-0.02}$	$0.022 \pm 0.021 \pm 0.009$	0.041 ± 0.020
348	$K^{*+}K^+K^-$	0.11 ± 0.09	$0.11 \pm 0.08 \pm 0.03$				0.11 ± 0.09
349	ϕK^{*+}	-0.01 ± 0.08	$0.00 \pm 0.09 \pm 0.04$	$-0.02 \pm 0.14 \pm 0.03$			-0.01 ± 0.08
351	$\phi K_1(1270)^+$	0.15 ± 0.20	$0.15 \pm 0.19 \pm 0.05$				0.15 ± 0.20
354	$\phi K_0^*(1430)^+$	0.04 ± 0.15	$0.04 \pm 0.15 \pm 0.04$				0.04 ± 0.15
355	$\phi K_2^*(1430)^+$	-0.23 ± 0.20	$-0.23 \pm 0.19 \pm 0.06$				-0.23 ± 0.20
359	$\phi\phi K^+$	-0.10 ± 0.08	-0.10 ± 0.08				-0.10 ± 0.08
363	$K^{*+}\gamma$	0.18 ± 0.29	$0.18 \pm 0.28 \pm 0.07$				0.18 ± 0.29
365	$K^+\eta\gamma$	-0.12 ± 0.07	$-0.09 \pm 0.10 \pm 0.01$	$-0.16 \pm 0.09 \pm 0.06$			-0.12 ± 0.07
367	$K^+\phi\gamma$	-0.13 ± 0.11 ‘	$-0.26 \pm 0.14 \pm 0.05$	$-0.03 \pm 0.11 \pm 0.08$			-0.13 ± 0.10
378	$\rho^+\gamma$	-0.11 ± 0.33		$-0.11 \pm 0.32 \pm 0.09$			-0.11 ± 0.33
379	$\pi^+\pi^0$	0.03 ± 0.04	$0.03 \pm 0.08 \pm 0.01$	$0.025 \pm 0.043 \pm 0.007$			0.026 ± 0.039
380	$\pi^+\pi^-\pi^+$	0.105 ± 0.029	$0.032 \pm 0.044^{+0.040}_{-0.037}$			$0.058 \pm 0.008 \pm 0.011$	0.057 ± 0.014
381	$\rho^0\pi^+$	$0.18^{+0.09}_{-0.17}$	$0.18 \pm 0.07^{+0.05}_{-0.15}$				$0.18^{+0.09}_{-0.17}$
383	$f_2(1270)\pi^+$	$0.41^{+0.31}_{-0.29}$	$0.41 \pm 0.25^{+0.18}_{-0.15}$				$0.41^{+0.31}_{-0.29}$
384	$\rho(1450)^0\pi^+$	$-0.06^{+0.36}_{-0.42}$	$-0.06 \pm 0.28^{+0.23}_{-0.32}$				$-0.06^{+0.36}_{-0.42}$
385	$f_0(1370)\pi^+$	0.72 ± 0.22	$0.72 \pm 0.15 \pm 0.16$				0.72 ± 0.22
387	$\pi^+\pi^-\pi^+(NR)$	$-0.14^{+0.23}_{-0.16}$	$-0.14 \pm 0.14^{+0.18}_{-0.08}$				$-0.14^{+0.23}_{-0.16}$
389	$\rho^+\pi^0$	0.02 ± 0.11	$-0.01 \pm 0.13 \pm 0.02$	$0.06 \pm 0.17^{+0.04}_{-0.05}$			0.02 ± 0.11
391	$\rho^+\rho^0$	-0.05 ± 0.05	$-0.054 \pm 0.055 \pm 0.010$	$0.00 \pm 0.22 \pm 0.03$			-0.051 ± 0.054
397	$\eta\pi^+$	-0.14 ± 0.07	$-0.03 \pm 0.09 \pm 0.03$	$-0.19 \pm 0.06 \pm 0.01$			-0.14 ± 0.05
398	$\eta\rho^+$	0.11 ± 0.11	$0.13 \pm 0.11 \pm 0.02$	$-0.04^{+0.34}_{-0.32} \pm 0.01$			0.11 ± 0.11
399	$\eta'\pi^+$	0.06 ± 0.16	$0.03 \pm 0.17 \pm 0.02$	$0.20^{+0.37}_{-0.36} \pm 0.04$			0.06 ± 0.15
400	$\eta'\rho^+$	0.26 ± 0.17	$0.26 \pm 0.17 \pm 0.02$				0.26 ± 0.17
401	$\omega\pi^+$	-0.04 ± 0.06 [1]	$-0.02 \pm 0.08 \pm 0.01$	$-0.02 \pm 0.09 \pm 0.01$			-0.02 ± 0.06
402	$\omega\rho^+$	-0.20 ± 0.09	$-0.20 \pm 0.09 \pm 0.02$				-0.20 ± 0.09
408	$b_1^0\pi^+$	0.05 ± 0.16	$0.05 \pm 0.16 \pm 0.02$				0.05 ± 0.16
417	$p\overline{p}\pi^+$	0.00 ± 0.04	$0.04 \pm 0.07 \pm 0.04$	$-0.17 \pm 0.10 \pm 0.02^{\ddagger}$			-0.04 ± 0.06
420	$p\overline{p}K^+$	-0.08 ± 0.04	$-0.16 \pm 0.08 \pm 0.04$	$-0.02 \pm 0.05 \pm 0.02^{\ddagger}$		$-0.047 \pm 0.036 \pm 0.007$	-0.051 ± 0.029
425	$p\overline{p}K^{*+}$	0.21 ± 0.16	$0.32 \pm 0.13 \pm 0.05$	$-0.01 \pm 0.19 \pm 0.02$			0.21 ± 0.11
428	$p\overline{\Lambda}\gamma$	0.17 ± 0.17		$0.17 \pm 0.16 \pm 0.05$			0.17 ± 0.17
429	$p\overline{\Lambda}\pi^0$	0.01 ± 0.17		$0.01 \pm 0.17 \pm 0.04$			0.01 ± 0.17
471	$K^+\ell\ell$	-0.02 ± 0.08	$-0.03 \pm 0.14 \pm 0.01^{\S}$	$0.04 \pm 0.10 \pm 0.02$			0.02 ± 0.08
472	$K^+e^+e^-$	0.14 ± 0.14		$0.14 \pm 0.14 \pm 0.03$			0.14 ± 0.14
473	$K^+\mu^+\mu^-$	-0.003 ± 0.033		$-0.05 \pm 0.13 \pm 0.03$		$0.012 \pm 0.017 \pm 0.001$ [2]	0.011 ± 0.017
478	$K^{*+}\ell\ell$	-0.09 ± 0.14	$0.01^{+0.26}_{-0.24} \pm 0.02$	$-0.13^{+0.17}_{-0.16} \pm 0.01$			$-0.09^{+0.14}_{-0.13}$
479	$K^{*+}e^+e^-$	$-0.14^{+0.23}_{-0.22}$		$-0.14^{+0.23}_{-0.22} \pm 0.02$			$-0.14^{+0.23}_{-0.22}$
480	$K^{*+}\mu^+\mu^-$	-0.12 ± 0.24		$-0.12 \pm 0.24 \pm 0.02$		$-0.035 \pm 0.024 \pm 0.003$ [2]	-0.036 ± 0.024
480	$\pi^+\mu^+\mu^-$					$-0.11 \pm 0.12 \pm 0.01$	-0.11 ± 0.12

† PDG takes the value from the *BABAR* amplitude analysis of $B^+ \to K^+K^-K^+$, while our numbers are from amplitude analyses of $B^+ \to K^+\pi^-\pi^+$.
‡ PDG swaps the Belle results corresponding to $A_{CP}(p\overline{p}\pi^+)$ and $A_{CP}(p\overline{p}K^+)$.
[1] PDG uses also a result from CLEO.
§ PDG uses also a previous result from *BABAR* ([820]);
[2] LHCb also quotes results in bins of $m(\ell^+\ell^-)^2$.

Table 207: *CP* asymmetries of charmless hadronic B^0 decays. Values in red (blue) are new published (preliminary) results since PDG2014.

RPP#	Mode	PDG2014 Avg.	*BABAR*	Belle	CDF	LHCb	Our Avg.
227	$K^+\pi^-$	-0.082 ± 0.006 [1]	$-0.107 \pm 0.016^{+0.006}_{-0.004}$	$-0.069 \pm 0.014 \pm 0.007$	$-0.083 \pm 0.013 \pm 0.004$	$-0.080 \pm 0.007 \pm 0.003$	-0.082 ± 0.006
230	$\eta' K^{*0}$	0.02 ± 0.23	$0.02 \pm 0.23 \pm 0.02$	$-0.22 \pm 0.29 \pm 0.07$			-0.07 ± 0.18
231	$\eta' K_0^*(1430)^0$	-0.19 ± 0.17	$-0.19 \pm 0.17 \pm 0.02$				-0.19 ± 0.17
232	$\eta' K_2^*(1430)^0$	0.14 ± 0.18	$0.14 \pm 0.18 \pm 0.02$				0.14 ± 0.18
234	ηK^{*0}	0.19 ± 0.05	$0.21 \pm 0.06 \pm 0.02$	$0.17 \pm 0.08 \pm 0.01$			0.19 ± 0.05
235	$\eta K_0^*(1430)^0$	0.06 ± 0.13	$0.06 \pm 0.13 \pm 0.02$				0.06 ± 0.13
236	$\eta K_2^*(1430)^0$	-0.07 ± 0.19	$-0.07 \pm 0.19 \pm 0.02$				-0.07 ± 0.19
241	$b_1^- K^+$	-0.07 ± 0.12	$-0.07 \pm 0.12 \pm 0.02$				-0.07 ± 0.12
246	ωK^{*0}	0.45 ± 0.25	$0.45 \pm 0.25 \pm 0.02$				0.45 ± 0.25
248	$\omega K_0^*(1430)^0$	-0.07 ± 0.09	$-0.07 \pm 0.09 \pm 0.02$				-0.07 ± 0.09
249	$\omega K_2^*(1430)^0$	-0.37 ± 0.17	$-0.37 \pm 0.17 \pm 0.02$				-0.37 ± 0.17
251	$K^+\pi^-\pi^0$	0.00 ± 0.06	$-0.030^{+0.045}_{-0.051} \pm 0.055$	$0.07 \pm 0.11 \pm 0.01$			$0.000^{+0.059}_{-0.061}$
252	$\rho^- K^+$	0.20 ± 0.11	$0.20 \pm 0.09 \pm 0.08$	$0.22^{+0.22+0.06}_{-0.23-0.02}$			0.20 ± 0.11
253	$\rho(1450)^- K^+$	-0.10 ± 0.33	$-0.10 \pm 0.32 \pm 0.09$				-0.10 ± 0.33
254	$\rho(1700)^- K^+$	-0.36 ± 0.61	$-0.36 \pm 0.57 \pm 0.23$				-0.36 ± 0.61
255	$K^+\pi^-\pi^0(NR)$	0.10 ± 0.18	$0.10 \pm 0.16 \pm 0.08$				0.10 ± 0.18
257	$K_0^*(1430)^0\pi^0$	-0.15 ± 0.11	$-0.15 \pm 0.10 \pm 0.04$				-0.15 ± 0.11
261	$K^0\pi^+\pi^-$	-0.01 ± 0.05	$-0.01 \pm 0.05 \pm 0.01$				-0.01 ± 0.05
264	$K^{*+}\pi^-$	-0.22 ± 0.06 [1]	$-0.24 \pm 0.07 \pm 0.02$ [2]	$-0.21 \pm 0.11 \pm 0.07$			-0.23 ± 0.06
265	$K_0^*(1430)^+\pi^-$	0.09 ± 0.07	$0.09 \pm 0.07 \pm 0.03$				0.09 ± 0.08
271	$K^{*0}\pi^0$	-0.15 ± 0.13	$-0.15 \pm 0.12 \pm 0.04$				-0.15 ± 0.13
278	$K^{*0}\pi^+\pi^-$	0.07 ± 0.05	$0.07 \pm 0.04 \pm 0.03$				0.07 ± 0.05
279	$K^{*0}\rho^0$	-0.06 ± 0.09	$-0.06 \pm 0.09 \pm 0.02$				-0.06 ± 0.09
280	$f_0(980)K^{*0}$	0.07 ± 0.10	$0.07 \pm 0.10 \pm 0.02$				0.07 ± 0.10
283	$a_1^- K^+$	-0.16 ± 0.12	$-0.16 \pm 0.12 \pm 0.01$				-0.16 ± 0.12
284	$K^{*+}\rho^-$	0.21 ± 0.15	$0.21 \pm 0.15 \pm 0.02$				0.21 ± 0.15
311	$K^{*0}K^+K^-$	0.01 ± 0.05	$0.01 \pm 0.05 \pm 0.02$				0.01 ± 0.05
312	ϕK^{*0}	0.00 ± 0.04	$0.01 \pm 0.06 \pm 0.03$	$-0.007 \pm 0.048 \pm 0.021$		$-0.015 \pm 0.032 \pm 0.10^{\dagger}$	-0.003 ± 0.038
314	$K^{*0}\pi^+K^-$	0.22 ± 0.39	$0.22 \pm 0.33 \pm 0.20$				0.22 ± 0.39
326	$\phi K_0^*(1430)^0$	0.12 ± 0.08	$0.20 \pm 0.14 \pm 0.06$	$0.093 \pm 0.094 \pm 0.017$			0.124 ± 0.081
333	$\phi K_2^*(1430)^0$	-0.11 ± 0.10	$-0.08 \pm 0.12 \pm 0.05$	$-0.155^{+0.152}_{-0.133} \pm 0.033$			$-0.113^{+0.102}_{-0.096}$
340	$K^{*0}\gamma$	-0.002 ± 0.015	$-0.016 \pm 0.022 \pm 0.007$			$0.008 \pm 0.017 \pm 0.009$	-0.002 ± 0.015
357	$\pi^0\pi^0$	0.43 ± 0.14	$0.43 \pm 0.26 \pm 0.05$	$0.44^{+0.52}_{-0.53} \pm 0.17$			0.43 ± 0.24
391	$a_1^\mp \pi^\pm$	-0.07 ± 0.06	$-0.07 \pm 0.07 \pm 0.02$	$-0.06 \pm 0.05 \pm 0.07$			-0.07 ± 0.06
400	$b_1^\mp \pi^\pm$	-0.05 ± 0.10	$-0.05 \pm 0.10 \pm 0.02$				-0.05 ± 0.10
412	$p\bar{p}K^{*0}$	0.05 ± 0.12	$0.11 \pm 0.13 \pm 0.06$	$-0.08 \pm 0.20 \pm 0.02$			0.05 ± 0.12
414	$p\bar{\Lambda}\pi^-$	0.04 ± 0.07	$-0.10 \pm 0.10 \pm 0.02$ [3]	$-0.02 \pm 0.10 \pm 0.03$			-0.06 ± 0.07
477	$K^{*0}\ell\ell$	-0.05 ± 0.10	$0.02 \pm 0.20 \pm 0.02$	$-0.08 \pm 0.12 \pm 0.02$			-0.05 ± 0.10
478	$K^{*0}e^+e^-$	-0.21 ± 0.19		$-0.21 \pm 0.19 \pm 0.02$			-0.21 ± 0.19
479	$K^{*0}\mu^+\mu^-$	-0.07 ± 0.04		$0.00 \pm 0.15 \pm 0.03$		$-0.035 \pm 0.024 \pm 0.003$ [4]	-0.034 ± 0.024

Measurements of time-dependent CP asymmetries are listed on the Unitarity Triangle home page. (http://www.slac.stanford.edu/xorg/hfag/triangle/index.html)

† Extracted from measured $\Delta A_{CP} = A_{CP}(\phi K^{*0}) - A_{CP}(J/\psi K^{*0}) = 0.015 \pm 0.032 \pm 0.005$.
[1] PDG uses also a result from CLEO.
[2] Average of *BABAR* results from $B^0 \to K^+\pi^-\pi^0$ and $B^0 \to K^0\pi^+\pi^-$.
[3] PDG quotes the opposite asymmetry.
[4] LHCb also quotes results in bins of $m(\ell^+\ell^-)^2$.

Table 208: *CP* asymmetries of charmless hadronic decays of $B^{\pm}/B^0$ admixture. Values in red (blue) are new published (preliminary) results since PDG2014.

RPP#	Mode	PDG2014 Avg.	*BABAR*	Belle	Our Avg.
65	$K^*\gamma$	$-0.003 \pm 0.017^{\ddagger}$	$-0.003 \pm 0.017 \pm 0.007$	$-0.015 \pm 0.044 \pm 0.012$	-0.005 ± 0.017
77	$s\gamma$	-0.008 ± 0.029	$0.017 \pm 0.019 \pm 0.010^{\S}$	$0.002 \pm 0.050 \pm 0.030$	0.015 ± 0.020
	$(s+d)\gamma$	-0.01 ± 0.05	$0.057 \pm 0.060 \pm 0.018^{1}$	$0.022 \pm 0.039 \pm 0.009$ *	0.032 ± 0.034
80	$s\eta$	$-0.13^{+0.04}_{-0.05}$		$-0.13 \pm 0.04^{+0.02}_{-0.03}$	$-0.13^{+0.04}_{-0.05}$
86	π^+X	0.10 ± 0.17	$0.10 \pm 0.16 \pm 0.05$		0.10 ± 0.17
121	$s\ell\ell$	-0.22 ± 0.26	$0.04 \pm 0.11 \pm 0.01$		0.04 ± 0.11
126	$K^*e^+e^-$	-0.18 ± 0.15		$-0.18 \pm 0.15 \pm 0.01$	-0.18 ± 0.15
128	$K^*\mu^+\mu^-$	-0.03 ± 0.13		$-0.03 \pm 0.13 \pm 0.02$	-0.03 ± 0.13
129	$K\ell\ell$	New	$-0.03 \pm 0.14 \pm 0.01$		-0.03 ± 0.14
130	$K^*\ell\ell$	-0.04 ± 0.07	$0.03 \pm 0.13 \pm 0.01^{\dagger}$	$-0.10 \pm 0.10 \pm 0.01$	-0.05 ± 0.08

§ *BABAR* also measures the difference in direct *CP* asymmetry for charged and neutral B mesons: $\Delta A_{CP} = +(5.0 \pm 3.9 \pm 1.5)\%$.
† Previous *BABAR* result is also included in the PDG Average.
1 There is another *BABAR* result using the recoil method [821], and a CLEO result [822] that are used in the PDG average
* Require $E_\gamma > 2.1$ GeV.
‡ PDG include also a result from CLEO.

Table 209: *CP* asymmetries of charmless hadronic B_s^0 decays. Values in red (blue) are new published (preliminary) results since PDG2014.

RPP#	Mode	PDG2014 Avg.	Belle	CDF	LHCb	Our Avg.
52	π^+K^-	0.28 ± 0.04		$0.22 \pm 0.07 \pm 0.02$	$0.27 \pm 0.04 \pm 0.01$	0.26 ± 0.04

Table 210: *CP* asymmetries of charmless hadronic Λ_b decays. Values in red (blue) are new published (preliminary) results since PDG2014.

RPP#	Mode	PDG2014 Avg.	CDF	LHCb	Our Avg.
21	$p\pi^-$	0.03 ± 0.18	$0.06 \pm 0.07 \pm 0.03$		0.06 ± 0.08
22	pK^-	0.37 ± 0.17	$-0.10 \pm 0.08 \pm 0.04$		-0.10 ± 0.09
–	$\overline{K}^0 p\pi^-$	New		$0.22 \pm 0.13 \pm 0.03$	0.22 ± 0.13
–	$\Lambda K^+\pi^-$	New		$-0.53 \pm 0.23 \pm 0.11$	-0.53 ± 0.26
–	ΛK^+K^-	New		$-0.28 \pm 0.10 \pm 0.07$	-0.28 ± 0.12

List of other measurements that are not included in the tables:

- In the paper [823], LHCb has measured the triple product asymmetries for the decays $\Lambda_b \to p\pi^-\pi^+\pi^-$ and $\Lambda_b \to p\pi^- K^+ K^-$.

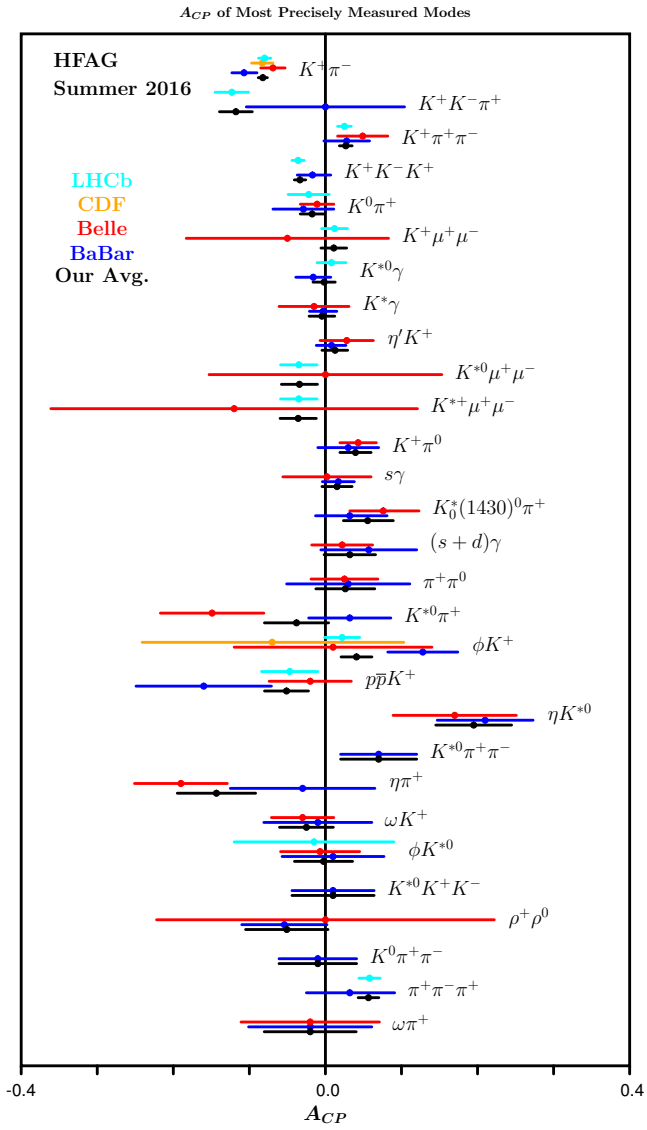

Figure 157: A_{CP} of most precisely measured modes.

7.7 Polarization measurements in *b*-hadron decays

In this section, compilations of polarization measurements in b-hadron decays are given. Tables 211 (212) detail measurements of the longitudinal fraction, f_L, in B^+ (B^0) decays, and Tables 213 (214) the results of the full angular analyses of B^+ (B^0) $\to \phi K^*$ decays. Table 215 gives results of the full angular analysis of $B^0 \to \phi K_2^{*0}(1430)$ decays. Tables 216 to 218 detail quantities of B_s^0 decays: f_L measurements, and observables from full angular analyses of decays to $\phi\phi$ and $\phi\overline{K}^{*0}$.

Figures 158 and 159 show a graphic representation of a selection of results shown in this section. For comments in the plots, marked with a symbol or a number, refer to the corresponding table.

Table 211: Longitudinal polarization fraction f_L for B^+ decays.Values in red (blue) are new published (preliminary) results since PDG2014.

RPP#	Mode	PDG2014 Avg.	*BABAR*	Belle	Our Avg.
282	ωK^{*+}	$0.41 \pm 0.18 \pm 0.05$	$0.41 \pm 0.18 \pm 0.05$		0.41 ± 0.19
285	$\omega K_2^*(1430)^+$	$0.56 \pm 0.10 \pm 0.04$	$0.56 \pm 0.10 \pm 0.04$		0.56 ± 0.11
312	$K^{*+}\rho^0$	$0.78 \pm 0.12 \pm 0.03$	$0.78 \pm 0.12 \pm 0.03$		0.78 ± 0.12
316	$K^{*0}\rho^+$	0.48 ± 0.08	$0.52 \pm 0.10 \pm 0.04$	$0.43 \pm 0.11^{+0.05}_{-0.02}$	0.48 ± 0.08
338	$K^{*+}\overline{K}^{*0}$	$0.75^{+0.16}_{-0.26} \pm 0.03$	$0.75^{+0.16}_{-0.26} \pm 0.03$		$0.75^{+0.16}_{-0.26}$
349	ϕK^{*+}	0.50 ± 0.05	$0.49 \pm 0.05 \pm 0.03$	$0.52 \pm 0.08 \pm 0.03$	0.50 ± 0.05
351	$\phi K_1(1270)^+$	$0.46^{+0.12+0.06}_{-0.13-0.07}$	$0.46^{+0.12+0.06}_{-0.13-0.07}$		$0.46^{+0.13}_{-0.15}$
355	$\phi K_2^*(1430)^+$	$0.80^{+0.09}_{-0.10} \pm 0.03$	$0.80^{+0.09}_{-0.10} \pm 0.03$		0.80 ± 0.10
391	$\rho^+\rho^0$	0.950 ± 0.016	$0.950 \pm 0.015 \pm 0.006$	$0.95 \pm 0.11 \pm 0.02$	0.950 ± 0.016
396	$\omega\rho^+$	$0.90 \pm 0.05 \pm 0.03$	$0.90 \pm 0.05 \pm 0.03$		0.90 ± 0.06

Table 212: Longitudinal polarization fraction f_L for B^0 decays. Values in red (blue) are new published (preliminary) results since PDG2014.

RPP#	Mode	PDG2014 Avg.	*BABAR*	Belle	LHCb	Our Avg.
246	ωK^{*0}	0.69 ± 0.13	$0.72 \pm 0.14 \pm 0.02$	$0.56 \pm 0.29^{+0.18}_{-0.08}$		0.70 ± 0.13
249	$\omega K_2^*(1430)^0$	$0.45 \pm 0.12 \pm 0.02$	$0.45 \pm 0.12 \pm 0.02$			0.45 ± 0.12
279	$K^{*0}\rho^0$	$0.40 \pm 0.08 \pm 0.11$	$0.40 \pm 0.08 \pm 0.11$			0.40 ± 0.14
284	$K^{*+}\rho^-$	$0.38 \pm 0.13 \pm 0.03$	$0.38 \pm 0.13 \pm 0.03$			0.38 ± 0.13
312	ϕK^{*0}	0.497 ± 0.025	$0.494 \pm 0.034 \pm 0.013$	$0.499 \pm 0.030 \pm 0.018$	$0.497 \pm 0.019 \pm 0.015$	0.497 ± 0.017
315	$K^{*0}\overline{K}^{*0}$	$0.80^{+0.10}_{-0.12} \pm 0.06$	$0.80^{+0.10}_{-0.12} \pm 0.06$			$0.80^{+0.12}_{-0.13}$
333	$\phi K_2^*(1430)^0$	$0.901^{+0.046}_{-0.058} \pm 0.037$	$0.901^{+0.046}_{-0.058} \pm 0.037$			$0.901^{+0.059}_{-0.069}$
386	$\rho^0\rho^0$	$0.75^{+0.11}_{-0.14} \pm 0.05$	$0.75^{+0.11}_{-0.14} \pm 0.05$	$0.21^{+0.18}_{-0.22} \pm 0.15$	$0.745^{+0.048}_{-0.058} \pm 0.034$	$0.714^{+0.055}_{-0.062}$
394	$\rho^+\rho^-$	$0.977^{+0.028}_{-0.024}$	$0.992 \pm 0.024^{+0.026}_{-0.013}$	$0.941^{+0.034}_{-0.040} \pm 0.030$		$0.978^{+0.025}_{-0.022}$
405	$a_1^\pm a_1^\mp$	$0.31 \pm 0.22 \pm 0.10$	$0.31 \pm 0.22 \pm 0.10$			0.31 ± 0.24

Table 213: Results of the full angular analyses of $B^+ \to \phi K^{*+}$. Values in red (blue) are new published (preliminary) results since PDG2014.

Parameter	PDG2014 Avg.	*BABAR*	Belle	Our Avg.
$f_\perp = \Lambda_{\perp\perp}$	0.20 ± 0.05	$0.21 \pm 0.05 \pm 0.02$	$0.19 \pm 0.08 \pm 0.02$	0.20 ± 0.05
$\phi_\parallel$	2.34 ± 0.18	$2.47 \pm 0.20 \pm 0.07$	$2.10 \pm 0.28 \pm 0.04$	2.34 ± 0.17
$\phi_\perp$	2.58 ± 0.17	$2.69 \pm 0.20 \pm 0.03$	$2.31 \pm 0.30 \pm 0.07$	2.58 ± 0.17
δ_0	$3.07 \pm 0.18 \pm 0.06$	$3.07 \pm 0.18 \pm 0.06$		3.07 ± 0.19
A_{CP}^0	$0.17 \pm 0.11 \pm 0.02$	$0.17 \pm 0.11 \pm 0.02$		0.17 ± 0.11
$A_{CP}^\perp$	$0.22 \pm 0.24 \pm 0.08$	$0.22 \pm 0.24 \pm 0.08$		0.22 ± 0.25
$\Delta\phi_\parallel$	$0.07 \pm 0.20 \pm 0.05$	$0.07 \pm 0.20 \pm 0.05$		0.07 ± 0.21
$\Delta\phi_\perp$	$0.19 \pm 0.20 \pm 0.07$	$0.19 \pm 0.20 \pm 0.07$		0.19 ± 0.21
$\Delta\delta_0$	$0.20 \pm 0.18 \pm 0.03$	$0.20 \pm 0.18 \pm 0.03$		0.20 ± 0.18

Angles (ϕ, δ) are in radians. BF, f_L and A_{CP} are tabulated separately.

Table 214: Results of the full angular analyses of $B^0 \to \phi K^{*0}$. Values in red (blue) are new published (preliminary) results since PDG2014.

Parameter	PDG2014 Avg.	*BABAR*	Belle	LHCb	Our Avg.
$f_\perp = \Lambda_{\perp\perp}$	0.228 ± 0.021	$0.212 \pm 0.032 \pm 0.013$	$0.238 \pm 0.026 \pm 0.008$	$0.221 \pm 0.016 \pm 0.013$	0.225 ± 0.015
$f_S(K\pi)$	New			$0.143 \pm 0.013 \pm 0.012$	0.143 ± 0.018
$f_S(KK)$	New			$0.122 \pm 0.013 \pm 0.008$	0.122 ± 0.015
$\phi_\parallel$	2.28 ± 0.08	$2.40 \pm 0.13 \pm 0.08$	$2.23 \pm 0.10 \pm 0.02$	$2.562 \pm 0.069 \pm 0.040$	2.430 ± 0.058
$\phi_\perp$	2.36 ± 0.09	$2.35 \pm 0.13 \pm 0.09$	$2.37 \pm 0.10 \pm 0.04$	$2.633 \pm 0.062 \pm 0.037$	2.527 ± 0.056
δ_0	2.88 ± 0.10	$2.82 \pm 0.15 \pm 0.09$	$2.91 \pm 0.10 \pm 0.08$		2.88 ± 0.10
$\phi_S(K\pi)$ †	New			$2.222 \pm 0.063 \pm 0.081$	2.222 ± 0.103
$\phi_S(KK)$ †	New			$2.481 \pm 0.072 \pm 0.048$	2.481 ± 0.087
A_{CP}^0	-0.01 ± 0.05	$0.01 \pm 0.07 \pm 0.02$	$-0.03 \pm 0.06 \pm 0.01$	$-0.003 \pm 0.038 \pm 0.005$	-0.007 ± 0.030
$A_{CP}^\perp$	-0.11 ± 0.09	$-0.04 \pm 0.15 \pm 0.06$	$-0.14 \pm 0.11 \pm 0.01$	$0.047 \pm 0.072 \pm 0.009$	-0.014 ± 0.057
$\mathcal{A}_{CP}^S(K\pi)$	New			$0.073 \pm 0.091 \pm 0.035$	0.073 ± 0.097
$\mathcal{A}_{CP}^S(KK)$	New			$-0.209 \pm 0.105 \pm 0.012$	-0.209 ± 0.106
$\Delta\phi_\parallel$	0.06 ± 0.11	$0.22 \pm 0.12 \pm 0.08$	$-0.02 \pm 0.10 \pm 0.01$	$0.045 \pm 0.068 \pm 0.015$	0.051 ± 0.053
$\Delta\phi_\perp$	0.10 ± 0.08	$0.21 \pm 0.13 \pm 0.08$	$0.05 \pm 0.10 \pm 0.02$	$0.062 \pm 0.062 \pm 0.006$	0.075 ± 0.050
$\Delta\delta_0$	0.13 ± 0.09	$0.27 \pm 0.14 \pm 0.08$	$0.08 \pm 0.10 \pm 0.01$		0.13 ± 0.08
$\Delta\phi_S(K\pi)$ †	New			$0.062 \pm 0.062 \pm 0.022$	0.062 ± 0.066
$\Delta\phi_S(KK)$ †	New			$0.022 \pm 0.072 \pm 0.004$	0.022 ± 0.072

Angles (ϕ, δ) are in radians. BF, f_L and A_{CP} are tabulated separately. † Original LHCb notation adapted to match similar existing quantities.

Table 215: Results of the full angular analyses of $B^0 \to \phi K_2^{*0}(1430)$. Values in red (blue) are new published (preliminary) results since PDG2014.

Parameter	PDG2014 Avg.	*BABAR*	Belle	Our Avg.
$f_\perp = \Lambda_{\perp\perp}$	$0.027^{+0.031}_{-0.025}$	$0.002^{+0.018}_{-0.002} \pm 0.031$	$0.056^{+0.050}_{-0.035} \pm 0.009$	$0.027^{+0.027}_{-0.024}$
$\phi_\parallel$	4.0 ± 0.4	$3.96 \pm 0.38 \pm 0.06$	$3.76 \pm 2.88 \pm 1.32$	3.96 ± 0.38
$\phi_\perp$	4.5 ± 0.4		$4.45^{+0.43}_{-0.38} \pm 0.13$	$4.45^{+0.45}_{-0.40}$
δ_0	3.46 ± 0.14	$3.41 \pm 0.13 \pm 0.13$	$3.53 \pm 0.11 \pm 0.19$	3.46 ± 0.14
A^0_{CP}	-0.03 ± 0.04	$-0.05 \pm 0.06 \pm 0.01$	$-0.016^{+0.066}_{-0.051} \pm 0.008$	$-0.032^{+0.043}_{-0.038}$
$A^\perp_{CP}$	$0.0^{+0.9}_{-0.7}$		$-0.01^{+0.85}_{-0.67} \pm 0.09$	$-0.01^{+0.85}_{-0.68}$
$\Delta\phi_\parallel$	-0.9 ± 0.4	$-1.00 \pm 0.38 \pm 0.09$	$-0.02 \pm 1.08 \pm 1.01$	-0.94 ± 0.38
$\Delta\phi_\perp$	-0.2 ± 0.4		$-0.19 \pm 0.42 \pm 0.11$	-0.19 ± 0.43
$\Delta\delta_0$	0.08 ± 0.09	$0.11 \pm 0.13 \pm 0.06$	$0.06 \pm 0.11 \pm 0.02$	0.08 ± 0.09

Angles (ϕ, δ) are in radians. BF, f_L and A_{CP} are tabulated separately.

Table 216: Longitudinal polarization fraction f_L for B_s^0 decays. Values in red (blue) are new published (preliminary) results since PDG2014.

RPP#	Mode	PDG2014 Avg.	CDF	LHCb	Our Avg.
51	$\phi\phi$	0.361 ± 0.022	$0.348 \pm 0.041 \pm 0.021$	$0.365 \pm 0.022 \pm 0.012$	0.361 ± 0.022
59	$K^{*0}\overline{K}^{*0}$	0.31 ± 0.13		$0.201 \pm 0.057 \pm 0.040$	0.201 ± 0.070
60	$\phi\overline{K}^{*0}$	0.51 ± 0.17		$0.51 \pm 0.15 \pm 0.07$	0.51 ± 0.17

Table 217: Results of the full angular analyses of $B_s^0 \to \phi\phi$. Values in red (blue) are new published (preliminary) results since PDG2014.

Parameter	PDG2014 Avg.	CDF	LHCb	Our Avg.
$f_\perp = \Lambda_{\perp\perp}$	0.306 ± 0.030	$0.365 \pm 0.044 \pm 0.027$	$0.291 \pm 0.024 \pm 0.010$	0.306 ± 0.023
$\phi_\parallel$	2.59 ± 0.15	$2.71^{+0.31}_{-0.36} \pm 0.22$	$2.57 \pm 0.15 \pm 0.06$	2.59 ± 0.15

The parameter ϕ is in radians. BF, f_L and A_{CP} are tabulated separately.

Table 218: Results of the full angular analyses of $B_s^0 \to \phi\overline{K}^{*0}$. Values in red (blue) are new published (preliminary) results since PDG2014.

Parameter	PDG2014 Avg.	LHCb	Our Avg.
$f_\perp = \Lambda_{\perp\perp}$		$0.28 \pm 0.12 \pm 0.03$	0.28 ± 0.12
f_0		$0.51 \pm 0.15 \pm 0.07$	0.51 ± 0.17
$f_\parallel$	0.21 ± 0.11	$0.21 \pm 0.11 \pm 0.02$	0.21 ± 0.11
$\phi_\parallel$ †	$1.75 \pm 0.53 \pm 0.29$	$1.75^{+0.59+0.38}_{-0.53-0.30}$	$1.75^{+0.70}_{-0.61}$

The parameter ϕ is in radians. BF, f_L and A_{CP} are tabulated separately.
† Converted from the measurement of $\cos(\phi_\parallel)$. PDG takes the smallest resulting asymmetric error as parabolic.

Table 219: Results of the full angular analyses of $B_s^0 \to K^{*0}\overline{K}^{*0}$. Values in red (blue) are new published (preliminary) results since PDG2014.

Parameter	PDG2014 Avg.	LHCb	Our Avg.
f_L	$0.31 \pm 0.12 \pm 0.04$	$0.201 \pm 0.057 \pm 0.040$	0.201 ± 0.070
$f_\parallel$		$0.215 \pm 0.046 \pm 0.015$	0.215 ± 0.048
$\lvert A_s^+\rvert^2$		$0.114 \pm 0.037 \pm 0.023$	0.114 ± 0.044
$\lvert A_s^-\rvert^2$		$0.485 \pm 0.051 \pm 0.019$	0.485 ± 0.054
$\lvert A_{ss}\rvert^2$		$0.066 \pm 0.022 \pm 0.007$	0.066 ± 0.023
$\delta_\parallel$		$5.31 \pm 0.24 \pm 0.14$	5.31 ± 0.28
$\delta_\perp - \delta_s^+$		$1.95 \pm 0.21 \pm 0.04$	1.95 ± 0.21
δ_s^-		$1.79 \pm 0.19 \pm 0.19$	1.79 ± 0.27
δ_{ss}		$1.06 \pm 0.27 \pm 0.23$	1.06 ± 0.35

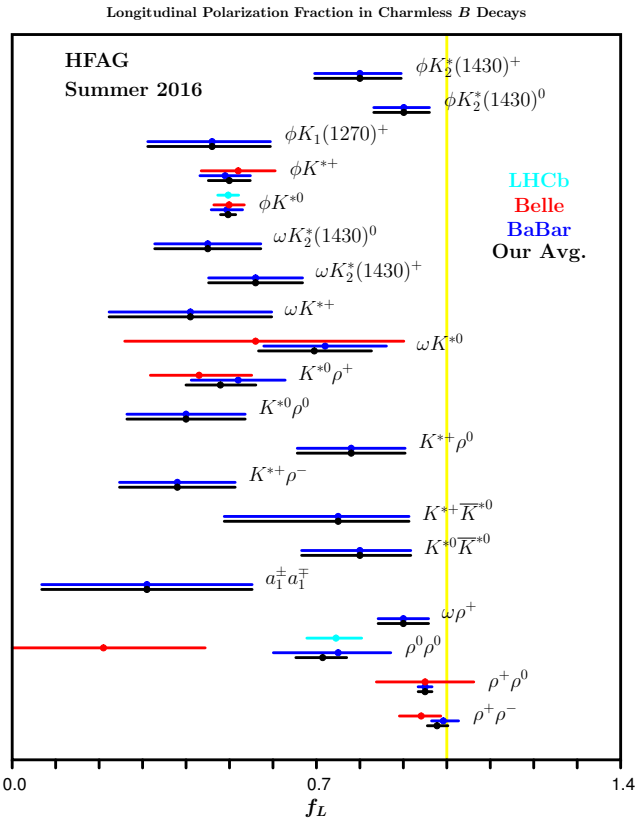

Figure 158: Longitudinal polarization fraction in charmless B decays

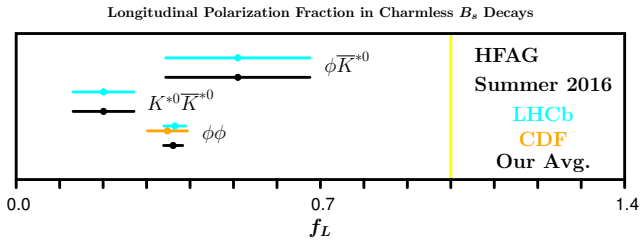

Figure 159: Longitudinal polarization fraction in charmless B_s decays

7.8 Decays of B_c^+ mesons

Table 220 detail branching fractions B_c^+ meson decays.

Table 220: Relative branching fractions (BF) of B_c^+ decays. Values in red (blue) are new published (preliminary) results since PDG2014.

RPP#	Mode	PDG2014 AVG.	CDF	LHCb	Our Avg.
	$f_c\mathcal{B}(B_c^+ \to K^+K^0)/f_u\mathcal{B}(B^+ \to K_S^0\pi^+)$	*		$< 5.8 \times 10^{-2}$	$< 5.8 \times 10^{-2}$
	$f_c\mathcal{B}(B_c^+ \to p\overline{p}\pi^+)/f_u$			$< 2.8 \times 10^{-8}$	$< 2.8 \times 10^{-8}$
	$\sigma(B_c^+)\mathcal{B}(B_c^+ \to K^+K^-\pi^+)/\sigma(B^+)^\dagger$			$< 15 \times 10^{-8}$	$< 15 \times 10^{-8}$

* PDG converts the LHCb result to $f_c\mathcal{B}(B_c^+ \to K^+K^0) < 4.6 \times 10^{-7}$;
† measured in the annililation region m$(K^-\pi^+) < 1.834$GeV$/c^2$

8 Charm physics

8.1 D^0-$\overline{D}^0$ mixing and CP violation

8.1.1 Introduction

In 2007 Belle [824] and *BABAR* [825] obtained the first evidence of D^0-$\overline{D}^0$ mixing, for which experiments had searched for more than two decades. These results were later confirmed by CDF [826] and more recently by LHCb [827]. There are now numerous measurements of D^0-$\overline{D}^0$ mixing with various levels of sensitivity. All measurements are input into a global fit to determine world average values of mixing parameters, CP-violation (CPV) parameters, and strong phases.

Our notation is as follows. The mass eigenstates are denoted $D_1 = p|D^0\rangle - q|\overline{D}^0\rangle$ and $D_2 = p|D^0\rangle + q|\overline{D}^0\rangle$, where we use the convention [828] $CP|D^0\rangle = -|\overline{D}^0\rangle$ and $CP|\overline{D}^0\rangle = -|D^0\rangle$. Thus in the absence of CP violation, D_1 is CP-even and D_2 is CP-odd. The weak phase ϕ is defined as $\mathrm{Arg}(q/p)$. The mixing parameters are defined as $x \equiv (m_1 - m_2)/\Gamma$ and $y \equiv (\Gamma_1 - \Gamma_2)/(2\Gamma)$, where m_1, m_2 and Γ_1, Γ_2 are the masses and decay widths for the mass eigenstates, and $\Gamma \equiv (\Gamma_1 + \Gamma_2)/2$.

The global fit determines central values and errors for ten underlying parameters. These consist of the mixing parameters x and y; indirect CPV parameters $|q/p|$ and ϕ; the ratio of decay rates $R_D \equiv [\Gamma(D^0 \to K^+\pi^-) + \Gamma(\overline{D}^0 \to K^-\pi^+)]/[\Gamma(D^0 \to K^-\pi^+) + \Gamma(\overline{D}^0 \to K^+\pi^-)]$; direct CPV parameters A_D, A_K, and A_π, as defined in Table 224; the strong phase difference δ between $\overline{D}^0 \to K^-\pi^+$ and $D^0 \to K^-\pi^+$ amplitudes; and the strong phase difference $\delta_{K\pi\pi}$ between $\overline{D}^0 \to K^-\rho^+$ and $D^0 \to K^-\rho^+$ amplitudes.

The fit uses 49 observables from measurements of $D^0 \to K^+\ell^-\nu$, $D^0 \to K^+K^-$, $D^0 \to \pi^+\pi^-$, $D^0 \to K^+\pi^-$, $D^0 \to K^+\pi^-\pi^0$, $D^0 \to K^0_S\pi^+\pi^-$, $D^0 \to \pi^0\pi^+\pi^-$, $D^0 \to K^0_S K^+K^-$, and $D^0 \to K^+\pi^-\pi^+\pi^-$ decays[48], and from double-tagged branching fractions measured at the $\psi(3770)$ resonance. Correlations among observables are accounted for by using covariance matrices provided by the experimental collaborations. Errors are assumed to be Gaussian, and systematic errors among different experiments are assumed to be uncorrelated unless specific correlations have been identified. We have checked this method with a second method that adds together three-dimensional log-likelihood functions for x, y, and δ obtained from several analyses; this combination accounts for non-Gaussian errors. When both methods are applied to the same set of measurements, equivalent results are obtained.

Mixing in heavy flavor systems such as those of B^0 and B^0_s is governed by a short-distance box diagram. In the D^0 system, however, this diagram is doubly-Cabibbo-suppressed relative to amplitudes dominating the decay width, and it is also GIM-suppressed. Thus the short-distance mixing rate is extremely small, and D^0-$\overline{D}^0$ mixing is expected to be dominated by long-distance processes. These are difficult to calculate, and theoretical estimates for x and y range over three orders of magnitude [829–832].

Almost all methods besides that of the $\psi(3770) \to \overline{D}D$ measurements [833] identify the flavor of the D^0 or $\overline{D}^0$ when produced by reconstructing the decay $D^{*+} \to D^0\pi^+$ or $D^{*-} \to \overline{D}^0\pi^-$. The charge of the pion, which has low momentum and is usually referred to as the "soft" pion, identifies the D flavor. For this decay $M_{D^*} - M_{D^0} - M_{\pi^+} \equiv Q \approx 6$ MeV, which is close to the threshold; thus analyses typically require that the reconstructed Q be small to suppress

[48] Charge-conjugate modes are implicitly included.

backgrounds. An LHCb measurement [834] of the difference between time-integrated CP asymmetries $A_{CP}(K^+K^-) - A_{CP}(\pi^+\pi^-)$ identifies the flavor of the D^0 by partially reconstructing $B \to D^0\mu^- X$ decays (and charge-conjugates); in this case the charge of the muon originating from the B decay identifies the flavor of the D^0.

For time-dependent measurements, the D^0 decay time is calculated as $(\vec{\mathbf{d}}\cdot\vec{\mathbf{p}})/p^2 \times M_{D^0}$, where $\vec{\mathbf{d}}$ is the displacement vector between the D^* and D^0 decay vertices, and $\vec{\mathbf{p}}$ is the reconstructed D^0 momentum. The D^* vertex position is taken to be the intersection of the D^0 momentum vector with the beamspot profile for e^+e^- experiments, and at the primary interaction vertex for $\overline{p}p$ and pp experiments [826, 827].

8.1.2 Input observables

The global fit determines central values and errors for ten underlying parameters using a χ^2 statistic. The fitted parameters are x, y, R_D, A_D, $|q/p|$, ϕ, δ, $\delta_{K\pi\pi}$, A_K and A_π. In the $D \to K^+\pi^-\pi^0$ Dalitz plot analysis [835] that provides sensitivity to x and y, the $\overline{D}{}^0 \to K^+\pi^-\pi^0$ isobar phases are determined relative to that for $\mathcal{A}(\overline{D}{}^0 \to K^+\rho^-)$, and the $D^0 \to K^+\pi^-\pi^0$ isobar phases are determined relative to that for $\mathcal{A}(D^0 \to K^+\rho^-)$. As the $\overline{D}{}^0$ and D^0 Dalitz plots are fitted independently, the phase difference $\delta_{K\pi\pi}$ between the two "normalizing amplitudes" cannot be determined from those fits. However, we can determine the phase difference in our global fit and include it as a fitted parameter.

All input measurements are listed in Tables 221-223. The observable $R_M = (x^2 + y^2)/2$ is measured in $D^0 \to K^+\ell^-\nu$ and $D^0 \to K^+\pi^-\pi^+\pi^-$ decays. For the former, we use in our global fit the world average value as calculated by HFAG [836]. The inputs used for this average [837–840] are plotted in Fig. 160. The observables $y_{CP} = (1/2)(|q/p| + |p/q|)y\cos\phi - (1/2)(|q/p| - |p/q|)x\sin\phi$ and $A_\Gamma = (1/2)(|q/p| - |p/q|)y\cos\phi - (1/2)(|q/p| + |p/q|)x\sin\phi$ are also HFAG world average values [836]; the inputs used for these averages are plotted in Figs. 161 and 162, respectively. The $D^0 \to K^+\pi^-$ measurements used are from Belle [841, 842], *BABAR* [825], CDF [843], and a recent result from LHCb [844]; earlier measurements have much less precision and are not used. The observables from $D^0 \to K^0_S\,\pi^+\pi^-$ decays are measured in two ways: assuming CP conservation (D^0 and $\overline{D}{}^0$ decays combined), and allowing for CP violation (D^0 and $\overline{D}{}^0$ decays fitted separately). The no-CPV measurements are from Belle [845], *BABAR* [846], and LHCb [847], but for the CPV-allowed case only Belle measurements [845] are available. The $D^0 \to K^+\pi^-\pi^0$ and $D^0 \to \pi^0\,\pi^+\pi^-$ results are from *BABAR* [835, 848], the $D^0 \to K^+\pi^-\pi^+\pi^-$ results are from LHCb [849], and the $\psi(3770) \to \overline{D}D$ results are from CLEOc [833].

The relationships between the observables and the fitted parameters are listed in Table 224. For each set of correlated observables we construct a difference vector $\vec{V}$ between measured values and those calculated from fitted parameters using these relations; *e.g.*, for $D^0 \to K^0_S\,\pi^+\pi^-$ decays, $\vec{V} = (\Delta x, \Delta y, \Delta|q/p|, \Delta\phi)$. The contribution of a set of observables to the fit χ^2 is calculated as $\vec{V}\cdot(M^{-1})\cdot\vec{V}^T$, where M^{-1} is the inverse of the covariance matrix for the measurement. Covariance matrices are constructed from the correlation coefficients among the measured observables. These correlation coefficients are also listed in Tables 221-223.

8.1.3 Fit results

The global fit uses MINUIT with the MIGRAD minimizer, and all errors are obtained from MINOS [866]. Four separate fits are performed: (*a*) assuming CP conservation, *i.e.*, fixing $A_D = 0$,

Table 221: Observables used in the global fit except those from $D^0 \to K^+\pi^-$ and those used for measuring direct CPV. The $D^0 \to K^+\pi^-\pi^0$ observables are $x'' \equiv x\cos\delta_{K\pi\pi} + y\sin\delta_{K\pi\pi}$ and $y'' \equiv -x\sin\delta_{K\pi\pi} + y\cos\delta_{K\pi\pi}$.

Mode	**Observable**	**Values**	**Correlation coefficients**
$D^0 \to K^+K^-/\pi^+\pi^-$,	y_{CP}	$(0.866 \pm 0.155)\%$	
$\phi\, K^0_S$ [836]	A_Γ	$(-0.014 \pm 0.052)\%$	
$D^0 \to K^0_S\,\pi^+\pi^-$ [845]	x	$(0.56 \pm 0.19\,^{+0.067}_{-0.127})\%$	$+0.012$
(Belle: no CPV)	y	$(0.30 \pm 0.15\,^{+0.050}_{-0.078})\%$	
$D^0 \to K^0_S\,\pi^+\pi^-$ [845]	$\lvert q/p\rvert$	$0.90\,^{+0.16+0.078}_{-0.15-0.064}$	
(Belle: no direct CPV)	ϕ	$(-6 \pm 11\,^{+4.2}_{-5.0})$ degrees	
$D^0 \to K^0_S\,\pi^+\pi^-$ [845]	x	$(0.58 \pm 0.19^{+0.0734}_{-0.1177})\%$	$\begin{pmatrix} 1 & 0.054 & -0.074 & -0.031 \\ 0.054 & 1 & 0.034 & -0.019 \\ -0.074 & 0.034 & 1 & 0.044 \\ -0.031 & -0.019 & 0.044 & 1 \end{pmatrix}$
	y	$(0.27 \pm 0.16^{+0.0546}_{-0.0854})\%$	
(Belle: direct CPV allowed)	$\lvert q/p\rvert$	$0.82\,^{+0.20+0.0807}_{-0.18-0.0645}$	
	ϕ	$(-13\,^{+12\,+4.15}_{-13\,-4.77})$ degrees	
$D^0 \to K^0_S\,\pi^+\pi^-$ [847]	x	$(-0.86\ \pm 0.53\ \pm 0.17)\%$	$+0.37$
(LHCb: no CPV)	y	$(0.03\ \pm 0.46\ \pm 0.13)\%$	
$D^0 \to K^0_S\,\pi^+\pi^-$ [846]			
$K^0_S\,K^+K^-$	x	$(0.16 \pm 0.23 \pm 0.12 \pm 0.08)\%$	0.0615
(*BABAR*: no CPV)	y	$(0.57 \pm 0.20 \pm 0.13 \pm 0.07)\%$	
$D^0 \to \pi^0\,\pi^+\pi^-$ [848]	x	$(1.5 \pm 1.2 \pm 0.6)\%$	-0.006
(*BABAR*: no CPV)	y	$(0.2 \pm 0.9 \pm 0.5)\%$	
$D^0 \to K^+\ell^-\nu$ [836]	$R_M = (x^2+y^2)/2$	$(0.0130 \pm 0.0269)\%$	
$D^0 \to K^+\pi^-\pi^0$ [835]	x''	$(2.61\,^{+0.57}_{-0.68}\ \pm 0.39)\%$	-0.75
	y''	$(-0.06\,^{+0.55}_{-0.64}\ \pm 0.34)\%$	
$D^0 \to K^+\pi^-\pi^+\pi^-$ [849]	$R_M/2$	$(4.8 \pm 1.8) \times 10^{-5}$	
$\psi(3770) \to \overline{D}D$ [833]	R_D	$(0.533 \pm 0.107 \pm 0.045)\%$	$\begin{pmatrix} 1 & 0 & 0 & -0.42 & 0.01 \\ & 1 & -0.73 & 0.39 & 0.02 \\ & & 1 & -0.53 & -0.03 \\ & & & 1 & 0.04 \\ & & & & 1 \end{pmatrix}$
	x^2	$(0.06 \pm 0.23 \pm 0.11)\%$	
(CLEOc)	y	$(4.2 \pm 2.0 \pm 1.0)\%$	
	$\cos\delta$	$0.81\,^{+0.22\,+0.07}_{-0.18\,-0.05}$	
	$\sin\delta$	$-0.01 \pm 0.41 \pm 0.04$	

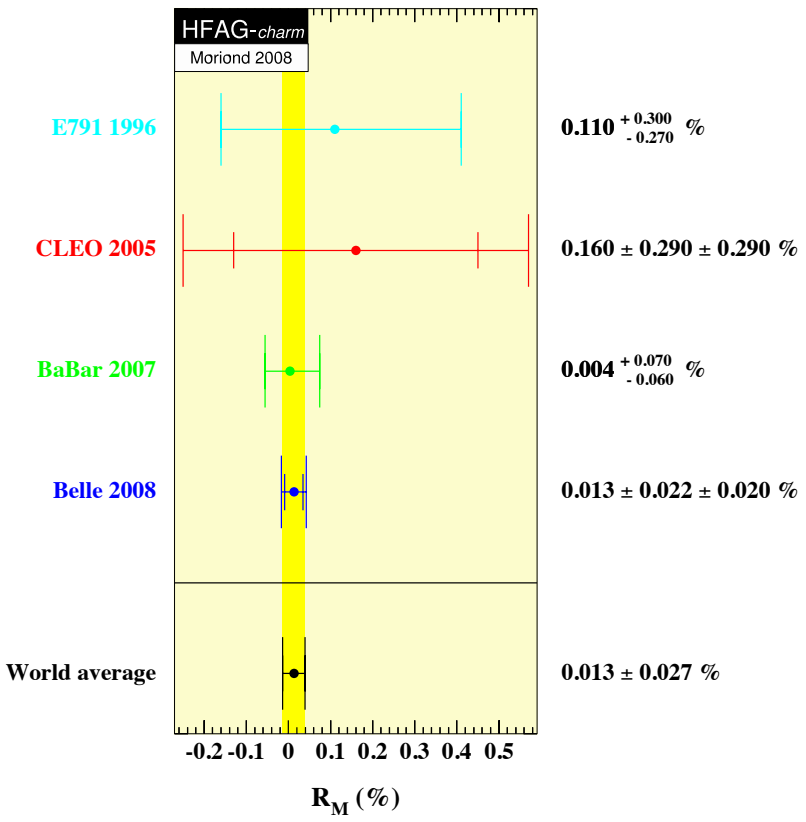

Figure 160: World average value of $R_M = (x^2 + y^2)/2$ from Ref. [836], as calculated from $D^0 \to K^+\ell^-\nu$ measurements [837–840].

$A_K = 0$, $A_\pi = 0$, $\phi = 0$, and $|q/p| = 1$; (*b*) assuming no direct CPV in doubly Cabibbo-suppressed (DCS) decays ($A_D = 0$) and fitting for parameters $(x, y, |q/p|)$ or (x, y, ϕ); (*c*) assuming no direct CPV in DCS decays and fitting for alternative parameters $x_{12} = 2|M_{12}|/\Gamma$, $y_{12} = \Gamma_{12}/\Gamma$, and $\phi_{12} = \mathrm{Arg}(M_{12}/\Gamma_{12})$, where M_{12} and Γ_{12} are the off-diagonal elements of the D^0-$\overline{D}{}^0$ mass and decay matrices, respectively; and (*d*) allowing full CPV (floating all parameters).

For the fits assuming no-direct-CPV in DCS decays, in addition to $A_D = 0$ we impose other constraints that reduce four independent parameters to three[49]. For fit *(b)* we impose the relation [868,869] $\tan\phi = (1-|q/p|^2)/(1+|q/p|^2) \times (x/y)$ in two ways: first we float parameters x, y, and ϕ and from these derive $|q/p|$; we then repeat the fit floating x, y, and $|q/p|$ and from these derive ϕ. The central values returned by the two fits are identical, but the first fit yields MINOS errors for ϕ, while the second fit yields MINOS errors for $|q/p|$. For no-direct-CPV fit *(c)*, we fit for underlying parameters x_{12}, y_{12}, and ϕ_{12}, and from these calculate x, y, $|q/p|$, and ϕ to which measured observables are compared. All fit results are listed in Table 225. For the CPV-allowed fit, individual contributions to the χ^2 are listed in Table 226. The total χ^2 is 76.8 for $49 - 10 = 39$ degrees of freedom.

Confidence contours in the two dimensions (x, y) or $(|q/p|, \phi)$ are obtained by allowing, for any point in the two-dimensional plane, all other fitted parameters to take their preferred values. The resulting 1σ-5σ contours are shown in Fig. 163 for the CP-conserving case, in Fig. 164 for the no-direct-CPV case, and in Fig. 165 for the CPV-allowed case. The contours

[49] One can also use Eq. (15) of Ref. [867] to reduce four parameters to three.

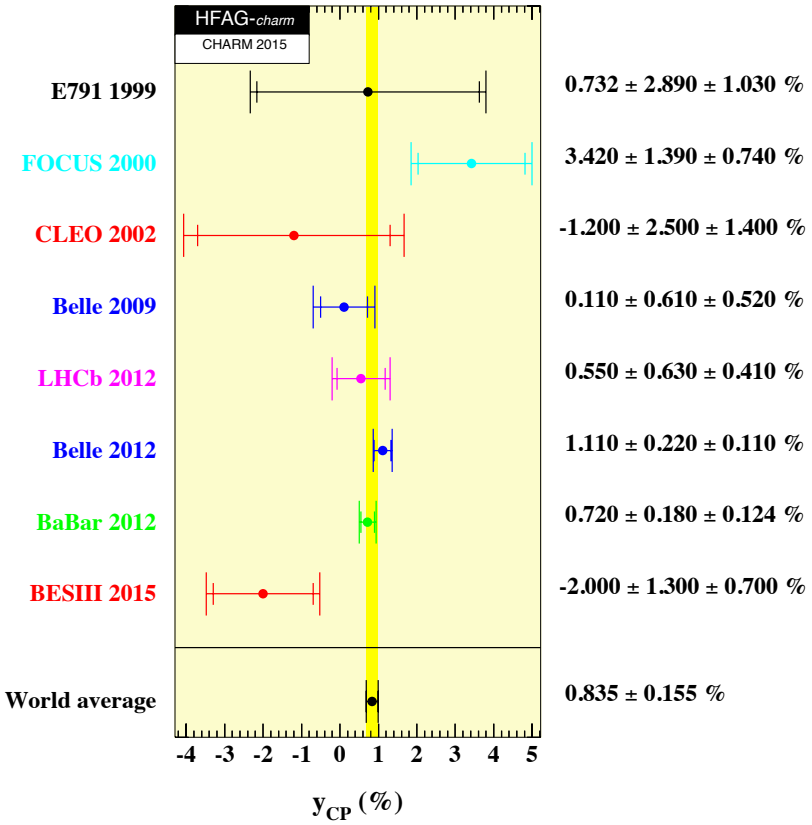

Figure 161: World average value of y_{CP} from Ref. [836], as calculated from $D^0 \to K^+K^-/\pi^+\pi^-$ measurements [855–862].

are determined from the increase of the χ^2 above the minimum value. One observes that the (x, y) contours for the no-CPV fit are very similar to those for the CPV-allowed fit. In the latter fit, the χ^2 at the no-mixing point $(x, y) = (0, 0)$ is 450 units above the minimum value, which, for two degrees of freedom, corresponds to a confidence level[50] (C.L.) $> 11.5\sigma$. Thus, no mixing is excluded at this high level. In the $(|q/p|, \phi)$ plot, the point $(1, 0)$ is within the 1σ contour; thus the data is consistent with CP conservation.

One-dimensional likelihood curves for individual parameters are obtained by allowing, for a fixed value of a selected parameter, all other fitted parameters to take their preferred values. The resulting functions $\Delta\chi^2 = \chi^2 - \chi^2_{\rm min}$ ($\chi^2_{\rm min}$ is the minimum value) are shown in Fig. 166. The points where $\Delta\chi^2 = 3.84$ determine 95% C.L. intervals for the parameters. These intervals are listed in Table 225.

8.1.4 Conclusions

From the fit results listed in Table 225 and shown in Figs. 165 and 166, we conclude that:

- the experimental data consistently indicate that D^0 mesons mix. The no-mixing point $x = y = 0$ is excluded at $> 11.5\sigma$. The parameter x differs from zero by 1.9σ, and y differs

[50] This is the limit of the CERNLIB PROB routine used for this calculation.

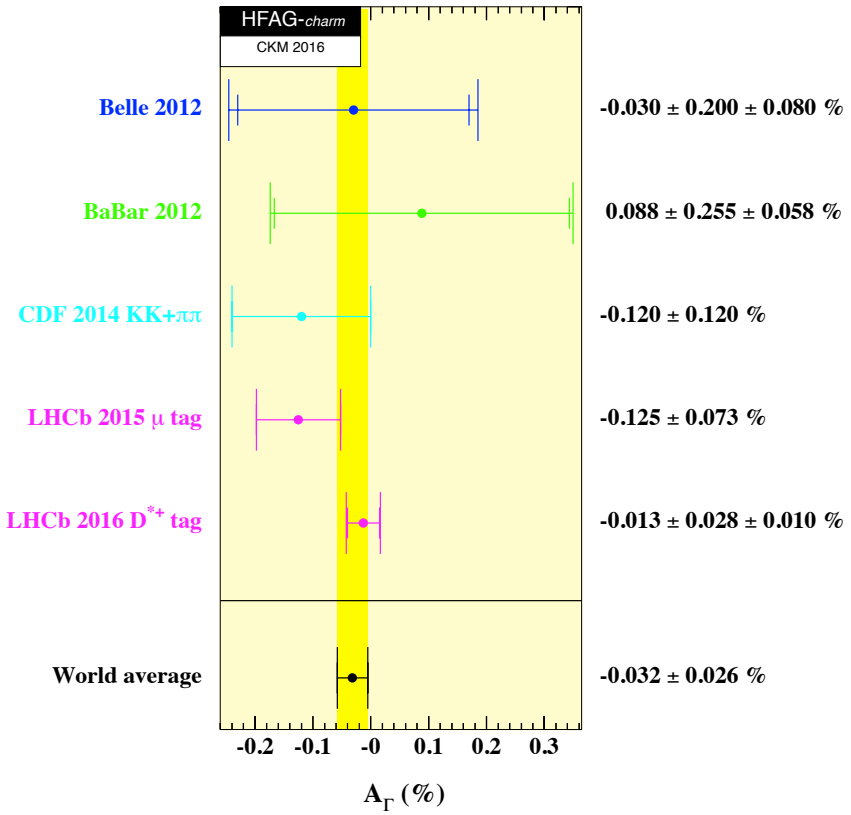

Figure 162: World average value of A_Γ from Ref. [836], as calculated from $D^0 \to K^+K^-$ and $D^0 \to \pi^+\pi^-$ measurements [860, 861, 863–865].

from zero by 9.4σ. This mixing is presumably dominated by long-distance processes, which are difficult to calculate. Thus unless it turns out that $|x| \gg |y|$ [829] (which is not indicated), it will be difficult to identify new physics from (x, y) alone.

- Since $y_{\rm CP}$ is positive, the CP-even state is shorter-lived as in the K^0-$\overline{K}{}^0$ system. However, since x also appears to be positive, the CP-even state is heavier, unlike in the K^0-$\overline{K}{}^0$ system.

- There is no evidence for CPV arising from D^0-$\overline{D}{}^0$ mixing ($|q/p| \neq 1$) or from a phase difference between the mixing amplitude and a direct decay amplitude ($\phi \neq 0$). The CDF experiment (and initially LHCb) measured a time-integrated asymmetry in $D^0 \to K^+K^-, \pi^+\pi^-$ decays that hints at direct CPV (see Table 223); however, recent measurements from LHCb with higher statistics disfavor this result and are consistent with zero.

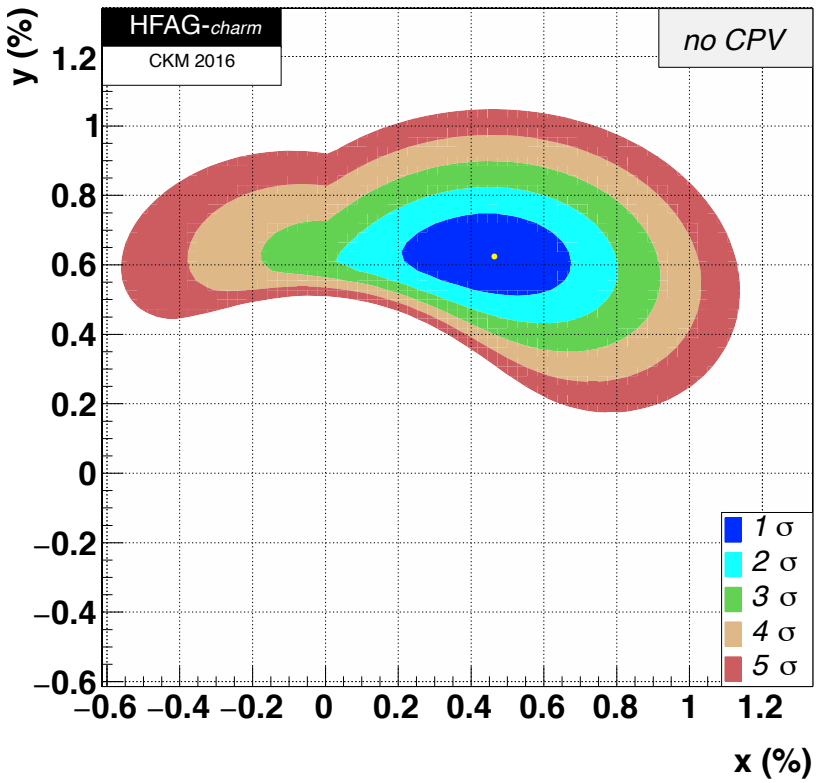

Figure 163: Two-dimensional contours for mixing parameters (x, y), for no CPV.

Table 222: $D^0 \to K^+\pi^-$ observables used for the global fit.

Mode	Observable	Values	Correlation coefficients
$D^0 \to K^+\pi^-$ [825] (*BABAR* 384 fb^{-1})	R_D	$(0.303 \pm 0.0189)\%$	$\begin{pmatrix} 1 & 0.77 & -0.87 \\ 0.77 & 1 & -0.94 \\ -0.87 & -0.94 & 1 \end{pmatrix}$
	x'^{2+}	$(-0.024 \pm 0.052)\%$	
	y'^{+}	$(0.98 \pm 0.78)\%$	
$\overline{D}{}^0 \to K^-\pi^+$ [825] (*BABAR* 384 fb^{-1})	A_D	$(-2.1 \pm 5.4)\%$	same as above
	x'^{2-}	$(-0.020 \pm 0.050)\%$	
	y'^{-}	$(0.96 \pm 0.75)\%$	
$D^0 \to K^+\pi^-$ [842] (Belle 976 fb^{-1} No CPV)	R_D	$(0.353 \pm 0.013)\%$	$\begin{pmatrix} 1 & 0.737 & -0.865 \\ 0.737 & 1 & -0.948 \\ -0.865 & -0.948 & 1 \end{pmatrix}$
	x'^{2}	$(0.009 \pm 0.022)\%$	
	y'	$(0.46 \pm 0.34)\%$	
$D^0 \to K^+\pi^-$ [841] (Belle 400 fb^{-1} CPV-allowed)	R_D	$(0.364 \pm 0.018)\%$	$\begin{pmatrix} 1 & 0.655 & -0.834 \\ 0.655 & 1 & -0.909 \\ -0.834 & -0.909 & 1 \end{pmatrix}$
	x'^{2+}	$(0.032 \pm 0.037)\%$	
	y'^{+}	$(-0.12 \pm 0.58)\%$	
$\overline{D}{}^0 \to K^-\pi^+$ [841] (Belle 400 fb^{-1} CPV-allowed)	A_D	$(2.3 \pm 4.7)\%$	same as above
	x'^{2-}	$(0.006 \pm 0.034)\%$	
	y'^{-}	$(0.20 \pm 0.54)\%$	
$D^0 \to K^+\pi^-$ [843] (CDF 9.6 fb^{-1} No CPV)	R_D	$(0.351 \pm 0.035)\%$	$\begin{pmatrix} 1 & 0.90 & -0.97 \\ 0.90 & 1 & -0.98 \\ -0.97 & -0.98 & 1 \end{pmatrix}$
	x'^{2}	$(0.008 \pm 0.018)\%$	
	y'	$(0.43 \pm 0.43)\%$	
$D^0 \to K^+\pi^-$ [844] (LHCb 3.0 fb^{-1} CPV-allowed)	R_D^+	$(0.3474 \pm 0.0081)\%$	$\begin{pmatrix} 1 & 0.823 & -0.920 \\ 0.823 & 1 & -0.962 \\ -0.920 & -0.962 & 1 \end{pmatrix}$
	x'^{2+}	$(0.0011 \pm 0.0065)\%$	
	y'^{+}	$(0.597 \pm 0.125)\%$	
$\overline{D}{}^0 \to K^-\pi^+$ [844] (LHCb 3.0 fb^{-1} CPV-allowed)	R_D^-	$(0.3591 \pm 0.0081)\%$	$\begin{pmatrix} 1 & 0.812 & -0.918 \\ 0.812 & 1 & -0.956 \\ -0.918 & -0.956 & 1 \end{pmatrix}$
	x'^{2-}	$(0.0061 \pm 0.0061)\%$	
	y'^{-}	$(0.450 \pm 0.121)\%$	

Table 223: Measurements of time-integrated CP asymmetries. The observable $A_{CP}(f) \equiv [\Gamma(D^0 \to f) - \Gamma(\overline{D}{}^0 \to f)]/[\Gamma(D^0 \to f) + \Gamma(\overline{D}{}^0 \to f)]$, and $\Delta\langle t\rangle$ is the difference between mean lifetimes for $D^0 \to K^+K^-$ and $D^0 \to \pi^+\pi^-$ decays (due to different trigger/reconstruction efficiencies).

Mode	**Observable**	**Values**	$\boldsymbol{\Delta\langle t\rangle/\tau_D}$
$D^0 \to h^+h^-$ [850]	$A_{CP}(K^+K^-)$	$(0.00 \pm 0.34 \pm 0.13)\%$	0
(*BABAR* 386 fb^{-1})	$A_{CP}(\pi^+\pi^-)$	$(-0.24 \pm 0.52 \pm 0.22)\%$	
$D^0 \to h^+h^-$ [851]	$A_{CP}(K^+K^-)$	$(-0.32 \pm 0.21 \pm 0.09)\%$	0
(Belle 976 fb^{-1})	$A_{CP}(\pi^+\pi^-)$	$(0.55 \pm 0.36 \pm 0.09)\%$	
$D^0 \to h^+h^-$ [852, 853]	$A_{CP}(K^+K^-) - A_{CP}(\pi^+\pi^-)$	$(-0.62 \pm 0.21 \pm 0.10)\%$	
(CDF 9.7 fb^{-1})	$A_{CP}(K^+K^-)$	$(-0.32 \pm 0.21)\%$	0.27 ± 0.01
	$A_{CP}(\pi^+\pi^-)$	$(0.31 \pm 0.22)\%$	
$D^0 \to h^+h^-$ [854] (LHCb 3.0 fb^{-1}, $D^{*+} \to D^0\pi^+$ tag)	$A_{CP}(K^+K^-) - A_{CP}(\pi^+\pi^-)$	$(-0.10 \pm 0.08 \pm 0.03)\%$	$0.1153 \pm 0.0007 \pm 0.0018$
$D^0 \to h^+h^-$ [834] (LHCb 3 fb^{-1}, $B \to D^0\mu^-X$ tag)	$A_{CP}(K^+K^-) - A_{CP}(\pi^+\pi^-)$	$(0.14 \pm 0.16 \pm 0.08)\%$	0.014 ± 0.004

Table 224: Left: decay modes used to determine fitted parameters x, y, δ, $\delta_{K\pi\pi}$, R_D, A_D, $|q/p|$, and ϕ. Middle: the observables measured for each decay mode. Right: the relationships between the observables measured and the fitted parameters. $\langle t \rangle$ is the mean lifetime for $D^0 \to K^+K^-$ or $D^0 \to \pi^+\pi^-$ decays.

Decay Mode	**Observables**	**Relationship**
$D^0 \to K^+K^-/\pi^+\pi^-$	y_{CP} A_Γ	$2y_{CP} = (\lvert q/p\rvert + \lvert p/q\rvert)\, y\cos\phi -$ $(\lvert q/p\rvert - \lvert p/q\rvert)\, x\sin\phi$ $2A_\Gamma = (\lvert q/p\rvert - \lvert p/q\rvert)\, y\cos\phi -$ $(\lvert q/p\rvert + \lvert p/q\rvert)\, x\sin\phi$
$D^0 \to K^0_S\,\pi^+\pi^-$	x y $\lvert q/p\rvert$ ϕ	
$D^0 \to K^+\ell^-\nu$	R_M	$R_M = (x^2+y^2)/2$
$D^0 \to K^+\pi^-\pi^0$ (Dalitz plot analysis)	x'' y''	$x'' = x\cos\delta_{K\pi\pi} + y\sin\delta_{K\pi\pi}$ $y'' = y\cos\delta_{K\pi\pi} - x\sin\delta_{K\pi\pi}$
"Double-tagged" branching fractions measured in $\psi(3770) \to DD$ decays	R_M y R_D $\sqrt{R_D}\cos\delta$	$R_M = (x^2+y^2)/2$
$D^0 \to K^+\pi^-$	$x'^2,\ y'$ $x'^{2+},\ x'^{2-}$ $y'^{+},\ y'^{-}$	$x' = x\cos\delta + y\sin\delta$ $y' = y\cos\delta - x\sin\delta$ $A_M \equiv (\lvert q/p\rvert^4 - 1)/(\lvert q/p\rvert^4 + 1)$ $x'^{\pm} = [(1 \pm A_M)/(1 \mp A_M)]^{1/4} \times$ $(x'\cos\phi \pm y'\sin\phi)$ $y'^{\pm} = [(1 \pm A_M)/(1 \mp A_M)]^{1/4} \times$ $(y'\cos\phi \mp x'\sin\phi)$
$D^0 \to K^+\pi^-/K^-\pi^+$ (time-integrated)	$\dfrac{\Gamma(D^0\to K^+\pi^-) + \Gamma(\overline{D}{}^0\to K^-\pi^+)}{\Gamma(D^0\to K^-\pi^+) + \Gamma(\overline{D}{}^0\to K^+\pi^-)}$ $\dfrac{\Gamma(D^0\to K^+\pi^-) - \Gamma(\overline{D}{}^0\to K^-\pi^+)}{\Gamma(D^0\to K^+\pi^-) + \Gamma(\overline{D}{}^0\to K^-\pi^+)}$	R_D A_D
$D^0 \to K^+K^-/\pi^+\pi^-$ (time-integrated)	$\dfrac{\Gamma(D^0\to K^+K^-) - \Gamma(\overline{D}{}^0\to K^+K^-)}{\Gamma(D^0\to K^+K^-) + \Gamma(\overline{D}{}^0\to K^+K^-)}$ $\dfrac{\Gamma(D^0\to \pi^+\pi^-) - \Gamma(\overline{D}{}^0\to \pi^+\pi^-)}{\Gamma(D^0\to \pi^+\pi^-) + \Gamma(\overline{D}{}^0\to \pi^+\pi^-)}$	$A_K + \frac{\langle t\rangle}{\tau_D}\,\mathcal{A}_{CP}^{\rm indirect} \quad (\mathcal{A}_{CP}^{\rm indirect} \approx -A_\Gamma)$ $A_\pi + \frac{\langle t\rangle}{\tau_D}\,\mathcal{A}_{CP}^{\rm indirect} \quad (\mathcal{A}_{CP}^{\rm indirect} \approx -A_\Gamma)$

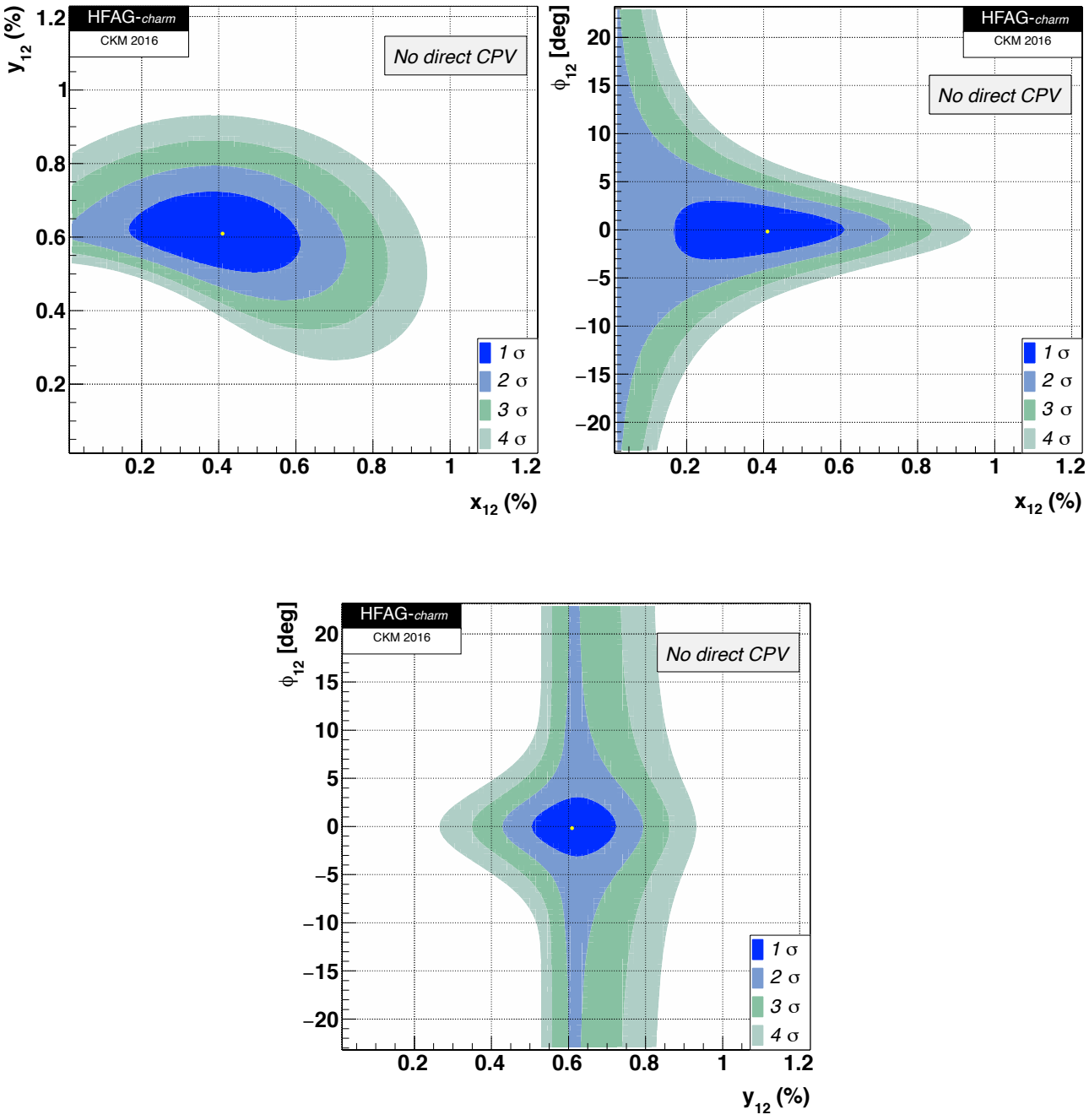

Figure 164: Two-dimensional contours for theoretical parameters (x_{12}, y_{12}) (top left), (x_{12}, ϕ_{12}) (top right), and (y_{12}, ϕ_{12}) (bottom), for no direct CPV.

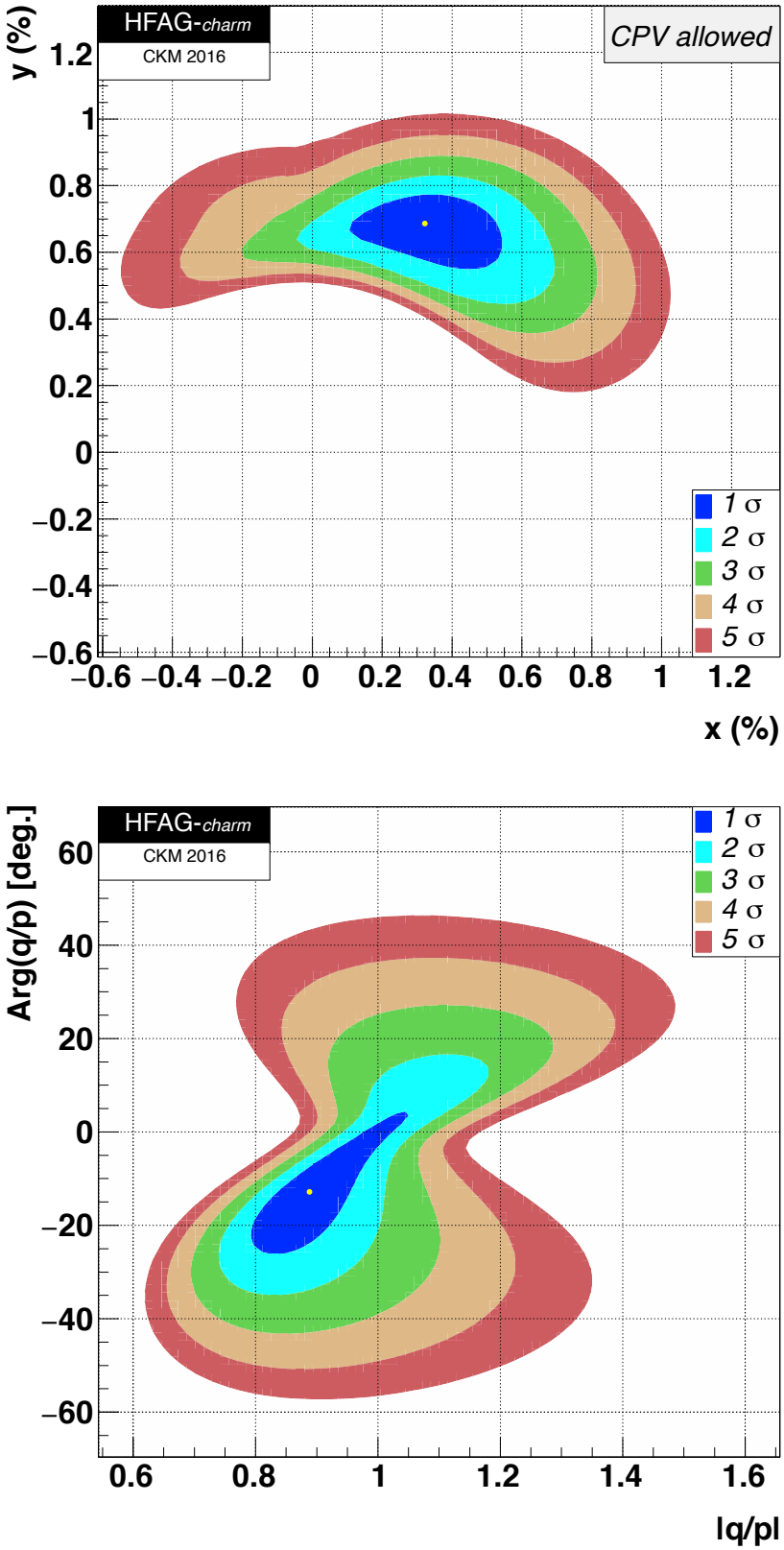

Figure 165: Two-dimensional contours for parameters (x, y) (top) and $(|q/p|, \phi)$ (bottom), allowing for CPV.

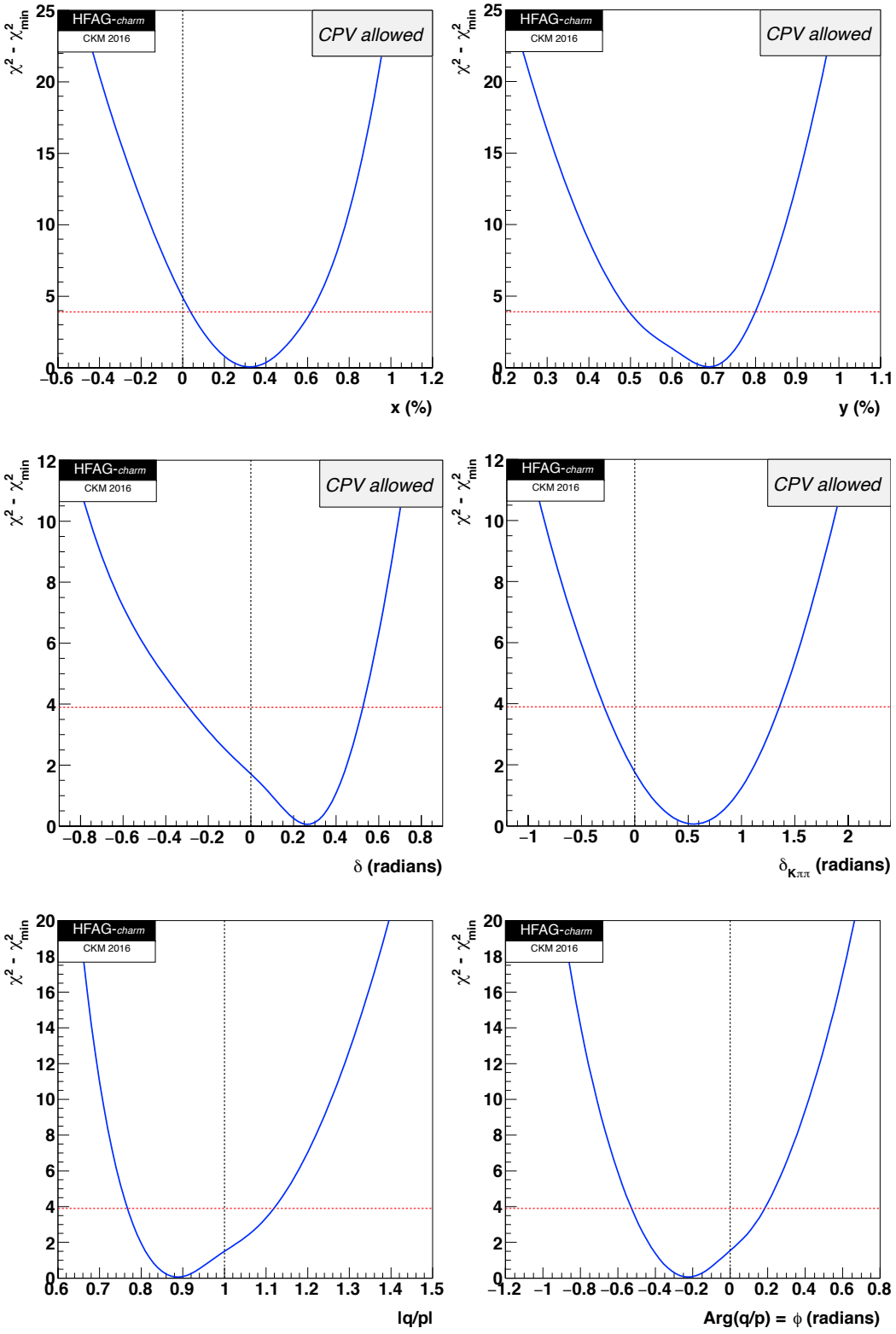

Figure 166: The function $\Delta\chi^2 = \chi^2 - \chi^2_{\rm min}$ for fitted parameters x, y, δ, $\delta_{K\pi\pi}$, $|q/p|$, and ϕ. The points where $\Delta\chi^2 = 3.84$ (denoted by dashed horizontal lines) determine 95% C.L. intervals.

Table 225: Results of the global fit for different assumptions concerning CPV.

Parameter	**No CPV**	**No direct CPV in DCS decays**	**CPV-allowed**	**CPV-allowed 95% C.L. Interval**
x (%)	$0.46^{+0.14}_{-0.15}$	$0.41^{+0.14}_{-0.15}$	0.32 ± 0.14	[0.04, 0.62]
y (%)	0.62 ± 0.08	0.61 ± 0.07	$0.69^{+0.06}_{-0.07}$	[0.50, 0.80]
$\delta_{K\pi}$ (°)	$8.0^{+9.7}_{-11.2}$	$4.8^{+10.4}_{-12.3}$	$15.2^{+7.6}_{-10.0}$	[−16.8, 30.1]
R_D (%)	$0.348^{+0.004}_{-0.003}$	$0.347^{+0.004}_{-0.003}$	$0.349^{+0.004}_{-0.003}$	[0.342, 0.356]
A_D (%)	–	–	-0.88 ± 0.99	[−2.8, 1.0]
$\lvert q/p \rvert$	–	0.999 ± 0.014	$0.89^{+0.08}_{-0.07}$	[0.77, 1.12]
ϕ (°)	–	$0.05^{+0.54}_{-0.53}$	$-12.9^{+9.9}_{-8.7}$	[−30.2, 10.6]
$\delta_{K\pi\pi}$ (°)	$20.4^{+23.3}_{-23.8}$	$22.6^{+24.1}_{-24.4}$	$31.7^{+23.5}_{-24.2}$	[−16.4, 77.7]
A_π(%)	–	0.02 ± 0.13	0.01 ± 0.14	[−0.25, 0.28]
A_K(%)	–	-0.11 ± 0.13	-0.11 ± 0.13	[−0.37, 0.14]
x_{12} (%)	–	$0.41^{+0.14}_{-0.15}$		[0.10, 0.67]
y_{12} (%)	–	0.61 ± 0.07		[0.47, 0.75]
ϕ_{12}(°)	–	-0.17 ± 1.8		[−5.3, 4.4]

Table 226: Individual contributions to the χ^2 for the CPV-allowed fit.

Observable	$\boldsymbol{\chi^2}$	$\boldsymbol{\sum \chi^2}$
y_{CP}	1.19	1.19
A_Γ	0.83	2.01
$x_{K^0\pi^+\pi^-}$ Belle	1.33	3.35
$y_{K^0\pi^+\pi^-}$ Belle	5.30	8.64
$\lvert q/p\rvert_{K^0\pi^+\pi^-}$ Belle	0.10	8.74
$\phi_{K^0\pi^+\pi^-}$ Belle	0.23	8.97
$x_{K^0\pi^+\pi^-}$ LHCb	4.51	13.48
$y_{K^0\pi^+\pi^-}$ LHCb	0.40	13.88
$x_{K^0h^+h^-}$ *BABAR*	0.36	14.24
$y_{K^0h^+h^-}$ *BABAR*	0.19	14.43
$x_{\pi^0\pi^+\pi^-}$ *BABAR*	0.77	15.20
$y_{\pi^0\pi^+\pi^-}$ *BABAR*	0.22	15.42
$(x^2+y^2)_{K^+\ell^-\nu}$	0.14	15.56
$x_{K^+\pi^-\pi^0}$ *BABAR*	7.10	22.67
$y_{K^+\pi^-\pi^0}$ *BABAR*	3.92	26.58
CLEOc		
$(x/y/R_D/\cos\delta/\sin\delta)$	10.53	37.12
$R_D^+/x'^{2+}/y'^+$ *BABAR*	11.13	48.25
$R_D^-/x'^{2-}/y'^-$ *BABAR*	6.04	54.29
$R_D^+/x'^{2+}/y'^+$ Belle	2.08	56.36
$R_D^-/x'^{2-}/y'^-$ Belle	3.22	59.58
$R_D/x'^2/y'$ CDF	1.29	60.87
$R_D^+/x'^{2+}/y'^+$ LHCb	0.58	61.46
$R_D^-/x'^{2-}/y'^-$ LHCb	1.65	63.11
$A_{KK}/A_{\pi\pi}$ *BABAR*	0.30	63.41
$A_{KK}/A_{\pi\pi}$ Belle	2.89	66.30
$A_{KK}/A_{\pi\pi}$ CDF	4.63	70.94
$A_{KK}-A_{\pi\pi}$ LHCb (D^* tag)	0.12	71.05
$A_{KK}-A_{\pi\pi}$ LHCb ($B^0\to D^0\mu X$ tag)	2.24	73.30
$(x^2+y^2)_{K^+\pi^-\pi^+\pi^-}$ LHCb	3.48	76.78

8.2 *CP* asymmetries

CP violation occurs if the decay rate for a particle differs from that of its *CP*-conjugate [870]. Such phenomena can be classified into two broad categories, termed *direct CP* violation and *indirect CP* violation [871]. Direct *CP* violation refers to $\Delta C = 1$ processes and can occur in both charged and neutral D decays. It results from interference between two different decay amplitudes (*e.g.*, a penguin and tree amplitude) that have different weak (CKM) and strong phases.[51] A difference in strong phases typically arises due to final-state interactions (FSI) [872]. A difference in weak phases arises from different CKM vertex couplings, as is often the case for spectator and penguin diagrams. Indirect *CP* violation refers to $\Delta C = 2$ processes and arises in D^0 decays due to D^0-$\overline{D}{}^0$ mixing. It can occur as an asymmetry in the mixing itself, or it can result from interference between a decay amplitude arising via mixing and a non-mixed amplitude.

The *CP* asymmetry is defined as the difference between D and $\overline{D}$ partial widths divided by their sum:

$$A_{CP} \;=\; \frac{\Gamma(D) - \Gamma(\overline{D})}{\Gamma(D) + \Gamma(\overline{D})}\,. \tag{214}$$

In the case of D^+ and D_s^+ decays, A_{CP} measures direct *CP* violation; in the case of D^0 decays, A_{CP} measures direct and indirect *CP* violation combined (see also Sec. 8.4).

In each experiment, care must be taken to correct for production and detection asymmetries. To take into account differences in production rates between D and $\overline{D}$ (which would affect the number of respective decays observed), some experiments (like FOCUS and E791) normalize to a Cabibbo-favored mode. In this case there is the additional benefit that most corrections due to reconstruction inefficiencies cancel out, reducing systematic uncertainties. An implicit assumption is that there is no measurable *CP* violation in the Cabibbo-favored normalizing mode. The *CP* asymmetry is calculated as

$$A_{CP} \;=\; \frac{\eta(D) - \eta(\overline{D})}{\eta(D) + \eta(\overline{D})}\,, \tag{215}$$

where (considering, for example, $D^0 \to K^-K^+$)

$$\eta(D) \;=\; \frac{N(D^0 \to K^-K^+)}{N(D^0 \to K^-\pi^+)}\,, \tag{216}$$

$$\eta(\overline{D}) \;=\; \frac{N(\overline{D}{}^0 \to K^-K^+)}{N(\overline{D}{}^0 \to K^+\pi^-)}\,. \tag{217}$$

Other experiments (like LHCb) determine A_{CP} through the relation:

$$A_{\rm meas} \;=\; A_{CP} + A_{\rm prod} + A_{\rm det}\,, \tag{218}$$

[51] The weak phase difference will have opposite signs for $D \to f$ and $\overline{D} \to \overline{f}$ decays, while the strong phase difference will have the same sign. As a result, squaring the total amplitudes to obtain the decay rates gives interference terms having opposite sign, *i.e.*, non-identical decay rates.

where $A_{\rm meas}$ is the measured asymmetry, $A_{\rm prod}$ is the asymmetry in the charm meson production, and $A_{\rm det}$ is due to difference in detection efficiencies between positevely and negatively charged hadrons.

Values of A_{CP} for D^+, D^0 and D_s^+ decays are listed in Tables 227, 228, 229, 230 and 231 respectively. In these tables we report asymmetries for the actual final state, *i.e.*, resonant substructure is implicitly included but not considered separately. The high accuracy of these measurements allows one to see and correct for *CP* violation due to the K^0-$\overline{K}^0$ system [873]. For example, the decay modes $D^+ \to (\overline{K^0}/K^0)K^+$ and $D_s^+ \to (\overline{K^0}/K^0)\pi^+$ (shown in Tables 227 and 231, respectively) are the modes $D^+ \to K_s K^+$ and $D_s^+ \to K_s\pi^+$ after subtracting for this effect.

Overall, *CP* asymmetry measurements have been carried out for 47 charm decay modes, and in several modes the sensitivity is well below 5×10^{-3}. There is currently no evidence for *CP* violation in the charm sector. The *CP* asymmetry observed in the mode $D^+ \to K_s^0\pi^+$ is consistent with what expected from the $K^0 - \overline{K}^0$ system [873], and thus it is not attributed to charm.

Taken together, the limits obtained for *CP* asymmetries in the charm sector pose tight constraints on new physics models.

Table 227: *CP* asymmetries $A_{CP} = [\Gamma(D^+) - \Gamma(D^-)]/[\Gamma(D^+) + \Gamma(D^-)]$ for two-body $D^\pm$ decays.

Mode	**Year**	**Collaboration**	$\boldsymbol{A_{CP}}$
$\boldsymbol{D^+ \to \mu^+\nu}$	2008	CLEO [874]	$+0.08 \pm 0.08$
$\boldsymbol{D^+ \to \pi^+\pi^0}$	2010	CLEO [875]	$+0.029 \pm 0.029 \pm 0.003$
$\boldsymbol{D^+ \to \pi^+\eta}$	2011	Belle [876]	$+0.0174 \pm 0.0113 \pm 0.0019$
	2010	CLEO [875]	$-0.020 \pm 0.023 \pm 0.003$
		COMBOS average	$+0.010 \pm 0.010$
$\boldsymbol{D^+ \to \pi^+\eta'}$	2011	Belle [876]	$-0.0012 \pm 0.0112 \pm 0.0017$
	2010	CLEO [875]	$-0.040 \pm 0.034 \pm 0.003$
		COMBOS average	-0.005 ± 0.011
$\boldsymbol{D^+ \to K^+\pi^0}$	2010	CLEO [875]	$-0.035 \pm 0.107 \pm 0.009$
$\boldsymbol{D^+ \to K^0_S\pi^+}$	2014	CLEO [877]	$-0.011 \pm 0.006 \pm 0.002$
	2012	Belle [878]	$-0.00363 \pm 0.00094 \pm 0.00067$
	2011	*BABAR* [879]	$-0.0044 \pm 0.0013 \pm 0.0010$
	2002	FOCUS [880]	$-0.016 \pm 0.015 \pm 0.009$
		COMBOS average	-0.0041 ± 0.0009
$\boldsymbol{D^+ \to K^0_S K^+}$	2013	*BABAR* [881]	$+0.0013 \pm 0.0036 \pm 0.0025$
	2013	Belle [882]	$-0.0025 \pm 0.0028 \pm 0.0014$
	2010	CLEO [875]	$-0.002 \pm 0.015 \pm 0.009$
	2002	FOCUS [880]	$+0.071 \pm 0.061 \pm 0.012$
		COMBOS average	-0.0011 ± 0.0025
$\boldsymbol{D^+ \to (\overline{K^0}/K^0)K^+}$	2014	LHCb [883]	$+0.0003 \pm 0.0017 \pm 0.0014$
	2013	*BABAR* [881]	$+0.0046 \pm 0.0036 \pm 0.0025$
	2013	Belle [882]	$-0.0008 \pm 0.0028 \pm 0.0014$
		COMBOS average	$+0.0011 \pm 0.0017$

Table 228: *CP* asymmetries $A_{CP} = [\Gamma(D^+) - \Gamma(D^-)]/[\Gamma(D^+) + \Gamma(D^-)]$ for three- and four-body $D^\pm$ decays.

Mode	**Year**	**Collaboration**	$\boldsymbol{A_{CP}}$
$\boldsymbol{D^+ \to \pi^+\pi^-\pi^+}$	2014	LHCb [884]	Dalitz plot analysis, no evidence for *CP* violation
	1997	E791 [885]	-0.017 ± 0.042 (stat.)
$\boldsymbol{D^+ \to K^-\pi^+\pi^+}$	2014	D0 [886]	$-0.0016 \pm 0.0015 \pm 0.0009$
	2014	CLEO [877]	$-0.003 \pm 0.002 \pm 0.004$
		COMBOS average	-0.0018 ± 0.0016
$\boldsymbol{D^+ \to K^0_S\pi^+\pi^0}$	2014	CLEO [877]	$-0.001 \pm 0.007 \pm 0.002$
$\boldsymbol{D^+ \to K^+K^-\pi^+}$	2014	CLEO [877]	$-0.001 \pm 0.009 \pm 0.004$
	2013	*BABAR* [887]	$+0.0037 \pm 0.0030 \pm 0.0015$
	2008	CLEO [888]	Dalitz plot analysis, no evidence for *CP* violation
	2000	FOCUS [889]	$+0.006 \pm 0.011 \pm 0.005$
	1997	E791 [885]	-0.014 ± 0.029 (stat.)
		COMBOS average	$+0.0032 \pm 0.0031$
$\boldsymbol{D^+ \to K^-\pi^+\pi^+\pi^0}$	2014	CLEO [877]	$-0.003 \pm 0.006 \pm 0.004$
$\boldsymbol{D^+ \to K^0_S\pi^+\pi^+\pi^-}$	2014	CLEO [877]	$+0.000 \pm 0.012 \pm 0.003$
$\boldsymbol{D^+ \to K^0_S K^+\pi^+\pi^-}$	2005	FOCUS [890]	$-0.042 \pm 0.064 \pm 0.022$

Table 229: *CP* asymmetries $A_{CP} = [\Gamma(D^0) - \Gamma(\overline{D}{}^0)]/[\Gamma(D^0) + \Gamma(\overline{D}{}^0)]$ for two-body $D^0, \overline{D}{}^0$ decays.

Mode	**Year**	**Collaboration**	$\boldsymbol{A_{CP}}$
$\boldsymbol{D^0 \to \pi^+\pi^-}$	2014	LHCb [834]	$-0.0020 \pm 0.0019 \pm 0.0010$
	2012	CDF [891]	$+0.0022 \pm 0.0024 \pm 0.0011$
	2008	*BABAR* [850]	$-0.0024 \pm 0.0052 \pm 0.0022$
	2012	Belle [892]	$+0.0043 \pm 0.0052 \pm 0.0012$
	2002	CLEO [857]	$+0.019 \pm 0.032 \pm 0.008$
	2000	FOCUS [889]	$+0.048 \pm 0.039 \pm 0.025$
	1998	E791 [893]	$-0.049 \pm 0.078 \pm 0.030$
		COMBOS average	$+0.0000 \pm 0.0015$
$\boldsymbol{D^0 \to \pi^0\pi^0}$	2014	Belle [894]	$-0.0003 \pm 0.0064 \pm 0.0010$
	2001	CLEO [895]	$+0.001 \pm 0.048$ (stat. and syst. combined)
		COMBOS average	-0.0003 ± 0.0064
$\boldsymbol{D^0 \to K^0_S\pi^0}$	2014	Belle [894]	$-0.0021 \pm 0.0016 \pm 0.0007$
	2001	CLEO [895]	$+0.001 \pm 0.013$ (stat. and syst. combined)
		COMBOS average	-0.0020 ± 0.0017
$\boldsymbol{D^0 \to K^0_S\eta}$	2011	Belle [896]	$+0.0054 \pm 0.0051 \pm 0.0016$
$\boldsymbol{D^0 \to K^0_S\eta'}$	2011	Belle [896]	$+0.0098 \pm 0.0067 \pm 0.0014$
$\boldsymbol{D^0 \to K^0_S K^0_S}$	2015	LHCb [897]	$-0.029 \pm 0.052 \pm 0.022$
	2001	CLEO [895]	-0.23 ± 0.19 (stat. and syst. combined)
		COMBOS average	-0.046 ± 0.054
$\boldsymbol{D^0 \to K^-\pi^+}$	2014	CLEO [877]	$+0.003 \pm 0.003 \pm 0.006$
$\boldsymbol{D^0 \to K^+K^-}$	2014	LHCb [834]	$-0.0006 \pm 0.0015 \pm 0.0010$
	2012	CDF [891]	$-0.0024 \pm 0.0022 \pm 0.0009$
	2008	*BABAR* [850]	$+0.0000 \pm 0.0034 \pm 0.0013$
	2012	Belle [892]	$-0.0043 \pm 0.0030 \pm 0.0011$
	2002	CLEO [857]	$+0.000 \pm 0.022 \pm 0.008$
	2000	FOCUS [889]	$-0.001 \pm 0.022 \pm 0.015$
	1998	E791 [893]	$-0.010 \pm 0.049 \pm 0.012$
		COMBOS average	-0.0016 ± 0.0012

Table 230: *CP* asymmetries $A_{CP} = [\Gamma(D^0) - \Gamma(\overline{D}{}^0)]/[\Gamma(D^0) + \Gamma(\overline{D}{}^0)]$ for three- and four-body $D^0, \overline{D}{}^0$ decays.

Mode	**Year**	**Collaboration**	$\boldsymbol{A_{CP}}$
$\boldsymbol{D^0 \to \pi^+\pi^-\pi^0}$	2008	*BABAR* [898]	$+0.0031 \pm 0.0041 \pm 0.0017$
	2008	Belle [899]	$+0.0043 \pm 0.0130$ (stat. and syst. combined)
	2005	CLEO [900]	$+0.01^{+0.09}_{-0.07} \pm 0.05$
		COMBOS average	$+0.0032 \pm 0.0042$
$\boldsymbol{D^0 \to K^-\pi^+\pi^0}$	2014	CLEO [877]	$+0.001 \pm 0.003 \pm 0.004$
$\boldsymbol{D^0 \to K^+\pi^-\pi^0}$	2005	Belle [901]	-0.006 ± 0.053 (stat.)
	2001	CLEO [902]	$+0.09^{+0.25}_{-0.22}$ (stat.)
		COMBOS average	-0.0014 ± 0.0517
$\boldsymbol{D^0 \to K^0_S\pi^+\pi^-}$	2012	CDF [903]	$-0.0005 \pm 0.0057 \pm 0.0054$
	2004	CLEO [904]	$-0.009 \pm 0.021^{+0.016}_{-0.057}$
		COMBOS average	-0.0008 ± 0.0077
$\boldsymbol{D^0 \to K^+K^-\pi^0}$	2008	*BABAR* [898]	$-0.0100 \pm 0.0167 \pm 0.0025$
$\boldsymbol{D^0 \to \pi^-\pi^-\pi^+\pi^+}$	2013	LHCb [905]	Amplitude analysis, no evidence for *CP* violation
$\boldsymbol{D^0 \to K^-\pi^+\pi^+\pi^-}$	2014	CLEO [877]	$+0.002 \pm 0.003 \pm 0.004$
$\boldsymbol{D^0 \to K^+\pi^-\pi^+\pi^-}$	2005	Belle [901]	-0.018 ± 0.044 (stat.)
$\boldsymbol{D^0 \to K^+K^-\pi^+\pi^-}$	2013	LHCb [905]	Amplitude analysis, no evidence for *CP* violation
	2012	CLEO [906]	Amplitude analysis, no evidence for *CP* violation
	2005	FOCUS [890]	$-0.082 \pm 0.056 \pm 0.047$

Table 231: *CP* asymmetries $A_{CP} = [\Gamma(D_s^+) - \Gamma(D_s^-)]/[\Gamma(D_s^+) + \Gamma(D_s^-)]$ for $D_s^\pm$ decays.

Mode	**Year**	**Collaboration**	$\boldsymbol{A_{CP}}$
$\boldsymbol{D_s^+ \to \mu^+\nu}$	2009	CLEO [907]	$+0.048 \pm 0.061$
$\boldsymbol{D_s^+ \to \pi^+\eta}$	2013	CLEO [908]	$+0.011 \pm 0.030 \pm 0.008$
$\boldsymbol{D_s^+ \to \pi^+\eta'}$	2013	CLEO [908]	$-0.022 \pm 0.022 \pm 0.006$
$\boldsymbol{D_s^+ \to K_s^0\pi^+}$	2013	*BABAR* [881]	$+0.006 \pm 0.020 \pm 0.003$
	2010	Belle [909]	$+0.0545 \pm 0.0250 \pm 0.0033$
	2010	CLEO [875]	$+0.163 \pm 0.073 \pm 0.003$
		COMBOS average	$+0.0311 \pm 0.0154$
$\boldsymbol{D_s^+ \to (\overline{K^0}/K^0)\pi^+}$	2014	LHCb [883]	$+0.0038 \pm 0.0046 \pm 0.0017$
	2013	*BABAR* [881]	$+0.003 \pm 0.020 \pm 0.003$
		COMBOS average	$+0.0038 \pm 0.0048$
$\boldsymbol{D_s^+ \to K_s^0K^+}$	2013	CLEO [908]	$+0.026 \pm 0.015 \pm 0.006$
	2013	*BABAR* [881]	$-0.0005 \pm 0.0023 \pm 0.0024$
	2010	Belle [909]	$+0.0012 \pm 0.0036 \pm 0.0022$
		COMBOS average	$+0.0008 \pm 0.0026$
$\boldsymbol{D_s^+ \to K^+\pi^0}$	2010	CLEO [875]	$+0.266 \pm 0.228 \pm 0.009$
$\boldsymbol{D_s^+ \to K^+\eta}$	2010	CLEO [875]	$+0.093 \pm 0.152 \pm 0.009$
$\boldsymbol{D_s^+ \to K^+\eta'}$	2010	CLEO [875]	$+0.060 \pm 0.189 \pm 0.009$
$\boldsymbol{D_s^+ \to \pi^+\pi^+\pi^-}$	2013	CLEO [908]	$-0.007 \pm 0.030 \pm 0.006$
$\boldsymbol{D_s^+ \to \pi^+\pi^0\eta}$	2013	CLEO [908]	$-0.005 \pm 0.039 \pm 0.020$
$\boldsymbol{D_s^+ \to \pi^+\pi^0\eta'}$	2013	CLEO [908]	$-0.004 \pm 0.074 \pm 0.019$
$\boldsymbol{D_s^+ \to K_s^0K^+\pi^0}$	2013	CLEO [908]	$-0.016 \pm 0.060 \pm 0.011$
$\boldsymbol{D_s^+ \to K_s^0K_s^0\pi^+}$	2013	CLEO [908]	$+0.031 \pm 0.052 \pm 0.006$
$\boldsymbol{D_s^+ \to K^+\pi^+\pi^-}$	2013	CLEO [908]	$+0.045 \pm 0.048 \pm 0.006$
$\boldsymbol{D_s^+ \to K^+K^-\pi^+}$	2013	CLEO [908]	$-0.005 \pm 0.008 \pm 0.004$
$\boldsymbol{D_s^+ \to K_s^0K^-\pi^+\pi^+}$	2013	CLEO [908]	$+0.041 \pm 0.027 \pm 0.009$
$\boldsymbol{D_s^+ \to K_s^0K^+\pi^+\pi^-}$	2013	CLEO [908]	$-0.057 \pm 0.053 \pm 0.009$
$\boldsymbol{D_s^+ \to K^+K^-\pi^+\pi^0}$	2013	CLEO [908]	$+0.000 \pm 0.027 \pm 0.012$

8.3 *T*-odd asymmetries

Measuring T-odd asymmetries provides an alternative way to search for *CP* violation in the charm sector, due to *CPT* invariance. T-odd asymmetries are measured using triple-product correlations and assuming the validity of the *CPT* theorem.

Triple-product correlations of the form $\vec{a} \cdot (\vec{b} \times \vec{c})$, where a, b, and c are spins or momenta, are odd under time reversal (T). In general, a triple-product formed using both momenta and spins, like

$$\vec{s_1} \cdot (\vec{p_2} \times \vec{p_3}) \tag{219}$$

is odd under T but even for P-conjugation.

Taking as an example the decay mode $D^0 \to K^+K^-\pi^+\pi^-$, one can form the triple-product correlation using the momenta of the final state particles. For a spinless decaying particle, such a correlation must necessarily involve at least four final-state particles. Defining for D^0 the T-odd correlation

$$C_T \equiv \vec{p}_{K^+} \cdot (\vec{p}_{\pi^+} \times \vec{p}_{\pi^-}) \,, \tag{220}$$

and the corresponding quantity for $\overline{D}{}^0$

$$\overline{C}_T \equiv \vec{p}_{K^-} \cdot (\vec{p}_{\pi^-} \times \vec{p}_{\pi^+}) \,, \tag{221}$$

one can measure the asymmetry

$$A_T \;=\; \frac{\Gamma(C_T > 0) - \Gamma(C_T < 0)}{\Gamma(C_T > 0) + \Gamma(C_T < 0)} \tag{222}$$

for D^0 decays and

$$\overline{A}_T \;=\; \frac{\Gamma(-\overline{C}_T > 0) - \Gamma(-\overline{C}_T < 0)}{\Gamma(-\overline{C}_T > 0) + \Gamma(-\overline{C}_T < 0)} \tag{223}$$

for $\overline{D}{}^0$ decays. In these expressions, Γ represents a partial width. These asymmetries can have a nonzero values because of FSI. On the other hand, one can construct the T-odd asymmetry

$$A_{T-\mathrm{odd}} \;\equiv\; \frac{A_T - \overline{A}_T}{2} \,, \tag{224}$$

which is nonzero only if *CP* violation is present (see Refs. [910–914]).

Recently, this topic has been revisited (see Refs. [915,916]) with the suggestion to use other asymmetries constructed from triple products in multi-body decay modes to probe the discrete symmetries C, P and *CP*. Up until now, experiments have measured only the variable defined by Eq. (224). (Note that this asymmetry is referred to in the literature by several names: $A_{T\,\mathrm{viol}}$, a_{CP}^{P}, and $a_{CP}^{T-\mathrm{odd}}$.)

Values of $A_{T-\mathrm{odd}}$ for numerous D^+, D_s^+, and D^0 decay modes are listed in Table 232. The first measurements were made by FOCUS, and subsequently *BABAR* reached a sensitivity of $\sim 1\%$. Currently the best sensitivity is from LHCb. However, despite this high precision ($< 1\%$) there is no evidence for *CP* violation.

Table 232: T-odd asymmetries $A_{T-odd} = (A_T - \overline{A}_T)/2$.

Mode	**Year**	**Collaboration**	$\boldsymbol{A_{T-odd}}$
$\boldsymbol{D^0 \to K^+K^-\pi^+\pi^-}$	2014	LHCb [917]	$+0.0018 \pm 0.0029 \pm 0.0004$
	2010	*BABAR* [918]	$+0.0010 \pm 0.0051 \pm 0.0044$
	2005	FOCUS [890]	$+0.010 \pm 0.057 \pm 0.037$
		COMBOS average	$+0.0017 \pm 0.0027$
$\boldsymbol{D^+ \to K^0_S K^+\pi^+\pi^-}$	2011	*BABAR* [919]	$-0.0120 \pm 0.0100 \pm 0.0046$
	2005	FOCUS [890]	$+0.023 \pm 0.062 \pm 0.022$
		COMBOS average	-0.0110 ± 0.0109
$\boldsymbol{D^+_s \to K^0_S K^+\pi^+\pi^-}$	2011	*BABAR* [919]	$-0.0136 \pm 0.0077 \pm 0.0034$
	2005	FOCUS [890]	$-0.036 \pm 0.067 \pm 0.023$
		COMBOS average	-0.0139 ± 0.0084

8.4 Interplay of direct and indirect CP violation

In decays of D^0 mesons, CP asymmetry measurements have contributions from both direct and indirect CP violation as discussed in Sec. 8.1. The contribution from indirect CP violation depends on the decay-time distribution of the data sample [869]. This section describes a combination of measurements that allows the extraction of the individual contributions of the two types of CP violation. At the same time, the level of agreement for a no-CP-violation hypothesis is tested. The observables are:

$$A_\Gamma \equiv \frac{\tau(\overline{D}{}^0 \to h^+h^-) - \tau(D^0 \to h^+h^-)}{\tau(\overline{D}{}^0 \to h^+h^-) + \tau(D^0 \to h^+h^-)}, \tag{225}$$

where h^+h^- can be K^+K^- or $\pi^+\pi^-$, and

$$\Delta A_{\rm CP} \equiv A_{\rm CP}(K^+K^-) - A_{\rm CP}(\pi^+\pi^-), \tag{226}$$

where $A_{\rm CP}$ are time-integrated CP asymmetries. The underlying theoretical parameters are:

$$\begin{aligned} a^{\rm dir}_{\rm CP} &\equiv \frac{|\mathcal{A}_{D^0\to f}|^2 - |\mathcal{A}_{\overline{D}{}^0\to f}|^2}{|\mathcal{A}_{D^0\to f}|^2 + |\mathcal{A}_{\overline{D}{}^0\to f}|^2}, \\ a^{\rm ind}_{\rm CP} &\equiv \frac{1}{2}\left[\left(\left|\frac{q}{p}\right| + \left|\frac{p}{q}\right|\right) x\sin\phi - \left(\left|\frac{q}{p}\right| - \left|\frac{p}{q}\right|\right) y\cos\phi\right], \end{aligned} \tag{227}$$

where $\mathcal{A}_{D\to f}$ is the amplitude for $D \to f$ [920]. We use the following relations between the observables and the underlying parameters [921]:

$$A_\Gamma = -a^{\rm ind}_{\rm CP} - a^{\rm dir}_{\rm CP} y_{\rm CP},$$

$$\Delta A_{\rm CP} = \Delta a^{\rm dir}_{\rm CP}\left(1 + y_{\rm CP}\frac{\overline{\langle t\rangle}}{\tau}\right) + a^{\rm ind}_{\rm CP}\frac{\Delta\langle t\rangle}{\tau} + \overline{a^{\rm dir}_{\rm CP}} y_{\rm CP}\frac{\Delta\langle t\rangle}{\tau}, \tag{228}$$

$$\approx \Delta a^{\rm dir}_{\rm CP}\left(1 + y_{\rm CP}\frac{\overline{\langle t\rangle}}{\tau}\right) + a^{\rm ind}_{\rm CP}\frac{\Delta\langle t\rangle}{\tau}. \tag{229}$$

The first relation constrains mostly indirect CP violation, and the direct CP violation contribution can differ for different final states. In the second relation, $\langle t\rangle/\tau$ denotes the mean decay time in units of the D^0 lifetime; ΔX denotes the difference in quantity X between K^+K^- and $\pi^+\pi^-$ final states; and $\overline{X}$ denotes the average for quantity X. We neglect the last term in this relation as all three factors are $\mathcal{O}(10^{-2})$ or smaller, and thus this term is negligible with respect to the other two terms. Note that $\Delta\langle t\rangle/\tau \ll \langle t\rangle/\tau$, and it is expected that $|a^{\rm dir}_{\rm CP}| < |\Delta a^{\rm dir}_{\rm CP}|$ because $a^{\rm dir}_{\rm CP}(K^+K^-)$ and $a^{\rm dir}_{\rm CP}(\pi^+\pi^-)$ are expected to have opposite signs [920].

A χ^2 fit is performed in the plane $\Delta a^{\rm dir}_{\rm CP}$ vs. $a^{\rm ind}_{\rm CP}$. For the *BABAR* result the difference of the quoted values for $A_{\rm CP}(K^+K^-)$ and $A_{\rm CP}(\pi^+\pi^-)$ is calculated, adding all uncertainties in quadrature. This may overestimate the systematic uncertainty for the difference as it neglects correlated errors; however, the result is conservative and the effect is small as all measurements are statistically limited. For all measurements, statistical and systematic uncertainties are added in quadrature when calculating the χ^2. We use the current world average value $y_{\rm CP} = (0.835 \pm 0.155)\%$ (see Sec. 8.1) and the measurements listed in Table 233.

Table 233: Inputs to the fit for direct and indirect CP violation. The first uncertainty listed is statistical, and the second is systematic.

Year	Experiment	Results	$\Delta\langle t\rangle/\tau$	$\langle t\rangle/\tau$	Reference
2012	*BABAR*	$A_\Gamma = (0.09 \pm 0.26 \pm 0.06)\%$	-	-	[861]
2016	LHCb prompt	$A_\Gamma(KK) = (-0.030 \pm 0.032 \pm 0.014)\%$	-	-	[865, 922]
		$A_\Gamma(\pi\pi) = (0.046 \pm 0.058 \pm 0.016)\%$	-	-	
2014	CDF	$A_\Gamma = (-0.12 \pm 0.12)\%$	-	-	[863]
2015	LHCb SL	$A_\Gamma = (-0.125 \pm 0.073)\%$	-	-	[864]
2015	Belle	$A_\Gamma = (-0.03 \pm 0.20 \pm 0.07)\%$	-	-	[923]
2008	*BABAR*	$A_{\rm CP}(KK) = (0.00 \pm 0.34 \pm 0.13)\%$			
		$A_{\rm CP}(\pi\pi) = (-0.24 \pm 0.52 \pm 0.22)\%$	0.00	1.00	[850]
2012	Belle prel.	$\Delta A_{\rm CP} = (-0.87 \pm 0.41 \pm 0.06)\%$	0.00	1.00	[924]
2012	CDF	$\Delta A_{\rm CP} = (-0.62 \pm 0.21 \pm 0.10)\%$	0.25	2.58	[853]
2014	LHCb SL	$\Delta A_{\rm CP} = (0.14 \pm 0.16 \pm 0.08)\%$	0.01	1.07	[834]
2016	LHCb prompt	$\Delta A_{\rm CP} = (-0.10 \pm 0.08 \pm 0.03)\%$	0.12	2.10	[854]

In this fit, $A_\Gamma(KK)$ and $A_\Gamma(\pi\pi)$ are assumed to be identical. This assumption is supported by all measurements to date. A significant relative shift due to final-state dependent A_Γ values between $\Delta A_{\rm CP}$ measurements with different mean decay times is excluded by these measurements.

The combination plot (see Fig. 167) shows the measurements listed in Table 233 for $\Delta A_{\rm CP}$ and A_Γ, where the bands represent $\pm 1\sigma$ intervals. The point of no CP violation (0,0) is shown as a filled circle, and two-dimensional 68% C.L., 95% C.L., and 99.7% C.L. regions are plotted as ellipses. The best fit value is indicated by a cross showing the one-dimensional errors.

From the fit, the change in χ^2 from the minimum value for the no-CPV point (0,0) is 4.7, which corresponds to a C.L. of 9.3×10^{-2} for two degrees of freedom. Thus the data are consistent with the no-CP-violation hypothesis at 9.3% C.L. This p-value corresponds to 1.7σ. The central values and $\pm 1\sigma$ uncertainties for the individual parameters are

$$\begin{aligned} a_{\rm CP}^{\rm ind} &= (0.030 \pm 0.026)\% \\ \Delta a_{\rm CP}^{\rm dir} &= (-0.134 \pm 0.070)\%. \end{aligned} \tag{230}$$

Compared to the previous average, the tension in the difference between direct CP violation in the two final states is reduced, while the common indirect CP violation moved away from the no-CP-violation point by about one standard deviation.

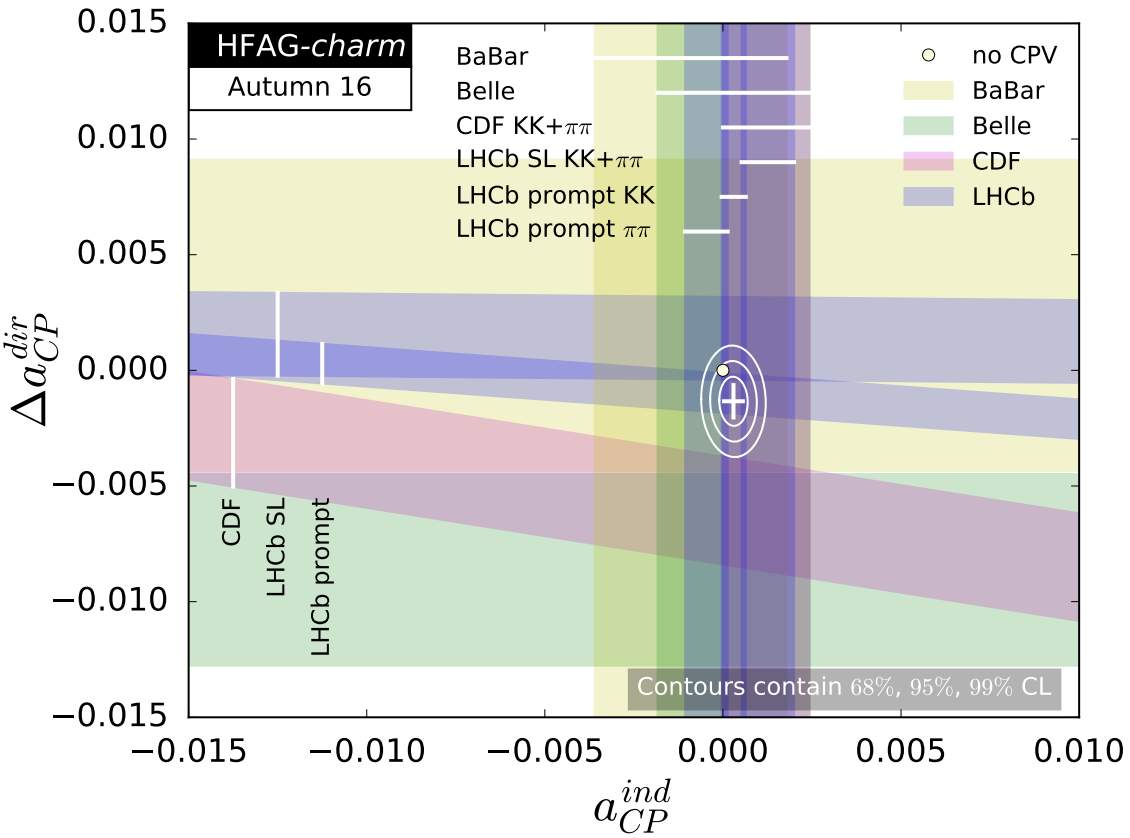

Figure 167: Plot of all data and the fit result. Individual measurements are plotted as bands showing their $\pm 1\sigma$ range. The no-CPV point (0,0) is shown as a filled circle, and the best fit value is indicated by a cross showing the one-dimensional uncertainties. Two-dimensional 68% C.L., 95% C.L., and 99.7% C.L. regions are plotted as ellipses.

8.5 Semileptonic decays

8.5.1 Introduction

Semileptonic decays of D mesons involve the interaction of a leptonic current with a hadronic current. The latter is nonperturbative and cannot be calculated from first principles; thus it is usually parameterized in terms of form factors. The transition matrix element is written

$$\mathcal{M} \;=\; -i\,\frac{G_F}{\sqrt{2}}\,V_{cq}\,L^\mu H_\mu\,, \tag{231}$$

where G_F is the Fermi constant and V_{cq} is a CKM matrix element. The leptonic current L^μ is evaluated directly from the lepton spinors and has a simple structure; this allows one to extract information about the form factors (in H_μ) from data on semileptonic decays [925]. Conversely, because there are no final-state interactions between the leptonic and hadronic systems, semileptonic decays for which the form factors can be calculated allow one to determine V_{cq} [2].

8.5.2 $D \to P\bar{\ell}\nu_\ell$ decays

When the final state hadron is a pseudoscalar, the hadronic current is given by

$$H_\mu \;=\; \langle P(p)|\bar{q}\gamma_\mu c|D(p')\rangle \;=\; f_+(q^2)\left[(p'+p)_\mu - \frac{m_D^2-m_P^2}{q^2}q_\mu\right] + f_0(q^2)\frac{m_D^2-m_P^2}{q^2}q_\mu\,, \tag{232}$$

where m_D and p' are the mass and four momentum of the parent D meson, m_P and p are those of the daughter meson, $f_+(q^2)$ and $f_0(q^2)$ are form factors, and $q = p' - p$. Kinematics require that $f_+(0) = f_0(0)$. The contraction $q_\mu L^\mu$ results in terms proportional to m_ℓ [926], and thus for $\ell = e$ the terms proportionals to q_μ in Eq. (232) are negligible. For light leptons only the $f_+(q^2)$ form factor is relevant and the differential partial width is

$$\frac{d\Gamma(D \to P\bar{\ell}\nu_\ell)}{dq^2\,d\cos\theta_\ell} \;=\; \frac{G_F^2|V_{cq}|^2}{32\pi^3}p^{*\,3}|f_+(q^2)|^2\sin\theta_\ell^2\,, \tag{233}$$

where p^* is the magnitude of the momentum of the final state hadron in the D rest frame, and θ_ℓ is the angle of the lepton in the $\ell\nu$ rest frame with respect to the direction of the pseudoscalar meson in the D rest frame.

8.5.3 Form factor parameterizations

The form factor is traditionally parameterized with an explicit pole and a sum of effective poles:

$$f_+(q^2) \;=\; \frac{f_+(0)}{(1-\alpha)}\left[\left(\frac{1}{1-q^2/m_{\rm pole}^2}\right) \;+\; \sum_{k=1}^{N}\frac{\rho_k}{1-q^2/(\gamma_k\,m_{\rm pole}^2)}\right], \tag{234}$$

where ρ_k and γ_k are expansion parameters and α is a parameter that normalizes the form factor at $q^2 = 0$, $f_+(0)$. The parameter $m_{\rm pole}$ is the mass of the lowest-lying $c\bar{q}$ resonance with the appropriate quantum numbers; this is expected to provide the largest contribution to the form factor for the $c \to q$ transition. The sum over N gives the contribution of higher mass states. For example, for $D \to \pi$ transitions the dominant resonance is expected to be $D^*(2010)$, and thus $m_{\rm pole} = m_{D^*(2010)}$. For $D \to K$ transitions, the dominant contribution is expected from $D_s^*(2112)$, with $m_{\rm pole} = m_{D_s^*(2112)}$.

8.5.4 Simple pole

Equation (234) can be simplified by neglecting the sum over effective poles, leaving only the explicit vector meson pole. This approximation is referred to as "nearest pole dominance" or "vector-meson dominance." The resulting parameterization is

$$f_+(q^2) \;=\; \frac{f_+(0)}{(1-q^2/m^2_{\rm pole})}\,. \tag{235}$$

However, values of $m_{\rm pole}$ that give a good fit to the data do not agree with the expected vector meson masses [927]. To address this problem, the "modified pole" or Becirevic-Kaidalov (BK) parameterization [928] was introduced. $m_{\rm pole}/\sqrt{\alpha_{\rm BK}}$ is interpreted as the mass of an effective pole, higher than $m_{\rm pole}$, thus it is expected that $\alpha_{\rm BK} < 1$.

The parameterization takes the form

$$f_+(q^2) \;=\; \frac{f_+(0)}{(1-q^2/m^2_{\rm pole})}\frac{1}{\left(1-\alpha_{\rm BK}\frac{q^2}{m^2_{\rm pole}}\right)}\,. \tag{236}$$

These parameterizations are used by several experiments to determine form factor parameters. Measured values of $m_{\rm pole}$ and $\alpha_{\rm BK}$ are listed in Tables 234 and 235 for $D \to K\ell\nu_\ell$ and $D \to \pi\ell\nu_\ell$ decays, respectively.

8.5.5 z expansion

An alternative series expansion around some value $q^2 = t_0$ to parameterize $f_+(q^2)$ can be used [925, 929–931]. This parameterization is model independent and satisfies general QCD constraints, being suitable for fitting experimental data. The expansion is given in terms of a complex parameter z, which is the analytic continuation of q^2 into the complex plane:

$$z(q^2,t_0) \;=\; \frac{\sqrt{t_+-q^2}-\sqrt{t_+-t_0}}{\sqrt{t_+-q^2}+\sqrt{t_+-t_0}}\,, \tag{237}$$

where $t_\pm \equiv (m_D \pm m_P)^2$ and t_0 is the (arbitrary) q^2 value corresponding to $z = 0$. The physical region corresponds to $\pm|z|_{max} = \pm 0.051$ for $D \to K\ell\nu_\ell$ and $= \pm 0.17$ for $D \to \pi\ell\nu_\ell$, using $t_0 = t_+(1-\sqrt{1-t_-/t_+})$.

The form factor is expressed as

$$f_+(q^2) \;=\; \frac{1}{P(q^2)\,\phi(q^2,t_0)}\sum_{k=0}^{\infty} a_k(t_0)[z(q^2,t_0)]^k\,, \tag{238}$$

where the $P(q^2)$ factor accommodates sub-threshold resonances via

$$P(q^2) \;\equiv\; \begin{cases} 1 & (D\to\pi) \\ z(q^2,M^2_{D_s^*}) & (D\to K)\,. \end{cases} \tag{239}$$

The "outer" function $\phi(t,t_0)$ can be any analytic function, but a preferred choice (see, *e.g.* Refs. [929, 930, 932]) obtained from the Operator Product Expansion (OPE) is

$$\begin{aligned}\phi(q^2,t_0) \;=\;& \alpha\left(\sqrt{t_+-q^2}+\sqrt{t_+-t_0}\right)\times \\ & \frac{t_+-q^2}{(t_+-t_0)^{1/4}}\,\frac{(\sqrt{t_+-q^2}\;+\;\sqrt{t_+-t_-})^{3/2}}{(\sqrt{t_+-q^2}+\sqrt{t_+})^5}\,,\end{aligned} \tag{240}$$

with $\alpha = \sqrt{\pi m_c^2/3}$. The OPE analysis provides a constraint upon the expansion coefficients, $\sum_{k=0}^{N} a_k^2 \leq 1$. These coefficients receive $1/M_D$ corrections, and thus the constraint is only approximate. However, the expansion is expected to converge rapidly since $|z| < 0.051$ (0.17) for $D \to K$ ($D \to \pi$) over the entire physical q^2 range, and Eq. (238) remains a useful parameterization. The main disadvantage as compared to phenomenological approaches is that there is no physical interpretation of the fitted coefficients a_K.

8.5.6 Three-pole formalism

An update of the vector pole dominance model has been developed for the $D \to \pi\ell\nu_\ell$ channel [933]. It uses information of the residues of the semileptonic form factor at its first two poles, the $D^*(2010)$ and $D^{*'}(2600)$ resonances. The form factor is expressed as an infinite sum of residues from $J^P = 1^-$ states with masses $m_{D_n^*}$:

$$f_+(q^2) = \sum_{n=0}^{\infty} \frac{\underset{q^2=m^2_{D_n^*}}{\text{Res}} f_+(q^2)}{m^2_{D_n^*} - q^2}\,, \tag{241}$$

with the residues given by

$$\underset{q^2=m^2_{D_n^*}}{\text{Res}} f_+(q^2) = \frac{1}{2} m_{D_n^*} f_{D_n^*} g_{D_n^* D\pi}\,. \tag{242}$$

Values of the f_{D^*} and $f_{D^{*\prime}}$ decay constants have been obtained by lattice QCD calculations, relative to f_D, with 2% and 28% precision, respectively [933]. The couplings to the $D\pi$ state, $g_{D^*D\pi}$ and $g_{D^{*\prime}D\pi}$, are extracted from measurements of the $D^*(2010)$ and $D^{*'}(2600)$ widths by *BABAR* and LHCb experiments [934–936]. Thus the contribution from the first pole is known with a 3% accuracy. The contribution from the $D^{*'}(2600)$ is determined with poorer accuracy, $\sim 30\%$, mainly due to lattice uncertainties. A *superconvergence* condition [937] is applied:

$$\sum_{n=0}^{\infty} \underset{q^2=m^2_{D_n^*}}{\text{Res}} f_+(q^2) = 0\,, \tag{243}$$

protecting the form factor behavior at large q^2. Within this model the first two poles are not sufficient to describe the data, and a third effective pole needs to be included.

One of the advantages of this phenomenological model is that it can be extrapolated outside the charm physical region, providing a method to extract the CKM matrix element V_{ub} using the ratio of the form factors of the $D \to \pi\ell\nu$ and $B \to \pi\ell\nu$ decay channels. It will be used once lattice calculations provide the form factor ratio $f^+_{B\pi}(q^2)/f^+_{D\pi}(q^2)$ at the same pion energy.

This form factor description can be extended to the $D \to K\ell\nu$ decay channel, considering the contribution of several $c\bar{s}$ resonances with $J^P = 1^-$. The first two pole masses contributing to the form factor correspond to the $D_s^*(2112)$ and $D_{s1}^*(2700)$ resonant states [314]. A constraint on the first residue can be obtained using information of the f_K decay constant [314] and the g coupling extracted from the D^{*+} width [934]. The contribution from the second pole can be evaluated using the decay constants from [938], the measured total width and the ratio of D^*K and DK decay branching fractions [314].

8.5.7 Experimental techniques and results

Different techniques by several experiments are used to measure D meson semileptonic decays with a pseudoscalar particle in the final state. The most recent results are provided by the *BABAR* [939] and BES III [940, 941] collaborations. Belle [942], *BABAR* [943] and CLEO-c [944, 945] collaborations have previously reported results. The Belle collaboration fully reconstructs the D events from the continuum under the $\Upsilon(4S)$ resonance, achieving a very good q^2 resolution ($\Delta q^2 = 15$ MeV^2) and low background level, but having a low efficiency. Using 282 fb^{-1}, about 1300 and 115 signal semileptonic decays are isolated for each lepton flavor (e and μ), respectively. The *BABAR* experiment uses a partial reconstruction technique where the semileptonic decays are tagged through the $D^{*+} \to D^0\pi^+$ decay. The D direction and neutrino energy is obtained using information from the rest of the event. With 75 fb^{-1} 74000 signal events in the $D^0 \to K^-e^+\nu$ mode are obtained. This technique provides larger statistics but a higher background level and poorer q^2 resolution (Δq^2 ranges from 66 to 219 MeV^2). In this case the measurement of the branching fraction is obtained by normalizing to the $D^0 \to K^-\pi^+$ decay channel and will benefit from future improvements in the determination of this reference channel. The measurement of the Cabibbo suppressed mode has been recently obtained using the same technique and 350 fb^{-1} data. 5000 $D^0 \to \pi^-e^+\nu$ signal events are reconstructed using this method [939].

The CLEO-c experiment uses two different methods to measure charm semileptonic decays. Tagged analyses [944] rely on the full reconstruction of $\Psi(3770) \to D\overline{D}$ events. One of the D mesons is reconstructed in a hadronic decay mode, the other in the semileptonic channel. The only missing particle is the neutrino so the q^2 resolution is very good and the background level very low. With the entire CLEO-c data sample, 818 pb^{-1}, 14123 and 1374 signal events are reconstructed for the $D^0 \to K^-e^+\nu$ and $D^0 \to \pi^-e^+\nu$ channels, and 8467 and 838 for the $D^+ \to \overline{K}^0e^+\nu$ and $D^+ \to \pi^0e^+\nu$ decays, respectively. Another technique without tagging the D meson in a hadronic mode ("untagged" in the following) has been also used by CLEO-c [945]. In this method, all missing energy and momentum in an event are associated with the neutrino four momentum, with the penalty of larger background as compared to the tagged method. Using the "tagged" method the BES III experiment measures the $D^0 \to K^-e^+\nu$ and $D^0 \to \pi^-e^+\nu$ decay channels. With 2.9 fb^{-1} they fully reconstruct 70700 and 6300 signal events for each channel, respectively [940]. In a separated analysis the BES III experiment measures also the D^+ decay mode into $D^+ \to K^0_Le^+\nu$ [941]. Using several tagged hadronic events they reconstruct 20100 semileptonic candidates.

Previous measurements were also performed by several experiments. Events registered at the $\Upsilon(4S)$ energy corresponding to an integrated luminosity of 7 fb^{-1} were analyzed by CLEO III [946]. Fixed targed photo-production experiments performed also measurements of the normalized form factor distribution (FOCUS [947]) and total decay rates (Mark-III [948], E653 [949, 950], E687 [951, 952], E691 [953], BES II [954, 955], CLEO II [956]). In the FOCUS fixed target photo-production experiment, D^0 semileptonic events were obtained from the decay of a D^{*+}, and the kaon or pion was reconstructed in the muon channel.

Results of the hadronic form factor parameters by the different groups are given in Tables 234 and 235 for m_{pole} and α_{BK}.

The z-expansion formalism has been used by *BABAR* [939, 943], BES III [957] and CLEO-c [944], [945]. Their fits uses the first three terms of the expansion, and the results for the ratios $r_1 \equiv a_1/a_0$ and $r_2 \equiv a_2/a_0$ are listed in Tables 236 and 237. These measurements correspond

Table 234: Results for $m_{\rm pole}$ and $\alpha_{\rm BK}$ from various experiments for $D^0 \to K^-\ell^+\nu$ and $D^+ \to \overline{K}^0\ell^+\nu$ decays.

$D \to K\ell\nu_\ell$ Expt.	Mode	Ref.	$m_{\rm pole}$ (GeV/c^2)	$\alpha_{\rm BK}$
CLEO III	$(D^0;\ \ell = e,\mu)$	[946]	$1.89 \pm 0.05^{+0.04}_{-0.03}$	$0.36 \pm 0.10^{+0.03}_{-0.07}$
FOCUS	$(D^0;\ \ell = \mu)$	[947]	$1.93 \pm 0.05 \pm 0.03$	$0.28 \pm 0.08 \pm 0.07$
Belle	$(D^0;\ \ell = e,\mu)$	[942]	$1.82 \pm 0.04 \pm 0.03$	$0.52 \pm 0.08 \pm 0.06$
BABAR	$(D^0;\ \ell = e)$	[943]	$1.889 \pm 0.012 \pm 0.015$	$0.366 \pm 0.023 \pm 0.029$
CLEO-c (tagged)	$(D^0, D^+;\ \ell = e)$	[944]	$1.93 \pm 0.02 \pm 0.01$	$0.30 \pm 0.03 \pm 0.01$
CLEO-c (untagged)	$(D^0;\ \ell = e)$	[945]	$1.97 \pm 0.03 \pm 0.01$	$0.21 \pm 0.05 \pm 0.03$
CLEO-c (untagged)	$(D^+;\ \ell = e)$	[945]	$1.96 \pm 0.04 \pm 0.02$	$0.22 \pm 0.08 \pm 0.03$
BESIII	$(D^0;\ \ell = e)$	[940]	$1.921 \pm 0.010 \pm 0.007$	$0.309 \pm 0.020 \pm 0.013$
BESIII	$(D^+;\ \ell = e)$	[941]	$1.953 \pm 0.044 \pm 0.036$	$0.239 \pm 0.077 \pm 0.065$

Table 235: Results for $m_{\rm pole}$ and $\alpha_{\rm BK}$ from various experiments for $D^0 \to \pi^-\ell^+\nu$ and $D^+ \to \pi^0\ell^+\nu$ decays.

$D \to \pi\ell\nu_\ell$ Expt.	Mode	Ref.	$m_{\rm pole}$ (GeV/c^2)	$\alpha_{\rm BK}$
CLEO III	$(D^0;\ \ell = e,\mu)$	[946]	$1.86^{+0.10+0.07}_{-0.06-0.03}$	$0.37^{+0.20}_{-0.31} \pm 0.15$
FOCUS	$(D^0;\ \ell = \mu)$	[947]	$1.91^{+0.30}_{-0.15} \pm 0.07$	–
Belle	$(D^0;\ \ell = e,\mu)$	[942]	$1.97 \pm 0.08 \pm 0.04$	$0.10 \pm 0.21 \pm 0.10$
CLEO-c (tagged)	$(D^0, D^+;\ \ell = e)$	[944]	$1.91 \pm 0.02 \pm 0.01$	$0.21 \pm 0.07 \pm 0.02$
CLEO-c (untagged)	$(D^0;\ \ell = e)$	[945]	$1.87 \pm 0.03 \pm 0.01$	$0.37 \pm 0.08 \pm 0.03$
CLEO-c (untagged)	$(D^+;\ \ell = e)$	[945]	$1.97 \pm 0.07 \pm 0.02$	$0.14 \pm 0.16 \pm 0.04$
BES III	$(D^0;\ \ell = e)$	[940]	$1.911 \pm 0.012 \pm 0.004$	$0.279 \pm 0.035 \pm 0.011$
BABAR	$(D^0;\ \ell = e)$	[939]	$1.906 \pm 0.029 \pm 0.023$	$0.268 \pm 0.074 \pm 0.059$

to using the standard outer function $\phi(q^2, t_0)$ of Eq. (240) and $t_0 = t_+\left(1 - \sqrt{1 - t_-/t_+}\right)$. This choice of t_0 constrains $|z|$ to vary between $\pm z_{max.}$

8.5.8 Combined results for the $D \to K\ell\nu_\ell$ channel

The q^2 distribution provided by each individual measurement is used to determine a combined result by performing a fit to the z-expansion formalism at second order. Results for the form factor normalization $f_+^K(0)|V_{cs}|$ and the shape parameters r_1 and r_2 for each individual measurement and for the combination is presented in Table 238. Measurements have been corrected with respect to the original ones using recent values from PDG [314]. This includes updated branching fractions of normalization channels, corrected CKM matrix elements and the D meson lifetime. The *BABAR* measurement has been corrected accounting for final-state radiation. The result for the $D^+ \to \overline{K}^0_L e^+\nu_e$ decay channel from BES III [941] is included as a constraint in the combined result since correlation matrices are not provided. Correlation coefficients of the parameters are quoted in the last column of Table 238. The χ^2 per degree of freedom is 114.7/101. Results are shown in Figure 170.

Combined values for the electron and muon channels are obtained in terms of $D \to Ke\nu_e$,

Table 236: Results for r_1 and r_2 from various experiments for the $D \to K\ell\nu_\ell$ decay channel. The correlation coefficient between these parameters is larger than 0.9.

Expt. $D \to K\ell\nu_\ell$	Mode	Ref.	r_1	r_2
BABAR	$(D^0; \ell = e)$	[943]	$-2.5 \pm 0.2 \pm 0.2$	$0.6 \pm 6.0 \pm 5.0$
CLEO-c (tagged)	$(D^0; \ell = e)$	[944]	$-2.65 \pm 0.34 \pm 0.08$	$13 \pm 9 \pm 1$
CLEO-c (tagged)	$(D^+; \ell = e)$	[944]	$-1.66 \pm 0.44 \pm 0.10$	$-14 \pm 11 \pm 1$
CLEO-c (untagged)	$(D^0; \ell = e)$	[945]	$-2.4 \pm 0.4 \pm 0.1$	$21 \pm 11 \pm 2$
CLEO-c (untagged)	$(D^+; \ell = e)$	[945]	$-2.8 \pm 6 \pm 2$	$32 \pm 18 \pm 4$
BES III	$(D^0; \ell = e)$	[940]	$-2.334 \pm 0.159 \pm 0.080$	$3.42 \pm 3.91 \pm 2.41$
BES III	$(D^+; \ell = e)$	[941]	$-2.23 \pm 0.42 \pm 0.53$	$11.3 \pm 8.5 \pm 8.7$

Table 237: Results for r_1 and r_2 from various experiments, for $D \to \pi\ell\nu_\ell$. The correlation coefficient between these parameters is larger than 0.9.

Expt. $D \to \pi\ell\nu_\ell$	Mode	Ref.	r_1	r_2
CLEO-c (tagged)	$(D^0; \ell = e)$	[944]	$-2.80 \pm 0.49 \pm 0.04$	$6 \pm 3 \pm 0$
CLEO-c (tagged)	$(D^+; \ell = e)$	[944]	$-1.37 \pm 0.88 \pm 0.24$	-4 ± 5 ± 1
CLEO-c (untagged)	$(D^0; \ell = e)$	[945]	$-2.1 \pm 0.7 \pm 0.3$	$-1.2 \pm 4.8 \pm 1.7$
CLEO-c (untagged)	$(D^+; \ell = e)$	[945]	$-0.2 \pm 1.5 \pm 0.4$	$-9.8 \pm 9.1 \pm 2.1$
BES III	$(D^0; \ell = e)$	[940]	$-1.85 \pm 0.22 \pm 0.07$	$-1.4 \pm 1.5 \pm 0.5$
BABAR	$(D^0; \ell = e)$	[939]	$-1.31 \pm 0.70 \pm 0.43$	$-4.2 \pm 4.0 \pm 1.9$

after having corrected the measurements with muons for the reduction of phase space and for the $f_0(q^2)$ contribution [958]. Channels with a D^0 or a D^+ are combined assuming isospin invariance and using physical meson and lepton masses. These combined results are noted as $D \to K\ell\nu_\ell$ in the following. Hadronic form factors are assumed to be the same for charged and neutral D mesons. Results for the $D^0 \to K^-\ell^+\nu_\ell$ and $D^+ \to \overline{K}^0\ell^+\nu_\ell$ decay channels are shown separately in Table 239 and Figure 169. Using the fitted parameters and integrating over the full q^2 range, the combined semileptonic branching fraction, expressed in terms of the D^0 decay channel gives:

$$\mathcal{B}(D^0 \to K^-\ell^+\nu_\ell) = (3.490 \pm 0.011 \pm 0.020)\% \tag{244}$$

Data from the different experiments are also fitted within the three-pole form factor formalism. Constraints on the first and second poles are imposed using information of the $D_s^*(2112)$ and $D_{s1}^*(2700)$ resonances. The superconvergence condition of Eq. 243 is applied. Results are presented in Table 240. Fitted parameters are the first two residues $\gamma_0^K = \underset{q^2=m^2_{D_s^*(2112)}}{\text{Res}} f_+^K(q^2)$ and $\gamma_1^\pi = \underset{q^2=m^2_{D_{s1}^*(2700)}}{\text{Res}} f_+^K(q^2)$ and an effective mass, $m_{D_{s\,\text{eff}}^{*\prime\prime}}$, accounting for higher mass hadronic contributions. It is found that the fitted effective third pole is larger than the mass of the second radial excitation, around 3.2 GeV, as expected. The contribution to the form factor

Table 238: Results of the fits to $D \to K\ell\nu_\ell$ measurements from several experiments, using the z-expansion formalism of the form factor at second order in the expansion. External inputs have been updated to the corresponding ones from PDG [314]. The correlation coefficients listed in the sixth column refer to $\rho_{12} \equiv \rho_{|V_{cs}|f_+^K(0),r_1}$, $\rho_{13} \equiv \rho_{|V_{cs}|f_+^K(0),r_2}$, and $\rho_{23} \equiv \rho_{r_1,r_2}$ and are for the total uncertainties (statistical $\oplus$ systematic). The result for the $D^+ \to \overline{K}^0_L e^+\nu_e$ decay channel from BES III [941] is included in the combined results as a constraint on the normalization, $|V_{cs}|f_+^K(0)$. The entry *others* refers to total decay rates measured by Mark-III [948], E653 [949, 950], E687 [951, 952], E691 [953], BES II [954, 955] and CLEO II [956].

Expt. $D \to K\ell\nu_\ell$	Mode	$\lvert V_{cs}\rvert f_+^K(0)$	r_1	r_2	$\rho_{12}/\rho_{13}/\rho_{23}$
BES III (tagged) [940]	(D^0)	0.7195(35)(43)	−2.33(16)(8)	3.4(4.0)(2.5)	−0.21/0.58/−0.81
CLEO-c (tagged) [944]	(D^0, D^+)	0.7189(64)(48)	−2.29(28)(27)	3.0(7.0)(1.0)	−0.19/0.58/−0.81
CLEO-c (untagged) [945]	(D^0, D^+)	0.7436(76)(79)	−2.57(33)(18)	23.9(8.9)(4.3)	−0.34/0.66/−0.84
BABAR [943]	(D^0)	0.7241(64)(60)	−2.45(20)(18)	−0.6(6.0)(3.8)	−0.36/0.59/−0.82
Belle [942]	(D^0)	0.700(19)	−3.06(71)	−3.3(17.9)	−0.20/0.66/−0.81
FOCUS [947] and others		0.724(29)	−2.54(75)	7.0(12.8)	−0.02/0.02/−0.97
Combined	(D^0, D^+)	**0.7226(22)(26)**	**−2.38(11)(6)**	**4.7(2.6)(1.4)**	**−0.19/0.51/−0.84**

Table 239: Results for the $D^0 \to K^-\ell^+\nu_\ell$ and $D^+ \to \overline{K}^0\ell^+\nu_\ell$ decays channels using the z-expansion formalism at second order.

Fit value	$D^0 \to K^-\ell^+\nu_\ell$	$D^+ \to \overline{K}^0\ell^+\nu_\ell$
$\lvert V_{cs}\rvert f_+^K(0)$	$0.7219 \pm 0.0024 \pm 0.0027$	$0.726 \pm 0.005 \pm 0.007$
r_1	$-2.41 \pm 0.11 \pm 0.07$	$-2.07 \pm 0.38 \pm 0.10$
r_2	$4.7 \pm 2.7 \pm 1.4$	$5.4 \pm 8.2 \pm 4.6$
$\rho_{12}/\rho_{13}/\rho_{23}$	$-0.19/0.51/-0.84$	$-0.10/0.39/-0.84$

by only the D_s^* resonance is disfavoured by the data. Figure 168 (left) shows the result of the fitted form factors for the z-expansion and three-pole parametrizations.

8.5.9 Combined results for the $D \to \pi\ell\nu_\ell$ channel

The combined result for the $D \to \pi\ell\nu_\ell$ decay channel is obtained from a fit to *BABAR*, Belle, BES III, and CLEO-c data, with updated input values from [314]. The available measurements are fitted in bins of q^2 to the z-expansion model at second order. Results of the individual fits for each experiment and the combined result are shown in Table 241. The χ^2 per degree of freedom of the combined fit is 51/55.

Using the fitted parameters and integrating over the full q^2 range, the combined semileptonic branching fraction, expressed in terms of the D^0 decay channel gives:

$$\mathcal{B}(D^0 \to \pi^-\ell^+\nu_\ell) = (2.891 \pm 0.030 \pm 0.022) \times 10^{-3} \tag{245}$$

Results of the three-pole model to the $D \to \pi\ell\nu_\ell$ data are shown in Table 242. Fitted parameters are the first two residues $\gamma_0^\pi = \operatorname*{Res}_{q^2=m_{D^*}^2} f_+^\pi(q^2)$ and $\gamma_1^\pi = \operatorname*{Res}_{q^2=m_{D^{*\prime}}^2} f_+^\pi(q^2)$ (which are constrained using present measurements of masses and widths of the $D^*(2010)$ and $D^{*\prime}(2600)$ mesons, and lattice computations of decay constants, following [933]), and an effective mass,

Table 240: Results of the three-pole model form factors obtained from a fit to all measurements. Fitted parameters are the first two residues γ_0^K and γ_1^K, which are constrained using present measurements of masses and widths of the D_s^* and D_{s1}^* mesons, and lattice computations of decay constants, and the effective mass, $m_{D_{s\,\mathrm{eff}}^{*\prime\prime}}$, accounting for higher mass hadronic contributions.

Parameter	Combined result ($D \to K\ell\nu_\ell$)
γ_0^K	4.85 ± 0.08 GeV^2
γ_1^K	-1.2 ± 0.30 GeV^2
$m_{D_{s\,\mathrm{eff}}^{*\prime\prime}}$	4.46 ± 0.26 GeV

Table 241: Results of the fits to $D \to \pi\ell\nu_\ell$ measurements from several experiments, using the z-expansion formalism of the form factor at second order in the expansion. External inputs are updated to the corresponding ones from PDG [314]. The correlation coefficients listed in the sixth column refer to $\rho_{12} \equiv \rho_{|V_{cd}|f_+^\pi(0),r_1}$, $\rho_{13} \equiv \rho_{|V_{cd}|f_+^\pi(0),r_2}$, and $\rho_{23} \equiv \rho_{r_1,r_2}$ and are for the total uncertainties (statistical $\oplus$ systematic).

Expt. $D \to \pi\ell\nu_\ell$	mode	$\lvert V_{cd}\rvert f_+^\pi(0)$	r_1	r_2	$\rho_{12}/\rho_{13}/\rho_{23}$
BES III (tagged) [940]	(D^0)	0.1422(25)(10)	−1.86(23)(7)	−1.24(1.51)(47)	−0.37/0.64/−0.93
CLEO-c (tagged) [944]	(D^0, D^+)	0.1507(42)(11)	−2.45(43)(9)	3.8(2.8)(6)	−0.43/0.67/−0.94
CLEO-c (untagged) [945]	(D^0, D^+)	0.1394(58)(25)	−1.71(62)(25)	−2.8(4.0)(1.6)	−0.50/0.69/−0.96
BABAR [943]	(D^0)	0.1381(36)(22)	−1.42(66)(45)	−3.5(3.7)(2.0)	−0.40/0.57/−0.97
Belle [942]	(D^0)	0.142(11)	−1.83(1.00)	1.5(6.5)	−0.30/0.59/−0.91
Combined	(D^0, D^+)	**0.1426(17)(8)**	**−1.95(18)(1)**	**−0.52(1.17)(32)**	**−0.37/0.63/−0.94**

$m_{D_{\mathrm{eff}}^{*\prime\prime}}$, accounting for higher mass hadronic contributions. The V_{cd} value enters in the fit; the value used is that prescribed by unitarity in Eq. 246. The χ^2 per degree of freedom of the combined fit is 57.5/57.

The result for the effective mass $m_{D_{\mathrm{eff}}^{*\prime\prime}}$ is larger than the mass of the second radially excited state with $J^P = 1^-$ (~ 3.11 GeV), indicating that more contributions are needed to explain the form factor. Figure 168 (right) shows the result of the combined form factor for the z-expansion and three-pole parameterizations.

8.5.10 V_{cs} and V_{cd} determination

Assuming unitarity of the CKM matrix, the values of the CKM matrix elements entering in charm semileptonic decays are known from the V_{ud}, V_{td} and V_{cb} elements [314]:

$$\begin{aligned} V_{cs} &= 0.97343 \pm 0.00015\,, \\ V_{cd} &= 0.22521 \pm 0.00061\,. \end{aligned} \tag{246}$$

Using the combined values of $f_+^K(0)|V_{cs}|$ and $f_+^\pi(0)|V_{cd}|$ in Tables 238 and 241, this leads to the form factor values:

$$\begin{aligned} f_+^K(0) &= 0.7423 \pm 0.0035\,, \\ f_+^\pi(0) &= 0.6327 \pm 0.0086\,, \end{aligned}$$

Table 242: Results of the three-pole model to *BABAR*, Belle, BES III and CLEO-c (tagged and untagged) data. Fitted parameters are the first two residues γ_0^π and γ_1^π, which are constrained using present measurements of masses and widths of the D^* and $D^{*'}$ mesons, and lattice computations of decay constants, and the effective mass, $m_{D^{*\prime\prime}_{\rm eff}}$, accounting for higher mass hadronic contributions.

Parameter	Combined result ($D \to \pi\ell\nu_\ell$)
γ_0^π	3.881 $\pm$ 0.093 GeV^2
γ_1^π	-1.18 $\pm$ 0.30 GeV^2
$m_{D^{*\prime\prime}_{\rm eff}}$	4.17 $\pm$ 0.42 GeV

which are in agreement with present lattice QCD computations [210]: $f_+^K(0) = 0.747 \pm 0.019$ and $f_+^\pi(0) = 0.666 \pm 0.029$ but more precise. If on the contrary one assumes the lattice QCD form factor values, one obtains for the CKM matrix elements using the combined results in Tables 238 and 241:

$$V_{cs} = 0.967 \pm 0.025\,,$$
$$V_{cd} = 0.2140 \pm 0.0097\,,$$

still compatible with unitarity of the CKM matrix.

8.5.11 $D \to V\bar{\ell}\nu_\ell$ decays

When the final state hadron is a vector meson, the decay can proceed through both vector and axial vector currents, and four form factors are needed. The hadronic current is $H_\mu = V_\mu + A_\mu$, where [926]

$$V_\mu = \langle V(p,\varepsilon)|\bar{q}\gamma_\mu c|D(p')\rangle = \frac{2V(q^2)}{m_D + m_V}\varepsilon_{\mu\nu\rho\sigma}\varepsilon^{*\nu}p'^\rho p^\sigma \tag{247}$$

$$\begin{aligned} A_\mu = \langle V(p,\varepsilon)|-\bar{q}\gamma_\mu\gamma_5 c|D(p')\rangle &= -i\,(m_D + m_V)A_1(q^2)\varepsilon_\mu^* \\ &+ i\frac{A_2(q^2)}{m_D + m_V}(\varepsilon^*\cdot q)(p' + p)_\mu \\ &+ i\,\frac{2m_V}{q^2}\left(A_3(q^2) - A_0(q^2)\right)[\varepsilon^*\cdot(p' + p)]q_\mu\,. \end{aligned} \tag{248}$$

In this expression, m_V is the daughter meson mass and

$$A_3(q^2) = \frac{m_D + m_V}{2m_V}A_1(q^2) - \frac{m_D - m_V}{2m_V}A_2(q^2)\,. \tag{249}$$

Kinematics require that $A_3(0) = A_0(0)$. Terms proportional to q_μ are only important for the case of τ leptons. Thus, only three form factors are relevant in these decays: $A_1(q^2)$, $A_2(q^2)$

and $V(q^2)$. The differential partial width is

$$\frac{d\Gamma(D \to V\bar{\ell}\nu_\ell)}{dq^2\, d\cos\theta_\ell} = \frac{G_F^2\,|V_{cq}|^2}{128\pi^3 m_D^2}\, p^*\, q^2 \times \left[\frac{(1-\cos\theta_\ell)^2}{2}|H_-|^2 + \frac{(1+\cos\theta_\ell)^2}{2}|H_+|^2 + \sin^2\theta_\ell |H_0|^2\right], \quad (250)$$

where $H_\pm$ and H_0 are helicity amplitudes given by

$$H_\pm = \frac{1}{m_D + m_V}\left[(m_D+m_V)^2 A_1(q^2) \mp 2m_D\, p^* V(q^2)\right] \quad (251)$$

$$H_0 = \frac{1}{|q|}\frac{m_D^2}{2m_V(m_D+m_V)} \times \left[\left(1 - \frac{m_V^2 - q^2}{m_D^2}\right)(m_D+m_V)^2 A_1(q^2) - 4p^{*2} A_2(q^2)\right]. \quad (252)$$

p^* is the magnitude of the three-momentum of the V system, measured in the D rest frame, and θ_ℓ is defined in Figure 171 for the electron case (θ_e). The left-handed nature of the quark current manifests itself as $|H_-| > |H_+|$. The differential decay rate for $D \to V\ell\nu$ followed by the vector meson decaying into two pseudoscalars is

$$\begin{aligned}\frac{d\Gamma(D\to V\ell\nu, V\to P_1P_2)}{dq^2 d\cos\theta_V d\cos\theta_\ell d\chi} = {} & \frac{3G_F^2}{2048\pi^4}|V_{cq}|^2 \frac{p^*(q^2)q^2}{m_D^2}\mathcal{B}(V\to P_1P_2) \times \\ & \Big\{(1+\cos\theta_\ell)^2\sin^2\theta_V |H_+(q^2)|^2 \\ & + (1-\cos\theta_\ell)^2\sin^2\theta_V |H_-(q^2)|^2 \\ & + 4\sin^2\theta_\ell\cos^2\theta_V |H_0(q^2)|^2 \\ & + 4\sin\theta_\ell(1+\cos\theta_\ell)\sin\theta_V\cos\theta_V\cos\chi H_+(q^2)H_0(q^2) \\ & - 4\sin\theta_\ell(1-\cos\theta_\ell)\sin\theta_V\cos\theta_V\cos\chi H_-(q^2)H_0(q^2) \\ & - 2\sin^2\theta_\ell\sin^2\theta_V\cos 2\chi H_+(q^2)H_-(q^2)\Big\}, \end{aligned} \quad (253)$$

where the angles θ_ℓ, θ_V, and χ are defined in Fig. 171.

Ratios between the values of the hadronic form factors expressed at $q^2 = 0$ are usually introduced:

$$r_V \equiv V(0)/A_1(0), \qquad r_2 \equiv A_2(0)/A_1(0)\,. \quad (254)$$

Table 243 lists measurements of r_V and r_2 from several experiments. Most of the measurements assume that the q^2 dependence of hadronic form factors is given by the simple pole ansatz. Some of these measurements do not consider a S-wave contribution and it is included in the measured values. The measurements are plotted in Fig. 172 which shows that they are all consistent.

8.5.12 S-wave component

In 2002 FOCUS reported [970] an asymmetry in the observed $\cos(\theta_V)$ distribution. This is interpreted as evidence for an S-wave component in the decay amplitude as follows. Since H_0

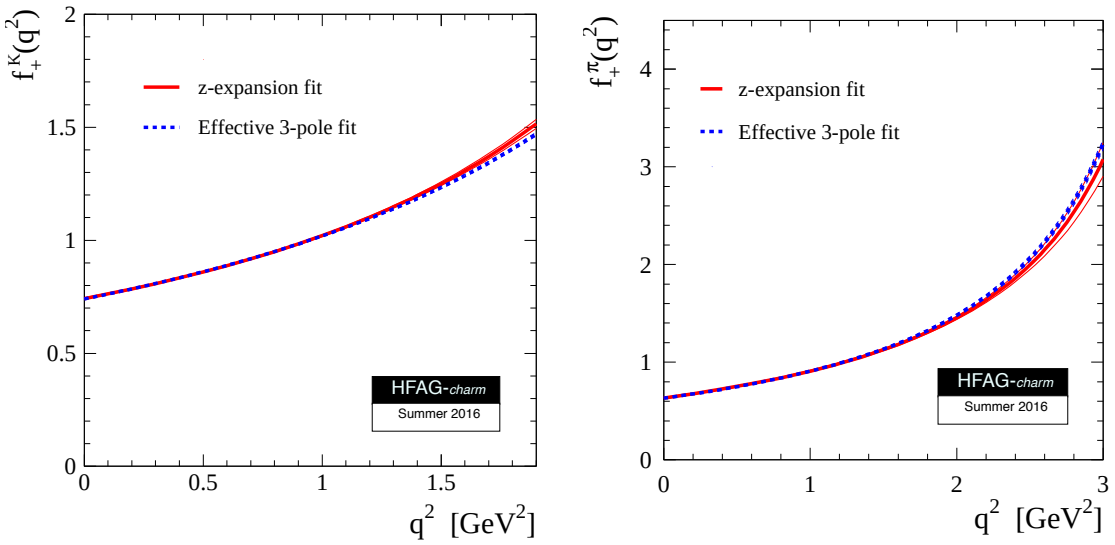

Figure 168: Form factors as function of q^2 for the $D \to K\ell\nu_\ell$ (left) and $D \to \pi\ell\nu_\ell$ (right) channels, obtained from a fit to all experimental data. Central values (central lines) and uncertainties (one σ deviation) are shown for the z-expansion and the 3-pole parameterization.

Table 243: Results for r_V and r_2 from various experiments.

Experiment	Ref.	r_V	r_2
$D^+ \to \overline{K}^{*0} l^+ \nu$			
E691	[959]	2.0± 0.6± 0.3	0.0± 0.5± 0.2
E653	[960]	2.00± 0.33± 0.16	0.82± 0.22± 0.11
E687	[961]	1.74± 0.27± 0.28	0.78± 0.18± 0.11
E791 (e)	[962]	1.90± 0.11± 0.09	0.71± 0.08± 0.09
E791 (μ)	[963]	1.84±0.11±0.09	0.75±0.08±0.09
Beatrice	[964]	1.45± 0.23± 0.07	1.00± 0.15± 0.03
FOCUS	[965]	1.504±0.057±0.039	0.875±0.049±0.064
$D^0 \to \overline{K}^0 \pi^- \mu^+ \nu$			
FOCUS	[966]	1.706±0.677±0.342	0.912±0.370±0.104
BABAR	[967]	$1.493 \pm 0.014 \pm 0.021$	$0.775 \pm 0.011 \pm 0.011$
$D_s^+ \to \phi\, e^+ \nu$			
BABAR	[968]	1.849±0.060±0.095	0.763±0.071±0.065
$D^0, D^+ \to \rho\, e\nu$			
CLEO	[969]	1.40±0.25±0.03	0.57±0.18±0.06

typically dominates over $H_\pm$, the distribution given by Eq. (253) is, after integration over χ, roughly proportional to $\cos^2\theta_V$. Inclusion of a constant S-wave amplitude of the form $A\,e^{i\delta}$ leads to an interference term proportional to $|AH_0 \sin\theta_\ell \cos\theta_V|$; this term causes an asymmetry in $\cos(\theta_V)$. When FOCUS fit their data including this S-wave amplitude, they obtained $A = 0.330 \pm 0.022 \pm 0.015$ GeV^{-1} and $\delta = 0.68 \pm 0.07 \pm 0.05$ [965].

More recently, both *BABAR* [968] and CLEO-c [971] have also found evidence for an f_0 component in semileptonic D_s decays.

8.5.13 Model-independent form factor measurement

Subsequently the CLEO-c collaboration extracted the form factors $H_+(q^2)$, $H_-(q^2)$, and $H_0(q^2)$ in a model-independent fashion directly as functions of q^2 [972] and also determined the S-wave form factor $h_0(q^2)$ via the interference term, despite the fact that the $K\pi$ mass distribution appears dominated by the vector $K^*(892)$ state. Their results are shown in Figs. 173 and 174. Plots in Fig. 174 clearly show that $H_0(q^2)$ dominates over essentially the full range of q^2, but especially at low q^2. They also show that the transverse form factor $H_t(q^2)$, which can be related to $A_3(q^2)$, is small compared to lattice gauge theory calculations and suggest that the form factor ratio $r_3 \equiv A_3(0)/A_1(0)$ is large and negative.

The product $H_0(q^2) \times h_0(q^2)$ is shown in Fig. 173 and clearly indicates the existence of $h_0(q^2)$, although it seems to fall faster with q^2 than $H_0(q^2)$. The other plots in this figure show that D- and F-wave versions of the S-wave $h_0(q^2)$ are not significant.

8.5.14 Detailed measurements of the $D^+ \to K^-\pi^+e^+\nu_e$ decay channel

BABAR [967] has selected a large sample of 244×10^3 signal candidates with a ratio $S/B \sim 2.3$ from an analyzed integrated luminosity of 347 fb^{-1}. With four particles emitted in the final state, the differential decay rate depends on five variables. In addition to the four variables defined in previous sections there is m^2, the mass squared of the $K\pi$ system. Apart from this last variable, the reconstruction algorithm does not provide a high resolution on the other measured quantities and a multi-dimensional unfolding procedure is not used to correct for efficiency and resolution effects. However, these limitations still allow an essentially model independent measurement of the differential decay rate. This is because, apart from the q^2 and mass dependence of the form factors, angular distributions are fixed by kinematics. In addition, present accurate measurements of $D \to P\bar{\ell}\nu_\ell$ decays have shown that the q^2 dependence of the form factors can be well described by several models as long as the corresponding model parameter(s) are fitted from data. This is even more true in $D \to V\bar{\ell}\nu_\ell$ decays because the q^2 range is reduced. To analyze the $D^+ \to K^-\pi^+e^+\nu_e$ decay channel it is assumed that all form factors have a q^2 variation given by the simple pole model and the effective pole mass value, $m_A = (2.63 \pm 0.10 \pm 0.13)$ GeV/c^2, is fitted for the axial vector form factors. This value is compatible with expectations when comparing with the mass of $J^P = 1^+$ charm mesons. Data are not sensitive to the effective mass of the vector form factor for which $m_V = (2.1 \pm 0.1)$ GeV/c^2 is used, nor to the effective pole mass of the scalar component for which m_A is used. For the mass dependence of the form factors, a Breit-Wigner with a mass dependent width and a Blatt-Weisskopf damping factor is used. For the S-wave amplitude, considering what was measured in $D^+ \to K^-\pi^+\pi^+$ decays, a polynomial variation below the $\overline{K}_0^*(1430)$ and a Breit-Wigner distribution, above are assumed. For the polynomial part, a linear term is sufficient to fit data.

It is verified that the variation of the S-wave phase is compatible with expectations from elastic $K\pi$ scattering, according to the Watson theorem. At variance with elastic scattering, a negative relative sign between the S- and P-waves is measured; this is compatible with the previous theorem. In Fig. 175, the measured S-wave phase is compared with the phase of the elastic, $I = 1/2$, $K\pi$ phase for different values of the $K\pi$ mass.

Contributions from other resonances decaying into $K^-\pi^+$ are considered. A small signal from the $\overline{K}^*(1410)$ is observed, compatible with expectations from τ decays and this component is included in the nominal fit. In total, 11 parameters are fitted in addition to the total number of signal events. They give a detailed description of the differential decay rate versus the 5 variables and corresponding matrices for statistical and systematic uncertainties are provided allowing to evaluate the compatibility of data with future theoretical expectations. Results of this analysis for the rates and few characteristics for S, P and D-waves are given in Table 244.

In Fig. 176, measured values from CLEO-c of the products $q^2H_0^2(q^2)$ and $q^2h_0(q^2)H_0(q^2)$ are compared with corresponding results from *BABAR* illustrating the difference in behavior of the scalar h_0 component and the helicity zero H_0 P-wave form factor. For this comparison, the plotted values from *BABAR* for the two distributions are fixed to 1 at $q^2 = 0$. The different behavior of $h_0(q^2)$ and $H_0(q^2)$ can be explained by their different dependence in the p^* variable.

Table 244: Detailed determination of the properties of the $D^+ \to K^-\pi^+e^+\nu_e$ decay channel, from *BABAR* [967]. The third error listed for the branching fractions corresponds to uncertainty in the branching fraction of the normalization channel ($D^+ \to K^-\pi^+\pi^+$). Values for $\mathcal{B}(D^+ \to \overline{K}^*(1410)^0/\overline{K}_2^*(1430)^0e^+\nu_e)$ are corrected for the $\overline{K}^{*0}$ branching fractions into $K^-\pi^+$.

Measurement	***BABAR* result**
$m_{K^*(892)^0}(\mathrm{MeV}/c^2)$	$895.4 \pm 0.2 \pm 0.2$
$\Gamma^0_{K^*(892)^0}(\mathrm{MeV}/c^2)$	$46.5 \pm 0.3 \pm 0.2$
$r_{BW}(\mathrm{GeV}/c)^{-1}$	$2.1 \pm 0.5 \pm 0.5$
r_V	$1.463 \pm 0.017 \pm 0.031$
r_2	$0.801 \pm 0.020 \pm 0.020$
$m_A(\mathrm{GeV}/c^2)$	$2.63 \pm 0.10 \pm 0.13$
$\mathcal{B}(D^+ \to K^-\pi^+e^+\nu_e)\,(\%)$	$4.04 \pm 0.03 \pm 0.04 \pm 0.09$
$\mathcal{B}(D^+ \to K^-\pi^+e^+\nu_e)_{\overline{K}^{*0}}\,(\%)$	$3.80 \pm 0.04 \pm 0.05 \pm 0.09$
$\mathcal{B}(D^+ \to K^-\pi^+e^+\nu_e)_{S-\mathrm{wave}}\,(\%)$	$0.234 \pm 0.007 \pm 0.007 \pm 0.005$
$\mathcal{B}(D^+ \to \overline{K}^*(1410)^0e^+\nu_e)\,(\%)$	$0.30 \pm 0.12 \pm 0.18 \pm 0.06$ (< 0.6 at 90% C.L.)
$\mathcal{B}(D^+ \to \overline{K}_2^*(1430)^0e^+\nu_e)\,(\%)$	$0.023 \pm 0.011 \pm 0.011 \pm 0.001$ (< 0.05 at 90% C.L.)

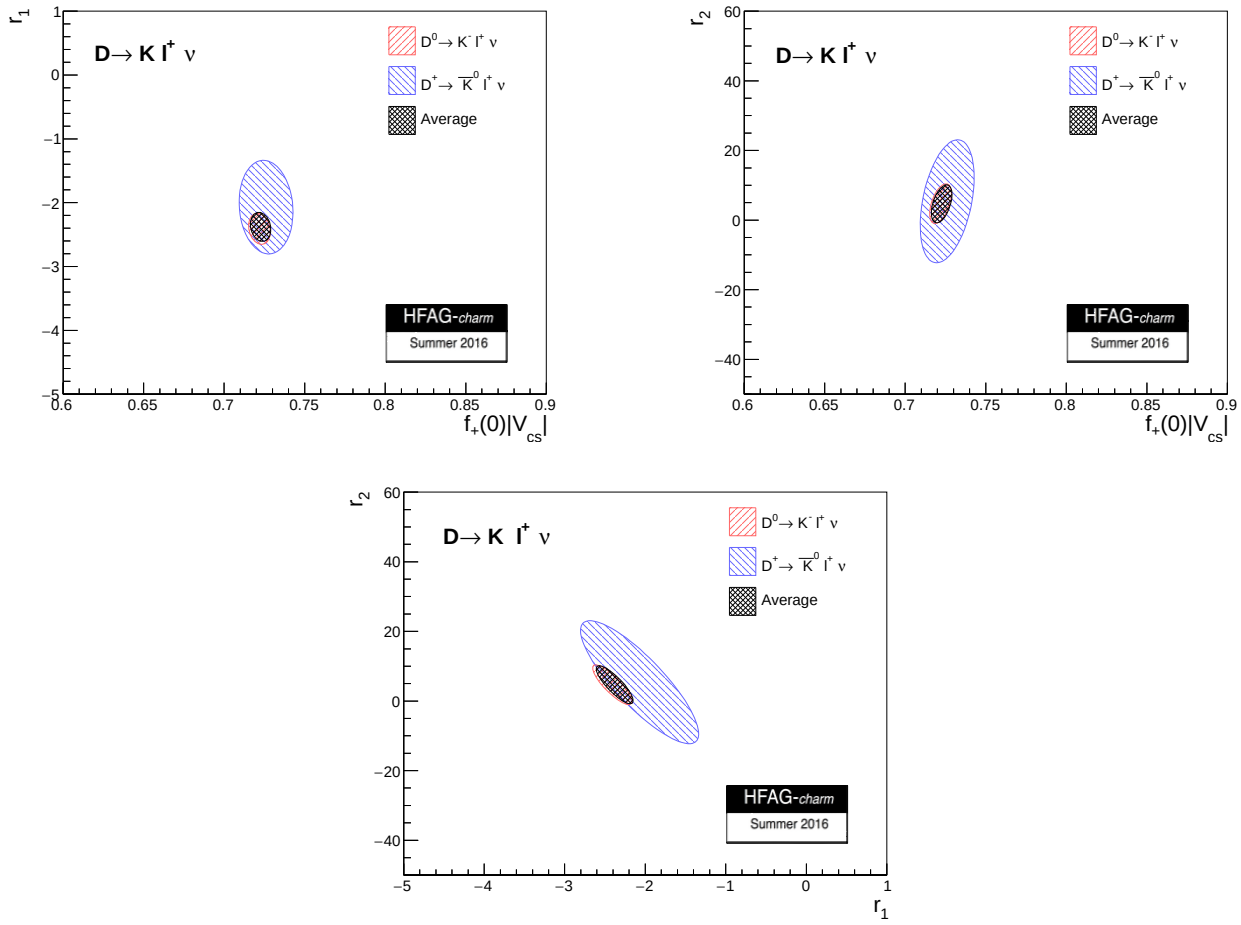

Figure 169: Results of the combined fit shown separately for the $D^0 \to K^-\ell^+\nu$ and $D^+ \to \overline{K}^0\ell^+\nu$ decay channels. Ellipses are shown for 68% C.L.

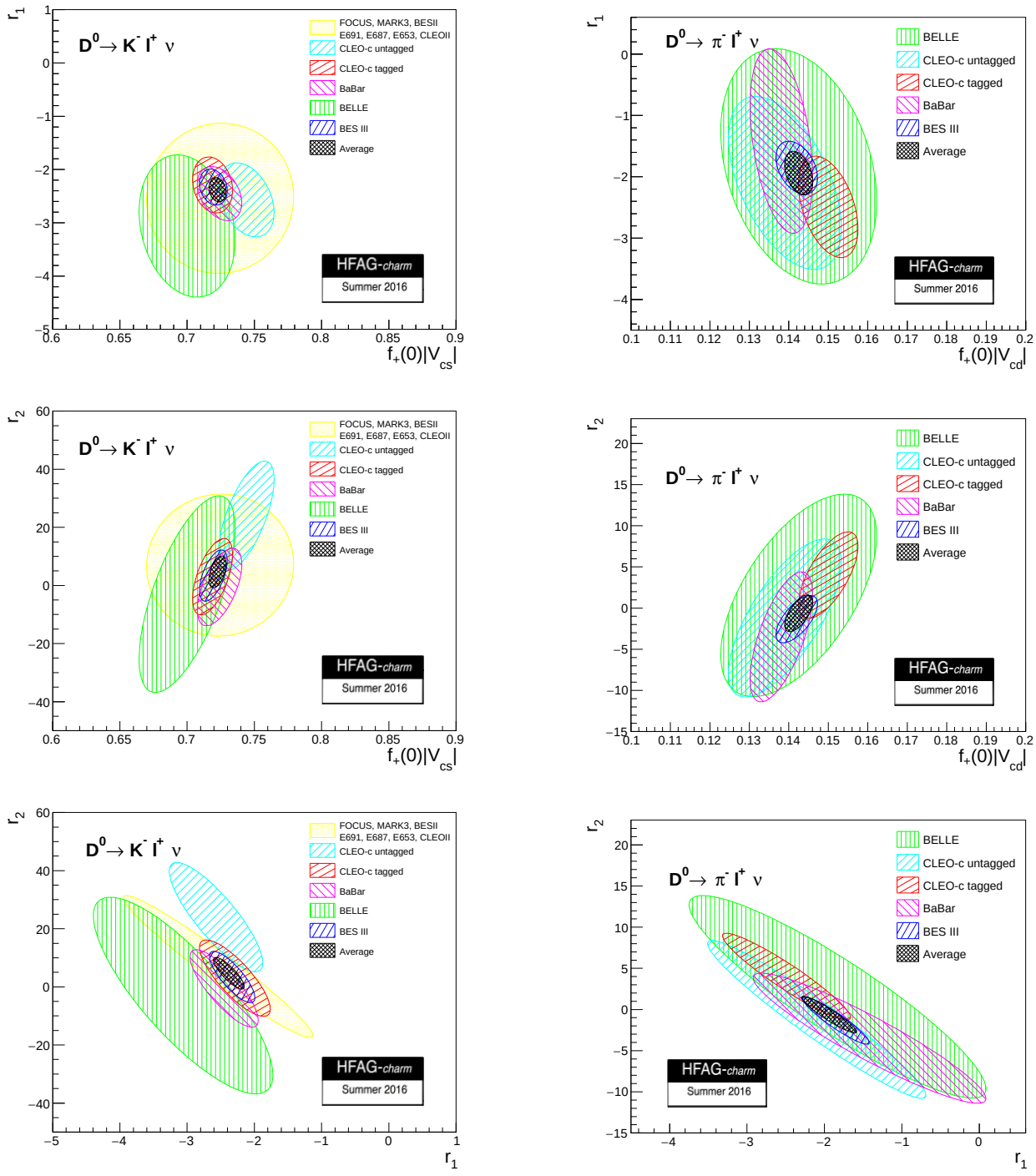

Figure 170: The $D^0 \to K^-\ell^+\nu$ (left) and $D^0 \to \pi^-\ell^+\nu$ (right) 68% C.L. error ellipses from the average fit of the 3-parameter z-expansion results.

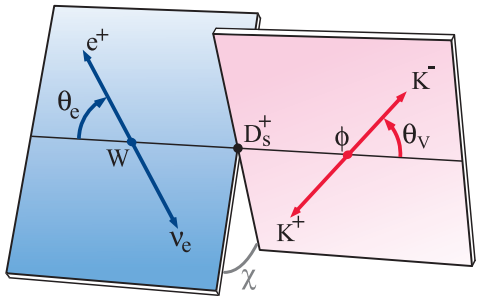

Figure 171: Decay angles θ_V, θ_ℓ and χ. Note that the angle χ between the decay planes is defined in the D-meson reference frame, whereas the angles θ_V and θ_ℓ are defined in the V meson and W reference frames, respectively.

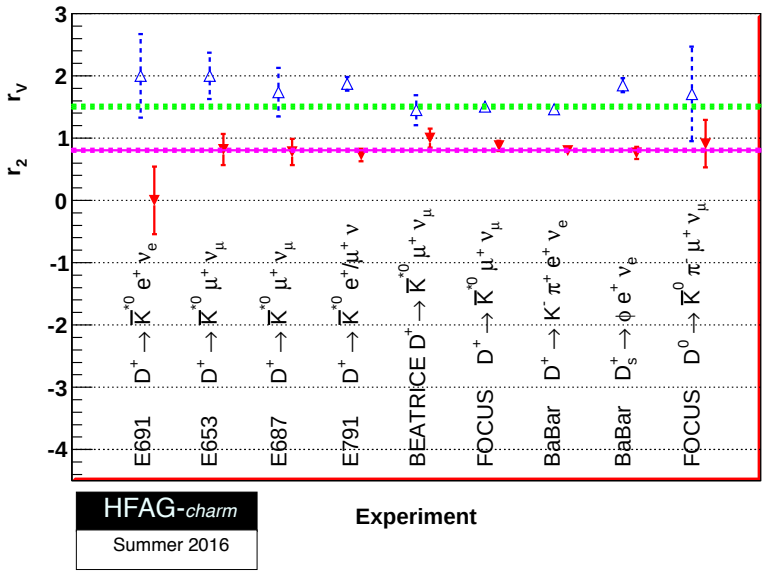

Figure 172: A comparison of r_2 (filled inverted triangles) and r_V (open triangles) values from various experiments. The first seven measurements are for $D^+ \to K^-\pi^+l^+\nu_l$ decays. Also shown as a line with 1-σ limits is the average of these. The last two points are D_s^+ decays and Cabibbo-suppressed D decays.

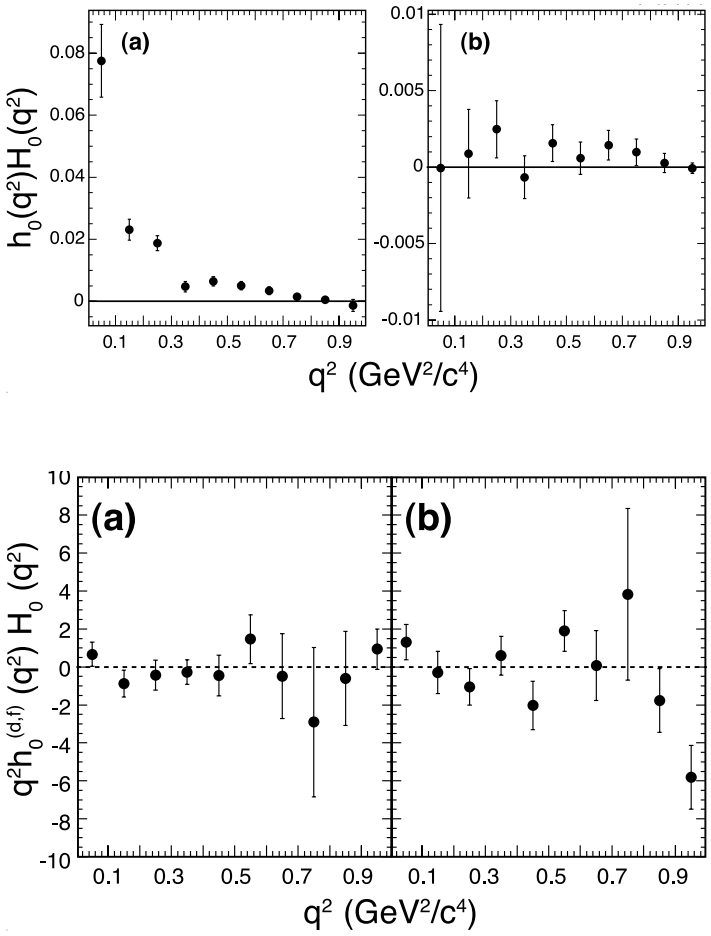

Figure 173: Model-independent form factors $h_0(q^2)$ measured by CLEO-c [972].

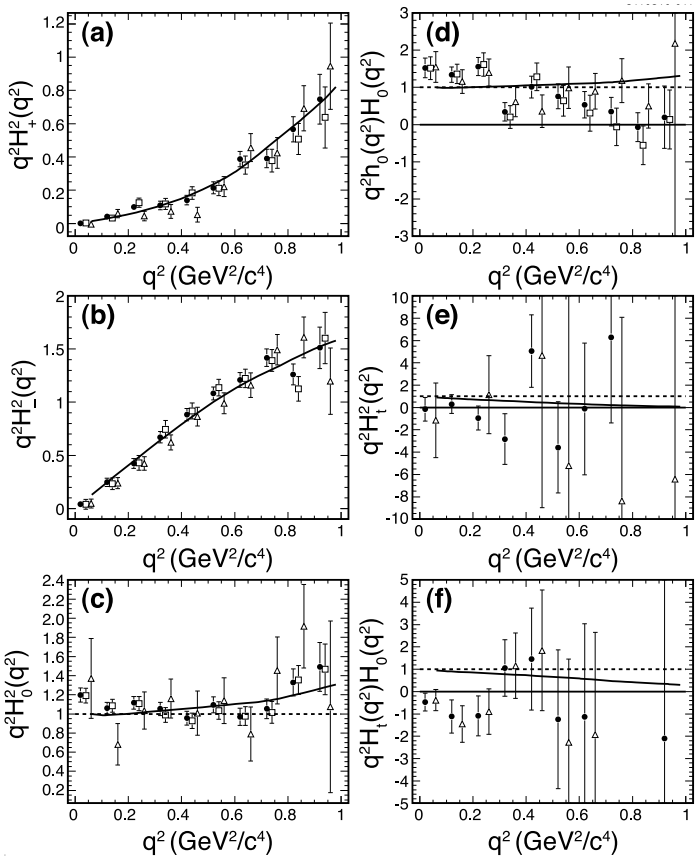

Figure 174: Model-independent form factors $H(q^2)$ measured by CLEO-c [972].

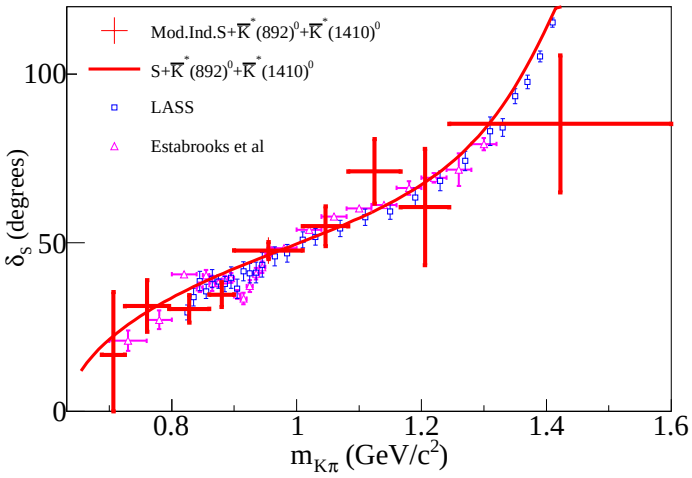

Figure 175: Points (full circles) give the *BABAR* S-wave phase variation assuming a signal containing S-wave, $\overline{K}^*(892)^0$ and $\overline{K}^*(1410)^0$ components [967]. Error bars include systematic uncertainties. The full line corresponds to a parameterized S-wave phase variation fitted on *BABAR* data. The phase variation measured in $K\pi$ scattering by Ref. [973] (triangles) and LASS [330] (squares), after correcting for $\delta^{3/2}$, are given.

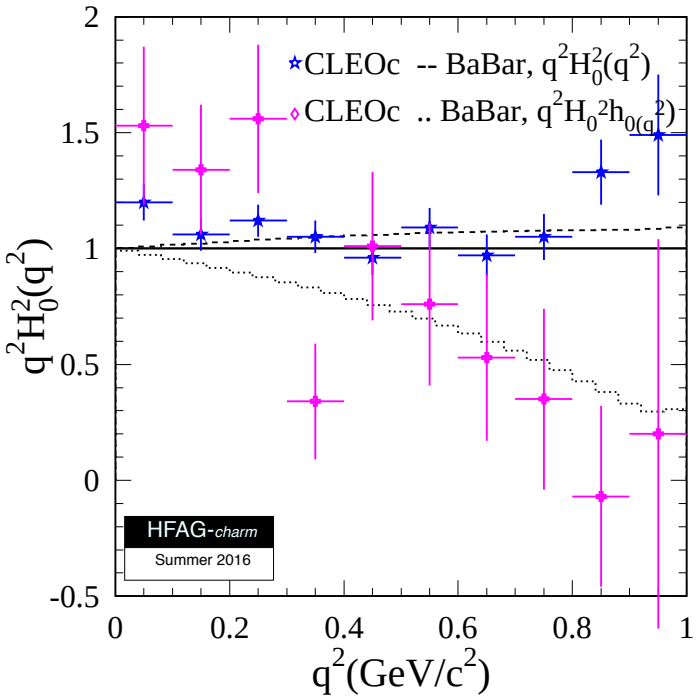

Figure 176: Comparison between CLEO-c and *BABAR* results for the quantities $q^2H_0^2(q^2)$ and $q^2h_0(q^2)H_0(q^2)$.

8.6 Leptonic decays

Purely leptonic decays of D^+ and D_s^+ mesons are among the simplest and theoretically cleanest probes of $c \to d$ and $c \to s$ quark flavor-changing transitions. The branching fraction of leptonic decays that proceed via the annihilation of the initial quark-antiquark pair ($c\overline{d}$ or $c\overline{s}$) into a virtual W^+ that finally materializes as an antilepton-neutrino pair ($\ell^+\nu_\ell$) is given in the Standard Model by

$$\mathcal{B}(D_q^+ \to \ell^+\nu_\ell) = \frac{G_F^2}{8\pi}\tau_{D_q} f_{D_q}^2 |V_{cq}|^2 m_{D_q} m_\ell^2 \left(1 - \frac{m_\ell^2}{m_{D_q}^2}\right)^2 . \quad (255)$$

Here, m_{D_q} is the D_q meson mass, τ_{D_q} is its lifetime, m_ℓ is the charged lepton mass, $|V_{cq}|$ is the magnitude of the relevant CKM matrix element, and G_F is the Fermi coupling constant. The parameter f_{D_q} is the D_q meson decay constant and is related to the wave-function overlap of the meson's constituent quark and anti-quark. Within the SM, the decay constants have been predicted using several methods, the most precise being the lattice gauge theory (LQCD) calculations. The Flavor Lattice Averaging Group [210] combines all LQCD calculations and provides averaged values for f_D and f_{D_s} (see Table 245) that are used within this section to extract the magnitudes of the V_{cd} and V_{cs} CKM matrix elements from experimentally measured branching fractions of $D^+ \to \ell^+\nu_\ell$ and $D_s^+ \to \ell^+\nu_\ell$ decays, respectively.

The leptonic decays of pseudoscalar mesons are suppressed by helicity conservation and their decay rates are thus proportional to the square of the charged lepton mass. Leptonic decays into electrons with $\mathcal{B} \lesssim 10^{-7}$ are not experimentally observable yet whereas decays to taus are favored over decays to muons. In particular, the ratio of the latter decays is equal to $R_{\tau/\mu}^{D_q} \equiv \mathcal{B}(D_q^+ \to \tau^+\nu_\tau)/\mathcal{B}(D_q^+ \to \mu^+\nu_\mu) = m_\tau^2/m_\mu^2 \cdot (1 - m_\tau^2/m_{D_q}^2)^2/(1 - m_\mu^2/m_{D_q}^2)^2 = 9.76 \pm 0.03$ in the case of D_s^+ decays and to 2.67 ± 0.01 in the case of D^+ decays based on the world average values of masses of the muon, tau and D_q meson given in Ref. [5]. Any deviation from this expectation could only be interpreted as violation of lepton universality in charged currents and would hence point to NP effects [974].

Averages presented within this subsection are weighted averages and correlations between measurements and dependencies on input parameters are taken into account. There is only one new experimental result on leptonic charm decays since our last report from 2014 – the preliminary measurements of $\mathcal{B}(D_s^+ \to \mu^+\nu_\mu)$ and $\mathcal{B}(D_s^+ \to \tau^+\nu_\tau)$ by BESIII collaboration [975]. The Lattice QCD calculations of the D and D_s meson decay constants have improved significantly since our last report and we use the latest averages of $N_f = 2 + 1 + 1$ calculations provided by

Table 245: The LQCD average for D and D_s meson decay constants and their ratio from the Flavor Lattice Averaging Group [210].

Quantity	Value
f_D	212.15 ± 1.45 MeV
f_{D_s}	248.83 ± 1.27 MeV
f_{D_s}/f_D	1.1716 ± 0.0032

Table 246: Experimental results and world averages for $\mathcal{B}(D^+ \to \ell^+\nu_\ell)$ and $f_D|V_{cd}|$. The first uncertainty is statistical and the second is experimental systematic. The third uncertainty in the case of $f_{D^+}|V_{cd}|$ is due to external inputs (dominated by the uncertainty of τ_D).

Mode	$\mathcal{B}$ (10^{-4})	$f_D\|V_{cd}\|$ (MeV)	Reference	
$\mu^+\nu_\mu$	$3.82 \pm 0.32 \pm 0.09$	$46.4 \pm 1.9 \pm 0.5 \pm 0.2$	CLEO-c	[874]
	$3.71 \pm 0.19 \pm 0.06$	$45.7 \pm 1.2 \pm 0.4 \pm 0.2$	BESIII	[976]
$\mu^+\nu_\mu$	$3.74 \pm 0.16 \pm 0.05$	$45.9 \pm 1.0 \pm 0.3 \pm 0.2$	Average	
$e^+\nu_e$	< 0.088 at 90% C.L.		CLEO-c	[874]
$\tau^+\nu_\tau$	< 12 at 90% C.L.		CLEO-c	[874]

the Flavour Lattice Averaging Group [210] in our determinations of the CKM matrix elements $|V_{cd}|$ and $|V_{cs}|$.

8.6.1 $D^+ \to \ell^+\nu_\ell$ decays and $|V_{cd}|$

We use measurements of the branching fraction $\mathcal{B}(D^+ \to \mu^+\nu_\mu)$ from CLEO-c [874] and BESIII [976] to calculate its world average (WA) value. We obtain

$$\mathcal{B}^{\rm WA}(D^+ \to \mu^+\nu_\mu) = (3.74 \pm 0.17) \times 10^{-4}, \tag{256}$$

from which we determine the product of the decay constant and the CKM matrix element to be

$$f_D|V_{cd}| = (45.9 \pm 1.1)\ \text{MeV}, \tag{257}$$

where the uncertainty includes the uncertainty on $\mathcal{B}^{\rm WA}(D^+ \to \mu^+\nu_\mu)$ and external inputs[52] needed to extract $f_D|V_{cd}|$ from the measured branching fraction using Eq. 255. Using the LQCD value for f_D from Table 245 we finally obtain the CKM matrix element V_{cd} to be

$$|V_{cd}| = 0.2164 \pm 0.0050(\text{exp.}) \pm 0.0015(\text{LQCD}), \tag{258}$$

where the uncertainties are from the experiments and lattice calculations, respectively. All input values and the resulting world averages are summarized in Table 246 and plotted in Fig. 177.

The upper limit on the ratio of branching fractions is found to be $R^D_{\tau/\mu} < 3.2$ at 90% C.L., which is just slightly above the SM expected value, 2.67 ± 0.01.

8.6.2 $D_s^+ \to \ell^+\nu_\ell$ decays and $|V_{cs}|$

We use measurements of the absolute branching fraction $\mathcal{B}(D_s^+ \to \mu^+\nu_\mu)$ from CLEO-c [907], *BABAR* [977], Belle [978], and BESIII [975], and obtain a WA value of

$$\mathcal{B}^{\rm WA}(D_s^+ \to \mu^+\nu_\mu) = (5.54 \pm 0.23) \times 10^{-3}. \tag{259}$$

[52] These values (taken from the PDG 2014 edition [314]) are $m_\mu = (0.1056583715 \pm 0.0000000035)$ GeV/c^2, $m_D = (1.86961 \pm 0.00009)$ GeV/c^2 and $\tau_D = (1040 \pm 7) \times 10^{-15}$ s.

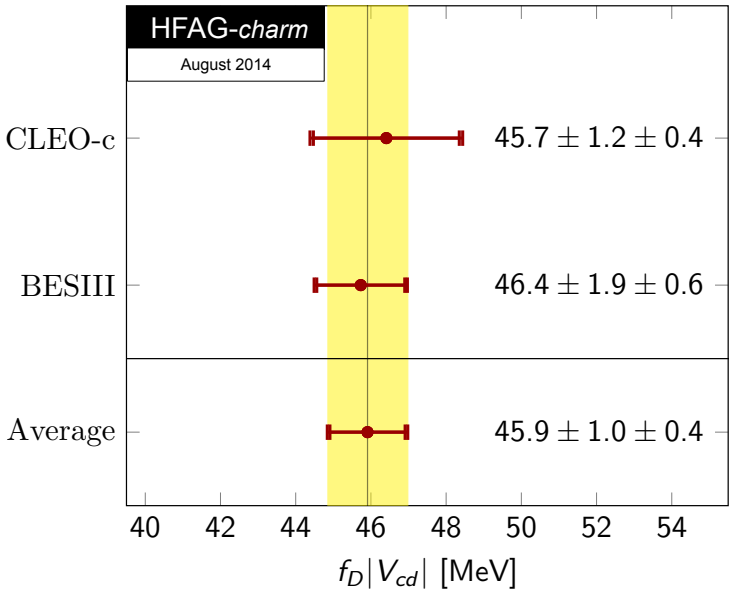

Figure 177: WA value for $f_D|V_{cd}|$. For each point, the first error listed is the statistical and the second error is the systematic error.

The WA value for $\mathcal{B}(D_s^+ \to \tau^+\nu_\tau)$ is also calculated from CLEO-c, *BABAR*, Belle, and BESIII measurements. CLEO-c made separate measurements for $\tau^+ \to e^+\nu_e\overline{\nu}_\tau$ [979], $\tau^+ \to \pi^+\overline{\nu}_\tau$ [907], and $\tau^+ \to \rho^+\overline{\nu}_\tau$ [980]; *BABAR* made separate measurements for $\tau^+ \to e^+\nu_e\overline{\nu}_\tau$ [977] and $\tau^+ \to \mu^+\nu_\mu\overline{\nu}_\tau$; Belle made separate measurements for $\tau^+ \to e^+\nu_e\overline{\nu}_\tau$, $\tau^+ \to \mu^+\nu_\mu\overline{\nu}_\tau$, and $\tau^+ \to \pi^+\overline{\nu}_\tau$ [978]; and BESIII made measurements using $\tau^+ \to \pi^+\overline{\nu}_\tau$ [975] decays. Combining all of them we obtain the WA value of

$$\mathcal{B}^{\rm WA}(D_s^+ \to \tau^+\nu_\tau) = (5.51 \pm 0.24) \times 10^{-2}. \tag{260}$$

The ratio of branching fractions is found to be

$$R^{D_s}_{\tau/\mu} = 9.95 \pm 0.57, \tag{261}$$

and is consistent with the value expected in the SM, 9.76 ± 0.03.

From the average values of branching fractions of muonic and tauonic decays we determine[53] the product of D_s meson decay constant and the $|V_{cs}|$ CKM matrix element to be

$$f_{D_s}|V_{cs}| = (250.3 \pm 4.5)\ \text{MeV}, \tag{262}$$

where the uncertainty is due to the uncertainties on $\mathcal{B}^{\rm WA}(D_s^+ \to \mu^+\nu_\mu)$ and $\mathcal{B}^{\rm WA}(D_s^+ \to \tau^+\nu_\tau)$ and the external inputs. All input values and the resulting world averages are summarized in Table 247 and plotted in Fig. 178. To obtain the averages given within this subsection and in Table 247 we have taken into account the correlations within each experiment[54] for the uncertainties related to: normalization, tracking, particle identification, signal and background parameterizations, and peaking background contributions.

[53] We use the following values (taken from PDG 2014 edition [314]) for external parameters entering Eq. 255: $m_\tau = (1.77686 \pm 0.00012)$ GeV/c^2, $m_{D_s} = (1.96830 \pm 0.00010)$ GeV/c^2 and $\tau_{D_s} = (500 \pm 7) \times 10^{-15}$ s.

[54] In the case of *BABAR* we use the covariance matrix from the errata of Ref. [977].

Table 247: Experimental results and world averages for $\mathcal{B}(D_s^+ \to \ell^+\nu_\ell)$ and $f_{D_s}|V_{cs}|$. The first uncertainty is statistical and the second is experimental systematic. The third uncertainty in the case of $f_{D_s}|V_{cs}|$ is due to external inputs (dominated by the uncertainty of τ_{D_s}). We have recalculated $\mathcal{B}(D_s^+ \to \tau^+\nu_\tau)$ quoted by CLEO-c and *BABAR* using the latest values for branching fractions of τ decays to electron, muon, or pion and neutrinos [5]. CLEO-c and *BABAR* include statistical uncertainty of number of D_s tags (denominator in the calculation of branching fraction) in the statistical uncertainty of measured $\mathcal{B}$. We subtract this uncertainty from the statistical one and add it to the systematic uncertainty.

Mode	$\mathcal{B}$ (10^{-2})	$f_{D_s}\|V_{cs}\|$ (MeV)	Reference	
$\mu^+\nu_\mu$	$0.565 \pm 0.044 \pm 0.020$	$250.8 \pm 9.8 \pm 4.4 \pm 1.8$	CLEO-c	[907]
	$0.602 \pm 0.037 \pm 0.032$	$258.9 \pm 8.0 \pm 6.9 \pm 1.8$	*BABAR*	[977]
	$0.531 \pm 0.028 \pm 0.020$	$243.1 \pm 6.4 \pm 4.6 \pm 1.7$	Belle	[978]
	$0.517 \pm 0.075 \pm 0.021$	$239.9 \pm 17.4 \pm 4.9 \pm 1.7$	BESIII	[975]
$\mu^+\nu_\mu$	$0.554 \pm 0.020 \pm 0.013$	$248.2 \pm 4.4 \pm 2.8 \pm 1.7$	Average	
$\tau^+(e^+)\nu_\tau$	$5.31 \pm 0.47 \pm 0.22$	$246.1 \pm 10.9 \pm 5.1 \pm 1.7$	CLEO-c	[980]
$\tau^+(\pi^+)\nu_\tau$	$6.46 \pm 0.80 \pm 0.23$	$271.4 \pm 16.8 \pm 4.8 \pm 1.9$	CLEO-c	[907]
$\tau^+(\rho^+)\nu_\tau$	$5.50 \pm 0.54 \pm 0.24$	$250.4 \pm 12.3 \pm 5.5 \pm 1.8$	CLEO-c	[979]
$\tau^+\nu_\tau$	$5.57 \pm 0.32 \pm 0.15$	$252.0 \pm 7.2 \pm 3.4 \pm 1.8$	CLEO-c	
$\tau^+(e^+)\nu_\tau$	$5.08 \pm 0.52 \pm 0.68$	$240.7 \pm 12.3 \pm 16.1 \pm 1.7$	*BABAR*	[977]
$\tau^+(\mu^+)\nu_\tau$	$4.90 \pm 0.46 \pm 0.54$	$236.4 \pm 11.1 \pm 13.0 \pm 1.7$		
$\tau^+\nu_\tau$	$4.95 \pm 0.36 \pm 0.58$	$237.6 \pm 8.6 \pm 13.8 \pm 1.7$	*BABAR*	
$\tau^+(e^+)\nu_\tau$	$5.37 \pm 0.33^{+0.35}_{-0.31}$	$247.4 \pm 7.6^{+8.1}_{-7.1} \pm 1.7$	Belle	[978]
$\tau^+(\mu^+)\nu_\tau$	$5.86 \pm 0.37^{+0.34}_{-0.59}$	$258.5 \pm 8.2^{+7.5}_{-13.0} \pm 1.8$		
$\tau^+(\pi^+)\nu_\tau$	$6.04 \pm 0.43^{+0.46}_{-0.40}$	$262.4 \pm 9.3^{+10.0}_{-8.7} \pm 1.8$		
$\tau^+\nu_\tau$	$5.70 \pm 0.21 \pm 0.31$	$254.9 \pm 4.7 \pm 6.9 \pm 1.8$	Belle	
$\tau^+(\pi^+)\nu_\tau$	$3.28 \pm 1.83 \pm 0.37$	$194 \pm 54 \pm 11 \pm 1$	BESIII	[975]
$\tau^+\nu_\tau$	$5.51 \pm 0.18 \pm 0.16$	$250.9 \pm 4.0 \pm 3.7 \pm 1.8$	Average	
$\mu^+\nu_\mu$ $\tau^+\nu_\tau$		$250.3 \pm 3.1 \pm 2.7 \pm 1.8$	Average	
$e^+\nu_e$	< 0.0083 at 90% C.L.		Belle	[978]

Using the LQCD value for f_{D_s} from Table 245 we finally obtain the CKM matrix element V_{cs} to be

$$|V_{cs}| = 1.006 \pm 0.018(\text{exp.}) \pm 0.005(\text{LQCD}), \tag{263}$$

where the uncertainties are from the experiments and lattice calculations, respectively.

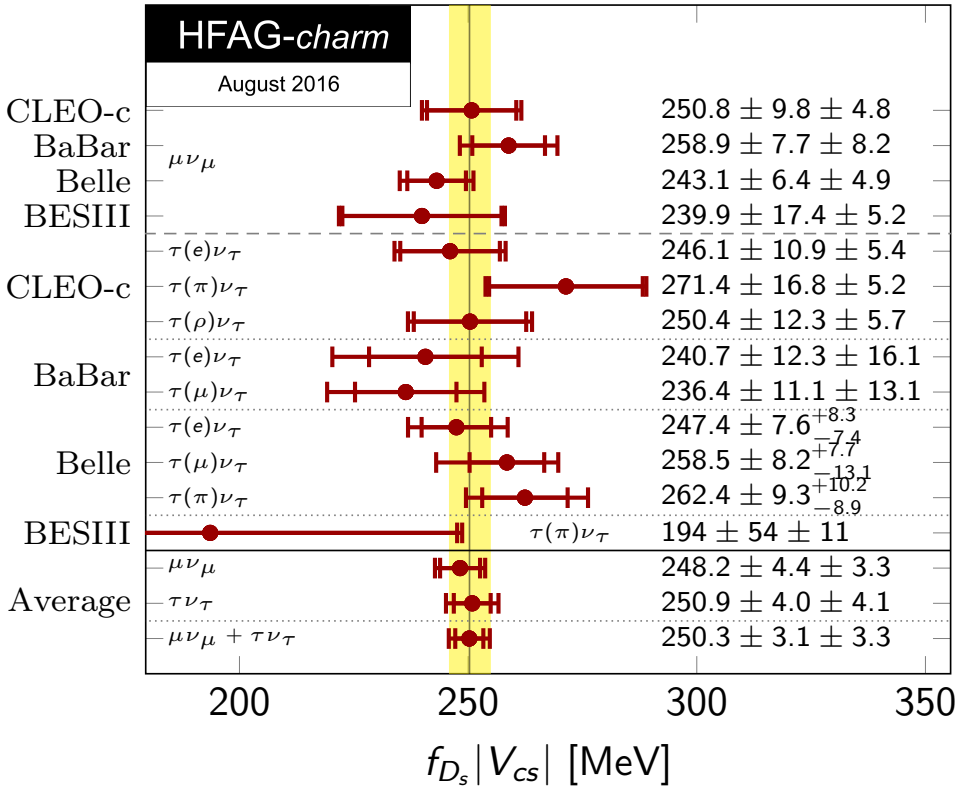

Figure 178: WA value for $f_{D_s}|V_{cs}|$. For each point, the first error listed is the statistical and the second error is the systematic error.

8.6.3 Comparison with other determinations of $|V_{cd}|$ and $|V_{cs}|$

Table 248 summarizes and Fig. 179 shows all determinations of the CKM matrix elements $|V_{cd}|$ and $|V_{cs}|$. As can be seen, the most precise direct determinations of these CKM matrix elements are those from leptonic and semileptonic $D_{(s)}$ decays. The values are in agreement within uncertainties with the values obtained from the global fit assuming CKM matrix unitarity.

8.6.4 Extraction of $D_{(s)}$ meson decay constants

Assuming unitarity of the CKM matrix, the values of the elements relevant in the case of (semi-)leptonic charm decays are known from the global fit of the CKM matrix, $|V_{cd}| = 0.22529^{+0.00041}_{-0.00032}$, and $|V_{cs}| = 0.973394^{+0.000074}_{-0.000096}$ [240]. These values can be used to extract the D and D_s meson decay constants from the experimentally measured products $f_D|V_{cd}|$ (Eq. 257) and $f_{D_s}|V_{cs}|$ (Eq. 262), respectively. This leads to the experimentally measured $D_{(s)}$ meson decay constants to be:

$$f_D^{\rm exp} = (203.7 \pm 4.9)\ {\rm MeV}, \quad (264)$$

$$f_{D_s}^{\rm exp} = (257.1 \pm 4.6)\ {\rm MeV}, \quad (265)$$

and the ratio of the constants is determined to be

$$f_{D_s}^{\rm exp}/f_D^{\rm exp} = 1.262 \pm 0.037. \quad (266)$$

Table 248: Average of the magnitudes of the CKM matrix elements $|V_{cd}|$ and $|V_{cs}|$ determined from the leptonic and semileptonic D and D_s decays. In the calculation of average values we assume 100% correlations in uncertainties due to LQCD. The values determined from neutrino scattering or W decays and determination from the global fit to the CKM matrix are given for comparison as well.

Method	Reference	Value
		$\lvert V_{cd}\rvert$
$D \to \ell\nu_\ell$	This section	$0.2164 \pm 0.0050(\text{exp.}) \pm 0.0015(\text{LQCD})$
$D \to \pi\ell\nu_\ell$	Section 8.5	$0.2141 \pm 0.0029(\text{exp.}) \pm 0.0093(\text{LQCD})$
$D \to \ell\nu_\ell$ $D \to \pi\ell\nu_\ell$	Average	0.216 ± 0.005
νN	PDG [5]	0.230 ± 0.011
Global CKM Fit	CKMFitter [240]	$0.22529^{+0.00041}_{-0.00032}$
		$\lvert V_{cs}\rvert$
$D_s \to \ell\nu_\ell$	This section	$1.006 \pm 0.018(\text{exp.}) \pm 0.005(\text{LQCD})$
$D \to K\ell\nu_\ell$	Section 8.5	$0.967 \pm 0.005(\text{exp.}) \pm 0.025(\text{LQCD})$
$D_s \to \ell\nu_\ell$ $D \to K\ell\nu_\ell$	Average	0.997 ± 0.017
$W \to c\bar{s}$	PDG [5]	$0.94^{+0.32}_{-0.26} \pm 0.13$
Global CKM Fit	CKMFitter [240]	$0.973394^{+0.000074}_{-0.000096}$

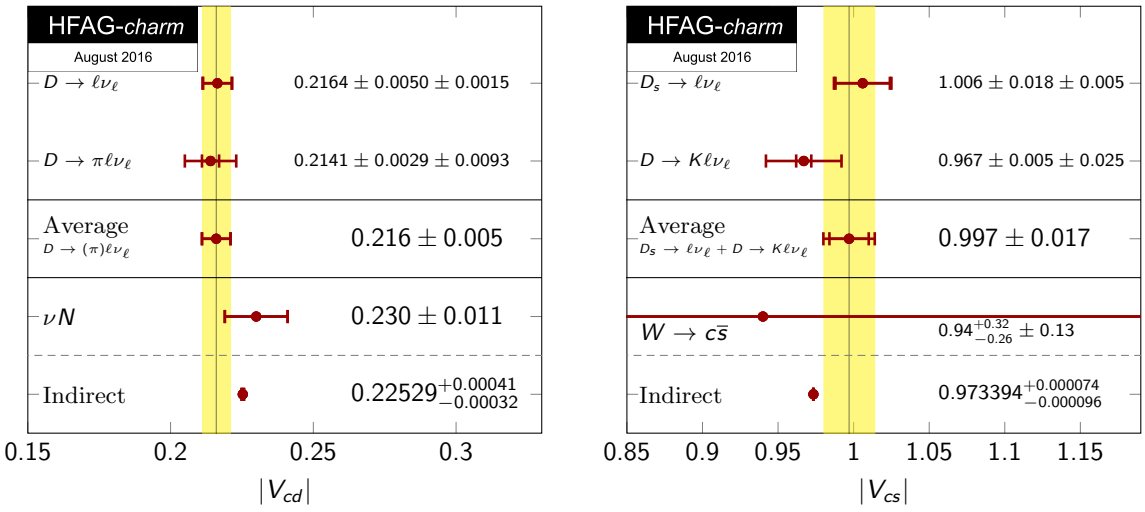

Figure 179: Comparison of magnitudes of the CKM matrix elements $|V_{cd}|$ (left) and $|V_{cs}|$ (right) determined from the (semi-)leptonic charm decays and from neutrino scattering data or W decays and determination from the global fit assuming CKM unitarity [240].

The values are in agreement with the LQCD determinations given in Table 245 within the uncertainties. The largest discrepancy is in the determinations of the ratio of the decay constants where the agreement is only at the level of 2.4σ.

8.7 Hadronic decays of D_s mesons

BABAR, CLEO-c and Belle collaborations have measured the absolute branching fractions of hadronic decays, $D_s^+ \to K^-K^+\pi^+$, $D_s^+ \to \overline{K}^0\pi^+$, and $D_s^+ \to \eta\pi^+$. The first two decay modes are the reference modes for the measurements of branching fractions of the D_s^+ decays to any other final state. Table 249 and Fig. 180 summarise the individual measurements and averaged values, which are found to be

$$\mathcal{B}^{\rm WA}(D_s^+ \to K^-K^+\pi^+) = (5.44 \pm 0.14)\%, \quad (267)$$
$$\mathcal{B}^{\rm WA}(D_s^+ \to \overline{K}^0\pi^+) = (3.00 \pm 0.09)\%, \quad (268)$$
$$\mathcal{B}^{\rm WA}(D_s^+ \to \eta\pi^+) = (1.71 \pm 0.08)\%, \quad (269)$$

where the uncertainties are total uncertainties. These averages are the same as in our previous report from 2014.

Table 249: Experimental results and world averages for branching fractions of $D_s^+ \to K^-K^+\pi^+$, $D_s^+ \to \overline{K}^0K^+$, and $D_s^+ \to \eta\pi^+$ decays. The first uncertainty is statistical and the second is experimental systematic. CLEO-c reports in Ref. [908] $\mathcal{B}(D_s^+ \to K_S^0K^+)$. We include it in the average of $\mathcal{B}(D_s^+ \to \overline{K}^0K^+)$ by using the relation $\mathcal{B}(D_s^+ \to \overline{K}^0K^+) \equiv 2\mathcal{B}(D_s^+ \to K_S^0K^+)$.

Mode	$\mathcal{B}$ (10^{-2})	Reference	
$K^-K^+\pi^+$	$5.78 \pm 0.20 \pm 0.30$	*BABAR*	[977]
	$5.55 \pm 0.14 \pm 0.13$	CLEO-c	[908]
	$5.06 \pm 0.15 \pm 0.21$	Belle	[978]
$K^-K^+\pi^+$	$5.44 \pm 0.09 \pm 0.11$	Average	
$\overline{K}^0K^+$	$3.04 \pm 0.10 \pm 0.06$	CLEO-c	[908]
	$2.95 \pm 0.11 \pm 0.09$	Belle	[978]
$\overline{K}^0K^+$	$3.00 \pm 0.07 \pm 0.05$	Average	
$\eta\pi^+$	$1.67 \pm 0.08 \pm 0.06$	CLEO-c	[908]
	$1.82 \pm 0.14 \pm 0.07$	Belle	[978]
$\eta\pi^+$	$1.71 \pm 0.07 \pm 0.08$	Average	

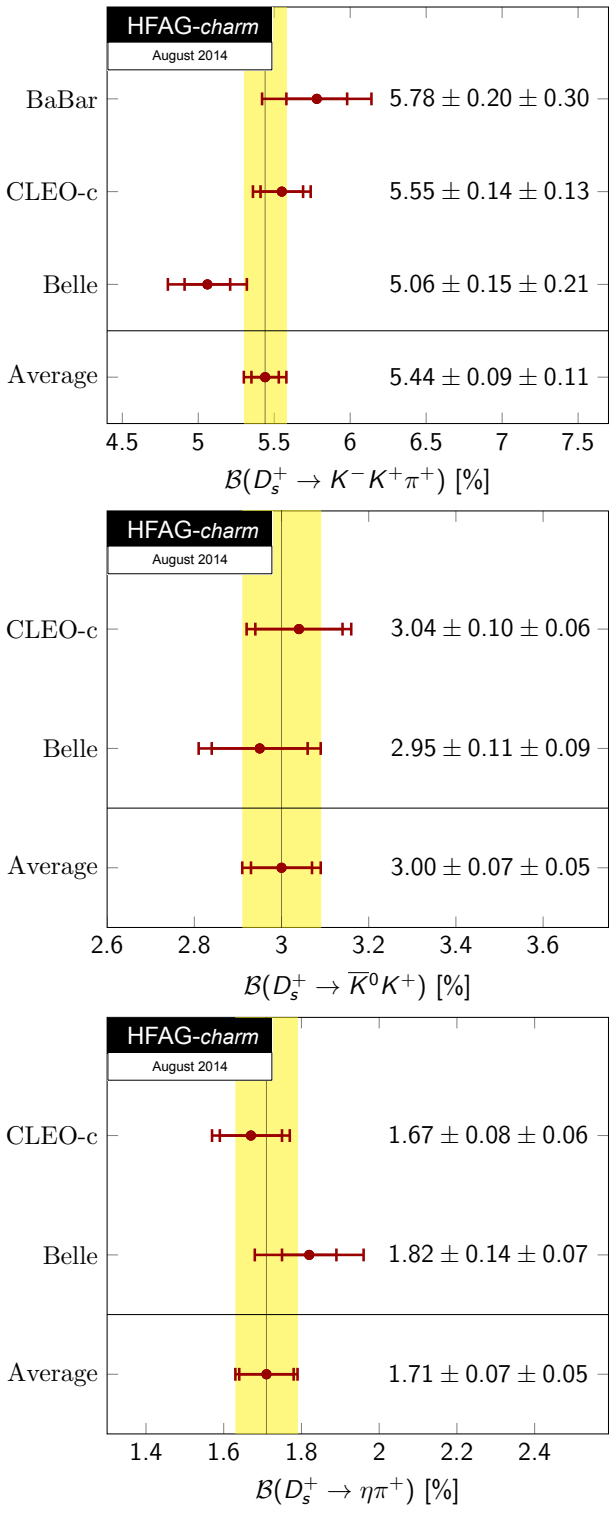

Figure 180: WA values for $\mathcal{B}(D_s^+ \to K^- K^+ \pi^+)$ (top), $\mathcal{B}(D_s^+ \to \overline{K}^0 \pi^+)$ (middle), $\mathcal{B}(D_s^+ \to \eta \pi^+)$ (bottom). For each point, the first error listed is the statistical and the second error is the systematic error.

8.8 Two-body hadronic D^0 decays and final state radiation

Measurements of the branching fractions for the decays $D^0 \to K^-\pi^+$, $D^0 \to \pi^+\pi^-$, and $D^0 \to K^+K^-$ have reached sufficient precision to allow averages with $\mathcal{O}(1\%)$ relative uncertainties. At these precisions, Final State Radiation (FSR) must be treated correctly and consistently across the input measurements for the accuracy of the averages to match the precision. The sensitivity of measurements to FSR arises because of a tail in the distribution of radiated energy that extends to the kinematic limit. The tail beyond $\sum E_\gamma \approx 30$ MeV causes typical selection variables like the hadronic invariant mass to shift outside the selection range dictated by experimental resolution, as shown in Fig. 181. While the differential rate for the tail is small, the integrated rate amounts to several percent of the total $h^+h^-(n\gamma)$ rate because of the tail's extent. The tail therefore translates directly into a several percent loss in experimental efficiency.

All measurements that include an FSR correction have a correction based on the use of PHOTOS [981–984] within the experiment's Monte Carlo simulation. PHOTOS itself, however, has evolved, over the period spanning the set of measurements. In particular, the incorporation of interference between radiation off the two separate mesons has proceeded in stages: it was first available for particle–antiparticle pairs in version 2.00 (1993), extended to any two-body, all-charged, final states in version 2.02 (1999), and further extended to multi-body final states in version 2.15 (2005). The effects of interference are clearly visible, as shown in Figure 181, and cause a roughly 30% increase in the integrated rate into the high energy photon tail. To evaluate the FSR correction incorporated into a given measurement, we must therefore note whether any correction was made, the version of PHOTOS used in correction, and whether the interference terms in PHOTOS were turned on.

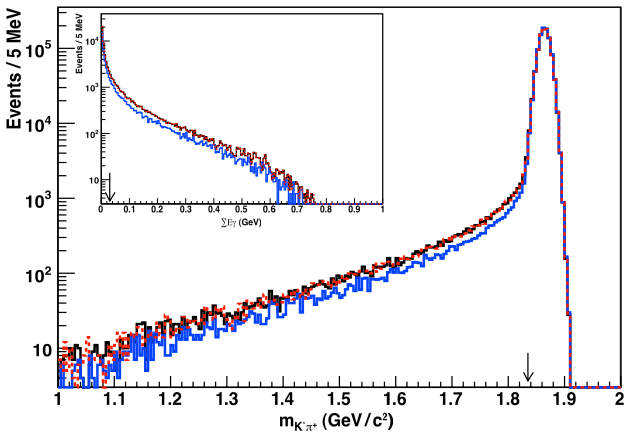

Figure 181: The $K\pi$ invariant mass distribution for $D^0 \to K^-\pi^+(n\gamma)$ decays. The 3 curves correspond to three different configurations of PHOTOS for modeling FSR: version 2.02 without interference (blue/grey), version 2.02 with interference (red dashed) and version 2.15 with interference (black). The true invariant mass has been smeared with a typical experimental resolution of 10 MeV/c^2. Inset: The corresponding spectrum of total energy radiated per event. The arrow indicates the $\sum E_\gamma$ value that begins to shift kinematic quantities outside of the range typically accepted in a measurement.

8.8.1 Branching fraction corrections

Before averaging the measured branching fractions, the published results are updated, as necessary, to the FSR prediction of PHOTOS 2.15 with interference included. The correction will always shift a branching fraction to a higher value: with no FSR correction or with no interference term in the correction, the experimental efficiency determination will be biased high, and therefore the branching fraction will be biased low.

Most of the branching fraction analyses used the kinematic quantity sensitive to FSR in the candidate selection criteria. For the analyses at the $\psi(3770)$, this variable was ΔE, the difference between the candidate D^0 energy and the beam energy (*e.g.* $E_K + E_\pi - E_{\rm beam}$ for $D^0 \to K^-\pi^+$). In the remainder of the analyses, the relevant quantity was the reconstructed hadronic two-body mass $m_{h^+h^-}$. To make the correction, we only need to evaluate the fraction of decays that FSR moves outside of the range accepted for the analysis.

The corrections were evaluated using an event generator (EvtGen [985]) that incorporates PHOTOS to simulate the portions of the decay process most relevant to the correction. We compared corrections determined both with and without smearing to account for experimental resolution. The differences were negligible, typically of $\mathcal{O}(1\%)$ of the correction itself. The immunity of the correction to resolution effects comes about because most of the long FSR-induced tail in, for example, the $m_{h^+h^-}$ distribution resides well away from the selection boundaries. The smearing from resolution, on the other hand, mainly affects the distribution of events right at the boundary.

For measurements incorporating an FSR correction that did not include interference, we update by assessing the FSR-induced efficiency loss for both the PHOTOS version and configuration used in the analysis and our nominal version 2.15 with interference. For measurements that published their sensitivity to FSR, our generator-level predictions for the original efficiency loss agreed to within a few percent of the correction. This agreement lends additional credence to the procedure.

Once the event loss from FSR in the most sensitive kinematic quantity is accounted for, the event loss from other quantities is very small. Analyses using D^* tags, for example, showed little sensitivity to FSR in the reconstructed $D^* - D^0$ mass difference: for example, in $m_{K^-\pi^+\pi^+} - m_{K^-\pi^+}$. Because the effect of FSR tends to cancel in the difference of the reconstructed masses, this difference showed a much smaller sensitivity than the two-body mass even before a two-body mass requirement. In the $\psi(3770)$ analyses, the beam-constrained mass distributions ($\sqrt{E^2_{\rm beam} - |\vec{p}_K + \vec{p}_\pi|^2}$) also show much smaller sensitivity than the two-body mass.

The FOCUS [986] analysis of the branching ratios $\mathcal{B}(D^0 \to \pi^+\pi^-)/\mathcal{B}(D^0 \to K^-\pi^+)$ and $\mathcal{B}(D^0 \to K^+K^-)/\mathcal{B}(D^0 \to K^-\pi^+)$ obtained yields using fits to the two-body mass distributions. FSR will both distort the low end of the signal mass peak, and will contribute a signal component to the low side tail used to estimate the background. The fitting procedure is not sensitive to signal events out in the FSR tail, which would be counted as part of the background.

A more complex toy Monte Carlo procedure was required to analyze the effect of FSR on the fitted yields, which were published with no FSR corrections applied. A detailed description of the procedure and results is available on the HFAG web site, and a brief summary is provided here. Determining the correction involved an iterative procedure in which samples of similar size to the FOCUS sample were generated and then fit using the FOCUS signal and background parameterizations. The MC parameterizations were tuned based on differences between the fits to the toy MC data and the FOCUS fits, and the procedure was repeated. These steps were

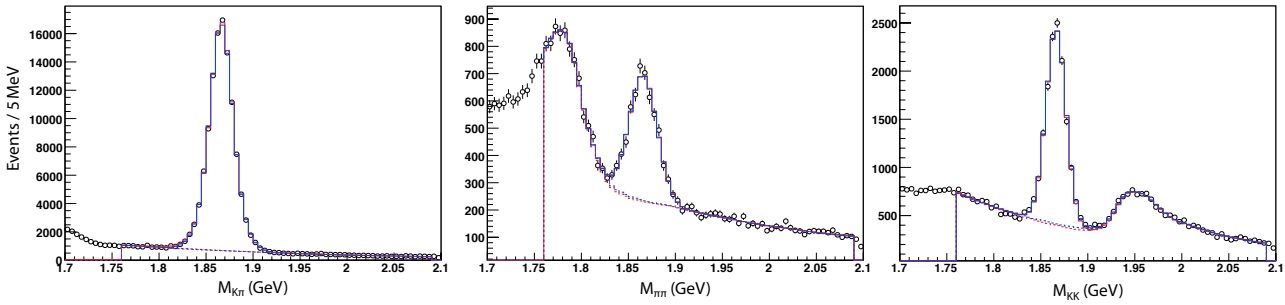

Figure 182: FOCUS data (dots), original fits (blue) and toy MC parameterization (red) for $D^0 \to K^-\pi^+$ (left), $D^0 \to \pi^+\pi^-$ (center), and $D^0 \to \pi^+\pi^-$ (right).

iterated until the fit parameters matched the original FOCUS parameters.

Table 250: The experimental measurements relating to $\mathcal{B}(D^0 \to K^-\pi^+)$, $\mathcal{B}(D^0 \to \pi^+\pi^-)$, and $\mathcal{B}(D^0 \to K^+K^-)$ after correcting to the common version and configuration of PHOTOS. The uncertainties are statistical and total systematic, with the FSR-related systematic estimated in this procedure shown in parentheses. Also listed are the percent shifts in the results from the correction, if any, applied here, as well as the original PHOTOS and interference configuration for each publication.

Experiment (acronym)	result (rescaled)	correction [%]	PHOTOS
$D^0 \to K^-\pi^+$			
CLEO-c 14 (CC14) [877]	$3.934 \pm 0.021 \pm 0.061(31)\%$	–	2.15/Yes
BABAR 07 (BB07) [987]	$4.035 \pm 0.037 \pm 0.074(24)\%$	0.69	2.02/No
CLEO II 98 (CL98) [988]	$3.920 \pm 0.154 \pm 0.168(32)\%$	2.80	none
ALEPH 97 (AL97) [989]	$3.930 \pm 0.091 \pm 0.125(32)\%$	0.79	2.0/No
ARGUS 94 (AR94) [990]	$3.490 \pm 0.123 \pm 0.288(24)\%$	2.33	none
CLEO II 93 (CL93) [991]	$3.960 \pm 0.080 \pm 0.171(15)\%$	0.38	2.0/No
ALEPH 91 (AL91) [992]	$3.730 \pm 0.351 \pm 0.455(34)\%$	3.12	none
$D^0 \to \pi^+\pi^-/D^0 \to K^-\pi^+$			
CLEO-c 10 (CC10) [875]	$0.0370 \pm 0.0006 \pm 0.0009(02)$	–	2.15/Yes
CDF 05 (CD05) [993]	$0.03594 \pm 0.00054 \pm 0.00043(15)$	–	2.15/Yes
FOCUS 02 (FO02) [986]	$0.0364 \pm 0.0012 \pm 0.0006(02)$	3.10	none
$D^0 \to K^+K^-/D^0 \to K^-\pi^+$			
CLEO-c 10 [875]	$0.1041 \pm 0.0011 \pm 0.0012(03)$	–	2.15/Yes
CDF 05 [993]	$0.0992 \pm 0.0011 \pm 0.0012(01)$	–	2.15/Yes
FOCUS 02 [986]	$0.0982 \pm 0.0014 \pm 0.0014(01)$	-1.12	none

The toy MC samples for the first iteration were based on the generator-level distribution of $m_{K^-\pi^+}$, $m_{\pi^+\pi^-}$, and $m_{K^+K^-}$, including the effects of FSR, smeared according to the original FOCUS resolution function, and on backgrounds generated using the parameterization from the final FOCUS fits. For each iteration, 400 to 1600 individual data-sized samples were generated and fit. The means of the parameters from these fits determined the corrections to the generator parameters for the following iteration. The ratio between the number of signal events generated and the final signal yield provides the required FSR correction in the final

iteration. Only a few iterations were required in each mode. Figure 182 shows the FOCUS data, the published FOCUS fits, and the final toy MC parameterizations. The toy MC provides an excellent description of the data.

The corrections obtained to the individual FOCUS yields were 1.0298 ± 0.0001 for $K^-\pi^+$, 1.062 ± 0.001 for $\pi^+\pi^-$, and 1.0183 ± 0.0003 for K^+K^-. These corrections tend to cancel in the branching ratios, leading to corrections of 1.031 ± 0.001 for $\mathcal{B}(D^0 \to \pi^+\pi^-)/\mathcal{B}(D^0 \to K^-\pi^+)$, and 0.9888 ± 0.0003 for $\mathcal{B}(D^0 \to K^+K^-)/\mathcal{B}(D^0 \to K^-\pi^+)$.

Table 250 summarizes the corrected branching fractions. The published FSR-related modeling uncertainties have been replaced by with a new, common, estimate based on the assumption that the dominant uncertainty in the FSR corrections comes from the fact that the mesons are treated like structureless particles. No contributions from structure-dependent terms in the decay process (*e.g.* radiation off individual quarks) are included in PHOTOS. Internal studies done by various experiments have indicated that in $K\pi$ decays, the PHOTOS corrections agree with data at the 20-30% level. We therefore attribute a 25% uncertainty to the FSR prediction from potential structure-dependent contributions. For the other two modes, the only difference in structure is the final state valence quark content. While radiative corrections typically come in with a $1/M$ dependence, one would expect the additional contribution from the structure terms to come in on time scales shorter than the hadronization time scale. In this case, you might expect $\Lambda_{\rm QCD}$ to be the relevant scale, rather than the quark masses, and therefore that the amplitude is the same for the three modes. In treating the correlations among the measurements this is what we assume. We also assume that the PHOTOS amplitudes and any missing structure amplitudes are relatively real with constructive interference. The uncertainties largely cancel in the branching fraction ratios. For the final average branching fractions, the FSR uncertainty on $K\pi$ dominates. Note that because of the relative sizes of FSR in the different modes, the $\pi\pi/K\pi$ branching ratio uncertainty from FSR is positively correlated with that for the $K\pi$ branching fraction, while the $KK/K\pi$ branching ratio FSR uncertainty is negatively correlated.

The $\mathcal{B}(D^0 \to K^-\pi^+)$ measurement of reference [994], the $\mathcal{B}(D^0 \to \pi^+\pi^-)/\mathcal{B}(D^0 \to K^-\pi^+)$ measurements of references [893] and [857], and the $\mathcal{B}(D^0 \to K^+K^-)/\mathcal{B}(D^0 \to K^-\pi^+)$ measurement of reference [857] are excluded from the branching fraction averages presented here. These measurements appear not to have incorporated any FSR corrections, and insufficient information is available to determine the 2-3% corrections that would be required.

8.8.2 Average branching fractions

The average branching fractions for $D^0 \to K^-\pi^+$, $D^0 \to \pi^+\pi^-$ and $D^0 \to K^+K^-$ are obtained from a single χ^2 minimization procedure, in which the three branching fractions are floating parameters. The central values are obtained from a fit in which the full covariance matrix – accounting for all statistical, systematic (excluding FSR), and FSR measurement uncertainties – is used. Table 251 presents the correlation matrix for this nominal fit. We then obtain the three reported uncertainties on those central values as follows: The statistical uncertainties are obtained from a fit using only the statistical covariance matrix. The systematic uncertainties are obtained by subtracting (in quadrature) the statistical uncertainties from the uncertainties determined via a fit using a covariance matrix that accounts for both statistical and systematic measurement uncertainties. The FSR uncertainties are obtained by subtracting (in quadrature) the uncertainties determined via a fit using a covariance matrix that accounts for both statistical

Table 251: The correlation matrix corresponding to the full covariance matrix. Subscripts h denote which of the $D^0 \to h^+h^-$ decay results from a single experiment is represented in that row or column.

	CC14	BB07	CL98	AL97	AR94	CL93	AL91	$FO02_\pi$	$CD05_\pi$	$CC10_\pi$	$FO02_K$	$CD05_K$	$CC10_K$
CC14	1.000	0.139	0.057	0.084	0.031	0.033	0.023	0.070	0.103	0.068	-0.019	-0.032	-0.085
BB07	0.139	1.000	0.035	0.051	0.019	0.020	0.014	0.042	0.062	0.041	-0.012	-0.019	-0.051
CL98	0.057	0.035	1.000	0.021	0.008	0.298	0.006	0.017	0.026	0.017	-0.005	-0.008	-0.021
AL97	0.084	0.051	0.021	1.000	0.011	0.012	0.116	0.025	0.038	0.025	-0.007	-0.012	-0.031
AR94	0.031	0.019	0.008	0.011	1.000	0.004	0.003	0.009	0.014	0.009	-0.003	-0.004	-0.011
CL93	0.033	0.020	0.298	0.012	0.004	1.000	0.003	0.010	0.015	0.010	-0.003	-0.005	-0.012
AL91	0.023	0.014	0.006	0.116	0.003	0.003	1.000	0.007	0.010	0.007	-0.002	-0.003	-0.009
$FO02_\pi$	0.070	0.042	0.017	0.025	0.009	0.010	0.007	1.000	0.031	0.021	-0.006	-0.010	-0.026
$CD05_\pi$	0.103	0.062	0.026	0.038	0.014	0.015	0.010	0.031	1.000	0.031	-0.009	-0.014	-0.038
$CC10_\pi$	0.068	0.041	0.017	0.025	0.009	0.010	0.007	0.021	0.031	1.000	-0.006	-0.010	-0.025
$FO02_K$	-0.019	-0.012	-0.005	-0.007	-0.003	-0.003	-0.002	-0.006	-0.009	-0.006	1.000	0.003	0.007
$CD05_K$	-0.032	-0.019	-0.008	-0.012	-0.004	-0.005	-0.003	-0.010	-0.014	-0.010	0.003	1.000	0.012
$CC10_K$	-0.085	-0.051	-0.021	-0.031	-0.011	-0.012	-0.009	-0.026	-0.038	-0.025	0.007	0.012	1.000

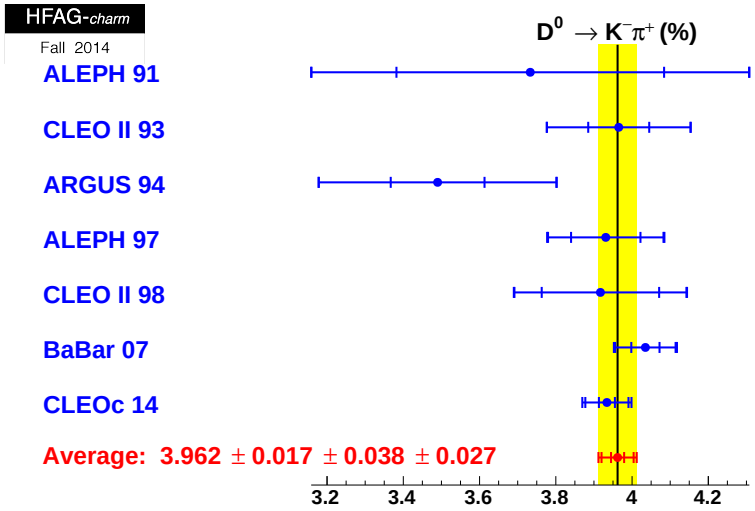

Figure 183: Comparison of measurements of $\mathcal{B}(D^0 \to K^-\pi^+)$ (blue) with the average branching fraction obtained here (red, and yellow band).

and systematic measurement uncertainties from the uncertainties determined via the fit using the full covariance matrix.

In forming the full covariance matrix, the FSR uncertainties are treated as fully correlated (or anti-correlated) as described above. For the covariance matrices involving systematic measurement uncertainties, ALEPH's systematic uncertainties in the θ_{D^*} parameter are treated as fully correlated between the ALEPH 97 and ALEPH 91 measurements. Similarly, the tracking efficiency uncertainties in the CLEO II 98 and the CLEO II 93 measurements are treated as fully correlated.

The averaging procedure results in a final χ^2 of 11.0 for 10 $(13-3)$ degrees of freedom. The branching fractions obtained are

$$\mathcal{B}(D^0 \to K^-\pi^+) = (3.962 \pm 0.017 \pm 0.038 \pm 0.027)\,\%, \quad (270)$$
$$\mathcal{B}(D^0 \to \pi^+\pi^-) = (0.144 \pm 0.002 \pm 0.002 \pm 0.002)\,\%, \quad (271)$$
$$\mathcal{B}(D^0 \to K^+K^-) = (0.399 \pm 0.003 \pm 0.005 \pm 0.002)\,\%\,. \quad (272)$$

The uncertainties, estimated as described above, are statistical, systematic (excluding FSR), and FSR modeling. The correlation coefficients from the fit using the total uncertainties are

	$K^-\pi^+$	$\pi^+\pi^-$	K^+K^-
$K^-\pi^+$	1.00	0.71	0.76
$\pi^+\pi^-$	0.71	1.00	0.53
K^+K^-	0.76	0.53	1.00

As the χ^2 would suggest and Fig. 183 shows, the average value for $\mathcal{B}(D^0 \to K^-\pi^+)$ and the input branching fractions agree very well. With the estimated uncertainty in the FSR modeling used here, the FSR uncertainty dominates the statistical uncertainty in the average, suggesting that experimental work in the near future should focus on verification of FSR with $\sum E_\gamma \gtrsim 100$ MeV. Note that the systematic uncertainty excluding FSR is still larger than the

Table 252: Evolution of the $D^0 \to K^-\pi^+$ branching fraction from a fit with no FSR corrections or correlations (similar to the average in the PDG 2016 update [5]) to the nominal fit presented here.

Modes fit	description	$\mathcal{B}(D^0 \to K^-\pi^+)$ (%)	χ^2/(deg. of freedom)
$K^-\pi^+$	PDG 2016 [5] equivalent	$3.930 \pm 0.017 \pm 0.042$	$4.5/(8-1) = 0.64$
$K^-\pi^+$	drop Ref. [994]	$3.938 \pm 0.017 \pm 0.042$	$4.5/(7-1) = 0.75$
$K^-\pi^+$	add FSR corrections	$3.955 \pm 0.017 \pm 0.038 \pm 0.018$	$3.5/(7-1) = 0.58$
$K^-\pi^+$	add FSR correlations	$3.956 \pm 0.017 \pm 0.038 \pm 0.027$	$3.6/(7-1) = 0.60$
all	–	$3.962 \pm 0.017 \pm 0.038 \pm 0.027$	$11.0/(13-3) = 1.10$

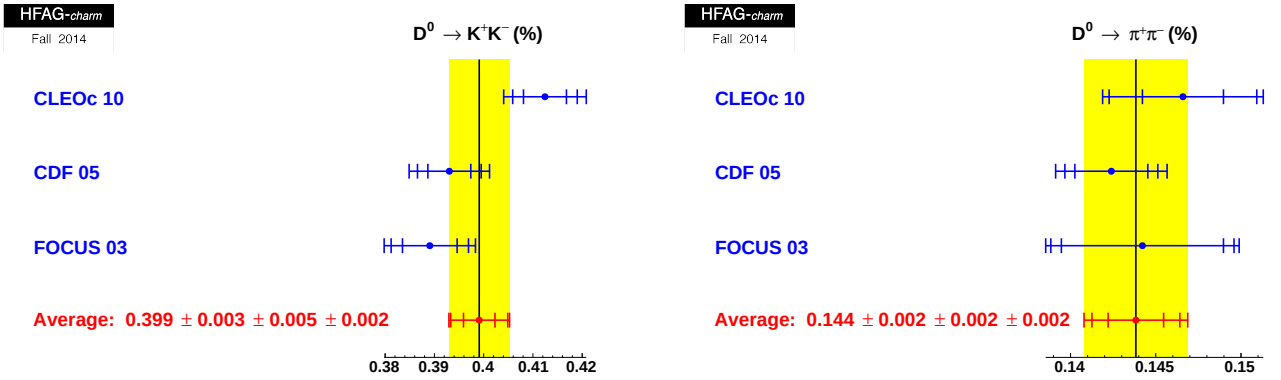

Figure 184: The $\mathcal{B}(D^0 \to K^+K^-)$ (left) and $\mathcal{B}(D^0 \to \pi^+\pi^-)$ (right) values obtained by scaling the measured branching ratios with the $\mathcal{B}(D^0 \to K^-\pi^+)$ branching fraction average obtained here. For the measurements (blue points), the error bars correspond to the statistical, systematic and $K\pi$ normalization uncertainties. The average obtained here (red point, yellow band) lists the statistical, systematics excluding FSR, and the FSR systematic.

FSR uncertainty; in the most precise measurements of these branching fractions, the largest systematic uncertainty is the uncertainty on the tracking efficiency. The $\mathcal{B}(D^0 \to K^+K^-)$ and $\mathcal{B}(D^0 \to \pi^+\pi^-)$ measurements inferred from the branching ratio measurements also agree well (Fig. 184).

The $\mathcal{B}(D^0 \to K^-\pi^+)$ average obtained here is approximately two statistical standard deviations higher than the 2016 PDG update average [5]. Table 252 shows the evolution from a fit similar to the PDG's (no FSR corrections or correlations, reference [994] included) to the average presented here. There are two main contributions to the difference. The branching fraction in reference [994] is low, and its exclusion shifts the result upwards. The dominant shift (+0.017%) is due to the FSR corrections, which as expected shift the result upwards.

There is no reason to presume that the effects of FSR should be different in $D^0 \to K^+\pi^-$ and $D^0 \to K^-\pi^+$ decays, as both decay to one charged kaon and one charged pion. Measurements of the relative branching fraction ratio between the doubly Cabibbo-suppressed decay $D^0 \to K^+\pi^-$ and the Cabibbo-favored decay $D^0 \to K^-\pi^+$ (R_D, determined in Section 8.1) are now approaching $\mathcal{O}(1\%)$ relative uncertainties. This makes it worthwhile to combine our R_D average

with the $\mathcal{B}(D^0 \to K^-\pi^+)$ average obtained in Equation 270, to provide measurements of the branching fraction:

$$\mathcal{B}(D^0 \to K^+\pi^-) = (1.379 \pm 0.023) \times 10^{-4} \text{ (assuming no } CPV\text{)}, \quad (273)$$

$$\mathcal{B}(D^0 \to K^+\pi^-) = (1.383 \pm 0.023) \times 10^{-4} \text{ (}CPV\text{ allowed)}. \quad (274)$$

Note that, by definition of R_D, these branching fractions do not include any contribution from Cabibbo-favored $\overline{D}^0 \to K^+\pi^-$ decays.

8.9 Excited $D_{(s)}$ mesons

Excited charm meson states have received increased attention since the first observation of states that could not be accommodated by QCD predictions [995–998]. Tables 253, 254 and 255 summarize recent measurements of the masses and widths of excited D and D_s mesons, respectively. If a preferred assignment of spin and parity was measured it is listed in the column J^P, where the label natural denotes $J^P = 0^-, 1^+, 2^- \ldots$ and unnatural $J^P = 0^+, 1^-, 2^+ \ldots$. If possible an average mass and width was calculated, which is listed in the gray shaded row. The calculation of the averages assumes no correlation between individual measurements. A summary of the averaged masses and widths is shown in Figure 185.

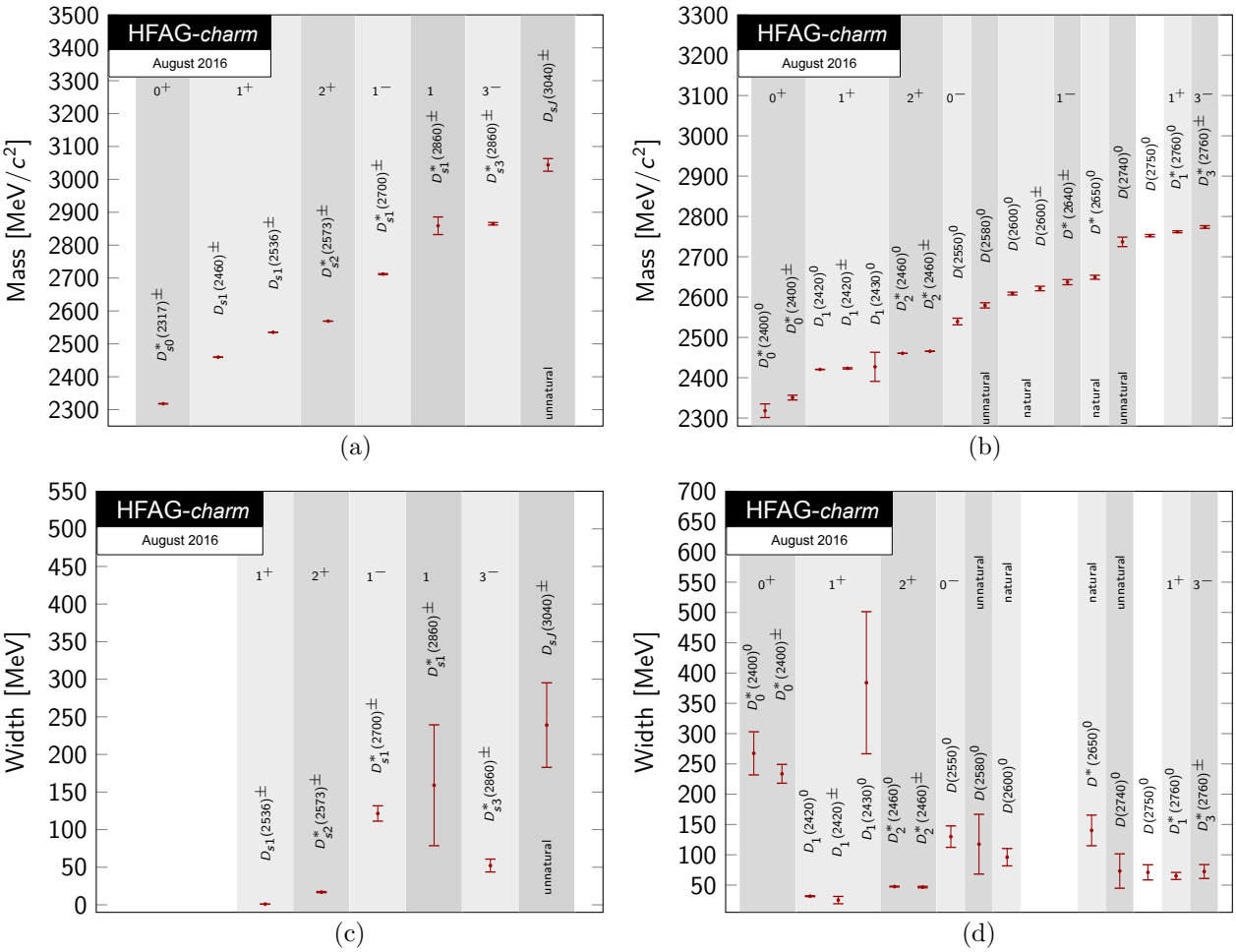

Figure 185: Averaged masses for D_s mesons are shown in subfigure (a) and for D mesons in subfigure (b). The average widths for D_s mesons are shown in subfigure (c) and for D mesons in subfigure (d). The vertical shaded regions distinguish between different spin parity states.

The masses and widths of narrow ($\Gamma < 50$ MeV) orbitally excited D mesons (denoted D^{**}), both neutral and charged, are well-established. Measurements of broad states ($\Gamma \sim 200$–400 MeV) are less abundant, as identifying the signal is more challenging. There is a slight discrepancy between the $D_0^*(2400)^0$ masses measured by the Belle [695] and FOCUS [999] experiments. No data exist yet for the $D_1(2430)^\pm$ state. Dalitz plot analyses of $B \to D^{(*)}\pi\pi$ decays strongly favor the assignments 0^+ and 1^+ for the spin-parity quantum numbers of the

$D_0^*(2400)^0/D_0^*(2400)^\pm$ and $D_1(2430)^0$ states, respectively. The measured masses and widths, as well as the J^P values, are in agreement with theoretical predictions based on potential models [481, 1000–1002].

Tables 256 and 257 summarize the branching fractions of B mesons decays to excited D and D_s states, respectively. It is notable that the branching fractions for B mesons decaying to a narrow D^{**} state and a pion are similar for charged and neutral B initial states, while the branching fractions to a broad D^{**} state and π^+ are much larger for B^+ than for B^0. This may be due to the fact that color-suppressed amplitudes contribute only to the B^+ decay and not to the B^0 decay (for a theoretical discussion, see Ref. [1003, 1004]). Measurements of individual branching fractions of D mesons are difficult due to the unknown fragmentation of $c\overline{c} \to D^{**}$ or due to the unknown $B \to D^{**}X$ branching fractions.

The discoveries of the $D_{s0}^*(2317)^\pm$ and $D_{s1}(2460)^\pm$ have triggered increased interest in properties of, and searches for, excited D_s mesons (here generically denoted D_s^{**}). While the masses and widths of $D_{s1}(2536)^\pm$ and $D_{s2}(2573)^\pm$ states are in relatively good agreement with potential model predictions, the masses of $D_{s0}^*(2317)^\pm$ and $D_{s1}(2460)^\pm$ states are significantly lower than expected (see Ref. [1005] for a discussion of $c\overline{s}$ models). Moreover, the mass splitting between these two states greatly exceeds that between the $D_{s1}(2536)^\pm$ and $D_{s2}(2573)^\pm$. These unexpected properties have led to interpretations of the $D_{s0}^*(2317)^\pm$ and $D_{s1}(2460)^\pm$ as exotic four-quark states [1006, 1007].

While there are few measurements of the J^P values of $D_{s0}^*(2317)^\pm$ and $D_{s1}(2460)^\pm$, the available data favor 0^+ and 1^+, respectively. A molecule-like (DK) interpretation of the $D_{s0}^*(2317)^\pm$ and $D_{s1}(2460)^\pm$ [1006, 1007] that can account for their low masses and isospin-breaking decay modes is tested by searching for charged and neutral isospin partners of these states; thus far such searches have yielded negative results. Therefore the subset of models that predict equal production rates for different charged states is excluded. The molecular picture can also be tested by measuring the rates for the radiative processes $D_{s0}^*(2317)^\pm/D_{s1}(2460)^\pm \to D_s^{(*)}\gamma$ and comparing to theoretical predictions. The predicted rates, however, are below the sensitivity of current experiments.

Another model successful in explaining the total widths and the $D_{s0}^*(2317)^\pm$ – $D_{s1}(2460)^\pm$ mass splitting is based on the assumption that these states are chiral partners of the ground states D_s^+ and D_s^* [1008]. While some measured branching fraction ratios agree with predicted values, further experimental tests with better sensitivity are needed to confirm or refute this scenario. A summary of the mass difference measurements is given in Table 258.

Measurements by *BABAR* [1009] and LHCb [1010] first indicated the existence of a strange-charm $D_{sJ}^*(2860)^\pm$ meson. An LHCb study of $B_s^0 \to \overline{D}^0 K^- \pi^+$ decays, in which they searched for excited D_s mesons [1011], showed with 10σ significance that this state is comprised of two different particles, one of spin 1 and one of spin 3. This represents the first measurement of a heavy flavored spin-3 particle, and the first observation B mesons decays to spin 3 particles. A subsequent study of D_{sJ} mesons by the LHCb collaboration [1012] supports the natural parity assignment for this state ($J^P = 3^-$). This study also shows weak evidence for a further structure at a mass around 3040 MeV/c^2 with unnatural parity, which was first hinted at by a Babar analysis [1009].

Recent evidence shows that the 1D family of charm resonances can be explored in the Dalitz plot analyses of B-meson decays in the same way as seen for the charm-strange resonances. The LHCb collaboration performed an analysis of $B^0 \to \overline{D}^0 \pi^+ \pi^-$ decays, in which they measured the spin-parity assignment of the state $D_3^*(2760)^\pm$, which was observed previously by *BABAR* [935]

and LHCb [936], to be $J^P = 3^-$. The measurement suggests a spectroscopic assignment of $^3D_3$. This is the second observation of a spin-3 charm meson.

Other observed excited D_s states include $D_{s1}(2700)^\pm$ and $D_{s2}(2573)^\pm$. The properties of both (mass, width, J^P) have been measured and determined in several analyses. A theoretical discussion [1013] investigates the possibility that the $D_{s1}(2700)^\pm$ could represent radial excitations of the $D_s^{*\pm}$. Similarly, the $D_{s1}(2860)^\pm$ and $D_{sJ}(3040)^\pm$ could be excitations of $D_{s0}^*(2317)^\pm$ and $D_{s1}(2460)^\pm$ or $D_{s1}(2536)^\pm$, respectively.

Table 259 summarizes measurements of the polarization amplitude A_D (sometimes also referred as helicity parameter), which describes the initial polarization of the D meson. In D^{**} meson decay the helicity distribution varies like $1 + A_D \cos^2\theta_H$, where θ_H is the angle in the D^* rest frame between the two pions emitted by decay $D^{**} \to D^*\pi$ and the $D^* \to D\pi$. The parameter is sensitive to possible S-wave contributions in the decay. In the case of an unpolarized D meson decay decaying purely via D-wave the polarization amplitude is predicted to give $A_D = 3$. Studies of the $D_1(2420)^0$ meson by the ZEUS and *BABAR* collaborations suggest that there is an S-wave admixture in the decay, which is contrary to Heavy Quark Effective Theory calculations [1014, 1015].

Table 253: Recent measurements of mass and width for different excited D_s mesons. The column J^P list the most significant assignment of spin and parity. If possible an average mass or width is calculated.

Resonance	J^P	Decay mode	Mass [MeV/c^2]	Width [MeV]	Measured by	Reference
		$D_s^+\pi^0$	$2319.6 \pm 0.2 \pm 1.4$		*BABAR*	[1016]
$D_{s0}^*(2317)^\pm$	0^+	$D_s^+\pi^0$	$2317.3 \pm 0.4 \pm 0.8$		*BABAR*	[998]
			2318.0 ± 0.8		Our average	
		$D_s^+\pi^0\gamma, D_s^+\gamma, D_s^+\pi^+\pi^-$	$2460.1 \pm 0.2 \pm 0.8$		*BABAR*	[1016]
$D_{s1}(2460)^\pm$	1^+	$D_s^+\pi^0\gamma$	$2458 \pm 1.0 \pm 1.0$		*BABAR*	[998]
			2459.6 ± 0.7		Our average	
		$D^{*+}K_S^0$	$2535.7 \pm 0.6 \pm 0.5$		DØ	[1017]
		$D^{*+}K_S^0, D^{*0}K^+$	$2534.78 \pm 0.31 \pm 0.40$		*BABAR*	[622]
		$D_s^+\pi^+\pi^-$	$2534.6 \pm 0.3 \pm 0.7$		*BABAR*	[1016]
		$D^{*+}K_S^0, D^{*0}K^+$	$2535.0 \pm 0.6 \pm 1.0$		E687	[1018]
		$D^{*0}K^+$	$2535.3 \pm 0.2 \pm 0.5$		CLEO	[1019]
$D_{s1}(2536)^\pm$	1^+	$D^{*+}K_S^0$	$2534.8 \pm 0.6 \pm 0.6$		CLEO	[1019]
		$D^{*0}K^+$	$2535.2 \pm 0.5 \pm 1.5$		ARGUS	[1020]
		$D^{*+}K_S^0$	$2535.6 \pm 0.7 \pm 0.4$		CLEO	[1021]
		$D^{*+}K_S^0$	$2535.9 \pm 0.6 \pm 2.0$		ARGUS	[1022]
		$D^{*+}K_S^0$		$0.92 \pm 0.03 \pm 0.04$	*BABAR*	[1023]
			2535.10 ± 0.26	0.92 ± 0.05	Our average	
		$D^0K^+, D^{*+}K_S^0$	$2568.39 \pm 0.29 \pm 0.26$	$16.9 \pm 0.5 \pm 0.6$	LHCb	[1024]
		$D^+K_S^0, D^0K^+$	$2569.4 \pm 1.6 \pm 0.5$	$12.1 \pm 4.5 \pm 1.6$	LHCb	[1025]
		$D^+K_S^0, D^0K^+$	$2572.2 \pm 0.3 \pm 1.0$	$27.1 \pm 0.6 \pm 5.6$	*BABAR*	[1026]
$D_{s2}^*(2573)^\pm$	2^+	D^0K^+	$2574.25 \pm 3.3 \pm 1.6$	$10.4 \pm 8.3 \pm 3.0$	ARGUS	[1027]
		D^0K^+	$2573.2^{+1.7}_{-1.6} \pm 0.9$	$16^{+5}_{-4} \pm 3$	CLEO	[1028]
			2569.08 ± 0.35	16.9 ± 0.8	Our average	
		$D^{*+}K_S^0, D^{*0}K^+$	$2732.3 \pm 4.3 \pm 5.8$	$136 \pm 19 \pm 24$	LHCb	[1012]
		D^0K^+	2699^{+14}_{-7}	127^{+24}_{-19}	*BABAR*	[1029]
		$D^{*+}K_S^0, D^{*0}K^+$	$2709.2 \pm 1.9 \pm 4.5$	$115.8 \pm 7.3 \pm 12.1$	LHCb	[1010]
$D_{s1}^*(2700)^\pm$	1^-	DK, D^*K	$2710 \pm 2^{+12}_{-7}$	$149 \pm 7^{+39}_{-52}$	*BABAR*	[1009]
		D^0K^+	$2708 \pm 9^{+11}_{-10}$	$108 \pm 2^{+36}_{-31}$	Belle	[718]
			2712.0 ± 1.5	121.5 ± 10.2	Our average	
$D_{s1}^*(2860)^\pm$	1	D^0K^+	$2859 \pm 12 \pm 24$	$159 \pm 23 \pm 77$	LHCb	[1011]
		$D^{*+}K_S^0, D^{*0}K^+$	$2867.1 \pm 4.3 \pm 1.9$	$50 \pm 11 \pm 13$	LHCb	[1012]
$D_{s3}^*(2860)^\pm$	3^-	D^0K^+	$2860.5 \pm 2.6 \pm 6.5$	$53 \pm 7 \pm 7$	LHCb	[1011]
			2865.0 ± 3.9	52.2 ± 8.6	Our average	
$D_{sJ}(3040)^\pm$	Unnatural	D^*K	$3044 \pm 8^{+30}_{-5}$	$239 \pm 35^{+46}_{-42}$	*BABAR* (m & Γ) + LHCb(J^P)	[1009]+ [1012]

Table 254: Recent measurements of mass and width for different excited D mesons. The column J^P list the most significant assignment of spin and parity. If possible an average mass or width is calculated.

Resonance	J^P	Decay mode	Mass [MeV/c^2]	Width [MeV]	Measured by	Reference
$D_0^*(2400)^0$	0^+	$D^+\pi^-$	$2297 \pm 8 \pm 20$	$273 \pm 12 \pm 48$	*BABAR*	[696]
		$D^+\pi^-$	$2308 \pm 17 \pm 32$	$276 \pm 21 \pm 63$	Belle	[695]
		$D^+\pi^-$	$2407 \pm 21 \pm 35$	$240 \pm 55 \pm 59$	Focus	[999]
			2318.2 ± 16.9	267.4 ± 35.6	Our average	
$D_0^*(2400)^\pm$	0^+	$D^0\pi^+$	$2349 \pm 6 \pm 1 \pm 4$	$217 \pm 13 \pm 5 \pm 12$	LHCb	[577]
		$D^0\pi^+$	$2360 \pm 15 \pm 12 \pm 28$	$255 \pm 26 \pm 20 \pm 47$	LHCb	[1030]
		$D^0\pi^+$	$2403 \pm 14 \pm 35$	$283 \pm 24 \pm 34$	Focus(m &Γ) + Belle(J^P)	[999] + [1031]
			2350.6 ± 5.9	233.7 ± 15.5	Our average	
$D_1(2420)^0$	1^+	$D^{*+}\pi^-$	$2419.6 \pm 0.1 \pm 0.7$	$35.2 \pm 0.4 \pm 0.9$	LHCb	[936]
		$D^{*+}\pi^-$	$2423.1 \pm 1.5^{+0.4}_{-1.0}$	$38.8 \pm 5^{+1.9}_{-5.4}$	Zeus	[1032]
		$D^{*+}\pi^-$	$2420.1 \pm 0.1 \pm 0.8$	$31.4 \pm 0.5 \pm 1.3$	*BABAR*	[935]
		$D^{*+}\pi^-$		$20.0 \pm 1.7 \pm 1.3$	CDF	[1033]
		$D^0\pi^+\pi^-$	$2426 \pm 3 \pm 1$	$24 \pm 7 \pm 8$	Belle	[601]
		$D^{*+}\pi^-$	$2421.4 \pm 1.5 \pm 0.9$	$23.7 \pm 2.7 \pm 4.0$	Belle	[695]
		$D^{*+}\pi^-$	$2421^{+1}_{-2} \pm 2$	20^{+6+3}_{-5-3}	CLEO	[1034]
		$D^{*+}\pi^-$	$2422 \pm 2 \pm 2$	$15 \pm 8 \pm 4$	E687	[1018]
		$D^{*+}\pi^-$	$2428 \pm 3 \pm 2$	23^{+8+10}_{-6-4}	CLEO	[1021]
		$D^{*+}\pi^-$	$2414 \pm 2 \pm 5$	$13 \pm 6^{+10}_{-5}$	ARGUS	[1035]
		$D^{*+}\pi^-$	$2428 \pm 8 \pm 5$	$58 \pm 14 \pm 10$	TPS	[1036]
			2420.5 ± 0.5	31.7 ± 0.7	Our average	
$D_1(2420)^\pm$	1^+	$D^{*0}\pi^+$	$2421.9 \pm 4.7^{+3.4}_{-1.2}$		Zeus	[1032]
		$D^+\pi^-\pi^+$	$2421 \pm 2 \pm 1$	$21 \pm 5 \pm 8$	Belle	[601]
		$D^{*0}\pi^+$	$2425 \pm 2 \pm 2$	$26^{+8}_{-7} \pm 4$	CLEO	[1037]
		$D^{*0}\pi^+$	$2443 \pm 7 \pm 5$	$41 \pm 19 \pm 8$	TPS	[1036]
			2423.2 ± 1.6	25.2 ± 6.0	Our average	
$D_1(2430)^0$	1^+	$D^{*+}\pi^-$	$2427 \pm 26 \pm 25$	$384^{+107}_{-75} \pm 74$	Belle	[695]
$D_2^*(2460)^0$	2^+	$D^{*+}\pi^-$	$2464.0 \pm 1.4 \pm 0.5 \pm 0.2$	$43.8 \pm 2.9 \pm 1.7 \pm 0.6$	LHCb	[701]
		$D^{*+}\pi^-$	$2460.4 \pm 0.4 \pm 1.2$	$43.2 \pm 1.2 \pm 3.0$	LHCb	[936]
		$D^+\pi^-$	$2460.4 \pm 0.1 \pm 0.1$	$45.6 \pm 0.4 \pm 1.1$	LHCb	[936]
		$D^{*+}\pi^-$, $D^+\pi^-$	$2462.5 \pm 2.4^{+1.3}_{-1.1}$	$46.6 \pm 8.1^{+5.9}_{-3.8}$	Zeus	[1032]
		$D^+\pi^-$	$2462.2 \pm 0.1 \pm 0.8$	$50.5 \pm 0.6 \pm 0.7$	*BABAR*	[935]
		$D^+\pi^-$	$2460.4 \pm 1.2 \pm 2.2$	$41.8 \pm 2.5 \pm 2.9$	*BABAR*	[696]
		$D^+\pi^-$		$49.2 \pm 2.3 \pm 1.3$	CDF	[1033]
		$D^+\pi^-$	$2461.6 \pm 2.1 \pm 3.3$	$45.6 \pm 4.4 \pm 6.7$	Belle	[695]
		$D^+\pi^-$	$2464.5 \pm 1.1 \pm 1.9$	$38.7 \pm 5.3 \pm 2.9$	Focus	[999]
		$D^+\pi^-$	$2465 \pm 3 \pm 3$	$28^{+8}_{-7} \pm 6$	CLEO	[1034]
		$D^+\pi^-$	$2453 \pm 3 \pm 2$	$25 \pm 10 \pm 5$	E687	[1018]
		$D^{*+}\pi^-$	$2461 \pm 3 \pm 1$	$20^{+9\ +9}_{-12-10}$	CLEO	[1021]
		$D^+\pi^-$	$2455 \pm 3 \pm 5$	15^{+13+5}_{-10-10}	ARGUS	[1038]
		$D^+\pi^-$	$2459 \pm 3 \pm 2$	$20 \pm 10 \pm 5$	TPS	[1036]
			2460.49 ± 0.17	47.52 ± 0.65	Our average	

Table 255: Recent measurements of mass and width for different excited D mesons. The column J^P list the most significant assignment of spin and parity. If possible an average mass or width is calculated.

Resonance	J^P	Decay mode	Mass [MeV/c^2]	Width [MeV]	Measured by	Reference
$D_2^*(2460)^\pm$	2^+	$D^0\pi^+$	$2468.6 \pm 0.6 \pm 0.0 \pm 0.3$	$47.3 \pm 1.5 \pm 0.3 \pm 0.6$	LHCb	[577]
		$D^0\pi^+$	$2465.6 \pm 1.8 \pm 0.5 \pm 1.2$	$46.0 \pm 3.4 \pm 1.4 \pm 2.9$	LHCb	[1030]
		$D^0\pi^+$	$2463.1 \pm 0.2 \pm 0.6$	$48.6 \pm 1.3 \pm 1.9$	LHCb	[936]
		$D^{*0}\pi^+$, $D^0\pi^+$	$2460.6 \pm 4.4^{+3.6}_{-0.8}$		Zeus	[1032]
		$D^0\pi^+$	$2465.4 \pm 0.2 \pm 1.1$		*BABAR*	[935]
		$D^0\pi^+$	$2465.7 \pm 1.8^{+1.4}_{-4.8}$	$49.7 \pm 3.8 \pm 6.4$	Belle	[1031]
		$D^0\pi^+$	$2467.6 \pm 1.5 \pm 0.8$	$34.1 \pm 6.5 \pm 4.2$	Focus	[999]
		$D^0\pi^+$	$2463 \pm 3 \pm 3$	$27^{+11}_{-8} \pm 5$	CLEO	[1037]
		$D^0\pi^+$	$2453 \pm 3 \pm 2$	$23 \pm 9 \pm 5$	E687	[1018]
		$D^0\pi^+$	$2469 \pm 4 \pm 6$		ARGUS	[1039]
			2465.55 ± 0.40	46.7 ± 1.2	Our average	
$D(2550)^0$	0^-	$D^{*+}\pi^-$	$2539.4 \pm 4.5 \pm 6.8$	$130 \pm 12 \pm 13$	*BABAR*	[935]
$D(2580)^0$	Unnatural	$D^{*+}\pi^-$	$2579.5 \pm 3.4 \pm 5.5$	$117.5 \pm 17.8 \pm 46.0$	LHCb	[936]
$D(2600)^0$	Natural	$D^+\pi^-$	$2608.7 \pm 2.4 \pm 2.5$	$93 \pm 6 \pm 13$	*BABAR*	[935]
$D(2600)^\pm$	Natural	$D^0\pi^+$	$2621.3 \pm 3.7 \pm 4.2$		*BABAR*	[935]
$D^*(2640)^\pm$	1^-	$D^{*+}\pi^+\pi^-$	$2637 \pm 2 \pm 6$		Delphi	[1040]
$D^*(2650)^0$	Natural	$D^{*+}\pi^-$	$2649.2 \pm 3.5 \pm 3.5$	$140.2 \pm 17.1 \pm 18.6$	LHCb	[936]
$D(2740)^0$	Unnatural	$D^{*+}\pi^-$	$2737.0 \pm 3.5 \pm 11.2$	$73.2 \pm 13.4 \pm 25.0$	LHCb	[936]
$D(2750)^0$		$D^{*+}\pi^-$	$2752.4 \pm 1.7 \pm 2.7$	$71 \pm 6 \pm 11$	*BABAR*	[935]
$D_1^*(2760)^0$	1^+	$D^+\pi^-$	$2781 \pm 18 \pm 11 \pm 6$	$177 \pm 32 \pm 20 \pm 7$	LHCb	[701]
		$D^{*+}\pi^-$	$2761.1 \pm 5.1 \pm 6.5$	$74.4 \pm 3.4 \pm 37.0$	LHCb	[936]
		$D^+\pi^-$	$2760.1 \pm 1.1 \pm 3.7$	$74.4 \pm 3.4 \pm 19.1$	LHCb	[936]
		$D^+\pi^-$	$2763.3 \pm 2.3 \pm 2.3$	$60.9 \pm 5.1 \pm 3.6$	*BABAR*	[935]
			2762.1 ± 2.4	65.1 ± 5.8	Our average	
$D_3^*(2760)^\pm$	3^-	$D^0\pi^+$	$2798 \pm 7 \pm 1 \pm 7$	$105 \pm 18 \pm 6 \pm 23$	LHCb	[577]
		$D^0\pi^+$	$2771.7 \pm 1.7 \pm 3.8$	$66.7 \pm 6.6 \pm 10.5$	LHCb	[936]
		$D^0\pi^+$	$2769.7 \pm 3.8 \pm 1.5$		*BABAR*	[935]
			2773.9 ± 3.3	72.3 ± 11.5	Our average	

Table 256: Product of B meson branching fraction and (daughter) excited D meson branching fraction.

Resonance	Decay	$\mathcal{B}r[10^{-4}]$	Measured by	Reference
$D_0^*(2400)^0$	$B^- \to D_0^*(2400)^0(\to D^+\pi^+)\pi^-$	$6.1 \pm 0.6 \pm 1.8$	Belle	[695]
		$6.8 \pm 0.3 \pm 2.0$	*BABAR*	[696]
		6.4 ± 1.4	Our average	
	$B^- \to D_0^*(2400)^0(\to D^+\pi^+)K^-$	$0.061 \pm 0.019 \pm 0.005 \pm 0.014 \pm 0.004$	LHCb	[701]
$D_0^*(2400)^\pm$	$\overline{B}^0 \to D_0^*(2400)^+(\to D^0\pi^+)\pi^-$	$0.77 \pm 0.05 \pm 0.03 \pm 0.03 \pm 0.04$	LHCb	[577]
		$0.60 \pm 0.13 \pm 0.27$	Belle	[1031]
		0.76 ± 0.07	Our average	
	$\overline{B}^0 \to D_0^*(2400)^+(\to D^0\pi^+)K^-$	$0.177 \pm 0.026 \pm 0.019 \pm 0.067 \pm 0.20$	LHCb	[1030]
$D_1(2420)^0$	$B^- \to D_1(2420)^0(\to D^{*+}\pi^-)\pi^-$	$6.8 \pm 0.7 \pm 1.3$	Belle	[695]
	$B^- \to D_1(2420)^0(\to D^0\pi^+\pi^-)\pi^-$	$1.85 \pm 0.29 \pm 0.27 \pm 0.41$	Belle	[601]
	$\overline{B}^0 \to D_1(2420)^0(\to D^{*+}\pi^-)\omega$	$0.7 \pm 0.2^{+0.1}_{-0.0} \pm 0.1$	Belle	[581]
$D_1(2420)^\pm$	$\overline{B}^0 \to D_1(2420)^+(\to D^+\pi^-\pi^+)\pi^-$	$0.89 \pm 0.15 \pm 0.22$	Belle	[601]
$D_1(2430)^0$	$B^- \to D_1(2430)^0(\to D^{*+}\pi^-)\pi^-$	$5.0 \pm 0.4 \pm 1.08$	Belle	[695]
	$\overline{B}^0 \to D_1(2430)^0(\to D^{*+}\pi^-)\omega$	$2.5 \pm 0.4^{+0.7+0.4}_{-0.2-0.1}$	Belle	[581]
$D_2^*(2460)^0$	$B^- \to D_2^*(2460)^0(\to D^+\pi^-)\pi^-$	$3.4 \pm 0.3 \pm 0.7$	Belle	[695]
		$3.5 \pm 0.2 \pm 0.5$	*BABAR*	[696]
		3.4 ± 0.3	Our average	
	$B^- \to D_2^*(2460)^0(\to D^{*+}\pi^-)\pi^-$	$1.8 \pm 0.3 \pm 0.4$	Belle	[695]
	$B^- \to D_2^*(2460)^0(\to D^{*+}\pi^-)\omega$	$0.4 \pm 0.1^{+0.0}_{-0.1} \pm 0.1$	Belle	[581]
	$B^- \to D_2^*(2460)^0(\to D^+\pi^+)K^-$	$0.232 \pm 0.011 \pm 0.006 \pm 0.010 \pm 0.016$	LHCb	[701]
$D_2^*(2460)^\pm$	$\overline{B}^0 \to D_2^*(2460)^+(\to D^0\pi^+)\pi^-$	$2.44 \pm 0.07 \pm 0.10 \pm 0.04 \pm 0.12$	LHCb	[577]
		$2.15 \pm 0.17 \pm 0.31$	Belle	[1031]
		2.38 ± 0.16	Our average	
	$\overline{B}^0 \to D_2^*(2460)^+(\to D^0\pi^+)K^-$	$0.212 \pm 0.010 \pm 0.011 \pm 0.011 \pm 0.25$	LHCb	[1030]
$D_1^*(2760)^0$	$B^- \to D_1^*(2760)^0(\to D^+\pi^+)K^-$	$0.036 \pm 0.009 \pm 0.003 \pm 0.007 \pm 0.002$	LHCb	[701]
$D_3^*(2760)^\pm$	$\overline{B}^0 \to D_3^*(2760)^0(\to D^0\pi^+)\pi^-$	$0.103 \pm 0.016 \pm 0.007 \pm 0.008 \pm 0.005$	LHCb	[577]

Table 257: Product of B meson branching fraction and (daughter) excited D_s meson branching fraction.

Resonance	Decay	$\mathcal{B}r[10^{-4}]$	Measured by	Reference
$D^*_{s0}(2317)^\pm$	$B^0 \to D^*_{s0}(2317)^+(\to D_s^+\pi^0)D^-$	$8.6^{+3.3}_{-2.6} \pm 2.6$	Belle	[624]
		$18.0 \pm 4.0^{+6.7}_{-5.0}$	*BABAR*	[625]
		$10.1^{+1.3}_{-1.2} \pm 1.0 \pm 0.4$	Belle	[626]
		10.2 ± 1.5	Our average	
	$B^+ \to D^*_{s0}(2317)^+(\to D_s^+\pi^0)\overline{D}^0$	$8.0^{+1.3}_{-1.2} \pm 1.0 \pm 0.4$	Belle	[626]
	$B^0 \to D^*_{s0}(2317)^+(\to D_s^+\pi^0)K^-$	$0.53^{+0.15}_{-0.13} \pm 0.16$	Belle	[602]
$D_{s1}(2460)^\pm$	$B^0 \to D_{s1}(2460)^+(\to D_s^{*+}\pi^0)D^-$	$22.7^{+7.3}_{-6.2} \pm 6.8$	Belle	[624]
		$28.0 \pm 8.0^{+11.2}_{-7.8}$	*BABAR*	[625]
		24.7 ± 7.6	Our average	
	$B^0 \to D_{s1}(2460)^+(\to D_s^{*+}\gamma)D^-$	$8.2^{+2.2}_{-1.9} \pm 2.5$	Belle	[624]
		$8.0 \pm 2.0^{+3.2}_{-2.3}$	*BABAR*	[625]
		8.1 ± 2.3	Our average	
	$D_{s1}(2460)^+ \to D_s^{*+}\pi^0$	$(56 \pm 13 \pm 9)\%$	*BABAR*	[615]
	$D_{s1}(2460)^+ \to D_s^{*+}\gamma$	$(16 \pm 4 \pm 3)\%$	*BABAR*	[615]
$D_{s1}(2536)^\pm$	$B^0 \to D_{s1}(2536)^+(\to D^{*0}K^+)D^-$	$1.71 \pm 0.48 \pm 0.32$	*BABAR*	[622]
	$B^0 \to D_{s1}(2536)^+(\to D^{*+}K^0)D^-$	$2.61 \pm 1.03 \pm 0.31$	*BABAR*	[622]
	$B^0 \to D_{s1}(2536)^+(\to D^{*0}K^+)D^{*-}$	$3.32 \pm 0.88 \pm 0.66$	*BABAR*	[622]
	$B^0 \to D_{s1}(2536)^+(\to D^{*+}K^0)D^{*-}$	$5.00 \pm 1.51 \pm 0.67$	*BABAR*	[622]
	$B^+ \to D_{s1}(2536)^+(\to D^{*0}K^+)\overline{D}^0$	$2.16 \pm 0.52 \pm 0.45$	*BABAR*	[622]
	$B^+ \to D_{s1}(2536)^+(\to D^{*+}K^0)\overline{D}^0$	$2.30 \pm 0.98 \pm 0.43$	*BABAR*	[622]
	$B^+ \to D_{s1}(2536)^+(\to D^{*0}K^+)\overline{D}^{*0}$	$5.46 \pm 1.17 \pm 1.04$	*BABAR*	[622]
	$B^+ \to D_{s1}(2536)^+(\to D^{*+}K^0)\overline{D}^{*0}$	$3.92 \pm 2.46 \pm 0.83$	*BABAR*	[622]
$D_{s2}(2573)^\pm$	$B^0 \to D_{s2}(2573)(\to D^0K^+)D^-$	$0.34 \pm 0.17 \pm 0.05$	*BABAR*	[1029]
	$B^+ \to D_{s2}(2573)(\to D^0K^+)\overline{D}^0$	$0.08 \pm 14 \pm 0.05$	*BABAR*	[1029]
$D_{s1}(2700)^\pm$	$B^+ \to D_{s1}(2700)^+(\to D^0K^+)\overline{D}^0$	$11.3 \pm 2.2^{+1.4}_{-2.8}$	Belle	[718]
		$5.02 \pm 0.71 \pm 0.93$	*BABAR*	[1029]
		5.83 ± 1.09	Our average	
	$B^0 \to D_{s1}(2700)^+(\to D^0K^+)D^-$	$7.14 \pm 0.96 \pm 0.69$	*BABAR*	[1029]

Table 258: Mass difference measurements for excited D mesons.

Resonance	Relative to	Δm [MeV/c^2]	Measured by	Reference
$D_1^*(2420)^0$	D^{*+}	$410.2 \pm 2.1 \pm 0.9$	Zeus	[1041]
		$411.7 \pm 0.7 \pm 0.4$	CDF	[1033]
		411.5 ± 0.8	Our average	
$D_1(2420)^\pm$	$D_1^*(2420)^0$	$4^{+2}_{-3} \pm 3$	CLEO	[1037]
$D_2^*(2460)^0$	D^+	$593.9 \pm 0.6 \pm 0.5$	CDF	[1033]
	D^{*+}	$458.8 \pm 3.7^{+1.2}_{-1.3}$	Zeus	[1041]
$D_2^*(2460)^\pm$	$D_2^*(2460)^0$	$3.1 \pm 1.9 \pm 0.9$	Focus	[999]
		$-2 \pm 4 \pm 4$	CLEO	[1037]
		$14 \pm 5 \pm 8$	ARGUS	[1039]
		3.0 ± 1.9	Our average	
$D_{s0}^*(2317)^\pm$	$D_s^\pm$	$348.7 \pm 0.5 \pm 0.7$	Belle	[997]
		$350.0 \pm 1.2 \pm 1.0$	CLEO	[996]
		$351.3 \pm 2.1 \pm 1.9$	Belle	[624]
		349.2 ± 0.7	Our average	
$D_{s1}(2460)^\pm$	$D_s^{*\pm}$	$344.1 \pm 1.3 \pm 1.1$	Belle	[997]
		$351.2 \pm 1.7 \pm 1.0$	CLEO	[996]
		$346.8 \pm 1.6 \pm 1.9$	Belle	[624]
		347.1 ± 1.1	Our average	
	$D_s^\pm$	$491.0 \pm 1.3 \pm 1.9$	Belle	[997]
		$491.4 \pm 0.9 \pm 1.5$	Belle	[997]
		491.3 ± 1.4	Our average	
$D_{s1}(2536)^\pm$	$D^*(2010)^\pm$	$524.83 \pm 0.01 \pm 0.04$	*BABAR*	[1023]
		$525.30^{+0.44}_{-0.41} \pm 0.10$	Zeus	[1041]
		$525.3 \pm 0.6 \pm 0.1$	ALEPH	[1042]
		524.84 ± 0.04	Our average	
	$D^*(2007)^0$	$528.7 \pm 1.9 \pm 0.5$	ALEPH	[1042]
$D_{s2}^*(2573)^\pm$	D^0	$704 \pm 3 \pm 1$	ALEPH	[1042]

Table 259: Measurements of polarization amplitudes for excited D mesons.

Resonance	A_D	Measured by	Reference
$D_1(2420)^0$	$7.8^{+6.7+4.6}_{-2.7-1.8}$	ZEUS	[1032]
	5.72 ± 0.25	*BABAR*	[935]
	$5.9^{+3.0+2.4}_{-1.7-1.0}$	ZEUS	[1041]
	$3.8 \pm 0.6 \pm 0.8$	*BABAR*	[487]
	5.61 ± 0.24	Our average	
$D_1(2420)^\pm$	$3.8 \pm 0.6 \pm 0.8$	*BABAR*	[487]
$D_2^*(2460)^0$	-1.16 ± 0.35	ZEUS	[1032]
$D(2750)^0$	-0.33 ± 0.28	*BABAR*	[935]

8.10 Charm baryons

In this section we summarize the present status of excited charmed baryons, decaying strongly or electromagnetically. We list their masses (or the mass difference between the excited baryon and the corresponding ground state), natural widths, decay modes, and assigned quantum numbers. The present ground-state measurements are: $M(\Lambda_c^+) = 2286.46 \pm 0.14$ MeV/c^2 measured by *BABAR* [1043], $M(\Xi_c^0) = 2470.85^{+0.28}_{-0.04}$ MeV/c^2 and $M(\Xi_c^+) = 2467.93^{+0.28}_{-0.40}$ MeV/c^2, both dominated by CDF [144], and $M(\Omega_c^0) = 2695.2 \pm 1.7$ MeV/c^2, doinated by Belle [1044]. Should these values change, so will some (but not all) of the values for the masses of the excited states.

Table 260 summarizes the excited Λ_c^+ baryons. The first two states, namely the $\Lambda_c(2595)^+$ and $\Lambda_c(2625)^+$, are well-established. Based on the measured masses and decay patterns, it is believed they are orbitally excited Λ_c^+ baryons with total angular momentum of the light quarks $L = 1$. Thus their quantum numbers are assigned to be $J^P = (\frac{1}{2})^-$ and $J^P = (\frac{3}{2})^-$, respectively. Their mass measurements are dominated by CDF [1045]: $M(\Lambda_c(2595)^+) = 2592.25 \pm 0.24 \pm 0.14$ MeV/c^2 and $M(\Lambda_c(2625)^+) = 2628.11 \pm 0.13 \pm 0.14$ MeV/c^2. Earlier measurements did not fully take into account the restricted phase-space of the $\Lambda_c(2595)^+$ decays.

The next two states, $\Lambda_c(2765)^+$ and $\Lambda_c(2880)^+$, were discovered by CLEO [1046] in the $\Lambda_c^+\pi^+\pi^-$ final state. CLEO found that some of these decays of the $\Lambda_c(2880)^+$ proceed via an intermediate $\Sigma_c(2445)^{++/0}\pi^{-/+}$. Later, *BABAR* [1047] observed that this state has also a D^0p decay mode. This was the first example of an excited charmed baryon decaying into a charm meson plus a baryon; all excited charmed baryon decays were found in final states comprising a charmed baryon and one or more light mesons. In the same analysis, *BABAR* observed for the first time an additional state, $\Lambda_c(2940)^+$, which decays into D^0p. Looking for the D^+p final state, *BABAR* found no signal; this implies that the $\Lambda_c(2880)^+$ and $\Lambda_c(2940)^+$ are really Λ_c^+ excited states rather than Σ_c excitations. Belle reported the result of an angular analysis that favors 5/2 for the $\Lambda_c(2880)^+$ spin hypothesis. Moreover, the measured ratio of branching fractions $\mathcal{B}(\Lambda_c(2880)^+ \to \Sigma_c(2520)\pi^\pm)/\mathcal{B}(\Lambda_c(2880)^+ \to \Sigma_c(2455)\pi^\pm) = (0.225 \pm 0.062 \pm 0.025)$, combined with theoretical predictions based on HQS [481, 1048], favor even parity. However this prediction is only valid if the p-wave portion of $\Sigma_c(2520)\pi$ is suppressed. The current open questions in the excited Λ_c^+ family include the determination of quantum numbers for the other states, and the nature of the $\Lambda_c(2765)^+$ state, in particular whether it is an excited Σ_c^+ or Λ_c^+. However, there is no doubt that the latter state exists, as it is clearly visible in Belle data.

Table 260: Summary of excited Λ_c^+ baryons.

Charmed Baryon Excited State	Mode	Mass (MeV/c^2)	Natural Width (MeV/c^2)	J^P
$\Lambda_c(2595)^+$	$\Lambda_c^+\pi^+\pi^-$, $\Sigma_c\pi$	2592.25 ± 0.28	$2.59 \pm 0.30 \pm 0.47$	$1/2^-$
$\Lambda_c(2625)^+$	$\Lambda_c^+\pi^+\pi^-$, $\Sigma_c\pi$	2628.11 ± 0.19	< 1.9	$3/2^-$
$\Lambda_c(2765)^+$	$\Lambda_c^+\pi^+\pi^-$, $\Sigma_c\pi$	2766.6 ± 2.4	50	??
$\Lambda_c(2880)^+$	$\Lambda_c^+\pi^+\pi^-$, $\Sigma_c\pi$, $\Sigma_c(2520)\pi$, D^0p	2881.53 ± 0.35	5.8 ± 1.1	$5/2^+$ (experimental evidence)
$\Lambda_c(2940)^+$	D^0p, $\Sigma_c\pi$	$2939.3^{+1.4}_{-1.5}$	17^{+8}_{-6}	??

Table 261 summarizes the excited $\Sigma_c^{++,+,0}$ baryons. The iso-triplets of $\Sigma_c(2455)^{++,+,0}$ and $\Sigma_c(2520)^{++,+,0}$ baryons are well-established. Belle [1049] precisely measured the mass differ-

ences (see above for the definition) and widths of the doubly charged and neutral members of this triplet. The short list of excited Σ_c baryons is completed by the triplet of $\Sigma_c(2800)$ states observed by Belle [1050]. Based on the measured masses and theoretical predictions [1051,1052], these states are thought to be members of the predicted Σ_{c2} $3/2^-$ triplet. From a study of resonant substructure in $B^- \to \Lambda_c^+ \overline{p}\pi^-$ decays, *BABAR* found a significant signal for $\Lambda_c^+\pi^-$ with a mean value higher than that measured by Belle by about 3σ (Table 261). The decay widths measured by Belle and *BABAR* are consistent, but it is an open question if the oberved state is the same as the Belle state.

Table 261: Summary of the excited $\Sigma_c^{++,+,0}$ baryon family.

Charmed Baryon Excited State	Mode	ΔM (MeV/c^2)	Natural Width (MeV/c^2)	J^P
$\Sigma_c(2455)^{++}$	$\Lambda_c^+\pi^+$	167.510 ± 0.17	$1.89\pm^{+0.09}_{-0.18}$	$1/2^+$
$\Sigma_c(2455)^{+}$	$\Lambda_c^+\pi^+$	166.4 ± 0.4	< 4.6 @ 90% C.L.	$1/2^+$
$\Sigma_c(2455)^{0}$	$\Lambda_c^+\pi^+$	167.29 ± 0.17	$1.83^{+0.11}_{-0.19}$	$1/2^+$
$\Sigma_c(2520)^{++}$	$\Lambda_c^+\pi^+$	$231.95^{+0.17}_{-0.12}$	$14.78 \pm +0.30_{-0.40}$	$3/2^+$
$\Sigma_c(2520)^{+}$	$\Lambda_c^+\pi^+$	231.0 ± 2.3	< 17 @ 90% C.L.	$3/2^+$
$\Sigma_c(2520)^{0}$	$\Lambda_c^+\pi^+$	$232.02^{+0.15}_{-0.14}$	$15.3^{+0.4}_{-0.5}$	$3/2^+$
$\Sigma_c(2800)^{++}$	$\Lambda_c^+\pi^+$	514^{+4}_{-6}	75^{+18+12}_{-13-11}	tentatively identified
$\Sigma_c(2800)^{+}$	$\Lambda_c^+\pi^0$	505^{+15}_{-5}	62^{+37+52}_{-23-38}	as members of the predicted
$\Sigma_c(2800)^{0}$	$\Lambda_c^+\pi^-$	519^{+5}_{-7}	72^{+22}_{-15}	Σ_{c2} $3/2^-$ isospin triplet?
	$\Lambda_c^+\pi^-$	$560 \pm 8 \pm 10$	86^{+33}_{-22}	

Table 262 summarizes the excited $\Xi_c^{+,0}$ and Ω_c^0 baryons. The list of excited Ξ_c baryons has several states, of unknown quantum numbers, having masses above 2900 MeV/c^2 and decaying into three different types of decay modes: $\Lambda_c/\Sigma_c n\pi$, $\Xi_c n\pi$ and the most recently observed ΛD. Some of these states ($\Xi_c(2970)^+$, $\Xi_c(3055)$ and $\Xi_c(3080)^{+,0}$) have been observed by both Belle [1053–1055] and *BABAR* [683] and are considered well-established. The $\Xi_c(2930)^0$ state decaying into $\Lambda_c^+K^-$ is seen only by *BABAR* [1056] and needs confirmation. The $\Xi_c(3123)^+$ observed by *BABAR* [683] in the $\Sigma_c(2520)^{++}\pi^-$ final state has not been confirmed by Belle [1054] with twice the statistics, and so its existence is in doubt.

Several of the width and mass measurements for the $\Xi_c(3055)$ and $\Xi_c(3080)$ iso-doublets are only in marginal agreement between experiments and decay modes. However, there seems little doubt that the differing measurements are of the same particle.

Belle [1057] has recently performed high statistics measurements of the Ξ_c', $\Xi_c(2645)$, $\Xi_c(2790)$, $\Xi_c(2815)$ and $\Xi_c(2970)$, leading to the most precise mass measurements of all five iso-doublets and the first significant width measurements of the $\Xi_c(2645)$, $\Xi_c(2790)$ and $\Xi_c(2815)$. The level of agreement in the different measurements of the mass and width of the $\Xi_c(2970)$, formerly named by the PDG as the $\Xi_c(2980)$, is not satisfactory. This leaves open the possibility of there being other resonances nearby or that threshold effects have not been fully understood. The present situation in the excited Ξ_c sector is summarized in in Table 262.

The excited Ω_c^0 doubly strange charmed baryon has been seen by both *BABAR* [1058] and Belle [1044]. The mass differences $\delta M = M(\Omega_c^{*0}) - M(\Omega_c^0)$ measured by the experiments are in good agreement and are also consistent with most theoretical predictions [1059–1062]. No higher mass Ω_c states have yet been observed.

Figure 186 shows the levels of excited charm baryons along with corresponding transitions between them, and also transitions to the ground states. We note that Belle and *BABAR* recently

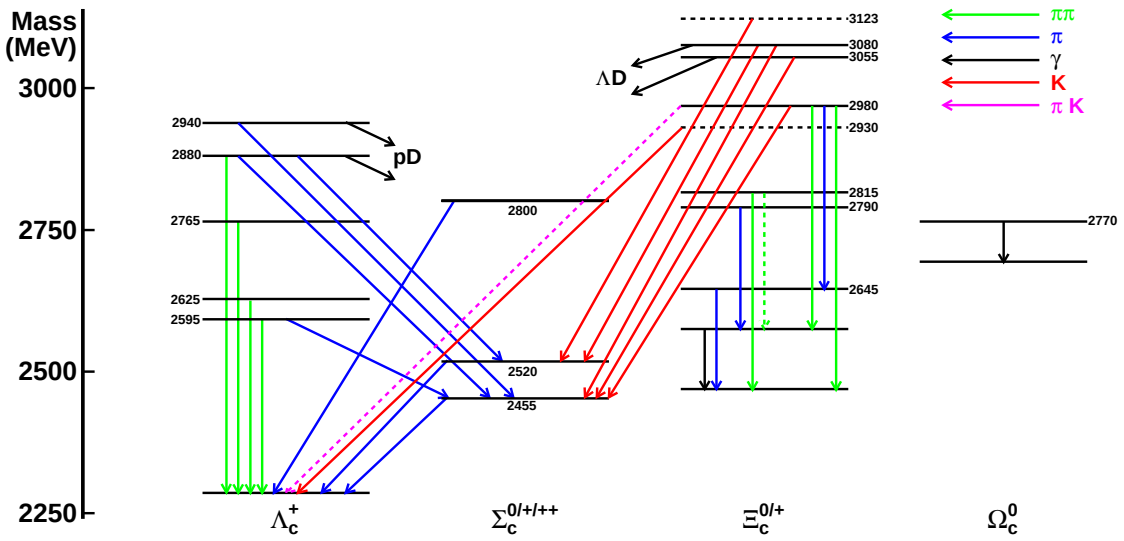

Figure 186: Level diagram for excited charm baryons.

discovered that transitions between families are possible, *i.e.*, between the Ξ_c and Λ_c^+ families of excited charmed baryons, and that highly excited states are found to decay into a non-charmed baryons and a D meson.

Table 262: Summary of excited $\Xi_c^{+,0}$ and Ω_c^0 baryon families. For the first four is-doublets, the mass difference with respect to the ground state is given, as the uncertainties are dominated by the uncertainty in the ground state mass. In the remaining cases, the uncertainty on the measurement of the excited state itself dominates.

Charmed Baryon Excited State	Mode	Mass Difference (MeV/c^2)	Natural Width (MeV/c^2)	J^P
$\Xi_c'^+$	$\Xi_c^+\gamma$	110.5 ± 0.4		$1/2^+$
$\Xi_c'^0$	$\Xi_c^0\gamma$	108.3 ± 0.4		$1/2^+$
$\Xi_c(2645)^+$	$\Xi_c^0\pi^+$	178.5 ± 0.1	2.1 ± 0.2	$3/2^+$
$\Xi_c(2645)^0$	$\Xi_c^+\pi^-$	174.7 ± 0.1	2.4 ± 0.2	$3/2^+$
$\Xi_c(2790)^+$	$\Xi_c'^0\pi^+$	320.7 ± 0.5	9 ± 1	$1/2^-$
$\Xi_c(2790)^0$	$\Xi_c'^+\pi^-$	323.8 ± 0.5	10 ± 1	$1/2^-$
$\Xi_c(2815)^+$	$\Xi_c(2645)^0\pi^+$	348.8 ± 0.1	2.43 ± 0.23	$3/2^-$
$\Xi_c(2815)^0$	$\Xi_c(2645)^+\pi^-$	349.4 ± 0.1	2.54 ± 0.23	$3/2^-$
Charmed Baryon Excited State	Mode	Mass (MeV/c^2)	Natural Width (MeV/c^2)	J^P
$\Xi_c(2930)^0$	$\Lambda_c^+K^-$	2931.6 ± 6	36 ± 13	??
$\Xi_c(2970)^+$	$\Lambda_c^+K^-\pi^+$, $\Sigma_c^{++}K^-$, $\Xi_c(2645)^0\pi^+$	2967.2 ± 0.8	21 ± 3	??
$\Xi_c(2970)^0$	$\Xi_c(2645)^+\pi^-$	2970.4 ± 0.8	28 ± 3	??
$\Xi_c(3055)^+$	$\Sigma_c^{++}K^-$,ΛD	3055.7 ± 0.4	8.0 ± 1.9	??
$\Xi_c(3055)^0$	ΛD	3059.0 ± 0.8	6.2 ± 2.4	??
$\Xi_c(3080)^+$	$\Lambda_c^+K^-\pi^+$, $\Sigma_c^{++}K^-$, $\Sigma_c(2520)^{++}K^-$, ΛD	3077.8 ± 0.3	3.6 ± 0.7	??
$\Xi_c(3080)^0$	$\Lambda_c^+K_S^0\pi^-$, $\Sigma_c^0K_S^0$, $\Sigma_c(2520)^0K_S^0$	3079.9 ± 1.0	5.6 ± 2.2	??
$\Omega_c(2770)^0$	$\Omega_c^0\gamma$	2765.9 ± 2.0	$70.7^{+0.8}_{-0.9}$	$3/2^+$

8.11 Λ_c^+ branching fractions

Charmed baryon decays play an important role in studies of weak and strong interactions and provide a crucial input in studies of exclusive and inclusive decay rate measurements of b-flavored mesons and baryons or the measurements of fragmentation fractions of charm and bottom quarks. Albeit their importance, the experimental input on branching fractions of Λ_c^+ baryons was scarce until 2014 when Belle published the first ever model-independent measurement of branching fractions of $\Lambda_c^+ \to pK^-\pi^+$ decays [1063] that improved the precision of previous model-dependent determinations by a factor of 5. The precisions of branching fractions of multiple hadronic Cabibbo-favored Λ_c^+ baryon decays have further been improved with the first direct measurement based on threshold data performed by BESIII [1064]. In addition, BESIII reported the first absolute measurement of branching fractions of the most favorable semi-leptonic mode $\Lambda_c^+ \to \Lambda e^+\nu_e$ [1065]. In this note, we present a global fit to branching fractions of the Cabbibo-favored Λ_c^+ decays taking into account many different experimental measurements.

The measurements listed in Table 263 have been used in a least χ^2 fit. The fitted quantities, branching fractions of twelve hadronic and one semileptonic Λ_c^+ decay, and the input measurements are labelled using the PDG Γ_n notation, where n is an integer number that matches the notation from the PDG 2014 edition [314]. Therefore, the fit output consists of 13 quantities – twelve hadronic and one semileptonic Λ_c^+ decay branching fraction. We have taken into account the correlations for the measurements from the same experiment for the systematic uncertainties related to: normalization, track finding efficiency, particle identification efficiency, π^0, K_S^0, and Λ reconstruction efficiencies. In the case of the simultaneous determination of twelve hadronic Λ_c^+ absolute branching fractions by BESIII [1064], we use the published correlation matrix.

The world average values for twelve hadronic and one semileptonic Λ_c^+ decay rates are given in Table 263. The overall χ^2 value of the global fit is 30.0 for 23 degrees of freedom, which corresponds to a p value of 0.149. Correlation matrix between the fitted branching fractions is shown in Fig. 187 and constraints from individual measurements for the pairs of fitted branching fractions are shown in Fig. 188. The branching fraction of the normalisation decay, $\Lambda_c^+ \to pK^-\pi^+$, is found to be

$$\mathcal{B}(\Lambda_c^+ \to pK^-\pi^+) = (6.46 \pm 0.24)\%.$$

Table 263: Experimental results and world averages for branching fractions of twelve hadronic and one semileptonic Λ_c^+ decay. The first uncertainty is statistical and the second is systematic.

Λ_c^+ branching fraction	Value	Reference
$\boldsymbol{\Gamma_1 = pK_S^0}$	$\boldsymbol{(1.59 \pm 0.07)\%}$	HFAG Fit
BESIII	$(1.52 \pm 0.08 \pm 0.03)\%$	[1064]
$\frac{\Gamma_1}{\Gamma_2} = \frac{pK_S^0}{pK^-\pi^+}$	$\boldsymbol{0.246 \pm 0.009}$	HFAG Fit
CLEO	$0.22 \pm 0.04 \pm 0.03$	[1066]
CLEO	$0.23 \pm 0.01 \pm 0.02$	[1067]
$\boldsymbol{\Gamma_2 = pK^-\pi^+}$	$\boldsymbol{(6.46 \pm 0.24)\%}$	HFAG Fit

Table 263 – continued from previous page

Λ_c^+ branching fraction	Value	Reference
Belle	$(6.84 \pm 0.24^{+0.21}_{-0.27})\%$	[1063]
BESIII	$(5.84 \pm 0.27 \pm 0.23)\%$	[1064]
$\boldsymbol{\Gamma_7 = pK_S^0\pi^0}$	$\boldsymbol{(2.03 \pm 0.12)\%}$	HFAG Fit
BESIII	$(1.87 \pm 0.13 \pm 0.05)\%$	[1064]
$\frac{\Gamma_7}{\Gamma_2} = \frac{pK_S^0\pi^0}{pK^-\pi^+}$	$\mathbf{0.314 \pm 0.017}$	HFAG Fit
CLEO	$0.33 \pm 0.03 \pm 0.04$	[1067]
$\boldsymbol{\Gamma_9 = pK_S^0\pi^+\pi^-}$	$\boldsymbol{(1.69 \pm 0.11)\%}$	HFAG Fit
BESIII	$(1.53 \pm 0.11 \pm 0.09)\%$	[1064]
$\frac{\Gamma_9}{\Gamma_2} = \frac{pK_S^0\pi^+\pi^-}{pK^-\pi^+}$	$\mathbf{0.261 \pm 0.013}$	HFAG Fit
CLEO	$0.22 \pm 0.06 \pm 0.02$	[1066]
CLEO	$0.26 \pm 0.02 \pm 0.03$	[1067]
$\boldsymbol{\Gamma_{10} = pK^-\pi^+\pi^0}$	$\boldsymbol{(5.05 \pm 0.29)\%}$	HFAG Fit
BESIII	$(4.53 \pm 0.23 \pm 0.30)\%$	[1064]
$\frac{\Gamma_{10}}{\Gamma_2} = \frac{pK^-\pi^+\pi^0}{pK^-\pi^+}$	$\mathbf{0.781 \pm 0.031}$	HFAG Fit
CLEO	$0.67 \pm 0.04 \pm 0.11$	[1067]
$\boldsymbol{\Gamma_{23} = \Lambda\pi^+}$	$\boldsymbol{(1.28 \pm 0.06)\%}$	HFAG Fit
BESIII	$(1.24 \pm 0.07 \pm 0.03)\%$	[1064]
$\frac{\Gamma_{23}}{\Gamma_2} = \frac{\Lambda\pi^+}{pK^-\pi^+}$	$\mathbf{0.198 \pm 0.008}$	HFAG Fit
CLEO	$0.18 \pm 0.03 \pm 0.03$	[1066]
ARGUS	$0.18 \pm 0.03 \pm 0.04$	[1068]
FOCUS	$0.217 \pm 0.013 \pm 0.020$	[1069]
$\boldsymbol{\Gamma_{24} = \Lambda\pi^+\pi^0}$	$\boldsymbol{(7.09 \pm 0.36)\%}$	HFAG Fit
BESIII	$(7.01 \pm 0.37 \pm 0.19)\%$	[1064]
$\frac{\Gamma_{24}}{\Gamma_2} = \frac{\Lambda\pi^+\pi^0}{pK^-\pi^+}$	$\mathbf{1.10 \pm 0.05}$	HFAG Fit
CLEO	$0.73 \pm 0.09 \pm 0.16$	[1070]
$\boldsymbol{\Gamma_{26} = \Lambda\pi^+\pi^-\pi^+}$	$\boldsymbol{(3.73 \pm 0.21)\%}$	HFAG Fit
BESIII	$(3.81 \pm 0.24 \pm 0.18)\%$	[1064]
$\frac{\Gamma_{26}}{\Gamma_2} = \frac{\Lambda\pi^+\pi^-\pi^+}{pK^-\pi^+}$	$\mathbf{0.577 \pm 0.022}$	HFAG Fit
CLEO	$0.65 \pm 0.11 \pm 0.12$	[1066]
FOCUS	$0.508 \pm 0.024 \pm 0.024$	[1069]
ARGUS	$0.61 \pm 0.16 \pm 0.04$	[1071]
$\boldsymbol{\Gamma_{39} = \Sigma^0\pi^+}$	$\boldsymbol{(1.31 \pm 0.07)\%}$	HFAG Fit

Table 263 – continued from previous page

Λ_c^+ branching fraction	Value	Reference
BESIII	$(1.27 \pm 0.08 \pm 0.03)\%$	[1064]
$\frac{\Gamma_{39}}{\Gamma_2} = \frac{\Sigma^0\pi^+}{pK^-\pi^+}$	**0.202 ± 0.009**	HFAG Fit
CLEO	$0.21 \pm 0.02 \pm 0.04$	[1070]
ARGUS	$0.17 \pm 0.06 \pm 0.04$	[1068]
$\frac{\Gamma_{39}}{\Gamma_{23}} = \frac{\Sigma^0\pi^+}{\Lambda\pi^+}$	**1.02 ± 0.03**	HFAG Fit
FOCUS	$1.09 \pm 0.11 \pm 0.19$	[1069]
BABAR	$0.997 \pm 0.015 \pm 0.051$	[1072]
$\Gamma_{40} = \Sigma^+\pi^0$	**$(1.25 \pm 0.09)\%$**	HFAG Fit
BESIII	$(1.18 \pm 0.10 \pm 0.03)\%$	[1064]
$\frac{\Gamma_{40}}{\Gamma_2} = \frac{\Sigma^+\pi^0}{pK^-\pi^+}$	**0.193 ± 0.014**	HFAG Fit
CLEO	$0.20 \pm 0.03 \pm 0.03$	[1073]
$\Gamma_{42} = \Sigma^+\pi^+\pi^-$	**$(4.64 \pm 0.24)\%$**	HFAG Fit
BESIII	$(4.25 \pm 0.24 \pm 0.20)\%$	[1064]
$\frac{\Gamma_{42}}{\Gamma_2} = \frac{\Sigma^+\pi^+\pi^-}{pK^-\pi^+}$	**0.719 ± 0.028**	HFAG Fit
CLEO	$0.74 \pm 0.07 \pm 0.09$	[1073]
$\Gamma_{48} = \Sigma^+\omega$	**$(1.77 \pm 0.21)\%$**	HFAG Fit
BESIII	$(1.56 \pm 0.20 \pm 0.07)\%$	[1064]
$\frac{\Gamma_{48}}{\Gamma_2} = \frac{\Sigma^+\omega}{pK^-\pi^+}$	**0.274 ± 0.031**	HFAG Fit
CLEO	$0.54 \pm 0.13 \pm 0.06$	[1073]
$\Gamma_{65} = \Lambda e^+\nu_e$	**$(3.18 \pm 0.32)\%$**	HFAG Fit
BESIII	$(3.63 \pm 0.38 \pm 0.20)\%$	[1065]
$\frac{\Gamma_{65}}{\Gamma_2} = \frac{\Lambda e^+\nu_e}{pK^-\pi^+}$	**0.492 ± 0.049**	HFAG Fit
CLEO	0.43 ± 0.08	[1074]
ARGUS	0.36 ± 0.14	[1075]

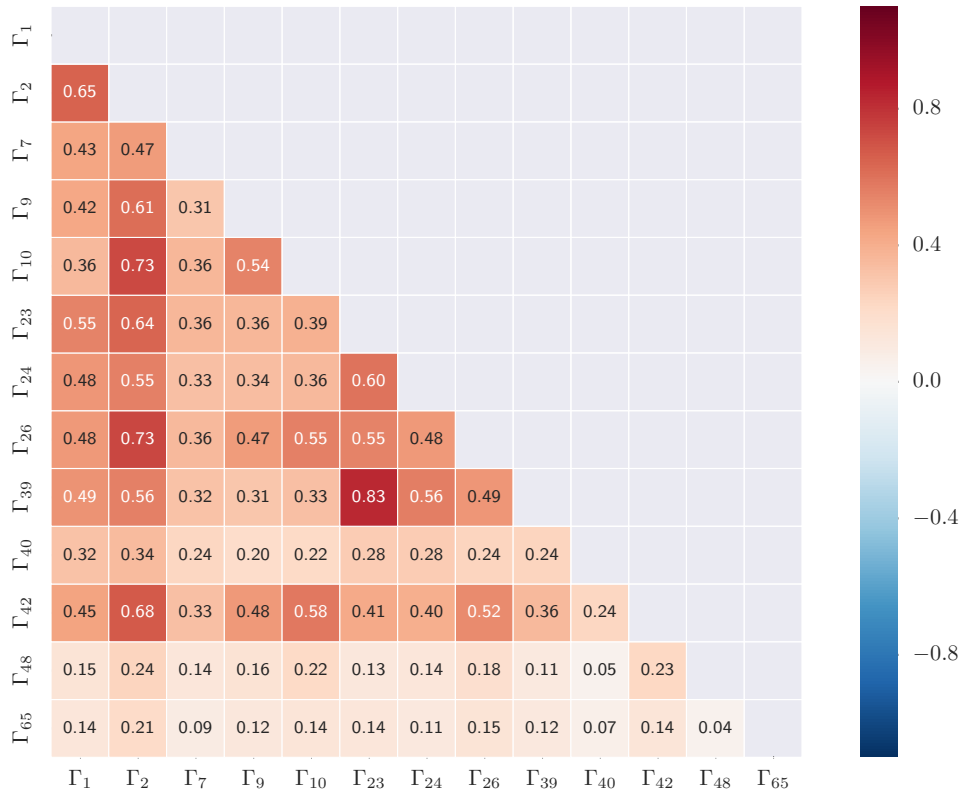

Figure 187: Correlation coefficients between averaged Λ_c^+ branching fractions.

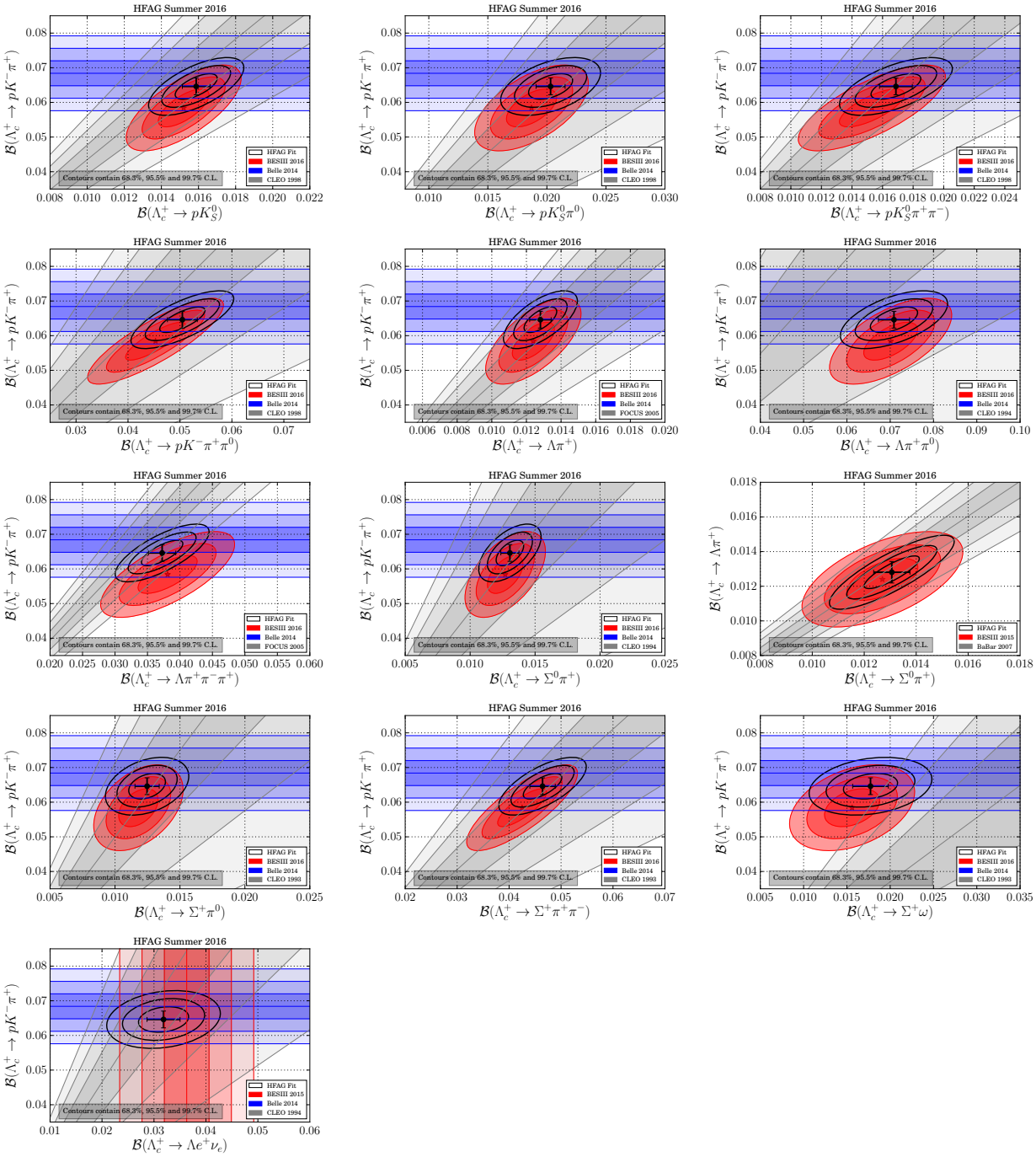

Figure 188: Plots of all individual measurements and the fitted averages. Individual measurements are plotted as bands (ellipses) showing their $\pm 1\sigma$, $\pm 2\sigma$, and $\pm 3\sigma$ ranges. The best fit value is indicated by a cross showing the one-dimensional errors. In cases where multiple ratio measurements exists (Γ_i/Γ_j) only the most precise one is plotted.

8.12 Rare and forbidden decays

This section provides a summary of rare and forbidden charm decays in tabular form. The decay modes can be categorized as flavor-changing neutral currents, lepton-flavor-violating, lepton-number-violating, and both baryon- and lepton-number-violating decays. Figures 189-191 plot the upper limits for D^0, D^+, D_s^+, and Λ_c^+ decays. Tables 264-267 give the corresponding numerical results. Some theoretical predictions are given in Refs. [1076–1083].

In several cases the rare-decay final states have been observed with the di-lepton pair being the decay product of a hadronic resonance. For these measurements the quoted limits are those expected for the non-resonant di-lepton spectrum. For the extrapolation to the full spectrum a phase-space distribution of the non-resonant component has been assumed. This applies to the CLEO measurement of the decays $D_{(s)}^+ \to (K^+\pi^+)e^+e^-$ [1084], to the D0 measurements of the decays $D_{(s)}^+ \to \pi^+\mu^+\mu^-$ [1085], and to the *BABAR* measurements of the decays $D_{(s)}^+ \to (K^+\pi^+)e^+e^-$ and $D_{(s)}^+ \to (K^+\pi^+)\mu^+\mu^-$, where the contribution from $\phi \to l^+l^-$ ($l = e, \mu$) has been excluded. In the case of the LHCb measurements of the decays $D^0 \to \pi^+\pi^-\mu^+\mu^-$ [1086] as well as the decays $D_{(s)}^+ \to \pi^+\mu^+\mu^-$ [1087] the contributions from $\phi \to l^+l^-$ as well as from $\rho, \omega \to l^+l^-$ ($l = e, \mu$) have been excluded.

Table 264: Upper limits at 90% C.L. for D^0 decays.

Decay	Limit $\times 10^6$	Experiment	Reference
$\gamma\gamma$	26.0	CLEO II	[1088]
	3.8	BESIII	[1089]
	2.2	*BABAR*	[1090]
	0.85	Belle	[1091]
e^+e^-	220.0	CLEO	[1092]
	170.0	Argus	[1093]
	130.0	Mark3	[1094]
	13.0	CLEO II	[1095]
	8.19	E789	[1096]
	6.2	E791	[1097]
	1.2	*BABAR*	[1098]
	0.079	Belle	[1099]
$\mu^+\mu^-$	70.0	Argus	[1093]
	44.0	E653	[1100]
	34.0	CLEO II	[1095]
	15.6	E789	[1096]
	5.2	E791	[1097]
	2.0	HERAb	[1101]
	1.3	*BABAR*	[1098]
	0.21	CDF	[1102]
	0.14	Belle	[1099]
	0.0062	LHCb	[1103]
$\pi^0e^+e^-$	45.0	CLEO II	[1095]
$\pi^0\mu^+\mu^-$	540.0	CLEO II	[1095]
	180.0	E653	[1100]

Table 264 – continued from previous page

Decay	Limit $\times 10^6$	Experiment	Reference
$\eta\, e^+e^-$	110.0	CLEO II	[1095]
$\eta\, \mu^+\mu^-$	530.0	CLEO II	[1095]
$\pi^+\pi^-e^+e^-$	370.0	E791	[1104]
$\rho^0 e^+e^-$	450.0	CLEO	[1092]
	124.0	E791	[1104]
	100.0	CLEO II	[1095]
$\pi^+\pi^-\mu^+\mu^-$	30.0	E791	[1104]
	0.55	LHCb	[1086]
$\rho^0\mu^+\mu^-$	810.0	CLEO	[1092]
	490.0	CLEO II	[1095]
	230.0	E653	[1100]
	22.0	E791	[1104]
$\omega\, e^+e^-$	180.0	CLEO II	[1095]
$\omega\, \mu^+\mu^-$	830.0	CLEO II	[1095]
$K^+K^-e^+e^-$	315.0	E791	[1104]
$\phi\, e^+e^-$	59.0	E791	[1104]
	52.0	CLEO II	[1095]
$K^+K^-\mu^+\mu^-$	33.0	E791	[1104]
$\phi\, \mu^+\mu^-$	410.0	CLEO II	[1095]
	31.0	E791	[1104]
$\overline{K}^0 e^+e^-$	1700.0	Mark3	[1105]
	110.0	CLEO II	[1095]
$\overline{K}^0\mu^+\mu^-$	670.0	CLEO II	[1095]
	260.0	E653	[1100]
$K^-\pi^+e^+e^-$	385.0	E791	[1104]
$\overline{K}^{*0}(892)e^+e^-$	140.0	CLEO II	[1095]
	47.0	E791	[1104]
$K^-\pi^+\mu^+\mu^-$	360.0	E791	[1104]
$\overline{K}^{*0}(892)\mu^+\mu^-$	1180.0	CLEO II	[1095]
	24.0	E791	[1104]
$\pi^+\pi^-\pi^0\mu^+\mu^-$	810.0	E653	[1100]
$\mu^\pm e^\mp$	270.0	CLEO	[1092]
	120.0	Mark3	[1106]
	100.0	Argus	[1093]
	19.0	CLEO II	[1095]
	17.2	E789	[1096]
	8.1	E791	[1097]
	0.81	*BABAR*	[1098]
	0.26	Belle	[1099]
	0.016	LHCb	[1107]
$\pi^0 e^\pm\mu^\mp$	86.0	CLEO II	[1095]
$\eta\, e^\pm\mu^\mp$	100.0	CLEO II	[1095]

Table 264 – continued from previous page

Decay	Limit $\times 10^6$	Experiment	Reference
$\pi^+\pi^- e^\pm\mu^\mp$	15.0	E791	[1104]
$\rho^0 e^\pm\mu^\mp$	66.0	E791	[1104]
	49.0	CLEO II	[1095]
$\omega\, e^\pm\mu^\mp$	120.0	CLEO II	[1095]
$K^+K^- e^\pm\mu^\mp$	180.0	E791	[1104]
$\phi\, e^\pm\mu^\mp$	47.0	E791	[1104]
	34.0	CLEO II	[1095]
$\overline{K}^0 e^\pm\mu^\mp$	100.0	CLEO II	[1095]
$K^-\pi^+ e^\pm\mu^\mp$	550.0	E791	[1104]
$K^{*0}(892) e^\pm\mu^\mp$	100.0	CLEO II	[1095]
	83.0	E791	[1104]
$\pi^\mp\pi^\mp e^\pm e^\pm$	112.0	E791	[1104]
$\pi^\mp\pi^\mp\mu^\pm\mu^\pm$	29.0	E791	[1104]
$K^\mp\pi^\mp e^\pm e^\pm$	206.0	E791	[1104]
$K^\mp\pi^\mp\mu^\pm\mu^\pm$	390.0	E791	[1104]
$K^\mp K^\mp e^\pm e^\pm$	152.0	E791	[1104]
$K^\mp K^\mp\mu^\pm\mu^\pm$	94.0	E791	[1104]
$\pi^\mp\pi^\mp e^\pm\mu^\pm$	79.0	E791	[1104]
$K^\mp\pi^\mp e^\pm\mu^\pm$	218.0	E791	[1104]
$K^\mp K^\mp e^\pm\mu^\pm$	57.0	E791	[1104]
$p\, e^-$	10.0	CLEO	[1108]
$\overline{p}\, e^+$	11.0	CLEO	[1108]

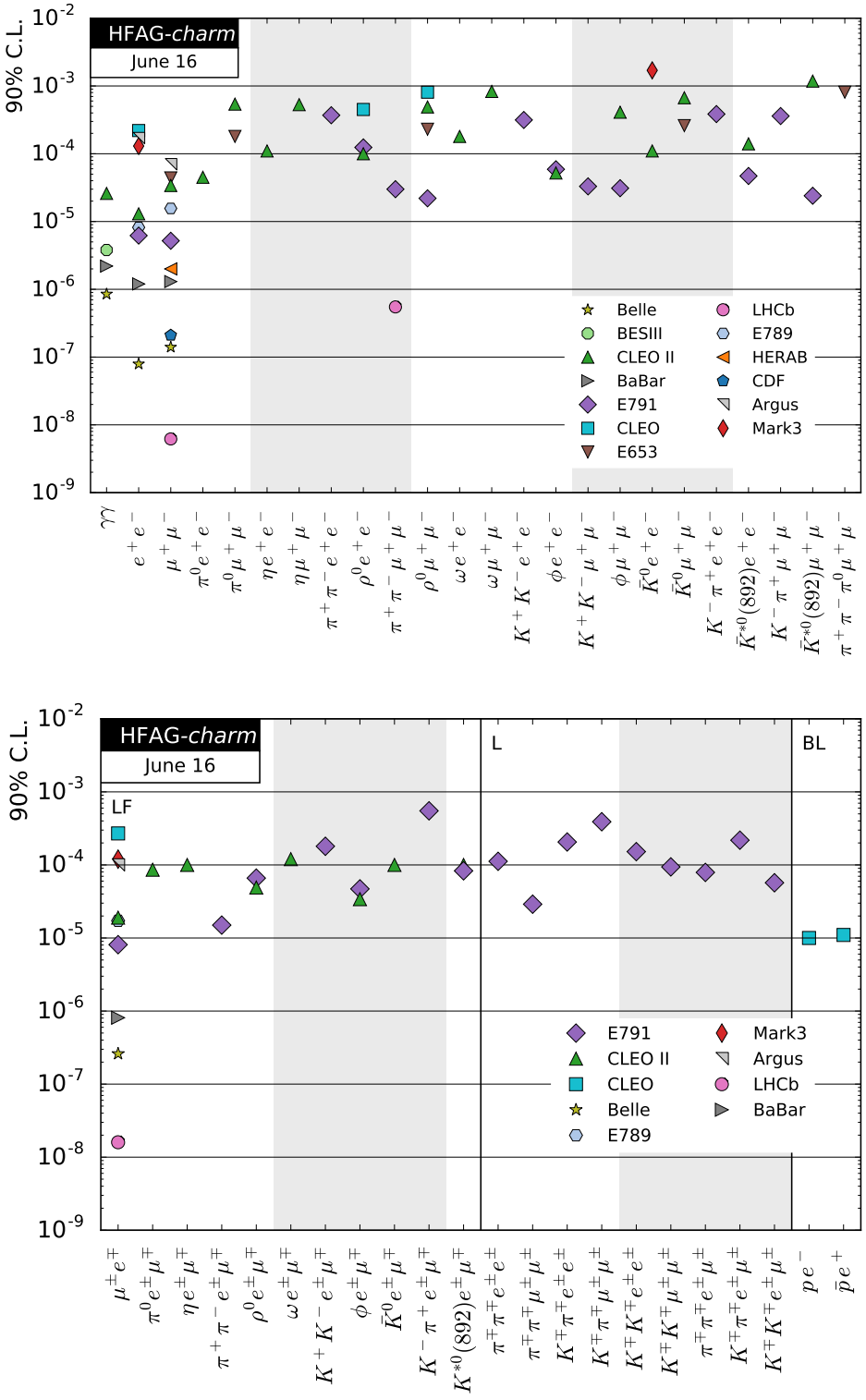

Figure 189: Upper limits at 90% C.L. for D^0 decays. The top plot shows flavor-changing neutral current decays, and the bottom plot shows lepton-flavor-changing (LF), lepton-number-changing (L), and both baryon- and lepton-number-changing (BL) decays.

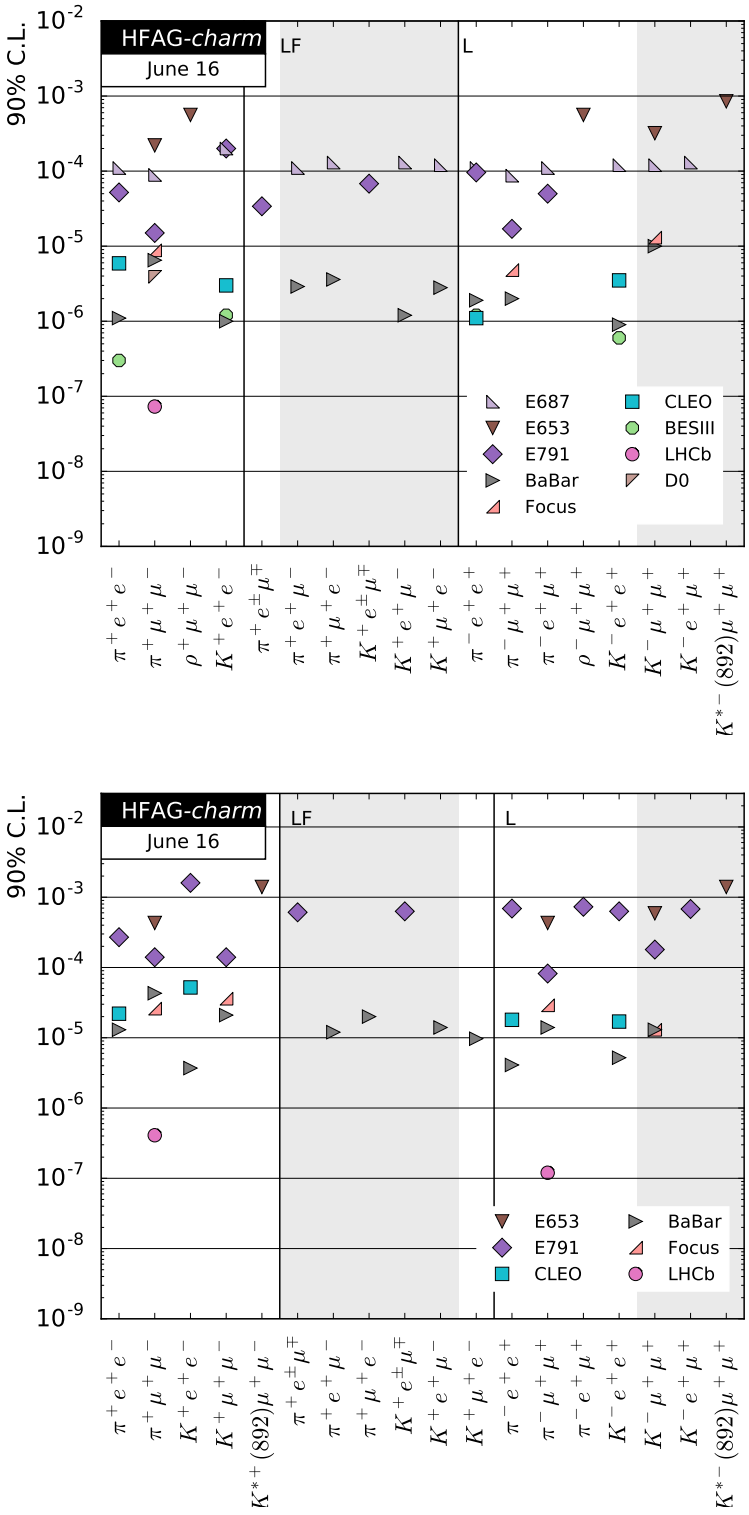

Figure 190: Upper limits at 90% C.L. for D^+ (top) and D_s^+ (bottom) decays. Each plot shows flavor-changing neutral current decays, lepton-flavor-changing decays (LF), and lepton-number-changing (L) decays.

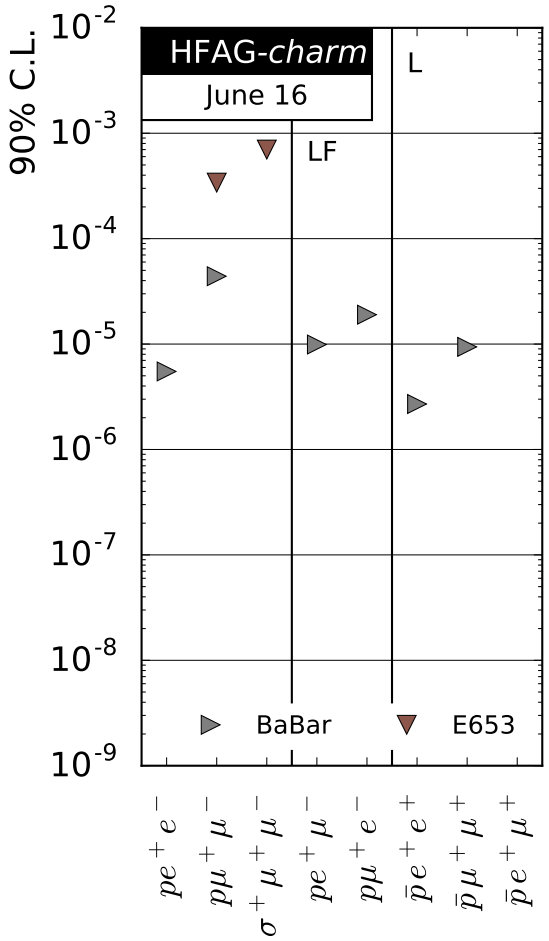

Figure 191: Upper limits at 90% C.L. for Λ_c^+ decays. Shown are flavor-changing neutral current decays, lepton-flavor-changing (LF) decays, and lepton-number-changing (L) decays.

Table 265: Upper limits at 90% C.L. for D^+ decays.

Decay	Limit $\times 10^6$	Experiment	Reference
$\pi^+e^+e^-$	110.0	E687	[1109]
	52.0	E791	[1097]
	5.9	CLEO	[1084]
	1.1	*BABAR*	[1110]
	0.3	BESIII	[1111]
$\pi^+\mu^+\mu^-$	220.0	E653	[1100]
	89.0	E687	[1109]
	15.0	E791	[1097]
	8.8	Focus	[1112]
	6.5	*BABAR*	[1110]
	3.9	D0	[1085]

Table 265 – continued from previous page

Decay	Limit $\times 10^6$	Experiment	Reference
	0.073	LHCb	[1087]
$\rho^+\mu^+\mu^-$	560.0	E653	[1100]
$K^+e^+e^-$	200.0	E687	[1109]
	3.0	CLEO	[1084]
	1.2	BESIII	[1111]
	1.0	*BABAR*	[1110]
$\pi^+e^\pm\mu^\mp$	34.0	E791	[1097]
$\pi^+e^+\mu^-$	110.0	E687	[1109]
	2.9	*BABAR*	[1110]
$\pi^+\mu^+e^-$	130.0	E687	[1109]
	3.6	*BABAR*	[1110]
$K^+e^\pm\mu^\mp$	68.0	E791	[1097]
$K^+e^+\mu^-$	130.0	E687	[1109]
	1.2	*BABAR*	[1110]
$K^+\mu^+e^-$	120.0	E687	[1109]
	2.8	*BABAR*	[1110]
$\pi^-e^+e^+$	110.0	E687	[1109]
	96.0	E791	[1097]
	1.9	*BABAR*	[1110]
	1.2	BESIII	[1111]
	1.1	CLEO	[1084]
$\pi^-\mu^+\mu^+$	87.0	E687	[1109]
	17.0	E791	[1097]
	4.8	Focus	[1112]
	2.0	*BABAR*	[1110]
	0.022	LHCb	[1087]
$\pi^-e^+\mu^+$	110.0	E687	[1109]
	50.0	E791	[1097]
$\rho^-\mu^+\mu^+$	560.0	E653	[1100]
$K^-e^+e^+$	120.0	E687	[1109]
	3.5	CLEO	[1084]
	0.9	*BABAR*	[1110]
	0.6	BESIII	[1111]
$K^-\mu^+\mu^+$	320.0	E653	[1100]
	120.0	E687	[1109]
	13.0	Focus	[1112]
	10.0	*BABAR*	[1110]
$K^-e^+\mu^+$	130.0	E687	[1109]
$K^{*-}(892)\mu^+\mu^+$	850.0	E653	[1100]

Table 266: Upper limits at 90% C.L. for D_s^+ decays.

Decay	Limit $\times 10^6$	Experiment	Reference

Table 266 – continued from previous page

Decay	Limit $\times 10^6$	Experiment	Reference
$\pi^+e^+e^-$	270.0	E791	[1097]
	22.0	CLEO	[1084]
	13.0	*BABAR*	[1110]
$\pi^+\mu^+\mu^-$	430.0	E653	[1100]
	140.0	E791	[1097]
	43.0	*BABAR*	[1110]
	26.0	Focus	[1112]
	0.41	LHCb	[1087]
$K^+e^+e^-$	1600.0	E791	[1097]
	52.0	CLEO	[1084]
	3.7	*BABAR*	[1110]
$K^+\mu^+\mu^-$	140.0	E791	[1097]
	36.0	Focus	[1112]
	21.0	*BABAR*	[1110]
$K^{*+}(892)\mu^+\mu^-$	1400.0	E653	[1100]
$\pi^+e^\pm\mu^\mp$	610.0	E791	[1097]
$\pi^+e^+\mu^-$	12.0	*BABAR*	[1110]
$\pi^+\mu^+e^-$	20.0	*BABAR*	[1110]
$K^+e^\pm\mu^\mp$	630.0	E791	[1097]
$K^+e^+\mu^-$	14.0	*BABAR*	[1110]
$K^+\mu^+e^-$	9.7	*BABAR*	[1110]
$\pi^-e^+e^+$	690.0	E791	[1097]
	18.0	CLEO	[1084]
	4.1	*BABAR*	[1110]
$\pi^-\mu^+\mu^+$	430.0	E653	[1100]
	82.0	E791	[1097]
	29.0	Focus	[1112]
	14.0	*BABAR*	[1110]
	0.12	LHCb	[1087]
$\pi^-e^+\mu^+$	730.0	E791	[1097]
$K^-e^+e^+$	630.0	E791	[1097]
	17.0	CLEO	[1084]
	5.2	*BABAR*	[1110]
$K^-\mu^+\mu^+$	590.0	E653	[1100]
	180.0	E791	[1097]
	13.0	*BABAR*	[1110]
$K^-e^+\mu^+$	680.0	E791	[1097]
$K^{*-}(892)\mu^+\mu^+$	1400.0	E653	[1100]

Table 267: Upper limits at 90% C.L. for Λ_c^+ decays.

Decay	Limit $\times 10^6$	Experiment	Reference
pe^+e^-	5.5	*BABAR*	[1110]

Table 267 – continued from previous page

Decay	Limit $\times 10^6$	Experiment	Reference
$p\mu^+\mu^-$	340.0	E653	[1100]
	44.0	*BABAR*	[1110]
$\sigma^+\mu^+\mu^-$	700.0	E653	[1100]
$pe^+\mu^-$	9.9	*BABAR*	[1110]
$p\mu^+e^-$	19.0	*BABAR*	[1110]
$\overline{p}\,e^+e^+$	2.7	*BABAR*	[1110]
$\overline{p}\,\mu^+\mu^+$	9.4	*BABAR*	[1110]

9 Tau lepton properties

We present world averages of a selection of τ lepton quantities with the goal to provide the best up-to-date determinations of the tests of the universality of the charged weak interaction (Section 9.2) and of the Cabibbo-Kobayashi-Maskawa (CKM) matrix coefficient $|V_{us}|$ from τ decays (Section 9.4). We concentrate our effort in the averages that benefit most from the adoption of the HFAG methodology [405], namely a global fit of the τ branching fractions that best exploits the available experimental information. Since the 2016 edition, the HFAG-Tau group has collaborated to the publication of the PDG τ lepton branching fraction fit and mini-review. The differences between the PDG 2016 fit and the fit presented here are detailed in Section 9.1.4.

All published statistical correlations are used, and a selection of measurements, particularly the most precise and the most recent ones, were studied to take into account the significant systematic dependencies from external parameters and common sources of systematic uncertainty.

Finally, we report in Section 9.5 the most up-to-date limits on the lepton-flavour-violating τ branching fractions and in Section 9.6 we determine the combined upper limits for the branching fractions that have multiple experimental results.

9.1 Branching fraction fit

A global fit of the available experimental measurements is used to determine the τ branching fractions, together with their uncertainties and statistical correlations. The τ branching fractions provide a test for theory predictions based on the Standard Model (SM) EW and QCD interactions and can be further elaborated to test the EW charged-current universality for leptons, to determine the CKM matrix coefficient $|V_{us}|$ and the QCD coupling constant α_s at the τ mass.

The measurements used in the fit are listed in Table 268 and consist of either τ decay mode branching fractions, labelled as Γ_i, or ratios of two τ decay mode branching fractions, labelled as Γ_i/Γ_j. A minimum χ^2 fit is performed for all the measured quantities and for some additional branching fractions and ratios of branching fractions, and all ft results are listed in Table 268. Some fitted quantities are equal to the ratio of two other fitted quantities, as documented with the notation Γ_i/Γ_j in Table 268. Some fitted quantities are sum of other fitted quantities, for instance $\Gamma_8 = B(\tau \to h^-\nu_\tau)$ is the sum of $\Gamma_9 = B(\tau \to \pi^-\nu_\tau)$ and $\Gamma_{10} = B(\tau \to K^-\nu_\tau)$. The symbol h is used to mean either a π or K. Section 9.1.7 lists all equations relating one quantity to the sum of other quantities. In the following, we refer to both types of relations between fitted quantities collectively as constraint equations or constraints. The fit χ^2 is minimized subject to all these above mentioned constraints. The fit procedure is equivalent to the one employed in the former HFAG reports [4, 222, 405].

9.1.1 Technical implementation of the fit procedure

The fit computes the quantities q_i by minimizing a χ^2 while respecting a series of equality constraints on the q_i. The χ^2 is computed using the measurements m_i and their covariance matrix E_{ij} as $\chi^2 = (m_i - A_{ik}q_k)^t E^{-1}_{ij}(m_j - A_{jl}q_l)$ where the model matrix A_{ij} is used to get the vector of the predicted measurements m'_i from the vector of the fit parameters q_j as $m'_i = A_{ij}q_j$.

In this particular implementation the measurements are grouped by the quantity that they measure, and all quantities with at least one measurement correspond to a fit parameter. Therefore, the matrix A_{ij} has one row per measurement m_i and one column per fitted quantity q_j, with unity coefficients for the rows and column that identify a measurement m_i of the quantity q_j, respectively. In summary, the fit requires:

$$\min(m_i - A_{ik}q_k)^t E_{ij}^{-1}(m_j - A_{jl}q_l), \tag{275}$$

$$\text{subjected to} \quad f_r(q_s) - c_r = 0, \tag{276}$$

where Eq. 276 defines the relations between the quantities q_i and its left term defines the respective constraint expressions. Using the method of Lagrange multipliers, a set of equations is obtained by taking the derivatives with respect to the fitted quantities q_k and the Lagrange multipliers λ_r of the sum of the χ^2 and the constraint expressions multiplied by the Lagrange multipliers λ_r, one for each constraint:

$$\min\left[(A_{ik}q_k - m_i)^t E_{ij}^{-1}(A_{jl}q_l - m_j) + 2\lambda_r(f_r(q_s) - c_r)\right] \tag{277}$$

$$(\partial/\partial q_k, \partial/\partial\lambda_r)[\text{expression above}] = 0 \tag{278}$$

Eq. 278 defines a set of equations for the vector of the unknowns (q_k, λ_r), some of which may be non-linear, in case of non-linear constraints. An iterative minimization procedure approximates at each step the non-linear constraint expressions by their first order Taylor expansion around the current values of the fitted quantities, $\overline{q}_s$:

$$f_r(q_s) - c_r = f_r(\overline{q}_s) + \left.\frac{\partial f_r(q_s)}{\partial q_s}\right|_{\overline{q}_s} (q_s - \overline{q}_s) - c_r, \tag{279}$$

which can be written as

$$B_{rs}q_s - c'_r, \tag{280}$$

where c'_r are the resulting constant known terms, independent of q_s at first order. After linearization, the differentiation by q_k and λ_r is trivial and leads to a set of linear equations

$$A^t_{ki}E^{-1}_{ij}A_{jl}q_l + B^t_{kr}\lambda_r = A^t_{ki}E^{-1}_{ij}m_j \tag{281}$$

$$B_{rs}q_s = c'_r, \tag{282}$$

which can be expressed as:

$$F_{ij}u_j = v_i \tag{283}$$

where $u_j = (q_k, \lambda_r)$ and v_i is the vector of the known constant terms running over the index k and then r in the right terms of Eq. 281 and Eq. 282, respectively. Solving the equation set in Eq. 283 by matrix inversion gives the the fitted quantities and their variance and covariance matrix, using the measurements and their variance and covariance matrix. The fit procedure starts by computing the linear approximation of the non-linear constraint expressions around the quantities seed values. With an iterative procedure, the unknowns are updated at each step by solving the equations and the equations are then linearized around the updated values, until the variation of the fitted unknowns is reduced below a numerically small threshold.

9.1.2 Fit results

The fit output consists of 135 fitted quantities that correspond to either branching fractions or ratios of branching fractions. The fitted quantities values and undertainties are listed in Table 268. The off-diagonal statistical correlation terms between a subset of 47 "basis quantities" are listed in Section 9.1.6. All the remaining statistical correlation terms can be obtained using the constraint equations listed in Table 268 and Section 9.1.7.

The fit has χ^2/d.o.f. = 137.3/123, corresponding to a confidence level CL = 17.84%. We use a total of 170 measurements to fit the above mentioned 135 quantities subjected to 88 constraints. Although the unitarity constraint is not applied, the fit is statistically consistent with unitarity, where the residual is $\Gamma_{998} = 1 - \Gamma_{\rm All} = (0.0355 \pm 0.1031) \cdot 10^{-2}$.

A scale factor of 5.44 (as in the three previous reports [4, 222, 405]) has been applied to the published uncertainties of the two severely inconsistent measurements of $\Gamma_{96} = \tau \to KKK\nu$ by *BABAR* and Belle. The scale factor has been determined using the PDG procedure, *i.e.* to the proper size in order to obtain a reduced χ^2 equal to 1 when fitting just the two Γ_{96} measurements.

For several old results, for historical reasons, the table lists the statistical errors formed from the quadratic sum of the statistical and systematic errors, setting the systematics errors to zero: this does not affect the fit result as the systematic and statistical errors are treated in the same way.

9.1.3 Changes with respect to the previous report

The following changes have been introduced with respect to the previous HFAG report [4].

Two old preliminary results have been removed:

- $\Gamma_{35} = B(\tau \to \pi K_S \nu)$, *BABAR* [1113],
- $\Gamma_{40} = B(\tau \to \pi K_S \pi^0 \nu)$, *BABAR* [1114].

They where announced in 2008 and 2009, respectively, but have not been published yet.

In the 2014 report, for several *BABAR* and Belle experimental results we used more precise numerical values than the published ones, using internal information from the Collaborations. We revert to the published figures in this report, as the improvements in the fit results were negligible. In so doing, we use in this report the same values that are used in the PDG 2016 fit.

The Belle result on $\tau^- \to K^0_S(\text{particles})^- \nu_\tau$ [1115] has been discarded, because it was determined that the published information does not permit a reliable determination of the correlations with the other results in the same paper. The correlations estimated for the HFAG 2014 report were inconsistent and made the covariance matrix of the results in the corresponding paper non positive-definite, as well as the overall correlation matrix for the branching ratio fit results. It has been found that the inconsistency had negligible impact on lepton universality and $|V_{us}|$ measurements.

The ALEPH result on Γ_{46} ($\tau^- \to \pi^- K^0 \overline{K}^0 \nu_\tau$) [1116] has been removed from the fit inputs, since it is the simply sum of twice $\Gamma_{47} = \pi^- K^0_S K^0_S \nu_\tau$ and $\Gamma_{48} = \pi^- K^0_S K^0_L \nu_\tau$ from the same paper, hence 100% correlated with them.

Several minor corrections have been applied to the constraints. The list of constraints included in the following fully documents the changes when compared with the same list in the

2014 edition. In some cases the relation equating one decay mode to a sum of modes included some minor terms that did not match the mode definitions. In other cases, the sum included modes with overlapping components. The effects on the 2014 fit results have been found to be modest with respect to the quoted uncertainties.

For instance, the definition of the total branching fraction has been updated as follows:

$$\begin{aligned}\Gamma_{\rm All} = \;& \Gamma_3+\Gamma_5+\Gamma_9+\Gamma_{10}+\Gamma_{14}+\Gamma_{16}+\Gamma_{20}+\Gamma_{23}+\Gamma_{27}+\Gamma_{28}+\Gamma_{30}+\Gamma_{35}+\Gamma_{37}+\Gamma_{40}+\Gamma_{42}+\\ & \Gamma_{47}\cdot(1+((\Gamma_{<K^0|K_L>}\cdot\Gamma_{<\overline{K}^0|K_L>})/(\Gamma_{<K^0|K_S>}\cdot\Gamma_{<\overline{K}^0|K_S>})))+\Gamma_{48}+\Gamma_{62}+\Gamma_{70}+\Gamma_{77}+\\ & \Gamma_{811}+\Gamma_{812}+\Gamma_{93}+\Gamma_{94}+\Gamma_{832}+\Gamma_{833}+\Gamma_{126}+\Gamma_{128}+\Gamma_{802}+\Gamma_{803}+\Gamma_{800}+\Gamma_{151}+\Gamma_{130}+\\ & \Gamma_{132}+\Gamma_{44}+\Gamma_{53}+\Gamma_{50}\cdot(1+((\Gamma_{<K^0|K_L>}\cdot\Gamma_{<\overline{K}^0|K_L>})/(\Gamma_{<K^0|K_S>}\cdot\Gamma_{<\overline{K}^0|K_S>})))+\Gamma_{51}+\\ & \Gamma_{167}\cdot(\Gamma_{\phi\to K^+K^-}+\Gamma_{\phi\to K_SK_L})+\Gamma_{152}+\Gamma_{920}+\Gamma_{821}+\Gamma_{822}+\Gamma_{831}+\Gamma_{136}+\Gamma_{945}+\Gamma_{805}\ .\end{aligned}$$

In the 2014 definition, the term $\Gamma_{78} = h^-h^-h^+3\pi^0\nu_\tau$ included the contributions of $\Gamma_{50} = \pi^-\pi^0K^0_SK^0_S\nu_\tau$ and $\Gamma_{132} = \pi^-\overline{K}^0\eta\nu_\tau$, which were already included. In the present definition, Γ_{78} has been replaced with modes whose sum corresponds to $\Gamma_{810} = 2\pi^-\pi^+3\pi^0\nu_\tau$ (ex. K^0). As in 2014, the total τ branching fraction $\Gamma_{\rm All}$ definition includes two modes that have overlapping final states, to a minor extent that we consider negligible:

$$\begin{aligned}&\Gamma_{50} = \pi^-\pi^0K^0_SK^0_S\nu_\tau\\ &\Gamma_{132} = \pi^-\overline{K}^0\eta\nu_\tau\ .\end{aligned}$$

Finally, we updated to the PDG 2015 results [314] all the parameters corresponding to the measurements systematic biases and uncertainties and all the parameters appearing in the constraint equations in Section 9.1.7 and Table 268.

9.1.4 Differences between the HFAG 2016 fit and the PDG 2016 fit

As is standard for the PDG branching fraction fits, the PDG 2016 τ branching fraction fit is unitarity constrained, while the HFAG 2016 fit is unconstrained.

The HFAG-Tau fit uses the ALEPH measurements of branching fractions defined according to the final state content of "hadrons" and kaons, where a "hadron" corresponds to either a pion or a kaon, since this set of results is closer to the actual experimental measurements and facilitates a more comprehensive treatment of the experimental results correlations [405]. The PDG 2016 fit on the other hand continues to use – as in the past editions – the ALEPH measurements of modes with pions and kaons, which correspond to the final set of published measurements of the collaboration. It is planned to eventually update the PDG fit to use the same ALEPH measurement set that is used by HFAG.

The HFAG 2016 fit, as in 2014, uses the ALEPH estimate for $\Gamma_{805} = B(\tau\to a_1^-(\to\pi^-\gamma)\nu_\tau)$, which is not a direct experimental measurement. The PDG 2016 fit uses the PDG average of $B(a_1\to\pi\gamma)$ as a parameter and defines $\Gamma_{805} = B(a_1\to\pi\gamma)\times B(\tau\to 3\pi\nu)$. As a consequence, the PDG fit procedure does not take into account the large uncertainty on $B(a_1\to\pi\gamma)$, resulting in an underestimated fit uncertainty on Γ_{805}. Therefore, in this case an appropriate correction has to be applied after the fit.

9.1.5 Branching ratio fit results and experimental inputs

Table 268 reports the τ branching ratio fit results and experimental inputs.

Table 268: HFAG Summer 2016 branching fractions fit results.

τ lepton branching fraction	**Fit value / Exp.**	**HFAG Fit / Ref.**
$\Gamma_1 = (\text{particles})^- \geq 0\,\text{neutrals} \geq 0\,K^0\,\nu_\tau$	0.8519 ± 0.0011	HFAG Summer 2016 fit
$\Gamma_2 = (\text{particles})^- \geq 0\,\text{neutrals} \geq 0\,K^0_L\,\nu_\tau$	0.8453 ± 0.0010	HFAG Summer 2016 fit
$\Gamma_3 = \mu^-\overline{\nu}_\mu\nu_\tau$	0.17392 ± 0.00040	HFAG Summer 2016 fit
$0.17319 \pm 0.00077 \pm 0.00000$	ALEPH	[1117]
$0.17325 \pm 0.00095 \pm 0.00077$	DELPHI	[1118]
$0.17342 \pm 0.00110 \pm 0.00067$	L3	[1119]
$0.17340 \pm 0.00090 \pm 0.00060$	OPAL	[1120]
$\dfrac{\Gamma_3}{\Gamma_5} = \dfrac{\mu^-\overline{\nu}_\mu\nu_\tau}{e^-\overline{\nu}_e\nu_\tau}$	0.9762 ± 0.0028	HFAG Summer 2016 fit
$0.9970 \pm 0.0350 \pm 0.0400$	ARGUS	[1121]
$0.9796 \pm 0.0016 \pm 0.0036$	*BABAR*	[1122]
$0.9777 \pm 0.0063 \pm 0.0087$	CLEO	[1123]
$\Gamma_5 = e^-\overline{\nu}_e\nu_\tau$	0.17816 ± 0.00041	HFAG Summer 2016 fit
$0.17837 \pm 0.00080 \pm 0.00000$	ALEPH	[1117]
$0.17760 \pm 0.00060 \pm 0.00170$	CLEO	[1123]
$0.17877 \pm 0.00109 \pm 0.00110$	DELPHI	[1118]
$0.17806 \pm 0.00104 \pm 0.00076$	L3	[1119]
$0.17810 \pm 0.00090 \pm 0.00060$	OPAL	[1124]
$\Gamma_7 = h^- \geq 0\,K^0_L\,\nu_\tau$	0.12023 ± 0.00054	HFAG Summer 2016 fit
$0.12400 \pm 0.00700 \pm 0.00700$	DELPHI	[1125]
$0.12470 \pm 0.00260 \pm 0.00430$	L3	[1126]
$0.12100 \pm 0.00700 \pm 0.00500$	OPAL	[1127]
$\Gamma_8 = h^-\nu_\tau$	0.11506 ± 0.00054	HFAG Summer 2016 fit
$0.11524 \pm 0.00105 \pm 0.00000$	ALEPH	[1117]
$0.11520 \pm 0.00050 \pm 0.00120$	CLEO	[1123]
$0.11571 \pm 0.00120 \pm 0.00114$	DELPHI	[1128]
$0.11980 \pm 0.00130 \pm 0.00160$	OPAL	[1129]
$\dfrac{\Gamma_8}{\Gamma_5} = \dfrac{h^-\nu_\tau}{e^-\overline{\nu}_e\nu_\tau}$	0.6458 ± 0.0033	HFAG Summer 2016 fit
$\Gamma_9 = \pi^-\nu_\tau$	0.10810 ± 0.00053	HFAG Summer 2016 fit
$\dfrac{\Gamma_9}{\Gamma_5} = \dfrac{\pi^-\nu_\tau}{e^-\overline{\nu}_e\nu_\tau}$	0.6068 ± 0.0032	HFAG Summer 2016 fit
$0.5945 \pm 0.0014 \pm 0.0061$	*BABAR*	[1122]

Table 268 – continued from previous page

τ lepton branching fraction	Fit value / Exp.	HFAG Fit / Ref.
$\Gamma_{10} = K^- \nu_\tau$	$(0.6960 \pm 0.0096) \cdot 10^{-2}$	HFAG Summer 2016 fit
$(0.6960 \pm 0.0287 \pm 0.0000) \cdot 10^{-2}$	ALEPH	[1130]
$(0.6600 \pm 0.0700 \pm 0.0900) \cdot 10^{-2}$	CLEO	[1131]
$(0.8500 \pm 0.1800 \pm 0.0000) \cdot 10^{-2}$	DELPHI	[1132]
$(0.6580 \pm 0.0270 \pm 0.0290) \cdot 10^{-2}$	OPAL	[1133]
$\frac{\Gamma_{10}}{\Gamma_5} = \frac{K^- \nu_\tau}{e^- \overline{\nu}_e \nu_\tau}$	$(3.906 \pm 0.054) \cdot 10^{-2}$	HFAG Summer 2016 fit
$(3.882 \pm 0.032 \pm 0.057) \cdot 10^{-2}$	*BABAR*	[1122]
$\frac{\Gamma_{10}}{\Gamma_9} = \frac{K^- \nu_\tau}{\pi^- \nu_\tau}$	$(6.438 \pm 0.094) \cdot 10^{-2}$	HFAG Summer 2016 fit
$\Gamma_{11} = h^- \geq 1\,\text{neutrals}\,\nu_\tau$	0.36973 ± 0.00097	HFAG Summer 2016 fit
$\Gamma_{12} = h^- \geq 1\,\pi^0\,\nu_\tau$ (ex. K^0)	0.36475 ± 0.00097	HFAG Summer 2016 fit
$\Gamma_{13} = h^- \pi^0 \nu_\tau$	0.25935 ± 0.00091	HFAG Summer 2016 fit
$0.25924 \pm 0.00129 \pm 0.00000$	ALEPH	[1117]
$0.25670 \pm 0.00010 \pm 0.00390$	Belle	[1134]
$0.25870 \pm 0.00120 \pm 0.00420$	CLEO	[1135]
$0.25740 \pm 0.00201 \pm 0.00138$	DELPHI	[1128]
$0.25050 \pm 0.00350 \pm 0.00500$	L3	[1126]
$0.25890 \pm 0.00170 \pm 0.00290$	OPAL	[1129]
$\Gamma_{14} = \pi^- \pi^0 \nu_\tau$	0.25502 ± 0.00092	HFAG Summer 2016 fit
$\Gamma_{16} = K^- \pi^0 \nu_\tau$	$(0.4327 \pm 0.0149) \cdot 10^{-2}$	HFAG Summer 2016 fit
$(0.4440 \pm 0.0354 \pm 0.0000) \cdot 10^{-2}$	ALEPH	[1130]
$(0.4160 \pm 0.0030 \pm 0.0180) \cdot 10^{-2}$	*BABAR*	[1136]
$(0.5100 \pm 0.1000 \pm 0.0700) \cdot 10^{-2}$	CLEO	[1131]
$(0.4710 \pm 0.0590 \pm 0.0230) \cdot 10^{-2}$	OPAL	[1137]
$\Gamma_{17} = h^- \geq 2\,\pi^0\,\nu_\tau$	0.10775 ± 0.00095	HFAG Summer 2016 fit
$0.09910 \pm 0.00310 \pm 0.00270$	OPAL	[1129]
$\Gamma_{18} = h^- 2\pi^0 \nu_\tau$	$(9.458 \pm 0.097) \cdot 10^{-2}$	HFAG Summer 2016 fit
$\Gamma_{19} = h^- 2\pi^0 \nu_\tau$ (ex. K^0)	$(9.306 \pm 0.097) \cdot 10^{-2}$	HFAG Summer 2016 fit
$(9.295 \pm 0.122 \pm 0.000) \cdot 10^{-2}$	ALEPH	[1117]
$(9.498 \pm 0.320 \pm 0.275) \cdot 10^{-2}$	DELPHI	[1128]
$(8.880 \pm 0.370 \pm 0.420) \cdot 10^{-2}$	L3	[1126]

Table 268 – continued from previous page

τ lepton branching fraction	Fit value / Exp.	HFAG Fit / Ref.
$\frac{\Gamma_{19}}{\Gamma_{13}} = \frac{h^- 2\pi^0 \nu_\tau \text{ (ex. } K^0)}{h^- \pi^0 \nu_\tau}$	0.3588 ± 0.0044	HFAG Summer 2016 fit
$0.3420 \pm 0.0060 \pm 0.0160$	CLEO	[1138]
$\Gamma_{20} = \pi^- 2\pi^0 \nu_\tau$ (ex. K^0)	$(9.242 \pm 0.100) \cdot 10^{-2}$	HFAG Summer 2016 fit
$\Gamma_{23} = K^- 2\pi^0 \nu_\tau$ (ex. K^0)	$(0.0640 \pm 0.0220) \cdot 10^{-2}$	HFAG Summer 2016 fit
$(0.0560 \pm 0.0250 \pm 0.0000) \cdot 10^{-2}$	ALEPH	[1130]
$(0.0900 \pm 0.1000 \pm 0.0300) \cdot 10^{-2}$	CLEO	[1131]
$\Gamma_{24} = h^- \geq 3\,\pi^0\,\nu_\tau$	$(1.318 \pm 0.065) \cdot 10^{-2}$	HFAG Summer 2016 fit
$\Gamma_{25} = h^- \geq 3\,\pi^0\,\nu_\tau$ (ex. K^0)	$(1.233 \pm 0.065) \cdot 10^{-2}$	HFAG Summer 2016 fit
$(1.403 \pm 0.214 \pm 0.224) \cdot 10^{-2}$	DELPHI	[1128]
$\Gamma_{26} = h^- 3\pi^0 \nu_\tau$	$(1.158 \pm 0.072) \cdot 10^{-2}$	HFAG Summer 2016 fit
$(1.082 \pm 0.093 \pm 0.000) \cdot 10^{-2}$	ALEPH	[1117]
$(1.700 \pm 0.240 \pm 0.380) \cdot 10^{-2}$	L3	[1126]
$\frac{\Gamma_{26}}{\Gamma_{13}} = \frac{h^- 3\pi^0 \nu_\tau}{h^- \pi^0 \nu_\tau}$	$(4.465 \pm 0.277) \cdot 10^{-2}$	HFAG Summer 2016 fit
$(4.400 \pm 0.300 \pm 0.500) \cdot 10^{-2}$	CLEO	[1138]
$\Gamma_{27} = \pi^- 3\pi^0 \nu_\tau$ (ex. K^0)	$(1.029 \pm 0.075) \cdot 10^{-2}$	HFAG Summer 2016 fit
$\Gamma_{28} = K^- 3\pi^0 \nu_\tau$ (ex. K^0, η)	$(4.283 \pm 2.161) \cdot 10^{-4}$	HFAG Summer 2016 fit
$(3.700 \pm 2.371 \pm 0.000) \cdot 10^{-4}$	ALEPH	[1130]
$\Gamma_{29} = h^- 4\pi^0 \nu_\tau$ (ex. K^0)	$(0.1568 \pm 0.0391) \cdot 10^{-2}$	HFAG Summer 2016 fit
$(0.1600 \pm 0.0500 \pm 0.0500) \cdot 10^{-2}$	CLEO	[1138]
$\Gamma_{30} = h^- 4\pi^0 \nu_\tau$ (ex. K^0, η)	$(0.1099 \pm 0.0391) \cdot 10^{-2}$	HFAG Summer 2016 fit
$(0.1120 \pm 0.0509 \pm 0.0000) \cdot 10^{-2}$	ALEPH	[1117]
$\Gamma_{31} = K^- \geq 0\,\pi^0 \geq 0\,K^0 \geq 0\,\gamma\nu_\tau$	$(1.545 \pm 0.030) \cdot 10^{-2}$	HFAG Summer 2016 fit
$(1.700 \pm 0.120 \pm 0.190) \cdot 10^{-2}$	CLEO	[1131]
$(1.540 \pm 0.240 \pm 0.000) \cdot 10^{-2}$	DELPHI	[1132]
$(1.528 \pm 0.039 \pm 0.040) \cdot 10^{-2}$	OPAL	[1133]
$\Gamma_{32} = K^- \geq 1\,(\pi^0 \text{ or } K^0 \text{ or } \gamma)\nu_\tau$	$(0.8528 \pm 0.0286) \cdot 10^{-2}$	HFAG Summer 2016 fit
$\Gamma_{33} = K^0_S(\text{particles})^- \nu_\tau$	$(0.9372 \pm 0.0292) \cdot 10^{-2}$	HFAG Summer 2016 fit
$(0.9700 \pm 0.0849 \pm 0.0000) \cdot 10^{-2}$	ALEPH	[1116]
$(0.9700 \pm 0.0900 \pm 0.0600) \cdot 10^{-2}$	OPAL	[1139]

Table 268 – continued from previous page

τ lepton branching fraction	Fit value / Exp.	HFAG Fit / Ref.
$\Gamma_{34} = h^- \overline{K}^0 \nu_\tau$	$(0.9865 \pm 0.0139) \cdot 10^{-2}$	HFAG Summer 2016 fit
$(0.8550 \pm 0.0360 \pm 0.0730) \cdot 10^{-2}$	CLEO	[1140]
$\Gamma_{35} = \pi^- \overline{K}^0 \nu_\tau$	$(0.8386 \pm 0.0141) \cdot 10^{-2}$	HFAG Summer 2016 fit
$(0.9280 \pm 0.0564 \pm 0.0000) \cdot 10^{-2}$	ALEPH	[1130]
$(0.8320 \pm 0.0025 \pm 0.0150) \cdot 10^{-2}$	Belle	[1115]
$(0.9500 \pm 0.1500 \pm 0.0600) \cdot 10^{-2}$	L3	[1141]
$(0.9330 \pm 0.0680 \pm 0.0490) \cdot 10^{-2}$	OPAL	[1142]
$\Gamma_{37} = K^- K^0 \nu_\tau$	$(0.1479 \pm 0.0053) \cdot 10^{-2}$	HFAG Summer 2016 fit
$(0.1580 \pm 0.0453 \pm 0.0000) \cdot 10^{-2}$	ALEPH	[1116]
$(0.1620 \pm 0.0237 \pm 0.0000) \cdot 10^{-2}$	ALEPH	[1130]
$(0.1480 \pm 0.0013 \pm 0.0055) \cdot 10^{-2}$	Belle	[1115]
$(0.1510 \pm 0.0210 \pm 0.0220) \cdot 10^{-2}$	CLEO	[1140]
$\Gamma_{38} = K^- K^0 \geq 0\, \pi^0\, \nu_\tau$	$(0.2982 \pm 0.0079) \cdot 10^{-2}$	HFAG Summer 2016 fit
$(0.3300 \pm 0.0550 \pm 0.0390) \cdot 10^{-2}$	OPAL	[1142]
$\Gamma_{39} = h^- \overline{K}^0 \pi^0 \nu_\tau$	$(0.5314 \pm 0.0134) \cdot 10^{-2}$	HFAG Summer 2016 fit
$(0.5620 \pm 0.0500 \pm 0.0480) \cdot 10^{-2}$	CLEO	[1140]
$\Gamma_{40} = \pi^- \overline{K}^0 \pi^0 \nu_\tau$	$(0.3812 \pm 0.0129) \cdot 10^{-2}$	HFAG Summer 2016 fit
$(0.2940 \pm 0.0818 \pm 0.0000) \cdot 10^{-2}$	ALEPH	[1116]
$(0.3470 \pm 0.0646 \pm 0.0000) \cdot 10^{-2}$	ALEPH	[1130]
$(0.3860 \pm 0.0031 \pm 0.0135) \cdot 10^{-2}$	Belle	[1115]
$(0.4100 \pm 0.1200 \pm 0.0300) \cdot 10^{-2}$	L3	[1141]
$\Gamma_{42} = K^- \pi^0 K^0 \nu_\tau$	$(0.1502 \pm 0.0071) \cdot 10^{-2}$	HFAG Summer 2016 fit
$(0.1520 \pm 0.0789 \pm 0.0000) \cdot 10^{-2}$	ALEPH	[1116]
$(0.1430 \pm 0.0291 \pm 0.0000) \cdot 10^{-2}$	ALEPH	[1130]
$(0.1496 \pm 0.0019 \pm 0.0073) \cdot 10^{-2}$	Belle	[1115]
$(0.1450 \pm 0.0360 \pm 0.0200) \cdot 10^{-2}$	CLEO	[1140]
$\Gamma_{43} = \pi^- \overline{K}^0 \geq 1\, \pi^0\, \nu_\tau$	$(0.4046 \pm 0.0260) \cdot 10^{-2}$	HFAG Summer 2016 fit
$(0.3240 \pm 0.0740 \pm 0.0660) \cdot 10^{-2}$	OPAL	[1142]
$\Gamma_{44} = \pi^- \overline{K}^0 \pi^0 \pi^0 \nu_\tau$ (ex. K^0)	$(2.340 \pm 2.306) \cdot 10^{-4}$	HFAG Summer 2016 fit
$(2.600 \pm 2.400 \pm 0.000) \cdot 10^{-4}$	ALEPH	[1143]
$\Gamma_{46} = \pi^- K^0 \overline{K}^0 \nu_\tau$	$(0.1513 \pm 0.0247) \cdot 10^{-2}$	HFAG Summer 2016 fit

Table 268 – continued from previous page

τ lepton branching fraction	Fit value / Exp.	HFAG Fit / Ref.
$\Gamma_{47} = \pi^- K^0_S K^0_S \nu_\tau$	$(2.332 \pm 0.065) \cdot 10^{-4}$	HFAG Summer 2016 fit
$(2.600 \pm 1.118 \pm 0.000) \cdot 10^{-4}$	ALEPH	[1116]
$(2.310 \pm 0.040 \pm 0.080) \cdot 10^{-4}$	*BABAR*	[1144]
$(2.330 \pm 0.033 \pm 0.093) \cdot 10^{-4}$	Belle	[1115]
$(2.300 \pm 0.500 \pm 0.300) \cdot 10^{-4}$	CLEO	[1140]
$\Gamma_{48} = \pi^- K^0_S K^0_L \nu_\tau$	$(0.1047 \pm 0.0247) \cdot 10^{-2}$	HFAG Summer 2016 fit
$(0.1010 \pm 0.0264 \pm 0.0000) \cdot 10^{-2}$	ALEPH	[1116]
$\Gamma_{49} = \pi^- K^0 \overline{K}^0 \pi^0 \nu_\tau$	$(3.540 \pm 1.193) \cdot 10^{-4}$	HFAG Summer 2016 fit
$\Gamma_{50} = \pi^- \pi^0 K^0_S K^0_S \nu_\tau$	$(1.815 \pm 0.207) \cdot 10^{-5}$	HFAG Summer 2016 fit
$(1.600 \pm 0.200 \pm 0.220) \cdot 10^{-5}$	*BABAR*	[1144]
$(2.000 \pm 0.216 \pm 0.202) \cdot 10^{-5}$	Belle	[1115]
$\Gamma_{51} = \pi^- \pi^0 K^0_S K^0_L \nu_\tau$	$(3.177 \pm 1.192) \cdot 10^{-4}$	HFAG Summer 2016 fit
$(3.100 \pm 1.100 \pm 0.500) \cdot 10^{-4}$	ALEPH	[1116]
$\Gamma_{53} = \overline{K}^0 h^- h^- h^+ \nu_\tau$	$(2.218 \pm 2.024) \cdot 10^{-4}$	HFAG Summer 2016 fit
$(2.300 \pm 2.025 \pm 0.000) \cdot 10^{-4}$	ALEPH	[1116]
$\Gamma_{54} = h^- h^- h^+ \geq 0\,\text{neutrals} \geq 0\,K^0_L\,\nu_\tau$	0.15215 ± 0.00061	HFAG Summer 2016 fit
$0.15000 \pm 0.00400 \pm 0.00300$	CELLO	[1145]
$0.14400 \pm 0.00600 \pm 0.00300$	L3	[1146]
$0.15100 \pm 0.00800 \pm 0.00600$	TPC	[1147]
$\Gamma_{55} = h^- h^- h^+ \geq 0\,\text{neutrals}\,\nu_\tau$ (ex. K^0)	0.14567 ± 0.00057	HFAG Summer 2016 fit
$0.14556 \pm 0.00105 \pm 0.00076$	L3	[1148]
$0.14960 \pm 0.00090 \pm 0.00220$	OPAL	[1149]
$\Gamma_{56} = h^- h^- h^+ \nu_\tau$	$(9.780 \pm 0.054) \cdot 10^{-2}$	HFAG Summer 2016 fit
$\Gamma_{57} = h^- h^- h^+ \nu_\tau$ (ex. K^0)	$(9.439 \pm 0.053) \cdot 10^{-2}$	HFAG Summer 2016 fit
$(9.510 \pm 0.070 \pm 0.200) \cdot 10^{-2}$	CLEO	[1150]
$(9.317 \pm 0.090 \pm 0.082) \cdot 10^{-2}$	DELPHI	[1128]
$\dfrac{\Gamma_{57}}{\Gamma_{55}} = \dfrac{h^- h^- h^+ \nu_\tau \text{ (ex. } K^0)}{h^- h^- h^+ \geq 0\,\text{neutrals}\,\nu_\tau \text{ (ex. } K^0)}$	0.6480 ± 0.0030	HFAG Summer 2016 fit
$0.6600 \pm 0.0040 \pm 0.0140$	OPAL	[1149]
$\Gamma_{58} = h^- h^- h^+ \nu_\tau$ (ex. K^0, ω)	$(9.408 \pm 0.053) \cdot 10^{-2}$	HFAG Summer 2016 fit
$(9.469 \pm 0.096 \pm 0.000) \cdot 10^{-2}$	ALEPH	[1117]

Table 268 – continued from previous page

τ lepton branching fraction	Fit value / Exp.	HFAG Fit / Ref.
$\Gamma_{59} = \pi^-\pi^+\pi^-\nu_\tau$	$(9.290 \pm 0.052) \cdot 10^{-2}$	HFAG Summer 2016 fit
$\Gamma_{60} = \pi^-\pi^+\pi^-\nu_\tau$ (ex. K^0)	$(9.000 \pm 0.051) \cdot 10^{-2}$	HFAG Summer 2016 fit
$(8.830 \pm 0.010 \pm 0.130) \cdot 10^{-2}$	*BABAR*	[1151]
$(8.420 \pm 0.000^{+0.260}_{-0.250}) \cdot 10^{-2}$	Belle	[1152]
$(9.130 \pm 0.050 \pm 0.460) \cdot 10^{-2}$	CLEO3	[1153]
$\Gamma_{62} = \pi^-\pi^-\pi^+\nu_\tau$ (ex. K^0, ω)	$(8.970 \pm 0.052) \cdot 10^{-2}$	HFAG Summer 2016 fit
$\Gamma_{63} = h^-h^-h^+ \geq 1\,\text{neutrals}\,\nu_\tau$	$(5.325 \pm 0.050) \cdot 10^{-2}$	HFAG Summer 2016 fit
$\Gamma_{64} = h^-h^-h^+ \geq 1\,\pi^0\,\nu_\tau$ (ex. K^0)	$(5.120 \pm 0.049) \cdot 10^{-2}$	HFAG Summer 2016 fit
$\Gamma_{65} = h^-h^-h^+\pi^0\nu_\tau$	$(4.790 \pm 0.052) \cdot 10^{-2}$	HFAG Summer 2016 fit
$\Gamma_{66} = h^-h^-h^+\pi^0\nu_\tau$ (ex. K^0)	$(4.606 \pm 0.051) \cdot 10^{-2}$	HFAG Summer 2016 fit
$(4.734 \pm 0.077 \pm 0.000) \cdot 10^{-2}$	ALEPH	[1117]
$(4.230 \pm 0.060 \pm 0.220) \cdot 10^{-2}$	CLEO	[1150]
$(4.545 \pm 0.106 \pm 0.103) \cdot 10^{-2}$	DELPHI	[1128]
$\Gamma_{67} = h^-h^-h^+\pi^0\nu_\tau$ (ex. K^0, ω)	$(2.820 \pm 0.070) \cdot 10^{-2}$	HFAG Summer 2016 fit
$\Gamma_{68} = \pi^-\pi^+\pi^-\pi^0\nu_\tau$	$(4.651 \pm 0.053) \cdot 10^{-2}$	HFAG Summer 2016 fit
$\Gamma_{69} = \pi^-\pi^+\pi^-\pi^0\nu_\tau$ (ex. K^0)	$(4.519 \pm 0.052) \cdot 10^{-2}$	HFAG Summer 2016 fit
$(4.190 \pm 0.100 \pm 0.210) \cdot 10^{-2}$	CLEO	[1154]
$\Gamma_{70} = \pi^-\pi^-\pi^+\pi^0\nu_\tau$ (ex. K^0, ω)	$(2.769 \pm 0.071) \cdot 10^{-2}$	HFAG Summer 2016 fit
$\Gamma_{74} = h^-h^-h^+ \geq 2\,\pi^0\,\nu_\tau$ (ex. K^0)	$(0.5135 \pm 0.0312) \cdot 10^{-2}$	HFAG Summer 2016 fit
$(0.5610 \pm 0.0680 \pm 0.0950) \cdot 10^{-2}$	DELPHI	[1128]
$\Gamma_{75} = h^-h^-h^+2\pi^0\nu_\tau$	$(0.5024 \pm 0.0310) \cdot 10^{-2}$	HFAG Summer 2016 fit
$\Gamma_{76} = h^-h^-h^+2\pi^0\nu_\tau$ (ex. K^0)	$(0.4925 \pm 0.0310) \cdot 10^{-2}$	HFAG Summer 2016 fit
$(0.4350 \pm 0.0461 \pm 0.0000) \cdot 10^{-2}$	ALEPH	[1117]
$\dfrac{\Gamma_{76}}{\Gamma_{54}} = \dfrac{h^-h^-h^+2\pi^0\nu_\tau\ (\text{ex. } K^0)}{h^-h^-h^+ \geq 0\,\text{neutrals} \geq 0\,K^0_L\,\nu_\tau}$	$(3.237 \pm 0.202) \cdot 10^{-2}$	HFAG Summer 2016 fit
$(3.400 \pm 0.200 \pm 0.300) \cdot 10^{-2}$	CLEO	[1155]
$\Gamma_{77} = h^-h^-h^+2\pi^0\nu_\tau$ (ex. K^0, ω, η)	$(9.759 \pm 3.550) \cdot 10^{-4}$	HFAG Summer 2016 fit
$\Gamma_{78} = h^-h^-h^+3\pi^0\nu_\tau$	$(2.107 \pm 0.299) \cdot 10^{-4}$	HFAG Summer 2016 fit
$(2.200 \pm 0.300 \pm 0.400) \cdot 10^{-4}$	CLEO	[1156]

Table 268 – continued from previous page

τ lepton branching fraction	Fit value / Exp.	HFAG Fit / Ref.
$\Gamma_{79} = K^- h^- h^+ \geq 0\,\text{neutrals}\,\nu_\tau$	$(0.6297 \pm 0.0141) \cdot 10^{-2}$	HFAG Summer 2016 fit
$\Gamma_{80} = K^- \pi^- h^+ \nu_\tau$ (ex. K^0)	$(0.4363 \pm 0.0073) \cdot 10^{-2}$	HFAG Summer 2016 fit
$\dfrac{\Gamma_{80}}{\Gamma_{60}} = \dfrac{K^- \pi^- h^+ \nu_\tau \text{ (ex. } K^0)}{\pi^- \pi^+ \pi^- \nu_\tau \text{ (ex. } K^0)}$	$(4.847 \pm 0.080) \cdot 10^{-2}$	HFAG Summer 2016 fit
$(5.440 \pm 0.210 \pm 0.530) \cdot 10^{-2}$	CLEO	[1157]
$\Gamma_{81} = K^- \pi^- h^+ \pi^0 \nu_\tau$ (ex. K^0)	$(8.726 \pm 1.177) \cdot 10^{-4}$	HFAG Summer 2016 fit
$\dfrac{\Gamma_{81}}{\Gamma_{69}} = \dfrac{K^- \pi^- h^+ \pi^0 \nu_\tau \text{ (ex. } K^0)}{\pi^- \pi^+ \pi^- \pi^0 \nu_\tau \text{ (ex. } K^0)}$	$(1.931 \pm 0.266) \cdot 10^{-2}$	HFAG Summer 2016 fit
$(2.610 \pm 0.450 \pm 0.420) \cdot 10^{-2}$	CLEO	[1157]
$\Gamma_{82} = K^- \pi^- \pi^+ \geq 0\,\text{neutrals}\,\nu_\tau$	$(0.4780 \pm 0.0137) \cdot 10^{-2}$	HFAG Summer 2016 fit
$(0.5800^{+0.1500}_{-0.1300} \pm 0.1200) \cdot 10^{-2}$	TPC	[1158]
$\Gamma_{83} = K^- \pi^- \pi^+ \geq 0\,\pi^0\,\nu_\tau$ (ex. K^0)	$(0.3741 \pm 0.0135) \cdot 10^{-2}$	HFAG Summer 2016 fit
$\Gamma_{84} = K^- \pi^- \pi^+ \nu_\tau$	$(0.3441 \pm 0.0070) \cdot 10^{-2}$	HFAG Summer 2016 fit
$\Gamma_{85} = K^- \pi^+ \pi^- \nu_\tau$ (ex. K^0)	$(0.2929 \pm 0.0067) \cdot 10^{-2}$	HFAG Summer 2016 fit
$(0.2140 \pm 0.0470 \pm 0.0000) \cdot 10^{-2}$	ALEPH	[1159]
$(0.2730 \pm 0.0020 \pm 0.0090) \cdot 10^{-2}$	*BABAR*	[1151]
$(0.3300 \pm 0.0010^{+0.0160}_{-0.0170}) \cdot 10^{-2}$	Belle	[1152]
$(0.3840 \pm 0.0140 \pm 0.0380) \cdot 10^{-2}$	CLEO3	[1153]
$(0.4150 \pm 0.0530 \pm 0.0400) \cdot 10^{-2}$	OPAL	[1137]
$\dfrac{\Gamma_{85}}{\Gamma_{60}} = \dfrac{K^- \pi^+ \pi^- \nu_\tau \text{ (ex. } K^0)}{\pi^- \pi^+ \pi^- \nu_\tau \text{ (ex. } K^0)}$	$(3.254 \pm 0.074) \cdot 10^{-2}$	HFAG Summer 2016 fit
$\Gamma_{87} = K^- \pi^- \pi^+ \pi^0 \nu_\tau$	$(0.1331 \pm 0.0119) \cdot 10^{-2}$	HFAG Summer 2016 fit
$\Gamma_{88} = K^- \pi^- \pi^+ \pi^0 \nu_\tau$ (ex. K^0)	$(8.115 \pm 1.168) \cdot 10^{-4}$	HFAG Summer 2016 fit
$(6.100 \pm 4.295 \pm 0.000) \cdot 10^{-4}$	ALEPH	[1159]
$(7.400 \pm 0.800 \pm 1.100) \cdot 10^{-4}$	CLEO3	[1160]
$\Gamma_{89} = K^- \pi^- \pi^+ \pi^0 \nu_\tau$ (ex. K^0, η)	$(7.761 \pm 1.168) \cdot 10^{-4}$	HFAG Summer 2016 fit
$\Gamma_{92} = \pi^- K^- K^+ \geq 0\,\text{neutrals}\,\nu_\tau$	$(0.1495 \pm 0.0033) \cdot 10^{-2}$	HFAG Summer 2016 fit
$(0.1590 \pm 0.0530 \pm 0.0200) \cdot 10^{-2}$	OPAL	[1161]
$(0.1500^{+0.0900}_{-0.0700} \pm 0.0300) \cdot 10^{-2}$	TPC	[1158]
$\Gamma_{93} = \pi^- K^- K^+ \nu_\tau$	$(0.1434 \pm 0.0027) \cdot 10^{-2}$	HFAG Summer 2016 fit
$(0.1630 \pm 0.0270 \pm 0.0000) \cdot 10^{-2}$	ALEPH	[1159]

Table 268 – continued from previous page

τ lepton branching fraction	Fit value / Exp.	HFAG Fit / Ref.
$(0.1346 \pm 0.0010 \pm 0.0036) \cdot 10^{-2}$	*BABAR*	[1151]
$(0.1550 \pm 0.0010^{+0.0060}_{-0.0050}) \cdot 10^{-2}$	Belle	[1152]
$(0.1550 \pm 0.0060 \pm 0.0090) \cdot 10^{-2}$	CLEO3	[1153]
$\frac{\Gamma_{93}}{\Gamma_{60}} = \frac{\pi^- K^- K^+ \nu_\tau}{\pi^- \pi^+ \pi^- \nu_\tau \text{ (ex. } K^0)}$	$(1.593 \pm 0.030) \cdot 10^{-2}$	HFAG Summer 2016 fit
$(1.600 \pm 0.150 \pm 0.300) \cdot 10^{-2}$	CLEO	[1157]
$\Gamma_{94} = \pi^- K^- K^+ \pi^0 \nu_\tau$	$(0.611 \pm 0.183) \cdot 10^{-4}$	HFAG Summer 2016 fit
$(7.500 \pm 3.265 \pm 0.000) \cdot 10^{-4}$	ALEPH	[1159]
$(0.550 \pm 0.140 \pm 0.120) \cdot 10^{-4}$	CLEO3	[1160]
$\frac{\Gamma_{94}}{\Gamma_{69}} = \frac{\pi^- K^- K^+ \pi^0 \nu_\tau}{\pi^- \pi^+ \pi^- \pi^0 \nu_\tau \text{ (ex. } K^0)}$	$(0.1353 \pm 0.0405) \cdot 10^{-2}$	HFAG Summer 2016 fit
$(0.7900 \pm 0.4400 \pm 0.1600) \cdot 10^{-2}$	CLEO	[1157]
$\Gamma_{96} = K^- K^- K^+ \nu_\tau$	$(2.174 \pm 0.800) \cdot 10^{-5}$	HFAG Summer 2016 fit
$(1.578 \pm 0.130 \pm 0.123) \cdot 10^{-5}$	*BABAR*	[1151]
$(3.290 \pm 0.170^{+0.190}_{-0.200}) \cdot 10^{-5}$	Belle	[1152]
$\Gamma_{102} = 3h^- 2h^+ \geq 0 \,\text{neutrals}\, \nu_\tau \text{ (ex. } K^0)$	$(0.0985 \pm 0.0037) \cdot 10^{-2}$	HFAG Summer 2016 fit
$(0.0970 \pm 0.0050 \pm 0.0110) \cdot 10^{-2}$	CLEO	[1162]
$(0.1020 \pm 0.0290 \pm 0.0000) \cdot 10^{-2}$	HRS	[1163]
$(0.1700 \pm 0.0220 \pm 0.0260) \cdot 10^{-2}$	L3	[1148]
$\Gamma_{103} = 3h^- 2h^+ \nu_\tau \text{ (ex. } K^0)$	$(8.216 \pm 0.316) \cdot 10^{-4}$	HFAG Summer 2016 fit
$(7.200 \pm 1.500 \pm 0.000) \cdot 10^{-4}$	ALEPH	[1117]
$(6.400 \pm 2.300 \pm 1.000) \cdot 10^{-4}$	ARGUS	[1164]
$(7.700 \pm 0.500 \pm 0.900) \cdot 10^{-4}$	CLEO	[1162]
$(9.700 \pm 1.500 \pm 0.500) \cdot 10^{-4}$	DELPHI	[1128]
$(5.100 \pm 2.000 \pm 0.000) \cdot 10^{-4}$	HRS	[1163]
$(9.100 \pm 1.400 \pm 0.600) \cdot 10^{-4}$	OPAL	[1165]
$\Gamma_{104} = 3h^- 2h^+ \pi^0 \nu_\tau \text{ (ex. } K^0)$	$(1.634 \pm 0.114) \cdot 10^{-4}$	HFAG Summer 2016 fit
$(2.100 \pm 0.700 \pm 0.900) \cdot 10^{-4}$	ALEPH	[1117]
$(1.700 \pm 0.200 \pm 0.200) \cdot 10^{-4}$	CLEO	[1156]
$(1.600 \pm 1.200 \pm 0.600) \cdot 10^{-4}$	DELPHI	[1128]
$(2.700 \pm 1.800 \pm 0.900) \cdot 10^{-4}$	OPAL	[1165]
$\Gamma_{106} = (5\pi)^- \nu_\tau$	$(0.7748 \pm 0.0534) \cdot 10^{-2}$	HFAG Summer 2016 fit
$\Gamma_{110} = X_s^- \nu_\tau$	$(2.909 \pm 0.048) \cdot 10^{-2}$	HFAG Summer 2016 fit

Table 268 – continued from previous page

τ lepton branching fraction	Fit value / Exp.	HFAG Fit / Ref.
$\Gamma_{126} = \pi^-\pi^0\eta\nu_\tau$	$(0.1386 \pm 0.0072) \cdot 10^{-2}$	HFAG Summer 2016 fit
$(0.1800 \pm 0.0447 \pm 0.0000) \cdot 10^{-2}$	ALEPH	[1166]
$(0.1350 \pm 0.0030 \pm 0.0070) \cdot 10^{-2}$	Belle	[1167]
$(0.1700 \pm 0.0200 \pm 0.0200) \cdot 10^{-2}$	CLEO	[1168]
$\Gamma_{128} = K^-\eta\nu_\tau$	$(1.547 \pm 0.080) \cdot 10^{-4}$	HFAG Summer 2016 fit
$(2.900^{+1.300}_{-1.200} \pm 0.700) \cdot 10^{-4}$	ALEPH	[1166]
$(1.420 \pm 0.110 \pm 0.070) \cdot 10^{-4}$	*BABAR*	[1169]
$(1.580 \pm 0.050 \pm 0.090) \cdot 10^{-4}$	Belle	[1167]
$(2.600 \pm 0.500 \pm 0.500) \cdot 10^{-4}$	CLEO	[1170]
$\Gamma_{130} = K^-\pi^0\eta\nu_\tau$	$(0.483 \pm 0.116) \cdot 10^{-4}$	HFAG Summer 2016 fit
$(0.460 \pm 0.110 \pm 0.040) \cdot 10^{-4}$	Belle	[1167]
$(1.770 \pm 0.560 \pm 0.710) \cdot 10^{-4}$	CLEO	[1171]
$\Gamma_{132} = \pi^-\overline{K}^0\eta\nu_\tau$	$(0.937 \pm 0.149) \cdot 10^{-4}$	HFAG Summer 2016 fit
$(0.880 \pm 0.140 \pm 0.060) \cdot 10^{-4}$	Belle	[1167]
$(2.200 \pm 0.700 \pm 0.220) \cdot 10^{-4}$	CLEO	[1171]
$\Gamma_{136} = \pi^-\pi^+\pi^-\eta\nu_\tau$ (ex. K^0)	$(2.184 \pm 0.130) \cdot 10^{-4}$	HFAG Summer 2016 fit
$\Gamma_{149} = h^-\omega \geq 0\,\text{neutrals}\,\nu_\tau$	$(2.401 \pm 0.075) \cdot 10^{-2}$	HFAG Summer 2016 fit
$\Gamma_{150} = h^-\omega\nu_\tau$	$(1.995 \pm 0.064) \cdot 10^{-2}$	HFAG Summer 2016 fit
$(1.910 \pm 0.092 \pm 0.000) \cdot 10^{-2}$	ALEPH	[1166]
$(1.600 \pm 0.270 \pm 0.410) \cdot 10^{-2}$	CLEO	[1172]
$\dfrac{\Gamma_{150}}{\Gamma_{66}} = \dfrac{h^-\omega\nu_\tau}{h^-h^-h^+\pi^0\nu_\tau\ (\text{ex. } K^0)}$	0.4332 ± 0.0139	HFAG Summer 2016 fit
$0.4310 \pm 0.0330 \pm 0.0000$	ALEPH	[1173]
$0.4640 \pm 0.0160 \pm 0.0170$	CLEO	[1150]
$\Gamma_{151} = K^-\omega\nu_\tau$	$(4.100 \pm 0.922) \cdot 10^{-4}$	HFAG Summer 2016 fit
$(4.100 \pm 0.600 \pm 0.700) \cdot 10^{-4}$	CLEO3	[1160]
$\Gamma_{152} = h^-\pi^0\omega\nu_\tau$	$(0.4058 \pm 0.0419) \cdot 10^{-2}$	HFAG Summer 2016 fit
$(0.4300 \pm 0.0781 \pm 0.0000) \cdot 10^{-2}$	ALEPH	[1166]
$\dfrac{\Gamma_{152}}{\Gamma_{54}} = \dfrac{h^-\omega\pi^0\nu_\tau}{h^-h^-h^+ \geq 0\,\text{neutrals} \geq 0\,K^0_L\,\nu_\tau}$	$(2.667 \pm 0.275) \cdot 10^{-2}$	HFAG Summer 2016 fit
$\dfrac{\Gamma_{152}}{\Gamma_{76}} = \dfrac{h^-\omega\pi^0\nu_\tau}{h^-h^-h^+2\pi^0\nu_\tau\ (\text{ex. } K^0)}$	0.8241 ± 0.0757	HFAG Summer 2016 fit

Table 268 – continued from previous page

τ lepton branching fraction	Fit value / Exp.	HFAG Fit / Ref.
$0.8100 \pm 0.0600 \pm 0.0600$	CLEO	[1155]
$\Gamma_{167} = K^- \phi \nu_\tau$	$(4.445 \pm 1.636) \cdot 10^{-5}$	HFAG Summer 2016 fit
$\Gamma_{168} = K^- \phi \nu_\tau$ ($\phi \to K^+ K^-$)	$(2.174 \pm 0.800) \cdot 10^{-5}$	HFAG Summer 2016 fit
$\Gamma_{169} = K^- \phi \nu_\tau$ ($\phi \to K^0_S K^0_L$)	$(1.520 \pm 0.560) \cdot 10^{-5}$	HFAG Summer 2016 fit
$\Gamma_{800} = \pi^- \omega \nu_\tau$	$(1.954 \pm 0.065) \cdot 10^{-2}$	HFAG Summer 2016 fit
$\Gamma_{802} = K^- \pi^- \pi^+ \nu_\tau$ (ex. K^0, ω)	$(0.2923 \pm 0.0067) \cdot 10^{-2}$	HFAG Summer 2016 fit
$\Gamma_{803} = K^- \pi^- \pi^+ \pi^0 \nu_\tau$ (ex. K^0, ω, η)	$(4.103 \pm 1.429) \cdot 10^{-4}$	HFAG Summer 2016 fit
$\Gamma_{804} = \pi^- K^0_L K^0_L \nu_\tau$	$(2.332 \pm 0.065) \cdot 10^{-4}$	HFAG Summer 2016 fit
$\Gamma_{805} = a_1^- (\to \pi^- \gamma) \nu_\tau$	$(4.000 \pm 2.000) \cdot 10^{-4}$	HFAG Summer 2016 fit
$(4.000 \pm 2.000 \pm 0.000) \cdot 10^{-4}$	ALEPH	[1117]
$\Gamma_{806} = \pi^- \pi^0 K^0_L K^0_L \nu_\tau$	$(1.815 \pm 0.207) \cdot 10^{-5}$	HFAG Summer 2016 fit
$\Gamma_{810} = 2\pi^- \pi^+ 3\pi^0 \nu_\tau$ (ex. K^0)	$(1.924 \pm 0.298) \cdot 10^{-4}$	HFAG Summer 2016 fit
$\Gamma_{811} = \pi^- 2\pi^0 \omega \nu_\tau$ (ex. K^0)	$(7.105 \pm 1.586) \cdot 10^{-5}$	HFAG Summer 2016 fit
$(7.300 \pm 1.200 \pm 1.200) \cdot 10^{-5}$	*BABAR*	[1174]
$\Gamma_{812} = 2\pi^- \pi^+ 3\pi^0 \nu_\tau$ (ex. K^0, η, ω, f_1)	$(1.344 \pm 2.683) \cdot 10^{-5}$	HFAG Summer 2016 fit
$(1.000 \pm 0.800 \pm 3.000) \cdot 10^{-5}$	*BABAR*	[1174]
$\Gamma_{820} = 3\pi^- 2\pi^+ \nu_\tau$ (ex. K^0, ω)	$(8.197 \pm 0.315) \cdot 10^{-4}$	HFAG Summer 2016 fit
$\Gamma_{821} = 3\pi^- 2\pi^+ \nu_\tau$ (ex. K^0, ω, f_1)	$(7.677 \pm 0.297) \cdot 10^{-4}$	HFAG Summer 2016 fit
$(7.680 \pm 0.040 \pm 0.400) \cdot 10^{-4}$	*BABAR*	[1174]
$\Gamma_{822} = K^- 2\pi^- 2\pi^+ \nu_\tau$ (ex. K^0)	$(0.596 \pm 1.208) \cdot 10^{-6}$	HFAG Summer 2016 fit
$(0.600 \pm 0.500 \pm 1.100) \cdot 10^{-6}$	*BABAR*	[1174]
$\Gamma_{830} = 3\pi^- 2\pi^+ \pi^0 \nu_\tau$ (ex. K^0)	$(1.623 \pm 0.114) \cdot 10^{-4}$	HFAG Summer 2016 fit
$\Gamma_{831} = 2\pi^- \pi^+ \omega \nu_\tau$ (ex. K^0)	$(8.359 \pm 0.626) \cdot 10^{-5}$	HFAG Summer 2016 fit
$(8.400 \pm 0.400 \pm 0.600) \cdot 10^{-5}$	*BABAR*	[1174]
$\Gamma_{832} = 3\pi^- 2\pi^+ \pi^0 \nu_\tau$ (ex. K^0, η, ω, f_1)	$(3.771 \pm 0.875) \cdot 10^{-5}$	HFAG Summer 2016 fit
$(3.600 \pm 0.300 \pm 0.900) \cdot 10^{-5}$	*BABAR*	[1174]
$\Gamma_{833} = K^- 2\pi^- 2\pi^+ \pi^0 \nu_\tau$ (ex. K^0)	$(1.108 \pm 0.566) \cdot 10^{-6}$	HFAG Summer 2016 fit
$(1.100 \pm 0.400 \pm 0.400) \cdot 10^{-6}$	*BABAR*	[1174]

Table 268 – continued from previous page

τ lepton branching fraction	Fit value / Exp.	HFAG Fit / Ref.
$\Gamma_{910} = 2\pi^-\pi^+\eta\nu_\tau$ ($\eta \to 3\pi^0$) (ex. K^0)	$(7.136 \pm 0.424) \cdot 10^{-5}$	HFAG Summer 2016 fit
$(8.270 \pm 0.880 \pm 0.810) \cdot 10^{-5}$	*BABAR*	[1174]
$\Gamma_{911} = \pi^-2\pi^0\eta\nu_\tau$ ($\eta \to \pi^+\pi^-\pi^0$) (ex. K^0)	$(4.420 \pm 0.867) \cdot 10^{-5}$	HFAG Summer 2016 fit
$(4.570 \pm 0.770 \pm 0.500) \cdot 10^{-5}$	*BABAR*	[1174]
$\Gamma_{920} = \pi^- f_1\nu_\tau$ ($f_1 \to 2\pi^-2\pi^+$)	$(5.197 \pm 0.444) \cdot 10^{-5}$	HFAG Summer 2016 fit
$(5.200 \pm 0.310 \pm 0.370) \cdot 10^{-5}$	*BABAR*	[1174]
$\Gamma_{930} = 2\pi^-\pi^+\eta\nu_\tau$ ($\eta \to \pi^+\pi^-\pi^0$) (ex. K^0)	$(5.005 \pm 0.297) \cdot 10^{-5}$	HFAG Summer 2016 fit
$(5.390 \pm 0.270 \pm 0.410) \cdot 10^{-5}$	*BABAR*	[1174]
$\Gamma_{944} = 2\pi^-\pi^+\eta\nu_\tau$ ($\eta \to \gamma\gamma$) (ex. K^0)	$(8.606 \pm 0.511) \cdot 10^{-5}$	HFAG Summer 2016 fit
$(8.260 \pm 0.350 \pm 0.510) \cdot 10^{-5}$	*BABAR*	[1174]
$\Gamma_{945} = \pi^-2\pi^0\eta\nu_\tau$	$(1.929 \pm 0.378) \cdot 10^{-4}$	HFAG Summer 2016 fit
$\Gamma_{998} = 1 - \Gamma_{\rm All}$	$(0.0355 \pm 0.1031) \cdot 10^{-2}$	HFAG Summer 2016 fit

9.1.6 Correlation terms between basis branching fractions uncertainties

The following tables report the correlation coefficients between basis nodes, in percent.

Table 269: Basis nodes correlation coefficients in percent, section 1.

Γ_5	23													
Γ_9	7	5												
Γ_{10}	3	5	1											
Γ_{14}	-13	-14	-12	-3										
Γ_{16}	0	-1	2	-1	-16									
Γ_{20}	-5	-5	-7	-1	-40	2								
Γ_{23}	0	0	0	-2	2	-13	-22							
Γ_{27}	-4	-3	-8	-1	0	3	-36	6						
Γ_{28}	0	0	0	-2	2	-13	5	-21	-29					
Γ_{30}	-5	-4	-11	-2	-9	0	6	0	-42	0				
Γ_{35}	0	0	0	0	0	0	0	1	0	1	0			
Γ_{37}	0	0	0	0	0	-2	1	-3	1	-3	0	-22		
Γ_{40}	0	0	0	0	0	1	0	1	-2	1	0	-12	4	
	Γ_3	Γ_5	Γ_9	Γ_{10}	Γ_{14}	Γ_{16}	Γ_{20}	Γ_{23}	Γ_{27}	Γ_{28}	Γ_{30}	Γ_{35}	Γ_{37}	Γ_{40}

Table 270: Basis nodes correlation coefficients in percent, section 2.

Γ_{42}	0	0	0	0	1	-3	1	-5	1	-5	0	2	-21	-20
Γ_{44}	0	0	0	0	0	0	0	0	0	0	0	-1	0	-4
Γ_{47}	0	0	0	0	0	0	0	0	0	0	0	-1	1	-4
Γ_{48}	0	0	0	0	0	0	0	0	0	0	0	-3	0	-2
Γ_{50}	0	0	0	0	0	0	0	-1	0	-1	0	0	7	0
Γ_{51}	0	0	0	0	0	0	0	0	0	0	0	-1	0	-1
Γ_{53}	0	0	0	0	0	0	0	0	0	0	0	0	0	0
Γ_{62}	-3	-5	8	0	-4	5	-7	-1	-5	-1	-5	0	0	0
Γ_{70}	-6	-6	-7	-1	-8	-1	-1	0	-1	0	3	0	0	0
Γ_{77}	-1	0	-3	-1	-2	0	0	0	2	0	2	0	0	0
Γ_{93}	-1	-1	3	0	-1	2	-1	0	-1	0	-1	0	0	0
Γ_{94}	0	0	0	0	0	0	0	0	0	0	0	0	0	0
Γ_{126}	0	0	0	0	0	0	-1	0	0	0	-2	0	0	0
Γ_{128}	0	0	1	0	0	1	0	-1	0	-1	0	0	0	0
	Γ_3	Γ_5	Γ_9	Γ_{10}	Γ_{14}	Γ_{16}	Γ_{20}	Γ_{23}	Γ_{27}	Γ_{28}	Γ_{30}	Γ_{35}	Γ_{37}	Γ_{40}

Table 271: Basis nodes correlation coefficients in percent, section 3.

Γ_{130}	0	0	0	0	0	0	0	0	0	0	0	0	0	0
Γ_{132}	0	0	0	0	0	0	0	0	0	0	0	0	0	0
Γ_{136}	0	0	0	0	0	0	0	0	0	0	0	0	0	0
Γ_{151}	0	0	0	0	0	0	0	0	0	0	0	0	0	0
Γ_{152}	-1	0	-3	-1	-2	0	-1	0	2	0	2	0	0	0
Γ_{167}	0	0	0	0	0	0	0	0	0	0	0	0	0	0
Γ_{800}	-2	-2	-2	0	-3	0	0	0	0	0	1	0	0	0
Γ_{802}	-1	-1	0	0	-1	0	-2	0	-2	0	-1	0	0	0
Γ_{803}	0	0	0	0	0	0	0	0	0	0	0	0	0	0
Γ_{805}	0	0	0	0	0	0	0	0	0	0	0	0	0	0
Γ_{811}	0	0	0	0	0	0	0	0	0	0	0	0	0	0
Γ_{812}	0	1	0	0	0	0	0	0	0	0	0	0	0	0
Γ_{821}	0	0	1	0	0	0	-1	0	0	0	-1	0	0	0
Γ_{822}	0	0	0	0	0	0	0	0	0	0	0	0	0	0
	Γ_3	Γ_5	Γ_9	Γ_{10}	Γ_{14}	Γ_{16}	Γ_{20}	Γ_{23}	Γ_{27}	Γ_{28}	Γ_{30}	Γ_{35}	Γ_{37}	Γ_{40}

Table 272: Basis nodes correlation coefficients in percent, section 4.

Γ_{831}	0	0	0	0	0	0	0	0	0	0	0	0	0	0
Γ_{832}	0	0	0	0	0	0	0	0	0	0	0	0	0	0
Γ_{833}	0	0	0	0	0	0	0	0	0	0	0	0	0	0
Γ_{920}	0	0	0	0	0	0	0	0	0	0	0	0	0	0
Γ_{945}	0	0	0	0	0	0	0	0	0	0	0	0	0	0
	Γ_3	Γ_5	Γ_9	Γ_{10}	Γ_{14}	Γ_{16}	Γ_{20}	Γ_{23}	Γ_{27}	Γ_{28}	Γ_{30}	Γ_{35}	Γ_{37}	Γ_{40}

Table 273: Basis nodes correlation coefficients in percent, section 5.

Γ_{44}	0													
Γ_{47}	1	0												
Γ_{48}	-1	-6	0											
Γ_{50}	5	0	-7	0										
Γ_{51}	0	-3	0	-6	0									
Γ_{53}	0	0	0	0	0	0								
Γ_{62}	0	0	1	0	0	0	0							
Γ_{70}	0	0	0	0	0	0	0	-20						
Γ_{77}	0	0	0	0	0	0	0	-1	-7					
Γ_{93}	0	0	0	0	0	0	0	14	-4	0				
Γ_{94}	0	0	0	0	0	0	0	0	-2	0	0			
Γ_{126}	0	0	1	0	0	0	0	1	0	-5	0	0		
Γ_{128}	0	0	1	0	0	0	0	2	0	0	1	0	4	
	Γ_{42}	Γ_{44}	Γ_{47}	Γ_{48}	Γ_{50}	Γ_{51}	Γ_{53}	Γ_{62}	Γ_{70}	Γ_{77}	Γ_{93}	Γ_{94}	Γ_{126}	Γ_{128}

Table 274: Basis nodes correlation coefficients in percent, section 6.

Γ_{130}	0	0	0	0	0	0	0	0	0	-1	0	0	1	1
Γ_{132}	0	0	0	0	0	0	0	0	0	0	0	0	2	1
Γ_{136}	0	0	0	0	0	0	0	0	-1	0	0	0	0	0
Γ_{151}	0	0	0	0	0	0	0	0	12	0	0	0	0	0
Γ_{152}	0	0	0	0	0	0	0	-1	-11	-64	0	0	0	0
Γ_{167}	0	0	0	0	0	0	0	-1	0	0	1	0	0	0
Γ_{800}	0	0	0	0	0	0	0	-8	-69	-2	-1	0	0	0
Γ_{802}	0	0	0	0	0	0	0	16	-6	0	0	0	0	0
Γ_{803}	0	0	0	0	0	0	0	-1	-19	0	0	-2	0	-1
Γ_{805}	0	0	0	0	0	0	0	0	0	0	0	0	0	0
Γ_{811}	0	0	0	0	0	0	0	0	0	0	0	0	0	0
Γ_{812}	0	0	0	0	-1	0	0	0	-1	0	0	0	0	0
Γ_{821}	0	0	0	0	0	0	0	0	-1	0	0	0	0	0
Γ_{822}	0	0	0	0	0	0	0	0	0	0	0	0	0	0
	Γ_{42}	Γ_{44}	Γ_{47}	Γ_{48}	Γ_{50}	Γ_{51}	Γ_{53}	Γ_{62}	Γ_{70}	Γ_{77}	Γ_{93}	Γ_{94}	Γ_{126}	Γ_{128}

Table 275: Basis nodes correlation coefficients in percent, section 7.

Γ_{831}	0	0	0	0	0	0	0	0	0	0	0	0	0	0
Γ_{832}	0	0	0	0	0	0	0	0	0	0	0	0	0	0
Γ_{833}	0	0	0	0	0	0	0	0	0	0	0	0	0	0
Γ_{920}	0	0	0	0	0	0	0	0	0	0	0	0	0	0
Γ_{945}	0	0	0	0	0	0	0	0	0	0	0	0	0	0
	Γ_{42}	Γ_{44}	Γ_{47}	Γ_{48}	Γ_{50}	Γ_{51}	Γ_{53}	Γ_{62}	Γ_{70}	Γ_{77}	Γ_{93}	Γ_{94}	Γ_{126}	Γ_{128}

Table 276: Basis nodes correlation coefficients in percent, section 8.

Γ_{132}	0													
Γ_{136}	0	0												
Γ_{151}	0	0	0											
Γ_{152}	0	0	0	0										
Γ_{167}	0	0	0	0	0									
Γ_{800}	0	0	0	-14	-3	0								
Γ_{802}	0	0	0	-2	0	1	-1							
Γ_{803}	0	0	0	-58	0	0	9	1						
Γ_{805}	0	0	0	0	0	0	0	0	0					
Γ_{811}	0	-1	20	0	0	0	0	0	0	0				
Γ_{812}	0	-2	-8	0	0	0	0	0	0	0	-16			
Γ_{821}	0	0	47	0	0	0	0	0	0	0	8	-4		
Γ_{822}	0	0	-1	0	0	0	0	0	0	0	0	0	-1	
	Γ_{130}	Γ_{132}	Γ_{136}	Γ_{151}	Γ_{152}	Γ_{167}	Γ_{800}	Γ_{802}	Γ_{803}	Γ_{805}	Γ_{811}	Γ_{812}	Γ_{821}	Γ_{822}

Table 277: Basis nodes correlation coefficients in percent, section 9.

Γ_{831}	0	0	39	0	0	0	0	0	0	0	14	-4	39	-1
Γ_{832}	0	0	3	0	0	0	0	0	0	0	2	0	3	0
Γ_{833}	0	0	-1	0	0	0	0	0	0	0	0	0	-1	0
Γ_{920}	0	0	21	0	0	0	0	0	0	0	3	-2	35	-1
Γ_{945}	0	-1	25	0	0	0	0	0	0	0	10	-11	10	0
	Γ_{130}	Γ_{132}	Γ_{136}	Γ_{151}	Γ_{152}	Γ_{167}	Γ_{800}	Γ_{802}	Γ_{803}	Γ_{805}	Γ_{811}	Γ_{812}	Γ_{821}	Γ_{822}

Table 278: Basis nodes correlation coefficients in percent, section 10.

Γ_{832}	-2				
Γ_{833}	-1	-1			
Γ_{920}	17	1	0		
Γ_{945}	17	2	0	4	
	Γ_{831}	Γ_{832}	Γ_{833}	Γ_{920}	Γ_{945}

9.1.7 Equality constraints

We list in the following the equality constraints that relate a branching fraction to a sum of branching fractions, which have been introduced in Section 9.1. In the constraint equations, the τ branching fractions are denoted with Γ_n labels. The equations include as coefficients the values of some non-tau branching fractions, denoted *e.g.* with the self-describing notation $\Gamma_{K_S\to\pi^0\pi^0}$. Some coefficients are probabilities corresponding to modulus square amplitudes describing quantum mixtures of states such as K^0, $\overline{K}^0$, K_S, K_L, denoted with *e.g.* $\Gamma_{<K^0|K_S>} = |<K^0|K_S>|^2$. All non-tau quantities are taken from the PDG 2015 [314] fits (when available) or averages, and are used without accounting for their uncertainties, which are however in general small with respect to the uncertainties on the τ branching fractions.

The following list does not include the constraints already introduced in Section 9.1, and listed in Table 268, where some measured ratios of branching fractions are expressed as ratios of two branching fractions.

$$\begin{aligned}
\Gamma_1 &= \Gamma_3 + \Gamma_5 + \Gamma_9 + \Gamma_{10} + \Gamma_{14} + \Gamma_{16} \\
&\quad + \Gamma_{20} + \Gamma_{23} + \Gamma_{27} + \Gamma_{28} + \Gamma_{30} + \Gamma_{35} \\
&\quad + \Gamma_{40} + \Gamma_{44} + \Gamma_{37} + \Gamma_{42} + \Gamma_{47} + \Gamma_{48} \\
&\quad + \Gamma_{804} + \Gamma_{50} + \Gamma_{51} + \Gamma_{806} + \Gamma_{126} \cdot \Gamma_{\eta\to\text{neutral}} \\
&\quad + \Gamma_{128} \cdot \Gamma_{\eta\to\text{neutral}} + \Gamma_{130} \cdot \Gamma_{\eta\to\text{neutral}} + \Gamma_{132} \cdot \Gamma_{\eta\to\text{neutral}} \\
&\quad + \Gamma_{800} \cdot \Gamma_{\omega\to\pi^0\gamma} + \Gamma_{151} \cdot \Gamma_{\omega\to\pi^0\gamma} + \Gamma_{152} \cdot \Gamma_{\omega\to\pi^0\gamma} \\
&\quad + \Gamma_{167} \cdot \Gamma_{\phi\to K_S K_L}
\end{aligned}$$

$$\begin{aligned}
\Gamma_2 &= \Gamma_3 + \Gamma_5 + \Gamma_9 + \Gamma_{10} + \Gamma_{14} + \Gamma_{16} \\
&\quad + \Gamma_{20} + \Gamma_{23} + \Gamma_{27} + \Gamma_{28} + \Gamma_{30} + \Gamma_{35} \cdot (\Gamma_{<\overline{K}^0|K_S>} \cdot \Gamma_{K_S\to\pi^0\pi^0} \\
&\quad + \Gamma_{<\overline{K}^0|K_L>}) + \Gamma_{40} \cdot (\Gamma_{<\overline{K}^0|K_S>} \cdot \Gamma_{K_S\to\pi^0\pi^0} + \Gamma_{<\overline{K}^0|K_L>}) + \Gamma_{44} \cdot (\Gamma_{<\overline{K}^0|K_S>} \cdot \Gamma_{K_S\to\pi^0\pi^0} \\
&\quad + \Gamma_{<\overline{K}^0|K_L>}) + \Gamma_{37} \cdot (\Gamma_{<\overline{K}^0|K_S>} \cdot \Gamma_{K_S\to\pi^0\pi^0} + \Gamma_{<\overline{K}^0|K_L>}) + \Gamma_{42} \cdot (\Gamma_{<\overline{K}^0|K_S>} \cdot \Gamma_{K_S\to\pi^0\pi^0} \\
&\quad + \Gamma_{<\overline{K}^0|K_L>}) + \Gamma_{47} \cdot (\Gamma_{K_S\to\pi^0\pi^0} \cdot \Gamma_{K_S\to\pi^0\pi^0}) + \Gamma_{48} \cdot \Gamma_{K_S\to\pi^0\pi^0} \\
&\quad + \Gamma_{804} + \Gamma_{50} \cdot (\Gamma_{K_S\to\pi^0\pi^0} \cdot \Gamma_{K_S\to\pi^0\pi^0}) + \Gamma_{51} \cdot \Gamma_{K_S\to\pi^0\pi^0} \\
&\quad + \Gamma_{806} + \Gamma_{126} \cdot \Gamma_{\eta\to\text{neutral}} + \Gamma_{128} \cdot \Gamma_{\eta\to\text{neutral}} + \Gamma_{130} \cdot \Gamma_{\eta\to\text{neutral}} \\
&\quad + \Gamma_{132} \cdot (\Gamma_{\eta\to\text{neutral}} \cdot (\Gamma_{<\overline{K}^0|K_S>} \cdot \Gamma_{K_S\to\pi^0\pi^0} + \Gamma_{<\overline{K}^0|K_L>})) + \Gamma_{800} \cdot \Gamma_{\omega\to\pi^0\gamma} \\
&\quad + \Gamma_{151} \cdot \Gamma_{\omega\to\pi^0\gamma} + \Gamma_{152} \cdot \Gamma_{\omega\to\pi^0\gamma} + \Gamma_{167} \cdot (\Gamma_{\phi\to K_S K_L} \cdot \Gamma_{K_S\to\pi^0\pi^0})
\end{aligned}$$

$$\begin{aligned}
\Gamma_7 &= \Gamma_{35} \cdot \Gamma_{<\overline{K}^0|K_L>} + \Gamma_9 + \Gamma_{804} + \Gamma_{37} \cdot \Gamma_{<K^0|K_L>} \\
&\quad + \Gamma_{10}
\end{aligned}$$

$$\Gamma_8 = \Gamma_9 + \Gamma_{10}$$

$$\begin{aligned}
\Gamma_{11} &= \Gamma_{14} + \Gamma_{16} + \Gamma_{20} + \Gamma_{23} + \Gamma_{27} + \Gamma_{28} \\
&\quad + \Gamma_{30} + \Gamma_{35} \cdot (\Gamma_{<K^0|K_S>} \cdot \Gamma_{K_S\to\pi^0\pi^0}) + \Gamma_{37} \cdot (\Gamma_{<K^0|K_S>} \cdot \Gamma_{K_S\to\pi^0\pi^0}) \\
&\quad + \Gamma_{40} \cdot (\Gamma_{<K^0|K_S>} \cdot \Gamma_{K_S\to\pi^0\pi^0}) + \Gamma_{42} \cdot (\Gamma_{<K^0|K_S>} \cdot \Gamma_{K_S\to\pi^0\pi^0}) \\
&\quad + \Gamma_{47} \cdot (\Gamma_{K_S\to\pi^0\pi^0} \cdot \Gamma_{K_S\to\pi^0\pi^0}) + \Gamma_{50} \cdot (\Gamma_{K_S\to\pi^0\pi^0} \cdot \Gamma_{K_S\to\pi^0\pi^0}) \\
&\quad + \Gamma_{126} \cdot \Gamma_{\eta\to\text{neutral}} + \Gamma_{128} \cdot \Gamma_{\eta\to\text{neutral}} + \Gamma_{130} \cdot \Gamma_{\eta\to\text{neutral}} \\
&\quad + \Gamma_{132} \cdot (\Gamma_{<K^0|K_S>} \cdot \Gamma_{K_S\to\pi^0\pi^0} \cdot \Gamma_{\eta\to\text{neutral}}) + \Gamma_{151} \cdot \Gamma_{\omega\to\pi^0\gamma} \\
&\quad + \Gamma_{152} \cdot \Gamma_{\omega\to\pi^0\gamma} + \Gamma_{800} \cdot \Gamma_{\omega\to\pi^0\gamma}
\end{aligned}$$

$$\begin{aligned}
\Gamma_{12} &= \Gamma_{128} \cdot \Gamma_{\eta\to 3\pi^0} + \Gamma_{30} + \Gamma_{23} + \Gamma_{28} + \Gamma_{14} \\
&\quad + \Gamma_{16} + \Gamma_{20} + \Gamma_{27} + \Gamma_{126} \cdot \Gamma_{\eta\to 3\pi^0} + \Gamma_{130} \cdot \Gamma_{\eta\to 3\pi^0}
\end{aligned}$$

$$\Gamma_{13} = \Gamma_{14} + \Gamma_{16}$$

$$\begin{aligned}
\Gamma_{17} &= \Gamma_{128} \cdot \Gamma_{\eta\to 3\pi^0} + \Gamma_{30} + \Gamma_{23} + \Gamma_{28} + \Gamma_{35} \cdot (\Gamma_{<K^0|K_S>} \cdot \Gamma_{K_S\to\pi^0\pi^0}) \\
&\quad + \Gamma_{40} \cdot (\Gamma_{<K^0|K_S>} \cdot \Gamma_{K_S\to\pi^0\pi^0}) + \Gamma_{42} \cdot (\Gamma_{<K^0|K_S>} \cdot \Gamma_{K_S\to\pi^0\pi^0}) \\
&\quad + \Gamma_{20} + \Gamma_{27} + \Gamma_{47} \cdot (\Gamma_{K_S\to\pi^0\pi^0} \cdot \Gamma_{K_S\to\pi^0\pi^0}) + \Gamma_{50} \cdot (\Gamma_{K_S\to\pi^0\pi^0} \cdot \Gamma_{K_S\to\pi^0\pi^0}) \\
&\quad + \Gamma_{126} \cdot \Gamma_{\eta\to 3\pi^0} + \Gamma_{37} \cdot (\Gamma_{<K^0|K_S>} \cdot \Gamma_{K_S\to\pi^0\pi^0}) + \Gamma_{130} \cdot \Gamma_{\eta\to 3\pi^0}
\end{aligned}$$

$$\Gamma_{18} = \Gamma_{23} + \Gamma_{35} \cdot (\Gamma_{<K^0|K_S>} \cdot \Gamma_{K_S \to \pi^0\pi^0}) + \Gamma_{20} + \Gamma_{37} \cdot (\Gamma_{<K^0|K_S>} \cdot \Gamma_{K_S \to \pi^0\pi^0})$$

$$\Gamma_{19} = \Gamma_{23} + \Gamma_{20}$$

$$\begin{aligned}\Gamma_{24} = {} & \Gamma_{27} + \Gamma_{28} + \Gamma_{30} + \Gamma_{40} \cdot (\Gamma_{<K^0|K_S>} \cdot \Gamma_{K_S \to \pi^0\pi^0}) \\ & + \Gamma_{42} \cdot (\Gamma_{<K^0|K_S>} \cdot \Gamma_{K_S \to \pi^0\pi^0}) + \Gamma_{47} \cdot (\Gamma_{K_S \to \pi^0\pi^0} \cdot \Gamma_{K_S \to \pi^0\pi^0}) \\ & + \Gamma_{50} \cdot (\Gamma_{K_S \to \pi^0\pi^0} \cdot \Gamma_{K_S \to \pi^0\pi^0}) + \Gamma_{126} \cdot \Gamma_{\eta \to 3\pi^0} + \Gamma_{128} \cdot \Gamma_{\eta \to 3\pi^0} \\ & + \Gamma_{130} \cdot \Gamma_{\eta \to 3\pi^0} + \Gamma_{132} \cdot (\Gamma_{<K^0|K_S>} \cdot \Gamma_{K_S \to \pi^0\pi^0} \cdot \Gamma_{\eta \to 3\pi^0})\end{aligned}$$

$$\begin{aligned}\Gamma_{25} = {} & \Gamma_{128} \cdot \Gamma_{\eta \to 3\pi^0} + \Gamma_{30} + \Gamma_{28} + \Gamma_{27} + \Gamma_{126} \cdot \Gamma_{\eta \to 3\pi^0} \\ & + \Gamma_{130} \cdot \Gamma_{\eta \to 3\pi^0}\end{aligned}$$

$$\begin{aligned}\Gamma_{26} = {} & \Gamma_{128} \cdot \Gamma_{\eta \to 3\pi^0} + \Gamma_{28} + \Gamma_{40} \cdot (\Gamma_{<K^0|K_S>} \cdot \Gamma_{K_S \to \pi^0\pi^0}) \\ & + \Gamma_{42} \cdot (\Gamma_{<K^0|K_S>} \cdot \Gamma_{K_S \to \pi^0\pi^0}) + \Gamma_{27}\end{aligned}$$

$$\Gamma_{29} = \Gamma_{30} + \Gamma_{126} \cdot \Gamma_{\eta \to 3\pi^0} + \Gamma_{130} \cdot \Gamma_{\eta \to 3\pi^0}$$

$$\begin{aligned}\Gamma_{31} = {} & \Gamma_{128} \cdot \Gamma_{\eta \to \text{neutral}} + \Gamma_{23} + \Gamma_{28} + \Gamma_{42} + \Gamma_{16} \\ & + \Gamma_{37} + \Gamma_{10} + \Gamma_{167} \cdot (\Gamma_{\phi \to K_S K_L} \cdot \Gamma_{K_S \to \pi^0\pi^0})\end{aligned}$$

$$\begin{aligned}\Gamma_{32} = {} & \Gamma_{16} + \Gamma_{23} + \Gamma_{28} + \Gamma_{37} + \Gamma_{42} + \Gamma_{128} \cdot \Gamma_{\eta \to \text{neutral}} \\ & + \Gamma_{130} \cdot \Gamma_{\eta \to \text{neutral}} + \Gamma_{167} \cdot (\Gamma_{\phi \to K_S K_L} \cdot \Gamma_{K_S \to \pi^0\pi^0})\end{aligned}$$

$$\begin{aligned}\Gamma_{33} = {} & \Gamma_{35} \cdot \Gamma_{<\overline{K}^0|K_S>} + \Gamma_{40} \cdot \Gamma_{<\overline{K}^0|K_S>} + \Gamma_{42} \cdot \Gamma_{<K^0|K_S>} \\ & + \Gamma_{47} + \Gamma_{48} + \Gamma_{50} + \Gamma_{51} + \Gamma_{37} \cdot \Gamma_{<K^0|K_S>} \\ & + \Gamma_{132} \cdot (\Gamma_{<\overline{K}^0|K_S>} \cdot \Gamma_{\eta \to \text{neutral}}) + \Gamma_{44} \cdot \Gamma_{<\overline{K}^0|K_S>} + \Gamma_{167} \cdot \Gamma_{\phi \to K_S K_L}\end{aligned}$$

$$\Gamma_{34} = \Gamma_{35} + \Gamma_{37}$$

$$\Gamma_{38} = \Gamma_{42} + \Gamma_{37}$$

$$\Gamma_{39} = \Gamma_{40} + \Gamma_{42}$$

$$\Gamma_{43} = \Gamma_{40} + \Gamma_{44}$$

$$\Gamma_{46} = \Gamma_{48} + \Gamma_{47} + \Gamma_{804}$$

$$\Gamma_{49} = \Gamma_{50} + \Gamma_{51} + \Gamma_{806}$$

$$\begin{aligned}\Gamma_{54} = {} & \Gamma_{35} \cdot (\Gamma_{<K^0|K_S>} \cdot \Gamma_{K_S \to \pi^+\pi^-}) + \Gamma_{37} \cdot (\Gamma_{<K^0|K_S>} \cdot \Gamma_{K_S \to \pi^+\pi^-}) \\ & + \Gamma_{40} \cdot (\Gamma_{<K^0|K_S>} \cdot \Gamma_{K_S \to \pi^+\pi^-}) + \Gamma_{42} \cdot (\Gamma_{<K^0|K_S>} \cdot \Gamma_{K_S \to \pi^+\pi^-}) \\ & + \Gamma_{47} \cdot (2 \cdot \Gamma_{K_S \to \pi^+\pi^-} \cdot \Gamma_{K_S \to \pi^0\pi^0}) + \Gamma_{48} \cdot \Gamma_{K_S \to \pi^+\pi^-} \\ & + \Gamma_{50} \cdot (2 \cdot \Gamma_{K_S \to \pi^+\pi^-} \cdot \Gamma_{K_S \to \pi^0\pi^0}) + \Gamma_{51} \cdot \Gamma_{K_S \to \pi^+\pi^-} \\ & + \Gamma_{53} \cdot (\Gamma_{<\overline{K}^0|K_S>} \cdot \Gamma_{K_S \to \pi^0\pi^0} + \Gamma_{<\overline{K}^0|K_L>}) + \Gamma_{62} + \Gamma_{70} \\ & + \Gamma_{77} + \Gamma_{78} + \Gamma_{93} + \Gamma_{94} + \Gamma_{126} \cdot \Gamma_{\eta \to \text{charged}} \\ & + \Gamma_{128} \cdot \Gamma_{\eta \to \text{charged}} + \Gamma_{130} \cdot \Gamma_{\eta \to \text{charged}} + \Gamma_{132} \cdot (\Gamma_{<\overline{K}^0|K_L>} \cdot \Gamma_{\eta \to \pi^+\pi^-\pi^0} \\ & + \Gamma_{<\overline{K}^0|K_S>} \cdot \Gamma_{K_S \to \pi^0\pi^0} \cdot \Gamma_{\eta \to \pi^+\pi^-\pi^0} + \Gamma_{<\overline{K}^0|K_S>} \cdot \Gamma_{K_S \to \pi^+\pi^-} \cdot \Gamma_{\eta \to 3\pi^0}) \\ & + \Gamma_{151} \cdot (\Gamma_{\omega \to \pi^+\pi^-\pi^0} + \Gamma_{\omega \to \pi^+\pi^-}) + \Gamma_{152} \cdot (\Gamma_{\omega \to \pi^+\pi^-\pi^0} + \Gamma_{\omega \to \pi^+\pi^-}) \\ & + \Gamma_{167} \cdot (\Gamma_{\phi \to K^+K^-} + \Gamma_{\phi \to K_S K_L} \cdot \Gamma_{K_S \to \pi^+\pi^-}) + \Gamma_{802} + \Gamma_{803} \\ & + \Gamma_{800} \cdot (\Gamma_{\omega \to \pi^+\pi^-\pi^0} + \Gamma_{\omega \to \pi^+\pi^-})\end{aligned}$$

$$\Gamma_{55} = \Gamma_{128} \cdot \Gamma_{\eta\to\text{charged}} + \Gamma_{152} \cdot (\Gamma_{\omega\to\pi^+\pi^-\pi^0} + \Gamma_{\omega\to\pi^+\pi^-}) + \Gamma_{78}$$
$$+ \Gamma_{77} + \Gamma_{94} + \Gamma_{62} + \Gamma_{70} + \Gamma_{93} + \Gamma_{126} \cdot \Gamma_{\eta\to\text{charged}}$$
$$+ \Gamma_{802} + \Gamma_{803} + \Gamma_{800} \cdot (\Gamma_{\omega\to\pi^+\pi^-\pi^0} + \Gamma_{\omega\to\pi^+\pi^-}) + \Gamma_{151} \cdot (\Gamma_{\omega\to\pi^+\pi^-\pi^0}$$
$$+ \Gamma_{\omega\to\pi^+\pi^-}) + \Gamma_{130} \cdot \Gamma_{\eta\to\text{charged}} + \Gamma_{168}$$

$$\Gamma_{56} = \Gamma_{35} \cdot (\Gamma_{<K^0|K_S>} \cdot \Gamma_{K_S\to\pi^+\pi^-}) + \Gamma_{62} + \Gamma_{93} + \Gamma_{37} \cdot (\Gamma_{<K^0|K_S>} \cdot \Gamma_{K_S\to\pi^+\pi^-})$$
$$+ \Gamma_{802} + \Gamma_{800} \cdot \Gamma_{\omega\to\pi^+\pi^-} + \Gamma_{151} \cdot \Gamma_{\omega\to\pi^+\pi^-} + \Gamma_{168}$$

$$\Gamma_{57} = \Gamma_{62} + \Gamma_{93} + \Gamma_{802} + \Gamma_{800} \cdot \Gamma_{\omega\to\pi^+\pi^-} + \Gamma_{151} \cdot \Gamma_{\omega\to\pi^+\pi^-}$$
$$+ \Gamma_{167} \cdot \Gamma_{\phi\to K^+K^-}$$

$$\Gamma_{58} = \Gamma_{62} + \Gamma_{93} + \Gamma_{802} + \Gamma_{167} \cdot \Gamma_{\phi\to K^+K^-}$$

$$\Gamma_{59} = \Gamma_{35} \cdot (\Gamma_{<K^0|K_S>} \cdot \Gamma_{K_S\to\pi^+\pi^-}) + \Gamma_{62} + \Gamma_{800} \cdot \Gamma_{\omega\to\pi^+\pi^-}$$

$$\Gamma_{60} = \Gamma_{62} + \Gamma_{800} \cdot \Gamma_{\omega\to\pi^+\pi^-}$$

$$\Gamma_{63} = \Gamma_{40} \cdot (\Gamma_{<K^0|K_S>} \cdot \Gamma_{K_S\to\pi^+\pi^-}) + \Gamma_{42} \cdot (\Gamma_{<K^0|K_S>} \cdot \Gamma_{K_S\to\pi^+\pi^-})$$
$$+ \Gamma_{47} \cdot (2 \cdot \Gamma_{K_S\to\pi^+\pi^-} \cdot \Gamma_{K_S\to\pi^0\pi^0}) + \Gamma_{50} \cdot (2 \cdot \Gamma_{K_S\to\pi^+\pi^-} \cdot \Gamma_{K_S\to\pi^0\pi^0})$$
$$+ \Gamma_{70} + \Gamma_{77} + \Gamma_{78} + \Gamma_{94} + \Gamma_{126} \cdot \Gamma_{\eta\to\text{charged}}$$
$$+ \Gamma_{128} \cdot \Gamma_{\eta\to\text{charged}} + \Gamma_{130} \cdot \Gamma_{\eta\to\text{charged}} + \Gamma_{132} \cdot (\Gamma_{<\overline{K}^0|K_S>} \cdot \Gamma_{K_S\to\pi^+\pi^-} \cdot \Gamma_{\eta\to\text{neutral}}$$
$$+ \Gamma_{<\overline{K}^0|K_S>} \cdot \Gamma_{K_S\to\pi^0\pi^0} \cdot \Gamma_{\eta\to\text{charged}}) + \Gamma_{151} \cdot \Gamma_{\omega\to\pi^+\pi^-\pi^0} + \Gamma_{152} \cdot (\Gamma_{\omega\to\pi^+\pi^-\pi^0}$$
$$+ \Gamma_{\omega\to\pi^+\pi^-}) + \Gamma_{800} \cdot \Gamma_{\omega\to\pi^+\pi^-\pi^0} + \Gamma_{803}$$

$$\Gamma_{64} = \Gamma_{78} + \Gamma_{77} + \Gamma_{94} + \Gamma_{70} + \Gamma_{126} \cdot \Gamma_{\eta\to\pi^+\pi^-\pi^0}$$
$$+ \Gamma_{128} \cdot \Gamma_{\eta\to\pi^+\pi^-\pi^0} + \Gamma_{130} \cdot \Gamma_{\eta\to\pi^+\pi^-\pi^0} + \Gamma_{800} \cdot \Gamma_{\omega\to\pi^+\pi^-\pi^0}$$
$$+ \Gamma_{151} \cdot \Gamma_{\omega\to\pi^+\pi^-\pi^0} + \Gamma_{152} \cdot (\Gamma_{\omega\to\pi^+\pi^-\pi^0} + \Gamma_{\omega\to\pi^+\pi^-}) + \Gamma_{803}$$

$$\Gamma_{65} = \Gamma_{40} \cdot (\Gamma_{<K^0|K_S>} \cdot \Gamma_{K_S\to\pi^+\pi^-}) + \Gamma_{42} \cdot (\Gamma_{<K^0|K_S>} \cdot \Gamma_{K_S\to\pi^+\pi^-})$$
$$+ \Gamma_{70} + \Gamma_{94} + \Gamma_{128} \cdot \Gamma_{\eta\to\pi^+\pi^-\pi^0} + \Gamma_{151} \cdot \Gamma_{\omega\to\pi^+\pi^-\pi^0}$$
$$+ \Gamma_{152} \cdot \Gamma_{\omega\to\pi^+\pi^-} + \Gamma_{800} \cdot \Gamma_{\omega\to\pi^+\pi^-\pi^0} + \Gamma_{803}$$

$$\Gamma_{66} = \Gamma_{70} + \Gamma_{94} + \Gamma_{128} \cdot \Gamma_{\eta\to\pi^+\pi^-\pi^0} + \Gamma_{151} \cdot \Gamma_{\omega\to\pi^+\pi^-\pi^0}$$
$$+ \Gamma_{152} \cdot \Gamma_{\omega\to\pi^+\pi^-} + \Gamma_{800} \cdot \Gamma_{\omega\to\pi^+\pi^-\pi^0} + \Gamma_{803}$$

$$\Gamma_{67} = \Gamma_{70} + \Gamma_{94} + \Gamma_{128} \cdot \Gamma_{\eta\to\pi^+\pi^-\pi^0} + \Gamma_{803}$$

$$\Gamma_{68} = \Gamma_{40} \cdot (\Gamma_{<K^0|K_S>} \cdot \Gamma_{K_S\to\pi^+\pi^-}) + \Gamma_{70} + \Gamma_{152} \cdot \Gamma_{\omega\to\pi^+\pi^-}$$
$$+ \Gamma_{800} \cdot \Gamma_{\omega\to\pi^+\pi^-\pi^0}$$

$$\Gamma_{69} = \Gamma_{152} \cdot \Gamma_{\omega\to\pi^+\pi^-} + \Gamma_{70} + \Gamma_{800} \cdot \Gamma_{\omega\to\pi^+\pi^-\pi^0}$$

$$\Gamma_{74} = \Gamma_{152} \cdot \Gamma_{\omega\to\pi^+\pi^-\pi^0} + \Gamma_{78} + \Gamma_{77} + \Gamma_{126} \cdot \Gamma_{\eta\to\pi^+\pi^-\pi^0}$$
$$+ \Gamma_{130} \cdot \Gamma_{\eta\to\pi^+\pi^-\pi^0}$$

$$\Gamma_{75} = \Gamma_{152} \cdot \Gamma_{\omega\to\pi^+\pi^-\pi^0} + \Gamma_{47} \cdot (2 \cdot \Gamma_{K_S\to\pi^+\pi^-} \cdot \Gamma_{K_S\to\pi^0\pi^0})$$
$$+ \Gamma_{77} + \Gamma_{126} \cdot \Gamma_{\eta\to\pi^+\pi^-\pi^0} + \Gamma_{130} \cdot \Gamma_{\eta\to\pi^+\pi^-\pi^0}$$

$$\Gamma_{76} = \Gamma_{152} \cdot \Gamma_{\omega\to\pi^+\pi^-\pi^0} + \Gamma_{77} + \Gamma_{126} \cdot \Gamma_{\eta\to\pi^+\pi^-\pi^0} + \Gamma_{130} \cdot \Gamma_{\eta\to\pi^+\pi^-\pi^0}$$

$$\Gamma_{78} = \Gamma_{810} + \Gamma_{50} \cdot (2 \cdot \Gamma_{K_S\to\pi^+\pi^-} \cdot \Gamma_{K_S\to\pi^0\pi^0}) + \Gamma_{132} \cdot (\Gamma_{<\overline{K}^0|K_S>} \cdot \Gamma_{K_S\to\pi^+\pi^-} \cdot \Gamma_{\eta\to 3\pi^0})$$

$$\begin{aligned}\Gamma_{79} = {} & \Gamma_{37} \cdot (\Gamma_{<K^0|K_S>} \cdot \Gamma_{K_S\to\pi^+\pi^-}) + \Gamma_{42} \cdot (\Gamma_{<K^0|K_S>} \cdot \Gamma_{K_S\to\pi^+\pi^-}) \\ & + \Gamma_{93} + \Gamma_{94} + \Gamma_{128} \cdot \Gamma_{\eta\to\text{charged}} + \Gamma_{151} \cdot (\Gamma_{\omega\to\pi^+\pi^-\pi^0} \\ & + \Gamma_{\omega\to\pi^+\pi^-}) + \Gamma_{168} + \Gamma_{802} + \Gamma_{803}\end{aligned}$$

$$\Gamma_{80} = \Gamma_{93} + \Gamma_{802} + \Gamma_{151} \cdot \Gamma_{\omega\to\pi^+\pi^-}$$

$$\Gamma_{81} = \Gamma_{128} \cdot \Gamma_{\eta\to\pi^+\pi^-\pi^0} + \Gamma_{94} + \Gamma_{803} + \Gamma_{151} \cdot \Gamma_{\omega\to\pi^+\pi^-\pi^0}$$

$$\begin{aligned}\Gamma_{82} = {} & \Gamma_{128} \cdot \Gamma_{\eta\to\text{charged}} + \Gamma_{42} \cdot (\Gamma_{<K^0|K_S>} \cdot \Gamma_{K_S\to\pi^+\pi^-}) + \Gamma_{802} \\ & + \Gamma_{803} + \Gamma_{151} \cdot (\Gamma_{\omega\to\pi^+\pi^-\pi^0} + \Gamma_{\omega\to\pi^+\pi^-}) + \Gamma_{37} \cdot (\Gamma_{<K^0|K_S>} \cdot \Gamma_{K_S\to\pi^+\pi^-})\end{aligned}$$

$$\begin{aligned}\Gamma_{83} = {} & \Gamma_{128} \cdot \Gamma_{\eta\to\pi^+\pi^-\pi^0} + \Gamma_{802} + \Gamma_{803} + \Gamma_{151} \cdot (\Gamma_{\omega\to\pi^+\pi^-\pi^0} \\ & + \Gamma_{\omega\to\pi^+\pi^-})\end{aligned}$$

$$\Gamma_{84} = \Gamma_{802} + \Gamma_{151} \cdot \Gamma_{\omega\to\pi^+\pi^-} + \Gamma_{37} \cdot (\Gamma_{<K^0|K_S>} \cdot \Gamma_{K_S\to\pi^+\pi^-})$$

$$\Gamma_{85} = \Gamma_{802} + \Gamma_{151} \cdot \Gamma_{\omega\to\pi^+\pi^-}$$

$$\begin{aligned}\Gamma_{87} = {} & \Gamma_{42} \cdot (\Gamma_{<K^0|K_S>} \cdot \Gamma_{K_S\to\pi^+\pi^-}) + \Gamma_{128} \cdot \Gamma_{\eta\to\pi^+\pi^-\pi^0} + \Gamma_{151} \cdot \Gamma_{\omega\to\pi^+\pi^-\pi^0} \\ & + \Gamma_{803}\end{aligned}$$

$$\Gamma_{88} = \Gamma_{128} \cdot \Gamma_{\eta\to\pi^+\pi^-\pi^0} + \Gamma_{803} + \Gamma_{151} \cdot \Gamma_{\omega\to\pi^+\pi^-\pi^0}$$

$$\Gamma_{89} = \Gamma_{803} + \Gamma_{151} \cdot \Gamma_{\omega\to\pi^+\pi^-\pi^0}$$

$$\Gamma_{92} = \Gamma_{94} + \Gamma_{93}$$

$$\Gamma_{96} = \Gamma_{167} \cdot \Gamma_{\phi\to K^+K^-}$$

$$\Gamma_{102} = \Gamma_{103} + \Gamma_{104}$$

$$\Gamma_{103} = \Gamma_{820} + \Gamma_{822} + \Gamma_{831} \cdot \Gamma_{\omega\to\pi^+\pi^-}$$

$$\Gamma_{104} = \Gamma_{830} + \Gamma_{833}$$

$$\begin{aligned}\Gamma_{106} = {} & \Gamma_{30} + \Gamma_{44} \cdot \Gamma_{<\overline{K}^0|K_S>} + \Gamma_{47} + \Gamma_{53} \cdot \Gamma_{<K^0|K_S>} \\ & + \Gamma_{77} + \Gamma_{103} + \Gamma_{126} \cdot (\Gamma_{\eta\to 3\pi^0} + \Gamma_{\eta\to\pi^+\pi^-\pi^0}) + \Gamma_{152} \cdot \Gamma_{\omega\to\pi^+\pi^-\pi^0}\end{aligned}$$

$$\begin{aligned}\Gamma_{110} = {} & \Gamma_{10} + \Gamma_{16} + \Gamma_{23} + \Gamma_{28} + \Gamma_{35} + \Gamma_{40} \\ & + \Gamma_{128} + \Gamma_{802} + \Gamma_{803} + \Gamma_{151} + \Gamma_{130} + \Gamma_{132} \\ & + \Gamma_{44} + \Gamma_{53} + \Gamma_{168} + \Gamma_{169} + \Gamma_{822} + \Gamma_{833}\end{aligned}$$

$$\Gamma_{149} = \Gamma_{152} + \Gamma_{800} + \Gamma_{151}$$

$$\Gamma_{150} = \Gamma_{800} + \Gamma_{151}$$

$$\Gamma_{168} = \Gamma_{167} \cdot \Gamma_{\phi\to K^+K^-}$$

$$\Gamma_{169} = \Gamma_{167} \cdot \Gamma_{\phi\to K_S K_L}$$

$$\Gamma_{804} = \Gamma_{47} \cdot ((\Gamma_{<K^0|K_L>} \cdot \Gamma_{<\overline{K}^0|K_L>})/(\Gamma_{<K^0|K_S>} \cdot \Gamma_{<\overline{K}^0|K_S>}))$$

$$\Gamma_{806} = \Gamma_{50} \cdot ((\Gamma_{<K^0|K_L>} \cdot \Gamma_{<\overline{K}^0|K_L>})/(\Gamma_{<K^0|K_S>} \cdot \Gamma_{<\overline{K}^0|K_S>}))$$

$$\Gamma_{810} = \Gamma_{910} + \Gamma_{911} + \Gamma_{811} \cdot \Gamma_{\omega\to\pi^+\pi^-\pi^0} + \Gamma_{812}$$

$$\Gamma_{820} = \Gamma_{920} + \Gamma_{821}$$

$$\Gamma_{830} = \Gamma_{930} + \Gamma_{831} \cdot \Gamma_{\omega\to\pi^+\pi^-\pi^0} + \Gamma_{832}$$

$$\Gamma_{910} = \Gamma_{136} \cdot \Gamma_{\eta\to 3\pi^0}$$

$$\Gamma_{911} = \Gamma_{945} \cdot \Gamma_{\eta\to\pi^+\pi^-\pi^0}$$

$$\Gamma_{930} = \Gamma_{136} \cdot \Gamma_{\eta\to\pi^+\pi^-\pi^0}$$

$$\Gamma_{944} = \Gamma_{136} \cdot \Gamma_{\eta\to\gamma\gamma}$$

$$\begin{aligned}
\Gamma_{\rm All} = {} & \Gamma_3 + \Gamma_5 + \Gamma_9 + \Gamma_{10} + \Gamma_{14} + \Gamma_{16} \\
& + \Gamma_{20} + \Gamma_{23} + \Gamma_{27} + \Gamma_{28} + \Gamma_{30} + \Gamma_{35} \\
& + \Gamma_{37} + \Gamma_{40} + \Gamma_{42} + \Gamma_{47} \cdot (1 + ((\Gamma_{<K^0|K_L>} \cdot \Gamma_{<\overline{K}^0|K_L>})/(\Gamma_{<K^0|K_S>} \cdot \Gamma_{<\overline{K}^0|K_S>}))) \\
& + \Gamma_{48} + \Gamma_{62} + \Gamma_{70} + \Gamma_{77} + \Gamma_{811} + \Gamma_{812} \\
& + \Gamma_{93} + \Gamma_{94} + \Gamma_{832} + \Gamma_{833} + \Gamma_{126} + \Gamma_{128} \\
& + \Gamma_{802} + \Gamma_{803} + \Gamma_{800} + \Gamma_{151} + \Gamma_{130} + \Gamma_{132} \\
& + \Gamma_{44} + \Gamma_{53} + \Gamma_{50} \cdot (1 + ((\Gamma_{<K^0|K_L>} \cdot \Gamma_{<\overline{K}^0|K_L>})/(\Gamma_{<K^0|K_S>} \cdot \Gamma_{<\overline{K}^0|K_S>}))) \\
& + \Gamma_{51} + \Gamma_{167} \cdot (\Gamma_{\phi\to K^+K^-} + \Gamma_{\phi\to K_S K_L}) + \Gamma_{152} + \Gamma_{920} \\
& + \Gamma_{821} + \Gamma_{822} + \Gamma_{831} + \Gamma_{136} + \Gamma_{945} + \Gamma_{805}
\end{aligned}$$

9.2 Tests of lepton universality

Lepton universality tests probe the Standard Model prediction that the charged weak current interaction has the same coupling for all lepton generations. The precision of such tests has been significantly improved since the 2014 edition by the addition of the Belle τ lifetime measurement [1175], while improvements from the τ branching fraction fit are negligible. We compute the universality tests as in the previous report by using ratios of the partial widths of a heavier lepton λ decaying to a lighter lepton ρ [1176],

$$\Gamma(\lambda \to \nu_\lambda \rho \overline{\nu}_\rho(\gamma)) = \frac{B(\lambda \to \nu_\lambda \rho \overline{\nu}_\rho)}{\tau_\lambda} = \frac{G_\lambda G_\rho m_\lambda^5}{192\pi^3} f\left(\frac{m_\rho^2}{m_\lambda^2}\right) R_W^\lambda R_\gamma^\lambda \ ,$$

where

$$G_\rho = \frac{g_\rho^2}{4\sqrt{2}M_W^2} \ , \qquad f(x) = 1 - 8x + 8x^3 - x^4 - 12x^2 \ln x \ ,$$

$$R_W^\lambda = 1 + \frac{3}{5}\frac{m_\lambda^2}{M_W^2} \ , \qquad R_\gamma^\lambda = 1 + \frac{\alpha(m_\lambda)}{2\pi}\left(\frac{25}{4} - \pi^2\right) \ .$$

We use $R_\gamma^\tau = 1 - 43.2 \cdot 10^{-4}$ and $R_\gamma^\mu = 1 - 42.4 \cdot 10^{-4}$ [1176] and M_W from PDG 2015 [314]. We use HFAG 2014 averages and PDG 2015 for the other quantities. Using pure leptonic processes we obtain

$$\left(\frac{g_\tau}{g_\mu}\right) = 1.0010 \pm 0.0015 \ , \qquad \left(\frac{g_\tau}{g_e}\right) = 1.0029 \pm 0.0015 \ , \qquad \left(\frac{g_\mu}{g_e}\right) = 1.0019 \pm 0.0014 \ .$$

Using the expressions for the τ semi-hadronic partial widths [1177] we obtain

$$\left(\frac{g_\tau}{g_\mu}\right)^2 = \frac{B(\tau \to h\nu_\tau)}{B(h \to \mu\overline{\nu}_\mu)} \frac{2m_h m_\mu^2 \tau_h}{(1+\delta R_{\tau/h}) m_\tau^3 \tau_\tau} \left(\frac{1 - m_\mu^2/m_h^2}{1 - m_h^2/m_\tau^2}\right)^2 \ ,$$

where $h = \pi$ or K and the radiative corrections are $\delta R_{\tau/\pi} = (0.16 \pm 0.12)\%$ and $\delta R_{\tau/K} = (0.90 \pm 0.22)\%$ [1177], we measure:

$$\left(\frac{g_\tau}{g_\mu}\right)_\pi = 0.9961 \pm 0.0027 \ , \qquad \left(\frac{g_\tau}{g_\mu}\right)_K = 0.9860 \pm 0.0070 \ .$$

Similar tests could be performed with decays to electrons, however they are less precise because the hadron two body decays to electrons are helicity-suppressed. Averaging the three g_τ/g_μ ratios we obtain

$$\left(\frac{g_\tau}{g_\mu}\right)_{\tau+\pi+K} = 1.0000 \pm 0.0014 \ ,$$

accounting for statistical correlations. Table 279 reports the statistical correlation coefficients for the fitted coupling ratios:

Table 279: Universality coupling ratios correlation coefficients (%).

	$\left(\frac{g_\tau}{g_\mu}\right)$	$\left(\frac{g_\tau}{g_e}\right)$	$\left(\frac{g_\mu}{g_e}\right)$	$\left(\frac{g_\tau}{g_\mu}\right)_\pi$
$\left(\frac{g_\tau}{g_e}\right)$	53			
$\left(\frac{g_\mu}{g_e}\right)$	-49	48		
$\left(\frac{g_\tau}{g_\mu}\right)_\pi$	24	26	2	
$\left(\frac{g_\tau}{g_\mu}\right)_K$	11	10	-1	6

Since there is 100% correlation between g_τ/g_e, g_μ/g_e and g_μ/g_e, the correlation matrix is expected to be positive semi-definite, with one eigenvalue equal to zero. Due to numerical inaccuracies, one eigenvalue is expected to be close to zero rather than exactly zero.

9.3 Universality improved $B(\tau \to e\nu\overline{\nu})$ and $R_{\rm had}$

We compute two quantities that are used in this report and have been traditionally used for further elaborations and tests involving the τ branching fractions:

- the "universality improved" experimental determination of $B_e = B(\tau \to e\nu\overline{\nu})$, which relies on the assumption that the Standard Model and lepton universality hold;

- the ratio $R_{\rm had}$ between the total branching fraction of the τ to hadrons and the universality improved B_e, which is the same as the ratio of the two respective partial widths.

Following Ref. [1178], we obtain a more precise experimental determination of B_e using the τ branching fraction to $\mu\nu\overline{\nu}$, B_μ, and the τ lifetime. We average:

- the B_e fit value Γ_5,
- the B_e determination from the $B_\mu = B(\tau \to \mu\nu\overline{\nu})$ fit value Γ_3 assuming that $g_\mu/g_e = 1$ hence (see also Section 9.2) $B_e = B_\mu \cdot f(m_e^2/m_\tau^2)/f(m_\mu^2/m_\tau^2)$,
- the B_e determination from the τ lifetime assuming that $g_\tau/g_\mu = 1$ hence $B_e = B(\mu \to e\overline{\nu}_e\nu_\mu)\cdot(\tau_\tau/\tau_\mu)\cdot(m_\tau/m_\mu)^5\cdot f(m_e^2/m_\tau^2)/f(m_e^2/m_\mu^2)\cdot(\delta_\gamma^\tau\delta_W^\tau)/(\delta_\gamma^\mu\delta_W^\mu)$ where $B(\mu \to e\overline{\nu}_e\nu_\mu) = 1$.

Accounting for statistical correlations, we obtain

$$B_e^{\rm uni} = (17.815 \pm 0.023)\%.$$

We use $B_e^{\rm uni}$ to obtain the ratio

$$R_{\rm had} = \frac{\Gamma(\tau \to \text{hadrons})}{\Gamma(\tau \to e\nu\overline{\nu})} = \frac{\Gamma_{\rm hadrons}}{B_e^{\rm uni}} = 3.6349 \pm 0.0082,$$

where $\Gamma(\tau \to \text{hadrons})$ and $\Gamma(\tau \to e\nu\overline{\nu})$ indicate the partial widths and $\Gamma_{\rm hadrons}$ is the total branching fraction of the τ to hadrons, or the total branching fraction in any measured final state minus the leptonic branching fractions, *i.e.* with our notation $\Gamma_{\rm hadrons} = \Gamma_{\rm All} - \Gamma_3 - \Gamma_5 = (64.76 \pm 0.10)\%$ (see Section 9.1 and Table 268 for the definitions of $\Gamma_{\rm All}$, Γ_3, Γ_5). We underline that this report's definition of $\Gamma_{\rm hadrons}$ corresponds to summing all τ hadronic decay modes, like in the previous report, rather than – as done elsewhere – subtracting the leptonic branching fractions from unity, *i.e.* $\Gamma_{\rm hadrons} = 1 - \Gamma_3 - \Gamma_5$.

9.4 $|V_{us}|$ measurement

The CKM matrix element $|V_{us}|$ is most precisely determined from kaon decays [1179] (see also Figure 192), and its precision is limited by the uncertainties of the lattice QCD estimates of $f_+^{K\pi}(0)$ and f_K/f_π. Using the τ branching fractions, it is possible to determine $|V_{us}|$ in an alternative way [1180] that does not depend on lattice QCD and has small theory uncertainties (as discussed in Section 9.4.1). Moreover, $|V_{us}|$ can be determined using the τ branching fractions similarly to the kaon case, using the same lattice QCD estimates, in order to check the overall experimental consistency.

In the following Sections 9.4.1, 9.4.2 and 9.4.3 we update the CKM coefficient $|V_{us}|$ determinations that were shown in the previous report using the 2015 determination of $|V_{ud}|$ [1181] and the updated averages from HFAG 2016 and PDG 2015 for the other quantities.

9.4.1 $|V_{us}|$ from $B(\tau \to X_s\nu)$

The τ hadronic partial width is the sum of the τ partial widths to strange and to non-strange hadronic final states, $\Gamma_{\rm had} = \Gamma_s + \Gamma_{\rm VA}$. The suffix "VA" traditionally denotes the sum of the τ partial widths to non-strange final states, which proceed through either vector or axial-vector currents.

Dividing any partial width Γ_x by the electronic partial width, Γ_e, we obtain partial width ratios R_x (which are equal to the respective branching fraction ratios B_x/B_e) for which $R_{\rm had} = R_s + R_{\rm VA}$. In terms of such ratios, $|V_{us}|$ is measured as [1180]

$$|V_{us}|_{\tau s} = \sqrt{R_s / \left[\frac{R_{\rm VA}}{|V_{ud}|^2} - \delta R_{\rm theory} \right]} \ ,$$

where $\delta R_{\rm theory}$ can be determined in the context of low energy QCD theory, partly relying on experimental low energy scattering data. The literature reports several calculations [1180,1182, 1183]. In this report we use Ref. [1180], whose estimated uncertainty size is in between the two other ones. We use the information in that paper and the PDG 2015 value for the s-quark mass $m_s = 95.00 \pm 5.00\,{\rm MeV}$ [314] to calculate $\delta R_{\rm theory} = 0.242 \pm 0.032$.

We proceed following the same procedure of the 2012 HFAG report [222], using the universality improved $B_e^{\rm uni} = (17.815 \pm 0.023)\%$ (see Section 9.3) to compute the R_x ratios, and using the sum of the τ branching fractions to strange and non-strange hadronic final states to compute R_s and $R_{\rm VA}$, respectively.

Using the τ branching fraction fit results with their uncertainties and correlations (Section 9.1), we compute $B_s = (2.909 \pm 0.048)\%$ (see also Table 280) and $B_{\rm VA} = B_{\rm hadrons} - B_s = (61.85 \pm 0.10)\%$, where $B_{\rm hadrons}$ is equal to $\Gamma_{\rm hadrons}$ defined in section 9.3. PDG 2015 averages are used for non-τ quantities, including $|V_{ud}| = 0.97417 \pm 0.00021$, which comes from Ref. [1184] like for the previous HFAG report.

We obtain $|V_{us}|_{\tau s} = 0.2186 \pm 0.0021$, which is 3.1σ lower than the unitarity CKM prediction $|V_{us}|_{\rm uni} = 0.22582 \pm 0.00091$, from $(|V_{us}|_{\rm uni})^2 = 1 - |V_{ud}|^2$ [5]. The $|V_{us}|_{\tau s}$ uncertainty includes a systematic error contribution of 0.47% from the theory uncertainty on $\delta R_{\rm theory}$. There is no significant change with respect to the previous HFAG report.

9.4.2 $|V_{us}|$ from $B(\tau \to K\nu)/B(\tau \to \pi\nu)$

We follow the same procedure of the HFAG 2012 report to compute $|V_{us}|$ from the ratio of branching fractions $B(\tau \to K^-\nu_\tau)/B(\tau \to \pi^-\nu_\tau) = (6.438 \pm 0.094) \cdot 10^{-2}$ from the equation

$$\frac{B(\tau \to K^-\nu_\tau)}{B(\tau \to \pi^-\nu_\tau)} = \frac{f_K^2 |V_{us}|^2}{f_\pi^2 |V_{ud}|^2} \frac{\left(1 - m_K^2/m_\tau^2\right)^2}{\left(1 - m_\pi^2/m_\tau^2\right)^2} R_{\tau K/\tau\pi}$$

We use $f_K/f_\pi = 1.1930 \pm 0.0030$ from the FLAG 2016 Lattice averages with $N_f = 2{+}1{+}1$ [210].

The ratio of radiative corrections $R_{\tau K/\tau\pi}$ is estimated as

$$R_{\tau K/\tau\pi} = \frac{R(\tau^- \to K^-\nu / K^- \to \mu^-\nu)}{R(\tau^- \to \pi^-\nu / \pi^- \to \mu^-\nu)} \cdot R(K^- \to \mu^-\nu \,/\, \pi^- \to \mu^-\nu) \ ,$$

where

$$\frac{R(\tau^- \to K^-\nu / K^- \to \mu^-\nu)}{R(\tau^- \to \pi^-\nu / \pi^- \to \mu^-\nu)} = \frac{1 + (0.90 \pm 0.22)\%}{1 + (0.16 \pm 0.12)\%} \quad [1185]$$

and

$$R(K^- \to \mu^-\nu \,/\, \pi^- \to \mu^-\nu) = 0.9930 \pm 0.0035 \quad [1186, 1187].$$

We compute $|V_{us}|_{\tau K/\pi} = 0.2231 \pm 0.0018$, 1.3σ below the CKM unitarity prediction.

Table 280: HFAG Summer 2016 τ branching fractions to strange final states.

Branching fraction	**HFAG Summer 2016 fit (%)**
$K^-\nu_\tau$	0.6960 ± 0.0096
$K^-\pi^0\nu_\tau$	0.4327 ± 0.0149
$K^-2\pi^0\nu_\tau$ (ex. K^0)	0.0640 ± 0.0220
$K^-3\pi^0\nu_\tau$ (ex. K^0, η)	0.0428 ± 0.0216
$\pi^-\overline{K}^0\nu_\tau$	0.8386 ± 0.0141
$\pi^-\overline{K}^0\pi^0\nu_\tau$	0.3812 ± 0.0129
$\pi^-\overline{K}^0\pi^0\pi^0\nu_\tau$ (ex. K^0)	0.0234 ± 0.0231
$\overline{K}^0 h^- h^- h^+\nu_\tau$	0.0222 ± 0.0202
$K^-\eta\nu_\tau$	0.0155 ± 0.0008
$K^-\pi^0\eta\nu_\tau$	0.0048 ± 0.0012
$\pi^-\overline{K}^0\eta\nu_\tau$	0.0094 ± 0.0015
$K^-\omega\nu_\tau$	0.0410 ± 0.0092
$K^-\phi\nu_\tau$ ($\phi \to K^+K^-$)	0.0022 ± 0.0008
$K^-\phi\nu_\tau$ ($\phi \to K^0_S K^0_L$)	0.0015 ± 0.0006
$K^-\pi^-\pi^+\nu_\tau$ (ex. K^0, ω)	0.2923 ± 0.0067
$K^-\pi^-\pi^+\pi^0\nu_\tau$ (ex. K^0, ω, η)	0.0410 ± 0.0143
$K^-2\pi^-2\pi^+\nu_\tau$ (ex. K^0)	0.0001 ± 0.0001
$K^-2\pi^-2\pi^+\pi^0\nu_\tau$ (ex. K^0)	0.0001 ± 0.0001
$X_s^-\nu_\tau$	2.9087 ± 0.0482

9.4.3 $|V_{us}|$ from $B(\tau \to K\nu)$

We determine $|V_{us}|$ from the branching fraction $B(\tau^- \to K^-\nu_\tau)$ using

$$B(\tau^- \to K^-\nu_\tau) = \frac{G_F^2 f_K^2 |V_{us}|^2 m_\tau^3 \tau_\tau}{16\pi\hbar} \left(1 - \frac{m_K^2}{m_\tau^2}\right)^2 S_{EW} \ .$$

We use $f_K = 155.6 \pm 0.4\,\text{MeV}$ from FLAG 2016 with $N_f = 2+1+1$ [210] and the radiative correction $S_{EW} = 1.02010 \pm 0.00030$ [1188]. We obtain $|V_{us}|_{\tau K} = 0.2223 \pm 0.0016$, which is 1.9σ below the CKM unitarity prediction. The physical constants have been taken from PDG 2015 (which uses CODATA 2014 [1189]).

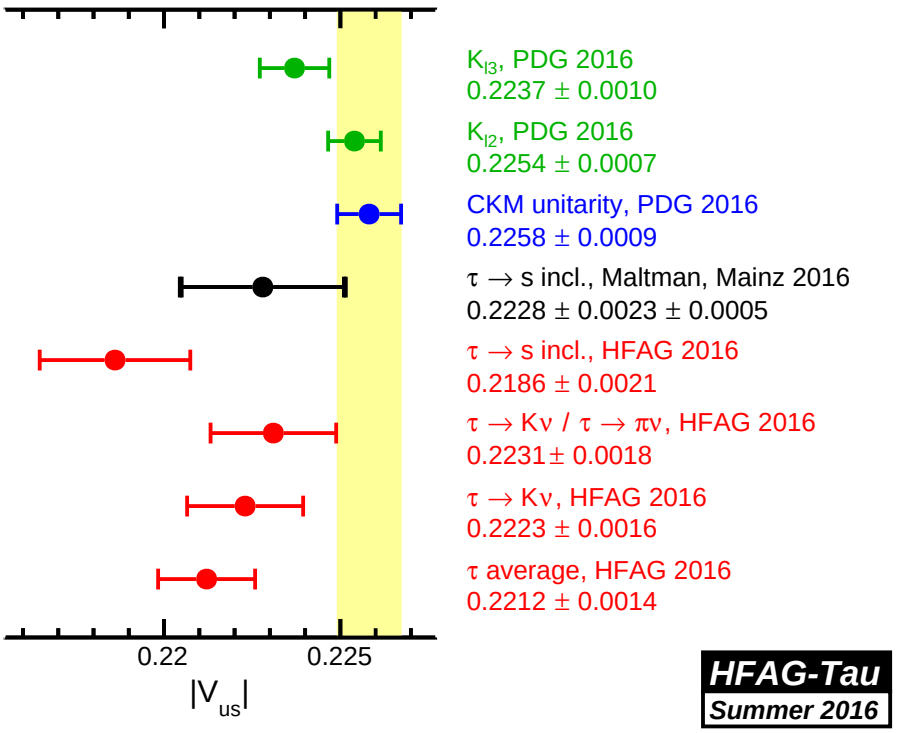

Figure 192: $|V_{us}|$ averages.

9.4.4 $|V_{us}|$ from τ summary

We summarize the $|V_{us}|$ results reporting the values, the discrepancy with respect to the $|V_{us}|$ determination from CKM unitarity, and an illustration of the measurement method:

$$
\begin{aligned}
|V_{us}|_{\rm uni} &= 0.22582 \pm 0.00091 && && [\text{from } \sqrt{1-|V_{ud}|^2} \quad (\text{CKM unitarity})] \ , \\
|V_{us}|_{\tau s} &= 0.2186 \ \pm 0.0021 && -3.1\sigma && [\text{from } \Gamma(\tau^- \to X_s^- \nu_\tau)] \ , \\
|V_{us}|_{\tau K/\pi} &= 0.2231 \ \pm 0.0018 && -1.3\sigma && [\text{from } \Gamma(\tau^- \to K^- \nu_\tau)/\Gamma(\tau^- \to \pi^- \nu_\tau)] \ , \\
|V_{us}|_{\tau K} &= 0.2223 \ \pm 0.0016 && -1.9\sigma && [\text{from } \Gamma(\tau^- \to K^- \nu_\tau)] \ .
\end{aligned}
$$

Averaging the three above $|V_{us}|$ determinations (taking into account all correlations due to the usage of the fitted τ branching fractions and the other mentioned inputs) we obtain:

$$
|V_{us}|_\tau = 0.2212 \pm 0.0014 \quad -2.8\sigma \quad [\text{average of 3 } |V_{us}| \ \tau \text{ measurements}] \ .
$$

We could not find a published estimate of the correlation of the uncertainties on f_K and f_K/f_π, but even if we assume $\pm 100\%$ correlation, the uncertainty on $|V_{us}|_\tau$ does not change more than about $\pm 5\%$.

Recent studies [1190, 1191] indicate that the currently used theory uncertainties for the $|V_{us}|$ determination from inclusive $\tau \to X_s \nu$ appear to be underestimated. This may explain the measured discrepancy with respect to $|V_{us}|$ determined from kaon decays and from $|V_{ud}|$ and the CKM matrix unitarity. The same studies propose an alternative determination of $|V_{us}|$ that uses the τ spectral functions in addition to the τ branching fractions. The resulting value of $|V_{us}|$ is consistent with the other $|V_{us}|$ determinations.

Figure 192 summarizes the $|V_{us}|$ results, reporting also recent determinations of $|V_{us}|$ from kaon decays [5], CKM matrix unitarity [5] and the above mentioned determination of $|V_{us}|$ from inclusive $\tau \to X_s \nu$ decays [1191].

9.5 Upper limits on τ LFV branching fractions

The Standard Model predicts that the τ LFV branching fractions be too small to be measured with the available experimental precision. We report in Table 281 and Figure 193 the up-to-date experimental upper limits on these branching fractions.

Table 281: Experimental upper limits on lepton flavour violating τ decays. The modes are grouped according to the particle content of their final states. Modes with baryon number violation are labelled with "BNV".

Decay mode	**Category**	**90% CL Limit**	**Exp.**	**Ref.**
$\Gamma_{156} = e^-\gamma$	$\ell\gamma$	$< 12.0 \cdot 10^{-8}$	Belle	[1192]
		$< 3.3 \cdot 10^{-8}$	*BABAR*	[1193]
$\Gamma_{157} = \mu^-\gamma$		$< 4.5 \cdot 10^{-8}$	Belle	[1192]
		$< 4.4 \cdot 10^{-8}$	*BABAR*	[1193]
$\Gamma_{158} = e^-\pi^0$	ℓP^0	$< 2.2 \cdot 10^{-8}$	Belle	[1194]
		$< 13.0 \cdot 10^{-8}$	*BABAR*	[1195]
$\Gamma_{159} = \mu^-\pi^0$		$< 2.7 \cdot 10^{-8}$	Belle	[1194]
		$< 11.0 \cdot 10^{-8}$	*BABAR*	[1195]
$\Gamma_{162} = e^-\eta$		$< 4.4 \cdot 10^{-8}$	Belle	[1194]
		$< 16.0 \cdot 10^{-8}$	*BABAR*	[1195]
$\Gamma_{163} = \mu^-\eta$		$< 2.3 \cdot 10^{-8}$	Belle	[1194]
		$< 15.0 \cdot 10^{-8}$	*BABAR*	[1195]
$\Gamma_{172} = e^-\eta'(958)$		$< 3.6 \cdot 10^{-8}$	Belle	[1194]
		$< 24.0 \cdot 10^{-8}$	*BABAR*	[1195]
$\Gamma_{173} = \mu^-\eta'(958)$		$< 3.8 \cdot 10^{-8}$	Belle	[1194]
		$< 14.0 \cdot 10^{-8}$	*BABAR*	[1195]
$\Gamma_{160} = e^- K^0_S$		$< 2.6 \cdot 10^{-8}$	Belle	[1196]
		$< 3.3 \cdot 10^{-8}$	*BABAR*	[1197]
$\Gamma_{161} = \mu^- K^0_S$		$< 2.3 \cdot 10^{-8}$	Belle	[1196]
		$< 4.0 \cdot 10^{-8}$	*BABAR*	[1197]
$\Gamma_{174} = e^- f_0(980)$	ℓS^0	$< 3.2 \cdot 10^{-8}$	Belle	[1198]
$\Gamma_{175} = \mu^- f_0(980)$		$< 3.4 \cdot 10^{-8}$	Belle	[1198]
$\Gamma_{164} = e^-\rho^0$	ℓV^0	$< 1.8 \cdot 10^{-8}$	Belle	[1199]
		$< 4.6 \cdot 10^{-8}$	*BABAR*	[1200]
$\Gamma_{165} = \mu^-\rho^0$		$< 1.2 \cdot 10^{-8}$	Belle	[1199]
		$< 2.6 \cdot 10^{-8}$	*BABAR*	[1200]
$\Gamma_{168} = e^- K^*(892)^0$		$< 3.2 \cdot 10^{-8}$	Belle	[1199]
		$< 5.9 \cdot 10^{-8}$	*BABAR*	[1200]

Table 281 – continued from previous page

Decay mode	Category	90% CL Limit	Exp.	Ref.
$\Gamma_{169} = \mu^- K^*(892)^0$		$< 7.2 \cdot 10^{-8}$	Belle	[1199]
		$< 17.0 \cdot 10^{-8}$	*BABAR*	[1200]
$\Gamma_{170} = e^- \overline{K}^*(892)^0$		$< 3.4 \cdot 10^{-8}$	Belle	[1199]
		$< 4.6 \cdot 10^{-8}$	*BABAR*	[1200]
$\Gamma_{171} = \mu^- \overline{K}^*(892)^0$		$< 7.0 \cdot 10^{-8}$	Belle	[1199]
		$< 7.3 \cdot 10^{-8}$	*BABAR*	[1200]
$\Gamma_{176} = e^- \phi$		$< 3.1 \cdot 10^{-8}$	Belle	[1199]
		$< 3.1 \cdot 10^{-8}$	*BABAR*	[1200]
$\Gamma_{177} = \mu^- \phi$		$< 8.4 \cdot 10^{-8}$	Belle	[1199]
		$< 19.0 \cdot 10^{-8}$	*BABAR*	[1200]
$\Gamma_{166} = e^- \omega$		$< 4.8 \cdot 10^{-8}$	Belle	[1199]
		$< 11.0 \cdot 10^{-8}$	*BABAR*	[1201]
$\Gamma_{167} = \mu^- \omega$		$< 4.7 \cdot 10^{-8}$	Belle	[1199]
		$< 10.0 \cdot 10^{-8}$	*BABAR*	[1201]
$\Gamma_{178} = e^- e^+ e^-$	$\ell\ell\ell$	$< 2.7 \cdot 10^{-8}$	Belle	[1202]
		$< 2.9 \cdot 10^{-8}$	*BABAR*	[1203]
$\Gamma_{181} = \mu^- e^+ e^-$		$< 1.8 \cdot 10^{-8}$	Belle	[1202]
		$< 2.2 \cdot 10^{-8}$	*BABAR*	[1203]
$\Gamma_{179} = e^- \mu^+ \mu^-$		$< 2.7 \cdot 10^{-8}$	Belle	[1202]
		$< 3.2 \cdot 10^{-8}$	*BABAR*	[1203]
$\Gamma_{183} = \mu^- \mu^+ \mu^-$		$< 2.1 \cdot 10^{-8}$	Belle	[1202]
		$< 3.3 \cdot 10^{-8}$	*BABAR*	[1203]
		$< 4.6 \cdot 10^{-8}$	LHCb	[1204]
		$< 37.6 \cdot 10^{-8}$	Atlas	[1205]
$\Gamma_{182} = e^- \mu^+ e^-$		$< 1.5 \cdot 10^{-8}$	Belle	[1202]
		$< 1.8 \cdot 10^{-8}$	*BABAR*	[1203]
$\Gamma_{180} = \mu^- e^+ \mu^-$		$< 1.7 \cdot 10^{-8}$	Belle	[1202]
		$< 2.6 \cdot 10^{-8}$	*BABAR*	[1203]
$\Gamma_{184} = e^- \pi^+ \pi^-$	ℓhh	$< 2.3 \cdot 10^{-8}$	Belle	[1206]
		$< 12.0 \cdot 10^{-8}$	*BABAR*	[1207]
$\Gamma_{186} = \mu^- \pi^+ \pi^-$		$< 2.1 \cdot 10^{-8}$	Belle	[1206]
		$< 29.0 \cdot 10^{-8}$	*BABAR*	[1207]
$\Gamma_{188} = e^- \pi^+ K^-$		$< 3.7 \cdot 10^{-8}$	Belle	[1206]
		$< 32.0 \cdot 10^{-8}$	*BABAR*	[1207]
$\Gamma_{194} = \mu^- \pi^+ K^-$		$< 8.6 \cdot 10^{-8}$	Belle	[1206]
		$< 26.0 \cdot 10^{-8}$	*BABAR*	[1207]
$\Gamma_{189} = e^- K^+ \pi^-$		$< 3.1 \cdot 10^{-8}$	Belle	[1206]
		$< 17.0 \cdot 10^{-8}$	*BABAR*	[1207]
$\Gamma_{195} = \mu^- K^+ \pi^-$		$< 4.5 \cdot 10^{-8}$	Belle	[1206]
		$< 32.0 \cdot 10^{-8}$	*BABAR*	[1207]
$\Gamma_{192} = e^- K^+ K^-$		$< 3.4 \cdot 10^{-8}$	Belle	[1206]

Table 281 – continued from previous page

Decay mode	Category	90% CL Limit	Exp.	Ref.
		$< 14.0 \cdot 10^{-8}$	*BABAR*	[1207]
$\Gamma_{198} = \mu^- K^+ K^-$		$< 4.4 \cdot 10^{-8}$	Belle	[1206]
		$< 25.0 \cdot 10^{-8}$	*BABAR*	[1207]
$\Gamma_{191} = e^- K^0_S K^0_S$		$< 7.1 \cdot 10^{-8}$	Belle	[1196]
$\Gamma_{197} = \mu^- K^0_S K^0_S$		$< 8.0 \cdot 10^{-8}$	Belle	[1196]
$\Gamma_{185} = e^+ \pi^- \pi^-$		$< 2.0 \cdot 10^{-8}$	Belle	[1206]
		$< 27.0 \cdot 10^{-8}$	*BABAR*	[1207]
$\Gamma_{187} = \mu^+ \pi^- \pi^-$		$< 3.9 \cdot 10^{-8}$	Belle	[1206]
		$< 7.0 \cdot 10^{-8}$	*BABAR*	[1207]
$\Gamma_{190} = e^+ \pi^- K^-$		$< 3.2 \cdot 10^{-8}$	Belle	[1206]
		$< 18.0 \cdot 10^{-8}$	*BABAR*	[1207]
$\Gamma_{196} = \mu^+ \pi^- K^-$		$< 4.8 \cdot 10^{-8}$	Belle	[1206]
		$< 22.0 \cdot 10^{-8}$	*BABAR*	[1207]
$\Gamma_{193} = e^+ K^- K^-$		$< 3.3 \cdot 10^{-8}$	Belle	[1206]
		$< 15.0 \cdot 10^{-8}$	*BABAR*	[1207]
$\Gamma_{199} = \mu^+ K^- K^-$		$< 4.7 \cdot 10^{-8}$	Belle	[1206]
		$< 48.0 \cdot 10^{-8}$	*BABAR*	[1207]
$\Gamma_{211} = \pi^- \Lambda$	BNV	$< 3.0 \cdot 10^{-8}$	Belle	[1208]
		$< 5.8 \cdot 10^{-8}$	*BABAR*	[1209]
$\Gamma_{212} = \pi^- \overline{\Lambda}$		$< 2.8 \cdot 10^{-8}$	Belle	[1208]
		$< 5.9 \cdot 10^{-8}$	*BABAR*	[1209]
$\Gamma_{213} = K^- \Lambda$		$< 4.2 \cdot 10^{-8}$	Belle	[1208]
		$< 15. \cdot 10^{-8}$	*BABAR*	[1209]
$\Gamma_{214} = K^- \overline{\Lambda}$		$< 3.1 \cdot 10^{-8}$	Belle	[1208]
		$< 7.2 \cdot 10^{-8}$	*BABAR*	[1209]
$\Gamma_{215} = p \mu^- \mu^-$		$< 44.0 \cdot 10^{-8}$	LHCb	[1210]
$\Gamma_{216} = \overline{p} \mu^+ \mu^-$		$< 33.0 \cdot 10^{-8}$	LHCb	[1210]

9.6 Combination of upper limits on τ LFV branching fractions

Combining upper limits is a delicate issue, since there is no standard and generally agreed procedure. Furthermore, the τ LFV searches published limits are extracted from the data with a variety of methods, and cannot be directly combined with a uniform procedure. It is however possible to use a single and effective upper limit combination procedure for all modes by re-computing the published upper limits with just one extraction method, using the published information that documents the upper limit determination: number of observed candidates, expected background, signal efficiency and number of analyzed τ decays.

We chose to use the CL_s method [1211] to re-compute the τ LFV upper limits, since it is well known and widely used (see the Statistics review of PDG 2013 [5]), and since the limits

computed with the CL_s method can be combined in a straightforward way (see below). The CL_s method is based on two hypotheses: signal plus background and background only. We calculate the observed confidence levels for the two hypotheses:

$$CL_{s+b} = P_{s+b}(Q \leq Q_{obs}) = \int_{-\infty}^{Q_{obs}} \frac{dP_{s+b}}{dQ} dQ, \tag{284}$$

$$CL_b = P_b(Q \leq Q_{obs}) = \int_{-\infty}^{Q_{obs}} \frac{dP_b}{dQ} dQ, \tag{285}$$

where CL_{s+b} is the confidence level observed for the signal plus background hypothesis, CL_b is the confidence level observed for the background only hypothesis, $\frac{dP_{s+b}}{dQ}$ and $\frac{dP_b}{dQ}$ are the probability distribution functions (PDFs) for the two corresponding hypothesis and Q is called the test statistics. The CL_s value is defined as the ratio between the confidence level for the signal plus background hypothesis to the confidence level for the background hypothesis:

$$CL_s = \frac{CL_{s+b}}{CL_b}. \tag{286}$$

When multiple results are combined, the PDFs in Equations 284 and 285 are the product of the individual PDFs,

$$CL_s = \frac{\prod_{i=1}^{N_{\text{chan}}} \sum_{n=0}^{n_i} \frac{e^{-(s_i+b_i)}(s_i+b_i)^n}{n!} \frac{\prod_{j=1}^{n} s_i S_i(x_{ij}) + b_i B_i(x_{ij})}{\prod_{j=1}^{n_i} B_i(x_{ij})}}{\prod_{i=1}^{n_{\text{chan}}} \sum_{n=0}^{n_i} \frac{e^{-b_i} b_i^n}{n!}}, \tag{287}$$

where N_{chan} is the number of results (or channels), and, for each channel i, n_i is the number of observed candidates, x_{ij} are the values of the discriminating variables (with index j), s_i and b_i are the number of signal and background events and S_i, B_i are the probability distribution functions of the discriminating variables. The expected signal s_i is related to the τ lepton branching fraction $B(\tau \to f_i)$ into the searched final state f_i by $s_i = N_i \epsilon_i B(\tau \to f_i)$, where N_i is the number of produced τ leptons and ϵ_i is the detection efficiency for observing the decay $\tau \to f_i$. For e^+e^- experiments, $N_i = 2\mathcal{L}_i \sigma_{\tau\tau}$, where $\mathcal{L}_i$ is the integrated luminosity and $\sigma_{\tau\tau}$ is the τ pair production cross section $\sigma(e^+e^- \to \tau^+\tau^-)$ [1212]. In experiments where τ leptons are produced in more complex multiple reactions, the effective N_i is typically estimated with Monte Carlo simulations calibrated with related data yields.

The extraction of the upper limits is performed using the code provided by Tom Junk [1213]. The systematic uncertainties are modeled in the Monte Carlo toy experiments by convolving the S_i and B_i PDFs with with Gaussian distributions corresponding to the nuisance parameters.

Table 282 reports the HFAG combinations of the τ LFV limits, together with the published limits, excluding the older and weaker CLEO limits. Since there is negligible gain in combining limits of very different strength, the combinations do not include the CLEO searches and we do not combine results for modes where the best limit is more than an order of magnitude better than the other limits. Figure 194 reports a graphical representation of the limits in Table 282.

Table 282: Combinations of upper limits on lepton flavour violating τ decay modes. The modes are grouped according to the particle content of their final states. Modes with baryon number violation are labelled with "BNV".

Decay mode	**Category**	**90% CL Limit**
$\Gamma_{156} = e^-\gamma$	$\ell\gamma$	$5.4 \cdot 10^{-8}$
$\Gamma_{157} = \mu^-\gamma$		$5.0 \cdot 10^{-8}$
$\Gamma_{160} = e^- K^0_S$	ℓP^0	$1.4 \cdot 10^{-8}$
$\Gamma_{161} = \mu^- K^0_S$		$1.5 \cdot 10^{-8}$
$\Gamma_{164} = e^-\rho^0$	ℓV^0	$1.5 \cdot 10^{-8}$
$\Gamma_{165} = \mu^-\rho^0$		$1.5 \cdot 10^{-8}$
$\Gamma_{166} = e^-\omega$		$3.3 \cdot 10^{-8}$
$\Gamma_{167} = \mu^-\omega$		$4.0 \cdot 10^{-8}$
$\Gamma_{168} = e^- K^*(892)^0$		$2.3 \cdot 10^{-8}$
$\Gamma_{169} = \mu^- K^*(892)^0$		$6.0 \cdot 10^{-8}$
$\Gamma_{170} = e^- \overline{K}^*(892)^0$		$2.2 \cdot 10^{-8}$
$\Gamma_{171} = \mu^- \overline{K}^*(892)^0$		$4.2 \cdot 10^{-8}$
$\Gamma_{176} = e^-\phi$		$2.0 \cdot 10^{-8}$
$\Gamma_{177} = \mu^-\phi$		$6.8 \cdot 10^{-8}$
$\Gamma_{178} = e^- e^+ e^-$	$\ell\ell\ell$	$1.4 \cdot 10^{-8}$
$\Gamma_{179} = e^-\mu^+\mu^-$		$1.6 \cdot 10^{-8}$
$\Gamma_{180} = \mu^- e^+\mu^-$		$9.8 \cdot 10^{-9}$
$\Gamma_{181} = \mu^- e^+ e^-$		$1.1 \cdot 10^{-8}$
$\Gamma_{182} = e^-\mu^+ e^-$		$8.4 \cdot 10^{-9}$
$\Gamma_{183} = \mu^-\mu^+\mu^-$		$1.2 \cdot 10^{-8}$
$\Gamma_{211} = \pi^-\Lambda$	BNV	$1.9 \cdot 10^{-8}$
$\Gamma_{212} = \pi^-\overline{\Lambda}$		$1.8 \cdot 10^{-8}$
$\Gamma_{213} = K^-\Lambda$		$3.7 \cdot 10^{-8}$
$\Gamma_{214} = K^-\overline{\Lambda}$		$2.0 \cdot 10^{-8}$

Table 283: Published information that has been used to re-compute upper limits with the CL_s method, *i.e.* the number of τ leptons produced, the signal detection efficiency and its uncertainty, the number of expected background events and its uncertainty, and the number of observed events. The uncertainty on the efficiency includes the minor uncertainty contribution on the number of τ leptons (typically originating on the uncertainties on the integrated luminosity and on the production cross-section). The additional limits used in the combinations (one from LHCb) have been determined with the CL_s method already in their publication.

Decay mode	**Exp.**	**Ref.**	N_τ **(millions)**	**efficiency (%)**	N_{bkg}	N_{obs}
$\Gamma_{156} = e^-\gamma$	*BABAR*	[1193]	963.2	3.90 ± 0.30	1.60 ± 0.40	0
$\Gamma_{156} = e^-\gamma$	Belle	[1192]	983.4	3.00 ± 0.10	5.14 ± 3.30	5
$\Gamma_{157} = \mu^-\gamma$	*BABAR*	[1193]	963.2	6.10 ± 0.50	3.60 ± 0.70	2
$\Gamma_{157} = \mu^-\gamma$	Belle	[1192]	983.4	5.07 ± 0.20	13.90 ± 5.00	10
$\Gamma_{160} = e^- K^0_S$	*BABAR*	[1197]	862	9.10 ± 1.73	0.59 ± 0.25	1
$\Gamma_{160} = e^- K^0_S$	Belle	[1196]	1273.6	10.20 ± 0.67	0.18 ± 0.18	0
$\Gamma_{161} = \mu^- K^0_S$	*BABAR*	[1197]	862	6.14 ± 0.20	0.30 ± 0.18	1
$\Gamma_{161} = \mu^- K^0_S$	Belle	[1196]	1273.6	10.70 ± 0.73	0.35 ± 0.21	0
$\Gamma_{164} = e^- \rho^0$	*BABAR*	[1200]	828.8	7.31 ± 0.20	1.32 ± 0.17	1
$\Gamma_{164} = e^- \rho^0$	Belle	[1199]	1554.2	7.58 ± 0.41	0.29 ± 0.15	0
$\Gamma_{165} = \mu^- \rho^0$	*BABAR*	[1200]	828.8	4.52 ± 0.40	2.04 ± 0.19	0
$\Gamma_{165} = \mu^- \rho^0$	Belle	[1199]	1554.2	7.09 ± 0.37	1.48 ± 0.35	0
$\Gamma_{166} = e^- \omega$	*BABAR*	[1201]	828.8	2.96 ± 0.13	0.35 ± 0.06	0
$\Gamma_{166} = e^- \omega$	Belle	[1199]	1554.2	2.92 ± 0.18	0.30 ± 0.14	0
$\Gamma_{167} = \mu^- \omega$	*BABAR*	[1201]	828.8	2.56 ± 0.16	0.73 ± 0.03	0
$\Gamma_{167} = \mu^- \omega$	Belle	[1199]	1554.2	2.38 ± 0.14	0.72 ± 0.18	0
$\Gamma_{168} = e^- K^*(892)^0$	*BABAR*	[1200]	828.8	8.00 ± 0.20	1.65 ± 0.23	2
$\Gamma_{168} = e^- K^*(892)^0$	Belle	[1199]	1554.2	4.37 ± 0.24	0.29 ± 0.14	0
$\Gamma_{169} = \mu^- K^*(892)^0$	*BABAR*	[1200]	828.8	4.60 ± 0.40	1.79 ± 0.21	4
$\Gamma_{169} = \mu^- K^*(892)^0$	Belle	[1199]	1554.2	3.39 ± 0.19	0.53 ± 0.20	1
$\Gamma_{170} = e^- \overline{K}^*(892)^0$	*BABAR*	[1200]	828.8	7.80 ± 0.20	2.76 ± 0.28	2
$\Gamma_{170} = e^- \overline{K}^*(892)^0$	Belle	[1199]	1554.2	4.41 ± 0.25	0.08 ± 0.08	0
$\Gamma_{171} = \mu^- \overline{K}^*(892)^0$	*BABAR*	[1200]	828.8	4.10 ± 0.30	1.72 ± 0.17	1
$\Gamma_{171} = \mu^- \overline{K}^*(892)^0$	Belle	[1199]	1554.2	3.60 ± 0.20	0.45 ± 0.17	1
$\Gamma_{176} = e^- \phi$	*BABAR*	[1200]	828.8	6.40 ± 0.20	0.68 ± 0.12	0
$\Gamma_{176} = e^- \phi$	Belle	[1199]	1554.2	4.18 ± 0.25	0.47 ± 0.19	0
$\Gamma_{177} = \mu^- \phi$	*BABAR*	[1200]	828.8	5.20 ± 0.30	2.76 ± 0.16	6
$\Gamma_{177} = \mu^- \phi$	Belle	[1199]	1554.2	3.21 ± 0.19	0.06 ± 0.06	1
$\Gamma_{178} = e^- e^+ e^-$	*BABAR*	[1203]	867.6	8.60 ± 0.20	0.12 ± 0.02	0
$\Gamma_{178} = e^- e^+ e^-$	Belle	[1202]	1437.4	6.00 ± 0.59	0.21 ± 0.15	0
$\Gamma_{179} = e^- \mu^+ \mu^-$	*BABAR*	[1203]	867.6	6.40 ± 0.40	0.54 ± 0.14	0
$\Gamma_{179} = e^- \mu^+ \mu^-$	Belle	[1202]	1437.4	6.10 ± 0.58	0.10 ± 0.04	0
$\Gamma_{180} = \mu^- e^+ \mu^-$	*BABAR*	[1203]	867.6	10.20 ± 0.60	0.03 ± 0.02	0
$\Gamma_{180} = \mu^- e^+ \mu^-$	Belle	[1202]	1437.4	10.10 ± 0.77	0.02 ± 0.02	0
$\Gamma_{181} = \mu^- e^+ e^-$	*BABAR*	[1203]	867.6	8.80 ± 0.50	0.64 ± 0.19	0
$\Gamma_{181} = \mu^- e^+ e^-$	Belle	[1202]	1437.4	9.30 ± 0.73	0.04 ± 0.04	0
$\Gamma_{182} = e^- \mu^+ e^-$	*BABAR*	[1203]	867.6	12.70 ± 0.70	0.34 ± 0.12	0
$\Gamma_{182} = e^- \mu^+ e^-$	Belle	[1202]	1437.4	11.50 ± 0.89	0.01 ± 0.01	0
$\Gamma_{183} = \mu^- \mu^+ \mu^-$	*BABAR*	[1203]	867.6	6.60 ± 0.60	0.44 ± 0.17	0
$\Gamma_{183} = \mu^- \mu^+ \mu^-$	Belle	[1202]	1437.4	7.60 ± 0.56	0.13 ± 0.20	0

Table 283 – continued from previous page

Decay mode	Exp.	Ref.	N_τ (millions)	efficiency (%)	$N_{\rm bkg}$	$N_{\rm obs}$
$\Gamma_{211} = \pi^- \Lambda$	*BABAR*	[1209]	435.6	12.20 ± 8.50	0.56 ± 0.56	0
$\Gamma_{211} = \pi^- \Lambda$	Belle	[1208]	1665.2	4.39 ± 0.36	0.31 ± 0.18	0
$\Gamma_{212} = \pi^- \overline{\Lambda}$	*BABAR*	[1209]	435.6	12.28 ± 8.50	0.42 ± 0.42	0
$\Gamma_{212} = \pi^- \overline{\Lambda}$	Belle	[1208]	1665.2	4.80 ± 0.39	0.21 ± 0.15	0
$\Gamma_{213} = K^- \Lambda$	*BABAR*	[1209]	435.6	9.47 ± 0.66	0.12 ± 0.12	1
$\Gamma_{213} = K^- \Lambda$	Belle	[1208]	1665.2	3.16 ± 0.27	0.42 ± 0.19	0
$\Gamma_{214} = K^- \overline{\Lambda}$	*BABAR*	[1209]	435.6	10.63 ± 0.74	0.26 ± 0.26	0
$\Gamma_{214} = K^- \overline{\Lambda}$	Belle	[1208]	1665.2	4.11 ± 0.35	0.31 ± 0.14	0

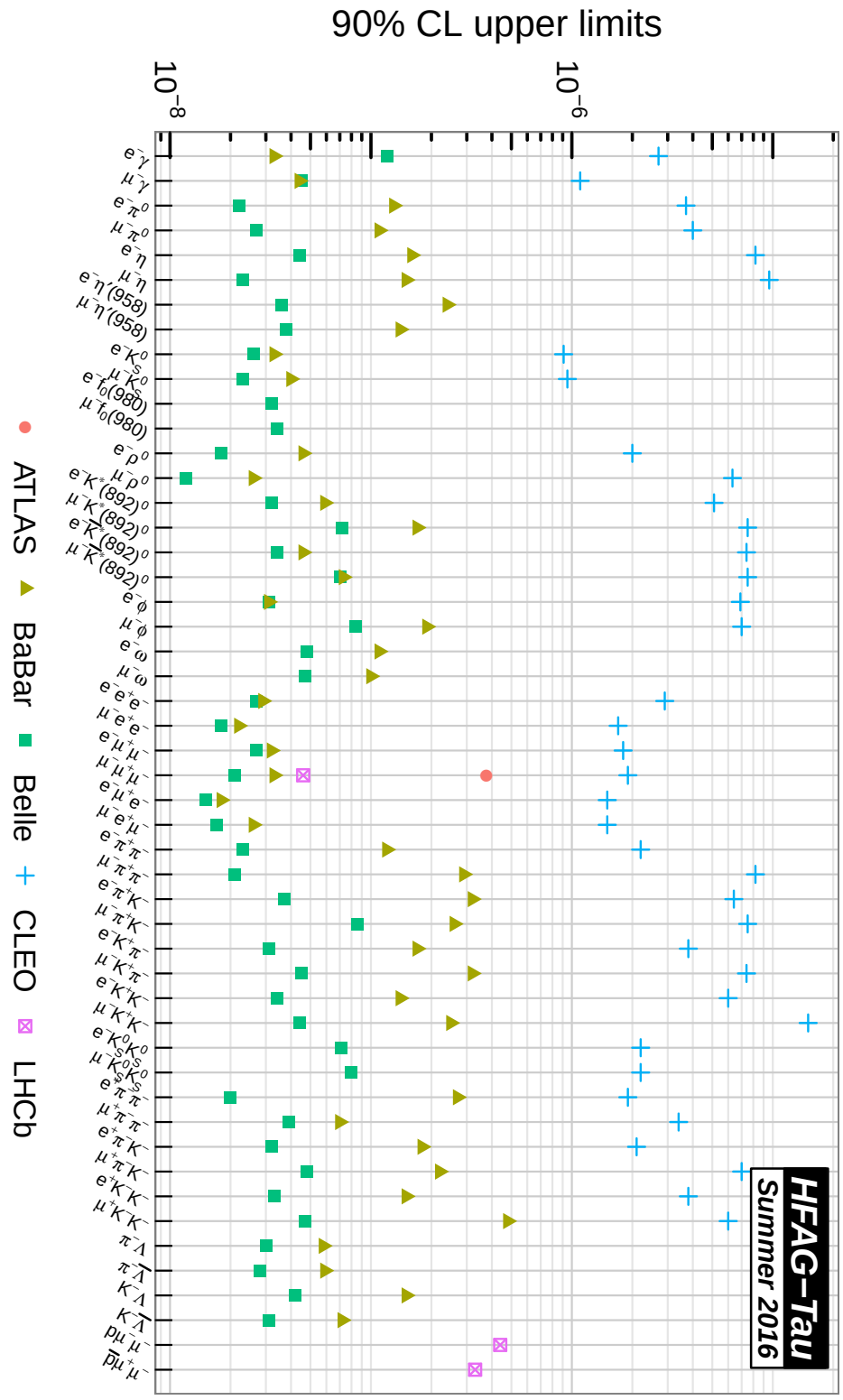

Figure 193: Tau lepton-flavor-violating branching fraction upper limits summary plot.

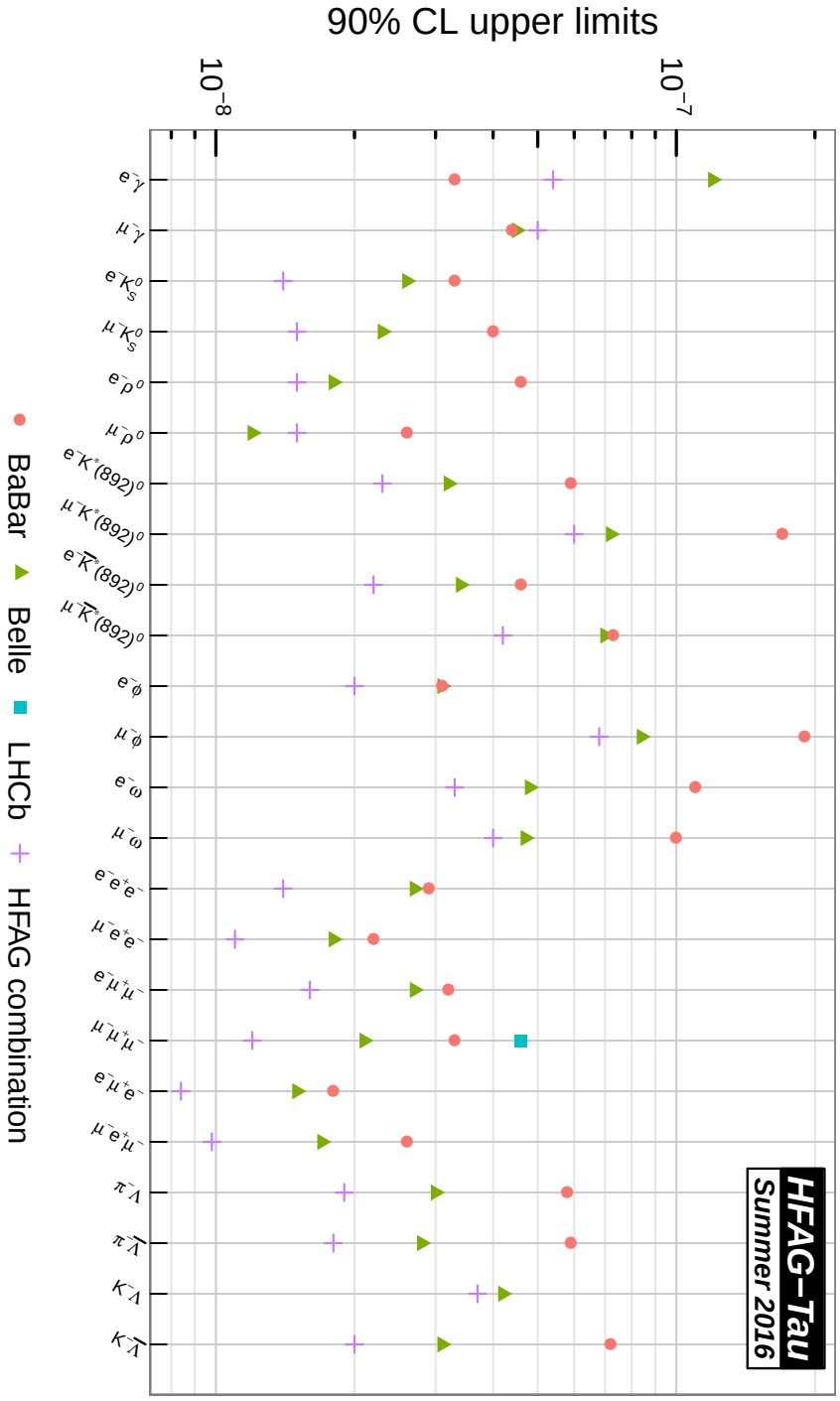

Figure 194: Tau lepton-flavour-violating branching fraction upper limits combinations summary plot. For each channel we report the HFAG combined limit, and the experimental published limits. In some cases, the combined limit is weaker than the limit published by a single experiment. This arises since the CL_s method used in the combination can be more conservative compared to other legitimate methods, especially when the number of observed events fluctuates below the expected background.

10 Summary

This article provides updated world averages for b-hadron properties using results available through summer 2016. A small selection of highlights of the results described in Sections 3-9 is given in Table 284.

Table 284: Selected world averages. Where two uncertainties are given the first is statistical and the second is systematic, except where indicated otherwise.

***b*-hadron lifetimes**	
$\tau(B^0)$	1.520 ± 0.004 ps
$\tau(B^+)$	1.638 ± 0.004 ps
$\overline{\tau}(B_s^0) = 1/\Gamma_s$	1.505 ± 0.005 ps
$\tau(B_{s\mathrm{L}})$	1.414 ± 0.006 ps
$\tau(B_{s\mathrm{H}})$	1.609 ± 0.010 ps
$\tau(B_c^+)$	0.507 ± 0.009 ps
$\tau(\Lambda_b^0)$	1.470 ± 0.010 ps
$\tau(\Xi_b^-)$	1.571 ± 0.040 ps
$\tau(\Xi_b^0)$	1.479 ± 0.031 ps
$\tau(\Omega_b^-)$	$1.64^{+0.18}_{-0.17}$ ps
B^0 and B_s^0 mixing / *CP* violation parameters	
Δm_d	0.5064 ± 0.0019 ps^{-1}
$\Delta\Gamma_d/\Gamma_d$	-0.002 ± 0.010
$\lvert q/p\rvert_d$	1.0009 ± 0.0013
Δm_s	17.757 ± 0.021 ps^{-1}
$\Delta\Gamma_s$	$+0.086 \pm 0.006$ ps^{-1}
$\lvert q/p\rvert_s$	1.0003 ± 0.0014
$\phi_s^{c\bar{c}s}$	-0.030 ± 0.033
Parameters related to Unitarity Triangle angles	
$\sin 2\beta \equiv \sin 2\phi_1$	0.691 ± 0.017
$\beta \equiv \phi_1$	$(21.9 \pm 0.7)^\circ$
$-\eta S_{\phi K_S^0}$	$0.74\,^{+0.11}_{-0.13}$
$-\eta S_{\eta' K^0}$	0.63 ± 0.06
$-\eta S_{K_S^0 K_S^0 K_S^0}$	0.72 ± 0.19
$\phi_s(\phi\phi)$	$-0.17 \pm 0.15 \pm 0.03$ rad
$-\eta S_{J/\psi\pi^0}$	0.93 ± 0.15
$-\eta S_{D^+D^-}$	0.84 ± 0.12
$-\eta S_{J/\psi\rho^0}$	$0.66\,^{+0.13\ +0.09}_{-0.12\ -0.03}$
$S_{K^*\gamma}$	-0.16 ± 0.22
$(S_{\pi^+\pi^-}, C_{\pi^+\pi^-})$	$(-0.68 \pm 0.04, -0.27 \pm 0.04)$
$(S_{\rho^+\rho^-}, C_{\rho^+\rho^-})$	$(-0.14 \pm 0.13, \quad 0.00 \pm 0.09)$
$a(D^{*\pm}\pi^\mp)$	-0.039 ± 0.010
$A_{CP}(B \to D_{CP+}K)$	0.111 ± 0.018

Selected world averages – continued from previous page.

$A_{\rm ADS}(B \to D_{K\pi} K)$	-0.415 ± 0.055
$\gamma \equiv \phi_3$	$(74.0\,^{+5.8}_{-6.4})^\circ$
Semileptonic B decay parameters	
$\mathcal{B}(\overline{B}^0 \to D^{*+}\ell^-\overline{\nu}_\ell)$	$(4.88 \pm 0.10)\%$
$\mathcal{B}(B^- \to D^{*0}\ell^-\overline{\nu}_\ell)$	$(5.59 \pm 0.19)\%$
$\eta_{\rm EW}\mathcal{F}(1)\lvert V_{cb}\rvert$	$(35.61 \pm 0.43) \times 10^{-3}$
$\lvert V_{cb}\rvert$ from $\overline{B} \to D^*\ell^-\overline{\nu}_\ell$	$(38.71 \pm 0.47_{\rm exp} \pm 0.59_{\rm th}) \times 10^{-3}$
$\mathcal{B}(\overline{B}^0 \to D^{+}\ell^-\overline{\nu}_\ell)$	$(2.20 \pm 0.10)\%$
$\mathcal{B}(B^- \to D^{0}\ell^-\overline{\nu}_\ell)$	$(2.33 \pm 0.10)\%$
$\eta_{\rm EW}\mathcal{G}(1)\lvert V_{cb}\rvert$	$(41.57 \pm 1.00) \times 10^{-3}$
$\lvert V_{cb}\rvert$ from $\overline{B} \to D\ell^-\overline{\nu}_\ell$	$(39.18 \pm 0.94_{\rm exp} \pm 0.31_{\rm th}) \times 10^{-3}$
$\mathcal{B}(\overline{B} \to X_c\ell^-\overline{\nu}_\ell)$	$(10.65 \pm 0.16)\%$
$\mathcal{B}(\overline{B} \to X\ell^-\overline{\nu}_\ell)$	$(10.86 \pm 0.16)\%$
$\lvert V_{cb}\rvert$ from $\overline{B} \to X\ell^-\overline{\nu}_\ell$	$(42.19 \pm 0.78) \times 10^{-3}$
$\mathcal{B}(\overline{B} \to \pi\ell^-\overline{\nu}_\ell)$	$(1.47 \pm 0.06) \times 10^{-4}$
$\lvert V_{ub}\rvert$ from $\overline{B} \to \pi\ell^-\overline{\nu}_\ell$	$(3.65 \pm 0.14) \times 10^{-3}$
$\lvert V_{ub}\rvert$ from $\overline{B} \to X_u\ell^-\overline{\nu}_\ell$	$(4.52 \pm 0.15_{\rm exp} \pm 0.13_{\rm th}) \times 10^{-3}$
$\lvert V_{ub}\rvert/\lvert V_{cb}\rvert$ from $\Lambda_b^0 \to p\mu^-\overline{\nu}_\mu/\Lambda_b^0 \to \Lambda_c^+\mu^-\overline{\nu}_\mu$	$0.080 \pm 0.004_{\rm exp} \pm 0.004_{\rm th}$
$\mathcal{R}(D) = \mathcal{B}(B \to D\tau\nu_\tau)/\mathcal{B}(B \to D\ell\nu_\ell)$	0.403 ± 0.047
$\mathcal{R}(D^*) = \mathcal{B}(B \to D^*\tau\nu_\tau)/\mathcal{B}(B \to D^*\ell\nu_\ell)$	0.310 ± 0.017
***b*-hadron to charmed hadron decays**	
$\mathcal{B}(\overline{B}^0 \to D^+\pi^-)$	$(2.65 \pm 0.15) \times 10^{-3}$
$\mathcal{B}(B^- \to D^0\pi^-)$	$(4.75 \pm 0.19) \times 10^{-3}$
$\mathcal{B}(\overline{B}_s^0 \to D_s^+\pi^-)$	$(3.03 \pm 0.25) \times 10^{-3}$
$\mathcal{B}(\Lambda_b^0 \to \Lambda_c^+\pi^-)$	$(4.30^{+0.36}_{-0.35}) \times 10^{-3}$
$\mathcal{B}(\overline{B}^0 \to J/\psi\overline{K}^0)$	$(0.863 \pm 0.035) \times 10^{-3}$
$\mathcal{B}(B^- \to J/\psi K^-)$	$(1.028 \pm 0.040) \times 10^{-3}$
$\mathcal{B}(\overline{B}_s^0 \to J/\psi\phi)$	$(1.00 \pm 0.09) \times 10^{-3}$
Rare B decays	
$\mathcal{B}(B_s^0 \to \mu^+\mu^-)$	$\left(2.8\,^{+0.07}_{-0.06}\right) \times 10^{-9}$
$\mathcal{B}(B^0 \to \mu^+\mu^-)$	$\left(0.39\,^{+0.16}_{-0.14}\right) \times 10^{-9}$
$\mathcal{B}(B \to X_s\gamma)$ ($E_\gamma > 1.6$ GeV)	$(3.32 \pm 0.16) \times 10^{-4}$
$\mathcal{B}(B^+ \to \tau^+\nu)$	$(1.06 \pm 0.19) \times 10^{-4}$
$R_K = \mathcal{B}(B^+ \to K^+\mu^+\mu^-)/\mathcal{B}(B^+ \to K^+e^+e^-)$ in $1.0 < m^2_{\ell^+\ell^-} < 6.0$ GeV$^2/c^4$	$0.745^{+0.090}_{-0.074} \pm 0.036$
$A_{CP}(B^0 \to K^+\pi^-)$, $A_{CP}(B^+ \to K^+\pi^0)$	-0.082 ± 0.006, 0.040 ± 0.021
$A_{CP}(B_s^0 \to K^-\pi^+)$	0.26 ± 0.04
Longitudinal polarisation of $B^0 \to \phi K^{*0}$	0.497 ± 0.017
Longitudinal polarisation of $B_s^0 \to \phi\phi$	0.361 ± 0.022
Observables in $B^0 \to K^{*0}\mu^+\mu^-$ decays in bins of $q^2 = m^2(\mu^+\mu^-)$	See Sec. 7.5

Selected world averages – continued from previous page.

D^0 mixing and CP violation parameters	
x	$(0.32 \pm 0.14)\%$
y	$(0.69\,^{+0.06}_{-0.07})\%$
$\delta_{K\pi}$	$(15.2\,^{+7.6}_{-10.0})^\circ$
A_D	$(-0.88 \pm 0.99)\%$
$\lvert q/p\rvert$	$0.89\,^{+0.08}_{-0.07}$
ϕ	$(-12.9\,^{+9.9}_{-8.7})^\circ$
x_{12} (no direct CP violation)	$(0.41\,^{+0.14}_{-0.15})\%$
y_{12} (no direct CP violation)	$(0.61 \pm 0.07)\%$
ϕ_{12} (no direct CP violation)	$(-0.17 \pm 1.8)^\circ$
$a_{CP}^{\rm ind}$	$(0.030 \pm 0.026)\%$
$\Delta a_{CP}^{\rm dir}$	$(-0.134 \pm 0.070)\%$
Leptonic D decays	
f_D	(203.7 ± 4.9) MeV
f_{D_s}	(257.1 ± 4.6) MeV
$\lvert V_{cd}\rvert$	$0.2164 \pm 0.0050_{\rm exp} \pm 0.0015_{\rm LQCD}$
$\lvert V_{cs}\rvert$	$1.006 \pm 0.018_{\rm exp} \pm 0.005_{\rm LQCD}$
Benchmark charm branching fractions	
$\mathcal{B}(\Lambda_c^+ \to pK^-\pi^+)$	$(6.46 \pm 0.24)\%$
$\mathcal{B}(D^0 \to K^-\pi^+)$	$(3.962 \pm 0.017 \pm 0.038 \pm 0.027_{\rm FSR})\%$
$\mathcal{B}(D^0 \to K^+\pi^-)/\mathcal{B}(D^0 \to K^-\pi^+)$	$(0.349\,^{+0.004}_{-0.003})\%$
$\mathcal{B}(D_s^+ \to K^+K^-\pi^+)$	$(5.44 \pm 0.09 \pm 0.11)\%$
τ parameters, lepton universality, and $\lvert V_{us}\rvert$	
g_μ/g_e	1.0019 ± 0.0014
g_τ/g_μ	1.0029 ± 0.0015
g_τ/g_e	1.0029 ± 0.0015
$\mathcal{B}_e^{\rm uni}$	$17.815 \pm 0.023\%$
$R_{\rm had}$	3.6349 ± 0.0082
$\lvert V_{us}\rvert$ from sum of strange branching fractions	0.2186 ± 0.0021
$\lvert V_{us}\rvert$ from $\mathcal{B}(\tau^- \to K^-\nu_\tau)/\mathcal{B}(\tau^- \to \pi^-\nu_\tau)$	0.2231 ± 0.0018
$\lvert V_{us}\rvert$ from $\mathcal{B}(\tau^- \to K^-\nu_\tau)$	0.2223 ± 0.0016
$\lvert V_{us}\rvert$ τ average	0.2212 ± 0.0014

Since the previous version of this writeup [4], the b-hadron lifetime and mixing averages have mostly made gradual progress in precision. Notable exceptions with significant improvement are the averages for the mass difference in the B^0–$\overline{B}^0$ system (Δm_d) and the CP violation parameter in B_s^0–$\overline{B}_s^0$ system ($|q/p|_s$). In total 11 new results (of which 10 from the LHC Run 1 data and 1 from the Tevatron data) have been incorporated in these averages. On the other hand, all results that remained unpublished and for which there is no publication plan, have been removed from the averages. The lifetime hierarchy for the most abundant weakly decaying b-hadron species is well established, with impressive precisions of 4 fs for the most common B^0, B^+ and B_s^0 mesons, and compatible with the expectations from the Heavy Quark

Expansion. However, statistics are still lacking for b-baryons heavier than Λ_b^0 (Ξ_b^-, Ξ_b^0, Ω_b, and all other yet-to-be-discovered b-baryons), but this will surely come from the LHC with sufficient time. A sizable value of the decay width difference in the B_s^0–$\overline{B}_s^0$ system is measured with a relative precision of 7% and is well predicted by the Standard Model (SM). In contrast, the experimental results for the decay width difference in the B^0–$\overline{B}^0$ system are not yet precise enough to distinguish the small (expected) value from zero. The masses differences in both systems are known very accurately, to the (few) per mil level. On the other hand, *CP* violation in the mixing of either system has not been observed yet, with asymmetries known within a couple per mil but still consistent both with zero and their SM predictions. A similar conclusion holds for the *CP* violation induced by B_s^0 mixing in the $b \to c\bar{c}s$ transition, although in this case the experimental precision on the corresponding weak phase is an order of magnitude larger, but now becoming just smaller than the SM central value. Many measurements are still dominated by statistical uncertainties and will improve once new results from the LHC Run 2 become available.

The measurement of $\sin 2\beta \equiv \sin 2\phi_1$ from $b \to c\bar{c}s$ transitions such as $B^0 \to J/\psi\, K_S^0$ has reached $< 2.5\,\%$ precision: $\sin 2\beta \equiv \sin 2\phi_1 = 0.691 \pm 0.017$. Measurements of the same parameter using different quark-level processes provide a consistency test of the Standard Model and allow insight into possible new physics. All results among hadronic $b \to s$ penguin dominated decays of B^0 mesons are currently consistent with the Standard Model expectations. Measurements of *CP* violation parameters in $B_s^0 \to \phi\phi$ allow a similar comparison to the value of $\phi_s^{c\bar{c}s}$; again, results are consistent with the SM expectation (which in this case is very close to zero). Among measurements related to the Unitarity Triangle angle $\alpha \equiv \phi_2$, results from the $\rho\rho$ system allow constraints at the level of $\approx 6^\circ$. These remain the strongest constraints, although results from all of *BABAR*, Belle and LHCb lead to good precision on the *CP* violation parameters in $B^0 \to \pi^+\pi^-$ decays. Knowledge of the third angle $\gamma \equiv \phi_3$ also continues to improve, with the current world average being $(74.0\,^{+5.8}_{-6.4})^\circ$. The precision is expected to improve further as more data becomes available at LHCb and Belle II.

In semileptonic B meson decays, the anomalies reported in the last version of the writeup have remained: The discrepancy between $|V_{cb}|$ measured with inclusive and exclusive decays is of the order of 3σ (3.2σ for $|V_{cb}|$ from $\overline{B} \to D^*\ell^-\overline{\nu}_\ell$, 2.4σ for $|V_{cb}|$ from $\overline{B} \to D\ell^-\overline{\nu}_\ell$). The difference between $|V_{ub}|$ measured with inclusive decays $\overline{B} \to X_u\ell^-\overline{\nu}_\ell$ and $|V_{ub}|$ from $\overline{B} \to \pi\ell^-\overline{\nu}_\ell$ has risen to 3.6σ. An important new contribution to the determination of the values of $|V_{ub}|$ and $|V_{cb}|$ comes from exclusive b-baryon decays. The largest anomaly however is observed in $B \to D^{(*)}\tau\nu_\tau$ decays: The combined discrepancy of the measured values of $\mathcal{R}(D^*)$ and $\mathcal{R}(D)$ to their standard model expectations is found to be 3.9σ.

The most important new measurements of rare b-hadron decays are coming from the LHC. Precision measurements of B_s^0 decays are particularly noteworthy, including several measurements of the longitudinal polarisation fraction from LHCb. ATLAS, CMS and LHCb have significantly improved the sensitivity to the $B_{(s)}^0 \to \mu^+\mu^-$ decays. Recently, CMS and LHCb published a combined analysis that allowed the first observation of the $B_s^0 \to \mu^+\mu^-$ decay to be obtained, and provided three standard deviations evidence of the $B^0 \to \mu^+\mu^-$ decay. The results are compatible with the SM predictions, and yield constrains on the parameter space of new physics models. CMS and LHCb have also performed angular analyses of the $B^0 \to K^{*0}\mu^+\mu^-$ decay, complementing, extending and improving on the precision of results from *BABAR* and Belle. One of the observables measured by LHCb, P_5', differs from the SM prediction by 3.7σ in one of the $m^2_{\mu^+\mu^-}$ intervals; results from Belle on this observable are

consistent but less precise. Improved measurements from LHCb and other experiments are keenly anticipated. A measurement of the ratio of branching fractions of $B^+ \to K^+\mu^+\mu^-$ and $B^+ \to K^+e^+e^-$ decays (R_K) has been made by LHCb. In the low $m^2_{\ell^+\ell^-}$ region, it differs from the standard model prediction by 2.6σ. Among the *CP* violating observables in rare decays, the "$K\pi$ puzzle" persists, and important new results have appeared in three-body decays. LHCb has produced many other results on a wide variety of decays, including b-baryon and B_c^+-meson decays. Belle and *BABAR* continue to produce new results though their output rates are dwindling. It will still be some years before we see new results from the upgraded SuperKEKB B factory and the Belle II experiment.

About 800 b to charm results from *BABAR*, Belle, CDF, D0, LHCb, CMS, and ATLAS reported in more than 200 papers are compiled in a list of over 600 averages. The huge samples of b hadrons that are available in contemporary experiments allows measurements of decays to states with open or hidden charm content with unprecedented precision. In addition to improvements in precision for branching fractions of $\overline{B}^0$ and B^- mesons, many new decay modes have been discovered. In addition, there is a rapidly increasing set of measurements available for $\overline{B}^0_s$ and B_c^- mesons as well as for b baryon decays.

In the charm sector, D^0–$\overline{D}^0$ mixing is now well-established and the emphasis has shifted to searching for *CP* violation. Measurements of 49 observables from the E791, FOCUS, Belle, *BABAR*, CLEO, BESIII, CDF, and LHCb experiments are input into a global fit for 10 underlying parameters, and the no-mixing hypothesis is excluded at a confidence level $> 11.5\sigma$. The mixing parameters x and y individually differ from zero by 1.9σ and 9.4σ, respectively. The world average value for the observable y_{CP} is positive, indicating that the *CP*-even state is shorter-lived as in the K^0–$\overline{K}^0$ system. The *CP* violation parameters $|q/p|$ and ϕ are consistent with the no-*CP* violation hypothesis within 1σ. Thus there is no evidence for *CP* violation arising from mixing ($|q/p| \neq 1$) or from a phase difference between the mixing amplitude and a direct decay amplitude ($\phi \neq 0$). In addition, the most recent data indicates no direct *CP* violation in $D^0 \to K^+K^-/\pi^+\pi^-$ decays; performing a global fit to all relevant measurements gives $\Delta a_{CP}^{\rm dir} = (-0.134 \pm 0.070)\%$. The world's most precise measurements of $|V_{cd}|$ and $|V_{cs}|$ are obtained from leptonic $D^+ \to \mu^+\nu$ and $D_s^+ \to \mu^+\nu/\tau^+\nu$ decays, respectively. These measurements have theoretical uncertainties arising from decay constants. However, calculations of decay constants within lattice QCD have improved such that the theory error is $< 1/3$ the experimental errors of the measurements.

Since 2016, HFAG provides the τ branching fraction fit averages for the PDG Review of Particle Physics. For the PDG, a unitarity constrained variant of the fit is performed, using only inputs that are published and included in the PDG. Two preliminary results used in the HFAG 2014 report have been removed both in the HFAG and in the PDG variants of the fit. A few minor imperfections of the 2014 fit have been corrected. There are no non-negligible changes to the lepton universality tests and to the $|V_{us}|$ determinations from the τ branching fractions. There is still a large discrepancy between $|V_{us}|$ from τ, $|V_{us}|$ from kaons and $|V_{us}|$ from $|V_{ud}|$ and CKM matrix unitarity, but there has been progress in the understanding of the theory at the base of the "$\tau \to s\nu$ inclusive" determination of $|V_{us}|$ and the related theory systematic uncertainty, which provides an explanation for the observed discrepancy. Just one more τ lepton-flavour-violating branching fraction upper limit has been published, and there are no changes to the combined upper limits.

11 Acknowledgments

We are grateful for the strong support of the ATLAS, *BABAR*, Belle, BES, CLEO, CDF, CMS, D0 and LHCb collaborations, without whom this compilation of results and world averages would not have been possible. The success of these experiments in turn would not have been possible without the excellent operations of the CESR, PEP-II, KEKB, Tevatron, BEPC and LHC accelerators, and fruitful collaborations between the accelerator groups and the experiments. We also recognise the interplay between theoretical and experimental communities that has provided a stimulus for many of the measurements in this document.

Our averages and this compilation have benefitted greatly from contributions to the Heavy Flavor Averaging Group from numerous individuals. We especially thank David Kirkby, Yoshihide Sakai, Simon Eidelman, Soeren Prell, and Gianluca Cavoto for their past leadership of HFAG. We are grateful to Paolo Gambino and Bob Kowalewski for assistance with averages that appear in Chapter 5; to Ruslan Chistov, Lawrence Gibbons, Bostjan Golob, and Milind Purohit for significant contributions to Chapter 8; and to Michel Davier for providing valuable input to Chapter 9. We also acknowledge the computing resources and support provided to HFAG by SLAC.

References

[1] N. Cabibbo, Phys. Rev. Lett. **10**, 531 (1963).

[2] M. Kobayashi and T. Maskawa, Prog. Theor. Phys. **49**, 652 (1973).

[3] D. Abbaneo *et al.* (ALEPH, CDF, DELPHI, L3, OPAL, and SLD collaborations), arXiv:hep-ex/0009052 (2000), CERN-EP-2000-096; arXiv:hep-ex/0112028 (2001), CERN-EP-2001-050.

[4] Y. Amhis *et al.* (Heavy Flavor Averaging Group), arXiv:1412.7515 [hep-ex] (2014).

[5] C. Patrignani *et al.* (Particle Data Group), Chin. Phys. **C40**, 100001 (2016).

[6] B. Aubert *et al.* (*BABAR* collaboration), Phys. Rev. Lett. **94**, 141801 (2005), arXiv:hep-ex/0412062 [hep-ex].

[7] B. Aubert *et al.* (*BABAR* collaboration), Phys. Rev. **D65**, 032001 (2002), arXiv:hep-ex/0107025.

[8] B. Aubert *et al.* (*BABAR* collaboration), Phys. Rev. **D69**, 071101 (2004), arXiv:hep-ex/0401028.

[9] J. P. Alexander *et al.* (CLEO collaboration), Phys. Rev. Lett. **86**, 2737 (2001), arXiv:hep-ex/0006002.

[10] S. B. Athar *et al.* (CLEO collaboration), Phys. Rev. **D66**, 052003 (2002), arXiv:hep-ex/0202033.

[11] N. C. Hastings *et al.* (Belle collaboration), Phys. Rev. **D67**, 052004 (2003), arXiv:hep-ex/0212033.

[12] B. Aubert *et al.* (*BABAR* collaboration), Phys. Rev. Lett. **95**, 042001 (2005), arXiv:hep-ex/0504001.

[13] B. Aubert *et al.* (*BABAR* collaboration), Phys. Rev. Lett. **96**, 232001 (2006), arXiv:hep-ex/0604031; A. Sokolov *et al.* (Belle collaboration), Phys. Rev. **D75**, 071103 (2007), arXiv:hep-ex/0611026; B. Aubert *et al.* (*BABAR* collaboration), Phys. Rev. **D78**, 112002 (2008), arXiv:0807.2014 [hep-ex].

[14] B. Barish *et al.* (CLEO collaboration), Phys. Rev. Lett. **76**, 1570 (1996).

[15] A. Drutskoy *et al.* (Belle collaboration), Phys. Rev. **D81**, 112003 (2010), arXiv:1003.5885 [hep-ex].

[16] G. S. Huang *et al.* (CLEO collaboration), Phys. Rev. **D75**, 012002 (2007), arXiv:hep-ex/0610035; this supersedes the results of Ref. [19].

[17] A. Drutskoy *et al.* (Belle collaboration), Phys. Rev. Lett. **98**, 052001 (2007), arXiv:hep-ex/0608015.

[18] S. Esen *et al.* (Belle collaboration), Phys. Rev. **D87**, 031101 (2013), arXiv:1208.0323.

[19] M. Artuso *et al.* (CLEO collaboration), Phys. Rev. Lett. **95**, 261801 (2005), arXiv:hep-ex/0508047.

[20] K. F. Chen *et al.* (Belle collaboration), Phys. Rev. Lett. **100**, 112001 (2008), arXiv:0710.2577 [hep-ex].

[21] A. Garmash *et al.* (Belle collaboration), Phys. Rev. **D91**, 072003 (2015), arXiv:1403.0992 [hep-ex]; this supersedes the $\Upsilon(nS)\pi^+\pi^-$ $(n = 1, 2, 3)$ results of Ref. [20].

[22] I. Adachi *et al.* (Belle collaboration), Phys. Rev. Lett. **108**, 032001 (2012), arXiv:1103.3419 [hep-ex].

[23] P. Krokovny *et al.* (Belle collaboration), Phys. Rev. **D88**, 052016 (2013), arXiv:1308.2646 [hep-ex].

[24] R. Louvot, PhD thesis #5213, EPFL, Lausanne, 2012, http://dx.doi.org/10.5075/epfl-thesis-5213.

[25] J. P. Lees *et al.* (*BABAR* collaboration), Phys. Rev. **D85**, 011101 (2012), arXiv:1110.5600 [hep-ex].

[26] J. Li *et al.* (Belle collaboration), Phys. Rev. Lett. **106**, 121802 (2011), arXiv:1102.2759 [hep-ex].

[27] R. Louvot *et al.* (Belle collaboration), Phys. Rev. Lett. **102**, 021801 (2009), arXiv:0809.2526 [hep-ex].

[28] P. Abreu *et al.* (DELPHI collaboration), Phys. Lett. **B289**, 199 (1992); P. D. Acton *et al.* (OPAL collaboration), Phys. Lett. **B295**, 357 (1992); D. Buskulic *et al.* (ALEPH collaboration), Phys. Lett. **B361**, 221 (1995).

[29] P. Abreu *et al.* (DELPHI collaboration), Z. Phys. **C68**, 375 (1995).

[30] R. Barate *et al.* (ALEPH collaboration), Eur. Phys. J. **C2**, 197 (1998).

[31] D. Buskulic *et al.* (ALEPH collaboration), Phys. Lett. **B384**, 449 (1996).

[32] J. Abdallah *et al.* (DELPHI collaboration), Eur. Phys. J. **C44**, 299 (2005), arXiv:hep-ex/0510023.

[33] P. Abreu *et al.* (DELPHI collaboration), Z. Phys. **C68**, 541 (1995).

[34] R. Barate *et al.* (ALEPH collaboration), Eur. Phys. J. **C5**, 205 (1998).

[35] J. Abdallah *et al.* (DELPHI collaboration), Phys. Lett. **B576**, 29 (2003), arXiv:hep-ex/0311005.

[36] T. Affolder *et al.* (CDF collaboration), Phys. Rev. Lett. **84**, 1663 (2000), arXiv:hep-ex/9909011.

[37] T. Aaltonen *et al.* (CDF collaboration), Phys. Rev. **D77**, 072003 (2008), arXiv:0801.4375 [hep-ex].

[38] T. Aaltonen *et al.* (CDF collaboration), Phys. Rev. **D79**, 032001 (2009), arXiv:0810.3213 [hep-ex].

[39] F. Abe *et al.* (CDF collaboration), Phys. Rev. **D60**, 092005 (1999).

[40] CDF collaboration, CDF note 10795, 2012, http://www-cdf.fnal.gov/physics/new/bottom/120420.blessed-BsJPsiPhi-BR/.

[41] V. M. Abazov *et al.* (D0 collaboration), Phys. Rev. Lett. **99**, 052001 (2007), arXiv:0706.1690 [hep-ex].

[42] V. M. Abazov *et al.* (D0 collaboration), Phys. Rev. Lett. **101**, 232002 (2008), arXiv:0808.4142 [hep-ex].

[43] T. Aaltonen *et al.* (CDF collaboration), Phys. Rev. **D80**, 072003 (2009), arXiv:0905.3123 [hep-ex].

[44] R. Aaij *et al.* (LHCb collaboration), Phys. Rev. **D85**, 032008 (2012), arXiv:1111.2357 [hep-ex]; the full covariance matrix of the measurements is available at https://cdsweb.cern.ch/record/1390838.

[45] R. Aaij *et al.* (LHCb collaboration), JHEP **04**, 001 (2013), arXiv:1301.5286 [hep-ex]; the numerical results and their full covariance matrix are available at http://cdsweb.cern.ch/record/1507868; this replaces R. Aaij *et al.* (LHCb collaboration), Phys. Rev. Lett. **107**, 211801 (2011), arXiv:1106.4435 [hep-ex].

[46] R. Aaij *et al.* (LHCb collaboration), JHEP **08**, 143 (2014), arXiv:1405.6842 [hep-ex].

[47] G. Aad *et al.* (ATLAS collaboration), Phys. Rev. Lett. **115**, 262001 (2015), arXiv:1507.08925 [hep-ex].

[48] X. Liu, W. Wang, and Y. Xie, Phys. Rev. **D89**, 094010 (2014), arXiv:1309.0313 [hep-ph].

[49] S. Schael *et al.* (ALEPH, CDF, DELPHI, L3, OPAL, and SLD collaborations, LEP electroweak working group, SLD electroweak and heavy flavour working groups), Phys. Rept. **427**, 257 (2006), arXiv:hep-ex/0509008; we use the $\langle x_E \rangle_b$ average given in Eq. 5.18 of this paper, as well as the $\overline{\chi}$ average of Eq. 5.39, obtained from a 10-parameter global fit of all electroweak data where the asymmetry measurements have been excluded.

[50] V. M. Abazov *et al.* (D0 collaboration), Phys. Rev. **D74**, 092001 (2006), arXiv:hep-ex/0609014.

[51] D. Acosta *et al.* (CDF collaboration), Phys. Rev. **D69**, 012002 (2004), arXiv:hep-ex/0309030; this supersedes the $\overline{\chi}$ value of Ref. [213].

[52] CDF collaboration, CDF note 10335, 2011, http://www-cdf.fnal.gov/physics/new/bottom/110127.blessed-chibar/.

[53] LHCb collaboration, LHCb-CONF-2013-011, 2013, https://cdsweb.cern.ch/record/1559262.

[54] M. Shifman, arXiv:hep-ph/0009131 [hep-ph] (2000).

[55] M. A. Shifman and M. B. Voloshin, Sov. Phys. JETP **64**, 698 (1986); J. Chay, H. Georgi, and B. Grinstein, Phys. Lett. **B247**, 399 (1990); I. I. Bigi, N. G. Uraltsev, and A. I. Vainshtein, Phys. Lett. **B293**, 430 (1992), arXiv:hep-ph/9207214, Erratum ibid. **B297**, 477 (1992).

[56] I. I. Bigi, arXiv:hep-ph/9508408 (1995); G. Bellini, I. I. Bigi, and P. J. Dornan, Phys. Rept. **289**, 1 (1997).

[57] M. Ciuchini, E. Franco, V. Lubicz, and F. Mescia, Nucl. Phys. **B625**, 211 (2002), arXiv:hep-ph/0110375; M. Beneke, G. Buchalla, C. Greub, A. Lenz, and U. Nierste, Nucl. Phys. **B639**, 389 (2002), arXiv:hep-ph/0202106; E. Franco, V. Lubicz, F. Mescia, and C. Tarantino, Nucl. Phys. **B633**, 212 (2002), arXiv:hep-ph/0203089.

[58] C. Tarantino, Eur. Phys. J. **C33**, s895 (2004), arXiv:hep-ph/0310241; F. Gabbiani, A. I. Onishchenko, and A. A. Petrov, Phys. Rev. **D68**, 114006 (2003), arXiv:hep-ph/0303235.

[59] F. Gabbiani, A. I. Onishchenko, and A. A. Petrov, Phys. Rev. **D70**, 094031 (2004), arXiv:hep-ph/0407004.

[60] A. Lenz, Int. J. Mod. Phys. **A30**, 1543005 (2015); A. Lenz, arXiv:1405.3601 [hep-ph] (2014).

[61] L. Di Ciaccio *et al.* (1996), internal note by former B lifetime working group, http://lepbosc.web.cern.ch/LEPBOSC/lifetimes/ps/final_blife.ps.

[62] D. Buskulic *et al.* (ALEPH collaboration), Phys. Lett. **B314**, 459 (1993).

[63] P. Abreu *et al.* (DELPHI collaboration), Z. Phys. **C63**, 3 (1994).

[64] P. Abreu *et al.* (DELPHI collaboration), Phys. Lett. **B377**, 195 (1996).

[65] J. Abdallah *et al.* (DELPHI collaboration), Eur. Phys. J. **C33**, 307 (2004), arXiv:hep-ex/0401025.

[66] M. Acciarri *et al.* (L3 collaboration), Phys. Lett. **B416**, 220 (1998).

[67] K. Ackerstaff *et al.* (OPAL collaboration), Z. Phys. **C73**, 397 (1997).

[68] K. Abe *et al.* (SLD collaboration), Phys. Rev. Lett. **75**, 3624 (1995), arXiv:hep-ex/9511005.

[69] D. Buskulic *et al.* (ALEPH collaboration), Phys. Lett. **B369**, 151 (1996).

[70] P. D. Acton *et al.* (OPAL collaboration), Z. Phys. **C60**, 217 (1993).

[71] F. Abe *et al.* (CDF collaboration), Phys. Rev. **D57**, 5382 (1998).

[72] ATLAS collaboration, ATLAS-CONF-2011-145, 2011, https://cdsweb.cern.ch/record/1389455.

[73] R. Barate *et al.* (ALEPH collaboration), Phys. Lett. **B492**, 275 (2000), arXiv:hep-ex/0008016.

[74] D. Buskulic *et al.* (ALEPH collaboration), Z. Phys. **C71**, 31 (1996).

[75] P. Abreu *et al.* (DELPHI collaboration), Z. Phys. **C68**, 13 (1995).

[76] W. Adam *et al.* (DELPHI collaboration), Z. Phys. **C68**, 363 (1995).

[77] P. Abreu *et al.* (DELPHI collaboration), Z. Phys. **C74**, 19 (1997).

[78] M. Acciarri *et al.* (L3 collaboration), Phys. Lett. **B438**, 417 (1998).

[79] R. Akers *et al.* (OPAL collaboration), Z. Phys. **C67**, 379 (1995).

[80] G. Abbiendi *et al.* (OPAL collaboration), Eur. Phys. J. **C12**, 609 (2000), arXiv:hep-ex/9901017.

[81] G. Abbiendi *et al.* (OPAL collaboration), Phys. Lett. **B493**, 266 (2000), arXiv:hep-ex/0010013.

[82] K. Abe *et al.* (SLD collaboration), Phys. Rev. Lett. **79**, 590 (1997).

[83] F. Abe *et al.* (CDF collaboration), Phys. Rev. **D58**, 092002 (1998), arXiv:hep-ex/9806018.

[84] D. E. Acosta *et al.* (CDF collaboration), Phys. Rev. **D65**, 092009 (2002).

[85] T. Aaltonen *et al.* (CDF collaboration), Phys. Rev. Lett. **106**, 121804 (2011), arXiv:1012.3138 [hep-ex]; these results replace the $\Lambda_b \to J/\psi\Lambda$ and $B^0 \to J/\psi K_S$ lifetime measurements of A. Abulencia *et al.* (CDF collaboration), Phys. Rev. Lett. **98**, 122001 (2007), arXiv:hep-ex/0609021, as well as the $B^0 \to J/\psi K^{*0}$ lifetime measurement of Ref. [312].

[86] V. M. Abazov *et al.* (D0 collaboration), Phys. Rev. Lett. **102**, 032001 (2009), arXiv:0810.0037 [hep-ex]; this replaces V. M. Abazov *et al.* (D0 collaboration), Phys. Rev. Lett. **95**, 171801 (2005), arXiv:hep-ex/0507084.

[87] V. M. Abazov *et al.* (D0 collaboration), Phys. Rev. **D85**, 112003 (2012), arXiv:1204.2340 [hep-ex]; this replaces V. M. Abazov *et al.* (D0 collaboration), Phys. Rev. Lett. **99**, 142001 (2007), arXiv:0704.3909 [hep-ex]; and V. M. Abazov *et al.* (D0 collaboration), Phys. Rev. Lett. **94**, 102001 (2005), arXiv:hep-ex/0410054.

[88] V. M. Abazov *et al.* (D0 collaboration), Phys. Rev. Lett. **114**, 062001 (2015), arXiv:1410.1568 [hep-ex]; this replaces V. M. Abazov *et al.* (D0 collaboration), Phys. Rev. Lett. **97**, 241801 (2006), arXiv:hep-ex/0604046.

[89] B. Aubert *et al.* (*BABAR* collaboration), Phys. Rev. Lett. **87**, 201803 (2001), arXiv:hep-ex/0107019.

[90] B. Aubert *et al.* (*BABAR* collaboration), Phys. Rev. Lett. **89**, 011802 (2002), arXiv:hep-ex/0202005, Erratum ibid. **89**, 169903 (2002).

[91] B. Aubert *et al.* (*BABAR* collaboration), Phys. Rev. **D67**, 072002 (2003), arXiv:hep-ex/0212017.

[92] B. Aubert *et al.* (*BABAR* collaboration), Phys. Rev. **D67**, 091101 (2003), arXiv:hep-ex/0212012.

[93] B. Aubert *et al.* (*BABAR* collaboration), Phys. Rev. **D73**, 012004 (2006), arXiv:hep-ex/0507054.

[94] K. Abe *et al.* (Belle collaboration), Phys. Rev. **D71**, 072003 (2005), arXiv:hep-ex/0408111.

[95] G. Aad *et al.* (ATLAS collaboration), Phys. Rev. **D87**, 032002 (2013), arXiv:1207.2284 [hep-ex].

[96] R. Aaij *et al.* (LHCb collaboration), JHEP **04**, 114 (2014), arXiv:1402.2554 [hep-ex].

[97] R. Aaij *et al.* (LHCb collaboration), Phys. Lett. **B736**, 446 (2014), arXiv:1406.7204 [hep-ex]; the $B_s^0 \to K^+K^-$ effective lifetime measurement replaces R. Aaij *et al.* (LHCb collaboration), Phys. Lett. **B716**, 393 (2012), arXiv:1207.5993 [hep-ex].

[98] T. Aaltonen *et al.* (CDF collaboration), Phys. Rev. **D83**, 032008 (2011), arXiv:1004.4855 [hep-ex].

[99] V. M. Abazov *et al.* (D0 collaboration), Phys. Rev. Lett. **94**, 182001 (2005), arXiv:hep-ex/0410052.

[100] CDF collaboration, CDF note 7514, 2005,
http://www-cdf.fnal.gov/physics/new/bottom/050224.blessed-bsemi-life/.

[101] CDF collaboration, CDF note 7386, 2005,
http://www-cdf.fnal.gov/physics/new/bottom/050303.blessed-bhadlife/.

[102] ATLAS collaboration, ATLAS-CONF-2011-092, 2011,
https://cdsweb.cern.ch/record/1363779.

[103] T. Jubb, M. Kirk, A. Lenz, and G. Tetlalmatzi-Xolocotzi, arXiv:1603.07770 [hep-ph] (2016); M. Artuso, G. Borissov, and A. Lenz, Rev. Mod. Phys. **88**, 045002 (2016), arXiv:1511.09466 [hep-ph]; these theory predictions are updates of the results of Ref. [104].

[104] A. Lenz and U. Nierste, arXiv:1102.4274 [hep-ph] (2011); and of A. Lenz and U. Nierste, JHEP **06**, 072 (2007), arXiv:hep-ph/0612167.

[105] M. Beneke, G. Buchalla, C. Greub, A. Lenz, and U. Nierste, Phys. Lett. **B459**, 631 (1999), arXiv:hep-ph/9808385.

[106] R. Aaij *et al.* (LHCb collaboration), Phys. Rev. Lett. **108**, 241801 (2012), arXiv:1202.4717 [hep-ex].

[107] R. Fleischer and R. Knegjens, Eur. Phys. J. **C71**, 1789 (2011), arXiv:1109.5115 [hep-ph].

[108] R. Barate *et al.* (ALEPH collaboration), Eur. Phys. J. **C4**, 367 (1998).

[109] P. Abreu *et al.* (DELPHI collaboration), Eur. Phys. J. **C18**, 229 (2000), arXiv:hep-ex/0105077.

[110] K. Ackerstaff *et al.* (OPAL collaboration), Eur. Phys. J. **C2**, 407 (1998), arXiv:hep-ex/9708023.

[111] D. Buskulic *et al.* (ALEPH collaboration), Phys. Lett. **B377**, 205 (1996).

[112] F. Abe *et al.* (CDF collaboration), Phys. Rev. **D59**, 032004 (1999), arXiv:hep-ex/9808003.

[113] P. Abreu *et al.* (DELPHI collaboration), Eur. Phys. J. **C16**, 555 (2000), arXiv:hep-ex/0107077.

[114] K. Ackerstaff *et al.* (OPAL collaboration), Phys. Lett. **B426**, 161 (1998), arXiv:hep-ex/9802002.

[115] T. Aaltonen *et al.* (CDF collaboration), Phys. Rev. Lett. **107**, 272001 (2011), arXiv:1103.1864 [hep-ex]; we consider that these results supersede those from the old CDF note 7386 [101], although the lifetime analysis of one of the modes ($B_s \to D_s\pi\pi\pi$) has not been updated.

[116] R. Aaij *et al.* (LHCb collaboration), Phys. Rev. Lett. **112**, 111802 (2014), arXiv:1312.1217 [hep-ex].

[117] R. Aaij *et al.* (LHCb collaboration), Phys. Rev. Lett. **113**, 172001 (2014), arXiv:1407.5873 [hep-ex].

[118] V. M. Abazov *et al.* (D0 collaboration), Phys. Rev. Lett. **94**, 042001 (2005), arXiv:hep-ex/0409043.

[119] R. Barate *et al.* (ALEPH collaboration), Phys. Lett. **B486**, 286 (2000).

[120] R. Aaij *et al.* (LHCb collaboration), Phys. Lett. **B707**, 349 (2012), arXiv:1111.0521 [hep-ex].

[121] R. Aaij *et al.* (LHCb collaboration), Phys. Lett. **B762**, 484 (2016), arXiv:1607.06314 [hep-ex].

[122] R. Aaij *et al.* (LHCb collaboration), Nucl. Phys. **B873**, 275 (2013), arXiv:1304.4500 [hep-ex].

[123] T. Aaltonen *et al.* (CDF collaboration), Phys. Rev. **D84**, 052012 (2011), arXiv:1106.3682 [hep-ex].

[124] V. M. Abazov *et al.* (D0 collaboration), Phys. Rev. **D94**, 012001 (2016), arXiv:1603.01302 [hep-ex].

[125] R. Aaij *et al.* (LHCb collaboration), Phys. Rev. **D87**, 112010 (2013), arXiv:1304.2600 [hep-ex]; this supersedes the following publications, R. Aaij *et al.* (LHCb collaboration), Phys. Rev. Lett. **108**, 101803 (2012), arXiv:1112.3183 [hep-ex]; R. Aaij *et al.* (LHCb collaboration), Phys. Lett. **B713**, 378 (2012), arXiv:1204.5675 [hep-ex]; R. Aaij *et al.* (LHCb collaboration), Phys. Lett. **B707**, 497 (2012), arXiv:1112.3056 [hep-ex]; this also replaces the $B_s^0 \to J/\psi\, f_0(980)$ result of R. Aaij *et al.* (LHCb collaboration), Phys. Rev. Lett. **109**, 152002 (2012), arXiv:1207.0878 [hep-ex].

[126] K. Hartkorn and H. G. Moser, Eur. Phys. J. **C8**, 381 (1999).

[127] R. Aaij *et al.* (LHCb collaboration), Phys. Lett. **B739**, 218 (2014), arXiv:1408.0275 [hep-ex].

[128] CDF collaboration, CDF note 7757, 2005, http://www-cdf.fnal.gov/physics/new/bottom/050707.blessed-bs-semi_life/.

[129] CDF collaboration, CDF note 8524, 2007, http://www-cdf.fnal.gov/physics/new/bottom/061130.blessed-bh-lifetime_v2/; all these preliminary results are superseded by Ref. [85, 312] except those on $B_s^0 \to J/\psi\phi$.

[130] D. Tonelli (for the CDF collaboration), arXiv:hep-ex/0605038 (2006).

[131] F. Abe *et al.* (CDF collaboration), Phys. Rev. Lett. **81**, 2432 (1998), arXiv:hep-ex/9805034.

[132] CDF collaboration, CDF note 9294, 2008, http://www-cdf.fnal.gov/physics/new/bottom/080327.blessed-BC_LT_SemiLeptonic/.

[133] A. Abulencia *et al.* (CDF collaboration), Phys. Rev. Lett. **97**, 012002 (2006), arXiv:hep-ex/0603027.

[134] V. M. Abazov *et al.* (D0 collaboration), Phys. Rev. Lett. **102**, 092001 (2009), arXiv:0805.2614 [hep-ex].

[135] T. Aaltonen *et al.* (CDF collaboration), Phys. Rev. **D87**, 011101 (2013), arXiv:1210.2366 [hep-ex].

[136] R. Aaij *et al.* (LHCb collaboration), Eur. Phys. J. **C74**, 2839 (2014), arXiv:1401.6932 [hep-ex].

[137] R. Aaij *et al.* (LHCb collaboration), Phys. Lett. **B742**, 29 (2015), arXiv:1411.6899 [hep-ex].

[138] P. Abreu *et al.* (DELPHI collaboration), Eur. Phys. J. **C10**, 185 (1999).

[139] P. Abreu *et al.* (DELPHI collaboration), Z. Phys. **C71**, 199 (1996).

[140] R. Akers *et al.* (OPAL collaboration), Z. Phys. **C69**, 195 (1996).

[141] F. Abe *et al.* (CDF collaboration), Phys. Rev. Lett. **77**, 1439 (1996).

[142] V. M. Abazov *et al.* (D0 collaboration), Phys. Rev. Lett. **99**, 182001 (2007), arXiv:0706.2358 [hep-ex].

[143] T. Aaltonen *et al.* (CDF collaboration), Phys. Rev. Lett. **104**, 102002 (2010), arXiv:0912.3566 [hep-ex].

[144] T. A. Aaltonen *et al.* (CDF collaboration), Phys. Rev. **D89**, 072014 (2014), arXiv:1403.8126 [hep-ex]; this replaces the $\Lambda_b \to J/\psi\,\Lambda$ lifetime result of Ref. [85], as well as the $\Xi_b^- \to J/\psi\,\Xi^-$ and $\Omega_b^- \to J/\psi\,\Omega^-$ lifetime results of Ref. [43].

[145] S. Chatrchyan *et al.* (CMS collaboration), JHEP **07**, 163 (2013), arXiv:1304.7495 [hep-ex].

[146] R. Aaij *et al.* (LHCb collaboration), Phys. Lett. **B734**, 122 (2014), arXiv:1402.6242 [hep-ex]; this replaces R. Aaij *et al.* (LHCb collaboration), Phys. Rev. Lett. **111**, 102003 (2013), arXiv:1307.2476 [hep-ex].

[147] R. Aaij *et al.* (LHCb collaboration), Phys. Lett. **B736**, 154 (2014), arXiv:1405.1543 [hep-ex].

[148] R. Aaij *et al.* (LHCb collaboration), Phys. Rev. Lett. **113**, 242002 (2014), arXiv:1409.8568 [hep-ex].

[149] R. Aaij *et al.* (LHCb collaboration), Phys. Rev. Lett. **113**, 032001 (2014), arXiv:1405.7223 [hep-ex].

[150] R. Aaij *et al.* (LHCb collaboration), Phys. Rev. **D93**, 092007 (2016), arXiv:1604.01412 [hep-ex].

[151] M. Beneke, G. Buchalla, and I. Dunietz, Phys. Rev. **D54**, 4419 (1996), arXiv:hep-ph/9605259; Y.-Y. Keum and U. Nierste, Phys. Rev. **D57**, 4282 (1998), arXiv:hep-ph/9710512.

[152] M. B. Voloshin, Phys. Rept. **320**, 275 (1999), arXiv:hep-ph/9901445; B. Guberina, B. Melic, and H. Stefancic, Phys. Lett. **B469**, 253 (1999), arXiv:hep-ph/9907468; M. Neubert and C. T. Sachrajda, Nucl. Phys. **B483**, 339 (1997), arXiv:hep-ph/9603202; I. I. Bigi, M. A. Shifman, and N. Uraltsev, Ann. Rev. Nucl. Part. Sci. **47**, 591 (1997), arXiv:hep-ph/9703290 [hep-ph].

[153] N. G. Uraltsev, Phys. Lett. **B376**, 303 (1996), arXiv:hep-ph/9602324; D. Pirjol and N. Uraltsev, Phys. Rev. **D59**, 034012 (1999), arXiv:hep-ph/9805488; P. Colangelo and F. De Fazio, Phys. Lett. **B387**, 371 (1996), arXiv:hep-ph/9604425; M. Di Pierro, C. T. Sachrajda, and C. Michael (UKQCD collaboration), Phys. Lett. **B468**, 143 (1999), arXiv:hep-lat/9906031.

[154] D. Buskulic *et al.* (ALEPH collaboration), Z. Phys. **C75**, 397 (1997).

[155] P. Abreu *et al.* (DELPHI collaboration), Z. Phys. **C76**, 579 (1997).

[156] J. Abdallah *et al.* (DELPHI collaboration), Eur. Phys. J. **C28**, 155 (2003), arXiv:hep-ex/0303032.

[157] M. Acciarri *et al.* (L3 collaboration), Eur. Phys. J. **C5**, 195 (1998).

[158] K. Ackerstaff *et al.* (OPAL collaboration), Z. Phys. **C76**, 417 (1997), arXiv:hep-ex/9707010.

[159] K. Ackerstaff *et al.* (OPAL collaboration), Z. Phys. **C76**, 401 (1997), arXiv:hep-ex/9707009.

[160] G. Alexander *et al.* (OPAL collaboration), Z. Phys. **C72**, 377 (1996).

[161] F. Abe *et al.* (CDF collaboration), Phys. Rev. Lett. **80**, 2057 (1998), arXiv:hep-ex/9712004; and Phys. Rev. **D59**, 032001 (1999), arXiv:hep-ex/9806026.

[162] F. Abe *et al.* (CDF collaboration), Phys. Rev. **D60**, 051101 (1999).

[163] F. Abe *et al.* (CDF collaboration), Phys. Rev. **D60**, 072003 (1999), arXiv:hep-ex/9903011.

[164] T. Affolder *et al.* (CDF collaboration), Phys. Rev. **D60**, 112004 (1999), arXiv:hep-ex/9907053.

[165] V. M. Abazov *et al.* (D0 collaboration), Phys. Rev. **D74**, 112002 (2006), arXiv:hep-ex/0609034.

[166] B. Aubert *et al.* (*BABAR* collaboration), Phys. Rev. Lett. **88**, 221802 (2002), arXiv:hep-ex/0112044; B. Aubert *et al.* (*BABAR* collaboration), Phys. Rev. **D66**, 032003 (2002), arXiv:hep-ex/0201020.

[167] B. Aubert *et al.* (*BABAR* collaboration), Phys. Rev. Lett. **88**, 221803 (2002), arXiv:hep-ex/0112045.

[168] Y. Zheng *et al.* (Belle collaboration), Phys. Rev. **D67**, 092004 (2003), arXiv:hep-ex/0211065.

[169] LHCb collaboration, LHCb-CONF-2011-010, 2011, https://cdsweb.cern.ch/record/1331124; this result has been published in Ref. [207].

[170] R. Aaij *et al.* (LHCb collaboration), Phys. Lett. **B719**, 318 (2013), arXiv:1210.6750 [hep-ex].

[171] R. Aaij *et al.* (LHCb collaboration), Eur. Phys. J. **C73**, 2655 (2013), arXiv:1308.1302 [hep-ex].

[172] R. Aaij *et al.* (LHCb collaboration), Eur. Phys. J. **C76**, 412 (2016), arXiv:1604.03475 [hep-ex].

[173] CDF collaboration, CDF note 8235, 2006, http://www-cdf.fnal.gov/physics/new/bottom/060406.blessed-semi_B0mix/.

[174] CDF collaboration, CDF note 7920, 2005, http://www-cdf.fnal.gov/physics/new/bottom/050804.hadr_B0mix/.

[175] H. Albrecht *et al.* (ARGUS collaboration), Z. Phys. **C55**, 357 (1992); H. Albrecht *et al.* (ARGUS collaboration), Phys. Lett. **B324**, 249 (1994).

[176] J. E. Bartelt *et al.* (CLEO collaboration), Phys. Rev. Lett. **71**, 1680 (1993).

[177] B. H. Behrens *et al.* (CLEO collaboration), Phys. Lett. **B490**, 36 (2000), arXiv:hep-ex/0005013.

[178] B. Aubert *et al.* (*BABAR* collaboration), Phys. Rev. Lett. **92**, 181801 (2004), arXiv:hep-ex/0311037; and Phys. Rev. **D70**, 012007 (2004), arXiv:hep-ex/0403002.

[179] T. Higuchi *et al.* (Belle collaboration), Phys. Rev. **D85**, 071105 (2012), arXiv:1203.0930 [hep-ex].

[180] T. Gershon, J. Phys. **G38**, 015007 (2011), arXiv:1007.5135 [hep-ph].

[181] M. Aaboud *et al.* (ATLAS collaboration), JHEP **06**, 081 (2016), arXiv:1605.07485 [hep-ex].

[182] J. Charles *et al.* (CKMfitter group), Phys. Rev. **D84**, 033005 (2011), arXiv:1106.4041 [hep-ph], with updated results and plots available at , http://ckmfitter.in2p3.fr; similar results are obtained by M. Bona *et al.* (UTfit collaboration), JHEP **10**, 081 (2006), arXiv:hep-ph/0606167, with updated results and plots available at , http://www.utfit.org.

[183] V. M. Abazov *et al.* (D0 collaboration), Phys. Rev. **D89**, 012002 (2014), arXiv:1310.0447 [hep-ex]; this updates V. M. Abazov *et al.* (D0 collaboration), Phys. Rev. **D84**, 052007 (2011), arXiv:1106.6308 [hep-ex]; which replaces V. M. Abazov *et al.* (D0 collaboration), Phys. Rev. **D82**, 032001 (2010), arXiv:1005.2757 [hep-ex]; as well as V. M. Abazov *et al.* (D0 collaboration), Phys. Rev. Lett. **105**, 081801 (2010), arXiv:1007.0395 [hep-ex]; these papers also supersede the search for CP violation in B^0 mixing of Ref. [50].

[184] U. Nierste, "Effect of $\Delta\Gamma$ on the dimuon asymmetry in B decays", presented at the 8th International Workshop on the CKM unitarity Triangle (CKM 2014), 2014.

[185] T. Aaltonen *et al.* (CDF collaboration), Phys. Rev. Lett. **109**, 171802 (2012), arXiv:1208.2967 [hep-ex]; this replaces T. Aaltonen *et al.* (CDF collaboration), Phys. Rev. **D85**, 072002 (2012), arXiv:1112.1726 [hep-ex]; as well as T. Aaltonen *et al.* (CDF collaboration), Phys. Rev. Lett. **100**, 161802 (2008), arXiv:0712.2397 [hep-ex]; and T. Aaltonen *et al.* (CDF collaboration), Phys. Rev. Lett. **100**, 121803 (2008), arXiv:0712.2348 [hep-ex].

[186] V. M. Abazov *et al.* (D0 collaboration), Phys. Rev. **D85**, 032006 (2012), arXiv:1109.3166 [hep-ex]; this replaces Ref. [86] and V. M. Abazov *et al.* (D0 collaboration), Phys. Rev. Lett. **101**, 241801 (2008), arXiv:0802.2255 [hep-ex]; as well as V. M. Abazov *et al.* (D0 collaboration), Phys. Rev. Lett. **98**, 121801 (2007), arXiv:hep-ex/0701012.

[187] G. Aad *et al.* (ATLAS collaboration), Phys. Rev. **D90**, 052007 (2014), arXiv:1407.1796 [hep-ex]; G. Aad *et al.* (ATLAS collaboration), JHEP **12**, 072 (2012), arXiv:1208.0572 [hep-ex].

[188] G. Aad *et al.* (ATLAS collaboration), JHEP **08**, 147 (2016), arXiv:1601.03297 [hep-ex].

[189] CMS collaboration, CMS-PAS-BPH-11-006, 2012, https://cds.cern.ch/record/1484686.

[190] V. Khachatryan *et al.* (CMS collaboration), Phys. Lett. **B757**, 97 (2016), arXiv:1507.07527 [hep-ex].

[191] R. Aaij *et al.* (LHCb collaboration), Phys. Rev. Lett. **114**, 041801 (2015), arXiv:1411.3104 [hep-ex]; this replaces any $B_s^0 \to J/\psi\, K^+K^-$, $B_s^0 \to J/\psi\, \phi$ or combined $\phi_s^{c\bar{c}s}$ result from Ref. [125].

[192] R. Aaij *et al.* (LHCb collaboration), Phys. Lett. **B762**, 253 (2016), arXiv:1608.04855 [hep-ex].

[193] S. Esen *et al.* (Belle collaboration), Phys. Rev. Lett. **105**, 201802 (2010), arXiv:1005.5177 [hep-ex].

[194] V. Abazov *et al.* (D0 collaboration), Phys. Rev. Lett. **102**, 091801 (2009), arXiv:0811.2173 [hep-ex].

[195] T. Aaltonen *et al.* (CDF collaboration), Phys. Rev. Lett. **100**, 021803 (2008).

[196] V. M. Abazov *et al.* (D0 collaboration), Phys. Rev. Lett. **99**, 241801 (2007), arXiv:hep-ex/0702049.

[197] A. Heister *et al.* (ALEPH collaboration), Eur. Phys. J. **C29**, 143 (2003).

[198] F. Abe *et al.* (CDF collaboration), Phys. Rev. Lett. **82**, 3576 (1999).

[199] J. Abdallah *et al.* (DELPHI collaboration), Eur. Phys. J. **C35**, 35 (2004), arXiv:hep-ex/0404013.

[200] G. Abbiendi *et al.* (OPAL collaboration), Eur. Phys. J. **C11**, 587 (1999), arXiv:hep-ex/9907061.

[201] G. Abbiendi *et al.* (OPAL collaboration), Eur. Phys. J. **C19**, 241 (2001), arXiv:hep-ex/0011052.

[202] K. Abe *et al.* (SLD collaboration), Phys. Rev. **D67**, 012006 (2003), arXiv:hep-ex/0209002.

[203] K. Abe *et al.* (SLD collaboration), Phys. Rev. **D66**, 032009 (2002), arXiv:hep-ex/0207048.

[204] K. Abe *et al.* (SLD collaboration), arXiv:hep-ex/0012043 (2000).

[205] A. Abulencia *et al.* (CDF collaboration), Phys. Rev. Lett. **97**, 242003 (2006), arXiv:hep-ex/0609040; this supersedes A. Abulencia *et al.* (CDF collaboration), Phys. Rev. Lett. **97**, 062003 (2006), arXiv:hep-ex/0606027.

[206] D0 collaboration, D0 note 5618-CONF v1.2, 2008, http://www-d0.fnal.gov/Run2Physics/WWW/results/prelim/B/B54/; D0 collaboration, D0 note 5474-CONF, 2007, http://www-d0.fnal.gov/Run2Physics/WWW/results/prelim/B/B51/; D0 collaboration, D0 note 5254-CONF, 2006, http://www-d0.fnal.gov/Run2Physics/WWW/results/prelim/B/B46/; these three notes supersede any previous preliminary results from D0 and replace V. M. Abazov *et al.* (D0 collaboration), Phys. Rev. Lett. **97**, 021802 (2006), arXiv:hep-ex/0603029.

[207] R. Aaij *et al.* (LHCb collaboration), Phys. Lett. **B709**, 177 (2012), arXiv:1112.4311 [hep-ex].

[208] R. Aaij *et al.* (LHCb collaboration), New J. Phys. **15**, 053021 (2013), arXiv:1304.4741 [hep-ex].

[209] A. Bazavov *et al.* (Fermilab Lattice, MILC collaboration), Phys. Rev. **D93**, 113016 (2016), arXiv:1602.03560 [hep-lat].

[210] S. Aoki *et al.*, arXiv:1607.00299 [hep-lat] (2016), see also http://itpwiki.unibe.ch/flag/.

[211] D. E. Jaffe *et al.* (CLEO collaboration), Phys. Rev. Lett. **86**, 5000 (2001), arXiv:hep-ex/0101006; this replaces the dilepton asymmetry measurement of Ref. [176].

[212] J. P. Lees *et al.* (*BABAR* collaboration), Phys. Rev. Lett. **114**, 081801 (2015), arXiv:1411.1842 [hep-ex]; this time-independent analysis replaces the time-dependent analysis of Ref. [217].

[213] F. Abe *et al.* (CDF collaboration), Phys. Rev. **D55**, 2546 (1997).

[214] CDF collaboration, CDF note 9015, 2007, http://www-cdf.fnal.gov/physics/new/bottom/070816.blessed-acp-bsemil/.

[215] R. Barate *et al.* (ALEPH collaboration), Eur. Phys. J. **C20**, 431 (2001).

[216] J. P. Lees *et al.* (*BABAR* collaboration), Phys. Rev. Lett. **111**, 101802 (2013), arXiv:1305.1575 [hep-ex]; this replaces M. Margoni (on behalf of the *BABAR* collaboration), arXiv:1301.0417 [hep-ex] (2013); and B. Aubert *et al.* (*BABAR* collaboration), arXiv:hep-ex/0607091 (2006).

[217] B. Aubert *et al.* (*BABAR* collaboration), Phys. Rev. Lett. **96**, 251802 (2006), arXiv:hep-ex/0603053; this is superseded by Ref. [212] and replaces B. Aubert *et al.* (*BABAR* collaboration), Phys. Rev. Lett. **88**, 231801 (2002), arXiv:hep-ex/0202041.

[218] E. Nakano *et al.* (Belle collaboration), Phys. Rev. **D73**, 112002 (2006), arXiv:hep-ex/0505017.

[219] M. Beneke, G. Buchalla, and I. Dunietz, Phys. Lett. **B393**, 132 (1997), arXiv:hep-ph/9609357; I. Dunietz, Eur. Phys. J. **C7**, 197 (1999), arXiv:hep-ph/9806521.

[220] V. M. Abazov *et al.* (D0 collaboration), Phys. Rev. **D86**, 072009 (2012), arXiv:1208.5813 [hep-ex].

[221] R. Aaij *et al.* (LHCb collaboration), Phys. Rev. Lett. **114**, 041601 (2015), arXiv:1409.8586 [hep-ex].

[222] Y. Amhis *et al.* (Heavy Flavor Averaging Group), arXiv:1207.1158 [hep-ex] (2012).

[223] V. Abazov *et al.* (D0 collaboration), Phys. Rev. Lett. **110**, 011801 (2013), arXiv:1207.1769 [hep-ex]; this replaces V. M. Abazov *et al.* (D0 collaboration), Phys. Rev. **D82**, 012003 (2010), arXiv:0904.3907 [hep-ex]; and also V. M. Abazov *et al.* (D0 collaboration), Phys. Rev. Lett. **98**, 151801 (2007), arXiv:hep-ex/0701007.

[224] R. Aaij *et al.* (LHCb collaboration), Phys. Rev. Lett. **117**, 061803 (2016), arXiv:1605.09768 [hep-ex]; this replaces R. Aaij *et al.* (LHCb collaboration), Phys. Lett. **B728**, 607 (2014), arXiv:1308.1048 [hep-ex].

[225] S. Descotes-Genon and J. F. Kamenik, Phys. Rev. **D87**, 074036 (2013), arXiv:1207.4483 [hep-ph], Erratum ibid. **D92**, 079903 (2015).

[226] M. Aaboud *et al.* (ATLAS collaboration), arXiv:1610.07869 [hep-ex] (2016).

[227] M. Beneke, G. Buchalla, A. Lenz, and U. Nierste, Phys. Lett. **B576**, 173 (2003), arXiv:hep-ph/0307344.

[228] R. Aaij *et al.* (LHCb collaboration), Phys. Lett. **B736**, 186 (2014), arXiv:1405.4140 [hep-ex]; this replaces any $B_s^0 \to J/\psi\,\pi^+\pi^-$ or $B_s^0 \to J/\psi\, f_0(980)$ result on *CP* violation from Ref. [125].

[229] R. Aaij *et al.* (LHCb collaboration), Phys. Rev. **D86**, 052006 (2012), arXiv:1204.5643 [hep-ex].

[230] R. Aaij *et al.* (LHCb collaboration), Phys. Rev. Lett. **113**, 211801 (2014), arXiv:1409.4619 [hep-ex].

[231] L.-L. Chau and W.-Y. Keung, Phys. Rev. Lett. **53**, 1802 (1984).

[232] L. Wolfenstein, Phys. Rev. Lett. **51**, 1945 (1983).

[233] A. J. Buras, M. E. Lautenbacher, and G. Ostermaier, Phys. Rev. **D50**, 3433 (1994), arXiv:hep-ph/9403384.

[234] C. Jarlskog, Phys. Rev. Lett. **55**, 1039 (1985).

[235] C. Jarlskog, Phys. Lett. **B615**, 207 (2005), arXiv:hep-ph/0503199.

[236] J. D. Bjorken, P. F. Harrison, and W. G. Scott, Phys. Rev. **D74**, 073012 (2006), arXiv:hep-ph/0511201.

[237] P. F. Harrison, S. Dallison, and W. G. Scott, Phys. Lett. **B680**, 328 (2009), arXiv:0904.3077 [hep-ph].

[238] P. H. Frampton and X.-G. He, Phys. Lett. **B688**, 67 (2010), arXiv:1003.0310 [hep-ph].

[239] P. H. Frampton and X.-G. He, Phys. Rev. **D82**, 017301 (2010), arXiv:1004.3679 [hep-ph].

[240] J. Charles *et al.*, Eur. Phys. J. **C41**, 1 (2005), arXiv:hep-ph/0406184, see also online updates, http://ckmfitter.in2p3.fr/.

[241] B. Aubert *et al.* (*BABAR* collaboration), Phys. Rev. Lett. **86**, 2515 (2001), arXiv:hep-ex/0102030.

[242] K. Abe *et al.* (Belle collaboration), Phys. Rev. Lett. **87**, 091802 (2001), arXiv:hep-ex/0107061.

[243] A. B. Carter and A. I. Sanda, Phys. Rev. **D23**, 1567 (1981).

[244] I. I. Y. Bigi and A. I. Sanda, Nucl. Phys. **B193**, 85 (1981).

[245] I. Dunietz, R. Fleischer, and U. Nierste, Phys. Rev. **D63**, 114015 (2001), arXiv:hep-ph/0012219.

[246] R. Aaij *et al.* (LHCb collaboration), Phys. Lett. **B742**, 38 (2015), arXiv:1411.1634 [hep-ex].

[247] B. Aubert *et al.* (*BABAR* collaboration), Phys. Rev. **D79**, 032002 (2009), arXiv:0808.1866 [hep-ex].

[248] P. Krokovny *et al.* (Belle collaboration), Phys. Rev. Lett. **97**, 081801 (2006), arXiv:hep-ex/0605023.

[249] B. Aubert *et al.* (*BABAR* collaboration), Phys. Rev. Lett. **99**, 231802 (2007), arXiv:0708.1544 [hep-ex].

[250] V. Vorobyev *et al.* (Belle collaboration), Phys. Rev. **D94**, 052004 (2016), arXiv:1607.05813 [hep-ex].

[251] J. Libby *et al.* (CLEO collaboration), Phys. Rev. **D82**, 112006 (2010), arXiv:1010.2817 [hep-ex].

[252] T. E. Browder, A. Datta, P. J. O'Donnell, and S. Pakvasa, Phys. Rev. **D61**, 054009 (2000), arXiv:hep-ph/9905425.

[253] B. Aubert *et al.* (*BABAR* collaboration), Phys. Rev. **D74**, 091101 (2006), arXiv:hep-ex/0608016 [hep-ex].

[254] J. Dalseno *et al.* (Belle collaboration), Phys. Rev. **D76**, 072004 (2007), arXiv:0706.2045 [hep-ex].

[255] R. Aaij *et al.* (LHCb collaboration), Phys. Rev. **D90**, 012003 (2014), arXiv:1404.5673 [hep-ex].

[256] J. R. Pelaez, Phys. Rept. **658**, 1 (2016), arXiv:1510.00653 [hep-ph].

[257] B. Aubert *et al.* (*BABAR* collaboration), Phys. Rev. Lett. **99**, 161802 (2007), arXiv:0706.3885 [hep-ex].

[258] Y. Nakahama *et al.* (Belle collaboration), Phys. Rev. **D82**, 073011 (2010), arXiv:1007.3848 [hep-ex].

[259] J. P. Lees *et al.* (*BABAR* collaboration), Phys. Rev. **D85**, 112010 (2012), arXiv:1201.5897 [hep-ex].

[260] A. Garmash *et al.* (Belle collaboration), Phys. Rev. **D71**, 092003 (2005), arXiv:hep-ex/0412066.

[261] B. Aubert *et al.* (*BABAR* collaboration), Phys. Rev. **D74**, 032003 (2006), arXiv:hep-ex/0605003 [hep-ex].

[262] B. Aubert *et al.* (*BABAR* collaboration), Phys. Rev. **D80**, 112001 (2009), arXiv:0905.3615 [hep-ex].

[263] J. Dalseno *et al.* (Belle collaboration), Phys. Rev. **D79**, 072004 (2009), arXiv:0811.3665 [hep-ex].

[264] A. Garmash *et al.* (Belle collaboration), Phys. Rev. Lett. **96**, 251803 (2006), arXiv:hep-ex/0512066.

[265] B. Aubert *et al.* (*BABAR* collaboration), Phys. Rev. **D72**, 072003 (2005), arXiv:hep-ex/0507004.

[266] B. Aubert *et al.* (*BABAR* collaboration), Phys. Rev. **D78**, 012004 (2008), arXiv:0803.4451 [hep-ex].

[267] A. E. Snyder and H. R. Quinn, Phys. Rev. **D48**, 2139 (1993).

[268] H. R. Quinn and J. P. Silva, Phys. Rev. **D62**, 054002 (2000), arXiv:hep-ph/0001290.

[269] B. Aubert *et al.* (*BABAR* collaboration), Phys. Rev. **D76**, 012004 (2007), arXiv:hep-ex/0703008.

[270] J. P. Lees *et al.* (*BABAR* collaboration), Phys. Rev. **D88**, 012003 (2013), arXiv:1304.3503 [hep-ex].

[271] A. Kusaka *et al.* (Belle collaboration), Phys. Rev. Lett. **98**, 221602 (2007), arXiv:hep-ex/0701015.

[272] A. Kusaka *et al.* (Belle collaboration), Phys. Rev. **D77**, 072001 (2008), arXiv:0710.4974 [hep-ex].

[273] B. Aubert *et al.* (*BABAR* collaboration), Phys. Rev. Lett. **99**, 071801 (2007), arXiv:0705.1190 [hep-ex].

[274] T. Aushev *et al.* (Belle collaboration), Phys. Rev. Lett. **93**, 201802 (2004), arXiv:hep-ex/0408051.

[275] M. Rohrken *et al.* (Belle collaboration), Phys. Rev. **D85**, 091106 (2012), arXiv:1203.6647 [hep-ex].

[276] B. Aubert *et al.* (*BABAR* collaboration), Phys. Rev. Lett. **91**, 201802 (2003), arXiv:hep-ex/0306030.

[277] C. C. Wang *et al.* (Belle collaboration), Phys. Rev. Lett. **94**, 121801 (2005), arXiv:hep-ex/0408003.

[278] B. Aubert *et al.* (*BABAR* collaboration), Phys. Rev. **D73**, 111101 (2006), arXiv:hep-ex/0602049.

[279] B. Aubert *et al.* (*BABAR* collaboration), Phys. Rev. **D71**, 112003 (2005), arXiv:hep-ex/0504035.

[280] O. Long, M. Baak, R. N. Cahn, and D. Kirkby, Phys. Rev. **D68**, 034010 (2003), arXiv:hep-ex/0303030.

[281] S. Bahinipati *et al.* (Belle collaboration), Phys. Rev. **D84**, 021101 (2011), arXiv:1102.0888 [hep-ex].

[282] F. J. Ronga *et al.* (Belle collaboration), Phys. Rev. **D73**, 092003 (2006), arXiv:hep-ex/0604013.

[283] R. Fleischer, Nucl. Phys. **B671**, 459 (2003), arXiv:hep-ph/0304027.

[284] R. Aaij *et al.* (LHCb collaboration), JHEP **11**, 060 (2014), arXiv:1407.6127 [hep-ex].

[285] D. Atwood, M. Gronau, and A. Soni, Phys. Rev. Lett. **79**, 185 (1997), arXiv:hep-ph/9704272.

[286] D. Atwood, T. Gershon, M. Hazumi, and A. Soni, Phys. Rev. **D71**, 076003 (2005), arXiv:hep-ph/0410036.

[287] B. Grinstein, Y. Grossman, Z. Ligeti, and D. Pirjol, Phys. Rev. **D71**, 011504 (2005), arXiv:hep-ph/0412019.

[288] B. Grinstein and D. Pirjol, Phys. Rev. **D73**, 014013 (2006), arXiv:hep-ph/0510104.

[289] M. Matsumori and A. I. Sanda, Phys. Rev. **D73**, 114022 (2006), arXiv:hep-ph/0512175.

[290] P. Ball and R. Zwicky, Phys. Lett. **B642**, 478 (2006), arXiv:hep-ph/0609037.

[291] F. Muheim, Y. Xie, and R. Zwicky, Phys. Lett. **B664**, 174 (2008), arXiv:0802.0876 [hep-ph].

[292] I. I. Y. Bigi and A. I. Sanda, Phys. Lett. **B211**, 213 (1988).

[293] M. Gronau and D. London., Phys. Lett. **B253**, 483 (1991).

[294] M. Gronau and D. Wyler, Phys. Lett. **B265**, 172 (1991).

[295] D. Atwood, I. Dunietz, and A. Soni, Phys. Rev. Lett. **78**, 3257 (1997), arXiv:hep-ph/9612433.

[296] D. Atwood, I. Dunietz, and A. Soni, Phys. Rev. **D63**, 036005 (2001), arXiv:hep-ph/0008090.

[297] A. Giri, Y. Grossman, A. Soffer, and J. Zupan, Phys. Rev. **D68**, 054018 (2003), arXiv:hep-ph/0303187.

[298] A. Poluektov *et al.* (Belle collaboration), Phys. Rev. **D70**, 072003 (2004), arXiv:hep-ex/0406067.

[299] A. Bondar and T. Gershon, Phys. Rev. **D70**, 091503 (2004), arXiv:hep-ph/0409281.

[300] D. Atwood and A. Soni, Phys. Rev. **D68**, 033003 (2003), arXiv:hep-ph/0304085.

[301] Y. Grossman, Z. Ligeti, and A. Soffer, Phys. Rev. **D67**, 071301 (2003), arXiv:hep-ph/0210433 [hep-ph].

[302] M. Nayak *et al.*, Phys. Lett. **B740**, 1 (2014), arXiv:1410.3964 [hep-ex].

[303] M. Gronau, Phys. Lett. **B557**, 198 (2003), arXiv:hep-ph/0211282.

[304] T. Gershon, Phys. Rev. **D79**, 051301 (2009), arXiv:0810.2706 [hep-ph].

[305] T. Gershon and M. Williams, Phys. Rev. **D80**, 092002 (2009), arXiv:0909.1495 [hep-ph].

[306] A. Bondar and A. Poluektov, Eur. Phys. J. **C47**, 347 (2006), arXiv:hep-ph/0510246.

[307] A. Bondar and A. Poluektov, Eur. Phys. J. **C55**, 51 (2008), arXiv:0801.0840 [hep-ex].

[308] T. Gershon, J. Libby, and G. Wilkinson, Phys. Lett. **B750**, 338 (2015), arXiv:1506.08594 [hep-ph].

[309] B. Aubert *et al.* (*BABAR* collaboration), Phys. Rev. Lett. **99**, 251801 (2007), arXiv:hep-ex/0703037.

[310] B. Aubert *et al.* (*BABAR* collaboration), Phys. Rev. **D76**, 031102 (2007), arXiv:0704.0522 [hep-ex].

[311] R. Itoh *et al.* (Belle collaboration), Phys. Rev. Lett. **95**, 091601 (2005), arXiv:hep-ex/0504030 [hep-ex].

[312] D. Acosta *et al.* (CDF collaboration), Phys. Rev. Lett. **94**, 101803 (2005), arXiv:hep-ex/0412057.

[313] R. Aaij *et al.* (LHCb collaboration), Phys. Rev. **D88**, 052002 (2013), arXiv:1307.2782 [hep-ex].

[314] K. Olive *et al.* (Particle Data Group), Chin. Phys. **C38**, 090001 (2014).

[315] M. Jung, Phys. Rev. **D86**, 053008 (2012), arXiv:1206.2050 [hep-ph].

[316] K. De Bruyn and R. Fleischer, JHEP **03**, 145 (2015), arXiv:1412.6834 [hep-ph].

[317] P. Frings, U. Nierste, and M. Wiebusch, Phys. Rev. Lett. **115**, 061802 (2015), arXiv:1503.00859 [hep-ph].

[318] B. Aubert *et al.* (*BABAR* collaboration), Phys. Rev. **D79**, 072009 (2009), arXiv:0902.1708 [hep-ex].

[319] B. Aubert *et al.* (*BABAR* collaboration), Phys. Rev. **D69**, 052001 (2004), arXiv:hep-ex/0309039.

[320] I. Adachi *et al.* (Belle collaboration), Phys. Rev. Lett. **108**, 171802 (2012), arXiv:1201.4643 [hep-ex].

[321] R. Barate *et al.* (ALEPH collaboration), Phys. Lett. **B492**, 259 (2000), arXiv:hep-ex/0009058.

[322] K. Ackerstaff *et al.* (OPAL collaboration), Eur. Phys. J. **C5**, 379 (1998), arXiv:hep-ex/9801022.

[323] A. A. Affolder *et al.* (CDF collaboration), Phys. Rev. **D61**, 072005 (2000), arXiv:hep-ex/9909003.

[324] R. Aaij *et al.* (LHCb collaboration), Phys. Rev. Lett. **115**, 031601 (2015), arXiv:1503.07089 [hep-ex].

[325] Y. Sato *et al.* (Belle collaboration), Phys. Rev. Lett. **108**, 171801 (2012), arXiv:1201.3502 [hep-ex].

[326] M. Bona *et al.* (UTfit collaboration), JHEP **07**, 028 (2005), arXiv:hep-ph/0501199, see also online updates, http://www.utfit.org/.

[327] E. Lunghi and A. Soni, Phys. Lett. **B666**, 162 (2008), arXiv:0803.4340 [hep-ph].

[328] G. Eigen, G. Dubois-Felsmann, D. Hitlin, and F. Porter, Phys. Rev. **D89**, 033004 (2014), arXiv:1301.5867 [hep-ex].

[329] I. Dunietz, H. R. Quinn, A. Snyder, W. Toki, and H. J. Lipkin, Phys. Rev. **D43**, 2193 (1991).

[330] D. Aston *et al.*, Nucl. Phys. **B296**, 493 (1988).

[331] M. Suzuki, Phys. Rev. **D64**, 117503 (2001), arXiv:hep-ph/0106354.

[332] B. Aubert *et al.* (*BABAR* collaboration), Phys. Rev. **D71**, 032005 (2005), arXiv:hep-ex/0411016.

[333] Y. Grossman and M. P. Worah, Phys. Lett. **B395**, 241 (1997), arXiv:hep-ph/9612269.

[334] R. Fleischer, Phys. Lett. **B562**, 234 (2003), arXiv:hep-ph/0301255.

[335] R. Fleischer, Nucl. Phys. **B659**, 321 (2003), arXiv:hep-ph/0301256.

[336] A. Abdesselam *et al.* (*BABAR* and Belle collaboration), Phys. Rev. Lett. **115**, 121604 (2015), arXiv:1505.04147 [hep-ex].

[337] A. Bondar, T. Gershon, and P. Krokovny, Phys. Lett. **B624**, 1 (2005), arXiv:hep-ph/0503174.

[338] F. Botella and J. Silva, Phys. Rev. **D71**, 094008 (2005), arXiv:hep-ph/0503136 [hep-ph].

[339] K. Vervink *et al.* (Belle collaboration), Phys. Rev. **D80**, 111104 (2009), arXiv:0901.4057 [hep-ex].

[340] B. Aubert *et al.* (*BABAR* collaboration), Phys. Rev. Lett. **101**, 021801 (2008), arXiv:0804.0896 [hep-ex].

[341] S. E. Lee *et al.* (Belle collaboration), Phys. Rev. **D77**, 071101 (2008), arXiv:0708.0304 [hep-ex].

[342] R. Aaij *et al.* (LHCb collaboration), arXiv:1608.06620 [hep-ex] (2016).

[343] J. P. Lees *et al.* (*BABAR* collaboration), Phys. Rev. **D86**, 112006 (2012), arXiv:1208.1282 [hep-ex].

[344] B. Kronenbitter *et al.* (Belle collaboration), Phys. Rev. **D86**, 071103 (2012), arXiv:1207.5611 [hep-ex].

[345] S. Fratina *et al.* (Belle collaboration), Phys. Rev. Lett. **98**, 221802 (2007), arXiv:hep-ex/0702031.

[346] R. Fleischer, Eur. Phys. J. **C10**, 299 (1999), arXiv:hep-ph/9903455 [hep-ph].

[347] K. De Bruyn, R. Fleischer, and P. Koppenburg, Eur. Phys. J. **C70**, 1025 (2010), arXiv:1010.0089 [hep-ph].

[348] R. Aaij *et al.* (LHCb collaboration), JHEP **06**, 131 (2015), arXiv:1503.07055 [hep-ex].

[349] R. Fleischer, Int. J. Mod. Phys. **A12**, 2459 (1997), arXiv:hep-ph/9612446.

[350] D. London and A. Soni, Phys. Lett. **B407**, 61 (1997), arXiv:hep-ph/9704277.

[351] M. Ciuchini, E. Franco, G. Martinelli, A. Masiero, and L. Silvestrini, Phys. Rev. Lett. **79**, 978 (1997), arXiv:hep-ph/9704274.

[352] T. Gershon and M. Hazumi, Phys. Lett. **B596**, 163 (2004), arXiv:hep-ph/0402097.

[353] Y. Grossman, Z. Ligeti, Y. Nir, and H. Quinn, Phys. Rev. **D68**, 015004 (2003), arXiv:hep-ph/0303171.

[354] M. Gronau and J. L. Rosner, Phys. Lett. **B564**, 90 (2003), arXiv:hep-ph/0304178.

[355] M. Gronau, Y. Grossman, and J. L. Rosner, Phys. Lett. **B579**, 331 (2004), arXiv:hep-ph/0310020.

[356] M. Gronau, J. L. Rosner, and J. Zupan, Phys. Lett. **B596**, 107 (2004), arXiv:hep-ph/0403287.

[357] H.-Y. Cheng, C.-K. Chua, and A. Soni, Phys. Rev. **D72**, 014006 (2005), arXiv:hep-ph/0502235.

[358] M. Gronau and J. L. Rosner, Phys. Rev. **D71**, 074019 (2005), arXiv:hep-ph/0503131.

[359] G. Buchalla, G. Hiller, Y. Nir, and G. Raz, JHEP **09**, 074 (2005), arXiv:hep-ph/0503151.

[360] M. Beneke, Phys. Lett. **B620**, 143 (2005), arXiv:hep-ph/0505075.

[361] G. Engelhard, Y. Nir, and G. Raz, Phys. Rev. **D72**, 075013 (2005), arXiv:hep-ph/0505194.

[362] H.-Y. Cheng, C.-K. Chua, and A. Soni, Phys. Rev. **D72**, 094003 (2005), arXiv:hep-ph/0506268.

[363] G. Engelhard and G. Raz, Phys. Rev. **D72**, 114017 (2005), arXiv:hep-ph/0508046.

[364] M. Gronau, J. L. Rosner, and J. Zupan, Phys. Rev. **D74**, 093003 (2006), arXiv:hep-ph/0608085.

[365] L. Silvestrini, Ann. Rev. Nucl. Part. Sci. **57**, 405 (2007), arXiv:0705.1624 [hep-ph].

[366] R. Dutta and S. Gardner, Phys. Rev. **D78**, 034021 (2008), arXiv:0805.1963 [hep-ph].

[367] M. Fujikawa *et al.* (Belle collaboration), Phys. Rev. **D81**, 011101 (2010), arXiv:0809.4366 [hep-ex].

[368] K. Abe *et al.* (Belle collaboration), Phys. Rev. **D76**, 091103 (2007), arXiv:hep-ex/0609006.

[369] B. Aubert *et al.* (*BABAR* collaboration), Phys. Rev. **D71**, 091102 (2005), arXiv:hep-ex/0502019.

[370] B. Aubert *et al.* (*BABAR* collaboration), Phys. Rev. **D79**, 052003 (2009), arXiv:0809.1174 [hep-ex].

[371] L. Šantelj *et al.* (Belle collaboration), JHEP **10**, 165 (2014), arXiv:1408.5991 [hep-ex].

[372] J. P. Lees *et al.* (*BABAR* collaboration), Phys. Rev. **D85**, 054023 (2012), arXiv:1111.3636 [hep-ex].

[373] K. F. Chen *et al.* (Belle collaboration), Phys. Rev. Lett. **98**, 031802 (2007), arXiv:hep-ex/0608039.

[374] V. Chobanova *et al.* (Belle collaboration), Phys. Rev. **D90**, 012002 (2014), arXiv:1311.6666 [hep-ex].

[375] B. Aubert *et al.* (*BABAR* collaboration), Phys. Rev. **D76**, 071101 (2007), arXiv:hep-ex/0702010.

[376] B. Aubert *et al.* (*BABAR* collaboration), Phys. Rev. **D78**, 092008 (2008), arXiv:0808.3586 [hep-ex].

[377] R. Fleischer, Phys. Lett. **B459**, 306 (1999), arXiv:hep-ph/9903456 [hep-ph].

[378] LHCb collaboration, LHCb-CONF-2016-018, 2016.

[379] R. Aaij *et al.* (LHCb collaboration), JHEP **10**, 183 (2013), arXiv:1308.1428 [hep-ex].

[380] R. Aaij *et al.* (LHCb collaboration), Phys. Lett. **B741**, 1 (2015), arXiv:1408.4368 [hep-ex].

[381] M. Raidal, Phys. Rev. Lett. **89**, 231803 (2002), arXiv:hep-ph/0208091 [hep-ph].

[382] R. Aaij *et al.* (LHCb collaboration), Phys. Rev. **D90**, 052011 (2014), arXiv:1407.2222 [hep-ex].

[383] B. Aubert *et al.* (*BABAR* collaboration), Phys. Rev. Lett. **97**, 171805 (2006), arXiv:hep-ex/0608036.

[384] Y. Nakahama *et al.* (Belle collaboration), Phys. Rev. Lett. **100**, 121601 (2008), arXiv:0712.4234 [hep-ex].

[385] S. Akar, PhD thesis, LPNHE, Université Pierre et Marie Curie - Paris VI, 2013, https://tel.archives-ouvertes.fr/tel-00998252.

[386] P. del Amo Sanchez *et al.* (*BABAR* collaboration), Phys. Rev. **D93**, 052013 (2016), arXiv:1512.03579 [hep-ex].

[387] J. Li *et al.* (Belle collaboration), Phys. Rev. Lett. **101**, 251601 (2008), arXiv:0806.1980 [hep-ex].

[388] B. Aubert *et al.* (*BABAR* collaboration), Phys. Rev. **D78**, 071102 (2008), arXiv:0807.3103 [hep-ex].

[389] Y. Ushiroda *et al.* (Belle collaboration), Phys. Rev. **D74**, 111104 (2006), arXiv:hep-ex/0608017.

[390] B. Aubert *et al.* (*BABAR* collaboration), Phys. Rev. **D79**, 011102 (2009), arXiv:0805.1317 [hep-ex].

[391] H. Sahoo *et al.* (Belle collaboration), Phys. Rev. **D84**, 071101 (2011), arXiv:1104.5590 [hep-ex].

[392] R. Aaij *et al.* (LHCb collaboration), arXiv:1609.02032 [hep-ex] (2016).

[393] Y. Ushiroda *et al.* (Belle collaboration), Phys. Rev. Lett. **100**, 021602 (2008), arXiv:0709.2769 [hep-ex].

[394] B. Aubert *et al.* (*BABAR* collaboration), Phys. Rev. **D76**, 052007 (2007), arXiv:0705.2157 [hep-ex].

[395] P. Vanhoefer *et al.* (Belle collaboration), Phys. Rev. **D93**, 032010 (2016), arXiv:1510.01245 [hep-ex].

[396] B. Aubert *et al.* (*BABAR* collaboration), Phys. Rev. **D78**, 071104 (2008), arXiv:0807.4977 [hep-ex].

[397] I. Adachi *et al.* (Belle collaboration), Phys. Rev. **D89**, 072008 (2014), arXiv:1212.4015 [hep-ex], Addendum ibid. **D89**, 119903 (2014).

[398] R. Aaij *et al.* (LHCb collaboration), Phys. Lett. **B747**, 468 (2015), arXiv:1503.07770 [hep-ex].

[399] B. Aubert *et al.* (*BABAR* collaboration), Phys. Rev. Lett. **98**, 181803 (2007), arXiv:hep-ex/0612050.

[400] B. Aubert *et al.* (*BABAR* collaboration), Phys. Rev. **D81**, 052009 (2010), arXiv:0909.2171 [hep-ex].

[401] J. P. Lees *et al.* (*BABAR* collaboration), Phys. Rev. **D87**, 052009 (2013), arXiv:1206.3525 [hep-ex].

[402] I. Adachi *et al.* (Belle collaboration), Phys. Rev. **D88**, 092003 (2013), arXiv:1302.0551 [hep-ex].

[403] J. Dalseno *et al.* (Belle collaboration), Phys. Rev. **D86**, 092012 (2012), arXiv:1205.5957 [hep-ex].

[404] M. Gronau and D. London, Phys. Rev. Lett. **65**, 3381 (1990).

[405] D. Asner *et al.* (Heavy Flavor Averaging Group), arXiv:1010.1589 [hep-ex] (2010).

[406] B. Aubert *et al.* (*BABAR* collaboration), Phys. Rev. Lett. **102**, 141802 (2009), arXiv:0901.3522 [hep-ex].

[407] H. J. Lipkin, Y. Nir, H. R. Quinn, and A. Snyder, Phys. Rev. **D44**, 1454 (1991).

[408] M. Gronau and J. Zupan, Phys. Rev. **D73**, 057502 (2006), arXiv:hep-ph/0512148.

[409] A. Bevan *et al.* (*BABAR* and Belle collaborations), Eur. Phys. J. **C74**, 3026 (2014), arXiv:1406.6311 [hep-ex].

[410] I. Dunietz, Phys. Lett. **B427**, 179 (1998), arXiv:hep-ph/9712401 [hep-ph].

[411] M.A. Baak, PhD thesis, Vrije U., Amsterdam, 2007, http://www-public.slac.stanford.edu/sciDoc/docMeta.aspx?slacPubNumber=slac-r-858.

[412] K. De Bruyn, R. Fleischer, R. Knegjens, M. Merk, M. Schiller, and N. Tuning, Nucl. Phys. **B868**, 351 (2013), arXiv:1208.6463 [hep-ph].

[413] M. Kenzie, M. Martinelli, and N. Tuning, Phys. Rev. **D94**, 054021 (2016), arXiv:1606.09129 [hep-ph].

[414] B. Aubert *et al.* (*BABAR* collaboration), Phys. Rev. **D77**, 071102 (2008), arXiv:0712.3469 [hep-ex].

[415] I. Dunietz and R. G. Sachs, Phys. Rev. **D37**, 3186 (1988), Erratum ibid. **D39**, 3515 (1989).

[416] R. Aleksan, I. Dunietz, and B. Kayser, Z. Phys. **C54**, 653 (1992).

[417] LHCb collaboration, LHCb-CONF-2016-015, 2016.

[418] J. Brod and J. Zupan, JHEP **01**, 051 (2014), arXiv:1308.5663 [hep-ph].

[419] P. del Amo Sanchez *et al.* (*BABAR* collaboration), Phys. Rev. **D82**, 072004 (2010), arXiv:1007.0504 [hep-ex].

[420] K. Abe *et al.* (Belle collaboration), Phys. Rev. **D73**, 051106 (2006), arXiv:hep-ex/0601032.

[421] T. Aaltonen *et al.* (CDF collaboration), Phys. Rev. **D81**, 031105 (2010), arXiv:0911.0425 [hep-ex].

[422] R. Aaij *et al.* (LHCb collaboration), Phys. Lett. **B760**, 117 (2016), arXiv:1603.08993 [hep-ex].

[423] B. Aubert *et al.* (*BABAR* collaboration), Phys. Rev. **D78**, 092002 (2008), arXiv:0807.2408 [hep-ex].

[424] B. Aubert *et al.* (*BABAR* collaboration), Phys. Rev. **D80**, 092001 (2009), arXiv:0909.3981 [hep-ex].

[425] LHCb collaboration, LHCb-CONF-2016-014, 2016.

[426] R. Aaij *et al.* (LHCb collaboration), Phys. Rev. **D92**, 112005 (2015), arXiv:1505.07044 [hep-ex].

[427] R. Aaij *et al.* (LHCb collaboration), Phys. Rev. **D90**, 112002 (2014), arXiv:1407.8136 [hep-ex].

[428] R. Aaij *et al.* (LHCb collaboration), Phys. Rev. **D93**, 112018 (2016), arXiv:1602.03455 [hep-ex].

[429] S. Malde *et al.*, Phys. Lett. **B747**, 9 (2015), arXiv:1504.05878 [hep-ex].

[430] R. Aaij *et al.* (LHCb collaboration), Phys. Rev. **D91**, 112014 (2015), arXiv:1504.05442 [hep-ex].

[431] P. del Amo Sanchez *et al.* (*BABAR* collaboration), Phys. Rev. **D82**, 072006 (2010), arXiv:1006.4241 [hep-ex].

[432] Y. Horii *et al.* (Belle collaboration), Phys. Rev. Lett. **106**, 231803 (2011), arXiv:1103.5951 [hep-ex].

[433] T. Aaltonen *et al.* (CDF collaboration), Phys. Rev. **D84**, 091504 (2011), arXiv:1108.5765 [hep-ex].

[434] J. P. Lees *et al.* (*BABAR* collaboration), Phys. Rev. **D84**, 012002 (2011), arXiv:1104.4472 [hep-ex].

[435] M. Nayak *et al.* (Belle collaboration), Phys. Rev. **D88**, 091104 (2013), arXiv:1310.1741 [hep-ex].

[436] B. Aubert *et al.* (*BABAR* collaboration), Phys. Rev. **D80**, 031102 (2009), arXiv:0904.2112 [hep-ex].

[437] K. Negishi *et al.* (Belle collaboration), Phys. Rev. **D86**, 011101 (2012), arXiv:1205.0422 [hep-ex].

[438] D. M. Asner *et al.* (CLEO collaboration), Phys. Rev. **D78**, 012001 (2008), arXiv:0802.2268 [hep-ex].

[439] N. Lowrey *et al.* (CLEO collaboration), Phys. Rev. **D80**, 031105 (2009), arXiv:0903.4853 [hep-ex].

[440] A. Poluektov *et al.* (Belle collaboration), Phys. Rev. **D81**, 112002 (2010), arXiv:1003.3360 [hep-ex].

[441] P. del Amo Sanchez *et al.* (*BABAR* collaboration), Phys. Rev. Lett. **105**, 121801 (2010), arXiv:1005.1096 [hep-ex].

[442] R. Aaij *et al.* (LHCb collaboration), Nucl. Phys. **B888**, 169 (2014), arXiv:1407.6211 [hep-ex].

[443] A. Poluektov *et al.* (Belle collaboration), Phys. Rev. **D73**, 112009 (2006), arXiv:hep-ex/0604054.

[444] R. Aaij *et al.* (LHCb collaboration), JHEP **08**, 137 (2016), arXiv:1605.01082 [hep-ex].

[445] B. Aubert *et al.* (*BABAR* collaboration), Phys. Rev. **D79**, 072003 (2009), arXiv:0805.2001 [hep-ex].

[446] R. A. Briere *et al.* (CLEO collaboration), Phys. Rev. **D80**, 032002 (2009), arXiv:0903.1681 [hep-ex].

[447] H. Aihara *et al.* (Belle collaboration), Phys. Rev. **D85**, 112014 (2012), arXiv:1204.6561 [hep-ex].

[448] R. Aaij *et al.* (LHCb collaboration), JHEP **10**, 97 (2014), arXiv:1408.2748 [hep-ex].

[449] K. Negishi *et al.* (Belle collaboration), PTEP **2016**, 043C01 (2016), arXiv:1509.01098 [hep-ex].

[450] R. Aaij *et al.* (LHCb collaboration), JHEP **06**, 131 (2016), arXiv:1604.01525 [hep-ex].

[451] R. Aaij *et al.* (LHCb collaboration), Phys. Lett. **B733**, 36 (2014), arXiv:1402.2982 [hep-ex].

[452] J. Insler *et al.* (CLEO collaboration), Phys. Rev. **D85**, 092016 (2012), arXiv:1203.3804 [hep-ex].

[453] J. P. Lees *et al.* (*BABAR* collaboration), Phys. Rev. **D87**, 052015 (2013), arXiv:1301.1029 [hep-ex].

[454] R. Aaij *et al.* (LHCb collaboration), arXiv:1611.03076 [hep-ex] (2016).

[455] M. Rama, Phys. Rev. **D89**, 014021 (2014), arXiv:1307.4384 [hep-ex].

[456] GammaCombo framework for combinations of measurements and computation of confidence intervals, CERN, http://gammacombo.hepforge.org/.

[457] R. Aaij *et al.* (LHCb collaboration), Phys. Lett. **B726**, 151 (2013), arXiv:1305.2050 [hep-ex].

[458] T. Evans, S. Harnew, J. Libby, S. Malde, J. Rademacker, and G. Wilkinson, Phys. Lett. **B757**, 520 (2016), arXiv:1602.07430 [hep-ex].

[459] R. Aaij *et al.* (LHCb collaboration), Phys. Rev. **D93**, 052018 (2016), arXiv:1509.06628 [hep-ex].

[460] J. P. Silva and A. Soffer, Phys. Rev. **D61**, 112001 (2000), arXiv:hep-ph/9912242 [hep-ph].

[461] Y. Grossman, A. Soffer, and J. Zupan, Phys. Rev. **D72**, 031501 (2005), arXiv:hep-ph/0505270 [hep-ph].

[462] I. Caprini, L. Lellouch, and M. Neubert, Nucl. Phys. **B530**, 153 (1998), arXiv:hep-ph/9712417.

[463] B semileptonic decays common input parameters, http://www.slac.stanford.edu/xorg/hfag/semi/summer16/common/common.param.summer16.

[464] N. E. Adam *et al.* (CLEO collaboration), Phys. Rev. **D67**, 032001 (2003), arXiv:hep-ex/0210040.

[465] B. Aubert *et al.* (*BABAR* collaboration), Phys. Rev. **D79**, 012002 (2009), arXiv:0809.0828 [hep-ex].

[466] B. Aubert *et al.* (*BABAR* collaboration), Phys. Rev. Lett. **100**, 231803 (2008), arXiv:0712.3493 [hep-ex].

[467] W. Dungel *et al.* (Belle collaboration), Phys. Rev. **D82**, 112007 (2010), arXiv:1010.5620 [hep-ex].

[468] B. Aubert *et al.* (*BABAR* collaboration), Phys. Rev. **D77**, 032002 (2008), arXiv:0705.4008 [hep-ex].

[469] D. Buskulic *et al.* (ALEPH collaboration), Phys. Lett. **B395**, 373 (1997).

[470] G. Abbiendi *et al.* (OPAL collaboration), Phys. Lett. **B482**, 15 (2000), arXiv:hep-ex/0003013.

[471] P. Abreu *et al.* (DELPHI collaboration), Phys. Lett. **B510**, 55 (2001), arXiv:hep-ex/0104026.

[472] J. Abdallah *et al.* (DELPHI collaboration), Eur. Phys. J. **C33**, 213 (2004), arXiv:hep-ex/0401023.

[473] J. A. Bailey *et al.*, Phys. Rev. **D89**, 114504 (2014), arXiv:1403.0635 [hep-lat].

[474] B. Aubert *et al.* (*BABAR* collaboration), Phys. Rev. Lett. **100**, 151802 (2008), arXiv:0712.3503 [hep-ex].

[475] J. E. Bartelt *et al.* (CLEO collaboration), Phys. Rev. Lett. **82**, 3746 (1999), arXiv:hep-ex/9811042.

[476] R. Glattauer *et al.* (Belle collaboration), Phys. Rev. **D93**, 032006 (2016), arXiv:1510.03657 [hep-ex].

[477] B. Aubert *et al.* (*BABAR* collaboration), Phys. Rev. Lett. **104**, 011802 (2010), arXiv:0904.4063 [hep-ex].

[478] J. A. Bailey *et al.* (MILC collaboration), Phys. Rev. **D92**, 034506 (2015), arXiv:1503.07237 [hep-lat].

[479] A. Sirlin, Nucl. Phys. **B196**, 83 (1982).

[480] D. Liventsev *et al.* (Belle collaboration), Phys. Rev. **D77**, 091503 (2008), arXiv:0711.3252 [hep-ex].

[481] N. Isgur and M. B. Wise, Phys. Rev. Lett. **66**, 1130 (1991).

[482] B. Aubert *et al.* (*BABAR* collaboration), Phys. Rev. Lett. **101**, 261802 (2008), arXiv:0808.0528 [hep-ex].

[483] D. Buskulic *et al.* (ALEPH collaboration), Z. Phys. **C73**, 601 (1997).

[484] G. Abbiendi *et al.* (OPAL collaboration), Eur. Phys. J. **C30**, 467 (2003), arXiv:hep-ex/0301018.

[485] A. Anastassov *et al.* (CLEO collaboration), Phys. Rev. Lett. **80**, 4127 (1998), arXiv:hep-ex/9708035.

[486] V. M. Abazov *et al.* (D0 collaboration), Phys. Rev. Lett. **95**, 171803 (2005), arXiv:hep-ex/0507046.

[487] B. Aubert *et al.* (*BABAR* collaboration), Phys. Rev. Lett. **103**, 051803 (2009), arXiv:0808.0333 [hep-ex].

[488] J. Abdallah *et al.* (DELPHI collaboration), Eur. Phys. J. **C45**, 35 (2006), arXiv:hep-ex/0510024.

[489] D. Benson, I. I. Bigi, T. Mannel, and N. Uraltsev, Nucl. Phys. **B665**, 367 (2003), arXiv:hep-ph/0302262.

[490] P. Gambino and N. Uraltsev, Eur. Phys. J. **C34**, 181 (2004), arXiv:hep-ph/0401063.

[491] P. Gambino, JHEP **09**, 055 (2011), arXiv:1107.3100 [hep-ph].

[492] A. Alberti, P. Gambino, K. J. Healey, and S. Nandi, Phys. Rev. Lett. **114**, 061802 (2015), arXiv:1411.6560 [hep-ph].

[493] C. W. Bauer, Z. Ligeti, M. Luke, A. V. Manohar, and M. Trott, Phys. Rev. **D70**, 094017 (2004), arXiv:hep-ph/0408002.

[494] B. Aubert *et al.* (*BABAR* collaboration), Phys. Rev. **D81**, 032003 (2010), arXiv:0908.0415 [hep-ex].

[495] B. Aubert *et al.* (*BABAR* collaboration), Phys. Rev. **D69**, 111104 (2004), arXiv:hep-ex/0403030.

[496] C. Schwanda *et al.* (Belle collaboration), Phys. Rev. **D75**, 032005 (2007), arXiv:hep-ex/0611044.

[497] P. Urquijo *et al.* (Belle collaboration), Phys. Rev. **D75**, 032001 (2007), arXiv:hep-ex/0610012.

[498] D. E. Acosta *et al.* (CDF collaboration), Phys. Rev. **D71**, 051103 (2005), arXiv:hep-ex/0502003.

[499] S. E. Csorna *et al.* (CLEO collaboration), Phys. Rev. **D70**, 032002 (2004), arXiv:hep-ex/0403052.

[500] K. Chetyrkin *et al.*, Phys. Rev. **D80**, 074010 (2009), arXiv:0907.2110 [hep-ph].

[501] B. Aubert *et al.* (*BABAR* collaboration), Phys. Rev. **D72**, 052004 (2005), arXiv:hep-ex/0508004.

[502] B. Aubert *et al.* (*BABAR* collaboration), Phys. Rev. Lett. **97**, 171803 (2006), arXiv:hep-ex/0607071 [hep-ex].

[503] A. Limosani *et al.* (Belle collaboration), Phys. Rev. Lett. **103**, 241801 (2009), arXiv:0907.1384 [hep-ex].

[504] S. Chen *et al.* (CLEO collaboration), Phys. Rev. Lett. **87**, 251807 (2001), arXiv:hep-ex/0108032 [hep-ex].

[505] P. Gambino and C. Schwanda, Phys. Rev. **D89**, 014022 (2014), arXiv:1307.4551 [hep-ph].

[506] C. Schwanda *et al.* (Belle collaboration), Phys. Rev. **D78**, 032016 (2008), arXiv:0803.2158 [hep-ex].

[507] R. Aaij *et al.* (LHCb collaboration), Nature Phys. **11**, 743 (2015), arXiv:1504.01568 [hep-ex].

[508] H. Ha *et al.* (Belle collaboration), Phys. Rev. **D83**, 071101 (2011), arXiv:1012.0090 [hep-ex].

[509] A. Sibidanov *et al.* (Belle collaboration), Phys. Rev. **D88**, 032005 (2013), arXiv:1306.2781 [hep-ex].

[510] P. del Amo Sanchez *et al.* (*BABAR* collaboration), Phys. Rev. **D83**, 032007 (2011), arXiv:1005.3288 [hep-ex].

[511] J. P. Lees *et al.* (*BABAR* collaboration), Phys. Rev. **D86**, 092004 (2012), arXiv:1208.1253 [hep-ex].

[512] C. Bourrely, I. Caprini, and L. Lellouch, Phys. Rev. **D79**, 013008 (2009), arXiv:0807.2722 [hep-ph], Erratum ibid. **D82**, 099902 (2010).

[513] A. Bharucha, JHEP **05**, 092 (2012), arXiv:1203.1359 [hep-ph].

[514] W. Detmold, C. Lehner, and S. Meinel, Phys. Rev. **D92**, 034503 (2015), arXiv:1503.01421 [hep-lat].

[515] R. N. Faustov and V. O. Galkin, Phys. Rev. **D94**, 073008 (2016), arXiv:1609.00199 [hep-ph].

[516] B. H. Behrens *et al.* (CLEO collaboration), Phys. Rev. **D61**, 052001 (2000), arXiv:hep-ex/9905056.

[517] N. E. Adam *et al.* (CLEO collaboration), Phys. Rev. Lett. **99**, 041802 (2007), arXiv:hep-ex/0703041.

[518] T. Hokuue *et al.* (Belle collaboration), Phys. Lett. **B648**, 139 (2007), arXiv:hep-ex/0604024.

[519] C. Schwanda *et al.* (Belle collaboration), Phys. Rev. Lett. **93**, 131803 (2004), arXiv:hep-ex/0402023 [hep-ex].

[520] J. P. Lees *et al.* (*BABAR* collaboration), Phys. Rev. **D87**, 032004 (2013), arXiv:1205.6245 [hep-ex].

[521] J. P. Lees *et al.* (*BABAR* collaboration), Phys. Rev. **D88**, 072006 (2013), arXiv:1308.2589 [hep-ex].

[522] R. Gray *et al.* (CLEO collaboration), Phys. Rev. **D76**, 012007 (2007), arXiv:hep-ex/0703042.

[523] B. Aubert *et al.* (*BABAR* collaboration), Phys. Rev. **D79**, 052011 (2009), arXiv:0808.3524 [hep-ex].

[524] B. Aubert *et al.* (*BABAR* collaboration), Phys. Rev. Lett. **101**, 081801 (2008), arXiv:0805.2408 [hep-ex].

[525] P. Urquijo *et al.* (Belle collaboration), Phys. Rev. Lett. **104**, 021801 (2010), arXiv:0907.0379 [hep-ex].

[526] J. P. Lees *et al.* (*BABAR* collaboration), Phys. Rev. **D86**, 032004 (2012), arXiv:1112.0702 [hep-ex].

[527] C. W. Bauer, Z. Ligeti, and M. E. Luke, Phys. Rev. **D64**, 113004 (2001), arXiv:hep-ph/0107074.

[528] M. Neubert, Phys. Rev. **D49**, 4623 (1994), arXiv:hep-ph/9312311.

[529] A. K. Leibovich, I. Low, and I. Z. Rothstein, Phys. Rev. **D61**, 053006 (2000), arXiv:hep-ph/9909404.

[530] B. O. Lange, M. Neubert, and G. Paz, JHEP **10**, 084 (2005), arXiv:hep-ph/0508178.

[531] B. Aubert *et al.* (*BABAR* collaboration), Phys. Rev. Lett. **96**, 221801 (2006), arXiv:hep-ex/0601046.

[532] V. B. Golubev, Y. I. Skovpen, and V. G. Luth, Phys. Rev. **D76**, 114003 (2007), arXiv:hep-ph/0702072.

[533] B. Aubert *et al.* (*BABAR* collaboration), Phys. Rev. **D73**, 012006 (2006), arXiv:hep-ex/0509040.

[534] R. V. Kowalewski and S. Menke, Phys. Lett. **B541**, 29 (2002), arXiv:hep-ex/0205038.

[535] B. Aubert *et al.* (*BABAR* collaboration), Phys. Rev. Lett. **95**, 111801 (2005), arXiv:hep-ex/0506036.

[536] A. Bornheim *et al.* (CLEO collaboration), Phys. Rev. Lett. **88**, 231803 (2002), arXiv:hep-ex/0202019.

[537] A. Limosani *et al.* (Belle collaboration), Phys. Lett. **B621**, 28 (2005), arXiv:hep-ex/0504046.

[538] H. Kakuno *et al.* (Belle collaboration), Phys. Rev. Lett. **92**, 101801 (2004), arXiv:hep-ex/0311048.

[539] I. Bizjak *et al.* (Belle collaboration), Phys. Rev. Lett. **95**, 241801 (2005), arXiv:hep-ex/0505088.

[540] B. O. Lange, M. Neubert, and G. Paz, Phys. Rev. **D72**, 073006 (2005), arXiv:hep-ph/0504071.

[541] S. W. Bosch, B. O. Lange, M. Neubert, and G. Paz, Nucl. Phys. **B699**, 335 (2004), arXiv:hep-ph/0402094.

[542] S. W. Bosch, M. Neubert, and G. Paz, JHEP **11**, 073 (2004), arXiv:hep-ph/0409115.

[543] M. Neubert, Eur. Phys. J. **C44**, 205 (2005), arXiv:hep-ph/0411027.

[544] M. Neubert, Phys. Lett. **B612**, 13 (2005), arXiv:hep-ph/0412241 [hep-ph].

[545] M. Neubert, Phys. Rev. **D72**, 074025 (2005), arXiv:hep-ph/0506245 [hep-ph].

[546] J. R. Andersen and E. Gardi, JHEP **01**, 097 (2006), arXiv:hep-ph/0509360.

[547] U. Aglietti, G. Ferrera, and G. Ricciardi, Nucl. Phys. **B768**, 85 (2007), arXiv:hep-ph/0608047.

[548] P. Gambino, P. Giordano, G. Ossola, and N. Uraltsev, JHEP **10**, 058 (2007), arXiv:0707.2493 [hep-ph].

[549] U. Aglietti, F. Di Lodovico, G. Ferrera, and G. Ricciardi, Eur. Phys. J. **C59**, 831 (2009), arXiv:0711.0860 [hep-ph].

[550] U. Aglietti, G. Ricciardi, and G. Ferrera, Phys. Rev. **D74**, 034004 (2006), arXiv:hep-ph/0507285.

[551] U. Aglietti, G. Ricciardi, and G. Ferrera, Phys. Rev. **D74**, 034005 (2006), arXiv:hep-ph/0509095.

[552] U. Aglietti, G. Ricciardi, and G. Ferrera, Phys. Rev. **D74**, 034006 (2006), arXiv:hep-ph/0509271.

[553] M. Duraisamy, P. Sharma, and A. Datta, Phys. Rev. **D90**, 074013 (2014), arXiv:1405.3719 [hep-ph].

[554] H. Na, C. M. Bouchard, G. P. Lepage, C. Monahan, and J. Shigemitsu (HPQCD collaboration), Phys. Rev. **D92**, 054510 (2015), arXiv:1505.03925 [hep-lat], Erratum ibid. **D93**, 119906 (2016).

[555] J. P. Lees *et al.* (*BABAR* collaboration), Phys. Rev. Lett. **109**, 101802 (2012), arXiv:1205.5442 [hep-ex].

[556] J. P. Lees *et al.* (*BABAR* collaboration), Phys. Rev. **D88**, 072012 (2013), arXiv:1303.0571 [hep-ex].

[557] J. F. Kamenik and F. Mescia, Phys. Rev. **D78**, 014003 (2008), arXiv:0802.3790 [hep-ph].

[558] S. Fajfer, J. F. Kamenik, and I. Nisandzic, Phys. Rev. **D85**, 094025 (2012), arXiv:1203.2654 [hep-ph].

[559] A. Matyja *et al.* (Belle collaboration), Phys. Rev. Lett. **99**, 191807 (2007), arXiv:0706.4429 [hep-ex].

[560] B. Aubert *et al.* (*BABAR* collaboration), Phys. Rev. Lett. **100**, 021801 (2008), arXiv:0709.1698 [hep-ex].

[561] I. Adachi *et al.* (Belle collaboration), arXiv:0910.4301 [hep-ex] (2009).

[562] A. Bozek *et al.* (Belle collaboration), Phys. Rev. **D82**, 072005 (2010), arXiv:1005.2302 [hep-ex].

[563] M. Huschle *et al.* (Belle collaboration), Phys. Rev. **D92**, 072014 (2015), arXiv:1507.03233 [hep-ex].

[564] R. Aaij *et al.* (LHCb collaboration), Phys. Rev. Lett. **115**, 111803 (2015), arXiv:1506.08614 [hep-ex], Addendum ibid. **115**, 159901 (2015).

[565] Y. Sato *et al.* (Belle collaboration), Phys. Rev. **D94**, 072007 (2016), arXiv:1607.07923 [hep-ex].

[566] A. Abdesselam *et al.* (2016), arXiv:1608.06391 [hep-ex].

[567] A. J. Lenz, J. Phys. **G41**, 103001 (2014), arXiv:1404.6197 [hep-ph].

[568] S. Choi *et al.* (Belle collaboration), Phys. Rev. Lett. **91**, 262001 (2003), arXiv:hep-ex/0309032 [hep-ex].

[569] R. Aaij *et al.* (LHCb collaboration), Phys. Rev. Lett. **110**, 222001 (2013), arXiv:1302.6269 [hep-ex].

[570] S. Choi *et al.* (Belle collaboration), Phys. Rev. Lett. **100**, 142001 (2008), arXiv:0708.1790 [hep-ex].

[571] R. Aaij *et al.* (LHCb collaboration), Phys. Rev. Lett. **112**, 222002 (2014), arXiv:1404.1903 [hep-ex].

[572] K. De Bruyn *et al.*, Phys. Rev. **D86**, 014027 (2012), arXiv:1204.1735 [hep-ph].

[573] S. Blyth *et al.* (Belle collaboration), Phys. Rev. **D74**, 092002 (2006), arXiv:hep-ex/0607029 [hep-ex].

[574] J. P. Lees *et al.* (*BABAR* collaboration), Phys. Rev. **D84**, 112007 (2011), arXiv:1107.5751 [hep-ex], Erratum ibid. **D87**, 039901 (2013).

[575] B. Aubert *et al.* (*BABAR* collaboration), Phys. Rev. **D75**, 031101 (2007), arXiv:hep-ex/0610027 [hep-ex].

[576] B. Aubert *et al.* (*BABAR* collaboration), Phys. Rev. **D74**, 111102 (2006), arXiv:hep-ex/0609033 [hep-ex].

[577] R. Aaij *et al.* (LHCb collaboration), Phys. Rev. **D92**, 032002 (2015), arXiv:1505.01710 [hep-ex].

[578] A. Satpathy *et al.* (Belle collaboration), Phys. Lett. **B553**, 159 (2003), arXiv:hep-ex/0211022 [hep-ex].

[579] G. Majumder *et al.* (Belle collaboration), Phys. Rev. **D70**, 111103 (2004), arXiv:hep-ex/0409008 [hep-ex].

[580] J. P. Lees *et al.* (*BABAR* collaboration), Phys. Rev. **D94**, 091101 (2016), arXiv:1609.06802 [hep-ex].

[581] D. Matvienko *et al.* (Belle collaboration), Phys. Rev. **D92**, 012013 (2015), arXiv:1505.03362 [hep-ex].

[582] B. Aubert *et al.* (*BABAR* collaboration), Phys. Rev. **D74**, 012001 (2006), arXiv:hep-ex/0604009 [hep-ex].

[583] J. Schumann *et al.* (Belle collaboration), Phys. Rev. **D72**, 011103 (2005), arXiv:hep-ex/0501013 [hep-ex].

[584] K. Abe *et al.* (Belle collaboration), Phys. Rev. Lett. **87**, 111801 (2001), arXiv:hep-ex/0104051 [hep-ex].

[585] B. Aubert *et al.* (*BABAR* collaboration), Phys. Rev. Lett. **95**, 171802 (2005), arXiv:hep-ex/0412040 [hep-ex].

[586] A. Drutskoy *et al.* (Belle collaboration), Phys. Lett. **B542**, 171 (2002), arXiv:hep-ex/0207041 [hep-ex].

[587] P. Krokovny *et al.* (Belle collaboration), Phys. Rev. Lett. **90**, 141802 (2003), arXiv:hep-ex/0212066 [hep-ex].

[588] B. Aubert *et al.* (*BABAR* collaboration), Phys. Rev. **D74**, 031101 (2006), arXiv:hep-ex/0604016 [hep-ex].

[589] B. Aubert *et al.* (*BABAR* collaboration), Phys. Rev. Lett. **96**, 011803 (2006), arXiv:hep-ex/0509036 [hep-ex].

[590] A. Das *et al.* (Belle collaboration), Phys. Rev. **D82**, 051103 (2010), arXiv:1007.4619 [hep-ex].

[591] B. Aubert *et al.* (*BABAR* collaboration), Phys. Rev. **D78**, 032005 (2008), arXiv:0803.4296 [hep-ex].

[592] N. Joshi *et al.* (Belle collaboration), Phys. Rev. **D81**, 031101 (2010), arXiv:0912.2594 [hep-ex].

[593] B. Aubert *et al.* (*BABAR* collaboration), Phys. Rev. **D73**, 071103 (2006), arXiv:hep-ex/0512031 [hep-ex].

[594] B. Aubert *et al.* (*BABAR* collaboration), Phys. Rev. Lett. **100**, 171803 (2008), arXiv:0707.1043 [hep-ex].

[595] R. Aaij *et al.* (LHCb collaboration), Phys. Rev. **D87**, 112009 (2013), arXiv:1304.6317 [hep-ex].

[596] R. Aaij *et al.* (LHCb collaboration), Phys. Rev. Lett. **109**, 131801 (2012), arXiv:1207.5991 [hep-ex].

[597] R. Aaij *et al.* (LHCb collaboration), Phys. Rev. **D84**, 092001 (2011), arXiv:1109.6831 [hep-ex], Erratum ibid. **D85**, 039904 (2011).

[598] R. Aaij *et al.* (LHCb collaboration), Phys. Rev. Lett. **108**, 161801 (2012), arXiv:1201.4402 [hep-ex].

[599] R. Aaij *et al.* (LHCb collaboration), Phys. Rev. **D86**, 112005 (2012), arXiv:1211.1541 [hep-ex].

[600] R. Aaij *et al.* (LHCb collaboration), JHEP **05**, 019 (2015), arXiv:1412.7654 [hep-ex].

[601] K. Abe *et al.* (Belle collaboration), Phys. Rev. Lett. **94**, 221805 (2005), arXiv:hep-ex/0410091 [hep-ex].

[602] A. Drutskoy *et al.* (Belle collaboration), Phys. Rev. Lett. **94**, 061802 (2005), arXiv:hep-ex/0409026 [hep-ex].

[603] K. Abe *et al.* (Belle collaboration), arXiv:hep-ex/0507064 [hep-ex] (2005).

[604] K. Abe *et al.* (Belle collaboration), Phys. Rev. Lett. **89**, 151802 (2002), arXiv:hep-ex/0205083 [hep-ex].

[605] P. del Amo Sanchez *et al.* (*BABAR* collaboration), Phys. Rev. **D85**, 092017 (2012), arXiv:1111.4387 [hep-ex].

[606] T. Medvedeva *et al.* (Belle collaboration), Phys. Rev. **D76**, 051102 (2007), arXiv:0704.2652 [hep-ex].

[607] Y.-W. Chang *et al.* (Belle collaboration), Phys. Rev. **D79**, 052006 (2009), arXiv:0811.3826 [hep-ex].

[608] J. P. Lees *et al.* (*BABAR* collaboration), Phys. Rev. **D89**, 112002 (2014), arXiv:1401.5990 [hep-ex].

[609] Y. Y. Chang *et al.* (Belle collaboration), Phys. Rev. Lett. **115**, no. 22, 221803 (2015), arXiv:1509.03034 [hep-ex].

[610] B. Aubert *et al.* (*BABAR* collaboration), Phys. Rev. **D73**, 112004 (2006), arXiv:hep-ex/0604037 [hep-ex].

[611] I. Adachi *et al.* (Belle collaboration), Phys. Rev. **D77**, 091101 (2008), arXiv:0802.2988 [hep-ex].

[612] P. del Amo Sanchez *et al.* (*BABAR* collaboration), Phys. Rev. **D83**, 032004 (2011), arXiv:1011.3929 [hep-ex].

[613] G. Gokhroo *et al.* (Belle collaboration), Phys. Rev. Lett. **97**, 162002 (2006), arXiv:hep-ex/0606055 [hep-ex].

[614] A. Zupanc *et al.* (Belle collaboration), Phys. Rev. **D75**, 091102 (2007), arXiv:hep-ex/0703040 [hep-ex].

[615] B. Aubert *et al.* (*BABAR* collaboration), Phys. Rev. **D74**, 031103 (2006), arXiv:hep-ex/0605036 [hep-ex].

[616] B. Aubert *et al.* (*BABAR* collaboration), Phys. Rev. **D67**, 092003 (2003), arXiv:hep-ex/0302015 [hep-ex].

[617] B. Aubert *et al.* (*BABAR* collaboration), Phys. Rev. **D71**, 091104 (2005), arXiv:hep-ex/0502041 [hep-ex].

[618] K. Abe *et al.* (Belle collaboration), arXiv:hep-ex/0508040 [hep-ex] (2005).

[619] B. Aubert *et al.* (*BABAR* collaboration), Phys. Rev. **D72**, 111101 (2005), arXiv:hep-ex/0510051 [hep-ex].

[620] R. Aaij *et al.* (LHCb collaboration), Phys. Rev. **D87**, 092007 (2013), arXiv:1302.5854 [hep-ex].

[621] CDF collaboration, CDF note 7925, 2006, https://www-cdf.fnal.gov/physics/new/bottom/060115.blessed-bddsdp/.

[622] B. Aubert *et al.* (*BABAR* collaboration), Phys. Rev. **D77**, 011102 (2008), arXiv:0708.1565 [hep-ex].

[623] T. Aushev *et al.* (Belle collaboration), Phys. Rev. **D83**, 051102 (2011), arXiv:1102.0935 [hep-ex], Erratum ibid. **D83**, 051102 (2011).

[624] P. Krokovny *et al.* (Belle collaboration), Phys. Rev. Lett. **91**, 262002 (2003), arXiv:hep-ex/0308019 [hep-ex].

[625] B. Aubert *et al.* (*BABAR* collaboration), Phys. Rev. Lett. **93**, 181801 (2004), arXiv:hep-ex/0408041 [hep-ex].

[626] S. K. Choi *et al.* (Belle collaboration), Phys. Rev. **D91**, 092011 (2015), arXiv:1504.02637 [hep-ex], Addendum ibid. **D92**, 039905 (2015).

[627] F. Abe *et al.* (CDF collaboration), Phys. Rev. Lett. **76**, 2015 (1996).

[628] K. Abe *et al.* (Belle collaboration), Phys. Rev. **D67**, 032003 (2003), arXiv:hep-ex/0211047 [hep-ex].

[629] K. Chilikin *et al.* (Belle collaboration), Phys. Rev. **D90**, 112009 (2014), arXiv:1408.6457 [hep-ex].

[630] F. Abe *et al.* (CDF collaboration), Phys. Rev. **D58**, 072001 (1998), arXiv:hep-ex/9803013 [hep-ex].

[631] R. Aaij *et al.* (LHCb collaboration), JHEP **07**, 140 (2014), arXiv:1405.3219 [hep-ex].

[632] T. Affolder *et al.* (CDF collaboration), Phys. Rev. Lett. **88**, 071801 (2002), arXiv:hep-ex/0108022 [hep-ex].

[633] P. del Amo Sanchez *et al.* (*BABAR* collaboration), Phys. Rev. **D82**, 011101 (2010), arXiv:1005.5190 [hep-ex].

[634] B. Aubert *et al.* (*BABAR* collaboration), Phys. Rev. Lett. **91**, 071801 (2003), arXiv:hep-ex/0304014 [hep-ex].

[635] K. Abe *et al.* (Belle collaboration), Phys. Rev. Lett. **87**, 161601 (2001), arXiv:hep-ex/0105014 [hep-ex].

[636] T. Iwashita *et al.* (Belle collaboration), PTEP **2014**, 043C01 (2014), arXiv:1310.2704 [hep-ex].

[637] B. Aubert *et al.* (*BABAR* collaboration), Phys. Rev. Lett. **93**, 041801 (2004), arXiv:hep-ex/0402025 [hep-ex].

[638] K. Abe *et al.* (Belle collaboration), arXiv:hep-ex/0308039 [hep-ex] (2003).

[639] R. Mizuk *et al.* (Belle collaboration), Phys. Rev. **D80**, 031104 (2009), arXiv:0905.2869 [hep-ex].

[640] V. Bhardwaj *et al.* (Belle collaboration), Phys. Rev. Lett. **111**, 032001 (2013), arXiv:1304.3975 [hep-ex].

[641] B. Aubert *et al.* (*BABAR* collaboration), Phys. Rev. Lett. **94**, 171801 (2005), arXiv:hep-ex/0501061 [hep-ex].

[642] B. Aubert *et al.* (*BABAR* collaboration), Phys. Rev. **D78**, 091101 (2008), arXiv:0808.1487 [hep-ex].

[643] V. Bhardwaj *et al.* (Belle collaboration), Phys. Rev. Lett. **107**, 091803 (2011), arXiv:1105.0177 [hep-ex].

[644] B. Aubert *et al.* (*BABAR* collaboration), Phys. Rev. Lett. **102**, 132001 (2009), arXiv:0809.0042 [hep-ex].

[645] V. Bhardwaj *et al.* (Belle collaboration), Phys. Rev. **D93**, 052016 (2016), arXiv:1512.02672 [hep-ex].

[646] J. P. Lees *et al.* (*BABAR* collaboration), Phys. Rev. **D85**, 052003 (2012), arXiv:1111.5919 [hep-ex].

[647] N. Soni *et al.* (Belle collaboration), Phys. Lett. **B634**, 155 (2006), arXiv:hep-ex/0508032 [hep-ex].

[648] F. Fang *et al.* (Belle collaboration), Phys. Rev. Lett. **90**, 071801 (2003), arXiv:hep-ex/0208047 [hep-ex].

[649] B. Aubert *et al.* (*BABAR* collaboration), Phys. Rev. **D76**, 092004 (2007), arXiv:0707.1648 [hep-ex].

[650] B. Aubert *et al.* (*BABAR* collaboration), Phys. Rev. **D70**, 011101 (2004), arXiv:hep-ex/0403007 [hep-ex].

[651] B. Aubert *et al.* (*BABAR* collaboration), Phys. Rev. **D78**, 012006 (2008), arXiv:0804.1208 [hep-ex].

[652] K. Abe *et al.* (Belle collaboration), arXiv:hep-ex/0408107 [hep-ex] (2004).

[653] B. Aubert *et al.* (*BABAR* collaboration), Phys. Rev. **D76**, 031101 (2007), arXiv:0704.1266 [hep-ex].

[654] M. Chang, Y. Duh, J. Lin, I. Adachi, K. Adamczyk, *et al.*, Phys. Rev. **D85**, 091102 (2012), arXiv:1203.3399 [hep-ex].

[655] R. Aaij *et al.* (LHCb collaboration), Phys. Rev. **D88**, 072005 (2013), arXiv:1308.5916 [hep-ex].

[656] R. Aaij *et al.* (LHCb collaboration), Phys. Rev. **D87**, 052001 (2013), arXiv:1301.5347 [hep-ex].

[657] R. Aaij *et al.* (LHCb collaboration), Phys. Rev. Lett. **112**, 091802 (2014), arXiv:1310.2145 [hep-ex].

[658] Y. Liu *et al.* (Belle collaboration), Phys. Rev. **D78**, 011106 (2008), arXiv:0805.3225 [hep-ex].

[659] R. Kumar *et al.* (Belle collaboration), Phys. Rev. **D78**, 091104 (2008), arXiv:0809.1778 [hep-ex].

[660] R. Aaij *et al.* (LHCb collaboration), Phys. Rev. **D92**, 112002 (2015), arXiv:1510.04866 [hep-ex].

[661] B. Aubert *et al.* (*BABAR* collaboration), Phys. Rev. **D70**, 091104 (2004), arXiv:hep-ex/0408018 [hep-ex].

[662] R. Aaij *et al.* (LHCb collaboration), JHEP **09**, 006 (2013), arXiv:1306.4489 [hep-ex].

[663] Q. Xie *et al.* (Belle collaboration), Phys. Rev. **D72**, 051105 (2005), arXiv:hep-ex/0508011 [hep-ex].

[664] B. Aubert *et al.* (*BABAR* collaboration), Phys. Rev. Lett. **90**, 231801 (2003), arXiv:hep-ex/0303036 [hep-ex].

[665] L. Zhang *et al.* (Belle collaboration), Phys. Rev. **D71**, 091107 (2005), arXiv:hep-ex/0503037 [hep-ex].

[666] B. Aubert *et al.* (*BABAR* collaboration), Phys. Rev. **D71**, 091103 (2005), arXiv:hep-ex/0503021 [hep-ex].

[667] F. Abe *et al.* (CDF collaboration), Phys. Rev. **D54**, 6596 (1996), arXiv:hep-ex/9607003 [hep-ex].

[668] R. Aaij *et al.* (LHCb collaboration), Nucl. Phys. **B867**, 547 (2013), arXiv:1210.2631 [hep-ex].

[669] R. Aaij *et al.* (LHCb collaboration), JHEP **01**, 024 (2015), arXiv:1411.0943 [hep-ex].

[670] R. Aaij *et al.* (LHCb collaboration), Eur. Phys. J. **C72**, 2118 (2012), arXiv:1205.0918 [hep-ex].

[671] R. Aaij *et al.* (LHCb collaboration), Nucl. Phys. **B871**, 403 (2013), arXiv:1302.6354 [hep-ex].

[672] B. Aubert *et al.* (*BABAR* collaboration), arXiv:0707.2843 [hep-ex] (2007).

[673] B. Aubert *et al.* (*BABAR* collaboration), Phys. Rev. Lett. **93**, 081801 (2004), arXiv:hep-ex/0404005 [hep-ex].

[674] B. Aubert *et al.* (*BABAR* collaboration), Phys. Rev. **D82**, 031102 (2010), arXiv:1007.1370 [hep-ex].

[675] N. Gabyshev *et al.* (Belle collaboration), Phys. Rev. **D66**, 091102 (2002), arXiv:hep-ex/0208041 [hep-ex].

[676] J. P. Lees *et al.* (*BABAR* collaboration), Phys. Rev. **D87**, 092004 (2013), arXiv:1302.0191 [hep-ex].

[677] J. P. Lees *et al.* (*BABAR* collaboration), Phys. Rev. **D91**, 031102 (2015), arXiv:1410.3644 [hep-ex].

[678] K. Park *et al.* (Belle collaboration), Phys. Rev. **D75**, 011101 (2007), arXiv:hep-ex/0608025 [hep-ex].

[679] N. Gabyshev *et al.* (Belle collaboration), Phys. Rev. Lett. **90**, 121802 (2003), arXiv:hep-ex/0212052 [hep-ex].

[680] B. Aubert *et al.* (*BABAR* collaboration), Phys. Rev. **D78**, 112003 (2008), arXiv:0807.4974 [hep-ex].

[681] B. Aubert *et al.* (*BABAR* collaboration), Phys. Rev. **D80**, 051105 (2009), arXiv:0907.4566 [hep-ex].

[682] R. Chistov *et al.* (Belle collaboration), Phys. Rev. **D74**, 111105 (2006), arXiv:hep-ex/0510074 [hep-ex].

[683] B. Aubert *et al.* (*BABAR* collaboration), Phys. Rev. **D77**, 012002 (2008), arXiv:0710.5763 [hep-ex].

[684] Y. Uchida *et al.* (Belle collaboration), Phys. Rev. **D77**, 051101 (2008), arXiv:0708.1105 [hep-ex].

[685] J. P. Lees *et al.* (*BABAR* collaboration), Phys. Rev. **D84**, 071102 (2011), arXiv:1108.3211 [hep-ex], Erratum ibid. **D85**, 039903 (2012).

[686] K. Abe *et al.* (Belle collaboration), Phys. Rev. Lett. **97**, 202003 (2006), arXiv:hep-ex/0508015 [hep-ex].

[687] J. P. Lees *et al.* (*BABAR* collaboration), Phys. Rev. **D89**, 071102 (2014), arXiv:1312.6800 [hep-ex].

[688] R. Aaij *et al.* (LHCb collaboration), Phys. Rev. Lett. **112**, 202001 (2014), arXiv:1403.3606 [hep-ex].

[689] B. Aubert *et al.* (*BABAR* collaboration), Phys. Rev. **D77**, 111101 (2008), arXiv:0803.2838 [hep-ex].

[690] R. Mizuk *et al.* (Belle collaboration), Phys. Rev. **D78**, 072004 (2008), arXiv:0806.4098 [hep-ex].

[691] B. Aubert *et al.* (*BABAR* collaboration), Phys. Rev. Lett. **96**, 052002 (2006), arXiv:hep-ex/0510070 [hep-ex].

[692] B. Aubert *et al.* (*BABAR* collaboration), Phys. Rev. **D71**, 031501 (2005), arXiv:hep-ex/0412051 [hep-ex].

[693] B. Aubert *et al.* (*BABAR* collaboration), Phys. Rev. **D79**, 112001 (2009), arXiv:0811.0564 [hep-ex].

[694] M. Iwabuchi *et al.* (Belle collaboration), Phys. Rev. Lett. **101**, 041601 (2008), arXiv:0804.0831 [hep-ex].

[695] K. Abe *et al.* (Belle collaboration), Phys. Rev. **D69**, 112002 (2004), arXiv:hep-ex/0307021 [hep-ex].

[696] B. Aubert *et al.* (*BABAR* collaboration), Phys. Rev. **D79**, 112004 (2009), arXiv:0901.1291 [hep-ex].

[697] B. Aubert *et al.* (*BABAR* collaboration), arXiv:hep-ex/0308026 [hep-ex] (2003).

[698] S. Swain *et al.* (Belle collaboration), Phys. Rev. **D68**, 051101 (2003), arXiv:hep-ex/0304032 [hep-ex].

[699] B. Aubert *et al.* (*BABAR* collaboration), Phys. Rev. **D73**, 111104 (2006), arXiv:hep-ex/0604017 [hep-ex].

[700] B. Aubert *et al.* (*BABAR* collaboration), Phys. Rev. Lett. **92**, 141801 (2004), arXiv:hep-ex/0308057 [hep-ex].

[701] R. Aaij *et al.* (LHCb collaboration), Phys. Rev. **D91**, 092002 (2015), arXiv:1503.02995 [hep-ex], Erratum ibid. **D93**, 119901 (2016).

[702] P. del Amo Sanchez *et al.* (*BABAR* collaboration), Phys. Rev. **D82**, 092006 (2010), arXiv:1005.0068 [hep-ex].

[703] R. Aaij *et al.* (LHCb collaboration), Phys. Rev. **D93**, 051101 (2016), arXiv:1512.02494 [hep-ex], Erratum ibid. **D93**, 119902 (2016).

[704] B. Aubert *et al.* (*BABAR* collaboration), Phys. Rev. **D72**, 011102 (2005), arXiv:hep-ex/0505099 [hep-ex].

[705] A. Abulencia *et al.* (CDF collaboration), Phys. Rev. Lett. **96**, 191801 (2006), arXiv:hep-ex/0508014 [hep-ex].

[706] Y. Horii *et al.* (Belle collaboration), Phys. Rev. **D78**, 071901 (2008), arXiv:0804.2063 [hep-ex].

[707] LHCb collaboration, LHCb-CONF-2011-031, 2011, https://cds.cern.ch/record/1363360.

[708] CDF collaboration, CDF note 8242, 2006, http://www-cdf.fnal.gov/physics/new/bottom/060420.blessed-BDK-decay/.

[709] B. Aubert *et al.* (*BABAR* collaboration), Phys. Rev. Lett. **92**, 202002 (2004), arXiv:hep-ex/0311032 [hep-ex].

[710] B. Aubert *et al.* (*BABAR* collaboration), Phys. Rev. **D71**, 031102 (2005), arXiv:hep-ex/0411091 [hep-ex].

[711] J. Wiechczynski *et al.* (Belle collaboration), Phys. Rev. **D80**, 052005 (2009), arXiv:0903.4956 [hep-ex].

[712] B. Aubert *et al.* (*BABAR* collaboration), Phys. Rev. Lett. **98**, 171801 (2007), arXiv:hep-ex/0611030 [hep-ex].

[713] R. Aaij *et al.* (LHCb collaboration), JHEP **02**, 043 (2013), arXiv:1210.1089 [hep-ex].

[714] B. Aubert *et al.* (*BABAR* collaboration), Phys. Rev. **D73**, 011103 (2006), arXiv:hep-ex/0512028 [hep-ex].

[715] P. Chen *et al.* (Belle collaboration), Phys. Rev. **D84**, 071501 (2011), arXiv:1108.4271 [hep-ex].

[716] O. Seon *et al.* (Belle collaboration), Phys. Rev. **D84**, 071106 (2011), arXiv:1107.0642 [hep-ex].

[717] G. Majumder *et al.* (Belle collaboration), Phys. Rev. Lett. **95**, 041803 (2005), arXiv:hep-ex/0502038 [hep-ex].

[718] J. Brodzicka *et al.* (Belle collaboration), Phys. Rev. Lett. **100**, 092001 (2008), arXiv:0707.3491 [hep-ex].

[719] K. Abe *et al.* (Belle collaboration), Phys. Rev. Lett. **93**, 051803 (2004), arXiv:hep-ex/0307061 [hep-ex].

[720] K. Abe *et al.* (Belle collaboration), arXiv:0708.2885 [hep-ex] (2007).

[721] K. Abe *et al.* (Belle collaboration), Phys. Lett. **B538**, 11 (2002), arXiv:hep-ex/0205021 [hep-ex].

[722] D. Acosta *et al.* (CDF collaboration), Phys. Rev. **D66**, 052005 (2002).

[723] H. Guler *et al.* (Belle collaboration), Phys. Rev. **D83**, 032005 (2011), arXiv:1009.5256 [hep-ex].

[724] B. Aubert *et al.* (*BABAR* collaboration), Phys. Rev. **D71**, 071103 (2005), arXiv:hep-ex/0406022 [hep-ex].

[725] K. Abe *et al.* (Belle collaboration), Phys. Rev. Lett. **88**, 031802 (2002), arXiv:hep-ex/0111069 [hep-ex].

[726] A. Vinokurova *et al.* (Belle collaboration), Phys. Lett. **B706**, 139 (2011), arXiv:1105.0978 [hep-ex].

[727] C.-H. Wu *et al.* (Belle collaboration), Phys. Rev. Lett. **97**, 162003 (2006), arXiv:hep-ex/0606022 [hep-ex].

[728] B. Aubert *et al.* (*BABAR* collaboration), Phys. Rev. **D72**, 051101 (2005), arXiv:hep-ex/0507012 [hep-ex].

[729] F. Fang *et al.* (Belle collaboration), Phys. Rev. **D74**, 012007 (2006), arXiv:hep-ex/0605007 [hep-ex].

[730] R. Aaij *et al.* (LHCb collaboration), Phys. Rev. **D85**, 091105 (2012), arXiv:1203.3592 [hep-ex].

[731] B. Aubert *et al.* (*BABAR* collaboration), Phys. Rev. Lett. **92**, 241802 (2004), arXiv:hep-ex/0401035 [hep-ex].

[732] B. Aubert *et al.* (*BABAR* collaboration), Phys. Rev. **D72**, 052002 (2005), arXiv:hep-ex/0507025 [hep-ex].

[733] R. Kumar *et al.* (Belle collaboration), Phys. Rev. **D74**, 051103 (2006), arXiv:hep-ex/0607008 [hep-ex].

[734] LHCb collaboration, LHCb-CONF-2011-030, 2011, https://cds.cern.ch/record/1362029.

[735] F. Abe *et al.* (CDF collaboration), Phys. Rev. Lett. **77**, 5176 (1996).

[736] A. Abulencia (CDF collaboration), Phys. Rev. **D79**, 112003 (2009), arXiv:0905.2146 [hep-ex].

[737] V. Abazov *et al.* (D0 collaboration), Phys. Rev. **D79**, 111102 (2009), arXiv:0805.2576 [hep-ex].

[738] R. Aaij *et al.* (LHCb collaboration), Eur. Phys. J. **C73**, 2462 (2013), arXiv:1303.7133 [hep-ex].

[739] J. P. Lees *et al.* (*BABAR* collaboration), Phys. Rev. **D86**, 091102 (2012), arXiv:1208.3086 [hep-ex].

[740] K. Abe *et al.* (Belle collaboration), arXiv:hep-ex/0505038 [hep-ex] (2005).

[741] B. Aubert *et al.* (*BABAR* collaboration), Phys. Rev. **D74**, 071101 (2006), arXiv:hep-ex/0607050 [hep-ex].

[742] B. Aubert *et al.* (*BABAR* collaboration), Phys. Rev. **D73**, 011101 (2006), arXiv:hep-ex/0507090 [hep-ex].

[743] R. Aaij *et al.* (LHCb collaboration), arXiv:1606.07895 [hep-ex] (2016).

[744] V. M. Abazov *et al.* (D0 collaboration), Phys. Rev. **D89**, 012004 (2014), arXiv:1309.6580 [hep-ex].

[745] T. Aaltonen *et al.* (CDF collaboration), arXiv:1101.6058 [hep-ex] (2011).

[746] T. Aushev *et al.* (Belle collaboration), Phys. Rev. **D81**, 031103 (2010), arXiv:0810.0358 [hep-ex].

[747] K. Abe *et al.* (Belle collaboration), Phys. Rev. Lett. **94**, 182002 (2005), arXiv:hep-ex/0408126 [hep-ex].

[748] R. Aaij *et al.* (LHCb collaboration), JHEP **06**, 115 (2012), arXiv:1204.1237 [hep-ex].

[749] R. Louvot *et al.* (Belle collaboration), Phys. Rev. Lett. **104**, 231801 (2010), arXiv:1003.5312 [hep-ex].

[750] R. Aaij *et al.* (LHCb collaboration), JHEP **06**, 130 (2015), arXiv:1503.09086 [hep-ex].

[751] R. Aaij *et al.* (LHCb collaboration), Phys. Rev. **D87**, 071101 (2013), arXiv:1302.6446 [hep-ex].

[752] R. Aaij *et al.* (LHCb collaboration), Phys. Rev. Lett. **116**, 161802 (2016), arXiv:1603.02408 [hep-ex].

[753] R. Aaij *et al.* (LHCb collaboration), Phys. Lett. **B706**, 32 (2011), arXiv:1110.3676 [hep-ex].

[754] R. Aaij *et al.* (LHCb collaboration), JHEP **08**, 005 (2015), arXiv:1505.01654 [hep-ex].

[755] A. Abulencia *et al.* (CDF collaboration), Phys. Rev. Lett. **98**, 061802 (2007), arXiv:hep-ex/0610045 [hep-ex].

[756] T. Aaltonen *et al.* (CDF collaboration), Phys. Rev. Lett. **103**, 191802 (2009), arXiv:0809.0080 [hep-ex].

[757] R. Aaij *et al.* (LHCb collaboration), Phys. Lett. **B727**, 403 (2013), arXiv:1308.4583 [hep-ex].

[758] T. Aaltonen *et al.* (CDF collaboration), Phys. Rev. Lett. **108**, 201801 (2012), arXiv:1204.0536 [hep-ex].

[759] R. Aaij *et al.* (LHCb collaboration), Phys. Rev. **D93**, 092008 (2016), arXiv:1602.07543 [hep-ex].

[760] J. Li *et al.* (Belle collaboration), Phys. Rev. Lett. **108**, 181808 (2012), arXiv:1202.0103 [hep-ex].

[761] R. Aaij *et al.* (LHCb collaboration), Phys. Rev. **D87**, no. 7, 072004 (2013), arXiv:1302.1213 [hep-ex].

[762] F. Thorne *et al.* (Belle collaboration), Phys. Rev. **D88**, no. 11, 114006 (2013), arXiv:1309.0704 [hep-ex].

[763] R. Aaij *et al.* (LHCb collaboration), Phys. Lett. **B713**, 172 (2012), arXiv:1205.0934 [hep-ex].

[764] T. Aaltonen *et al.* (CDF collaboration), Phys. Rev. **D83**, 052012 (2011), arXiv:1102.1961 [hep-ex].

[765] R. Aaij *et al.* (LHCb collaboration), JHEP **11**, 082 (2015), arXiv:1509.00400 [hep-ex].

[766] LHCb collaboration, LHCb-CONF-2011-025, 2011, https://cds.cern.ch/record/1353270.

[767] R. Aaij *et al.* (LHCb collaboration), Phys. Rev. Lett. **108**, 151801 (2012), arXiv:1112.4695 [hep-ex].

[768] V. M. Abazov *et al.* (D0 collaboration), Phys. Rev. **D86**, 092011 (2012), arXiv:1204.5723 [hep-ex].

[769] CDF collaboration, CDF note 10795, 2012, http://www-cdf.fnal.gov/physics/new/bottom/120420.blessed-BsJPsiPhi-BR/.

[770] R. Aaij *et al.* (LHCb collaboration), Phys. Lett. **B698**, 115 (2011), arXiv:1102.0206 [hep-ex].

[771] A. Abulencia *et al.* (CDF collaboration), Phys. Rev. Lett. **96**, 231801 (2006), arXiv:hep-ex/0602005 [hep-ex].

[772] R. Aaij *et al.* (LHCb collaboration), JHEP **03**, 040 (2016), arXiv:1601.05284 [hep-ex].

[773] R. Aaij *et al.* (LHCb collaboration), Phys. Lett. **B747**, 484 (2015), arXiv:1503.07112 [hep-ex].

[774] V. M. Abazov *et al.* (D0 collaboration), Phys. Rev. **D85**, 011103 (2012), arXiv:1110.4272 [hep-ex].

[775] V. Khachatryan *et al.* (CMS collaboration), Phys. Lett. **B756**, 84 (2016), arXiv:1501.06089 [hep-ex].

[776] R. Aaij *et al.* (LHCb collaboration), Phys. Rev. **D89**, 092006 (2014), arXiv:1402.6248 [hep-ex].

[777] E. Solovieva *et al.* (Belle collaboration), Phys. Lett. **B726**, 206 (2013), arXiv:1304.6931 [hep-ex].

[778] R. Aaij *et al.* (LHCb collaboration), Phys. Rev. **D87**, 112012 (2013), arXiv:1304.4530 [hep-ex].

[779] G. Aad *et al.* (ATLAS collaboration), Eur. Phys. J. **C76**, 4 (2016), arXiv:1507.07099 [hep-ex].

[780] R. Aaij *et al.* (LHCb collaboration), JHEP **09**, 075 (2013), arXiv:1306.6723 [hep-ex].

[781] R. Aaij *et al.* (LHCb collaboration), JHEP **11**, 094 (2013), arXiv:1309.0587 [hep-ex].

[782] LHCb collaboration, LHCb-CONF-2011-040, 2011, https://cds.cern.ch/record/1368193.

[783] R. Aaij *et al.* (LHCb collaboration), Phys. Rev. Lett. **108**, 251802 (2012), arXiv:1204.0079 [hep-ex].

[784] V. Khachatryan *et al.* (CMS collaboration), JHEP **01**, 063 (2015), arXiv:1410.5729 [hep-ex].

[785] R. Aaij *et al.* (LHCb collaboration), Phys. Rev. **D92**, 072007 (2015), arXiv:1507.03516 [hep-ex].

[786] LHCb collaboration, LHCb-CONF-2011-017, 2011, https://cds.cern.ch/record/1336254.

[787] R. Aaij *et al.* (LHCb collaboration), Phys. Rev. Lett. **111**, 181801 (2013), arXiv:1308.4544 [hep-ex].

[788] R. Aaij *et al.* (LHCb collaboration), Phys. Rev. **D89**, 032001 (2014), arXiv:1311.4823 [hep-ex].

[789] R. Aaij *et al.* (LHCb collaboration), Chin. Phys. **C40**, 011001 (2016), arXiv:1509.00292 [hep-ex].

[790] F. Abe *et al.* (CDF collaboration), Phys. Rev. **D55**, 1142 (1997).

[791] V. M. Abazov *et al.* (D0 collaboration), Phys. Rev. **D84**, 031102 (2011), arXiv:1105.0690 [hep-ex].

[792] G. Aad *et al.* (ATLAS collaboration), Phys. Lett. **B751**, 63 (2015), arXiv:1507.08202 [hep-ex].

[793] R. Aaij *et al.* (LHCb collaboration), JHEP **07**, 103 (2014), arXiv:1406.0755 [hep-ex].

[794] R. Aaij *et al.* (LHCb collaboration), JHEP **05**, 132 (2016), arXiv:1603.06961 [hep-ex].

[795] G. Aad *et al.* (ATLAS collaboration), Phys. Rev. **D89**, 092009 (2014), arXiv:1404.1071 [hep-ex].

[796] T. Aaltonen *et al.* (CDF collaboration), Phys. Rev. **D85**, 032003 (2012), arXiv:1112.3334 [hep-ex].

[797] A. Abulencia *et al.* (CDF collaboration), Phys. Rev. Lett. **98**, 122002 (2007), arXiv:hep-ex/0601003 [hep-ex].

[798] R. Aaij *et al.* (LHCb collaboration), Phys. Rev. Lett. **115**, 241801 (2015), arXiv:1510.03829 [hep-ex].

[799] R. Aaij *et al.* (LHCb collaboration), JHEP **10**, 143 (2013), arXiv:1307.7648 [hep-ex].

[800] R. Aaij *et al.* (LHCb collaboration), JHEP **06**, 115 (2015), arXiv:1503.07138 [hep-ex].

[801] R. Aaij *et al.* (LHCb collaboration), Phys. Rev. Lett. **114**, 062004 (2015), arXiv:1411.4849 [hep-ex].

[802] R. Aaij *et al.* (LHCb collaboration), JHEP **05**, 161 (2016), arXiv:1604.03896 [hep-ex].

[803] V. Khachatryan *et al.* (CMS and LHCb collaborations), Nature **522**, 68 (2015), arXiv:1411.4413 [hep-ex].

[804] R. Aaij *et al.* (LHCb collaboration), JHEP **09**, 179 (2015), arXiv:1506.08777 [hep-ex].

[805] O. Buchmuller and H. Flacher, Phys. Rev. **D73**, 073008 (2006), arXiv:hep-ph/0507253 [hep-ph].

[806] B. Aubert *et al.* (*BABAR* collaboration), Phys. Rev. **D81**, 051101 (2010), arXiv:0912.2453 [hep-ex].

[807] I. Adachi *et al.* (Belle collaboration), Phys. Rev. Lett. **110**, 131801 (2013), arXiv:1208.4678 [hep-ex].

[808] R. Aaij *et al.* (LHCb collaboration), Phys. Rev. Lett. **112**, 161801 (2014), arXiv:1402.6852 [hep-ex].

[809] R. Aaij *et al.* (LHCb collaboration), JHEP **05**, 159 (2013), arXiv:1304.3035 [hep-ex].

[810] R. Aaij *et al.* (LHCb collaboration), JHEP **10**, 034 (2015), arXiv:1509.00414 [hep-ex].

[811] R. Aaij *et al.* (LHCb collaboration), JHEP **05**, 082 (2014), arXiv:1403.8045 [hep-ex].

[812] A. Abdesselam *et al.* (Belle collaboration), arXiv:1604.04042 [hep-ex] (2016).

[813] R. Aaij *et al.* (LHCb collaboration), JHEP **04**, 064 (2015), arXiv:1501.03038 [hep-ex].

[814] J. T. Wei *et al.* (Belle collaboration), Phys. Rev. Lett. **103**, 171801 (2009), arXiv:0904.0770 [hep-ex].

[815] J. P. Lees *et al.* (*BABAR* collaboration), Phys. Rev. **D93**, 052015 (2016), arXiv:1508.07960 [hep-ex].

[816] R. Aaij *et al.* (LHCb collaboration), JHEP **02**, 104 (2016), arXiv:1512.04442 [hep-ex].

[817] V. Khachatryan *et al.* (CMS collaboration), Phys. Lett. **B753**, 424 (2016), arXiv:1507.08126 [hep-ex].

[818] Y. Sato *et al.* (Belle collaboration), Phys. Rev. **D93**, 032008 (2016), arXiv:1402.7134 [hep-ex], Addendum ibid. **D93**, 059901 (2016).

[819] R. Aaij *et al.* (LHCb collaboration), arXiv:1609.04736 [hep-ex] (2016).

[820] B. Aubert *et al.* (*BABAR* collaboration), Phys. Rev. Lett. **102**, 091803 (2009), arXiv:0807.4119 [hep-ex].

[821] B. Aubert *et al.* (*BABAR* collaboration), Phys. Rev. **D77**, 051103 (2008), arXiv:0711.4889 [hep-ex].

[822] T. E. Coan *et al.* (CLEO collaboration), Phys. Rev. Lett. **86**, 5661 (2001), arXiv:hep-ex/0010075 [hep-ex].

[823] R. Aaij *et al.* (LHCb collaboration), arXiv:1609.05216 [hep-ex] (2016).

[824] M. Staric *et al.* (Belle collaboration), Phys. Rev. Lett. **98**, 211803 (2007), arXiv:hep-ex/0703036.

[825] B. Aubert *et al.* (*BABAR* collaboration), Phys. Rev. Lett. **98**, 211802 (2007), arXiv:hep-ex/0703020.

[826] T. Aaltonen *et al.* (CDF collaboration), Phys. Rev. Lett. **100**, 121802 (2008), arXiv:0712.1567 [hep-ex].

[827] R. Aaij *et al.* (LHCb collaboration), Phys. Rev. Lett. **111**, 251801 (2013), arXiv:1309.6534 [hep-ex].

[828] S. Bergmann, Y. Grossman, Z. Ligeti, Y. Nir, and A. A. Petrov, Phys. Lett. **B486**, 418 (2000), arXiv:hep-ph/0005181 [hep-ph].

[829] I. I. Y. Bigi and N. G. Uraltsev, Nucl. Phys. **B592**, 92 (2001), arXiv:hep-ph/0005089.

[830] A. A. Petrov, arXiv:hep-ph/0311371 (2003).

[831] A. A. Petrov, Nucl. Phys. Proc. Suppl. **142**, 333 (2005), arXiv:hep-ph/0409130.

[832] A. F. Falk, Y. Grossman, Z. Ligeti, Y. Nir, and A. A. Petrov, Phys. Rev. **D69**, 114021 (2004), arXiv:hep-ph/0402204.

[833] D. Asner *et al.* (CLEO collaboration), Phys. Rev. **D86**, 112001 (2012), arXiv:1210.0939 [hep-ex].

[834] R. Aaij *et al.* (LHCb collaboration), JHEP **07**, 041 (2014), arXiv:1405.2797 [hep-ex].

[835] B. Aubert *et al.* (*BABAR* collaboration), Phys. Rev. Lett. **103**, 211801 (2009), arXiv:0807.4544 [hep-ex].

[836] Heavy Flavor Averaging Group collaboration, Heavy Flavor Averaging Group: charm physics parameters, http://www.slac.stanford.edu/xorg/hfag/charm/index.html.

[837] E. M. Aitala *et al.* (Fermilab E791 collaboration), Phys. Rev. Lett. **77**, 2384 (1996), arXiv:hep-ex/9606016.

[838] C. Cawlfield *et al.* (CLEO collaboration), Phys. Rev. **D71**, 077101 (2005), arXiv:hep-ex/0502012.

[839] B. Aubert *et al.* (*BABAR* collaboration), Phys. Rev. **D76**, 014018 (2007), arXiv:0705.0704 [hep-ex].

[840] U. Bitenc *et al.* (Belle collaboration), Phys. Rev. **D77**, 112003 (2008), arXiv:0802.2952 [hep-ex].

[841] L. M. Zhang *et al.* (Belle collaboration), Phys. Rev. Lett. **96**, 151801 (2006), arXiv:hep-ex/0601029.

[842] B. Ko *et al.* (Belle collaboration), Phys. Rev. Lett. **112**, 111801 (2014), arXiv:1401.3402 [hep-ex].

[843] T. A. Aaltonen *et al.* (CDF collaboration), Phys. Rev. Lett. **111**, 231802 (2013), arXiv:1309.4078 [hep-ex].

[844] R. Aaij *et al.* (LHCb collaboration), arXiv:1611.06143 [hep-ex] (2016).

[845] T. Peng *et al.* (Belle collaboration), Phys. Rev. **D89**, 091103 (2014), arXiv:1404.2412 [hep-ex].

[846] P. del Amo Sanchez *et al.* (*BABAR* collaboration), Phys. Rev. Lett. **105**, 081803 (2010), arXiv:1004.5053 [hep-ex].

[847] R. Aaij *et al.* (LHCb collaboration), JHEP **04**, 033 (2016), arXiv:1510.01664 [hep-ex].

[848] J. P. Lees *et al.* (*BABAR* collaboration), Phys. Rev. **D93**, 112014 (2016), arXiv:1604.00857 [hep-ex].

[849] R. Aaij *et al.* (LHCb collaboration), Phys. Rev. Lett. **116**, 241801 (2016), arXiv:1602.07224 [hep-ex].

[850] B. Aubert *et al.* (*BABAR* collaboration), Phys. Rev. Lett. **100**, 061803 (2008), arXiv:0709.2715 [hep-ex].

[851] B. R. Ko (Belle collaboration), arXiv:1212.5320 [hep-ex] (2012).

[852] CDF collaboration, CDF note 10784, 2012, http://www-cdf.fnal.gov/physics/new/bottom/120216.blessed-CPVcharm10fb/.

[853] T. Aaltonen *et al.* (CDF collaboration), Phys. Rev. Lett. **109**, 111801 (2012), arXiv:1207.2158 [hep-ex].

[854] R. Aaij *et al.* (LHCb collaboration), Phys. Rev. Lett. **116**, 191601 (2016), arXiv:1602.03160 [hep-ex].

[855] E. M. Aitala *et al.* (Fermilab E791 collaboration), Phys. Rev. Lett. **83**, 32 (1999), arXiv:hep-ex/9903012.

[856] J. M. Link *et al.* (FOCUS collaboration), Phys. Lett. **B485**, 62 (2000), arXiv:hep-ex/0004034.

[857] S. E. Csorna *et al.* (CLEO collaboration), Phys. Rev. **D65**, 092001 (2002), arXiv:hep-ex/0111024.

[858] A. Zupanc *et al.* (Belle collaboration), Phys. Rev. **D80**, 052006 (2009), arXiv:0905.4185 [hep-ex].

[859] R. Aaij *et al.* (LHCb collaboration), JHEP **04**, 129 (2012), arXiv:1112.4698 [hep-ex].

[860] M. Staric (Belle collaboration), arXiv:1212.3478 [hep-ex] (2012).

[861] J. P. Lees *et al.* (*BABAR* collaboration), Phys. Rev. **D87**, 012004 (2013), arXiv:1209.3896 [hep-ex].

[862] M. Ablikim *et al.* (BESIII collaboration), Phys. Lett. **B744**, 339 (2015), arXiv:1501.01378 [hep-ex].

[863] T. A. Aaltonen *et al.* (CDF collaboration), Phys. Rev. **D90**, 111103 (2014), arXiv:1410.5435 [hep-ex].

[864] R. Aaij *et al.* (LHCb collaboration), JHEP **04**, 043 (2015), arXiv:1501.06777 [hep-ex].

[865] LHCb collaboration, LHCb-CONF-2016-009, 2016, https://cds.cern.ch/record/2220079.

[866] F. James, MINUIT – Function Minimization and Error Analysis, Reference Manual Version 94.1, CERN Program Library Long Writeup D506, http://wwwasdoc.web.cern.ch/wwwasdoc/minuit/minmain.html.

[867] Y. Grossman, Y. Nir, and G. Perez, Phys. Rev. Lett. **103**, 071602 (2009), arXiv:0904.0305 [hep-ph].

[868] M. Ciuchini, E. Franco, D. Guadagnoli, V. Lubicz, M. Pierini, *et al.*, Phys. Lett. **B655**, 162 (2007), arXiv:hep-ph/0703204 [hep-ph].

[869] A. L. Kagan and M. D. Sokoloff, Phys. Rev. **D80**, 076008 (2009), arXiv:0907.3917 [hep-ph].

[870] I. I. Y. Bigi and A. I. Sanda, Camb. Monogr. Part. Phys. Nucl. Phys. Cosmol. **9**, 1 (2000).

[871] Y. Nir, arXiv:hep-ph/9911321 (1999).

[872] F. Buccella, M. Lusignoli, G. Miele, A. Pugliese, and P. Santorelli, Phys. Rev. **D51**, 3478 (1995), arXiv:hep-ph/9411286.

[873] Y. Grossman and Y. Nir, JHEP **04**, 002 (2012), arXiv:1110.3790 [hep-ph].

[874] B. I. Eisenstein *et al.* (CLEO collaboration), Phys. Rev. **D78**, 052003 (2008), arXiv:0806.2112 [hep-ex].

[875] H. Mendez *et al.* (CLEO collaboration), Phys. Rev. **D81**, 052013 (2010), arXiv:0906.3198 [hep-ex].

[876] E. Won *et al.* (Belle collaboration), Phys. Rev. Lett. **107**, 221801 (2011), arXiv:1107.0553 [hep-ex].

[877] G. Bonvicini *et al.* (CLEO collaboration), Phys. Rev. **D89**, 072002 (2014), arXiv:1312.6775 [hep-ex].

[878] B. R. Ko *et al.* (Belle collaboration), Phys. Rev. Lett. **109**, 021601 (2012), arXiv:1203.6409 [hep-ex].

[879] P. del Amo Sanchez *et al.* (*BABAR* collaboration), Phys. Rev. **D83**, 071103 (2011), arXiv:1011.5477 [hep-ex].

[880] J. M. Link *et al.* (FOCUS collaboration), Phys. Rev. Lett. **88**, 041602; 159903(E) (2002), arXiv:hep-ex/0109022.

[881] J. P. Lees *et al.* (*BABAR* collaboration), Phys. Rev. **D87**, 052012 (2013), arXiv:1212.3003 [hep-ex].

[882] B. R. Ko *et al.* (Belle collaboration), JHEP **02**, 098 (2013), arXiv:1212.6112 [hep-ex].

[883] R. Aaij *et al.* (LHCb collaboration), JHEP **10**, 25 (2014), arXiv:1406.2624 [hep-ex].

[884] R. Aaij *et al.* (LHCb collaboration), Phys. Lett. **B728**, 585 (2014), arXiv:1310.7953 [hep-ex].

[885] E. M. Aitala *et al.* (Fermilab E791 collaboration), Phys. Lett. **B403**, 377 (1997), arXiv:hep-ex/9612005.

[886] V. M. Abazov *et al.* (D0 collaboration), Phys. Rev. **D90**, 111102 (2014), arXiv:1408.6848 [hep-ex].

[887] J. P. Lees *et al.* (*BABAR* collaboration), Phys. Rev. **D87**, 052010 (2013), arXiv:1212.1856 [hep-ex].

[888] P. Rubin *et al.* (CLEO collaboration), Phys. Rev. **D78**, 072003 (2008), arXiv:0807.4545 [hep-ex].

[889] J. M. Link *et al.* (FOCUS collaboration), Phys. Lett. **B491**, 232 (2000), arXiv:hep-ex/0005037.

[890] J. M. Link *et al.* (FOCUS collaboration), Phys. Lett. **B622**, 239 (2005), arXiv:hep-ex/0506012.

[891] T. Aaltonen *et al.* (CDF collaboration), Phys. Rev. **D85**, 012009 (2012), arXiv:1111.5023 [hep-ex].

[892] M. Staric *et al.* (Belle collaboration), Phys. Lett. **B670**, 190 (2008), arXiv:0807.0148 [hep-ex].

[893] E. M. Aitala *et al.* (Fermilab E791 collaboration), Phys. Lett. **B421**, 405 (1998), arXiv:hep-ex/9711003.

[894] N. K. Nisar *et al.* (Belle collaboration), Phys. Rev. Lett. **112**, 211601 (2014), arXiv:1404.1266 [hep-ex].

[895] G. Bonvicini *et al.* (CLEO collaboration), Phys. Rev. **D63**, 071101 (2001), arXiv:hep-ex/0012054.

[896] B. R. Ko *et al.* (Belle collaboration), Phys. Rev. Lett. **106**, 211801 (2011), arXiv:1101.3365 [hep-ex].

[897] R. Aaij *et al.* (LHCb collaboration), JHEP **10**, 055 (2015), arXiv:1508.06087 [hep-ex].

[898] B. Aubert *et al.* (*BABAR* collaboration), Phys. Rev. **D78**, 051102 (2008), arXiv:0802.4035 [hep-ex].

[899] K. Arinstein (Belle collaboration), Phys. Lett. **B662**, 102 (2008), arXiv:0801.2439 [hep-ex].

[900] D. Cronin-Hennessy *et al.* (CLEO collaboration), Phys. Rev. **D72**, 031102 (2005), arXiv:hep-ex/0503052.

[901] X. C. Tian *et al.* (Belle collaboration), Phys. Rev. Lett. **95**, 231801 (2005), arXiv:hep-ex/0507071.

[902] G. Brandenburg *et al.* (CLEO collaboration), Phys. Rev. Lett. **87**, 071802 (2001), arXiv:hep-ex/0105002.

[903] T. Aaltonen *et al.* (CDF collaboration), Phys. Rev. **D86**, 032007 (2012), arXiv:1207.0825 [hep-ex].

[904] D. M. Asner *et al.* (CLEO collaboration), Phys. Rev. **D70**, 091101 (2004), arXiv:hep-ex/0311033.

[905] R. Aaij *et al.* (LHCb collaboration), Phys. Lett. **B726**, 623 (2013), arXiv:1308.3189 [hep-ex].

[906] M. Artuso *et al.* (CLEO collaboration), Phys. Rev. **D85**, 122002 (2012), arXiv:1201.5716 [hep-ex].

[907] J. Alexander *et al.* (CLEO collaboration), Phys. Rev. **D79**, 052001 (2009), arXiv:0901.1216 [hep-ex].

[908] P. Onyisi *et al.* (CLEO collaboration), Phys. Rev. **D88**, 032009 (2013), arXiv:1306.5363 [hep-ex].

[909] B. R. Ko, E. Won, *et al.* (Belle collaboration), Phys. Rev. Lett. **104**, 181602 (2010), arXiv:1001.3202 [hep-ex].

[910] E. Golowich and G. Valencia, Phys. Rev. **D40**, 112 (1989).

[911] I. I. Y. Bigi, arXiv:hep-ph/0107102 (2001).

[912] W. Bensalem, A. Datta, and D. London, Phys. Rev. **D66**, 094004 (2002), arXiv:hep-ph/0208054.

[913] W. Bensalem and D. London, Phys. Rev. **D64**, 116003 (2001), arXiv:hep-ph/0005018.

[914] W. Bensalem, A. Datta, and D. London, Phys. Lett. **B538**, 309 (2002), arXiv:hep-ph/0205009.

[915] A. J. Bevan, arXiv:1506.04246 [hep-ex] (2015).

[916] G. Durieux and Y. Grossman, Phys. Rev. **D92**, 076013 (2015), arXiv:1508.03054 [hep-ph].

[917] R. Aaij *et al.* (LHCb collaboration), JHEP **10**, 005 (2014), arXiv:1408.1299 [hep-ex].

[918] P. del Amo Sanchez *et al.* (*BABAR* collaboration), Phys. Rev. **D81**, 111103 (2010), arXiv:1003.3397 [hep-ex].

[919] J. P. Lees *et al.* (*BABAR* collaboration), Phys. Rev. **D84**, 031103 (2011), arXiv:1105.4410 [hep-ex].

[920] Y. Grossman, A. L. Kagan, and Y. Nir, Phys. Rev. **D75**, 036008 (2007), arXiv:hep-ph/0609178 [hep-ph].

[921] M. Gersabeck, M. Alexander, S. Borghi, V. Gligorov, and C. Parkes, J. Phys. **G39**, 045005 (2012), arXiv:1111.6515 [hep-ex].

[922] LHCb collaboration, LHCb-CONF-2016-010, 2016, https://cds.cern.ch/record/2220093.

[923] M. Staric *et al.* (Belle collaboration), Phys. Lett. **B753**, 412 (2016), arXiv:1509.08266 [hep-ex].

[924] B. Ko (Belle collaboration), PoS **ICHEP2012**, 353 (2013), arXiv:1212.1975.

[925] T. Becher and R. J. Hill, Phys. Lett. **B633**, 61 (2006), arXiv:hep-ph/0509090 [hep-ph].

[926] F. J. Gilman and R. L. Singleton, Phys. Rev. **D41**, 142 (1990).

[927] R. J. Hill, eConf **C060409**, 027, arXiv:hep-ph/0606023 [hep-ph] (2006).

[928] D. Becirevic and A. B. Kaidalov, Phys. Lett. **B478**, 417 (2000), arXiv:hep-ph/9904490 [hep-ph].

[929] C. G. Boyd, B. Grinstein, and R. F. Lebed, Phys. Rev. Lett. **74**, 4603 (1995), arXiv:hep-ph/9412324 [hep-ph].

[930] C. G. Boyd and M. J. Savage, Phys. Rev. **D56**, 303 (1997), arXiv:hep-ph/9702300 [hep-ph].

[931] M. C. Arnesen, B. Grinstein, I. Z. Rothstein, and I. W. Stewart, Phys. Rev. Lett. **95**, 071802 (2005).

[932] C. Bourrely, B. Machet, and E. de Rafael, Nucl. Phys. **B189**, 157 (1981).

[933] D. Becirevic, A. L. Yaouanc, A. Oyanguren, P. Roudeau, and F. Sanfilippo, arXiv:1407.1019 [hep-ph] (2014).

[934] J. P. Lees *et al.* (*BABAR* collaboration), Phys. Rev. **D88**, 052003 (2013), arXiv:1304.5009 [hep-ex], Erratum ibid. **D88**, 079902 (2013).

[935] P. del Amo Sanchez *et al.* (*BABAR* collaboration), Phys. Rev. **D82**, 111101 (2010), arXiv:1009.2076 [hep-ex].

[936] R. Aaij *et al.* (LHCb collaboration), JHEP **09**, 145 (2013), arXiv:1307.4556.

[937] G. Burdman and J. Kambor, Phys. Rev. **D55**, 2817 (1997), arXiv:hep-ph/9602353 [hep-ph].

[938] D. Becirevic, A. Le Yaouanc, L. Oliver, J.-C. Raynal, P. Roudeau, and J. Serrano, Phys. Rev. **D87**, 054007 (2013), arXiv:1206.5869 [hep-ph].

[939] J. P. Lees *et al.* (*BABAR* collaboration), Phys. Rev. **D91**, 052022 (2015), arXiv:1412.5502 [hep-ex].

[940] M. Ablikim *et al.* (BESIII collaboration), Phys. Rev. **D92**, 072012 (2015), arXiv:1508.07560 [hep-ex].

[941] M. Ablikim *et al.* (BESIII collaboration), Phys. Rev. **D92**, 112008 (2015), arXiv:1510.00308 [hep-ex].

[942] L. Widhalm *et al.* (Belle collaboration), Phys. Rev. Lett. **97**, 061804 (2006), arXiv:hep-ex/0604049 [hep-ex].

[943] B. Aubert *et al.* (*BABAR* collaboration), Phys. Rev. **D76**, 052005 (2007), arXiv:0704.0020 [hep-ex].

[944] D. Besson *et al.* (CLEO collaboration), Phys. Rev. **D80**, 032005 (2009), arXiv:0906.2983 [hep-ex].

[945] S. Dobbs *et al.* (CLEO collaboration), Phys. Rev. **D77**, 112005 (2008), arXiv:0712.1020 [hep-ex].

[946] G. Huang *et al.* (CLEO collaboration), Phys. Rev. Lett. **94**, 011802 (2005), arXiv:hep-ex/0407035 [hep-ex].

[947] J. Link *et al.* (FOCUS collaboration), Phys. Lett. **B607**, 233 (2005), arXiv:hep-ex/0410037 [hep-ex].

[948] J. Adler *et al.* (MARK-III collaboration), Phys. Rev. Lett. **62**, 1821 (1989).

[949] K. Kodama *et al.* (Fermilab E653 collaboration), Phys. Rev. Lett. **66**, 1819 (1991).

[950] K. Kodama *et al.* (Fermilab E653 collaboration), Phys. Lett. **B336**, 605 (1994).

[951] P. L. Frabetti *et al.* (Fermilab E687 collaboration), Phys. Lett. **B364**, 127 (1995).

[952] P. L. Frabetti *et al.* (Fermilab E687 collaboration), Phys. Lett. **B315**, 203 (1993).

[953] J. C. Anjos *et al.* (Tagged Photon Spectrometer collaboration), Phys. Rev. Lett. **62**, 1587 (1989).

[954] M. Ablikim *et al.* (BES collaboration), Phys. Lett. **B597**, 39 (2004), arXiv:hep-ex/0406028 [hep-ex].

[955] M. Ablikim *et al.* (BES collaboration), arXiv:hep-ex/0610019 [hep-ex] (2006).

[956] A. Bean *et al.* (CLEO collaboration), Phys. Lett. **B317**, 647 (1993).

[957] Y. Zheng (BESIII collaboration). presented at the 37th International Conference on High Energy Physics (ICHEP 2014), 2014.

[958] J. G. Korner and G. A. Schuler, Z. Phys. **C46**, 93 (1990).

[959] J. Anjos *et al.* (Fermilab E691 collaboration), Phys. Rev. Lett. **65**, 2630 (1990).

[960] K. Kodama *et al.* (Fermilab E653 collaboration), Phys. Lett. **B274**, 246 (1992).

[961] P. Frabetti *et al.* (Fermilab E687 collaboration), Phys. Lett. **B307**, 262 (1993).

[962] E. Aitala *et al.* (Fermilab E791 collaboration), Phys. Rev. Lett. **80**, 1393 (1998), arXiv:hep-ph/9710216 [hep-ph].

[963] E. Aitala *et al.* (Fermilab E791 collaboration), Phys. Lett. **B440**, 435 (1998), arXiv:hep-ex/9809026 [hep-ex].

[964] M. Adamovich *et al.* (BEATRICE collaboration), Eur. Phys. J. **C6**, 35 (1999).

[965] J. Link *et al.* (FOCUS collaboration), Phys. Lett. **B544**, 89 (2002), arXiv:hep-ex/0207049 [hep-ex].

[966] J. Link *et al.* (FOCUS collaboration), Phys. Lett. **B607**, 67 (2005), arXiv:hep-ex/0410067 [hep-ex].

[967] P. del Amo Sanchez *et al.* (*BABAR* collaboration), Phys. Rev. **D83**, 072001 (2011), arXiv:1012.1810 [hep-ex].

[968] B. Aubert *et al.* (*BABAR* collaboration), Phys. Rev. **D78**, 051101 (2008), arXiv:0807.1599 [hep-ex].

[969] H. Mahlke, eConf **C0610161**, 014 (2006), arXiv:hep-ex/0702014 [hep-ex].

[970] J. Link *et al.* (FOCUS collaboration), Phys. Lett. **B535**, 43 (2002), arXiv:hep-ex/0203031 [hep-ex].

[971] K. M. Ecklund *et al.* (CLEO collaboration), Phys. Rev. **D80**, 052009 (2009), arXiv:0907.3201 [hep-ex].

[972] R. A. Briere *et al.* (CLEO collaboration), Phys. Rev. **D81**, 112001 (2010), arXiv:1004.1954 [hep-ex].

[973] P. Estabrooks *et al.*, Nucl. Phys. **B133**, 490 (1978).

[974] A. Filipuzzi, J. Portoles, and M. Gonzalez-Alonso, Phys. Rev. **D85**, 116010 (2012), arXiv:1203.2092 [hep-ph].

[975] M. Ablikim *et al.* (BESIII collaboration), Phys. Rev. **D94**, 072004 (2016), arXiv:1608.06732 [hep-ex].

[976] M. Ablikim *et al.* (BESIII collaboration), Phys. Rev. **D89**, 051104 (2014), arXiv:1312.0374 [hep-ex].

[977] P. del Amo Sanchez *et al.* (*BABAR* collaboration), Phys. Rev. **D82**, 091103 (2010), arXiv:1008.4080 [hep-ex].

[978] A. Zupanc *et al.* (Belle collaboration), JHEP **09**, 139 (2013), arXiv:1307.6240 [hep-ex].

[979] P. Naik *et al.* (CLEO collaboration), Phys. Rev. **D80**, 112004 (2009), arXiv:0910.3602 [hep-ex].

[980] P. Onyisi *et al.* (CLEO collaboration), Phys. Rev. **D79**, 052002 (2009), arXiv:0901.1147 [hep-ex].

[981] E. Barberio, B. van Eijk, and Z. Was, Comput. Phys. Commun. **66**, 115 (1991).

[982] E. Barberio and Z. Was, Comput. Phys. Commun. **79**, 291 (1994).

[983] P. Golonka and Z. Was, Eur. Phys. J. **C45**, 97 (2006), arXiv:hep-ph/0506026.

[984] P. Golonka and Z. Was, Eur. Phys. J. **C50**, 53 (2007), arXiv:hep-ph/0604232.

[985] EVTGEN-V00-11-07, 2005, http://inspirehep.net/record/707695.

[986] J. M. Link *et al.* (FOCUS collaboration), Phys. Lett. **B555**, 167 (2003), arXiv:hep-ex/0212058.

[987] B. Aubert *et al.* (*BABAR* collaboration), Phys. Rev. Lett. **100**, 051802 (2008), arXiv:0704.2080 [hep-ex].

[988] M. Artuso *et al.* (CLEO collaboration), Phys. Rev. Lett. **80**, 3193 (1998), arXiv:hep-ex/9712023.

[989] R. Barate *et al.* (ALEPH collaboration), Phys. Lett. **B403**, 367 (1997).

[990] H. Albrecht *et al.* (ARGUS collaboration), Phys. Lett. **B340**, 125 (1994).

[991] D. S. Akerib *et al.* (CLEO collaboration), Phys. Rev. Lett. **71**, 3070 (1993).

[992] D. Decamp *et al.* (ALEPH collaboration), Phys. Lett. **B266**, 218 (1991).

[993] D. E. Acosta *et al.* (CDF collaboration), Phys. Rev. Lett. **94**, 122001 (2005), arXiv:hep-ex/0504006.

[994] T. E. Coan *et al.* (CLEO collaboration), Phys. Rev. Lett. **80**, 1150 (1998), arXiv:hep-ex/9710028.

[995] B. Aubert *et al.* (*BABAR* collaboration), Phys. Rev. Lett. **90**, 242001 (2003), arXiv:hep-ex/0304021 [hep-ex].

[996] D. Besson *et al.* (CLEO collaboration), Phys. Rev. **D68**, 032002 (2003), arXiv:hep-ex/0305100 [hep-ex], Erratum ibid. **D75**, 119908 (2007).

[997] K. Abe *et al.* (Belle collaboration), Phys. Rev. Lett. **92**, 012002 (2004), arXiv:hep-ex/0307052 [hep-ex].

[998] B. Aubert *et al.* (*BABAR* collaboration), Phys. Rev. **D69**, 031101 (2004), arXiv:hep-ex/0310050 [hep-ex].

[999] J. M. Link *et al.* (FOCUS collaboration), Phys. Lett. **B586**, 11 (2004), arXiv:hep-ex/0312060 [hep-ex].

[1000] S. Godfrey and N. Isgur, Phys. Rev. **D32**, 189 (1985).

[1001] S. Godfrey and R. Kokoski, Phys. Rev. **D43**, 1679 (1991).

[1002] P. Schweitzer, S. Boffi, and M. Radici, Phys. Rev. **D66**, 114004 (2002), arXiv:hep-ph/0207230 [hep-ph].

[1003] F. Jugeau, A. Le Yaouanc, L. Oliver, and J.-C. Raynal, Phys. Rev. **D72**, 094010 (2005), arXiv:hep-ph/0504206 [hep-ph].

[1004] P. Colangelo, F. De Fazio, and R. Ferrandes, Mod. Phys. Lett. **A19**, 2083 (2004), arXiv:hep-ph/0407137 [hep-ph].

[1005] R. N. Cahn and J. D. Jackson, Phys. Rev. **D68**, 037502 (2003), arXiv:hep-ph/0305012 [hep-ph].

[1006] T. Barnes, F. E. Close, and H. J. Lipkin, Phys. Rev. **D68**, 054006 (2003), arXiv:hep-ph/0305025 [hep-ph].

[1007] H. Lipkin, Phys. Lett. **B580**, 50 (2004), arXiv:hep-ph/0306204 [hep-ph].

[1008] W. A. Bardeen, E. J. Eichten, and C. T. Hill, Phys. Rev. **D68**, 054024 (2003), arXiv:hep-ph/0305049 [hep-ph].

[1009] B. Aubert *et al.* (*BABAR* collaboration), Phys. Rev. **D80**, 092003 (2009), arXiv:0908.0806 [hep-ex].

[1010] R. Aaij *et al.* (LHCb collaboration), JHEP **10**, 151 (2012), arXiv:1207.6016 [hep-ex].

[1011] R. Aaij *et al.* (LHCb collaboration), Phys. Rev. Lett. **113**, 162001 (2014), arXiv:1407.7574 [hep-ex].

[1012] R. Aaij *et al.* (LHCb collaboration), JHEP **02**, 133 (2016), arXiv:1601.01495 [hep-ex].

[1013] T. Matsuki, T. Morii, and K. Sudoh, Eur. Phys. J. **A31**, 701 (2007), arXiv:hep-ph/0610186 [hep-ph].

[1014] N. Isgur and M. B. Wise, Phys. Lett. **B232**, 113 (1989).

[1015] M. Neubert, Phys.Rept. **245**, 259 (1994), arXiv:hep-ph/9306320 [hep-ph].

[1016] B. Aubert *et al.* (*BABAR* collaboration), Phys. Rev. **D74**, 032007 (2006), arXiv:hep-ex/0604030 [hep-ex].

[1017] V. M. Abazov *et al.* (D0 collaboration), Phys. Rev. Lett. **102**, 051801 (2009), arXiv:0712.3789 [hep-ex].

[1018] P. L. Frabetti *et al.* (Fermilab E687 collaboration), Phys. Rev. Lett. **72**, 324 (1994).

[1019] J. P. Alexander *et al.* (CLEO collaboration), Phys. Lett. **B303**, 377 (1993).

[1020] H. Albrecht *et al.* (ARGUS collaboration), Phys. Lett. **B297**, 425 (1992).

[1021] P. Avery *et al.* (CLEO collaboration), Phys. Rev. **D41**, 774 (1990).

[1022] H. Albrecht *et al.* (ARGUS collaboration), Phys. Lett. **B230**, 162 (1989).

[1023] J. P. Lees *et al.* (*BABAR* collaboration), Phys. Rev. **D83**, 072003 (2011), arXiv:1103.2675 [hep-ex].

[1024] R. Aaij *et al.* (LHCb collaboration), Phys. Rev. **D90**, 072003 (2014), arXiv:1407.7712 [hep-ex].

[1025] R. Aaij *et al.* (LHCb collaboration), Phys. Lett. **B698**, 14 (2011), arXiv:1102.0348 [hep-ex].

[1026] B. Aubert *et al.* (*BABAR* collaboration), Phys. Rev. Lett. **97**, 222001 (2006), arXiv:hep-ex/0607082 [hep-ex].

[1027] H. Albrecht *et al.* (ARGUS collaboration), Z. Phys. **C69**, 405 (1996).

[1028] Y. Kubota *et al.* (CLEO collaboration), Phys. Rev. Lett. **72**, 1972 (1994), arXiv:hep-ph/9403325 [hep-ph].

[1029] J. P. Lees *et al.* (*BABAR* collaboration), Phys. Rev. **D91**, 052002 (2015), arXiv:1412.6751 [hep-ex].

[1030] R. Aaij *et al.* (LHCb collaboration), Phys. Rev. **D92**, 012012 (2015), arXiv:1505.01505 [hep-ex].

[1031] A. Kuzmin *et al.* (Belle collaboration), Phys. Rev. **D76**, 012006 (2007), arXiv:hep-ex/0611054 [hep-ex].

[1032] H. Abramowicz *et al.* (ZEUS collaboration), Nucl. Phys. **B866**, 229 (2013), arXiv:1208.4468 [hep-ex].

[1033] A. Abulencia *et al.* (CDF collaboration), Phys. Rev. **D73**, 051104 (2006), arXiv:hep-ex/0512069 [hep-ex].

[1034] P. Avery *et al.* (CLEO collaboration), Phys. Lett. **B331**, 236 (1994), arXiv:hep-ph/9403359 [hep-ph].

[1035] H. Albrecht *et al.* (ARGUS collaboration), Phys. Lett. **B232**, 398 (1989).

[1036] J. C. Anjos *et al.* (Tagged Photon Spectrometer collaboration), Phys. Rev. Lett. **62**, 1717 (1989).

[1037] T. Bergfeld *et al.* (CLEO collaboration), Phys. Lett. **B340**, 194 (1994).

[1038] H. Albrecht *et al.* (ARGUS collaboration), Phys. Lett. **B221**, 422 (1989).

[1039] H. Albrecht *et al.* (ARGUS collaboration), Phys. Lett. **B231**, 208 (1989).

[1040] P. Abreu *et al.* (DELPHI collaboration), Phys. Lett. **B426**, 231 (1998).

[1041] S. Chekanov *et al.* (ZEUS collaboration), Eur. Phys. J. **C60**, 25 (2009), arXiv:0807.1290 [hep-ex].

[1042] A. Heister *et al.* (ALEPH collaboration), Phys. Lett. **B526**, 34 (2002), arXiv:hep-ex/0112010 [hep-ex].

[1043] B. Aubert *et al.* (*BABAR* collaboration), Phys. Rev. **D72**, 052006 (2005), arXiv:hep-ex/0507009 [hep-ex].

[1044] E. Solovieva *et al.* (Belle collaboration), Phys. Lett. **B672**, 1 (2009), arXiv:0808.3677 [hep-ex].

[1045] T. Aaltonen *et al.* (CDF collaboration), Phys. Rev. **D84**, 012003 (2011), arXiv:1105.5995 [hep-ex].

[1046] M. Artuso *et al.* (CLEO collaboration), Phys. Rev. Lett. **86**, 4479 (2001), arXiv:hep-ex/0010080 [hep-ex].

[1047] B. Aubert *et al.* (*BABAR* collaboration), Phys. Rev. Lett. **98**, 012001 (2007), arXiv:hep-ex/0603052 [hep-ex].

[1048] H.-Y. Cheng and C.-K. Chua, Phys. Rev. **D75**, 014006 (2007), arXiv:hep-ph/0610283 [hep-ph].

[1049] S. H. Lee *et al.* (Belle collaboration), Phys. Rev. **D89**, 091102 (2014), arXiv:1404.5389 [hep-ex].

[1050] R. Mizuk *et al.* (Belle collaboration), Phys. Rev. Lett. **94**, 122002 (2005), arXiv:hep-ex/0412069 [hep-ex].

[1051] L. Copley, N. Isgur, and G. Karl, Phys. Rev. **D20**, 768 (1979), Erratum ibid. **D23**, 817 (1981).

[1052] D. Pirjol and T.-M. Yan, Phys. Rev. **D56**, 5483 (1997), arXiv:hep-ph/9701291 [hep-ph].

[1053] R. Chistov *et al.* (Belle collaboration), Phys. Rev. Lett. **97**, 162001 (2006), arXiv:hep-ex/0606051 [hep-ex].

[1054] Y. Kato *et al.* (Belle collaboration), Phys. Rev. **D89**, 052003 (2014), arXiv:1312.1026 [hep-ex].

[1055] Y. Kato *et al.* (Belle collaboration), Phys. Rev. **D94**, 032002 (2016), arXiv:1605.09103 [hep-ex].

[1056] B. Aubert *et al.* (*BABAR* collaboration), Phys. Rev. **D77**, 031101 (2008), arXiv:0710.5775 [hep-ex].

[1057] J. Yelton *et al.* (Belle collaboration), Phys. Rev. **D94**, 052011 (2016), arXiv:1607.07123 [hep-ex].

[1058] B. Aubert *et al.* (*BABAR* collaboration), Phys. Rev. Lett. **97**, 232001 (2006), arXiv:hep-ex/0608055 [hep-ex].

[1059] J. L. Rosner, Phys. Rev. **D52**, 6461 (1995), arXiv:hep-ph/9508252 [hep-ph].

[1060] L. Y. Glozman and D. Riska, Nucl. Phys. **A603**, 326 (1996), arXiv:hep-ph/9509269 [hep-ph].

[1061] E. E. Jenkins, Phys. Rev. **D54**, 4515 (1996), arXiv:hep-ph/9603449 [hep-ph].

[1062] L. Burakovsky, J. T. Goldman, and L. Horwitz, Phys. Rev. **D56**, 7124 (1997), arXiv:hep-ph/9706464 [hep-ph].

[1063] A. Zupanc *et al.* (Belle collaboration), Phys. Rev. Lett. **113**, 042002 (2014), arXiv:1312.7826 [hep-ex].

[1064] M. Ablikim *et al.* (BESIII collaboration), Phys. Rev. Lett. **116**, 052001 (2016), arXiv:1511.08380 [hep-ex].

[1065] M. Ablikim *et al.* (BESIII collaboration), Phys. Rev. Lett. **115**, 221805 (2015), arXiv:1510.02610 [hep-ex].

[1066] P. Avery *et al.* (CLEO collaboration), Phys. Rev. **D43**, 3599 (1991).

[1067] M. S. Alam *et al.* (CLEO collaboration), Phys. Rev. **D57**, 4467 (1998), arXiv:hep-ex/9709012 [hep-ex].

[1068] H. Albrecht *et al.* (ARGUS collaboration), Phys. Lett. **B274**, 239 (1992).

[1069] J. M. Link *et al.* (FOCUS collaboration), Phys. Lett. **B624**, 22 (2005), arXiv:hep-ex/0505077 [hep-ex].

[1070] P. Avery *et al.* (CLEO collaboration), Phys. Lett. **B325**, 257 (1994).

[1071] H. Albrecht *et al.* (ARGUS collaboration), Phys. Lett. **B207**, 109 (1988).

[1072] B. Aubert *et al.* (*BABAR* collaboration), Phys. Rev. **D75**, 052002 (2007), arXiv:hep-ex/0601017 [hep-ex].

[1073] Y. Kubota *et al.* (CLEO collaboration), Phys. Rev. Lett. **71**, 3255 (1993).

[1074] T. Bergfeld *et al.* (CLEO collaboration), Phys. Lett. **B323**, 219 (1994), arXiv:hep-ph/9403326 [hep-ph].

[1075] H. Albrecht *et al.* (ARGUS collaboration), Phys. Lett. **B269**, 234 (1991).

[1076] G. Burdman, E. Golowich, J. L. Hewett, and S. Pakvasa, Phys. Rev. **D66**, 014009 (2002), arXiv:hep-ph/0112235 [hep-ph].

[1077] S. Fajfer, A. Prapotnik, S. Prelovsek, P. Singer, and J. Zupan, Nucl. Phys. Proc. Suppl. **115**, 93 (2003), arXiv:hep-ph/0208201 [hep-ph].

[1078] S. Fajfer, N. Kosnik, and S. Prelovsek, Phys. Rev. **D76**, 074010 (2007), arXiv:0706.1133 [hep-ph].

[1079] E. Golowich, J. Hewett, S. Pakvasa, and A. A. Petrov, Phys. Rev. **D79**, 114030 (2009), arXiv:0903.2830 [hep-ph].

[1080] A. Paul, I. I. Bigi, and S. Recksiegel, Phys. Rev. **D82**, 094006 (2010), arXiv:1008.3141 [hep-ph], Erratum ibid. **D83**, 019901 (2011).

[1081] A. Borisov, arXiv:1112.3269 [hep-ph] (2011).

[1082] R.-M. Wang, J.-H. Sheng, J. Zhu, Y.-Y. Fan, and Y. Gao, Int. J. Mod. Phys. **A29**, 1450169 (2014).

[1083] S. de Boer and G. Hiller, Phys. Rev. **D93**, 074001 (2016), arXiv:1510.00311 [hep-ph].

[1084] P. Rubin *et al.* (CLEO collaboration), Phys. Rev. **D82**, 092007 (2010), arXiv:1009.1606 [hep-ex].

[1085] V. Abazov *et al.* (D0 collaboration), Phys. Rev. Lett. **100**, 101801 (2008), arXiv:0708.2094 [hep-ex].

[1086] R. Aaij *et al.* (LHCb collaboration), Phys. Lett. **B728**, 234 (2014), arXiv:1310.2535 [hep-ex].

[1087] R. Aaij *et al.* (LHCb collaboration), Phys. Lett. **B724**, 203 (2013), arXiv:1304.6365 [hep-ex].

[1088] T. Coan *et al.* (CLEO collaboration), Phys. Rev. Lett. **90**, 101801 (2003), arXiv:hep-ex/0212045 [hep-ex].

[1089] M. Ablikim *et al.* (BESIII collaboration), Phys. Rev. **D91**, 112015 (2015), arXiv:1505.03087 [hep-ex].

[1090] J. P. Lees *et al.* (*BABAR* collaboration), Phys. Rev. **D85**, 091107 (2012), arXiv:1110.6480 [hep-ex].

[1091] N. K. Nisar *et al.* (Belle collaboration), Phys. Rev. **D93**, 051102 (2016), arXiv:1512.02992 [hep-ex].

[1092] P. Haas *et al.* (CLEO collaboration), Phys. Rev. Lett. **60**, 1614 (1988).

[1093] H. Albrecht *et al.* (ARGUS collaboration), Phys. Lett. **B209**, 380 (1988).

[1094] J. Adler *et al.* (MARK-III collaboration), Phys. Rev. **D37**, 2023 (1988), Erratum ibid. **D40**, 3788 (1989).

[1095] A. Freyberger *et al.* (CLEO collaboration), Phys. Rev. Lett. **76**, 3065 (1996).

[1096] D. Pripstein *et al.* (Fermilab E789 collaboration), Phys. Rev. **D61**, 032005 (2000), arXiv:hep-ex/9906022 [hep-ex].

[1097] E. Aitala *et al.* (Fermilab E791 collaboration), Phys. Lett. **B462**, 401 (1999), arXiv:hep-ex/9906045 [hep-ex].

[1098] B. Aubert *et al.* (*BABAR* collaboration), Phys. Rev. Lett. **93**, 191801 (2004), arXiv:hep-ex/0408023 [hep-ex].

[1099] M. Petric *et al.* (Belle collaboration), Phys. Rev. **D81**, 091102 (2010), arXiv:1003.2345 [hep-ex].

[1100] K. Kodama *et al.* (Fermilab E653 collaboration), Phys. Lett. **B345**, 85 (1995).

[1101] I. Abt *et al.* (HERA-B collaboration), Phys. Lett. **B596**, 173 (2004), arXiv:hep-ex/0405059 [hep-ex].

[1102] T. Aaltonen *et al.* (CDF collaboration), Phys. Rev. **D82**, 091105 (2010), arXiv:1008.5077 [hep-ex].

[1103] R. Aaij *et al.* (LHCb collaboration), Phys. Lett. **B725**, 15 (2013), arXiv:1305.5059 [hep-ex].

[1104] E. Aitala *et al.* (Fermilab E791 collaboration), Phys. Rev. Lett. **86**, 3969 (2001), arXiv:hep-ex/0011077 [hep-ex].

[1105] J. Adler *et al.* (MARK-III collaboration), Phys. Rev. **D40**, 906 (1989).

[1106] J. Becker *et al.* (MARK-III collaboration), Phys. Lett. **B193**, 147 (1987).

[1107] R. Aaij *et al.* (LHCb collaboration), Phys. Lett. **B754**, 167 (2016), arXiv:1512.00322 [hep-ex].

[1108] P. Rubin *et al.* (CLEO collaboration), Phys. Rev. **D79**, 097101 (2009), arXiv:0904.1619 [hep-ex].

[1109] P. Frabetti *et al.* (Fermilab E687 collaboration), Phys. Lett. **B398**, 239 (1997).

[1110] J. P. Lees *et al.* (*BABAR* collaboration), Phys. Rev. **D84**, 072006 (2011), arXiv:1107.4465 [hep-ex].

[1111] M.-G. Zhao (BESIII collaboration), arXiv:1605.08952 [hep-ex] (2016).

[1112] J. Link *et al.* (FOCUS collaboration), Phys. Lett. **B572**, 21 (2003), arXiv:hep-ex/0306049 [hep-ex].

[1113] B. Aubert *et al.* (*BABAR* collaboration), Nucl. Phys. Proc. Suppl. **189**, 193 (2009), arXiv:0808.1121 [hep-ex].

[1114] S. Paramesvaran (*BABAR* collaboration), arXiv:0910.2884 [hep-ex] (2009).

[1115] S. Ryu *et al.* (Belle collaboration), Phys. Rev. **D89**, 072009 (2014), arXiv:1402.5213 [hep-ex].

[1116] R. Barate *et al.* (ALEPH collaboration), Eur. Phys. J. **C4**, 29 (1998), http://cdsweb.cern.ch/record/346304.

[1117] S. Schael *et al.* (ALEPH collaboration), Phys. Rept. **421**, 191 (2005), arXiv:hep-ex/0506072 [hep-ex], HFAG-tau uses measurements of $\tau \to hX$ and $\tau \to KX$ and obtains $\tau \to \pi X$ by difference; the measurement of $\mathcal{B}\left(\tau^- \to 3h^- 2h^+ \pi^0 \nu_\tau \text{ (ex.}K^0\text{)}\right)$ has been read as $(2.1 \pm 0.7 \pm 0.6) \times 10^{-4}$ whereas PDG11 uses $(2.1 \pm 0.7 \pm 0.9) \times 10^{-4}$.

[1118] P. Abreu *et al.* (DELPHI collaboration), Eur. Phys. J. **C10**, 201 (1999).

[1119] M. Acciarri *et al.* (L3 collaboration), Phys. Lett. **B507**, 47 (2001), arXiv:hep-ex/0102023 [hep-ex].

[1120] G. Abbiendi *et al.* (OPAL collaboration), Phys. Lett. **B551**, 35 (2003), arXiv:hep-ex/0211066 [hep-ex].

[1121] H. Albrecht *et al.* (ARGUS collaboration), Z. Phys. **C53**, 367 (1992).

[1122] B. Aubert *et al.* (*BABAR* collaboration), Phys. Rev. Lett. **105**, 051602 (2010), arXiv:0912.0242 [hep-ex].

[1123] A. Anastassov *et al.* (CLEO collaboration), Phys. Rev. **D55**, 2559 (1997), Erratum ibid. **D58**, 119903 (1998).

[1124] G. Abbiendi *et al.* (OPAL collaboration), Phys. Lett. **B447**, 134 (1999), arXiv:hep-ex/9812017 [hep-ex].

[1125] P. Abreu *et al.* (DELPHI collaboration), Z. Phys. **C55**, 555 (1992).

[1126] M. Acciarri *et al.* (L3 collaboration), Phys. Lett. **B345**, 93 (1995).

[1127] G. Alexander *et al.* (OPAL collaboration), Phys. Lett. **B266**, 201 (1991).

[1128] J. Abdallah *et al.* (DELPHI collaboration), Eur. Phys. J. **C46**, 1 (2006), arXiv:hep-ex/0603044 [hep-ex].

[1129] K. Ackerstaff *et al.* (OPAL collaboration), Eur. Phys. J. **C4**, 193 (1998), arXiv:hep-ex/9801029 [hep-ex].

[1130] R. Barate *et al.* (ALEPH collaboration), Eur. Phys. J. **C10**, 1 (1999), arXiv:hep-ex/9903014 [hep-ex].

[1131] M. Battle *et al.* (CLEO collaboration), Phys. Rev. Lett. **73**, 1079 (1994), arXiv:hep-ph/9403329 [hep-ph].

[1132] P. Abreu *et al.* (DELPHI collaboration), Phys. Lett. **B334**, 435 (1994).

[1133] G. Abbiendi *et al.* (OPAL collaboration), Eur. Phys. J. **C19**, 653 (2001), arXiv:hep-ex/0009017 [hep-ex].

[1134] M. Fujikawa *et al.* (Belle collaboration), Phys. Rev. **D78**, 072006 (2008), arXiv:0805.3773 [hep-ex].

[1135] M. Artuso *et al.* (CLEO collaboration), Phys. Rev. Lett. **72**, 3762 (1994), arXiv:hep-ph/9404310 [hep-ph].

[1136] B. Aubert *et al.* (*BABAR* collaboration), Phys. Rev. **D76**, 051104 (2007), arXiv:0707.2922 [hep-ex].

[1137] G. Abbiendi *et al.* (OPAL collaboration), Eur. Phys. J. **C35**, 437 (2004), arXiv:hep-ex/0406007 [hep-ex].

[1138] M. Procario *et al.* (CLEO collaboration), Phys. Rev. Lett. **70**, 1207 (1993).

[1139] R. Akers *et al.* (OPAL collaboration), Phys. Lett. **B339**, 278 (1994).

[1140] T. Coan *et al.* (CLEO collaboration), Phys. Rev. **D53**, 6037 (1996).

[1141] M. Acciarri *et al.* (L3 collaboration), Phys. Lett. **B352**, 487 (1995).

[1142] G. Abbiendi *et al.* (OPAL collaboration), Eur. Phys. J. **C13**, 213 (2000), arXiv:hep-ex/9911029 [hep-ex].

[1143] R. Barate *et al.* (ALEPH collaboration), Eur. Phys. J. **C11**, 599 (1999), arXiv:hep-ex/9903015 [hep-ex].

[1144] J. P. Lees *et al.* (*BABAR* collaboration), Phys. Rev. **D86**, 092013 (2012), arXiv:1208.0376 [hep-ex].

[1145] H. Behrend *et al.* (CELLO collaboration), Phys. Lett. **B222**, 163 (1989).

[1146] B. Adeva *et al.* (L3 collaboration), Phys. Lett. **B265**, 451 (1991).

[1147] H. Aihara *et al.* (TPC/Two Gamma collaboration), Phys. Rev. **D35**, 1553 (1987).

[1148] P. Achard *et al.* (L3 collaboration), Phys. Lett. **B519**, 189 (2001), arXiv:hep-ex/0107055 [hep-ex].

[1149] R. Akers *et al.* (OPAL collaboration), Z. Phys. **C68**, 555 (1995).

[1150] R. Balest *et al.* (CLEO collaboration), Phys. Rev. Lett. **75**, 3809 (1995).

[1151] B. Aubert *et al.* (*BABAR* collaboration), Phys. Rev. Lett. **100**, 011801 (2008), arXiv:0707.2981 [hep-ex].

[1152] M. Lee *et al.* (Belle collaboration), Phys. Rev. **D81**, 113007 (2010), arXiv:1001.0083 [hep-ex].

[1153] R. A. Briere *et al.* (CLEO collaboration), Phys. Rev. Lett. **90**, 181802 (2003), arXiv:hep-ex/0302028 [hep-ex].

[1154] K. Edwards *et al.* (CLEO collaboration), Phys. Rev. **D61**, 072003 (2000), arXiv:hep-ex/9908024 [hep-ex].

[1155] D. Bortoletto *et al.* (CLEO collaboration), Phys. Rev. Lett. **71**, 1791 (1993).

[1156] A. Anastassov *et al.* (CLEO collaboration), Phys. Rev. Lett. **86**, 4467 (2001), arXiv:hep-ex/0010025 [hep-ex].

[1157] S. Richichi *et al.* (CLEO collaboration), Phys. Rev. **D60**, 112002 (1999), arXiv:hep-ex/9810026 [hep-ex].

[1158] D. A. Bauer *et al.* (TPC/Two Gamma collaboration), Phys. Rev. **D50**, 13 (1994).

[1159] R. Barate *et al.* (ALEPH collaboration), Eur. Phys. J. **C1**, 65 (1998).

[1160] K. E. Arms *et al.* (CLEO collaboration), Phys. Rev. Lett. **94**, 241802 (2005), arXiv:hep-ex/0501042 [hep-ex].

[1161] G. Abbiendi *et al.* (OPAL collaboration), Eur. Phys. J. **C13**, 197 (2000), arXiv:hep-ex/9908013 [hep-ex].

[1162] D. Gibaut *et al.* (CLEO collaboration), Phys. Rev. Lett. **73**, 934 (1994).

[1163] B. Bylsma *et al.*, Phys. Rev. **D35**, 2269 (1987).

[1164] H. Albrecht *et al.* (ARGUS collaboration), Phys. Lett. **B202**, 149 (1988).

[1165] K. Ackerstaff *et al.* (OPAL collaboration), Eur. Phys. J. **C8**, 183 (1999), arXiv:hep-ex/9808011 [hep-ex].

[1166] D. Buskulic *et al.* (ALEPH collaboration), Z. Phys. **C74**, 263 (1997).

[1167] K. Inami *et al.* (Belle collaboration), Phys. Lett. **B672**, 209 (2009), arXiv:0811.0088 [hep-ex].

[1168] M. Artuso *et al.* (CLEO collaboration), Phys. Rev. Lett. **69**, 3278 (1992).

[1169] P. del Amo Sanchez *et al.* (*BABAR* collaboration), Phys. Rev. **D83**, 032002 (2011), arXiv:1011.3917 [hep-ex].

[1170] J. E. Bartelt *et al.* (CLEO collaboration), Phys. Rev. Lett. **76**, 4119 (1996).

[1171] M. Bishai *et al.* (CLEO collaboration), Phys. Rev. Lett. **82**, 281 (1999), arXiv:hep-ex/9809012 [hep-ex].

[1172] P. S. Baringer *et al.* (CLEO collaboration), Phys. Rev. Lett. **59**, 1993 (1987).

[1173] D. Buskulic *et al.* (ALEPH collaboration), Z. Phys. **C70**, 579 (1996).

[1174] J. P. Lees *et al.* (*BABAR* collaboration), Phys. Rev. **D86**, 092010 (2012), arXiv:1209.2734 [hep-ex].

[1175] K. Belous *et al.* (Belle collaboration), Phys. Rev. Lett. **112**, 031801 (2014), arXiv:1310.8503 [hep-ex].

[1176] W. Marciano and A. Sirlin, Phys. Rev. Lett. **61**, 1815 (1988).

[1177] R. Decker and M. Finkemeier, Phys. Lett. **B334**, 199 (1994).

[1178] M. Davier, A. Hocker, and Z. Zhang, Rev. Mod. Phys. **78**, 1043 (2006), arXiv:hep-ph/0507078 [hep-ph].

[1179] M. Antonelli *et al.*, Eur. Phys. J. **C69**, 399 (2010), arXiv:1005.2323 [hep-ph].

[1180] E. Gamiz, M. Jamin, A. Pich, J. Prades, and F. Schwab, Nucl. Phys. Proc. Suppl. **169**, 85 (2007), arXiv:hep-ph/0612154.

[1181] J. C. Hardy and I. S. Towner, Phys. Rev. **C91**, 025501 (2015), arXiv:1411.5987 [nucl-ex].

[1182] E. Gamiz, M. Jamin, A. Pich, J. Prades, and F. Schwab, PoS **KAON**, 008 (2008), arXiv:0709.0282 [hep-ph].

[1183] K. Maltman, Nucl. Phys. Proc. Suppl. **218**, 146 (2011), arXiv:1011.6391 [hep-ph].

[1184] J. C. Hardy and I. S. Towner, Phys. Rev. **C79**, 055502 (2009), arXiv:0812.1202 [nucl-ex].

[1185] R. Decker and M. Finkemeier, Nucl. Phys. **B438**, 17 (1995), arXiv:hep-ph/9403385.

[1186] W. J. Marciano, Phys. Rev. Lett. **93**, 231803 (2004), arXiv:hep-ph/0402299.

[1187] M. Finkemeier, Phys. Lett. **B387**, 391 (1996), arXiv:hep-ph/9505434 [hep-ph].

[1188] J. Erler, Rev. Mex. Fis. **50**, 200 (2004), arXiv:hep-ph/0211345.

[1189] P. J. Mohr, D. B. Newell, and B. N. Taylor, Rev. Mod. Phys. **88**, 035009 (2016), arXiv:1507.07956.

[1190] K. Maltman, R. J. Hudspith, R. Lewis, C. E. Wolfe, and J. Zanotti, arXiv:1510.06954 [hep-ph] (2015).

[1191] K. Maltman. presented at the workshop 'Determination of the Fundamental Paramaters in QCD, Mainz', 2016.

[1192] K. Hayasaka *et al.* (Belle collaboration), Phys. Lett. **B666**, 16 (2008), arXiv:0705.0650 [hep-ex].

[1193] B. Aubert *et al.* (*BABAR* collaboration), Phys. Rev. Lett. **104**, 021802 (2010), arXiv:0908.2381 [hep-ex].

[1194] K. Hayasaka (Belle collaboration), J. Phys. Conf. Ser. **335**, 012029 (2011).

[1195] B. Aubert *et al.* (*BABAR* collaboration), Phys. Rev. Lett. **98**, 061803 (2007), arXiv:hep-ex/0610067 [hep-ex].

[1196] Y. Miyazaki *et al.* (Belle collaboration), Phys. Lett. **B692**, 4 (2010), arXiv:1003.1183 [hep-ex].

[1197] B. Aubert *et al.* (*BABAR* collaboration), Phys. Rev. **D79**, 012004 (2009), arXiv:0812.3804 [hep-ex].

[1198] Y. Miyazaki *et al.* (Belle collaboration), Phys. Lett. **B672**, 317 (2009), arXiv:0810.3519 [hep-ex].

[1199] Y. Miyazaki (Belle collaboration), Phys. Lett. **B699**, 251 (2011), arXiv:1101.0755 [hep-ex].

[1200] B. Aubert *et al.* (*BABAR* collaboration), Phys. Rev. Lett. **103**, 021801 (2009), arXiv:0904.0339 [hep-ex].

[1201] B. Aubert *et al.* (*BABAR* collaboration), Phys. Rev. Lett. **100**, 071802 (2008), arXiv:0711.0980 [hep-ex].

[1202] K. Hayasaka *et al.* (Belle collaboration), Phys. Lett. **B687**, 139 (2010), arXiv:1001.3221 [hep-ex].

[1203] J. P. Lees *et al.* (*BABAR* collaboration), Phys. Rev. **D81**, 111101 (2010), arXiv:1002.4550 [hep-ex].

[1204] R. Aaij *et al.* (LHCb collaboration), JHEP **02**, 121 (2015), arXiv:1409.8548 [hep-ex].

[1205] G. Aad *et al.* (ATLAS collaboration), Eur. Phys. J. **C76**, 232 (2016), arXiv:1601.03567 [hep-ex].

[1206] Y. Miyazaki *et al.* (Belle collaboration), Phys. Lett. **B719**, 346 (2013), arXiv:1206.5595 [hep-ex].

[1207] B. Aubert *et al.* (*BABAR* collaboration), Phys. Rev. Lett. **95**, 191801 (2005), arXiv:hep-ex/0506066 [hep-ex].

[1208] K. Hayasaka (Belle collaboration), Nucl. Phys. Proc. Suppl. **169**, 225 (2012).

[1209] G. Lafferty (*BABAR* collaboration), Nucl. Phys. Proc. Suppl. **169**, 186 (2007).

[1210] R. Aaij *et al.* (LHCb collaboration), Phys. Lett. **B724**, 36 (2013), arXiv:1304.4518 [hep-ex].

[1211] A. L. Read, J. Phys. **G28**, 2693 (2002).

[1212] S. Banerjee, B. Pietrzyk, J. M. Roney, and Z. Was, Phys. Rev. **D77**, 054012 (2008), arXiv:0706.3235 [hep-ph].

[1213] CDF collaboration, CDF note 8128, 2007,
http://www-cdf.fnal.gov/physics/statistics/notes/cdf8128_mclimit_csm_v2.pdf.